An Ecological Assessment of the Jordan River: 2013-2018

Volume I

Physical and Chemical Integrity

Prepared by
Theron Miller, PhD
WFWQC
And
David Richards, PhD
OreoHelix Ecological

Prepared for
Wasatch Front Water Quality Council

August 2019

Executive Summary

Introduction

The Jordan River, named after the biblical River Jordan, is a unique river that originates from shallow, highly-regulated Utah Lake, the last freshwater remnant of pluvial Lake Bonneville. It flows from the lake for approximately 51 miles as it is fed by numerous cold-water Wasatch Front Range tributaries until it ultimately nourishes several impounded and sheetflow wetlands reliant on its waters on the southern fringe of Farmington Bay, Great Salt Lake. The physical, chemical, and biological integrity of the Jordan River that make up its ecological integrity are intimately linked via feedback loops that do not act independently. It is now apparent to the Council that the river's ecological integrity has been debased.

In this volume, Volume I we present our research and findings on the physical and chemical integrity of the Jordan River. In Volume II, we present our research and findings on the biological integrity of the river.

Physical and Chemical Integrity Research

The physical integrity of the Jordan River has been greatly altered by the iniquity of human development throughout its entire length. It has been straightened, channelized and constrained by levees. Large portions are dredged regularly (every 3-6 years) to remove the large sediment load delivered from upstream and tributary sources. It is also vastly dewatered at two locations (at mile 21, the Turner Dam and at mile 37, the Surplus Canal Diversion near 2100 S) and its natural flow regime has been severely dampened and altered. Connectivity to cold-water mountain tributaries has been predominately curtailed and connectivity with its floodplain eliminated. Surplus Canal diverts on average about 75% of the river's flow with an annual range from 50% during low flow periods to near 100% during high flow events such as above-average spring runoff or severe storm events. During spring runoff, 90% of this diverted water may be further shunted to the Goggin drain to protect the levee system of the Farmington Bay Waterfowl Management Area and the approximate two dozen private duck clubs that utilize Jordan River water. These physical impairments have unquestionably affected and compromised the Jordan River's chemical and biological integrity.

The lower Jordan River was first added to Utah's §303(d) list of impaired waters in 1998. The cause was identified as low dissolved oxygen (DO) and the source was listed as excessive nutrients. Investigations for the TMDL began in the early 2000s, however additional data collection and evaluation by Division of Water Quality staff did not begin in earnest until about 2008. In 2009 the Jordan River/Farmington Bay Water Quality Council (Council) was organized to perform research and monitoring that would provide greater understanding of the Jordan River ecosystem and further elucidate the cause of low DO in the lower Jordan. This effort initially focused on habitat limitations associated with the channelization, dewatering and poor substrate quality as a result of clay, silt, sand and organic matter deposition (physical integrity).
Water quality monitoring also began in 2009 with 12 sites along the mainstem, the mouths of major tributaries and the effluent of the POTWs that discharge to the river. Constituents included total and dissolved nutrients, including total and ortho-P nitrate, nitrite, TKN and ammonia,

major ions and other basic water quality parameters such as BOD, TDS and VSS (chemical integrity). A multiprobe sonde was used to measure temperature, DO, conductivity and pH at the same sites and time where water quality samples were collected. These parameters are particularly important with regard to the low DO impairment and the original unfounded claim in the 1998 Integrated Report that elevated nutrients, caused elevated primary production (algal growth) and were the cause of the low DO impairment.

Field studies during 2009 focused on basic habitat characteristic and biological quality, including performing the Stream Visual Assessment Protocol (SVAP; US Natural Resources Conservation Service, 1993) (**Chapter 1: "A Visual Assessment of the Jordan River, 2009.").** This project documented degraded physical integrity and how it related to biological integrity, including elevated turbidity and generally very poor habitat characterized by channelization throughout the entire river, excessive scouring and embeddedness upstream from 2100 S and deposition of sediments downstream from 2100 S, all as a result of the 50 to > 95% of stream water being diverted to the Surplus Canal and the ever-declining stream gradient.

After these initial observations, several projects were conducted to begin characterizing and quantify the effects of these physical conditions. Initial studies focused on the effect of turbidity on light penetration and the effect of scouring or smothering on the periphyton community and the types and sources of algae that was being transported downstream (**Chapter 2: "Light Attenuation and Nutrients in the Jordan River and Their Relationship to Periphyton and Phytoplankton Communities").** SVAP results also raised questions as to the actual cause of low DO and we hypothesized that vast amounts of organic material were being deposited along with the inorganic sands, silts and clays in the lower Jordan River. Therefore, in 2010, we also began an intensive coarse particulate organic matter (CPOM) sampling program at several sites in the mainstem and the major tributaries, starting at the mouth of the major canyons and this continued until 2016 (**Chapter 3: "Coarse Particulate Organic Matter Measurements in the Jordan River and its Major Tributaries, 2010 – 2015".)** During 2010, the Council also initiated long-term deployment of data recording sondes fitted with temperature, DO, pH and conductivity probes and later probes that measure fluorescing dissolved organic carbon in order to understand these responses to the frequency, season and severity of flow regimes associated with low DO events (**Chapter 4: "Diel Patterns of Dissolved Oxygen, Fluorescing Dissolved Organic Matter and Turbidity and Their Relationship to Seasonal Runoff and Storm Events in the Jordan River")**. In addition, this report includes updated versions of the original 2013 compendium. These studies were followed by more detailed investigation of sediment oxygen demand as the primary source of oxygen depletion and sediment interactions, transformations and fluxes of nutrients and methane (**Chapter 5: "Sediment oxygen Demand, Nutrient Flux, Organic Matter Processing and Methane Release from the Lower Jordan River."**) Finally, we supported an exploratory study to investigate microbial activity with regard to nutrient availability and assimilation and an attempt to identify relative sources of organic carbon (POTW vs instream algal growth vs terrestrial organic litter)(**Chapter 6: "Nitrogen sources and transformations and Microbial community response to energy and nutrient availability in the Jordan River."**).

The following results were documented from these physical and chemical integrity studies (Chapters 1 – 6).

1. The SVAP study documented the great majority of the river to be drastically modified by channelization to contain and facilitate the movement of floodwaters. Also, the river continues to transport large quantities of loose alluvial material from the Jordan Narrows reach and from all the tributaries within Salt Lake Valley. This ranges from large gravels and cobbles transported during runoff and stormwater flows to continuous transport of small sand, silt and clay in the bedload. This results in a high degree of scouring as well as embeddedness (75-90%) at all locations upstream from 2100 S. Most of this transported material is deposited below the Surplus Canal diversion, including large quantities of organic matter, mostly in the form of leaves, seeds and grass clippings flushed to the river in tributaries and storm drains. This organic material immediately begins to decompose, consuming oxygen and producing large amounts of methane and ammonia.

2. Identification of these scouring and depositional zones prompted the quantification of periphyton and water column algae at multiple locations throughout the Jordan River. Periphyton accumulation was very slow on all substrates for the first 8 weeks of the study. Most of the samplers as well as sediment surface was smothered by several cm of organic and inorganic debris that was transported from upstream sources. This resulted in wildly different results of algal growth and Chl a production. Water column algal species were also identified. The water column was dominated by periphyton that had been sluffed off the sediment surface during spring and summer. However, during July and August, Utah Lake cyanobacteria, including Anabaena and Aphanizomenon, dominated the water column in great numbers. Moreover, except for some patchy growth of the filamentous green alga, *Chladophora glomerata*, in the Narrows, minimal additional algal growth was found to occur throughout the entire length and there was no correlation to the nutrient load delivered by any single POTW discharge or the accumulated result of all of the POTW discharges in the lower reaches of the river.

3. A concurrent study was performed to address the question of whether the turbidity limited light to the degree that algal growth was inhibited. A submarine photometer was used to measure light penetration several times at several locations along the river. While light attenuation curves were steep and light intensity was generally reduced to about 10% or less, all sites had sufficient light to remain above the compensation point (the point at which algal/oxygen production equals respiration) at the bottom.

4. This led to the hypothesis that the large amount of organic matter comes from terrestrial sources, including leaves, seeds, twigs, grass clippings, etc. from tributaries and storm drains, as well as the mainstem. Further, the 60% diversion or more to the

Surplus Canal dewaters the channel sufficiently to transform the river from largely erosional to almost exclusively a depositional river. The contribution of this organic matter, particularly as CPOM, was quantified with monthly measurements in both the mainstem and in major tributaries during the years of 2010 to 2016. This allowed quantification of the CPOM transport in very dry years, wet years and normal years of precipitation and snowpack. In addition, CPOM transport values were generally corroborated by the organic matter modeling of Epstein et al. 2015. Clearly, loads of CPOM are flow-dependent, with annual loads ranging from ~20,000 kg yr^{-1} reaching to LJR during low-flow years to > 2,000,000 kg CPOM yr^{-1} during high-flow years.

5. A PhD dissertation (Hogsett 2015) and subsequent calibration of the QUAL2Kw model linked the apparent low DO to elevated SOD that had become enriched with organic matter from upstream tributary and stormwater sources. Further, high flow events were found to mobilize some of these sediments, including underlying layers that contain oxygen-demanding methane, ammonia and hydrogen sulfide, causing severe depletion of oxygen to as low as 0 mg L^{-1}.

6. The last study concerning chemical integrity of the Jordan River was led by Dr. Jennifer Follstadt-Shah in an effort to understand the dynamics of organic matter decomposition and bacterial nutrient use in the water column. Using a recently developed technique of evaluating ratios of "eco-enzymes", a name assigned to enzymes that adjust their activity in response to nutrient availability, she found that enzyme activity varies throughout the year, suggesting that at various times, these bacteria increase their effort to acquire P or N or C. It was also suggested that elevated concentrations of these nutrients might indicate that decomposition of organic carbon and utilization of nutrients is continually occurring at a "maximum rate".

The Future of the Jordan River and Use Attainability Analysis

All of our research to date had shown that the Jordan River's ecological integrity has be severely compromised by human activity and that initiation of a Use Attainability Analysis strongly be considered. To illustrate this, we use our findings on just one aspect of the types of impairment the river faces and is as follows: The acute DO standard of 4.0 mg L^{-1} has continued to be violated only during and immediately following rare and substantial storm events, or during periods when the Surplus Canal diversion gates at 2100 S were closed in anticipation of imminent storm threats, but which never materialized. This occasionally leaves the channel below 2100 S substantially dewatered and stagnant. For example, the mean daily DO fell below the 5.5 mg L^{-1} mean 7-day chronic standard on two occasions and this included the several days of recovery from a major storm event. During non-storm periods in late summer the daily mean DO dropped below 5.5 when river flows fell below about 120 cfs and water temperature reached 24-25 ^{0}C, but none of these episodes lasted 7 days. Nevertheless, there are circumstances when

the acute standard is violated but the true chronic standard (7-day or 30-day) are not violated. The question for interpretation and policy clarification is whether these acute episodes constitute 10% of samples and, more importantly, whether such standards should apply. In other words, these DO excursions are the result of un-mitigatable conditions, including: natural, ephemeral, intermittent, or (controlled) low-flow conditions or water levels prevent the attainment of the use (CFR § 131.10(g) factor number 2); Human-caused conditions prevent the attainment of the use (CFR § 131.10(g) factor number 3); which is related to the overarching problem that: hydrologic modifications, particularly the diversion of 60 to 90% + of the flow to the surplus canal, preclude the attainment of the use, and it is not feasible to restore the water body to its original condition or to operate such modification in a way that would result in the attainment of the use (CFR § 131.10(g) factor number 4); and this dewatering has also caused: physical conditions related to the natural features of the water body, such as the lack of a proper substrate, cover, flow, depth, pools, riffles, and the like, unrelated to [chemical] water quality, preclude attainment of aquatic life protection uses (CFR § 131.10(g) factor number 5). The river is further impacted by the frequent (every 3-5 years for any particular reach), that is necessary to remove the accumulated debris to provide channel flow. This directly removes critical biological and physical features of the river that would be necessary for ecological integrity. Moreover, this dredging will proceed in perpetuity. Indeed, four out of the six (g) factors (when only one factor is required), qualify the Lower Jordan River for a Use Attainability Analysis whereby the beneficial use and/or site-specific standard should be altered and developed appropriately. This issue needs to be championed by the Council and collaboratively addressed with DWQ.

Chapter 1

An Assessment of the Jordan River Using The Stream Visual Assessment Protocol

Prepared by

Theron Miller

Wasatch Front Water Quality Council

August 2019

Table of Contents

List of Figures

List of Tables

Introduction

The Stream Visual Assessment Protocol (SVAP; US Department of Agriculture 1998) rates 15 different characteristics that provide an assessment of the aquatic fish and macroinvertebrate habitat, riparian condition, the presence or absence of aquatic macroinvertebrates, algal or macrophyte blooms, and the general appearance of water quality and clarity of the river.

Methods

This SVAP was performed during May 2009 on the entire length of the river. We divided the river into 29 segments or reaches. Each reach was divided into sub-reaches, which were approximately 0.25-mile-long resulting in a total of 161 sub-reaches. Two teams assessed the river, one team on the west bank and one on the east bank. After each sub-reach was surveyed, both teams stopped and filled out a data sheet, scoring each variable according to the SVAP protocol (site reference). The variables assessed included channel condition, hydrologic alteration, riparian zone, bank stability, water appearance, nutrient enrichment, barriers to fish movement, instream fish cover, pools, invertebrate habitat and if applicable canopy cover, manure presence, salinity, riffle embeddedness, and macroinvertebrates observed. Each assessment element is rated with a value of 1 to 10 with scoring descriptions given in the protocol for each element assessed. In addition to these elements, river width was estimated, usually paced off where bridges were available, land use was recorded, dominant substrate was assessed, and weather conditions were recorded. In addition to performing the SVAP protocol all inflows and outflows as well as sites where bank erosion or other severe alteration had occurred were photographed and GPS coordinates was recorded. This information may be used for future analysis of nonpoint and storm water sources of contaminants.

Our approach was a slight modification of the original SVAP in order to gain a more accurate and specific assessment of the Jordan River. Due to visibility restrictions and sometimes drastic variation between the two banks, riparian condition was scored for each bank independently by the team assessing that bank. These scores were then averaged to gain a more accurate representation of the river as a whole. Bank stability was scored in the same manner. According to the SVAP protocol, deep streams or streams with low visibility should not be assessed for pools. Therefore, although pools were very rare, they were generally not scored due to the low visibility inherent to the Jordan River. Macroinvertebrates were scored whenever access to their habitat was possible. After a review of this section of the SVAP protocol, it was determined that additional useful information could be derived from macroinvertebrate observations. The SVAP protocol lists the most common macroinvertebrates and separates them into three groups according to their pollution sensitivity; Group I taxa being the most sensitive and group III taxa being the most tolerant. The SVAP scoring accounts for the sensitivity of the dominant group type and the overall abundance and diversity of the macroinvertebrate community. If, however, one species in the group I (sensitive) taxa were found in great abundance but it is the only species found, it was unclear how this would rate because the high abundance and its group I taxa categorization would indicate a high score whereas the lack of diversity would indicate a lower score. Since this is not a particularly uncommon problem in the Jordan River, additional rubrics were added to account for the percentage of the reach with macroinvertebrate habitat, macroinvertebrate diversity, macroinvertebrate abundance/patchiness, and the dominant macroinvertebrate group taxa. Each of these areas was then scored separately. A minimum of

five substrate samples was collected before abundance/ patchiness was scored. To further increase accuracy, abundance scores were directly correlated with the number of macroinvertebrates found in an area 2.5 x 2.5 inches on the substrate being observed. An effort was made to spend 15 to 25 minutes looking at different invertebrate habitats such as cobble, woody debris and root mats to gain an accurate representation of the macroinvertebrates present. Scores for each element are added together and then divided by the number of elements scored to give an overall rating of the river. Due to our alterations made for the macroinvertebrate assessment, these scores were assessed separately so that the results obtained from SVAP would be comparable to those obtained by other stream assessments made with this same protocol. Although careful measures were taken to ensure the most accurate assessment possible, unusually high spring flows during 2019 caused difficulty in sampling some of the parameters such as bottom substrate size and macroinvertebrate species composition.

At the beginning of the assessment the river was reaching some of the highest flows measured since 1983-1984 (US Geological Survey data). June of 2009 was also one of the wettest Junes on record. Our reassessment later in spring and early summer helped to overcome or explain this variability. Since each team scored the river independently, scores could be compared to assess accuracy and consistency in scoring. Once the entire river had been assessed, 10% of the river's reaches were randomly chosen for reassessment. Each team resurveyed the side to which it was originally assigned. A t-test was performed to provide a statistical comparison of scores with those originally obtained. Several reaches were also chosen and reassessed with the opposite team performing the assessment to evaluate any variation that may have been introduced by the team variability. In both reassessments the difference was insignificant. The reassessment also included the participation of two scientists from Utah's Division of Water Quality, one of which had performed SVAP on multiple streams. This was to assure that our crew was surveying and scoring the SVAP protocol in similar fashion as DWQ would and hence our data and conclusions would be acceptable to DWQ.

Although there are numerous tributaries and discharges to the river, the river is highly regulated with multiple dams and diversions. Therefore, its flow varies dramatically between various reaches (Figure 1). Due to the unusually long, wet spring and flow regulation, a drop in water level by as much as 1 meter was observed in some areas during our assessment. These variables undoubtedly affected either directly or indirectly the scores given throughout the assessment.

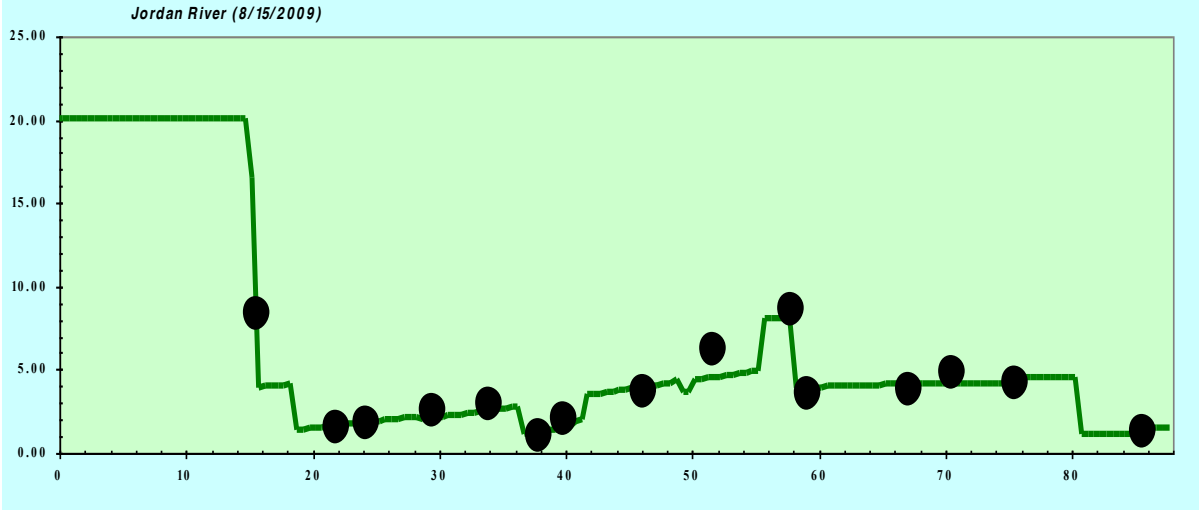

Figure 1. Flow (y-axis in m^3/s) variation along the Jordan River Utah Lake to Farmington Bay (Distance from Utah Lake = x-axis in km). The two major diversions are the Turner Dam (km 13) and the Surplus Canal Diversion (km 60). This graph was generated using the 2009-calibrated QUAL2Kw model for the Jordan River.

Results

Channel Condition

Average scores for each reach are reported in Figure 2. From the headwaters at Utah Lake to 2100 S channel condition varies from quite good to very poor. Below 2100 S. the channel condition rated very poor. Seven of the ten reaches in this section had an average sub-reach score of 1, meaning that >50% of the sub-reach had either riprap or was channelized (Figure 2). In this case, extensive channelization was the primary problem. Dikes or levees were also preventing access to the flood plain.

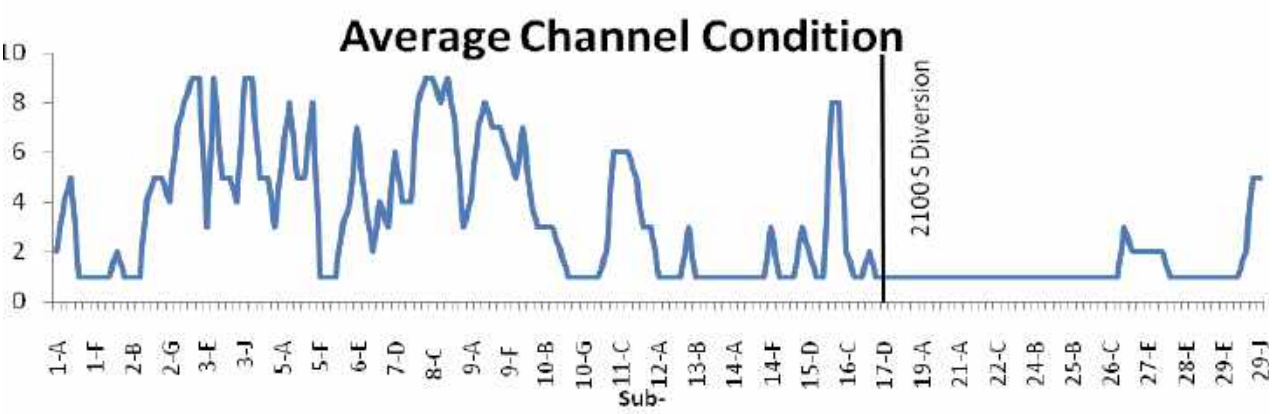

Figure 2. Average SVAP channel condition scores for each sub-reach on the Jordan River.

Hydraulic Alteration

The river rated poorly for hydrologic alteration with few exceptions (See Figure 3). These scores were based on flooding frequency estimates. The flow of the river is highly regulated and the

landscape it flows though is largely developed. In many areas the river was within 50 meters of homes, yards, buildings and parking lots, or running through golf courses, and hence, has little floodplain remaining. The river is contained or incised throughout the great majority of its length, limiting the flows from forming proper channel configuration and from performing its normal functions such developing normal meanders or sinuosity, developing natural pool and riffle areas and shaping and maintaining healthy floodplains for filtration and sediment deposition.

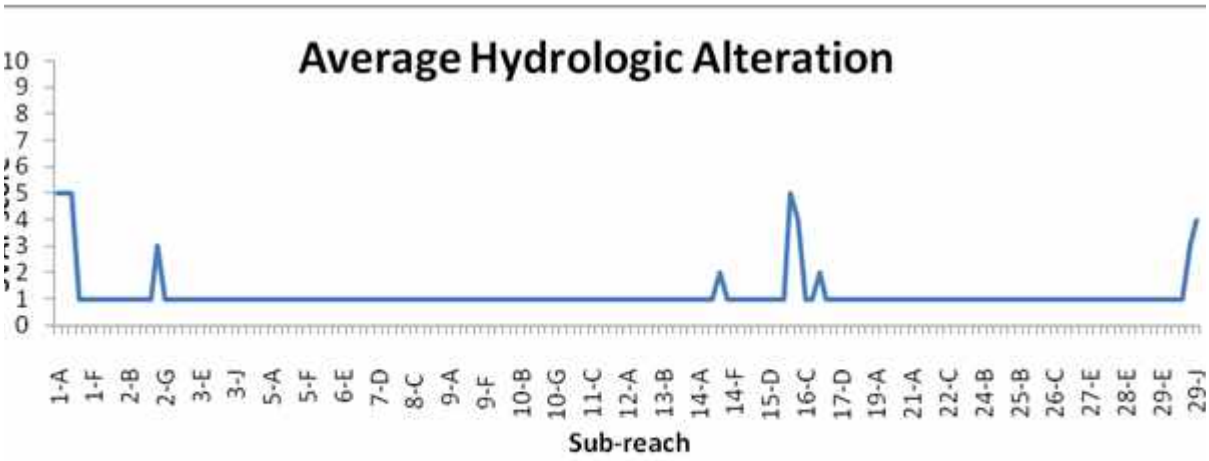

Figure 3. Hydrologic Alteration scores for the Jordan River by sub-reach.

Riparian Zone

The quality of the riparian zone was highly variable. Some sections of the river had natural vegetation extending more than a channel width on each side. Again, it is notable that below 2100 S there is a noticeable decrease in the riparian zone ratings although this in not the only section of the river that is severely limited in this way (see Figures 4 and 5). There are several areas where the riparian quality was scored fairly high, but the number of sub-reaches that scored from 1 to 5 was 3.7 times more frequent than those that scored in the 6-10 range.

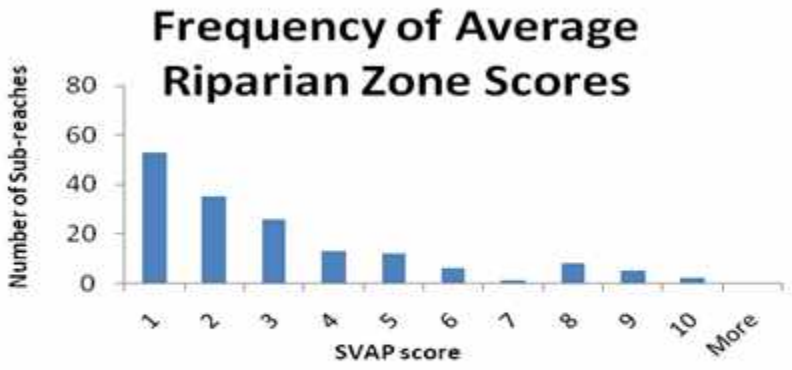

Figure 4. Sub-reaches and their correlated SVAP scores.

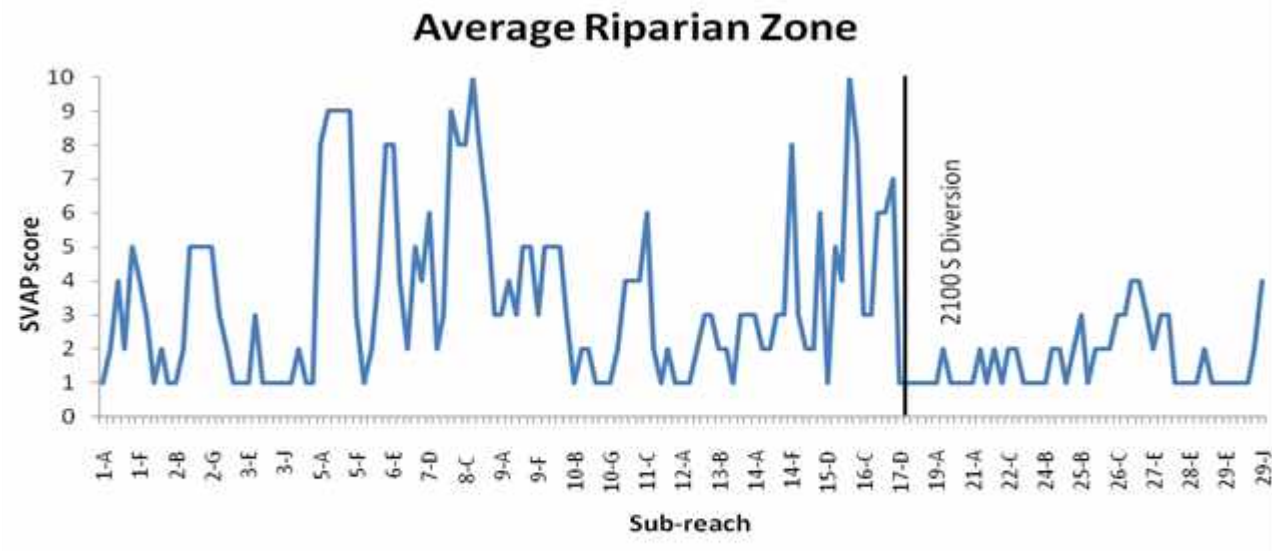

Figure 5. Sub-reaches and their correlated Riparian Zone SVAP scores for the Jordan River. Average scores were obtained by averaging the west and east bank scores for each sub-reach. The line divides up and downstream at 2100S. in Salt Lake City. Sub-reach A1 is at Utah Lake.

Bank Stability

Scoring for bank stability is based on indicators of bank erosion, potential for bank sloughing and the ability of existing bank cover (rocks, brush or trees) to keep banks stable. Bank stability was scored for each bank independently and both the west and east bank showed a high amount of variability, with the most common scores being in the range of 3-6 (Figures 6, 7 and 8). These scores reflect the many areas that are actively eroding and adding suspended and bedload sediment to the river.

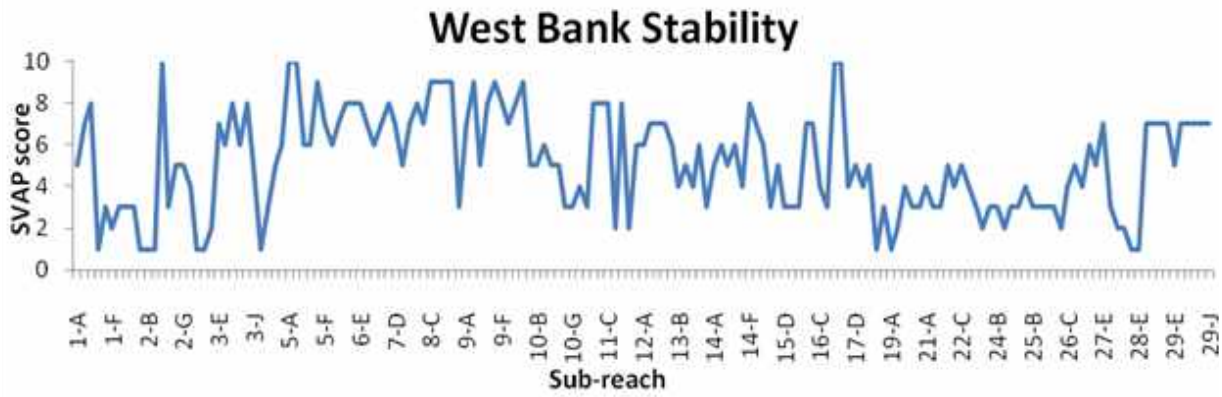

Figure 6. Bank Stability SVAP scores obtained for the west bank of the Jordan River.

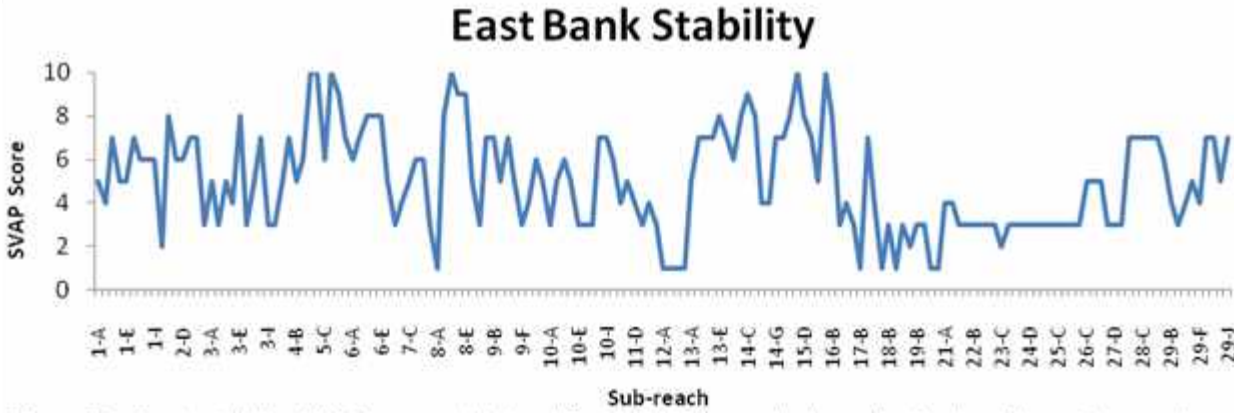

Figure 7. Bank stability SVAP scores obtained for each sub-reach along the Jordan River. Sub-reach A1 is at Utah Lake.

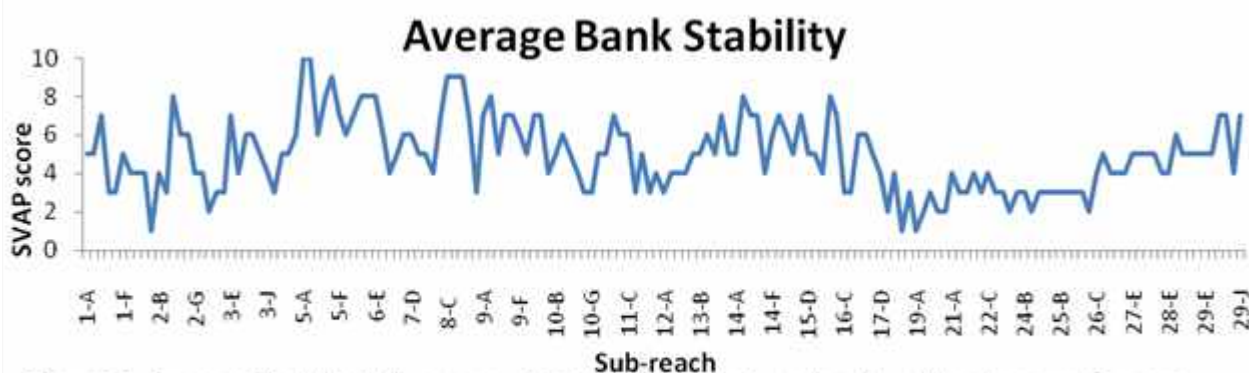

Figure 8. Average Bank Stability scores obtained by averaging east and west bank scores for each sub-reach of the Jordan River.

Average Water Appearance

Water appearance scores were based on the depth of transparency and is an indicator of the turbidity or cloudiness of the water. A score of three was the most common and is given when an objects visible depth is 0.5-1.5 ft (See Figure 9). Water appearance scores did not vary greatly throughout the entire length of the river nor over the duration of the study. However, in October after irrigation releases from Utah Lake were cut off, water became somewhat clearer as the suspended solids settled out and no new sources were delivered from Utah Lake. It is important to note here that the greatest source of turbidity is the inorganic suspended and colloidal solids from Utah Lake. This became apparent, for example, during 2009 where the Utah Lake surface elevation remained below the compromise level at the end of irrigation season. The compromise level is defined as the point at which water begins to free-flow over the weirs at the Utah Lake pump station. Below this elevation, water can be released through controlled gates or, as lake level further declines, water is pumped into the Jordan River in order to meet irrigation water rights. At the end of irrigation season, the pumps are shut off, eliminating Utah Lake as a source of water to the Jordan River.

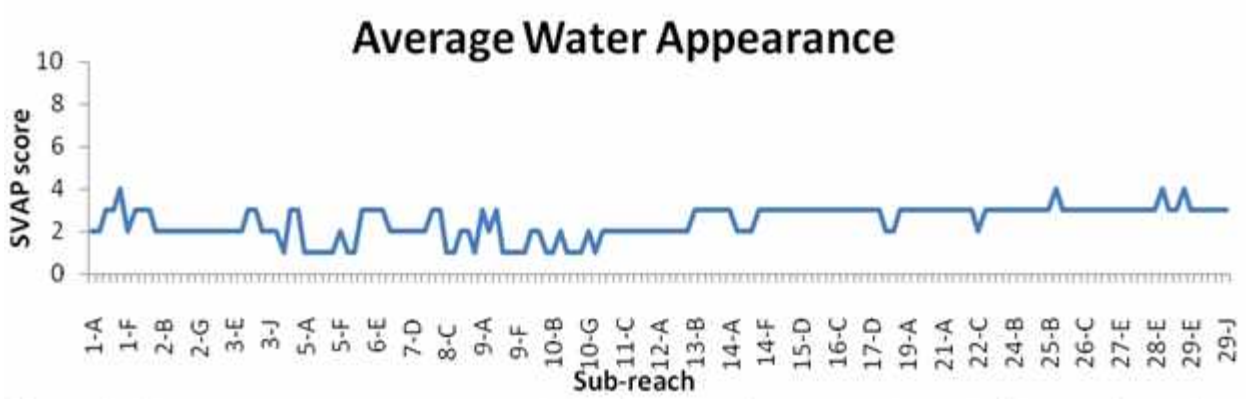

Figure 9. Average Water Appearance SVAP score. Average was obtained by averaging east and west bank scores for each sub-reach.

Nutrient Enrichment

According to SVAP, the types and amounts of aquatic vegetation in the water often indicate nutrient enrichment. High levels of nutrients (especially phosphorus and nitrogen) can promote an overabundance of algae and floating and rooted macrophytes. The river received an average nutrient enrichment score of 7 indicating fairly clear or slightly greenish colored water with moderate algal growth on stream substrates (See Figure 10). Unique to the Jordan River is the gray coloration, which is due to the formation of calcite minerals that form in Utah Lake as a result of elevated pH. These minerals range from suspended to colloidal in nature, depending on the exact type of mineral formed and hence, results in very limited to very slow settling out of the water column. The exact types of minerals, including the phosphorus content, that are formed in Utah Lake is the subject of ongoing research currently being performed in Dr. Greg Carling's lab at BYU (for example, see Randall 2018). Hence, the moderate score, in light of the fact that phosphorus and nitrogen, occurs in relatively high concentrations, are due to the mitigating factors of high turbidity (low light penetration), unstable substrate or scouring by sand and silt and large areas of continual deposition downstream.

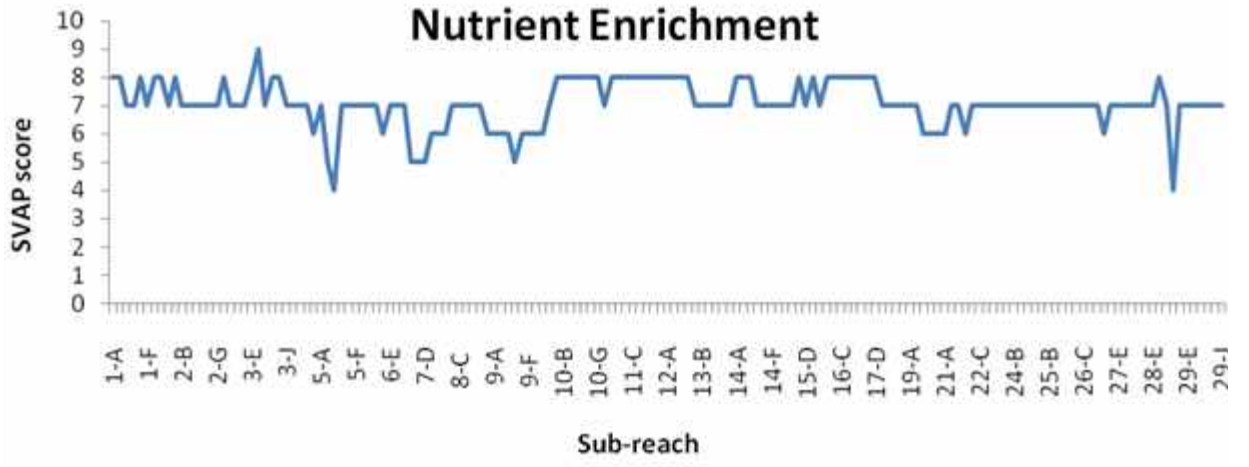

Figure 10. SVAP scores for nutrient enrichment by sub-reach for the Jordan River.

Barriers to Fish Movement

Barriers to fish movement were found in several locations. According to the SVAP protocol a sub-reach containing a barrier to fish movement would rate a 1, a sub-reach with a barrier to fish

movement within 3 miles would rate a score of 3 and any section of the river where no fish barriers were present or within 3 miles rated a 10. The number and location of barriers to fish movement along the Jordan River can be seen in Figure 11.

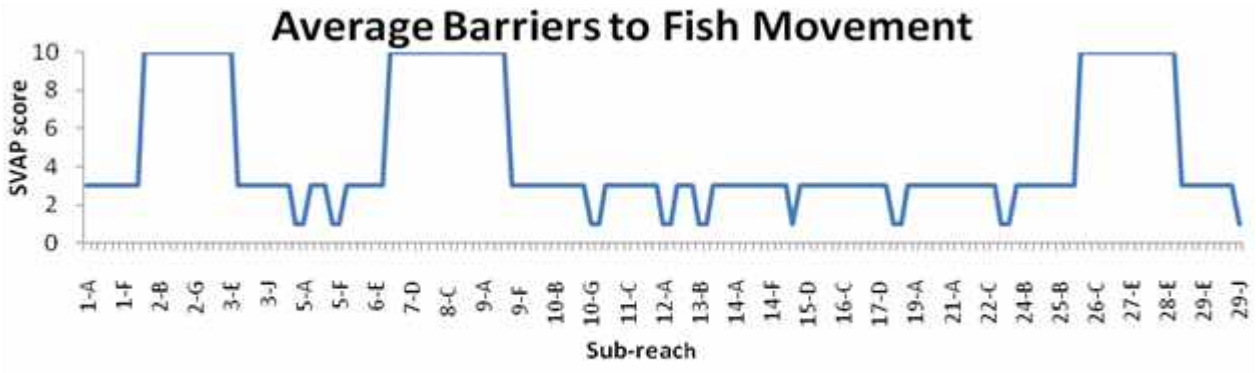

Figure 11. SVAP scores by sub-reach for barriers to fish movement along the Jordan River. Each score of 1 represents a fish barrier or drop > 1 ft in height. Sub-reach A1 is at Utah Lake.

Instream Fish Cover

Instream fish cover is scored according to the number of cover types available. These include deep pools, boulders, large woody debris, thick root mats, overhanging vegetation undercut banks, dense root mats, riffles and deep backwater pools. The scores were highly variable for fish cover with the urbanized reaches of the river receiving the lowest scores (Figure 12).

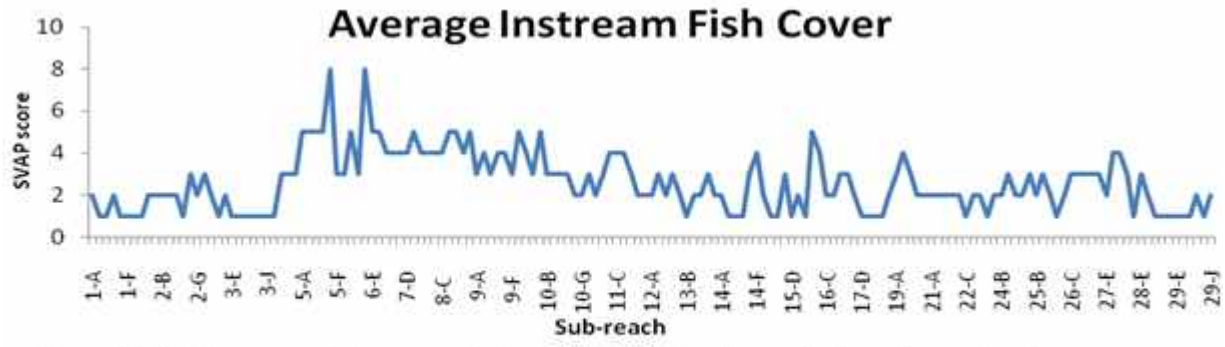

Figure 12. SVAP scores for instream fish cover for each sub-reach along the Jordan River.

Insect/Invertebrate Habitat

The insect and invertebrate habitat also received highly variable scores (Figure 13). Scores were based on the number of habitat types available but the number of habitat types needed for a good score was fewer than the number needed for a good fish cover score. Invertebrate habitat types include: fine woody debris, leaf packs, submerged logs, cobble, boulders and coarse gravel. Much of the habitat that would otherwise be available for invertebrates was covered by a layer of silt or organic sediment.

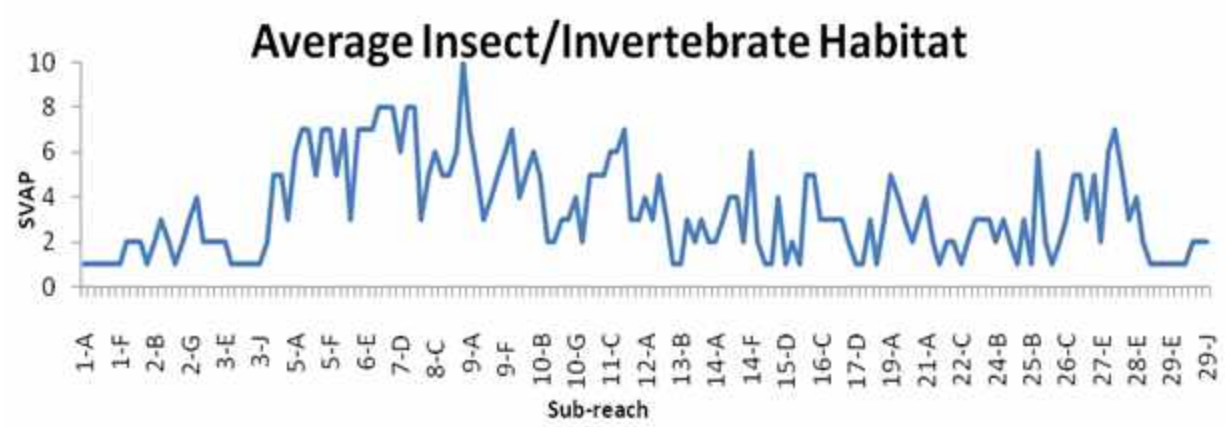

Figure 13. SVAP scores for macroinvertebrates. Averages were obtained by averaging east and west bank scores for invertebrate habitat.

The following five elements were only scored when applicable; canopy cover, manure presence, salinity, riffle embeddedness, and macroinvertebrates observed. Canopy cover, according to the SVAP protocol, should not be assessed if the active channel width is greater than 50ft or if the woody vegetation is naturally absent such as in a wet meadow, etc. Only 58 of the 161 sites had a river width of 50 feet or less. Of these, two sub-reaches scored a 10 while all others were scored a 1. All sub-reaches were given a score despite river width. Of the 103 sub-reaches that were not counted because river width exceeded 50 feet, none scored above a 1.

Canopy Cover

The scores for canopy cover was obtained by averaging scores obtained from the east and west banks. Sub-reaches are not to be scored if the river width is > 50ft or if woody vegetation is naturally absent. Also, cold and warm water fisheries differ in their respective optimal shading conditions and were scored according to different rubrics. Where Canopy cover was scored, all sub-reaches received a score of 1 except for two sub-reaches, which received a score of 10 (Figure 14).

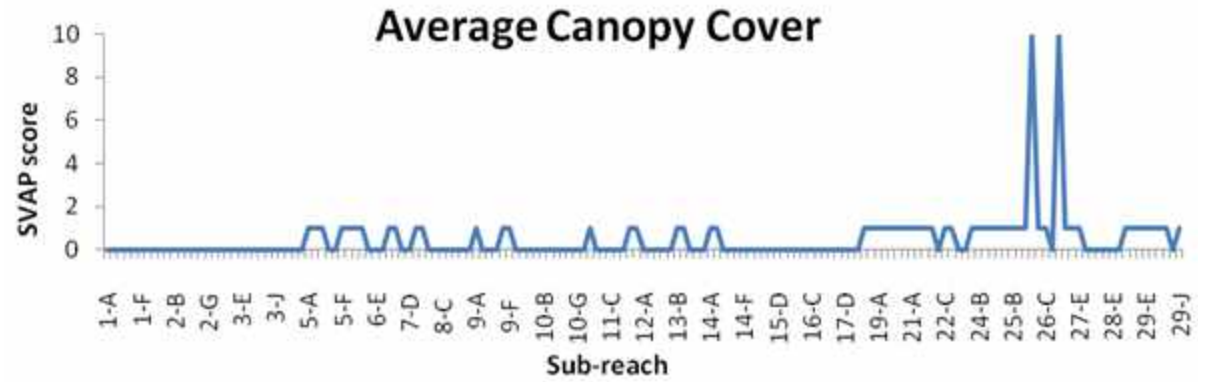

Figure 14. SVAP Average Canopy Cover scores. Average score for east and west banks combined. Score of 0 = NA.

Manure Presence

Manure presence is not scored unless livestock operations or human waste discharges are present. Of the 161 sub-reaches, 33 were scored for manure presence and of these, all were

confined to 7 areas (see Figure 15). Twenty-two of the 33 sub-reaches scored a 5 and the remaining 11 scored between 1 and 4. A score of 5 is given when there is evidence of livestock access to the riparian zone.

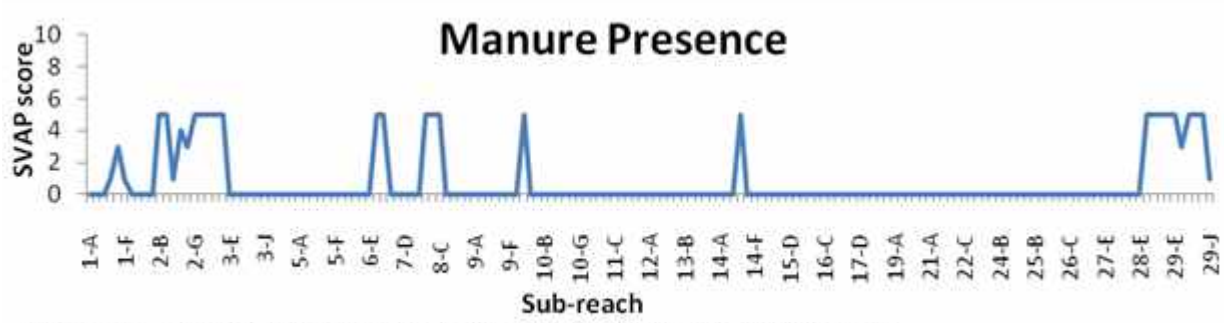

Figure 15. SVAP Manure Presence scores. A score of 0 = NA.

Salinity

According to the SVAP protocol salinity should be assessed only when elevated salinity from anthropogenic sources is known to occur in the stream, and thus salinity was not assessed.

Riffle embeddedness

Outside of the narrows and down to about the 9000 South street crossing, the Jordan River is almost completely void of riffles. Thus, riffle embeddedness was not scored. However, where patches of cobbles existed, even within the narrows, it was evident that 75% to 90% of cobbles were embedded in a sand/silt/clay matrix.

Macroinvertebrates

Macroinvertebrates were assessed using four elements; habitat, abundance, diversity, and dominant group type. During the analysis of these scores, only a weak correlation was found between any two elements (see Table 1). One of the significant variables that need to be understood with invertebrate sampling is that some macroinvertebrate types are more abundant during certain times of the year while others are common at other times of the year. Our assessment was performed over the course of about one and a half month, so our sampling could have overlapped periods where natural seasonal succession may have resulted in species shifts. In addition, due to the prolonged spring rainy season, Utah Lake releases were near 2500 CFS (approximately 3X average spring flows), until late June. At that time, flows were reduced to the normal 700 CFS range within just 24 hours (simply by the shutting the gates at Utah Lake). The combination of above-average and prolonged spring flows, followed by the rapid decline in flows, along with natural seasonal succession, introduced considerable variability to the macroinvertebrate data. it is unclear how this affected the elements that were observed and scored over the course of the study.

Table 1. Correlation coefficients calculated between the habitat metric and various invertebrate metrics.

Correlation Coefficients	
Habitat vs. Diversity	0.42

Habitat vs. Abundance	**0.15**
Habitat vs. Dom. Grp. Type	**-0.12**
Diversity vs. Abundance	**0.45**
Diversity vs. Dom. Grp. Type	**0.31**
Abundance vs. Dom Grp. Type	**0.31**

Overall SVAP score

The ranking of scores is broken down into four categories. A score < 6.0 = Poor, a score between 6.1 and 7.4 = Fair, a score between 7.5 and 8.9 = Good, and a score >9.0 = Excellent. Out of 161 sub-reaches, 158 rated poor and 3 rated fair. The average overall score was 3.53 ± 0.98 (see Figure 16).

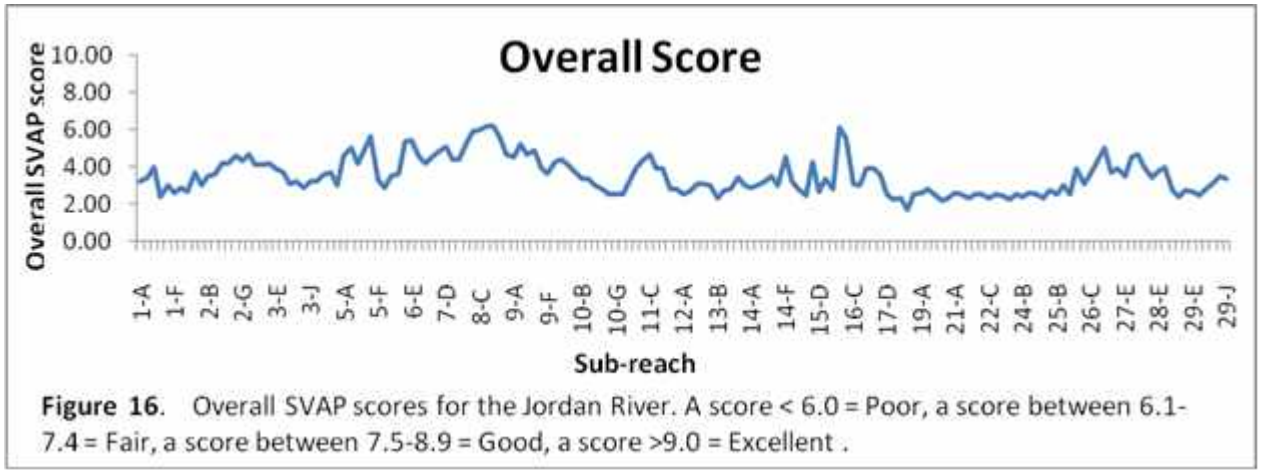

Figure 16. Overall SVAP scores for the Jordan River. A score < 6.0 = Poor, a score between 6.1-7.4 = Fair, a score between 7.5-8.9 = Good, a score >9.0 = Excellent .

Figure 16. SVAP Overall scores for the Jordan River. A score < 6.0 = Poor; 6.1 to 7.4 = Fair; 7.5 to 8.9 = Good; > 9.0 = Excellent.

Discussion

The Stream Visual Assessment Protocol provides a semi-quantitative assessment of the river and provides for identification of specific problems in specific areas. For example, channelization was given significantly lower scores below 2100 S in Salt Lake City than those given for the upper portion of the river. In general stream meandering generally increases as the gradient decreases. Meandering enables the stream to perform its natural functions such as deposition of sediments on flood plains on the inside of meander bends and the development and maintenance of habitat for fish, aquatic insects, and aquatic plants (SVAP). The Jordan River is channelized to the greatest extent in the lower portion of the river where due to the gradient of the valley, the meandering should be the greatest. The riparian zone also scored noticeably lower than the rest of the river below 2100 S. With site-specific information about the quality of the riparian zone, sites for restoration can be more easily identified. Improving the riparian zone would in turn increase its ability to reduce the amount of pollutants that reach the river in surface runoff, help

control erosion, provide a cooler microclimate during the summer for aquatic organisms, and provide habitat for fish and insects.

The hydraulic alteration scores, low for the whole river, were largely based on the frequency of flooding, but the river's flow is regulated by levees, channelization, diversions and dredging to maintain channel capacity and flooding of river water into floodplains rarely occurs and in large sections of the river. No functional floodplain exists. Bankfull flows, as well as flooding, are important to maintaining channel shape and function. The land through which the river flows is developed in many areas, structures or levees are too close to the river along the great majority of the river, precluding any floodplain development. (see Figure 17). Large sections of the river, however, are still undeveloped where more natural flows and flooding could possibly be allowed to help the river regain some of its natural function.

Figure 17. An example of a constricted floodplain and the resultant potential for back erosion. Photo was taken in reach 13 of the Jordan River.

During the SVAP survey, releases from Utah Lake were maintained at extraordinarily high flows from early May until mid-June. This was the first year in at least a decade that Utah Lake has exceeded the "compromise" level where released water quantities above that required to meet downstream water demands. As such we believe that up to 1.5 ft (45 cm) of sediment that had accumulated over the years became re-suspended and was transported down the river. Because sediment accumulation had occurred in even the very upper reaches of the river, we believe that much of this sediment was likely delivered to the river from highly turbid Utah Lake. This cycle of deposition and re-suspension of sediments likely occurs to some degree each year as Utah Lake releases are terminated each fall and then restarted each spring. Other sources such as bank erosion and nonpoint source runoff would occur on a similar cyclic basis and contribute to the sediment load as well (e.g. see Figures 17 and 18). Large amounts of suspended solids may block sunlight from reaching aquatic plants and periphyton and when it settles, it smothers cobble and woody debris that would otherwise serve as insect habitat (Figure 19). Identifying and controlling these sources of suspended solids and organic debris should be a priority in the Jordan River restoration effort. Providing clean, stable substrate would provide for primary

production, as well as invertebrate habitat which, in turn would enhance the aquatic food chain for fish.

Figure 18. An example of an actively sloughing and eroding bank. This bank was about 15 feet (4 m) high. Photo was taken in reach 4.

Figure 19. An example of silt and organic sediment deposited on a piece of woody debris that was taken from the Jordan River in reach 27.

Chapter 2

Light Attenuation and Nutrients in the Jordan River and Their Relationship to Periphyton and Phytoplankton Communities

Prepared by

Theron Miller

Wasatch Front Water Quality Council

August 2019

Table of Contents

List of Figures

List of Tables

Introduction

The lower reaches of the Jordan River were assessed as being impaired for low dissolved oxygen (DO) in 1998. As such, the Utah Division of Water Quality is currently preparing the TMDL. The TMDL is required to identify the sources of the impairment as well as allocate pollutant load reductions that will improve the DO deficiency and restore fully supporting status to the impaired reach.

The Jordan River represents the first TMDL for a Utah stream that is nearly completely "urbanized". Straightened, narrow channels with highly restricted floodplains and frequent dredging characterize such streams and particularly the Jordan River. The prevalent private ownership and the zoning laws has allowed considerable commercial and housing development and parking lot construction immediately adjacent to the main stem and its many tributaries as they leave Forest Service land and enter the Salt Lake Valley. Consequently, the riparian corridor is severely restricted and mostly non-functional. This allows extensive bank erosion and incision of the main and tributary channels, which become most obvious during spring and stormwater runoff. The river also suffers from severe hydrologic modification, including several points of diversion (including 85% to 95% diversions by the Turner and Point Dams in the narrows, followed by tributary, groundwater, storm water and POTW inflow and then another diversion of 50 to >90% to the surplus canal near the 2100 South crossing.

Another significant problem with the Jordan River is the delivery of high concentrations of algae and TSS from shallow (mean depth ~2 m), eutrophic, Utah Lake. Water leaving Utah Lake contains 45 to 100 mg L^{-1} TSS and 15 to about 90 ug L^{-1} (depending on season), chlorophyll a. Total volatile suspended solids (VSS) at the Utah Lake outlet is consistently near 10 mg L^{-1}) (Wasatch Front Water Quality Council data, 2009, 2014, Cirrus Environmental 2009).

Another factor that strongly influences the persistence, effect and fate of the TSS in the Jordan River is the steady decline in the stream gradient. This gradient ranges from approximately 15 ft per mile (3 m per km) through the narrows to approximately 1.5 ft per mile (0.3 m per km) at its terminus as it enters the impounded wetlands of Farmington Bay. Substrate size distribution responds appropriately with large gravel, cobble and boulders dominating the narrows (between Thanksgiving Point and about 14600 South). There is a gradual decline in substrate size to mostly large gravel interspersed with occasional cobble from 14600 to approximately 7200 South, large and medium gravel from 7200 South to approximately 5400 South and a gradual decline from medium gravel to sand between 5400 South and 2100 South (Bio-West (1980; personal observations; see Chapter 1). Below 2100 South (after an average of about 85% of the flow has been diverted to the surplus canal), the substrate is dominated by silt and clay with some areas of sand. This dramatic decline in volume results in a decline in velocity (in addition to the ever-declining stream gradient) and allows for the TSS and most of course particulate organic matter (CPOM) transported in the water column or as part of the bedload to begin settling at the bottom. As such, the last 15 miles (25 km) of the river channel is overwhelmingly a depositional reach as the velocity slows to 5 - 15 cm s^{-1} and the bottom is increasingly

dominated by unstable silts and clays filled with settling particulate organic matter. These various impacts on the Jordan River are critically important in dictating the degree to which Utah lake phytoplankton persists in the river as well the ability of periphyton to colonize the various substrates that are scoured in upstream sections and smothered in downstream sections.

The presence of these severe habitat impairments complicates the determination of just what further impacts might be attributed to the four POTWs that discharge considerable loads of phosphorus and nitrogen to the Jordan River. These POTWs are located at approximately 13500 South, 7200 South, Mill Creek/Jordan River near 3100 South and just below Center St. in Bountiful. The two southern most plants, Jordan Basin and South Valley are design with BNR and thus discharge at or below 1 mg P/L. These point sources of nutrients help in raising and maintaining P to 0.1 to 0.5 mg L^{-1} and total nitrogen (mostly as NO_3) intermittently up to about 5 mg L^{-1}. These concentrations of nutrients have the potential to maintain or even increase the high concentrations of chlorophyll a that are delivered from Utah Lake.

It is apparent that these adverse factors induce inhibitory responses with regard to primary production and standing crop of both the Utah Lake phytoplankton as well as periphyton growth within the river. This chapter investigates the relationships between turbidity, unstable substrate and nutrients and the ability to grow or support both phytoplankton and periphytic growth of algae in the Jordan River.

In the first year of our studies (1999), our objectives were three-fold: 1) to understand the contribution of Utah Lake phytoplankton to the water column biomass and its proportion of the water column algal community in Jordan River; 2) and how far downstream do these species occur in the river; and 3) Are these assemblages influenced by the South Valley and Central Valley water reclamation facilities? These observations prompted the measurement periphyton growth both on artificial substrate (slate tiles) as well as on natural ambient cobble-sized substrate.

In addition, the characteristic high turbidity and calculations that predict the potential for much higher Chl a concentrations (based on instream P concentrations), led to the hypotheses that light limitation and unstable substrate significantly impede periphyton and phytoplankton growth in the river. To begin testing these hypotheses, we measured water column light intensity at several stations throughout the Jordan River during the summer of 2010.

Methods

Light Measurements

Twenty-one stations were selected for light measurements to represent the entire distance of the Jordan River, including immediately downstream from the Utah Lake outlet, within the narrows, and multiple locations throughout the middle and lower reaches of the river (Table 1.). In addition, one site was sampled on the Surplus Canal about 3 miles downstream from the 2100 S. diversion for comparison of transparency of the water left in the river channel.

Sites were selected that provided open exposure to the water surface (no shading from trees or the stream bank) and measurements were made between the hours of 1000 and 1500 and at times absent of cloud cover in order to capture the highest intensity of the daylight hours.

The sensor frame was mounted to a 2 m aluminum rod, which allowed the frame to be held in a stable position to a maximum depth of about 1.2 m. Irradiance values were measured every 0.2 m from the surface to the bottom or to 1.2 m.

Light attenuation coefficients were calculated for each curve developed at each sampling event, using the equation:

$$I_z = I_o \, e^{-kz}$$

Where I_o is the irradiance just below the water surface, I_z is the irradiance at a specified depth (z) in question, and k is the light extinction coefficient of the waterbody. We calculated the extinction coefficient by using the same exponential model but derived from the regression curves of measured depth profile data. We then used the median values for k and the I_o (y intercept) values to calculate a final extinction equation and subsequent I_z values and the associated percentage of surface irradiance at various depths.

Periphyton and Phytoplankton Measurements

Water column algae samples were collected monthly during 2009 from the Utah Lake outlet, the narrows near Thanksgiving Point, and near the bridges at 14600 S, 9000 S, 7800 S, 6400 S, 3300 S, 2100 S, 900 S, 400 S, 300 N, 1800 N, Center St, Legacy Nature Preserve and Burnham Dam. Some sampling was also conducted upstream and downstream from the Central Valley Reclamation Facility discharge in Mill Creek. Samples were collected in 500 mL plastic bottles, immediately stored on ice and delivered to the Rushforth Lab on the day of sampling.

During 2010, we installed artificial substrate samplers, which consisted of 12-inch (30.5 cm) square slate tiles from a local hardware store. These tiles were fastened to steel brackets that were constructed from 1-inch angle iron and these brackets were fastened to stakes made from ½-inch rebar (see Figure 3). Two tiles were fastened to each rebar stake such that the bottom tile lay flush with the sediment surface and the top tile was set at about 15 cm above the bottom but at a right angle to the bottom tile. We chose this arrangement to evaluate the influence of either scouring by the mobile bed load material or smothering by sediment deposition as compared to a tile suspended at about mid-depth, which hypothetically, would not be exposed to such severe

scouring or burial. One tile was positioned upstream and one downstream from the stake to avoid shading. Tiles were placed at the same locations as for the water column samples. The tiles were placed in the river on about June 6 and sampling began three weeks later. We also collected periphyton samples from natural cobble substrates at each site, where available, for comparison with the periphytic community that developed on the artificial substrate.

Sample collection included the use of a small section of 2-inch (5.1 cm) PVC pipe or a similar-sized hole in flexible gasket material that served as a template to identify a quantitative area to determine growth and standing crop on an aerial basis. Samples were collected in triplicate and composited. The periphyton was removed using a razor blade or toothbrush followed by rinsing the brushed area into a 500 mL sample bottle. Where natural (ambient), cobble-sized, stable, substrate occurred in the vicinity of the tile placement, a similar scraping was collected from the exposed surface of the rock. Samples were transported on ice to the South Valley Water Reclamation Facility lab where the Chlorophyll a was collected on glass fiber filters and analyzed using the ethanol extraction method (EPA Method 446). Sample collection occurred approximately every two weeks until October 9, 2010.

Grab samples for nutrient analysis were collected during each sampling event to determine if there was any relation between Chlorophyll a and nutrients discharged to the river. A chain of custody sheet was prepared for each sampling event and delivered to the appropriate lab. The Chl *a* samples were frozen until analysis, which was within about 30 days. Portions of the water quality samples were immediately filtered upon arrival for the determination of dissolved P. These samples were transported to the Central Valley Water Reclamation Facility Lab. Nutrients and other basic parameters have been sampled each month since May, 2009. This intense sampling was intended to describe monthly, seasonal and annual variability that might be associated with flows and the annual growing, senescing and dormant seasons.

Results

Light Transmissivity

Sample sites included from the Utah Lake outlet to downstream from Burnham Dam. Between two and seven measurements were made at each sampling location between July and October. Representative graphs of the light extinction profiles are depicted in Figure 1, determined at the 3300 South Site. Depending on the date and specific location, the depth was between 1 and 1.2 m. The equation reflects the August 19 measurements and the R^2 value (0.99) is typical of the regression curves generated from these data throughout this study. Regression plots of the remainder of the sampling sites are listed in the appendix of this chapter.

A summary of the maximum depth that light transmission was measured and other important endpoints of light intensity are presented in Table 2. The 5% and 1% depths are listed because these represent the range of values reported as the compensation point (where primary production = respiration; see Discussion). Note that in all cases, except for the narrows site, greater than 1% of the surface light reached the bottom or the maximum measurable depth (1.2 m). Also, except for two of the most downstream stations (Center St., and 500 m below Burnham

Dam), and the Surplus Canal, light at the bottom of the remaining sites was at or above 5% of surface irradiance. In other words, the calculated depth at which the 5% level would be reached is deeper than the depth of the river at most of the sampling stations. This is important in that is indicates that most of the river should in a net positive state of primary production. Alternatively, however, other critical physical characteristics such as scouring and particularly smothering or burial at downstream sites could preclude the river from achieving net primary production. Hogsett and Goel, as discussed in Chapter 5, examined this possibility further.

Table 2. Sample locations and number of individual light profiles measured in the Jordan River and the Surplus Canal.

Site	Number of Times sampled			
	July	August	Sept.	Oct
Utah Lake outlet	3	2		
Narrows (Thanksgiving Point)	3	2	1	
14600 South	3	2	1	1
9000 South		2	1	
7800 South	3	3		
7200 South	3	3		
6400 South		2		
5400 South	3	3		
3900 South		3		
3300 South	3	3		
2100 South	3	3	1	1
1700 South		2		
California Ave (1300 South)	3	3		
900 South	3	3		
400 South		1		
North Temple		1		
300 North		2		
1800 North		2		
Center Street (Bountiful)	2	3		1
500 m downstream of S. Davis S. POTW		2		
500 m downstream of Burnham Dam		3		
Surplus Canal near airport	2	3		

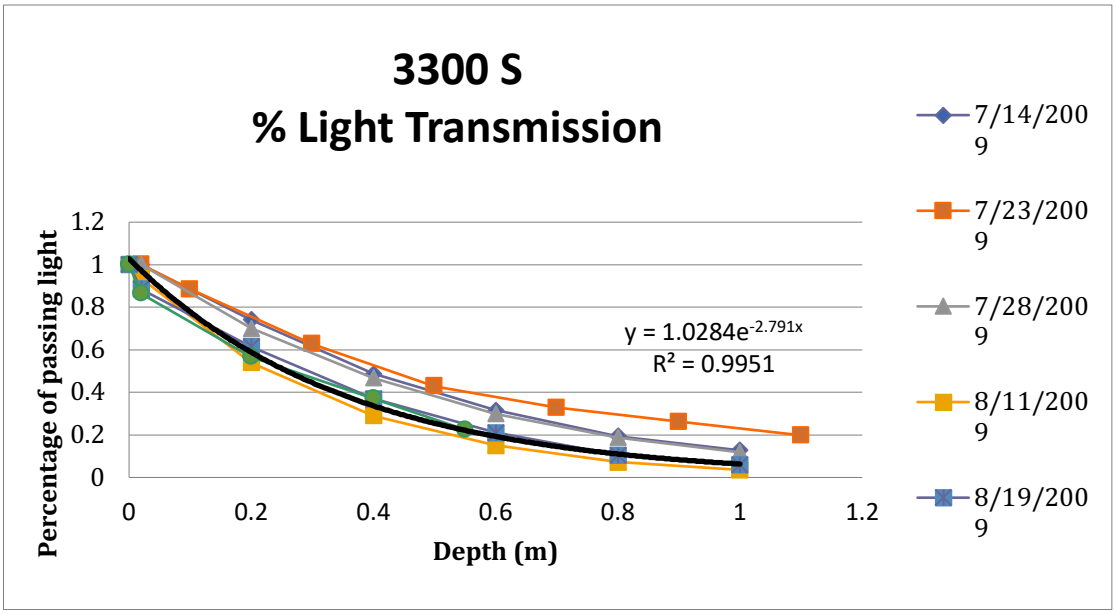

Figure 20. Light extinction profiles measured in the Jordan River at the 3300 South site. Measurements are reported as a percentage of reduction of light intensity at increasing depths. The displayed equation represents light attenuation values measured on Aug. 19, 2009.

Table 3. Maximum depth of light intensity measured at each sampling location and the associated percentage of the surface light intensity. For comparison, depths at which 5% and 1% intensity are reported as calculated from the light extinction curve. Note that nearly all sites, except at the Narrows, retained at least 5% of surface irradiance all the way to the bottom (see text).

Site	Max depth (m)	% of surf. Ir. at bottom (m)	Depth at 5% of Surf. Ir. (m)*	Depth at 1% of Surf. Ir.* (m)
Utah L. outlet	1	5	1.0	1.5
Narrows	1.2	0.5	0.7	1.1
14600 S.	1.0	5	1.0	1.5
9000 S.	0.4	35	1.1	1.7
7800 S.	0.9	13	1.3	2.0
7200 S.	0.8	16	1.3	1.9
6400 S	0.6	21	1.3	2.0
5400 S.	0.6	24	1.2	1.9
3900 S.	0.4	26	0.9	1.4
3300 S.	1.1	8	1.3	2.1
2100 S	0.8	24	1.6	2.4
1700 S.	0.8	11	1.1	1.7
900 S.	1.0	7	1.15	1.8
North Temple	0.5	27	1.1	1.6
300 N.	0.5	23	0.85	1.3
1800 N.	0.6	17	1.0	1.5
Center St.	1.0	3	0.8	1.3
500 m Bl. S. Davis S. POTW	0.8	5	0.8	1.2
500 m Bl. Burnham Dam	1.0	2	0.75	1.2
Surplus Canal at airport	1.0	3	0.8	1.3

*These are predicted values derived from the regression equation.

Phytoplankton and other Algae Suspended in the Water Column

Identification and quantification of phytoplankton and periphyton data are summarized by Rushforth and Rushforth (2009a and 2009b). These reports are appended to this report. Monthly samples of the water column indicated that a majority of the suspended algal community in the Jordan River water column came from Utah Lake and these taxa clearly dominated the community throughout the entire River length (Figure 2). The only exception was the month of June, when the biomass of suspended algae was relatively very low. In this sample, soft algae (Chlorophyta) dominated upstream sites (delivered from Utah Lake) while diatoms mostly dominated downstream sites. Notably, however, the diatoms that were present largely consisted of periphyton (attached) taxa that had become dislodged from benthic substrate. This supports the hypothesis that periphyton is continually being scoured by the moving bedload material.

The community continued to shift with summer succession as the population of in Utah Lake experienced a large bloom of Cyanobacteria (mostly Aphanezomenon) starting in July. The population of Chlorophytes and diatoms remained relatively stable as the Aphanezomenon population grew from non-detectable to several orders of magnitude larger that the other algae. The dramatic reduction in the Cyanobacteria downstream at 7800 S (Figure 2) is the result of the average of 97% diversion of the river by Turner Dam, followed by dilution with groundwater as well as several tributaries. Evidence of large groundwater entry has been described by CH2MHill (2005). Also, locally placed piezometers have demonstrated positive hydrostatic pressure at several locations in the upper and middle reaches of the river, suggesting positive groundwater inflow to the river (Mitch Hogsett, University of Utah, personal communication).

Another key observation is that after the reduction in biovolume at Turner Dam, there was no further reduction of these taxa, even at locations downstream from 2100 S., Chl *a* values followed a similar pattern (Figure 2). Further, it is notable that the 25 ug/L Chl *a* concentration in Utah Lake outlet water is indicative of eutrophic (nutrient enriched) conditions. But yet, following the Turner Dam diversion, the 10 ug/L Chl *a* concentration is actually indicative of oligotrophic to mesotrophic conditions (i.e. nutrient poor to a medium trophic status). But in this transition from a lake to a river environment, one would expect algal growth to transition from a phytoplankton-dominated/lake community to a periphyton-dominated stream community (See next section). Finally, the fact that we did not see any significant reduction in biovolume downstream from the Turner Dam diversion, and including downstream from the Surplus Canal diversion, provides notable evidence that settling of these algal cells is minute and immeasurable. Consequently, these sources of organic matter provide a very minor contribution to the very high sediment oxygen demand- values that were measured by Goel 2010; Chapter 5).

a.

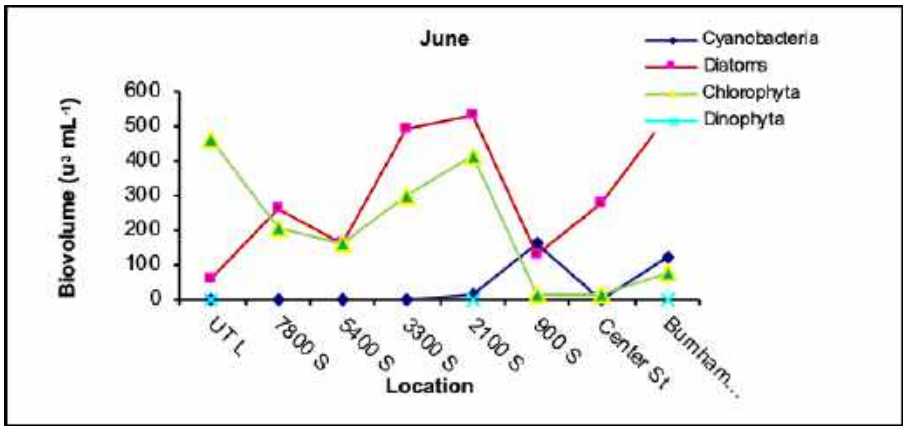

b.

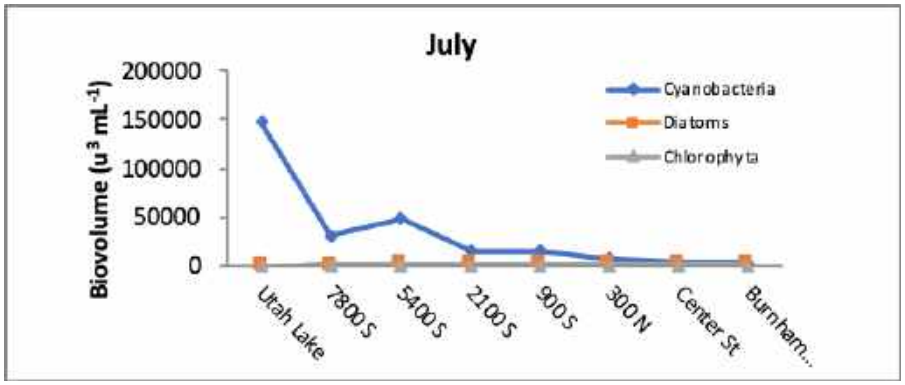

c.

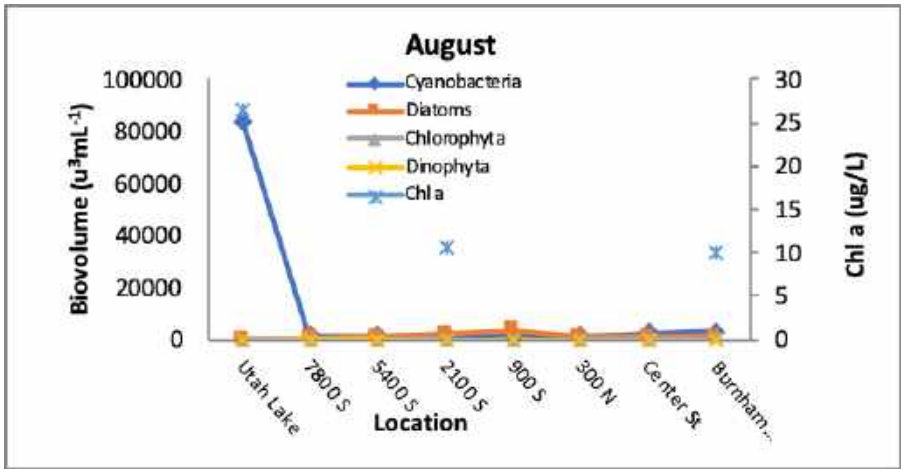

Figure 21. A summary the biovolumes (times 1000) of major taxa groups in water column measured at select sites representing the upper, middle and lower reaches of the Jordan River. Note different units in the Y -axis scale between June and July as the Cyanophyte population in Utah Lake began to bloom. Yet, biovolumes of Cyanobacteria declined by nearly 2 orders of magnitude as it traveled down the river in July and August. Although diatoms increased from about 100,000 to 900,000 between Utah Lake and 2100 S in July, this biovolume was only about 0.6% of that of the Cyanobacteria. In addition, the increase in diatoms was largely composed of dislodged pennate diatoms. Note Chlorophyll a followed the same trend as the Cyanobacteria. Data were compiled from Rushforth and Rushforth (2009).

d.

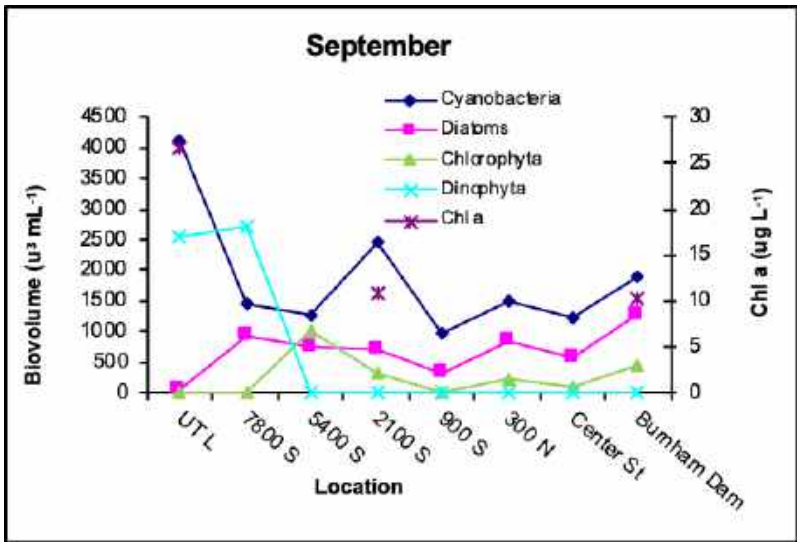

e.

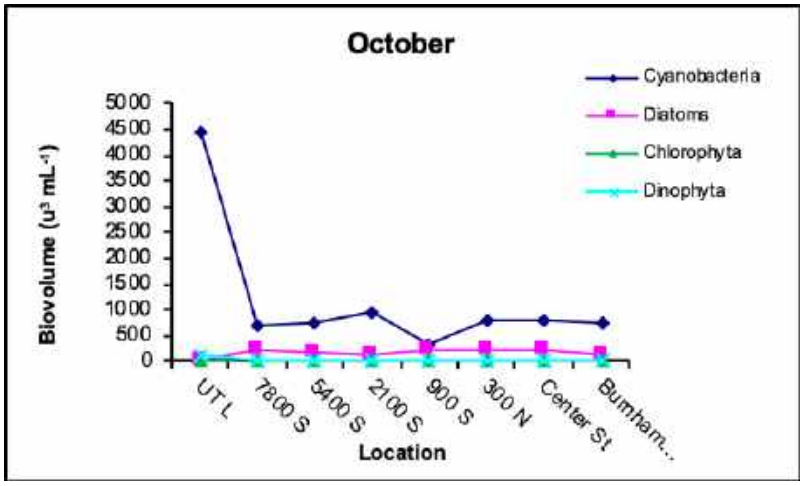

Figure 2. Continued.

Periphyton Growth on Natural and Artificial Substrates

Periphyton biomass was measured on an approximate biweekly basis from June 6 to October 1, 2010. Samples were collected from slate tiles and natural cobble-size substrate, when it was present, at each sampling site. The tiles were installed during the week of June 7 and the sample collections at each location convened on June 29. This provided an initial incubation of 22 days prior to sampling. A Summary of Chl *a* concentrations for each site is presented in Figure 3. Initial observations indicated that periphyton colonization was just beginning to occur at all sample locations. The greatest Chl a density occurred on the ambient substrate at 9000 S, 7800 S (upstream from the South Valley Facility discharge) and 5400 S (downstream from the South Valley Facility discharge). Chl *a* concentrations on both the suspended and bottom tiles at each sample site were substantially lower than the ambient substrate, suggesting that even 22 days were not sufficient for the artificial substrates to reach equilibrium with adjacent natural substrates. At sites upstream from 2100 S, algal growth remained minimal (less that 50 mg/m^2)

until early to mid-August. This was unexpected, but is probably related to the exceptionally variable runoff that occurred during the spring and early summer (Figure 4). Flows periodically reached about 3 times that of normal flows, and at times fell below normal flows. These erratic flows would mobilize and scour substrates, followed by periods of deposition and then repeating - restricting periphytic growth until flows stabilized in the middle of July.

Despite the low Chl *a* values in the early samples, the suspended tiles contained slightly higher concentrations than the bottom tiles, supporting the hypothesis that the periphyton colonies established on the bottom tiles were more impacted from scouring or sedimentation. The only exception to this trend was the samples collected at Legacy Nature Preserve. The tile placed at this LNP site consistently showed greater Chl *a* concentrations than the suspended tile. Initially, this might appear to support the idea that suspended algae, from Utah Lake, or dislodged algae from upstream locations are finally settling out of the water column at this calm, depositional location. However, measurements of Chl a, biovolume and cell counts throughout the length of the Jordan River indicate that the algal cells remain suspended in the water column, even in this slow-moving segment of the river (Figure 2; Rushforth and Rushforth, 2009). Moreover, Chl *a* concentrations rapidly fell from ca. 60 to 90 ug L^{-1} at the Utah Lake outlet down to 10 -25 ug L^{-1} at the bottom of the Narrows and remain at this oligotrophic to mesotrophic range for the entire length of the River (Cirrus 2009).

Samples collected later did not show a relationship between suspended and bottom tiles. Only two of the sample locations (1700 S and LNP), demonstrated significant differences (two-tailed T-test; $p < 0.05$) between the suspended and bottom tiles placed at each site. Of these however, only the samples collected from the 1700 S site supported the hypothesis that suspended tiles would provide for greater growth of periphyton because of less bedload scouring or deposition and perhaps slightly greater light conditions.

Bedload movement and settling were key factors periphyton colonization and is directly in flow velocity. Figure 4 shows the variability in flows that occurred downstream from The Surplus Canal Diversion Dam and this diversion dam greatly stabilizes downstream flows in the channel. This stability in the channel is misleading in that the greater flows that reach the diversion dam are still transporting high bedloads. But the fact that the gate that controls releases to the channel releases flows at the bottom, while the diverted water releases flows over the top of the weir, directs the bedload to the channel, resulting to a nearly continual supply of unstable sand, silt and clay (Figure 5). Moreover, due to the mandate for flood control through the Rose Park community in Northern Salt Lake City, excess flows from spring runoff or summer storms, are nearly completely diverted to the Surplus Canal. Because the gate at the dam is manually operated, increased flow diversion may begin after elevated flows begin. As well, however, dewatering of the channel may occur in anticipation of flooding flows or because post-storm adjustment to widen the gate may be delayed. In turn, flow variability is likely the major cause of the very large variability in our periphyton samples.

The highly variable flow began to stabilize by about mid-July. Hence, the repeating pattern of settling, then resuspension of bedload material clearly diminished. This is the likely reason for such a late season peak in benthic algal biomass, for both artificial and natural substrates. The peak in algal biomass values occurring after the first part of August also indicates that the

scouring or smothering are dominant stressors on the periphyton community when flows are normal to above-average. In other words, this peak in biomass occurred 4 to 6 weeks after summer solstice, when the photoperiod and sun angle had diminished substantially, but could still provide for growth in primary production. However, this peak was very short-lived. By mid-September, Chl *a* values had diminished substantially, reflecting the shorter photoperiod and lower sun angle during the fall season as flows remained relatively stable.

There were two notable exceptions to this trend: 1) At the 2100 site, periphyton growing on the ambient rock was always less than 100 mg Chl *a* m^{-2} (i.e. it never experienced the July peak as with most of the other sites) and was most often below 50 mg Chl *a* m^{-2}. These values were not only low compared to the tiles at this site but were low compared to the other sites as well. We attributed these low values to the moving/scouring bedload as well as extreme embeddedness of the cobble-sized substrate by sand and silt that filled the interstitial spaces. Indeed, during most visits the bottom tile was covered with sand that had been recently deposited at this site since the previous sampling visit (i.e. we carefully removed the sand or silt material from the tile after each sample event to allow potential periphyton colonization), showing how mobile and available this material is to either scour or deposit (Figure 5) and even when river flows are at average summer levels. In addition, the rebar stake and tile clamps frequently accumulated large amounts of debris, including branches and strands of macrophytes. This material could also have scoured the tiles (by sweeping back and forth in the current), or perhaps shaded the tiles – which also could have caused the widely variable results. However, the similar low biomass on the ambient cobbles suggests that scouring is the primary cause of low tile colonization, as well as on the ambient substrate. The second notable exception occurred at the Legacy Nature Preserve site, where the bottom tile nearly always had greater Chl *a* concentrations and often had 3-4 times more Chl *a* than the top tile. Further, although organic-rich sediment accumulated on both the top and bottom tiles (Figures 3 and 5), there was substantially more sediment (several cm) accumulated on the bottom tile. We initially considered the high Chl *a* values on the bottom tiles to be an artifact of the elevated deposition rates and possibly the settling of dead or dying algae (See Figure 5) (e.g. Baker (2010, reported similar high values for Chl *a*). However, Dr. Sam Rushforth (personal communication) suggested that there are motile species of a type of the golden diatoms, Division Chrysophyta that could be responsible for the high Chl *a* measurements. Members of this group are highly adapted to organic-rich sediments in that they have flagella, and hence are motile – even within the sediments. In addition, if they are covered or shaded, they can assume a heterotrophic existence where they can obtain organic carbon from particulate and dissolved organic matter, rather than photosynthesis when they can actually contribute to the sediment oxygen demand. Conversely, they can also migrate to the sediment surface where, because they have retained their Chl *a*, they can rapidly convert to an autotrophic existence and photosynthetically acquire their energy. This could explain how very high concentrations of Chl *a* occur in an area that is characterized as depositional but consists of high proportions of organic matter. This will receive additional attention in summer of 2019.

a.

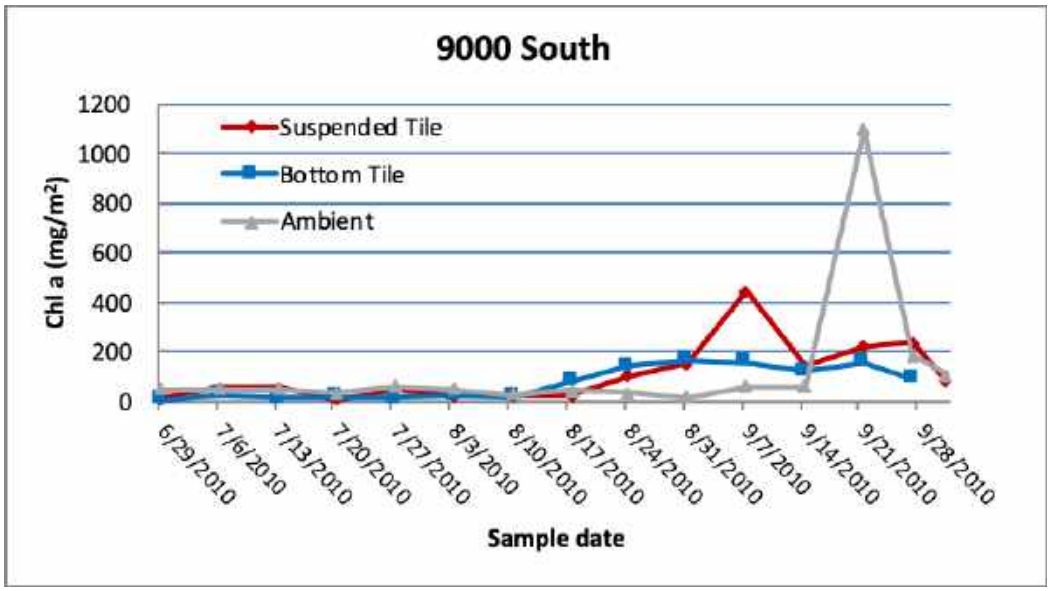

b.

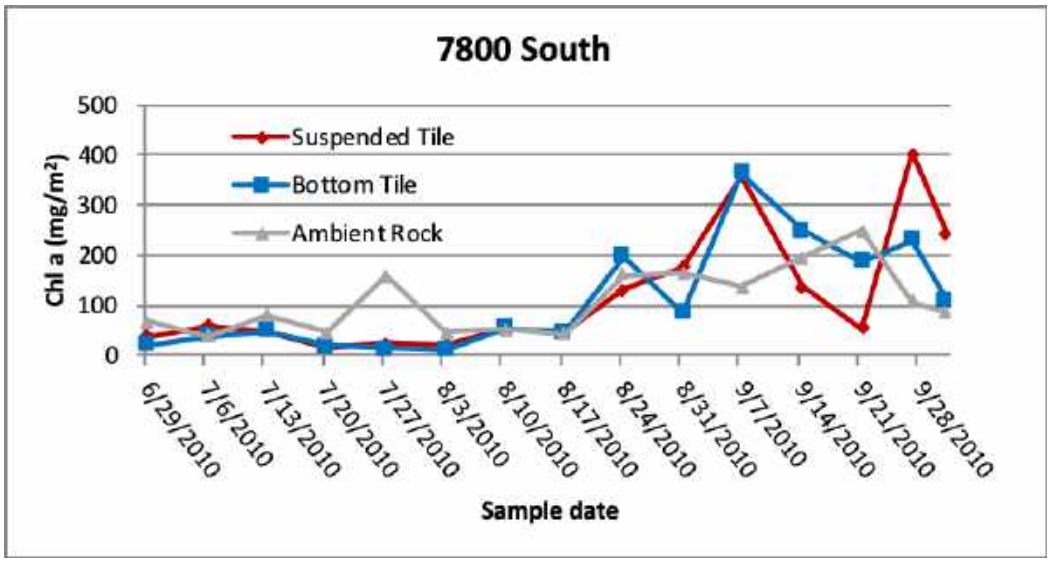

Figure 22. Benthic chlorophyll a measurements collected throughout the growing season from artifical (slate tile) substrates and from natural cobble stones located at various locations upstream and downstream from the Surplus Canal diversion at 2100 South; at 9000 S (a.), 7800 S (b.), 5400 S (c.), 2100 S (d.), 1700 S (e.), 300 N (d.) and in the Legacy Nature Preserve (e.). Tiles were deployed on approximately June 6. At each site, one tile was attached at the bottom to conform to the natural substrate surface so that it would experience the scouring (or burial) effects similar to that of the adjacent substrate. A second tile was suspended approximately 15 cm above the bottom to avoid these "bottom affects." Ambient samples were collected from adjacent natural cobble-sized rock. These rocks were difficult to find at 1700 and were nonexistant at further downstream sites. All samples were collected in triplicate and each triplicate sample was analysed in triplicate in the South Valley Water Reclamation Facility Laboratory.

c.

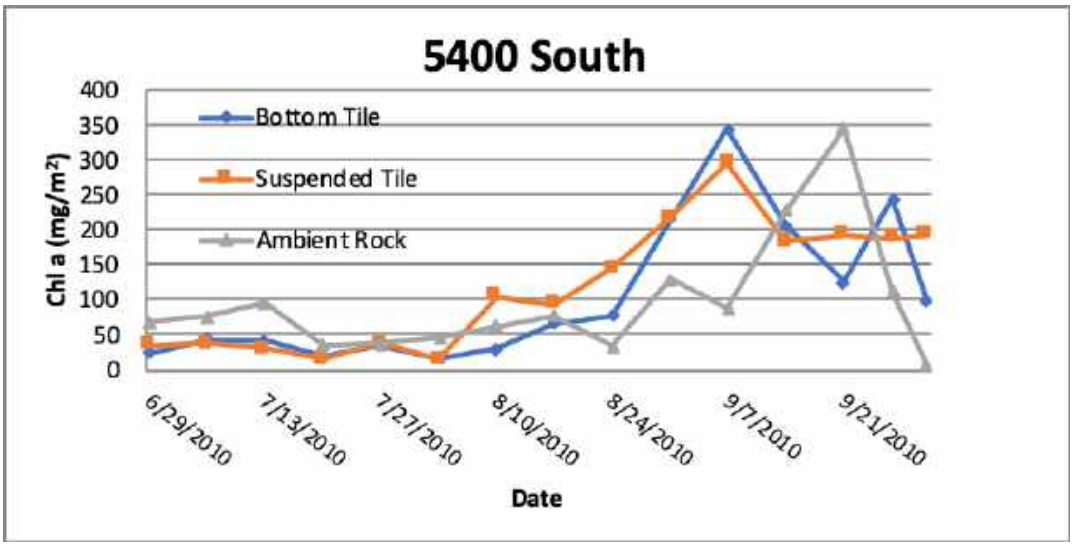

d.

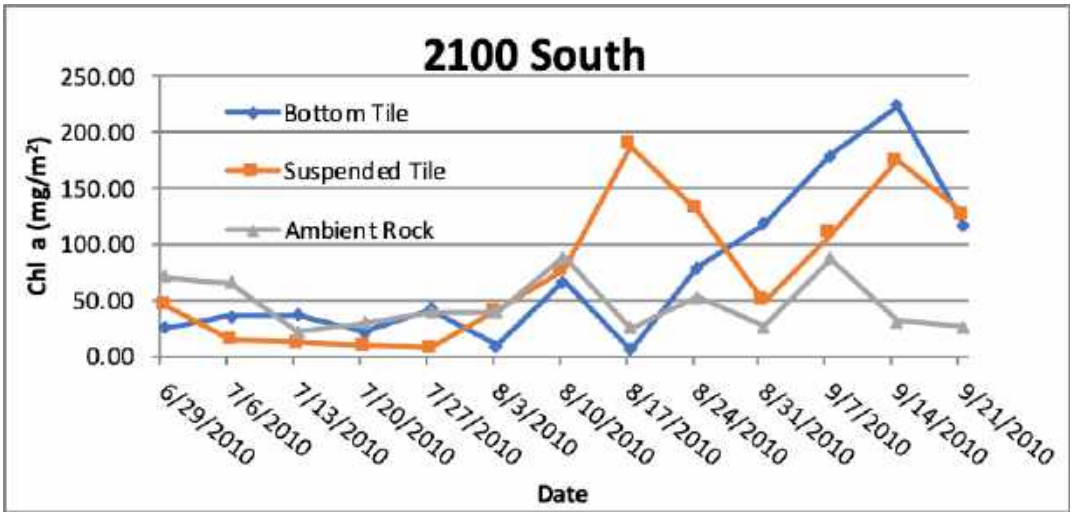

e.

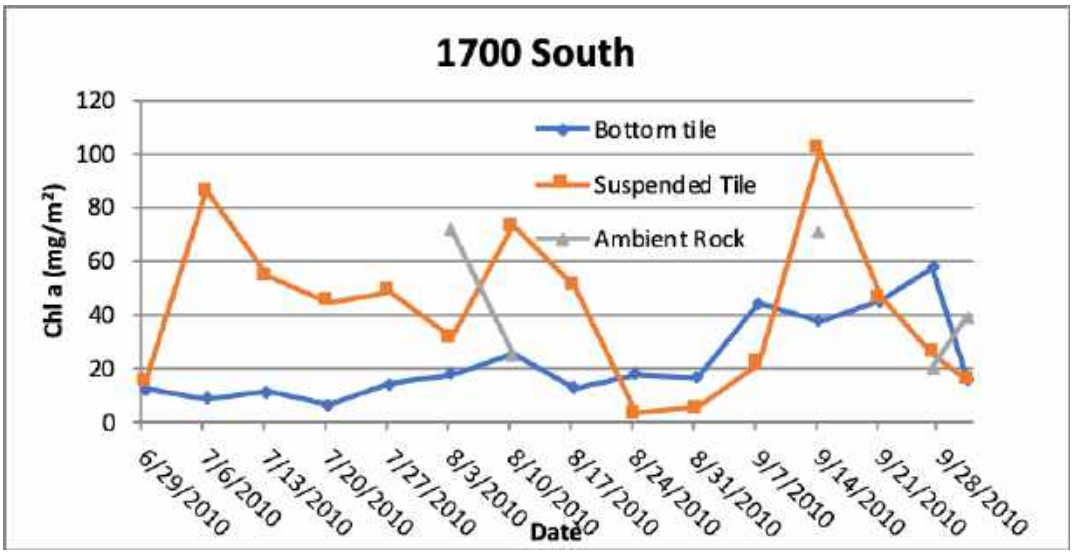

Figure 3. Continued.

f.

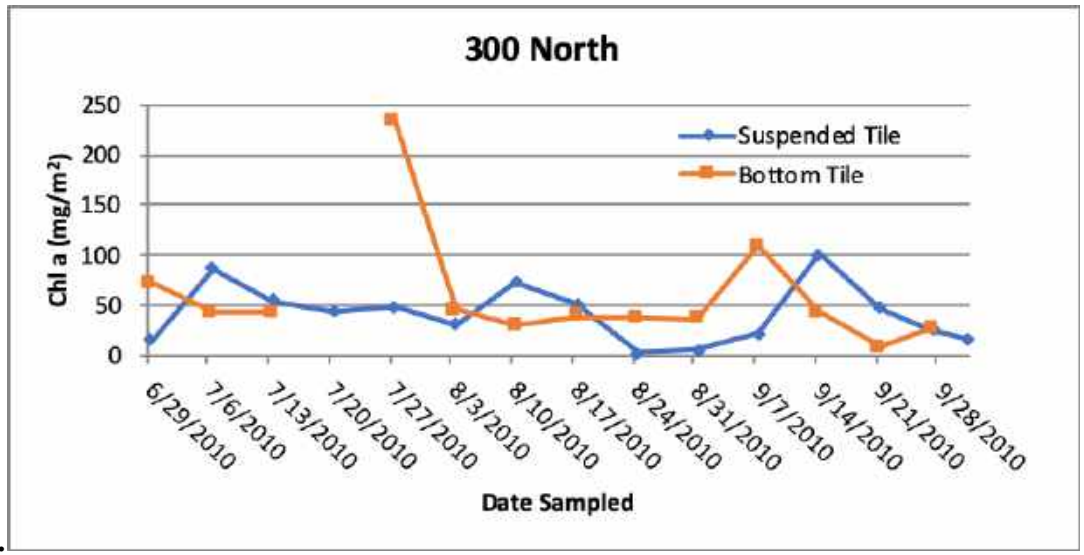

g.

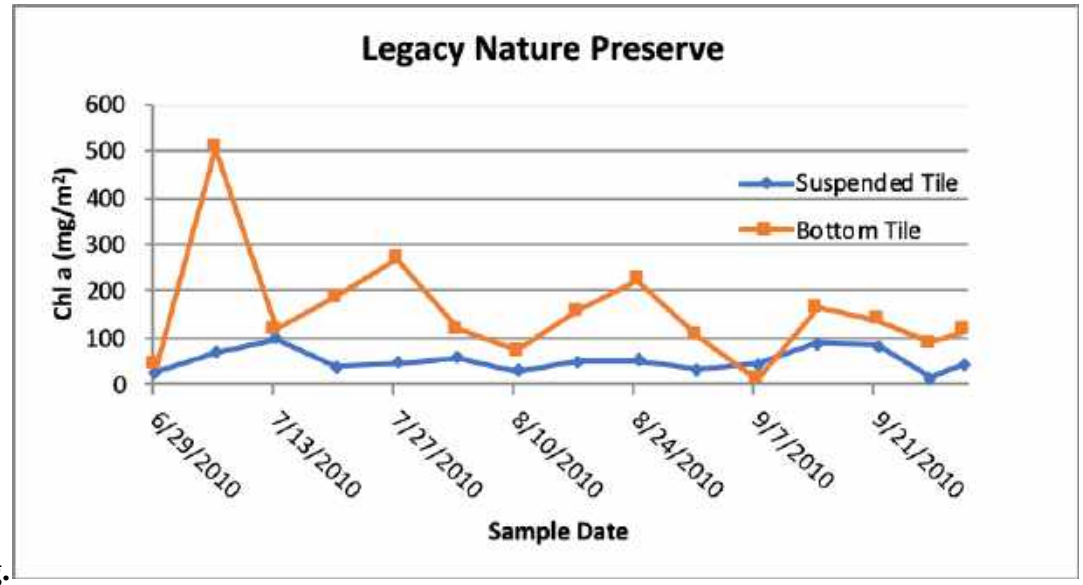

Figure 3. Continued.

The middle photograph depicts the typical conditions at 2100 S during July. Sand would continually accumulate on the tiles, precluding the possibility of substantial periphyton growth. The bottom photograph illustrates the deposition of fine inorganic sediments mixed with fine organic material from the disintegration and partial decomposition of organic matter. The location of the triplicate samples can be identified in the top and bottom photographs.

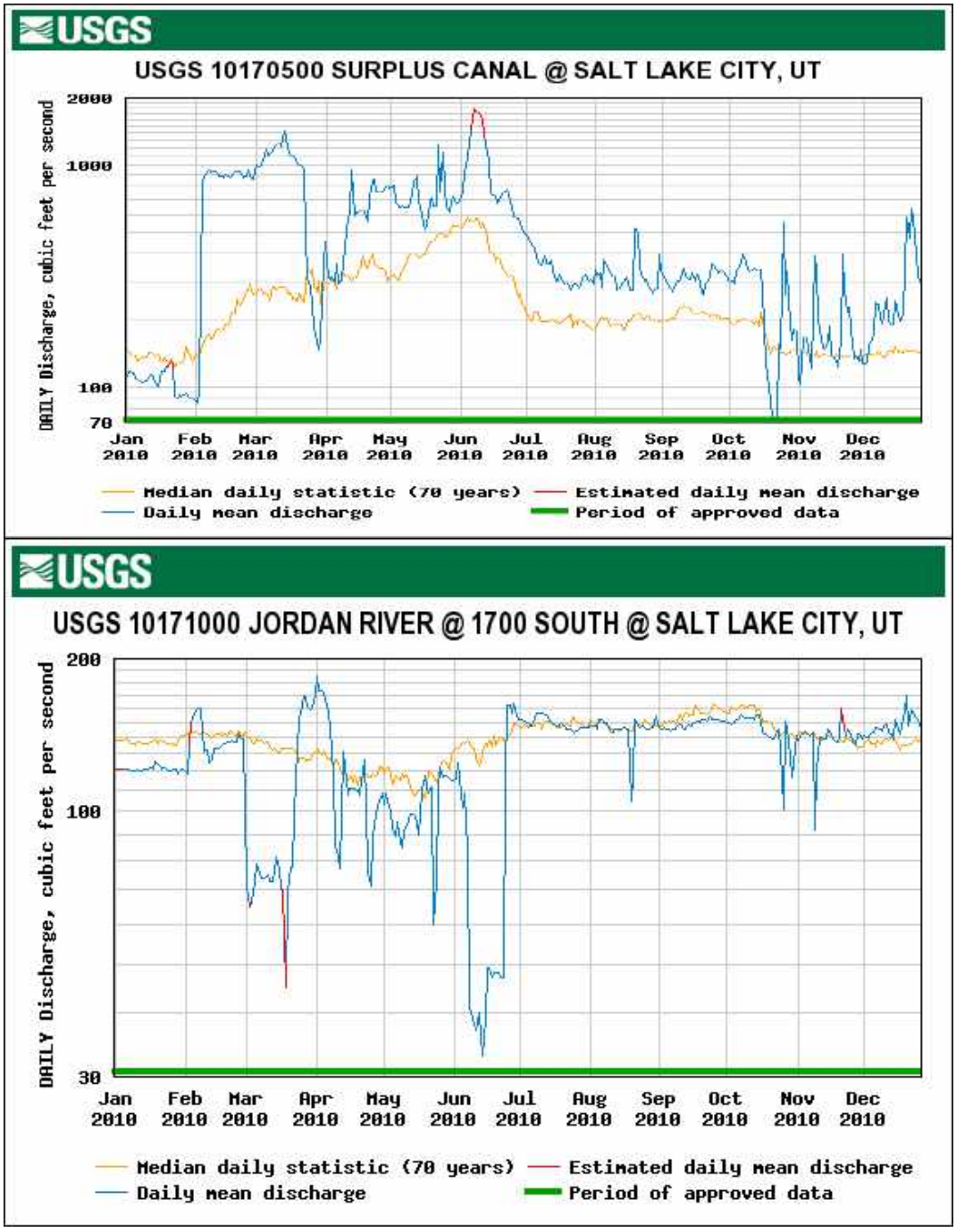

Figure 23. Flow measurements in the Surplus Canal and at 1700 S during 2010. Flows were unusually highly variable upstream and downstream from the diversion.

Figure 24. Representative photographs of periphytic algal growth and types of sediment deposition that occur in the Jordan River. Top: Tile retrieved from the river at 5400 South. Middle: Tile retrieved from the river immediately downstream from the 2100 S diversion. Bottom: Tile retrieved from the river in the Legacy Nature Preserve. Note triplicate samples have been collected in the top and bottom photos.

As an interesting comparison, Utah DWQ has conducted a public survey using photographs of benthic algal growth, as a potential assessment tool, to determine if there is an aesthetic threshold based on the appearance of the growth or density of benthic algae (DWQ 2012). This survey was fashioned after the Montana DEQ public survey of fishermen and other recreationists (Suplee et al. 2009). Montana DEQ has actually adapted this survey technique into an assessment tool. Both the Montana and Utah surveys identified the threshold chlorophyll a concentration to be at 150 mg Chlorophyll a m^{-2} (the percent of respondents identifying favorable conditions fell from about 78% desirable to about 35% desirable between 150 and 200 mg chlorophyll a m^{-2} (see Figures 6, 7 and 8). The Chl *a* samples collected from the deposits on the bottom tile at Legacy Nature Preserve often exceeded that collected from the substrate depicted in Figures 7 (150 mg m^{-2}) and 8 (240 mg m^{-2}). Yet, there were no visible algae on the Legacy NP sample. These illustrations clearly demonstrate the variety of benthic algae and the different conditions where they may flourish. Obviously, an assessment tool based on a visual assessment of green algae would not be appropriate where organic-rich sediments occur in depositional zones. Future studies on the biological and oxygen dynamics in this depositional reach will continue and will include verification of the presence and activity of these unique diatoms.

Overall, these data and photographs, demonstrate the inability of the Jordan River, both upstream and downstream from 2100 S to support extensive communities of periphyton. Most samples from the tiles and natural substrate contain much less Chl *a* than the Montana photographs that depict even hyper-eutrophic conditions. These data support the suggestion that the Jordan River, particularly downstream from 2100 S is severely habitat limited as a result of erratic flows, dewatering, and accumulation of inorganic and organic sediments.

Figure 25. Photograph used by Montana DEQ and Utah DWQ to depict 150 mg chlorophyll *a* m^{-2} of benthic algae in the public survey of recreational users of rivers and streams.

Figure 26. Photograph used by Montana DEQ and Utah DWQ to depict 200 mg Chlorophyll *a* m^{-2} of benthic algae in the public survey of recreational users of rivers and streams.

Figure 27. Photograph used by Montana DEQ and Utah DWQ to depict 240 mg chlorophyll *a* m^{-2} of benthic algae in the public survey of recreational users of rivers and streams.

The second question we asked was: Do the nutrient inputs from the South Valley Water Reclamation or the Central Valley Water Reclamation Facilities alter (enhance) the algal biomass downstream from their respective discharge points. The South Valley facility discharges at about 7600 South, downstream from the 7800 South sampling station and about three miles upstream from the 5400 South sampling station. The Central Valley facility discharges to Mill Creek approximately 600 m upstream from the Mill Creek confluence with Jordan River. Other than during spring runoff, the Central Valley discharge, which averages about 80 CFS, comprises the majority of flow in lower Mill Creek. Mill Creek enters the Jordan River approximately 4500 m (3 miles) downstream from the 5400 South sampling station and about 1200 m upstream from the 2100 South sampling site. Mill Creek comprises between 1/5 and 1/3 of the Jordan River, depending on season and upstream flow.

I arranged the data to illustrate the upstream/downstream differences during each sampling event to determine whether there were any changes in algal biomass downstream from these two discharges. The mean summer total inorganic nitrogen (TIN) and total phosphorus (TP) are also plotted for comparison to benthic algal biomass (Figures 9, 10, 11, 12, 13, 14 and 15). Mean summer nutrient values are plotted for purposes of simplification and the fact that there was little variability in nutrient concentrations across the summer months (i.e. The standard deviation of the summer (May to September) total P concentrations was consistently about 1/10 of the mean values at all sampling stations; The standard deviation of the nitrate and ammonia concentrations were consistently about ¼ to 1/3 of the mean summer values at all stations). Regression analysis was performed between TIN or TP and each sample type (suspended tile, bottom tile and ambient substrate) for each date. There were no significant relationships between nutrient concentrations and any of the sample types for any of the dates sampled ($p>0.1$). Rather, field observations (e.g. Figures 4 and 5) and Chl a values indicated that there were frequent episodes of scouring or smothering by sand or organic silts and clays that inhibited periphyton colonization and chlorophyll a concentrations. Overall, the samples collected at 9000 and 7800 exhibited the most consistently high values for Chl a. These sites were located above the South Valley POTW. This occurred despite the fact that downstream sites have much higher nutrient concentrations. Undoubtedly, the repetitive scouring and deposition played a significant role in impeding periphyton growth in the river.

a.

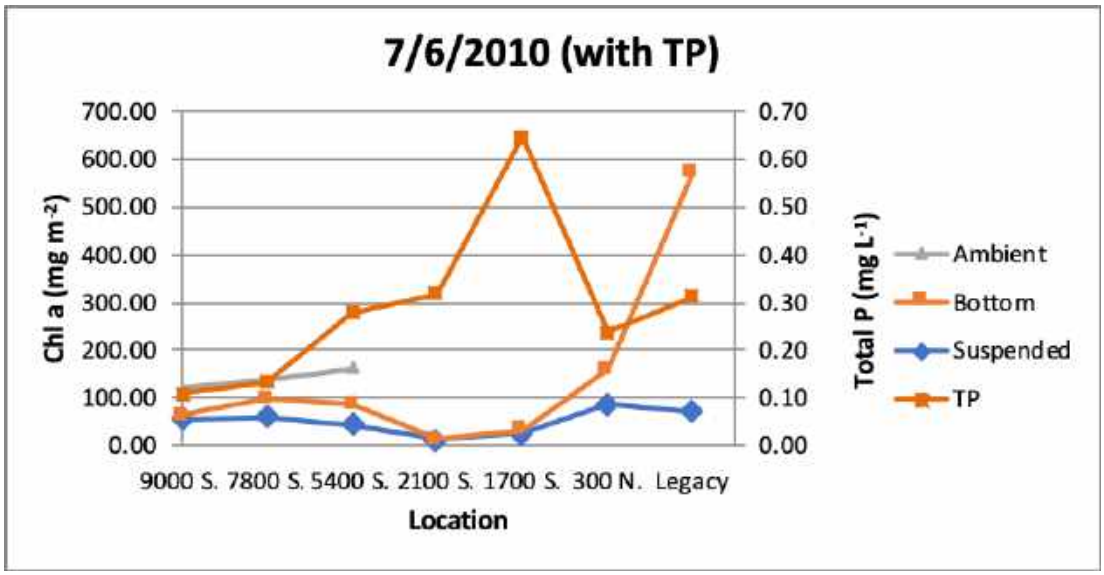

b.

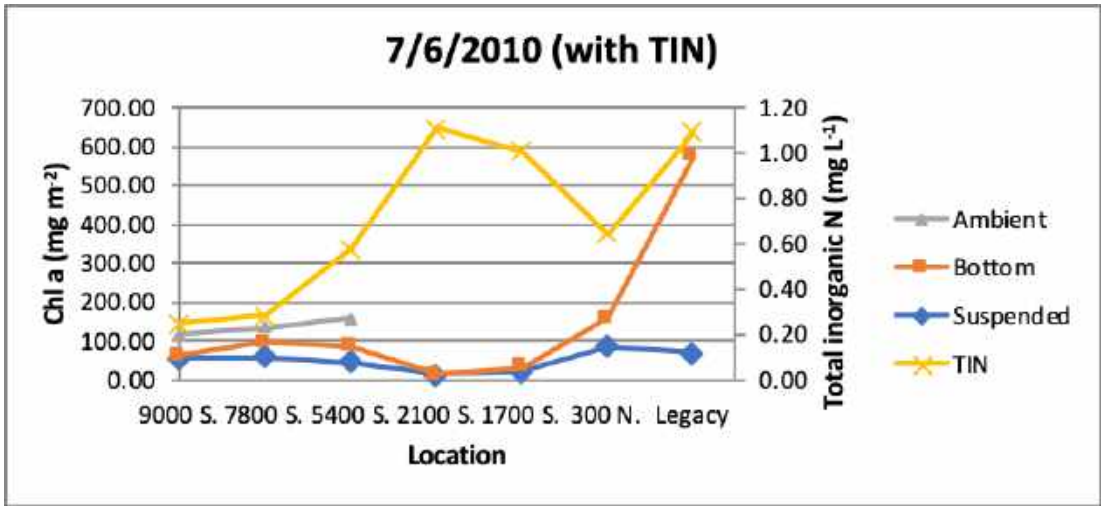

Figure 28. Benthic Chl *a* measured on July 6, 2010 and mean summer (monthly, May to September), values for total phosphorus (TP; a.) and total inorganic nitrogen (TIN; b.) at selected locations along the Jordan River. Ambient natural substrate could not be found at or below 2100 S on this date.

a.

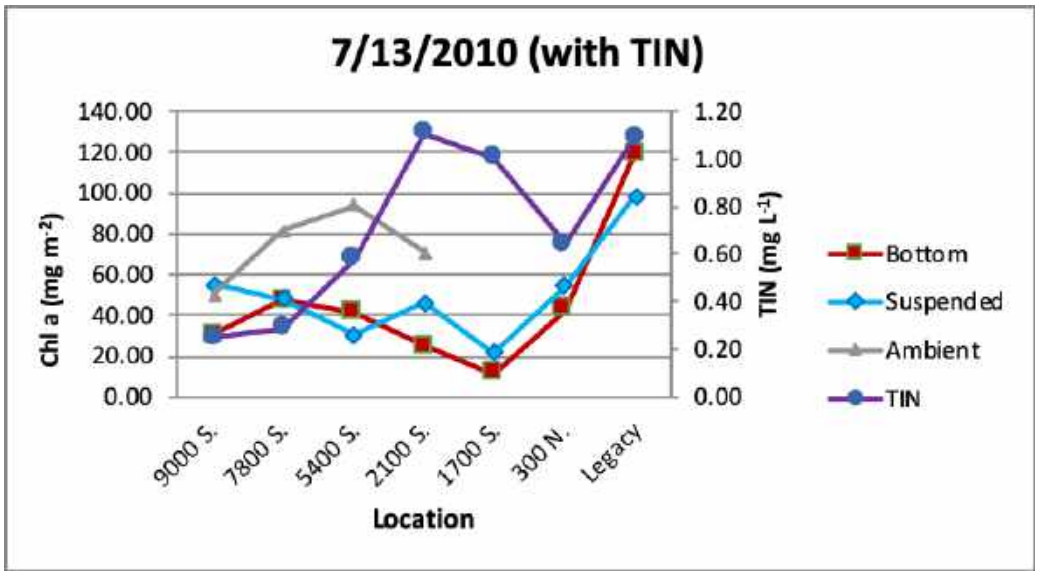

b.

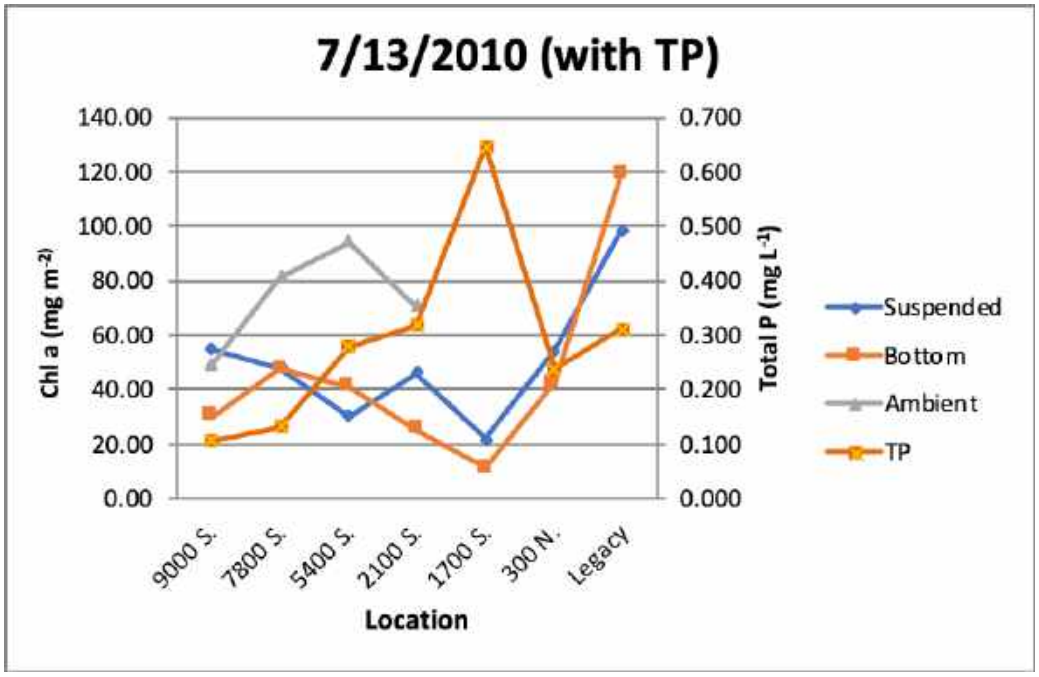

Figure 29. Benthic chlorophyll a measured on July 13, 2010 and mean summer (monthly, May to September), values for total inorganic nitrogen (TN) and total phosphorus (TP; b.), at selected locations along the Jordan River. Ambient natural substrate could not be found at sampling sites below 2100 S.

a.

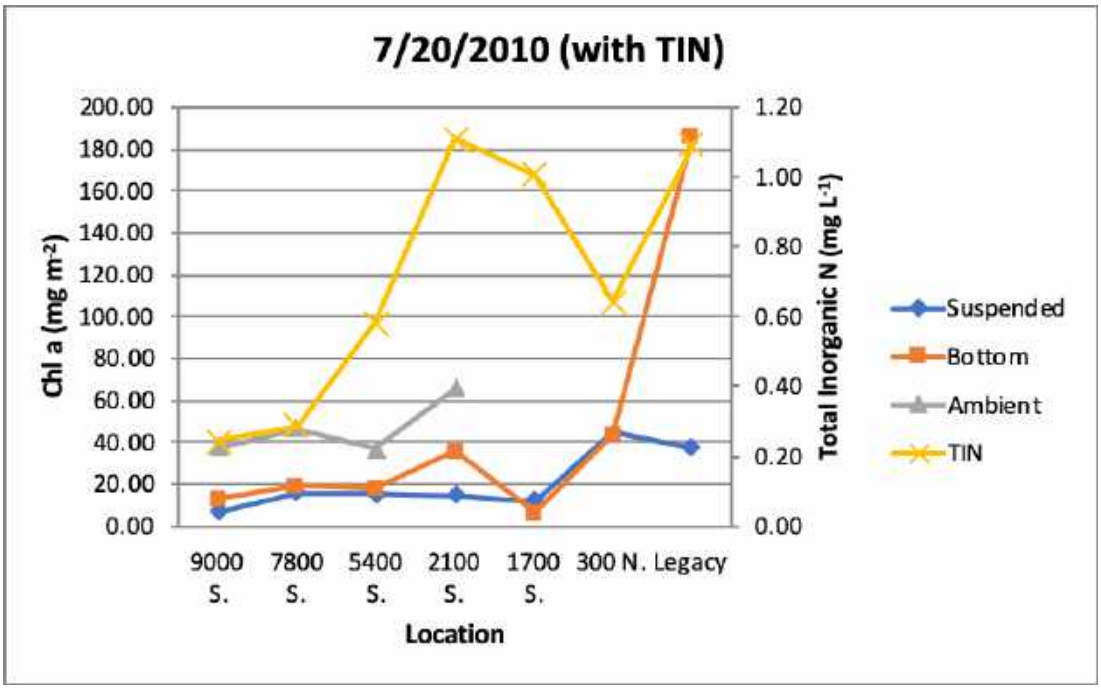

b.

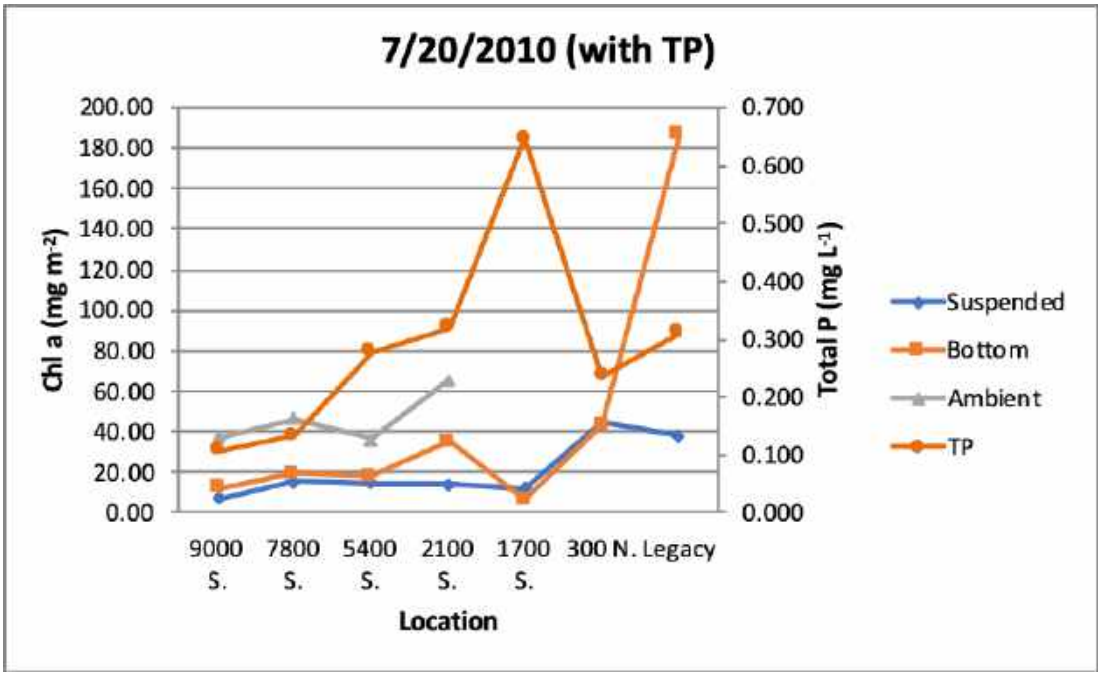

Figure 30. Benthic chlorophyll a measured on July 20, 2010 and mean summer (monthly, May to September), values for total inorganic nitrogen (TN a.) and total phosphorus (TP; b.), at selected locations along the Jordan River. Ambient natural substrate could not be found at sampling sites below 2100 S.

a.

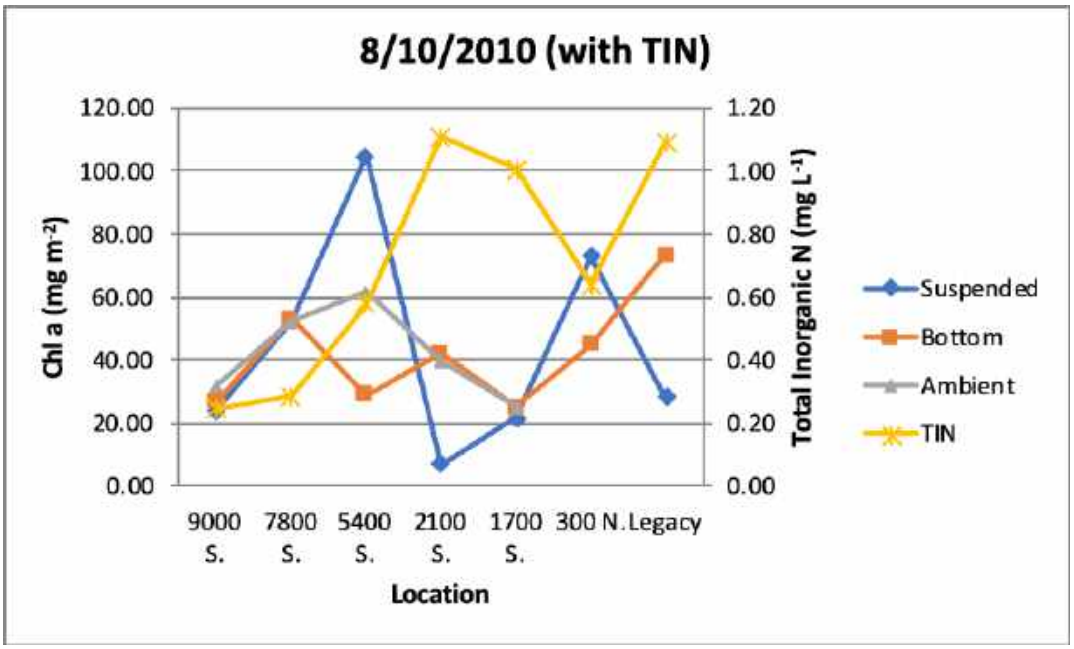

b.

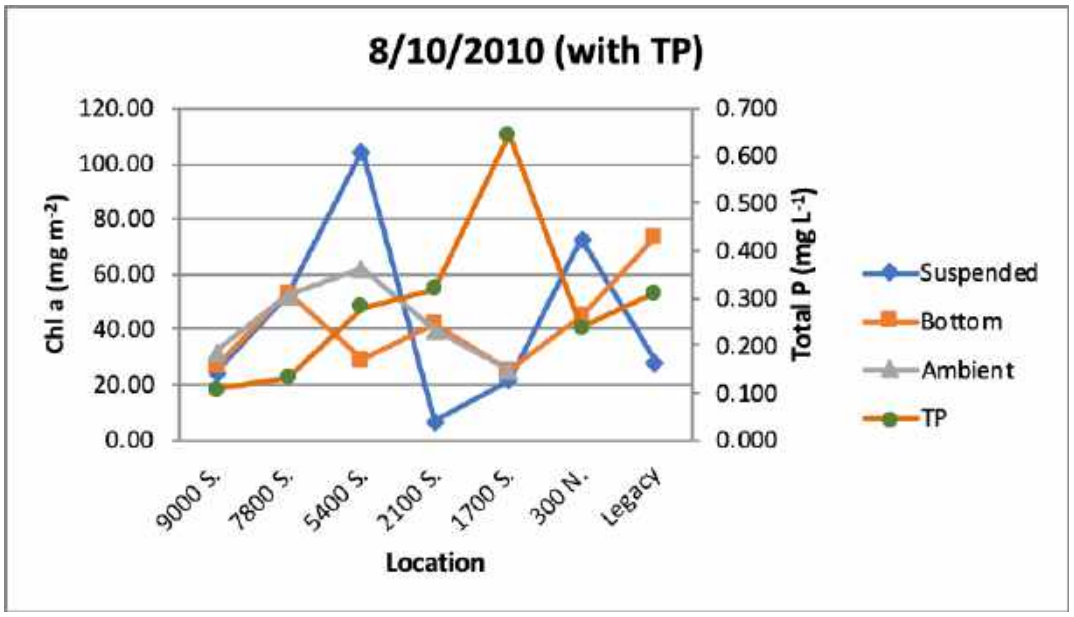

Figure 31. Benthic chlorophyll a measured July 20, 2010 and mean summer (monthly, May to September), values for total inorganic nitrogen (TN; a.) and total phosphorus (TP; b.), at selected locations along the Jordan River. Ambient natural substrate was found as far downstream as 1700 S on this date, although little colonization by periphyton had occurred.

a.

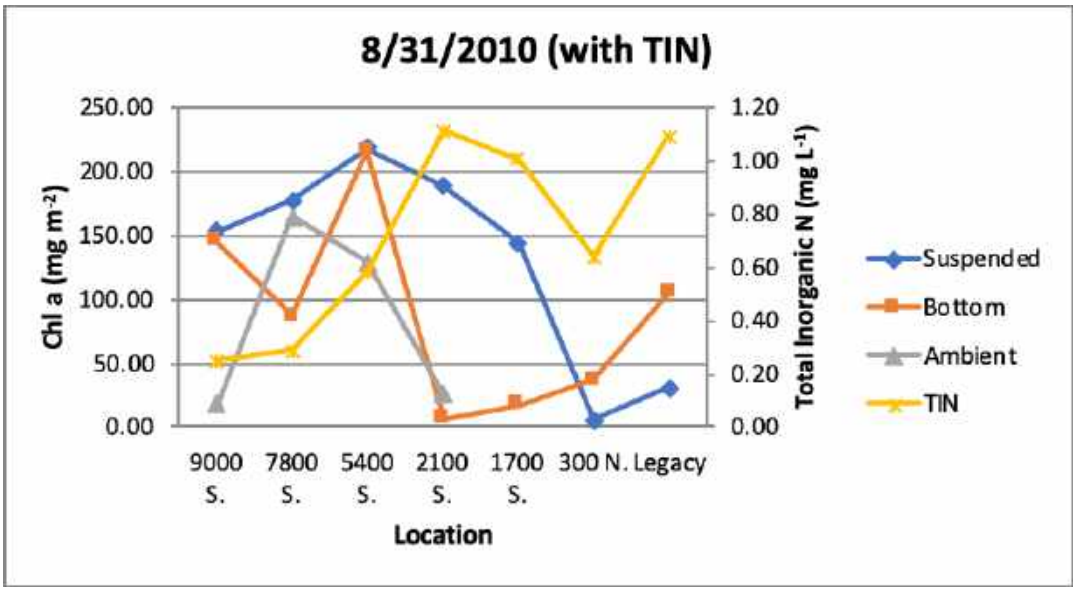

b.

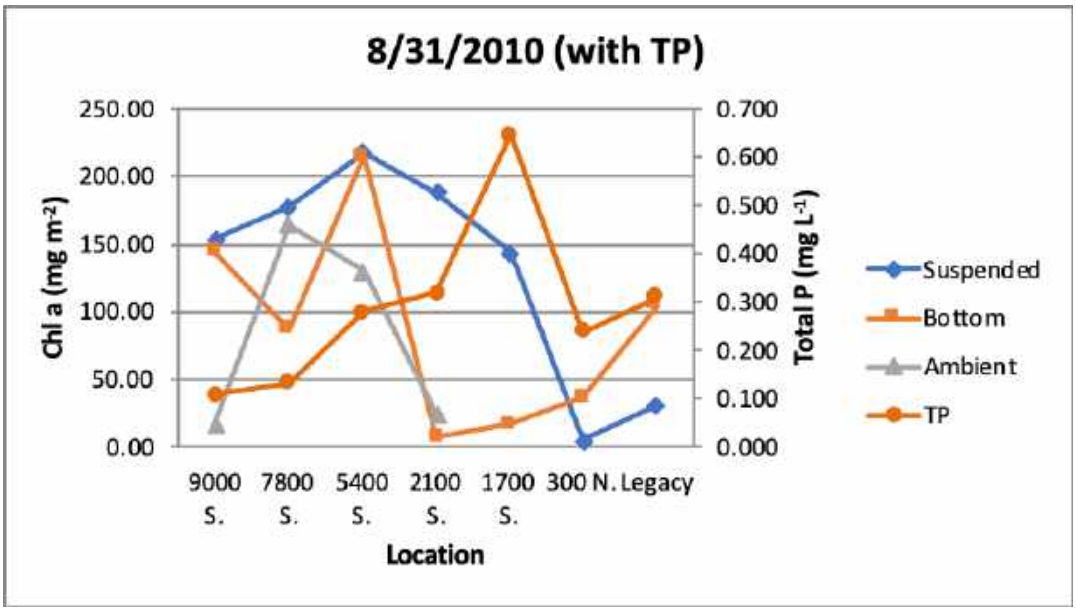

Figure 32. Benthic Chl *a* measured on July 20, 2010 and mean summer (monthly, May to September), values for total inorganic nitrogen (TN; a.) and total phosphorus (TP; b.), at selected locations along the Jordan River. Ambient natural substrate could not be found at sampling sites below 2100 S at this time and chlorophyll a values at 2100 S were relatively very low – suggesting that considerable scouring was still occurring. The suspended tile at 2100 S and 1700 S accumulated about as much Chlorophyll a as upstream sites at this time, suggesting that bedload sand and silt was still scouring the bottom tile and the ambient substrate.

a.

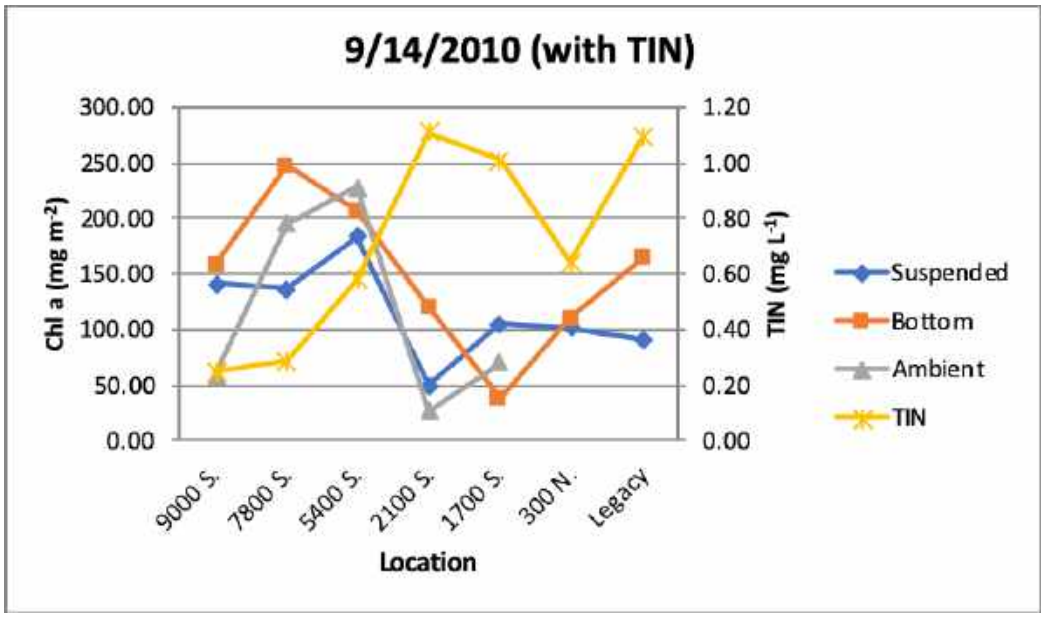

b.

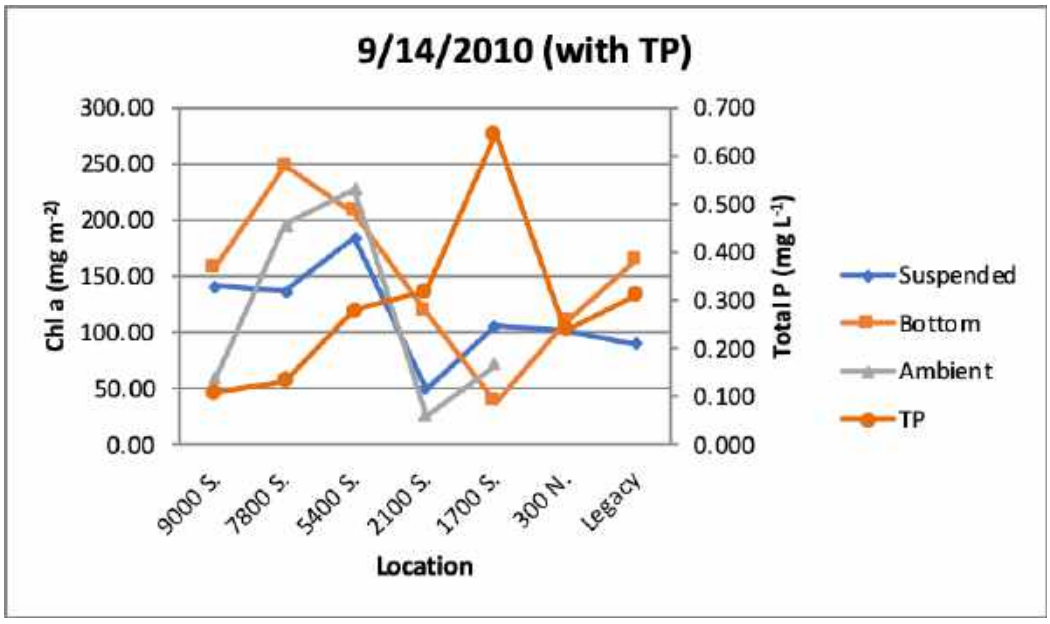

Figure 33. Benthic chlorophyll a measured on September 14, 2010 and mean summer (monthly, May to September), values for total inorganic nitrogen (TN; a.) and total phosphorus (TP; b.), at selected locations along the Jordan River. Ambient natural substrate could be found as far downstream as 1700 S at this time although chlorophyll a values at 2100 S and 1700 were relatively low compared to upstream samples – suggesting that considerable scouring was still occurring. Similarly, the accumulation on the suspended tile at 2100 S and 1700 S declined considerably from the previous sample on 8/31 (Figure 12), perhaps due to a scouring event or to declining intensity and length of the photoperiod during this fall sample.

a.

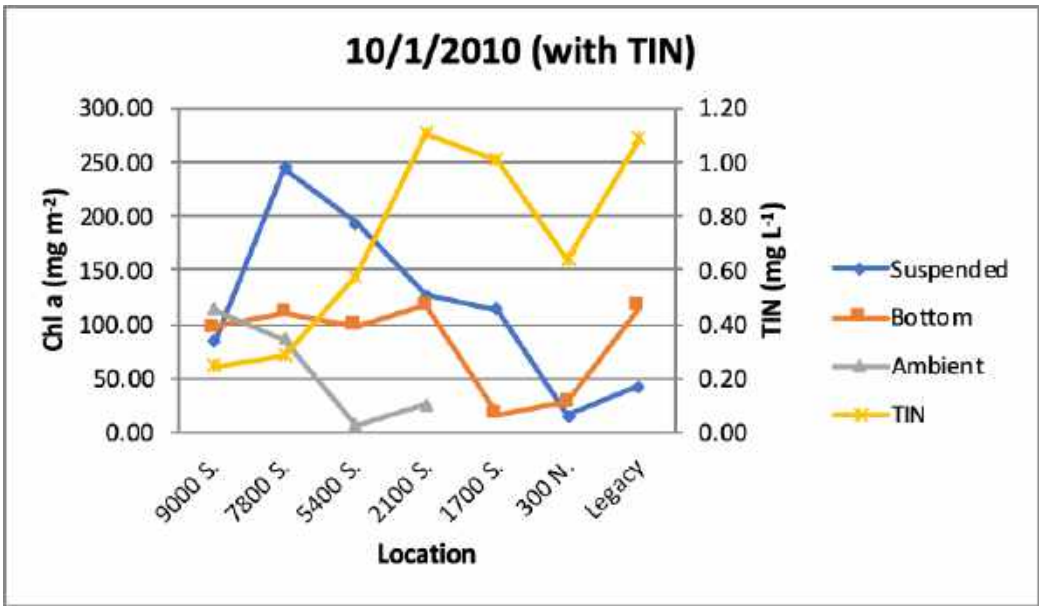

b.

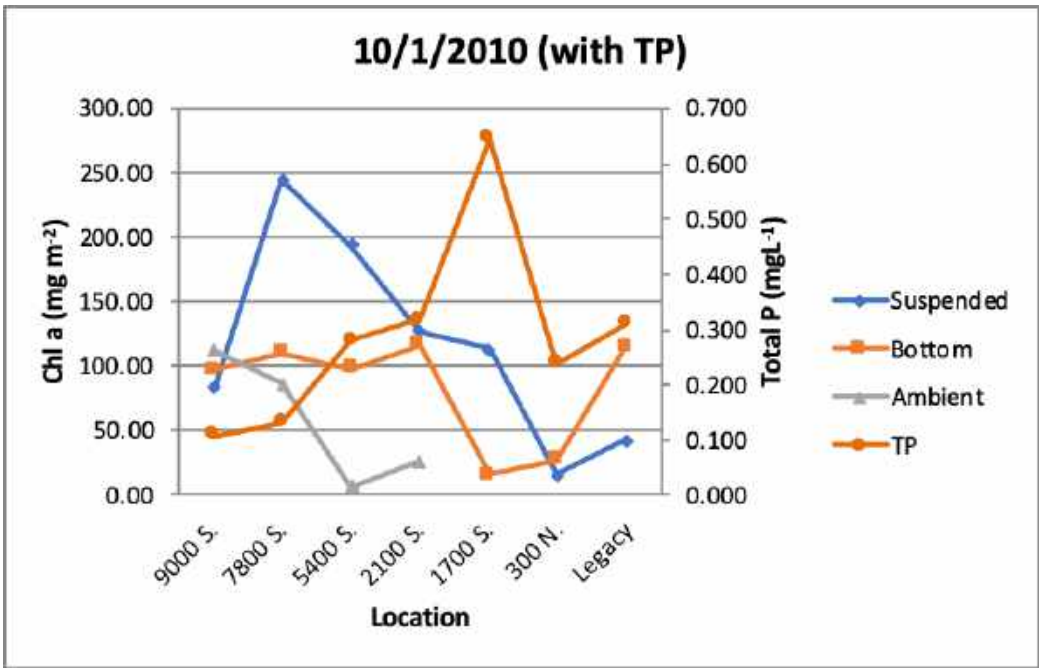

Figure 34. Benthic Chl *a* measured on September 14, 2010 and mean summer (monthly, May to September), values for total inorganic nitrogen (TN; a.) and total phosphorus (TP; b.), at selected locations along the Jordan River. Ambient natural substrate could be found as far downstream as 21 S at this time although chlorophyll a values at 2100 S and 5400 S were relatively low compared to upstream samples and samples from the previous month. The suspended tile at 7800 S was the only sample that was comparable to previous months. This again suggests that considerable scouring was still occurring, although further declining photoperiod and sun angle could also play a role.

Additional Water Quality Monitoring

As mentioned above, there was little temporal change in phosphorus or nitrogen during the 2010 Tile experiments. Yet, we have continued to monitor the various nutrient concentrations as well as the parameters that are related to the low DO impairment other parameters throughout the last 10 years in order to elucidate any long-term trends that might be occurring. In summary, of this information, I chose to report summary data from 2010, 2011, 2013, 2015, 2016 and 2018. These years represent flows during normal years, drought years and above-normal years. For example, 2010 flow was very near the multi-year average (Figure 16). Year 2011 was a notable very wet year, 2013 was very dry and 2015, 2016 and 2018 also had below average flows but were nearer to the long-term average. It was important to determine if these variable flows had any influence on constituent concentrations, such as increased dilution (reduction in concentrations) or in concentrating constituents during drought years. Notably, there was no reduction in TSS or VSS with the elevated flows recorded in 2011. Rather TSS was elevated at all sites, and even with the slight dilution from Little Cottonwood and Big Cottonwood Creeks TSS concentrations increased to new highs at downstream locations.

Notably, VSS remains very low and stable at about 5 mg L^{-1}. Furthermore, during 2015 and 2016, The VSS in Mill Creek was actually much lower than that in Jordan River, indicating that the Central Valley WRF often dilutes and improves the quality of Jordan River with respect to VSS and TSS. This is important in that the Phase I TMDL identified VSS as the primary pollutant of concern with the recommendation that reductions in VSS could be used to control the DO deficit. As such, the TMDL identified the POTWs as necessary to reduce VSS by several fold in order to reduce the DO deficit. Furthermore, the fact that VSS concentrations in every year are either maintained or actually increase (e.g. 2011) at lower Jordan River sites indicates that there is no net loss or significant settling of VSS to contribute to the sediment oxygen demand, as was also assumed in the Phase I report. Therefore, this data suggests that any reduction in VSS in the adjacent POTWs, at a potential cost of many 10s of millions of dollars would likely have no positive impact on VSS or DO. Additional evidence for this misunderstanding is provided in subsequent sections and chapters that discuss organic matter budgets and coarse particulate matter.

The inorganic nitrogen species and TKN are shown in Figure 17. With the exception of nitrate values, there was no difference in the nitrogen species between the normal or elevated flows of 2010 and 2011 compared to the subsequent low-flow drought years. Nitrate values were generally about 50% less during 2010 and 2011 than during other years. In all years following 2011 (drought years), nitrate was consistently between 4 and 5 mg L^{-1}. With the exception of the State Canal, ammonia remained consistently less than 1 mg L^{-1}. Ammonia in Mill Creek ranged up to about 1 mg L^{-1} and the site in the State Canal, below the SDSD N ranged up to about 2 mg L^{-1}. Notably the discharge from the S. Davis North Plant is only 900 m above the final diversion and distribution of State Canal water to impoundments of the FBWMA. This is worth mentioning as the healthy community of benthic nitrifiers and denitrifiers in the impoundments rapidly drop the ammonia to less that 1 mg L^{-1} and nitrate to non-detectable in most samples – rendering the impoundments nitrogen limited. This will be discussed further in the wetlands chapter that will be reported in Volume III of this update.

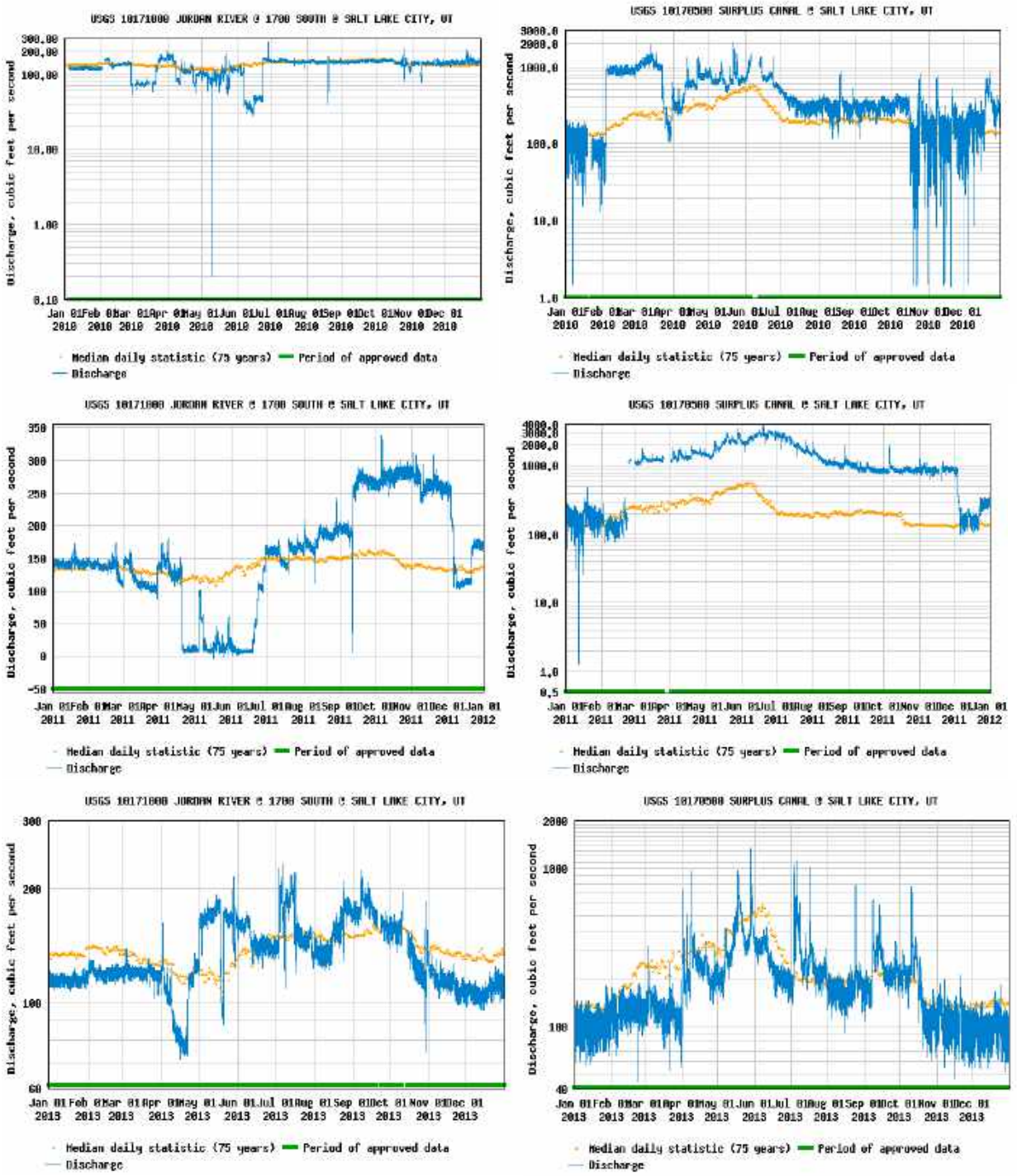

Figure 35. Monthly (Blue) and long-term average flows (Gold) for the Jordan River at 1700 S. (left) and the Surplus Canal (right) for 2010, 2011, 2013, 2015, 2016 and 2018.

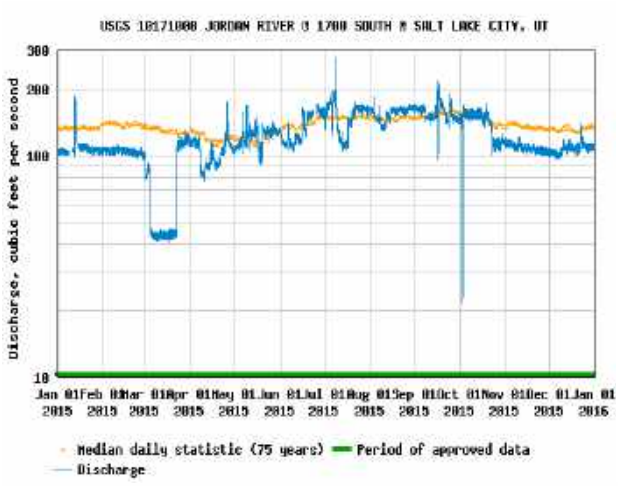
USGS 10171000 JORDAN RIVER @ 1700 SOUTH @ SALT LAKE CITY, UT
Discharge, cubic feet per second
300
200
100
10
Jan 01 2015
Feb 01 2015
Mar 01 2015
Apr 01 2015
May 01 2015
Jun 01 2015
Jul 01 2015
Aug 01 2015
Sep 01 2015
Oct 01 2015
Nov 01 2015
Dec 01 2015
Jan 01 2016
Median daily statistic (75 years)
Period of approved data
Discharge

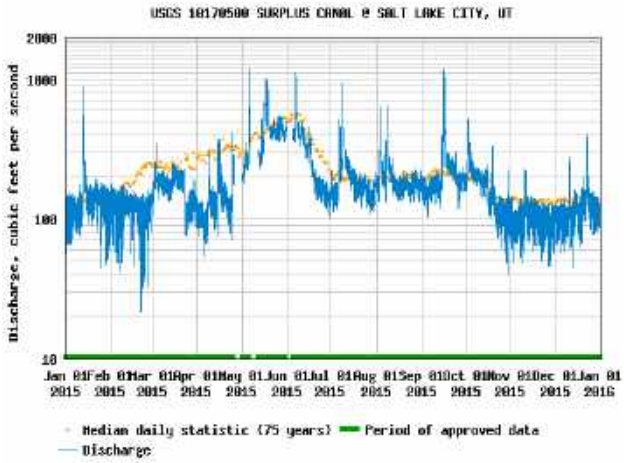
USGS 10170500 SURPLUS CANAL @ SALT LAKE CITY, UT
Discharge, cubic feet per second
2000
1000
100
10
Jan 01 2015
Feb 01 2015
Mar 01 2015
Apr 01 2015
May 01 2015
Jun 01 2015
Jul 01 2015
Aug 01 2015
Sep 01 2015
Oct 01 2015
Nov 01 2015
Dec 01 2015
Jan 01 2016
Median daily statistic (75 years)
Period of approved data
Discharge

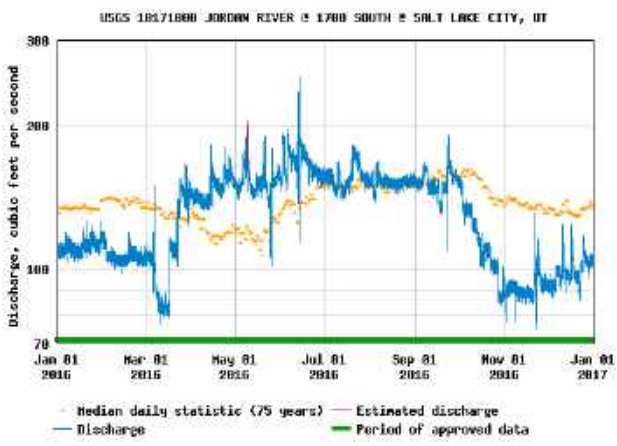
USGS 10171000 JORDAN RIVER @ 1700 SOUTH @ SALT LAKE CITY, UT
Discharge, cubic feet per second
300
200
100
70
Jan 01 2016
Mar 01 2016
May 01 2016
Jul 01 2016
Sep 01 2016
Nov 01 2016
Jan 01 2017
Median daily statistic (75 years)
Estimated discharge
Discharge
Period of approved data

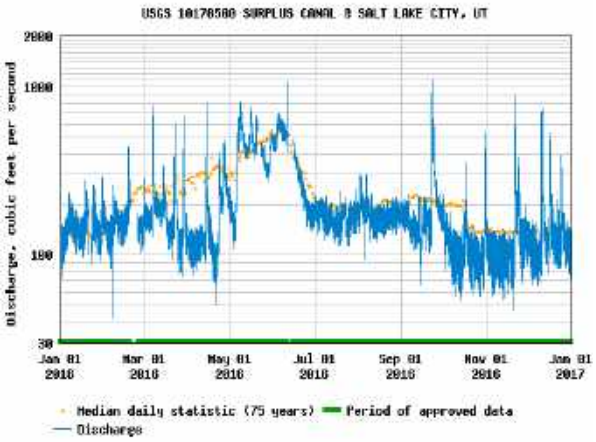
USGS 10170500 SURPLUS CANAL @ SALT LAKE CITY, UT
Discharge, cubic feet per second
2000
1000
100
50
Jan 01 2016
Mar 01 2016
May 01 2016
Jul 01 2016
Sep 01 2016
Nov 01 2016
Jan 01 2017
Median daily statistic (75 years)
Period of approved data
Discharge

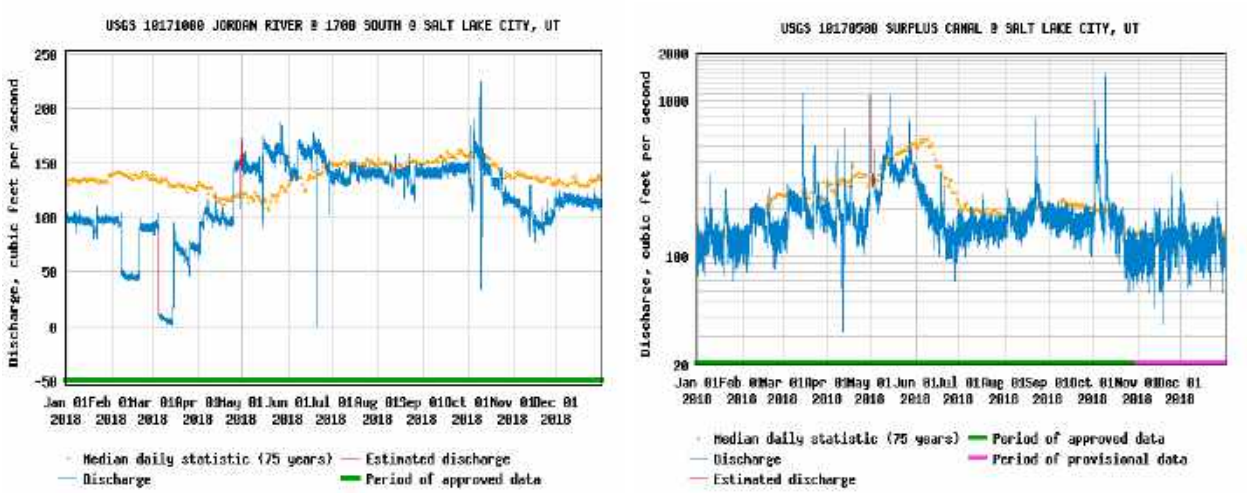

Figure 16, Continued

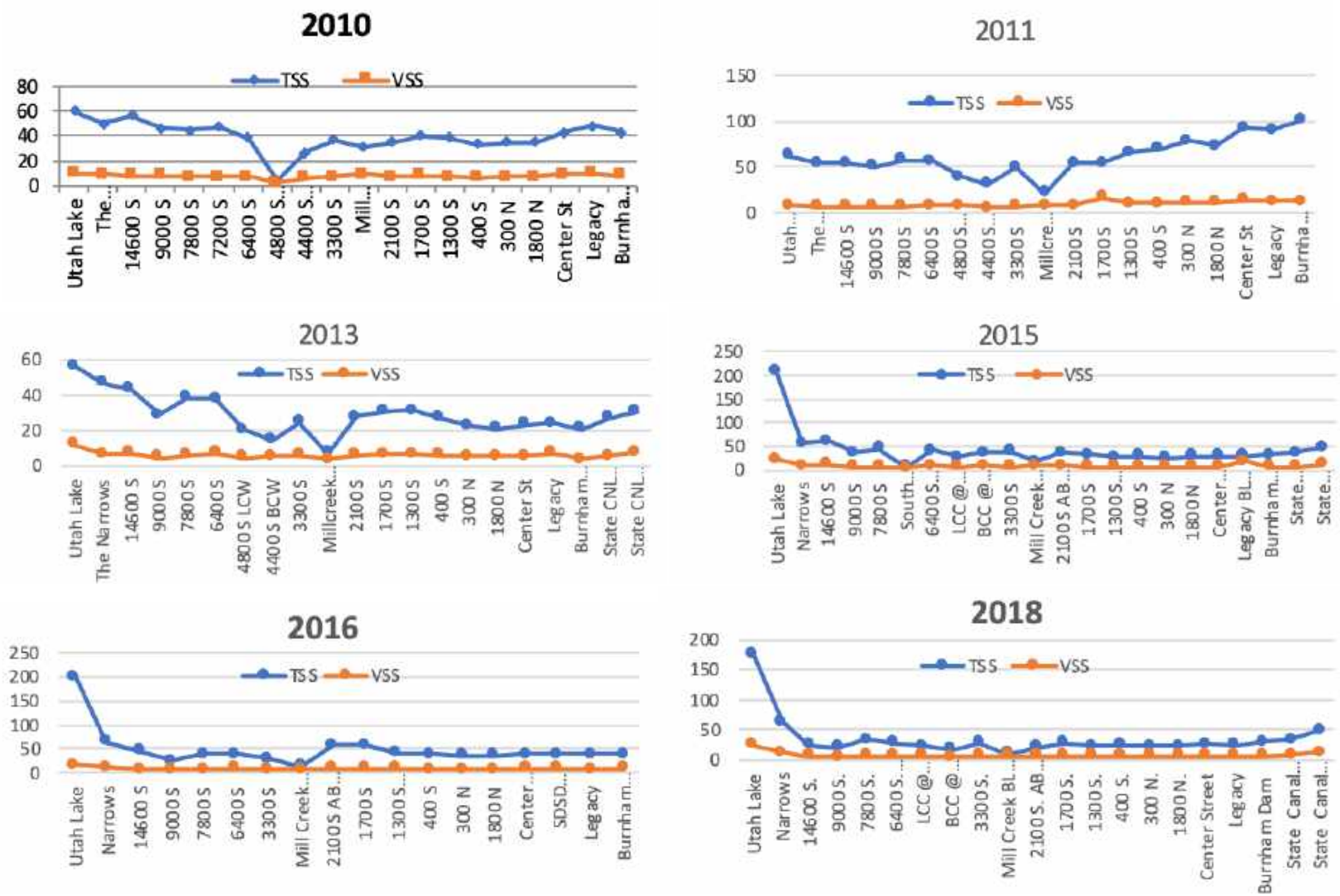

Figure 36. Annual average total suspended solids (TSS) and volatile suspended solids (VSS) at the mainstem sampling sites and at the mouth of Big and Little Cottonwood Creeks during 2010, 2011, 2013, 2015, 2016 and 2018. All values are in mg L^{-1}. Note: scales differ.

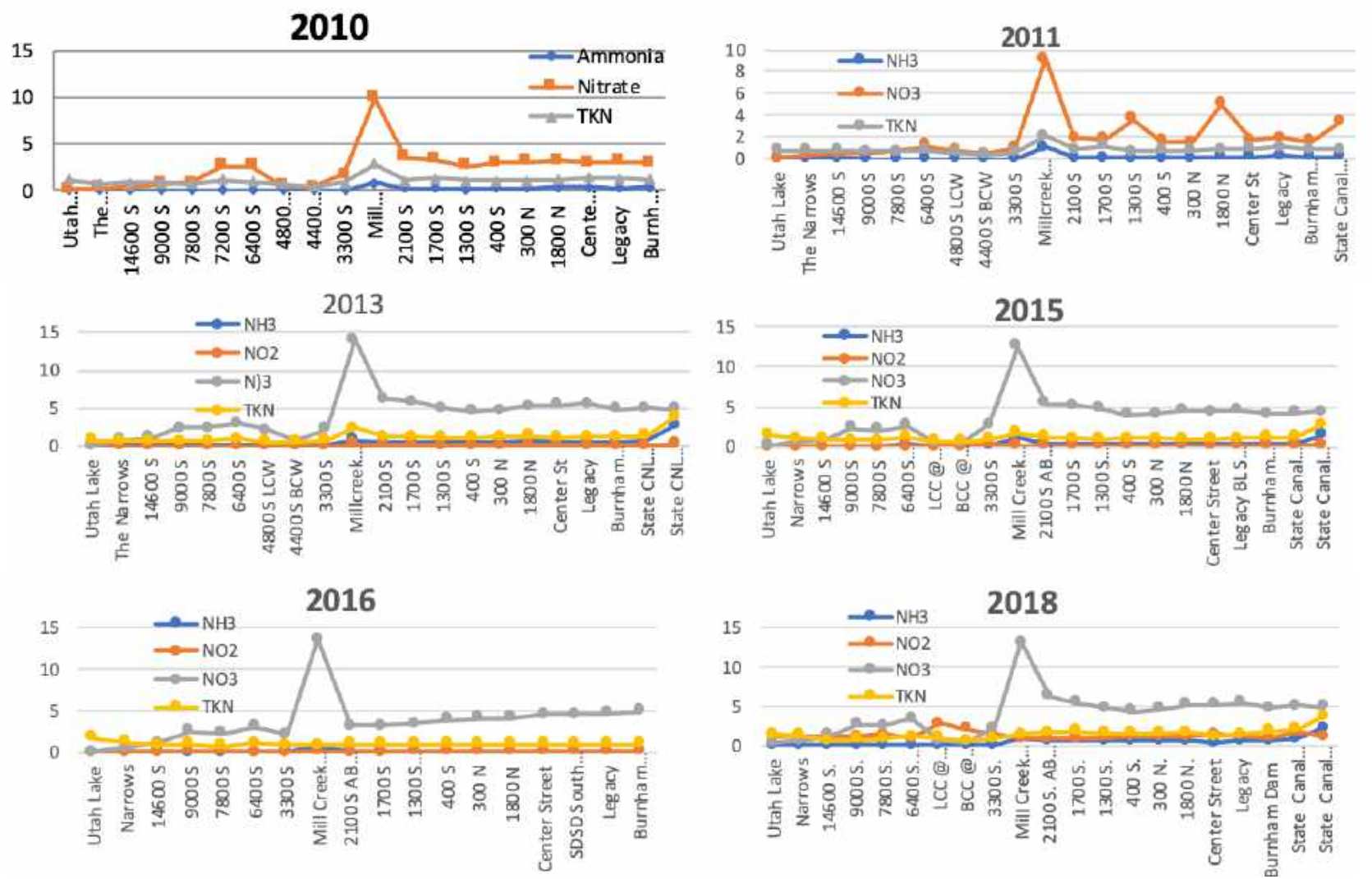

Figure 37. Annual average ammonia, nitrite, nitrate and TKN at the mainstem sampling sites and at the mouth of Big and Little Cottonwood Creeks during 2010, 2011, 2013, 2015, 2016 and 2018. All values are in mg L^{-1}. Note: scales differ.

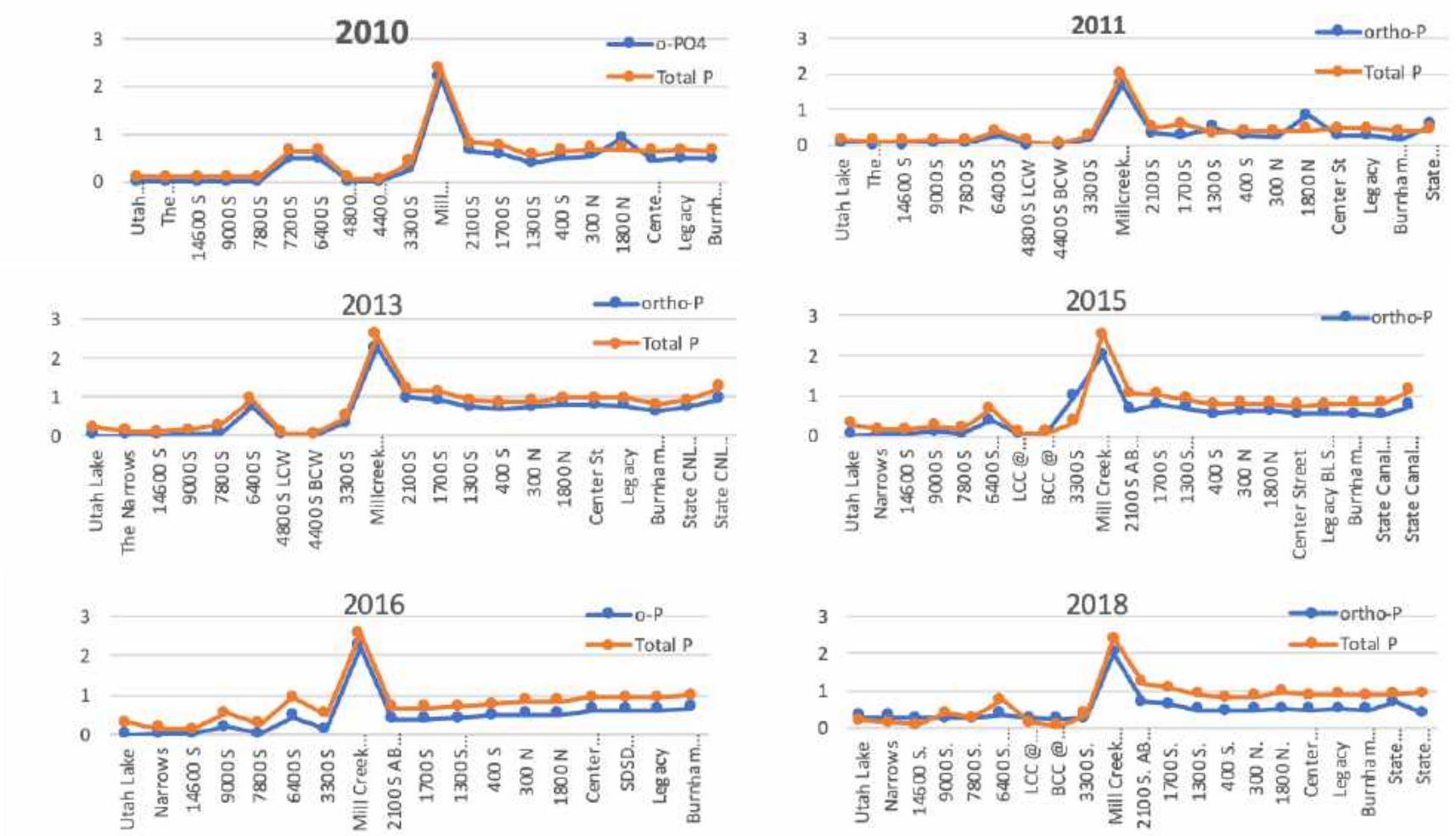

Figure 38. Annual average total and ortho-phosphate at the mainstem sampling sites and at the mouth of Big and Little Cottonwood Creeks during 2010, 2011, 2013, 2015, 2016 and 2018. All values are in mg L^{-1}. Note: scales differ.

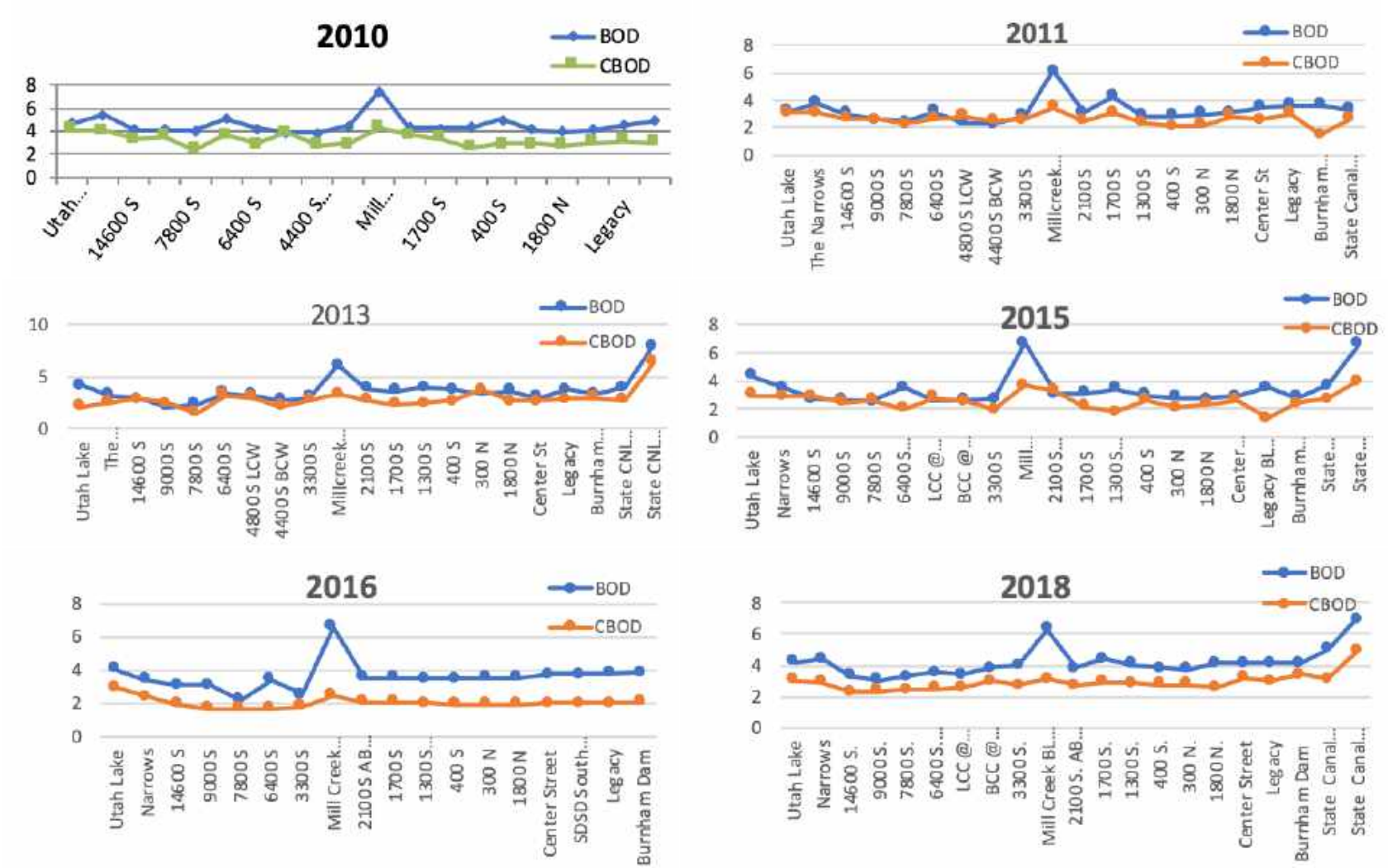

Figure 39. Annual average BOD and CBOD at the mainstem sampling sites and at the mouth of Big and Little Cottonwood Creeks during 2010, 2011, 2013, 2015, 2016 and 2018. All values are in mg L^{-1}. Note: scales differ.

The concentrations of total and ortho-P behaved similar to the nitrogen species throughout the study period. During 2011 the peak in P in Mill Creek was about 0.5 mg L^{-1} lower during 2011, while P concentrations at most river sites was about ½ those measured during 2011.

Discussion

While we believe the impedance of light by the turbidity is an important factor limiting primary production in the water column, reduction in Chl a in the upper portion of the river appears largely to be the result of the approximate 95% diversion of river water by Turner Dam, followed by dilution with shallow ground water and downstream tributaries. Notably however, despite this dilution in Chl a, turbidity itself remains quite stable throughout the entire river. For example, Rushforth and Rushforth (2010) recorded a dramatic decline in water column algae at progressive distances downstream. The biovolumes of Utah Lake species fell to about 1% of those at the Utah Lake outlet. Further, although Cyanobacteria dominated the phytoplankton community, the water column began carrying a substantial amount (up to 500,000 u^3 L^{-1}) of dislodged periphytic diatoms, suggesting that the periphyton was being scoured off of the substrate. Similarly, recent studies by Baker (2009) found that artificial nutrient-diffusing substrates acquired highly variable results during 21-day incubations at 20 locations in the main stem and tributaries. Generally, some samplers that were placed upstream from 2100 S. had quite high amounts of Chl *a*, while other samplers had very little. Overall these variable results were independent of where samplers were placed with regard to the location of the POTW discharges (i.e. whether placed upstream or within reaches that had elevated nutrients). Most of the higher amounts of Chl *a* were measured in the higher gradient portions upstream from all the POTW discharges. This high variability also supports the random likelihood that samplers were being scoured by the TSS or bedload sand, silt and clay particles.

The primary focus of this study is to understand the attenuation of light in the water column at various locations on the Jordan River and its effect upon the algal growth in the river. The hypothesis being tested is that light limitation inhibits phytoplankton and periphyton growth in the river vs the effect of scouring or smothering by the mobilized (upstream sites) or settling (downstream sites). Yet, the evidence indicates that all three factors are at play in the Jordan River. The rapid attenuation of light to near the compensation point at the bottom at all sites clearly indicates that substantial light limitation is occurring, while the embeddedness (at upstream sites) – suggesting that significant scouring is occurring upstream and the complete smothering (at downstream sites) also clearly reduce the ability for periphyton production. Furthermore, this is part of the larger hypothesis that periphyton and phytoplankton primary production and biomass in the river is not sufficient to cause excessive respiration or decomposition that leads to the oxygen deficits/DO impairment experienced at downstream locations. Rather, oxygen deficits result from sediment oxygen demand (SOD) that results from organic matter delivered to the river from urban sources, including seeds, leaves, grass clippings, etc. from adjacent properties and storm drains throughout the urbanized valley that reaches the river and its tributaries (see Chapters 4 and 6). Although the light attenuation curves reported here are relatively steep, and light intensity near the bottom is greatly

diminished, they do indicate that sufficient light to support net primary production reaches nearly all of the river bottom. This suggests that under the normal flows of summer, but particularly during winter, when Utah Lake water is shut off, (the clearest water and lowest flow conditions), there is sufficient light penetration to support net positive primary production by both phytoplankton and periphyton communities. This phenomenon has been confirmed by the many measurements of SOD and water column OD by Hogsett (2015; Chapter 6).

In other words, the light reaching the bottom was generally greater than the estimated intensity needed to maintain the compensation point (threshold for net positive primary production). These estimates range from 1% to 5% of the incident radiation striking the surface. For example, Hill and Fanta (2007) exposed periphyton communities to various combinations of low light intensities and phosphorus in large flow-through laboratory streams. Growth rates became limited by light ranging from 12-88 umole m^{-2} s^{-1}. Among all of our sampling stations, the 1% of surface light intensity ranged from 7 to 16 umole m^{-2} s^{-1} and the 5% light intensity ranged from 66 to 85 umole m^{-2} s^{-1}.

Notably, these ranges are also similar to the threshold for light measured for the filamentous periphyton, *Cladophora glomerata* in natural stream and lake populations. Graham et al. (1982) and Lester et al. (1998) found light limitation occurred at 25 to 44 umole m^{-2} s^{-1}. Lorenz et al. (1991) used these light intensities to predict and effectively map the distribution of *Cladophora* stands in littoral zones of the Great Lakes. This narrower range marks the 2% to 4% range of surface light intensity under direct sunlight measured in the Jordan River. By comparison most of the measurement sites in the Jordan River experienced higher irradiance values near the bottom. Therefore, while some light limitation may occur, most of the river's water column and sediment surface receive sufficient light for net accumulation of periphyton or phytoplankton.

Despite the presence of sufficient light, the phytoplankton populations from Utah Lake rapidly and drastically diminish at successive sites below the Utah Lake outlet (Figure 2). The biovolume of the most common taxa, Cyanobacteria, decreases by more than 99% within the first approximate 30 miles of the river (ca. 1.5 travel days).

These data suggest that there is considerable divergence between the photosynthetically available light throughout the water column, and the decline of the phytoplankton biomass, including cyanobacteria, downstream from the Utah Lake outlet. This indicates that the Turner Dam diversion removes the great majoring of phytoplankton and that it never recovers at downstream sites. Further, although some periphyton is dislodged from the stable upstream substrates, this scouring doesn't nearly replace the biomass that is delivered from Utah Lake and this is despite sufficient, although perhaps not optimal light intensity penetrating the entire water column. For example, Cyanobacteria don't become light-limited until the intensity falls below 12-18 umol m^{-2} s^{-1} or the 1% light level (Van Liere and Walsby 1982) and are also well known to tolerate the relatively intense light near lake surfaces, e.g. Whitton and Potts (2000). Further, the turbidity (measured as both TSS or light attenuation curves) remains relatively consistent from the Utah Lake outfall to the Jordan River terminus (see Appendix) – suggesting that these algae are exposed to similar light conditions as that of Utah Lake.

In addition to the major diversion at Turner Dam, there is also considerable dilution from returning ground water, tributaries and POTW discharges (CH2MHill 2005, Borup and Haws, 1999). Notable evidence that supports this "diversion and dilution" concept is the very large number of the same species, *Anabaena spiroides* and *Aphanizomenon flos-aquae,* in the east side tributaries and their occurrence in the same ratio as water leaving Utah Lake. This also suggests that there may not be a lot of die-off – even as water is diverted and carried in the canals and eventually returned in at least two of the main tributaries to the Jordan River (Little Cottonwood and Mill Creeks; Rushforth and Rushforth 2010). Therefore, although there appears to be sufficient light intensity to maintain the Utah Lake phytoplankton populations, there doesn't appear to be additional growth of phytoplankton in the river.

The relatively low production by periphyton was also very dynamic. For example, common periphyton taxa, including pennate and centric diatoms and the ubiquitous green alga, *Cladophora glomerata,* do become marginally established where stable substrate occurs in the upper river reaches. However, periphyton communities remain sparse, even where suitable cobble and boulder substrates occur and particularly in relation to the apparent availability of light and the elevated concentrations of nitrogen and phosphorus. This scarcity, particularly in light of the abundant P and N concentrations, confirms the hypothesis that: 1) The elevated concentrations of suspended and bedload sediments from Utah Lake, bank erosion and various nonpoint sources, remain in dynamic equilibrium between suspension in the water column and being transported as bedload throughout the entire river. Therefore, there is a continual source of unstable sand, silt and clay that is carried by even normal stream flows (Bio-West 1987, personal observations). This unstable sediment serves to continually dislodge the developing periphyton communities, which then become suspended in the water column (Figure 3; Rushforth and Rushforth, 2010) and also cause extreme embeddedness of 80 to 90% of the substrate that is stable-further reducing the available surface area for colonization; 2) Numerous observations and our periphyton scrapings indicated that substantial quantities of sand, silt and clay material had become embedded/entangled even within the periphyton strands and stalks themselves. For example, the mucilaginous secretions of diatoms provide for a "sticky" biofilm that can accumulate silt and clay particles (personal observations). Such particles also become entrapped by the branched filaments of *Chladophora*, apparently limiting its filamentous growth to just a few cm in length.

With the exception of the 1700 S. area, nearly the entire river bottom below 2100 S is depositional in nature. Attempts to perform periphyton colonization studies using nutrient diffusing substrates (Baker 2009) resulted in nearly all of the canisters becoming covered with 1- 4 cm of sediment and several samplers were lost in the accumulating sediment. Samplers placed upstream from 2100 S. yielded extremely variable results with some of the artificial substrate samplers accumulating substantial quantities of Chl a, while other samplers accumulating only traces of Chl a (Baker 2009).

The settling and shifting of fine organic and inorganic sediments appear to be the primary reasons why periphyton colonization does not occur in the downstream reaches. Rather, these reaches are dominated by a heterotrophic microbial system that is based on the

decomposition of organic matter delivered from upstream sources, including Utah Lake and the many tributaries (Chapters 4 and 6).

Overall, the light profiles provide valuable information relating to primary production in the river. Generally, while light rapidly attenuates through the water column, sufficient light (remaining above the compensation point) occurs to provide for periphyton or phytoplankton growth throughout the entire river, and particularly at depths shallower than 2 m. The other constraining factor is that the river is likely too turbulent for the phytoplankton to fully optimize their morphological and physiological acclimation to the light [e.g. Kohler (1992) suggested that *Microcystis* takes two days to adapt to the high irradiances typical of surface blooms]. Even in the slow-moving portions of the river, the turbulence would randomly transport phytoplankton between the top and bottom several times each day. The extent that this differs from the turbulence on Utah Lake plankton is unknown. However, because TSS, VSS and the light profiles remain quite stable as the water travels downstream, light and turbulence conditions in the Jordan River likely remain quite similar to those in Utah Lake.

These data also help elucidate the question of the contribution of either phytoplankton or periphyton growth in the upper and middle reaches of the river toward the organic loading and potential for deposition downstream from 2100 S. For example, the Jordan River TMDL Phase II: Draft Technical Memo: Critical Conditions, Endpoints, and Permissible Loads on the Jordan River (Stantec and Cirrus 2010) suggests: "nutrients may be responsible for increased algal growth and subsequent detritus levels within the Jordan River above 2100 South that add to the loads of TSS." However, a review of Figure 2 and the original data from Rushforth and Rushforth (2010) indicate that the greatest reduction of Utah Lake algal biomass occurs upstream from 2100 south. Further, these cells would be collected in the monthly VSS and TSS samples, which again remain stable or slightly increase with distance downstream, indicating that there is very little or no additional particulate organic carbon being delivered to the river from autochthonous sources (above that which is already being delivered to the river by Utah Lake). Finally, the biomass of diatoms actually increases slightly downstream from 2100 S. This is contrary to the hypothesis that these cells are dying and depositing and adding to the SOD downstream. Rather, this slight increase could be supplied from the three tributaries in this reach that are likely also contributing dislodged diatoms to the Jordan River. These and the other tributaries including the return of Utah Lake water from exchanges with Mill Creek and Big Cotton Creeks. are likely replacing the VSS that is being removed by the large diversions. Sources of this additional/replacement VSS are likely the partially decomposed leaves, seeds, grass litter and perhaps from the many tributaries and stormwater flows.

Notably, the concentrations of VSS do not vary (settle) substantially from upstream to downstream sites, nor from month to month or year to year (Figure 17). Alternatively, we have a large data set documenting the delivery and settling of CPOM in the lower Jordan River (Chapter 3). Sparse populations of periphyton in reaches that possess both ample light and relatively stable substrate suggest that the benthic community is largely influenced by the continual or intermittent settling and scouring of the unstable sand, silt and clay material. Further evidence of this characteristic is the low numbers of

macroinvertebrate grazers such as members of the caddisfly and mayfly orders (Peterson and Miller 2010, Bio-West, Inc., 1987, 1992). But perhaps most damaging to this ecosystem is the continual need to dredge the channel at various locations (e.g. near the mouth of Mill Creek, Little Cottonwood Creek and 1700 S.) and along most of the downstream channel, every few years. This degradation of Jordan River habitat has been discussed in greater detail by Filbert and Holden (1992), Biowest, et al. (1987) and Holden and Crist (1986) and in several of our Chapters in Volume II: Biological Integrity. This present study, in conjunction with those of Rushforth and Rushforth (2009) and Baker (2009) adds important information that helps us understand the complex interactions within this urban river. Based upon this new information, additional studies were initiated to focus on:

1. Quantifying the proportion of VSS or fine particulate organic matter (FPOM) at the Utah Lake outlet and subsequent delivery of FPOM and CPOM from downstream tributaries. We need to understand the fraction of the organic material that is composed of living cells vs. detritus (Chapter 6).
2. Quantifying the components of primary production/community respiration/SOD in reaches that possess quantifiable periphyton vs reaches that are primarily depositional in nature, This should be performed using both the two-station – upstream-downstream technique for primary production and community respiration as well as the more site-specific respirometer method (chamber technique) to compare individual site primary production/respiration in reaches located upstream and downstream from 2100 S. (See Bott, 2007; Chapter 6).

Literature Cited

Baker, M. 2009. Summary and Interpretation of 2009 Jordan River Chlorophyll Bioassay Results. Technical Memorandum to Utah Division of Water Quality and South Valley Water Reclamation District. 4 pp. plus Appendices.

Bio-west, Inc., Callister, Duncan and Nebeker, R.L. Dahl, Hydroqual, Inc., W.M. Lewis and Zorc, Rissetto and Weaver. 1987. Proposed 208 plan water quality standards modification for the lower Jordan River. 225 pp.

Borup, B. and N. Haws. 1999. Jordan River flow analysis. Civil and Environmental Engineering Department. Brigham Young University, Provo, Utah. Prepared for the State of Utah, Department of Environmental Quality, Division of Water Quality.

Bott, T.L. 2007. Primary productivity and community respiration. pp. 663-690. In: Haur, F.R. and G. A. Lamberti (eds.). Methods in stream ecology. Second Edition. Elsevier.

Cirrus Ecological Solutions, LC and Stantec Consulting, 2010. Jordan River TMDL Phase II:Draft Technical Memo: Critical conditions, endpoints and permissible loads in the Jordan River. Report to Utah Division of Water Quality. 39 pp.

Holden, P.B. and L.W. Crist. 1987. Fishery and macroinvertebrate studies of the Jordan River in Salt Lake county November 1987. Report to Central Valley Water Reclamation Facility Board. 95 pp.

Cirrus Environmental Consultants. 2009 Jordan River TMDL: Public Draft Work Element 2 – Pollutant Identification and Loading. Report to Utah Division of Water Quality. 212 pp.

CH2M Hill. 2005. Jordan River Return Flow Study. Report to Recycled Water Coalition.

Filbert, R. and P.B. Holden. 1992. Fishery investigations of the lower Jordan River, Utah Final Report, 1988-1991. Report to Central Valley Water Reclamation Facility Board. 73 pp.

Goel, R. 2010. Sediment oxygen demand and reaeration rates in the Jordan River. Draft report to the Utah Division of Water Quality and Central Davis Sewer District. 16 pp.

Graham, J. M., M. T. Auer, R. P. Canale, and J. P. Hoffmann. 1982. Ecological studies and mathematical modeling of *Cladophora* in Lake Huron: 4. Photosynthesis and respiration as functions of light and temperature. J. Great Lakes Res., 8(1): 100-111.

Hill, W. R. and S. E. Fanta. 2007. Phosphorus and light colimit periphyton growth at subsaturating irradiances. Freshwater Biology 53(2):215-225.

Kohler. J. 1992. Influence of turbulent mixing on growth and primary production of *Microcystis aeruginosa* in the hypertrophic Bautzen Reservoir. Arch. Hydrobiol. 123:413-429.

Lester, W. W., Adams, M. S., and Farmer, A. M. 1988. Effects of light and temperatureon photosynthesis of the nuisance alga Cladophora glomerata (L.) Kutz from Green Bay, Lake Michigan. New Phytol. 109: 53-58.

Lorenz, R. C., Monaco, M. E., and Herdendorf, C. E. 1991. Minimum light requirements of substrate colonization by *Cladophora glomerata*. J. Great Lakes Res. 17: 536-542.

Peterson J. and T.G. Miller. 2010. Stream Visual Assessment Protocol results and interpretation for the Jordan River, 2009.

Van Liere, L and A.E. Walsby. 1982. Interactions of Cyanobacteria with light. In: Carr, N.G. and Whitton, B.A. (eds.). The biology of Cyanobacteria. pp. 9-45. Blackwell Scientific Publications. Oxford.

Whitton, B.A. and M. Potts. 2000. The Ecology of Cyanobacteria: their diversity in time and space. Kluwer Academic Publishers. Netherlands. 699 pp.

Appendix

The following graphs summarize the light extinction profiles at the water quality sampling stations in the Jordan River and the Surplus Canal during summer and fall, 2009. The graphs include measured light intensity values as well as percentage of light intensity as a function of depth. The equations posted on the graphs represent an exponential regression model for one of the listed attenuation curves.

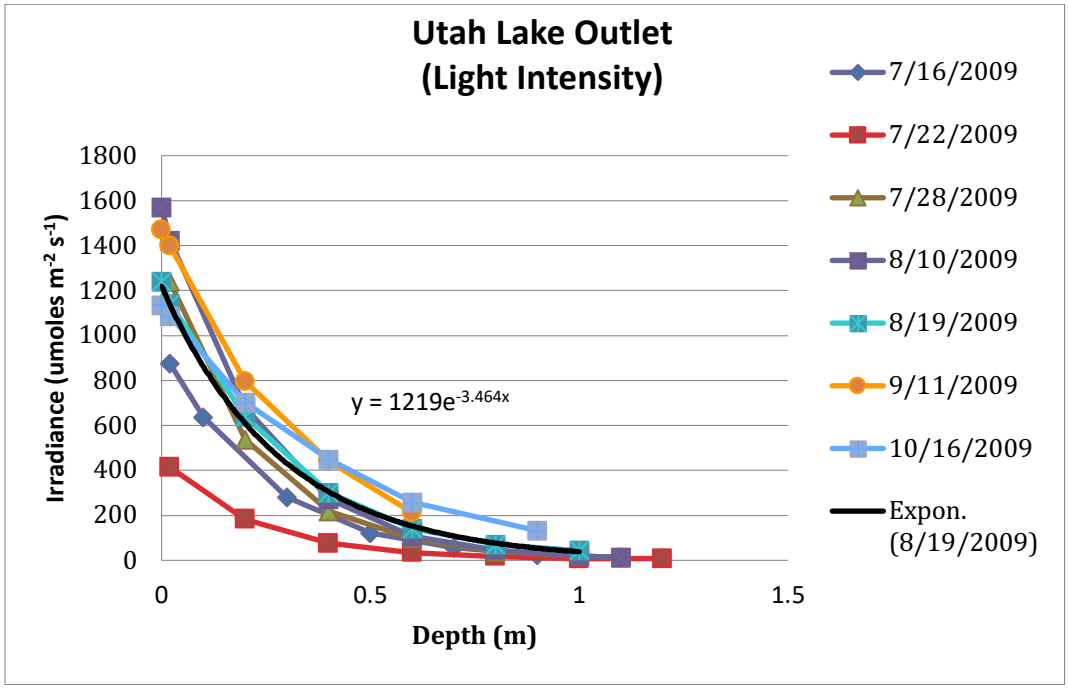

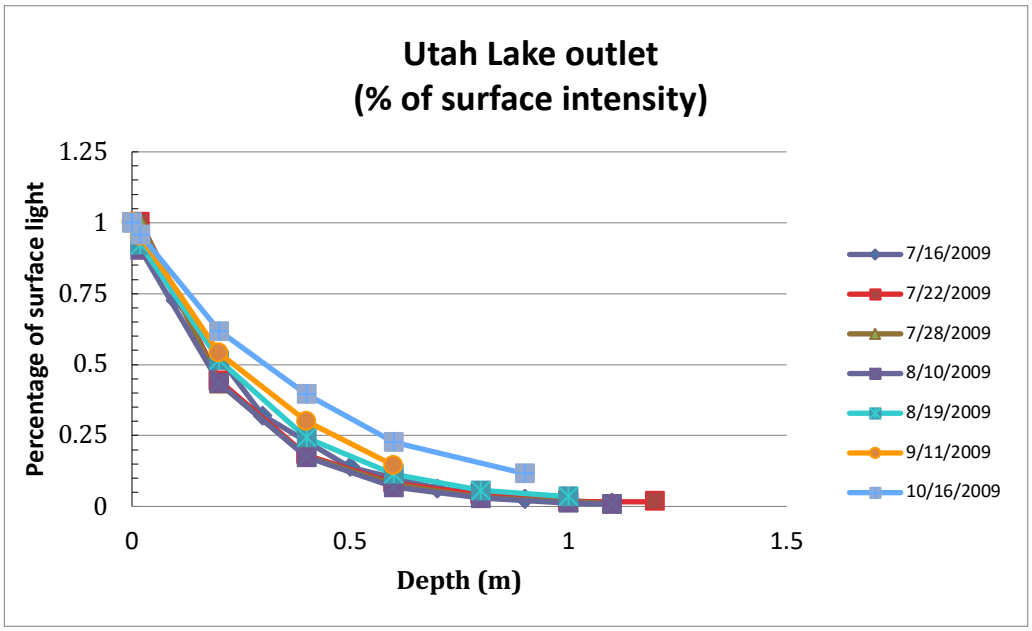

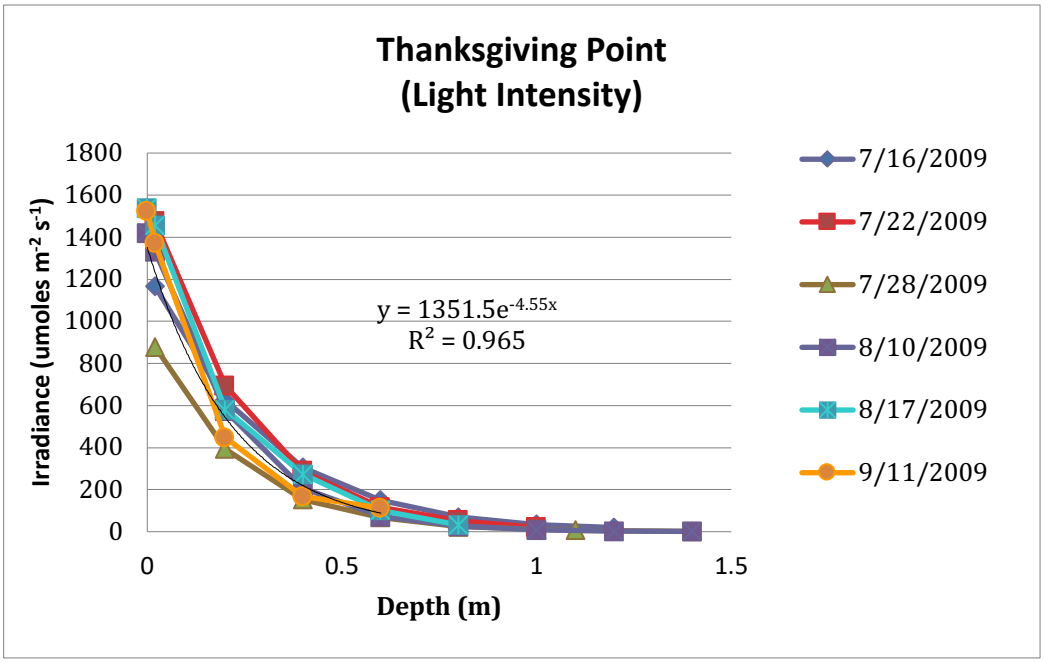
Thanksgiving Point
(Light Intensity)
Irradiance (umoles m-2 s-1)
1800
1600
1400
1200
1000
800
600
400
200
0
0
0.5
1
1.5
Depth (m)
y = 1351.5e-4.55x
R2 = 0.965
7/16/2009
7/22/2009
7/28/2009
8/10/2009
8/17/2009
9/11/2009

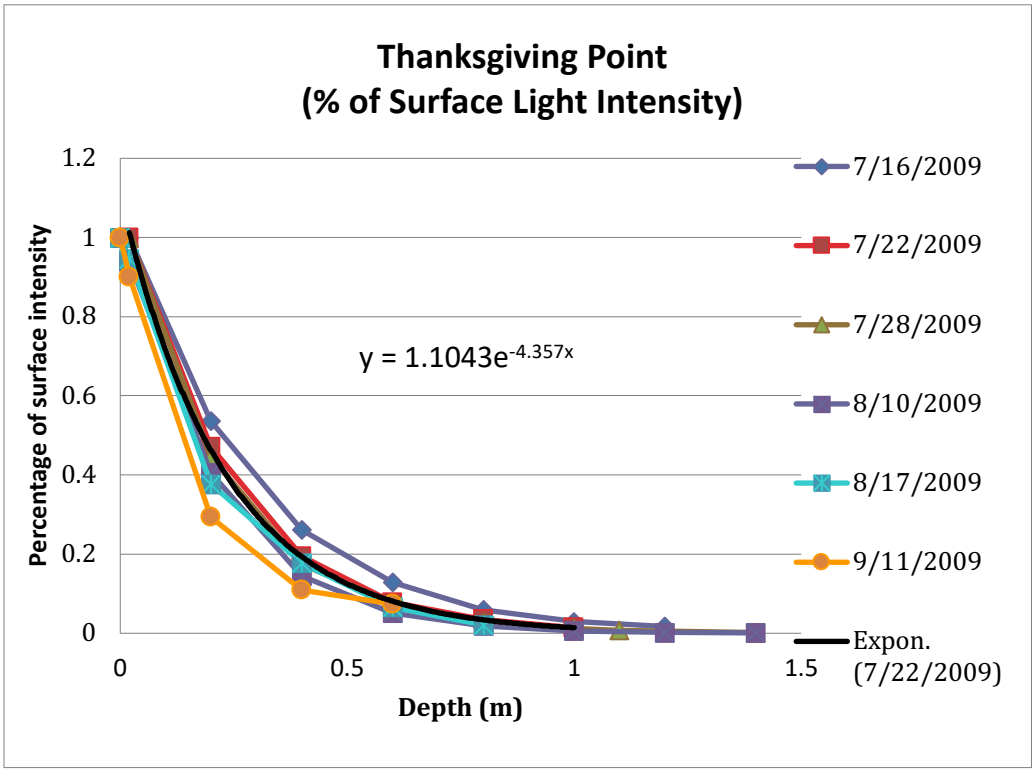
Thanksgiving Point
(% of Surface Light Intensity)
Percentage of surface intensity
1.2
1
0.8
0.6
0.4
0.2
0
0
0.5
1
1.5
Depth (m)
y = 1.1043e-4.357x
7/16/2009
7/22/2009
7/28/2009
8/10/2009
8/17/2009
9/11/2009
Expon. (7/22/2009)

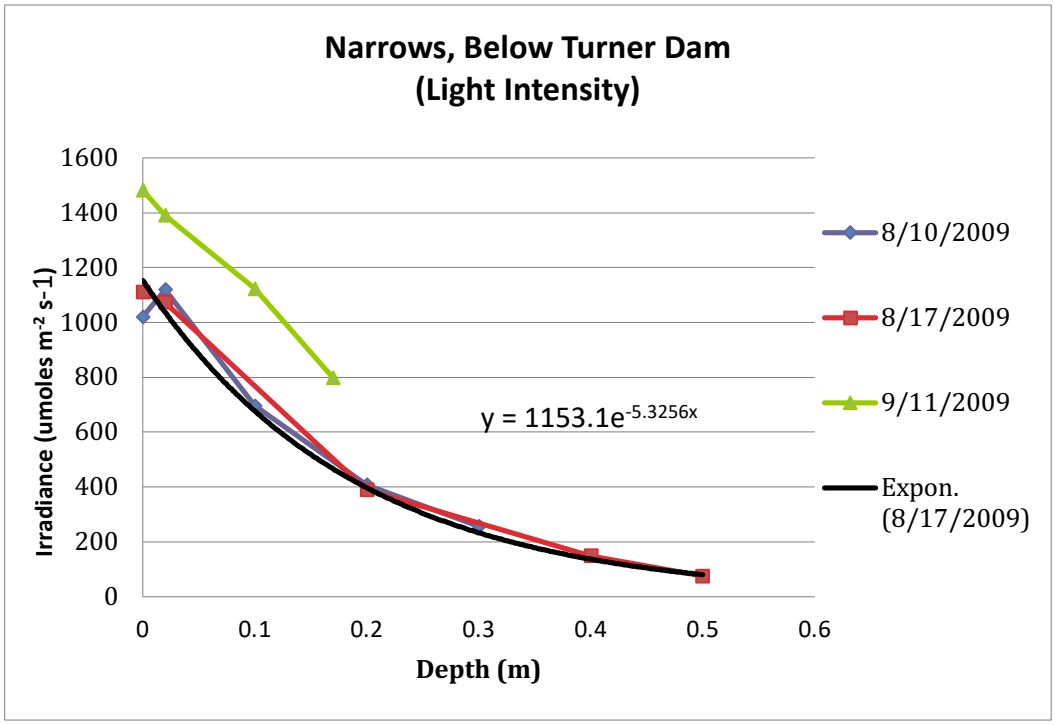
Narrows, Below Turner Dam
(Light Intensity)
Irradiance (umoles m-2 s-1)
1600
1400
1200
1000
800
600
400
200
0
0
0.1
0.2
0.3
0.4
0.5
0.6
Depth (m)
y = 1153.1e-5.3256x
8/10/2009
8/17/2009
9/11/2009
Expon. (8/17/2009)

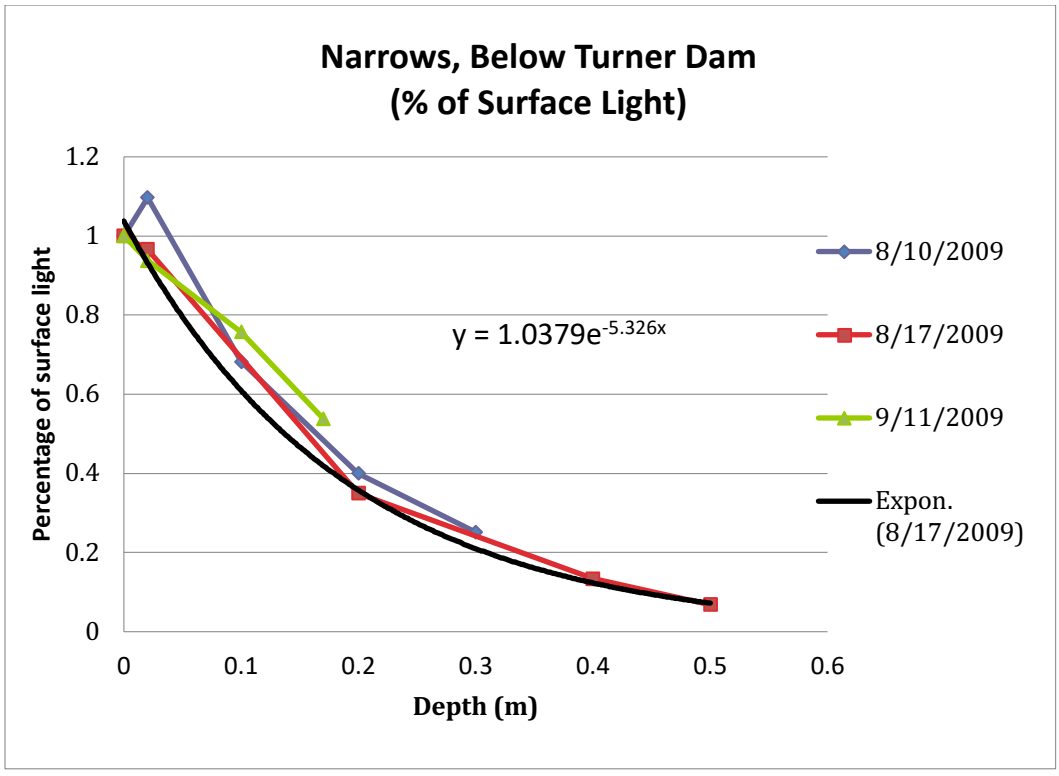
Narrows, Below Turner Dam
(% of Surface Light)
Percentage of surface light
1.2
1
0.8
0.6
0.4
0.2
0
0
0.1
0.2
0.3
0.4
0.5
0.6
Depth (m)
y = 1.0379e-5.326x
8/10/2009
8/17/2009
9/11/2009
Expon. (8/17/2009)

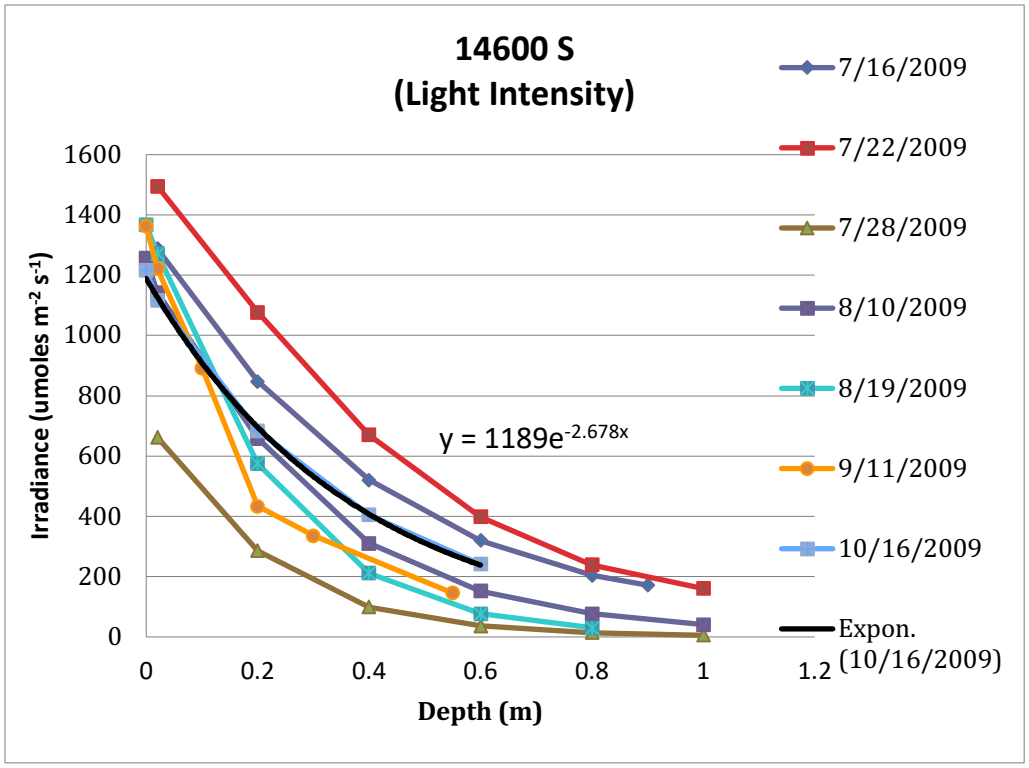
14600 S
(Light Intensity)
Irradiance (umoles m-2 s-1)
1600
1400
1200
1000
800
600
400
200
0
0
0.2
0.4
0.6
0.8
1
1.2
Depth (m)
y = 1189e-2.678x
7/16/2009
7/22/2009
7/28/2009
8/10/2009
8/19/2009
9/11/2009
10/16/2009
Expon. (10/16/2009)

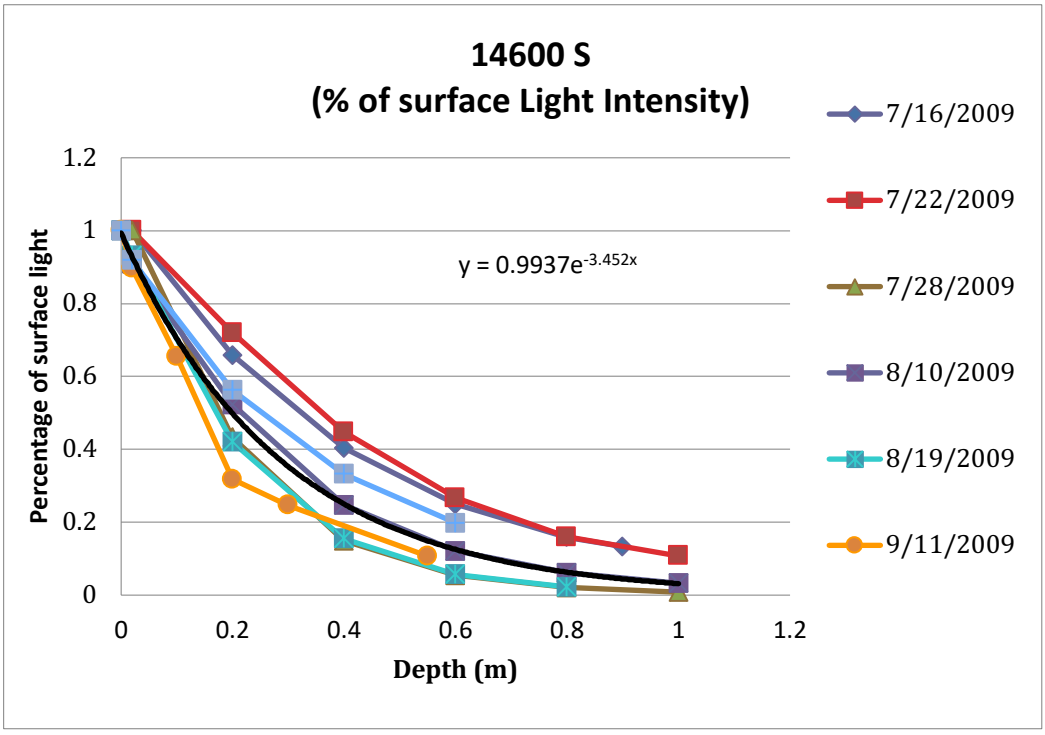
14600 S
(% of surface Light Intensity)
Percentage of surface light
1.2
1
0.8
0.6
0.4
0.2
0
0
0.2
0.4
0.6
0.8
1
1.2
Depth (m)
y = 0.9937e-3.452x
7/16/2009
7/22/2009
7/28/2009
8/10/2009
8/19/2009
9/11/2009

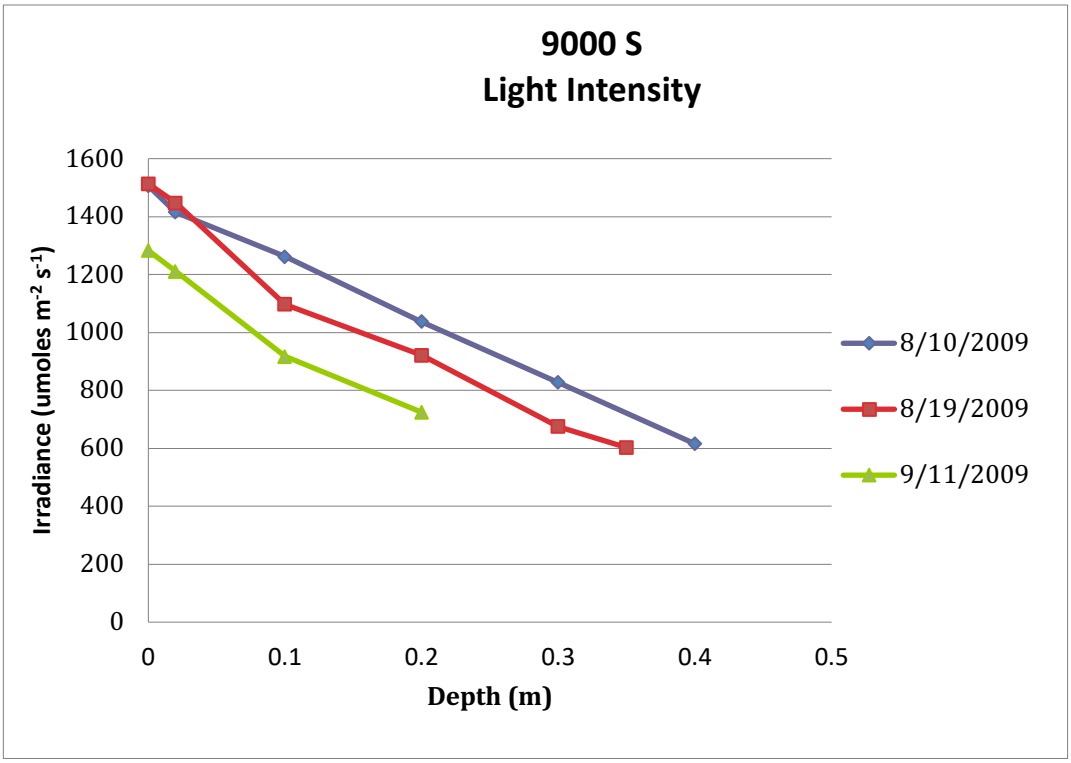
9000 S
Light Intensity
Irradiance (umoles m-2 s-1)
1600
1400
1200
1000
800
600
400
200
0
0
0.1
0.2
0.3
0.4
0.5
Depth (m)
8/10/2009
8/19/2009
9/11/2009

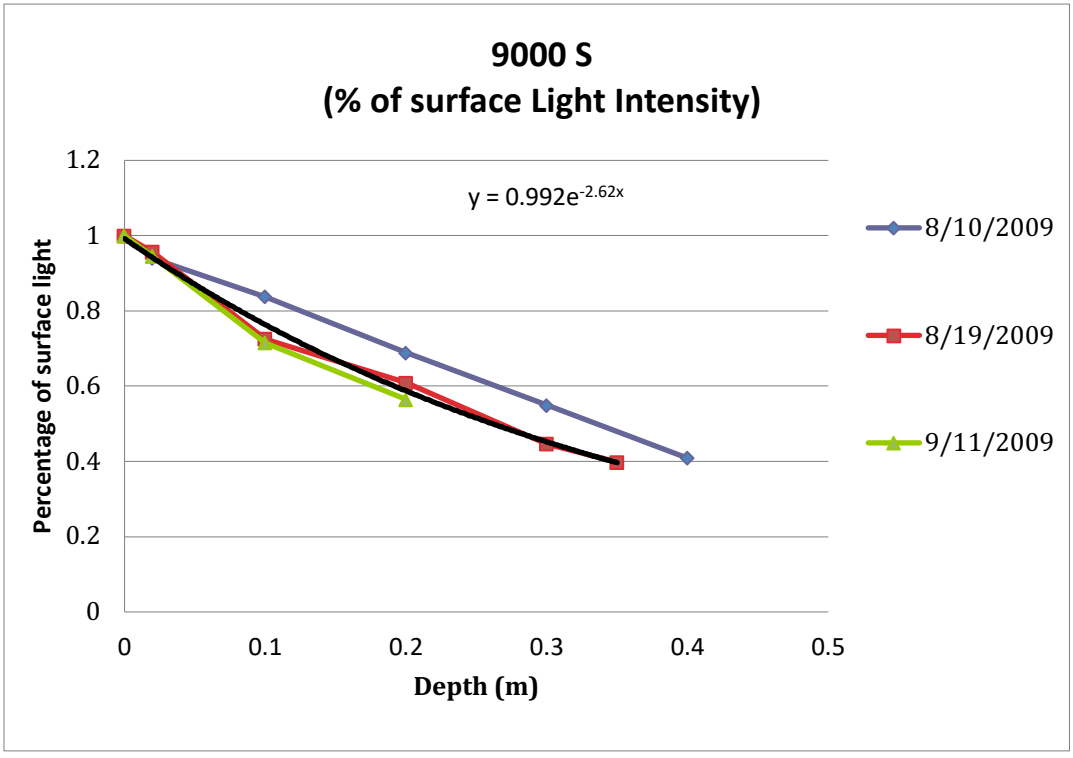
9000 S
(% of surface Light Intensity)
y = 0.992e-2.62x
Percentage of surface light
1.2
1
0.8
0.6
0.4
0.2
0
0
0.1
0.2
0.3
0.4
0.5
Depth (m)
8/10/2009
8/19/2009
9/11/2009

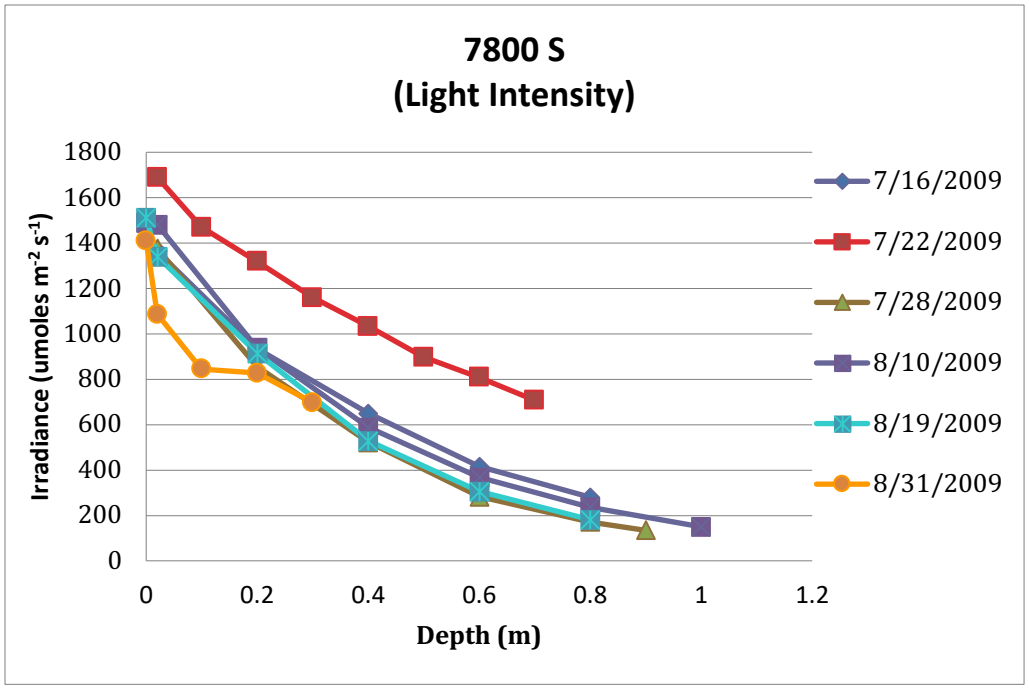
7800 S
(Light Intensity)
Irradiance (umoles m-2 s-1)
1800
1600
1400
1200
1000
800
600
400
200
0
0
0.2
0.4
0.6
0.8
1
1.2
Depth (m)
7/16/2009
7/22/2009
7/28/2009
8/10/2009
8/19/2009
8/31/2009

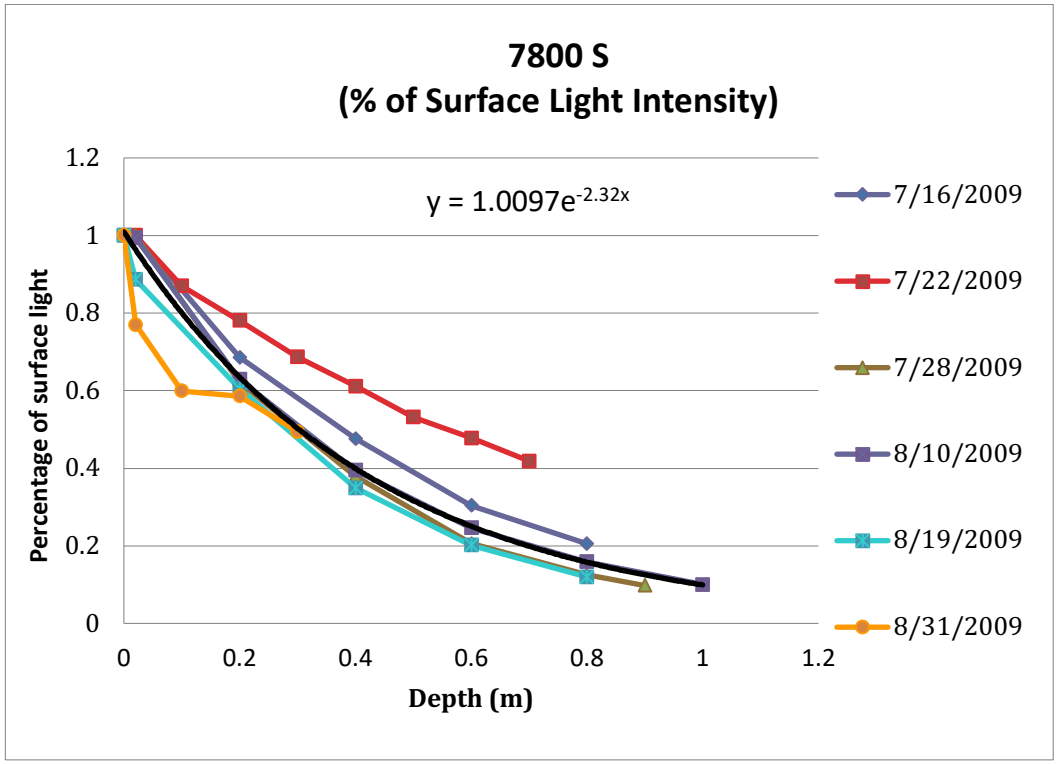
7800 S
(% of Surface Light Intensity)
y = 1.0097e-2.32x
Percentage of surface light
1.2
1
0.8
0.6
0.4
0.2
0
0
0.2
0.4
0.6
0.8
1
1.2
Depth (m)
7/16/2009
7/22/2009
7/28/2009
8/10/2009
8/19/2009
8/31/2009

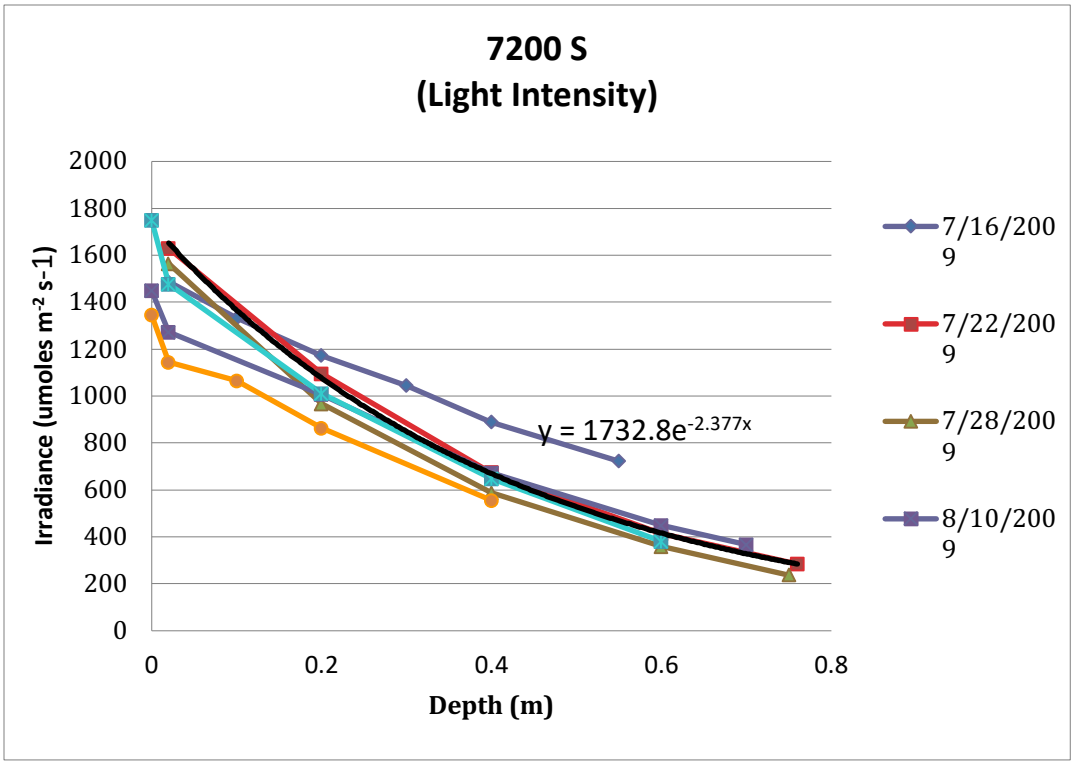
7200 S
(Light Intensity)
Irradiance (umoles m-2 s-1)
2000
1800
1600
1400
1200
1000
800
600
400
200
0
0
0.2
0.4
0.6
0.8
Depth (m)
y = 1732.8e-2.377x
7/16/2009
7/22/2009
7/28/2009
8/10/2009

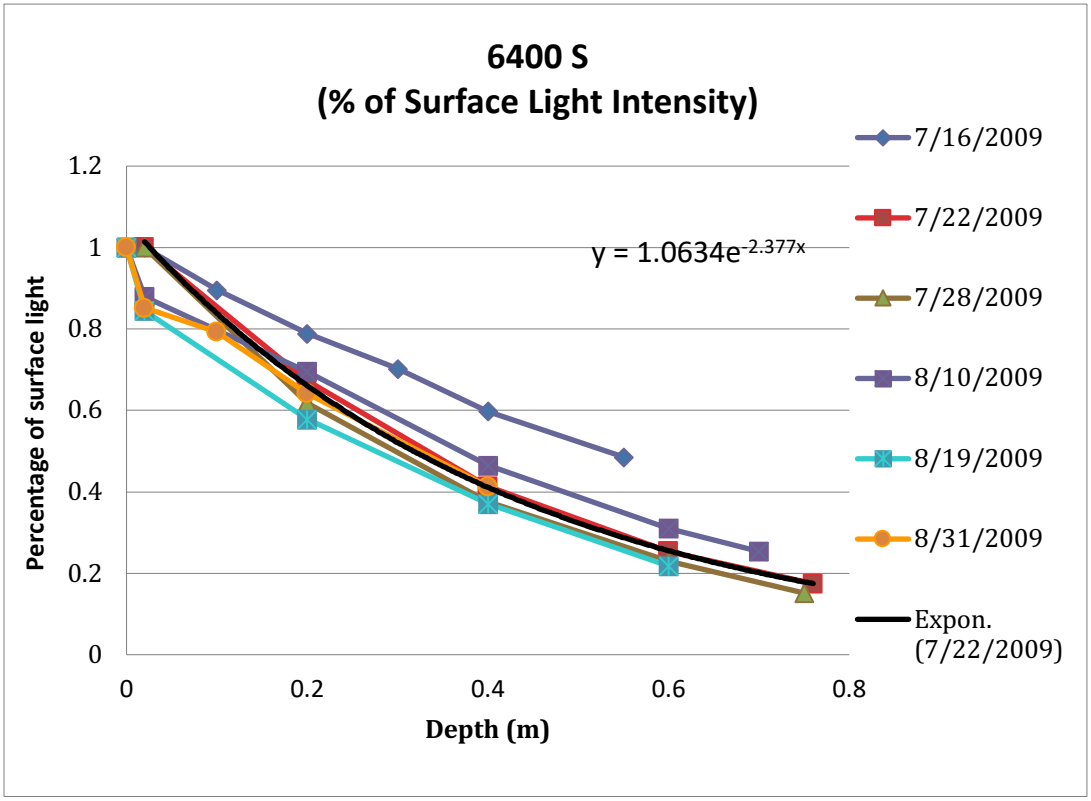
6400 S
(% of Surface Light Intensity)
Percentage of surface light
1.2
1
0.8
0.6
0.4
0.2
0
0
0.2
0.4
0.6
0.8
Depth (m)
y = 1.0634e-2.377x
7/16/2009
7/22/2009
7/28/2009
8/10/2009
8/19/2009
8/31/2009
Expon. (7/22/2009)

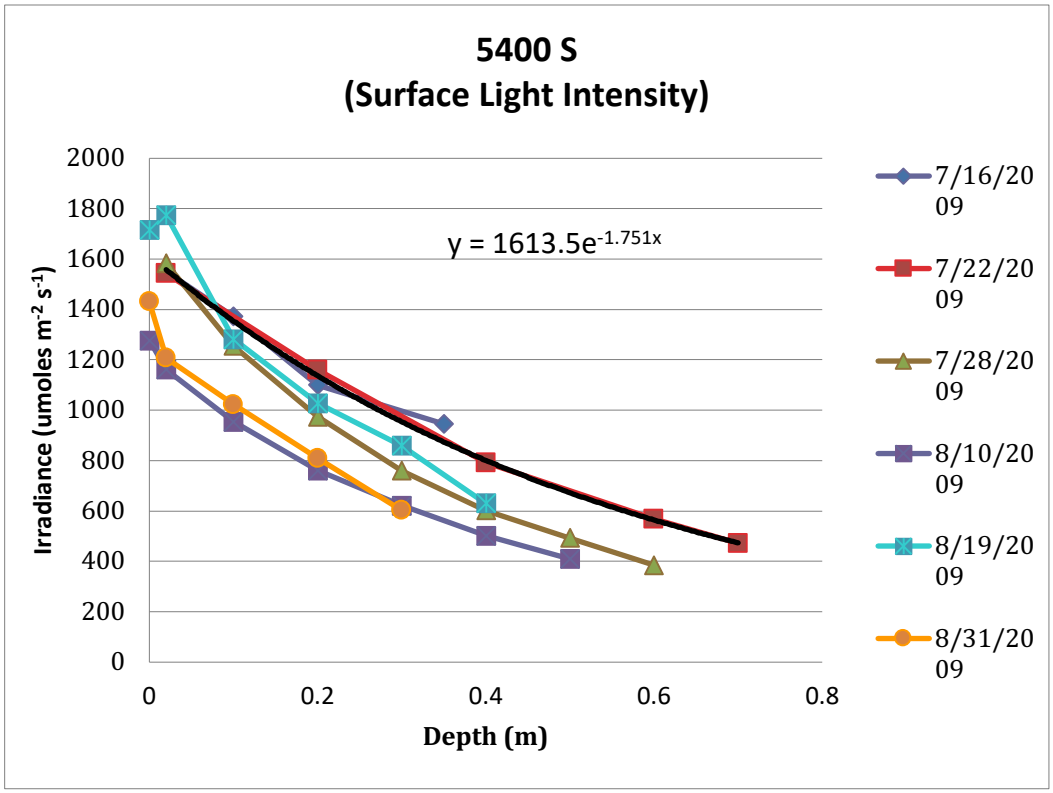
5400 S
(Surface Light Intensity)
y = 1613.5e-1.751x
Irradiance (umoles m-2 s-1)
Depth (m)
2000
1800
1600
1400
1200
1000
800
600
400
200
0
0
0.2
0.4
0.6
0.8
7/16/2009
7/22/2009
7/28/2009
8/10/2009
8/19/2009
8/31/2009

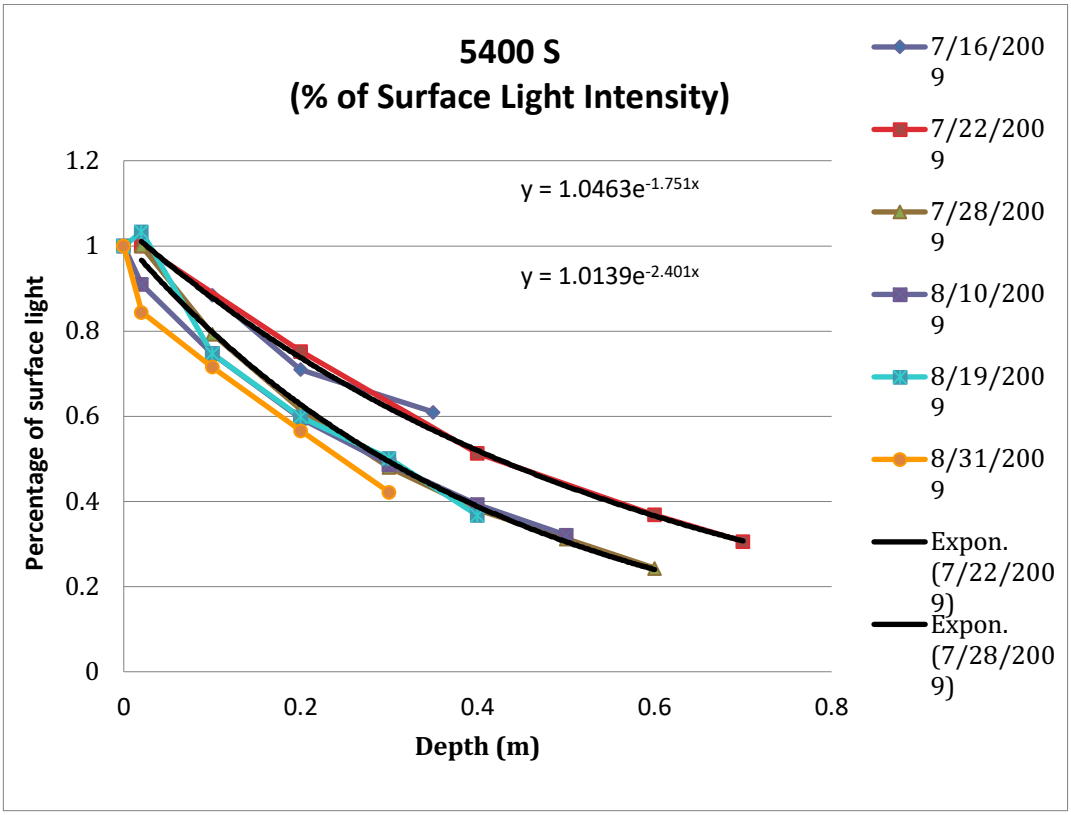
5400 S
(% of Surface Light Intensity)
y = 1.0463e-1.751x
y = 1.0139e-2.401x
Percentage of surface light
Depth (m)
1.2
1
0.8
0.6
0.4
0.2
0
0
0.2
0.4
0.6
0.8
7/16/2009
7/22/2009
7/28/2009
8/10/2009
8/19/2009
8/31/2009
Expon. (7/22/2009)
Expon. (7/28/2009)

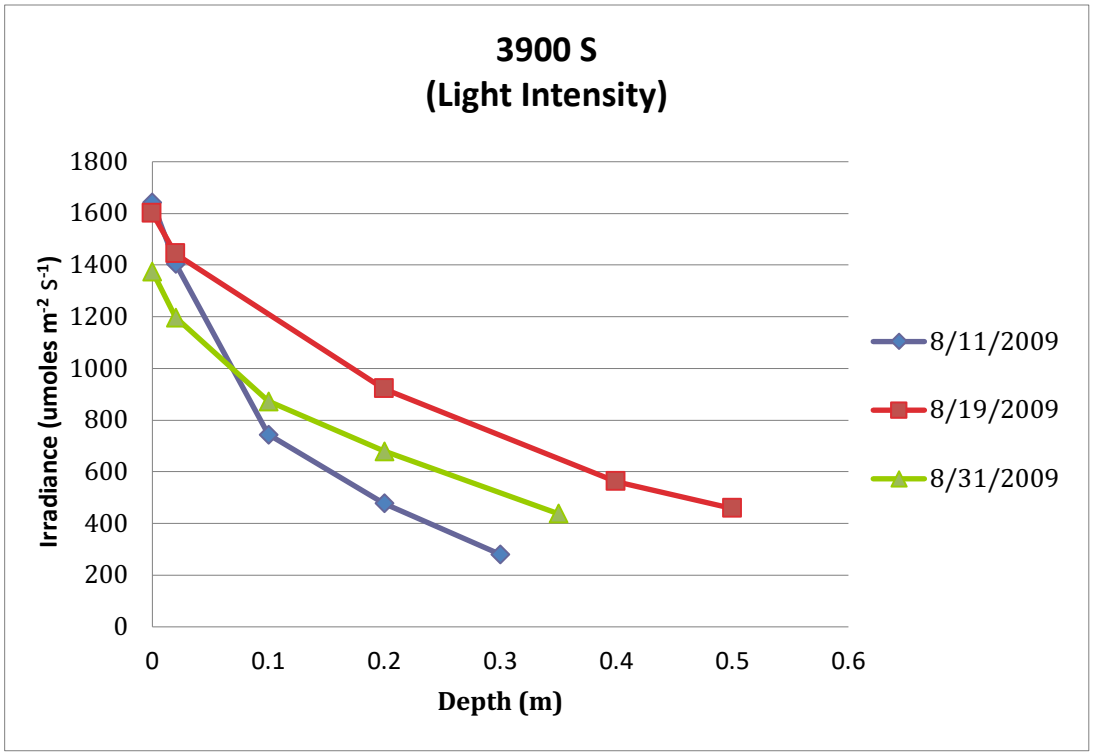
3900 S
(Light Intensity)
Irradiance (umoles m-2 S-1)
1800
1600
1400
1200
1000
800
600
400
200
0
0
0.1
0.2
0.3
0.4
0.5
0.6
Depth (m)
8/11/2009
8/19/2009
8/31/2009

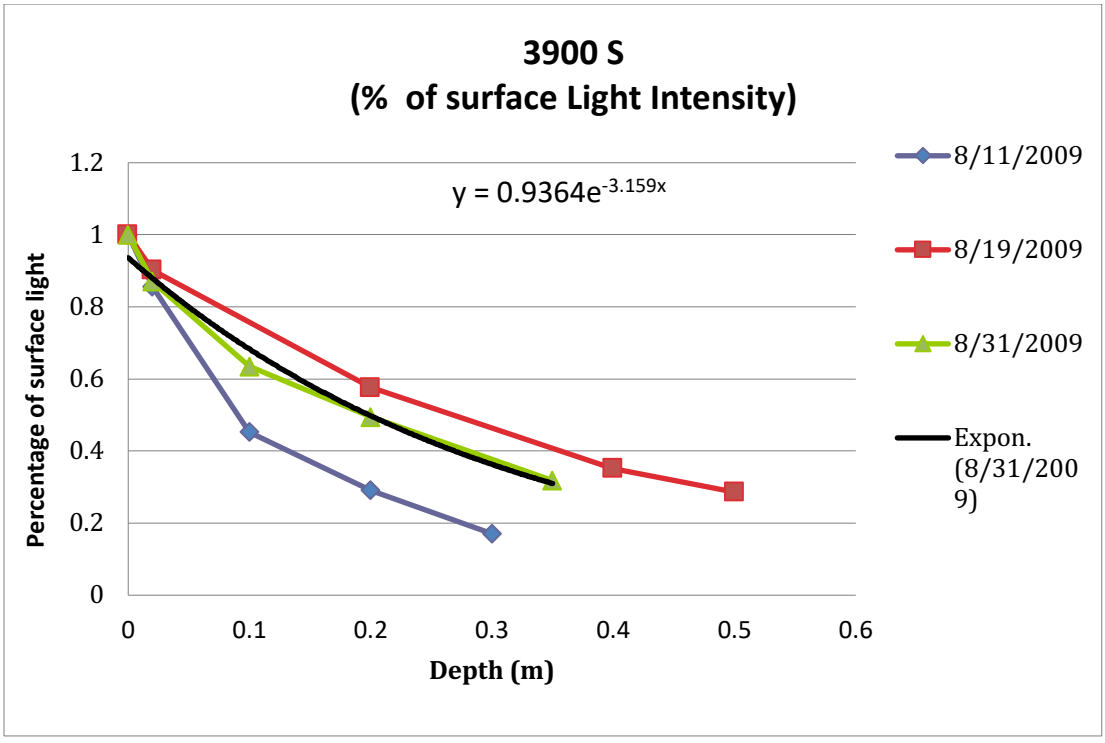
3900 S
(% of surface Light Intensity)
y = 0.9364e-3.159x
Percentage of surface light
1.2
1
0.8
0.6
0.4
0.2
0
0
0.1
0.2
0.3
0.4
0.5
0.6
Depth (m)
8/11/2009
8/19/2009
8/31/2009
Expon. (8/31/2009)

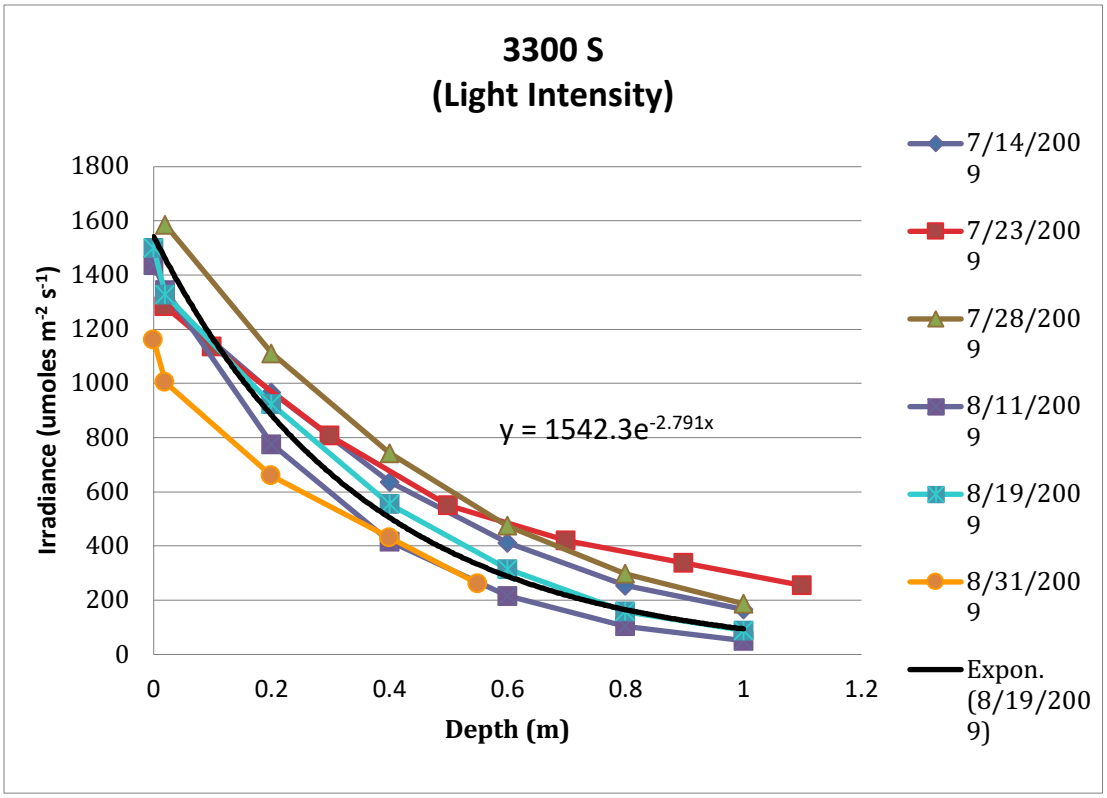
3300 S
(Light Intensity)
Irradiance (umoles m-2 s-1)
1800
1600
1400
1200
1000
800
600
400
200
0
0
0.2
0.4
0.6
0.8
1
1.2
Depth (m)
y = 1542.3e-2.791x
7/14/2009
7/23/2009
7/28/2009
8/11/2009
8/19/2009
8/31/2009
Expon. (8/19/2009)

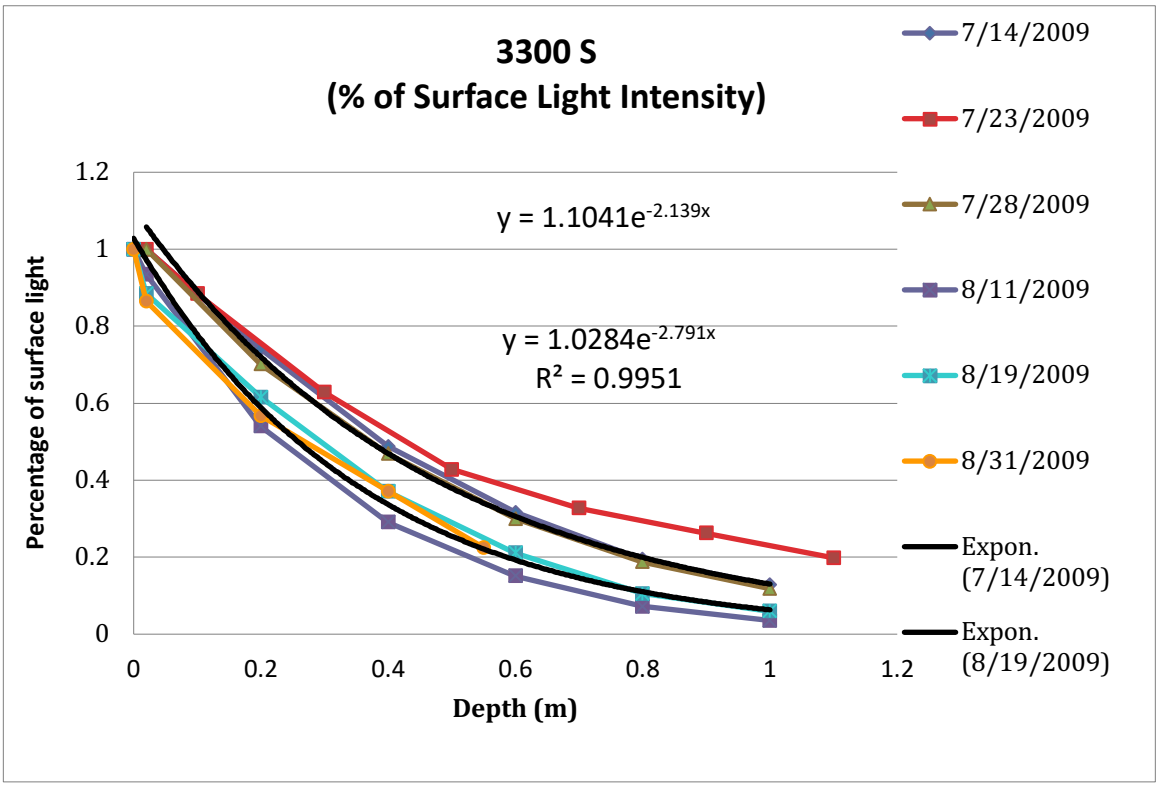
3300 S
(% of Surface Light Intensity)
Percentage of surface light
1.2
1
0.8
0.6
0.4
0.2
0
0
0.2
0.4
0.6
0.8
1
1.2
Depth (m)
y = 1.1041e-2.139x
y = 1.0284e-2.791x
R² = 0.9951
7/14/2009
7/23/2009
7/28/2009
8/11/2009
8/19/2009
8/31/2009
Expon. (7/14/2009)
Expon. (8/19/2009)

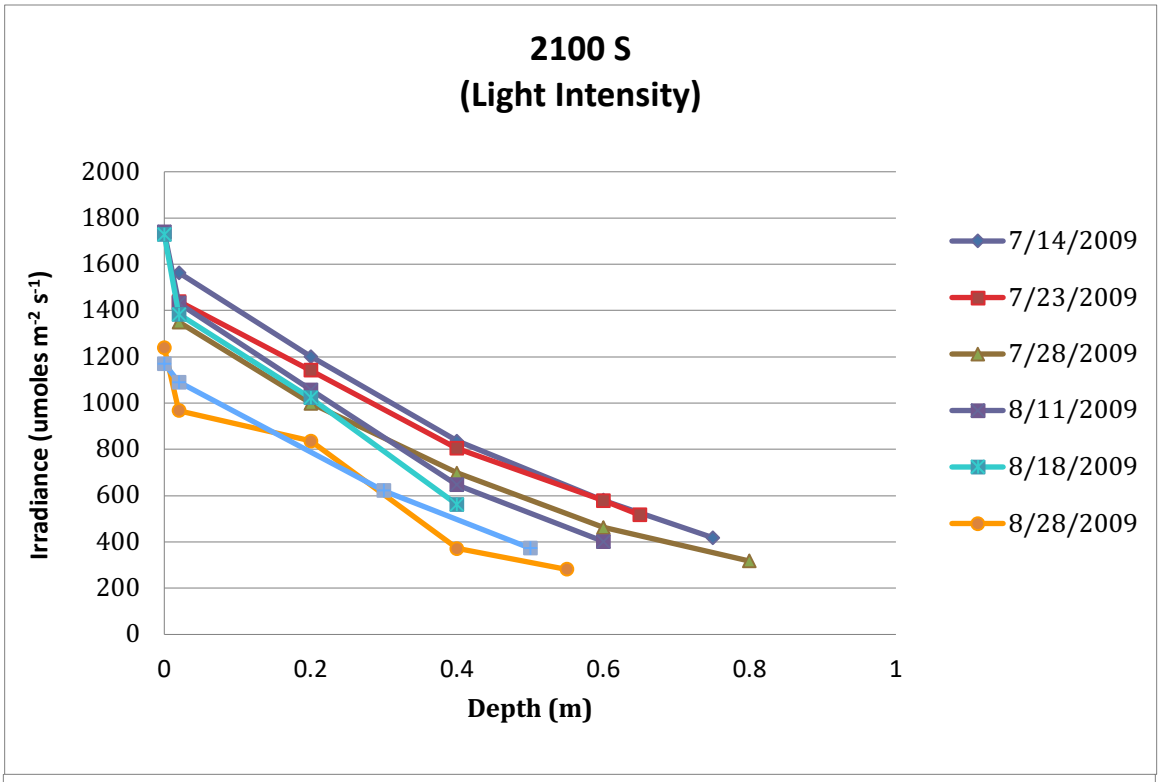
2100 S
(Light Intensity)
Irradiance (umoles m-2 s-1)
2000
1800
1600
1400
1200
1000
800
600
400
200
0
0
0.2
0.4
0.6
0.8
1
Depth (m)
7/14/2009
7/23/2009
7/28/2009
8/11/2009
8/18/2009
8/28/2009

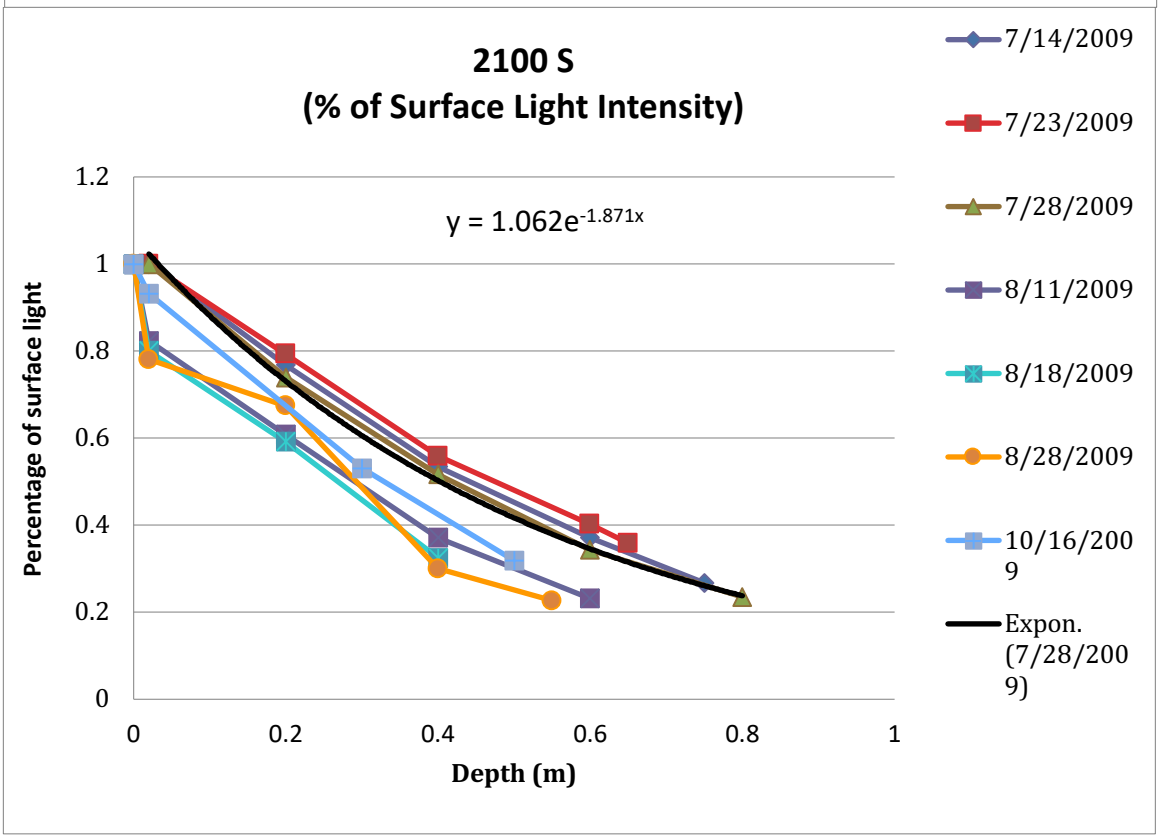
2100 S
(% of Surface Light Intensity)
y = 1.062e-1.871x
Percentage of surface light
1.2
1
0.8
0.6
0.4
0.2
0
0
0.2
0.4
0.6
0.8
1
Depth (m)
7/14/2009
7/23/2009
7/28/2009
8/11/2009
8/18/2009
8/28/2009
10/16/2009
Expon. (7/28/2009)

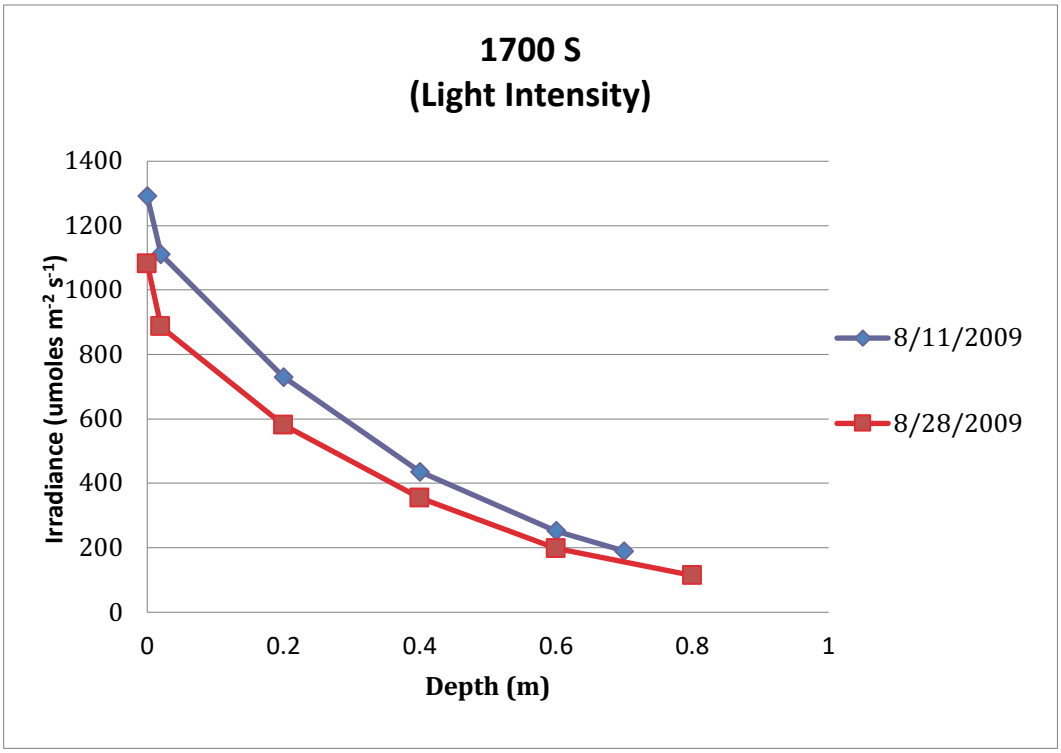
1700 S
(Light Intensity)
Irradiance (umoles m-2 s-1)
1400
1200
1000
800
600
400
200
0
0
0.2
0.4
0.6
0.8
1
Depth (m)
8/11/2009
8/28/2009

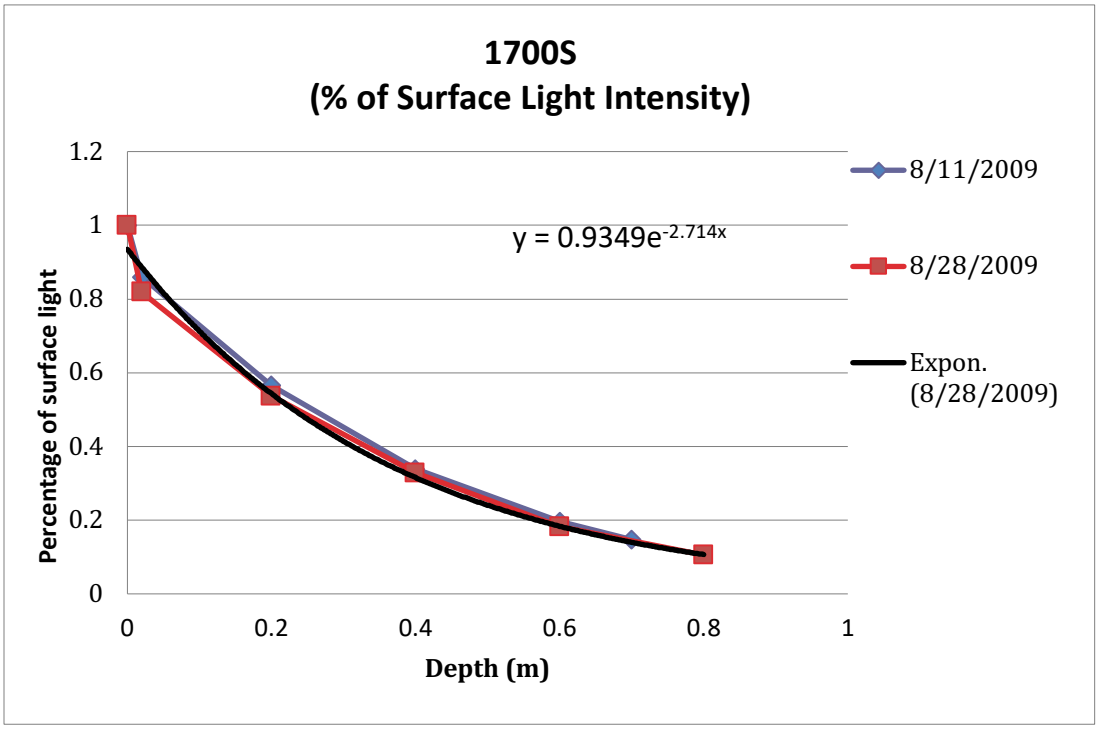
1700S
(% of Surface Light Intensity)
Percentage of surface light
1.2
1
0.8
0.6
0.4
0.2
0
0
0.2
0.4
0.6
0.8
1
Depth (m)
y = 0.9349e-2.714x
8/11/2009
8/28/2009
Expon. (8/28/2009)

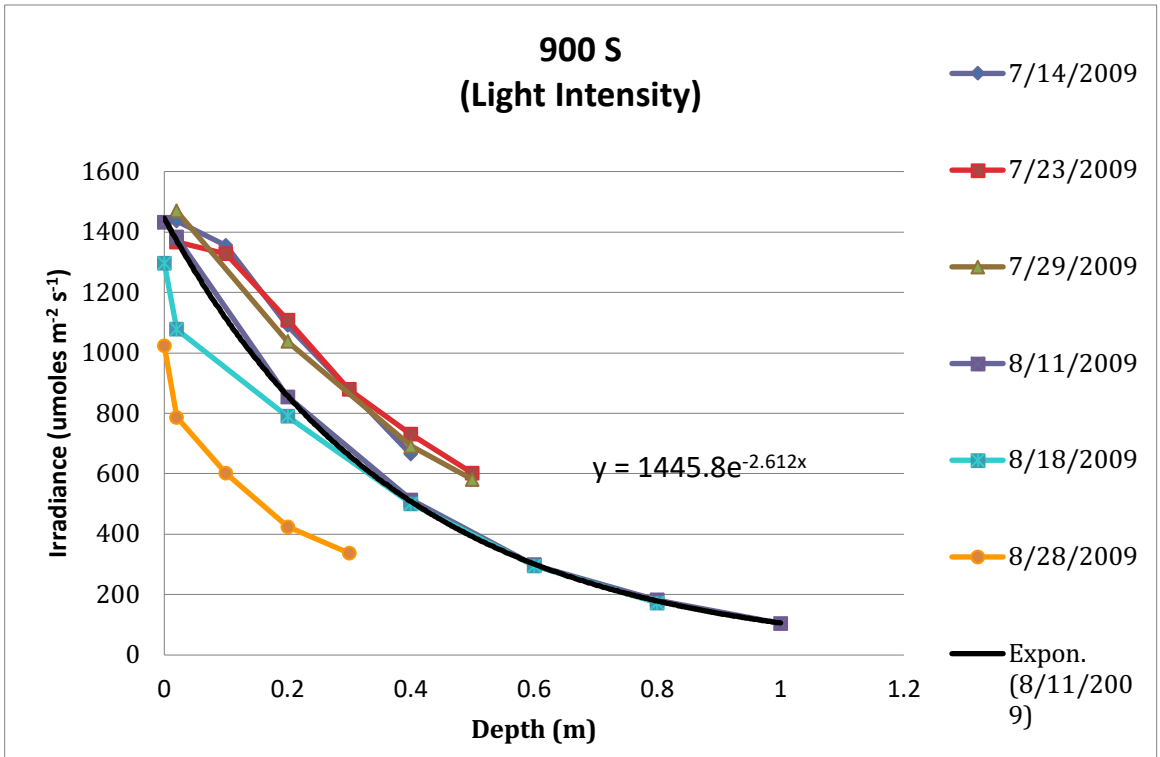
900 S
(Light Intensity)
Irradiance (umoles m-2 s-1)
1600
1400
1200
1000
800
600
400
200
0
0
0.2
0.4
0.6
0.8
1
1.2
Depth (m)
y = 1445.8e-2.612x
7/14/2009
7/23/2009
7/29/2009
8/11/2009
8/18/2009
8/28/2009
Expon. (8/11/2009)

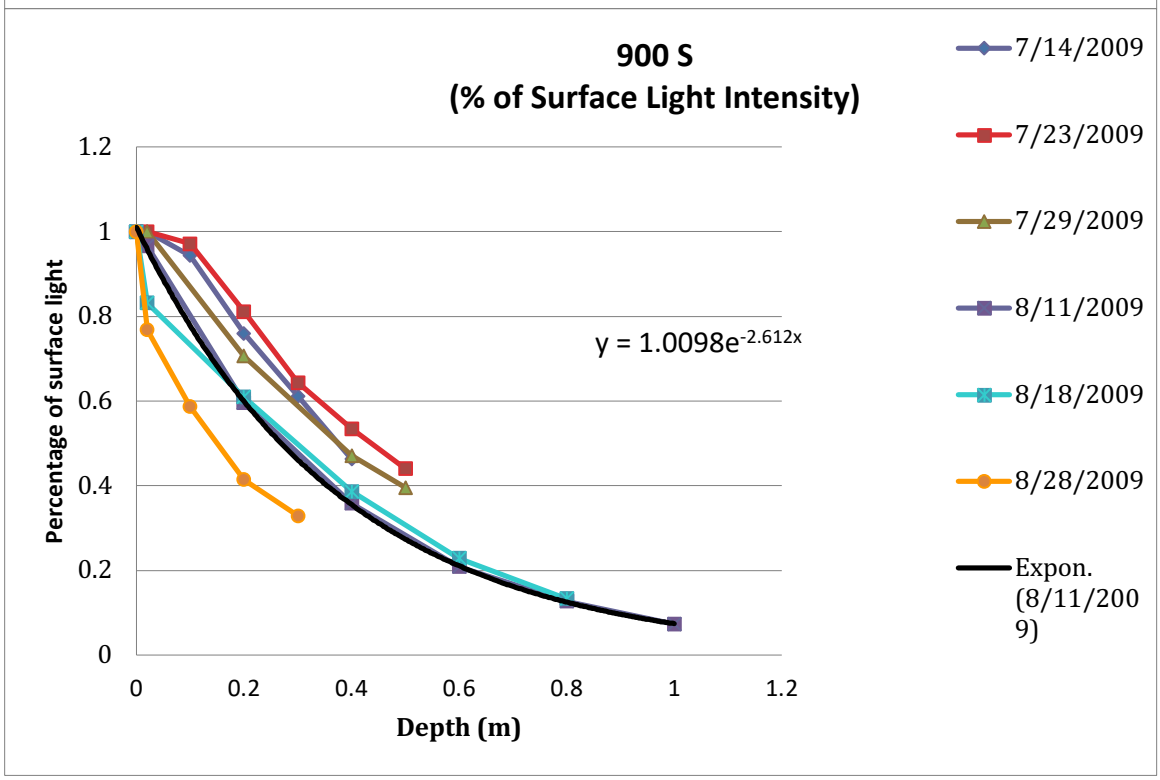
900 S
(% of Surface Light Intensity)
Percentage of surface light
1.2
1
0.8
0.6
0.4
0.2
0
0
0.2
0.4
0.6
0.8
1
1.2
Depth (m)
y = 1.0098e-2.612x
7/14/2009
7/23/2009
7/29/2009
8/11/2009
8/18/2009
8/28/2009
Expon. (8/11/2009)

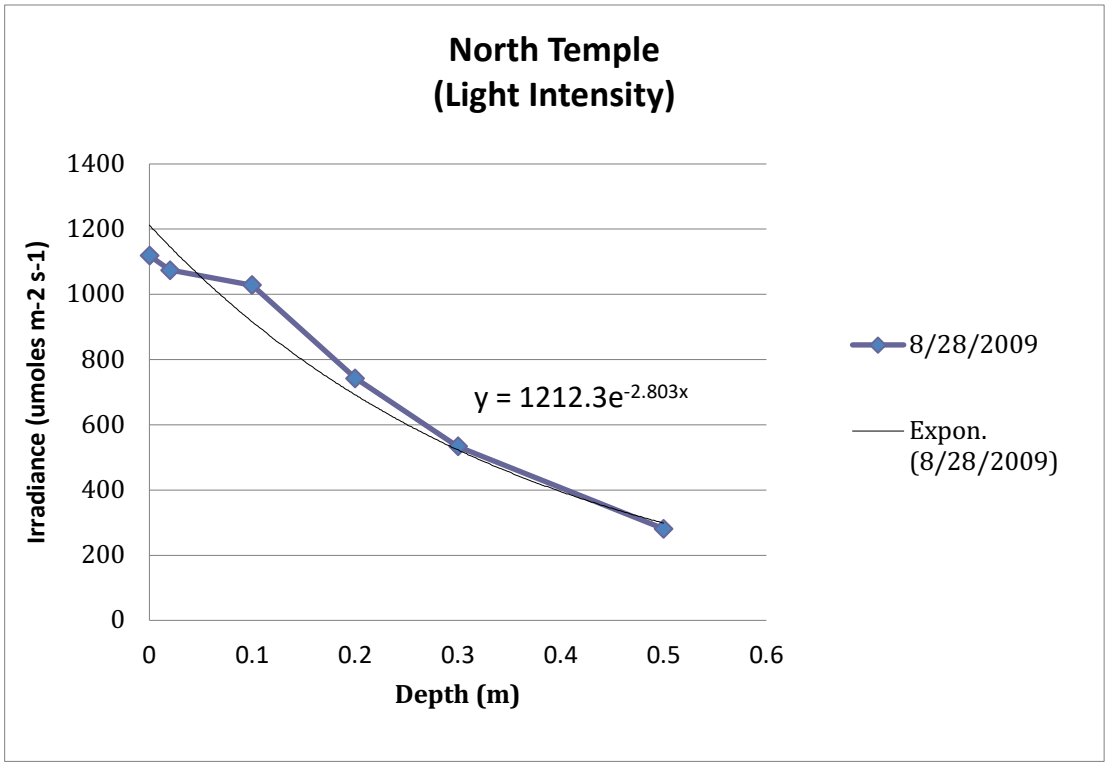
North Temple
(Light Intensity)
Irradiance (umoles m-2 s-1)
1400
1200
1000
800
600
400
200
0
0
0.1
0.2
0.3
0.4
0.5
0.6
Depth (m)
y = 1212.3e-2.803x
8/28/2009
Expon. (8/28/2009)

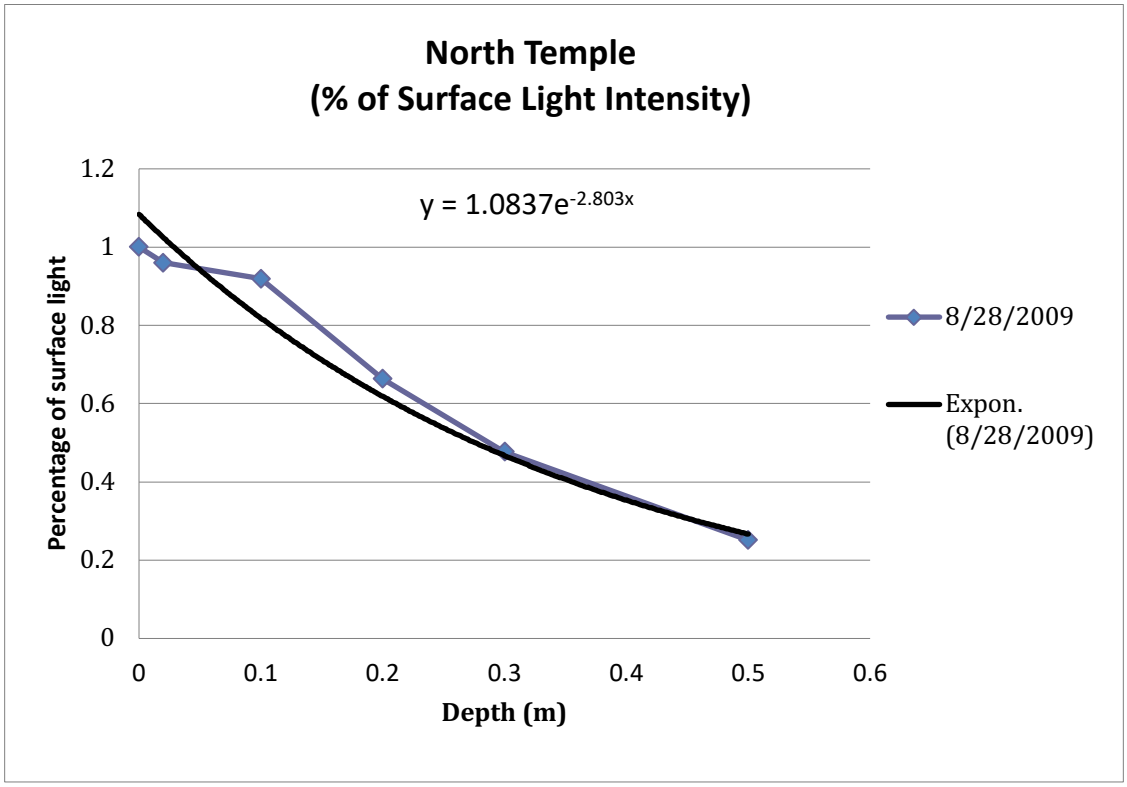
North Temple
(% of Surface Light Intensity)
Percentage of surface light
1.2
1
0.8
0.6
0.4
0.2
0
0
0.1
0.2
0.3
0.4
0.5
0.6
Depth (m)
y = 1.0837e-2.803x
8/28/2009
Expon. (8/28/2009)

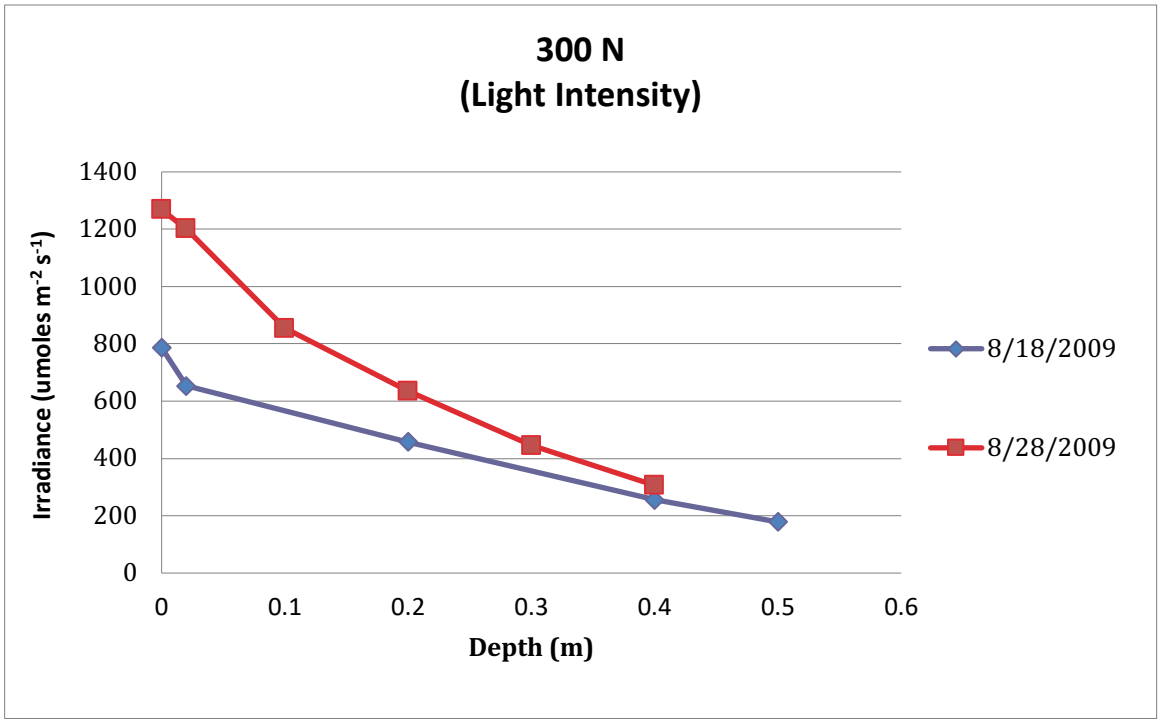
300 N
(Light Intensity)
Irradiance (umoles m-2 s-1)
1400
1200
1000
800
600
400
200
0
0
0.1
0.2
0.3
0.4
0.5
0.6
Depth (m)
8/18/2009
8/28/2009

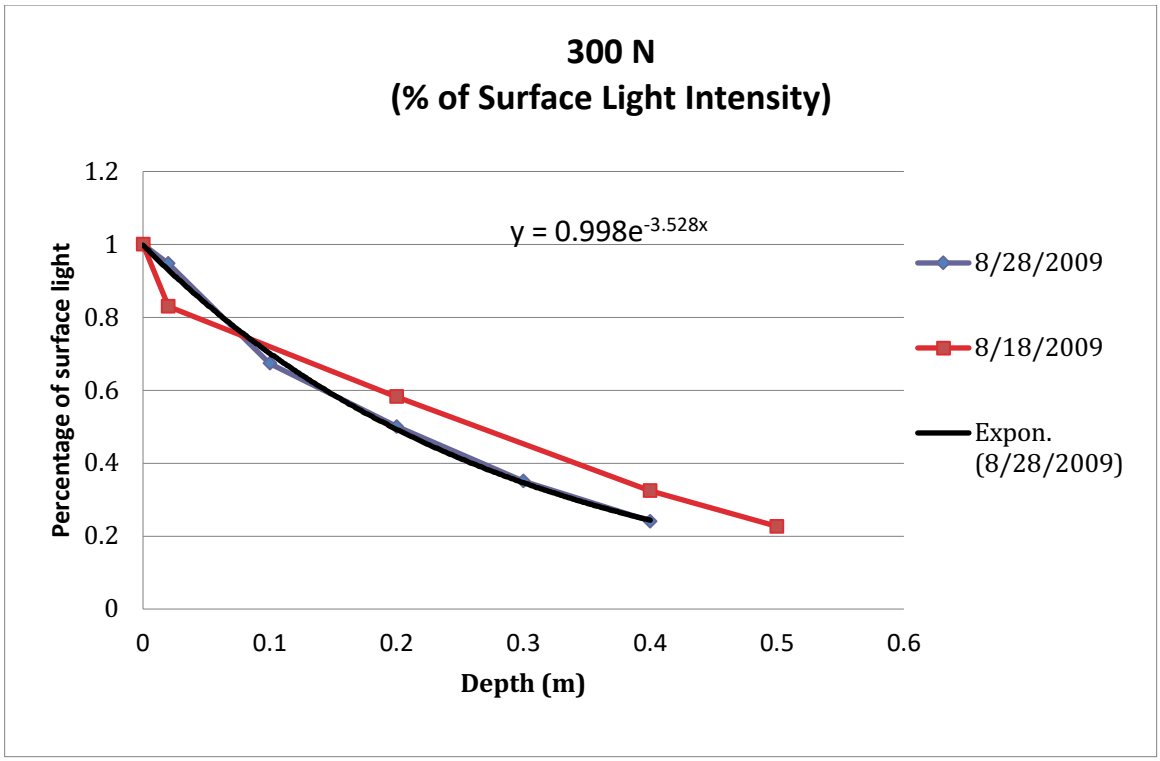
300 N
(% of Surface Light Intensity)
Percentage of surface light
1.2
1
0.8
0.6
0.4
0.2
0
y = 0.998e-3.528x
0
0.1
0.2
0.3
0.4
0.5
0.6
Depth (m)
8/28/2009
8/18/2009
Expon. (8/28/2009)

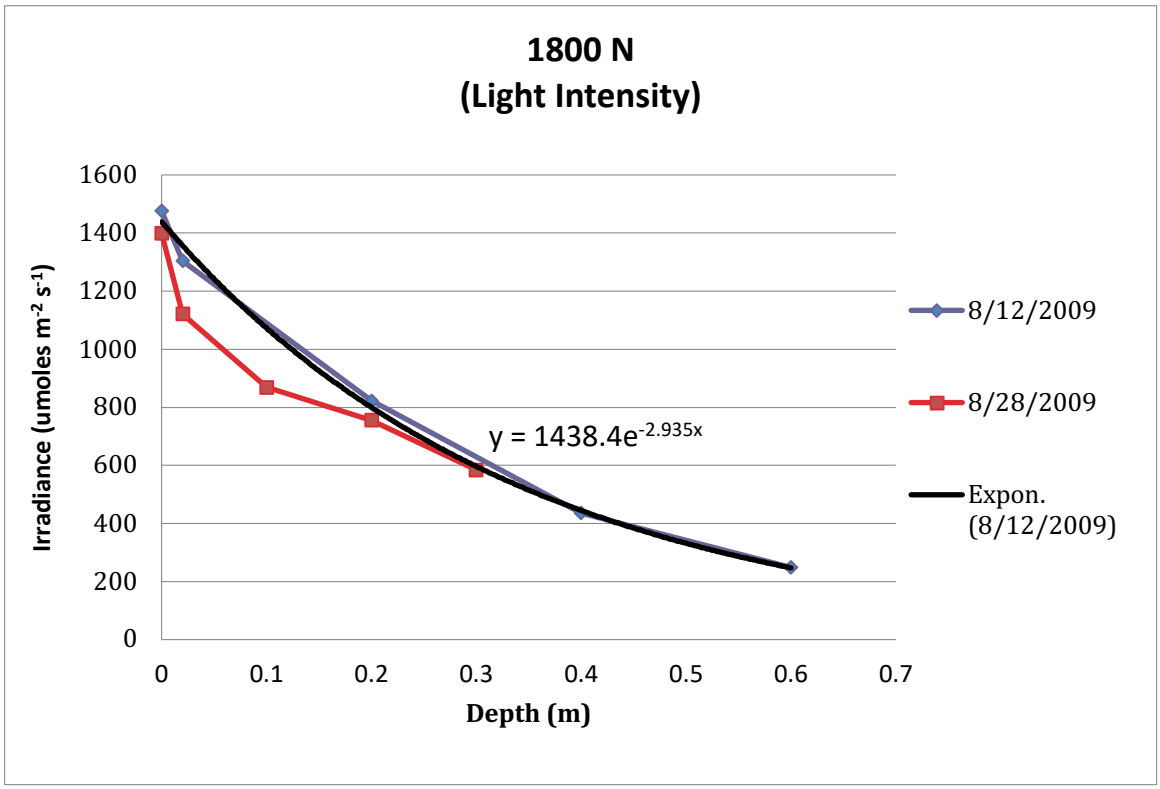
1800 N
(Light Intensity)
Irradiance (umoles m-2 s-1)
1600
1400
1200
1000
800
600
400
200
0
0
0.1
0.2
0.3
0.4
0.5
0.6
0.7
Depth (m)
y = 1438.4e-2.935x
8/12/2009
8/28/2009
Expon. (8/12/2009)

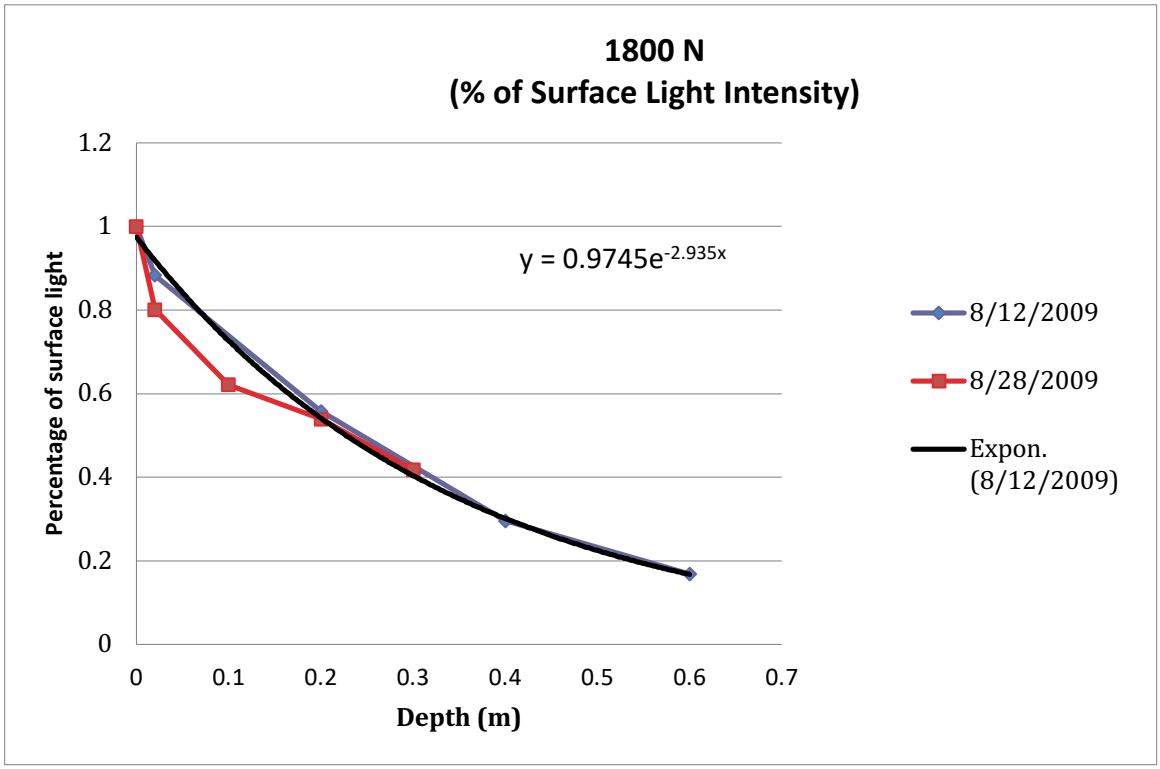
1800 N
(% of Surface Light Intensity)
Percentage of surface light
1.2
1
0.8
0.6
0.4
0.2
0
0
0.1
0.2
0.3
0.4
0.5
0.6
0.7
Depth (m)
y = 0.9745e-2.935x
8/12/2009
8/28/2009
Expon. (8/12/2009)

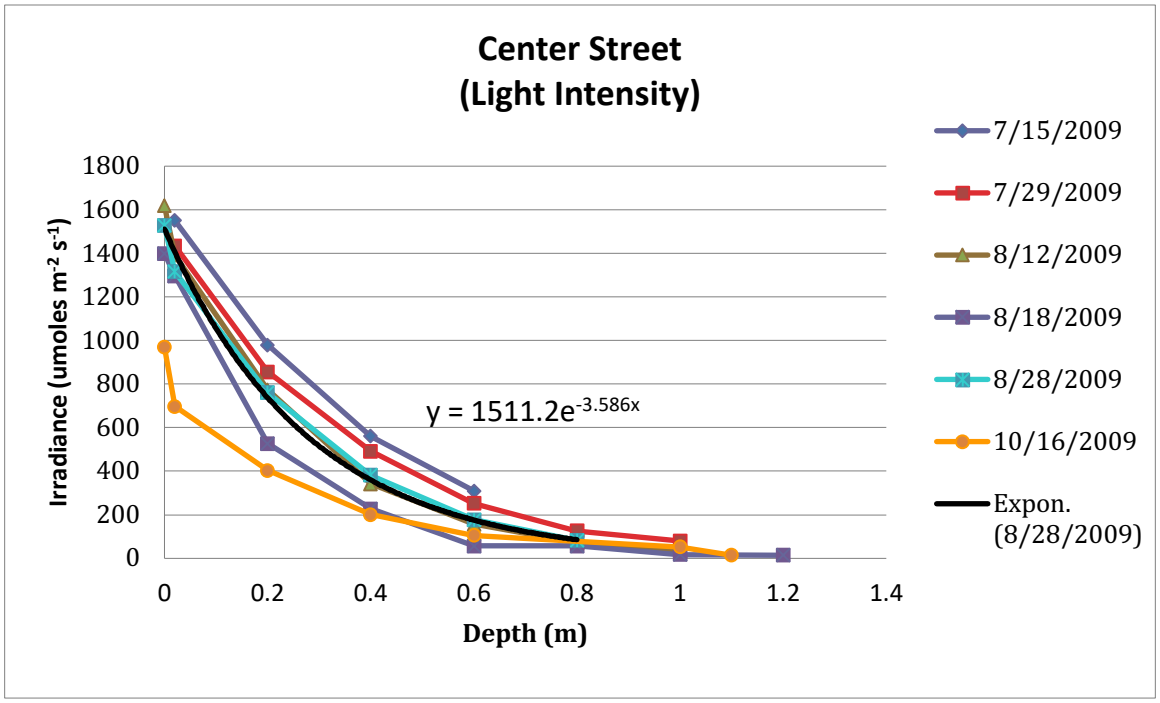
Center Street
(Light Intensity)
Irradiance (umoles m-2 s-1)
1800
1600
1400
1200
1000
800
600
400
200
0
0
0.2
0.4
0.6
0.8
1
1.2
1.4
Depth (m)
y = 1511.2e-3.586x
7/15/2009
7/29/2009
8/12/2009
8/18/2009
8/28/2009
10/16/2009
Expon. (8/28/2009)

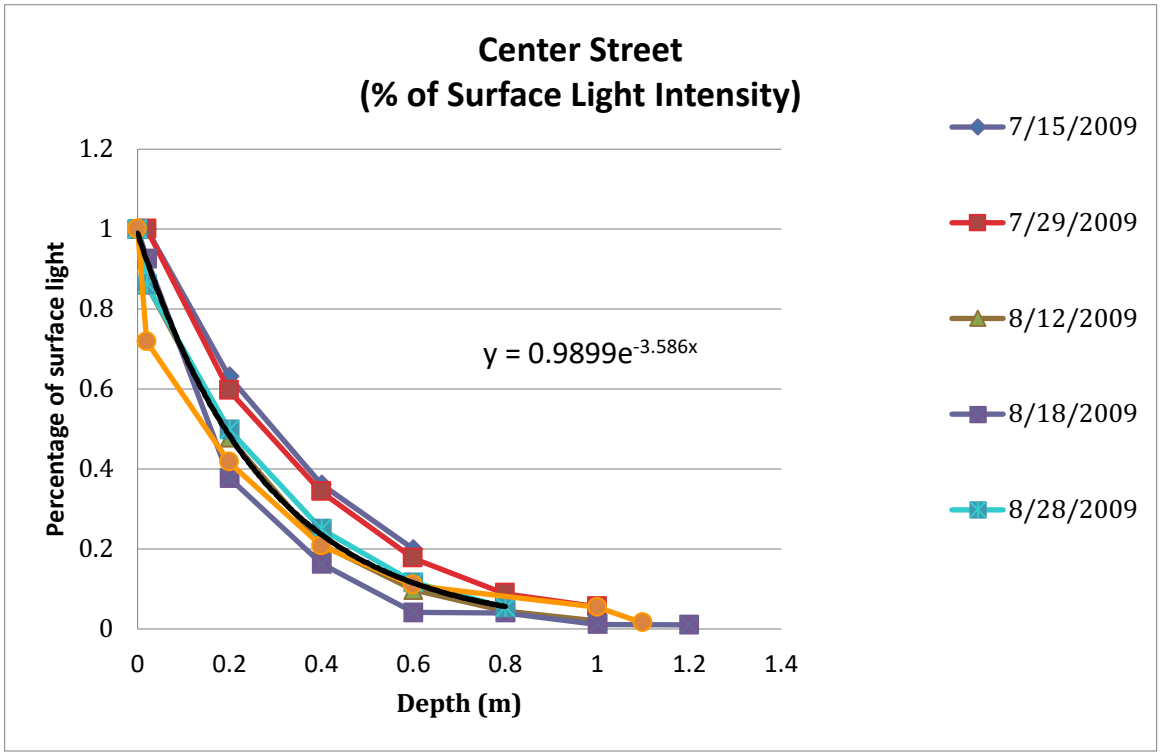
Center Street
(% of Surface Light Intensity)
Percentage of surface light
1.2
1
0.8
0.6
0.4
0.2
0
0
0.2
0.4
0.6
0.8
1
1.2
1.4
Depth (m)
y = 0.9899e-3.586x
7/15/2009
7/29/2009
8/12/2009
8/18/2009
8/28/2009

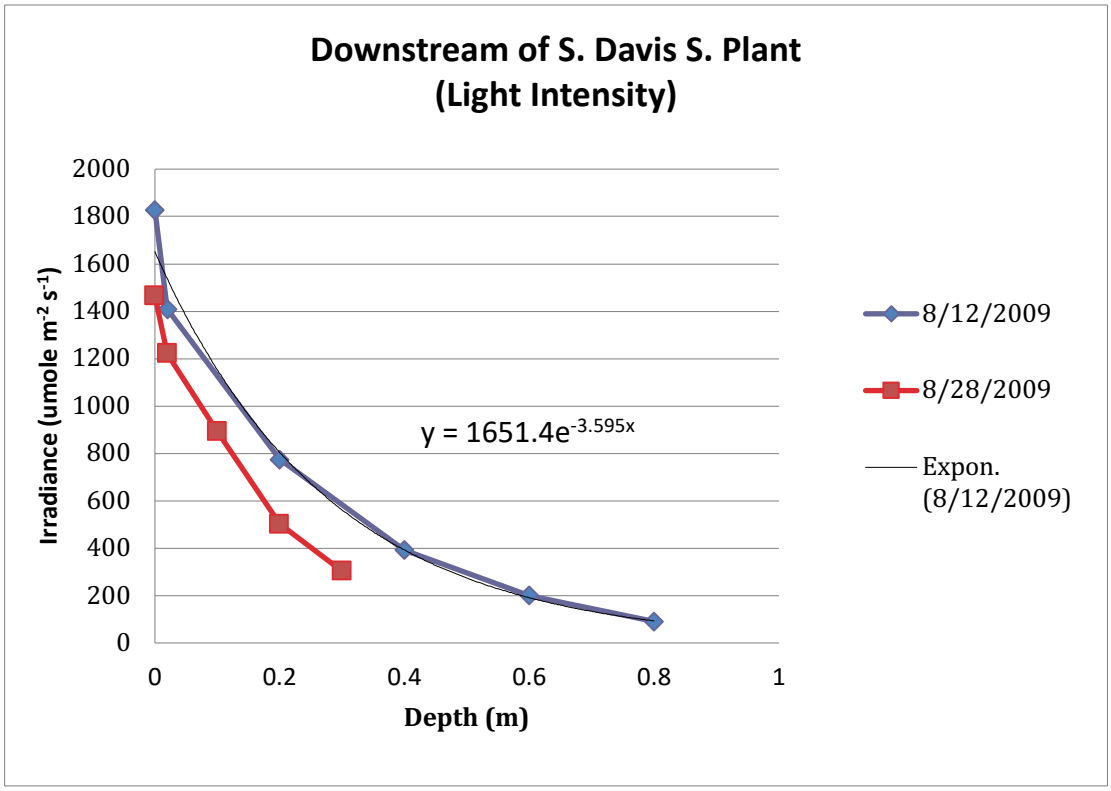
Downstream of S. Davis S. Plant
(Light Intensity)
Irradiance (umole m-2 s-1)
2000
1800
1600
1400
1200
1000
800
600
400
200
0
0
0.2
0.4
0.6
0.8
1
Depth (m)
y = 1651.4e-3.595x
8/12/2009
8/28/2009
Expon.
(8/12/2009)

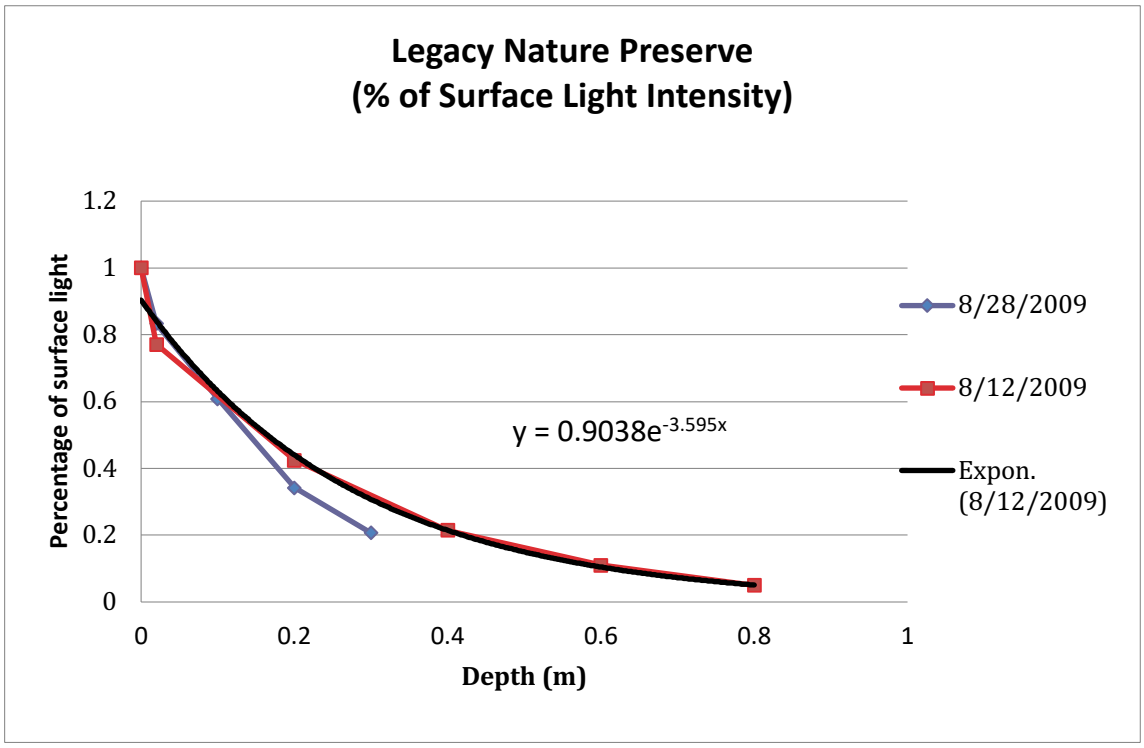
Legacy Nature Preserve
(% of Surface Light Intensity)
Percentage of surface light
1.2
1
0.8
0.6
0.4
0.2
0
0
0.2
0.4
0.6
0.8
1
Depth (m)
y = 0.9038e-3.595x
8/28/2009
8/12/2009
Expon.
(8/12/2009)

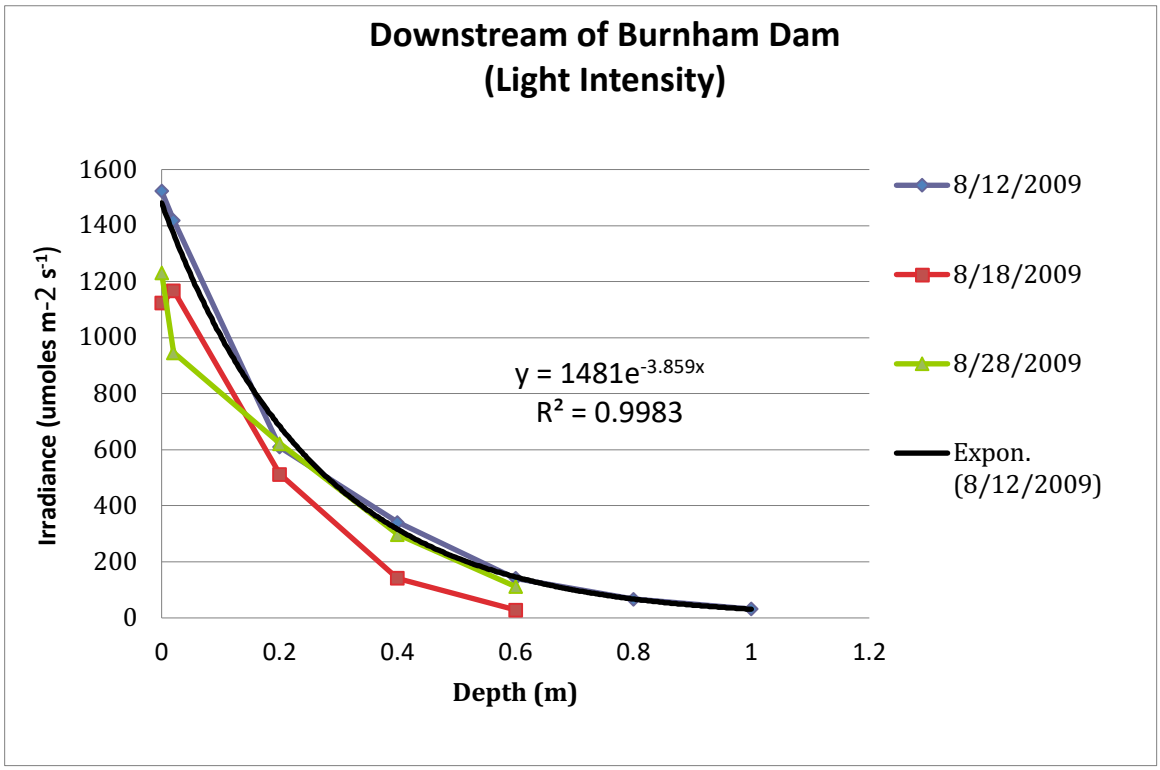
Downstream of Burnham Dam
(Light Intensity)
Irradiance (umoles m-2 s-1)
1600
1400
1200
1000
800
600
400
200
0
0
0.2
0.4
0.6
0.8
1
1.2
Depth (m)
y = 1481e-3.859x
R² = 0.9983
8/12/2009
8/18/2009
8/28/2009
Expon. (8/12/2009)

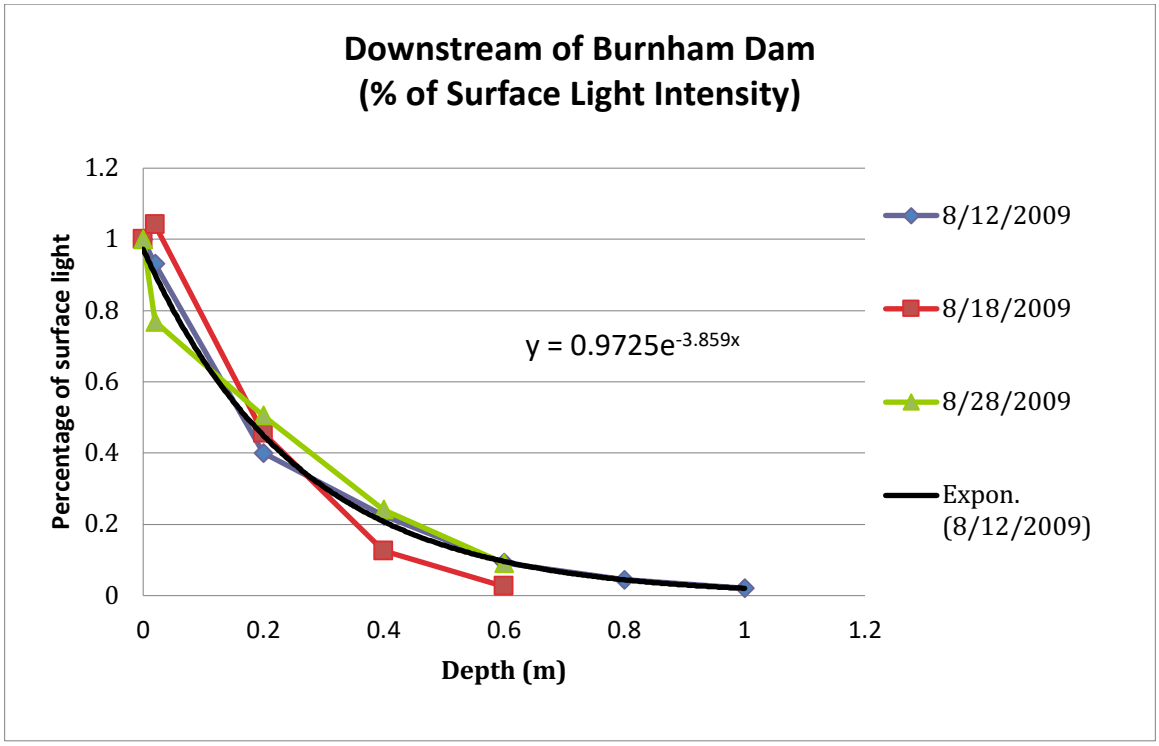
Downstream of Burnham Dam
(% of Surface Light Intensity)
Percentage of surface light
1.2
1
0.8
0.6
0.4
0.2
0
0
0.2
0.4
0.6
0.8
1
1.2
Depth (m)
y = 0.9725e-3.859x
8/12/2009
8/18/2009
8/28/2009
Expon. (8/12/2009)

CHAPTER 3

Coarse Particulate Organic Matter Measurements in the Jordan River and its Major Tributaries, 2010 – 2015

Theron Miller

Wasatch Front Water Quality Council

August 2019

Table of Contents

List of Figures

List of Tables

Introduction

The most widely accepted paradigm for the cause of dissolved oxygen deficits in lakes and streams is the assumed linkage to elevated nutrients (i.e. eutrophication) and increased temperature. In certain situations, elevated nutrients can cause excessive algal blooms which in turn are known to consume oxygen during respiration or eventual decomposition. Early drafts of the Jordan River TMDL accepted this paradigm and claimed that the occasional violations of the dissolved oxygen (DO) standard were caused by excessive nutrients entering the river. This claim was questioned in 2009 by the Wasatch Front Water Quality Council (Council). In addition to initiating an extensive water quality monitoring program, Council field technicians performed the Stream Visual Assessment Protocol (SVAP) during the summer of 2009 to begin understanding the physical and chemical characteristics of the river and particularly downstream from 2100 (the reach that was designated as impaired for DO; see Chapter 1). Starting in 2009, the Council also started deploying data recording sondes fitted with DO, temperature, pH and conductivity probes and permanent installation of similar probes with real-time cellular connections to the internet took place in 2013.

Two important and related characteristics were initially identified from these efforts:

1) DO violations are limited to the lower reaches of the river (near and below 300 N). These locations are downstream from the diversion of 55% to >95% of the flow to the Surplus Canal (One of the primary purposes of the Surplus Canal is to divert Storm water and high spring flows to avoid flooding downstream neighborhoods);
2) This severe reduction in flow, velocity and turbulence, reduces reaeration potential, allows the settling of suspended and bedload organic debris, leaving the river bottom dominated by depositional zones with depths of 30 to 100 cm of organic debris among the clay and silt particles that exists in various stages of decomposition. In turn, measured sediment oxygen demand (SOD) values from decomposing organic matter are among the highest values measured across the nation (Goel 2010, Hogsett, 2015).

Initially these high values of SOD were thought to be the result of settled algae that had been dislodged from upstream substrates and from Utah Lake. However, our frequent monitoring of algal species, chlorophyll a (Chl a), algal biomass and VSS all contradicted this assumption. Indeed, similar concentrations of algal biomass, Chl a, TSS and VSS were measured at Utah Lake, the top of the segment (2100 S), and at the end of the segment (Burnham Dam), indicating that organic matter comprised of algal biomass or measured as VSS did not settle out of the water column, further indicating that it does not contribute to SOD.

Rather, these observations prompted us to measure the load of this coarse particulate organic matter (CPOM) delivered from tributaries and carried down the main channel in an effort to account for its potential contribution to SOD and the oxygen deficit. There are no published methods for directly measuring CPOM. The limited literature on this subject most often focuses on the ability of certain stream segments to retain “artificial”

CPOM in the form of small dowel segments or dumping measured quantities of non-native leaves so that the proportion of such leaves that are retained within a stream can be identified (e.g. see Quinn et al. 2007). This chapter focuses on initial methods development (2010) and a refinement (2011, 2012) used to estimate CPOM loading with major tributaries and along the main stem of the Jordan River.

Methods

CPOM sampling was performed monthly from April to November in 2010 and monthly throughout 2011 and 2012. In addition, during the high flow periods of the spring and during the heavy leaf fall periods of September to November of 2011, samples were collected biweekly to more accurately account for the higher CPOM delivery periods. Up to four sites were identified in each of the major tributaries, City, Emigration, Mill, Big Cottonwood and Little Cottonwood creeks. The sample sites in each tributary included one at the canyon mouth, and one as close to the confluence with the Jordan River as possible. Additional sites were included to evaluate the efficacy of constructed debris basins/ponds in removing CPOM. Additionally, sample sites were identified in the Lower Jordan to assess the quantity of organic matter delivered to the lower Jordan and its potential to settle out of the water column throughout the lower portions of the river.

During relatively low-flow (non-spring runoff) conditions (< approximately 300 CFS), samples were collected with a standard 10 x 18-inch sweep net. The only mesh available during 2010 to 2012 was 500 µm whereas the standard separation between FPOM (VSS) and CPOM is defined using a 1 mm mesh size. Therefore, samples were immediately rinsed in a 1 mm- mesh soil sieve for accurate separation of particle sizes. At each site, samples were collected at ¼, ½ and ¾ distance across a perpendicular transect. Where or when the stream depth was > approximately 30 cm, and floating debris was visible, samples were collected with the net at the surface and with the net resting on the bottom in order to collect floating debris as well as bed load and suspended material. The top and bottom samples were composited when collected. In addition, samples collected at ¼, ½ and ¾ distance across the stream were composited and this process was performed in triplicate. The duration of sample collection was timed in order to calculate the load and the duration of each "set" was adjusted in order to collect sufficient sample for accurate measurement as well as to limit sample volume to < approximately 200 g dry weight to facilitate sample handling, drying and combustion in the laboratory. Concentration or mass of the organic debris was determined by dividing the sample mass by the product of the stream velocity x net dimensions x sampling duration. During high flows or during the autumn leaf fall, typical duration of net placement was 10 to 30 seconds. During low flow conditions of winter and summer, net placement was extended to 60 seconds or more in order to collect sufficient sample volume. During high flow conditions (> approximately 300 CFS), we used a 3-inch trash pump. About ½ of the cross-linkages of the intake screen were removed to facilitate the uptake of the debris. The intake screen was weighted with approximately 40-pounds of steel plates to ensure that the screen remained on the stream bottom. Sample collections from the surface were not performed during these high flows because the turbulence caused sufficient mixing that the leaf material was rapidly saturated and was assumed to be distributed randomly throughout the water column. Also, because of this homogeneity, sample collection was only

performed near the center of the channel. The discharge volume from the pump was measured using a 55-gallon barrel and each of triplicate samples included ten volumes (550 gallons) of water. Similarly, this material was sieved using the 1 mm soil sieve to collect the CPOM fraction.

Where samples were collected near stream gauges, these flow measurements were used to calculate loads. Where stream gauge data were not available, channel dimensions were measured and velocity measurements were performed using a Valeport mechanical flow meter.

Results and Discussion

There were three principle tasks in this effort to characterize CPOM: 1) Develop a representative and repeatable method for measuring CPOM concentrations and loads; 2) Determine loads delivered to the Jordan River from the major tributaries; and 3) Understand the persistence or attenuation of CPOM as it travels down the Jordan River and particularly downstream from 2100 S.

There is no standard protocol for CPOM sampling. Our CPOM program began in 2010 with designing and testing methods for sample collection. The only rule we adhered to was the basic definition of CPOM being that fraction of organic matter that is retained by 1 mm mesh size. Otherwise, it was a challenge to collect a representative and measurable sample without having to require the laboratory personnel to subdivide samples in order to use the drying and combustion chambers. Thirdly, it was important to collect samples during high flow events because these were the conditions of greatest CPOM transport. However, it was impossible to safely sample deep swift water, so we developed a sampling method using a 3-inch trash pump that could be operated from a bridge deck (Figure 1). We tested the comparability of sampling with a sweep net vs the trash pump (Figure 2). For most sampling events the results were comparable. The single outlier revealed in sample 7 of the sweep net was a larger piece of branch that weighed more than 100 g dry weight. Hence, it was small enough to be collected in the net but would have been too large to fit through the approximate 4 cm mesh size of the trash pump intake screen. Woody debris of this size and even much larger was common during high flow events. Therefore, it became apparent that collecting CPOM using these manageable techniques provides only a very conservative estimate of the total annual CPOM load.

Figure 40. Photographs illustrating the two techniques used for sampling coarse particulate organic matter. With either technique the water was initially filtered through the same net, followed by screening with a 1-mm soil sieve.

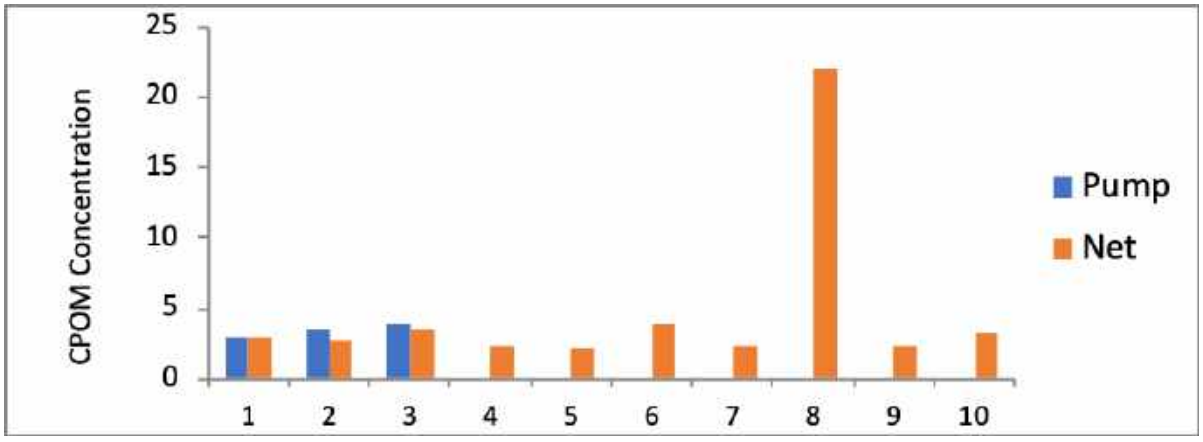

Figure 41. A comparison of samples collected by the trash pump and by the sweep net. Each pump sample consisted of filtering 550 gallons (filling a 55-gallon drum 10 times). The net sample number 8 collected a large stick, which was not uncommon throughout the entire sampling program. See text for details.

Tributary samples

Tributary sampling was conducted for two purposes. First, we wanted to estimate the monthly, seasonal and annual CPOM loads from the major tributaries. Second, we were interested in the effectiveness of debris basins or man-made ponds that were constructed in some of the tributaries.

City Creek

City Creek is a small tributary that flows out of City Creek Canyon. At the mouth of the canyon, approximately 0.5 mile upstream from Memory Grove, there are two small ponds, approximately 1/4 acre in size (Figure 3). Despite their small size, we chose to sample upstream and downstream in 2010 to evaluate the ability of these small basins to remove CPOM. Figure 4 illustrates the effectiveness of CPOM removal during this relative low flow year.

Figure 42. Image depicting the two small debris basins located near the mouth of City Creek Canyon.

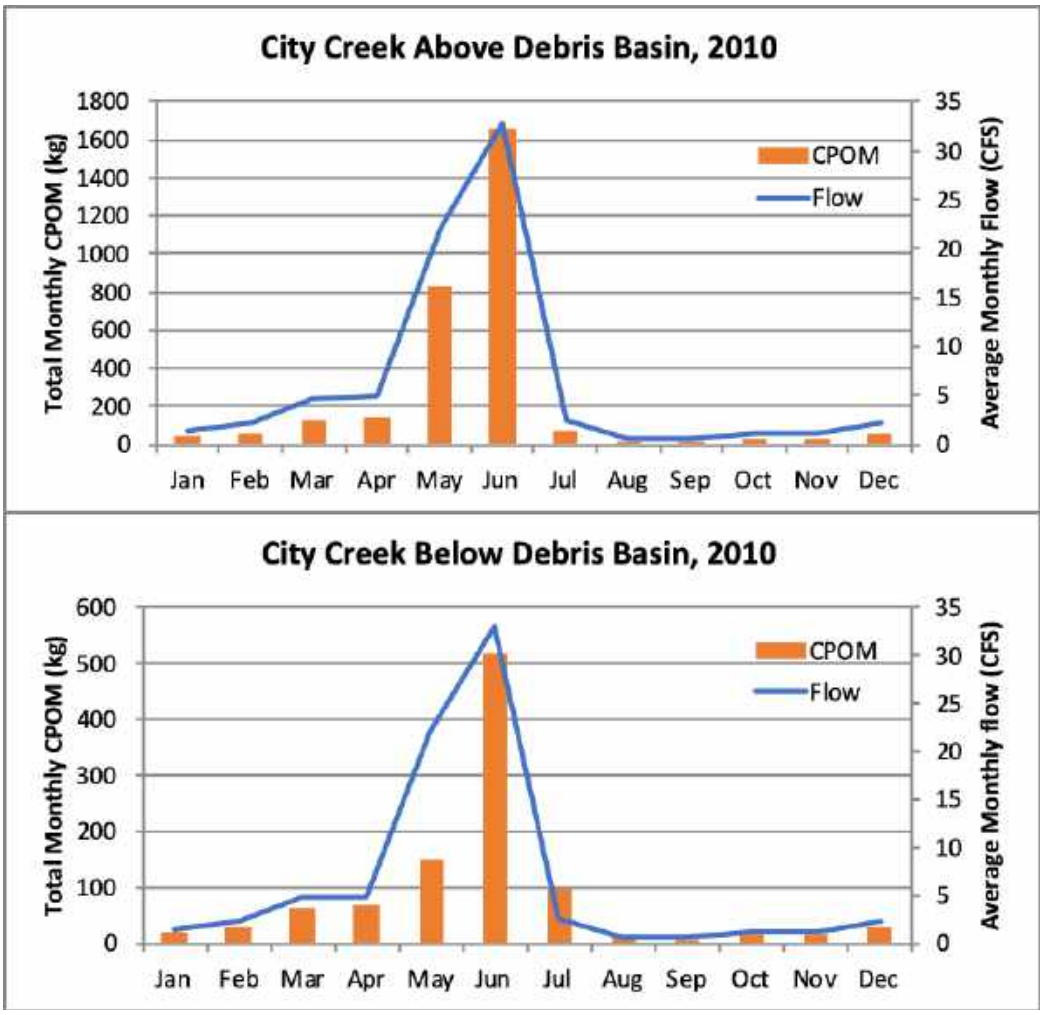

Figure 43. Monthly CPOM values in City Creek during 2010. Top: Samples collected approximately 100 m upstream from the debris basins; Bottom: Samples collected approximate 50 m downstream from the basins.

The two small debris basins reduced the CPOM load by about 2/3. This suggests that if these debris basins are maintained that substantial quantities of the CPOM can be removed and prevented from settling in and affecting downstream segments. Data collected during 2011 and 2012 are illustrated in Figure 5. During these years sampling was only performed at a point downstream from both debris basins. Because City Creek is directed to an underground culvert not far below Memory Grove, we feel that samples collected from this location provide an estimate of CPOM that is delivered to the Lower Jordan River near North Temple Street.

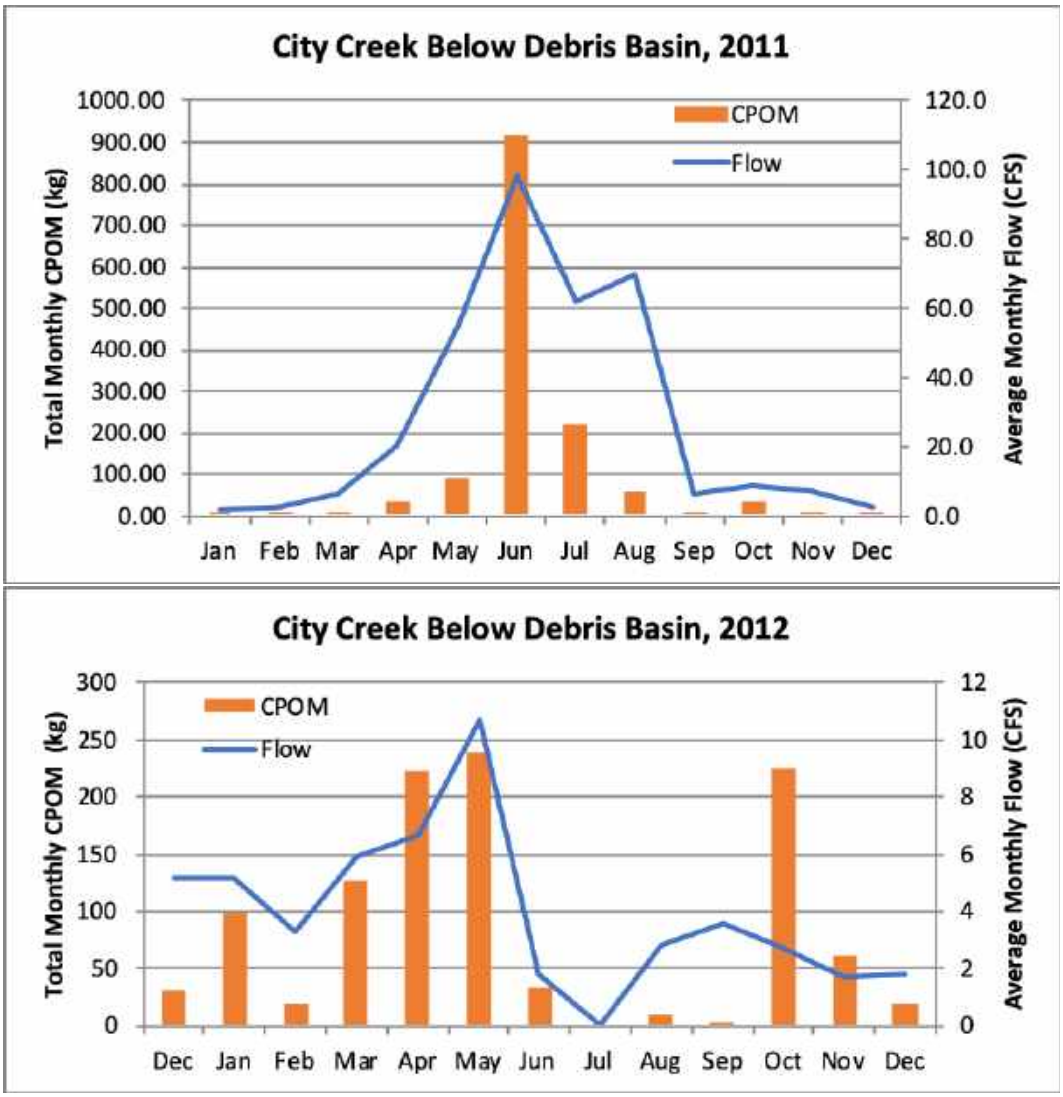

Figure 44. Monthly measurements of CPOM during 2011 and 2012 in City Creek. Samples were collected downstream from the small debris basins in Memory Grove.

It should be noted that rainfall and snowpack during 2010 was near the long-term average for the Wasatch front. Rainfall and snowpack during 2011 was approximately 30% above average while that for 2012 was about 30% below average. Therefore, the CPOM load during 2011 above the debris basins was likely much larger than that delivered in 2010, further suggesting that the debris basins were quite effective in reducing organic matter loads to the Jordan River. The CPOM loads during 2012 was predictably low.

Emigration Creek

Emigration is also a small tributary to the Jordan River and it is also directed underground shortly after it enters Salt Lake Valley. It also has a small debris basin at the mouth of the canyon. Our upstream sampling station was located approximately 1 mile upstream from the canyon mouth near the kiosk where fees are collected. The downstream sampling location was immediately below the debris basin. Similar to the

effectiveness of the basins in City Creek, CPOM was drastically reduced by the debris basin at the mouth of Emigration Canyon (Figure 6). Emigration, Red Butte and Parleys creeks are united into one culvert and flow under the city streets until they discharge to the Jordan River at 1300 S or through an overflow channel that discharges at 900 S.

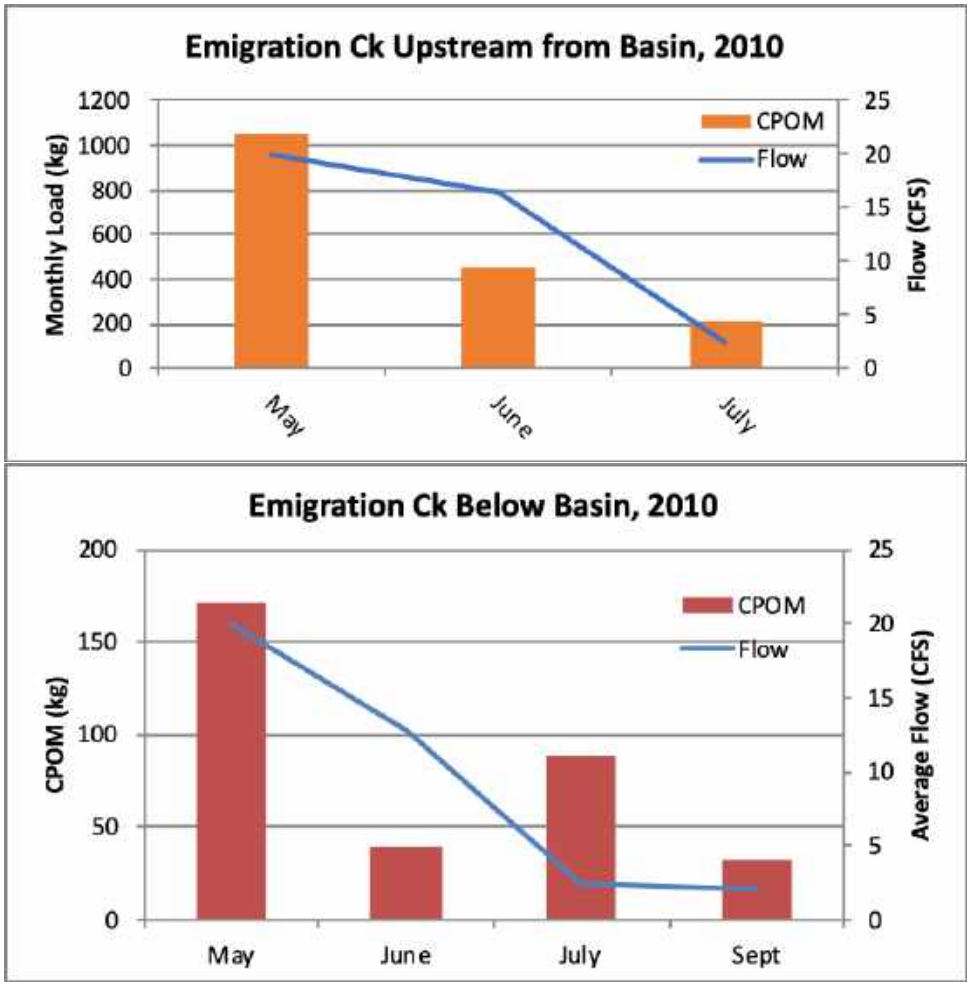

Figure 45. Monthly measurements of CPOM during 2011 and 2012 in Emigration Creek.

Mill Creek

Mill Creek is another small tributary to the Jordan River. It forms the next canyon south of Parleys Canyon. Again, it had similar flows and contains two smaller debris basins, although they are located about 3 and 4 miles out from the canyon mouth. The stream intermittently flows above ground and through underground culverts. Figure 7 illustrates the 2010 data collected upstream and downstream from the 1300 E basin.

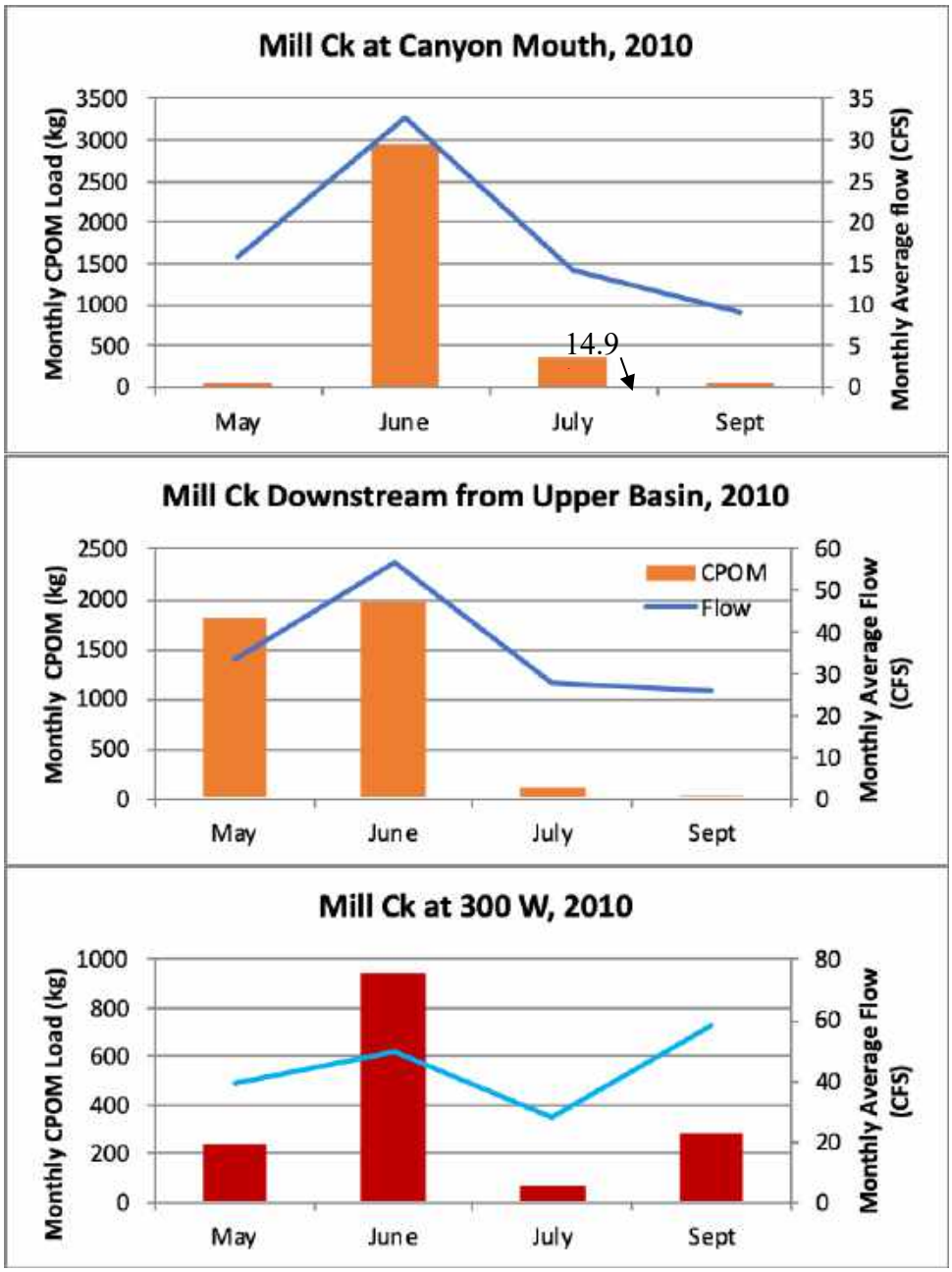

Figure 46. Monthly measurements of CPOM during 2011 and 2012 in Mill Creek.

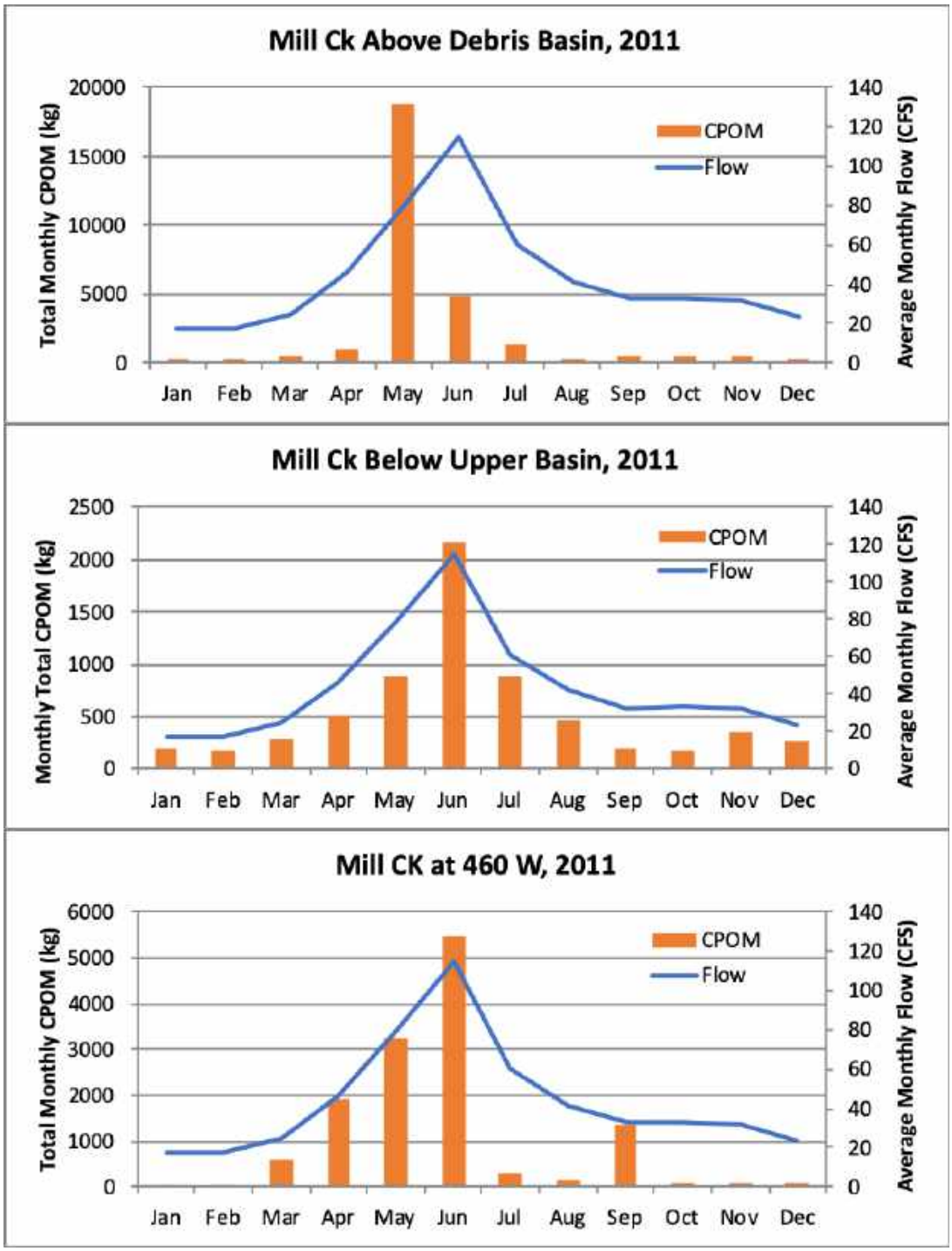

Figure 7. Continued. The unexpected high value in May above the debris basin was due to the collection of a large stick in the sweep net.

The debris basins again significantly reduced the amount of CPOM that is delivered to the Jordan River. Similar samples were collected during 2012 (Figure 8). It should be noted that rainfall and snowpack were much less than average, resulting in considerably less flows than during 2011. These low flows led to predictably low CPOM values at the

canyon mouth. The channel gains consider flow as it travels toward the Jordan River. There are unusually high levels of CPOM above the 900 E debris basin even though flows are minimal. In addition, CPOM levels were elevated for the last three months. The fact that flows were diminished suggests that material was delivered anthropogenically at a location between the mouth of the canyon and 900 E.

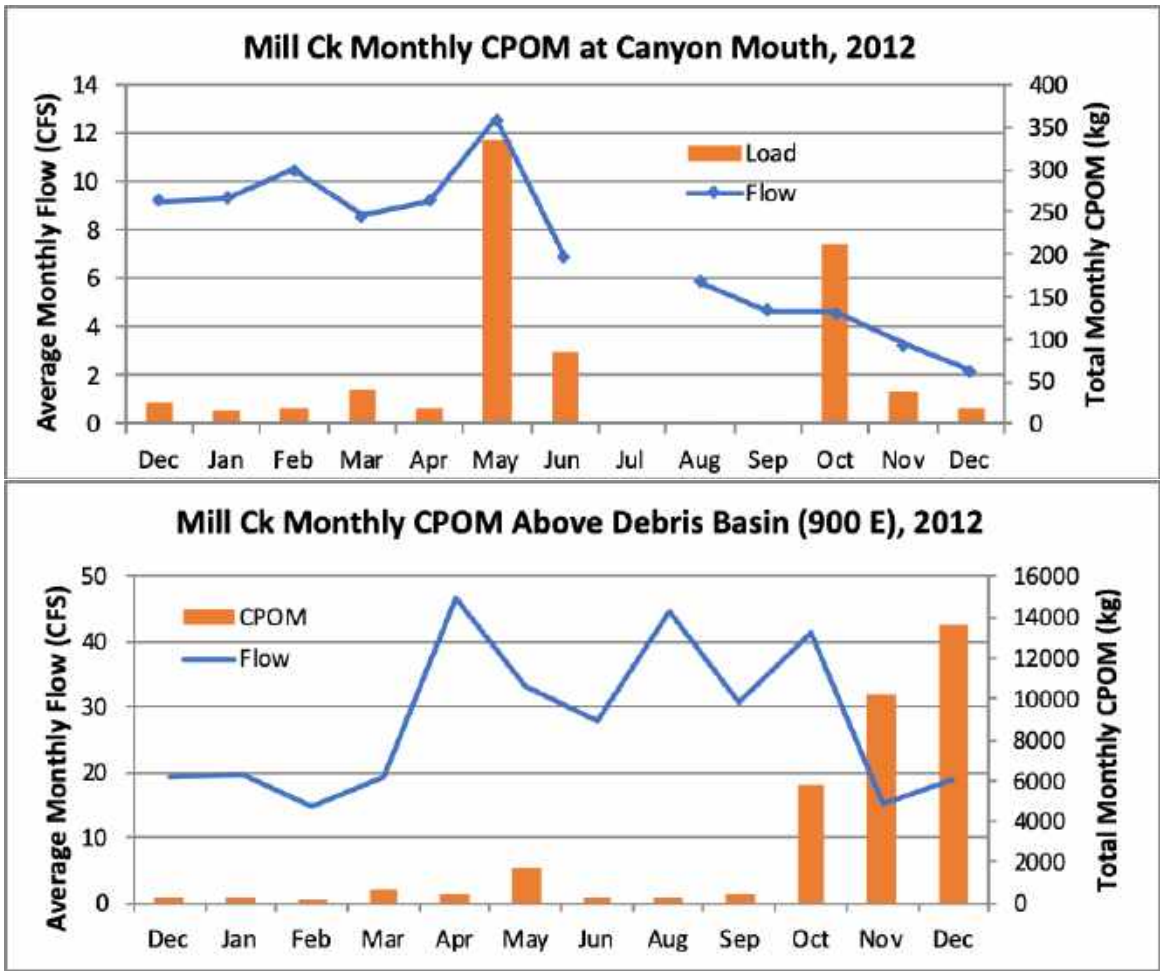

Figure 47. Monthly flow and CPOM values at four sites in Mill Creek during 2012. Mill Creek has two debris basins, immediately downstream from 900 E and immediately upstream from 500 E. Note the large increase in CPOM at 900 E and 500 E in October November and December, despite the low seasonal flow.

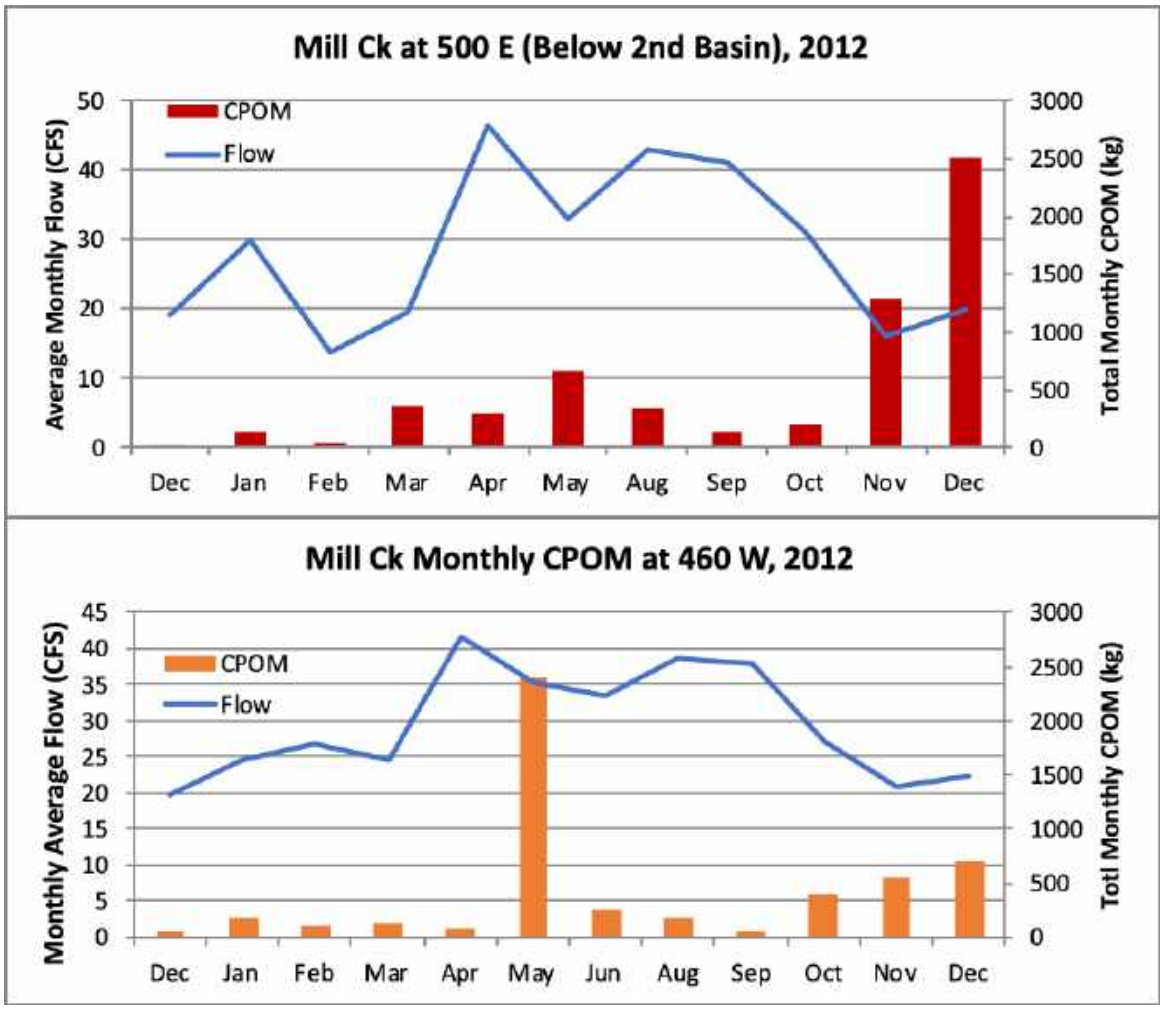

Figure 8. Continued. Monthly flow and CPOM values for Mill Creek during 2012.

Big Cottonwood Creek

Big Cottonwood Creek is one of the two major tributaries to the Jordan River. It was also subject to both extremely high and low flows. Again, it should be noted that 2010 represented a low runoff year, 2011 represented an above-average runoff year and 2012 represented another low runoff year. Both the highest flow and highest CPOM loads occurred in June for all three years. Even with the low flow years of 2010 and 2012, substantial CPOM loads are carried out of Big Cottonwood Canyon. During 2010, approximately 40,000 kg of CPOM was transported to the debris basin at the canyon mouth (Figure 9.a). Notably, however, the debris basin had sufficient residence time to provide for considerable removal of CPOM (Figure 9.b).

a. b.

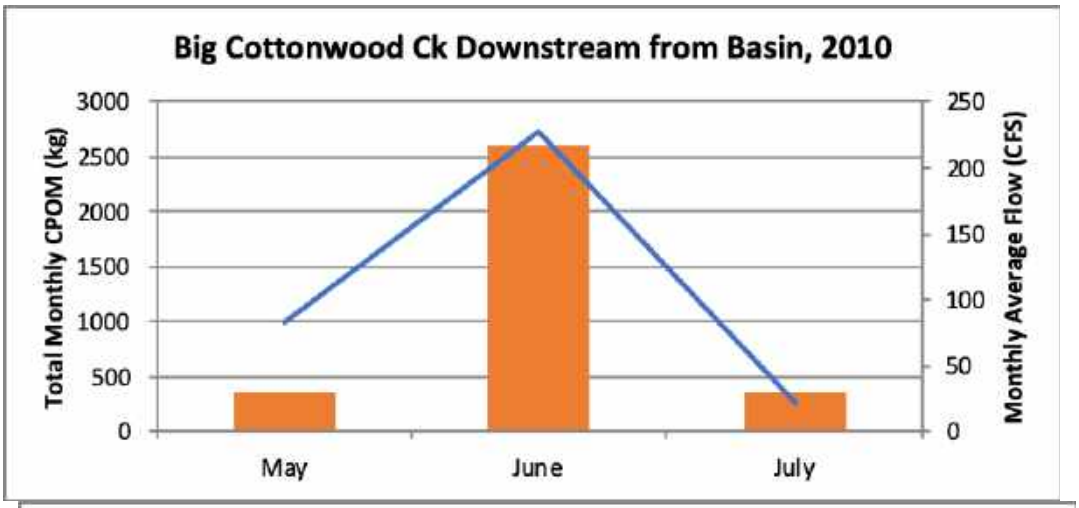

c.

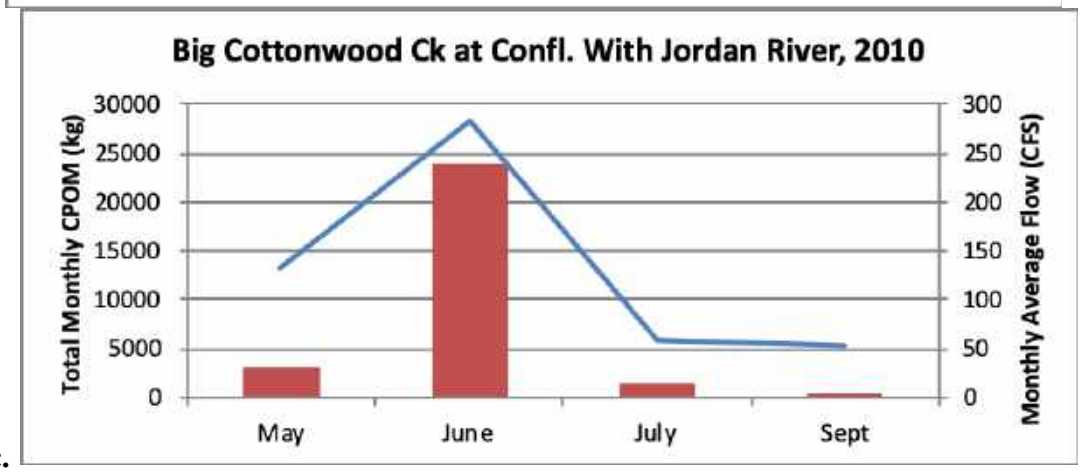

Figure 48. Flow and CPOM at selected sites along Big Cottonwood Creek during 2010, 2011, and 2012. The debris basin was located approximately 800 m (1/2 mile) below the canyon mouth.

d.

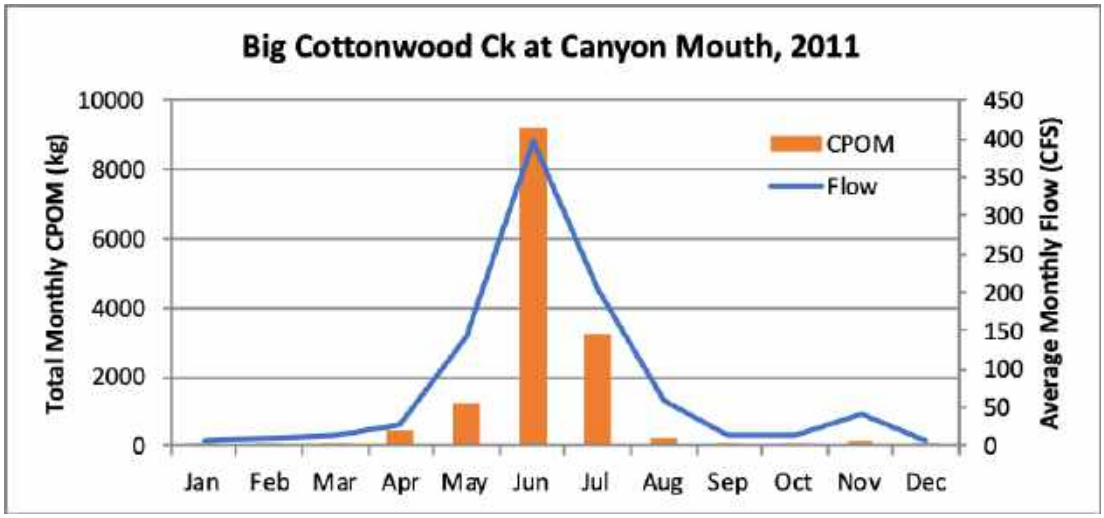

e.

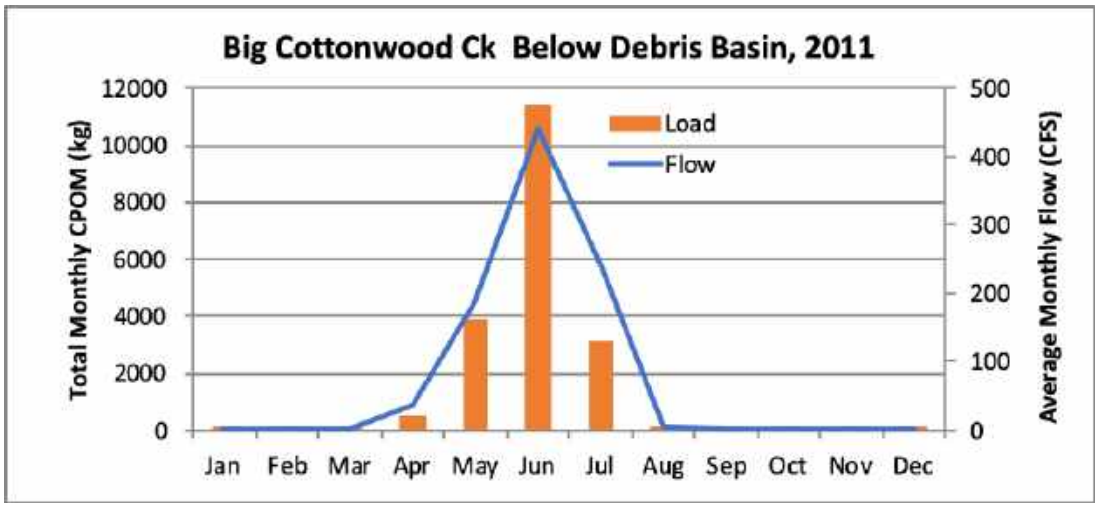

f.

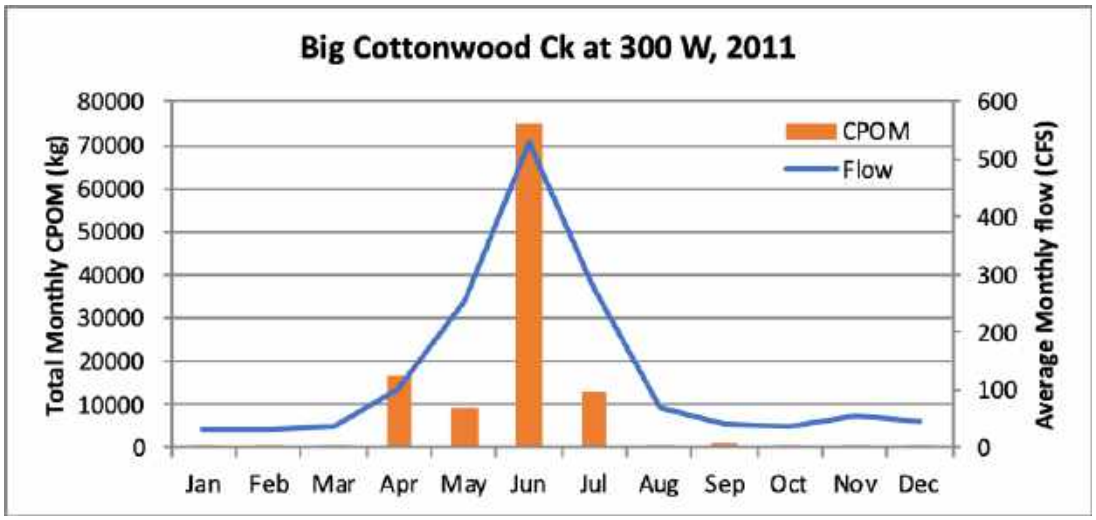

Figure 9. Continued. Note in Figure 9 f. CPOM values for Oct. Nov. and Dec. were very low (13, 5 and 2.2 kg respectively).

g.

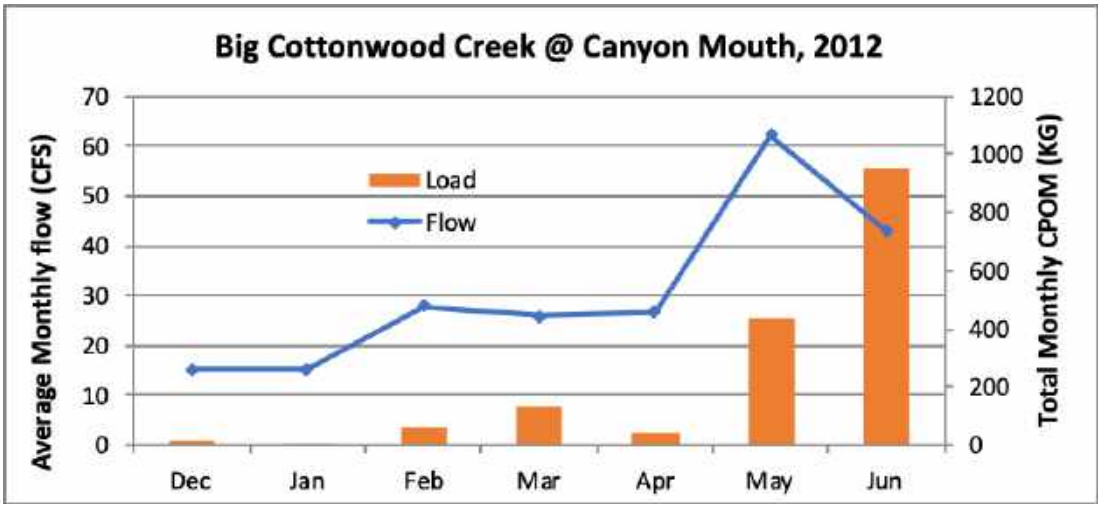

h.

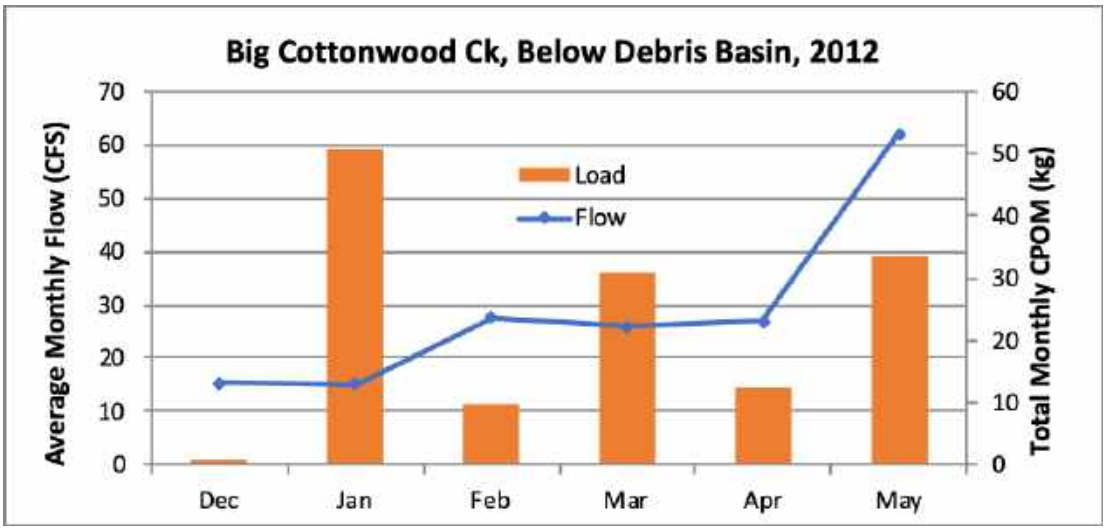

i.

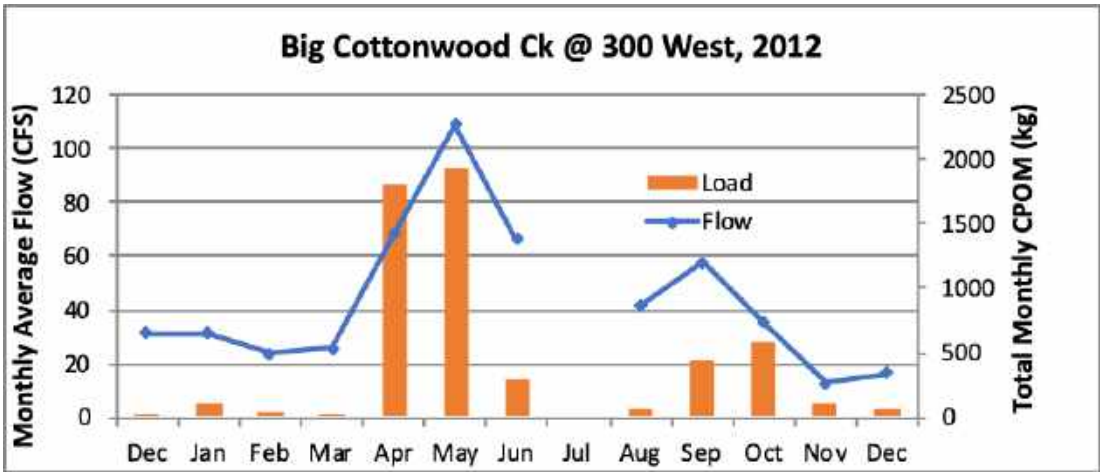

Figure 9, Continued. Note, the creek was totally dewatered immediately below the debris basin after May, but then some return flows occurred by fall and continued carrying CPOM.

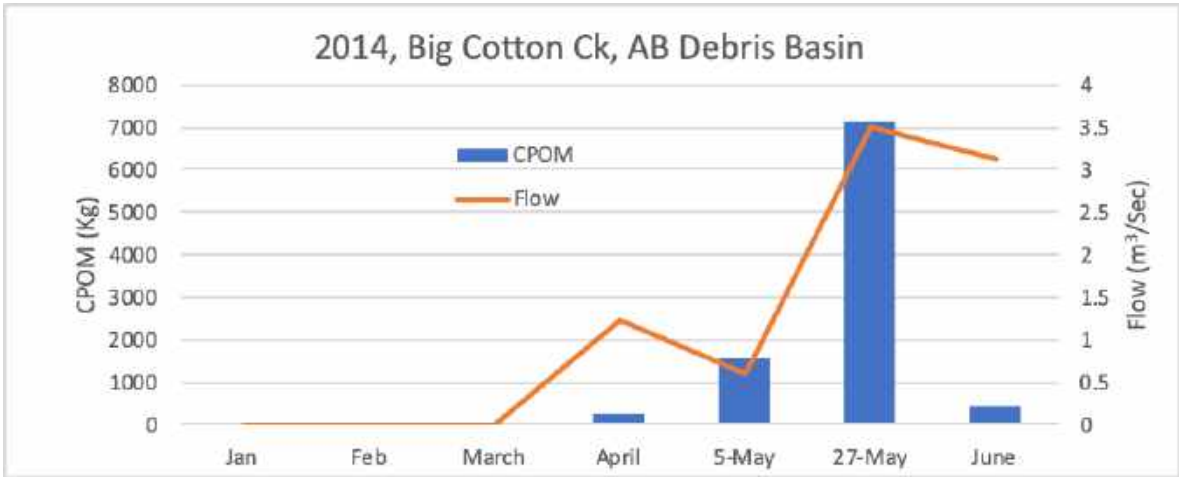

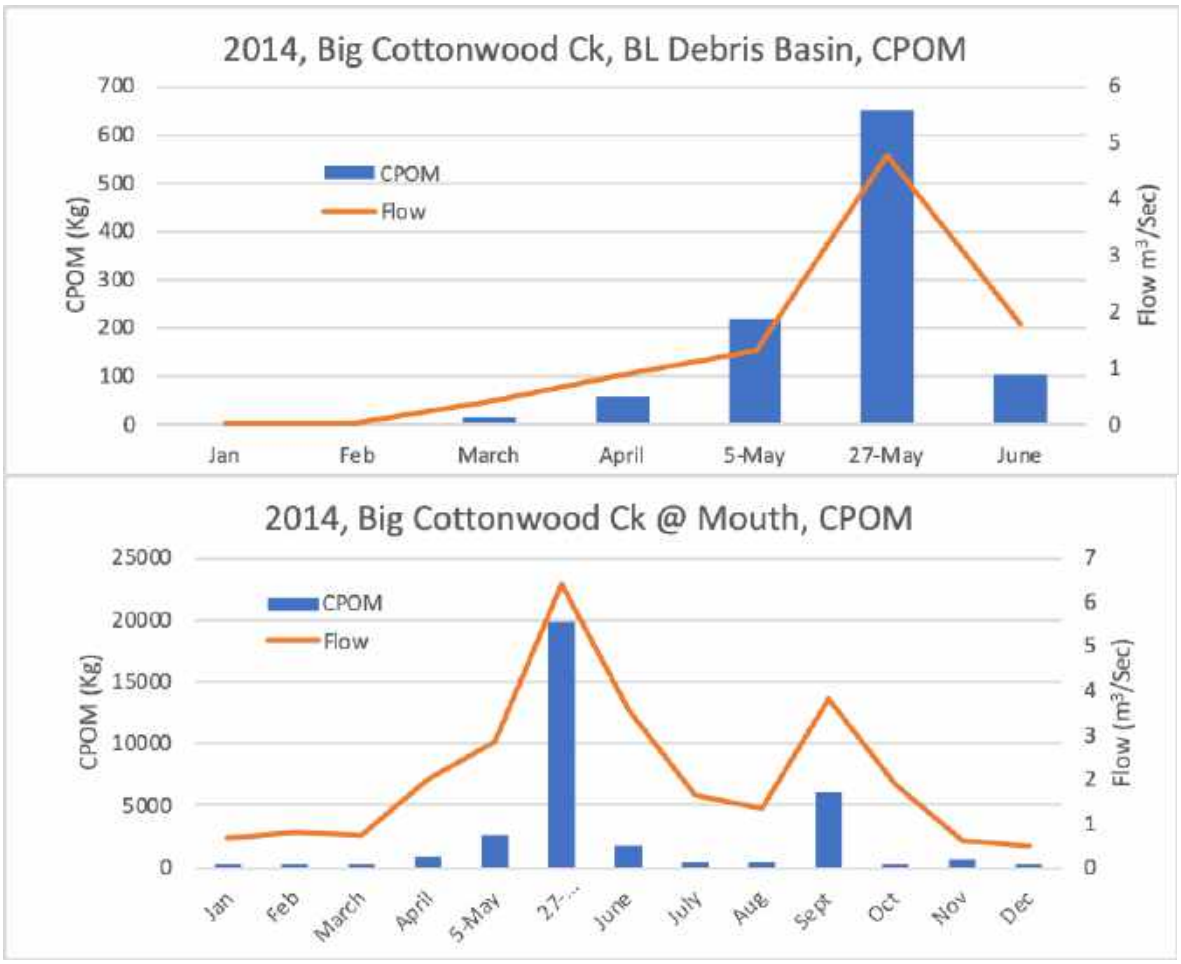

While the inflow delivered an estimated 40,000 kg during June, the outflow from the basin only carried 2,500 kg during June, a reduction of 94% (Figure 9b.). This reveals the effectiveness of debris basins if they provide sufficient residence time and are maintained. Despite the observed effectiveness of the debris basin during spring of 2010, Big Cottonwood Creek acquired considerable CPOM downstream of the debris basin (up to 25,000 kg during June) as it flowed through the urbanized section of the creek. This sampling site was located immediately upstream from the confluence of Big Cottonwood Ck and the Jordan River, indicating that this large load entered the Jordan River.
Flows were substantially greater during the greater snowpack year of 2011 (Figure 9, d., e. and f.). Yet, there was an unexpected lower load of CPOM. The CPOM samples for June were collected on June 8, which was relatively early on the ascending limb of the hydrograph during this specific year. This would have been before the creek reached or exceeded bankfull, whereby much more leaf and grass material that would have been deposited during the previous fall would be mobilized and transported by the creek. Also notable, the debris basin was ineffective in removing CPOM during this period. It is likely that either the increased flow did not provide adequate retention time, and/or the debris basin was relatively full of sediment and had not been dredged prior to the 2011 runoff season. Most notable, as with 2010, there was significant accrual of CPOM

between the debris basin, and 300 W. The estimated CPOM load for the month at 300 W (and was undoubtedly delivered to the Jordan River) was near 75,000 kg (Figure 9 f.). This sample was collected about two weeks after sampling was performed at the canyon mouth, which was very close to the timing of peak flows in Big Cottonwood Creek. Flows during 2012 were substantially below average. The channel was completely dewatered by June at the canyon mouth and by May at the site below the debris basin. There were measurable flows at 300 W, which included a moderate amount of CPOM during May and June. The flow further diminished throughout the remainder of the year and this low flow undoubtedly contributed to the very low CPOM measurements, even though the months of leaf litter falling during September, October and November- suggesting that much of the leaf litter fell on the banks.

The flows during 2014 were about 40% higher than those of 2012 but still only about 30% of that during 2011. Predictably CPOM loads were proportional between these flows. About 20,000 kg flowed by the mouth during the spring of 2014, while 2000 kg flowed by the mouth the spring of 2012 and 70,000 kg flowed by the mouth during the spring of 2011 (Figures 8, 9 and 10)

Little Cottonwood Creek

Little Cottonwood Creek behaved very similar to Big Cottonwood Creek. There is a small debris basin located just upstream from the diversion at the canyon mouth. This debris basin removed approximately ½ of the CPOM coming out of the canyon during 2010 (Figure 10). The snowpack was slightly below average during the 2010 spring with peak flows occurring during June. During 2011, runoff included much higher peak flow and this flow was sustained through both June and July.

a.

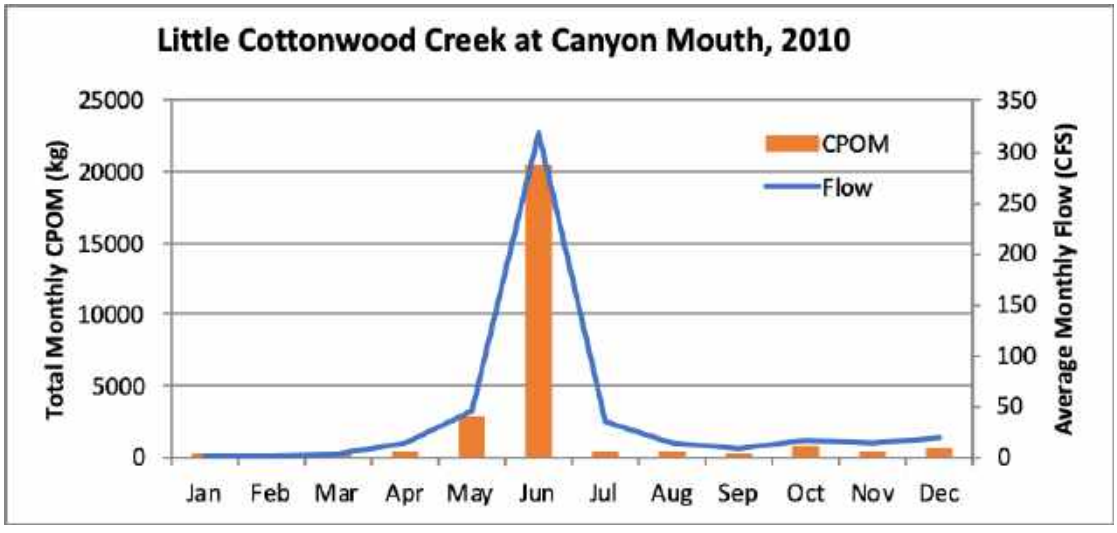

b.

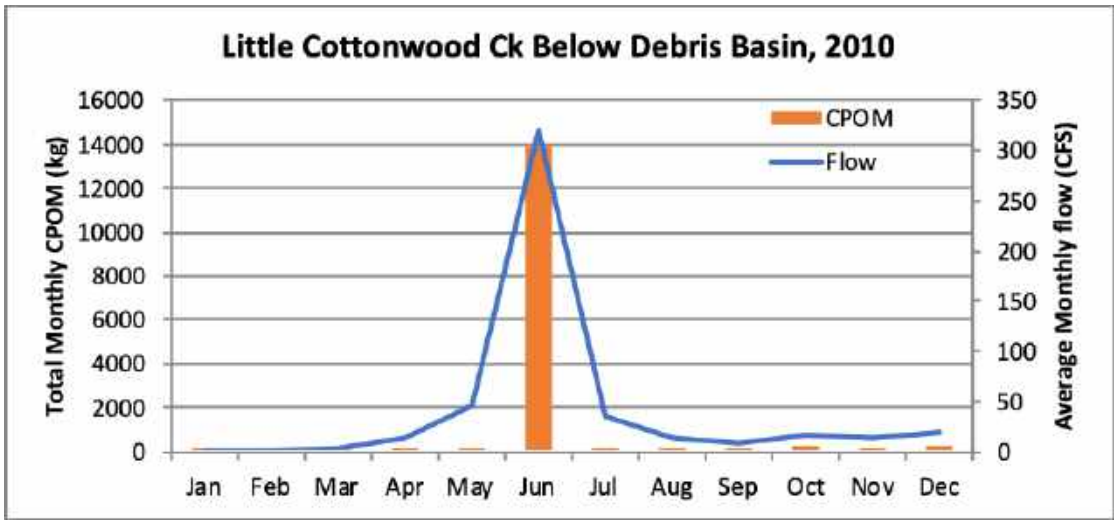

c.

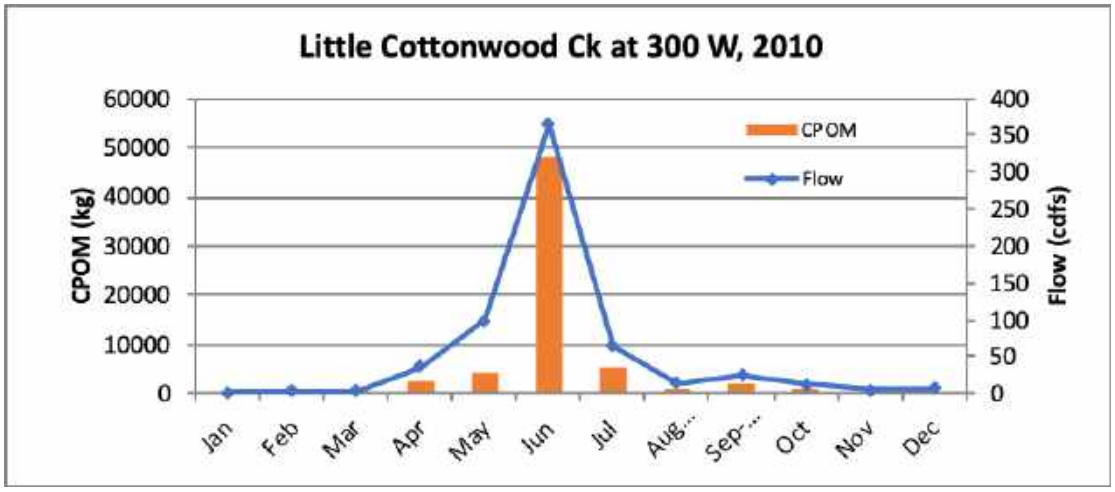

Figure 49. Flow and CPOM at selected sites along Little Cottonwood Creek. The debris basin was relatively small (approximately 0.5 hectare; 1 acre) located approximately 800 m (1/2 mile below the canyon mouth.

d.

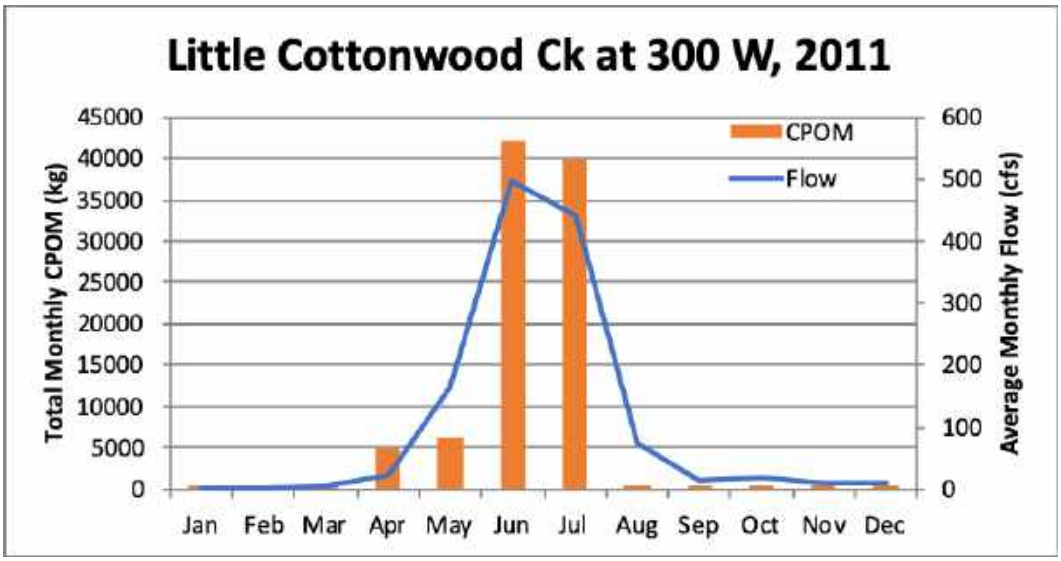

e.

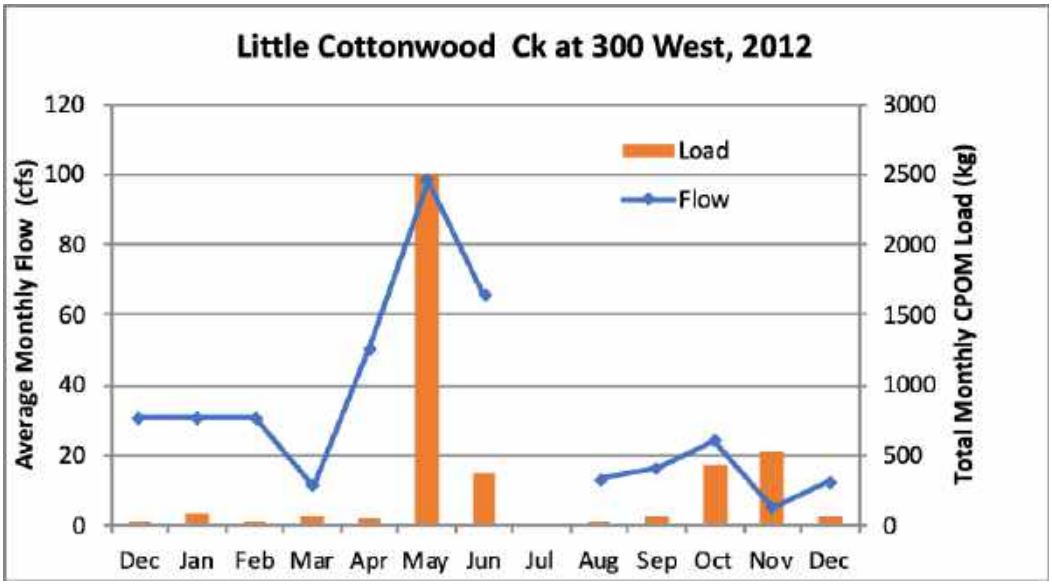

Figure 11, d and e. CPOM measurements and mean monthly flow at 300 W, approximately 800 m (0.5 mile) upstream from the confluence with the Jordan River. Note difference in axis scales between 2011 and 2012 graphs.

2012 was another low snowpack, low runoff year which resulted in much lower CPOM loading that during 2011. CPOM loads were directly correlated to flows and notably the fall loading that had occurred in Mill Creek and City Creek was not observed or was greatly diminished in both Little Cottonwood and Big Cottonwood Creeks. This may have been due to the timing of sampling or perhaps also due to the relatively low flows of late summer and fall of 2012. Also, as with Big Cottonwood Creek there are many 10s of thousands of kg of CPOM transported during the high spring flows and again, the creek picked up substantial amounts of CPOM as it flowed through the valley floor.

Jordan River

The Jordan River was sampled at several sites to understand the timing of delivery and the magnitude of CPOM loading to and transport within the lower Jordan River. For example, large quantities of CPOM are transported to the Jordan River upstream from the 2100 S diversion. Yet, most of this material is delivered during periods of high flow and particularly from those tributaries that join the Jordan River upstream from 2100 S. This presents an important and complicated conundrum. For example, it is during high flow events that up to 90% or more of the Jordan River is diverted to the Surplus Canal (Figure 11 a. and b). Under extremely high flow conditions, the gates are nearly completely closed (Figure 11). Initially this suggests that the great majority of CPOM is diverted with the majority of the flow. However, it is also important to note that the gate in the diversion dam provides only for a bottom release to the downstream river channel. This is opposite the top-water release of water diverted to the surplus canal. It is also important to note that on several occasions and throughout the Jordan River and its tributaries, we observed that even the freshly fallen leaves and twigs only require minutes to maybe an hour to become saturated and thereby quite rapidly sink to where the majority of CPOM is carried as organic bedload material. Therefore, a relatively smaller proportion of the CPOM may actually to pass over the top of the dam and down the Surplus Canal (depending on the local hydraulics and potential for upwelling at the weir itself). Alternatively, it is possible, that when the gate is open even slightly, a greater proportion of the organic bedload will continue down the channel rather than being diverted.

The reason why so much of the flow is diverted is that tributaries that deliver water downstream from 2100 S add considerable flows. These include the 1300 S and 900 S conduits from Emigration, Red Butte and Parleys creeks and the North Temple conduit that similarly transports City Creek water under Salt Lake City. Hence, flows are diverted to the surplus canal to provide channel capacity for these tributaries. These flows are apparent from the measurements made at 500 N (vs flow measured at 1700 S), which are those graphed and used to estimate downstream loads. Figure 13 illustrates the flows and CPOM loads in the lower Jordan River during 2011 and 2012.

a.

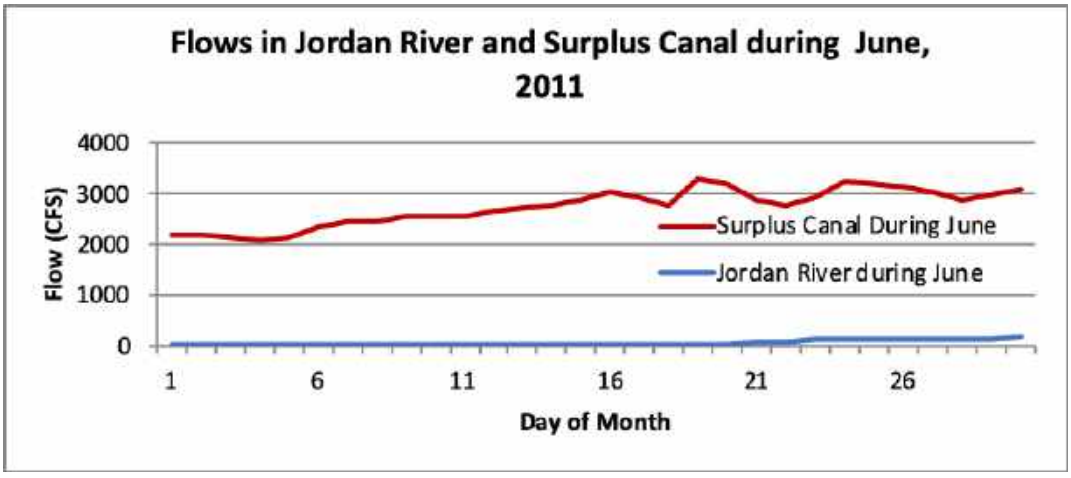

b.

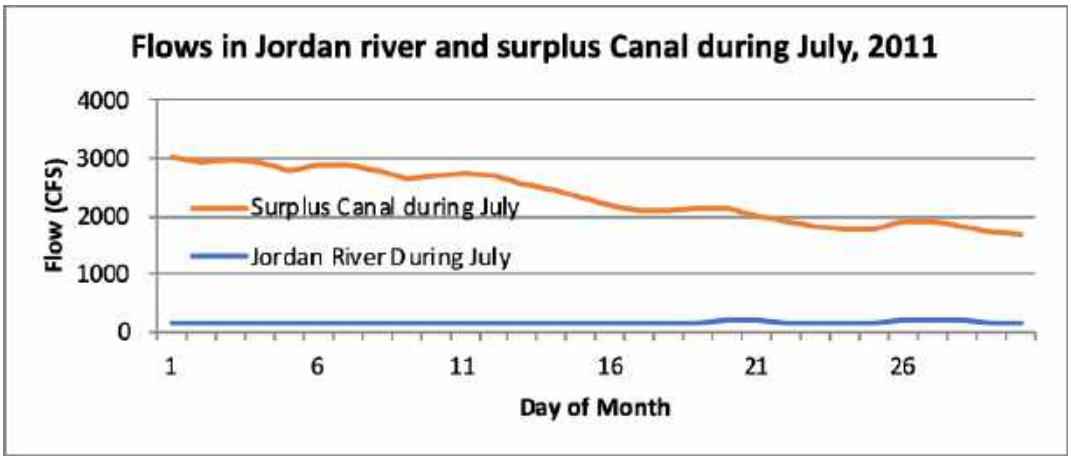

Figure 50. A comparison of flows measured in the Surplus Canal at the SLC International Airport and the Jordan River at 1700 S, during June (a) and July (b).

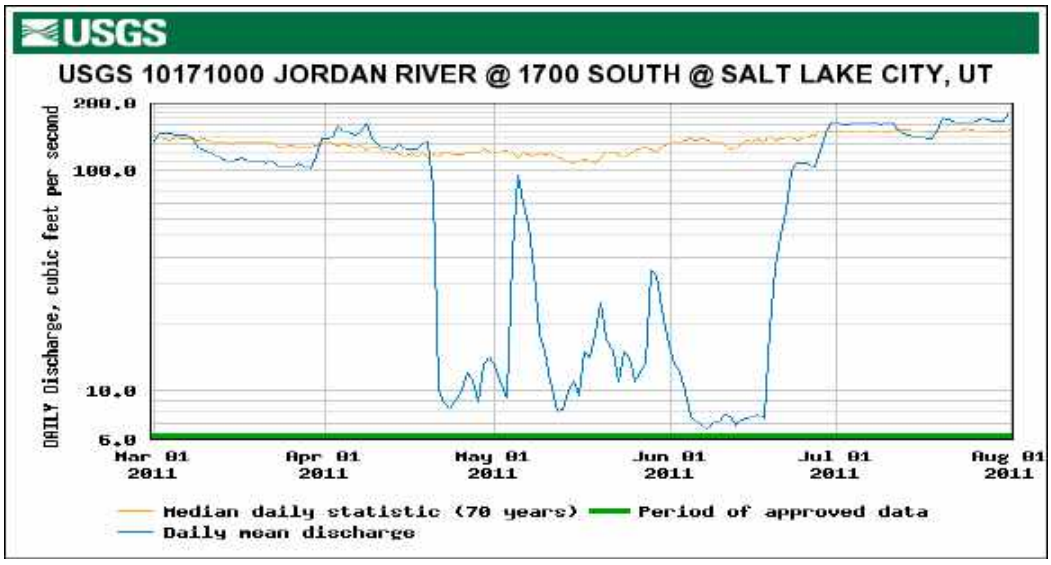

Figure 51. USGS flow data recorded at 1700 S from March through July 2011. Note how flow was restricted during the peak runoff months of May and June.

An example of a low water year was the 2012 (Figure 13). Snow pack during the winter 2011/2012 was at about 70% of average. This led to a much lower runoff and hence a much lower proportion of the Jordan River was diverted to the Surplus Canal. As a result, the CPOM loads were also much lower than the 2011 year (see below).

There are two distinct flow regimes associated with the 2012 season. The first is that the greatest flows during 2012 occurred from the end of January through April. Note that peak flows occurred in February and March, as more water was released from Utah Lake to provide additional capacity for possible additonal high runoff flows in 2012. However, spring runoff flows were much lower than expected prompting the water managers to change their management strategy and begin conserving water in Utah Lake, thus altering and restricting normal seasonal flows. Indeed, by June, when flows are normally peaking,

they were very much less than 2011 values and had fallen to a stable range near 175 CFS at 1700 S (Figure 13). It is also informative to provide similar detailed daily flow for the months June and July. These are included in Figure 14. Comparison with Figure 11 reveals the dramatic differences in flow regime that can occur from year to year.

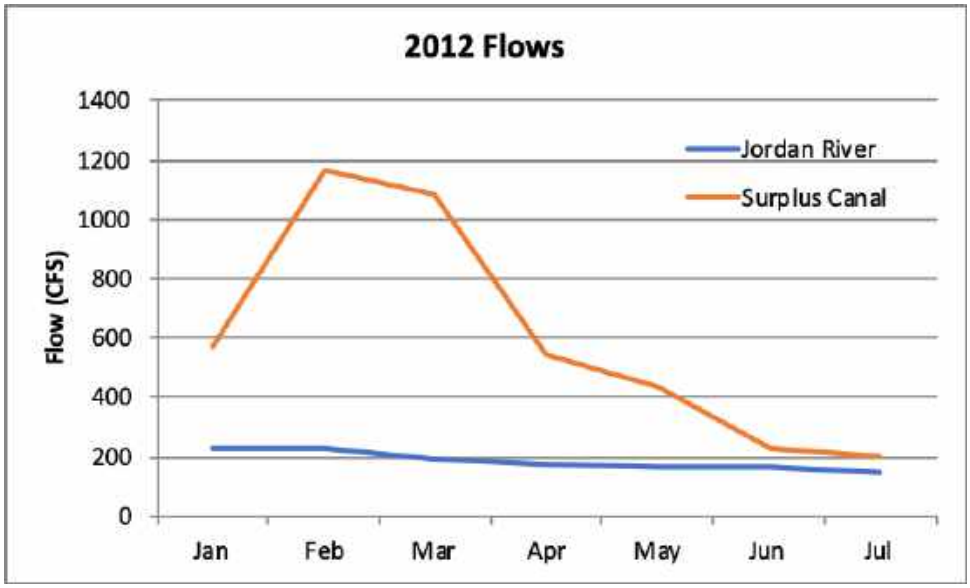

Figure 52. Mean monthly flows in the Surplus Canal and in the Jordan River at 1700 S During 2012. Note unusual peak flows occurred during February and March rather than during normal timing for spring runoff. See text for more details.

a.

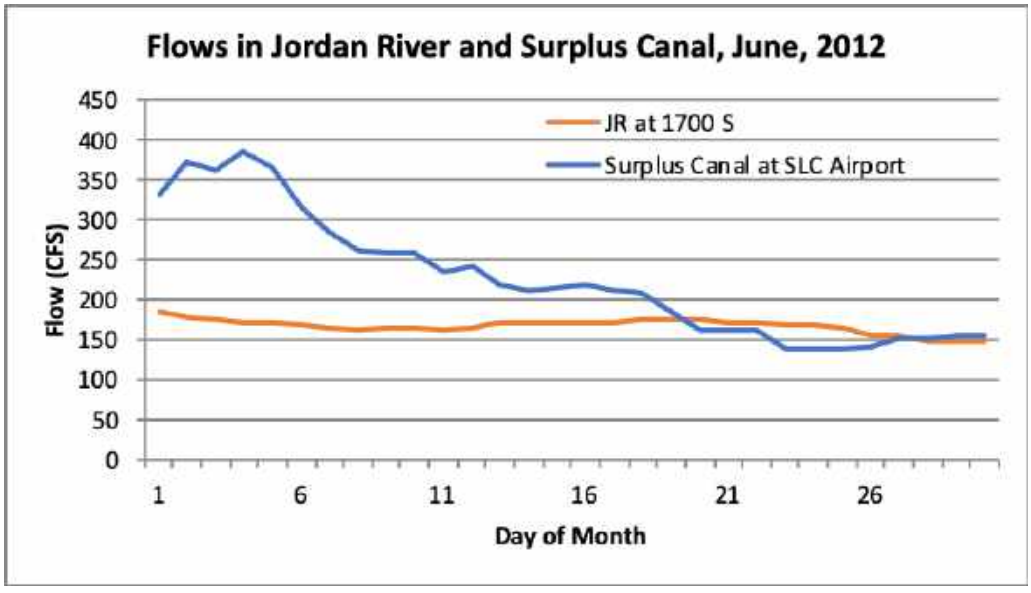

b.

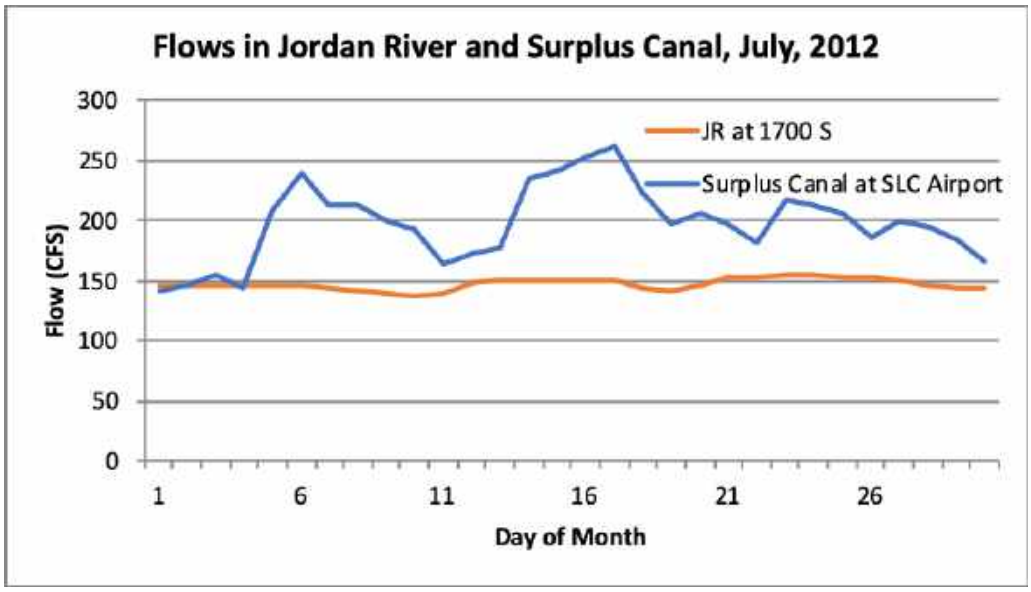

Figure 53. USGS flow recordings in the Jordan River at 1700 S and the Surplus Canal during June (a) and July (b) of 2012.

CPOM loads responded as expected to these different flow regimes. Flow and CPOM loads in the Jordan River during 2011 are illustrated in Figure 15. CPOM loads were generally correlated to flows. Some notable characteristics include; 1) Total flows (combined Surplus Canal and the 1700 S flows) remained near or above 3000 CFS for about 3 weeks during June and July (Figure 11). Yet, a greater proportion of water was allowed down the Jordan River channel starting on about June 23 and continuing throughout July. This greater flow down the channel apparently carried a greater load of CPOM, even though total flow began to diminish after the first week in July. This is likely related to the point made above, wherein the bottom discharge of the diversion dam leading to the lower Jordan River is carrying a disproportionate higher load of CPOM relative to the actual total flow because the CPOM is primarily being carried as bedload and hence is more easily directed to the bottom release of the gate leading to the river channel. Contrarily, the flow diverted to the Surplus Canal flows over the top of the weir which is about 2 m above the stream bottom. Overall, several hundred thousand kg of CPOM were likely transported to the lower Jordan River.

Figure 15 also reveals the immense quantities of CPOM that settled out of the water column during 2011 between 1700 S and 300 N, even though there were additional tributary contributions from Red Butte, Emigration and City Creeks. For example, 40,000 to 70,000 kg of CPOM typically passed 1700 S while only 8,000 to 16,000 kg passed the 300 N site per month. Many tens of thousands of kg of CPOM settled to the bottom of the Jordan River each month during 2011. The implications of this mass settling is discussed in Chapter 5.

During 2012 the sampling effort was increased to included monthly samples. Overall flows were much less than during 2011, although similar flow-related patterns of CPOM

were observed during 2012 (Figure 16). Again, despite the diversion of most of the flows, a considerably elevated load of CPOM was associated with the increase in spring flows. For example, there were two CPOM samples collected during January, 2012. The first was collected January 5, when total flows (1700 S and Surplus Canal flows totaled 595 CFS) and the CPOM load was measured at 1.2 mg/ft3 at 1700 S. If flows had been sustained at this value, the total CPOM load for January would have been 511 kg. However, the second CPOM sample was collected on January 25, one day after flows had increased by 50% to 879 CFS. These were the highest flows experienced by the river since the spring of 2011 and hence it is likely that this increase had begun to pick up additional CPOM lying in backwaters or on the banks. If this flow and CPOM load had been sustained for the entire month of January, the total monthly CPOM load would have been estimated to be 10,367 kg. The mean of these two values was 5,439 kg (Figure 16), perhaps an accurate reflection of actual January loads. These data further support the idea that, although the great majority of water is diverted to the Surplus Canal during high flows, there are considerable quantities of CPOM that continue moving down the channel as well as additional quantities delivered by Immigration, Parley's, Red Butte and City Creeks and the downstream reaches of the main stem that flow through the Rose Park neighborhood and North Salt Lake. In turn, and contrary to the January peak in CPOM, the June CPOM peak was likely due to the natural runoff and increase in CPOM loading from the tributaries (Figures 8, 9 and 10). CPOM values measured during autumn were elevated once again and were correlated to the annual leaf fall from riparian zones along tributaries, storm drains and the main stem. Notably, these autumn values were similar to those measured during 2011 – as was the actual stream flow.

We continued sampling for CPOM during 2013, 2014 and 2015. These additional data were collected in order to capture additional potential variability due to flows streamside management or changes in land use. Notably, drought, with very low flows continued throughout these years. As a result, CPOM remained quite consistent with 2012 data, all of which represented a smaller CPOM load compared to that collected during 2011. Nevertheless, many thousands of kg of CPOM are delivered annually to the Jordan River. For example the 2014 data for Big Cottonwood Creek shows both the effectiveness of the large debris basin at the mouth of the canyon, the effectiveness of that debris basin in reducing CPOM loads and yet the large addition of CPOM as the Creek passes through urbanized neighborhoods toward the Jordan River.

The early years of data raised concern by the Utah Division of Water Quality as to the quantity of CPOM delivered to the lower Jordan River and the link to the SOD. Therefore, UDWQ contracted to Dr. Michelle Baker of USU to perform a similar study to ours during 2013. We shared our sampling methods with Dr. Baker and although we sampled similar sites on the main stem, Dr. Baker's group did not sample tributaries. Also Dr. Baker's group sampled less frequently and at different times than us. Nevertheless, our results were quite similar. Table 2 shows the difference between the two teams. Our group consistently showed higher loads, but with the high variability in

this type of sampling (one or two twigs in the sample net can easily double the quantity of CPOM. For this reason, our team always collected at least triplicate samples and determined the mean. In addition, we often sampled twice per month during spring runoff to ensure we were appropriately characterizing flows and loads.

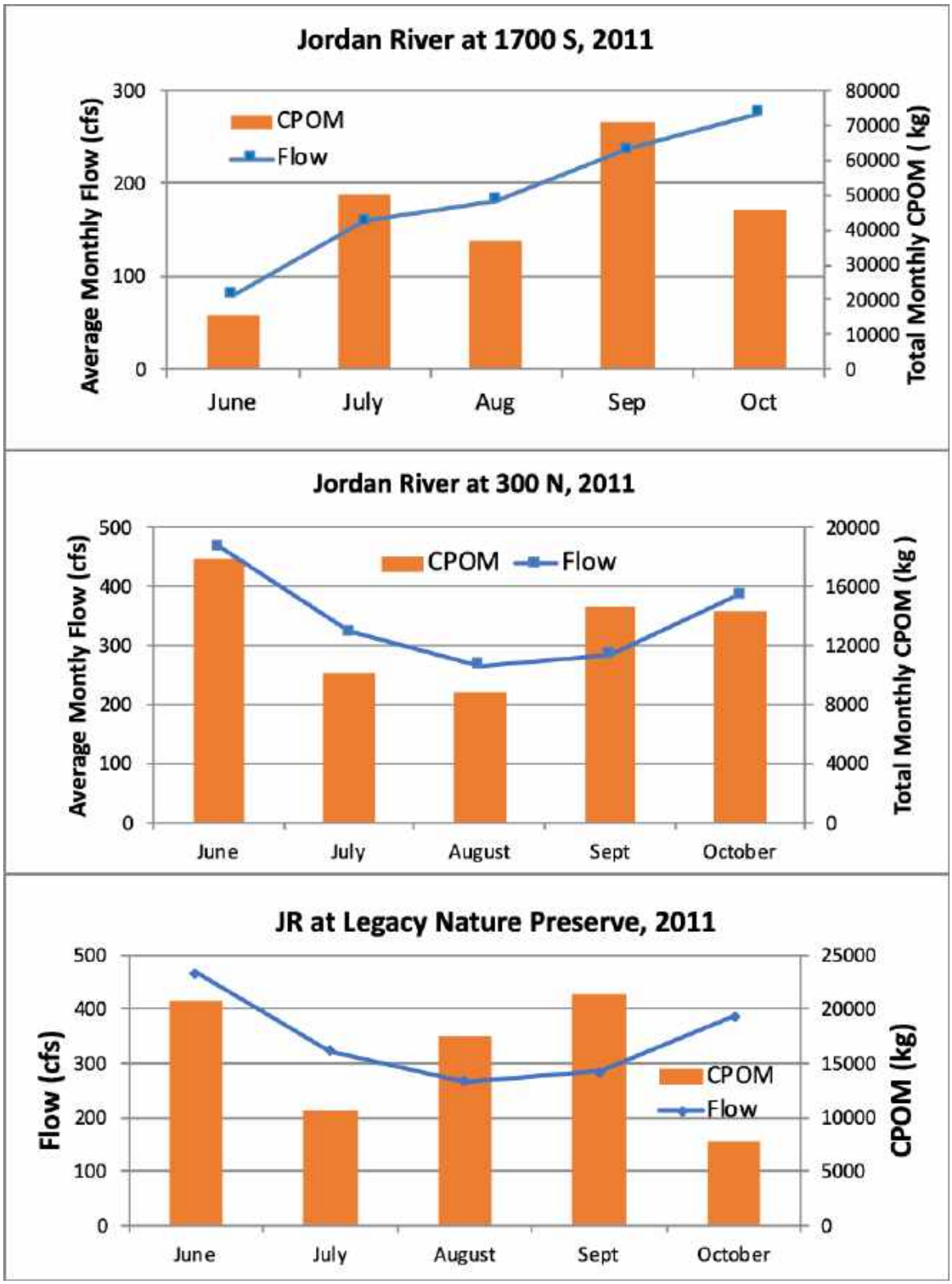

Figure 54. Flow and CPOM measurements made at 1700 S (a.), 300 N (b.), and Burnham Dam (c.) during 2011. Flow measurement data was collected from the Salt Lake County gage at 500 N.

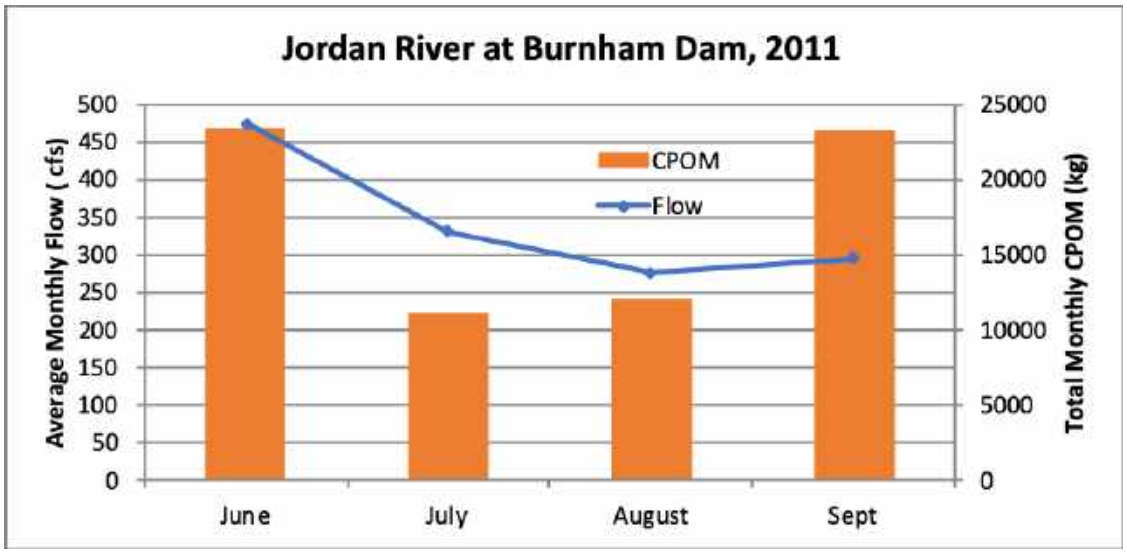

Figure 15. Continued.

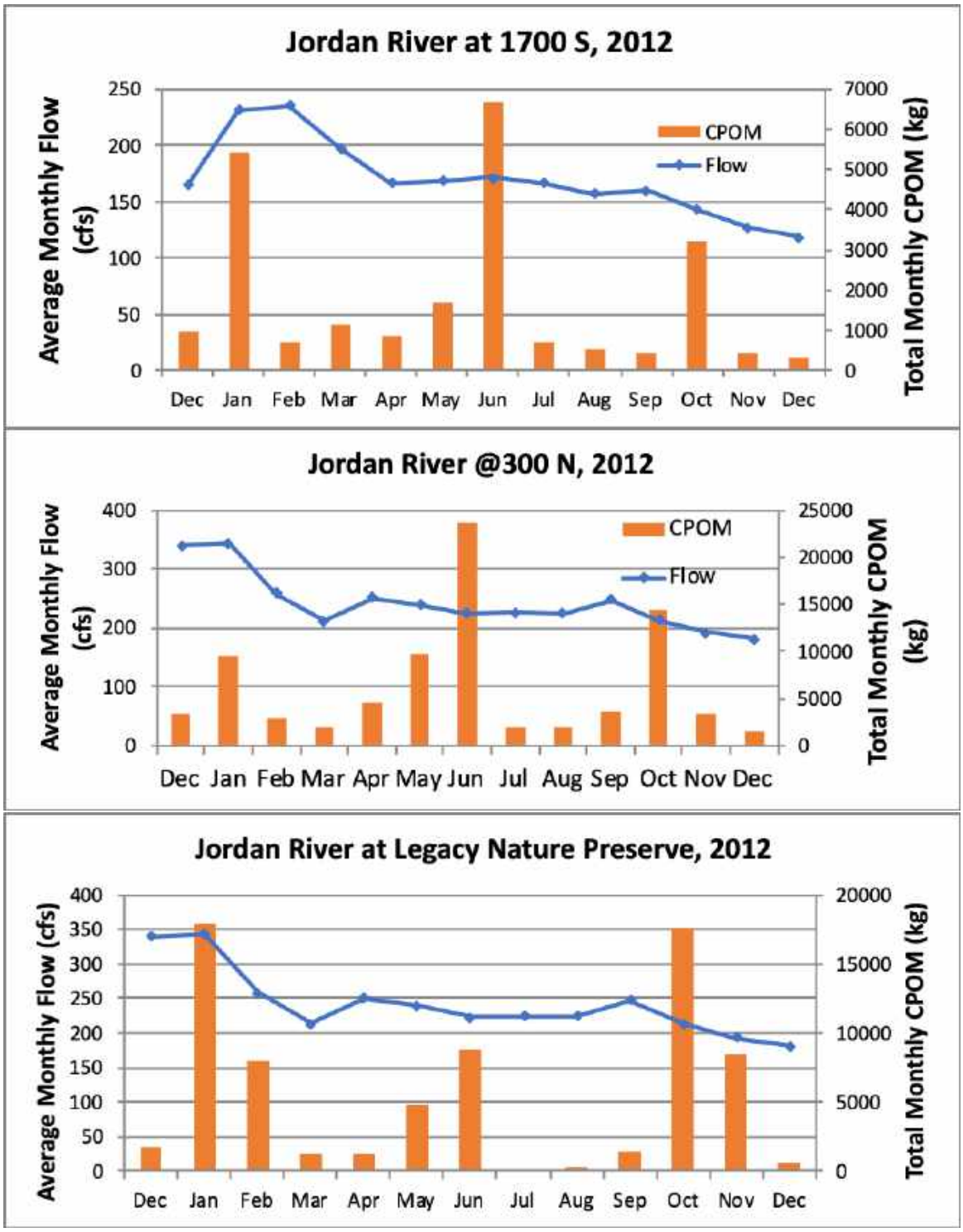

Figure 55. Monthly measurements of flow and CPOM at 1700 S (a.), 300 N (b.) and Legacy Nature Preserve (c.) during 2012. During the higher flow periods of January, February and March, and during August, September and October, CPOM samples were collected twice monthly.

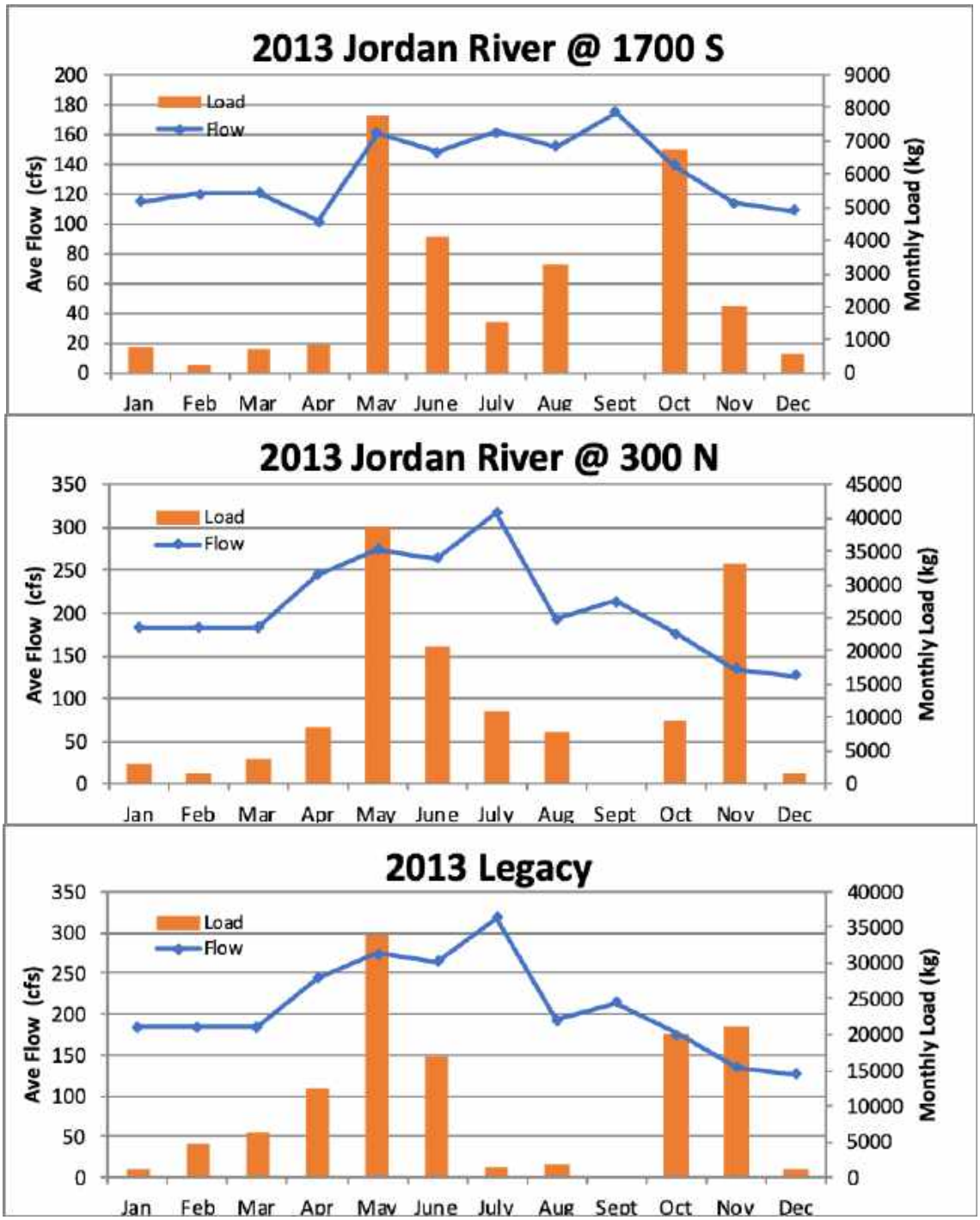

Figure 56. Monthly measurements of flow and CPOM at 1700 S (a.), 300 N (b.) and Legacy Nature Preserve (c.) during 2013. CPOM loads predictably increased during the higher flow periods of April, May and June.

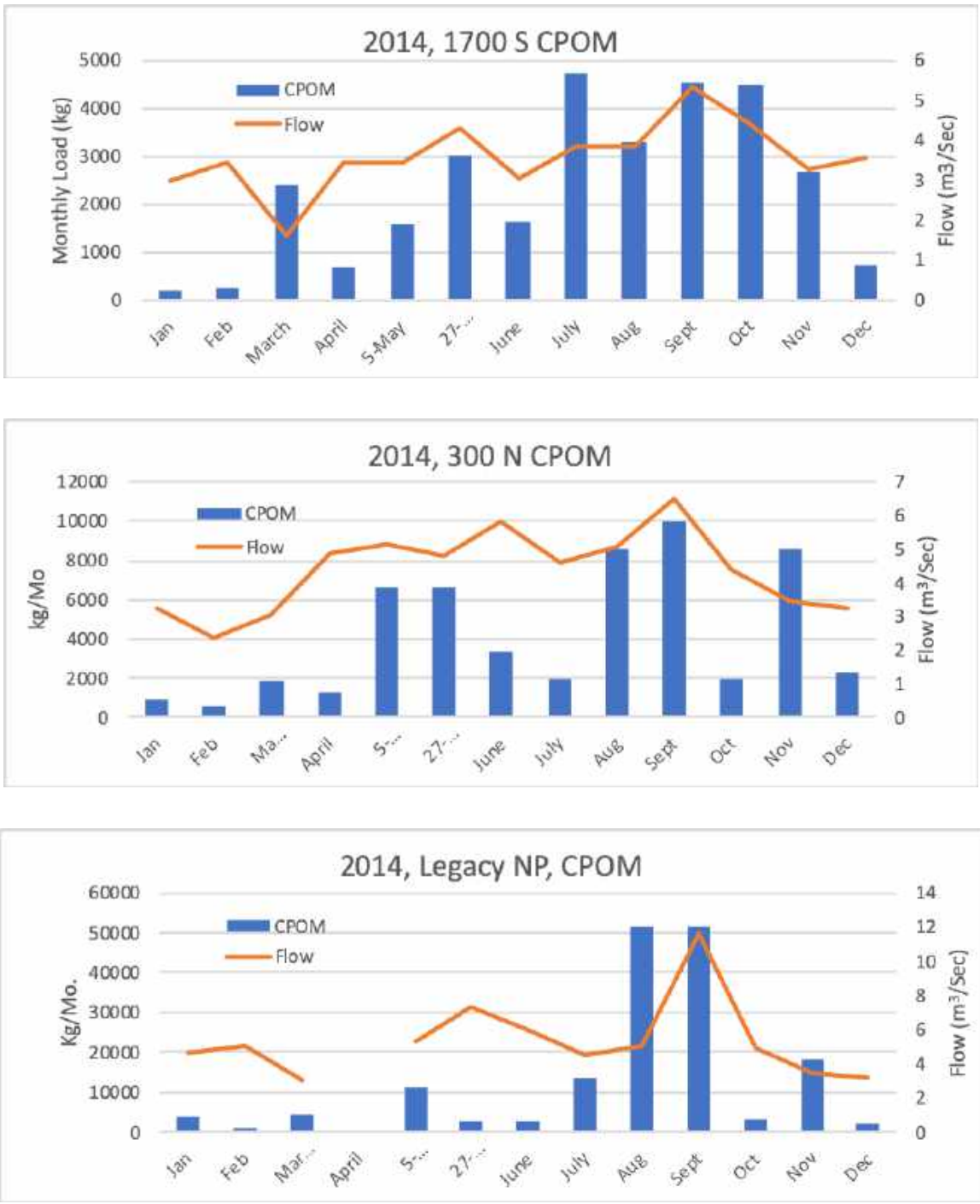

Figure 57. Monthly measurements of flow and CPOM at 1700 S (a.), 300 N (b.) and Legacy Nature Preserve (c.) during 2014. Notice the relatively low spring flows and concomitant low POM loadings. August and September flows increased, dramatically increasing the CPOM loading during fall.

The general pattern appears to be driven by the magnitude of spring runoff in combination with seeds, grass litter and other urban refuse deliberately or inadvertently running down storm drains or over the backyard fence. Secondly, there is commonly a

fall surge of CPOM that accompanies late summer storms where flood flows reach bankfull and pick up additional litter that had fallen during spring and summer and particularly where spring flows were below normal.

Table 4. Comparison of CPOM measurements between a high runoff year (2011) and a low runoff year (2013) and between CPOM measurements between two different teams.

	2011 WFWQC		2013 WFWQC		Epstein et al 2013
	AFDM	kg C	AFDM	kg C	kg C
1700 S	218712	72175	33954	11205	6023
300 N	62119	20499	139433	46013	8592
Legacy	74836	24696	121547	40110	14373

Except for the June samples of 2012, CPOM loads downstream from 1700 S fell considerably, indicating that large quantities settled out of the water column. There was very little change in CPOM between Legacy Nature Preserve and Burnham Dam. Overall, however, it is apparent that the CPOM loading during 2012 was much lower than 2011 and this was most likely due to the general lower flow conditions.
Overall, monthly sampling reveals a bi-modal pattern of elevated CPOM loads. These are: 1) during spring runoff when elevated stream flows pick up/mobilize additional organic debris (leaves, twigs, seeds, grass, etc.), that fell onto stream banks during the previous autumn or perhaps tossed onto stream banks by adjacent land owners; and 2) during the autumn season when deciduous trees are losing their leaves. The total annual - as well as seasonal transport of CPOM varies directly with the magnitude of the spring runoff or the occurrence and magnitude of autumn rain events. Based upon the magnitude of such flows, the total annual CPOM delivered to and carried by the Jordan River may exceed 200,000 kg per year. This estimate should be considered conservative during high runoff years – particularly based on the fact that generally only one sample event was performed per month and such sampling occurred at random with respect to when peak flows actually occurred. this estimate may also be considered excessive during low runoff year as much of the leaf litter will remain on the banks until higher flows occur.

A general trend seems to be that the highest loads are at the mouth of the canyon and at the confluence with the Jordan River. We only have data at the confluence for the three larger tributaries due to the 2010 oil spill in Red Butte Creek. A total load estimate for the combined flow of the smaller tributaries, City Creek, Emigration, and Parleys and Red Butte would be 20,000 kg/year, but this is with the assumption that Parley's and Red Butte Creeks have roughly the same load as the City Creek and Emigration Creek.
The total combined load at the canyon mouth sites for Big Cottonwood, Little Cottonwood, and Mill creeks may reach 100,000 kg/year during normal to high runoff years. A reasonable estimate of the combined CPOM loading at their confluence sites is

200,000 kg/year during normal to high runoff years. Conversely, loads may be half or less of these amounts during low runoff years.

While there is evidence that even small debris basins can be quite efficient at removing CPOM, (for example, in Mill Creek and Big Cottonwood Creek) it is also evident that considerable maintenance is required to maintain these removal rates. Further, despite the effectiveness of these debris basins, considerable CPOM enters these tributaries downstream of the debris basins and enters the Jordan River.

Finally, these data provide clear evidence that there are huge quantities of CPOM being delivered to the many tributaries, storm drains and main stem of the Jordan River and that this CPOM is being delivered and deposited throughout the lower reaches of the river. In turn, disintegration and decomposition of this organic matter in depositional areas is in sufficient quantities and rates as to cause the elevated SOD values that have been observed in the Lower Jordan River.

One of the most important points to understand in the study of CPOM transport and settling and subsequent oxidation is that there are different types of decomposition. For example, the QUAL2Kw model assumes that all organic carbon oxidation is performed aerobically. Yet, as we have discovered through surveys and the seminal work by Hogsett, (2015; Chapter 6), is that considerable decomposition includes the ultimate reduction of organic carbon to methane. In addition, all sites downstream from 1700 S are characterized as soft, organic rich anaerobic sediments that continue for at least 1 m. In this condition OM is converted to methane. This is critical in that the oxidation of methane requires 6.7 times or oxygen than the oxidation of glucose (Figure 19) Therefore, the assumption in the Phase I report (Cirrus 2010), that, according to the QUAL2Kw model, all organic carbon is oxidized aerobically, is false. Moreover, data on TSS and VSS and BOD (Chapter 2), indicates that the VSS does not settle and the BOD in the water column remains virtually the same throughout the river. Finally, the work performed by Hogsett (2015) has identified SOD as the primary source of oxygen loss in the river (Figure 20).

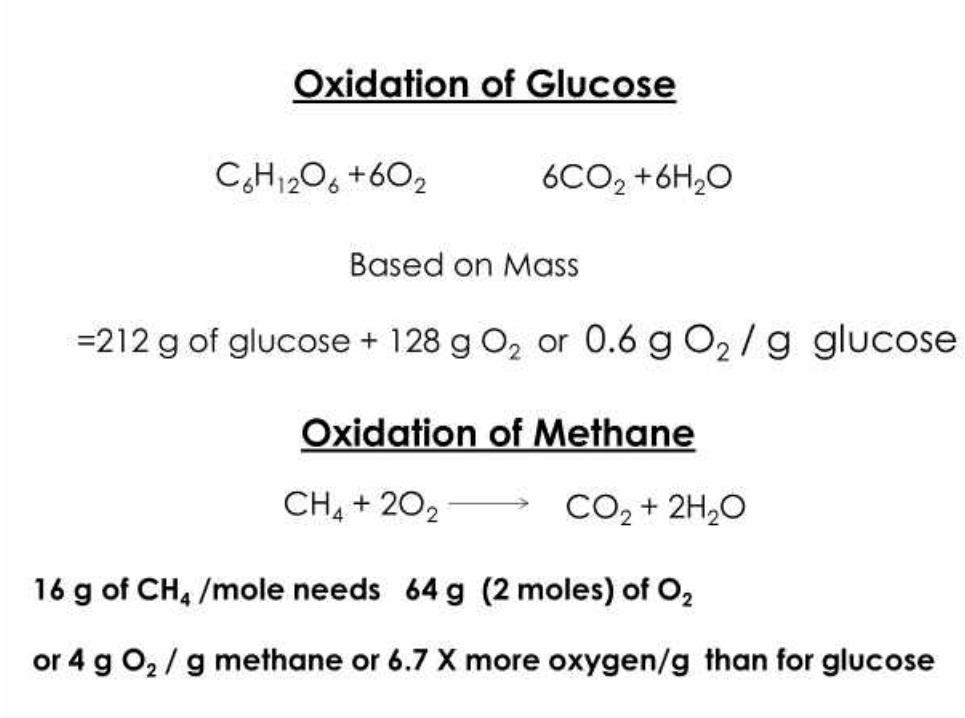

Figure 58. Display of the basic chemical reactions and oxygen demand in the oxidation of glucose and the oxidation of methane. Note the oxidation of methane requires 6.7 times more oxygen per gram for complete oxidation than glucose.

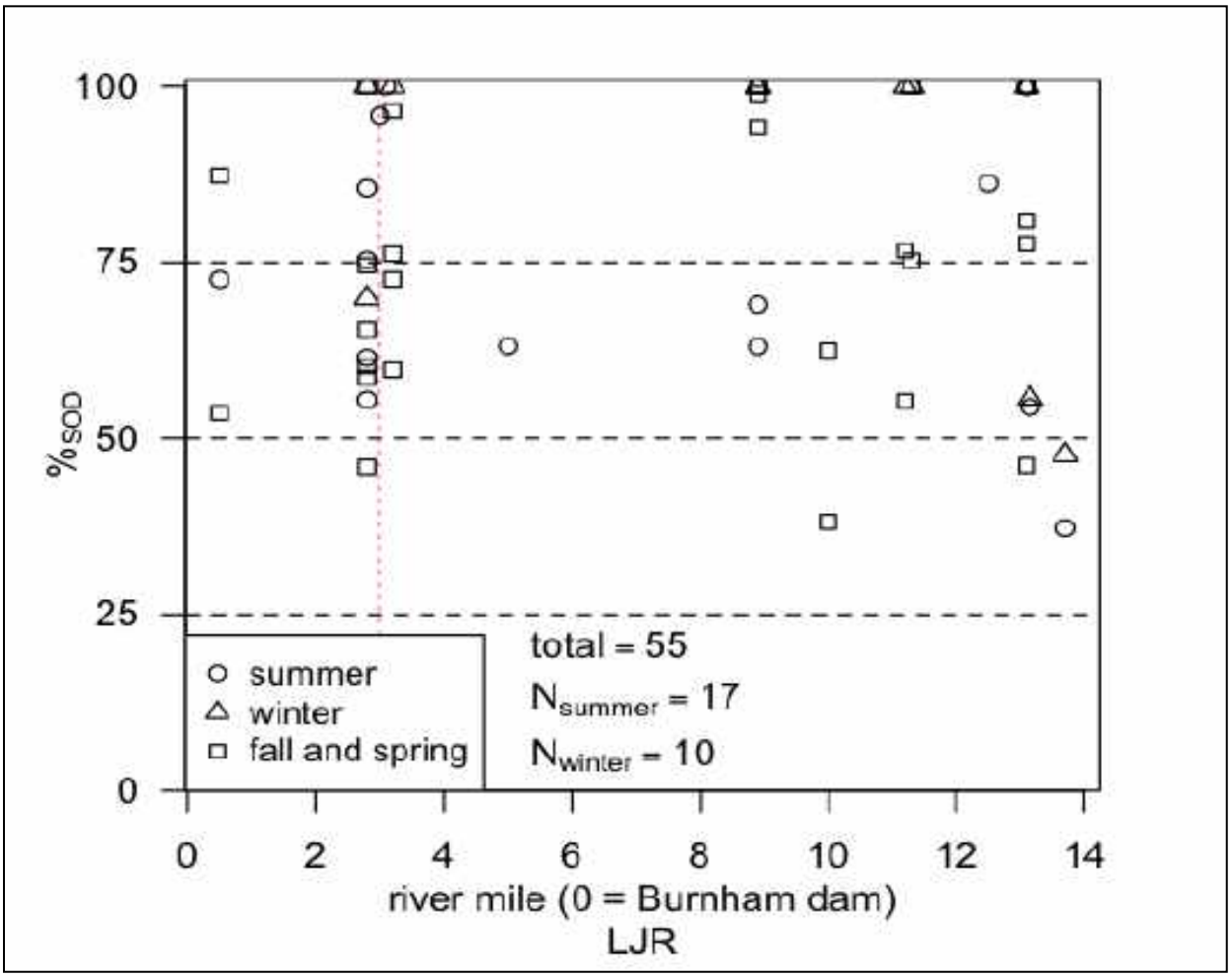

Figure 59. Measurements of SOD in the Lower portion of the Jordan River. Note that the vast majority of oxygen depletion in the river is the direct result of SOD (From Hogsett, 2015)

Out of 57 SOD sampling events, all but 5 demonstrated SOD as the primary source of oxygen loss and several sites demonstrated 100% of oxygen loss was due to SOD. Moreover, Hogsett, measured methane flux to the water column. These data and observations clearly demonstrate that the settled organic matter (i.e. CPOM), causing the production of methane and subsequent SOD, is the primary cause of oxygen depletion on an everyday basis. Finally, under normal flow conditions, even this large delivery of CPOM and SOD does not typically cause the DO to fall below the acute or even chronic DO criterion. Rather, the low DO events are due to the period storm events that mobilize sediments and methane; or the occasional event where the Surplus Canal diversion gate is lowered in order to prevent flood flows from entering the lower Jordan River in anticipation of a flood event and such flood flows do not occur – leaving the lower Jordan River in a series of mostly stagnant pools.

References

CH2MHILL. 2005. Modeling Water resources of the Jordan River. Report for the Recycled Water Coalition.

Cirrus Ecological Solutions and Stantec Consulting. 2011. Jordan River TMDL Water Quality Study. Report to Utah Department of Environmental Quality, Division of Water Quality

Hogsett, M. 2015 Water quality and sediment biogeochemistry in the urban Jordan River UT. PhD Thesis. University of Utah. 293 p.

Quinn, J.M., N. R. Phillips and S. M. Parkyn. 2007. Factors influencing retention of coarse particulate organic matter in streams. Earth Surface Processes and Landforms. 32: 1186-1203.

Chapter 4

Diel Patterns of Dissolved Oxygen, Fluorescing Dissolved Organic Matter and Turbidity and Their Relationship to Seasonal Runoff and Storm Events in the Jordan River

Prepared by

Theron G. Miller

Wasatch Front Water Quality Council

August 2019

Table of Contents

List of Figures

Introduction

Large quantities of both organic and inorganic material are delivered to the Jordan River regularly (Chapters 3 and 4). The inorganic silt -to very fine to large sand -to gravel fractions are largely deposited upstream from the 2100 S diversion. This deposition follows a continuum from larger to smaller substrate size as the channel gradient gradually decreases through the valley. Chronic severe dewatering of the Jordan River channel at the 2100 S diversion to the Surplus Canal vastly reduces stream velocity and allows for the settling of small sand, silt and clays as well as substantial quantities of coarse particulate organic material (CPOM). These materials are also deposited along a continuum from larger to smaller particle sizes and density or mass of organic matter as the channel velocity further decreases. The great majority of the Jordan River downstream of 2100 S. is characterized as a depositional zone of inorganic fine material and CPOM.

There are notable nutrient inputs from Utah Lake and three POTWs along the middle and lower reaches of the river and these high nutrient concentrations had been blamed for the occasional low DO violations in the lower Jordan River. The naïve paradigm of this linkage is that nutrients cause excessive algal blooms (or benthic periphytic growth). In turn this large biomass experiences considerable evening respiration rates and, upon senescence, contributes to further oxygen consumption as decomposition proceeds. The Jordan River is one anomaly. actual water column (phytoplankton) and benthic chlorophyll a (Chl a) concentrations (attached algal communities) are far less developed than the potential growth that the nutrients provide for (Jordan River Phase I TMDL, 2010), which is far less algal biomass that has been associated with low DO excursions (e.g. Smith and Peidrahita, 1988). The relatively low benthic algal biomass can be attributed to the near-constant shifting and scouring of the unstable bedload material upstream from 2100 S, as well as the shifting and near-constant settling and smothering of benthic communities downstream from the 2100 S diversion. These factors inhibit the establishment of substantial quantities of periphytic growth. In turn, these low quantities of periphyton led to the search for other possible causes for the occasional DO violations that are known to occur.

Early on, there were two important observations: 1) The depositional sediments below the 2100 S diversion are rich in organic material that exists in many stages of decomposition (from identifiable leaves, twigs, seeds, etc. to black unconsolidated organic mud layers rich in sulfide odors). Release of considerable amounts of gas bubbles, undoubtedly comprised of methane, hydrogen sulfide, ammonia or N_2 gases, were observed while sampling. The majority of these gases have potentially huge contributions to BOD; or sediment oxygen demand (SOD) if the aerobic/anaerobic interface occurs below the sediment surface; and 2) The low DO excursions have irregular patterns - on a diel basis or seasonally as most of them appear to be associated with isolated storm events. Hence, the occasional violations of the DO standards do not agree with the paradigm that links low DO excursions to diel patterns of elevated evening respiration or to the eventual elongated periods of depressed DO due to decomposing of

dead algal cells. These observations led to a detailed investigation of the other sources of organic matter (i.e. VSS and CPOM; Chapters 3 and 4), and how this organic matter ultimately affects the DO patterns and the occasional violations of the DO standard.

Our group has performed standard measures of organic matter and oxygen dynamics, including BOD, CBOD, and VSS since 2009. These parameters remain quite stable throughout the year while the DO record shows considerable variability. In other words, these parameters were not correlated with the DO record except for the rare occasion when samples were collected during storm events. Yet, the Phase I TMDL (Utah DWQ, 2011) identified VSS as the pollutant of primary concern by assuming that this VSS is the source of sediment oxygen demand (SOD), by assuming that all VSS settles out of the water column. However, our data shows that VSS is high at the Utah Lake outlet and, although there may be some exchange of VSS between the sediment and water column, there is no net loss from the water column throughout the entire river. Hence, this investigation was extended to include the potential contribution of CPOM to the benthic organic matter and the subsequent elevated sediment oxygen demand; and finally, to its contribution to the episodic low DO events. The deposition and fate of sediment organic matter remains of critical importance. This chapter begins to elucidate the fate of settled organic matter and the important role that it plays in the oxygen dynamics of the river.

Summary of Methods

On average, 25 sites were sampled monthly along the Jordan River, at the mouth of major tributaries, the surplus canal and upstream and downstream from The South Valley, Central Valley, and South Davis South and South Davis North facilities. All water quality samples were collected as grabs, immediately placed on ice and transported to the Central Valley Water Reclamation Facility Laboratory where all analysis were performed following EPA methods. In addition, In-Situ® data recording sondes were placed in specific locations starting in 2009 to start recording DO, pH, temperature and conductivity. These sondes were used primarily during summer months, from 2009 to May, 2013 and were primarily set at 2100 S, 300 N, inside the Legacy Nature Preserve and at Burnham Dam. In May of 2013 these sondes were replaced by permanently installed YSI (model) sondes fitted with solar panels and real-time cellular transmission of data to a secure web site at 15-minute intervals. These sondes were installed at 9 locations (Utah Lake outlet, 3300 S, 2100 S, Surplus Canal at the SLC airport, 800 S, 300 N, Center Street (Cudahay Lane) and Burnham Dam). sondes. Of these nine sondes, six are fitted with the four standard parameters mentioned above and a turbidity probe. The other three sondes included the five probes plus chlorophyll a and fluorescing dissolved organic matter (FDOM). In addition to comparison of the data between the probes at a single station, these data can track episodic events from upstream to downstream and in relation to the flow, BOD and VSS data throughout the river and major tributaries. All sondes were calibrated every 30 days to maintain QA goals. Throughout the calibration procedures very little drift of any of the parameters was recorded.

Results and Discussion

Total suspended solids, volatile suspended solids, biological oxygen demand and carbonaceous biological oxygen demand

One of our initial goals was to characterize the seasonal and annual variability and sources of TSS, VSS, BOD, CBOD and nutrients. Here I summarize those parameters that are related to the oxygen dynamics of the River. Figure 1 includes the mean of monthly, and some cases biweekly samples of TSS, VSS, BOD and CBOD for the entire length of the Jordan River from May to December of 2009. There are some points worth noting. The Jordan River is initially controlled at the outlet of Utah Lake. It flows through low gradient agricultural and then increasingly urbanized landscapes until just upstream from Thanksgiving Point. At that point the gradient increases substantially as the river flows through the Narrows.

a.

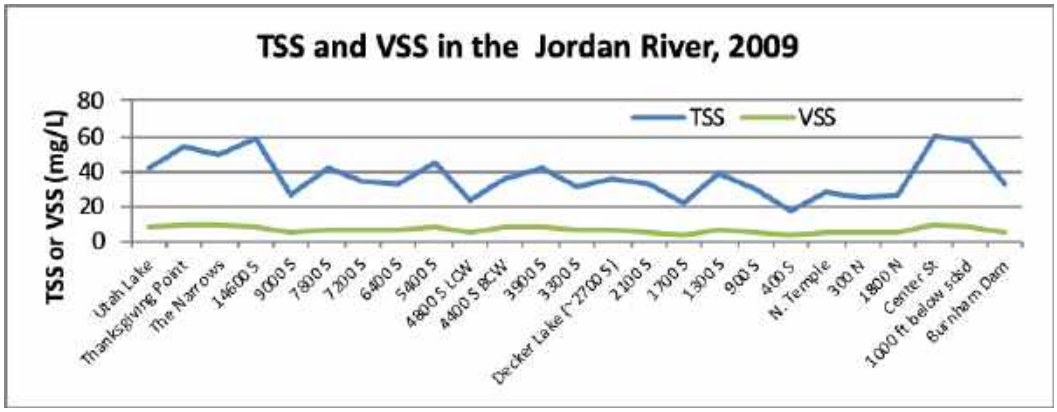

b.

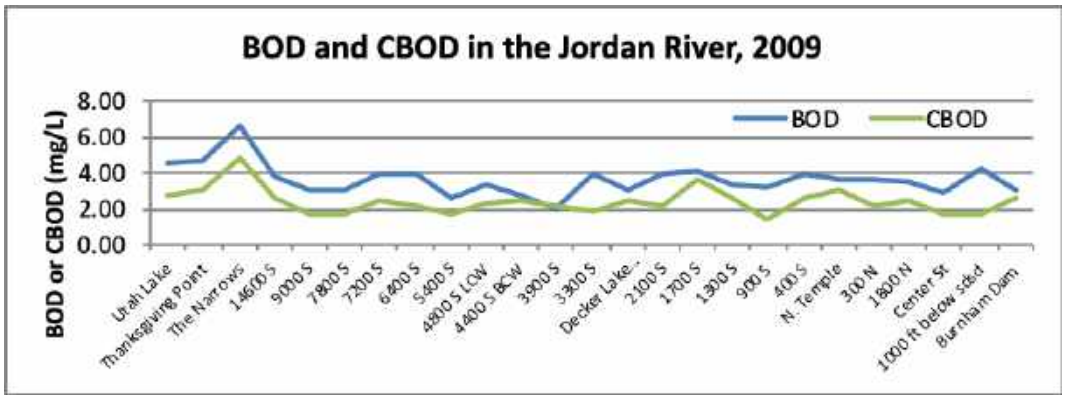

Figure 60. Mean concentrations of total suspended solids and volatile dissolved solids (a.) and BOD and CBOD (b.) in the Jordan River during 2009. Data include the means of monthly samples collected May through December. The peak in TSS at Center St and Burnham Dam was due to a single spike in the river samples measured on July 29 of 299 mg/L. The small peak in BOD and CBOD at the Narrows was due to a single grab sample on August 11 of 13.6 mg/L and 8.6 mg/L for BOD and CBOD respectively.

This is a "gaining" reach as there are known sources of springs/groundwater. This reach also flows through loose alluvial material and during 2009 and 2010, active construction of the Frontrunner train was occurring immediately adjacent to the river through the entire area of the Narrows. This was a constant source of inorganic TSS, although not so much VSS. The South Valley Water Reclamation Facility discharges to the Jordan

between 7800 S and 7200 S and grab samples were collected from the effluent on the same day that other river samples were collected. The mean value of BOD for the South Valley plant was 3.1 mg/L, equal to the mean value measured at 7800 S. Therefore, the small increase in BOD between 7800 S and 7200 S was not likely due to the discharge of the South Valley plant. In addition, the sites labeled 4800 S LCW and 4400 S BCW represent samples collected from Little Cottonwood and Big Cottonwood creeks respectively, immediately upstream from their confluence with the Jordan River. Despite the apparent dilution from these tributaries, the mean TSS, VSS and BOD in the Jordan River increased slightly between 5400 S and 3300 S. Similarly, the Decker Lake sample was collected from the Decker Lake outlet immediately upstream from its confluence with the Jordan River. Mill Creek, which receives the discharge from the Central Valley Water Reclamation Facility, enters the Jordan River at about 2700 S. During low flow periods of the year (basically all months except May and June), the majority of Mill Creek flow (50 to 80%) is comprised of the Central Valley discharge. In turn, Mill Creek comprises about 1/3 of the Jordan River flow during low-flow periods. Yet, the discharge of Mill Creek has no perceptible influence on the BOD or CBOD in the Jordan River. The mean BOD and CBOD are virtually identical between 3300 S (upstream from Mill Creek), and 2100 S (downstream from Mill Creek; Figure 1 b.). The downstream TSS is also similar to upstream values and the mean VSS downstream was actually lower by a small amount (from 6.6 to 5.4 mg/L; Figure 1 a.). Because of the recent interest on influence of Central Valley Water Reclamation Facility on Mill Creek and the Jordan River, Figure 2 provides more detail of these important water quality parameters. Except for the August 11 sample, Mill Creek upstream from the discharge point was lower in BOD than the downstream location. The effluent elevated the BOD somewhat, but the data were variable, including a lower BOD than the downstream site in Mill Creek (Figure 2). Similarly, VSS was much higher downstream from the discharge than in the effluent itself. This was certainly unexpected and led us to investigate the source of this additional BOD and VSS. Our field technicians had observed a storm drain that discharged immediately adjacent to the 900 W bridge was flowing during most sampling events, even though there had been no recent rainfall events. Further, this discharge was quite turbid and discolored the stream water as it mixed. More recently, during a site visit with DWQ personnel during December 2013, discolored water was discharging from this same culvert. We now believe that this discharge was the cause of increased turbidity, VSS and BOD downstream from the Central Valley facility discharge. In turn, this additional load of BOD and VSS is substantial and contributes to Jordan River loading when it is flowing. It may be discharges like this that contribute to the overall variability of these constituents in the Jordan River. Overall, however, and despite this contribution of Mill Creek's load to the Jordan River, the BOD and VSS experience little change from upstream conditions. There is a slight increase in BOD during August, September, and October from upstream to downstream of the Mill Creek confluence and a slight reduction in BOD during November and December. There was very little change in VSS from upstream to downstream during the entire sampling period.

a.

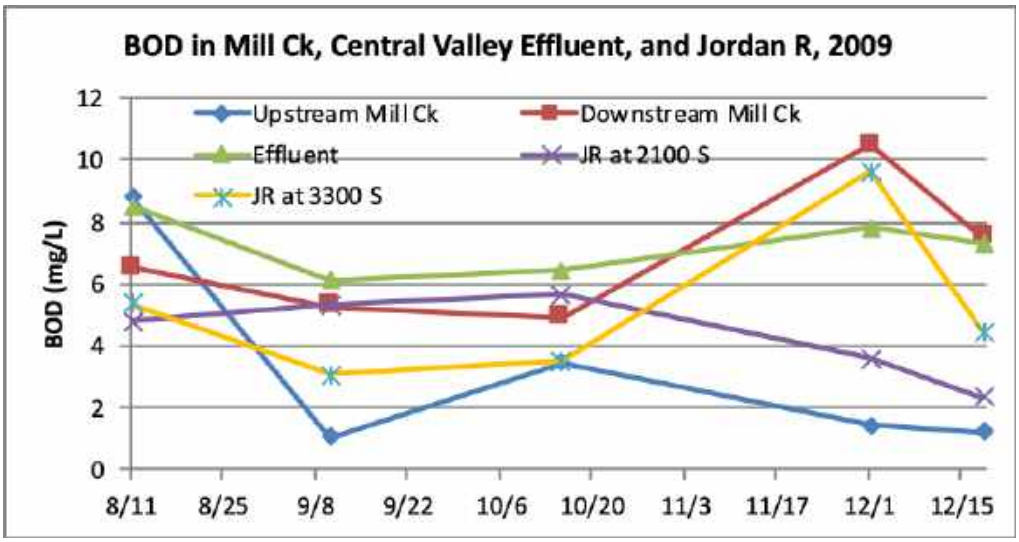

b.

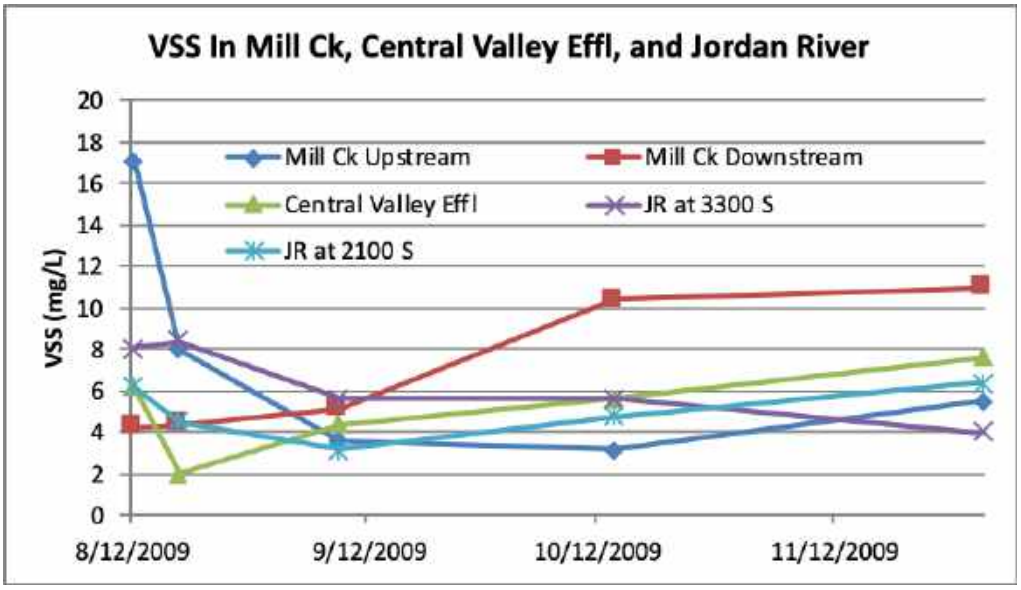

Figure 61. Detailed tracking of BOD (a.) and VSS (b.) at sampling sites in Mill Creek, located upstream and downstream from the Central Valley Water Reclamation Facility, the facility effluent itself and in the Jordan River upstream and downstream from the confluence with Mill Creek.

Similar samples were collected during 2010. These data are summarized in Figure 3. Average concentrations TSS and VSS were very similar to the 2009 samples. TSS remained relatively high through the narrows during 2010 as construction on the light rail train was continuing. Also similar to 2009, there was a general rise in TSS downstream from Center Street although VSS remained quite stable throughout the entire River. The dip in both TSS and VSS at 4800 S LCW is again, from sampling in Little Cottonwood Creek immediately above the confluence with the Jordan River.

a.

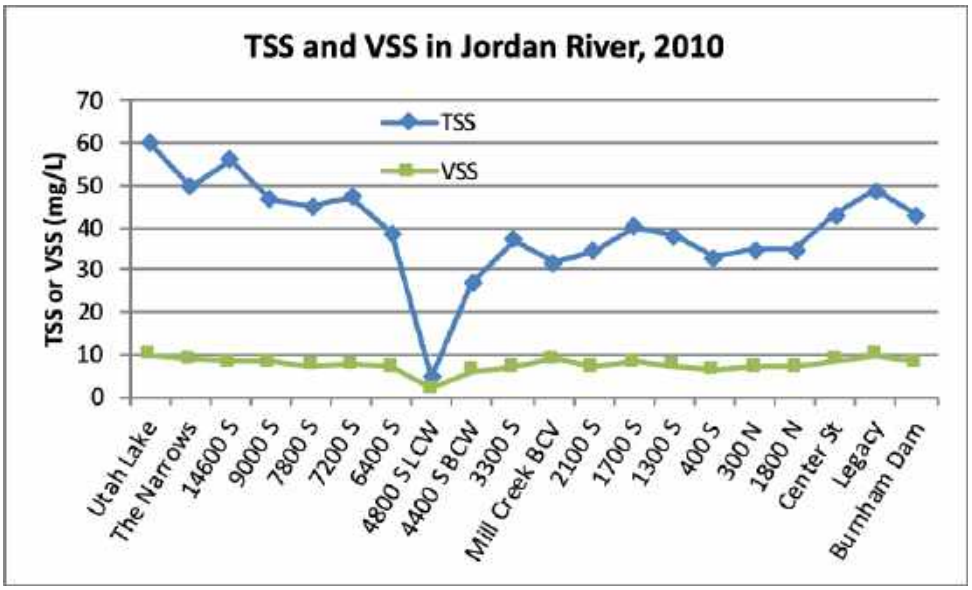

b.

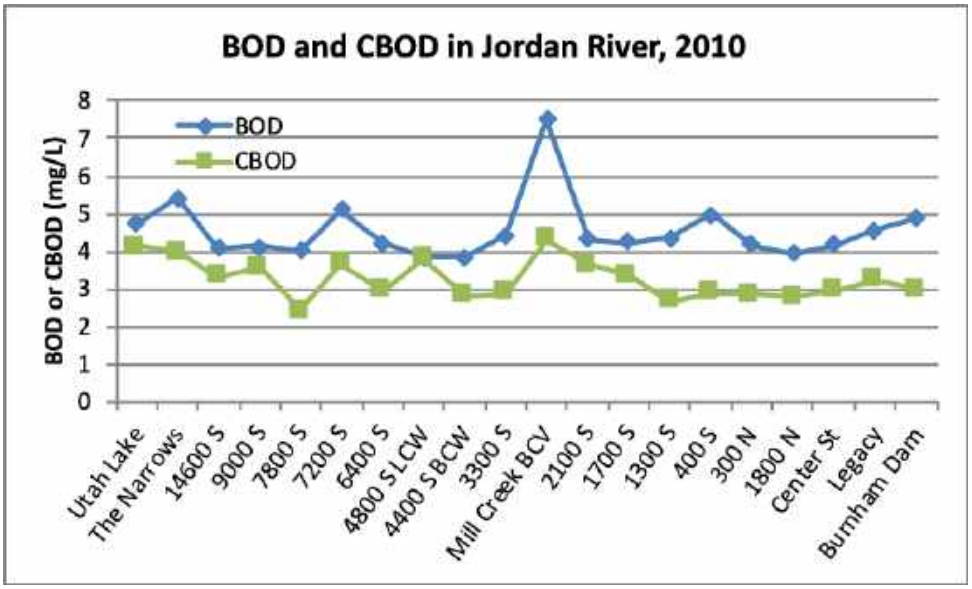

Figure 62. Mean of monthly total dissolved solids and volatile dissolved solids (a.) and BOD and CBOD (b.) samples in the Jordan River during 2010. Data include the means of monthly samples collected January through December.

The annual average concentration of BOD and CBOD in Mill Creek was also elevated during 2010. However, this was due to two very high measurements that likely also attributed to the storm drain near the 900 West Bridge (See figure 4). In the 2010 monthly data set, the average values in Mill Creek downstream from the Central Valley facility are also included (Figure 4). While some BOD and CBOD are being added from the Central Valley Discharge, the downstream values are often greater that the Central Valley discharge itself – indicating additional source(s) such as the illicit release from the storm drain described above.

a.

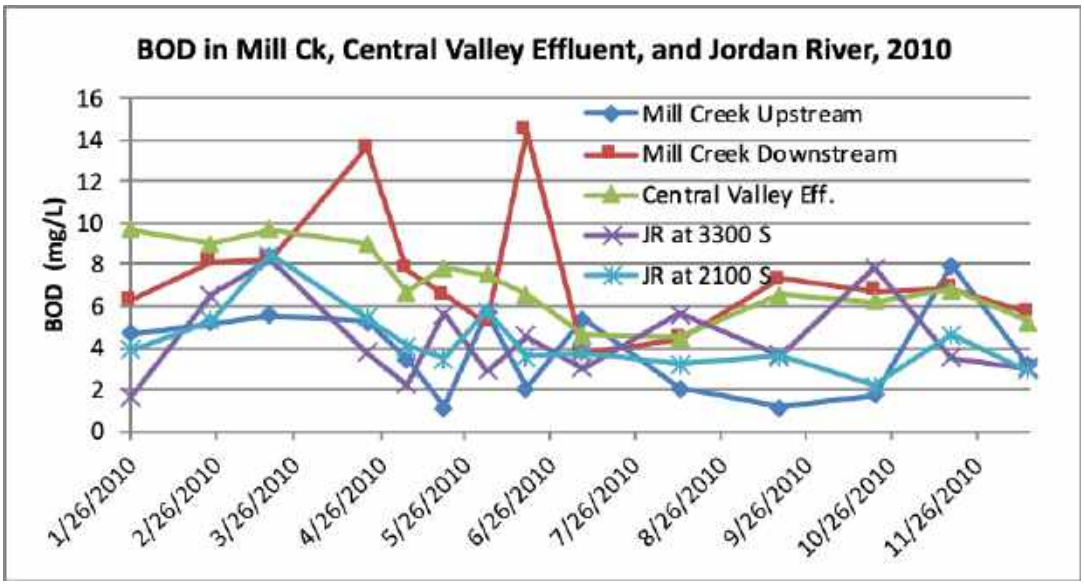

b.

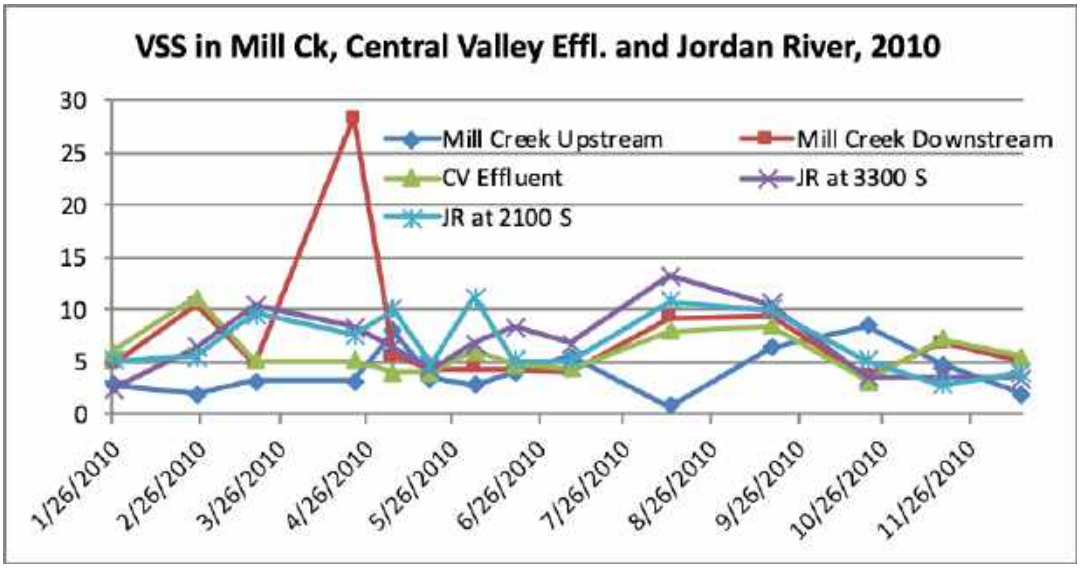

Figure 63. Detailed tracking of BOD (a.) and VSS (b.) at sampling sites in Mill Creek, located upstream and downstream from the Central Valley Water Reclamation Facility, the facility effluent itself and in the Jordan River upstream and downstream from the confluence with Mill Creek.

The two spikes in BOD downstream from the Central Valley discharge, in April and in June, reached much higher values than effluent concentrations. This suggests again, that the storm drain that discharges near the 900 W Bridge, or perhaps one of more of the others that discharge in the same vicinity are adding some BOD to Mill Creek.

Even so, neither the POTW effluent or the storm drain(s) appear to have a significant influence on the Jordan River downstream from the Mill Creek confluence. The BOD averages about 4 mg/L throughout the entire length of the river. The VSS was very similar between all sampling locations throughout the year. The only exception was the spike in VSS in the April sample collected downstream from the Central Valley effluent.

This was the same timing and location of the April spike in BOD. Finally, it should be noted that overall flows during 2009 were close to the long-term average for the Jordan River and surrounding watershed. The 2010 flows were only about 70% of normal flows. Although this would reduce overall loads and dilution capability, there was not a discernible difference in concentrations.

The 2011 data were similar to the previous years. BOD and CBOD remained in the 2.5 to 4 mg/L range throughout the length of the river (Figure 5). The TSS was somewhat higher and continued to increase through the downstream locations. Flows were about 40% above normal during 2011 due to a very wet and late spring. Indeed, for about three weeks, flows down the surplus canal were approaching the 1984 all time high record flows (USGS stream flow historic data). These unusually high flows likely suspended additional inorganic sediments (silt and clay material) that would normally be more stable under normal flows and velocities. Notably, the TSS actually increased at downstream locations, indicating that the resuspension of these fine inorganic materials was continually increasing in zones that were typically dominated by the settling of this material under the normal flows. Interestingly, there was not a concomitant increase in the VSS, which suggests that the two are independent (Figure 5).

We evaluated the local site-specific characteristics of BOD and VSS in lower Mill Creek again during 2011 (Figure 6). BOD and VSS were similar to previous years. There was an excursion of BOD in the April sample in the Central Valley Facility discharge that was also apparent in the downstream Mill Creek Sample. Also, BOD was elevated in the November and December samples, although this was not reflected as strongly in the downstream samples. In addition to the increase of BOD in April, there was an increase in VSS in the upstream Mill Creek samples later in the spring of 2011. This increase was likely associated with the unusually high runoff, but notably, was diluted by the lower VSS concentrations of the Central Valley Facility effluent. However, other than these brief excursions, BOD and VSS did not vary from previous years in either Mill Creek or the Jordan River.

a.

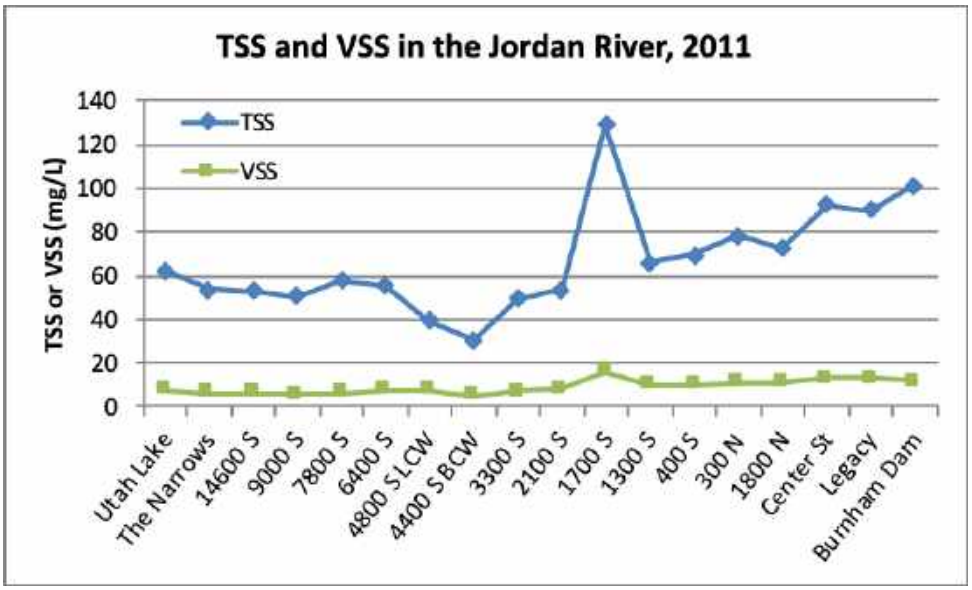

b.

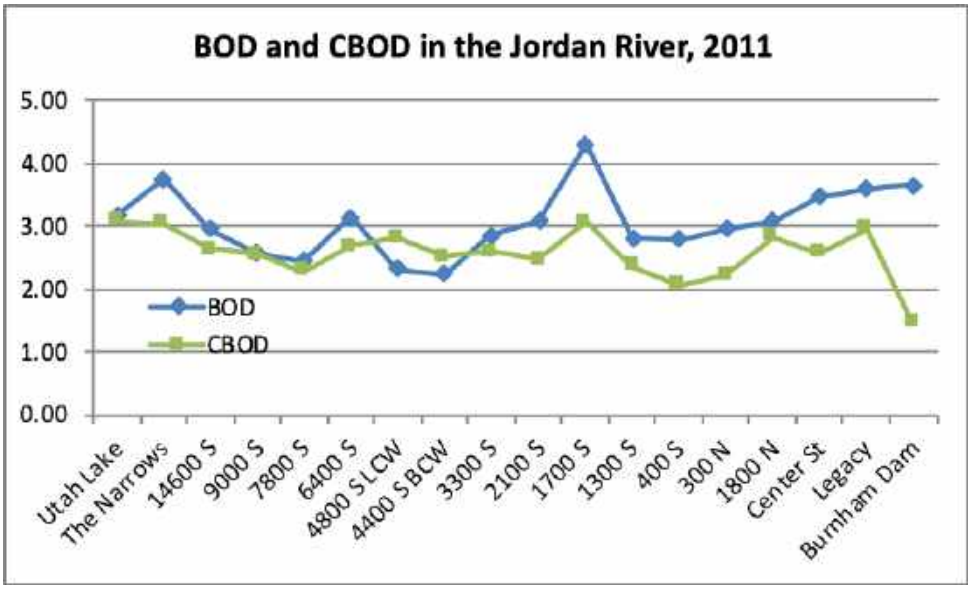

Figure 64. Mean of monthly total dissolved solids and volatile dissolved solids (a.) and BOD and CBOD (b.) samples in the Jordan River during 2010. Data include the means of monthly samples collected January through December. Fifteen samples were collected from each site and included at least one sample each month.

a.

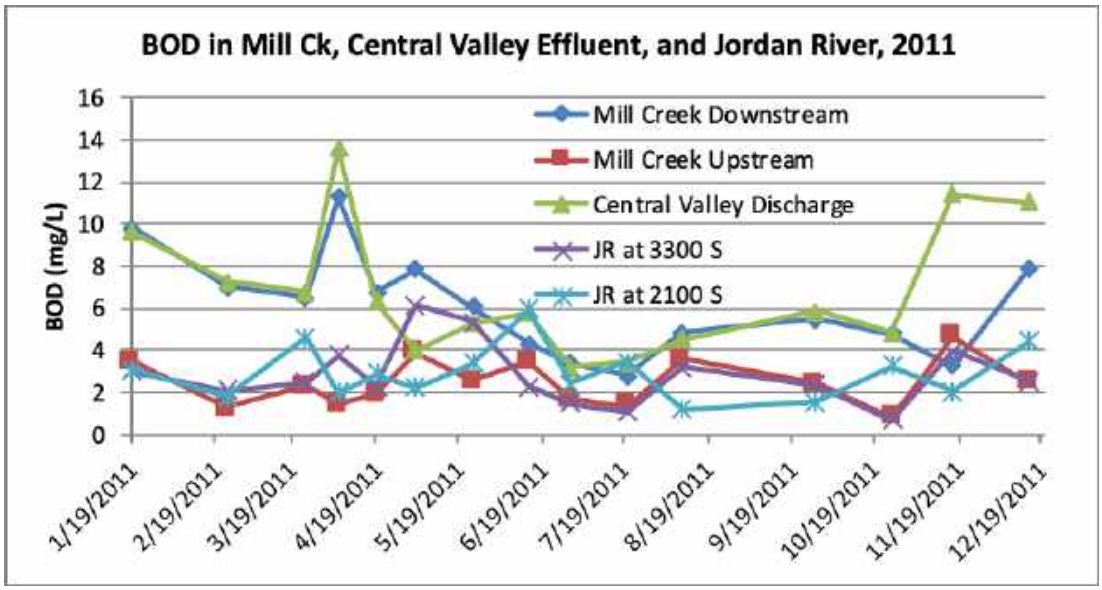

b.

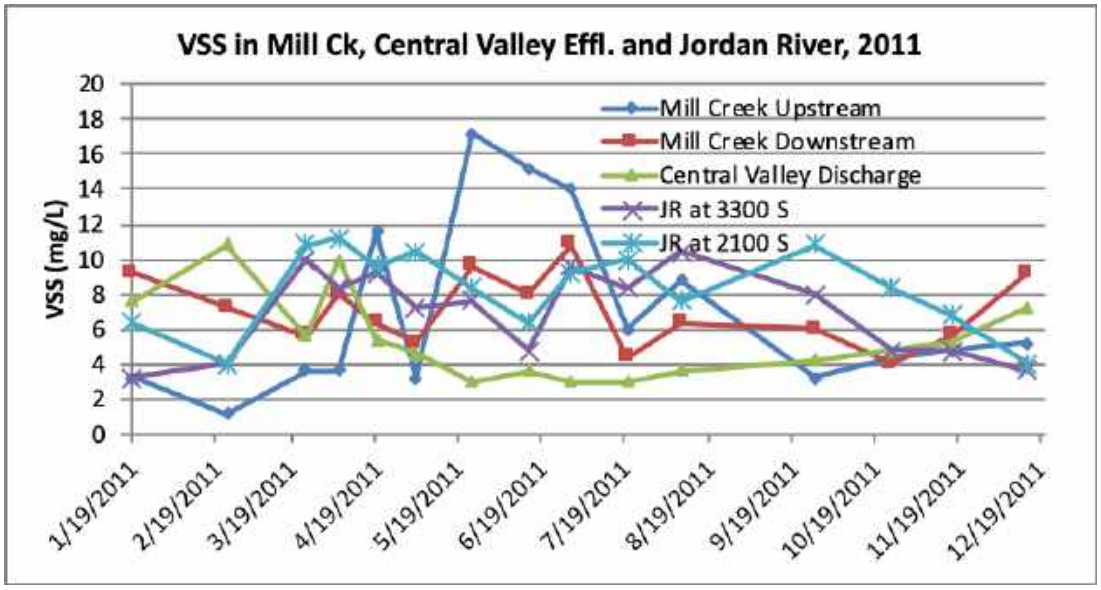

Figure 65. Detailed record of BOD (a.) and VSS (b.) at sampling sites in Mill Creek, located upstream and downstream from the Central Valley Water Reclamation Facility discharge, the facility effluent itself and in the Jordan River upstream and downstream from the confluence with Mill Creek during 2011. Data represent approximate monthly grab samples.

During 2012 flows were once again below average. For 2012 data, the BOD, CBOD and VSS are reported separately for winter and summer to determine if season or temperature influenced these characteristics of the river. BOD and CBOD are illustrated in Figure 7. There were clearly no seasonal differences between BOD or CBOD.

a.

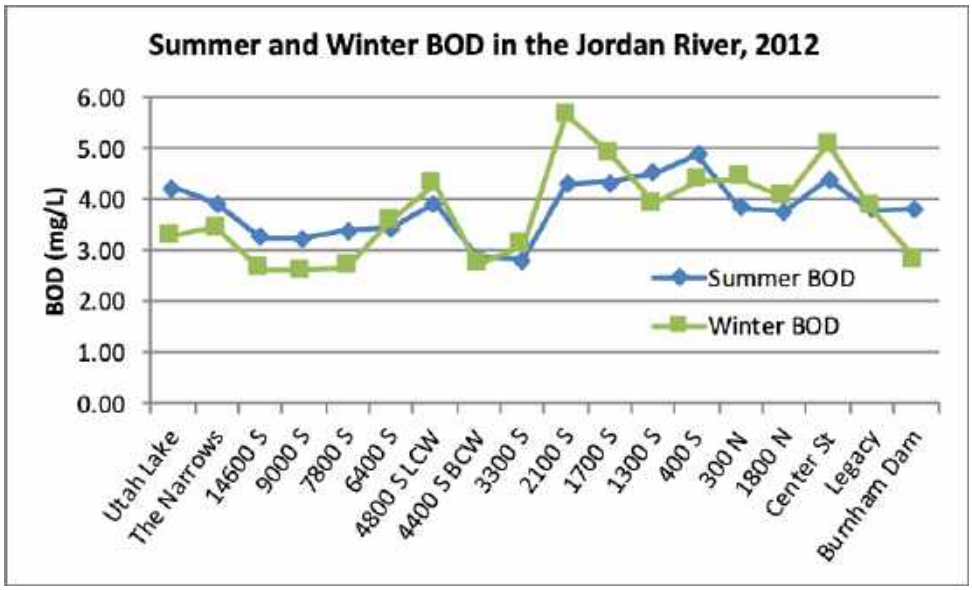

b.

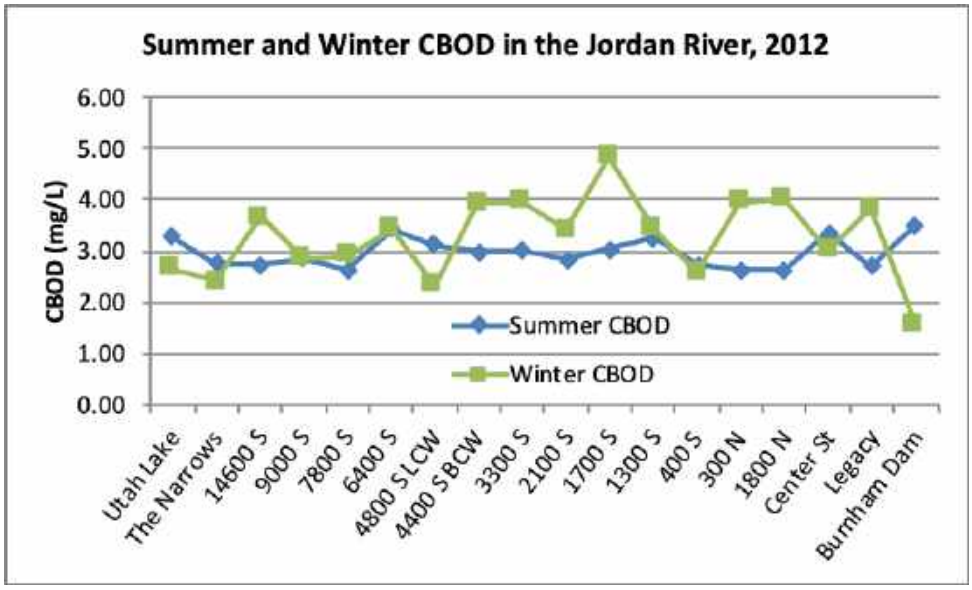

Figure 66. Mean of monthly BOD (a.) and CBOD (b.) samples collected from the Jordan River during 2012. Fifteen samples were collected from each site and included at least one sample each month.

Seasonal separation of TSS and VSS data was also performed (Figure 8). In these graphs, summer sampling was defined as May through October and winter was defined as November through April. As such, the elevated spring runoff months were likely responsible for the elevated VSS and TSS. Summer values were elevated until about the area of the Surplus Canal diversion where the channel and Surplus Canal flows would be more equalized and hence might be expected to moderate the difference between seasons. It should also be noted that for both seasons, Little Cottonwood and Big Cottonwood creeks contained lower concentrations of VSS and TSS. Yet, the samples collected at 3300 S were similar to those collected upstream from these two tributaries- suggesting there was not a lot of dilution.

a.

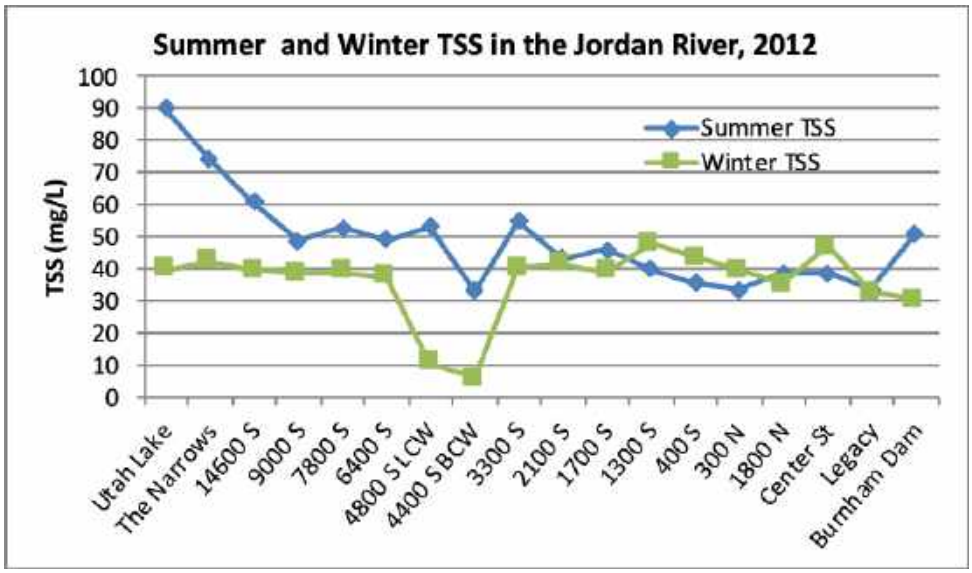

b.

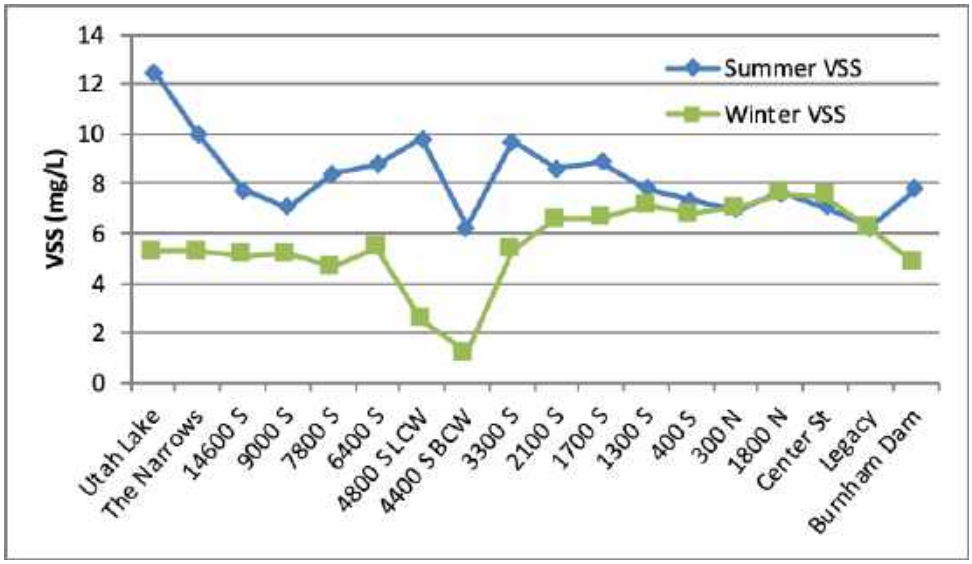

Figure 67. Mean of monthly TSS (a.) and VSS (b.) samples collected from the Jordan River during 2012. Fifteen samples were collected from each site and included at least one sampling event each month.

DO and Temperature Recordings

Another key goal of the Council was to elucidate the dissolved oxygen dynamics in the reach that DWQ listed as impaired and more fully ascertain whether this reach should actually be listed as impaired. In their assessment decision, the DWQ did not use EPA's recommended dissolved oxygen assessment method (described in EPA's Water Quality Criteria for Dissolved Oxygen, 1986 document) to determine beneficial use support before they concluded that the lower reach is impaired. As such, we requested all of the available data that DWQ used for this assessment. Figure 9 illustrates a summary of all of the instantaneous data collected at Cudahy Lane (the designated compliance point). The acute water quality standard is 4.0 mg/L. To account for natural variability and to satisfy concerns over measurement accuracy and to avoid type I (false positive) errors, the

assessment criteria states that if 10 percent or greater of the sample data acquired during the assessment period is less than the 4.0 mg/L standard, the water body is impaired. Because the Integrated Report (305(b) assessment and 303(d) list of impaired waters) is submitted every two years to EPA, an assessment period is usually the 2-year period prior to the reporting year, but data within the previous five-year period is often used. A minimum of ten samples must be used and is preferably collected within a one-year time period and the data are expected to represent seasonal data. In some cases, if ten samples have not been collected during the previous two years, the assessment period is extended to five years. Yet, "data as old as ten years may be used if information is available to validate that there has not been a significant disturbance in the watershed during the ten years that would significantly change the results of the assessment." We reviewed all of the data that DWQ provided and a summary of this data collected at Center Street (the compliance point) is presented in Figure 9. Over the 14-year period of record, there were five violations of the 4.0 mg/L standard. Further, all of these violations occurred during drought years when low flows allow greater stream warming and provide for less turbulence and surface reaeration. In addition, the overall lower mass of water in the stream channel causes it to be more exposed to sediment oxygen demand and susceptible to short-term changes in DO. Such extremely low flow data are displayed for the summer and fall of 2008 in Figure 10. Flows were held to only 40 to 80 CFS during the normal runoff period of May and June and remained below about 140 CFS for the remainder of the year. Hence, any CPOM that was transported to this lower reach settled and proceeded to decompose, along with the previous years' CPOM-contributing to elevated SOD values. For comparison, there has never been a recorded DO violation in the Surplus Canal, where the majority of water is diverted, even though this is the exact same water as that which continues down the river channel.

We also received data from the State Canal, a constructed canal that transports water from the Burnham Dam to Farmington Bay Waterfowl Management Area (Figure 11). This site used to be included in the assessment process. In this case there were only two violations of the 4.0 mg/L DO standard and they occurred during the same low-flow period of 2008.

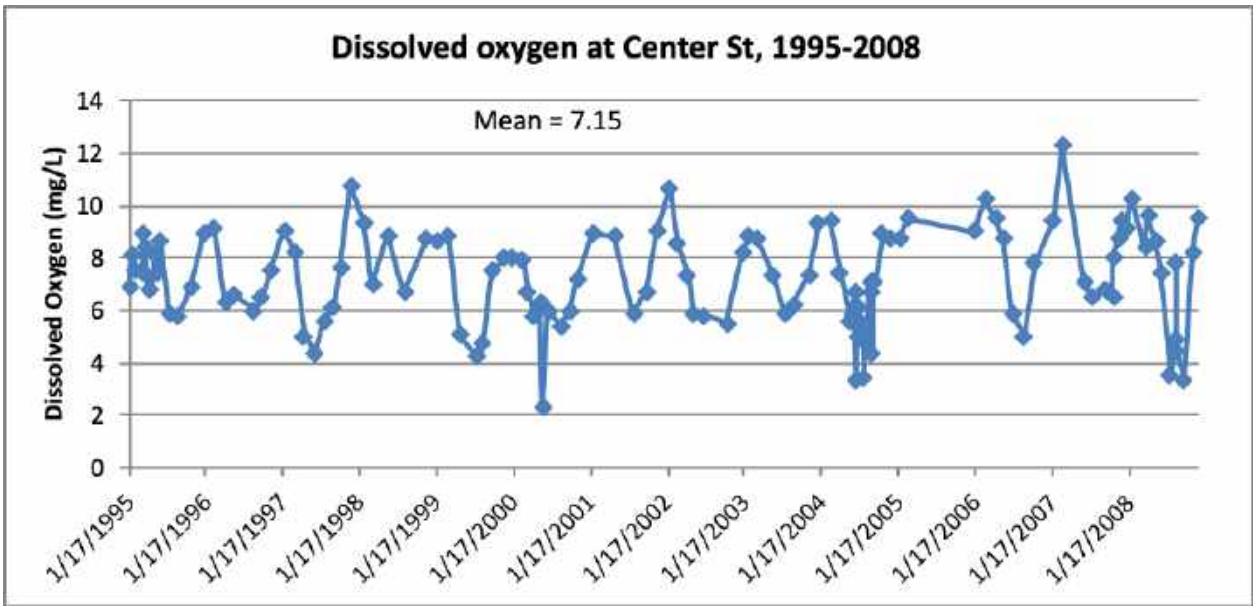

Figure 68. Dissolved oxygen recordings in the Jordan River at Cudahy Lane (Center Street) from 1995 to 2008. Note a total of 5 violations of the DO criterion or 4% of the 125 samples collected.

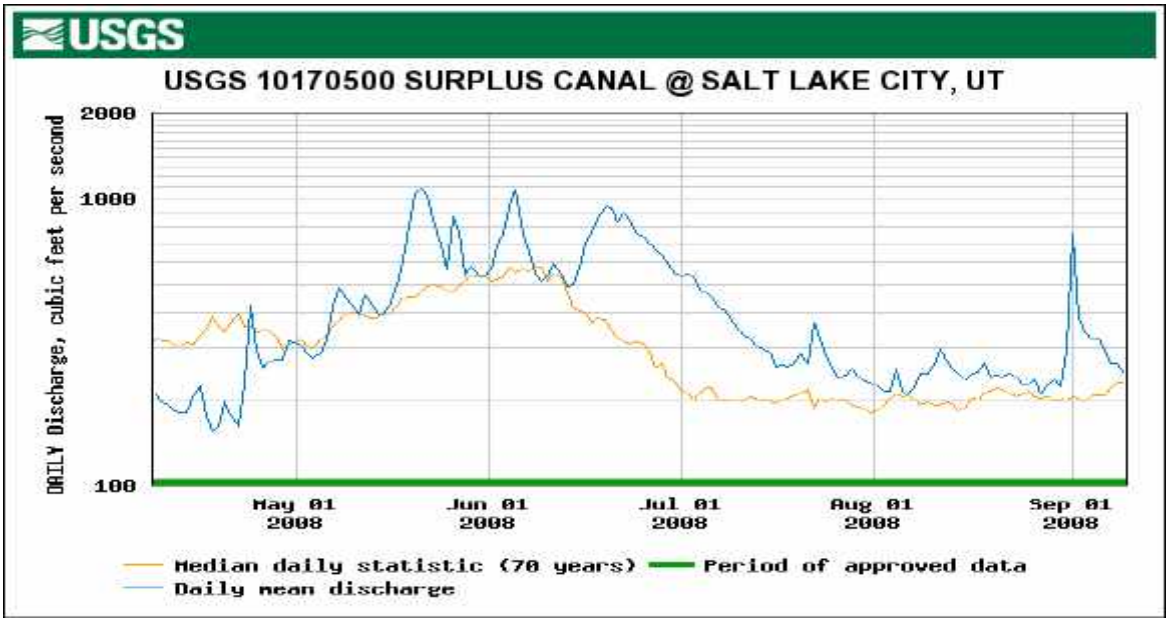

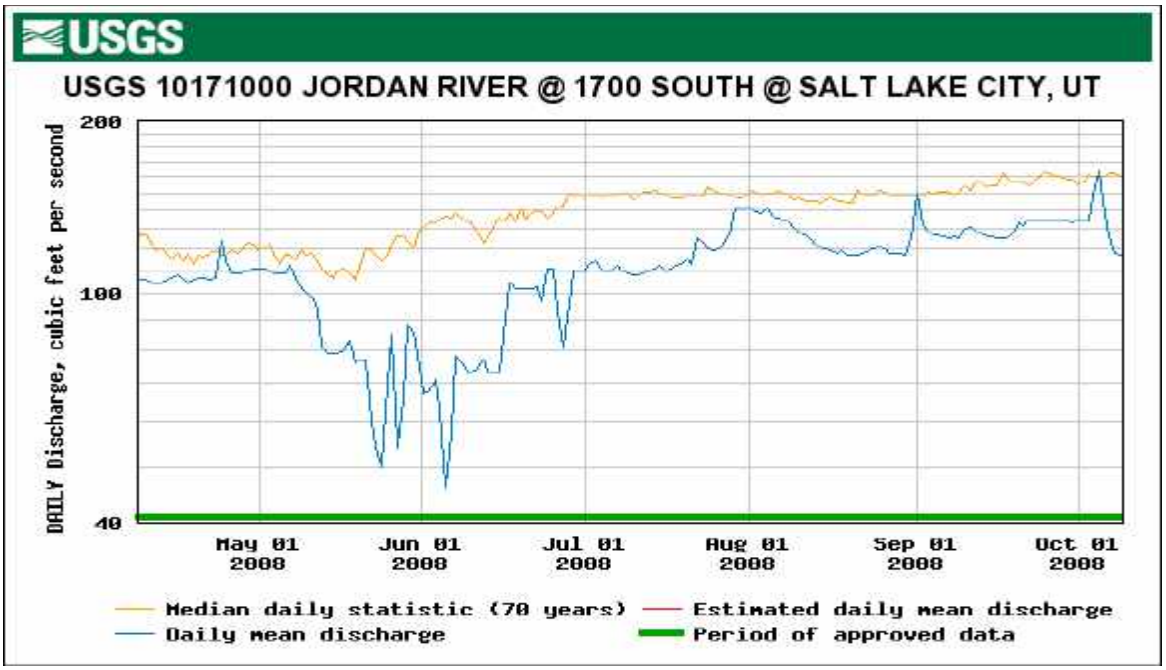

Figure 69. USGS flows recorded in the Surplus Canal (upper) and at 1700 S (lower), during 2008. Note although above average flows occurred in the surplus Canal, only very minimal flows were allowed to continue down the river channel – particularly during the normal runoff period. Flows were held at less than half the average flows for the entire year exacerbating warmer temperatures, lower re-aeration and elevated SOD rates.

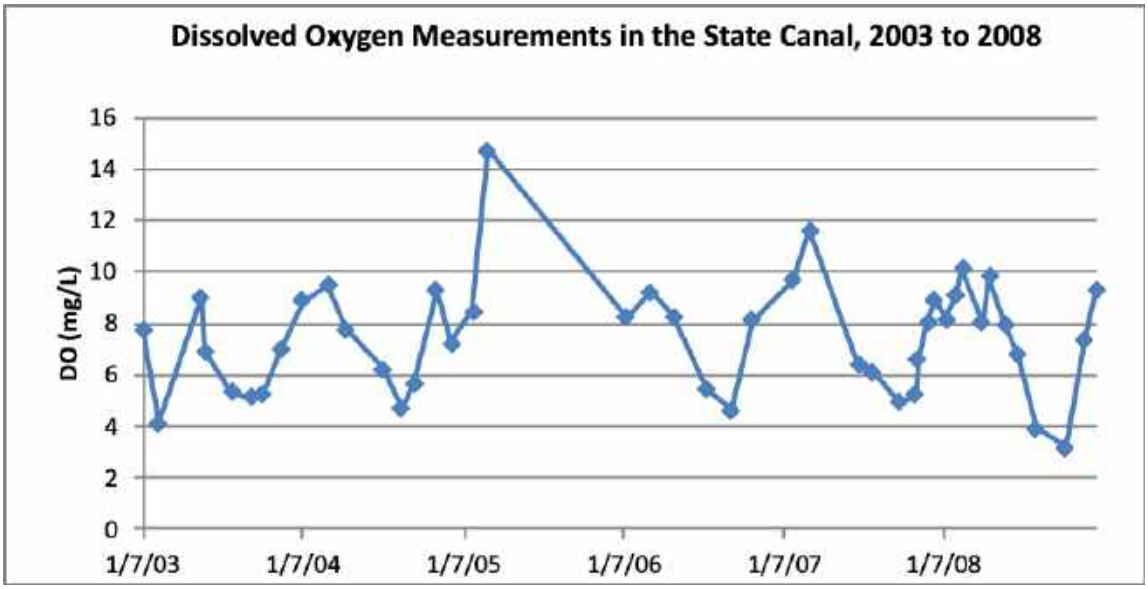

Figure 70. Dissolved oxygen measurements in the State Canal. Note only two violations throughout this six-year period.

This was 4.5% of the total sample data. Data from the Jordan River at Center Street and the State Canal were used by the state DWQ in the determination that the lower Jordan River was impaired. Yet, these data clearly indicate that with the low number of exceedences, there is no apparent violation of the DO standard. However, DWQ also

used these data to assess against the chronic criterion and used this comparison to justify that the lower Jordan was impaired. However, DWQ did not use EPA's recommended methodology for making such a determination. Instead, DWQ developed a unique but controversial, and imprecise manner of applying grab sample data to the more stringent 7-day and 30-day average criteria. The 2008 Integrated Report states "Dissolved oxygen follows a diurnal cycle with the highest values occurring during the day. The AU (assessment unit) is listed on the 303(d) list if two or more samples are less than the 30-day standard and if the standard is violated in more than 10% of the samples." This creates a defacto rule that allows the much more stringent chronic criteria to be used in place of the acute criterion for assessment purposes. Not only is this imprecise, but it is directly discordant to the methods prescribed in EPA's criteria document for dissolved oxygen (US EPA 1986). Briefly the document states "If daily cycles of dissolved oxygen are essentially sinusoidal, a reasonable daily average is calculated from the day's high and low dissolved oxygen values. A time-weighted average may be required if the dissolved oxygen cycles are decidedly non-sinusoidal.

Determining the magnitude of the daily dissolved oxygen cycles requires at least two appropriately timed measurements daily and characterizing the shape of the cycle requires several more appropriately spaced measurements." (US EPA 1986). Because EPA recognized the importance of a longer-term chronic criterion, it provided these specific instructions for calculating this value. Clearly, this method would need to be used to develop a truly accurate assessment against the 7-day or 30-day average. Also, it is obvious that these instructions were provided prior to the availability of data recording sondes, but also prior to the listing of the Lower Jordan as impaired, so these instructions were available prior to the assessment decision.

Also, recording data sondes have been available now for at least ten year and DWQ has owned such probes for nearly that long. Yet, no effort has been made to either acquire the necessary data according to EPA's instructions, or to use the sondes to confirm whether the lower Jordan actually violates the 7-day or 30-day chronic criterion. Where such a high profile and expensive TMDL would be imminent, this simple confirming step should have been required. Further yet, with DWQ's apparent belief in the paradigm that low DO concentrations result from eutrophication, all of the POTWs along the Jordan River would be held accountable as the source of nutrients and subjected to extremely expensive (in the range of $1,000,000,000 total) upgrades or new construction costs for advanced nutrient removal. With such a price tag at stake, which would essentially double most sewer rates, along the Wasatch Front, DWQ should have performed additional monitoring and analyses to document that there was truly an impairment based upon EPA's assessment protocols. Because of this paucity of essential data, whether the lower Jordan River belongs on the 303(d) actually remains dubious.

Yet, because there were actually an insufficient number of acute DO violations, the initial drafts of the TMDL and even the Phase I TMDL document erroneously reported numerous violations of the chronic 5.5 mg/L criterion based on its arbitrary assessment method. This prompted the Council to purchase and deploy recording data sondes to begin collecting the appropriate data to elucidate the frequency, duration, and cause(s) of

low DO and ascertain whether conditions exist that qualify the lower Jordan to be listed as impaired. These sondes were deployed throughout most months of the year.

Monitoring sites located upstream and downstream from 2100 S were included, although greater emphasis was placed on sites below 2100 S because this is the reach identified as impaired and indeed experienced episodes of low DO. Following are representative graphs of data collected during the critical summer months.

A total of four sondes were deployed at these various locations 2009 to 2012. Most of these sondes were fitted with temperature and DO probes only. One sonde was fitted with temperature, DO and pH. One of the first recordings was performed August 18 at 2100 S. Even though this deployment lasted for only 20 hours it reveals the typical diel pattern of DO and pH (Figure 12). The swing from the late afternoon peak to the early morning minimum is the result of the cessation of photosynthesis and oxygen production. Respiration continues, however, consuming oxygen while producing and releasing CO_2 which also lowers the pH. In the morning hours, after the sun angle is high enough to penetrate the water column with enough light energy, photosynthesis resumes. Shortly thereafter, there is enough oxygen produced to overcome the rate of respiration, causing the oxygen to rise again. Hence the daily DO minimum actually occurs shortly after sunrise.

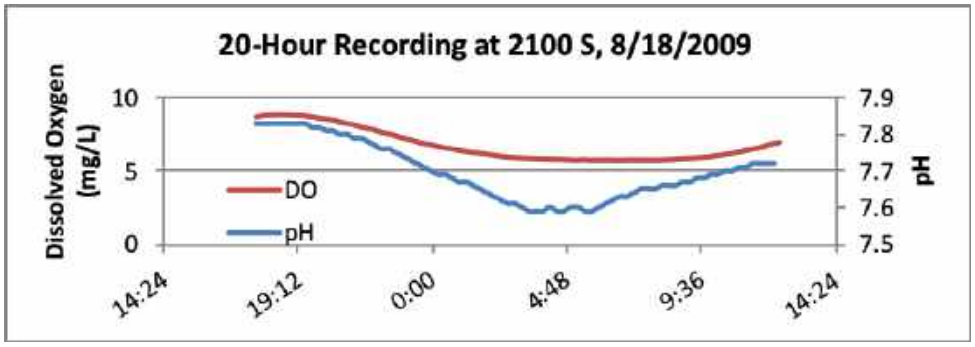

Figure 71. Twenty-hour recording of DO and pH at 2100 S, August 18, 2009.

A second DO recording was performed at 2100 S later in August (Figure 13). Maximum and minimum values were similar to the earlier recording. However, the recording performed at 400 S during this same time period indicated that while the range between maximal and minimum values remained at about 3 mg/L, the range was actually much lower with maximum and minimum values between about 7.6 and 4.7 respectively, (Figure 4.13). At sampling stations further downstream the diel range of DO began to decrease, as well as the average DO concentration. At Center St the difference between the maximum and minimum values was less that 2.5 mg/L with the maximum and minimum values ranging between about 6.2 and 5.2. (Figure 4.14 a.) At Burnham Dam, the range further declined to a fluctuation of about 1 mg/L (Figure 4.14 b.). More notable however, the maximum and minimum of this range declined to between 5.5 mg/L and 4.5 mg/L respectively.

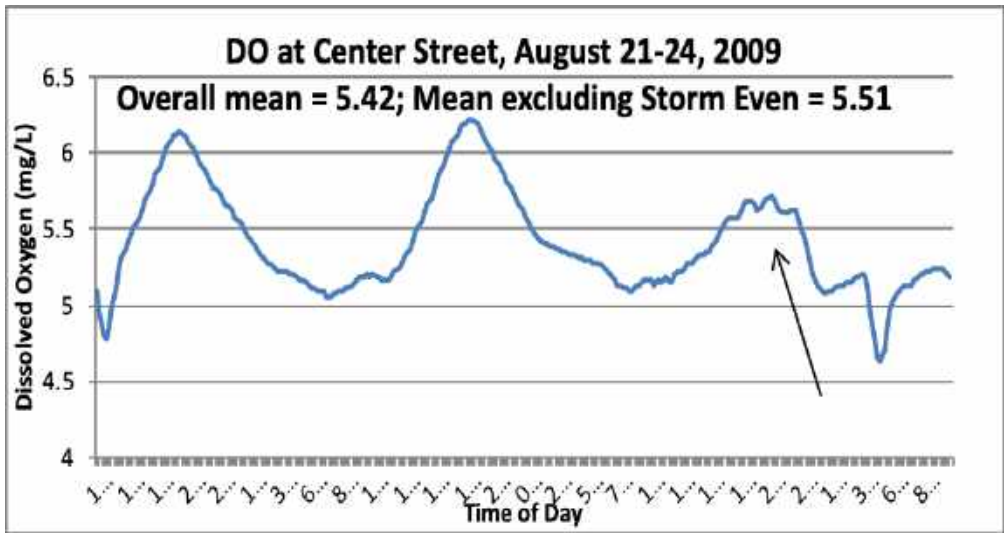

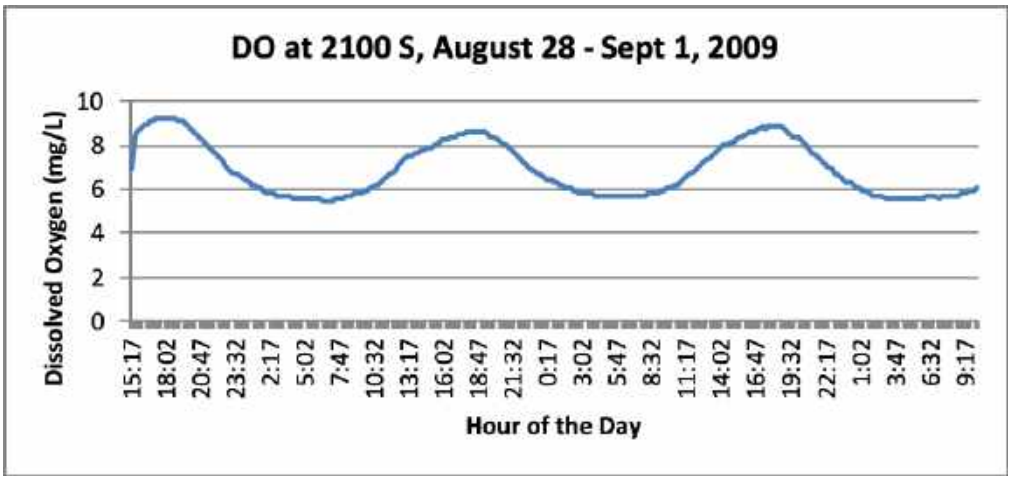

Figure 72. Record of DO between August 28 and September 1, 2009.

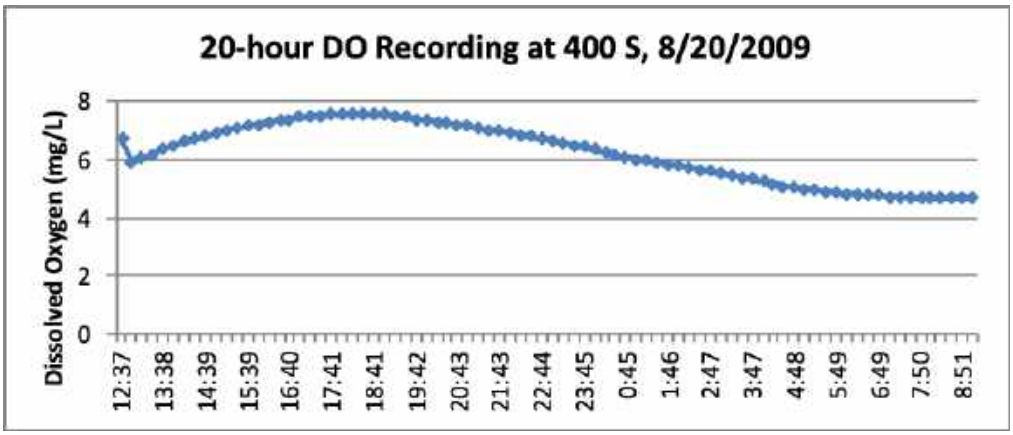

Figure 73. Twenty-hour recording of DO starting on 8/20, 2009 at 400 S.

a.

b.

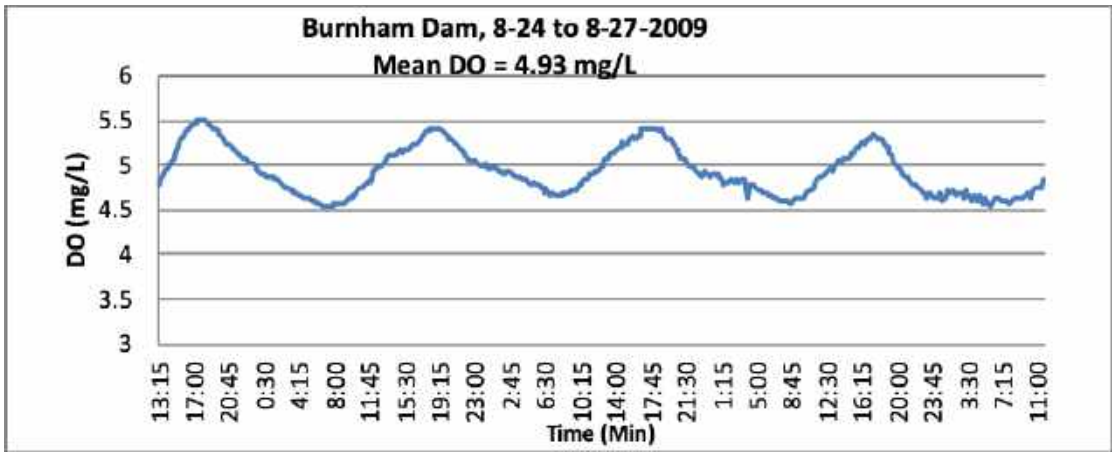

Figure 74. Dissolved oxygen records measured at Center St. (a.) and at Burnham Dam (b.), during late August 2009. Both the range and the average of DO declined between these two stations and between these and upstream stations.

Flows during this time period and the previous few weeks averaged about 250 CFS in the Surplus Canal (USGS stream flow data; Figure 15) and averaged about 220 CFS at the Salt Lake County 500 N gage (data not shown). This was somewhat above average late summer flows. However, spring flows during 2009 started in early May and continued until early July and ranged between 3 and 4 times average spring runoff. This above-average runoff undoubtedly transported above average and considerable quantities of suspended and bedload organic debris to the lower Jordan even though the majority of flow was diverted to the Surplus Canal (See Chapter 3, 2011 CPOM data).

Settling/deposition would similarly occur following these high flows as large amounts of organic sediments have been documented starting with the SVAP study of 2009 (See Chapter 1) and observed in virtually every sampling event since that time. Also, as mid to late summer flows diminished, this fresh sediment smothers any existing benthic algae, limiting primary production to the remnants of Utah Lake algal populations and a small amount of dislodged periphyton from upstream sources that remained in the water column (See Chapter 3). These low flows also reduced the effectiveness of surface reaeration as turbulence diminished which limited the frequency of surface boundary reformation (See Chapter 5). We have hypothesized, as with other researchers, that if greater flows were allowed to remain in the lower Jordan River Channel, this would provide for more effective flushing and less settling of organic matter. In turn, this might reduce the magnitude of sediment oxygen demand and improve reaeration rates. Although it is possible to maintain somewhat higher flows in the channel, these flows are limited by the potential for flooding adjacent neighborhoods and, hence, the requirement to maintain some channel capacity in the event of thunderstorms in the local Salt Lake City watersheds. Nevertheless, the level to which elevated flows can be maintained is the subject of a proposed study by River Network and DWQ. The data acquired thus far indicates that this continual diversion and dewatering of the channel diminishes the flushing ability and exacerbates the sedimentation of fine sediments and organic debris. This greatly degrades the aquatic habitat, both physically and with respect to the DO because of elevated SOD.

Such man-caused or natural degradation of aquatic habitat conditions have been addressed in the Code of Federal Regulations with respect to the ability to achieve Clean Water Act goals and this has become one of the issues raised by the Council to the Utah DWQ. Specifically, in addition to questioning the initial action of listing the Jordan River based on the number of DO violation, we also raise the question of whether to beneficial uses are being maintained due to severe habitat alteration and dewatering. The over-arching issue is the diversion of the great majority of flow, and particularly the potential flushing flows. Even under low flow conditions at least half of the water is still diverted. Although this provides water for vast acreages of wetland habitat and prevents flooding of northern Salt Lake City neighborhoods, this diversion drastically dewaters the river which severely alters its aquatic habitat.

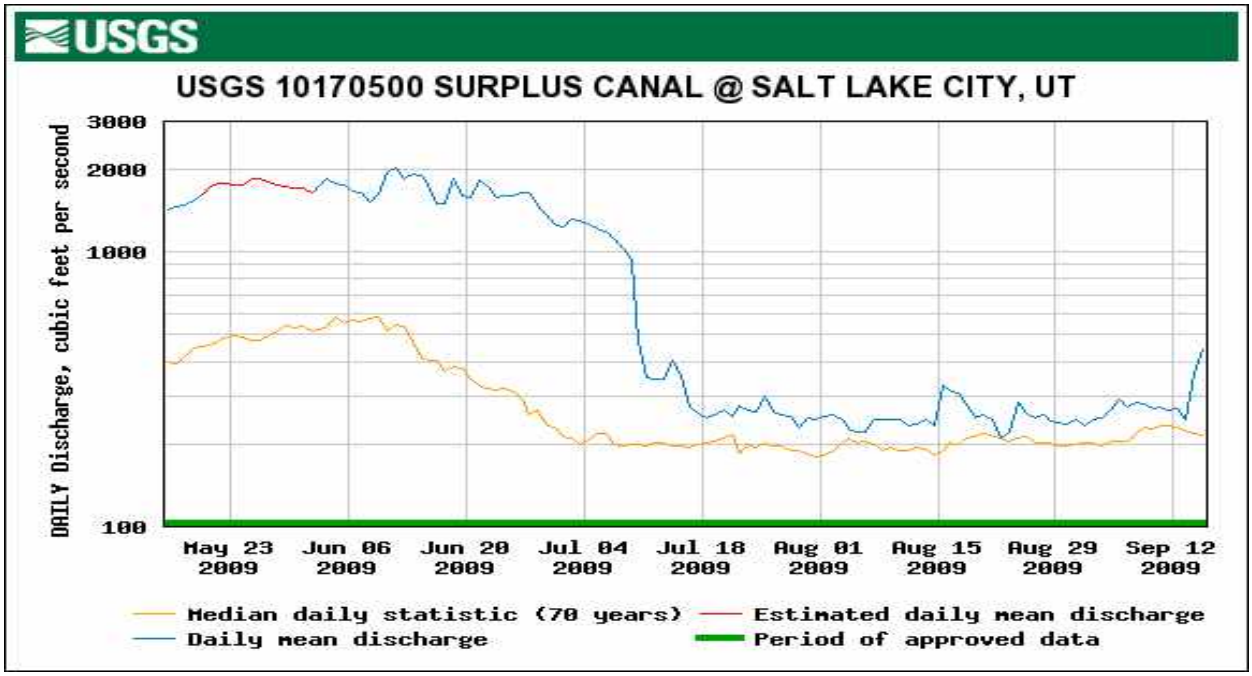

Figure 75. Spring and summer flows measured in the Surplus Canal during 2009. The yellow (lower) tracing is the 70-year median value.

To account for natural background conditions or man-caused impacts on streams which prevent the water body from achieving water quality goals, the Clean Water Act provides for off ramps or exemptions to 303(d) listing of impaired waters (40 CFR § 131.10(g). These (g) factors include a list of physical or chemical conditions that prevent the attainment of designated beneficial use. In other words, these "g factors" constitute irreparable impacts that cannot be restored or would cause undue economic hardship on the community. Performing a Use Attainability Analysis is the proper procedure for this determination. The lower Jordan River qualifies for at least three of the six "g" factor off ramps: Factor number (2) "Natural, ephemeral, intermittent or low flow conditions or water levels prevent the attainment of the use, unless these conditions may be compensated for by the discharge of sufficient volume of effluent discharges without violating State water conservation requirements to enable uses to be met"; Factor number

(4) “Dams, diversions or other types of hydrologic modifications preclude the attainment of the use, and it is not feasible to restore the water body to its original condition or to operate such modification in a way that would result in the attainment of the use”; and Factor number (5) “Physical conditions related to the natural features of the water body, such as the lack of a proper substrate, cover, flow, depth, pools, riffles, and the like, unrelated to water quality, preclude attainment of aquatic life protection uses”. Due to the dominance of the 2100 S diversion, these factors are inextricably linked.

The Council began addressing Factor (5) with the Stream Visual Assessment Protocol (Chapter 1) in 2009 and documented severely degraded habitat due to channelization, frequent dredging, riparian loss, dewatering and sedimentation. Factors (2) and (4) are of equal importance. An illustration of the impact of the 2100 S diversion on the hydrology (Factor 4), of the Jordan River is displayed in Figure 16. The diversion of flow represents a significant impact in that any flows above base flow (150-175 CFS) is diverted to the Surplus Canal; Prevention of flushing flows allows increased settling of organic and inorganic debris that has been identified as the cause of high sediment oxygen demand values Chapter 3. As well, there are times when nearly all flows are diverted to the Surplus Canal in anticipation of a storm event in Salt Lake City’s watershed (Figure 17).

a.

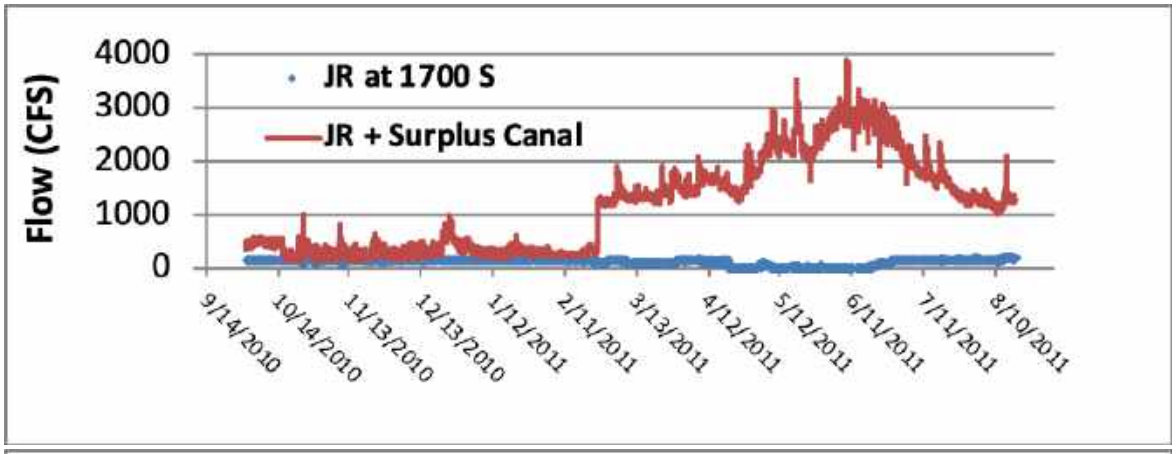

b.

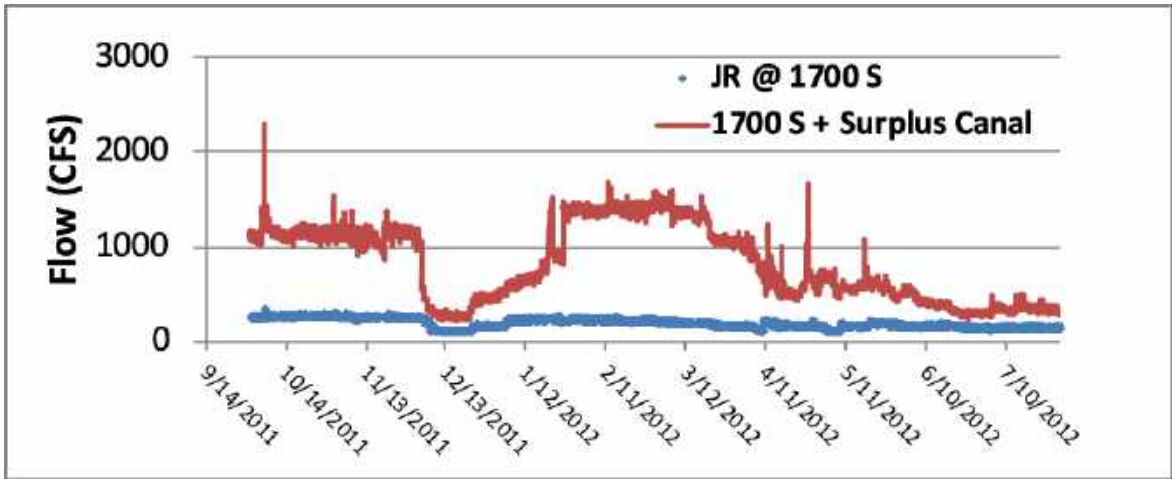

Figure 76. Detailed recordings of flow measured at 1700 S and the combination of this flow with the Surplus Canal flow. Figure 16a. is the annual flow from September of 2010 to September of 2011.

Note the near-record flows during June (exceeding 3000 CFS) yet flows in the river channel were reduced to between 20 and 100 CFS – eliminating the potential for beneficial flushing flows through the lower Jordan River. (b.) is a continuation of (a.) and ends at August 1, 2012. Because of the accumulation of water in Utah Lake from the high 2011 flows, water was released throughout most of the winter to create additional capacity in anticipation of potential high spring flows in 2012. However, this did not occur, resulting in unnatural and very low runoff flows during the 2012 spring.

This severe loss of flow from the channel transforms the lower Jordan River into a nearly exclusively depositional segment. The slow laminar flow has filled in potential pool areas with fine silts and clays that are mixed with 5-15% organic debris (Mitch Hogset, University of Utah, personal communication). These fine anaerobic sediments preclude colonization by a variety of stream organisms typical a stream with diverse particle sizes, proper pool to riffle ratios and a proper riparian corridor. Additional evaluation of Factors (2) and (4) included deployment of recording sondes in the Surplus Canal, as well as the lower Jordan River. Except for the rare occasion when storm water collects in watersheds and storm drains that flow through the city, the water in the Canal is identical to the water in the river channel. Yet, the Canal has never experienced a violation of the acute or 30-day average DO criteria. A representative recording is illustrated in Figure 18.

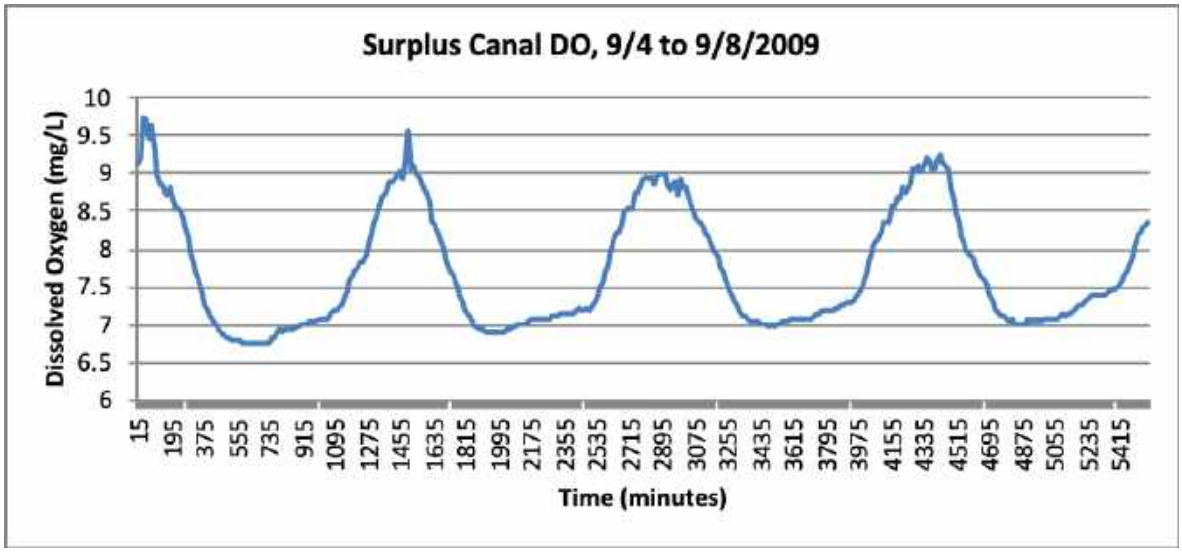

Figure 77. Dissolved oxygen concentrations recorded in the Surplus Canal at the USGS gage near the Salt Lake City international airport.

Contrary to the lower river, the greater velocity, depth and mass of water results in greater atmospheric reaeration, a much lower settling rate of organic debris and a greater volume of water that is removed from the exposure to even this lower sediment oxygen demand (greater volume:sediment surface ratio; See Chapter 6).

Additional late spring, summer and fall DO and temperature recordings were made during 2010, 2011 and 2012 using the portable data recording sondes. Dissolved oxygen concentrations at 2100 S remained near saturation throughout the summer even though temperatures increased to above 20 C (Figure 19).

Figure 20. is the first recording of DO during a high flow event – a common event that highly influences the oxygen dynamics of the lower Jordan River. This was a relatively small storm event which resulted in a relatively small dip in DO. There was an increase in flows at the USGS Surplus Canal gage of about 35% (from 210 to 282 CFS) on August 24, although elevated flows were not observed at 1700 S or the 500 N gage. This suggests that the storm event occurred in one or more of the local watersheds that join the Jordan River upstream from the surplus Canal diversion (e.g. the Cottonwood canyons). Yet, although the Surplus Canal received all the increased flow, the elevated concentrations of the highly reactive organic carbon that was mobilized during the storm was still in the water that continued down the river channel as well. This dissolved organic carbon has been found to correspond to a rapid and often deep depression in DO in the lower reaches of the river (See Permanent Data Sonde section below).

a.

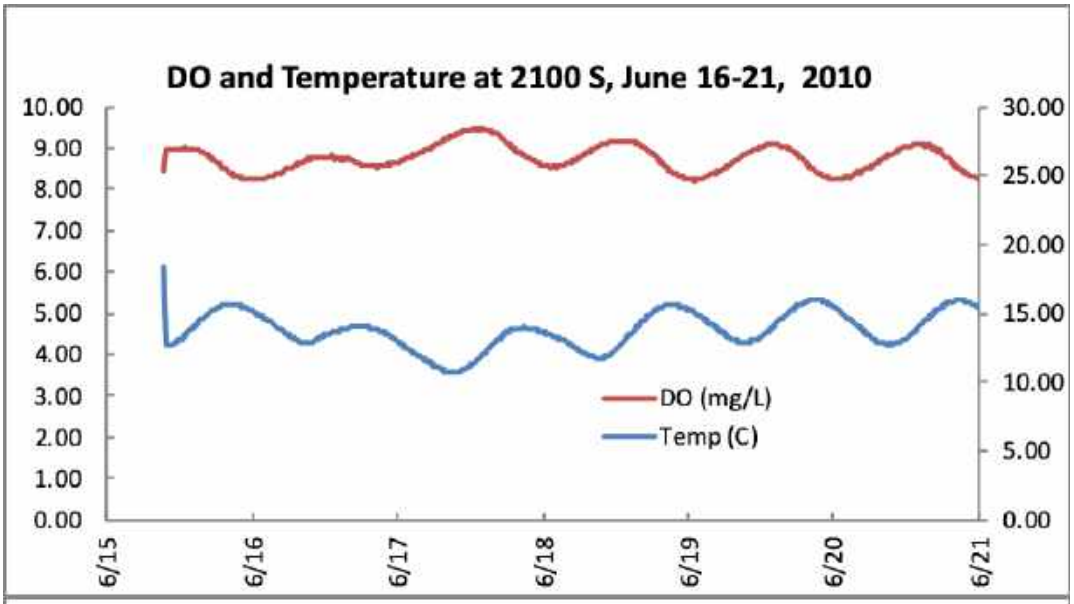

b.

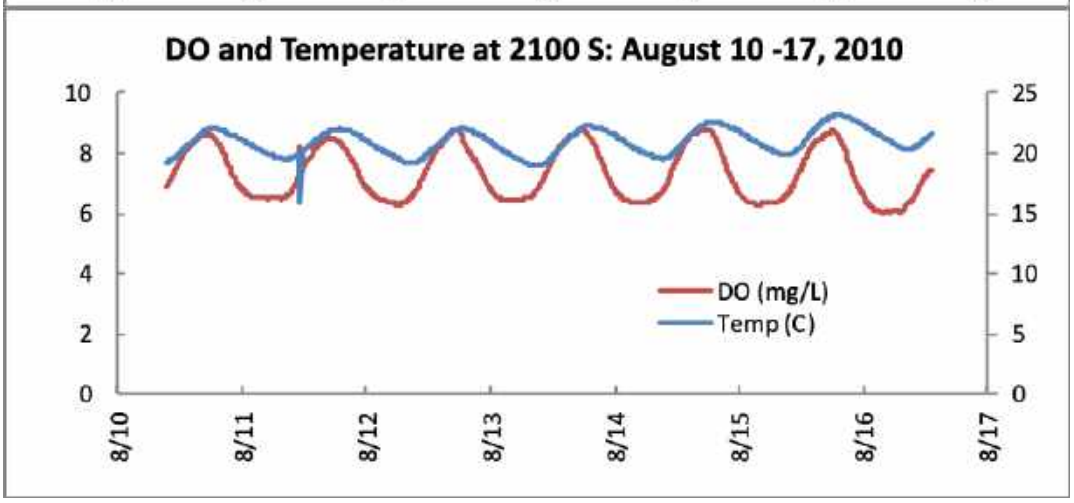

Figure 78. Dissolved oxygen and temperature recorded at 2100 S during June (a.) and August (b.).

At 1700 S there were three excursions from the typical sinusoidal diel pattern for DO (Figure 20). The two earlier events were of short duration and were not correlated with changes in the flow pattern. These short-term aberations were not uncommon and perhaps are likely due to short-term disturbance of the sediment upstream or perhaps to an occassional illicit dumping of organic chemicals. The low-DO event recorded on August 20 was of longer duration and was accompanied with a typical reduction in stream temperature. Indeed, the USGS flow record indicates a high-flow event on that day (Figure 21).

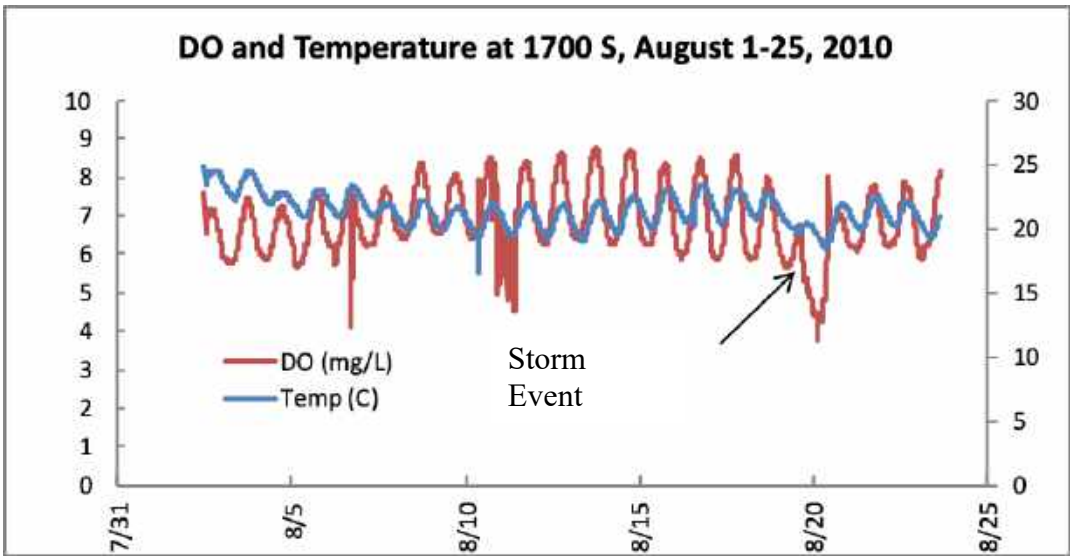

Figure 79. DO and Temperature values recorded August 1 to 25, 2010 at 1700 S.

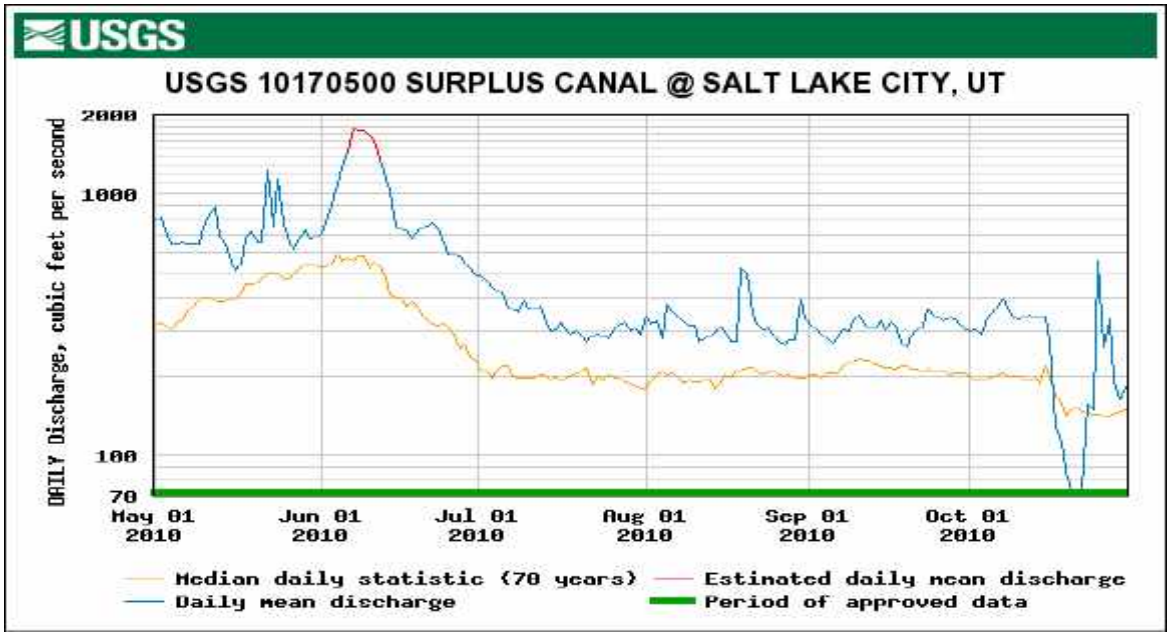

Figure 80. Recorded flows in the Surplus Canal near the Salt Lake City international airport from May 1 to October 30, 2010. Note the y axis is on a log scale.

Additional recordings of DO and temperature were conducted at Center St and Burnham Dam. The average and diel range of DO was noticably less than that recorded at 1700 S. Dissolved oxygen at Center St ranged from 5.2 to 6.2 during most of the recording. However, a storm event occurred on 8/23 to 8/24 which depressed the DO and reduced the temperature (Figure 22). This storm event was also recorded in the USGS data (Figure 20) where flows in the Surplus Canal doubled for a short duration.

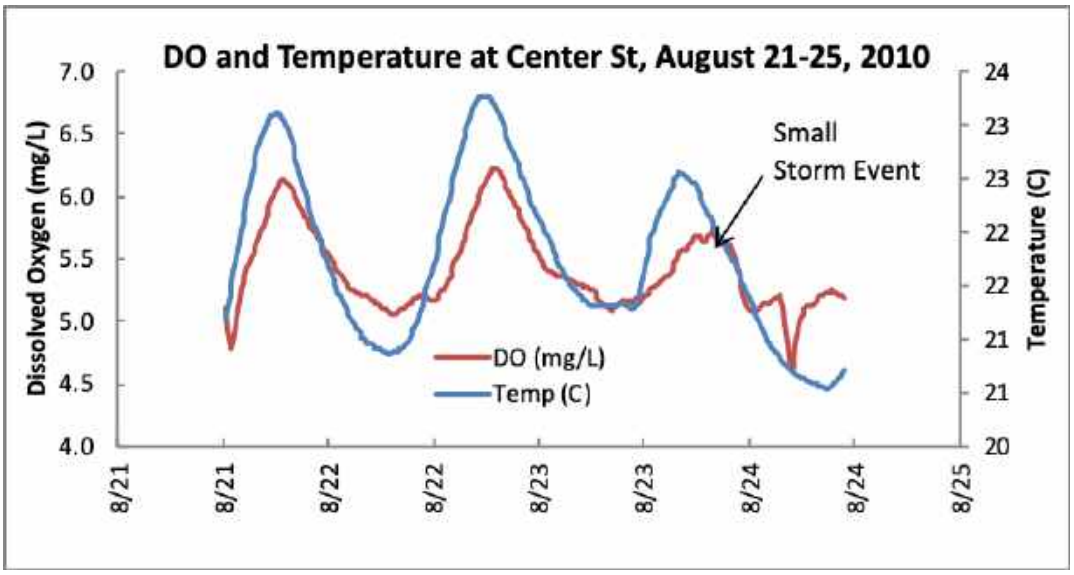

Figure 81. Dissolved oxygen and temperature recorded at Center St from August 21 to August 24, 2010.

Flows at the 500 N gage were not available during the summer of 2010 due to maintenance requirements and the shut down due to the Chevron oil spill. By the end of September, the temperature had declined by several degrees and although the daily range of DO continued to fluctuate only by about 1 mg/L, the average DO increased considerably. At 300 N the average DO was approximately 7 mg/L (Figure 23). Dissolved oxygen at Burnham Dam had increased to an average of about 6.3 mg/L (Figure 24). There was another minor storm event that occurred between 9/22 and 9/24, an occurrence that was also recorded in the USGS data (Figure 24).

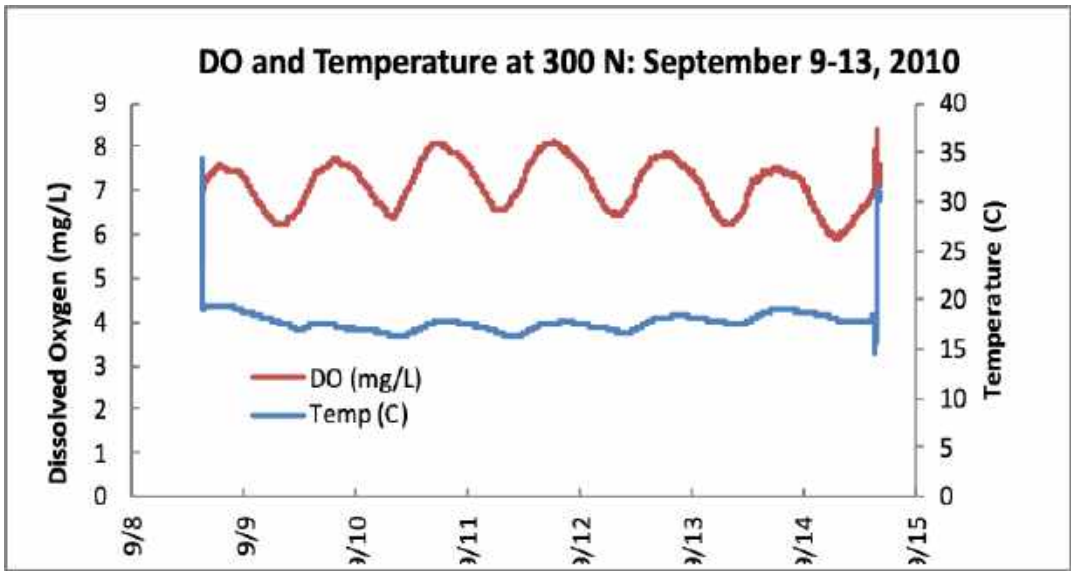

Figure 82. Temperature and DO values recorded at 300 N from September 9 to 13, 2010.

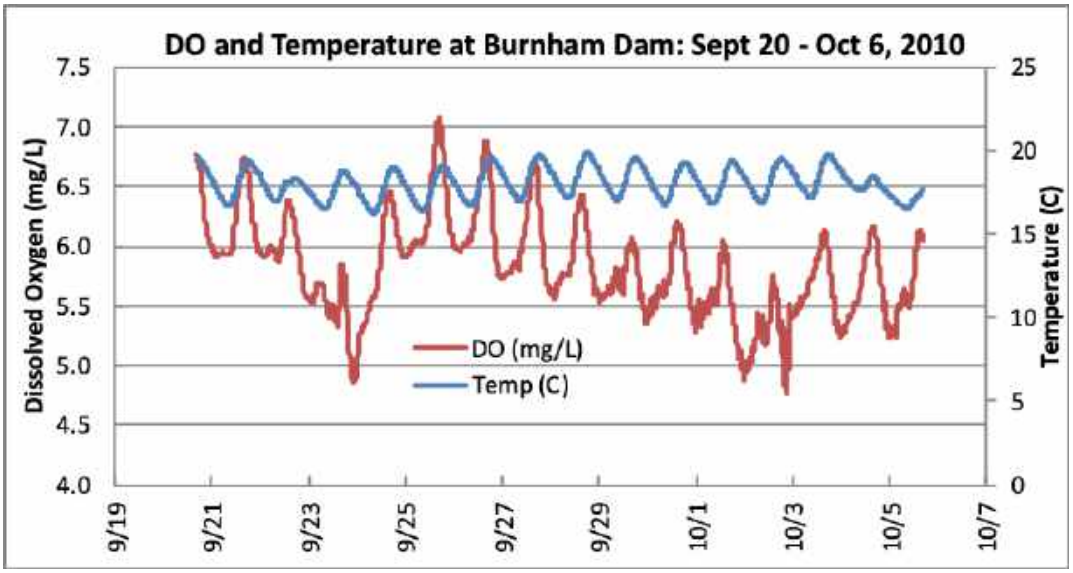

Figure 83. Dissolved oxygen and temperature recorded September 20 to October 6, 2010 in the Jordan River at Burnham Dam.

The sonde that was placed at Burnham Dam was to be deployed from July to October. Apparently however, the diminishing flows through July allowed for sediments to accumulate. The probe sensors became buried shortly after deployment and even though data was downloaded, batteries changed and probes recalibrated approximately every two weeks, the sondes were reattached at the same height on the stake. However, with the poor water clarity, and extremely soft new sediments it went unnoticed that the tip of the sonde was being reset just a few cm below the surface of the sediments. Of course, this invalidated most all the late July and August data.

Additional recordings were performed during 2011 and 2012. Sondes were deployed nearly every month of the year. However, for the sake of brevity, only recordings where

storm flows and low DO episodes were likely to occur are reported here. Figure 25 displays the diel patterns of DO, along with temperature or pH during June, July and August at Legacy Nature Preserve.

a.

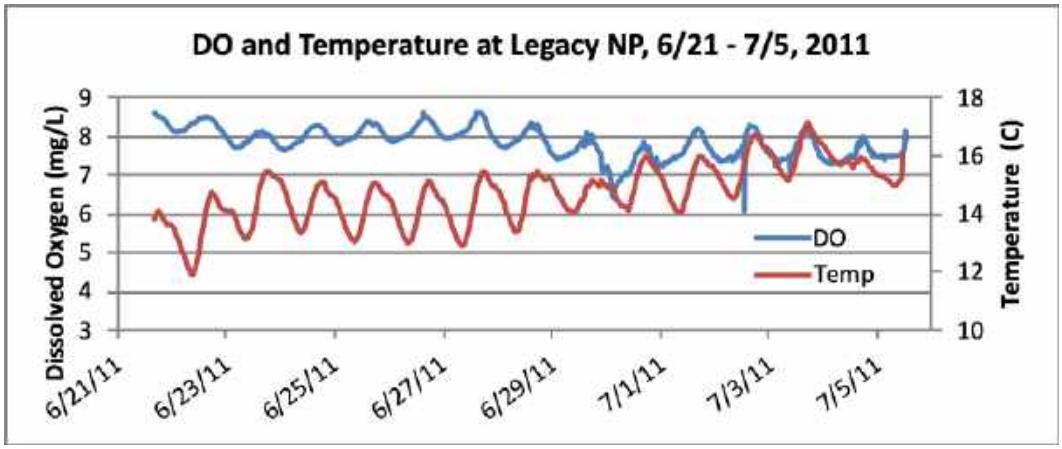

b.

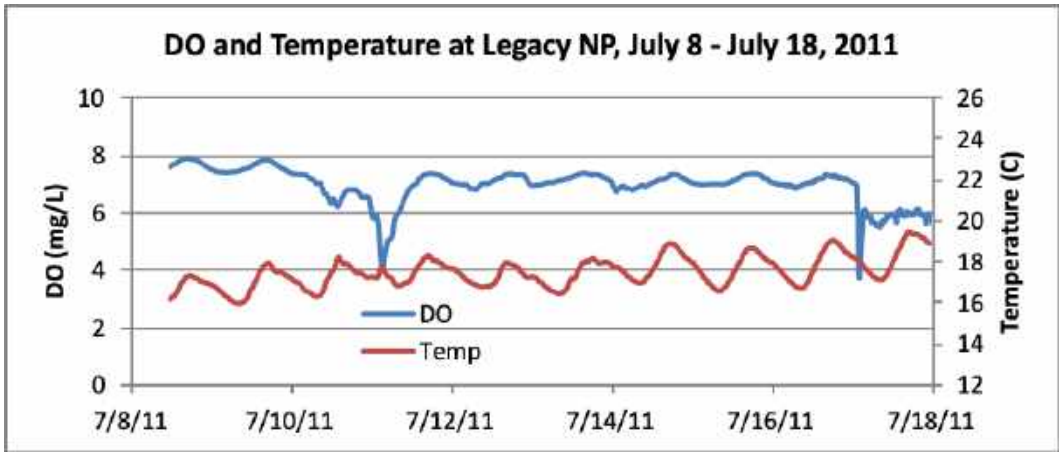

c.

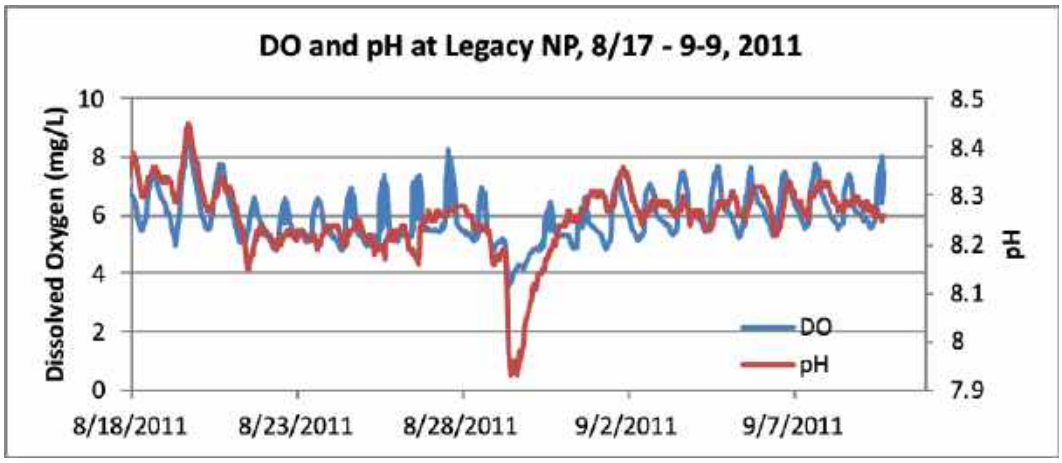

Figure 84. DO, temperature and pH values recorded at Legacy Nature Preserve during June, July and August 2011.

There was always a general trend that as water temperatures warmed up, DO values declined. However, this was also related to the fact the flows were diminishing to

summer minimum values during this same time. Such low flows are of critical concern. They lead to diminished reaeration rates, greater exposure to the SOD (the sediment surface area to volume ratio increases) and the warming temperatures will continually enhance biochemical reactions (respiration rates) (Figure 25a.). The DO continued to decline as temperature increased through July. Also at this time the flow rapidly decreased from near-record highs of 3000 CFS in the Surplus Canal to the 2011 summer minimum flows of about 320 CFS. This was about double the normal summer flows through the lower Jordan River and, except for the occasional storm events, these elevated flows maintained the DO above the minimum DO standard (4.0 mg/L), as well as above the 7-day and 30-day standard. Still though, these low DO dips are important to note. For example, when flows increased a relatively small amount for the short duration of August 28-29, (Figure 26.), there was a concurrent reduction in DO in the lower Jordan, suggesting that these short-term spikes in flow are mobilizing some highly reactive organic compounds, likely from the stormwater vaults, drains, etc. that immediately consume oxygen. Overall, however, mean DO values remained at or above 6 mg/L during 2011– likely as a result of the much-higher than average summer flows.

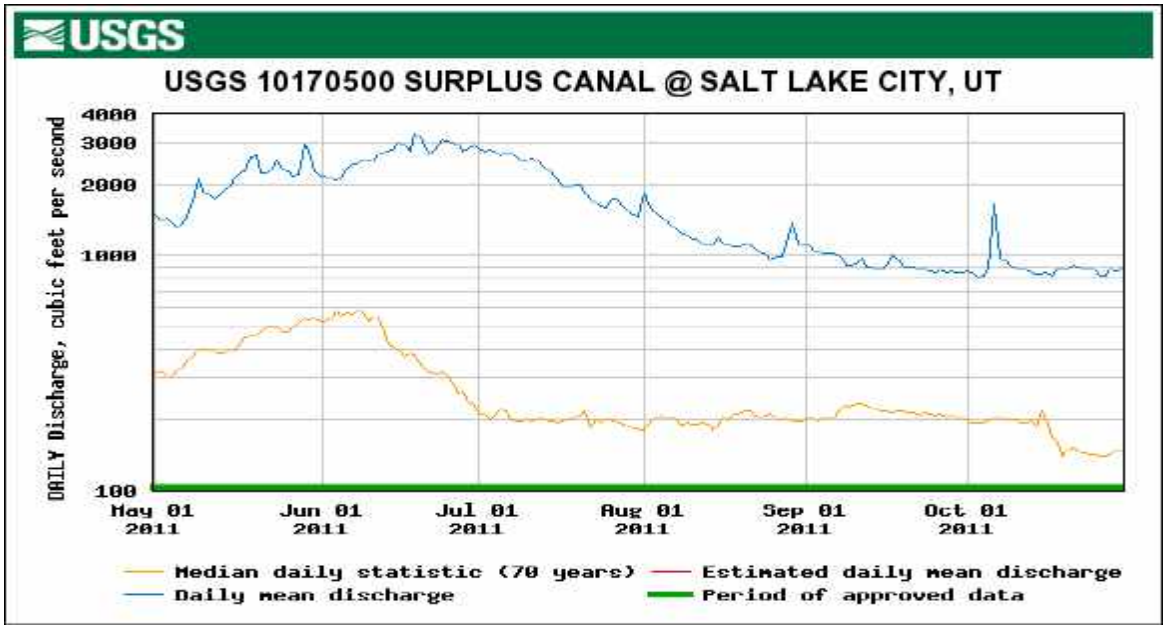

Figure 85. Flow recorded in the Surplus Canal at the Salt Lake City International Airport from May 1 to October 30, 2011.

In most respects the data sonde recordings of 2012 were similar to the previous three years. However, the hydrograph was significantly altered from normal winter and spring flows. Utah Lake elevation was still well above the compromise line as a result of the very high 2011 flows, so substantial releases were made during winter when normally there is no water released from the lake. As described above, these releases were made in anticipation for potential high runoff flows in the 2012 spring. However, the 2011/2012 snowpack was well below normal and the high and sustained winter and early spring releases ended up being the highest flows of the year (Figure 27). Normal spring flows were below normal as a result of Utah Lake retaining much of the runoff flows.

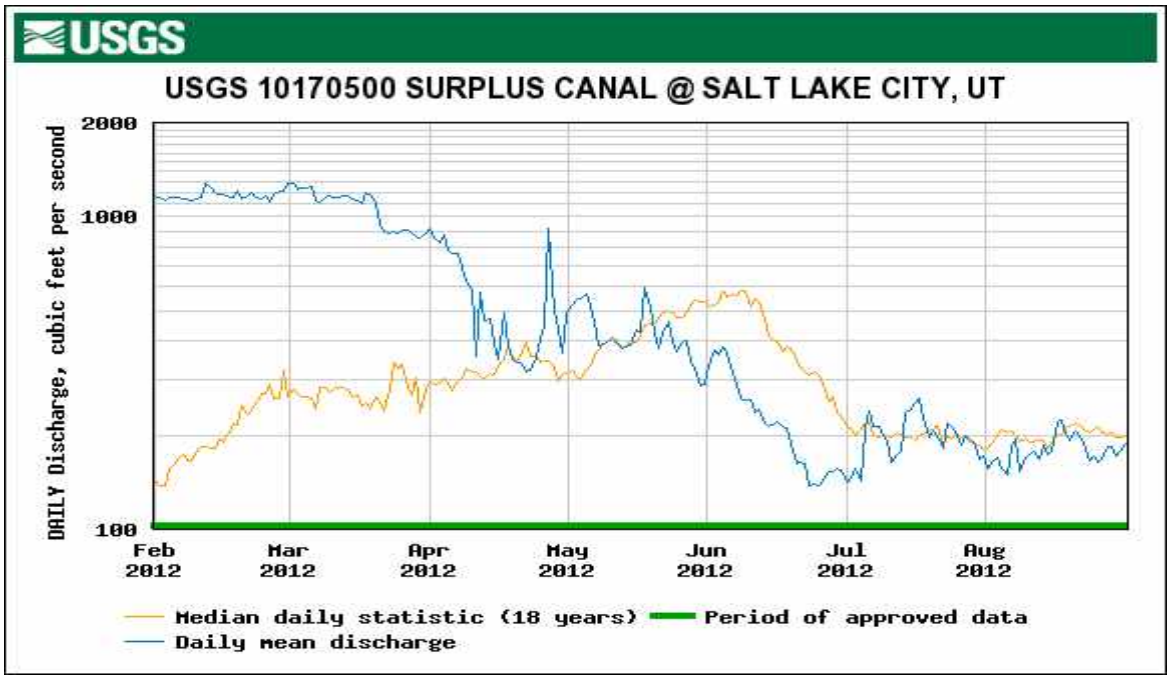

Figure 86. Hydrograph of the Surplus Canal from February 1 to August 31, 2012.

During 2012 there was again a correlation between increasing temperature values and decreasing mean daily DO concentrations (Figure 28a.) There were two recognizable storm events that were recorded during spring and summer 2012. One occurred on about July 6 and was recorded by the probe set at 300 N (Figure 28a.). It took several days for the DO pattern to recover to pre-storm values (until about July 13) at which time the mean DO began to decrease again. Elevated and erratic flows occurred again, starting on July 13, which lasted for several more days (Figure 27) and DO began to decline once again (Figure 28). This elevated flow also caused a decrease in stream temperature (Figure 28a). As flows declined in June (Figure 27), the stream temperature began to increase again, and this increase was accompanied by continued decline in DO (Figure 28a). Figure 28b. is a continuation of Figure 28a. However, between these two recordings the probes were removed, cleaned and recalibrated and the batteries replaced – all according to the manufacturer's recommendations. In fact, except for the DO probe, all of the probes remained very stable. But after the probes were replaced, the DO began recording values that averaged about 1.5 mg/L higher (Figure 28b.). This same pattern occurred between the recordings of Figure 28b. and 28c. All other parameters (e.g. pH and temperature) remained predictably in their same ranges. We attributed this decline to the buildup of biofilm with its associated debris on the new optical DO probe.

a.

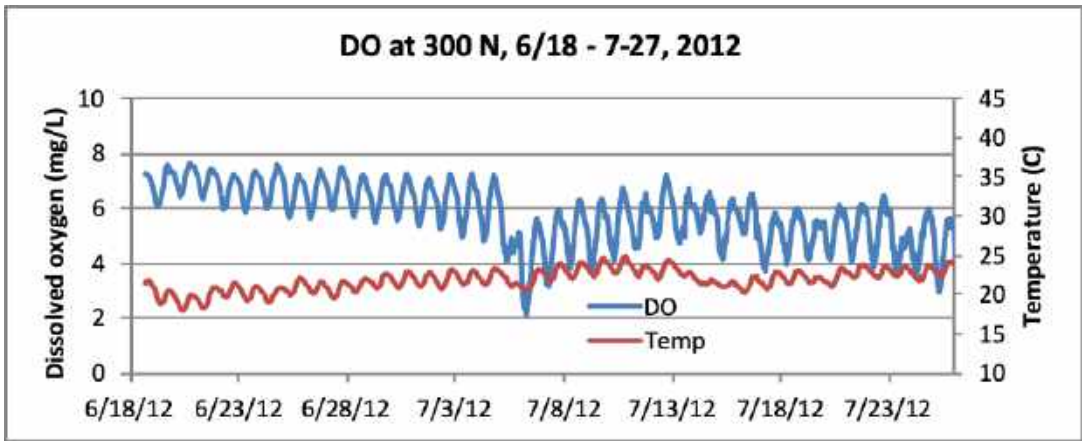

b.

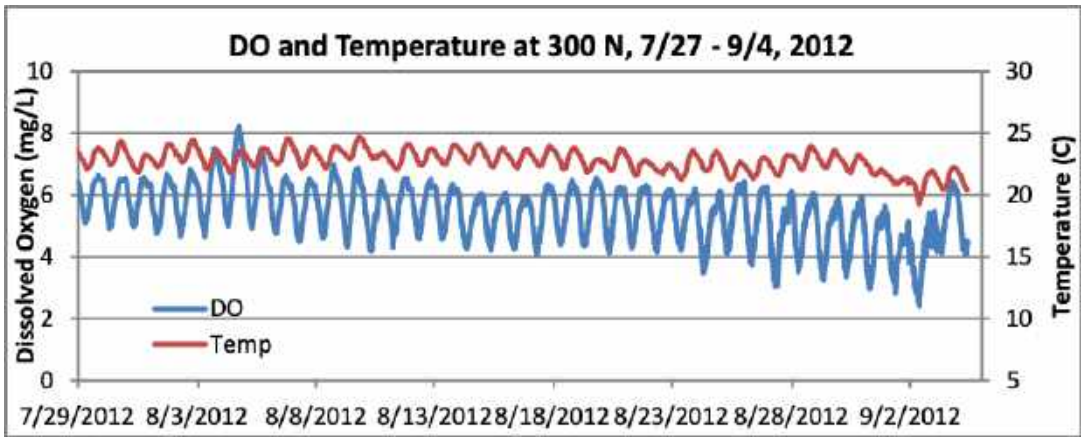

c.

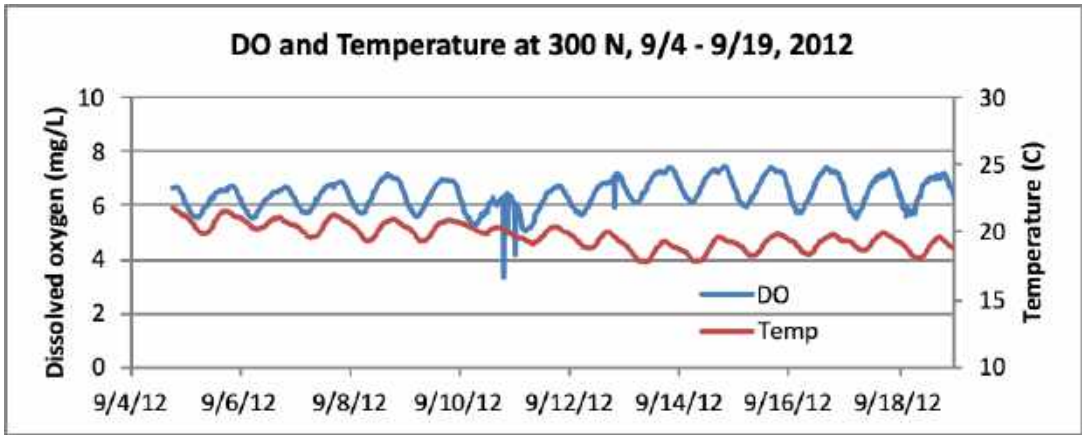

Figure 87. Dissolved oxygen and temperature recordings at 300 N. Note, b. and c. are a continuation of the previous record. The sonde was removed, cleaned, recalibrated and replaced in the river at the end of each record.

This biofilm was clearly visible and was carefully removed when the probe was serviced. However, we believe that this film gradually accumulates, obscures the optical pathway and weakens the signal to the detector. The 2012 year was the first time these long-term deployments (i.e. greater than 2-3 weeks) were performed and because we knew the batteries lasted this long, we tried this monthly cleaning as a time-and-materials-saving practice. We later increased our cleaning schedule to once every two weeks as we did not

believe the biofilm interference during this time-scale caused any inexplicable decline in DO.

The other storm event occurred on May 26/27 at Burnham Dam (Figure 29). This high flow event was not recorded in the stream gage data from the USGS Surplus Canal gage (Figure 26) or from the 1700 S USGS gage (data not shown). However, the Salt Lake County gage at 500 N recorded an increase from about 230 CFS to 380 CFS during this time-indicating that a local storm occurred in one or more of the City Creek, Red Butte, Immigration, or Parleys Creek watersheds. The drop in DO on 6/6 was associated with another high-flow event recorded at the USGS gage on the Surplus Canal. However, elevated flows were not recorded at the 500 N gage. This adds further support to the concept that, although elevated flows are diverted over the top of the weir to the Surplus Canal, the exact same constituents (i.e. mobilized sediment-derived oxygen consuming compounds), are passing through the gate and are affecting downstream conditions in the lower Jordan River channel.

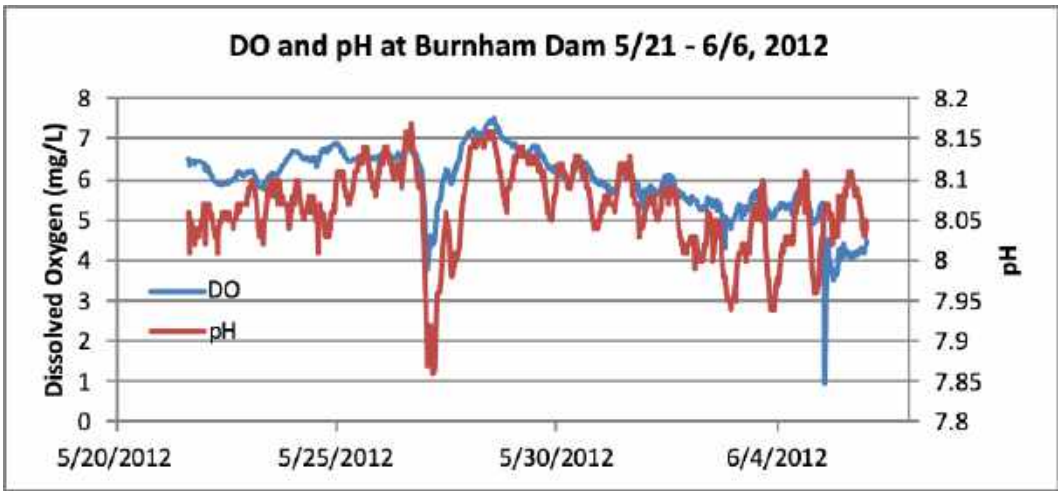

Figure 88. Dissolved oxygen and temperature recorded at Burnham Dam, May 21 – June 6, 2012.

The same high flow event and DO sag recorded at 300 N on July 6, 2012 (Figure 28a.) was recorded by the sonde set at Burnham Dam (Figure 30a). However, while the DO at 300 N only fell to about 2.0 mg/L, the DO at Burnham Dam fell to 0 mg/L for a few minutes. It also took several days for the DO at Burnham Dam to recover to approximate pre-storm values. Also, as described above, the gradual decline in DO to a mean of about 3 mg/L was likely due to the accumulation of biofilm and associated debris (i.e. the deployment extended beyond the 3-4-week period). Cleaning and recalibration of the probes immediately followed by re-deployment resulted in much higher DO values (about 5 mg/L), than the previous several days (Figure 30b.). Notably, if the recording where interference by the biofilm is disregarded, the average DO remained slightly above the 30-day average chronic criterion – even on a moving average basis. The probes that were permanently installed in 2013 are fitted with automatic wipers that clean the sensor surfaces immediately prior to recording of data, eliminating the fouling problem (see below).

a.

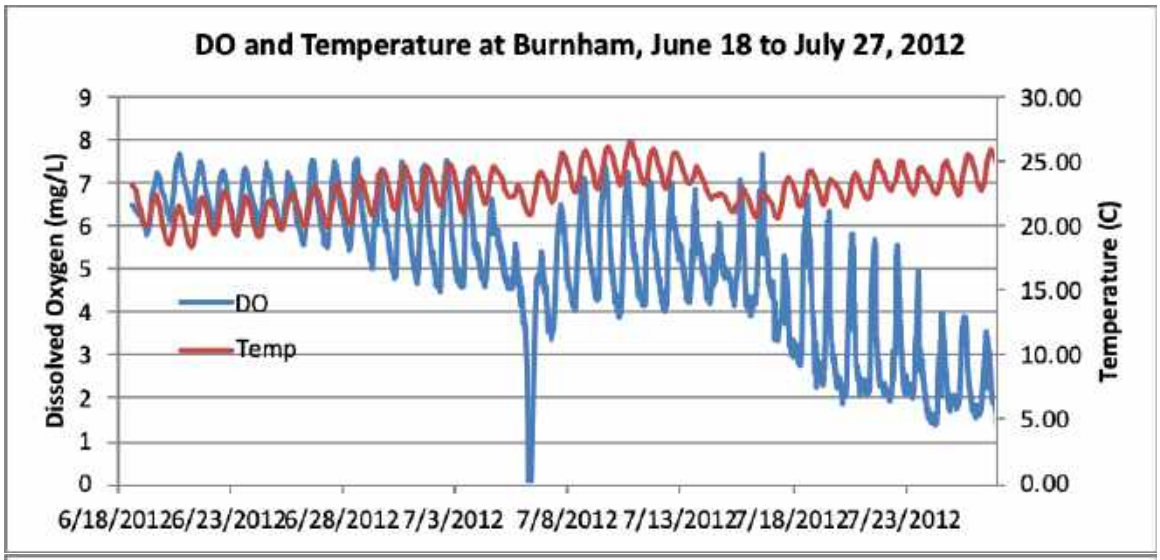

b.

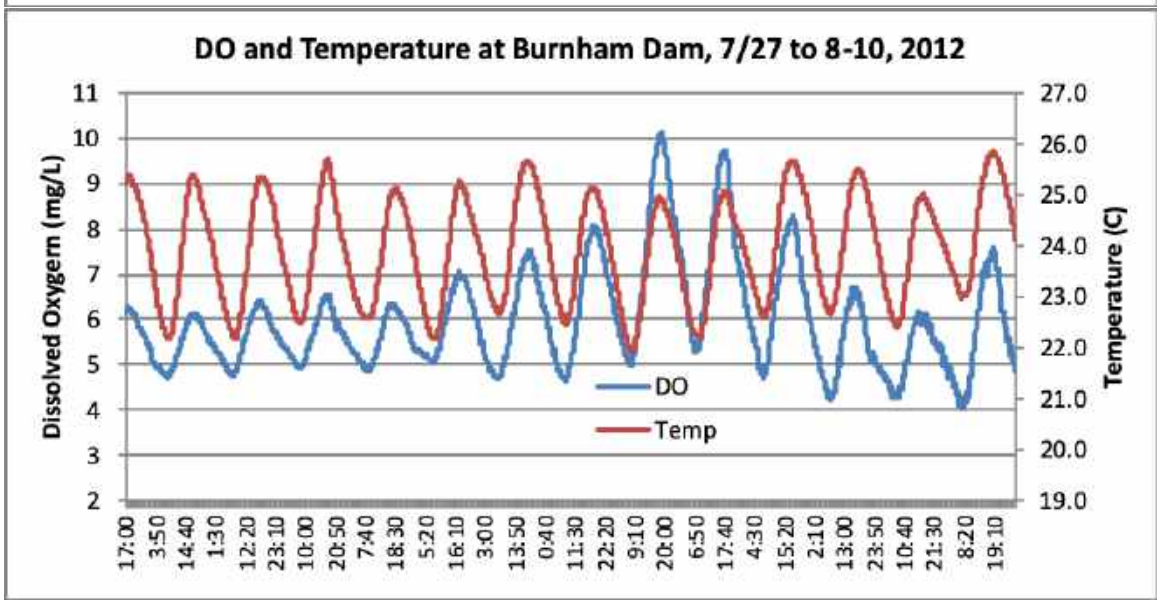

Figure 89. Dissolved oxygen and temperature in the Jordan River at Burnham Dam from June 18 to July 27 (a.) and from July 27 to August 10 (b.), 2012. Note that the DO probe was cleaned, recalibrated and replaced on July 27, resulting in much higher DO values. See text above for explanation.

Placement and Recordings from Permanent Sondes

In March 2013 the Council installed an array of 8 data recording sondes. Five of these sondes are fitted with DO, Temperature, pH and conductivity, and turbidity. In addition to these parameters, the other three were fitted with fluorescing dissolved organic matter (FDOM) and chlorophyll a. Notably, these new sondes were fitted with wiper blades that rotate several times just a few seconds before the parameter values are recorded and these recordings are again, scheduled for every 15 minutes. This resolved one of the biggest issues we found with long-term deployment of the portable sondes – that of fouling the probes with excessive biofilm accumulation. These sondes are permanently mounted on

bridge crossings, or concrete abutments or footings and are fitted with solar panels and cellular transmission equipment. The primary purposes of these installations are twofold: 1) provide long term indisputable records of these basic water quality parameters primarily with respect to the frequency, duration and degree of DO violations of water quality standards; and 2) to provide associated records of water quality changes that may be associated with such DO excursions. For example, as indicated in several recordings above, DO excursions are associated with storm events. In addition, there may be occasions in the lower, high-depositional reaches of the river where unusually low, late summer flows combine with warm temperatures and high SOD rates to drive the daily mean DO below the 5.5 mg/L 7-day or 30-day average DO standard for a few days. However, as with the July 4 and July 7 storm events, several days may be required for the DO to recover to pre-storm values and thus far, regular/seasonal violations of the 7-day or 30-day standards have not been observed outside of these storm events. Again, because such events, and resultant DO sags and recovery times are unavoidable; this supports the question as to whether an impairment due to a true DO standard violation exists. This further supports the suggestion that a UAA is warranted based on hydrologic diversion to extremely low levels that are accompanied by unavoidable summer storm events that depress the DO.

Following are selected recordings of DO, temperature, turbidity and FDOM during normal to low flows, as well as during storm events at several sites are included. Particular attention is paid to 2100 S, 300 N and Center Street – the extended reach of the Lower Jordan River that is currently listed as impaired. Center Street is of particular value because this is the compliance point – or the location at which assessment against water quality standards is performed for the entire reach below 2100 S.

Figure 31 is a recording at 2100 S from June 15 to July 3. After about June 25 temperature is trending upward quite rapidly and the pH range is expanding. Before June 25, DO was experiencing a diel range from about 5.5 mg/L to very near saturation at 9.5 mg/L. This indicates the presence of both significant primary production as well as considerable respiration. The rising temperature logically increases biological activity as indicated by an increasing range of pH. Elevated daytime pH is a result of the consumption of CO_2 and HCO_3 during photosynthesis (primary production), while respiration of both algae and heterotrophic bacteria during evening releases CO_2 – decreasing pH. Further, however, although there is increasing primary production throughout this time, the peak of the DO curve remains

a.

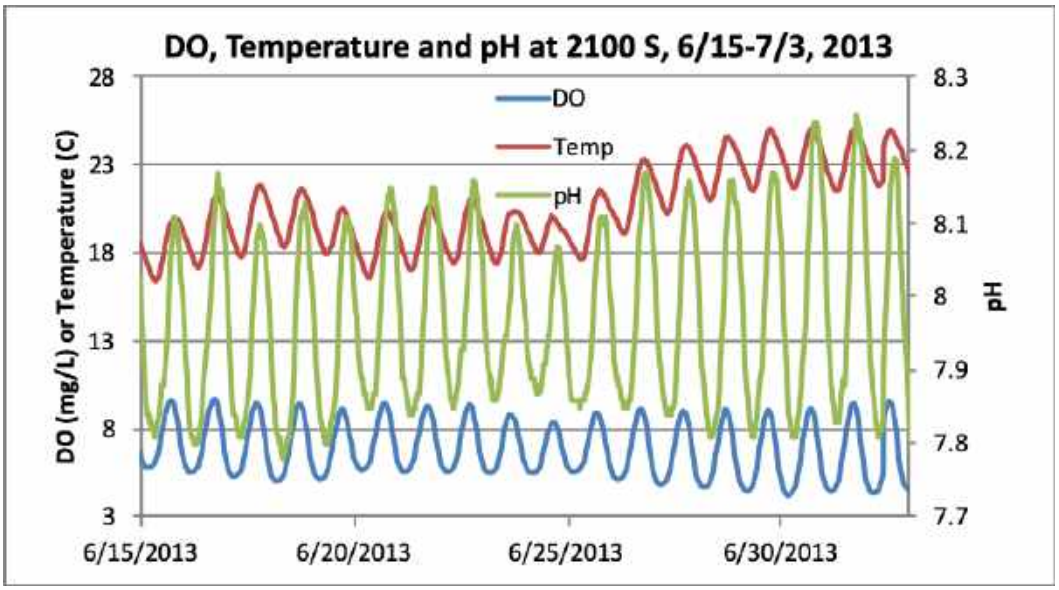

b.

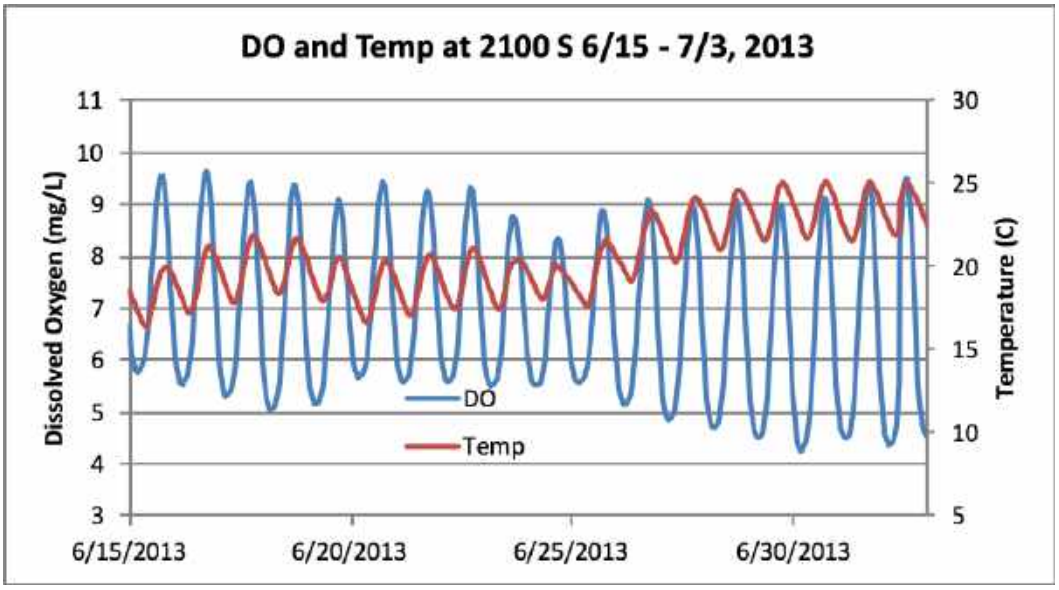

Figure 90. Recordings of dissolved oxygen, temperature and pH (a.) and dissolved oxygen and temperature (b.) at 2100 S from June 15 to July 3, 2013. The pH record in (b.) was removed to more clearly illustrate the relationship between DO and temperature.

Flat. Yet, the minimum DO values continue to sag further each day until it reaches a minimum of about 4.5 (Figure 31b.). This same phenomenon occurred at 300N (Figure 31a.). However, while the temperature values were nearly identical, as were the minimum values in DO, the maximum values in DO also declined- causing a decrease in the daily mean DO. These dips and even average values for DO are substantially below saturation, which would increase the rate of atmospheric oxygen transfer. This suggests that of the daily balance, respiration has a greater influence on DO than photosynthesis or atmospheric reaeration and this is particularly true for 300 N (Figure 32a.) and Center St (Figure 32b.), where there were both lower DO maxima and minima.

a.

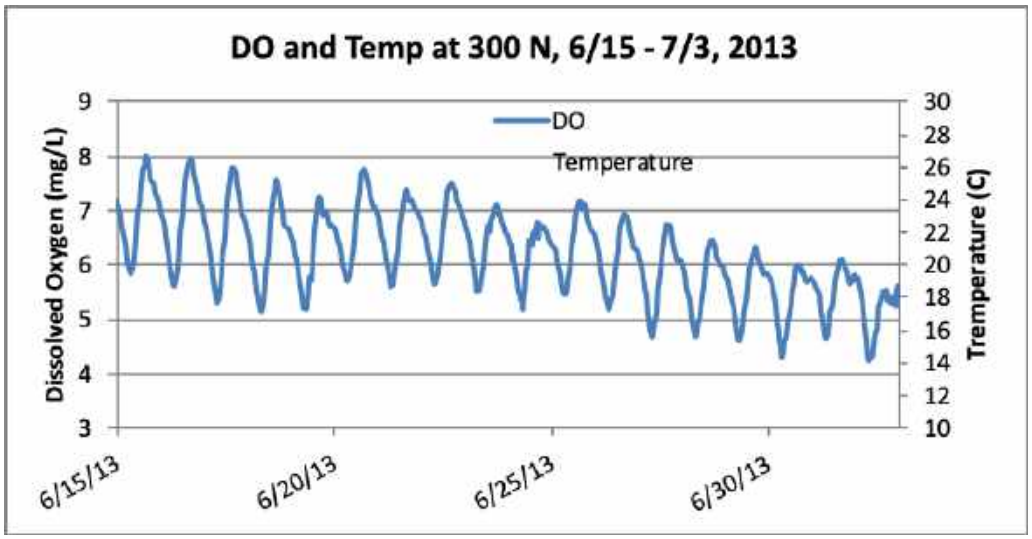

b.

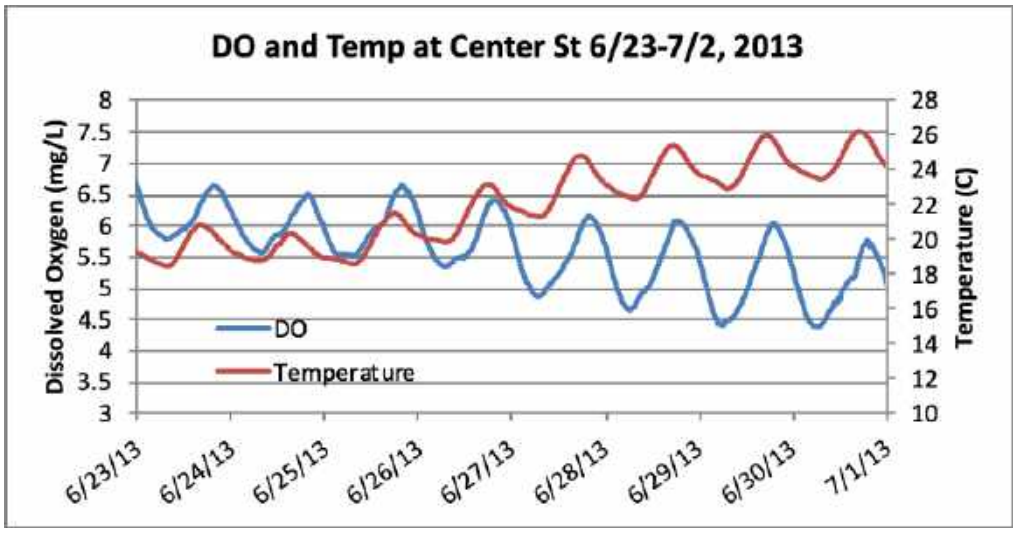

Figure 91. Recordings of dissolved oxygen and temperature in the Jordan River at the 300 N Foot Bridge and at the Center St crossing during June and early July, 2013.

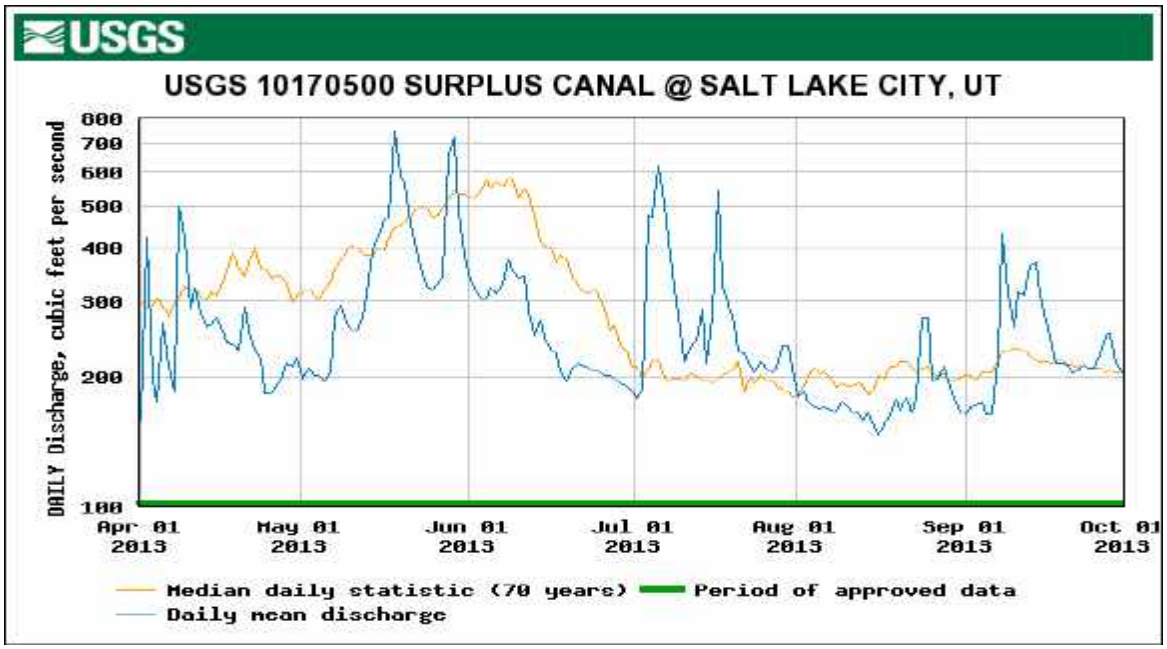

Figure 92. Flows recorded in the Surplus Canal, April 1 to October 1, 2013.

The tracings that include July 4 are of particular interest as there are several important observations from these graphs. First, a large storm event occurred during the afternoon of July 4, when flows actually approached the spring runoff level (Figure 33). Figures 34a. and 34b. are both included to display the flow management that occurred at the 2100 S diversion to the Surplus Canal. Also note that these figures reflect the instantaneous flow while figure 33 is a plot of the daily average flows. The river peaked at just over 200 CFS while the combined Surplus and river flow peaked at nearly 1000 CFS (Figure 33). This high-flow event dramatically affected various aspects of the water quality of the river. Most notable, there was an obvious sag in DO at 2100 S that occurred simultaneously with the high flow from a storm event and the depth and duration of this sag worsened at downstream stations. Secondly, there was a large increase in fluorescing dissolved organic matter (FDOM) that was concurrent with the elevated flows and with the DO sag and this correlation continued at downstream stations (Figures 35 and 36, 37 and 38).

a.

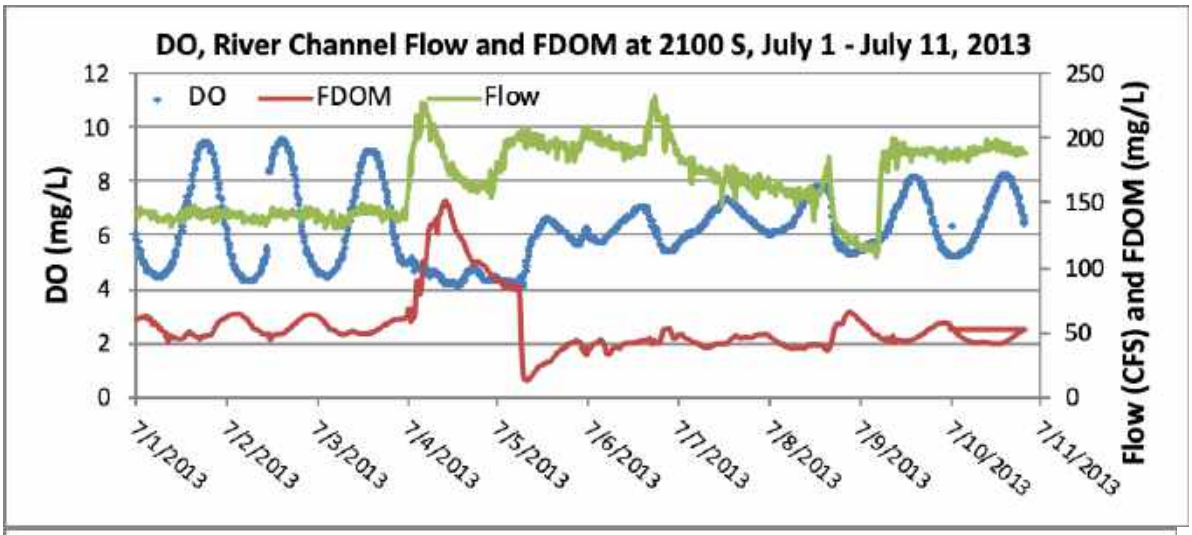

b.

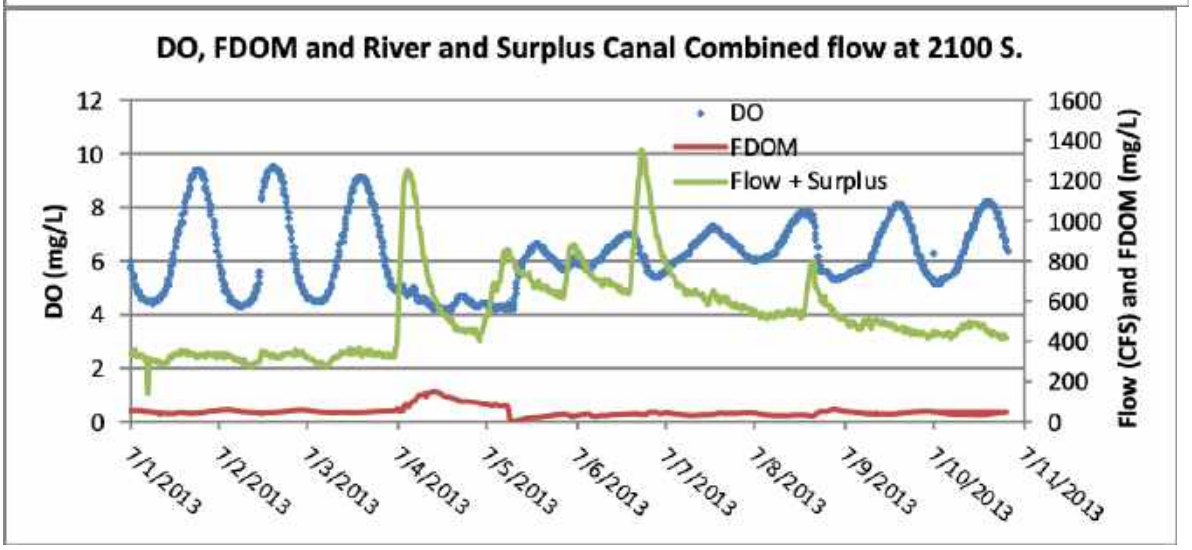

Figure 93. Dissolved oxygen, fluorescing dissolved organic matter and flow at 2100 S. The river channel flow is illustrated in (a.) while the combined river and surplus Canal flow is illustrated in (b.).

Tracking pH had not been a high priority in previous studies. Indeed, it was always thought that with the high alkalinity of Utah Lake, came the strong buffering capacity that stabilizes pH between about 8.0 and 8.3. Yet the storm event dropped pH temporarily all the way down to 7.28 (Figure 35). This suggests that large amount of CO_2 has been produced and released from the anaerobic sediments and the immediate oxidation of reduced organic compounds and ammonia and the concomitant release of H^+ ions in addition to CO_2. It was also apparent that the degree of the oxygen depletion worsened with downstream distance.

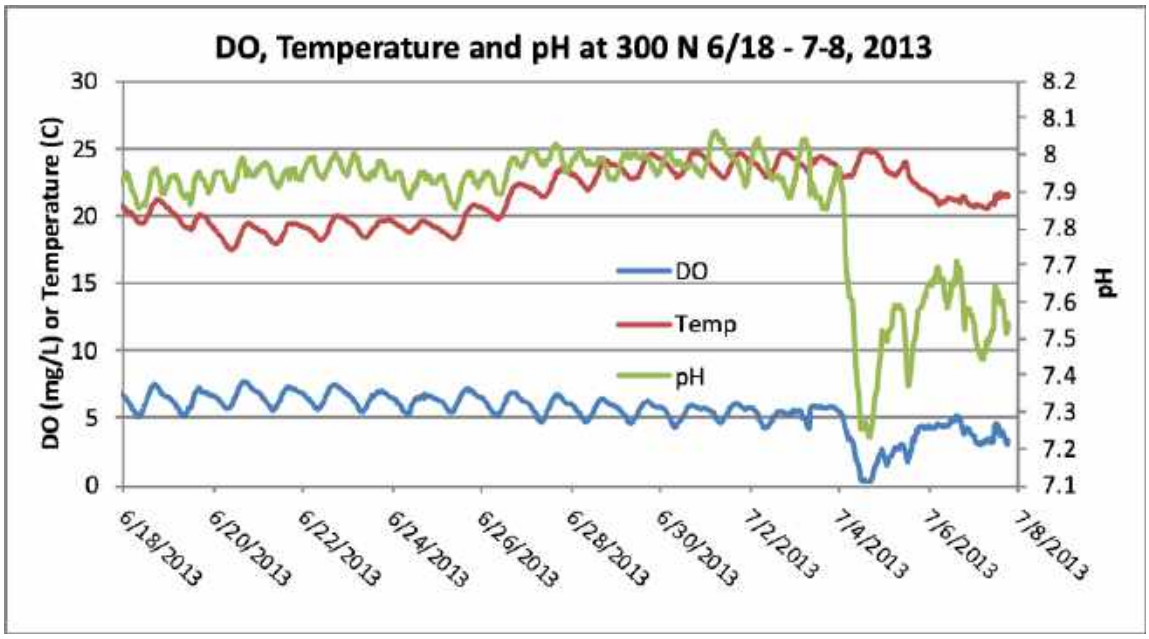

Figure 94. DO temperature and pH in the Jordan River at the 300 N foot bridge. Flow is removed from this graph to more clearly illustrate the change in pH associated with the high flow event.

This is undoubtedly due to continual oxygen consumption and CO_2 consumption in the water column as it travels downstream as well as the potential for increased mobilization of local sediments, including chemically reduced, oxygen-demanding compounds as the high flow reached these sites. For example, while the USGS gage recorded flows of about 200 CFS and 1700 S, the 500 N gage recorded flows exceeding 500 CFS. Hence, additional flow/scouring ability as well as mobilized sediments within the local storm drains and tributaries provided additional labile organic compounds for immediate oxidation. Accordingly, the longest period of anoxia (about fourteen hours) occurred at Center St.

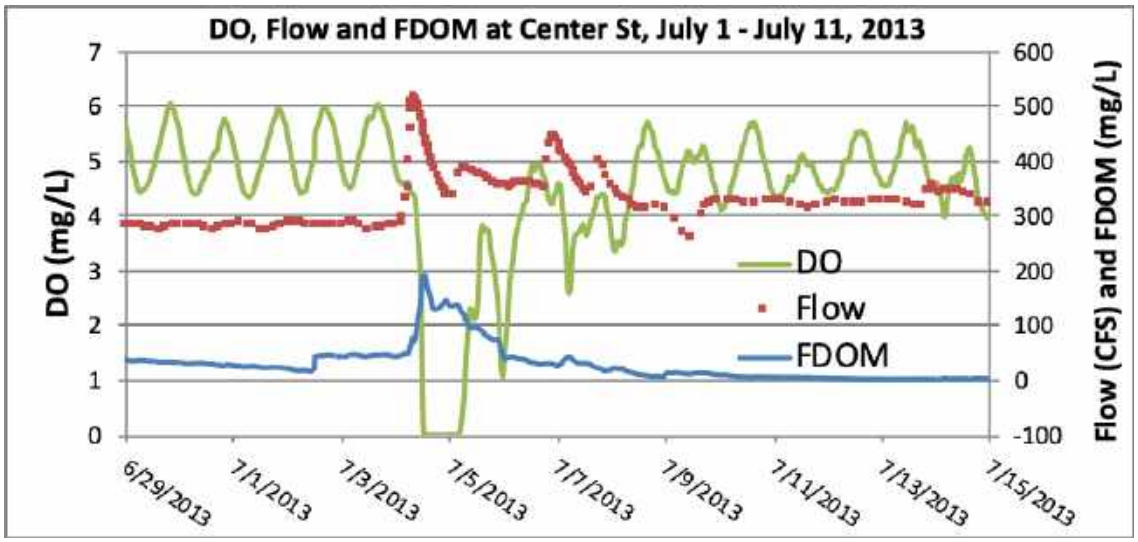

Figure 95. DO, fluorescing dissolved organic matter, and flow in the Jordan River at the Center St. crossing. Note exactly correlated timing of the arrival of high flow, elevated FDOM and DO decline. Flows recorded in this graph were obtained from the 500 N gage operated by Salt Lake County.

There were other high flow events that were associated with abrupt declines in DO. A record of these high flow events from upstream watersheds was best recorded in the Surplus Canal because that's where all of the "excess" flows are diverted (refer to figure 33). As described above, flows measured at 500 north crossing account for additional contributions from tributaries and storm flows that enter the river downstream from 2100 S.

Figure 37 displays DO recordings in late August and September at Center St. Both of these events were marked with increased flows measured at the Surplus Canal, although there was also an increase in flows measured at 500 N - from an average of about 190 CFS to about 300 CFS (data not shown). It should be mentioned that it is difficult and very time-consuming to align County flow data from 500 N with our sonde data, because the flow gage only records flow events that are different from the previous time step. Hence, there are occasions where recordings have skipped 30 to 200 minutes or more.

Also, it appears likely that the high flows that occurred on July 4 mobilized and removed a considerable amount of the oxygen-demanding organic compounds that had accumulated in the river, tributaries, and storm drains up until that time. For example, the DO sag recorded at all three sites during the July 7 high flow event was not nearly as low as that caused by the high flow event of July 4 – even though flows were slightly higher on July 7 (Figures 34, 35 and 36). However, this "cleansing" affect is brief. For example, the prominent low-DO event marked on July 4 occurred only about 5 weeks after higher spring flows had occurred in late May. This suggests that there is both considerable settling of "fresh" organic debris and that decomposition progresses rapidly to form the amount of reduced and labile organic matter that would be necessary to cause such low DO events. In turn, this labile organic matter consists of dissolved organic carbon (here measured as FDOM), that readily diffuses to the water column in storm water vaults and the countless other pools that are created by the incongruities throughout the storm drain

system and underground conduits that transport tributary and storm water. Hence the initial storm surge or flushing flow first transports the stagnant water and we believe that this initial flush is the cause of the instantaneous drop in DO that occurs simultaneously with arrival of elevated flows at our monitoring sites. Thereafter, if flows reach a high-enough values, they can be remobilized the sediments themselves from the stormwater vaults, etc. and cause lingering low DO values as well as contribute to the turbidity. As storm flows subside, these organic-rich sediments will also settle and resume forming highly reactive organic compounds that will accumulate in pore spaces and diffuse into surface water. As a further example of the rapid formation of labile dissolve organic carbon, high flow events also occurred in August and September and even though the magnitude of these elevated flows were much less than the July 4/7 flows, there was still a substantial reduction in DO. The September flow was slightly higher than the August flow (Figure 33), resulting in a predictable mobilization of greater amounts of FDOM and a concomitant greater sag in DO (Figure 36). Further, this occurred even though seasonal temperatures were beginning to cool down.

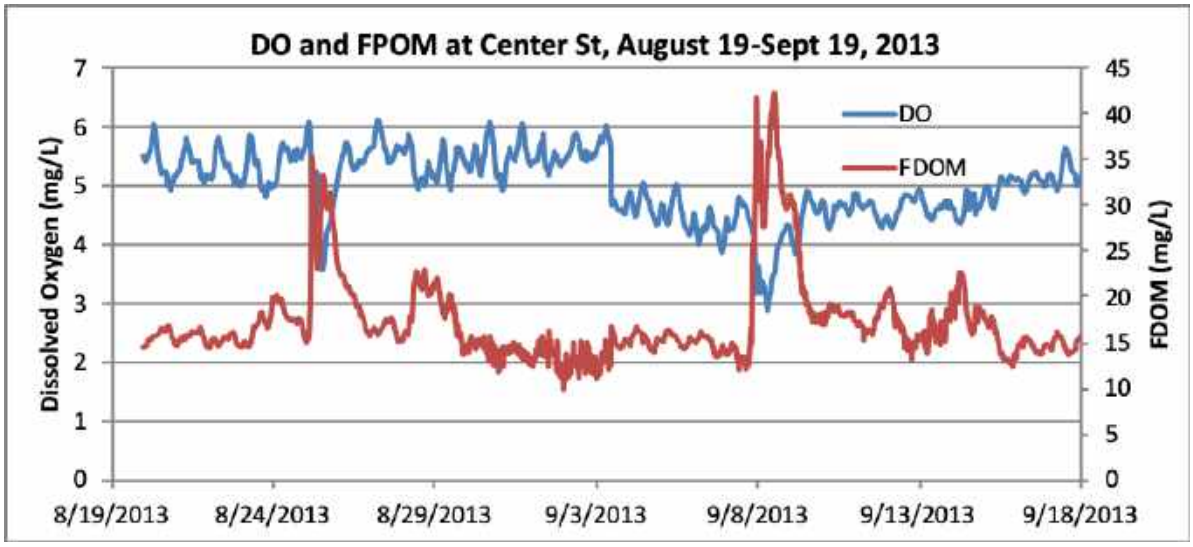

Figure 96. Dissolved oxygen and FDOM at Center St. from August 19 to September 19, 2013.

Is There a Role of VSS/Turbidity in Determining Oxygen Depletion?

It was originally assumed that the drop in DO during high flow events was the result of mobilized volatile suspended solids (VSS). Figure 38 is a time-correlated record of turbidity, a reasonable surrogate for VSS, at locations upstream and downstream from 2100 S during the July 4 storm event. Between each site, there is a 30 to 120-minute lag time – indicating the travel time of this high-turbidity event. First, there is a dramatic decline in turbidity between the 3300 S and 2100 S sites. This is likely due to settling of inorganic and organic material within the fore bay of the diversion dam for the Surplus Canal. Additional settling occurs with downstream distance until the value at Center St is a small fraction of that experienced at 3300 S or 2100 S. In fact, the second high flow event on July 6/7, which had similar high flows as on July 4-5 (see Figure 33), caused relatively tiny peaks at 3300 S and 2100 S, and resulted in no measurable increase in

turbidity at 300 N or Center St, again suggesting that the July 4 event was a major flushing/cleansing flow that removed a lot of both organic and inorganic material.

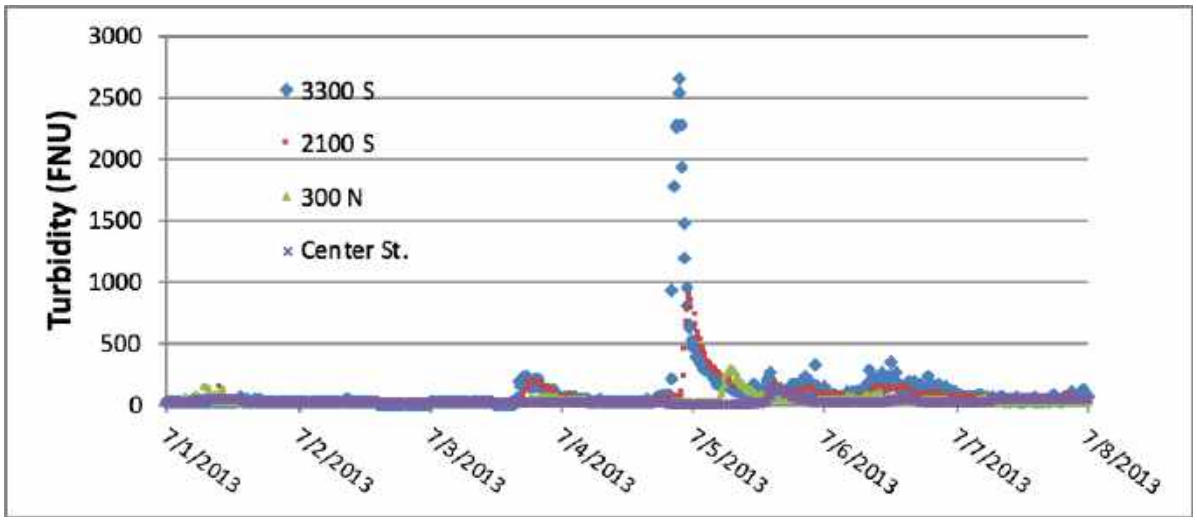

Figure 97. Time-correlated record of turbidity and 3300 S and successive monitoring stations downstream. Note how peaks could be identified with time and downstream distance as this "plug" or turbidity travelled downstream.

Secondly, a more detailed and time related recording of turbidity and DO at 300 N during the July 4 storm event shows that while the DO initially dropped at the onset of the first (small) peak in turbidity, the DO continued to drop while the turbidity was declining to near pre-storm values (Figure 39). The second and much higher peak in turbidity on July 5 is largely inexplicable. There was a concurrent slight increase in flow and slight increase in FDOM, along with a small decrease in DO. However, careful review of the data indicates that this drop in DO is initially occurring simply because it is night time. However, The DO actually begins to increase again at 02:40 - long before sunrise and at the exact moment that the turbidity is peaking. So, although these two parameters appear to co-vary, it is hard to imagine that the source of turbidity was actually a strong-enough oxidant as to raise the river DO during the middle of night. Regardless of whether there is a relationship, it has no predictable value with regard to DO values.

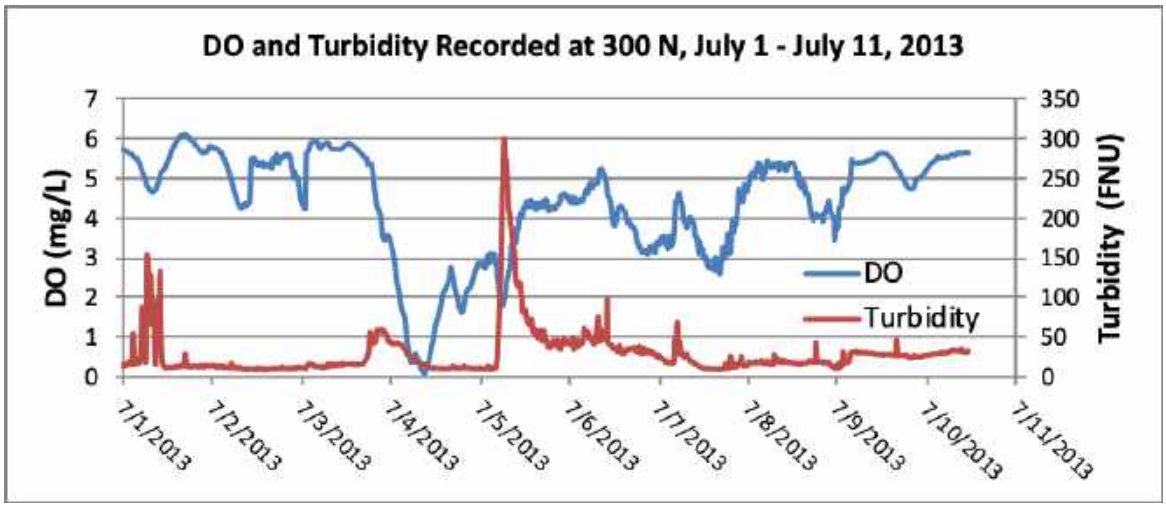

Figure 98. Recording of dissolved oxygen and turbidity at 300 N, July 1 – July 10, 2013.

A much more detailed illustration of the relationship between DO, FDOM and Turbidity is displayed in Figure 39. Particularly, this is the site that experienced the greatest impact on DO.

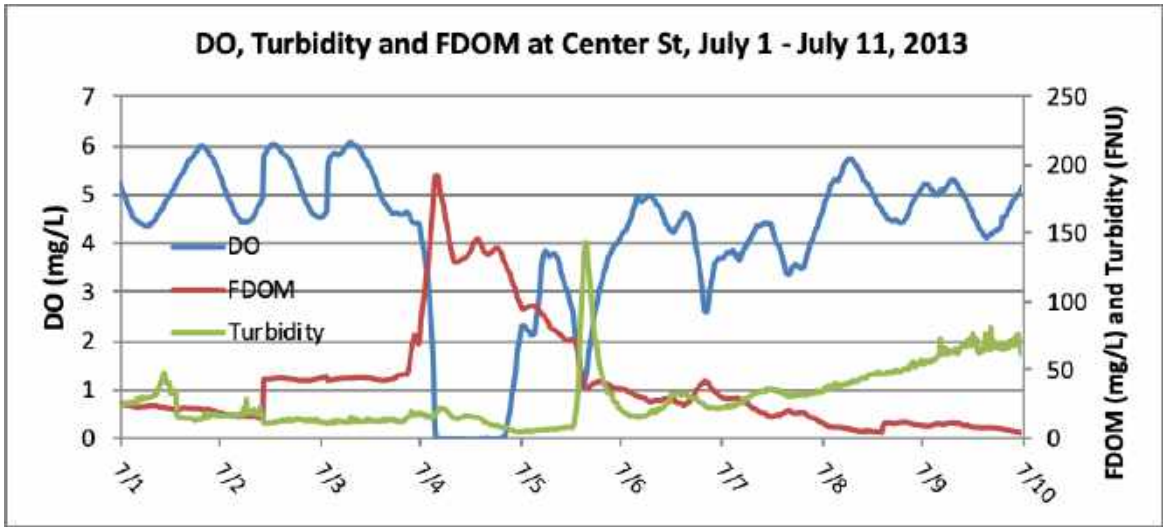

Figure 99. Recording of DO, turbidity and FDOM at Center St, July 1 to July 11, 2013.

Although there is some movement in the turbidity there is a much stronger relationship between DO and FDOM, suggesting that the fluorescing dissolved organic matter is a much more accurate surrogate than turbidity for the organic compounds that are actually responsible for the low-DO events. Additional recordings in 2014, 2015, 2016 2017 and 2018 displays a similar reaction to high flow events. Two examples, Figures 41 and 42 show the same relationship between high flow spikes and DO and FDOM.

a.

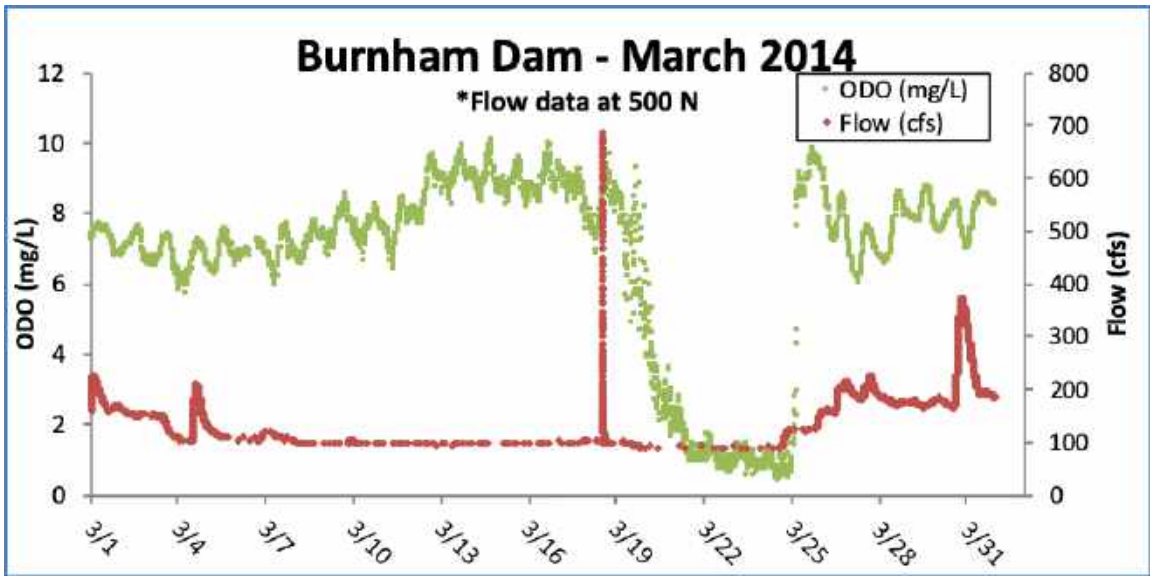

b.

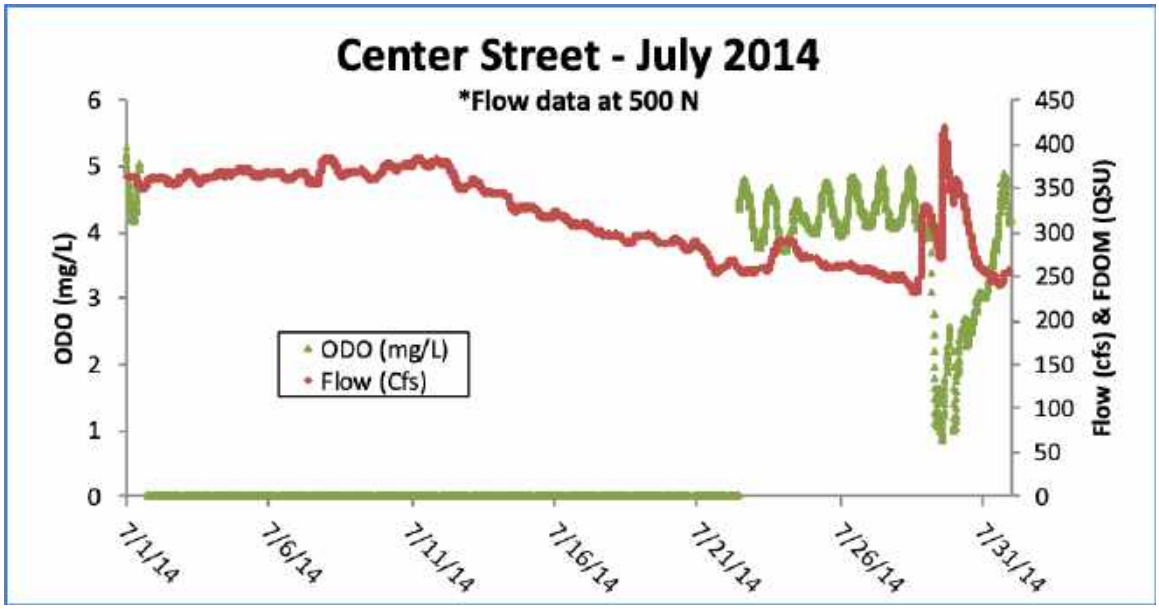

Figure 100. The effect of a spike in flow on dissolved oxygen March 18 (a.) and July 27, 2014 (b.). Note, even though there may be a relatively short interval between high flow events, the resultant immediate sag in DO is evident.

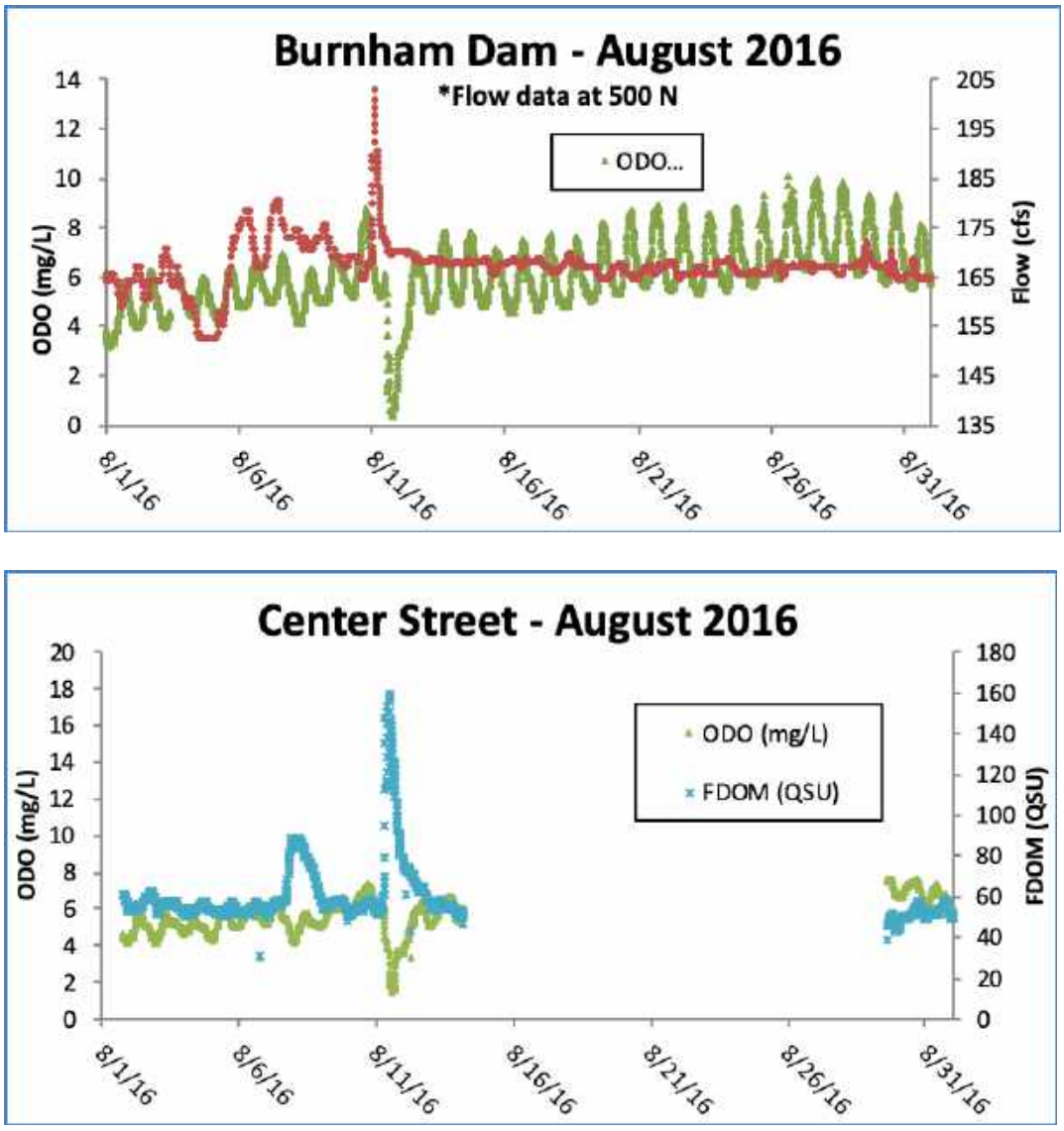

Figure 101. Flow and DO data (a.) and DO and FDOM data (b.) during the high flow even of August 11, 2014.

Although the fluorescing fraction of the total amount of dissolved organic matter (FDOM) is an unknown fraction of the total dissolved organic carbon, it has been shown to be a convenient and predictable surrogate for the portion that is highly reactive with oxygen. In general, various DOM fractions fluoresce within a broad excitation range from 250 and 400 nm and a broad emission range from 350 to 500 nm (Stedmon et al. 2003). Stedmon et al. (2003) were able to isolate specific fractions of DOC based on the adjustment of excitation and emission spectra. The results reveal that at least five different fluorescent DOM fractions are present (in significant amounts) in their study watershed and that the relative composition is dependent on the source (e.g. agricultural runoff, forest soil, aquatic production). Four different allochthonous fluorescent groups and one autochthonous fluorescent group were identified. Stedman et al. (2003) concluded that use of scanning spectroscopy allows the ability to trace the different fractions of the DOM pool and represents a significant advance within the fields of

aquatic ecology and chemistry and will prove to be useful for catchment management. Cory and Kaplan (2012) reviewed the recent literature and suggested that all of the studies suggest that the proportion of the amino acid–like fluorescence components relative to the total FDOM pool represents a proxy for the biodegradable fraction of DOM, while amounts of fluorescent moieties associated with the humic fraction of DOM are a proxy for slowly cycling, more recalcitrant DOM.

The FDOM sensor used in our Sonde is adjusted to excite at 365 nm and detect an emission wavelength of 480 nm. This is somewhat in the mid-range, and thus reacts to both recalcitrant and labile compounds (YSI technical team, personal communication). Also the fact that the fluorescence signal from one or more similar components may be greater than that from other components of the total FDOM does not equate to the first having a higher concentration than the other, only higher fluorescence (Stedmon and Bro 2008). This suggests that engagement in studies that use a scanning UV spectrophotometer and the necessary DOC and TOC analyses to better characterize the source needs to be a part of the study. It would be particularly informative to elucidate the sources of the organic matter (i.e. allochthonous vs autochthonous) and which fraction may be more labile and hence responsible for the DO sag. For example, Baker (2001) was able to distinguish the FDOM signature on streams receiving POTW effluent from those that didn't. He identified the labile compounds as being metabolized within several hours. These were identified as within the smaller molecular weight fraction that includes fulvic acid, amino acids and peptides within the humic substances. It should be pointed out, however, that in our data the dissolved oxygen rapidly began to sag nearly instantaneously with the arrival of the FDOM signal and the elevated flow. This indicates that the organic compounds consumed in the low DO event were extremely reactive. It has been speculated that this fast reaction must be the result of COD and not biological.

However, it seems improbable that a chemical oxidant that could react so quickly and powerfully wouldn't absolutely decimate the biological community in the river. A logical alternative is methane oxidation. For example, I have observed the destruction of several mg/L of methane (CH_4) begin within minutes of introducing oxygen to anaerobic hypolimnetic samples of eutrophic lakes in Northern Alberta and nearly complete removal of about 10 mg /L of methane within an hour (personal observations). In addition, two moles of O_2 are required to oxidize one mole of CH_4, making this a highly oxygen-demanding reaction. Other biologically-mediated reactions are nearly as fast (i.e. nitrification of ammonia and oxidation of H_2S). Finally, research performed by Goel and Hogsett (Chapter 5), has revealed the presence and flux of considerable amounts of CH_4 and NH_4 to the water column from undisturbed sediments of the lower Jordan River. It is most likely that the first flush of stormwater moves stagnant anaerobic methane-rich water that overlies organic sediments in stormwater vaults, oil/water separators and other incongruities in storm drains and underground tributary conduits. In turn, when these large concentrations of labile compounds reach the Jordan River, they immediately depress the Jordan River DO. Secondly, if storm flows are sufficiently high, the organic-rich sediments that had previously settled in the same stormwater vaults, oil/water separators, etc. will be mobilized and transported to the river, including additional reduced and labile compounds that are contained in these anaerobic sediments. These

sediments will re-settle as storm flows diminish and the water reaches the low-velocity, lower reaches of the river. Evidence for this phenomenon includes the several days required for the Jordan River DO to recover to pre-storm ranges (Figures 38, 39, 40 and 41), and the 30-100 cm or organic-rich sediments present throughout the lower Jordan River. Because this can occur multiple times throughout a summer season, renewed accumulation and decomposition begins immediately following a high-flow event –likely even on the descending limb of any peak flow in the hydrograph. New research by the Council will focus on 1) following the methods of Stedmon et al. (2012) to determine if allochthonous vs autochthonous sources of dissolved organic carbon can be determined in the Jordan River watershed and 2) identifying the compounds within the DOM that are responsible for such immediate consumption of oxygen.

Finally, while certain BMPs may improve water quality, another critical outcome of this study will be the assembly of the type of information prescribed in 40 CFR §131.10(g), to write a scientifically sound Use Attainability Analysis that will document the severe consequences associated with extreme flows, extreme diversions, and the transport and deposition of large amounts of inorganic sediments and organic debris (CP0M). Particularly there is no conceivable way to eliminate the deposition and accumulation of inorganic and organic debris during or following storm events as flows subside and the lower Jordan is so massively dewatered (>90% or more). Further, there is already an active dredging program designed to remove accumulated sediments. Yet, our data reveals that mobilization, deposition, decomposition cyclex continuously as even high flow events just a few days apart result in the same FDOM/DO response (Figure 38). Under these current managed flow conditions, spring runoff and each storm event, of almost any size, will continue to cause short-term excursions of DO and occasional violation of the acute dissolved oxygen criteria and perhaps even the chronic DO criteria.

Recommendations

Overall, the inability to control the delivery, accumulation and decomposition of organic debris will preclude the ability to consistently maintain water quality standards for DO. While debris basins have been shown to be effective in eliminating some CPOM (Chapter 3), their success depends on sizing the basin large enough to provide sufficient retention time to allow for settling. In addition, an active means of removing accumulated material is essential to avoid rapid filling of the basin with excessive debris, precluding success. In addition, the continued sampling of tributaries, particularly Big Cottonwood and Mill Creeks has demonstrated that stream reaches downstream from debris basins rapidly collect and transport large amounts of CPOM along with inorganic sands, silts and clays from the unconsolidated alluvial sediment that comprises the East Bench of Salt Lake Valley. Therefore, it is apparent that numerous debris basins, with regular maintenance schedules, including real-time dredging during high flow events, would be necessary to more effectively remove this debris. However, this kind of effort, in coordination with other BMPs, such as creating bioswales, and installing more oil/water/sediment separators on public and private properties would be essential. Yet, because the costs and participation of these projects would be enormous, several tens to hundreds of millions of dollars (the success would be proportional to the funds

dedicated), to acquire private lands and perform these installations, public "buy in" would be a major obstacle.

Another alternative, and much less costly would be a major overhaul of the surplus Canal diversion dam. This renovation would include constructing a wier-type structure that provides for water over-toping the dam – much like the weir that currently controls the flow down the Surplus Canal; only that the flow-control gate would regulate flow over the dam instead of underneath. This change in design would create and improve the settling properties of the forebay – turning it into a much more effective settling basin than currently exists. Secondly, the current dam provides about 8 feet of hydraulic head. The bottom release basically "wastes" this valuable potential stream gradient. We propose to modify the stream channel to take advantage of this "gift" by elevating the stream bed to the approximate 8 ft height and provide enough fill to create a gradient of 3 to 4 ft per mile for the next 2-4 miles to the vicinity of the Pacific Corp diversion. Two to three additional sedimentation basins should be construction along the flow path to collect additional debris in localized, specifically designed basins for easy debris removal. Hence, any CPOM that flows over the weir, will continue to be transported to the designated sedimentation basins – rather than being deposited along every inch of the stream bottom. This will reduce the need to dredge many miles of stream bottom, destroying the benthic biota and destroying stream habitat in general and trampling miles of stream bank and piling thousands of tons of sediment that needs to dry for several weeks before final removal – only to be repeated every 2 – 3 years. In addition, the stream bed should be covered with appropriately-sized cobble and gravel (suited for stability in the resulting increased velocity), Finally, and most importantly, this greater gradient will provide for a tremendous improvement in natural re-aeration and enhanced "processing" of stream BOD and potential SOD. Ultimately these processes will likely maintain DO above existing criteria, greatly enhance aquatic habitat and biota and return the river to some semblance of its natural condition, help attain State designated beneficial uses, and improve ecological integrity as designated by the Clean Water Act. This entire project may cost 40 to 50 million dollars. However, this is a small fraction of what is planned or is currently being constructed for the misguided goal of improving DO using the assumption that reducing POTW nutrients will somehow improve the DO.
In the meantime, with the stream conditions that currently exist, and in cooperation with DWQ we need to modify and improve the DO assessment criteria to align more appropriately with EPA guidelines and move forward with a Use Attainability Analysis to remove the lower Jordan River from the 303(d) list. Also, the Council suggests that DWQ coordinate to further the investigation new innovative alternatives merits of installing an aeration system which could mitigate these storm-caused DO excursions and late summer, low flow DO sags.

References

Baker, A. 2001. Fluorescence Excitation−Emission Matrix Characterization of Some Sewage-Impacted Rivers *Environ. Sci. Technol. 35* (5): 948–953

Cory, RM and LA Kaplan. 2012. Biological lability of streamwater fluorescent dissolved organic matter. *Limol. Oceanogr*. 57(5): 1347-1360.

CH2M Hill. 2005. Jordan River Return Flow Study. Report to Recycled Water Coalition.

Hogsett, M. 2015. Water quality and sediment biogeochemistry in the urban Jordan River, UT. PhD Dissertation, University of Utah.

Smith, DW and RH Piedrahita. 1988. The relation between phytoplankton and dissolved oxygen in fish ponds. *Aquaculture* 68 (3): 249-265

Stedmon, CA, S Markager and R Bro. 2003. Tracing dissolved organic matter in aquatic environments using a new approach to fluorescence spectroscopy. *Marine Chemistry* 82: 239-254.

Stedmon, CA and R Bro. 2008. Characterizing dissolved organic matter fluorescence with parallel factor analysis: a tutorial. *Limnol. Oceanogr*. : Methods 6: 572-579.

Chapter 5

Sediment oxygen Demand, Nutrient Flux, Organic Matter Processing And Methane Release from the Lower Jordan River

Prepared by

Theron Miller, PhD

Wasatch Front Water Quality Council

August 2019

Table of Contents

Introduction

Due to its urban setting and neglect, the Jordan River has been characterized as one of the most impaired and modified streams in the US (Richards 2018). It has been straightened, channelized and constrained by levees in all but tiny reaches of its entire course and its natural flow regime conceded. It is diverted and dewatered at multiple locations, receives wastewater, urban runoff and stormwater flows that contain huge loads of organic matter as well as inorganic sediments from the mostly alluvial landscape of the Salt Lake Valley. The regular accumulation of this material requires frequent dredging at the mouths of major tributaries as well and dewater sections downstream from the Surplus Canal diversion. The low gradient and dewatering at 2100 S leads to excessive unnatural deposition of organic matter, mostly in the form of coarse particulate organic matter (CPOM) and continuous aerobic and anaerobic decomposition leads to some of the highest sediment oxygen demand (SOD) values measured anywhere. Chapter 5 characterizes the nature of episodic DO sags that relate to stormwater flows and the resuspension of fine sediments and exposure of underlying anaerobic sediments that contain large quantities of oxygen-demanding methane, hydrogen sulfide and ammonia. The purpose of this research was to better understand the underlying causes of DO deficits found in the lower Jordan River. The primary goals of this chapter were focused on identifying and quantifying nutrient and methane fluxes across the sediment-water interface. In addition, these fluxes are related to macronutrient dynamics, sediment methane production and characteristics of sediment organic matter. These characteristics are summarized here based on the 2015 PhD dissertation by Mitchel Hogsett. His work was supported by both Utah DWQ and the Wasatch Front Water Quality Council. His Dissertation is appended to this chapter (Appendix B).

Sediment Oxygen Demand (SOD)

Council scientists and UDWQ first suspected SOD to be an important factor in the oxygen dynamics of the Jordan River in 2009 and one of our first contracts with Dr. Ramesh Goel at the University of Utah focused on SOD measurements (Appendix a). Immediately following Goel's findings the Jordan River Technical Advisory Committee sought to modify the QUAL2Kw model with appropriately prescribed SOD and methane flux values as a critical matter of calibrating the model against actual measured DO values in the river. Here is a summary of the SOD Project.

The review of organic matter composition and sources presented by Hogsett, (2015; Appendix b.), provides important background information and a comprehensive explanation of the importance of organic matter in creating sediment oxygen demand:

> "It is accepted that the DOM is responsible for the majority of the SOD associated with the decomposition of organic material, but over time CPOM is converted to FPOMand eventually DOM, resulting in a constant flux of DOM from organically enriched sediments (Hauer and Lamberti 2007, pg. 273). Sediment oxygen demand (SOD) accounts for the depletion of dissolved oxygen due to the decomposition of settled organic matter (OM), the respiration of benthic flora and fauna, and the biotic

and abiotic oxidation of reduced inorganic chemical species diffusing from the sediments (Utley et al. 2008; Todd et al. 2009; Walker and Snodgrass 1986). The degradation of OM is the ultimate source of SOD either directly, such as decay at the sediment–water interface, or indirectly, such as the flux of reduced chemicals from sediments. SOD is also a function of the quality of OM present, the microbial community responsible for OM degradation, ecosystem metabolism, and the hospitality of the general environment to support the microbial and macroinvertebrate community (Young et al. 2008; Webster and Benfield 1986).

Terrestrial OM (litterfall)

Terrestrial forests can deposit 200–800 g-OM/m2/year as litterfall worldwide and production rates are dependent on the availability of sun and water, which are directly related to latitude and precipitation (Meentemeyer et al. 1982). Litterfall includes all annual loadings of OM derived from trees and shrubs including leafs, bark, seeds, and branches. The vast majority, over 70%, of terrestrial litterfall occurs during autumn as leaf litter in temperate zones (Meentemeyer et al. 1982). 44% of the annual organic load in a section of the forested Bear Brook, NH was due to autumn leaf litter (Fisher and Likens 1973). Over 70% of the OM loads to three headwater streams were from leaf fall, but only 3% of OM exports were CPOM, indicating a high conversion of CPOM to FPOM to DOM (Wallace et al. 1995; Cushing et al. 1993). In the deciduous forest streams of Eastern U.S., 86% of the organic carbon load was CPOM and 58% of the annual leaf litter load occurred in autumn (Webster et al. 1995),

Initial leaf decomposition of dry leaves can occur rapidly with 17% of the carbon being leached into the water column as DOM in the first 3 days (Mcdowell and Fisher 1976). Up to 25% of the mass of dry leaves can leach within 24 hours of being submerged in water, while fresh cut green leafs do not leach as rapidly (Gessner et al. 1999; Webster and Benfield 1986). The leaf litter decomposition rate has been estimated to be 1 year in most lotic systems, resulting in a steady-state leaf litter deposition/decomposition process over an annual cycle (Fisher and Likens 1973). Leaf litter will undergo structural decomposition and mineralization carried out by a consortium of macroinvertebrates, fungi, and bacteria with dominant populations dictated by the prevailing ambient environmental conditions (Gessner et al. 1999). In Portugal's urban Ave River, fungi were responsible for 34% of leaf carbon losses, while bacteria removed 7.5% in alder leaf packs over a 42-day instream incubation period (Pascoal and Cassio 2004). The majority of leaf decomposition in urban streams was found to be a result of the microbial community, not macroinvertebrate shredders (Imberger et al. 2008). Within a couple days, submerged leafs are initially colonized by fungus followed by bacteria, whereas macrophyte debris are initially colonized by bacteria (Webster and Benfield 1986).

The majority of nutrient spiraling and CPOM degradation studies have been conducted in small streams (1st to 3rd order) in relatively undisturbed aquatic

> environments (Ensign and Doyle 2006). The 4th order Jordan River fits into neither of these categories, but it does receive urban stormwater conveyed via creeks. The macroinvertebrate shredders indicative of high water quality (WQ) are not present in the fine sediments of the Lower Jordan River (LJR), but can be found among the gravel and cobbles present in the Upper Jordan R. Urban streams are typically dominated by disturbance-tolerant macroinvertebrates composed primarily of oligochaetes (aquatic worms) and chironomids (midges) (Walsh et al. 2005)"

This is the case for the Jordan River (see Macroinvertebrate Chapters 9 -13, Volume II: Biological Integrity). Hogsett continues:

> "Urban environments are largely impervious to runoff resulting in dust, organic matter, and pollutants being transported to the downstream surface water through stormwater conduits (Heaney and Huber 1984). Secondary growth of fungus and biofilms will colonize and degrade terrestrial OM during dry periods in stormwater conveyance systems and can flush out during rain events (Ellis 1977).
>
> Stormwater conveyance systems typically bypass the riparian zone where nutrient removal and sediment retention naturally occur, thereby increasing pollutant loads to the receiving stream (Hatt et al. 2004). Benthic leaf litter in an urbanized stream with an efficient stormwater conveyance system was composed primarily of nonnative tree species planted along streets in Australia (Miller and Boulton 2005). The specie of leaf influences the rate of OM turnover, and nonnative species can influence benthic metabolism since macroinvertebrate diversity is very low in many urban streams. This lack of aquatic macroinvertebrate diversity can result in an overloading of OM to the system due to the lack of higher life forms capable of preconditioning additional substrate (Ryder and Miller 2005). Through urbanization, the Salt Lake valley has been ordained with nonnative deciduous shade trees lining impervious streets. This seasonal urban stormwater load of leaf organic matter may add to the organic loading to the Lower Jordan River."

The original 2009 study (Goel 2014) included sites throughout most of the river. These sites were selected based on locations of tributary confluences and POTW discharge points. The basic design included setting chambers with an open bottom, to provide contact of the overlying water in the chamber to be in contact with the sediment and another chamber set beside the open-bottom chamber fitted with a watertight plate. This chamber quantifies only water column oxygen depletion, which is subtracted from open chamber value – yielding the SOD value. The open chamber design was deployed in duplicate for each experiment.

Additional SOD chambers with important modifications were constructed and provided by the WFWQC for subsequent SOD measurements but also for determination of Net Daily Metabolism (NDM) which is a measure of whether a site has a net positive oxygen production or a net negative oxygen production. In other words, whether the site has a net increase in DO or decrease in DO due to heterotrophic (oxygen consuming) microbial activity. For these tests, the chambers were constructed of clear acrylic plastic and trays

were constructed which were filled with ambient substrate, representative of the surrounding substrate at a particular site and allowed to incubate or recolonize natural benthic microbial communities of periphyton or bacteria for three weeks. At that time the trays were carefully placed in the clear chambers and incubated in either dark or light conditions. Wrapping the chamber in black plastic bags created dark conditions. In this manner, community respiration (excluding photosynthesis) could be measured for a period of hours. This was followed by removal of the plastic bags for an additional several hours to measure primary production/oxygen production. Subtraction of the respiration value from the primary production value determines to what degree there is net primary production or net community respiration.

The following is Table 12 from Hogsett (2015), which is a summary of the 142 individual SOD measurements performed by Hogsett (2015).

Table 12. 2009–2013 mean seasonal SOD (g-DO/m^2/d). From Hogsett (2015). Note: 142 SOD chamber installations in the Jordan River.

Site	Mile	Reach	Mean SOD	SD	N
State Canal			-6.57	2.2	2
Burnham	0.5	1	-2.15	1.5	5
LNP NE	2.8	1	-2.13	0.8	21
LNP SW	3	1	-2.92	0.6	2
LNP Upper-N	3.1	1	-2.19	0.1	2
Cudahy Ln	3.2	1	-2.58	0.8	10
1700 N	5	2	-2.06	0.3	2
300 N	8.9	2	-1.82	1.0	17
700 S	10	3	-1.42	0.3	4
900 S-N	11.2	3	-1.66	0.6	5
900 S-S	11.3	3	-1.12	0.4	6
1300 S	12.5	3	-2.26		1
1700 S-N	13.1	3	-1.72	1.0	15
1700 S-S	13.15	3	-1.07	0.5	3
2100 S	13.7	3	-1.49	0.6	3
2300 S	13.7	4	-2.44	1.4	4
2600 S	14.7	4	-4.69		1
2780 S-E	15	4	-2.60	1.7	4
2780 S-W	15.1	4	-2.81	0.6	3
3600 S	16.8	4	-0.97	0.5	2
5400 S	20.9	4	-3.27	2.4	9
7600 S	23.9	5	-3.45	2.5	5
7800 S	24.1	5	-1.30	1.2	3
9000 S	26	5	-1.35	0.7	7
SR-154	34.1	6	-1.77	1.0	2

Site	Mile	Reach	Mean SOD	SD	N
14600 S	37	7	-1.90	0.3	2

The 4-year standard deviations (SD) for in the LJR (Reaches 1–3) were equal to or less than 1.0 g-DO/m2/d for all sites except Burnham Dam, where one chamber measured -4.8 g-DO/m2/d. The high SD in the downstream State Canal was a result of one chamber measuring an extremely high SOD of -8.13 g-DO/m2/d.

With this information the Jordan River TAC voted to prescribe additional relatively very high SOD values ranging between 2 and 3.5 g O_2/M^2/Day for the calibration of the QUAL2Kw model.

A modification of the chamber apparatus was then developed using trays that were filled with ambient natural substrate and incubated for 3 weeks in the river to recolonize with benthic flora and fauna. These trays were then carefully placed in the chambers subsequent SOD measurements. This was an important modification as hyporheic exchange of water has been documented to occur at different locations in the river (CH2MHill 2005; Borup and Haws 1999). Use of the trays in sealed chambers eliminated this variable. The following figure (Figure 45 in Hogsett, 2015) displays the relationship between "tray oxygen demand" in the chamber and chamber that were connected with the sediment surface.

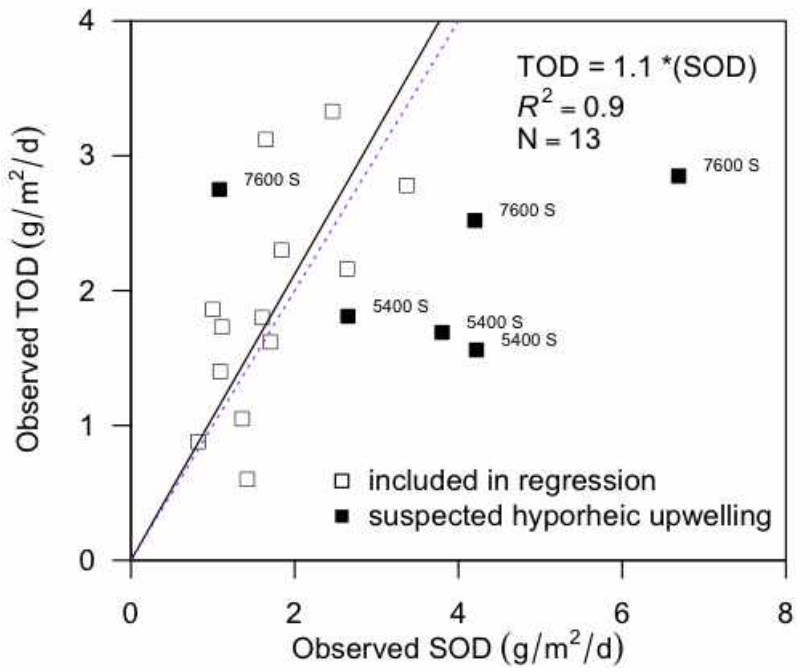

Fig. 45. TOD:SOD relationship

Net daily metabolism (NDM) was also determined using diel DO curves at a single station in the river. As described in Hogsett (2015):

> "To estimate stream GPP, the maximum daytime DO deficit or surplus can be normalized to depth and photoperiod using a half-sinusoid model to account for the changing rates of photosynthesis in relation to the solar flux (Chapra 2008). Finally, the
> dark respiration normalized to the photoperiod is subtracted to account for daytime respiration masked by DO production. NDM is expressed as the sum of DO fluxes from
> GPP and CR24, similar to the NDM chamber equations.
> $P\text{m} = K(C\text{max} - C\text{sat})d$
> $P\text{m} = maximum\ net\ flux\ of\ DO\ from\ primary\ production\ g\ DO\ /m^2\ day$
> $C\text{max} = maximum\ daytime\ DO\ concentration\ mg\ DO/L$
> $C\text{max} - C\text{sat} = maximum\ daytime\ DO\ surplus\ mg\ DO\ /L$
> $GPP = (P\text{m} * 2f/\pi) - (f * CR24)$
> $GPP = gross\ daily\ stream\ DO\ production\ (g\ DO\ /m^2\ day)$
> $f = photoperiod\ ,\ fraction\ of\ day\ recieving\ sunlight\ (d)$
> $\pi = 3.14$
> $NDM = GPP + CR24$
> $NDM = net\ daily\ metabolism\ (g\ DO\ /m^2\ day)$
>
> As shown in the example equations below, the CR24, GPP, and NDM was -7.2, 8.5, and 1.3 g/m2/d for the 9000 S site, respectively. A positive NDM indicates that OM is being produced in abundance and is a source of OM to downstream hydraulic
> reaches.
>
> $CR24 = (6\ day^{-1}) - (1.5\ mg\ DO\ /L)\ (0.8\ m) = -7.2\ g\ DO/m^2\ day$
> $P\text{m} = 6\ day^{-1}\ (2.8\ mg\ DO\ /L)\ 0.8\ m = 13.4\ g\ DO/\ m^2\ day$
>
> $GPP = P\text{m}(\ 2 * 13\ hr/24\ hr/\ \pi) - CR24\ (\ 13\ hr/24\ hr) = 8.5\ g\ DO/m^2\ day$
> $NDM = 8.5 - 7.2\ g\ DO/m^2\ day = 1.3\ g\ DO/m^2\ day$
>
> The LJR had a net DO consumption, while the UJR had a net DO production in these examples."

The extensive work of Hogsett (2015) provided a rare comparison between the two methods of calculation Net Daily Metabolism. Figure 53 of the dissertation is provided below.

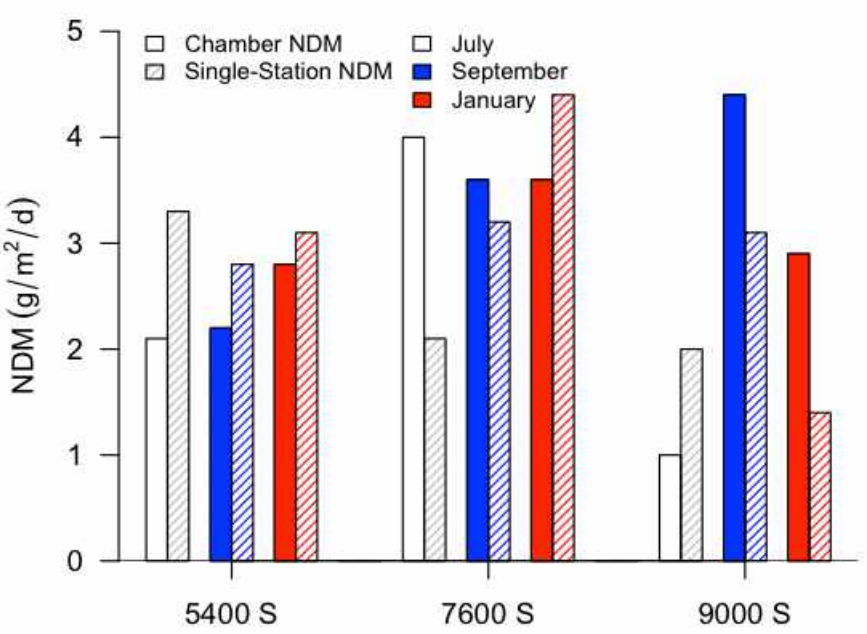

Fig. 53. UJR Chamber and single-station GW adjusted NDM estimates

The graph displays seasonal measurements among three stations located upstream from the Surplus Canal Diversion. Knowing the many sources of variability, from different days of sampling and perhaps different flows, depths and sediment characteristics among the local conditions, the results are notably quite comparable.

Figure 54 of Hogsett (2015) shows the same comparison but for sites located in the lower Jordan River. He attributed the overestimation of chamber GPP compared to single-station estimate in the LJR to the deeper river depths (>1m) resulting in greater biases towards sampling the benthos in shallower locations where the chambers could be more easily installed. As such, the 1700 S site data was nearly identical between methods, likely as a result of more uniform substrate and stream depths across the channel (personal observations). Nonetheless, the comparison of these different methods reveals the benefits and weaknesses that need to be considered for each one.

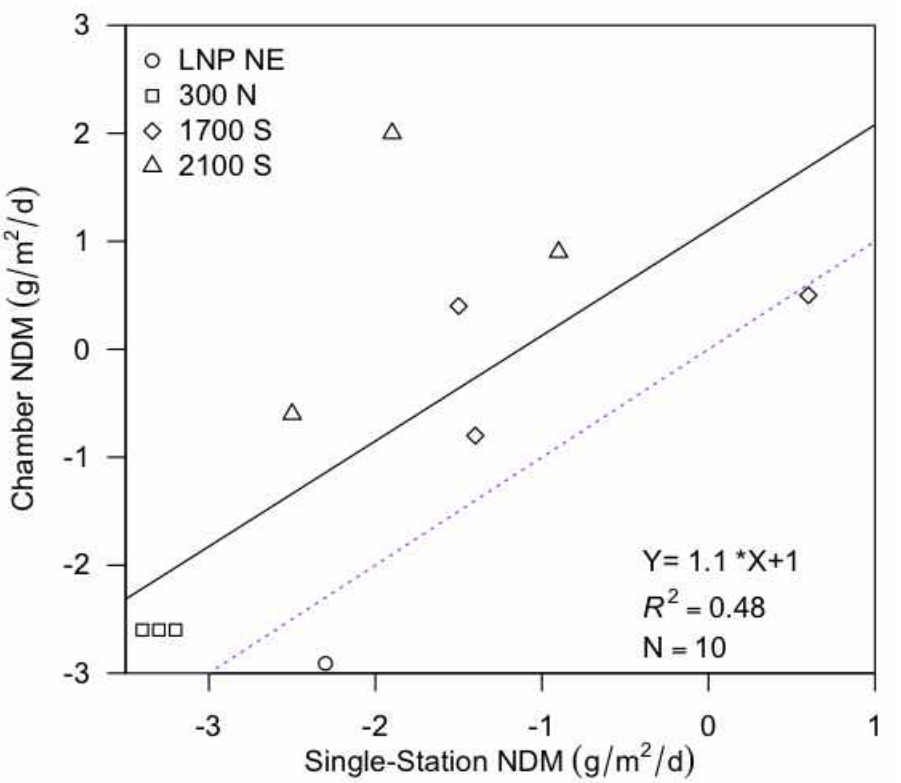

Fig. 54. Chamber vs. Single-station NDM relationship Note: summer LNP NE data not included

Hogsett concluded:

> "Overall, the NDM chambers tended to overestimate NDM in the LJR, but are very useful in isolating the sediments from the WC to determine the relative light and dark metabolic rates and fluxes. In addition, the use of chambers removes the requirement of knowing the reaeration coefficient, groundwater intrusion fluxes, and groundwater DO concentrations. By coupling multiple chamber NDM estimates with a large collection of diurnal DO NDM estimates, a great deal of information about the surface water in question can be obtained due to the strengths and weaknesses of both methods to estimate stream metabolism."

Hogsett (2015) also noted:

> "No direct correlations between POTW discharges and SOD were noted, suggesting that nutrients and organic matter are quickly distributed downstream, making it difficult to link increases in SOD directly to point discharges (Utley et al. 2008). Increases in SOD were recorded following the South Valley Water Reclamation Facility and Central Valley Water Reclamation Facility (CVWRF) discharges, but these increases in SOD cannot be directly tied to the discharges of these facilities. Large amounts of deposition occur in the slow moving backwaters of the Surplus Canal diversion dam, and this was attributed to the elevated SOD measured downstream of the CVWRF discharge. Indirectly the POTWs are influencing SOD by discharging the macronutrients nitrogen and phosphorus. The abundance of these macronutrients may be contributing to the eutrophication of the

> Jordan River, resulting in an indirect OM load via primary production in the water column and benthos (Stringfellow et al. 2009)."

A further explanation of Hogsett's (2015) conclusion is that the final clarifiers of the POTWs remove all but the smallest and least dense of suspended organic particles. Moreover, even the slow-moving Jordan River has enough velocity and turbulence to maintain this VSS in suspension to the terminus of the river, Further, the quantity/concentration of this fine particulate matter is equal to the concentration of VSS leaving Utah Lake and which also remains stable throughout the entire river (See Chapter 2). Also, while this was apparent in Stringfellow et al. (2009), SOD and the NDM results indicate that the lower Jordan River has a very low level – to net negative levels of primary production. Periphyton and Chl a results presented in Chapter 2 also indicate low quantities of standing crop, and CPOM collections throughout the river indicated that while some filamentous algae is dislodged from upstream sites (Epstein et al. 2015), relatively low quantities of identifiable algae occurred at sites below 2100 S (Epstein et al. 2015, Chapter 3). Alternatively, CPOM samples were mostly composed of seeds, leaves, grass clippings and twigs and these materials were most often described in the most recently deposited organic material in the lower Jordan River.

Additionally, although not empirically quantified as of yet, high densities of the Asian clam, Corbicula likely effect TSS by preferentially filtering and utilizing the smaller organic particles and biodepositing other TSS into the sediments. These ecosystem engineers also may be directly and indirectly affecting periphyton assemblages both spatially and temporally (see Chapter: A snail, a clam, and the River Jordan, Volume II).

While this would seemingly "let nutrients off the hook" for stimulating primary production, recent studies have addressed the stimulation of heterotrophic processes (obtaining carbon for metabolism and growth from existing organic matter, rather than photosynthesis) also consume oxygen by the addition of nutrients [(e.g. see review by and Tank and Dodds (2003) and Gulis and Suberkropp (2002)]. In such cases, the amount of organic carbon may exceed the stoichiometric concentrations of N or P, or both, for optimal growth, suggesting that reducing N and P concentrations might mitigate some of the elevated SOD experienced particularly in the Lower Jordan River. The Council sponsored a project that began researching this dilemma (Follstad-Shah et al.; Chapter 7).

Hence, the debate continues; Should we place emphasis on reduction of OM in the form of CPOM that settles and decomposes in depositional zones (i.e. by building numerous sedimentation basins) or should we focus on nutrient reductions from well-known sources (the low hanging fruit), such as our POTWs, in hopes that by limiting these nutrients, we can reduce oxygen-consuming heterotrophic activity. Either of these alternatives would cost hundreds of millions of dollars for even a chance for success and in support of the latter, Council members have volunteered to comply with nutrient reduction to 1 mg/L in our discharges. Yet, the question will inevitably arise: is this enough of a nutrient reduction to reduce the oxygen demand in the sediments?

Because the South Valley and Jordan Basin facilities have already met the 1 mg/L limit and an average of 60-70% of Central Valley's discharged is currently diverted to the Surplus Canal (via the normal diversion of the Jordan River), it is most likely that the current effluent limit of 1 mg/L will not result in any meaningful reduction in SOD or water column BOD. The greatest financial concern is that the regulatory community will simply say that the reductions were not enough and, rather than focus on the other important, but less quantifiable and currently less controllable nonpoint and stormwater sources, will try to force the POTW community to even lower and exponentially more expensive effluent limits.

Yet, hopefully, after fair thought and consideration, the alternative of modifying the Surplus Canal diversion dam and appropriate channel modifications to take advantage of the hydraulic head created by the dam, city and county managers and the regulatory community will investigate and approve the modifications that will enhance natural reaeration, provide enhanced oxygenation and turbulence for organic matter decomposition, reduce and focus channel dredging to a few specifically designed basins and improve overall substrate stability and aquatic habitat. This more appropriately addresses the three goals of the Clean Water Act: to protect and restore the physical, chemical and biological integrity of our nation's waters, and State designated beneficial uses.

Sediment organic matter

Sediment core samples were also collected to determine the proportion of organic matter in the sediments (Hogsett 2015). Samples were also partitioned into coarse particulate organic matter and fine particulate organic matter (FPOM). The following figure displays the percentage of volatile solids (VS) that occurred as CPOM, in relation to a perpendicular stream profile and with depth. Generally, there is a decrease in CPOM percentage with depth, indicating that increased time and burial since deposition, the more physical disintegration and biological decomposition occurs. Notably, Burnham Dam sediments had very little CPOM across the width of the river and sediment OM was composed of fine particulate organic matter (FPOM). This data is also in accordance with the River Continuum, as finer, less dense material would tend to drift further downstream as well as the additional time being exposed to disintegration and decomposition. In addition, the LJR has very high densities of the invasive clam, Corbicula that can often be more instrumental in sediment organic matter decomposition and recycling of nutrients from the water column through the sediments than bacteria or any other organism (see Chapter: A snail, a clam, and the River Jordan, Volume II).

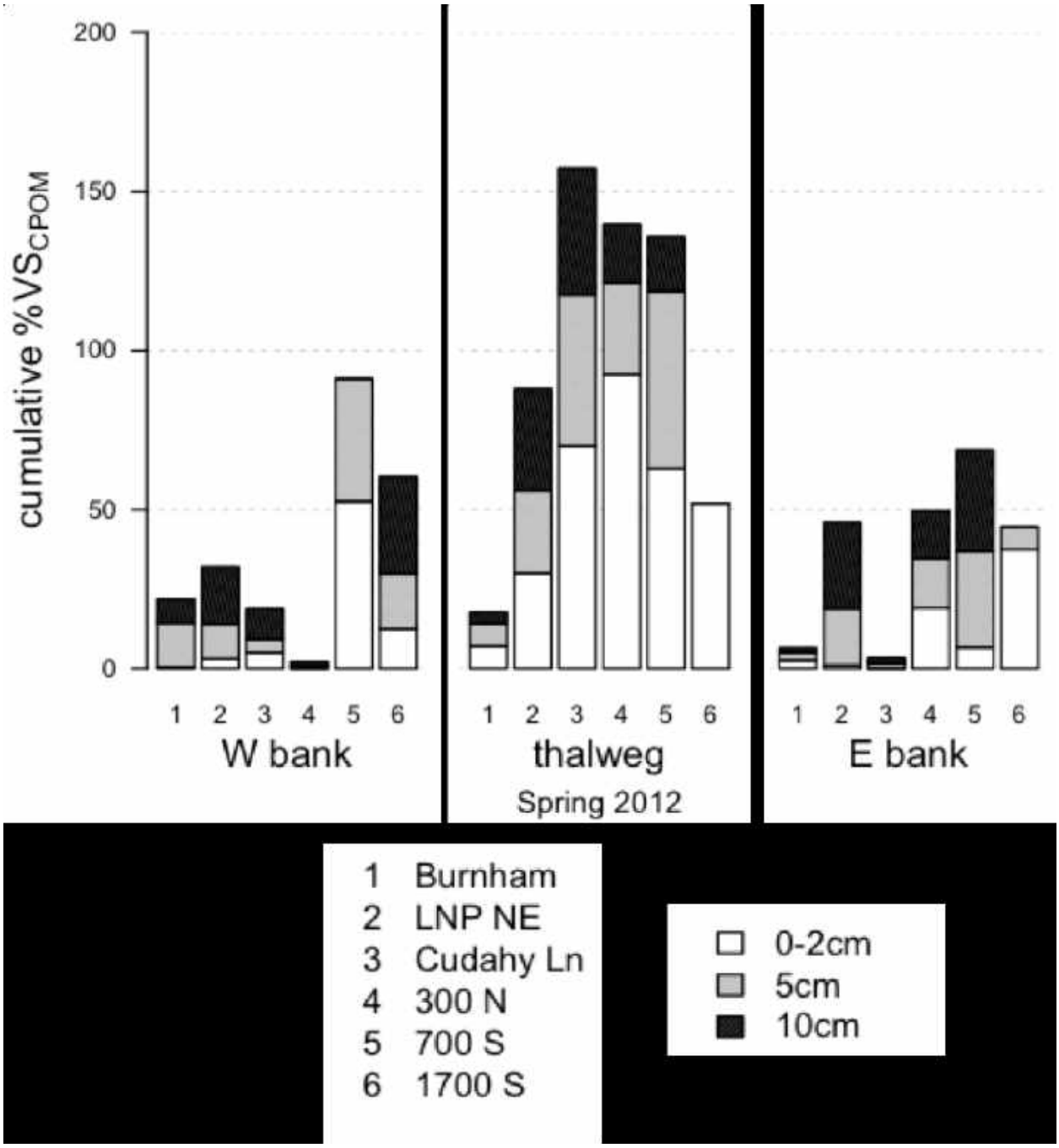

Fig. 62. River-wide cumulative sediment %VSCPOM

Nutrient flux calculations

Similar to the SOD calculations, nutrient fluxes were calculated using the normalization equation for sediment area and chamber volume while subtracting the water column rates (Chiaro et al. 1980).

Initially, three water column samples were analyzed for nutrients during the time that the flux measurements were being made (Table 22 below).

Table 22. Ambient dissolved nutrient concentration during nutrient flux sampling (mg/L)

site	date	NH_4-N	NO_2-N	NO_3-N	TIN	PO_4-P	N:P
State Canal	2/6/13	3	0.3	6.3	9.6	0.95	22
Burnham	6/12/12	0.13	0.06	3.76	4	0.53	17
Burnham	6/14/13	0.33	0.13	2.95	3.4	0.55	14
LNP NE	6/3/10	1.49	0.23	0.06	1.8	0.12	33
LNP NE	4/3/12	0.4	0.08	1.83	2.3	0.29	18
LNP NE	6/15/12	0.39	0.16	3.95	4.5	0.65	15
LNP NE	6/15/13	0.33	0.11	3.1	3.5	0.53	15
Cudahy	6/3/10	1.33	0.24	0.06	1.6	0.1	36
Cudahy	6/13/12	0.21	0.15	3.53	3.9	0.61	14
Cudahy	6/13/13	0.27	0.16	2.96	3.4	0.56	13
300 N	6/7/10	0.06		0.59	0.7	0.07	21
300 N	4/14/12	0.17	0.08	2.31	2.6	0.43	13
300 N	6/12/13	0.1	0.06	2.42	2.6	0.43	13
700 S	6/14/12	0.1	0.07	3.32	3.5	0.58	13
700 S	6/10/13	0.11	0.05	2.17	2.3	0.36	14
900 S-N	6/8/10	0.05		0.57	0.6	0.11	12
900 S-S	6/8/10	0.08		0.64	0.7	0.1	16
1700 S-N	5/24/10	0.08	0.05	1.16	1.3	0.12	24
1700 S-N	4/16/12	0.13	0.07	2.1	2.3	0.49	10
1700 S-N	6/10/13	0.06		2.93	3	0.46	14
2600 S	6/2/10	5.64	1.13	0.22	7	0.29	53
5400 S	1/12/11	0.04		3.91	4	0.74	12
7600 S	1/15/11	0.03		1.85	1.9	0.1	42
9000 S	1/20/11	0.04		1.67	1.7	0.1	38
LJR avg.		0.31	0.11	2.13	2.5	0.37	15

A total of 16 sampling events were performed or three years to generate the sediment flux values in Table 23 of Hogsett (2015). Positive values represent the efflux into the water column while negative numbers indicate influx or loss to the sediments. Notably at every site ammonia was being produced and released to the water column indicating a considerable rate of decomposition of protein or DNA-containing compounds. In addition, recent sampling and analysis of the benthic community by Dr. Richards has indicated that considerable amounts of ammonia are being released and oxygen consumed by the Asiatic clam, Corbicula. Because clams were never included in the sediment chamber experiments, the results of these experiments should be considered conservative estimates of ammonia flux to the water column. (see Chapter 13, Volume II: "A snail, a clam, and the River Jordan").

Furthermore, compared to the high nitrate concentrations listed in Table 22, it is noteworthy that there continued to be a net loss of nitrate to the sediments. This denitrification was sufficient to generate a net loss of total inorganic nitrogen (TIN) from the water column. Also notable, except for the Burnham site, there was a net efflux of P – indicating substantial decomposition of organic matter in the sediments. This loss of P from the sediments suggests that P is not limiting to the active benthic microbial community. Furthermore, when the nutrient concentrations in Table 22 are converted to moles, the N:P ratio listed in the final column appears to be correct (i.e. the Redfield ratio based on molality = 106C: 16N: 1P). Consequently, results indicate that the loss of nitrogen (due to denitrification) and the addition of P to the water column provides for a general equilibrium of the Redfield Ratio showing co-limitation. This is contrary to the Hogsett dissertation conclusion that P is limiting and further P reduction in the POTWs would be beneficial.

Table 23. Average sediment nutrient fluxes in the Lower Jordan River

average sediment flux ($g/m^2/d$)

site	NH_4-N	NO_3-N	TIN	PO_4-P
Burnham	0.03	-0.69	-0.66	-0.08
LNP NE	0.04	-0.11	-0.09	0.06
Cudahy Ln	0.22	-0.28	-0.13	0.07
DWQ	0.04	-0.03	0.00	0.05
700 S	0.07	-0.27	-0.20	0.06
1700 S-N	0.14	-0.14	-0.04	0.11

Note: data from 16 sampling events over 3 years

The total annual contribution or removal of nutrient fluxes are shown in Hogsett (2015) Table 25. The sediments add over 5,000 kg of phosphate-P and 12,000 kg of ammonia-N to the LJR, but remove over 33,000 kg of nitrate-N from the water column. This results in the sediments removing roughly 21,000 kg of dissolved nitrogen from the water column annually.

Table 25. Sediment nutrient loads to the Lower Jordan River Sediment Nutrient

	Reach 1	Reach 2	Reach 3	LJR load
NH_4-N	6,455	1,352	4,332	12,139
NO_3-N	-23,738	-985	-8,343	-33,065
TIN	-17,283	368	-4,010	-20,925
PO_4-P	1,051	1,839	2,112	5,002

Note: data from 16 sampling events over 3 years

Although not quantified, Corbicula is also responsible for much of the removal of nitrate-N from the water column into the sediments and phosphate-P and ammonia-N release into the water column (see Chapter: A snail, a clam, and the River Jordan).

Sediment methane flux

The denitrification processes are complex as several organic compounds have been identified as important electron donors. The case described by Hogsett (2015), is perhaps oversimplified as it implies that anaerobic methane oxidation is a key pathway to the overall oxidation of methane.

Hogsett (2019) states:

> Methane produced in organically enriched sediments can be utilized as a readily biodegradable substrate (rbCOD) for some heterotrophic denitrifying bacteria. This results in a much lower theoretical DO requirement of 1.71 g-O2/g-N for the complete nitrification and denitrification process utilizing ammonia and methane produced during the anaerobic decomposition of OM (Chapra 2008).

The following equations are used as an example:

$$5/8CH4 + HNO3 \rightarrow 5/8CO2 + 1/2N2 + 7/4H2O$$
$$NH3 + 3/4O2 \rightarrow 1/2N2 + 6/4H2O$$

Hogsett (2015) further states:

> This is important because methane can be oxidized using either nitrite or nitrate as an electron acceptor instead of DO, thereby decreasing the ambient DO demand required for the direct oxidation of both methane and ammonia independently (Chapra 2008, pg. 459). This results in an additional nitrogenous oxygen demand of roughly 11% of the carbon oxygen demand, compared to 30% when nitrate is not used as an electron
> acceptor during methane oxidation. This is important in degraded urban rivers since nitrate is typically in abundance due to POTW discharges and can be utilized to oxidize sediment produced methane.

However, this may be an oversimplification of the fate of methane as there are several substrates that are available and are utilized by denitrifiers (including, but not limited to methanol, ethanol, acetate and other small chained fatty acids and proteins (e.g. see Lopez 2011, Eisentraeger, et al 2001, Beauchamp et al. 1989, among others) as electron donors. As these carbon sources are also extremely abundant in urban streams and, although much of the stoichiometry remains to be worked out, they also will compete thermodynamically in donating electrons to the denitrification process.

Moreover, Chapra and Pelletier 2003, for their QUAL2Kw model simplifies SOD as the sum of nitrification and methane oxidation. While additional electron donors and accepters are involved in aerobic and anaerobic methane and ammonia and nitrate reduction Chapra and Peletier (2003) use these reactions to describe dominant contributions to SOD. Accordingly, these reactions can be summarized as follows:

For ammonia oxidation:

$$NH_3 + 1.5O_2 \rightarrow NO2 * H + H_2O$$

And secondly:

$$NO_2 + 0.5O2 \rightarrow NO_3$$

Together the ratio of oxygen to nitrogen consumed during nitrification [= 4.57 gO_2/gN]

This is important that Hogsett (2015)(Table 25) estimated that lower Jordan River sediments produce 12,139 kg of ammonia. Thus 55,475 kg of DO are consumed annual in the lower Jordan just from oxidizing the ammonia produced in Jordan River sediments. As mentioned above, much of the ammonia production and oxygen consumption can be attributed to Corbicula excretion that was not measured by Hogsett (2015).

Table 25. Sediment nutrient loads to the Lower Jordan River Sediment Nutrient loading (kg/year)

	Reach 1	Reach 2	Reach 3	LJR load
NH_4-N	6,455	1,352	4,332	12,139
NO_3-N	-23,738	-985	-8,343	-33,065
TIN	-17,283	368	-4,010	-20,925
PO_4-P	1,051	1,839 2,112		5,002

Note: Based on 16 measurements over 3 years

Methane chemistry and metabolism are more complicated. While anaerobic methane oxidation pathways involving different terminal electron acceptors such as NO_3, SO_4, and oxides of Fe and Mn are thermodynamically possible, their reaction rates are considerably lower than that of aerobic oxidation (Lopes et al. 2011). Alternatively, the oxidation of methane by methanotrophic bacteria is the major pathway for methane oxidation and oxygen consumption. Lopes et. al. (2011) found that the aerobic methane oxidation rate to CO_2 and H_2O was more than 2 orders of magnitude faster than anaerobic oxidation of methane as an electron donor to denitrification in a meromictic lake. Scheutz, et al. 2007, describes how methane is oxidized in this process in detail. An alternative and simplified equation of the process is shown below:

$$CH_4 + 2O_2 \rightarrow CO_2 + 2H_2O$$

This direct pathway by many methanotrophs is important in that:

16 g of CH_4 /mole needs 64 g (2 moles) of O_2 or 4 g O_2 / g methane

As compared to the oxidation of glucose:

$$C_6H_{12}O_6 + 6O_2 \rightarrow 6CO_2 + 6H_2O$$

Or based on moles:

212 g of glucose needs 128 g O_2 or 0.6 g O_2 / g glucose

In other words, the oxidation of methane requires 6.7 times more oxygen that the oxidation of glucose.

Therefore, while anaerobic methane oxidation may participate in nitrate reduction, it is much more likely to be oxidized directly by methanotrophic bacteria and together, methane, and ammonia oxidation are not only the primary sources of SOD (Chapra and Pelletier 2003); they represent huge quantities of oxygen loss in the lower Jordan River.

Conclusion

In conclusion, there is no question that the primary source of oxygen demand is SOD and that the primary source of SOD is the vast amount of CPOM that is transported to and settles in the depositional zones of the lower Jordan River. However, direct and indirect biotic pathways and spiraling of CPOM to SOD to O_2 demand have been ineffectually measured and are not completely understood. From a water quality management perspective, the next step is to determine if occasional low O_2 levels negatively affect Clean Water Act ecological integrity or State designated beneficial uses i.e. “warm water game fishery and aquatic life they depend on” or are the biota in the Jordan River more limited by other factors.

Literature Cited

Beauchamp E.G., Trevors J.T., Paul J.W. (1989) Carbon Sources for Bacterial Denitrification. In: Stewart B.A. (eds) Advances in Soil Science. Advances in Soil Science, vol 10. Springer, New York, NY

Borup, B. and N. Haws. 1999. Jordan River Flow Analyses. Brigham Young University, Civil and Environmental Engineering Department, Provo, Utah. Prepared for State of Utah, Department of Environmental Quality, Division of Water Quality.

Chapra, S.C. and Pelletier, G.J. 2003. QUAL2K: A Modeling Framework for Simulating River and Stream Water Quality: Documentation and Users Manual. Civil and Environmental Engineering Dept., Tufts University, Medford, MA., Steven.Chapra@tufts.edu

Christensson, M., L. Ewa, and W. Thomas. 1994. A comparison between ethanol and methanol as carbon sources for denitrification. Wat. Sci. Technol. 30(6): 83-90.

CH2M Hill. 2005. Jordan River Return Flow Study. Report to Recycled Water Coalition.

Dodds W. K. 2007, Trophic state, eutrophication and nutrient criteria in streams. TRENDS in Ecology and Evolution Vol.22 No.12

Eisentraeger, A., P. Klag, E. Heymann and W. Dott. 2001. Denitrification of groundwater with methane as sole hydrogen donor. Water Research. 35: 2261-2267

Goel, R., S. Abedin and S. Teeters. 2014. Understanding Nitrogen Dynamics at Selected Sites in The Jordan River and The Great Salt Lake Wetlands. Report to the Wasatch Front Water Quality Council.

Gulis, V. and Suberkropp, K. (2002) Effect of inorganic nutrients on relative contributions of fungi and bacteria to carbon flow from submerged decomposing leaf litter. Microb. Ecol. 45, 11–19

Hogsett, M.C. 2015. Water quality and sediment biogeochemistry in the urban Jordan River, UT. PhD Thesis. University of Utah. 293 p.

Lopes, F. Eric Viollier, A. Thiam, Gil Michard, G. Abril, et al.. Biogeochemical modelling of anaerobic vs. aerobic methane oxidation in a meromictic crater lake (Lake Pavin, France). Applied Geochemistry, Elsevier, 2011, 26, pp.1919-1932.

Scheutz, C., P. Kjeldsen, J. E. Bogner, A. De Visscher, J. Gebert, H. A. Hilger, M. Huber-Humer and K. Spokas. 2009. Microbial methane oxidation processes and

technologies for mitigation of landfill gas emissions. Waste Manag Res 2009 27: 409. Online at: http://wmr.sagepub.com/content/27/5/409

Tank, J.L. and Dodds, W.K. (2003) Responses of heterotrophic and autotrophic biofilms to nutrients in ten streams. Freshw. Biol. 48, 1031–1049

Chapter 6

Nitrogen sources and transformations *and* Microbial community response to energy *and* nutrient availability in the Jordan River

J. Follstad-Shah, R. Smith, R. Gabor, S. Weintraub, Y. Jameel & M. Navidomskis

With Introduction and Comments Prepared by

Theron G. Miller

Wasatch Front Water Quality Council

August 2019

Table of Contents

Introduction

The Wasatch Front Water Quality Council also funded a study to investigate microbial activity as it relates to nutrient transformations and oxygen consumption. Microbial communities are responsible for the majority of organic matter and nutrient transformations in streams and rivers (Mallin et al. 2011, Sinsabaugh and Follstad Shah 2012), although when bivalves (e.g. Corbicula) are present at high densities, microbial community effects are altered, reduced, or even circumvented through bivalves (see Chapter X: A snail, a clam, and the River Jordan). Heterotrophic activity can deplete oxygen as discussed in Chapter 6. However, the debate continues as to whether the majority of organic matter supplied to the Jordan River is due to instream or autotrophic primary production or from terrestrial or allochthonous sources such as leaves, grass, seeds etc. or from POTW effluents. Furthermore, the quality of organic matter within the system has not been well characterized. It also is unclear whether microbial communities in the Jordan River are limited by an imbalance in organic matter, nitrogen and/or phosphorus at various times or locations, despite generally high supply of these resources or are influenced by bivalves. Highlights of the Follstad et al. 2017 report are presented below as quoted from the report (indented). The full report is attached.

Methods

A variety of methods were used in this investigation. As the authors (Follstad et al. 2017) explain:

> "Wastewater effluent is often nutrient rich and enriched in δ 15N compared with other sources such as precipitation, fertilizer and soil N, due to mass-dependent fractionation during waste production (Kendall et al. 2007). Denitrification within aquatic habitats can further enrich δ 15N within the water column as microbes preferentially use 14N (Kendall et al. 2007). Hence, we are using measures of riverine nutrient concentrations, hydrologic flow volume, and stable isotope analyses (natural abundance) to quantify the contribution of effluent to N loading to the river, compared with other sources (Research Question 1), the degree to which N is transformed downstream via biotic processes (Research Question 2), and the extent to which biota assimilate N from WRF inputs (Research Question 3). We are using a mass balance approach to quantify WRF contributions of nutrients and water to the river, based on nutrient concentrations within the river and effluent sources combined with flow volumes for the river and effluent discharge (Research Question 1). We are quantifying changes in the natural abundance of 15N-NO3 in the water column downstream of the Central Valley WRF to determine if denitrification is occurring along the Jordan River flowpath, which would result in a loss of N gas to the atmosphere (Research Question 2). We are measuring the natural abundance of 15N in particulate organic matter within the water column, biofilms, and sediments to infer whether N inputs from WRFs are being assimilated by biota within the Jordan River (Research Question 3).

Elemental content and stable isotopes of biofilms, organic matter, and sediment

> "We are quantifying the natural abundance of a suite of stable isotopes (2H, 13C, and 15N) and the C:N ratios of biofilms, fine particulate organic matter (FPOM) in the water column and sediments (13C and 15N only), and senesced leaves of riparian plants to infer whether organic matter within Jordan River is primarily of aquatic or terrestrial origin (Research Question 4). This suite of stable isotopes was chosen for several reasons. First, the natural abundance of deuterium (2H) produced in aquatic (-250 0/00) vs. terrestrial (-150 0/00) habitats generally differs by ~ 100 dell units (0/00; Doucett et al. 2007). Second, measurement of 13C and 15N combined with C:N ratios also can distinguish between organic matter derived from algal vs. terrestrial production (Finlay and Kendall 2007). Third, measurement of 13C and 15N may help to determine if organic matter has an anthropogenic signature. Human diets are now rich in products derived from corn, a C4 plant that is more enriched (-13 0/00) in 13C relative to C3 plants (-27 0/00), such as riparian shrubs and trees, and freshwater autotrophs (-18 to -35 0/00; Finlay and Kendall 2007). In addition, fecal matter is typically enriched in 15N (+15-20 0/00) relative to the atmosphere or N fixed by biota (0 0/00; Kendall et al. 2007)."

Ecoenzyme expression and excitation-emission matrices

> "We are inferring the quality of organic C fueling microbial community metabolism (Research Question 5) using two complementary approaches: measurement of ecoenzyme activity rates associated with the hydrolysis of labile and recalcitrant organic matter (Table 2) and quantification of dissolved organic C (DOC) concentrations combined with multi-wave fluorescence spectroscopy to create excitation-emission matrices (EEMs). Microbes generally express more POX relative to BG when available organic matter is recalcitrant (Sinsabaugh and Follstad Shah 2011). EEMs represent a simple index used to identify the types of organic matter present in samples and distinguish between likely sources of organic matter to rivers (McKnight et al. 2001). Microbes generally produce and release enzymes proportional to energy or nutrient requirements (Sinsabaugh and Follstad Shah 2012; Table 2). When the availability of energy and nutrient resources meet microbial maintenance and growth demands, the ratios of ecoenzymes related to C, N, and P resources is approximately 1:1:1 (Sinsabaugh et al. 2009). Deviations from these ratios indicate whether microbial communities are energy or nutrient limited (Sinsabaugh andFollstad Shah 2012). We have measured the activity rates of five ecoenzymes associated with microbial acquisition of C, N, and P using high throughput fluorescence spectroscopy to address whether these resources are balanced or imbalanced relative to microbial stoichiometric requirements (Research Question 6)."

Important Findings of Follstad et al. 2017

In the intensively sampled reach there was a positive correlation between $\delta^{15}N\text{-}NO_3$ and $\delta^{18}O\text{-}NO_3$ for water samples collected in spring along ($r^2 = 0.67$; Fig. 6 of the report). The slope for this relationship was 0.45, which is close to the value (0.50), expected if N is being transformed via denitrification along the downstream flowpath. This supports the large denitrification values reported by Hogdsett, (2015). However, samples became less enriched in $^{15}N\text{-}NO_3$ along the flowpath, suggesting either that N fixation is occurring or novel inputs of less enriched in 15N-NO3 are entering the system (e.g., leaf litter from N_2-fixing species, such as Russian olive [*Elaeagnus angustifolia*], groundwater recharge; Follstad -Shaw et al. 2017); or possibly $N\text{-}NO_3$ spiralling through the ecosystem by Corbicula. Alternatively, however, this reduction in enrichment may be due to nitrification and denitrification of organic matter from terrestrial sources (i.e. the more natural leaf, seed, grass, etc. material that is delivered in the 10s to 100s of thousands of kg each year from riparian and tributary sources (see Chapter 3). Analyses of $\delta^{15}N\text{-}NO_3$ and $\delta^{18}ONO_3$ for water samples collected in summer and fall do not show this trend, however. When combined with longitudinal trends in $\delta^{15}N\text{-}NO_3$ and $\delta^{18}O\text{-}NO_3$ Follstad-Shah et al. 2017 "suggests that denitrification does not have a strong impact on nitrate removal in the water column. Instead, nitrification may be favored". However, this data conflicts with the ammonia and nitrate flux data presented for multiple years and seasons by Hogsett (2015). This conflict suggests further work needs to be done on this important subject including the effects of Corbicula, which were not addressed by either Hogsett (2015) or Follstad et al 2017.

Is wastewater effluent a source of N for in-stream biota?

The Follstad et al. 2017 report states:

> "$\delta^{15}N$ of fine particulate organic matter (POM) measured in our study was quite variable, ranging from 3-12 ‰ (Fig. 7). $\delta^{15}N$ of POM derived from effluent discharged from the Jordan Valley WRF consistently had lower (depleted) values than the river, while effluent discharged from the Central Valley WRF consistently had higher (enriched) values than the river. Effluent from the South Valley WRF had $\delta^{15}N$ of POM values lower than the river in spring and fall, but higher values in summer. $\delta^{15}N$ of POM values just downstream of WRFs sometimes declined in response to lower effluent inputs (e.g., downstream of Jordan Valley WRF in fall), but sometimes increased (e.g., downstream of Jordan Valley WRF in summer) relative to upstream river $\delta^{15}N$ of POM signatures. These data indicate we cannot correlate $\delta^{15}N$ of POM signatures to effluent discharge. However, downstream of the Central Valley WRF, $\delta^{15}N$ of POM values were always enriched, suggesting a consistent influence of effluent inputs on POM signatures at this location. It is possible these differences are due to differences in technology used at the various WRFs along the river."

In fact, the two upstream plants, Jordan Basin and South Valley employ biological nutrient removal. It would be interesting to investigate the reason for this discrepancy, as many papers have cited different $\delta^{15}N$: $\delta^{14}N$ signatures between terrestrial carbon sources and organic carbon in POTW discharges. At this point, however, stable isotopes do not

appear to be very useful in identifying relative sources (i.e. human vs natural or plant) of N.

The Follstad et al. 2017report also states:

> "δ15N of POM values measured in 2013 (Kelso and Baker 2017) and 2016 were of a similar range but values in 2016 were usually more enriched relative to values in 2013 (Fig. 7). $\delta^{15}N$ of POM values for both 2013 and 2016 were much more depleted relative to $\delta^{15}N$ of DOM measured in 2013 (Kelso and Baker 2017). $\delta^{15}N$ of DOM was 6 ‰ greater downstream of the Central Valley WRF relative to upstream in summer of 2013. These data suggest that the N signature of effluent discharge is more evident in the river's DOM pool as compared to the POM pool. However, we do not have data on the $\delta^{15}N$ of DOM within effluent, so this conclusion is uncertain. We have not reported $\delta^{13}C$ values of POM or C:N ratio of POM because many of our samples had highly enriched $\delta^{13}C$ values, suggesting contamination of carbonates within the POM matrix presumably due to suspended solids in the river. We could not correct for these carbonates through acid digestion given the small quantity of POM collected on filters."

The lack of effluent DOM data, as well as the inability to correct for the high carbonate concentrations, are two serious shortcomings of this study. While the Council tried to negotiate additional data collection to complete this data set, these questions remain unanswered.

Are substrates supporting microbial community metabolism in the Jordan River primarily of terrestrial or aquatic origin?

The Follstad et al. 2017report states:

> "We did not find distinction between the $\delta^{2}H$ values of biofilms and riparian vegetation, as expected (Figs. 8-9). Contamination of biofilms by entrained sediment enriched in ^{2}H is one possible reason for this outcome. However, we found that FPOM $\delta^{2}H$ values were similar in both 2013 (measured by J. Kelso) and 2016 (our study) (Fig. 9). FPOM from both years of sample collection and DOM (measured in 2013 by J. Kelso) also had similar $\delta^{2}H$ values (Fig. 9). Mean annual flow in the Jordan River at 1700 S. was 20.6 ft3 s^{-1} for 2013 and 34.6 ft3 s^{-1} for 2016 (USGS 2017). Differences in flow in these years may have altered the relative contribution of terrestrial vs. aquatic sources to dissolved and particulate organic matter pools, but it is not possible to distinguish between contributions from various sources without isotopic distinction in biofilm and riparian vegetation end-members.
>
> Fluorescence Index (FI) is one type of index that can be calculated from excitation-emission matrices (EEMs). FI values from Antarctica (a purely microbial source) are approximately 1.8- 2.0. FI values from the Suwannee River (with intact wetland) are approximately 1.1-1.2. Hence, lower FI values are associated with plant material and higher FI values are associated with microbial biomass or

material sourced from microbes. The Jordan River has very high FI values – as high or higher than values observed from microbe dominated communities of Antarctica (Fig. 10). These results suggest that microbes may constitute a significant fraction of dissolved organic carbon (DOC) in the water column. However, EEMs have not been commonly used in urban river systems. Such systems may contain constituents that augment FI values relative to systems without large human populations. That said, our results spurred us to examine the methods used to generate FI values, which may lead to a modification of the analysis used to measure FI. We will re-analyze our data, should this modification be deemed appropriate. Regardless of the actual value of FI, our data suggest that WRFs influence FI values, given that FI values were generally elevated downstream of WRFs relative to upstream sites. Lowest FI values in the Jordan River were observed just downstream of Utah Lake, upstream of the Jordan Basin WRF, and in the Unit 1 wetland. Higher rates of primary production in all of these areas relative to other parts of the Jordan River may be one mechanism leading to similarity in FI values. FI values were lowest in the Jordan River in spring, during high hydrologic flow, and generally increased through summer and fall. Highest FI values in fall as compared to other seasons suggest terrestrial sources do not contribute significantly to dissolved organic matter loads, contrary to previous reports (UDWQ 2015)."

What is the quality of the organic matter within the Jordan River?

The Follstad-Shah report states:

> High FI values (Fig. 10), as discussed previously, suggest that DOC in the Jordan River water column is very labile. BG:POX ratios (Fig. 11) also show much greater rates of ecoenzyme expression related acquisition of C from labile sources (i.e., glucose) relative to more recalcitrant sources (i.e., lignin). Ecoenzyme expression was measured on unfiltered water samples, so these data are reflective of both dissolved and particulate forms of organic matter.

Are microbial communities in the Jordan River limited by C, N, and/or P?

The Follstad-Shah report states:

> Ecoenzyme activities in water derived from the river, effluent, oil drain, and wetland were highly variable both spatially and temporally (Fig. 11).

An explanation of the abbreviations for the ecoenzymes are displayed in Table 2, shown below:

Table 2. Microbial ecoenzymes and their ecological roles.

Ecoenzyme	Code	Ecological Role

β-1,4-glucosidase	BG	Carbon acquisition via cellulose degradation; hydrolyzes glucose from cellobiose
β-1,4-N-acetylglucosaminidase	NAG	Carbon and nitrogen acquisition via chitin and peptidoglycan degradation; hydrolyzes glucosamine from chitobiose
Leucine aminopeptidase	LAP	Nitrogen acquisition via proteolysis; hydrolyzes leucine and other hydrophobic amino acids from the N terminus of polypeptides
Acid (alkaline) phosphatase	AP	Phosphorus acquisition via hydrolysis of phosphate from phosphosaccharides or phospholipids
Phenol oxidase	POX	C acquisition via the oxidative degradation of lignin

The report states:

> "Activities of ecoenzymes associated with C and N acquisition (BG, NAG+LAP) were high in effluent, resulting in elevated activities downstream. This pattern was not evident with respect to activities of ecoenzymes associated with P acquisition (AP). AP activities along the river's flow path in summer were the mirror opposite of activities in spring and fall, while longitudinal patterns of BG and NAG+LAP were generally similar through time. Regression analyses of ecoenzyme activities (Fig. 12) showed consistent positive relationships between C and N acquisition, explaining between 54-85% of the variation. Slopes had values less than 1, suggesting the river is more limited with respect to N relative to C. Relationships between C and P acquisition and N and P acquisition were positive in summer, but explained less variation (27% for C:P, 11% for N:P). These positive relationships in summer may result from higher temperatures driving higher metabolic rates, and thus higher growth rates (Sinsabaugh and Follstad Shah 2011). High growth rate requires greater P uptake given that ribosomes are rich in P. In contrast, negative relationships were evident in spring and 2017 fall, explaining between 15-26% of the variation. Negative relationships in spring and fall are indicative of greater allocation to P relative to C and N, which typically occurs when P is limiting growth. Hence, ecoenzyme expression in the water column of the Jordan River shows that microbial communities perceive differences in resource supply relative to metabolic needs and are responding most to P availability.
>
> Ecoenzyme activities in sediment derived from the river, oil drain, and wetland were highly variable both spatially and temporally (Fig. 13). However, longitudinal variation in patterns of BG, NAG+LAP, and AP showed greater concordance as compared to patterns in the water column. Correlation in longitudinal patterns were supported by consistent positive relationships in relationships between BG vs. NAG+LAP, BG vs. AP, and NAG+LAP vs. AP, which explained between 11-51%

of the variation (data not shown). BG vs. NAG+LAP and BG vs. AP slopes were close to or greater than 1, indicating either matched allocation of energy to C and N acquisition or greater allocation of energy towards C acquisition. NAG+LAP vs. AP slopes were approximately 1 in spring and fall, indicating matched allocation of energy to N and P acquisition, but 0.74 in summer indicative of greater allocation to P when growth rate demands are highest.

In summary, microbial communities in the water column and sediment differ with respect to C, which is in adequate supply in the water column but appears to be limiting in the sediment in some seasons. Microbial communities in the water column and sediment are similar because N appears to be in adequate supply and both communities are limited with respect to P at some times of the year."

Conclusions

While these new techniques may be useful in natural (i.e. more pristine) streams and rivers, these data indicate that that substantial limitations exist in the urbanized Jordan River. Of particular concern, most all indicators used, vary with seasonality, therefore, no conclusive statements could be made. In addition, the use of stable isotopes provided little useful information. Although not useful for discerning relative sources of organic carbon, the conclusion that: Differences in flow between the sample years (2013 vs 2016) may have altered the relative contribution of terrestrial vs. aquatic sources to dissolved and particulate organic matter pools is useful information as it is likely a key variable that needs to be accounted for. In this case thus far, "it is not possible to distinguish between contributions from various sources without isotopic distinction in biofilm and riparian vegetation end-members."

Finally, it seems unlikely that any particular nutrient could be limiting and the indication that this limitation may vary between seasons supports this conclusion. Moreover, it is well known that the vast majority (80 to 95%) of P in POTW effluents is ortho-P or soluble reactive P. As such because the Jordan River is close to being effluent dominated, depending on season, there is always plenty of ortho-P throughout the river and concentrations of either ammonia or nitrate, as well as dissolved organic carbon follow suit. Thus, the indication that one or the other nutrient may be limiting at different locations of time is likely based on unexamined and unexplained factors that influenced variability in the data (e.g. bivalve or other benthic biota ecology, measurement error, etc.) and should not be used as support for controlling specific nutrients. The ultimate futility of such nutrient controls is further discussed in Chapter 3 and Chapter 5.

WATER QUALITY AND SEDIMENT BIOGEOCHEMISTRY

IN THE URBAN JORDAN RIVER, UT

by

Mitchell Clay Hogsett

A thesis submitted to the faculty of
The University of Utah
in partial fulfillment of the requirements for the degree of

Doctor of Philosophy

Department of Civil and Environmental Engineering

The University of Utah

May 2015

The University of Utah Graduate School

STATEMENT OF DISSERTATION APPROVAL

The dissertation of **Mitchell Clay Hogsett**

has been approved by the following supervisory committee members:

Ramesh Goel	, Chair	**7-30-2014** Date Approved
Otakuye Conroy–Ben	, Member	**7-30-2014** Date Approved
Michelle Baker	, Member	**7-31-2014** Date Approved
Theron Miller	, Member	**7-30-2014** Date Approved
Carl Adams	, Member	**7-30-2014** Date Approved
Steve Burian	, Member	**8-2-2014**

and by **Michael Barber**, Chair/Dean of

the Department/College/School of **Civil & Environmental Engineering**

and by David B. Kieda, Dean of The Graduate School.

ABSTRACT

Urban rivers are plagued with a variety of ailments ranging from hydraulic modifications, organic matter enrichment, loss of biodiversity, toxic pollutant loads, and chronically low dissolved oxygen (DO) concentrations. Utah's Jordan River is no exception, and the purpose of this research was to better understand the chronic DO deficits found in the lower river flowing through Salt Lake City. The primary goals were focused on identifying and quantifying DO dynamics in the water column and at the sediment-water interface, macronutrient dynamics, sediment methane production, sediment organic matter (OM) standing stocks, size speciation of sediment OM, and the estimation of OM loads associated with primary production in the Upper Jordan River. Solids, liquids, and gases were investigated to identify linkages and to conduct mass balances on both DO and OM to better understand the urban Jordan River.

TABLE OF CONTENTS

LIST OF ACRONYMS

AOB	ammonia oxidizing bacteria
BOD	biochemical oxygen demand
BOD_5	5-day biochemical oxygen demand
cfs	cubic feet per second
C	carbon
Chl-a	chlorophyll-a
C:N:P	carbon to nitrogen to phosphorus molar ratio
COD	chemical oxygen demand
CPOM	course particulate organic matter
CR_{24}	24-hour community respiration
DO	dissolved oxygen
DOC	dissolved organic carbon
DOM	dissolved organic matter
DP	dissolved phosphorus, orthophosphate
FPOM	fine particulate organic matter
GBD	gas bubble deterioration
GBT	gas bubble trauma
GPP	24-hour gross primary production
GW	groundwater
LJR	Lower Jordan River
LNP	Legacy Nature Preserve
LWD	large woody debris
NPP	net primary production
NDM	net daily metabolism
NBOD	nitrogenous biochemical oxygen demand
NOB	nitrite oxidizing bacteria
OM	organic matter
ORP	oxidation-reduction potential
POM	particulate organic matter
POTW	publicly owned treatment works
ppmV	volumetric parts per million
rbCOD	readily biodegradable chemical oxygen demand
SCUBA	self contained underwater breathing apparatus
SD	standard deviation
SOD	sediment oxygen demand
STORET	Storage and Retrieval identification number
STP	standard temperature and pressure
TDS	total dissolved solids

TSS	total suspended solids
TMDL	total maximum daily load
TIN	total inorganic nitrogen (sum of nitrite, nitrate, and ammonia nitrogen)
TN	total nitrogen
TP	total phosphorus
UBOD	ultimate biochemical oxygen demand
UJR	Upper Jordan River
USEPA	United Stated Environmental Protection Agency
USGS	United States Geological Survey
Utah DWQ	Utah Division of Water Quality
WC	water column
WRF	water reclamation facility
WQ	water quality
WWTP	wastewater treatment plant
%TS	percent total solids
%VS	percent volatile solids

LIST OF COMMOMLY USED PARAMETERS

$CH_{4,OD}$	oxygen demand required to oxidize sediment methane flux (g DO/m^2/day)
$CPOM_{aer,stretch}$	standing stock of sediment CPOM (kg OM)
CR_{24}	24-hour community respiration (g DO/m^2/day)
CR_{GW}	low DO groundwater intrusion flux (g DO/m^2/day)
$CR_{GW,24}$	24-hour community respiration adjusted for GW intrusion (g DO/m^2/day)
GPP	gross primary production (g DO/m^2/day)
NDM	net daily metabolism (g DO/m^2/day)
NDM_{adj}	Single-station NDM adjusted for low DO GW intrusion (g DO/m^2/day)
OM_{aerial}	standing stock of sediment organic matter (g OM/m^2)
$OM_{aer,stretch}$	standing stock of sediment OM matter (kg OM)
SOD	sediment oxygen demand flux (g DO/m^2/day)
SOD_{20}	sediment oxygen demand flux normalized to 20°C (g DO/m^2/day)
TDS	total dissolved solids, salt content (mg salt/L)
TOD	tray oxygen demand flux (g DO/m^2/day)
TPP	tray gross primary production (g DO/m^2/day)
TSS	total suspended solids (mg solids/L)
VSS	volatile suspended solids (mg burnable/L)
WC_{dark}	water column dark respiration rate (g DO/m^3/day)
WC_{light}	water column gross primary production rate (g DO/m^3/day)
$\%_{SOD}$	percent of nighttime DO deficit associated with the sediments
%TOC	percent total organic carbon (mass organic carbon/mass dry sediment) • also referred to as TOC
%TS	percent total solids (mass dry sediment/mass wet sediment) • also referred to as $\%TS_{bulk}$ and TS
%VS	percent volatile solids (mass burnable/mass dry sediment) • also referred to as $\%VS_{bulk}$ and VS
$\%VS_{bulk\ avg}$	three sample average %VS across width of river
$\%VS_{wet}$	percent volatile solids of wet sediment (mass burnable/mass wet sediment)
$\%VS_{CPOM}$	percent of VS as CPOM (mass burnable CPOM/mass burnable dry sed.)
Q_{10}	change in rate of metabolism for 10°C temperature change

ACKNOWLEDGEMENTS

I would like to thank my advisor Dr. Ramesh Goel for the opportunities, guidance, and support during both my masters and doctorate research. I would also like to thank my lab mates for their input, help, and friendship. A special thanks to the Utah Division of Water Quality and the Jordan River/Farmington Bay Water Quality Council for funding this research while providing equipment, training, and insight. I would like to show my appreciation to Dr. Theron Miller for introducing me to a variety of field sampling methods and sharing his knowledge regarding water quality in the Wasatch Front. Finally, I would like to thank my committee members for their valuable suggestions, criticisms, and perspectives.

CHAPTER 1

INTRODUCTION

The Jordan River flows from Utah Lake along the urbanizing Wasatch Front before entering a complex of constructed wetlands and finally draining into the terminal Great Salt Lake. Utah's Jordan River is a highly managed urban river that has been the recipient of both anthropogenic and natural pollutants. In recent years, there has been a growing awareness concerning the issues influencing the health and function of the Jordan River. These issues include channelization, urban stormwater runoff, industrial/municipal wastewater discharges, eutrophication, loss of riparian habitat, excessive incision/sedimentation, flow diversions, agricultural diffuse runoff, and water management. It is important to recognize that the continued growth and urbanization in the Salt Lake Valley will add to the load of waste and pollutants that will eventually find their way into the Jordan River.

The Jordan River has been classified as impaired in the lower three hydraulic reaches in terms of dissolved oxygen (DO) and *E. Coli*. (Utah DWQ 2013, Table 1.1). DO impairments can result in a variety of both acute and chronic water quality (WQ) problems. These problems include bad smells, degradation of the native aquatic community, problematic nutrient/toxicant transformations, and fish kills that can result from individual events, such as a large algal bloom die off (Tenore 1972; Heaney and Huber 1984; Dauer et al. 1992). This applied research will focus on identifying and

quantifying DO dynamics occurring in the water column and at the sediment–water interface.

There are many different water quality (WQ) models available to visualize the function and health of a lotic system (Cox 2003). The QUAL2kw model was adopted by the Utah Division of Water Quality (Utah DWQ) as a platform to store, share, and model WQ data collected from the Jordan River. During the Utah DWQ modeling efforts, the sediments were identified as a potential source of the river's chronic DO deficits. Models are extremely useful, but they require large amounts of planning, stakeholder involvement, and field-collected data for meaningful calibration (Beck 1987; Refsgaard et al. 2007; Cox 2003).

As part of this research, the field measured parameters sediment oxygen demand (SOD), methane, ammonium, and orthophosphate sediment fluxes can be directly incorporated into the QUAL2kw model framework (Pelletier et al. 2006). The measured water column (WC) nitrification rates, water column dark respiration (WC_{dark}), sediment denitrification fluxes, and net daily metabolism (NDM) can be directly compared to model outputs. The sediment standing stock of organic matter (OM) can be used to describe the existing OM present in the system that is not included in the QUAL2kw algorithm (Cox 2003).

A variety of factors can directly or indirectly contribute to DO deficits in a lotic system; the most important is the presence of organic matter in the water column and sediments (Edwards and Rolley 1965; Streeter and Phelps 1958). Bacteria utilize DO during OM degradation, and an additional DO demand is required for the oxidation of ammonia associated with organic nitrogen degradation (Fair et al. 1941). The ambient

DO concentrations in streams can be heavily influenced by sediment–water interactions, including periphyton respiration/primary production, OM decay, and the oxidation of reduced chemicals such as ammonia, sulfide, and methane.

The Jordan River experiences both "chronic" and "acute" DO deficits (Utah DWQ 2013). The chronic ailment is hypothesized to be a result of "steady state" OM decomposition in the sediments and WC. This requires a year-round source of OM to maintain a "steady state" DO deficit. Acute DO deficits in surface and marine waters are typically associated with a large algal bloom die-off (Diaz and Rosenberg 2008; Paerl et al. 1998). Acute DO deficits have been observed in the Lower Jordan River (LJR), and the most recent event occurred in July of 2013 following a large storm event (Theron Miller 2013, personal communication). This may have been a result of the impervious surface "first flush" phenomena, the disturbance of organically enriched instream sediments, or from reduced dissolved chemical species originating from rotting OM in the conduits being introduced into the Jordan River (Gromaire-Mertz et al. 1999; Deletic 1998; Bertrand-Krajewski et al. 1998). Terrestrial particulate OM transported into the LJR during storm events will eventually contribute to the steady state chronic DO deficits.

Similar to DO, the dynamics and availability of the macronutrients nitrogen and phosphorus are very important in understanding the pollution status of surface waters (Vollenweider 1971; Fisher et al. 1982). Excessive nutrient loads from point and nonpoint sources can lead to the eutrophication and subsequent degradation of water quality. The instream sources and sinks of nutrients are important to quantify for the successful management of surface waters. Ammonium, nitrate, and orthophosphate

dynamics occurring in the WC and at the sediment–water interface can be decoupled using chambers to isolate the potentially very different metabolisms (Forja and Gomex-Parra 1998). For example, the sediments may be a source of ammonium and phosphate due to OM decomposition while removing publicly owned treatment works (POTW) nitrate loads through sediment denitrification (Fisher et al. 2005; DeSimone and Howes 1996; Pauer and Auer 2000). Comparing external nutrient loads and internal cycling rates will allow insight to how the Jordan River may respond to future POTW nutrient discharge concentrations.

As surface waters become excessively productive due to anthropogenic activities, or eutrophication, WQ will deteriorate (Hilton et al. 2006). Benthic and WC primary production result in supersaturated ambient DO concentrations (>125%) in the Upper Jordan River (UJR), suggesting that instream produced OM from the UJR is a source of organic matter to the DO impaired Lower Jordan River (LJR). Net daily metabolism (NDM) in the Upper and Lower Jordan River were compared using two different methods due to the challenges associated with characterizing a 52-mile 4th order stream. Light-dark chamber techniques were used to decouple the effects of reaeration while using DO as a surrogate for OM production and respiration (Bott et al. 1978; Odum 1956). Since chambers can only be placed near the riverbanks in water less than 1 meter deep, single-station diurnal DO techniques were also utilized to provide a better understanding of NDM at a reach based scale to include macrophytes and thalweg metabolisms (Chapra and Di Torro 1991; Chapra 1991).

Having an understanding of the standing stock of sediment OM is important for multiple reasons. Sediment OM will decay at varying rates while consuming DO, cycling

nutrients, and producing reduced chemical byproducts that may negatively influence stream health (Fair et al. 1941). The standing stock of sediment OM across the width of the river at seven locations was measured using the parameters total solids (%TS), volatile solids (%VS), total organic carbon (%TOC), and sediment density. A %TOC:%VS ratio for the LJR was developed to better understand the amount of carbon present in sediment OM. A relationship between SOD and %VS specific to the Lower Jordan River was also developed to allow easy estimation of SOD based on surface sediment OM.

OM loads to lotic environments are both autochthonous (instream production) and allochthonous (external) (Minshall 1978). Sources of allochthonous OM in an urban environment include litterfall transported over impervious surfaces and through stormwater conduits to downstream surface waters (Goonetilleke et al. 2005). Fresh litterfall, macrophytes debris, seeds, and sticks that are larger than 1 mm in size are classified as course particulate organic matter (CPOM) (Cummins 1974). Through the speciation of sediment OM in terms of CPOM and fine particulate organic matter (FPOM) while removing sticks, the CPOM portion was assumed to be terrestrial leaf litter and aquatic vegetation. The sources of FPOM were inconclusive since FPOM includes algae, bacteria, diatoms, fungus, small worms, and partially decomposed CPOM.

Swamp gas, a combination of methane and carbon dioxide, is produced during the anaerobic decay of OM in sediments (Segers 1998). In oxic surface waters, the vast majority of sediment diffused methane is oxidized at the oxic-anoxic-anaerobic interfaces within the sediments (Fenzel et al. 1990). If occurring, sediment methane production will contribute an oxygen demand leading to an increase in SOD (Di Toro et al. 1990).

Laboratory methods were utilized to maintain complete anaerobiosis to measure sediment methane production rates, which were then used to estimate sediment methane fluxes in the Jordan River.

Through the investigation and quantification of the previously mentioned WQ parameters, multiple mass balances on DO, OM, and nutrients were conducted. The data collected during this research can be used directly by the Utah DWQ to aid in populating the Jordan River QUAL2kw model, provides additional information about the Jordan River not predicted using the QUAL2kw model, and includes information relevant to future researchers investigating the Jordan River.

CHAPTER 2

PROBLEM STATEMENT AND RESEARCH OBJECTIVES

2.1 Problem Statement

The basis for this PhD research was to investigate dissolved oxygen (DO) dynamics and ambient water quality (WQ) with respect to sediment biogeochemistry in Utah's Jordan River. The goals of this research are two fold. The first was to increase the working knowledge concerning sediment oxygen demand (SOD), nutrient fluxes, sediment organic matter, methane fluxes, and net daily metabolism (NDM) in an urban river system. The second goal was to provide in situ WQ data to help regulatory agencies and stakeholders in understanding instream processes while contributing to the Jordan River TMDL development process.

SOD measurements conducted during my Master's research suggested that sediment processes drive ambient DO deficits in the Lower Jordan River (LJR). Further investigation was required to isolate and quantify these DO consuming processes. In addition to characterizing the sediments in the LJR, the upstream DO unimpaired lotic environment was investigated to better understand the entire Jordan River system. It is hypothesized that sediment OM enrichment is the driving factor in ambient DO deficits in the LJR, and this research characterized and quantified various reservoirs of OM and instream degradation processes.

2.2 Research Objectives

The basis of my doctoral research and the specific hypotheses are listed below.

Hypothesis 1: SOD is driven by sediment organic matter type and concentration in the Lower Jordan River: sediments containing more fine particulate organic matter will exert more SOD than those containing more coarse particulate organic matter at similar organic carbon concentrations, and sediment organic content is more important in estimating seasonal SOD rates compared to ambient water column temperature.

Hypothesis 2: In situ factors such as ambient pH, DO, and benthic community structure can significantly influence nutrient fluxes from sediments.

Hypothesis 3: %TOC and %VS are positively correlated with SOD, and both %TOC and %VS can be used as a surrogate for SOD in the Lower Jordan River (not the Upper Jordan River).

Hypothesis 4: Biogas (methane and carbon dioxide) production in the sediments of the Lower Jordan River is a significant DO consumer at the sediment–water interface.

To test these hypotheses, the following objectives were formulated and accomplished:

Objective 1: Measure seasonal SOD at locations representative of hydraulic reach based sediment characteristics, downstream and upstream of wastewater and stormwater discharge points and in other local surface waters.

Objective 2: Evaluate the flux and fate of nutrients as they interact with the sediments and WC using SOD chambers during in situ conditions and after manipulating chamber DO and pH.

Objective 3: Evaluate the contribution of primary production to DO dynamics and

organic carbon fixation using transparent SOD chambers and diurnal ambient water quality data.

Objective 4: Obtain sediment core samples at locations selected for SOD studies and quantify the bulk sediments and fine/coarse particulate organic matter in terms of %TOC, %TS, %VS, and $\%VS_{wet}$ to establish correlations between SOD and these parameters.

Objective 5: Evaluate methane fluxes from the sediments in the Lower Jordan River.

2.3 Research Contributions

Fig. 1 provides the WQ parameters investigated during this research and expected linkages. These parameters can be included into existing WQ models and mass balances. The sediment and WQ relationships investigated during this research are briefly described in terms of application.

The SOD:%VS relationship provides an alternative method to estimate Sediment Oxygen Demand (SOD) in silty sediments using standardized volatile solids (%VS) measurements. This relationship can be utilized by POTW, educational, and governmental laboratories that do not have the materials and expertise needed to directly measure SOD. The decomposition of organic matter has long been recognized as the driving factor contributing to SOD. Previous relationships required estimating aerial concentrations of OM, which requires knowledge of the depth of the biologically active sediment layer or benthal deposit. The proposed relationship is based solely on the organic portion of the top 2 cm of the surficial sediments and allows the rapid processing of large amounts of samples.

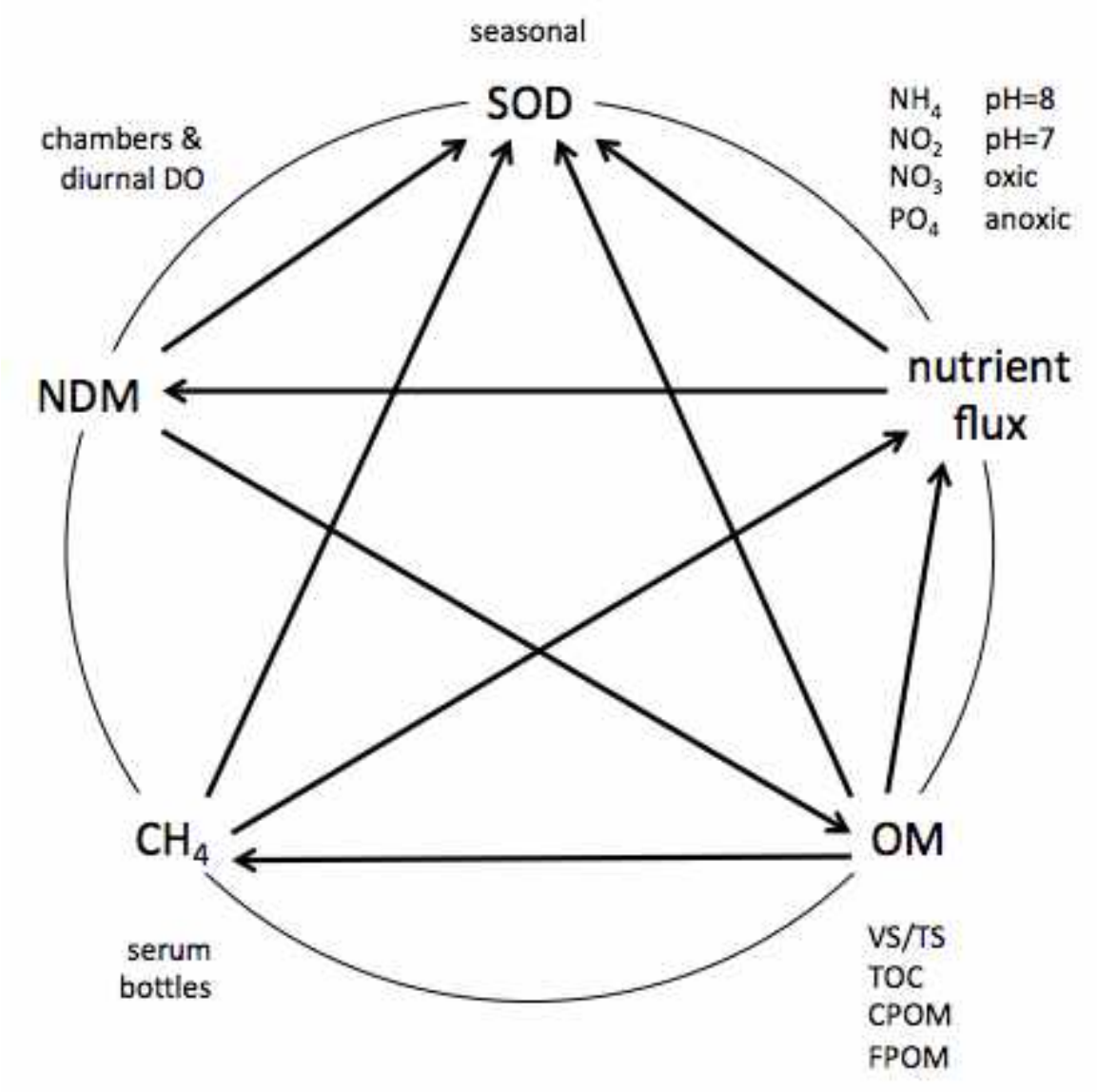

Fig. 1. Research parameters and expected linkages

Quantifying nitrogen and phosphorus sediment fluxes and water column rates allows the estimation of nutrient cycling and internal loadings. These fluxes can be compared to POTW nutrient loads to determine the relative contributions of internal versus external nutrient loadings.

The quantification of net daily metabolism (NDM) allows instream OM production and decomposition estimates. This information can be used to predict UJR OM loads resulting from eutrophication to the DO impaired LJR.

Percent total solids (%TS) is the percent solids matter in a wet sediment, and percent volatile solids (%VS) is the percent OM of the dry solids. The %VS:%TS relationship will aid in describing the surface sediments in the Jordan River, allow the calculation of sediment wet density, and provide a specific range to utilize the SOD:%VS relationship proposed in this study.

%VS measurements can be complicated by a variety of factors including lab protocols, sampling techniques, and the presence of inorganic carbon and clays (Heiri et al. 2001; Dean 1974). Carbonates and clay minerals are abundant in the alkaline Great Salt Lake Valley, and total organic carbon (%TOC) was measured to validate %VS as a surrogate for OM in the Jordan River.

By removing sticks from sediment samples, the course particulate organic matter (CPOM) represents terrestrial leaf and macrophyte debris before being degraded to less than 1 mm in size. Measuring both CPOM and the bulk OM found in the sediments may provide insight regarding the sources of OM to different stretches of the LJR. The fine particulate organic matter (FPOM) fraction represents degraded CPOM, periphyton, and subsurface microbes.

By measuring SOD and the flux of methane from the sediments, the relative contribution of methane oxidation in the benthos in relation to SOD can be calculated. Methane fluxes result in an ambient oxygen demand and are indicative of sediment OM enrichment.

CHAPTER 3

LITERATURE REVIEW

3.1 Water Quality in Lotic Systems

3.1.1 Earth's water resources

The majority of Earth's surface is covered with water (Fig. 2), but only 2.5% of the Earth's water resources are considered fresh, or having low total dissolved solids (TDS <500 mg/L). Only 0.3% of Earth's fresh water is surface water, and 0.007% is considered easily collectable surface water. Rivers account for an estimated 0.00015% of the Earth's total water (Gleick 1993). These rivers and streams are responsible for channeling hydraulic energy from the uplands to the oceans as an important part of the world's ongoing water cycle (Gleick 1993, Shiklomanov chapter).

Rivers play a vital role in both terrestrial and aquatic biology by providing diverse ecosystems, habitat, clean water, energy, and a constant supply of minerals and organic matter (Allan 1995; Naiman and Bilby 1998). Within a lotic system, or moving surface water, the water column and sediments dynamically interact in response to upstream influences while providing an environment responsible for maintaining a functioning aquatic ecosystem.

Surface waters provide potable water and many recreational benefits to society, yet more than 50% of America's surface waters are designated as impaired for various reasons (USEPA 2010b; USEPA 2006). 42% of the nation's sampled wadeable streams

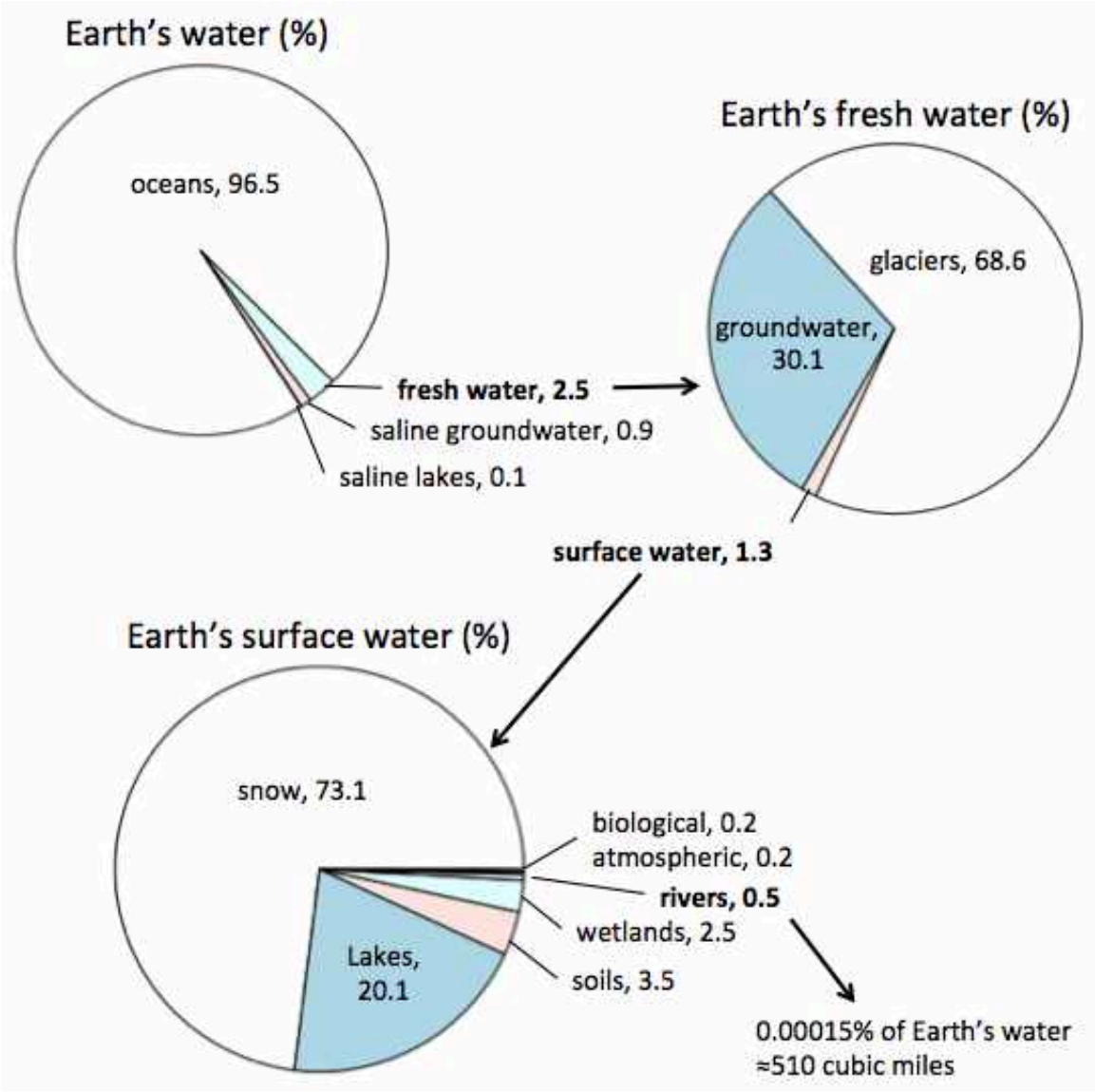

Fig. 2. General breakdown of the Earth's water resources
Note: adapted from Gleick 1993, Chapter 2

are classified as “poor” in terms of biological condition with only 28% characterized as “good” (USEPA 2006). The Western United States has the best biological condition with 45% of wadeable stream miles considered good and 27% considered as poor (USEPA 2006). Organic enrichment and contaminant inputs from urban and industrial discharges, aquaculture, stormwater, and agricultural runoff are stressors to surface water health. Water quality deterioration due to nutrients, organic carbon, and other pollutants is a widespread problem threatening the sustainability of global water resources while increasing the cost of potable water treatment (Makepeace et al. 1995).

The degradation of Earth’s rivers is not an isolated problem in the United States, but a global challenge since all rivers flow downstream to lakes, estuaries, bays, fjords, seas, and oceans. The obvious, yet socially complex, consequences are portrayed in the dead zones present in the Gulf of Mexico and rapidly declining water quality in Washington’s Puget Sound, where these habitats have historically been recognized as highly productive, important, and diverse ecosystems (Dodds 2006; Diaz and Rosenberg 2008).

3.1.2 Urban rivers

An important factor contributing to the degradation of surface water quality is urbanization (Bernhardt and Palmer 2007; Paul and Meyer 2001). Urbanization directly affects the water quality (WQ) of surface waters due to a variety of anthropogenic activities (Walsh et al. 2005). Common hydrological, biological, and chemical problems contributing to decreased WQ in urban rivers has been coined “urban stream syndrome” (Walsh et al. 2005). Urban rivers suffer from many ailments, including increased stormwater runoff resulting in flashy hydrographs, increased water temperature, loss of

riparian habitat, channelization, hydraulic manipulations, excessive sedimentation/incision, nutrient induced eutrophication, organic pollution, toxins, nonnative species invasion, and the general degradation of the upstream watershed (Booth 1990; Hilton et al. 2006; Sweeney et al. 2004, Pimentel et al. 2005; Paul and Meyer 2001; Meyer et al. 2005; Groffman et al. 2003).

Historically, water engineering and management practices focused on water quantity for agricultural, culinary, and flood control purposes. Management of the quality of surface waters have focused on "end of pipe" approaches that work great for flow quantity engineering, but have proved mostly ineffective for surface water quality management (Goonetilleke et al. 2005).

The sediment spatial heterogeneities characteristic of flowing waters include runs, rapids, riffles, pools, and depositional zones associated with river meanders. The diversity of flow regimes in a natural river results in patchiness of OM and the benthic community, leading to increased biodiversity (Casas 1996). Urban rivers tend to have a homogeneous bedform compared to the predevelopment conditions of the watershed due to the loss of riffles and meanders associated with channelization, stream incision, and sediment deposition (Miller and Boulton 2005).

The ability for a river ecosystem to assimilate nutrients, sediment, organics, and toxins is an important factor contributing to surface water quality and is compromised downstream of poorly planned urbanization (Bernhardt and Palmer 2007; Paul and Meyer 2001).

3.1.3 Total Maximum Daily Load (TMDL) studies

Section 303(d) of the Clean Water Act requires states, territories, and tribes to develop lists of impaired waters that are polluted based on the standards set by state and federal regulatory agencies. A Total Maximum Daily Load (TMDL) calculation for specific pollutants is performed to determine the pollutant load a specific surface water can receive without impairing the designated beneficial uses of that waterbody. In this context, the Clean Water Act requires a TMDL study to be undertaken for each pollutant responsible for the impairment of a surface waterbody. After the pollutant of concern is identified, a TMDL study determines the pollutant load allocations that can be discharged from both point and nonpoint sources. A complete TMDL study requires extensive monitoring, modeling, and laboratory and field scale experiments. Once appropriate loads are determined, management strategies can be developed and implemented to reduce the daily load of pollutants until the waterbody is brought back into compliance with water quality standards. The final stage of a TMDL includes load allocations and decision-making associated with revised pollutant discharge permits (Stackelberg and Neilson 2012; Boyd 2000).

3.2 Introduction to the Jordan River, Utah

3.2.1 The Great Basin, Lake Bonneville, and Great Salt Lake

The Great Basin is the largest endorheic, or landlocked, watershed in North America, extending North-South from Oregon to Southern California and East-West from central Utah to Eastern California. Within the Great Basin, lies the Great Salt Lake, which claims the title of the world's fourth largest terminal lake. The Great Salt Lake is a remnant of the historic freshwater Lake Bonneville that once filled the Wasatch Front

with water up to 1,000 feet deep (Spencer et al. 1984). Fig. 3 provides a map of Utah's current rivers with the historic Lake Bonneville shaded pink. The Great Salt Lake, Jordan River, and Utah Lake are located within the boundaries of the historic Lake Bonneville.

Since the watershed is terminal, the Great Salt Lake behaves like an evaporation pond and can have salinities ranging from 5–27% depending on location and lake level. For comparison, the world's oceans have an average salinity of roughly 3.5%. The three main sources of freshwater to the Great Salt Lake are the Bear (avg. flow 25 m^3/s), Weber (avg. flow 10 m^3/s), and Jordan Rivers (avg. flow 15 m^3/s), which contribute over 1 million tons of new salt to the Great Salt Lake annually. The Bear, Weber, and Jordan Rivers contribute roughly 50%, 20%, and 30% of the annual freshwater to the Great Salt Lake.

The Great Salt Lake proper is too saline for fish to live, and the primary aquatic life are brine shrimp (*Artemia*), shore flies (Ephydridae), and algae. Although the water column is very inhospitable for higher life forms, the wetlands surrounding the Great Salt Lake provide invaluable habitat for migratory waterfowl and shorebirds for feeding, mating, and resting on the Pacific Flyway extending from Alaska to Patagonia. The Great Salt Lake wetlands account for roughly 75% of Utah's wetlands and are concentrated along the northern and eastern shores receiving water from the Wasatch Mountains.

Utah Lake, the origin of the Jordan River, has a surface area of roughly 390 km^2 (145 square mile) and a storage capacity just shy of a million acre-feet (902,400 ac-ft). It is a shallow lake with an average depth of approximately 9–10 feet during normal reservoir operating conditions (Utah DWQ 2007). Utah Lake is the largest natural freshwater lake in the western United States in terms of surface area and has a maximum

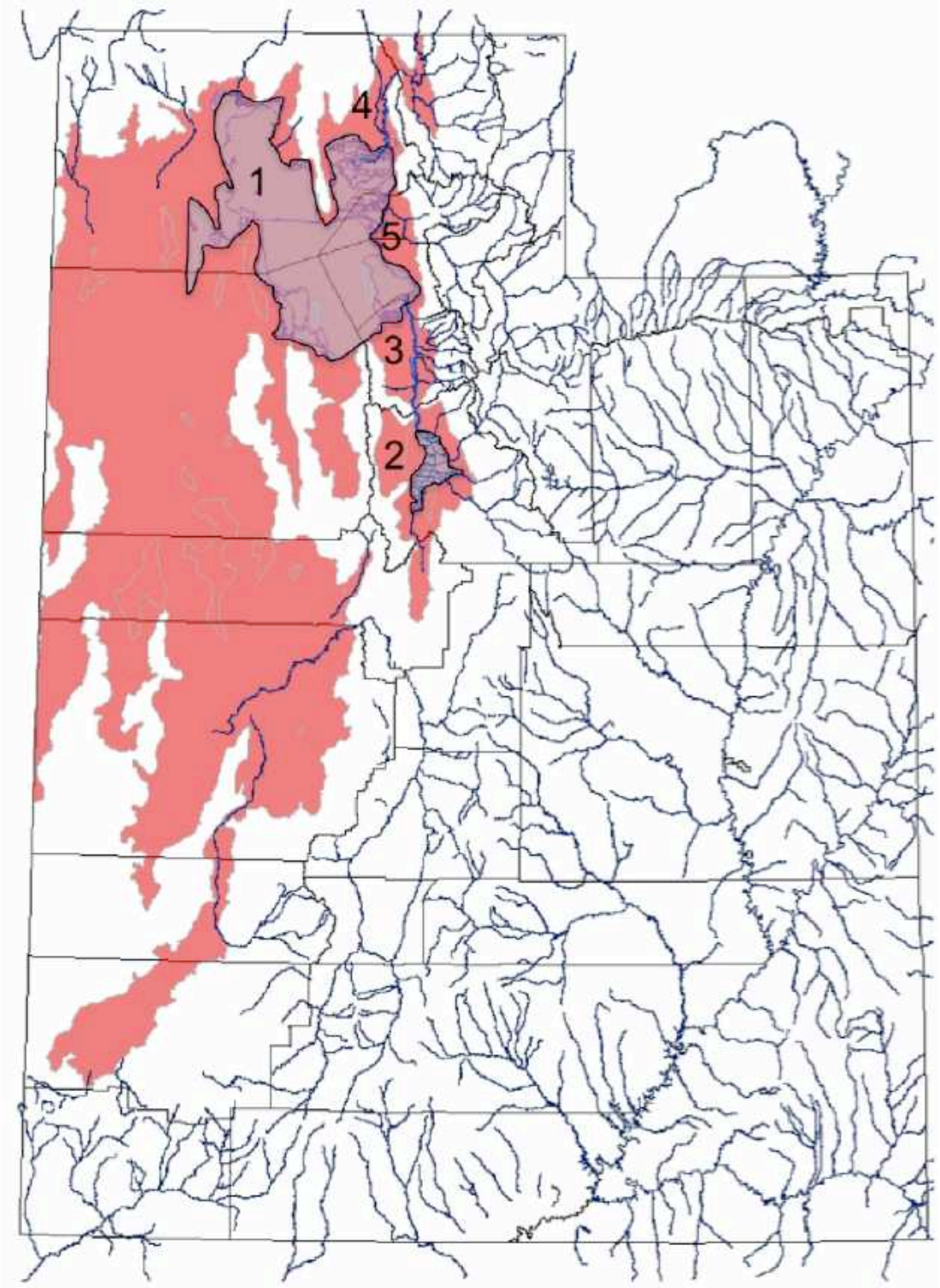

Fig. 3. Historic Lake Bonneville (shaded) and current lotic waters in Utah State
Note: 1 = Great Salt Lake, 2 = Utah Lake, 3 = Jordan River,
4 = Bear River, and 5 = Weber River

length and width of 24 and 13 miles, respectively.

Utah Lake is managed at a lake elevation of 4,489 feet above sea level, resulting in tributaries and groundwater inputs being the source of water to the Upper Jordan River (UJR) during the winter months. This results in much lower flows and decreased turbidity in the UJR during the winter months.

3.2.2 Utah's Jordan River

Utah's 4th order Jordan River flows 52 miles south to north from Utah Lake through the urbanized Salt Lake Valley before entering a series of managed wetlands before finally discharging into the terminal Great Salt Lake. Fig. 4 provides a general overview of the Jordan River with counties, municipalities, and a parcel map to visualize areas of urban development and population density.

The Jordan River passes through three counties, 15 municipalities, and 10 diversion dams/weirs and receives the direct discharge of three municipal wastewater treatment plants (WWTP). In addition, the Jordan River receives sediment and pollutant inputs from an 800 square mile watershed with the lowlands rapidly being urbanized while contributing additional untreated diffuse runoff.

The four mountain water tributaries to the Lower Jordan River include City Creek, Red Butte Creek, Emigration Creek, and Parleys Creek. All four of these tributaries have been incorporated into stormwater conveyance systems and piped below Salt Lake City as shown by the red circle in Fig. 5. The complete loss of habitat and stream function occurs when a river is enclosed in pipes by removing the stream from daylight, floodplains, hyporheic exchanges, and the riparian zone (Miller and Boulton 2005; Boughton and Neller 1981). Potable water is collected in the mountains from

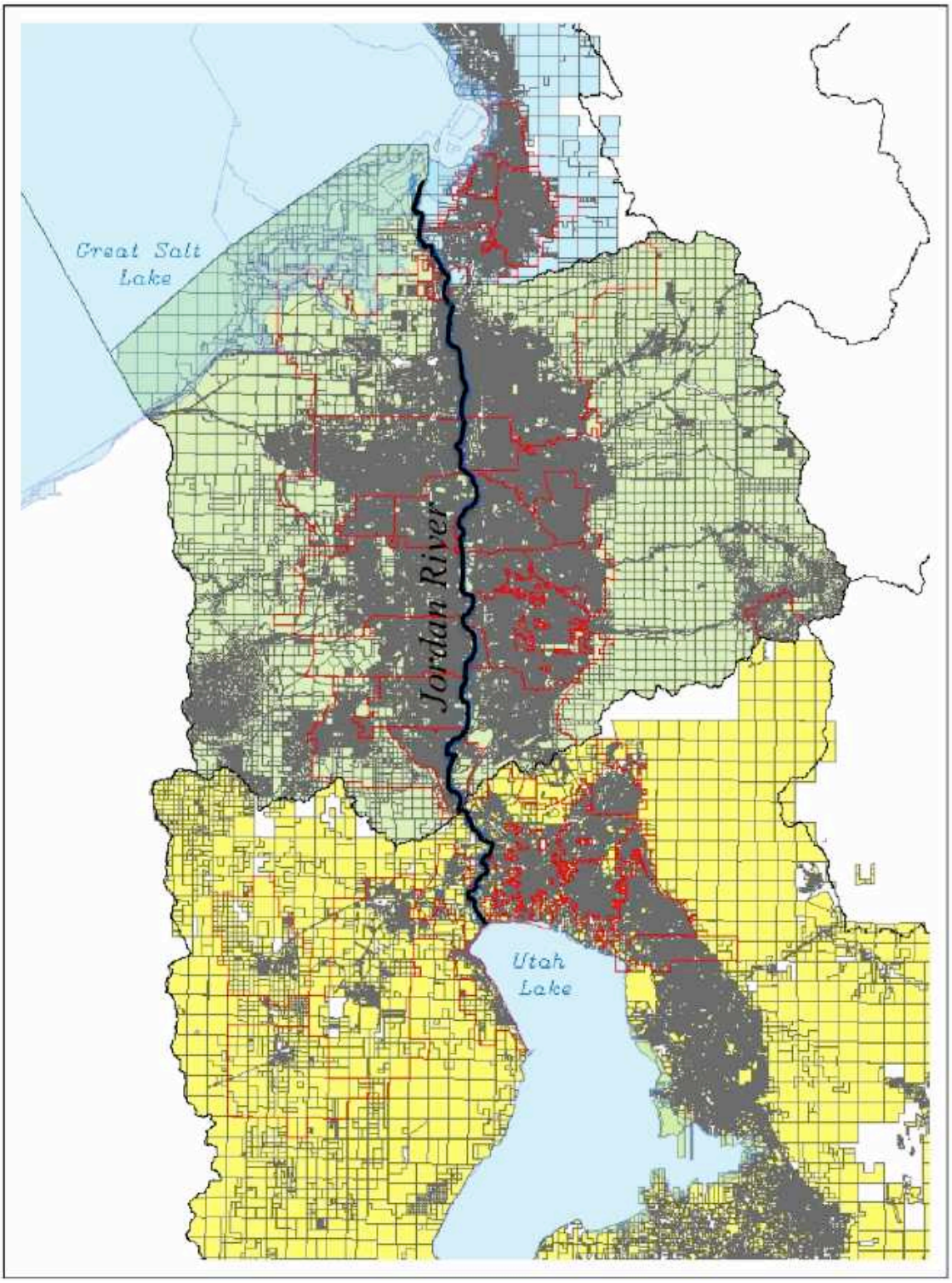

Fig. 4. Parcel map (property lines) for Davis, Salt Lake, and Utah Counties

Fig. 5. Primary tributaries to the Jordan River
Note: the red circle indicates streams piped underneath Salt Lake City and incorporated into stormwater conveyance system; orange diamonds identify bridge crossings

these streams, but these tributaries have historically been modified and managed as a conduit for stormwater conveyance, thereby losing all function as a stream before discharging into the Lower Jordan River (LJR).

Fig. 6 provides municipal WWTP locations along the Jordan River and upstream Utah Lake. The three POTWs directly discharging into the Jordan River at the time of this research include South Davis-South WWTP, Central Valley Water Reclamation Facility (WRF), and South Valley WRF. WWTPs discharging into Utah Lake indirectly add nutrients to the downstream Jordan River as suspended OM present as living phytoplankton and dead sestonic matter.

3.2.3 The Upper and Lower Jordan River

The urban Jordan River has been highly modified due to channelization, loss of riparian habitat, an extensive low head dam water diversion network, and upstream impoundments associated with Utah Lake, Deer Creek reservoir, and Jordanelle reservoir. Upstream diversions mitigate spring flooding and divert water for agriculture and potable uses. Fig. 7 provides a map showing dams and weirs located on the Jordan River and the complex canal network utilizing Jordan River and Utah Lake water.

The Surplus Canal diversion located at 2100 S was built to mitigate flooding in Salt Lake City during spring runoff and during large storm events. Roughly 72% (standard deviation (SD) = 16%) of the Jordan River's annual flow is diverted to the west towards the Great Salt Lake via the Surplus Canal. Due to the large removal of water from the Lower Jordan River at the Surplus Canal diversion, the Jordan River has been subdivided into two distinct sections in this dissertation. The Upper Jordan River (UJR) extends from Utah Lake to the Surplus Canal diversion and the Lower Jordan River

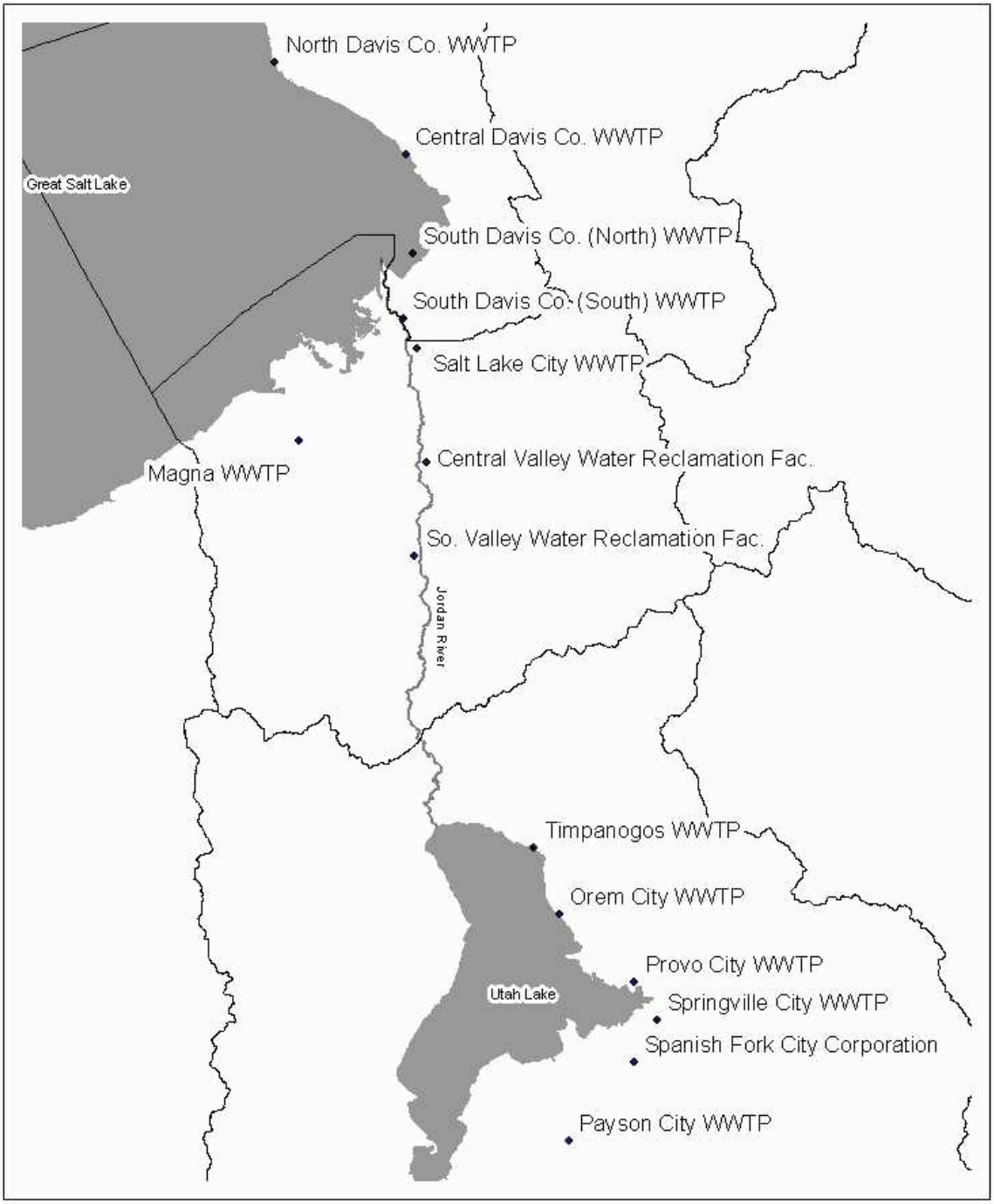

Fig. 6. WWTPs discharging to Utah Lake, Jordan River, and Great Salt Lake

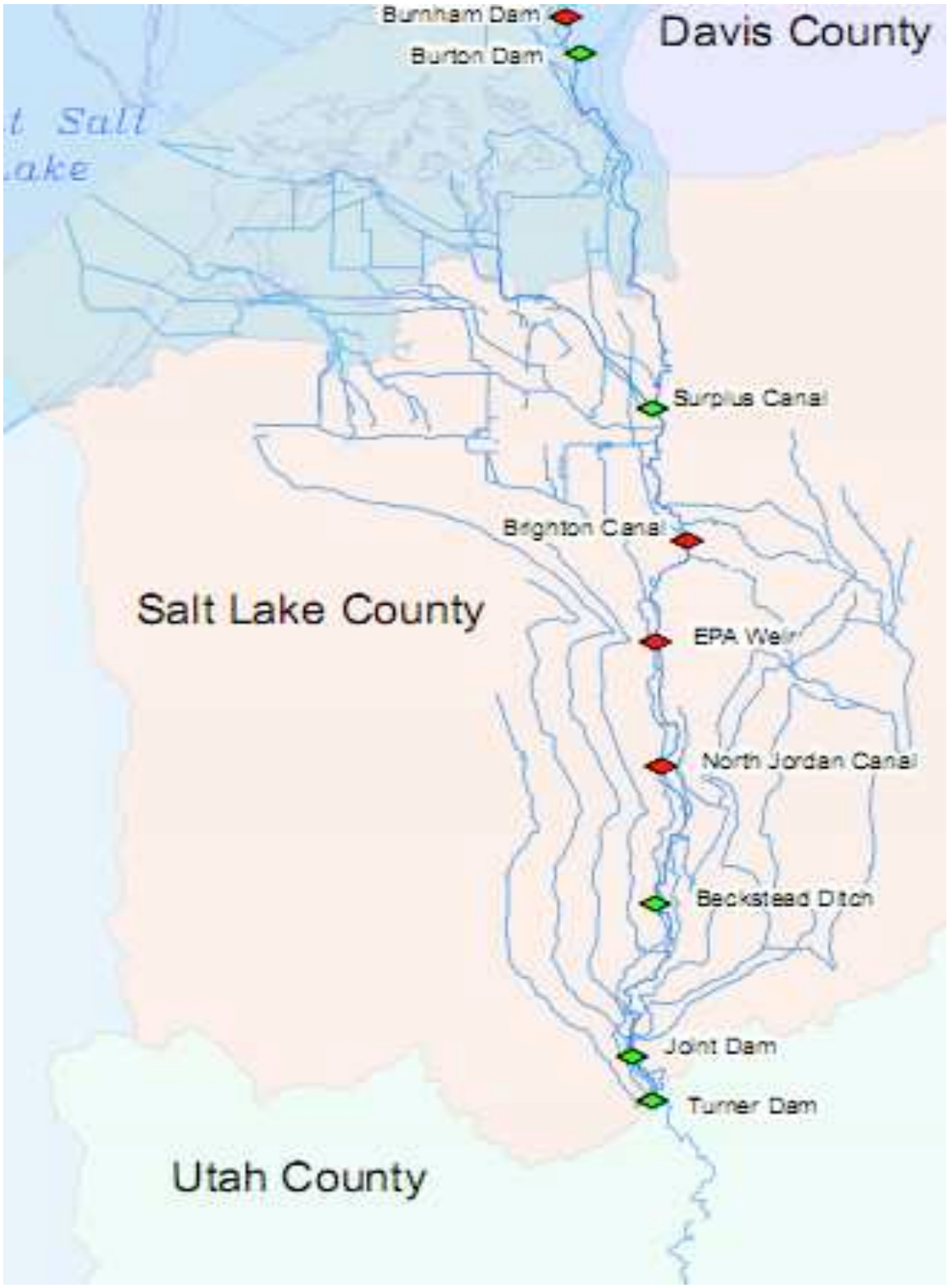

Fig. 7. Major diversions, canals, and flow control structures

(LJR) is located downstream of the diversion. This distinction in important since the Lower Jordan River does not experience the annual flow variations typical of a lotic system due to the decoupling of flows from the Upper Jordan River at the Surplus Canal diversion.

Fig. 8 provides mean daily stream flow rates for the Surplus Canal, UJR, and LJR over the time period of 2007–2012. Flow data were measured at the Surplus Canal overflow weir (purple line, United States Geologic Survey (USGS) station 10170500) and near the start of the Lower Jordan River at 1700 S (red line, USGS station 10171000). The Upper River data (blue line) were calculated by summing the mean daily flow for the previously mentioned sites.

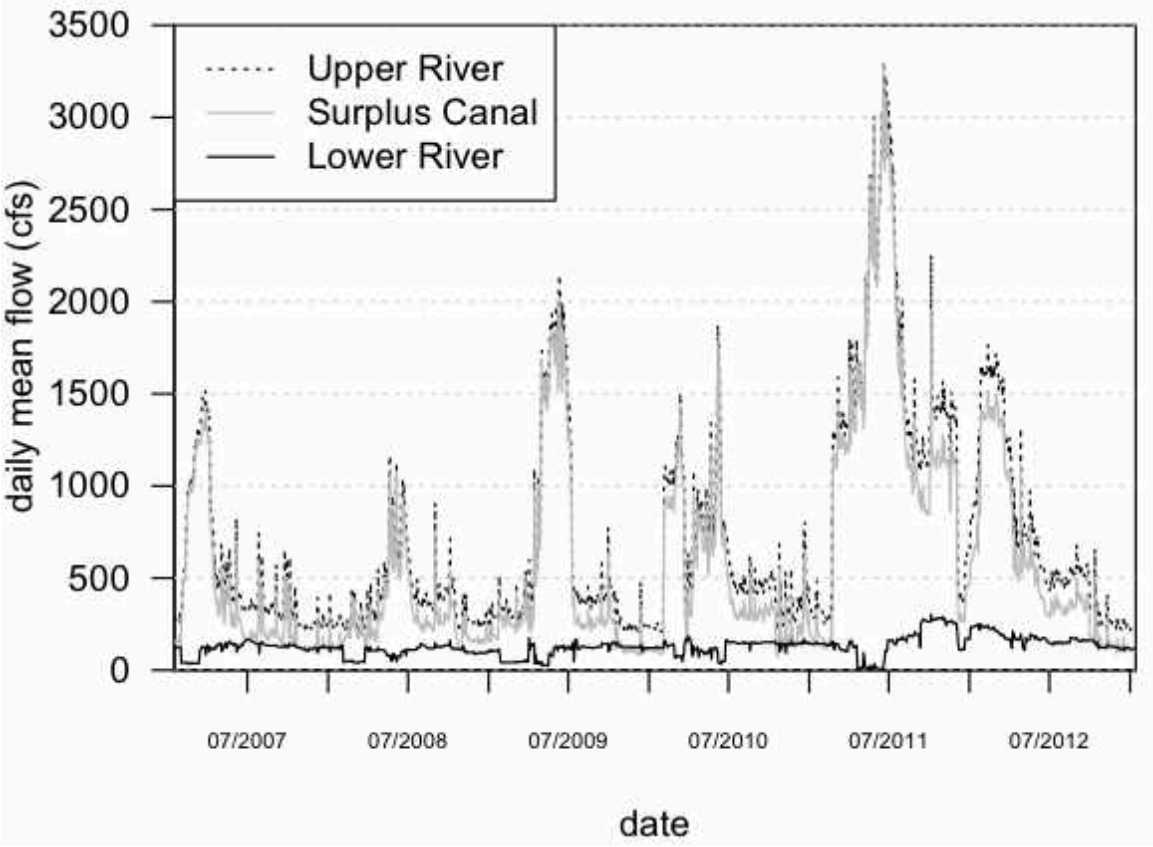

Fig. 8. Upper Jordan River, Lower Jordan River, and Surplus Canal annual flows

The annual mean daily flow rates observed during this time period for the Upper Jordan River, Surplus Canal, and Lower Jordan River were 704 (SD = 571), 576 (SD = 569), and 128 cfs (SD = 52), respectively. The relatively low flow rates and low standard deviation characteristic of the Lower Jordan River highlights its "tamed" nature. The maximum mean daily flow rate observed in the LJR over this time period was 303 cfs.

During large storm events the underflow weir allowing water into the LJR may be closed by Salt Lake City engineers to accommodate the flashy hydrographs associated with the impervious urban areas draining into the LJR. This can result in periods of little or no flow entering the LJR at 2100 S.

The six flow rate spikes in the UJR coincide with spring runoff, and the maximum mean daily flow rate of 3300 cubic feet per second (cfs) measured in 2011 was a result of the large mountain snowpack in the region (Fig. 8). The annual variations in the Jordan River are highlighted during this event where flows in the Upper Jordan River exceeded 850 cfs for 9 straight months from the managed release of water from Utah Lake into the Jordan River (Feb. 24, 2011, through Dec. 3, 2011).

The Jordan River has been partitioned into eight hydraulic reaches for assessment purposes. Multiple of these reaches have been classified as impaired for the designated uses of secondary recreational contact (2B), cold and warm water fisheries (3A, 3B), and agriculture (4). WQ indicators including E. coli, temperature, DO, and total dissolved solids (TDS) did not fulfill the standards associated with the designated uses (Utah DWQ 2013, Table 1.1). Impaired reaches of the Jordan River are provided in Table 1 and a map of the designated reaches is provided in Fig. 9.

Table 1. Jordan River hydraulic reach descriptions and impairments

Reach #	Description	Impairment
1	Burton dam to Davis County line (Cudahy Ln.)	3B
2	Cudahy Ln. to North Temple St. (City Creek tributary)	2B, 3B
3	North Temple St. to 2100 S (Surplus Canal)	2B, 3B
4	2100 S to 6400 S (Mill, Big and Little Cottonwood Cr.)	4
5	6400 S to 7800 S (Midvale Slag Superfund site)	2B, 3A, 4
6	7800 S to Bluffdale Rd. (14600 S)	3A
7	Bluffdale Rd. to Salt Lake County line (Traverse Mtns.)	3A, 4
8	Salt Lake County line to Utah Lake	3A, 4

Note: adapted from Utah DWQ 2013, Table 1.1

3.3 Dissolved Oxygen Dynamics

3.3.1 Dissolved Oxygen (DO)

Dissolved oxygen (DO) impairments can be chronic as well as acute with extreme cases typically associated with individual events, such as a large algal bloom. This rapid increase in aquatic biomass eventually dies and settles to the sediments where it depletes ambient DO as organic matter undergoes bacterial decomposition in the benthic zone. The effects of highly organic sediments on ambient stream DO can be significant (Baity 1938; Rudolfs 1932). The presence of low DO itself does not mean that DO is a pollutant (Utley et al. 2008; Todd et al. 2009). Instead, low DO provides an indication of other activities, which may have triggered the low DO (Parr and Mason 2004; Stringfellow et al. 2009). Dissolved oxygen impairments can result in a variety of nuisance and problematic water quality (WQ) issues, including bad smells, degradation of the aquatic community, problematic toxicant chemical transformations, and fish kills.

Managing WQ using DO as an indicator parameter is common practice, and the pollution status of surface waters can be assessed through DO dynamics. DO is important since all aquatic fauna require oxygen for respiration, and low concentrations will stress,

Fig. 9. Jordan River hydraulic reaches

inhibit, and kill the native aquatic community. As a general rule of thumb, DO concentrations less than 50% saturation are stressful to most aquatic communities.

The use of new technologies such as luminescent dissolved oxygen probes allows diurnal monitoring of the ambient water column for identifying water quality impairments and collecting baseline data. These WQ monitoring probes allow large amounts of data to be confidently and efficiently collected over multiday time periods to better understand the daily fluctuations in DO and stream metabolism.

The actual DO saturation concentration is influenced by temperature, atmospheric pressure, and salinity. Fig. 10 provides the relationship between fresh water at sea level

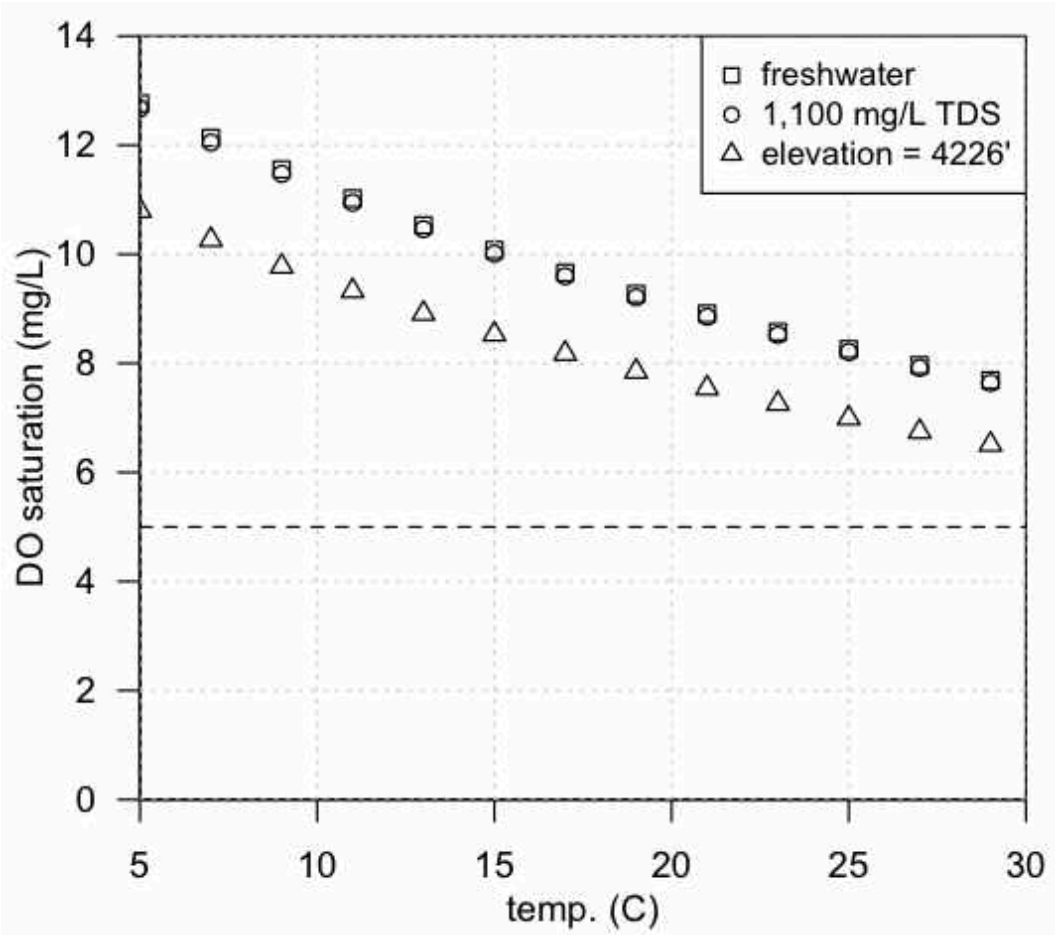

Fig. 10. DO in relation to temperature, salinity, and elevation above sea level

(squares), water having a salinity similar to the Jordan River of 1,100 mg TDS/L at sea level (circles), and Jordan River water at an elevation of 4226 feet (triangles). The dotted line represents 5 mg-DO/L, a common ambient DO level expected to be maintained in flowing waters to provide a healthy aquatic environment. DO saturation decreases with temperature, resulting in the majority of low DO events occurring in late summer in warm waters. In addition to decreasing ambient DO saturation, warmer temperatures increase stream metabolic rates.

Fig. 11 provides a general schematic of the biotic and abiotic DO consuming activities occurring in a river ecosystem during nighttime hours. These include

1) phytoplankton respiration
2) decay of instream flora/fauna
3) hyporheic exchanges
4) benthic respiration
5) flux of reduced chemical species
6) biochemical oxygen demand (BOD)
7) decay of course particulate organic matter (CPOM)
8) decay of fine particulate organic matter (FPOM)
9) respiration of fauna
10) macrophyte respiration

It should be noted that 1 and 10 will produce more DO than is utilized for respiration during daytime hours as a result of photosynthesis. Number 4 may produce a net positive flux of DO during daylight if periphyton are present on the surface of the benthic zone.

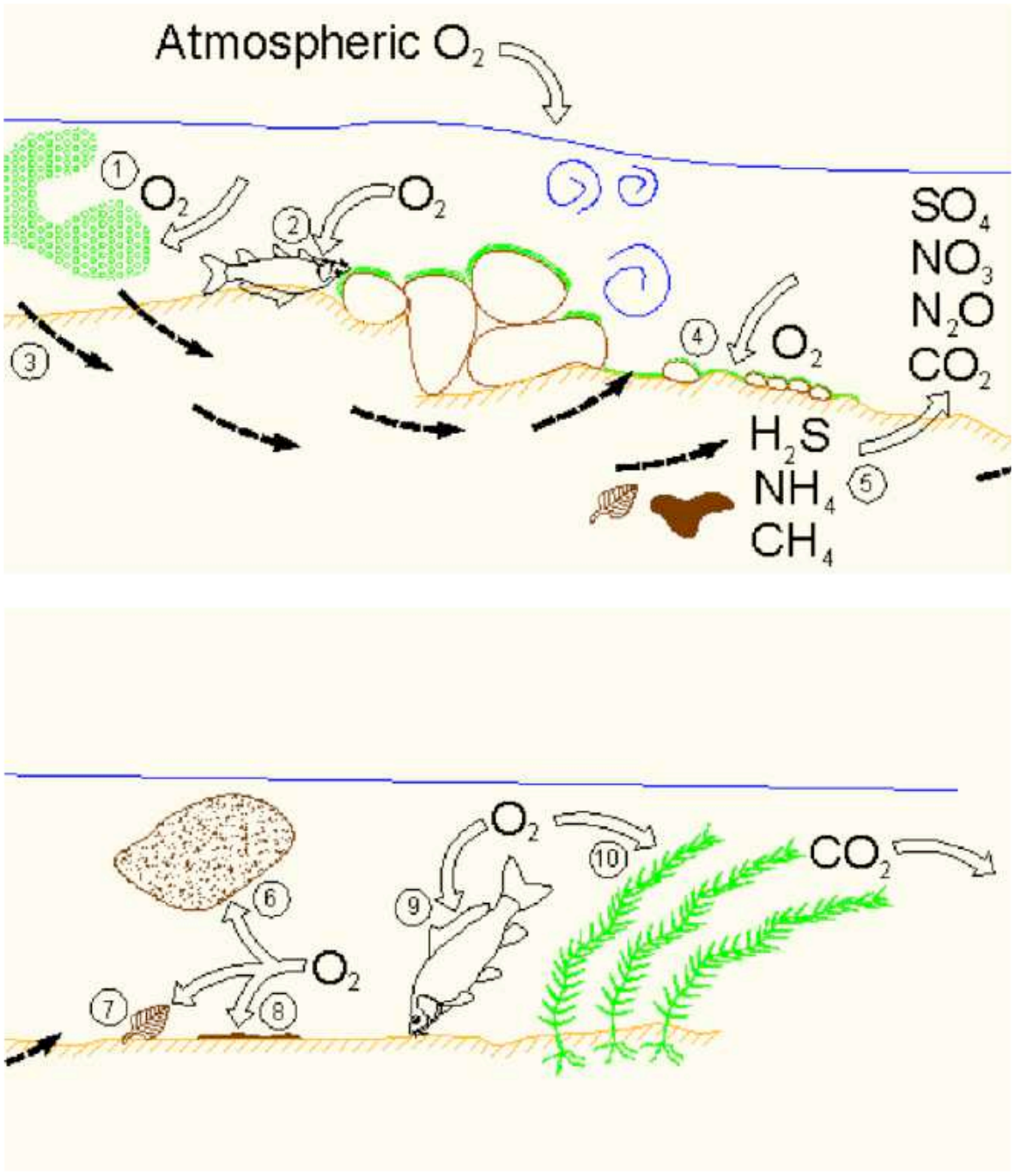

Fig. 11. Typical DO consuming activities occurring in the water column and at the sediment–water interface in a river system during nighttime

3.3.2 Reaeration

The replenishment of DO into the water column from atmospheric reaeration and daytime biological photosynthesis are constantly occurring at varying rates to achieve equilibrium between the ambient river DO deficit, or surplus, and atmospheric oxygen. The reaeration potential in a well-mixed surface water is generally expressed as a 1st order reaeration coefficient. As a result, the rate of physical reaeration increases in response to increased ambient DO deficits (Deatrick et al. 2007; Copeland and Duffer 1964). Since oxygen is considered to be poorly soluble in water due to a relatively high Henry's constant, approximately 0.8 atm*m^3/mole, ambient river DO levels may remain chronically low in slow moving and organically enriched sections (Chapra 2008, pg. 376).

Physical reaeration rates increase with any type of disturbance at the air-water interface. Disturbances increase the surface area of this interface allowing more atmospheric oxygen to diffuse across the air-water interface. Any form of turbulence to the water column, including wind, waves, rainfall, rapids, riffles, snags, and weirs, all increase reaeration locally.

Common techniques used to determine reaeration coefficients include conservative gas and dye injection into the stream (Tsivoglou et al. 1968), floating of a nitrogen gas filled diffusion dome (Cavinder 2002), diurnal models utilizing ambient DO profiles (Chapra and Di Toro 1991), and predictive equations based on stream depth, velocity, and slope (Bowie et al. 1985). All these techniques have advantages and challenges. For example, gas injection studies require substantial infrastructure including gas and dye sources, injection and sampling methods, and laboratory equipment to

quantify gas and dye concentrations. The gas injection method can become very expensive and labor intensive when investigating rivers with substantial flows. Diffusion dome studies are less expensive and can be utilized in large rivers, but cannot be employed in extremely turbulent or shallow conditions. Diurnal DO models are inexpensive and can estimate net daily metabolism, but can be heavily influenced by groundwater inputs and hyporheic exchanges (Hall and Tank 2005). Predictive equations are free, simple, and require only a small amount of initial data, but can be grossly misleading if incorrect assumptions are made in equation selection and parameter inputs.

A great deal of effort has been directed towards the generation of predictive equations used to estimate reaeration coefficients, and many of these equations have been produced using data acquired from rivers and streams with very distinct characteristics. As a result, the efficient use of predictive equations for the estimation of reaeration coefficients requires additional information regarding their history and appropriate use (Bowie et al. 1985). The O'Connor and Dobbins equation was developed using empirical observations in slow deep channels, 0.31–9 meters deep and 0.16–0.5 m/sec flow velocities, to estimate reaeration using a ratio based on steam velocity and depth (O'Connor and Dobbins 1958). The Churchill equation was generated from a dissolved oxygen mass balance following the release of low DO water from several dams and back calculating reaeration rates based on the ambient river waters' ability to achieve saturation downstream. Average depths and stream velocities used in the Churchill study were 0.6–3.4 meters and 0.6–1.6 m/sec, respectively (Churchill et al. 1962). The Owens and Gibbs equation was produced by deoxygenating several streams using sodium sulfite and measuring the increase in DO as water flowed downstream. Average depths and

stream velocities utilized in the Owens and Gibbs equation were 0.1–3.4 meters and 0.03–0.6 m/sec, respectively. This information was combined with Churchill's observations to develop Owens and Gibbs final equation (Owens et al. 1964).

It is common practice to use the O'Connor and Dobbins equation to predict reaeration coefficients in rivers that are relatively deep and slow moving, although other studies have shown that this equation overestimates reaeration in very slow moving sections (Leu et al. 1997). The Churchill equation applies best to relatively deep rivers characterized by elevated stream velocities, and the Owens and Gibbs equation is best suited for fast flowing shallow streams (Covar 1976; Zison et al. 1978).

Table 2 presents reaeration coefficients normalized to 20 centigrade for the various stretches of the Jordan River measured with a diffusion dome while floating down the thalweg (Hogsett and Goel 2013).

Fig. 12 provides the relationship between the diffusion dome measured reaeration coefficients and commonly used predictive equations (Covar 1976). The Float # in Table 2 is in relation to the float sections presented in Fig. 13. The parameters river depth and

Table 2. Reaeration coefficients for the Jordan River

River section	Reach #	$K_{2,20}$ (1/day)	Float #
1700 N to LNP NE	1 & 2	0.6	1 & 1b
1700 S to 900 S	3	4.2	2
3300 S to 2100 S	3 & 4	7.0	3
5400 S to 4170 S	4	5.1	4
9000 S to 7800 S	5 & 6	17.7	5
12600 S to 10600 S	6	11.0	6
Lehi	8	3.4	7

Note: $K_{2,20}$ = Reaeration coefficient normalized to 20 °C
1b = reaeration coefficient measured twice

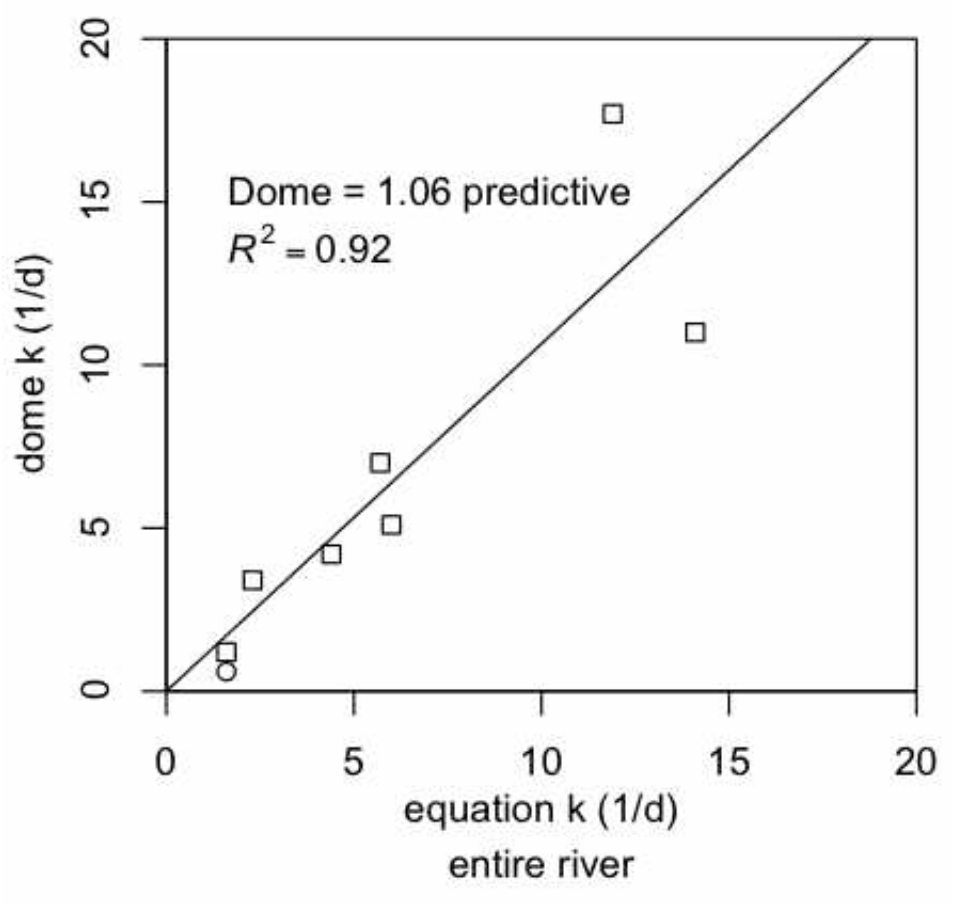

Fig. 12. Measured reaeration coefficients vs. suggested predictive equations

flow velocity were measured during the diffusion dome experiments. The diffusion dome reaeration coefficients were very similar to predictive equations within the range of k between 2 to 6 day^{-1}.

The low k value measured in Reach 1 is most likely a result of wind-induced reaeration becoming more important in this relatively slow moving hydraulic reach (Banks 1977; Cerco 1989). Reach 1 is located in the flood plains of the Great Salt Lake and receives minimal riparian buffering from wind and weather moving across the lake. The k estimate for wind induced reaeration in a shallow estuary 1 meter deep is 0.6 d^{-1} with an average wind speed of 8 mile/hour (Ro and Hunt 2006). The combination of

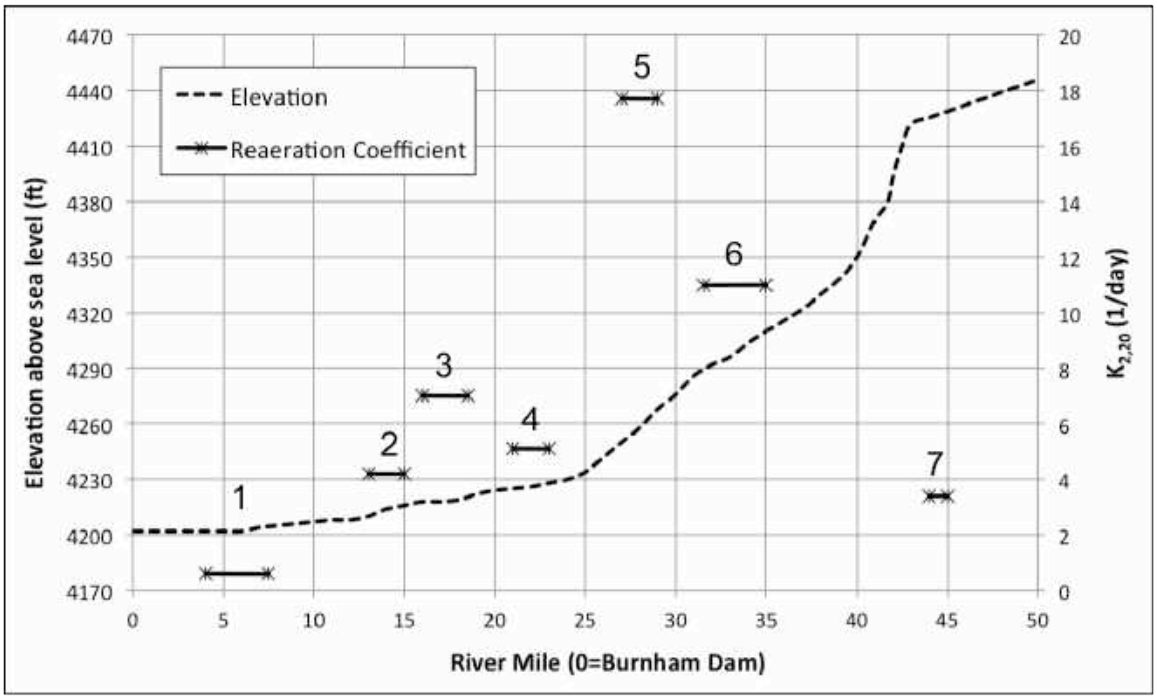

Fig. 13. Measured reaeration coefficients and elevation gradient for the Jordan River
Note: elevation profile adapted from Jensen 1986, Fig. 7

water and wind turbulence results in a k = 1.2 d^{-1} in Reach 1. This wind adjusted reaeration coefficient in Reach 1 was used for all calculations in the followings sections of this thesis.

Fig. 13 provides the elevation profile for the Jordan River and associated reaeration coefficients. It is obvious from Fig. 13 that the potential for reaeration is greater in the steeper midsection of the UJR and much lower in first 20 miles where the topography is relatively flat. Other reaeration studies conducted on the Jordan River estimated coefficients of 1.8 and 9.5 1/d for the sections between 1800 N–4800 S (river mile 5–21) and 4800 S–12300 S (river mile 21–34), respectively (Stephensen 1984). The low reaeration coefficient associated with Hydraulic Reach 8 is a result of its location in the slow moving backwaters above Turner Dam and downstream of Utah Lake.

3.3.3 Biochemical Oxygen Demand (BOD)

Surface and wastewater are routinely tested for biochemical oxygen demand (BOD) and chemical oxygen demand (COD) to characterize the waters' organic pollution status. COD tests entail oxidizing all organic carbon in a water sample using a strong acid and heat during a short time period (hours), while BOD tests utilize bacteria and DO to biologically oxidize organic carbon over much longer time scales (days).

BOD tests are typically carried out over a 5-day period under dark conditions to curtail photosynthesis. A 5-day testing period, BOD_5, is the standard due to 1st order reaction kinetics resulting in long time periods required to measure the ultimate BOD (UBOD). Since organic carbon comes in many qualities (glucose vs. cellulose), the UBOD will always be less than the COD measurements due the recalcitrant nature of biologically structural OM.

During this research the zero order parameter water column dark respiration (WC_{dark}) was used to describe the oxygen demand of the Jordan River. The units are per day as opposed to BOD_5. This is a beneficial timescale since river water is constantly moving downstream while interacting with changing environments.

3.3.4 Sediment Oxygen Demand (SOD)

Sediment oxygen demand (SOD) accounts for the depletion of dissolved oxygen due to the decomposition of settled organic matter (OM), the respiration of benthic flora and fauna, and the biotic and abiotic oxidation of reduced inorganic chemical species diffusing from the sediments (Utley et al. 2008; Todd et al. 2009; Walker and Snodgrass 1986). The degradation of OM is the ultimate source of SOD either directly, such as decay at the sediment–water interface, or indirectly, such as a sediment flux of reduced

chemicals. To complicate the parameter, SOD is also a function of the quality of OM present, the microbial community responsible for OM degradation, ecosystem metabolism, and the hospitality of the general environment to support the microbial and macroinvertebrate community (Young et al. 2008; Webster and Benfield 1986). The vast majority of the aquatic microbial population lives in the sediments with only a small fraction present in the water column (Ellis et al. 1998). The sediment–water interface, or benthic zone, and hyporheic zone are responsible for the majority of heterotrophic activity in stream ecosystems (Pusch et al. 1998). As a result, the SOD associated with organically enriched river sediments can be responsible for over 90% of the ambient oxygen deficit (Matlock et al. 2003; Hogsett and Goel 2013).

SOD can be measured in the laboratory using sediment cores as well as in situ using chamber methods. In situ measurements are preferred over laboratory scale experiments to avoid uncertainties associated with disturbing the sediments during collection, transportation, and testing. Mathematical modeling, using tools such as QUAL2Kw, are commonly used to simulate natural systems and predict DO dynamics based on field measurements of SOD and other parameters (Pelletier at al. 2006; Utley et al. 2008). Models that underestimate SOD or a lack of field sampling can greatly misrepresent diurnal DO profiles in streams.

Sources of organic matter contributing to SOD include the sedimentation of suspended solids originating from point dischargers; settled suspended solids associated with diffuse runoff, sloughed periphyton, and phytoplankton biomass that has settled to the river bottom; organic rich sediments that have eroded from upstream; organics traveling along the bottom of the river as bedload; and cryptic microbial growth.

Sources of phototrophic biomass (algae, macrophytes, diatoms, and cyanobacteria) to the Jordan River include Utah Lake, tributaries, and growth occurring within the mainstem of the Jordan River. Potential contributions to SOD resulting from the decomposition of phototrophic biomass within a river system can be large since tributaries and lake headwaters can be a consistent source of algal inoculum and sestonic particulate organic matter (Stringfellow et al. 2009). Other sources of organic material include nonpoint urban runoff and stormwater that can contribute additional organic matter during storm events and snowmelts (Goonetilleke et al. 2005; Paul and Meyer 2001).

In addition to the oxidation of organic compounds within the benthic zone and underlying sediments, the oxidation of inorganic compounds can contribute to SOD (Di Tora et al. 1990; Gelda et al. 1995; Wang 1981). Reduced compounds such as methane, ammonia, hydrogen sulfide, iron (II), and manganese (II) can be oxidized during transition from the anaerobic/anoxic zone within the sediments to the aerobic environment at the sediment–water interface.

Table 3 presents common electron acceptors utilized by sediment microbes as environmental conditions become more reductive. The last column provides an estimate of the redox potential (E_O) required for these reactions to become biologically favorable.

The significance is that after DO is depleted from sediment pore water, both abiotic reactions and biological respiration continue to occur, resulting in different chemical byproducts and nutrient cycling pathways that will eventually lead to an oxygen demand upon diffusion into the surface water.

The anaerobic sediment metabolism contributing to SOD is controlled, or limited,

Table 3. Preferred/available electron acceptors at decreasing redox potential

Substrate	Product	E_0 (mV)
$O_2 + H_2$	$2H_2O$	+330
$2NO_3^- + 5H_2 + 2H^+$	$N_2 + 6H_20$	+220
$NO_3 + 4H_2 + 2H^+$	$NH_4^+ + 3H_2O$	+220
$MnO_2 + H^2 + 2H^+$	$Mn^{2+} + 2H_2O$	+200
$2Fe(OH)^3 + H_2 + 4H^+$	$2Fe^{2+} + 6H_2O$	+120
$SO_4^2- + 4H_2$	$S^{2-} + 4H_2O$	-150
$CO_2 + 4H_2$	$CH_4 + 2H_2O$	-250

Note: adapted from Wetzel 2001, pg. 639

by the biogeochemical reactions and mass transport of dissolved ions and gasses through the sediments and across the sediment–water interface, assuming no hyporheic exchanges (Higashino et al. 2004). In sediments not conducive to hyporheic exchanges (silts and clays), the sediment boundary layer depths can be very thin, millimeters to centimeters.

The three most influential physical parameters influencing SOD in rivers are water temperature, water velocity, and the depth of the water column (Truax et al. 1995; Ziadat and Berdanier 2004). Lower temperatures result in a decrease in the metabolic rate of most microbes, and it is assumed that SOD rates will decrease accordingly. The water column depth is important since deeper depths are associated with slow moving waters, which have less mixing and decreased fluxes of DO to the benthic zone. At low flow velocities, DO transfer across the water–sediment interface is assumed to be the limiting factor driving SOD. It has been shown that SOD increases linearly within the flow velocity range between 0–10 cm/sec (Mackenthun and Stefan 1998). As velocities increase, SOD increases to a point where the dissolved oxygen consuming activities occurring within the sediments become the limiting factor and SOD rates reach a maximum (Nakamura and Stefan 1994). For perspective, the thalweg of the Lower Jordan River in Reach 1 has a mean velocity around 30 cm/sec, or three times greater

than required to overcome DO transfer limitations across the sediment–water interface. Further increases in water velocity can resuspend fine sediments within the water column. The resuspension of fine sediments due to elevated flow velocities temporarily increases BOD and SOD while exposing interstitial and sediment bound nutrients to the surface water (Malecki et al. 2004).

In addition to the various parameters contributing to DO consumption, many heterogeneities occurring within the sediment substrate can dramatically affect SOD locally. Variations in SOD are also expected to vary seasonally as flows, temperature, aquatic community structure, and sedimentation patterns change over the annual cycle.

3.3.5 SOD models

Previous researchers have developed relationships between SOD and various surrogates for OM. Prior to the Clean Water Act it was shown that the surficial 1 cm of sewage sludge may be aerobic, but the subsurface sludge is undergoing an anaerobic metabolism (Baity 1938). Baity's SOD predictive equation was based on the depth of the sewage sludge deposit. Fair, Moore, and Thomas (1941) developed a relationship based on aerial estimates of OM present in sewage sludge deposits found in a New England stream. Both of these relationships were developed before the Clean Water Act and an important variable was the depth of sludge layer. There are many challenges in accurately estimating the SOD contributing depth of the sludge layer including the "quality" of the OM matter (Fair et al. 1941; Di Toro et al. 1990; Gardiner et al. 1984; Barcelona 1983).

Gardiner et al. (1984) developed a relationship between sediment chemical oxygen demand (COD) and SOD in Green Bay sediments. Once again, the depth of the active sludge layer was required, and application of this relationship quickly becomes

complicated. Butts (1974) produced a relationship between chamber measured SOD in the Upper Illinois Waterway using data collected at 22 sites based on percent total solids (%TS) and percent volatile solids (%VS) of surface mud. Other methods to estimate SOD include the flux of reduced chemicals methane, sulphide, ammonia, and ferrous iron with these parameters accounting for 42%, 50%, 7%, and <1% of the SOD in anaerobic sediments, respectively (Gelda et al. 1995).

3.3.6 Primary Production (PP)

Terrestrial and aquatic primary production provide the organic matter required to support a healthy functioning food web in lotic ecosystems. Primary production results in the generation of OM and DO using the ambient solar flux as an energy source and bicarbonate as the carbon source according to the following general equation (Hauer and Lamberti 2007, pg. 664).

$$6CO_2 + 12H_2O + \text{sunlight} \rightarrow 6O_2 + C_6H_{12}O_6 + 6H_2O$$

This results in diurnal fluctuations in ambient DO concentrations and can lead to supersaturated conditions during the day. In addition, dissolved organic carbon (DOC) can be added to the stream during algal photosynthesis. Up to a 1/3 of the ambient water column DOC can be from algae during periods of peak photosynthesis creating diurnal biological DOC loadings (Kaplan and Bott 1982). As the sun falls below the horizon and photosynthesis ceases, algae, cyanobacteria, macrophytes, diatoms, and other primary producers utilize a portion of the organic carbon produced during daylight hours to support their nighttime metabolism (Hauer and Lamberti 2007, pg. 663). As a result, a net consumption of DO by the primary producers occurs in the absence of sunlight. This

results in lower DO concentrations in the nighttime and early morning hours compared to daytime values.

During photosynthesis, a portion of the reduced organic material is utilized for organism maintenance and survival, or autotrophic respiration (R_a). Organic carbon stored as biomass for growth and reproduction is referred to as net primary productivity (NPP). The gross primary productivity (GPP) is estimated by the following equation (Hauer and Lamberti 2007, pg. 663):

$$GPP = NPP + R_a$$

The net daily metabolism (NDM) can be defined as the change in dissolved oxygen per day as a result of both gross primary production and community respiration (CR_{24}) (Hauer and Lamberti 2007, pg. 665).

$$NDM = GPP - CR_{24}$$

3.3.7 DO supersaturation

Although DO is required for the aquatic respiration of eukaryotic fauna, too much DO can be deadly. This can occur in highly DO supersaturated waters as a direct result from excessive primary production leading to gas bubble trauma (GBT) or gas bubble deterioration (GBD). This potentially fatal phenomenon is typically associated with dinitrogen gas and large hydrostatic pressure changes. GBD is synonymous with the "bends" experienced by SCUBA (self contained underwater breathing apparatus) divers who have spent too much time deep underwater. If the diver swims to the surface too quickly, nitrogen gas bubbles may form within the bloodstream, potentially leading to

injury or death. Fig. 14 provides the saturation concentrations of nitrogen and oxygen in relation to temperature at sea level. Notice that the atmosphere is roughly 80% nitrogen, yet DO concentrations are not 5 times smaller in magnitude.

The United States Environmental Protection Agency (USEPA) has suggested a "total gas" supersaturation limit of 110% in shallow surface waters due to the acute mortality of sensitive fish species during reproduction and the year-round chronic stress to other species (Bouk et al. 1976; USEPA 1986). At a water temperature of 20 °C with nitrogen in equilibrium with the atmosphere, a DO concentration of 130% saturation

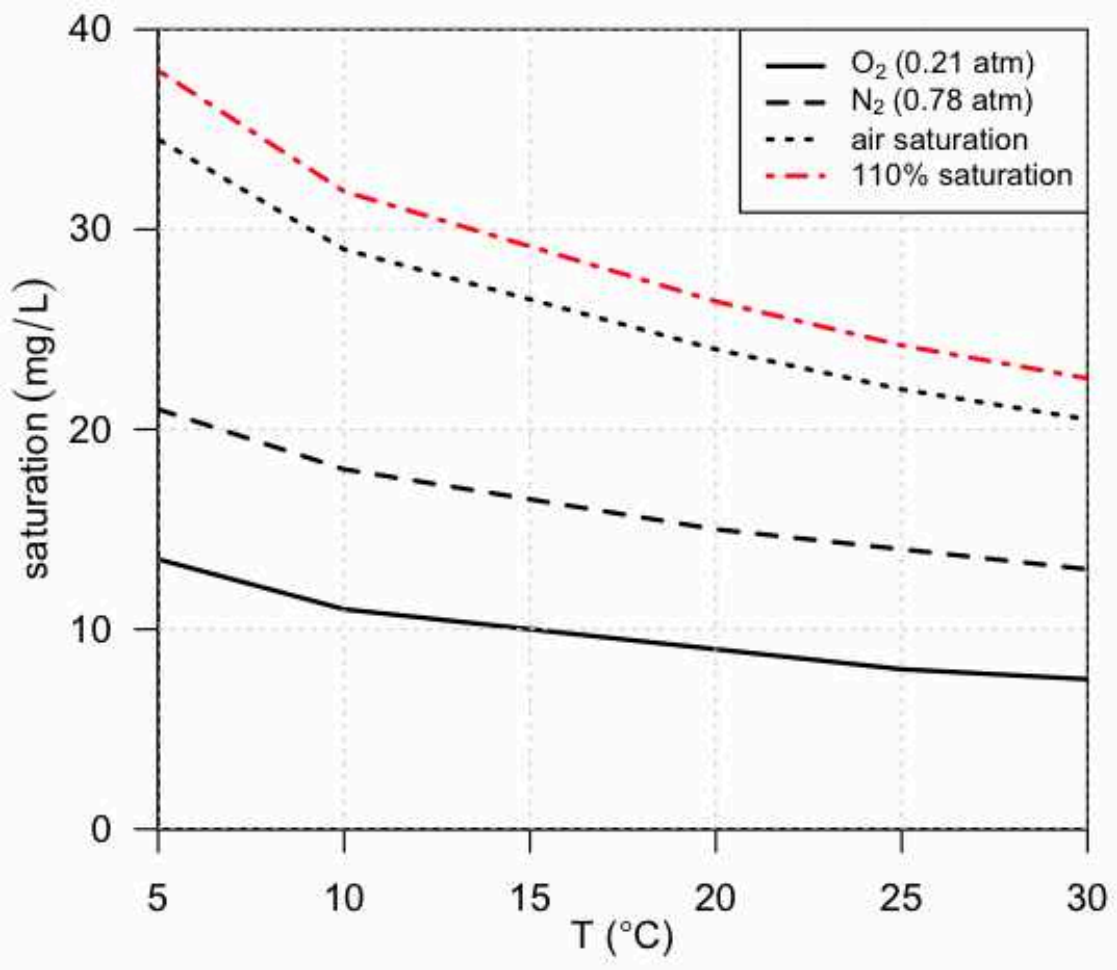

Fig. 14. Nitrogen and DO saturation concentrations

results in a "total gas" supersaturation value greater than 110%. DO saturation concentrations in the UJR have been routinely observed to peak at >130% and have been recorded as high as 150%. These high DO concentrations suggest eutrophication and may be stressful to the aquatic community (Renfro 1963). Fig. 15 shows oxygen bubbles forming in clear chambers when exposed to sunlight. These oxygen bubbles were produced in the benthos during photosynthesis in the UJR at a chamber DO concentration of 150% saturation.

3.3.8 Diurnal DO profiles

Odum (1956) originally introduced the in situ oxygen and gas monitoring techniques that are commonly used to estimate organic carbon fixation due to primary production. During the daytime, photosynthesis ensues and ambient DO concentrations increase. As the sun falls below the horizon, photosynthesis ceases and DO drops due to dark respiration until ambient DO concentrations reach equilibrium with the atmosphere, which is a function of the reaeration coefficient.

The characterization of the water column has long been standardized. BOD bottles measuring the nighttime respiration of the water column can be coupled with chlorophyll-A measurements and "light" bottles measuring DO production due to photosynthesis to estimate the water column's contribution to both CR_{24} and GPP (Wetzel and Likens 1979, Ch. 14). Measuring the metabolism of the benthos requires additional sampling protocols and parameters to separate the water column from the sediments.

Fig. 16 and 17 show two typical, and nearly identical, diurnal dissolved oxygen profiles measured in Reach 1 and 6 of the Jordan River. Reach 1 is where the river is

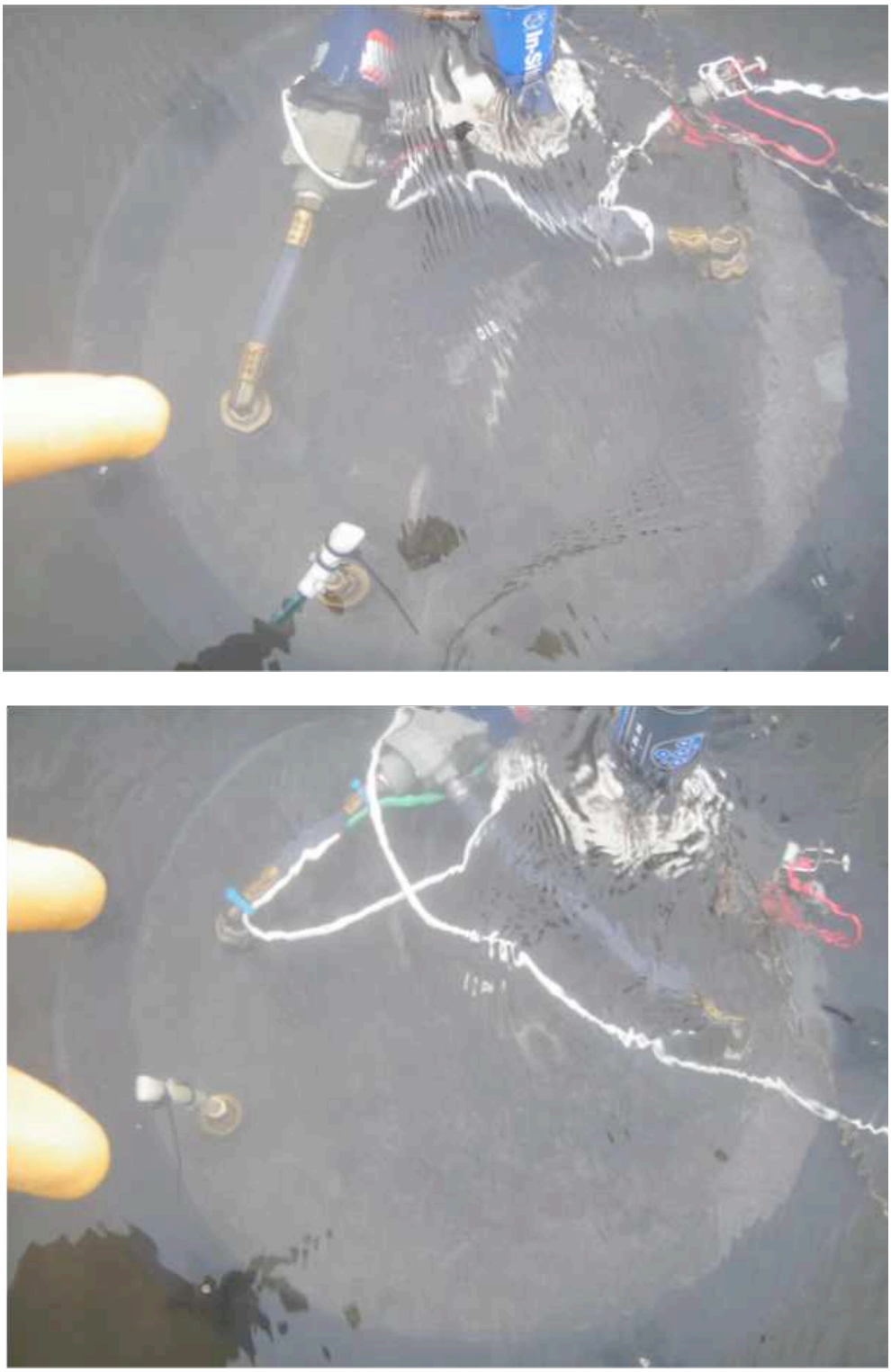

Fig. 15. Gas bubbles forming in closed chambers from supersaturated DO due to benthic photosynthesis (oxygen gas build up on right side of chambers)

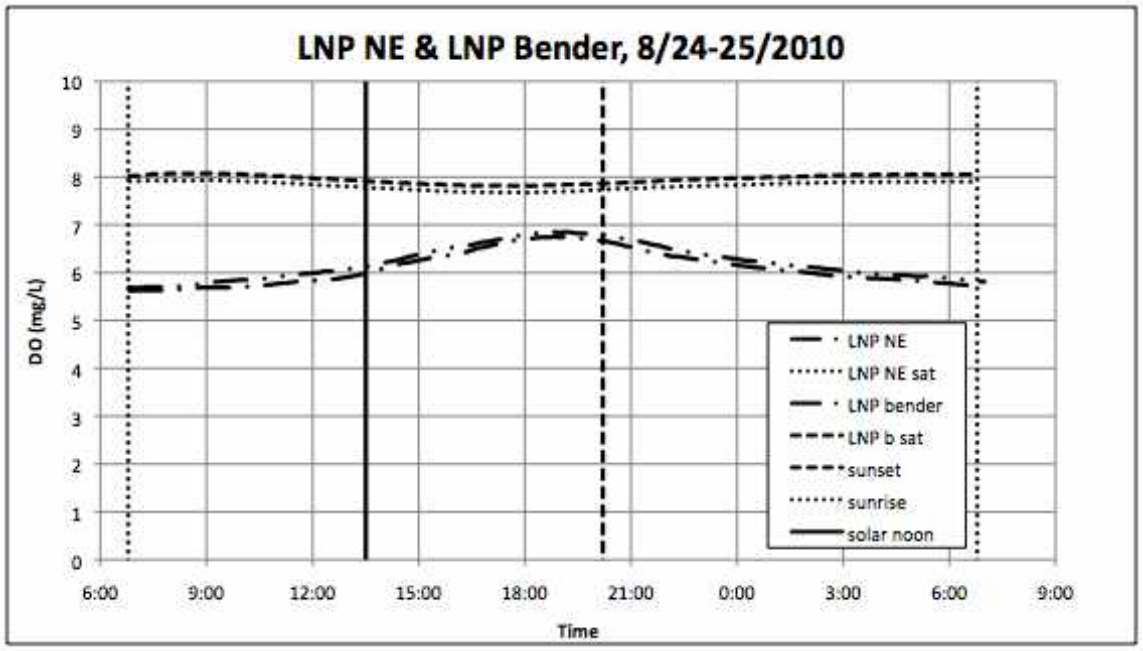

Fig. 16. Diurnal DO fluctuations in the Lower Jordan River

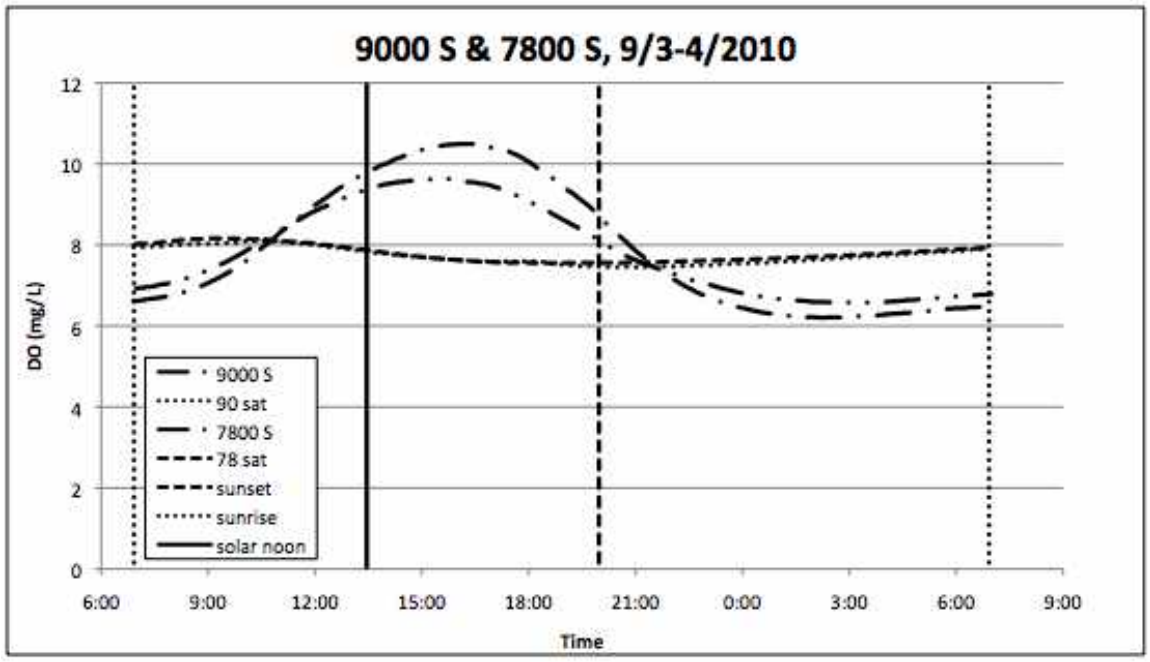

Fig. 17. Diurnal DO fluctuations in the Upper Jordan River

impaired in terms of DO. The chronic DO impairment assigned to Reach 1 by the Utah DWQ is a result of this diurnal DO deficit.

Dissolved oxygen is a byproduct of photosynthesis, and Fig. 17 shows no shortage of dissolved oxygen in the Upper Jordan River during the daylight hours. The 9000 S site reached 135% DO saturation in early September, which was greater than the 110% total gas supersaturation that will cause stress to the aquatic community (Bouk et al. 1976; USEPA 1986).

3.3.9 Eutrophication

> In its course from the source to the sea, the progressive eutrophication of a river water by drainage from cultivated and inhabited districts is an almost inevitable natural process. There are some rivers, however, which, by drainage from densely populated areas, receive excessive amounts of organic matter so that the river is said to be polluted. (Butcher 1947, pg. 186)

The word eutrophication originates from the Latin language meaning "good nourishment." The concept of eutrophication describes the general, yet predictable, degradation of a surface water due to excessive plant, algae, cyanobacteria, and biofilm growth resulting from anthropogenic loadings of nitrogen and phosphorus. Although primary production creates the OM necessary to support the aquatic food chain, if too much OM is produced, the aquatic system may not be able to "function" under the burden of the sequential OM decay.

The general ecological state of surface waters can be described using a trophic state index. In general, oligotrophic systems have very little nutrients and minimal aquatic biomass and tend to have very clear cold water. Oligotrophic systems are typically found in mountain lakes, and the headwaters of lotic systems and are socially "prized" for their perceived beauty and excellent cold-water fisheries. Mesotrophic

systems have more nutrients and aquatic biomass compared to an oligotrophic state. Eutrophic systems are characterized by high nutrient concentrations, poor visibility, high primary production, and variable DO concentrations (Wetzel 2001). Eutrophic ecosystems tend to by plagued by chronic nighttime DO deficits and may experience fish kills during acute events, such as an algal bloom die off or the turnover of a stratified lake where the hypolimnion has become anoxic. Hypereutrophic systems have very high primary production, low aquatic biomass diversity, and very low DO at night. Hypereutrophic systems tend to be very inhospitable due to temporary anoxia and become dominated by cyanobacteria (Chapman and Schelske 1997).

The idea of nutrient based eutrophication due to external anthropogenic loadings was originally identified, quantified, and confirmed in lake systems (Vollenweider 1971; Vollenweider 1976). During the 1990s, water quality managers agreed on the following list (Table 4) of observed changes in a lotic system indicating eutrophication (Hilton et al. 2006; Hilton and Irons 1998).

Water quality parameters commonly used to identify the degree of eutrophication, or trophic state, in lakes include total nitrogen (TN), total phosphorus (TP), Chlorophyll-a (Chl-a), and water clarity (turbidity or secchi depth) (Carlson 1977). Excessive

Table 4. Apparent cues eutrophication is occurring

1	Excessive growth of phytoplankton
2	Excessive growth of periphyton
3	Excessive growth of macrophytes (noted by flood defense engineers)
4	Reduced diversity of macrophytes
5	Shift from macrophyte dominance to benthic, filamentous or planktonic algae
6	Acute low DO events (typically at night)
7	Large pH fluctuations
8	Reoccurring cyanobacteria blooms
9	Water appears green or brown colored

phytoplankton and degraded water clarity are typically feedback from external nutrient loads. Rivers require a different perspective and deviations in sampling protocols to describe the trophic state compared to lakes (Dodds 2007). Table 5 provides a proposed trophic state index for streams that includes benthic characteristics (Dodds 1998). Instead of water clarity, benthic chlorophyll-a is used since rivers are much shallower than lakes, leading to the benthos playing a much larger role in GPP. This is evident by the max benthic Chl-a boundaries being 6–7 times larger than the sestonic, or suspended, fraction in a stream 1 meter deep (Table 5). In addition, water clarity becomes less important in rivers due to ample light reaching the benthos and the large amounts of inert total suspended solids (TSS) transported in lotic systems.

Applying Table 5 to the Jordan River, sestonic Chlorophyll-a (Chl-a) concentrations in the UJR were considered eutrophic in the August of 2006 while the LJR WC was mesotrophic (Utah DWQ 2013, pg. 31). Chl-a accounts for 1–2% of phytoplankton OM, and water column concentrations greater than 25 μg Chl-a/L are considered eutrophic in lakes (Dodds et al. 1998). Jordan River ambient dissolved nitrogen and phosphorus concentrations are typically higher than the eutrophic boundary downstream of WWTP discharges during base flows. In addition, the majority of the

Table 5. Stream Trophic State

	Stream trophic state boundaries	
parameter	oligotrophic-mesotrophic	mesotrophic-eutrophic
mean benthic Chl-a (mg/m^2)	20	70
max benthic Chl-a (mg/m^2)	60	200
sestonic Chl-a (μg/L)	10	30
TN (mg/L)	0.7	1.5
TP (mg/L)	0.025	0.075

Note: adapted from Dodds et al. 1998

phototrophic biomass identified in the Jordan River by Dr. Rushforth during the summer months was cyanophyta, a cyanobacteria also found in the upstream Utah Lake, which is another "apparent cue" of eutrophication suggested in Table 4 (Utah DWQ 2013, pg. 47).

Total phosphorus (TP) present primarily as dissolved phosphorus (DP) in lakes immediately following spring turnover has been shown to be directly related to summertime WC chlorophyll-a concentrations (mg-P:mg Chl-a = 1:1) (Dillon and Rigler 1974). The voluntary reduction in phosphate detergents by soap manufacturers in the 1970s from 12% to 5% decreased POTW effluent discharges by several mg-P/L, improving downstream WQ by reducing eutrophication (Lee et al. 1978; Litke 1999). Lake Erie, once known as the "dead lake" due to eutrophication has been reborn into a functioning waterbody in terms of its trophic state and fish communities following phosphorus abatement over a timescale of 3 decades (Ludsin et al. 2001). The diversion of POTW nutrient loads into Puget Sound led to the rehabilitation of the eutrophic Lake Washington while improving habitat for the freshwater lifecycle of native pacific salmon (Edmondson and Lehman 1981), although it should be noted that dilution is NOT the solution to macronutrient pollution, and the Puget Sound will now need to assimilate this additional nutrient loading. The United States Environmental Protection Agency (USEPA) has established a recommended limit for ambient total phosphorus (TP) concentrations of 0.1 mg-P/L for flowing waters, 0.05 mg-P/L for streams that enter lakes, and 0.025 mg-P/L in lakes and reservoirs (Mueller and Helsel 1996).

A recent report produced by the United States Geological Survey (USGS) reviewing nationwide surface and ground water quality data from 1992–2004 concluded

that ambient stream nutrient concentrations did not change appreciably even with a growing emphasis on nutrient removal from point sources. This was attributed to the large nonpoint source nutrient loadings that have yet to be adequately addressed, let alone identified (Dubroysky et al. 2010). Over 90% of the 190 urban and agricultural streams studied significantly exceeded nutrient background concentrations. Agricultural streams received the largest nutrient loads and had median total nitrogen (TN) concentrations of 4 mg-N/L, while urban streams had 1.5 mg-N/L. Total phosphorus concentrations were on average 0.25 mg-P/L in anthropogenically influenced surface waters. Natural background concentrations were 0.58 mg-N/L and 0.04 mg-P/L, roughly 6 times less, highlighting the amount of macronutrients humans add to our surface waters in both rural and urban settings under our current social practices (Dubroysky et al. 2010).

As of 2008, five states have adopted nutrient standards for all rivers and streams, and nine additional states regulate selected streams. The remaining 36 states, including Utah, have not adopted numeric criteria in the ongoing effort to improve and protect water quality (USEPA 2008).

3.4 Organic Matter (OM)

3.4.1 OM in the aquatic environment

Eutrophication results in the excessive production of organic matter (OM), but additional sources include the natural "background" instream production, terrestrial watershed loads, riparian vegetation loads, and urban stormwater loads. Organic matter can enter a stream through multiple pathways (Pusch et al. 1998):

- allochthonous point and nonpoint surface loads derived from terrestrial primary production

- dissolved organic carbon (DOC) from subsurface or hyporheic inputs
- downstream sediment migration during high flow events
- autochthonous primary production
- instream cycling of existing organic matter

The accumulation of excessive amounts of OM as a sediment sludge layer due to eutrophication and external OM loads is a long known problem and has been coined "benthal deposits" (Fillos and Swanson 1975). The "life cycle" of benthal deposits can be compared to the sludge production and stabilization occurring in a modern day biological wastewater treatment plant (WWTP) process where an external organic load (facility influent) initially undergoes a settling step similar to a depositional zone in a river. Microorganisms mineralize and recycle the settled OM into new viable organisms to perpetuate the process under aerobic, anoxic, and anaerobic conditions. Over time, the OM becomes more recalcitrant and the rate of carbon turnover slows. These processes are occurring within river sediments, and OM will become stabilized similar to WWTP biosolids following anaerobic digestion. Similar to anaerobic digesters, methane, ammonia, hydrogen sulfide, and other reduced chemicals are produced during anaerobic sediment decomposition, thereby transforming a portion of the OM into soluble and mobile oxygen consuming chemical species. As a result, SOD is ultimately a result of the "quality and quantity" of OM present in the surficial sediments.

3.4.2 OM size fractionation

In the most basic form of OM characterization, organic matter can be differentiated as dissolved organic matter (DOM) or particulate organic matter (POM). Organic matter classified as POM can be further characterized as fine particulate OM

(FPOM) and course particulate OM (CPOM) depending on the size of the particle. CPOM is defined as those particles larger than a 1 mm diameter, and FPOM includes all organic particles with diameters between 0.45 μm and 1 mm in size.

3.4.3 Dissolved Organic Matter (DOM)

Dissolved organic matter (DOM) is ever present in the aquatic environment and provides the carbon and electron source for heterotrophic microbes (Spencer et al. 2007; Baines and Pace 1991). DOM plays a crucial role in carbon and nutrient cycling as high molecular weight DOM is utilized for cell growth and maintenance while being further broken down to low molecular weight DOM (Amon and Benner 1996). The concentration of DOM in riverine systems varies on diurnal, seasonal, and annual cycles. Seasonal and annual variations are typically associated with hydrologic inputs, while daily fluctuations have been linked to primary production. It has been estimated that 13% of the inorganic carbon fixed to organic carbon during planktonic photosynthesis is lost to the ambient water through extracellular release (Baines and Pace 1991).

It is accepted that the DOM is responsible for the majority of the SOD associated with the decomposition of organic material, but over time CPOM is converted to FPOM and eventually DOM, resulting in a constant flux of DOM from organically enriched sediments (Hauer and Lamberti 2007, pg. 273).

3.4.4 Particulate organic matter (FPOM, CPOM, and LWD)

CPOM can be present in pockets or layers within the sediments due to seasonal loadings and erosion patterns. Autumn leaf loadings to a stream can become buried beneath inorganic sediments to be mineralized throughout the following year (Pusch et al.

1998). Highly recalcitrant large woody debris (LWD) does not directly contribute to DO dynamics in running waters. Wood requires years to decades to decompose due to its high lignin content and low surface area to volume ratio (Melillo et al. 1983; Webster and Benfield 1986). LWD is a valuable aquatic habitat in terms of substrate for biofilm growth and habitat for higher aquatic life forms.

3.4.5 Terrestrial OM (litterfall)

Terrestrial forests deposit 200–800 g-OM/m^2/year as litterfall and production rates are dependent on the availability of sun and water, which are directly related to latitude and precipitation (Meentemeyer et al. 1982). Litterfall includes all annual loadings of OM derived from trees and shrubs including leafs, bark, seeds, and branches. The vast majority, over 70%, of terrestrial litterfall occurs during autumn as leaf litter (Meentemeyer et al. 1982). The role of seasonal organic matter loads associated with autumn leaf litter accounted for 44% of the annual organic load in a section of the forested Bear Brook, NH (Fisher and Likens 1973). Over 70% of the OM loads to three headwater steams were from leaf fall, but only 3% of OM exports were CPOM, indicating a high conversion of CPOM to FPOM to DOM (Wallace et al. 1995; Cushing et al. 1993). In the deciduous forest streams of Eastern U.S., 86% of the organic carbon load was CPOM, and 58% of the annual leaf litter load occurred in autumn (Webster et al. 1995).

Initial leaf decomposition of dry leafs can occur rapidly with 17% of the carbon being leached into the water column as DOM in the first 3 days (Mcdowell and Fisher 1976). Up to 25% of the mass of dry leafs can leach within 24 hours of being submerged in water, while fresh cut green leafs do not leach as rapidly (Gessner et al. 1999; Webster

and Benfield 1986). The leaf litter decomposition rate has been estimated to be 1 year in most lotic systems, resulting in a steady-state leaf litter deposition/decomposition process over an annual cycle (Fisher and Likens 1973).

Leaf litter will undergo structural decomposition and mineralization carried out by a consortium of macroinvertebrates, fungi, and bacteria with dominant populations dictated by the prevailing ambient environmental conditions (Gessner et al. 1999). In Portugal's urban Ave River, fungi were responsible for 34% of leaf carbon losses, while bacteria removed 7.5% in alder leaf packs over a 42-day instream incubation period (Pascoal and Cassio 2004). The majority of leaf decomposition in urban streams was found to be a result of the microbial community, not macroinvertebrate shredders (Imberger et al. 2008). Within a couple days, submerged leafs are initially colonized by fungus followed by bacteria, whereas macrophyte debris are initially colonized by bacteria (Webster and Benfield 1986).

3.4.6 Urban OM

The majority of nutrient spiraling and CPOM degradation studies have been conducted in small streams (1st to 3rd order) in relatively undisturbed aquatic environments (Ensign and Doyle 2006). The 4th order Jordan River fits into neither of these categories, but it does receive urban stormwater conveyed via creeks. The macroinvertebrate shredders indicative of high water quality (WQ) are not present in the fine sediments of the LJR, but can be found among the gravel and cobbles present in the UJR. Urban streams are typically dominated by disturbance-tolerant macroinvertebrates composed primarily of oligochaetes and chironomids, or aquatic worms and midges (Walsh et al. 2005).

Urban environments are largely impervious resulting in dust, organic matter, and pollutants being transported to the downstream surface water through stormwater conduits (Heaney and Huber 1984). Secondary growth of fungus and biofilms will colonize and degrade terrestrial OM during dry periods in stormwater conveyance systems and can flush out during rain events (Ellis 1977).

Stormwater conveyance systems typically bypass the riparian zone where nutrient removal and sediment retention naturally occur, thereby increasing pollutant loads to the receiving stream (Hatt et al. 2004). Benthic leaf litter in an urbanized stream with an efficient stormwater conveyance system was composed primarily of nonnative tree species planted along streets in Australia (Miller and Boulton 2005). The specie of leaf influences the rate of OM turnover, and nonnative species can influence benthic metabolism since macroinvertebrate diversity is very low in many urban streams. This lack of aquatic macroinvertebrate diversity can result in an overloading of OM to the system due to the lack of higher life forms capable of preconditioning additional substrate (Ryder and Miller 2005). Through urbanization, the Salt Lake valley has been ordained with nonnative deciduous shade trees lining impervious streets. This seasonal urban stormwater load of leaf organic matter may add to the organic loading to the Lower Jordan River.

3.5 Nutrient Cycling and Transformations

3.5.1 Aquatic nutrient dynamics

Fig. 18 provides a general overview of organic matter (OM) and nutrient cycling occurring in a lotic system in the water column and at the sediment–water interface. The following list describes the nutrient dynamics shown in Fig. 18.

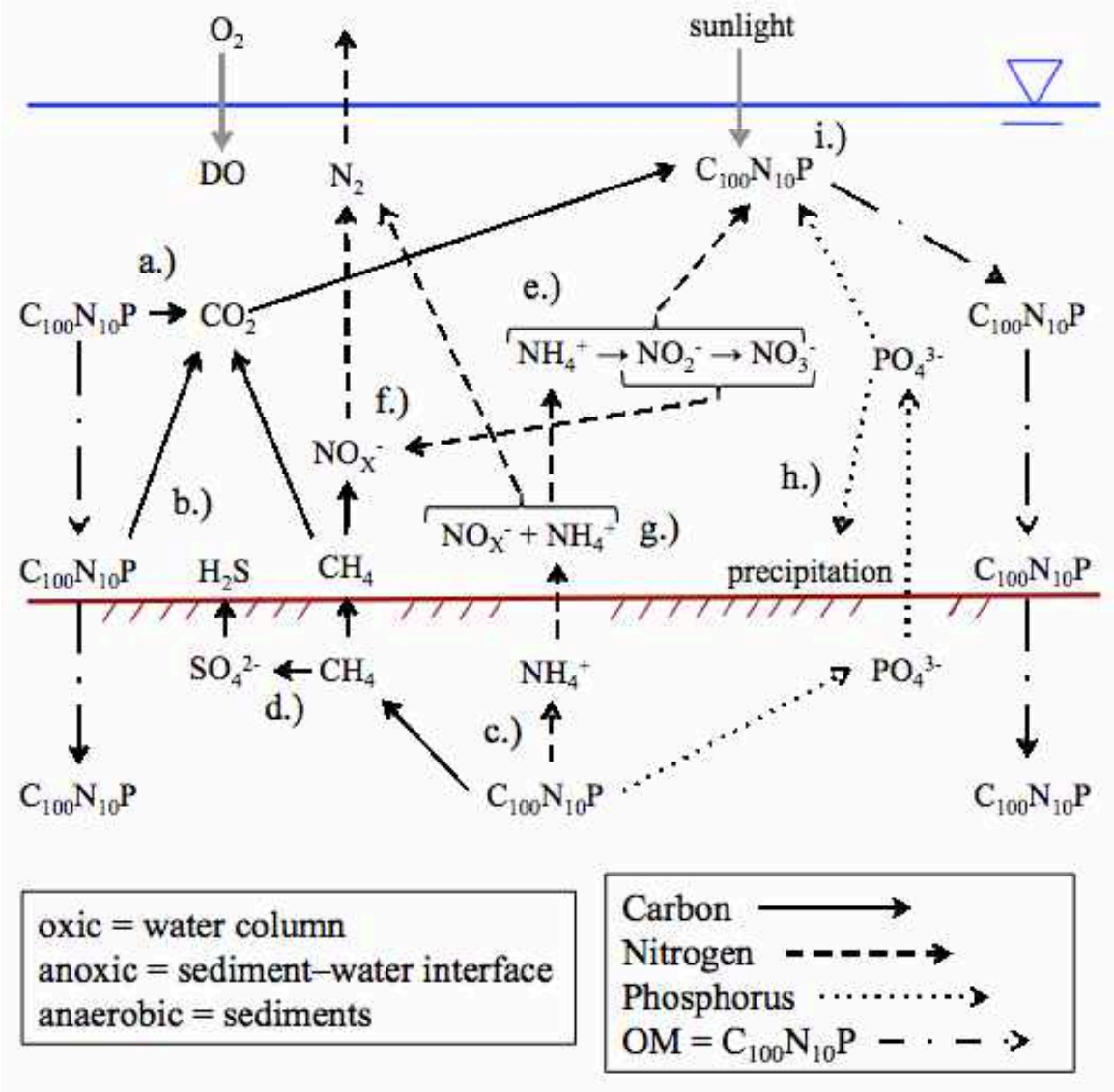

Fig. 18. Nutrient cycling dynamics

a.) biochemical oxygen demand (BOD), sestonic OM is oxidized in the water column and phytoplankton respire

b.) sediment oxygen demand (SOD), OM settles and is oxidized in the benthos and periphyton respire

c.) sediment anaerobic decay, OM becomes buried and a portion of the organic-C is reduced to methane and carbon dioxide while releasing

ammonium and phosphate to the water column as a sediment flux

d.) the low oxidation reduction potential (ORP) of the sediment pore water, fueled by OM decay, can lead to the reduction of other compounds (methane and other reduced chemicals diffuse out of the sediments contributing to SOD)

e.) nitrogenous biochemical oxygen demand (NBOD), Ammonium is oxidized to nitrate in the water column

f.) denitrification can occur at the sediment–water interface with methane being the readily biodegradable carbon and electron source (rbCOD)

g.) anaerobic ammonium oxidation (ANAMMOX) utilizes nitrite or nitrate and ammonium to produce N_2 gas

h.) orthophosphate may precipitate or sorb to the sediments in the alkaline Jordan River

i.) instream primary production cycles dissolved nitrogen and phosphorus into an organic form to start the process over, see step a.)

3.5.2 Particulate OM decay into dissolved nutrients

In a lotic aquatic environment, particulate OM (POM) is physically broken down with a portion of the POM and DOM being swept downstream and the remainder being consumed by heterotrophs producing additional OM and CO_2. The cycling of carbon (C), nitrogen (N), and phosphorus (P) associated with OM decay in the aquatic environment is referred to as nutrient spiraling (Newbold et al. 1981; Newbold et al. 1982; Ensign and Doyle 2006).

The majority of the carbon, nitrogen, and phosphorus cycling is a result of the

element entering an organic phase through direct assimilation or other biologically mediated processes. As a result, biologically active environments are conducive to nutrient cycling, and the preferred energy source for microbes living in the sediments are reduced carbon (Fischer et al. 2002). OM fuels the microbial community and acts as a stockpile of nutrients to become biologically available over time as the OM is degraded.

3.5.3 Methane (CH_4)

An estimated 37% of the current methane loads to the atmosphere are associated with natural systems, with wetlands being the largest source (USEPA 2010). Rivers and estuaries contribute 0.9% of the estimated natural loadings and 0.3% of total loadings to the atmosphere (USEPA 2010). The majority of natural sources of methane are biologically mediated resulting from methanogenesis occurring in wet environments with low redox potential and a source of biodegradable OM. These environments include surface water sediments, wetlands, WWTPs, landfills, rice paddies, and the guts of ruminants (four-stomached animals). Other major sources of methane to the atmosphere include the extraction of natural gas, fossil fuel combustion, and wildfires (USEPA 2010).

Once methane has entered the atmosphere, a single molecule is estimated to last 9–12 years until being oxidized to CO_2 in the troposphere (USEPA 2010). Methane is an important greenhouse gas influencing climate change and has a global warming potential 25 times greater than CO_2 over a 100-year period. The current atmospheric concentration of 1.7 ppmV methane is twice as high compared to preindustrial revolution concentrations. Carbon dioxide is currently at 400 ppmV, or 0.04%, and was 280 ppmV prior to the industrial revolution.

Methane is soluble in water at 1 atm (100%) at standard temperature and pressure (STP) to a concentration of 22 mg-CH_4/L. Methane is poorly soluble and has a Henry's equilibrium constant k_H = 1.3x10^{-3} (M/atm) (Stumm and Morgan 1996).

$$k_H = {}^{[C_a]}/_{p_a} \qquad (1)$$

k_H = Henry's equilibrium constant
$[C_a]$ = molar concentration dissolved in water
p_a = partial pressure in gas phase

For perspective, if 1 liter (L) of water saturated with dissolved methane was placed in a 2 L airtight container (i.e., 1 L water and 1 L headspace) and allowed to come into equilibrium at STP, 30 parts of methane would enter the gas phase for every 1 part remaining dissolved in the liquid. The k_H values for other common atmospheric gases are provided in Table 6 along with the relative percentage of the atmosphere and corresponding dissolved concentrations at STP in contact with atmospheric air. Atmospheric methane dissolving into surface waters results in negligible BOD since the atmospheric concentration is so low. Dissolved methane found in surface waters is typically associated with anaerobic decay occurring in the sediments. Hydrogen sulphide is the most soluble gas in Table 6 and when found in surface water suggests sediment

Table 6. Equilibrium constants of select compounds

	$K_{25°C}$ (M/atm)	% atmos	equalibrium (mg/L)
CH_4	1.29x10-3	0.00017	0.00004
O_2	1.26x10-3	21	8.5
N_2	6.61x10-4	78	14.4
H_2S	1.05x10-1		

Adapted from Stumm and Morgan 1996

OM decomposition and low redox potentials. Hydrogen sulphide can be smelled when silty sediments are physically disturbed in the LJR.

3.5.4 Diffusion and ebullition

Methane fluxes at the sediment–water interface can be very different than at the water–atmosphere interface due to water column oxidation, advection transport, and ebullition (Huttunen et al. 2006). Over 95% of the sediment derived methane flux across the air-water interface into the atmosphere in a hypereutrophic lake was due to ebullition, not sediment diffusion (Casper et al. 2000). In a study of eutrophic shallow lakes, 40–60% of atmospheric methane fluxes were due to ebullition (Bastviken et al. 2004). Increases in sediment methane ebullition have been observed in lakes during periods of quickly dropping barometric pressure (Casper et al. 2000; Bastviken et al. 2004). Deeper water column depths result in sediments that release less methane as ebullition, and shallow water column depths of 0–2 meters resulted in the highest swamp gas ebullition fluxes (Bastviken et al. 2004).

3.5.5 Nitrogen

As microbes utilize DO during the oxic degradation of organic matter, an additional DO demand is required for the subsequent oxidation of ammonium associated with organic nitrogen (Fair et al. 1941). The oxygen demand required for nitrification can add an additional 30% to the oxygen demand associated with only organic carbon. Ammonium produced during the decomposition of organic material within the sediments requires 4.57 g-O_2/g-N to complete the two-step biological nitrification process ($NH_4^+ \rightarrow NO_2^- \rightarrow NO_3^-$) according to the following stoichiometric equations (Tchobanoglous et al.

2003):

$$\text{(Nitritation)} \quad 2NH_4^+ + 3O_2 \rightarrow 2NO_2^- + 4H^+ + 2H_2O$$

$$\text{(Nitratation)} \quad 2NO_2^- + O_2 \rightarrow 2NO_3^-$$

$$\text{(combined Nitrification)} \quad NH_4^- + 2O_2 \rightarrow NO_3^- + 2H^+ + H_2O$$

The first metabolism, nitritation, is carried out by autotrophic nitrosobacteria, also known as ammonia oxidizing bacteria (AOB) utilizing 3.43 g-O_2/g-NH_4^+-N to produce nitrite. Nitrite is toxic in the aquatic environment and does not accumulate in healthy lotic systems due to the rapid oxidation to nitrate by autotrophic nitrobacteria, or nitrite oxidizing bacteria (NOB). The oxidation of nitrite, or nitratation, requires 1.14 g-O_2/g-NO_2^--N. Ambient nitrite concentrations in surface waters are typically less than 0.002 mg NO_2-N/L due to the close proximity in the environment of these two different bacteria (Lewis et al. 1986). Nitrate is the most common form of dissolved nitrogen found in aerobic surface waters. Nitrate will eventually be reduced or bioassimilated by phototrophs and bacteria during cell growth and can be utilized as an electron acceptor under low DO conditions during microbial denitrification.

Methane produced in organically enriched sediments can be utilized as a readily biodegradable substrate (rbCOD) for some heterotrophic denitrifying bacteria. This results in a much lower theoretical DO requirement of 1.71 g-O_2/g-N for the complete nitrification and denitrification process utilizing ammonia and methane produced during the anaerobic decomposition of OM (Chapra 2008). The following equations provide stoichiometric equations for methane driven denitrification, and the combined processes of nitrification and denitrification utilizing methane from decaying OM:

$$^{5}/_{8}CH_4 + HNO_3 \rightarrow {}^{5}/_{8}CO_2 + {}^{1}/_{2}N_2 + {}^{7}/_{4}H_2O$$

$$NH_3 + {}^{3}/_{4}O_2 \rightarrow {}^{1}/_{2}N_2 + {}^{6}/_{4}H_2O$$

This is important because methane can be oxidized using either nitrite or nitrate as an electron acceptor instead of DO, thereby decreasing the ambient DO demand required for the direct oxidation of both methane and ammonia independently (Chapra 2008, pg. 459). This results in an additional nitrogenous oxygen demand of roughly 11% of the carbon oxygen demand, compared to 30% when nitrate is not used as an electron acceptor during methane oxidation. This is important in degraded urban rivers since nitrate is typically in abundance due to POTW discharges and can be utilized to oxidize sediment produced methane.

3.5.6 Phosphorus

Most aquatic systems are capable of storing large amounts of phosphorus (P) within the sediments and act as a P sink as sedimentation ensues. The storage and/or release of sediment bound phosphorus is influenced by sediment mineralogy, sediment OM content, ambient water chemistry, and the benthic community (Wetzel 2001, pg. 245). In hard water rivers, the solubility of inorganic phosphorus decreases as pH exceeds 8.5, and precipitation can be driven by photosynthesis in highly productive environments (Olsen et al. 2009).

There are four principal methods that phosphorus may enter the sediments of a surface water:

- sedimentation of phosphorus rich minerals
- sorption/precipitation of inorganic P with iron, manganese, clays,

carbonates, and amorphous oxyhydroxides

- bioassimilation of dissolved P via aquatic biota
- sedimentation of organic P from both autochthonous and allochthonous sources

The sedimentation of phosphorus rich minerals is typically associated with watershed geology. The immobilization of dissolved P through sorption and precipitation is influenced by sediment geochemistry and ambient water quality. The bioassimilation of dissolved P is associated with cell growth. The death and subsequent sedimentation of phototrophs and autochthonous OM introduced into the surface water removes phosphorus from the water column, but contributes to SOD and positive sediment phosphate fluxes over the long term. All aquatic life relies on phosphorus, but excessive availability is linked to eutrophication (Marsden 1989).

3.5.7 C:N:P ratios

Oceanic planktonic biomass samples have very similar carbon, nitrogen, and phosphorus molar ratios and can be generalized according to the Redfield Ratio expressed in moles (Table 7) (Redfield 1934). The significance of this observation was that the ambient oceanic water column C:N:P molar ratio was 106:16:1, the same as the ratios found in many of the living phytoplankton. The C:N:P molar ratios found in Table 7 are organized in terms of nitrogen enrichment, with WWTP influent containing the highest concentration of organic nitrogen and wood having the least.

Organic matter found in organically enriched river sediments and sludge are composed of 3–5% organic nitrogen in terms of dry mass (Baity 1938; Fair et al. 1941; Rudolfs 1932; McDonnell and Hall 1969). Terrestrial soils have a C:N ratio of 14 while

Table 7. Organic C:N:P molar ratios found in the environment

	organic C:N:P molar ratios				
	C	N	P	C:N	reference
WWTP influent	53	13	1	4	Tchobanoglous et al. 2003, pg. 558
WWTP bacteria	65	13	1	5	Tchobanoglous et al. 2003, pg. 558
oceanic algae	106	16	1	7	Redfield 1934
soil bacteria	60	7	1	9	Cleveland and Liptzin 2007
river mud	117	10		12	Rolley and Owens 1967
grass clippings	>120	10		>12	Humanure Handbook 2005
terrestrial soil	186	13	1	14	Cleveland and Liptzin 2007
cow manure	190	10		19	Humanure Handbook 2005
foliage	1,212	28	1	43	Mcgroddy et al. 2004
leaf litter	3,007	45	1	67	Mcgroddy et al. 2004
cardboard	>4,000	10		>400	Humanure Handbook 2005
wood	>5,600	10		>560	Humanure Handbook 2005

river and estuarine muds tend to be more nitrogen enriched with a ratio of 11.7 (Rolley and Owens 1967). Soil bacteria have a slightly lower C:N ratio of 8.5, and wastewater bacteria typically have C:N ratios around 5:1, while POTW influent has an average ratio of 4:1 (Cleveland and Liptzin 2007; Tchobanoglous et al. 2003, Table 3–15, pg. 558). It is worth noting that the macronutrient N:P ratios for WWTP bacteria are the same as the influent wastewater used to grow the microbes during biological wastewater treatment, similar to Redfield's observation that plankton have similar stoichiometry to the "soup" they grew in.

CHAPTER 4

MATERIALS AND METHODS

4.1 Sediment Oxygen Demand (SOD)

4.1.1 SOD sampling locations

Sediment oxygen demand (SOD) sampling locations were preselected based on hydraulic reaches, tributaries, stormwater outfalls, and the proximity to WWTP point discharges. Recommendations from the Utah Division of Water Quality (Utah DWQ) and other stakeholders were incorporated into site selection. A list of sampled sites for SOD and a short description is provided in Table 8.

4.1.2 SOD chamber details

Three aluminum SOD chambers, one Control and two Testing, were utilized in the Jordan River SOD study. A fourth chamber was brought to each site as a spare in the case of pump failures or other unforeseen circumstances. The top section of each chamber consisted of a lid housing the pump, plumbing, water sampling tube, water quality probe connection, and attachments for ropes used to lift the SOD chamber out of the water. A submersible pump was mounted on each chamber to circulate water inside the chamber at a predetermined flow rate of 11 L/min at an average flow velocity of 8 cm/sec. The influent and effluent ends of the plumbing were located inside the chamber and were connected to a polyvinyl chloride (PVC) water distribution system. The

Table 8. SOD sampling locations and descriptions

2009, 2010, 2011, 2012, and 2013 SOD Study Sites			
Mile	Reach	Site Name	Description
0.1	1	Burnham	100 m upstream of Burnham Dam, end of Reach 1
2.8	1	LNP NE	0.3 miles downstream of South Davis WWTP
3	1	LNP SW	350' downstream of South Davis WWTP
3.2	1	Cudahy Ln	450' upstream of South Davis-S WWTP
8.9	2	300 N	downstream of City Cr./stormwater
10.7	3	700 S	downstream of 900 S stormwater/tributary discharge
11.2	3	900 S-N	175' downstream of the stormwater discharge
11.3	3	900 S-S	185' upstream of the stormwater discharge
13.1	3	1700 S	downstream of the Surplus Canal diversion dam
13.7	3	2100 S	350' downstream of the Surplus Canal diversion
14.3	4	2300 S	1000' upstream of the Surplus Canal diversion
14.8	4	2600 S	1,350' downstream of Mill Cr.
15	4	2780 S	downstream of Mill Cr. (E and W banks)
16.8	4	3650 S	above Mill Cr. and below Big Cottonwood Cr.
20.9	4	5400 S	200' upstream of the 5400 S bridge
24	5	7600 S	70' downstream of the flow control structure
24.1	5	7800 S	100' upstream of the 7800 S bridge
26	6	9000 S	100' upstream of the 9000 S bridge
34.1	6	SR 154	upstream of the SR 154 bridge
46.2	7	14600 S	0.65 miles upstream of the 14600 S bridge
52	8	US-73	0.4 miles upstream of the US-73 bridge

distribution pipe, or diffuser, contained 10 small holes to evenly distribute the re-circulated flow within the chamber

Both the Control and Testing SOD chamber configurations were identical in construction and operation except for the bottom sections. The lids were attached to the chambers via coupling flange, bolts, and a neoprene gasket. In the Control chamber configuration, the bottom of the chamber was sealed to measure oxygen consumption

associated with the water column only. In the Testing SOD chamber configuration, the bottom was open and the river water contained in the chamber was in constant contact with the river sediments during the experimental period. Thus, the Testing SOD chamber measured DO consumption associated with the sediments as well as in the water column. Before use in the field, each chamber was carefully tested in the lab for water tightness and the ability of the submersible pump to effectively circulate water within the chamber. Lab scale testing was accomplished using a large livestock-watering trough filled with tap water.

The original Control chamber (which measured WC_{dark}) had a working volume of 44 liters, and the Testing SOD chambers had working volumes of 38 liters. This discrepancy in volumes is a result of the additional space provided in the Control chamber that is not seated 1½" into the sediments. The SOD calculation accounts for these variations in volume when calculating SOD fluxes. A smaller Control chamber having a volume of 38 L replaced the larger original chamber in 2010. When deployed, the Testing SOD chambers encapsulated a sediment area of 0.16 m^2. Fig. 19 provides a general schematic of the SOD chambers deployed.

Water quality probes, or sondes (probe in French) were provided by the Utah Division of Water Quality. The probes utilized were In-Situ Inc. model Troll 9500, capable of measuring DO, temperature, conductivity, pH, and barometric pressure. All sensors were utilized during sampling, but only DO and temperature were used directly while calculating oxygen demands. Conductivity was used to determine when the probes were placed in the water and when they were taken out. The probes were quality control checked and calibrated, if necessary, in the lab before all sampling events.

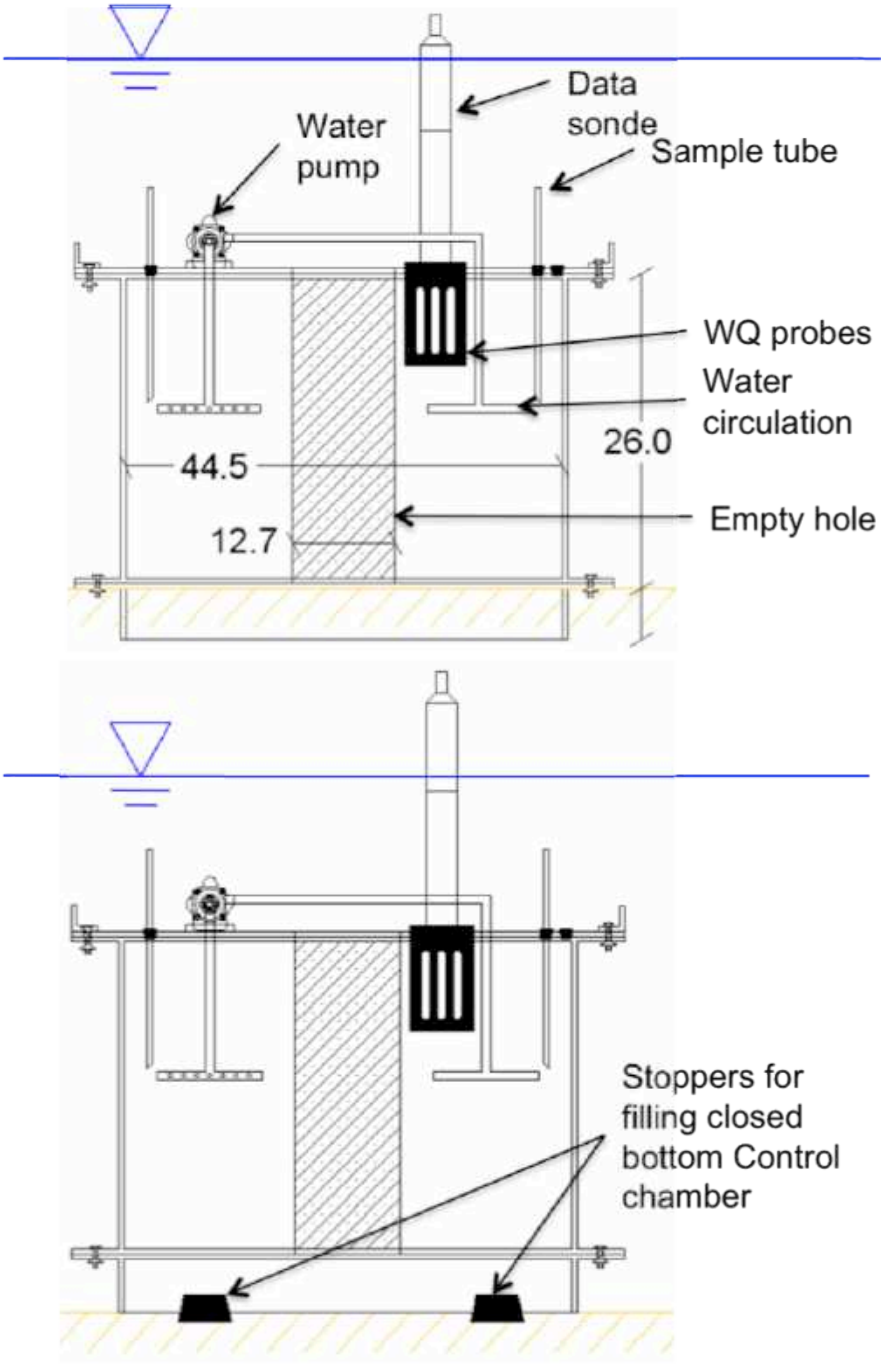

Fig. 19. Testing (top) and WC (bottom) SOD chamber schematics
Note: dimensions in cm

4.1.3 SOD chamber deployment

SOD sampling locations were positioned on the inside of river bends and along straight sections of the Jordan River. Safety issues were addressed by sampling on the inside of meanders since the fast flowing deep water (thalweg), steep riverbanks, and associated riverbank undercutting were avoided. Sampling locations were chosen to represent the sediment substrate characteristics corresponding to that particular stretch of the Jordan River. For example, if the typical sediments were silty muck, sand, or gravel, then the chambers were deployed in sediments having those characteristics.

A great deal of time was allotted to walking both the riverbanks and within the Jordan River proper to locate suitable SOD sampling locations that were reasonable representations of the particular section of river under consideration. The time spent walking the Jordan River allowed for a better understanding of the sediment characteristics and provided an opportunity to locate any obstructions that may cause potential safety issues or SOD chamber deployment problems such as rebar, barbed wire, construction debris, riprap, shopping carts, submerged logs, etc.

After the exact location of SOD chamber deployment was determined, the water quality probes were turned on for data collection. The author deployed all SOD chambers to minimize sediment disturbances and to provide consistency in the chamber deployment protocol.

The Control chamber was placed first due to the additional time required for the Control chamber to reach a stable DO reading. Two large stoppers were removed from the bottom of the Control chamber, and the chamber was immersed in the river sideways and allowed to fill with ambient river water. Deviations in the filling angle were required

at sites that were too shallow to completely submerge the Control chamber perpendicularly. If possible, the Control chamber was filled sideways in a deeper section of the river immediately downstream or off to the side to minimize sediment disturbances.

After filling the Control chamber with river water, the chamber was flipped upside down while keeping the chamber completely submerged. The pump was turned on to purge any trapped air out of the pump and associated plumbing. After 10–15 seconds of running the pump, the pump was turned off and any remaining air in the Control chamber was allowed to escape by removing a small stopper located on the bottom outer edge of the chamber in the tilted position. After all air had been removed from the Control chamber, all three stoppers were replaced while keeping the Control chamber completely submerged. It is necessary to remove all air from the chambers if accurate oxygen depletion rates are to be measured. Air left in the system contains oxygen that will slowly dissolve into the chamber water, leading to an underestimation of respiration.

The Control chamber was then carefully placed on top of the sediments while taking great care not to disturb the surrounding area. Depending on the slope of the river bottom and flow velocities, the Control chamber was attached to a wood stake hammered into the sediments to stop downstream chamber drift. After the Control chamber was situated, the water quality probe was submerged into the water, gently swirled to remove air bubbles attached to the probes, and screwed into the probe housing on the Control chamber lid. After placement of the water quality sonde, the water circulation pump was turned on for the remainder of the testing period.

Similar to the Control chamber, the two Testing chambers were filled with river

water and flipped upside down while running the pumps to remove any air trapped in the pump and plumbing. After 10–15 seconds, the pumps were turned off and the Testing chambers were then flipped right side up while keeping the chambers submerged. The Testing chambers were deployed upstream of the Control chamber to ensure undisturbed sediments. After placing the Testing chambers into the sediments by hand and body weight, proper placement was confirmed by carefully checking the coupling flange connecting the bottom sections of the Testing chambers. Seating the chambers to a depth of 1½" was achieved by setting the coupling flange of the chambers parallel to the surrounding sediments.

Obstructions such as rocks, riprap, logs, urban garbage, etc., were commonly encountered, and the Testing chamber was redeployed upstream to ensure a proper seal in the river sediments. After seating the two Testing chambers, the water quality probes were installed and the pumps were turned on. To ensure the pumps were working correctly during the testing period, the pumps were periodically touched by hand, foot, or stick to feel for vibrations indicating the pumps were on.

4.1.4 Calculation of SOD and WC_{dark}

The sediment oxygen demand (SOD) fluxes and dark water column respiration (WC_{dark}) rates were calculated using the following equations (Butts 1974; Butts 1978; Murphy and Hicks 1986; Chiaro et al. 1980):

$$SOD = 1.44\left({}^{V}/_{A}\right)(b_{SOD} - b_{WC}) \qquad (2)$$

$SOD = Sediment\ Oxygen\ Demand\ \left({}^{g}/_{m^2\ day}\right)$
$1.44 = unit\ conversion\ \left({}^{mg}/_{L\ min} \rightarrow {}^{g}/_{L\ day}\right)$
$V = volume\ of\ SOD\ and\ WC\ chambers\ (38\ L)$

$A = sediment\ area\ within\ the\ chamber\ (0.16\ m^2)$
$b_{SOD} = bulk\ DO\ depletion\ rate\ in\ SOD\ chamber\ \left({}^{mg}/_{L\ min}\right)$
$b_{WC} = DO\ depletion\ rate\ in\ WC\ chamber\ \left({}^{mg}/_{L\ min}\right)$

$$WC_{dark} = 1440(b_{wc}) \quad (3)$$

$WC_{dark} = DO\ depletion\ rate\ in\ WC\ chamber\ \left({}^{g}/_{m^3\ day}\right)$
$1440 = unit\ conversion\ \ \left({}^{mg}/_{L\ min} \rightarrow {}^{g}/_{m^3\ day}\right)$

WC_{dark} is the volumetric oxygen consumption rate measured in the Control chamber and represents the dark respiration associated with the water column. This parameter is comparable to a 1-day biochemical oxygen demand (BOD) test having no nitrification inhibitor. SOD is expressed as a two-dimensional flux associated with the sediments and benthos since the oxygen demand required by the water column has been subtracted. The working volumes and sediment areas were constant since the Testing chambers were placed to a uniform depth of 1½". The SOD fluxes were initially calculated for both of the Testing chambers and then averaged for further analysis and oxygen mass balances. A flow diagram for the procedures used to calculate SOD is provided in Fig. 20.

A prior warning concerning the presentation of the dark respiration parameters SOD and WC_{dark} needs to be addressed. SOD is the amount of oxygen utilized by the sediments, which is typically represented in the literature as a positive flux. Alternatively, from the perspective of the river water and when performing DO mass balances, this is a loss of DO and will be a negative flux. As a result, many of the graphs in this dissertation represent SOD and WC_{dark} as positive values since this was easier to visualize, but all tables and mass balances are from the perspective of the ambient water column and are

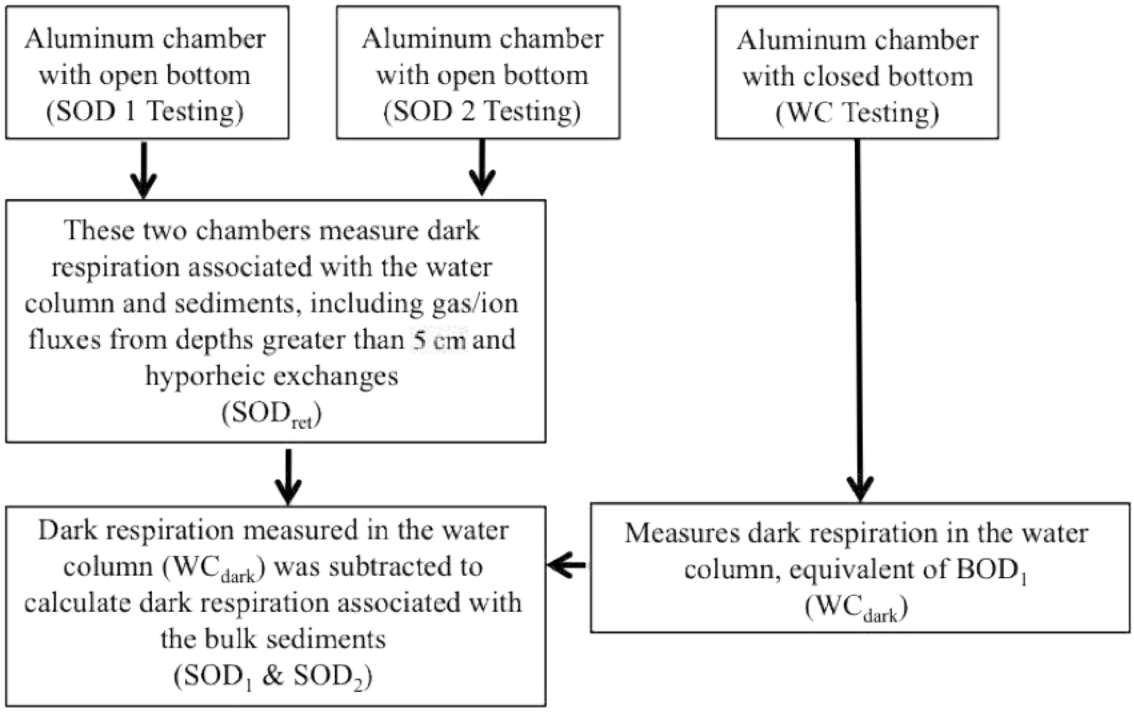

Fig. 20. Dark respiration (SOD and WC_{dark}) calculation flow diagram

presented as negative values.

SOD values found in literature are typically normalized to 20 °C (SOD_{20}) using the following modified van 't Hoff form of the Arrhenius equation based on ambient water temperature (Berthelson et al. 1996; Chapra 2008, Table 2.3):

$$SOD_{20} = \frac{SOD}{\theta^{t-20}} \qquad (4)$$

$SOD_{20} = SOD\ normalized\ to\ 20\ ℃$
$t = observed\ temperature\ (℃)$
$\theta = temperature\ normalization\ coefficient$
$1.065 = (Berthelson\ et\ al. 1996)$
$1.08 = (Chapra\ 2008)$
$1.047 = WC\ BOD\ decomposition\ (Chapra\ 2008)$

The ambient DO deficit is a result of various biogeochemical activities occurring in the water column and at the sediment–water interface. Through the use of chambers,

these parameters are decoupled, and the percent of the ambient oxygen demand associated with the sediments ($\%_{SOD}$) can be calculated accordingly:

$$\%_{SOD} = \left(\frac{SOD}{SOD + (WC_{dark}) * d}\right) 100 \quad (5)$$

$$d = mean\ river\ depth\ at\ the\ sampled\ site\ (m)$$

The mean river-wide depth at each site was calculated after mapping river cross sections in the Lower Jordan River and estimated in the Upper Jordan River by walking across the river while noting depth.

4.1.5 Utah Lake SOD

SOD and WC_{dark} measurements were performed in Utah Lake to characterize the sediments and water column in the large shallow waterbody draining to the Jordan River. Fig. 21 provides a general overview of Utah Lake, the surrounding topography, municipalities, and SOD sampling locations.

The site names, geographical coordinates, USEPA assigned STOrage and RETrieval (STORET) sampling identification numbers, and dates sampled are provided in Table 9. SOD measurements in the Jordan River did not require special arrangements due to the shallow water depths at most locations. However, the water depth in Utah Lake was 4 meters at some locations. Utah Lake SOD sampling required the use of SCUBA gear, a custom made sampling barge to deploy the chambers, and an anchored float tube to carry the deep cycle 12V battery. The barge was constructed in a fashion such that it was easy to transport from the University of Utah to Utah Lake, light enough to be carried by one person, convenient and straightforward for the nuances of sampling SOD,

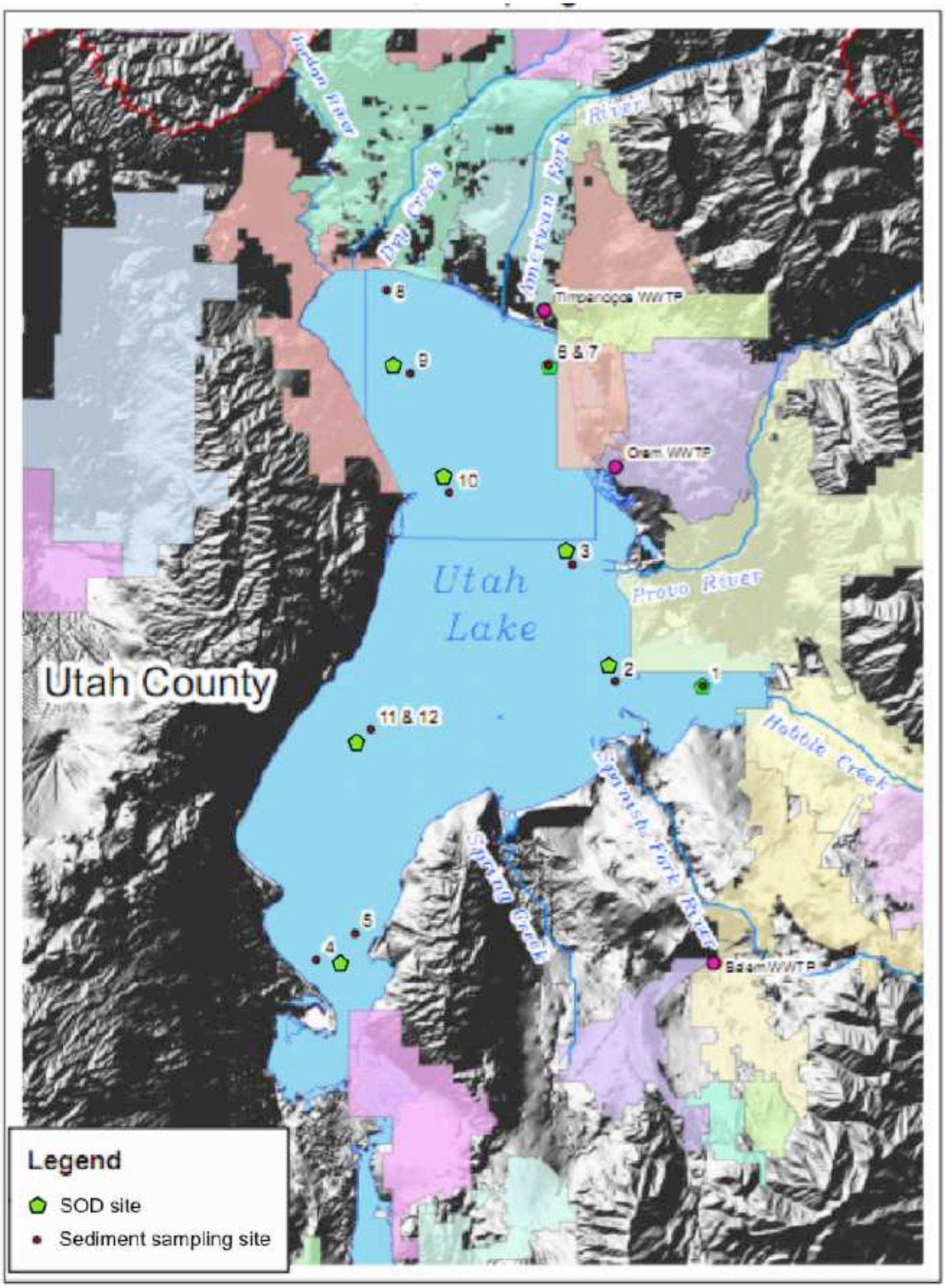

Fig. 21. Utah Lake SOD and sediment sampling sites

Table 9. Utah Lake SOD sampling sites and dates

site #	Location	Easting	Northing	STORET #	Date
1	Provo Bay	441119	4449033	4917450	9/14/10
2	Entrance to Provo Bay	437811	4448947	4917770	8/3/12
3	1.3 miles W of Provo River	435143	4454575	4917390	8/2/12
5	Goshen Bay	425157	4437673	4917620	8/3/12
6	0.5 miles W of Geneva Steel	434005	4463666	4917320	9/24/10
9	2 miles E of Saratoga Springs	426061	4466105	4917520	9/30/11
10	1 mile E of Pelican Point	429499	4457869	4917370	8/4/12
12	Goshen Bay entrance	425054	4445601	4917500	8/4/12

durable, and to minimize any disturbance to the sediments during chamber deployment by providing a stable lowering and lifting function (Fig. 22).

The motorboat used to access Utah Lake SOD sites was anchored further away from the chambers than the length of anchor line utilized to secure the vessel. As a general nautical rule, 10 feet of anchor line is required for every 1 foot of water depth. Changing wind directions causes the boat to arc around the anchor, posing a collision hazard to the SCUBA diver upon resurfacing in the turbid water. This was learned through experience. Fig. 23 shows the chambers being deployed outside the anchor radius

Fig. 22. SOD chamber deployment barge being built (left) and final product

Fig. 23. SOD chamber deployment barge (left) and float tube used to carry the battery to power SOD chamber pumps (right)

and the final setup with three chambers deployed while powered by the battery on the anchored float tube.

4.1.6 State Canal SOD

The purpose of conducting SOD in State Canal was to obtain SOD values for extremely organically enriched sediments and to evaluate SOD downstream of the Jordan River. The State Canal sampling site was located downstream of the South Davis County-North wastewater treatment plant (WWTP) discharge and upstream of the Bountiful Pond "tributary" (Fig. 24). SOD was measured off the west bank in water 1 meter deep. State Canal was roughly 2 meters deep center channel at this location. Sediment cores were taken at the SOD site and from the bridge west of the parking lot.

4.2 Chamber Net Daily Metabolism (NDM)

4.2.1 Chamber NDM sampling locations

Seven sites were selected to evaluate the dark and light metabolisms of both the water column and benthos. The LNP NE and 300 N sites where located within Reaches 1 and 2 where DO deficits are routinely observed during daylight hours. The 2100 S site was located just below the Surplus Canal diversion and signifies the beginning of the

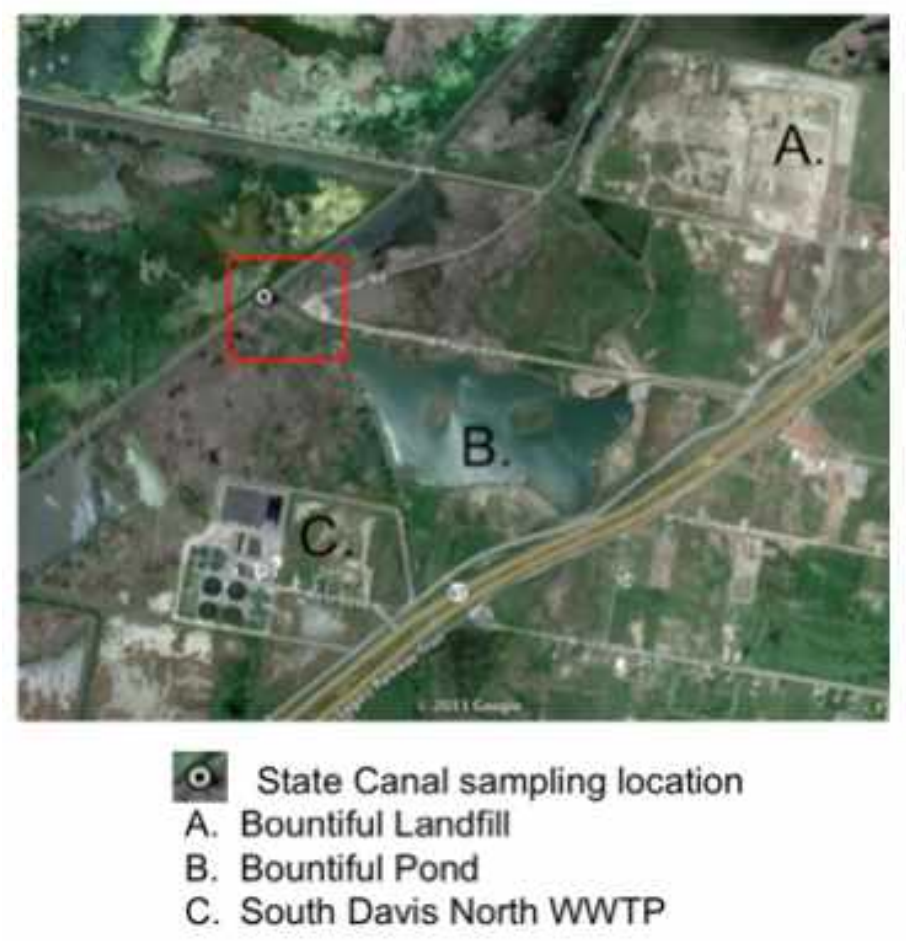

Fig. 24. State Canal sampling site

Lower Jordan River. The 1700 S site was located downstream of the 2100 S site and provided a comparison of sediment composition as the average size decreased from sandy gravel to sand. The 5400 S site was located in the Upper Jordan River downstream of the South Valley WRF discharge. The 7600 S site was located upstream of all online WWTP direct discharges to the Jordan River in a cobble dominated substrate conducive to periphyton growth. The 9000 S site was also located above all online WWTPs and had sediments composed of sands to investigate the potential for periphyton to colonize this mobile substrate. All sites except for the 7600 S and 2100 S sites have been used for previous SOD studies and allow direct comparisons.

4.2.2 NDM chamber details

To measure water column and benthic dark respiration and light metabolisms, custom chambers were constructed of transparent bulletproof plastic (Lexan) by the South Davis-S WWTP machine shop. The NDM chambers were built to be directly comparable to the existing SOD chambers, and all chambers had a working volume of 38 L and encapsulated a sediment area of 0.16 m^2 (Fig. 25).

Unlike the aluminum SOD chambers, which were open at the bottom, the NDM chambers were closed at the bottom. Hence, the Testing NDM chamber and the Control NDM chamber were the exact same in construction. At the time of testing, however, a preincubated sediment tray containing local sediment was placed in the Testing NDM

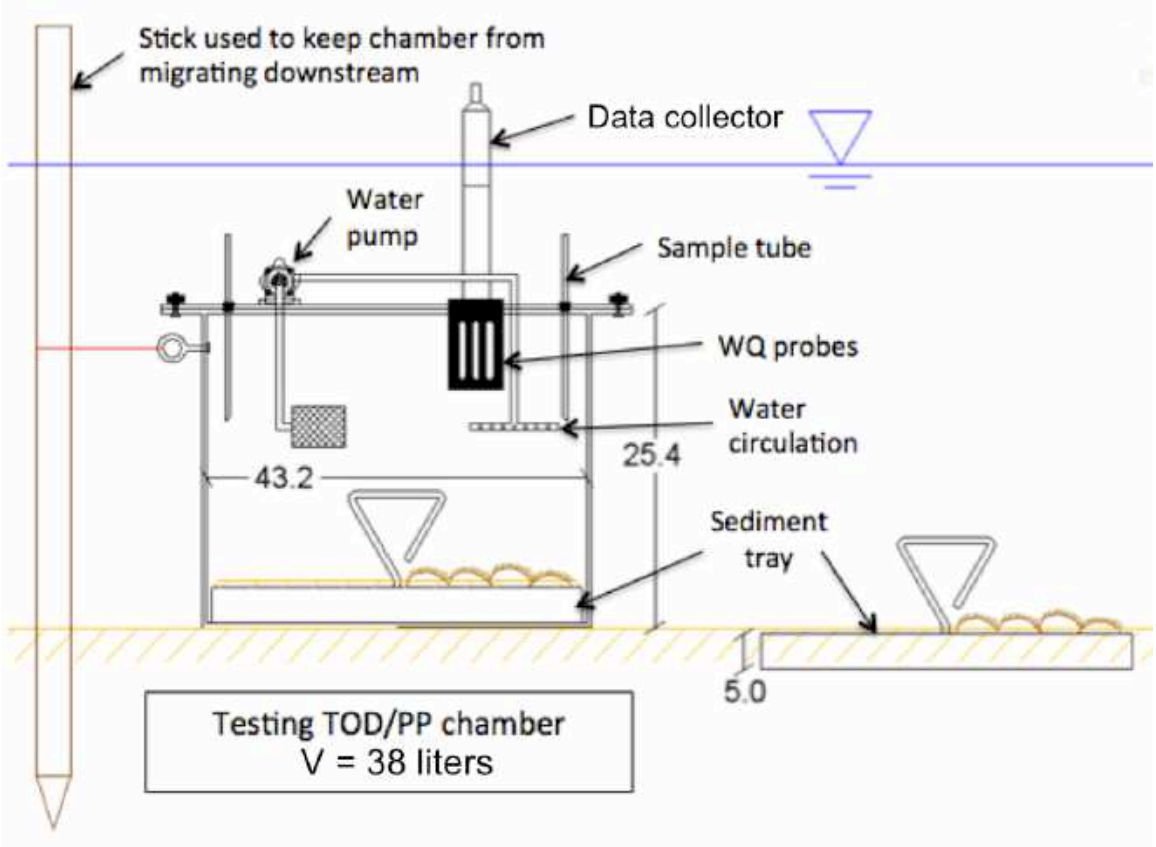

Fig. 25. NDM chamber in use and tray incubation

chambers.

The use of sediment trays allowed for the study of a wide range of undisturbed substrates ranging from silts, sands, gravel, cobbles, and detritus. The top 5 cm of local sediments were transferred to the sediment trays by shovel. The trays were then buried to allow roughly 1 cm of sediments above the lip of the tray to reduce localized flow variations (Hauer and Lamberti 2007, Ch. 28). The trays were then allowed to sit within the river for a minimum of 3 weeks to allow recolonization of the benthic community, including both heterotrophs and autotrophs (Bott et al. 1985). While the trays were left in the river bottom, bedload CPOM (leafs, phragmites stalks, detached macrophytes, sticks, etc.) and anthropogenic litter needed to be regularly removed from the tray handles protruding from the sediments.

In addition, the sites needed to be regularly visited to confirm that the trays did not erode out of the sediments due to fluctuating stream velocities. If the lids of the trays were observed above the sediments, the trays were carefully removed without disturbing the contents, holes redug, and the trays replaced. The tray handles where thoroughly cleaned with a steel wool pad before chamber testing to remove any benthic growth present on the exposed sediment tray handle. After the recolonization period, the sediment trays were carefully removed and placed in the closed bottom clear chambers for the primary production and dark respiration experiments.

The use of sealed chambers containing sediment trays allows the measurement of both heterotrophic and autotrophic respiration and abiotic processes occurring at the sediment–water interface while excluding hyporheic exchanges, groundwater intrusion, and deep sediment gas fluxes (Grace and Imberger 2006). In addition, the trays allowed

the measurement of sediment dark respiration in cobble sediments that SOD chambers cannot be deployed in due to erosive flow velocities and poor chamber sealing. Fig. 26 shows sediment trays containing silt in Reach 1 (left) and gravel at 7600 S located in the Upper Jordan River (right).

4.2.3 NDM chamber deployment

At each site a total of five chambers were installed, two aluminum open bottom SOD chambers and three transparent closed bottom NDM chambers. Two of the closed bottom transparent NDM chambers were used to measure tray oxygen demand (TOD) and tray gross primary production (TPP) and contained sediment trays. These chambers measured respiration rates under dark conditions and the net oxygen production rates under sunlit conditions. The transparent NDM chambers were initially covered with two black bags to measure dark respiration associated with the aquatic community present in the sediment trays and in the water column. The third clear chamber was filled with ambient river water and initially covered with two black plastic bags to measure water

Fig. 26. Silts and cobbles following incubation in the Jordan River

column dark respiration (WC_{dark}). Under dark conditions this chamber acted as the control for the two aluminum SOD chambers and the two black-bagged NDM chambers containing sediment trays. After initially measuring dark respiration, the black bags where removed from the three clear chambers by carefully cutting the bags with a knife. In this way, the NDM chambers measured oxygen depletion and net production in the absence and presence of sunlight throughout the day. The three NDM chambers were initially covered with black plastic bags for 120–180 minutes depending on the length of the photoperiod. The length of the photoperiod is important since sampling occurred both in the summer and winter months. The chambers were deployed for a total of 4~6 hours.

Sediment tray dark respiration, or tray oxygen demand (TOD), was initially measured in the NDM chambers during the morning hours. Dark respiration needs to be measured before light metabolism (primary production) within the productive Jordan River because chamber studies require a DO deficit, and supersaturated DO conditions are typically encountered in the UJR shortly after sunrise. Supersaturated DO at the beginning of testing will result in oxygen bubbles forming on the top and sides of the chamber, skewing results since these bubbles will redissolve as a DO deficit develops within the chambers under dark conditions. Therefore, the chambers were initially filled with ambient river water with a DO deficit during the morning hours for all experiments. Another advantage to measuring respiration before production is that the DO levels in the chambers are allowed to decrease further before measuring primary production, allowing longer testing times before the chamber reaches DO saturation.

The black bags were removed close to solar noon (approximately 1:00 PM in summer and 11:30 AM in the winter) to measure light metabolism with the assumption

that the maximum rate of primary production in the benthos and water column was occurring at this time. After the water contained in the chambers becomes DO saturated, the measured rate of DO production is underestimated since much of the oxygen occurs as gas bubbles, not dissolved oxygen.

4.2.4 Calculation of WC_{dark}, TOD, WC_{light}, and TPP

Similar to the SOD calculations, WC_{dark} is the dark respiration rate in the water column measured using the black-bagged transparent chamber containing only river water. TOD is the tray oxygen demand and is calculated using the black-bagged transparent chambers containing sediment trays under dark conditions. TOD is similar to SOD except that it does not account for methane fluxes from deeper than 1.5", hyporheic exchanges, or low DO groundwater intrusion. Both autotrophic and heterotrophic dark respiration in the sediments and water column are assumed to occur at a consistent rate throughout the diurnal period. Therefore, the dark respiration oxygen depletion rates TOD and WC_{dark} can be used directly in NDM estimates and are calculated using the SOD equations.

Photosynthesis only occurs during daytime at varying rates; therefore, the maximum rate of photosynthesis was measured midday. The maximum net rate of sediment tray primary production ($TP_{m,net}$) and the maximum net rate of water column primary production ($WCP_{m,net}$) were calculated using the following equations based on chamber DO depletion and production rates under light conditions. Notice that when TOD is subtracted, TPP_m increases since respiration is an oxygen sink. Also note that the $WC_{light,m}$ is the net rate measured in the chamber and does not have WC_{dark} subtracted at this stage.

$$TPP_m = \left[1.44\,{}^{V}/_{A}\left(TPP_{m,bulk} - WC_{light,m}\right)\right] - TOD \quad (6)$$

$TPP_m = maximum\ rate\ of\ sediment\ tray\ PP\ \left({}^{g}/_{m^2\ day}\right)$

$TPP_{m,bulk} = maximum\ rate\ of\ sediment\ tray\ bulk\ PP\ \left({}^{mg}/_{L\ min}\right)$

$WC_{light,m,} = maximum\ \ rate\ of\ water\ column\ net\ PP\ \left({}^{mg}/_{L\ min}\right)$

$TOD = sediment\ tray\ oxygen\ demand\ \left({}^{g}/_{m^2\ day}\right)$

Since TPP_m and $WC_{light,m}$ were measured midday and are assumed to be the maximum rate of photosynthesis, they cannot be directly compared to SOD, TOD, and WC_{dark} respiration rates. Therefore, both TPP_m and $WC_{light,m}$ were converted to gross average daily oxygen production rates by normalizing the maximum rate to a Gaussian curve over the length of the photoperiod to calculate the final parameters TPP and WC_{light} using the following equations (Chapra 2008, pg. 436):

$$TPP = TPP_m\left({}^{2f}/_{\pi}\right) \quad (7)$$

$TPP = avg.daily\ sediment\ tray\ PP\ \left({}^{g}/_{m^2\ day}\right)$

$TPP_m = maximum\ rate\ of\ sediment\ tray\ bulk\ PP\ \left({}^{g}/_{m^2\ day}\right)$

$f = photoperiod\ , fraction\ of\ day\ recieving\ sunlight\ (d)$

$\pi = 3.14$

$$WC_{light} = (WC_{light,m} - WC_{dark})\left({}^{2f}/_{\pi}\right) \quad (8)$$

$WC_{light} = avg.daily\ water\ column\ PP\ \left({}^{g}/_{m^2\ day}\right)$

After normalizing the maximum oxygen production rates to a 24-hr average based on the length of the photoperiod, SOD, TOD, and TPP can be directly compared. By dividing TPP by TOD a general benthic indication of heterotrophic (<1) or autotrophic (>1) conditions can be obtained. This ratio can also be applied to the water column to determine the degree of autotrophy:heterotrophy associated with seston and phytoplankton (Vannote et al. 1980).

Although the parameters TPP and WC_{light} are represented as gross fluxes and rates, they do not account for increases in phototroph respiration during photosynthesis. This was not a consideration in the context of a river DO mass balance since the phototrophs may respire and photosynthesize at rates higher than measured, but they are utilizing DO that they produced, and the final NDM answer will be the same (Grace and Imberger 2006). The final chamber derived NDM flux was calculated accordingly:

$$NDM = TOD + TPP + \left(WC_{dark} + WC_{light}\right) * d \qquad (9)$$

$NDM = chamber\ measured\ net\ daily\ metabolism\ \left({}^{g\ DO}/_{m^2 * day}\right)$
$d = mean\ riverwide\ depth\ (m)$

If a volumetric NDM rate is desired instead of a flux, divide the sediment parameters by mean river depth and sum the water column parameters. The schematic in Fig. 27 shows the complete protocol for light and dark metabolism chamber measurements used during this research.

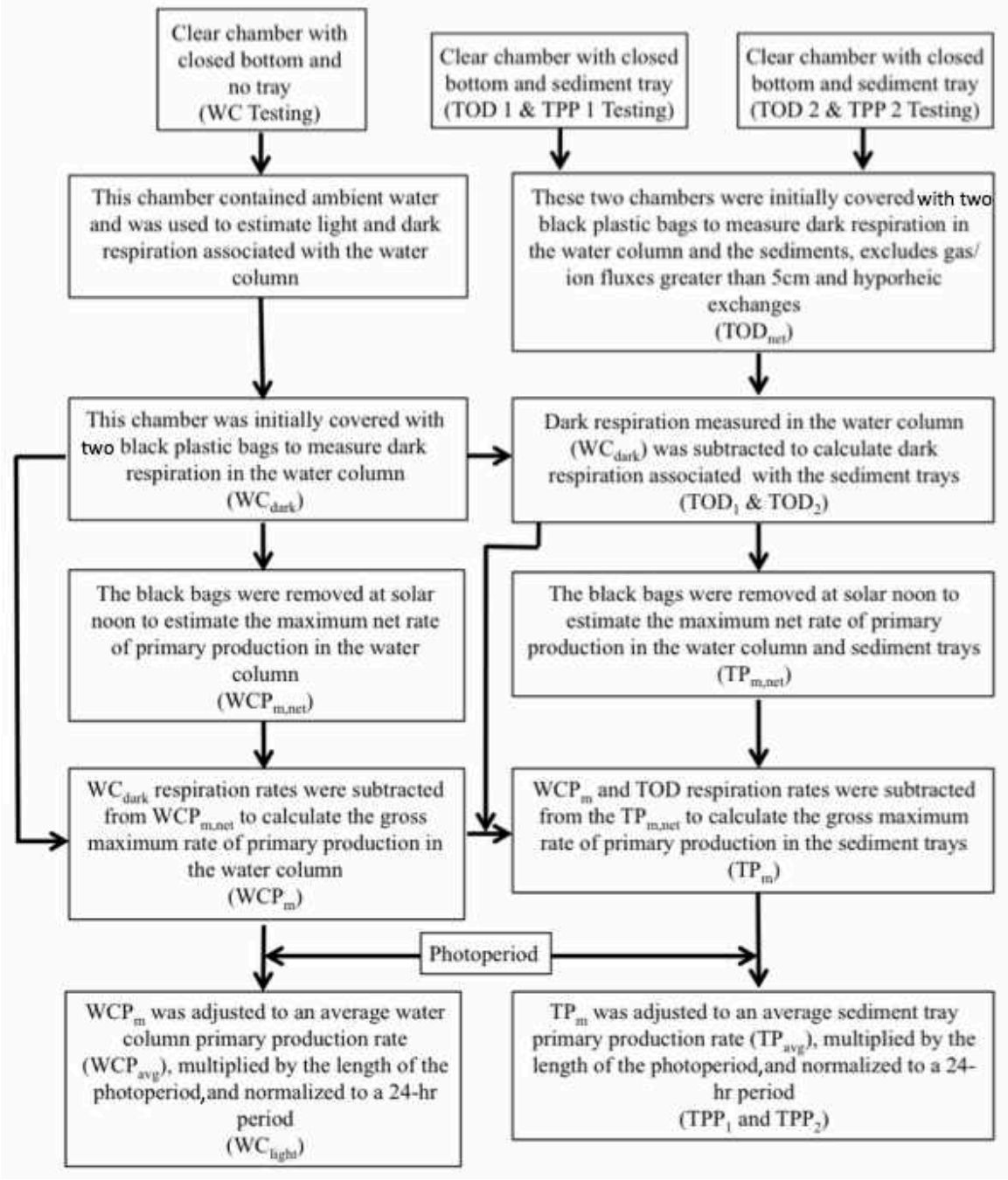

Fig. 27. General schematic of the experimental strategy used for chamber NDM

4.3 Estimating NDM using Diurnal DO Curves

4.3.1 Calculation of single-station GPP, CR_{24}, and NDM

Diurnal DO curves can be used to estimate stream metabolism based on the nighttime DO deficit, daytime DO deficit or surplus, length of photoperiod, and reaeration coefficient (Chapra and Di Toro 1991; Chapra 2008; Odum 1956). Diurnal DO models initially calculate a nighttime respiration rate and normalize this rate over a 24-hour cycle with the assumption that respiration is occurring at a constant rate during the daytime (CR_{24}). Net primary production (NPP) is measured during daytime, and GPP is estimated by including the contribution of the "constant" respiration during the photoperiod to estimate GPP. Ambient DO measurements in the Jordan River were collected every 5 minutes using In-Situ Troll 9500 data sondes.

There are many diurnal DO NDM models available, and a variety were used including single-station excel, upstream-downstream excel, Bob Hall's single-station R model, and basic equations (Hauer and Lamberti 2007, ch. 28). The single-station basic equations, or "visual" analysis, was ultimately used since it provides the same answers without the need of a computer, as long as the reaeration coefficient is known.

Fig. 28 provides an example diurnal DO profile for a stream metabolism estimate in the UJR where the reaeration coefficient is 6, the length of photoperiod is 13 hours, and the average depth is 0.8 meters.

The nighttime steady state DO deficit was -1.5 mg-DO/L, and this respiration rate is assumed to be constant throughout the 24-hour cycle. After multiplying the reaeration coefficient by the ambient nighttime DO deficit and normalizing to the mean river depth, CR_{24} is estimated.

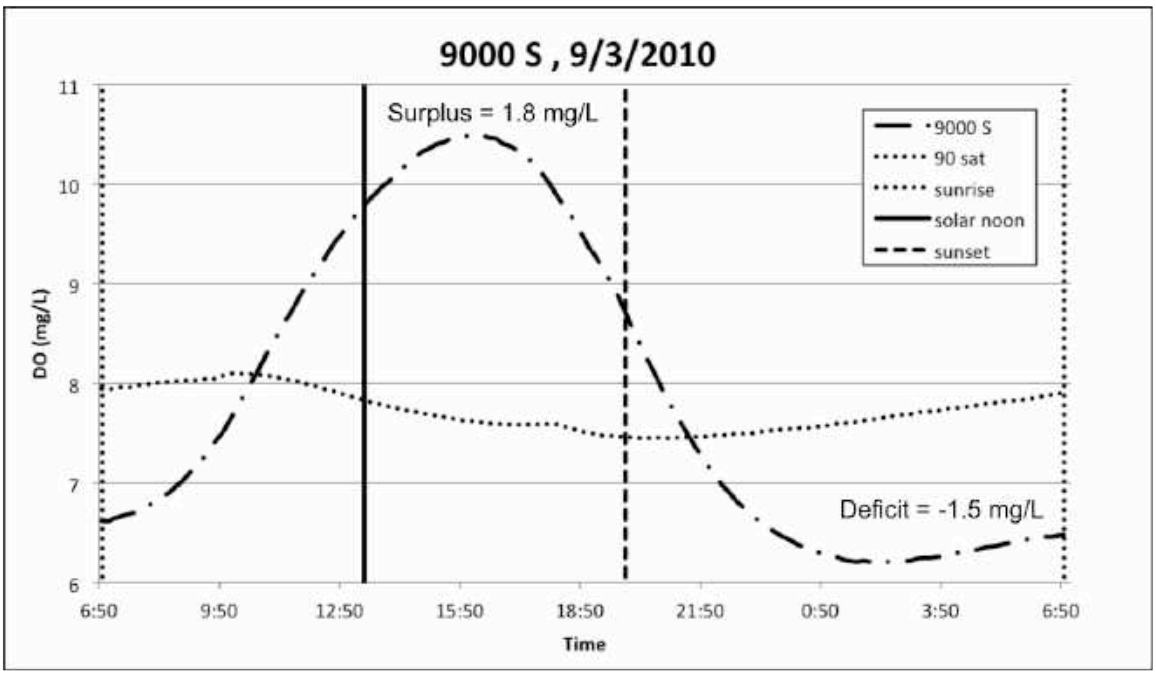

Fig. 28. Visual NDM estimate from diurnal DO curve in UJR

$$CR_{24} = K(C_{night} - C_{sat})d \quad (10)$$

$CR_{24} = community\ respiration\ \left({}^{g\ DO}/_{m^2\ day}\right)$

$K = reaeration\ coefficient\ \left({}^{1}/_{day}\right)$

$C_{night} = steady\ state\ or\ lowest\ nighttime\ DO\ concentration\ \left({}^{mg\ DO}/_{L}\right)$

$C_{sat} = saturation\ at\ time\ of\ C_{night}\ \left({}^{mg\ DO}/_{L}\right)$

$C_{night} - C_{sat} = nighttime\ DO\ deficit\ \left({}^{mg\ DO}/_{L}\right)$

$d = mean\ stream\ depth\ (m)$

To estimate stream GPP, the maximum daytime DO deficit or surplus can be normalized to depth and photoperiod using a half-sinusoid model to account for the changing rates of photosynthesis in relation to the solar flux (Chapra 2008). Finally, the

dark respiration normalized to the photoperiod is subtracted to account for daytime respiration masked by DO production. NDM is expressed as the sum of DO fluxes from GPP and CR_{24}, similar to the NDM chamber equations.

$$P_m = K(C_{max} - C_{sat})d \quad (11)$$

$P_m = maximum\ net\ flux\ of\ DO\ from\ primary\ production\ \left({}^{g\ DO}/_{m^2\ day}\right)$
$C_{max} = maximum\ daytime\ DO\ concentration\ \left({}^{mg\ DO}/_{L}\right)$
$C_{max} - C_{sat} = maximum\ daytime\ DO\ surplus\ \left({}^{mg\ DO}/_{L}\right)$

$$GPP = \left(P_m * {}^{2f}/_{\pi}\right) - (f * CR_{24}) \quad (12)$$

$GPP = gross\ daily\ stream\ DO\ production\ \left({}^{g\ DO}/_{m^2\ day}\right)$
$f = photoperiod\ , fraction\ of\ day\ recieving\ sunlight\ (d)$
$\pi = 3.14$

$$NDM = GPP + CR_{24} \quad (13)$$

$NDM = net\ daily\ metabolism\ \left({}^{g\ DO}/_{m^2\ day}\right)$

As shown in the example equations below, the CR_{24}, GPP, and NDM was -7.2, 8.5, and 1.3 $g/m^2/d$ for the 9000 S site, respectively (Fig. 28). A positive NDM indicates that OM is being produced in abundance and is a source of OM to downstream hydraulic reaches.

$$CR_{24} = (6\ day^{-1})\left(-1.5\ {}^{mg\ DO}/_{L}\right)(0.8\ m) = -7.2\ {}^{g\ DO}/_{m^2\ day}$$

$$P_m = (6\ day^{-1})\left(2.8\ {}^{mg\ DO}/_{L}\right)(0.8\ m) = 13.4\ {}^{g\ DO}/_{m^2\ day}$$

$$GPP = P_m\left(2 * {}^{13\ hr}/_{24\ hr}/_{\pi}\right) - CR_{24}\left({}^{13\ hr}/_{24\ hr}\right) = 8.5\ {}^{g\ DO}/_{m^2\ day}$$

$$NDM = (8.5 - 7.2)\ {}^{g\ DO}/_{m^2\ day} = 1.3\ {}^{g\ DO}/_{m^2\ day}$$

Fig. 29 shows a diurnal DO profile for the LJR in Reach 1 where a DO deficit is typical over the 24-hour cycle. The nighttime DO deficit was -2.3 mg-DO/L, and the daytime surplus, or deficit in this example, was -0.9 mg-DO/L. The reaeration coefficient was 1.2 d^{-1}, length of photoperiod was 13 hours, and the average depth was 1.2 meters.

The CR_{24}, GPP, and NDM were -3.3, 1.3, and -2.0 g-DO/m^2/d, respectively. Reach 1 in the LJR was heterotrophic in this example.

$$CR_{24} = (1.2\ day^{-1})\left(-2.3\ {}^{mg\ DO}/_{L}\right)(1.2\ m) = -3.3\ {}^{g\ DO}/_{m^2\ day}$$

$$P_m = (1.2\ day^{-1})\left(-0.9\ {}^{mg\ DO}/_{L}\right)(1.2\ m) = -1.3\ {}^{g\ DO}/_{m^2\ day}$$

$$GPP = P_m\left(2 * {}^{13\ hr}/_{24\ hr}/_{\pi}\right) - CR_{24}\left({}^{13\ hr}/_{24\ hr}\right) = 1.3\ {}^{g\ DO}/_{m^2\ day}$$

$$NDM = (1.3 - 3.3)\ {}^{g\ DO}/_{m^2\ day} = -2.0\ {}^{g\ DO}/_{m^2\ day}$$

The LJR had a net DO consumption, while the UJR had a net DO production in these examples. Using diurnal DO profiles, the NDM chamber experiments can be compared to alternative methods for estimating stream metabolism.

4.3.2 Adjusting single-station NDM for groundwater intrusion

Groundwater (GW) is known to enter the UJR, and if the groundwater is low in DO, then the dilution of ambient DO due to the influx of GW will overestimate CR_{24},

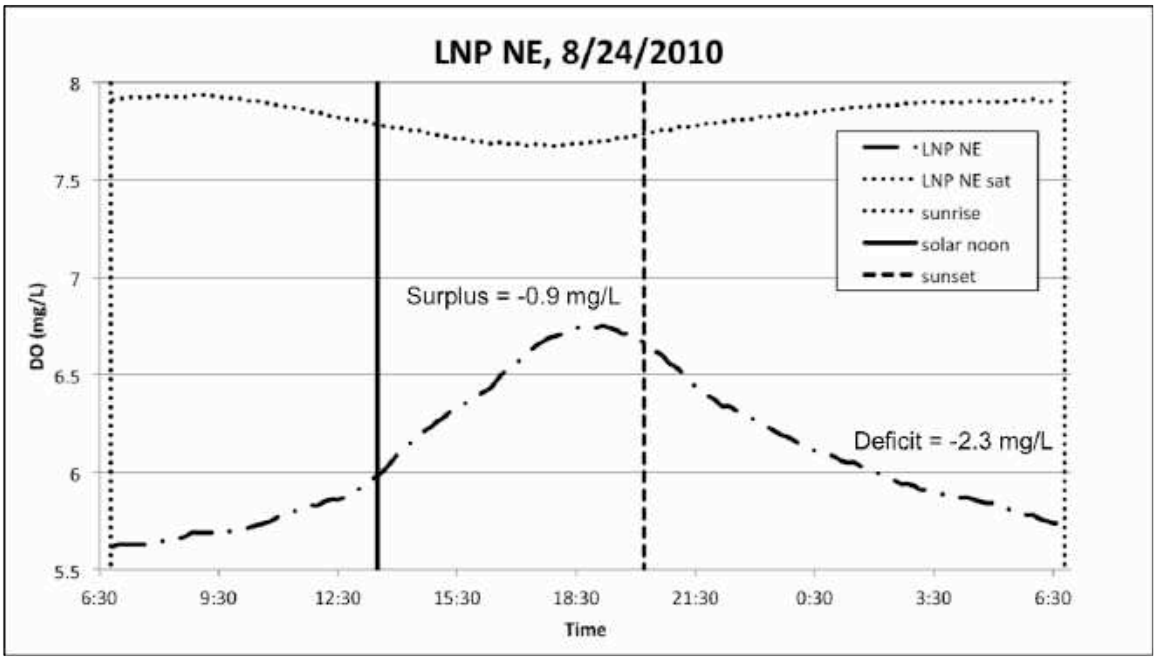

Fig. 29. Visual NDM estimate from diurnal DO curve in LJR

leading to an underestimation of NDM using the single-station diurnal DO method (Hall and Tank 2005). This hydraulic DO dilution process is shown in Fig. 30.

Estimates of groundwater intrusion in the UJR are provided in the Jordan River TMDL as a percentage of total flow (Utah DWQ 2013, Fig. 1.4). Groundwater DO concentrations were measured using minipiezometers at 30, 60, and 90 cm depths in the gravel and sand sediments of the UJR (Bridge 2005; Malcom et al. 2004). Using river flow rates, the percentage of flow from groundwater, groundwater DO concentrations, stream velocity, length of river under consideration, and average width, the DO deficit associated with anoxic GW can be expressed as a flux (CR_{GW}) using the following relationship.

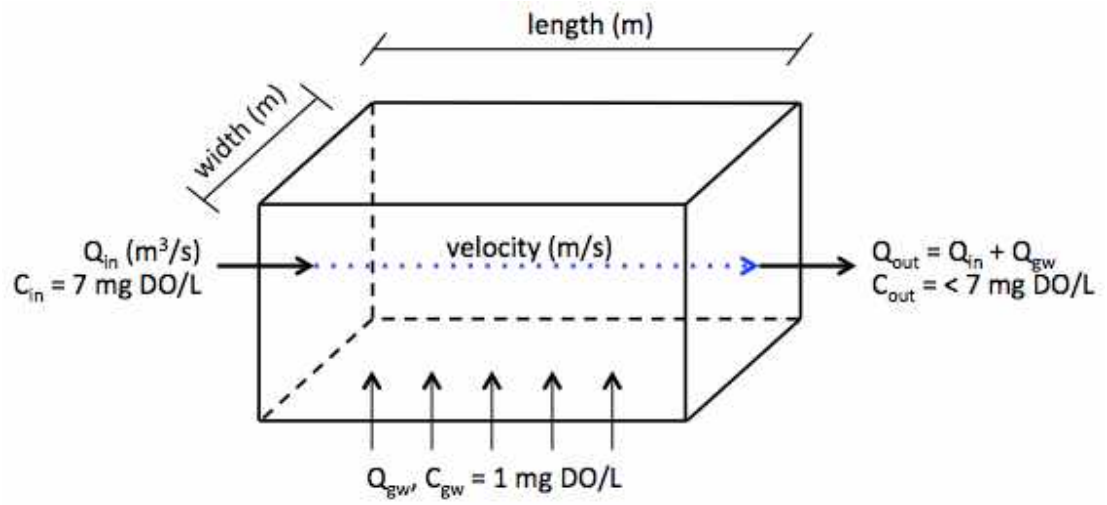

Fig. 30. Groundwater DO dilutions

$$CR_{GW} = \frac{(Q * x) * \%_{GW} * (C_{GW} - C_S)}{l * w} * \left(\frac{v * x}{l}\right) * 1\ day \quad (14)$$

$CR_{GW} = negative\ sediment\ DO\ flux\ due\ to\ GW\ \left({}^{g\ DO}/_{m^2\ day}\right)$

$Q = river\ flow\ rate\ at\ end\ of\ hydraulic\ reach\ \left({}^{m^3}/_{sec}\right)$

$x = unit\ conversion, 86{,}400 = \frac{60\ sec}{min} * \frac{60\ min}{hr} * \frac{24\ hr}{day}, \left({}^{sec}/_{day}\right)$

$\%_{GW} = ratio\ of\ GW\ flow\ in\ relation\ to\ Q\ \left({}^{\%}/_{100}\right)$

$C_{GW} = DO\ concentration\ of\ GW\ \left({}^{mg\ DO}/_{L}\right)$

$C_S = DO\ saturation\ concentration\ in\ ambient\ river\ \left({}^{mg\ DO}/_{L}\right)$

$C_{GW} - C_S = GW\ DO\ deficit\ \left(-{}^{mg\ DO}/_{L}\right)$

$l = hydraulic\ reach\ length\ (m)$
$w = mean\ hydraulic\ reach\ width\ (m)$
$v = river\ velocity\ ({}^{m}/_{sec})$

$\left(\frac{v * x}{l}\right) * 1\ day = number\ of\ times\ flow\ passes\ over\ sediments$

The parameter CR_{gw} can then be subtracted from the CR_{24} estimate obtained from the single-station method to separate the biological DO consuming activities occurring at the sediment–water interface from groundwater DO dilutions. This is important since this research focuses on using DO as a surrogate for OM dynamics, and hydraulic dilutions may horribly underestimate NDM results. The final equation for estimating NDM using a single-station method adjusted for GW dilutions is provided below.

$$NDM_{adj} = GPP + (CR_{24} - CR_{GW}) \quad (15)$$

Table 10 provides information used to estimate CR_{GW} to account for hydraulic DO dilutions associated with GW intrusion in the Upper Jordan River. During baseflow conditions, roughly 15% of the Upper Jordan River's flow is comprised of groundwater above 9000 S, and 5% of the flow is GW downstream until the confluence of Little Cottonwood Creek (LCC) (Utah DWQ 2013, Fig. 1.4).

Table 10. GW intrusion parameters used to adjust single-station model

parameters for UJR GW DO dilutions in single-station model					
	Q (m^3/sec)	length (m)	width (m)	v (m/s)	CR_{GW} (g DO/m^2/d)
above 9000 S	4	22,000	13	0.6	-2.6
9000 S-LCC	3	10,000	17	0.6	-2.4

LCC = Little Cottonwood Creek tributary
flow, length and velocity (v) data from Aug 2009 QUAL2kw (Utah DWQ)
tributaries were not included in flow
since rivers are moving, used v to calculate HRT for calculations
15% GW above 9000 S (TMDL, Fig. 1.4)
5% GW above 9000 S (TMDL, Fig. 1.4)
GW has a DO concentration of 1 mg-DO/L

4.4 Nutrient Fluxes

4.4.1 Nutrient flux sampling locations

Nutrient Fluxes were measured at the same time as SOD in the LJR during the 2010, 2012, and 2013 summer sampling seasons.

4.4.2 Nutrient flux protocols

Jordan River nutrient dynamics were measured by utilizing the contained volume of water provided by the SOD chambers to monitor changes in dissolved nitrogen and phosphorus concentrations (Callender and Hammond 1982). Three samples were taken at 90-minute intervals during the 3-hour SOD testing period. It should be noted that the environmental conditions investigated while measuring nutrient dynamics represent the dark metabolism and do not include the daytime dynamics associated with biological assimilation due to photosynthesis.

To measure sediment nutrient fluxes during anoxic conditions, the SOD chamber was injected with a slurry of sodium sulphite and trace amounts of cobalt chloride to scavenge DO in the chamber while producing sulphate according to the following chemical reaction.

$$2{SO_3}^{2-} + O_2 \rightarrow 2{SO_4}^{2-}$$

The sulphite slurry was made immediately before injection with 20 mL of ambient river water and preweighed vials of salt to drop the DO concentration by 1 mg-DO/L in the 38 L chamber. The amount of salt added to the slurry to achieve zero DO in the chamber was determined in the field using the ambient DO concentration measured at the beginning of testing. Removing 7 mg-DO/L increases the sulphate concentration in

the chamber by 44 mg-SO_4/L. Background sulphate concentrations in the Jordan River are greater than 150 mg-SO_4/L, and it was assumed that the relatively small increase in sulphate concentration would not negatively influence biological activity.

For pH manipulations, 2N hydrochloric acid was injected into the chamber. The exact amount of acid required to drop the chamber pH to 7 was determined in the field by titrating a sediment core with 26 cm of overlying water, which is the same as the height of the SOD chamber when installed. Background chloride concentrations in the Jordan River are higher than 150 mg-Cl^-/L, and it was assumed that the addition of chloride would not negatively influence biological activity.

Nutrient flux samples were taken via syringe from a closable sampling tube incorporated into the SOD chamber lid. Initially, 20 mL was extracted and discarded to account for the 10 mL of river water present in the sampling tube. An additional 50 mL was then extracted for dissolved nutrient analysis. After collecting the water sample, the sampling tube was then pinched off via hose clamp to ensure no interaction between the ambient river water and the encapsulated water within the SOD chamber. Water quality samples were immediately filtered using a 0.45-micron filter before storage on ice for lab analysis.

Water samples were analyzed for ammonia-N, nitrite-N, nitrate-N, and orthophosphate-P using ion-exchange chromatography and photometric methods. All samples were filtered, cooler stored, and analyzed within 48-hours following sample collection. Nitrite-N, nitrate-N, and phosphate-P concentrations were analyzed using ion exchange chromatography (IC) per USEPA standard method 300.0 A. Ammonia-N was analyzed using the colorimetric HACH method 10205.

4.4.3 Nutrient flux calculations

Similar to the SOD calculations, nutrient fluxes were calculated using the normalization equation for sediment area and chamber volume while subtracting the water column rates (Chiaro et al. 1980).

4.5 Sediment Organic Matter

This portion of research focused on sediment organic matter (OM) and organic carbon to evaluate whether the common measurement percent volatile solids (%VS) can be used as a surrogate for SOD. Particular focus was given to coarse and particulate organic matter in the sediments to better characterize the black muck found in the Lower Jordan River. In addition, the standing stock of organic matter in the sediments was estimated based on depth in the sediment column. Fig. 31 presents an overview of the methodology and relationships that were utilized.

4.5.1 %TS, %VS, and %TOC sampling locations

To account for the differences in OM found in depositional zones and the thalweg, samples were collected across the width of the river at each sampling location. The details of the sampled sites are provided in Table 11.

4.5.2 Sediment core collection and depth partitioning

Sediment samples were collected using a 3’ long 2” inner diameter acrylic open-barrel core, or open-drive sampler (Glew et al. 2001, Ch. 5). To access sediments in the thalweg of the river, an additional 3’ or 6’ custom-made sediment core extension was used depending on the depth of the water column. The core sampler was pushed into the sediments and a #11 stopper inserted into the top of the coring unit to allow removal of

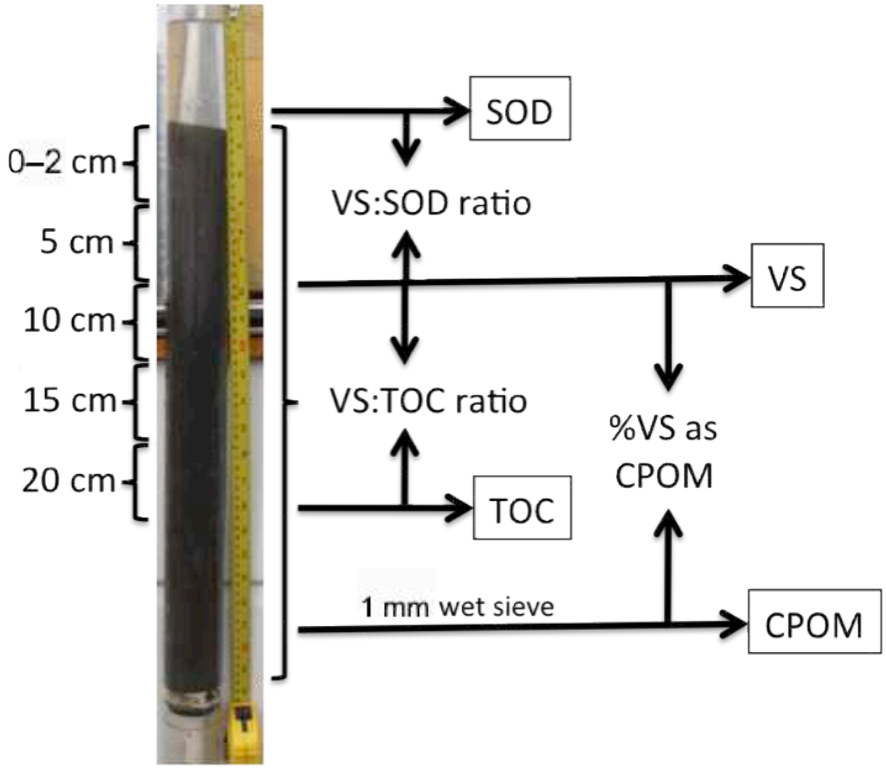

Fig. 31. Sediment core characterization relationships

Table 11. Site descriptions for 2012/2013 sampling

Reach	Site name	Description
1	Burnham Dam	end of the Lower Jordan River (before diversion to State Canal and managed wetlands)
1	LNP NE	below South Davis-S WWTP discharge
1	Cudahy Ln	above South Davis-S WWTP discharge (Reach 1–2 boundary)
2	300 N	below City Creek tributary/stormwater discharge
3	700 S	below Parleys, Emigration, and Red Butte Cr. tributaries/stormwater discharge
3	1700 S	near the beginning of the Lower Jordan River

an intact sediment core. Another stopper was inserted into the bottom of the core tube during transportation to the riverbank. Sediment core samples were extracted onsite using a 2" outer diameter plunger inserted into the bottom of the coring unit and pushed upwards (Glew 1988). This allowed sediment samples to be collected at specific depths within the sediment column.

Depth specific core samples were collected in 50 mL vials and stored on ice until analysis. Roughly 40 mL of sediment was collected at each depth while characterizing each 2 cm subsample.

$$V = \pi R^2 H = 40.5\ cm^3 \approx 40\ mL$$

$V = volume\ of\ wet\ sediment\ sample\ (mL)$
$R = inner\ radius\ of\ core\ sampler\ (2\ inches)$
$H = height\ of\ sample\ collected\ (2\ cm)$

Core samples were collected in deep water using a float tube and rope strung across the river. Fig. 32 provides a general schematic of the sediment core sampling protocol in the field.

The removable sediment core extension is critical for deep water (>1 meter deep) sampling for two reasons:

1. to remove the water column head from the core sampler since this extra weight will push out the sediment core when removed from the water
2. to minimize the distance the core needs to be extruded (i.e., 3' vs. 9'), to limit sediment disturbances, and to make the extrusion process easier and capable of being accomplished by one person.

Fig. 33 shows the sediment core extension being used in the Legacy Nature Preserve in Reach 1 where depths can exceed 1.5 meters in the thalweg. Intact sediment

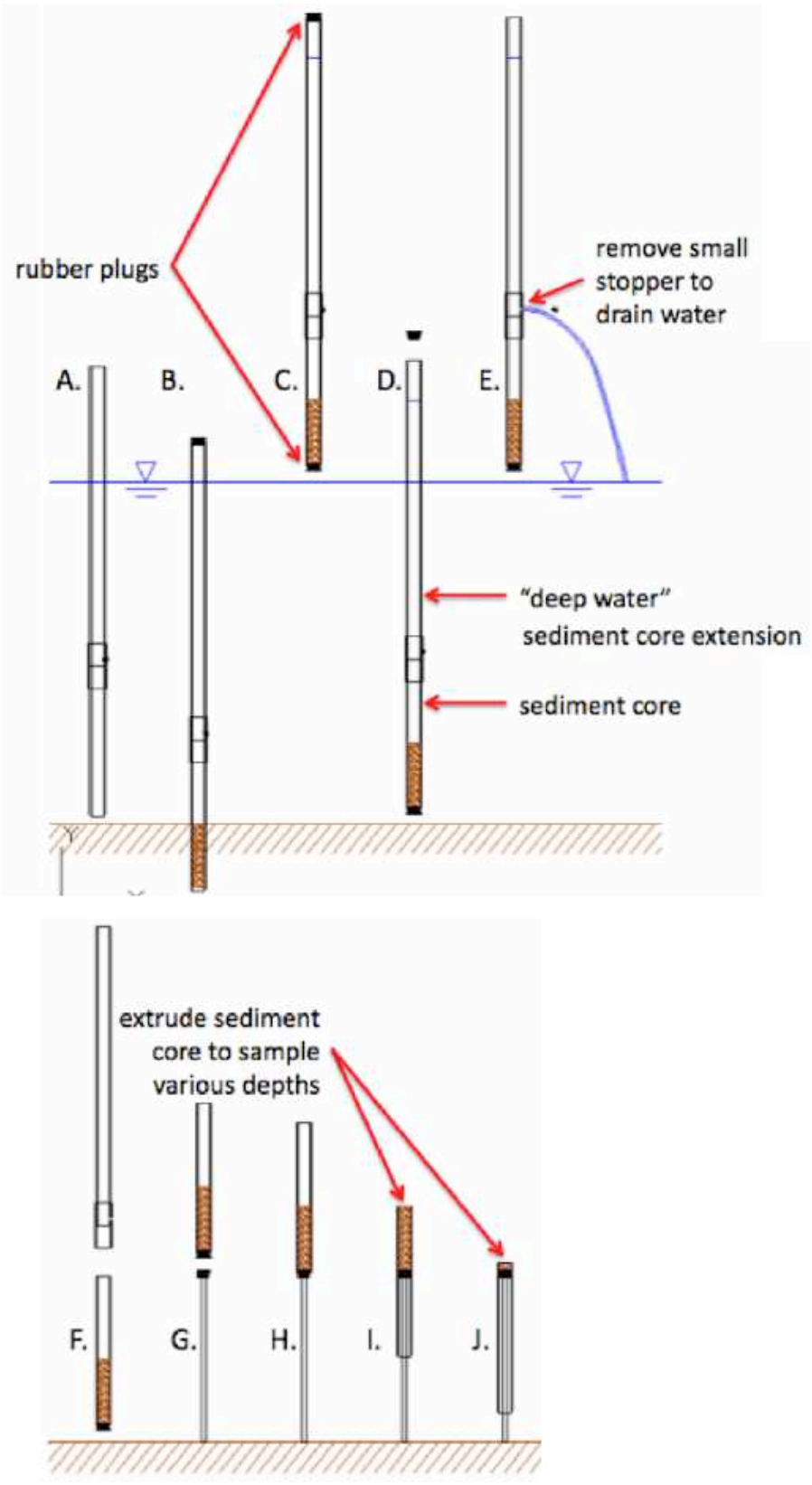

Fig. 32. Midriver multipiece sediment core sampler

Fig. 33. Midriver sediment core sampling
Note: tape measure and rope strung across river (left) and removing water from the sediment core extension (right)

cores were subsampled in the field to include the top 0–2 cm of the surficial sediments and at 5 cm increments thereafter. Sticks and plastic were removed from the samples during collection since these objects will be measured as %VS, but they do not add to the ambient DO deficit. The rationale for collecting the top 0–2 cm as opposed to 1 cm while characterizing surficial sediments was to remove sampling bias associated with benthic growth covering the sediments that will inflate sediment OM estimates.

4.5.3 %TS and %VS calculations

Percent total solids (%TS) and percent volatile solids (%VS) were measured according to USEPA Method 1684 and Standard Methods (APHA 2005). The first 187 sediment samples were analyzed in duplicate for %TS and %VS. Due to the high reproducibility, duplicates were not performed on the following samples. Calculations

used to quantify sediment %TS, %VS, and the VS of the wet sediment ($\%VS_{wet}$) are provided below.

$$\%TS_{bulk} = \frac{(A - B)\times 100}{C - B} \quad (1)$$

$$\%VS_{bulk} = \frac{(A - D)\times 100}{A - B} \quad (2)$$

$$\%VS_{wet} = \%VS_{bulk} \times \left({}^{\%TS_{bulk}}/_{100}\right) \quad (3)$$

$\%TS_{bulk} = total\ solids\ of\ bulk\ wet\ sediments\ \left({}^{kg\ dry}/_{kg\ wet}\right)$

$\%VS_{bulk} = volatile\ solids\ of\ dried\ bulk\ sediments\ \left({}^{kg\ burnable}/_{kg\ dry}\right)$

$\%VS_{wet} = volatile\ solids\ of\ bulk\ wet\ sediments\ \left({}^{kg\ burnable}/_{kg\ wet}\right)$

$A = weight\ of\ dried\ residue + dish\ (mg)$
$B = weight\ of\ dish\ (mg)$
$C = weight\ of\ wet\ sample + dish\ (mg)$
$D = weight\ of\ residue\ and\ dish\ after\ combustion\ (mg)$
(APHA 2005)

4.5.4 CPOM and FPOM measurement and calculations

Sediment course and fine particulate matter (CPM and FPM) were separated from the bulk sediments by wet sieving (1 mm sieve) using a stream of tap water as not to destroy the structure of any course particulate organic matter (CPOM). CPM samples were then subjected to %TS, %VS, and %TOC analysis to determine the OM fraction. The final parameters of $\%VS_{CPOM}$ and $\%VS_{FPOM}$ represent the percentage of the bulk %VS present as either course or fine particulate OM. Equations used to quantify the amount of course and fine organic matter are provided on the following page.

$$\%TS_{CPM} = \frac{(A_{CPM} - B)\times 100}{C_{CPM} - B} \quad (4)$$

$$\%VS_{CPM} = \frac{(A_{CPM} - D_{CPM})\times 100}{A_{CPM} - B} \quad (5)$$

$$\%VS_{CPOM,wet} = \frac{(A_{CPM} - D_{CPM})\times 100}{C_{CPM} - B} \quad (6)$$

$$\%VS_{CPOM} = \frac{VS_{CPOM,wet}\times 100}{VS_{wet}} \quad (7)$$

$$C_{CPM} = B + F - G \quad (8)$$

$$\%VS_{FPOM} = 100\% - \%VS_{CPOM} \quad (9)$$

$\%TS_{CPM} = TS\ of\ CPM\ in\ bulk\ wet\ sediments\ \left({}^{kg\ dry}/_{kg\ wet}\right)$

$\%VS_{CPM} = VS\ of\ CPM\ in\ dried\ bulk\ sediments\ \left({}^{kg\ burnable}/_{kg\ dry}\right)$

$\%VS_{CPOM,wet} = VS\ of\ CPOM\ in\ bulk\ wet\ sediments\ \left({}^{kg\ burnable}/_{kg\ wet}\right)$

$\%VS_{CPOM} = VS\ of\ CPOM\ as\ a\ percentage\ of\ VS_{bulk}\ \left({}^{kg\ CPOM}/_{kg\ VS}\right)$

$\%VS_{FPOM} = VS\ of\ FPOM\ as\ a\ percentage\ of\ VS_{bulk}\ \left({}^{kg\ FPOM}/_{kg\ VS}\right)$

$A_{CPM} = weight\ of\ dried\ wet\ sieved\ CPM\ residue + dish\ (mg)$
$B = weight\ of\ dish\ (mg)$
$C_{CPM} = weight\ of\ bulk\ wet\ sample + dish\ (mg)$
$F = weight\ of\ bulk\ wet\ sample + plastic\ dish\ (mg)$
$G = weight\ of\ plastic\ dish\ (mg)$
$D_{CPM} = weight\ of\ CPM\ residue\ and\ dish\ after\ combustion\ (mg)$

4.5.5 %TOC measurement and calculations

Sediment percent total organic carbon (%TOC) of the bulk sediments was measured using a Shimadzu TOC-V with SSM-5000A solids sampling module. Percent total carbon (%TC) was measured by combusting a 200–400 mg dry sediment sample at 900 °C, volatilizing both inorganic and organic carbon, and measuring CO_2 evolution via infrared spectroscopy. Percent inorganic carbon (%IC) was measured at 200 °C using 85% phosphoric acid to evolve CO_2. %TOC was initially measured via the following relationship:

$$\%TOC = \%TC - \%IC \quad (10)$$

Due to challenges associated with inorganic carbon being present at higher concentrations than organic carbon in the alkaline sediments, the protocol was adjusted by using a 5% hydrochloric acid (HCl) pretreatment to remove inorganic carbon (Leipe et al. 2010). After confirming methods, all samples were acid pretreated to improve reliability in %TOC analysis in the alkaline sediments using the relationship.

$$\%TOC = \%TC_{HCl\ pretreated} \quad (11)$$

4.5.6 Sediment OM standing stock calculations

Aerial OM standing stocks can be estimated using the following equation to account for pore water and sediment wet density. A dry bulk density of 1.6 kg/L, representative of fine quartz sand, was used in all calculations. The following equations were used to estimate the amount of OM present in a square meter at a 2.5 cm depth at the surface and 5 cm sectional depths for subsurface sediment OM estimates.

$$OM_{aerial} = Y\left\{\left[\rho_w * \left(1 - \frac{\%TS}{100}\right)\right] + \left[\rho_s * \left(\frac{\%TS}{100}\right)\right]\right\}\left(\frac{L}{10^3\ cm^3}\right) d \left(\frac{10^4\ cm^2}{m^2}\right)$$

$$OM_{aerial} = Y\left\{\left[\rho_w * \left(1 - \frac{\%TS}{100}\right)\right] + \left[\rho_s * \left(\frac{\%TS}{100}\right)\right]\right\} d(10) \quad (12)$$

$OM_{aerial} = standing\ stock\ of\ OM\ x\ cm\ deep\ \left({}^{g\ OM}/_{m^2}\right)$

$Y = \frac{10\ g * (\%VS_{wet})}{kg\ wet\ sediment} = \left(\frac{g\ OM}{kg\ wet\ sediment}\right)$

$\rho_w = density\ of\ water = 1\ {}^{kg}/_{L}$

$\rho_s = dry\ bulk\ density = 1.6\ {}^{kg}/_{L}\ \left(sand = 1.6\ {}^{g}/_{cm^3}\right)$

$d = depth\ of\ active\ sediment\ layer$
$surface = 2.5\ cm\ and\ subsurface = 5\ cm$

After calculating aerial sediment standing stocks of OM, these values can be applied to the Jordan River using the average length and width of each hydraulic reach.

$$OM_{aer,stretch} = (OM_{aerial} * L * w) * \left({}^{kg}/_{1000\ g}\right) \quad (13)$$

$OM_{aer,stretch} = standing\ stock\ of\ OM\ along\ each\ stretch\ (kg\ OM)$
$L = length\ of\ river\ under\ consideration\ (m)$
$w = river\ width\ (m)$

Finally, the depth specific loads can be summed to estimate the cumulative OM present at different sediment column depths.

4.6 Sediment Methane Gas Fluxes

4.6.1 Sediment gas flux sampling locations

Sediment methane and carbon dioxide fluxes were measured at the CPOM sampling locations in the LJR during the Spring of 2012. An additional methane study was conducted in State Canal during the Spring of 2013.

4.6.2 Sediment gas flux sampling protocols

The poor solubility of methane was utilized by subjecting a sediment–water slurry to headspace gas extraction protocols commonly used for dissolved gas analysis. The dissolved methane fraction was considered insignificant due to the vortexing of the serum bottle sediment samples directly before analysis, and the low water volume to gas headspace ratio (V_{liquid}:$V_{headspace}$ = 0.2 for %TS = 50%, or 150 molecules CH_4 in the gas phase for every one dissolved methane molecule in the pore water).

Serum bottle sediment methane production batch tests were conducted by adding a known mass of wet sediments into a 75 mL serum bottle to a volume slightly less than 30 mL. Jordan River water was then added to the serum bottle so that the final volume of the sediment/water mixture was 30 mL, with 45 mL of headspace to allow standardized use of the ideal gas equation. The addition of LJR water was used only to provide the correct headspace volume, and the addition of water was kept to a minimum (<10 ml). In addition to simplifying Henry's Gas Law, the large relative headspace is required since multiple gas samples will be taken from each serum bottle during the experimental period, and negative relative pressures need to be avoided. Blank, or control, serum bottles containing only DI water where the only serum bottles that maintained a negative relative pressure during analysis, as expected. The serum bottles were capped with 20

mm aluminum crimp caps and 20 mm butyl rubber-teflon faced septa.

After sealing the bottles, the sediment slurry and headspace where purged for 15-minutes with nitrogen gas while gently mixing the slurry every 5-minutes to create anaerobic conditions. 26-gauge needles were used both for nitrogen purging and headspace gas analysis to minimize the size of puncture holes in the septa during multiple day testing to limit positive pressure induced headspace losses and potential atmospheric contamination. Since positive headspace pressures are produced during anaerobic decay, atmospheric contamination did not influence results. Figures 34 and 35 show prepared sediment serum bottles for the Burnham Dam site having silty muck sediments and the 700 S site having more sandy sediments.

The sediment serum bottles were left undisturbed to incubate at 20 °C in a dark cabinet for a time period of 5 days. 5 minutes before headspace gas chromatography analysis, the serum bottles were completely mixed by vortexing at a speed between 2–4 (per the speed dial) for 2 minutes while taking great care not to contaminate the septa bottom with sediment (Scientific Industries, Vortex Genie-2).

The samples were mixed prior to gas analysis to measure the maximum rate of

Fig. 34. Burnham Dam serum bottles (silt and muck)

Fig. 35. 700 S serum bottles (sand and silt)

sediment methane production while removing the gas-sediment diffusion complexities. Following vortexing, the headspace relative pressure was measured via manometer and 26-gauge hypodermic needle (Fisher Scientific, Traceable manometer). 200 microliter gas samples were collected with a gas tight syringe (Hamilton #81156) and injected into an Agilent Technology gas chromatograph 7890A with a thermal conductivity detector (TCD) at a detector temperature of 150 °C. Gas separation was carried out using a 30 meter capillary column (Agilent GS-Carbonplot) at an isothermal oven temperature (30 °C) over a 5-minute time interval. The carrier gas was helium at 27 cm/sec with an injector temperature of 185 °C and 1:30 split. The methane peak was at 2.6 minutes and carbon dioxide occurred at 4 minutes. The calibration curves for CH_4 and CO_2 were within the range of 0.02–25% in terms of partial pressure of the gas sample. The methane and carbon dioxide percentages were then used in the following gas equations. The percent of carbon dioxide can be substituted for methane in the following equations to estimate sediment production of the more soluble CO_2.

4.6.3 Sediment gas flux calculations

The ideal gas law is required to calculate the number of moles of methane (CH_4) present in the headspace of the serum bottle.

$$PV = nRT \quad (14)$$

$P = pressure\ (Pa)$
$V = volume\ (m^3)$
$n = moles\ of\ gas$
$R = gas\ constant = 8.314\ \left({}^{J}/_{K * mol}\right)$
$J = joule\ (Pa * m^3)$
$T = temperature\ (K)$

The following equations provide the parameters and units required to utilize the ideal gas law in this serum bottle study. Absolute pressure was calculated as the sum of atmospheric and relative headspace pressures.

$$\mu mol\ CH^4 = \frac{\left\{(P_{amb} + P_{HS})\left(10^3\ {}^{Pa}/_{kPa}\right)\right\}\left\{(V_{HS})\left({}^{L}/_{10^3\ mL}\right)\left(\frac{m^3}{10^3\ L}\right)\right\}\left\{\left(10^6\ {}^{\mu mol}/_{mole}\right)\left({}^{\%CH_4}/_{10^2}\right)\right\}}{\left(8.314\ {}^{J}/_{K * mol}\right)(T_{amb})}$$

$$\mu mol\ CH^4 = \frac{(P_{amb} + P_{HS})(V_{HS})(\%CH_4)(10)}{(8.314)(T_{amb})} \quad (15)$$

$\mu mol\ CH_4 = micromoles\ methane\ in\ headspace\ of\ bottle$
$P_{amb} = ambient\ atmospheric\ pressure\ (kPa) \cong 85.6$
$P_{HS} = serum\ bottle\ headspace\ pressure\ (kPa)$
$V_{HS} = serum\ bottle\ headspace\ volume\ (mL)$
$\%CH_4 = headspace\ methane\ as\ percent\ volume\ (GC\ output)$
$T_{amb} = ambient\ room\ temperature\ (K) \cong 293$

After determining the number of micromoles of methane produced in the sediment bottle, this value was normalized to wet sediment mass and days of incubation to calculate the wet sediment methane production rate (Y).

$$Y = \frac{(\mu mol\ CH_4)\left({}^{mol}/_{10^6\ \mu mol}\right)}{(m_{wet})\left({}^{kg}/_{10^3}\right)(t)} = \frac{mol\ CH_4}{(m_{wet})(t)(10^3)} \quad (16)$$

$$Y = \frac{mol\ CH_4}{(kg\ wet\ sediment)(day)}$$

$t = time\ (days)$
$m_{wet} = wet\ mass\ of\ sediments\ (g)$

Similar to sediment OM, the gravimetric methane production rate was converted to an aerial flux by incorporating the wet bulk density and depth of the sediment layer. For comparison reasons, this molar flux was converted into a SOD equivalent assuming that all methane is oxidized at the sediment water interface ($CH_{4,OD}$).

$$CH_{4,OD} = Y\left(\frac{16\ g\ CH_4}{mol}\right)\left(\frac{64\ g\ O_2}{16\ g\ CH_4}\right)\left\{\left[\rho_w * \left(1 - \frac{\%TS}{100}\right)\right] + \left[\rho_s * \left(\frac{\%TS}{100}\right)\right]\right\}\left(\frac{L}{10^3\ cm^3}\right) d\left(\frac{10^4\ cm^2}{m^2}\right)$$

$$CH_{4,OD} = Y(64\ g\ O_2)\left\{\left[\rho_w * \left(1 - \frac{\%TS}{100}\right)\right] + \left[\rho_s * \left(\frac{\%TS}{100}\right)\right]\right\} d(10) \quad (17)$$

$CH_{4,OD} = SOD\ associated\ with\ CH_4\ \left({}^{g\ DO}/_{m^2 * day}\right)$
$\rho_w = density\ of\ water = 1\ {}^{kg}/_{L}$
$\rho_s = dry\ bulk\ density = 1.6\ {}^{kg}/_{L}\ \left(sand = 1.6\ {}^{g}/_{cm^3}\right)$
$d = depth\ of\ active\ sediment\ layer$
$surface = 2.5\ cm\ and\ subsurface = 5\ cm$

To investigate temperature effects on methanogenesis, a Q_{10} study was conducted. The Q_{10} coefficient is an unitless ratio used to describe the change in a biological metabolism following a 10 °C temperature change. Sediment Q_{10} ratios can easily be measured while investigating methane production using serum bottle techniques.

$$Q_{10} = \left(\frac{R_2}{R_1}\right)^{10/(T_2 - T_1)} \quad (18)$$

$Q_{10} = unitless\ ratio$
$R = observed\ rate$
$T =$ temperature (°C)

The samples used in the Q_{10} study were collected during the winter and immediately monitored under "cold" conditions to minimize sampling artifacts associated with temperature changes to the original samples. Sediment serum bottles were initially stored for 2 days at 4 °C in a refrigerator to measure winter methane production, followed by 2 days at 20 °C in a dark cabinet to mimic summer conditions.

CHAPTER 5

RESULTS AND DISCUSSIONS

5.1 Sediment Oxygen Demand (SOD)

5.1.1 Jordan River SOD

SOD was measured at 27 locations along the length of the Jordan River and during different seasons. During SOD measurements, many types of sediments capable of exerting elevated oxygen demands were encountered including clays, silty mucks, sands, gravels, and cobbles. Duplicate SOD chambers were installed at each location to account for sediment heterogeneity. Fig. 36 provides the relationship between the duplicate SOD chambers for all chamber deployments. The blue dots represent sampling events in the Lower Jordan River (LJR). The sediments in the LJR were surprisingly homogeneous at individual sites and had a 1.05:1 relationship (circles) between the duplicate SOD chambers in the silty muck sediments characteristic of Reaches 1 and 2. The extremely homogeneous sediments found in Utah Lake (triangles) resulted in duplicate SOD chambers giving very reproducible DO fluxes. The small squares represent chamber installations in the Upper Jordan River (UJR). These sites had much more heterogeneous sediments composed of sand and gravel, and duplicate SOD fluxes were more variable.

Table 12 summarizes average SOD fluxes measured between 2009–2013 for all sites. Also included is the number of chamber placements (N) and the standard deviation (SD) of SOD measured over four years. In Table 12, the negative values indicate that

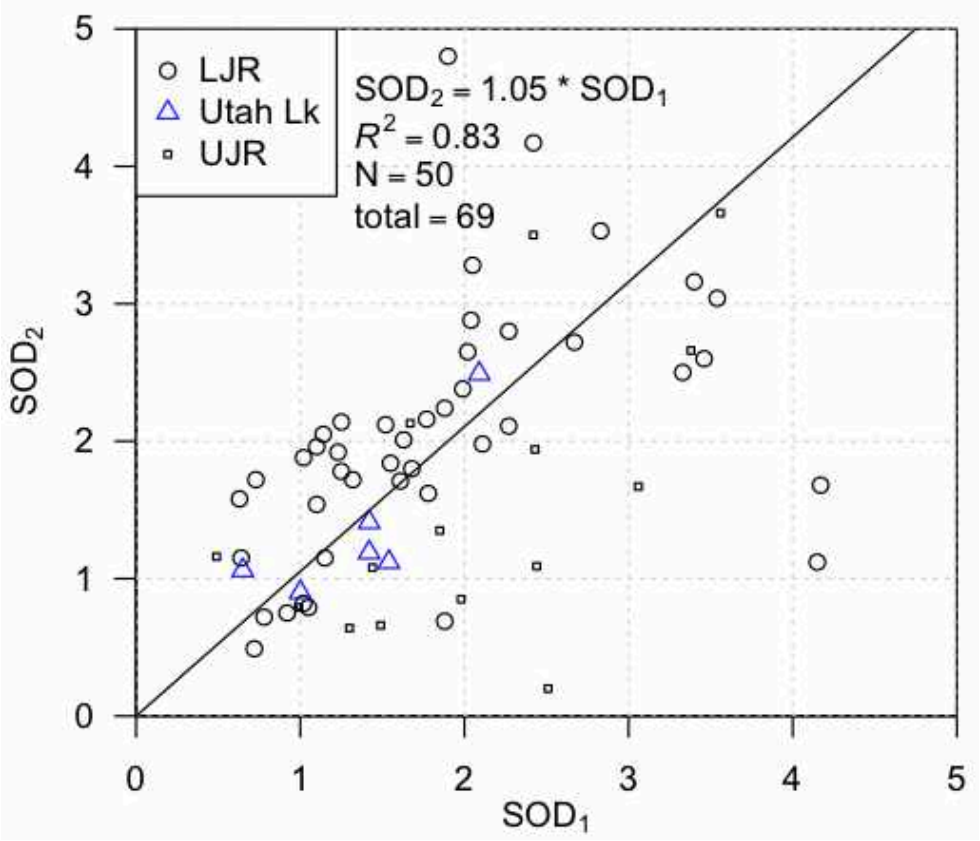

Fig. 36. Duplicate SOD chamber consistency

ambient DO was being consumed by the sediments. Appendix A provides additional SOD and WC_{dark} data. As a general rule, SOD values greater than -1 g-DO/m^2/d are associated with organically enriched sediments (Chapra 2008, pg. 452). The USEPA broadly classifies a SOD less than -1 g-DO/m^2/d as low and greater than -1 g-DO/m^2/d as high (USEPA 1985). Except for the 3600 S site, all sites in the Jordan River had an average SOD greater than -1 g-DO/m^2/d, signifying the presence of either organically enriched sediments or the presence of other biogeochemical activities consuming oxygen.

The 4-year standard deviation (SD) for in the LJR (Reaches 1–3) were equal to or less than 1.0 g-DO/m^2/d for all sites except Burnham Dam, where one chamber measured -4.8 g-DO/m^2/d. The high SD in the downstream State Canal was a result of one chamber

Table 12. Jordan River SOD

2009–2013 mean seasonal SOD (g-DO/m^2/d)					
site	mile	reach	mean SOD	SD	N
State Canal			-6.57	2.2	2
Burnham	0.5	1	-2.15	1.5	5
LNP NE	2.8	1	-2.13	0.8	21
LNP SW	3	1	-2.92	0.6	2
LNP Upper-N	3.1	1	-2.19	0.1	2
Cudahy Ln	3.2	1	-2.58	0.8	10
1700 N	5	2	-2.06	0.3	2
300 N	8.9	2	-1.82	1.0	17
700 S	10	3	-1.42	0.3	4
900 S-N	11.2	3	-1.66	0.6	5
900 S-S	11.3	3	-1.12	0.4	6
1300 S	12.5	3	-2.26		1
1700 S-N	13.1	3	-1.72	1.0	15
1700 S-S	13.15	3	-1.07	0.5	3
2100 S	13.7	3	-1.49	0.6	3
2300 S	13.7	4	-2.44	1.4	4
2600 S	14.7	4	-4.69		1
2780 S-E	15	4	-2.60	1.7	4
2780 S-W	15.1	4	-2.81	0.6	3
3600 S	16.8	4	-0.97	0.5	2
5400 S	20.9	4	-3.27	2.4	9
7600 S	23.9	5	-3.45	2.5	5
7800 S	24.1	5	-1.30	1.2	3
9000 S	26	5	-1.35	0.7	7
SR-154	34.1	6	-1.77	1.0	2
14600 S	37	7	-1.90	0.3	2
US-73	46.2	8	-1.51	0.9	4

Note: 142 SOD chamber installations in the Jordan River

measuring an extremely high SOD of -8.13 g-DO/m^2/d.

The most intriguing SOD results were obtained at sites located in the UJR where the sediments where dominated by gravel and sand substrates. The high SOD observed in Reaches 4 and 5 of the UJR are hypothesized to be a result of hyporheic upwelling or groundwater intrusion into the SOD chamber, not sediment OM decay (Hall and Tank 2005; Brunke and Gonser 1997).

Table 13 provides generalized benthic conditions based on 103 SOD measurements conducted in Illinois streams (Butts and Evans 1978). Table 13 refers to fine sediments, not coarse sands and gravels. These values provide an indication of the pollution status of the sediment in terms of organic matter enrichment based on measured SOD fluxes.

To obtain a snapshot of all SOD measurements with respect to the pollution status of the sediments, Fig. 37 provides all SOD fluxes measured in the Jordan River in relation to river mile. The three vertical lines represent the boundaries between Reaches 1–3. SOD measurements in the LJR were routinely classified as “moderately polluted” (65% of measurements) and Reach 1 was considered “polluted” in terms of organic

Table 13. Sediment condition for different SOD fluxes

SOD	Sediment condition
< -0.4	clean
-0.4 to -0.8	moderately clean
-0.8 to -1.6	slightly degraded
-1.6 to -2.4	moderately polluted
-2.4 to -4.0	polluted
-4.0 to -8.0	heavily polluted
> -8.0	sewage sludge like

adapted from Butts and Evans 1978, Table 13
20 °C fluxes

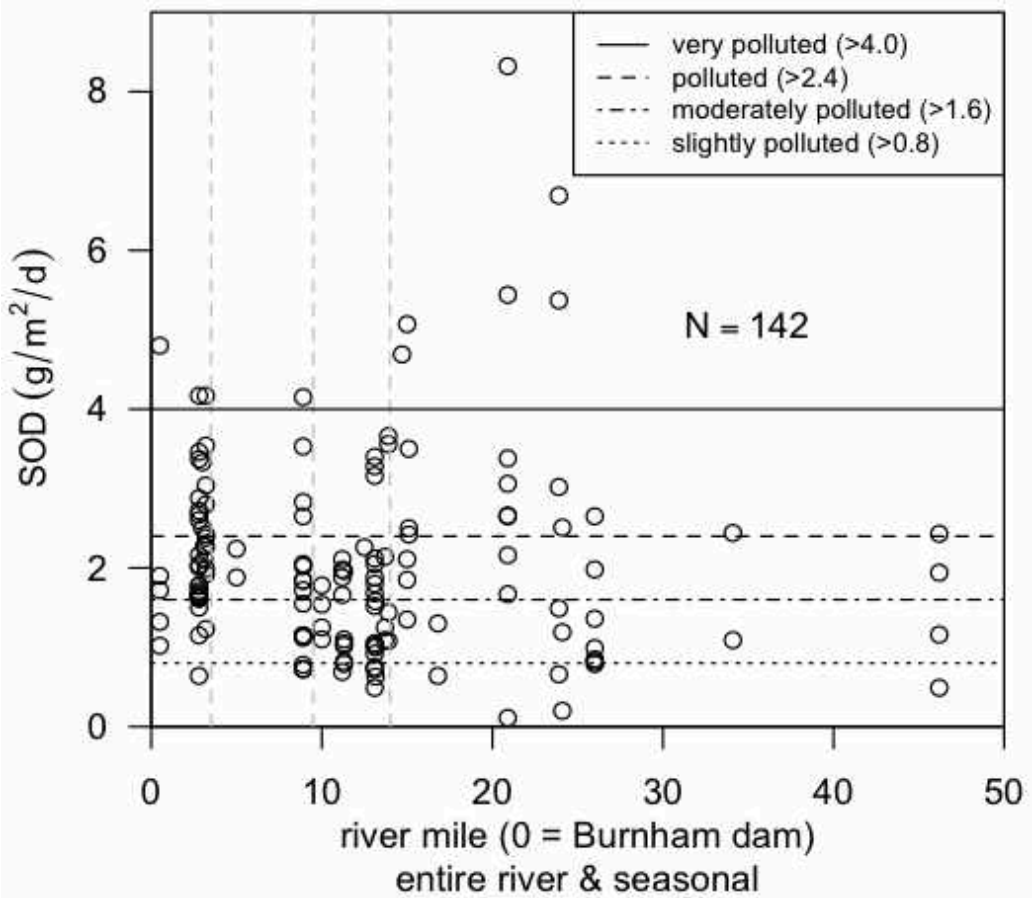

Fig. 37. All SOD data collected in the Jordan River
Note: presented from north to south along the Jordan River

matter (OM) enrichment (40% of measurements). The four SOD fluxes greater than -5 g-DO/m^2/d near mile 20 were measured in gravel sediments, and the sediment pollution status proposed by Table 13 does not apply. Hyporheic upwelling or groundwater intrusion was hypothesized to be the driving parameter in the reduction of DO in the open bottomed SOD chambers, not biological and abiotic processes occurring at the sediment–water interface.

Table 14 provides Reach based average SOD fluxes measured between 2009 and 2013. Hydraulic reach average SOD values were greater than -1.5 throughout the length of the Jordan River. Since the UJR and LJR are very different in terms of topography,

Table 14. Reach based average SOD values

Annual average SOD (g-DO/m^2/d)	
Reach 1	-2.29
Reach 2	-1.85
Reach 3	-1.53
Reach 4, backwater	-2.77
Reach 4, above BW	-2.85
Reach 5	-2.64
Reach 6	-1.77
Reach 8	-1.51

sediment type, and annual streamflow, these sections of the Jordan River will be addressed independently in the following sections.

Table 15 provides SOD fluxes measured in other degraded surface waters in the United States. Additional factors including BOD, flow velocity, reaeration potential, and river depth will dictate whether anoxia will occur in a slow moving river. From Table 15, it can be concluded that SOD fluxes measured in Reach 1 were similar to those found in aerated catfish ponds used for aquaculture, suggesting sediment organic enrichment (Berthelson et al. 1996). All hydraulic reaches in the Jordan River had average SOD fluxes higher than the Salem River, which is considered eutrophic, and had sediment oxygen demands similar to the Klamath and Lower Willamette Rivers that were characterized as having chronically low ambient DO. The extremely high SOD flux of -19.5 g-DO/m^2/d was measured prior to the Clean Water Act in river sediments capable of maintaining anoxic ambient conditions in the Lower Willamette River.

5.1.2 SOD Lower Jordan River

Fig. 38 provides a box plot for average SOD measured in the LJR. SOD increases with distance downstream in the LJR, consistent with the observed ambient DO

Table 15. Comparisons of SOD in other degraded surface waters

Surface Water	State	mean SOD_{20} ($g/m^2/d$)	N	STD DEV	Reference and notes
Saddle River	NJ	-1.3	5		1
Salem River	NJ	-1.5	6		2
Passaic River	NJ	-0.9	11	0.94	3
Arroyo Colorado River	TX	-0.6		0.38	4
7 blackwater streams	GA	-1.4	24		5
Klamath River	OR	-1.8	22		6
Lower Willamette River	OR	-2.1	45	0.57	7
Catfish ponds	MS	-2.5	86	0.93	8
Shrimp ponds		-6			9
Lower Willamette River	OR	-19.5			10
Reach 1, Jordan River	UT	-2.3	40	0.89	11

Reference and notes

1 (Heckathorn and Gibs 2010) eutrophic
2 (Heckathorn and Gibs 2010) eutrophic
3 (Urchin and Ahlert 1983) poor urban WQ
4 (Matlock et al. 2003) chronic low DO and fish kills
5 (Utley et al. 2008) chronic low DO
6 (Doyle and Lynch 2005) chronic low DO
7 (Caldwell and Doyle 1995) anoxic
8 (Berthelson et al. 1996) aquaculture
9 (Madenjian et al. 1990) aquaculture
10 (Thomas 1970) anoxic, before Clean Water Act
11 this study, chronic low DO

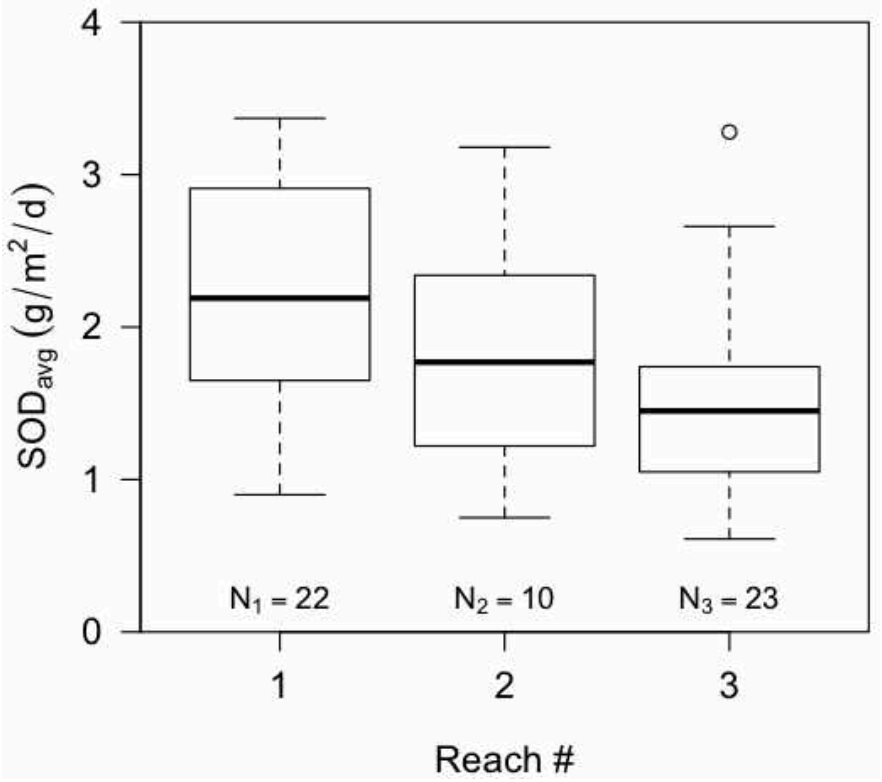

Fig. 38. LJR reach average SOD fluxes

deficit in the LJR (Utah DWQ 2013).

Hydraulic Reach 1 had sediments composed of fine silts and detritus that were easily penetrated with a sediment core sampler to depths greater than 60 cm in depositional zones and released considerable amounts of swamp gas when disturbed. Swamp gas, predominately methane and carbon dioxide, is commonly found in the sediments of stagnant and slow moving water bodies and is produced during the anaerobic decomposition of organic material. The diffusion of these reduced compounds, including methane, ammonia, and hydrogen sulfide increases SOD as these compounds are oxidized near the sediment–water interface (Di Toro et al. 1990).

Hydraulic Reach 1 is located within the historic Great Salt Lake flood plain and is a natural location for large amounts of sedimentation. Burnham Dam and the network of

canals, and weirs used to distribute freshwater to the downstream impounded wetlands creates a backwater effect in Hydraulic Reach 1. This backwater results in decreased flow velocities and increased settling of suspended matter. The accumulation of settled materials in natural systems typically occurs during the low flows associated with the summer and fall months (Whittemore 2004). Most rivers and streams in their natural state experience scouring of the benthos during the spring runnoff and during storm events (Lytle and Poff 2004; Biggs and Close 1989; Casey 1990; Naiman and Bibly 1998). These events do not regularly occur on the LJR due to the Surplus Canal diversion that routes the majority of the UJR's flow away from Salt Lake City. The managed flows resulting from the Surplus Canal diversion enhance sediment and particulate organic matter deposition due to decreased stream energy (Allan 1995). The depressed flow rates decrease reaeration potential and increase the hydraulic retention time in the LJR, resulting in additional time for the sediments to deplete DO from the water column (Parr and Mason 2003).

5.1.3 SOD Upper Jordan River

Correlations between SOD and sediment OM in gravel and sandy gravel sediments were not observed in this study, although SOD was almost always greater than -1 g-DO/m^2/d in the UJR. It has been suggested that clean sands have a SOD of -1 g-DO/m^2/d and dirty sands have a SOD of -2 g-DO/m^2/d based on visual observations (Butts 1974). SOD fluxes as high -5 and -8 g-DO/m^2/d were measured in clean gravel sediments in the UJR where there are swift flows and no DO impairment. SOD associated with gravel sediments may be attributed to the respiration of heterotrophic biofilms and autotrophs living on the surface of the gravel (Reid et al. 2006). These

biofilms attached to gravel and cobble substrate act very similar to the trickling filters used by many local municipal wastewater treatment facilities. Alternatively, the elevated SOD fluxes measured in Hydraulic Reaches 4 and 5 may be the result of localized upwelling of low DO water through the gravely substrate associated with the hyporheic activity or groundwater intrusion (Boulton et al. 1998; Wright et al. 2005).

5.1.4 Effect of land use and POTW discharges on SOD

Direct correlations between land use and SOD were not observed in the Jordan River, which has been noted in other SOD studies (Utley et al. 2008). Although SOD steadily increased in the LJR below the Surplus Canal diversion, sedimentation patterns driven by the natural topography of the LJR are most likely responsible for the consistent downstream increases in SOD. Flatter topography is associated with increased SOD due to enhanced settling of OM, but topography does not describe the sources of OM contributing to SOD.

No direct correlations between POTW discharges and SOD were noted, suggesting that nutrients and organic matter are quickly distributed downstream, making it difficult to link increases in SOD directly to point discharges (Utley et al. 2008). Increases in SOD were recorded following the South Valley Water Reclamation Facility and Central Valley Water Reclamation Facility (CVWRF) discharges, but these increases in SOD cannot be directly tied to the discharges of these facilities. Large amounts of deposition occur in the slow moving backwaters of the Surplus Canal diversion dam, and this was attributed to the elevated SOD measured downstream of the CVWRF discharge. Indirectly the POTWs are influencing SOD by discharging the macronutrients nitrogen and phosphorus. The abundance of these macronutrients may be contributing to the

eutrophication of the Jordan River, resulting in an indirect OM load via primary production in the water column and benthos (Stringfellow et al. 2009).

High SOD fluxes have been observed in rivers that receive minimal inputs of organic matter from point sources. These natural sources of potential SOD originate from particulate organics that are transported downstream from erosion and detritus entering the river system via runoff. Anthropogenic nonpoint discharges from construction, agriculture, and untreated urban stormwater runoff are undoubtedly contributing to the water quality issues in the Jordan River.

5.1.5 Water column oxygen demand (WC_{dark})

Fig. 39 provides the volumetric DO demand utilized by the water column (WC_{dark}) for each sampling event with the winter observations presented as "*" symbols. The vertical dashed lines indicated hydraulic reach boundaries in the LJR. The UJR had WC_{dark} demands higher than the LJR. This may be attributed to the biochemical oxygen demand (BOD) required to oxidize soluble and suspended OM in the water column or the respiration of phytoplankton and sloughed periphyton (metaphyton) in the swift flowing water conducive to suspended solids transport.

Oxygen demands associated with the water column were highest in the UJR and immediately downstream of the POTW discharge at the 1700 S, 2100 S, and 5400 S sites. This is most noticeable in the winter months when warm wastewater effluent increases the ambient river temperature and associated water column metabolism. The respiration rates measured in the water column decreased dramatically during the winter at sites less influenced by the warm WWTP effluent. Many of the winter sampling events resulted in the WC having zero oxygen demand.

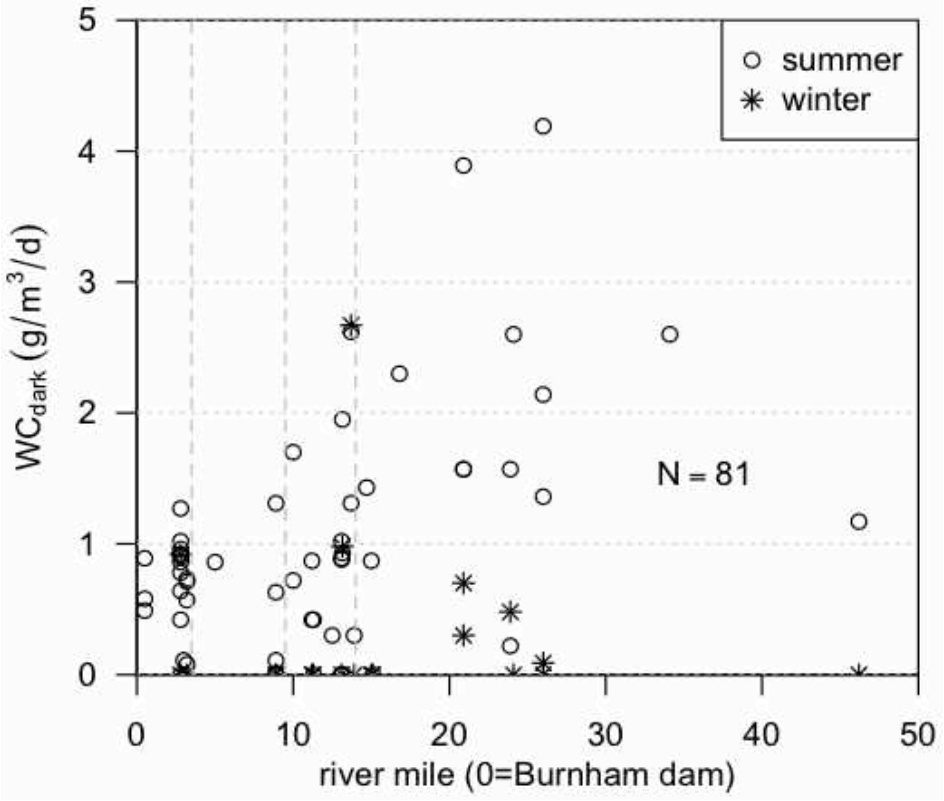

Fig. 39. WC_{dark} oxygen demand for the Jordan River

5.1.6 $\%_{SOD}$ of ambient DO deficit

SOD can account for the majority of ambient DO deficits in shallow water bodies (USEPA 1985). Ambient DO deficits in the Jordan River are heavily influenced by SOD throughout the 52-mile long river. Fig. 40 provides a graphical representation of $\%_{SOD}$ in relation to river mile in the LJR with the assumption that the flow managed LJR mean river depths are consistent throughout the year. The dotted red vertical line identifies the South Davis-South POTW discharge to the Lower Jordan River, and the various symbols identify seasons sampled with summer being the critical time period when ambient DO is the lowest.

SOD accounted for over 50% of the ambient DO deficit during 84% of the sampling events in the LJR (N = 46) and over 75% of the DO deficit during 58% of the

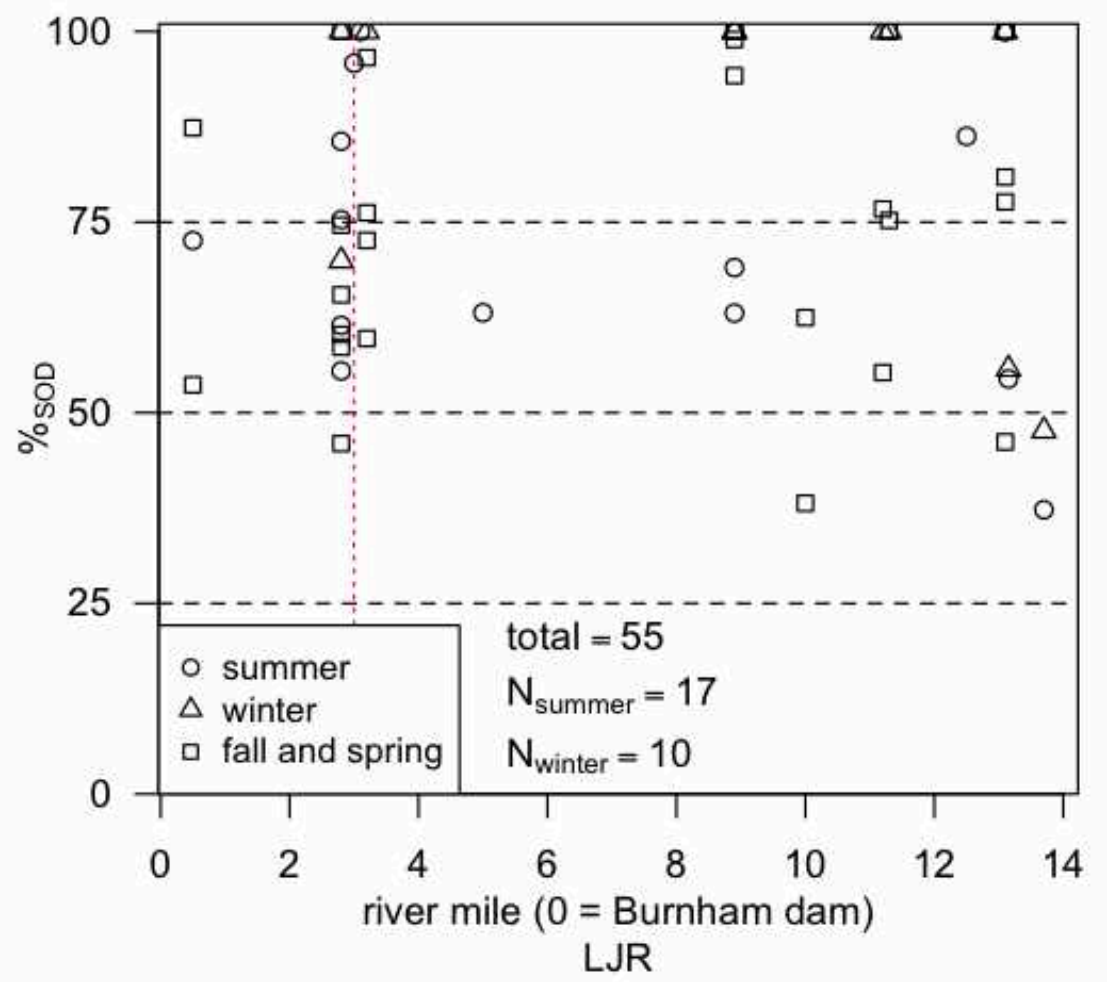

Fig. 40. Percent of ambient oxygen demand associated with sediments (LJR)

sampling events (N = 32). SOD in the DO impaired Arroyo Colorado River accounted for roughly 84% of ambient oxygen demand (N = 15) (Matlock et al. 2003). Many other rivers and shallow surface waters have shown that SOD is a driving parameter in ambient DO deficits (Rutherford et al. 1991; Todd et al. 2009). In general, the shallower the depth of the water column, the more important SOD becomes in relation to ambient DO deficits given similar sediment characteristics (Ziadat and Berdanier 2004). The LJR will most likely continue to experience chronic DO deficits until the sediments become less active in terms of SOD.

Fig. 41 provides $\%_{SOD}$ for all sampling events in the UJR under the assumption that the depths in the UJR decrease by 25% during the winter compared to summer baseflow conditions. The red vertical lines identify the Central Valley WRF and South Valley WRF discharges. The four star-shaped data points identify the sampling events where anoxic upwelling was suspected. These data points are considered "skewed" in this particular analysis since the introduction of low DO water originating from an external source should not be considered an instream biological process. This idea is revisited in Sections 5.2.1 and 5.3.2. Upstream of all online WWTP discharges, SOD accounted for less than 50% of ambient oxygen demand during summertime conditions during six of the seven sampling events

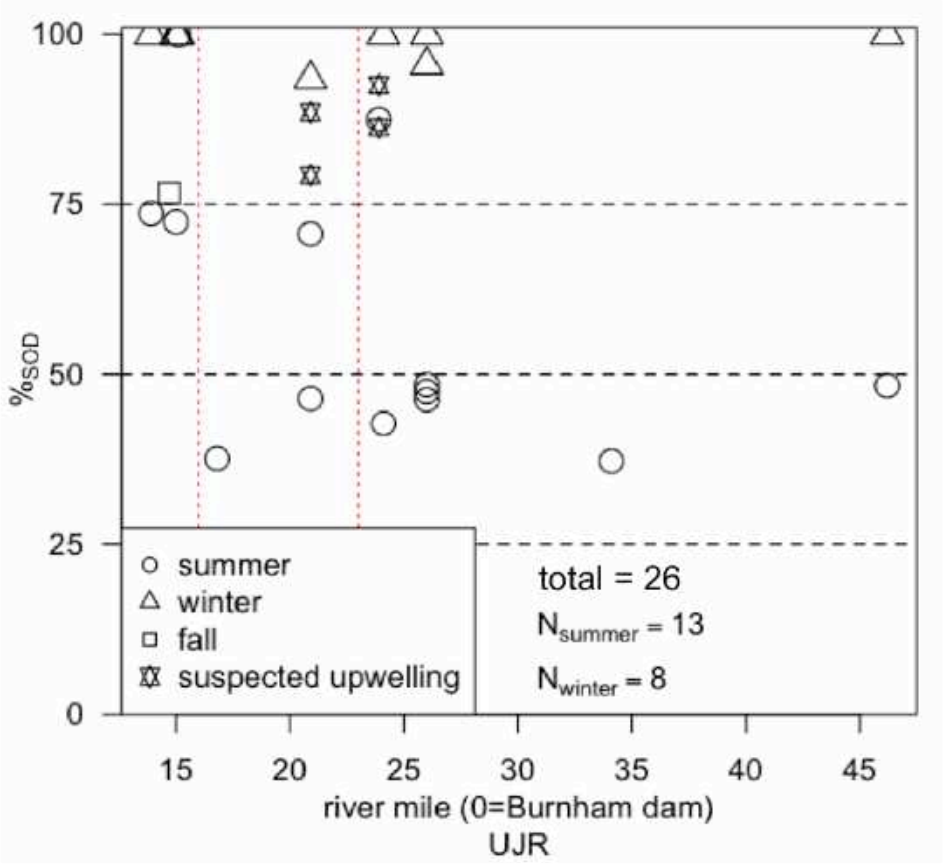

Fig. 41. Percent of ambient oxygen demand associated with sediments (UJR)

5.1.7 Temperature dependence of SOD and WC_{dark}

The dark metabolism of the water column decreased with temperature during the winter months (Fig. 39), but the sediments did not follow the anticipated Van der Hoff model reductions in metabolism due to decreased water temperature. The lack of a clear trend between SOD and ambient river temperature is highlighted in Fig. 42 where SOD did not decrease during the winter months as anticipated. The black squares represent summer measured SOD fluxes normalized to 20 °C (y-axis) using a temperature normalization coefficient (k) of 1.065. The reason the temperature normalized summer

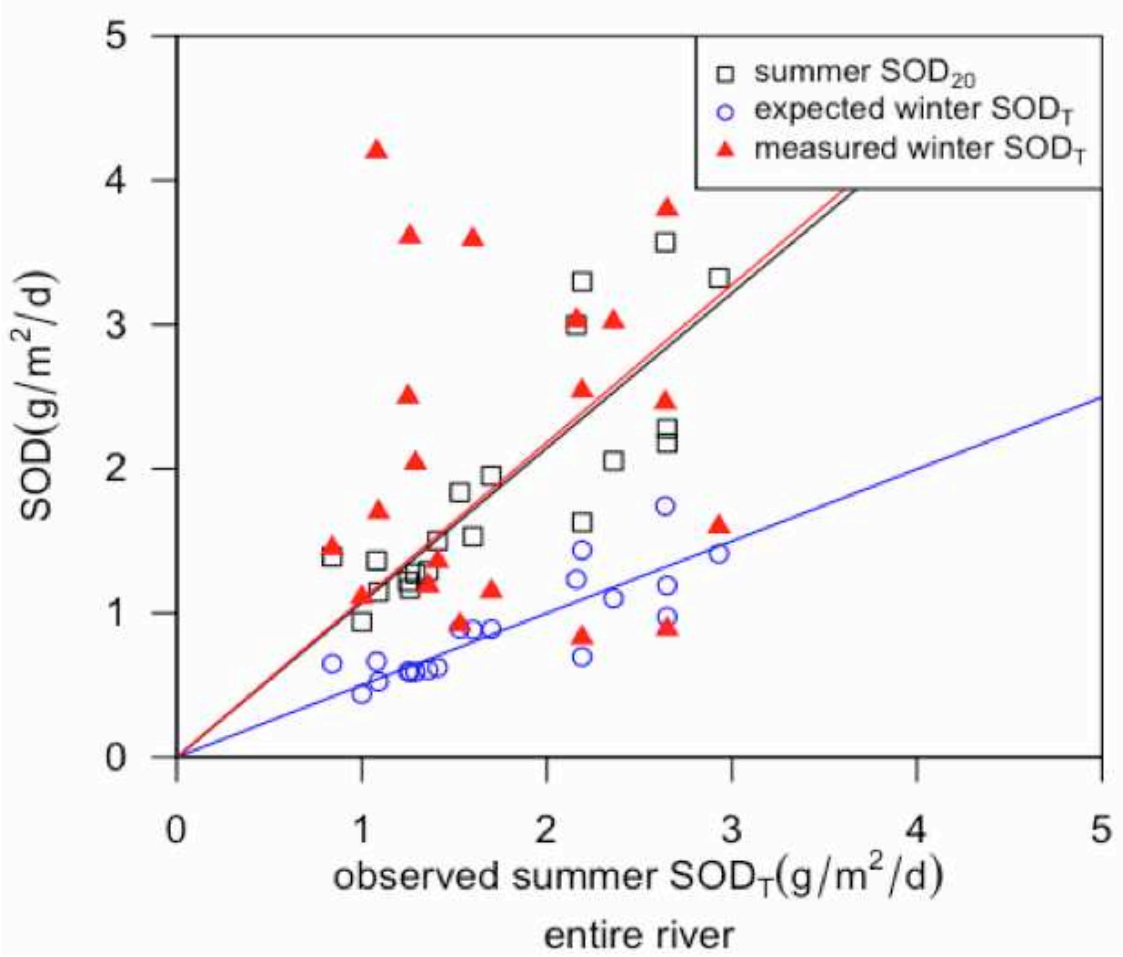

Fig. 42. SOD and temperature

observations (black squares) are at a near 1:1 ratio (SOD_{20}:SOD) is a result of ambient river temperatures being very close to 20 °C during summer sampling. The blue circles represent the expected wintertime SOD fluxes based on temperature normalization to the measured ambient winter temperatures. The red triangles identify the measured winter SOD fluxes. During the winters of 2009 and 2010, 46% and 71% of the sites had winter SOD fluxes higher than the observed summer values, respectively.

These deviations from accepted temperature normalization equations cannot be accounted for by adjusting the temperature normalization coefficient since no relationship was observed in regards to ambient water temperature, except that SOD remained elevated throughout the year.

The elevated winter SOD fluxes observed in both the Upper and Lower Jordan River are hypothesized to be a result of multiple contributing factors:

- groundwater upwelling may add low DO water to the UJR. This would be measured as SOD, but is not a biological process occurring at the sediment–water interface (see chamber NDM and single-station NDM estimates, Sections 5.2.1 and 5.3.2)
- decreased wintertime UJR flow rates coupled with decreased turbidity results in a more hospitable environment for periphyton growth due to less benthic scouring (see winter TPP, Section 5.2.3)
- the autumn deciduous leaf shedding throughout the watershed adds a seasonal OM load compromised of natural and urban OM (see CPOM, Section 5.4.3 and riparian OM load estimate 5.7.6)
- river-mud bacteria and other microbes live in a very inhospitable

environment and are most likely very tolerant to changing environmental conditions (see Seasonal NDM, Section 5.2.3)

- diffusion of reduced chemicals from the surface sediments is the rate limiting parameter for SOD during all seasons (see Q_{10} methanogens, Section 5.6.5)

5.1.8 Utah Lake SOD

The outlet of Utah Lake is the source of the Jordan River; therefore, lake water quality (WQ) directly affects WQ in the downstream Jordan River. SOD was measured at eight sites throughout the large shallow lake to characterize oxygen demands.

Ambient water quality conditions measured at each site are provided in Table 16. The elevated pH and supersaturated DO at the Provo Bay site are a result of primary production in the isolated bay receiving water from Hobble Creek, not the Provo River as the name would suggest. All sites visited during the afternoon hours had supersaturated ambient DO concentrations, even at sites located in the center of the lake. Ambient pH values were greater than 8.5 at all sites. Values greater than 9.0 were coupled with supersaturated ambient DO and were associated with water column primary production

Table 16. Ambient conditions at time of SOD sampling

site	%DO sat.	pH	temp. (°C)	depth (m)
Provo Bay	165	9.6	17.1	1
Provo Bay entrance	129	9	23.5	1
outside marina	81	8.6	22.5	3
Goshen Bay	73	9	22	1
Geneva Steel	110	8.6	18.3	2
Utah Lake Outlet	91	8.6	19.1	2.2
Pelican Point	114	8.9	23	3
Goshen Bay entrance	88	8.6	22.9	3

(phytoplankton). The highest pH values were observed in the shallow sites where water column depths were roughly 1 meter.

Table 17 shows the two-chamber average SOD, WC_{dark}, and chamber calculated nighttime ambient DO depletion rates. The SOD flux describes the amount of DO consumed at the two-dimensional sediment–water interface, and the WC_{dark} is presented as a volumetric rate to be comparable with BOD measurements. The ambient column is presented as a volumetric rate. The "ambient" values were calculated by normalizing SOD to a volumetric rate using lake water depth and summing the SOD and WC rates. Ambient volumetric rates represent the DO dynamics from the perspective of the water column, which is useful because most WQ scientists think in terms of volumetric rates and concentrations. When the WC is deeper than 1 meter, as is the case in most lakes, the sediments become less influential to ambient DO dynamics in unstratified lakes. It should be noted that lake stratification may result in an anoxic hypolimnion over the course of months, not days, but Utah Lake does not experience seasonal stratification.

The highly productive Provo Bay had the highest SOD flux measured in Utah Lake and the visually green water in the isolated hypereutrophic bay had the highest

Table 17. Observed SOD, WC, and estimated ambient DO depletion rates

site	SOD_{avg} g-DO/m^2/d	WC g-DO/m^3/d	ambient g-DO/m^3/d	$\%_{SOD}$
Provo Bay	-4.61	-6.66	-11.3	41
Provo Bay entrance	-1.42	-3.45	-4.9	29
outside marina	-1.49	-2.28	-2.8	18
Goshen Bay	-1.67	-3.4	-5.1	33
Geneva Steel	-2.04	-1.9	-2.9	35
Utah Lake Outlet	-1.03	-1.28	-1.7	27
Pelican Point	-1.06	-4.17	-4.5	8
Goshen Bay entrance	-0.9	-1.11	-1.4	21

WC_{dark} rate measured during this research. WC_{dark} rates measured in Utah Lake were two to 10 times higher than typically measured in the LJR. The senescence, settling, and decay of the phytoplankton respiring to create this extremely high WC_{dark} oxygen demand are the source of the high SOD of -4.6 g-DO/m^2/d measured in Provo Bay.

The sites located near the shores of Utah Lake (Provo Bay entrance, outside marina, Goshen Bay, and Geneva Steel) all had SOD fluxes ranging from -1.4 to -2 g-DO/m^2/d. The deep water sites located offshore (Utah Lake Outlet, Pelican Point, and Goshen Bay entrance) had decreased SOD fluxes ranging from -0.9 to -1.06 g-DO/m^2/d. The decreased SOD in the middle of Utah Lake compared to locations near townships suggests that sediment organic matter enrichment due to eutrophication is ongoing and more pronounced near civilization.

The $\%_{SOD}$ was less than 50% at all sites due to the increased WC depths associated with a lake compared to a river. In addition, the water column in Utah Lake was visually green from phytoplankton during sampling, which was not observed in the Jordan River. The decay of OM derived from phytoplankton is the source of SOD in Utah Lake and is most likely an OM load to the downstream Jordan River in the form of suspended seston and viable phytoplankton cells.

5.1.9 SOD:%VS relationship

Sediment volatile solids (%VS) was measured during 37 chamber installations in the Jordan River to investigate a surface sediment SOD:%VS relationship as an alternative method to estimate SOD using standard laboratory protocols. Correlations between SOD and %VS were observed in the fine silts and sands found in the LJR, Surplus Canal backwater, and in the downstream State Canal (Fig. 43). The backwaters

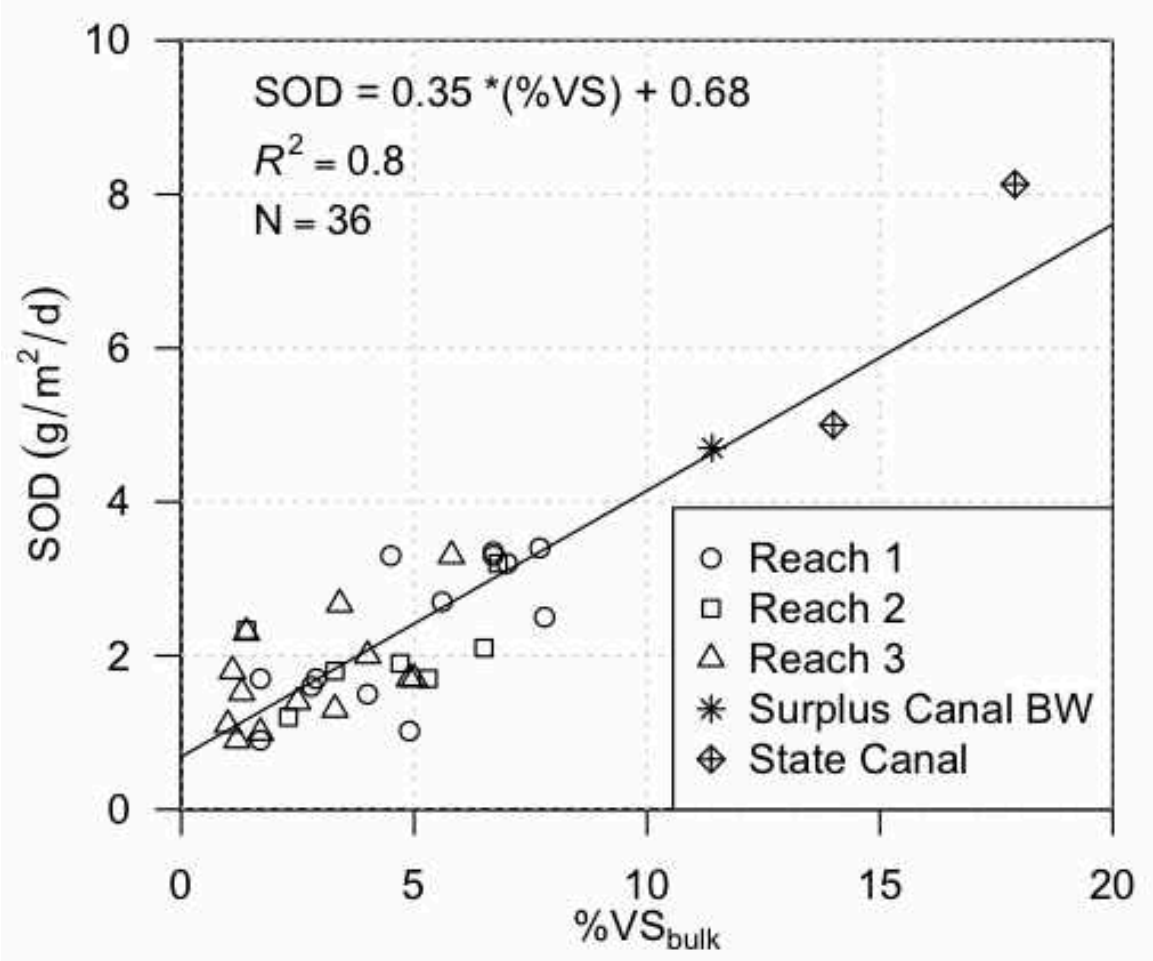

Fig. 43. SOD and %VS relationship in the Lower Jordan River
Note: 0–2 cm sediment depth

of the Surplus Canal diversion dam and State Canal are depositional zones and represent areas of enhanced deposition in the Jordan River. The top 0–2 cm of the surficial sediments were used in this regression since these are the sediments composed of the most recent deposition and contain the benthic community directly interacting with the ambient water. The standard error of the proposed SOD:VS relationship was +/-0.6 g-DO/m^2/d. The relationship between SOD and %VS of the top 0–2 cm of the surficial sediments was

$$SOD = 0.35(\%VS) + 0.68 \quad (19)$$

Other studies have developed general relationships between SOD and various surrogates for OM. These previous empirical equations had a square-root relationship between SOD and sediment OM parameters (Di Toro et al. 1990). The equation proposed in this research was not forced through zero through the use of a more complex regression with the goal to simplify the relationship and due to the fact that a SOD of zero has yet to be measured in the Jordan River.

Butts (1974) encountered silty sediments having %TS and %VS ranging from 30–80% and 1–25%, respectively and he produced the following relationship:

$$SOD = 6.5(\%TS^{-0.46})(\%VS^{0.38}) \quad (20)$$

Fig. 44 compares the Butts (1974) SOD model with LJR data. The pink linear equation represents Butts equation with %TS back calculated using the LJR 0–2 cm %VS:%TS relationship (see Section 5.4.2).

The Butts 1974 equation underestimated SOD in the LJR at fluxes greater than -2.5 g-DO/m^2/d. A SOD greater than -2.5 suggests polluted sediments and provides a strong indication that the sediments are negatively influencing WQ (Butts and Evans 1978).

In summary, the SOD:VS relationship for the Jordan River can be utilized to easily estimate SOD in silty sediments using standard methods for modeling purposes. This relationship could also be used to set goals for the reduction of SOD in the LJR in terms of surface sediment OM enrichment.

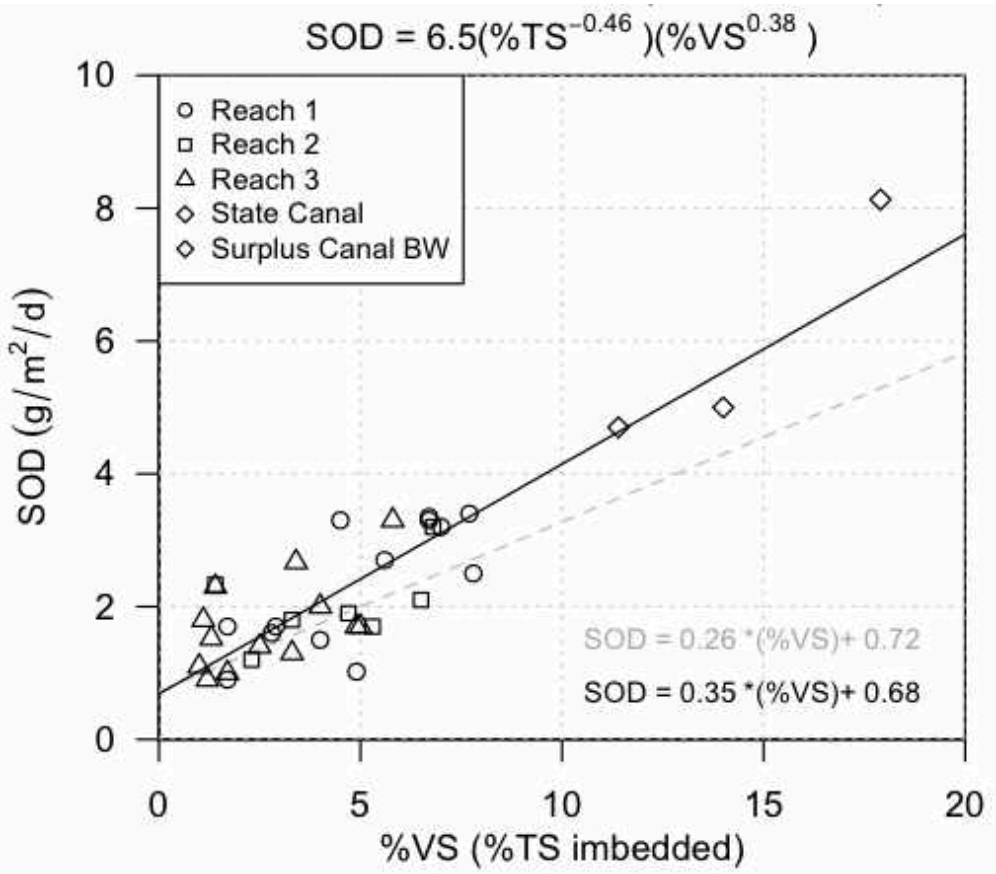

Fig. 44. SOD predictions using Butts (1974) equation

5.2 Chamber Net Daily Metabolism (NDM)

5.2.1 NDM and SOD chamber comparison

SOD measures the sediment oxygen demand utilizing open bottom aluminum chambers and tray oxygen demand (TOD) is the oxygen consumption associated with a sediment tray in a completely enclosed NDM chamber. SOD chambers measure oxygen consumption in the top 1.5" of the sediment column and include the oxidation of reduced gases diffusing from buried sediments and oxygen deficiencies associated with hyporheic exchanges and groundwater upwelling. TOD does not account for hyporheic exchanges, groundwater upwelling, or the diffusion of sediment gases deeper than 1.5".

Fig. 45 provides the relationship between TOD and SOD during 19 sampling

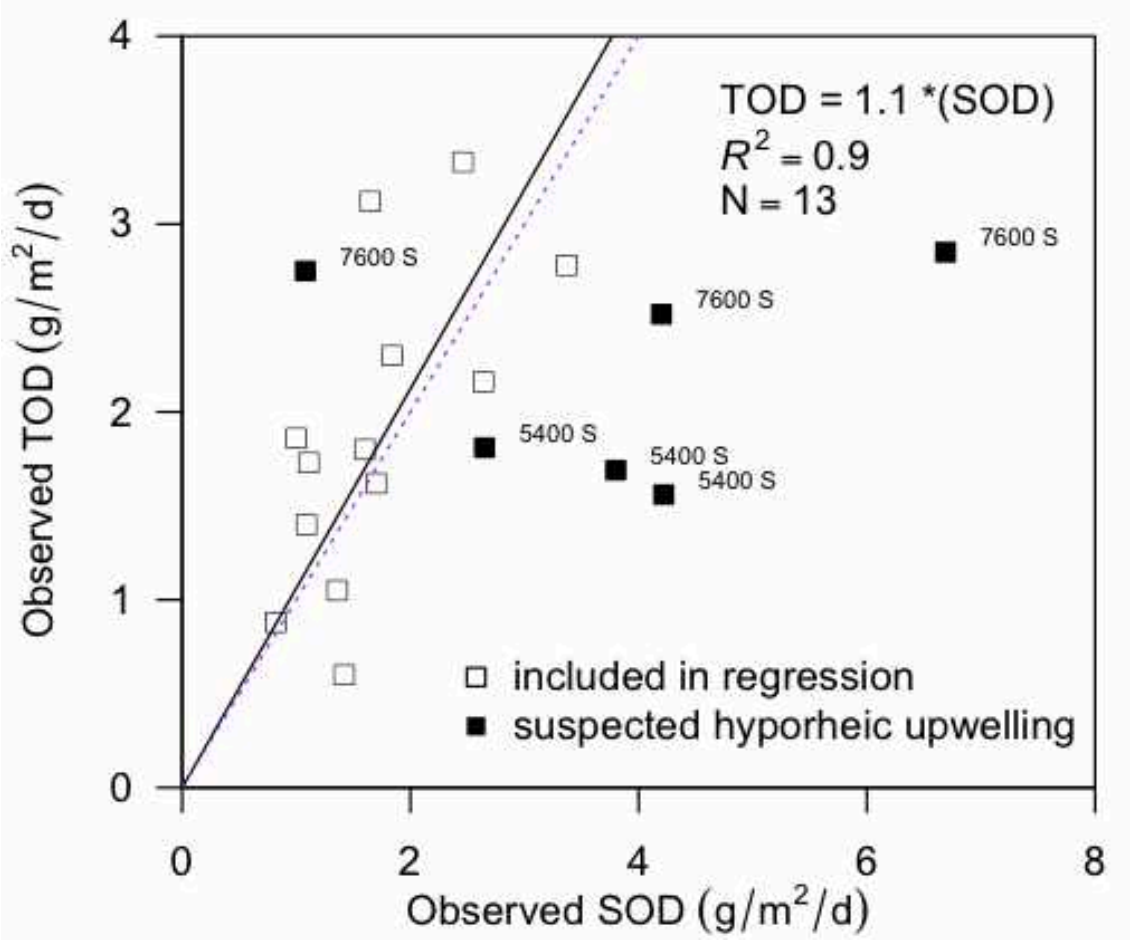

Fig. 45. TOD:SOD relationship

events where both styles of chambers were simultaneously deployed. Both chamber types produced very similar sediment oxygen demands in the silty muck sediments characteristic of the LJR and had a TOD:SOD relationship of 1.1:1 (hollow squares). Surprisingly, the SOD chambers measured much higher oxygen demands in the gravel sediments in the UJR (solid black squares). This was not expected, as any potential sampling error was originally anticipated to be associated with the SOD chambers measuring decreased oxygen demands due to the possibility of a poor seal in the gravel substrate. The sites suspected of low DO upwelling were not included in the regression presented in Fig. 45 (six sampling events).

Evidence of potential hyporheic upwelling or groundwater intrusion is shown as the black square data points in Fig. 45. The extremely high SOD flux greater than -6 $g/m^2/d$ measured during the July sampling event at the 7600 S site suggested upwelling of DO depleted water in the clean gravel sediments. Following this observation, the SOD chambers were placed near zones of suspected upwelling at the 5400 S and 7600 S sites.

The 1700 S site had TOD fluxes greater than the closed bottom SOD chambers. This trend was also observed at the 2100 S site during the August sampling event. This may be a result of heterogeneities in the benthic community and sediment substrate. It is also possible that ambient river water was able to enter the chamber via localized hyporheic flow under the lip of the SOD chamber in the sand and gravel sediments. Sediments were composed of clean gravels and sands at 2100 S, turning into sands at the 1700 S-S site.

5.2.2 NDM chamber dark and light metabolism

Table 18 provides average TOD, gross sediment tray primary production (TPP), WC_{dark}, gross water column primary production (WC_{light}), ambient water temperature, and length of the photoperiod for all NDM chamber sampling events. The sites were visited three times during midsummer, late summer, and winter to investigate seasonal effects on stream metabolism. Negative values indicate that DO is consumed and positive values indicate oxygen production. The sediment parameters are presented as fluxes and the water column is provided as volumetric rates.

The lowest TPP fluxes were measured at 300 N. The 300 N site was located along a straight channelized section of the LJR that is relatively deep (0.75 meters at the bank), experiencing bank undercutting, and is abutted by a veneer of riparian vegetation. The

Table 18. TOD, TPP, WC_{dark}, and WC_{light} measurements

		(g DO/m^2/d)		(g DO/m^3/d)		(°C)	(hrs)
Site	Date	TOD	TPP	WC_{dark}	WC_{light}	temp.	photoperiod
LNP NE	7/16/10	-2.8	4.7	-0.8	1.2	22.3	14.8
LNP NE	8/24/10	-1.8	2.7	-0.9	1.9	20.5	13.4
LNP NE	12/25/11	-3.3	1.2	-0.8	0.1	8.7	9.3
300 N	7/15/10	-2.3	1.8	-0.6	0.5	20.5	14.8
300 N	8/13/10	-2.2	0.2	-1.1	0.6	18.4	13.9
300 N	1/6/11	-1.8	0.7	0.0	0.0	6.6	9.4
1700 S	7/14/10	-1.9	1.0	-0.8	2.2	21.0	14.8
1700 S	8/26/10	-1.2	1.5	-1.6	1.7	20.4	13.3
1700 S	1/3/11	-1.7	1.5	-0.8	0.2	7.9	9.3
2100 S	7/13/10	-2.8	2.5	-1.1	2.7	21.3	14.9
2100 S	8/25/10	-1.4	3.2	-2.2	2.6	19.2	13.4
2100 S	1/7/11	-1.6	2.2	-2.3	0.5	7.7	9.4
5400 S	7/19/11	-1.8	3.5	-1.3	1.8	22.5	14.7
5400 S	9/2/10	-1.6	2.8	-1.3	2.6	18.6	13.0
5400 S	1/12/11	-1.7	4.1	-0.6	1.2	9.7	9.5
7600 S	7/20/10	-2.8	7.4	-1.3	1.1	21.0	14.7
7600 S	9/1/11	-2.8	5.8	-0.2	1.5	16.5	13.1
7600 S	1/15/11	-2.5	5.6	-0.4	1.1	8.5	9.6
9000 S	7/21/10	-0.9	2.0	-1.1	1.0	21.0	15.7
9000 S	9/3/10	-0.1	1.4	-1.8	5.8	18.6	13.0
9000 S	1/20/11	-1.0	3.2	-0.1	1.0	6.0	9.7

low benthic primary production measured at this site was attributed to the increased WC depth, presence of riparian vegetation intercepting the ambient solar flux, and a northwesterly flow direction increasing the amount of shading provided by the riparian vegetation.

The highest TPP rates were observed at the 7600 S site, which had cobble substrate conducive to periphyton colonization and was located upstream of all online WWTPs discharging to the Jordan River. Elevated TPP rates in the UJR (5400 S, 7600 S, and 9000 S) are a result of the relatively swift and shallow hydraulics and larger sediment

substrate capable of providing an anchor point for benthic organisms (Minshall et al. 1992). The benthic zone was visually covered with biofilms throughout the length of the Jordan River.

Algal biofilms in the benthos typically dominate primary production in most streams (Pusch et al. 1998). Net primary production of periphyton in other rivers ranged from <0.03–10 g-DO/m^2/day with most rivers sections producing less than 1.3 g-DO/m^2/day (Webster et al. 1995). The Jordan River benthic zone was more active in terms of primary production than the average river, and the UJR had benthic photosynthesis fluxes comparable to other eutrophic rivers (Webster et al. 1995).

Benthic gross primary production was higher than expected in Reach 1 at the LNP NE site and TPP fluxes were similar to those found in the UJR, and this will be discussed in more detail in the following sections.

Both WC_{dark} and WC_{light} were the highest following WWTP discharges at the 5400 S, 2100 S, and LNP NE sites, indicating that WWTP nutrient loads stimulate water column eutrophication in the Jordan River.

There were no trends in TPP decreasing with ambient water temperature in the UJR during the winter months, as was noted in the seasonal SOD study (Section 5.1.7). Turbidity of the ambient river water decreased dramatically during winter low flows.

This coupled with less bedload migrating downstream during the winter months most likely resulted in less scouring, creating an environment conducive to the elevated winter TPP fluxes observed in the UJR. Fig. 46 provides two pictures taken 4 days apart (Jan. 11 and 15, 2011) at the 9000 S site. These pictures provide a visual perspective regarding how fast the benthic community was growing during the winter months. The

Fig. 46. Periphyton regrowth during winter conditions at 9000 S (before and after)

surface benthic layer was scraped with a shovel to expose the clean gravel beneath (left), and the benthic community was recolonized within 4 days (right), highlighting the amount of biological activity occurring at the sediment–water interface in the Jordan River.

It should be noted that the turbidity of the Jordan River increased dramatically following a mild snowmelt while sampling at the 9000 S site. This observed increase in turbidity still resulted in winter TPP fluxes greater than measured in summer. Although many of the TPP fluxes measured during winter conditions were similar to the summer values, the maximum rate of photosynthesis was higher in the winter months before being (Table 18).

Fig. 47 provides a stacked bar chart for benthic and water column respiration and production during the July, September, and winter sampling events. The WC rates were normalized to the mean river depth for direct comparison with sediment fluxes. The water column is presented as the light grey and dark grey bars, and the sediments are colored white and black. The sum of WC_{light} and TPP is the chamber calculated gross primary production (GPP) flux in terms of DO. The sum of WC_{dark} and TOD is the chamber

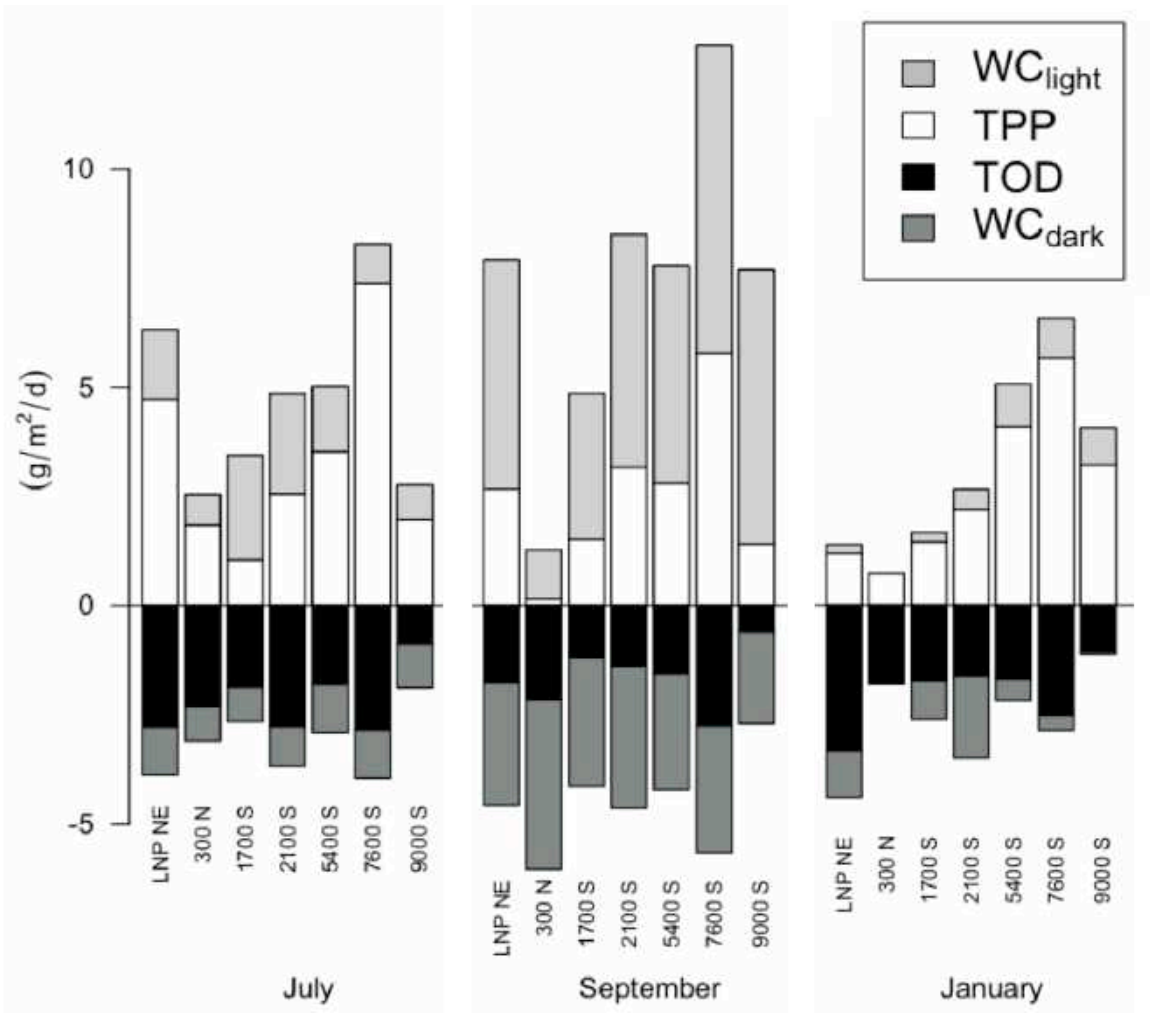

Fig. 47. GPP and CR_{24} during summer and winter
Note: GPP = TPP + WC_{light} and CR_{24} = TOD + WC_{dark}

calculated 24-hour community respiration (CR_{24}).

Phytoplankton and broken apart metaphyton present in the water column were responsible for the majority of the production and respiration during the critical time period during late summer (grey bars, September). This suggests that upstream eutrophication is a significant source of seasonal OM to the LJR. In addition, WC_{light} was elevated at the 9000 S and 7600 S sites located upstream of all WWTP discharges during late summer suggesting that Utah Lake may be a source of phytoplankton to the UJR (see

Utah Lake WC_{dark}, Section 5.1.8). Alternatively, the phytoplankton is sloughed periphyton, or metaphyton, growing upstream of 9000 S in the Upper Jordan River.

The benthic community was responsible for the vast majority of the primary production measured in the Jordan River during early summer and winter. Periphyton can be the largest and most active standing stock of algal biomass in a lotic system, requiring sediment–sampling protocols to properly quantify (Dodds 2006; Minshall et al. 1992).

The seasonal NDM chamber derived degree of autotrophy is provided in Fig. 48, where the UJR was autotrophic year round. The significance is that a ratio greater than 1 implies OM is being produced faster than it is being degraded, creating a source of OM to downstream reaches. The 1700 S and 2100 S sites in Reach 3 were autotrophic during the

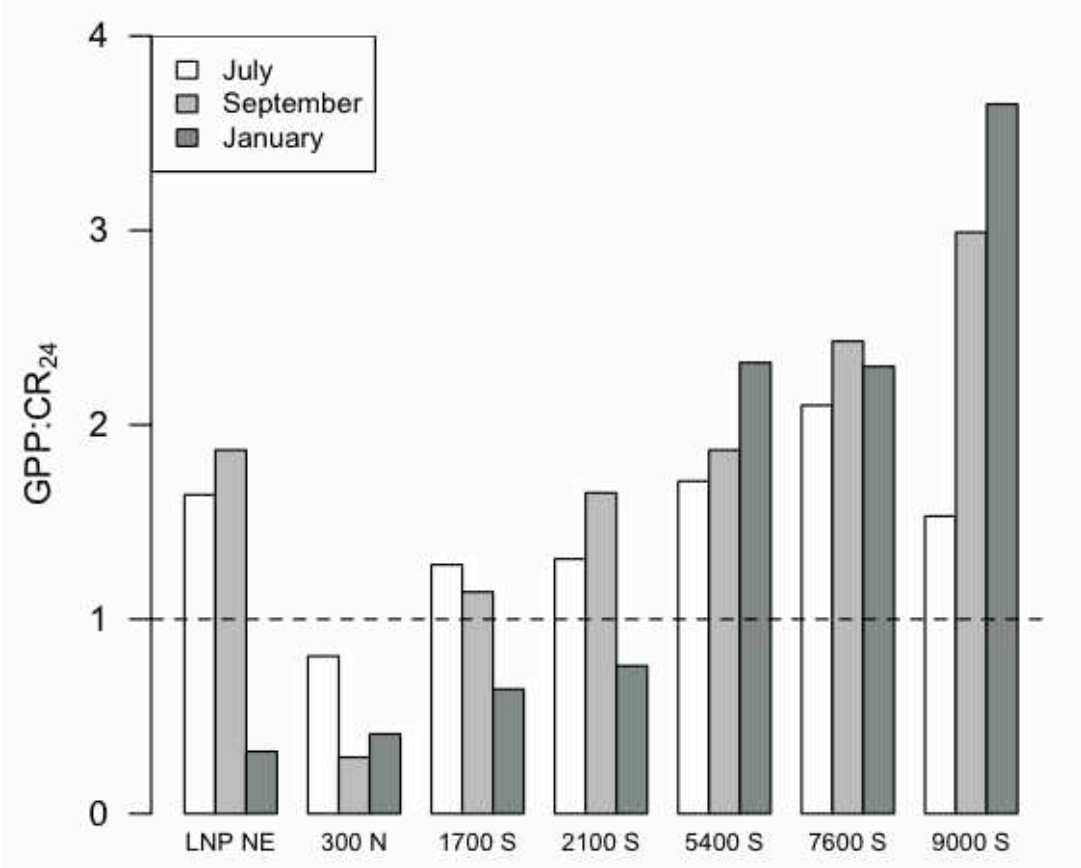

Fig. 48. Seasonal GPP:CR24 ratios

summer, and all sites in the LJR were heterotrophic during the winter.

The unexpected autotrophic conditions measured at the LNP NE site during the summer are a result of periphyton mats covering the sediments in the shallow sampling location. Unfortunately, NDM chamber sampling cannot be conducted in the 1.5 to 2 meter deep thalweg in Reach 1, which created a sampling bias towards "easy to access" productive sediments. Although the author does not believe that Reach 1 is autotrophic, the take home message is that the benthic zone was active in terms of primary production throughout the Jordan River.

5.2.2 Chamber Net Daily Metabolism (NDM)

Fig. 49 provides a bar chart for the chamber measured NDM. The UJR was a year-round source of instream-produced OM to the downstream LJR and Surplus Canal. The LJR became more heterotrophic with distance downstream, and all sites in the LJR were net DO consumers during the winter months. The positive NDM at the LNP NE site was a result of abundant periphyton growth on the silty sediments that became detached and floated to the surface in the afternoon due to oxygen gas production. This periphyton was assumed to be isolated to the shallow depositional zones in Reach 1, not in the thalweg. The overestimation of NDM using chambers is associated with the requirement of relatively shallow sampling locations in a medium sized river and is most likely a sampling artifact at all sites (Bott et al. 1978). As a result, the NDM estimates provided by chamber studies should be viewed as conservatively high.

The three season average chamber NDM metabolism parameters are provided in Table 19. The benthos were responsible for 50–87% of the CR_{24} and GPP in the Jordan River. The seasonal site average percent of CR_{24} and GPP associated with the benthos

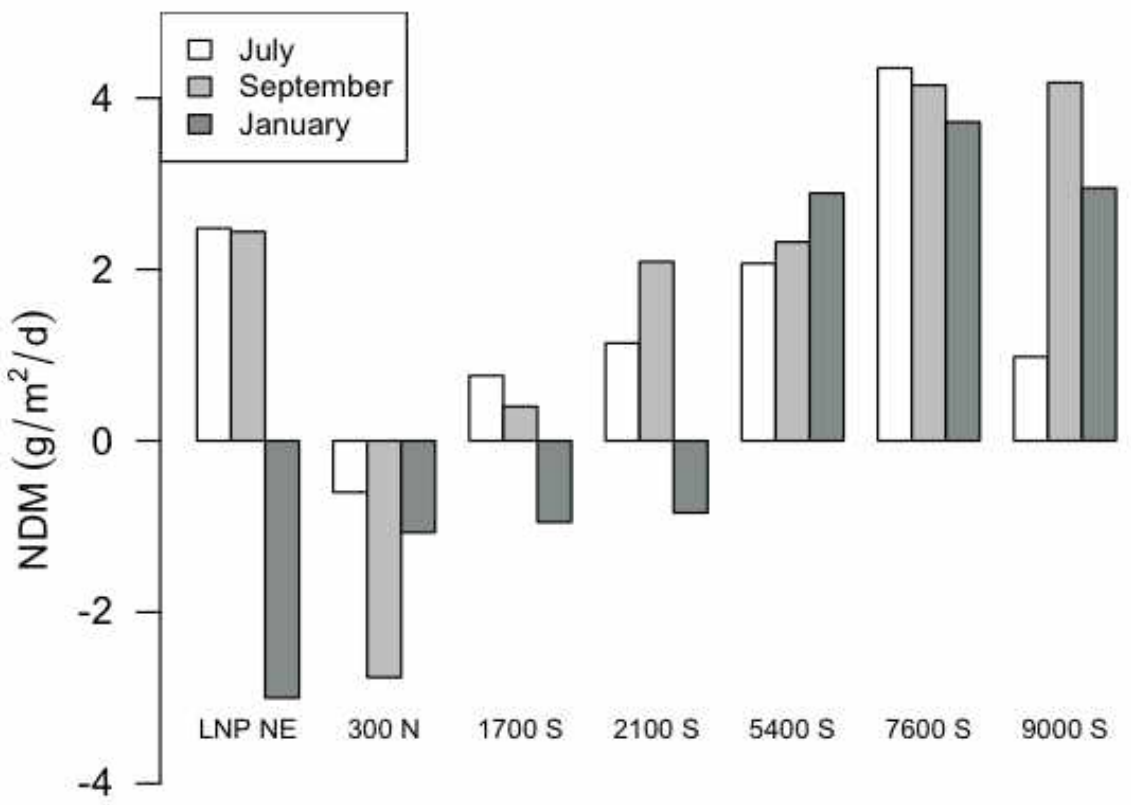

Fig. 49. Seasonal NDM

Table 19. Annual average chamber NDM

	average annual chamber NDM fluxes						
	(g DO/m^2/d)		(g DO/m^3/d)		(g DO/m^2/d)		
Site	TOD	TPP	WC_{dark}	WC_{light}	GPP	CR_{24}	NDM
LNP NE	-2.6	2.9	-0.8	1.1	4.2	-3.6	0.5
300 N	-2.1	0.9	-0.6	0.4	1.4	-2.8	-1.4
1700 S	-1.6	1.3	-1.1	1.4	2.6	-2.6	0.0
2100 S	-1.9	2.6	-1.9	1.9	4.0	-3.2	0.8
5400 S	-1.7	3.5	-1.1	1.9	4.9	-2.5	2.4
7600 S	-2.7	6.3	-0.6	1.3	7.2	-3.2	4.0
9000 S	-0.7	2.2	-1.0	2.6	4.2	-1.4	2.7

was 67% and 65%, respectively, for the entire length of the Jordan River. As was noted in the SOD study (Section 5.1.7), the benthos were responsible for the majority of the biological activity in the Jordan River.

5.3 Single-Station Diurnal DO Stream Metabolism

5.3.1 Diurnal DO profiles in the Jordan River

Fig. 50 shows the consistency in the UJR stream metabolism at the 9000 S and 7800 S sites over a 5-day period in late summer. The daytime ambient DO surplus peaks midday around 2 mg-DO/L (130% saturation), and during nighttime hours a deficit of roughly -2 mg-DO/L occurs (75% saturation). The increase in ambient DO following 0:00 does not influence the ambient DO deficit and is the result of the stream temperature decreasing during nighttime, resulting in an increase in ambient DO saturation in the well-mixed UJR. The sinusoidal nature in DO concentrations is very consistent,

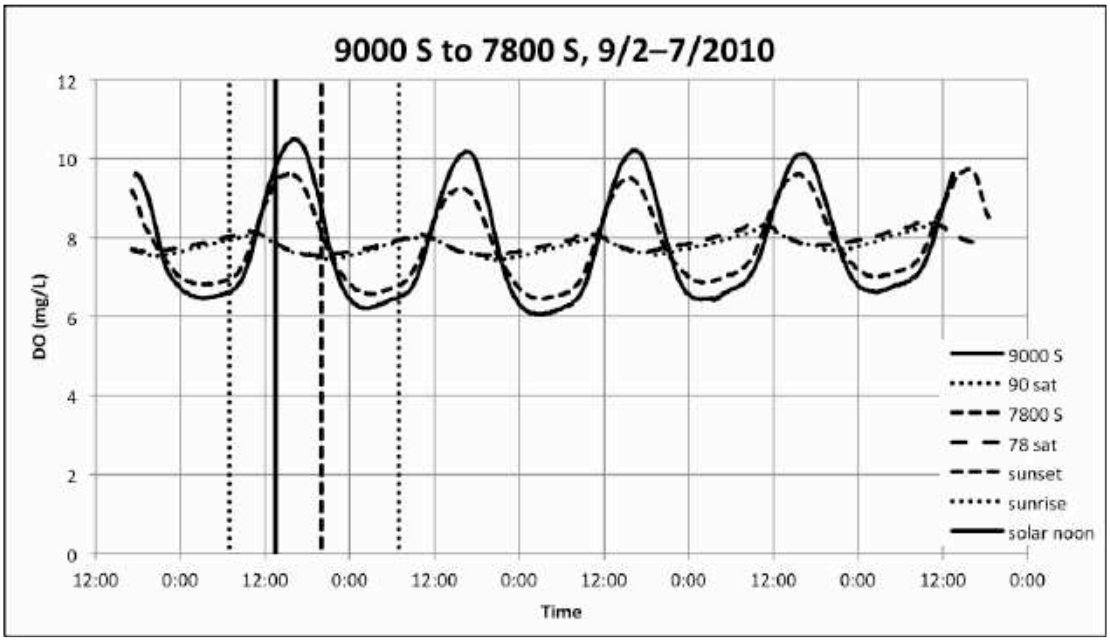

Fig. 50. 5-day diurnal DO profiles for the Upper Jordan River

indicating that both of these sites have a consistent diurnal metabolism.

Fig. 51 provides 24-hour DO profiles for additional sites in the UJR during the spring of 2012. All sites were supersaturated throughout the photoperiod with the 5400 S site reaching 156% saturation, indicating that the UJR may be a significant source of instream produced OM to the DO impaired LJR.

The Lehi site is located in Reach 8 near the outlet of Utah Lake and has the smallest diurnal DO swing and smallest reaeration coefficient in the UJR. The reason that the Lehi site remained supersaturated with DO throughout the night until 4:00 AM and did not begin to show signs of photosynthesis until 4 hours after sunrise is hypothesized to be result of Utah Lake phytoplankton. The diurnal DO profiles measured near the outlet of the lake were most likely the DO dynamics occurring in the eutrophic water column of Utah Lake before discharging into the Jordan River. This resulted in the diurnal DO data collected at the Lehi site being unsuitable for the stream metabolism analysis.

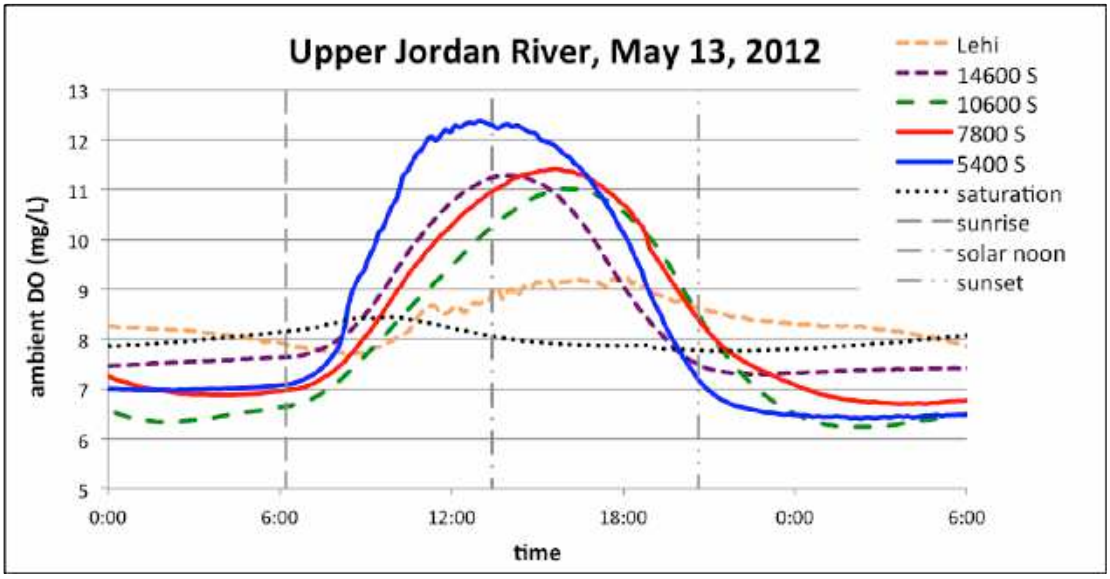

Fig. 51. May 2012 diurnal DO profiles for the Upper Jordan River

Fig. 52 shows diurnal DO curves collected in the LJR in early summer. The 700 S site was supersaturated for roughly 6 hours of the day and daytime DO deficits continued to increase with distance downstream of the Surplus Canal diversion. Interestingly, the nighttime DO deficit was -2 mg-DO/L at all four of these sites in the LJR independent of the different mean depths and reaeration coefficients. This constant DO deficit is the reason the LJR is considered chronically impaired for DO and is vulnerable to acute DO depletion events.

5.3.2 Single-station NDM model comparison

Diurnal DO models are excellent tools to characterize, document, and estimate autotrophic:heterotrophic ratios in lotic systems, and they can be used to estimate CR_{24}, GPP, and NDM if the reaeration coefficient is known. Limitations include that diurnal models will not differentiate between SOD or BOD, nor will they isolate the primary production associated with periphyton and phytoplankton. In addition, groundwater

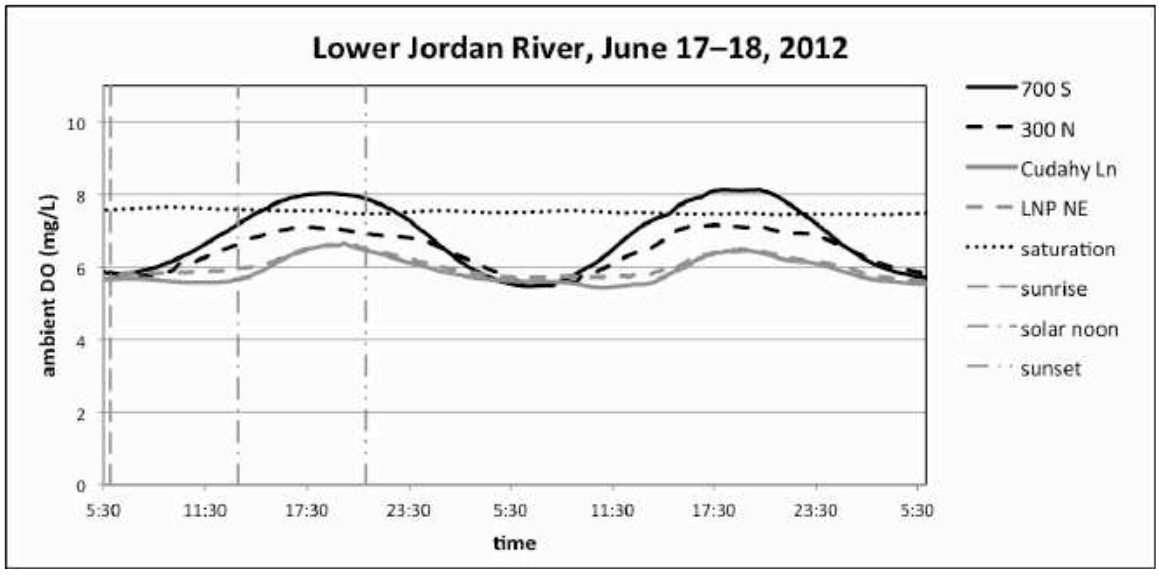

Fig. 52. Typical diurnal DO profiles for the Lower Jordan River

(GW) intrusion having a DO deficit will overestimate respiration while underestimating NDM if not accounted for when using the single-station method (Hall and Tank 2005). It has been suggested that rivers having more than 5% of their flow composed of GW should be sampled for NDM using chamber methods (Grace and Imberger 2006). The use of multiple methods, chambers and single-station calculations, to estimate NDM in the Jordan River provided both insight to the flaws of each method and added confidence to the general conclusions obtained using each method.

Provided in Table 20 are flux estimates of GPP, CR_{24}, and NDM based on diurnal DO profiles measured in the UJR utilizing the single-station method. The first set of parameters provides stream metabolic rates based on measured, or apparent, diurnal signatures, and the second list was adjusted for GW intrusion having a DO concentration of 1 mg-DO/L.

The river-wide mean depth (d) in meters and reaeration coefficient (k) are provided beneath the site name. The mean depth at each site was estimated by walking across the width of the river at each site in the UJR. The reaeration coefficients used in the UJR single-station NDM estimates are a combination of diffusion dome measured and predictive equations provided in the Literature Review (Section 3.3.2). NDM estimates neglecting the effects of GW intrusion and potential hyporheic exchanges estimated an average NDM of +0.1 g-DO/m^2/day in the UJR. This flux is slightly positive, but neutral enough to be overlooked as a large source of OM to the LJR.

An estimated 15% of the baseflow above 9000 S, and 5% between 9000 S and the Little Cottonwood Creek tributary are associated with GW intrusion (Utah DWQ 2013, Fig. 1.4). Under this scenario, -2.6 and -2.4 g-DO/m^2/d of the single-station estimated

Table 20. UJR Single-Station and GW adjusted model NDM outputs

		Single-Station model (g DO/m^2/d)			GW adjusted (g DO/m^2/d)		
	date	GPP	CR_{24}	NDM	GPP	$CR_{24,GW}$	NDM
14600 S	5/13/12	7.7	-5.9	1.8	7.7	-3.3	4.4
d = 0.3, k = 10	6/10/12	9.4	-8.7	0.7	9.4	-6.1	3.3
10600 S	5/13/12	12.1	-12	0.1	12.1	-9.4	2.7
d = 0.5, k = 6	6/10/12	6.2	-7.7	-1.5	6.2	-5.1	1.1
	7/24/12	8.7	-10.2	-1.5	8.7	-7.6	1.1
9000 S	7/20/10	7.8	-8.4	-0.6	7.8	-5.8	2.0
d = 0.8, k = 6	9/2/10	9.3	-8.8	0.5	9.3	-6.2	3.1
	1/16/11	9.5	-10.7	-1.2	9.5	-8.1	1.4
	1/15/12	1.1	-2	-0.9	1.1	0.6	1.7
7800 S	9/2/10	6.3	-6.55	-0.25	6.3	-4.2	2.1
d = 0.8, k = 6	1/16/11	8.3	-7.5	0.8	8.3	-5.1	3.2
	5/13/12	13.1	-11.45	1.65	13.1	-9.1	4.0
	6/10/12	6.6	-8.4	-1.8	6.6	-6.0	0.6
	7/24/12	13.3	-14	-0.7	13.3	-11.6	1.7
7600 S	9/2/10	2.65	-4.2	-1.55	2.7	-1.8	0.8
d = 0.8, k = 6	1/11/11	6.7	-4.7	2	6.7	-2.3	4.4
5400 S	6/5/10	5.9	-5	0.9	5.9	-2.6	3.3
d = 0.8, k = 5	9/2/10	2.7	-2.3	0.4	2.7	0.1	2.8
	1/21/11	5.1	-4.4	0.7	5.1	-2.0	3.1
	5/13/12	12.1	-9.6	2.5	12.1	-7.2	4.9
	6/10/12	8	-6.5	1.5	8.0	-4.1	3.9
	7/24/12	10.1	-9.4	0.7	10.1	-7.0	3.1
average		7.6	-7.4	0.1	7.6	-5.0	2.6

above 9000 S GW uses -2.6 g-DO/m^2/d
below 9000 S GW uses -2.4 g-DO/m^2/d

community respiration is a result of GW intrusion upstream and downstream of 9000 S, respectively. The positive GW adjusted CR_{24} fluxes measured at the 9000 S site in January and the 5400 S site in September do not reflect reality since photosynthesis cannot occur during the nighttime and are assumed to be a result of the generalized assumptions used to calculate GW contributions in this analysis. They were included in the average values in Table 20 since the same assumptions were used in all GW adjusted values. This resulted in a GW adjusted average autotrophic NDM of 2.6 g-DO/m^2/d in the

UJR. Appendix B provides diurnal DO profiles used in the single-station NDM analysis.

Fig. 53 provides a comparison between the chamber measured NDM and the single-station GW adjusted NDM estimate in the UJR. The elevated chamber NDM measured at the 7600 S and 9000 S sites are most likely a result of the sampling locations being closer to the banks where benthic communities are subjected to less scouring and shallow water depths (Bott et al. 1997; Bott et al. 1978; Grace and Imberger 2006).

The single-station NDM estimates for the LJR are provided in Table 21 and were not adjusted for GW intrusion. The average model estimates for NDM in Reaches 3, 2, and 1 were -1.5, -2.7, and -2.6 g-DO/m^2/d, respectively. The decrease in NDM with distance downstream in the LJR agrees with observations that SOD and ambient DO

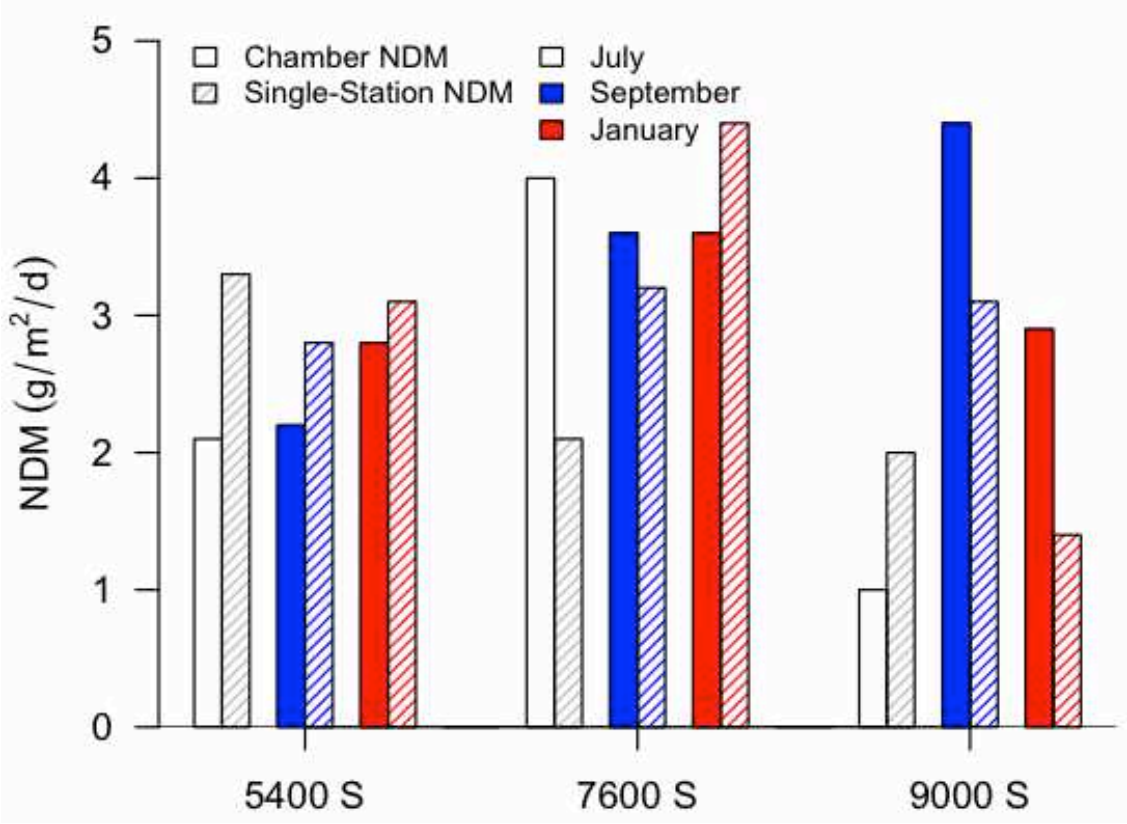

Fig. 53. UJR Chamber and single-station GW adjusted NDM estimates

Table 21. LJR Single-station model NDM outputs

		LJR Single-station (g DO/m^2/d)		
	date	GPP	CR_{24}	NDM
2100 S	7/6/10	3.1	-4	-0.9
d = 0.8, k = 6	8/25/10	4.3	-6.2	-1.9
	1/21/11	3.2	-5.7	-2.5
	8/23/12	11.6	-12.5	-0.9
1700 S	7/7/10	6.6	-6	0.6
d = 0.9, k = 4	8/25/10	4.3	-5.8	-1.5
	1/21/11	3.3	-4.7	-1.4
700 S, d = 1.3, k = 4	6/18/12	6.6	-10.3	-3.7
300 N	8/30/10	1.9	-5.2	-3.3
d = 1.3, k = 1.2	6/18/12	3.5	-5.5	-2
500 N	8/23/12	4.4	-7.6	-3.2
700 N	8/30/10	1.5	-4.9	-3.4
1700 N	7/16/10	3.8	-5.3	-1.5
Cudahy Ln	6/18/12	2.9	-6.1	-3.2
d = 1.5, k = 1.2	8/23/12	4.2	-8	-3.8
LNP NE	7/15/10	3.4	-6.4	-3
d = 1.2, k = 1.2	8/25/10	2.2	-4.4	-2.2
	6/18/12	2	-4.3	-2.3
Bender	8/25/10	2.2	-4.3	-2.1
Burnham	5/26/10	1.3	-3.4	-2.1
d = 1, k = 1.2	8/23/12	4.2	-6.2	-2

d = mean depth (m)
k = reaeration coeff. (1/day)

deficits increase with distance downstream.

Fig. 54 provides the relationship between chamber NDM and the single-station model NDM for the LJR. The lack of an equivalent ratio when comparing data in the LJR is a result of GPP being overestimated in the NDM chambers in the relatively deep slow moving LJR. This is shown by the regression line crossing the y-axis at +1 (y = 1.1x + 1). A 1:1 relationship is shown as the dotted line for reference. The overestimation of chamber GPP compared to single-station estimate in the LJR is pronounced due to the deeper river depths (>1m) resulting in greater biases towards sampling the benthos in

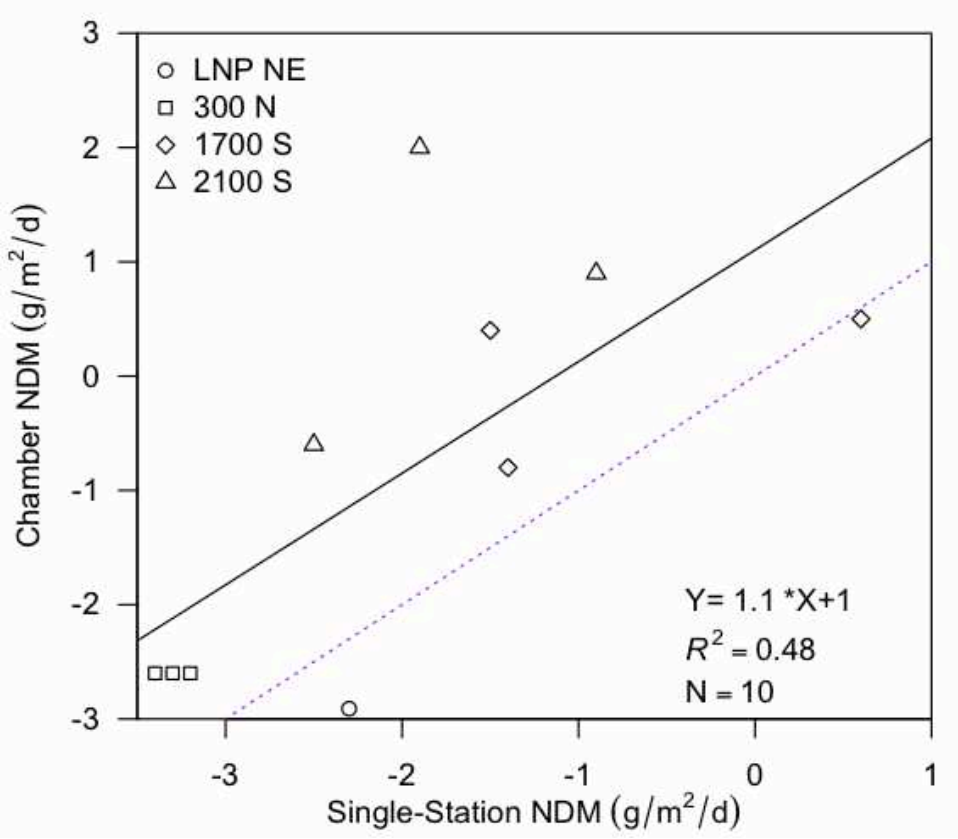

Fig. 54. Chamber vs. Single-station NDM relationship
Note: summer LNP NE data not included

shallow areas more conducive to benthic growth compared to the thalweg (Grace and Imberger 2006).

Overall, the NDM chambers tended to overestimate NDM in the LJR, but are very useful in isolating the sediments from the WC to determine the relative light and dark metabolic rates and fluxes. In addition, the use of chambers removes the requirement of knowing the reaeration coefficient, GW intrusion fluxes, and GW DO concentrations. By coupling multiple chamber NDM estimates with a large collection of diurnal DO NDM estimates, a great deal of information about the surface water in question can be obtained due to the strengths and weaknesses of both methods to estimate stream metabolism.

5.4 Sediment Organic Matter

5.4.1 Sediment %TOC

The commonly used sediment characterization measurement volatile solids (%VS) is a surrogate for organic matter (OM). Total organic carbon (%TOC) is another common sediment OM parameter, but is much more time consuming, challenging, and expensive compared to %VS. These challenges are compounded in sediments having a high inorganic carbon content, such as those found in the alkaline Great Salt Lake valley. Combustible OM is composed of carbon, hydrogen, and oxygen, and a relationship between sediment %TOC and %VS was produced to confirm that %VS measurements were a viable method to estimate OM in Jordan River sediments. In addition, this information was used to identify how much of the OM was present as organic carbon.

Fig. 55 provides the relationship compiled from 28 depth integrated sediment cores between sediment %TOC and %VS in the LJR. The LJR had a %TOC:%VS range between 0.4 to 0.6, similar to the range found in other sediments (Schumacher 2002; Dean 1974). The LJR had a mean %TOC:%VS ratio of 0.5, which is a common assumption used to correlate organic carbon and OM in sediments (Beaudoin 2003; Ball 1964). Site specific %TOC data can be found in Appendix D.

Easily biodegradable organic matter includes viable bacteria and phytoplankton containing 47–50% carbon (Tchobanoglous et al. 2003, Table 7-4). Cellulose, $C_6H_{12}O_5$, a major component of terrestrial leafs, macrophytes, and algal biofilms, is 44% carbon as dry mass. Pure bacteria cultures have %TOC:%VS ratios between 0.45–0.50 and wastewater bacteria found in activated sludge processes are generalized as 53% carbon in terms of dry OM (Bratbak and Dundras 1984; Tchobanoglous et al. 2003, pg. 558).

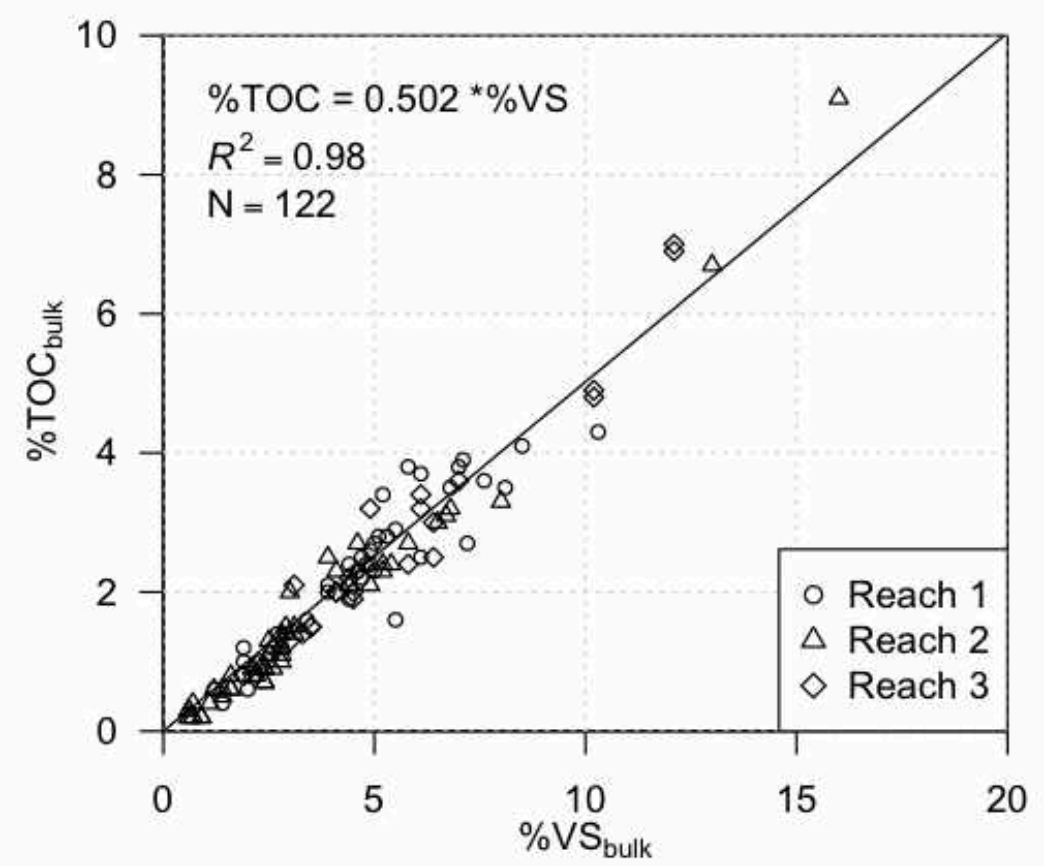

Fig. 55. LOI to %TOC conversion for the Lower Jordan River

Although the sources of sediment OM were not identified based on organic carbon content, the ratio agrees with other researchers across a wide range of %VS in the LJR.

The strong correlation between %TOC and %VS allows OM to be confidently measured using %VS protocols in the LJR. The primary advantage to using %VS as a surrogate for OM is the ease of processing large amounts of samples with minimal time, effort, and monetary overhead (Konen et al. 2002).

Previous researchers found the %TOC:%VS relationship to be nonlinear for %VS greater than 25%, but sediments this organically enriched were not encountered in the LJR (Leipe et al. 2010). Sediments exceeding 25% VS most likely do exist in the Jordan River, but will be found in areas of localized sedimentation, such as the backwaters of the

Surplus Canal and other diversion dams. Early researchers reported poor repeatability for samples less than 10% VS, but the relationship was very strong in the LJR (Mackereth 1966).

5.4.2 Sediment %TS and %VS

Fig. 56 provides photos of sediments found in the LJR. Note the dark color and sludge-like appearance of the sediments found in Reach 1. The surface sludge layer overlying dirty course sand at the 2300 S site is referred to as a benthal deposit.

The top 0–2 cm of the sediment column was less consolidated than depths 5 cm and deeper where the sediments had a higher bulk density (Fig. 57). The top 0–2 cm of the LJR sediment column consisted of a silty-muck benthal deposit overlaying more consolidated sediments. Similar to the principle of superposition used to describe sediments on a geologic scale, the surficial sediments are composed of the most recently deposited, or disturbed, material (Glew et al. 2001). Site specific %VS and %TS data are provided in Appendix B.

Studies relating SOD to OM prior to the Clean Water Act worked with benthal deposits having %TS as low as 10% and %VS ranging from 10–20%. Whereas Jordan River surface sediments where "cleaner" and range from 20–80% TS and 1–18% VS.

The relationships for surface (0–2 cm, R^2 = 0.89) and subsurface (5+ cm, R^2 = 0.79) sediment %VS and %TS in the Lower Jordan River where

$$\%VS_{surface} = -9.7 * (\ln \%TS) + 43 \quad (21)$$

$$\%VS_{subsurface} = -15.5 * (\ln \%TS) + 69 \quad (22)$$

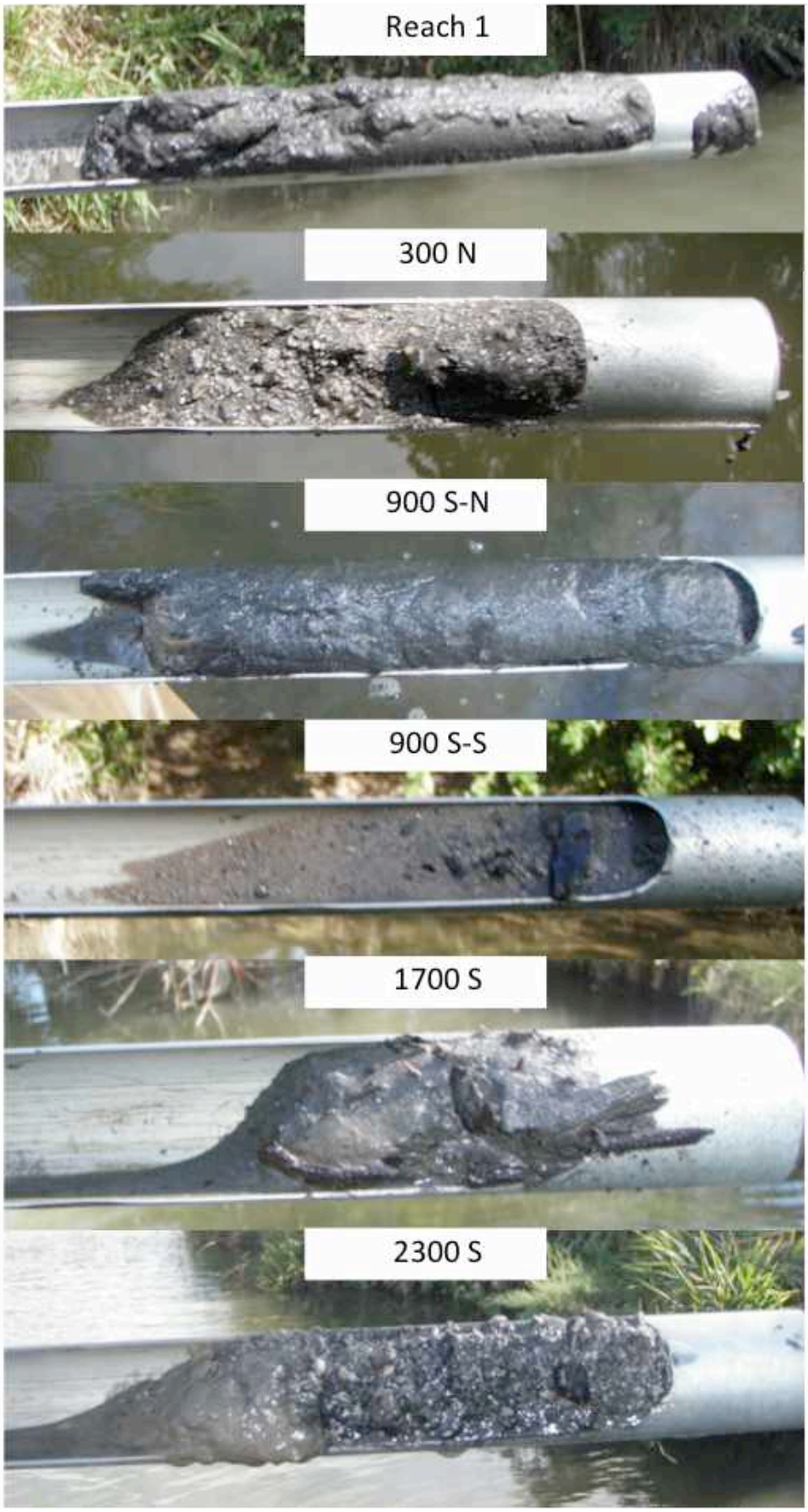

Fig. 56. Sediments found in the Lower Jordan River and Surplus Canal backwater

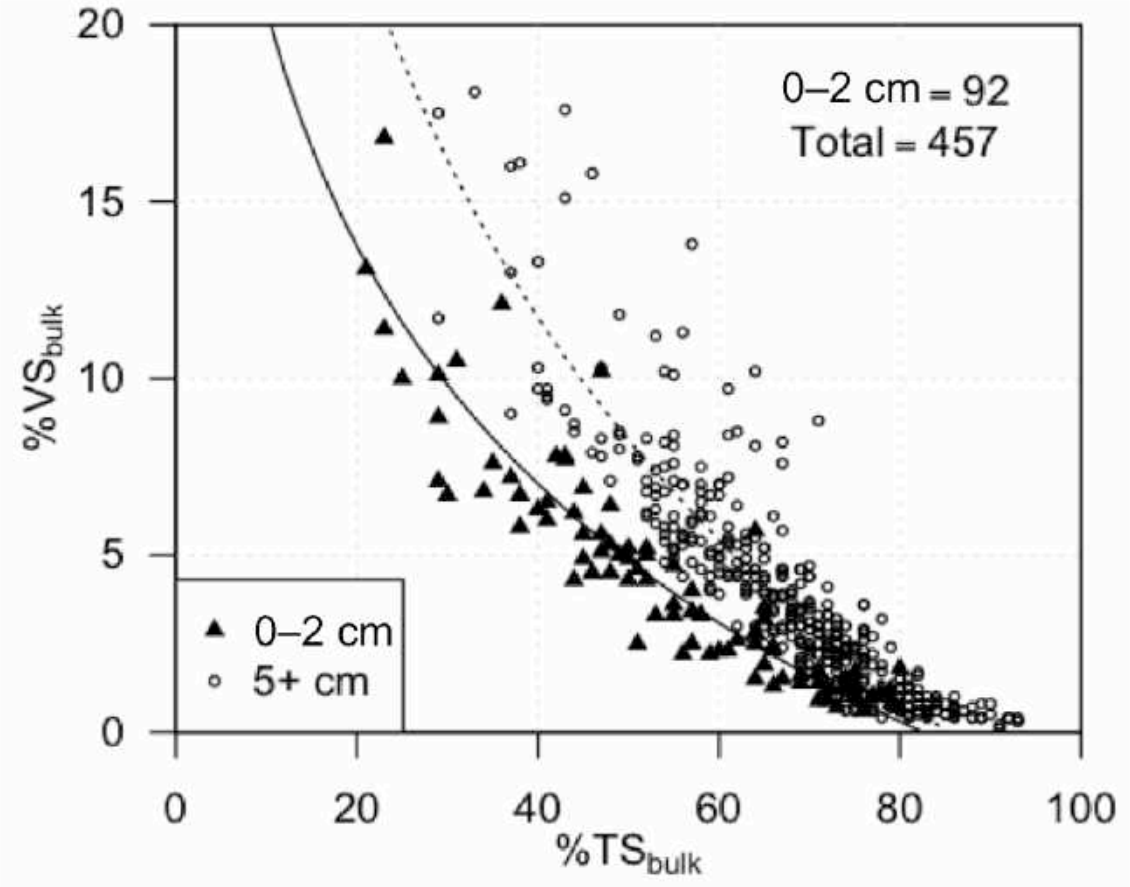

Fig. 57. Jordan River %VS and %TS relationship

The parameter %TS describes the water content, or how "muddy" the sediment is. This becomes a very important parameter when calculating the standing stock, or amount of OM present in the wet sediments, since the water content is required to calculate a bulk wet density. This parameter changes with both depth and %VS in the Jordan River.

Presented in Fig. 58 are hydraulic reach based average sediment %TS in terms of depth in the sediment column. The two important trends to note are that %TS increases with depth, and %TS increases significantly in the coarse sand and gravels found in Reaches 4–6. Increases in %TS with increasing sediment column depth are due to

- more consolidated sediments

- gas production in the organically enriched sediments displaces pore water leading to dryer sediments (field observation)

%VS is defined as the percentage of the %TS that is combustible, or OM. The higher the %VS the more "mucky" the sediments become. Fig. 59 provides hydraulic reach average sediment %VS from over 500 samples collected in the Jordan River. The average %VS was consistently within the range of 3–6% in the top 10 cm of the sediment column in Reaches 1 and 2. Average bulk sediment %VS decreased more than an order of magnitude upstream of the Surplus Canal backwater. The most organically enriched sediments where found in the backwater of the Surplus Canal in Reach 4. %VS

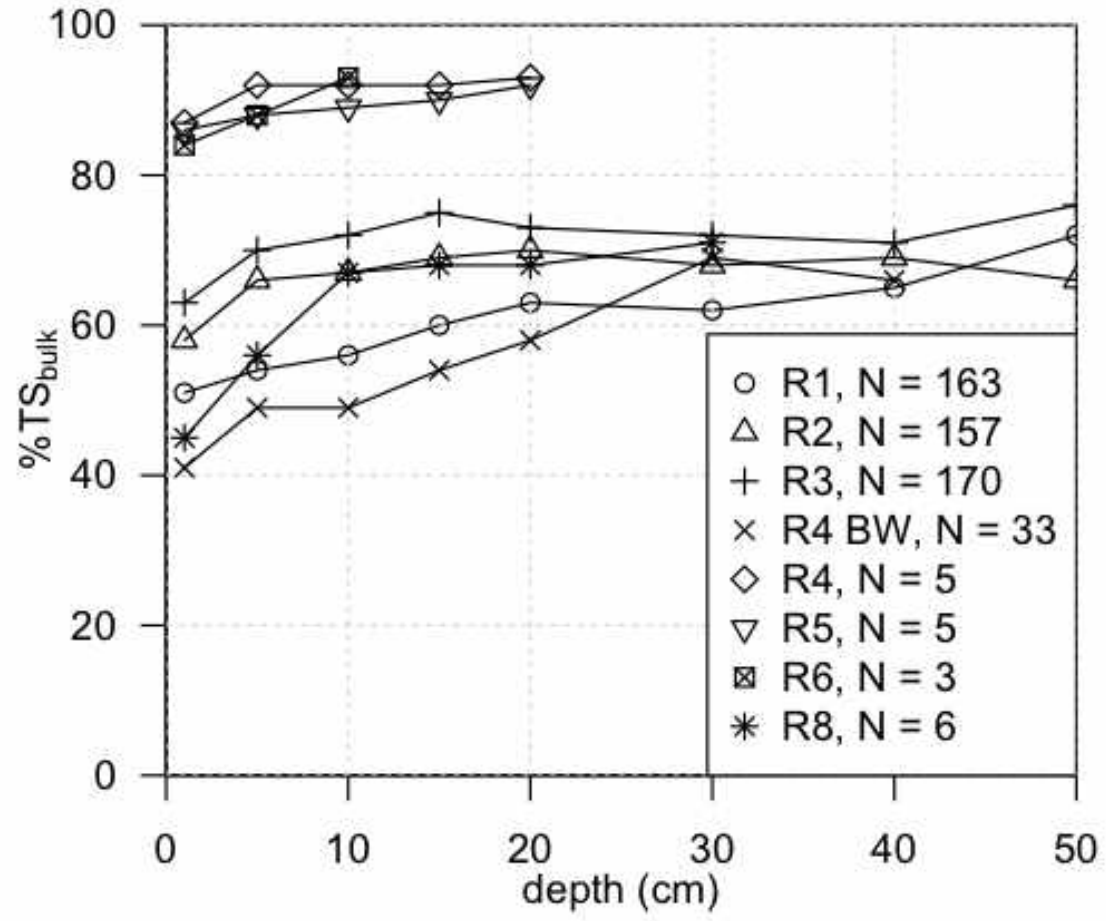

Fig. 58. Reach average sediment %TS

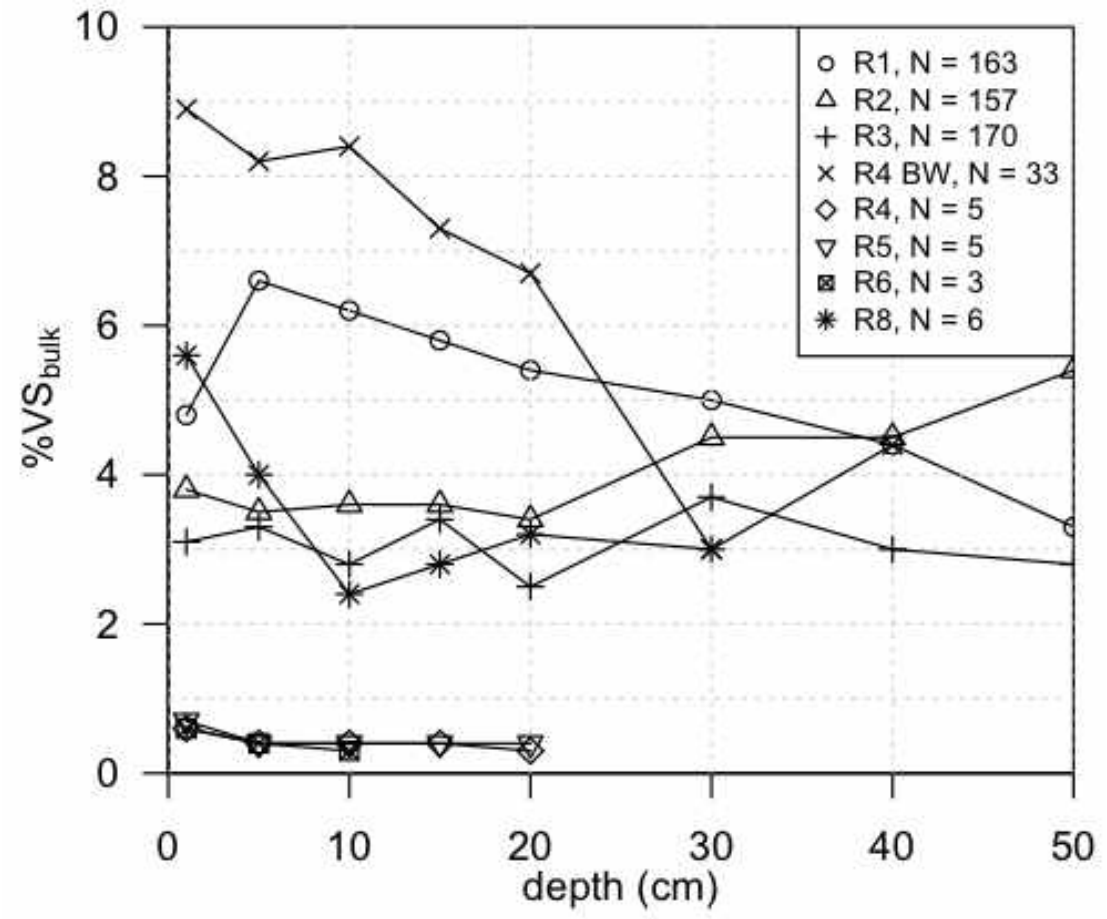

Fig. 59. Reach average sediment %VS

consistently increased in the fine sediments downstream of the Surplus Canal Diversion in the LJR. These increases are observed throughout the depth of the sediment column. In the limited number of observations made in Reach 8, near the outlet of Utah Lake, the benthal deposits had %VS similar to Reach 1 suggesting that Utah Lake is a source of OM to the downstream Jordan River.

In the LJR, sediments with %VS greater than 5% were visually observed to release swamp gas when disturbed, and %VS greater than 10% was accompanied by sporadic gas ebullition from undisturbed sediments. Ebullition was visually observed in the Surplus Canal backwaters and at the 1300 S stormwater and tributary discharge.

Sands and gravels collected in free flowing sections of the UJR had %VS less than 0.7% (5400 S, 7600 S, and 9000 S (N = 11)).

Fig. 60 provides a bar chart for the depth integrated cumulative $\%VS_{bulk}$ taken from three locations across the width of the river at 0–2, 5, and 10 cm depths. Sediment OM present at depths greater 0–2 cm provide information about the historical OM loading to the LJR. The 10 cm cumulative $\%VS_{bulk}$ consistently increased with distance downstream from the Surplus Canal diversion both in the thalweg and near the east bank. The exception was the LNP NE east bank site where large amounts of new sand were visually observed following the high water event of 2011. The thalweg in Reach 1 (sites 1–3) was not scoured to a sand layer, implying that the sediments across the entire width of the river are contributing to SOD and ambient DO deficits.

Fig. 61 provides the depth integrated average $\%VS_{bulk}$ of the sediments taken from the three locations across the width of the river. During the Spring 2012 sampling event the surface sediments (0–2 cm) had less $\%VS_{bulk}$ than the 5 and 10 cm depths in Reach 1. The unusually large snowpack in the winter of 2010–2011 resulted in a "managed" spring runoff lasting for 12 months in the UJR. It is hypothesized that the surface sediments encountered during the Spring 2012 sampling event were the deposition of inorganic sediments associated with upstream erosion and sediment displacement. As a general trend, the river-wide average sediment %VS increases as the LJR flows downstream from the Surplus Canal diversion. River-wide sediment characterization data are provided in Appendix D.

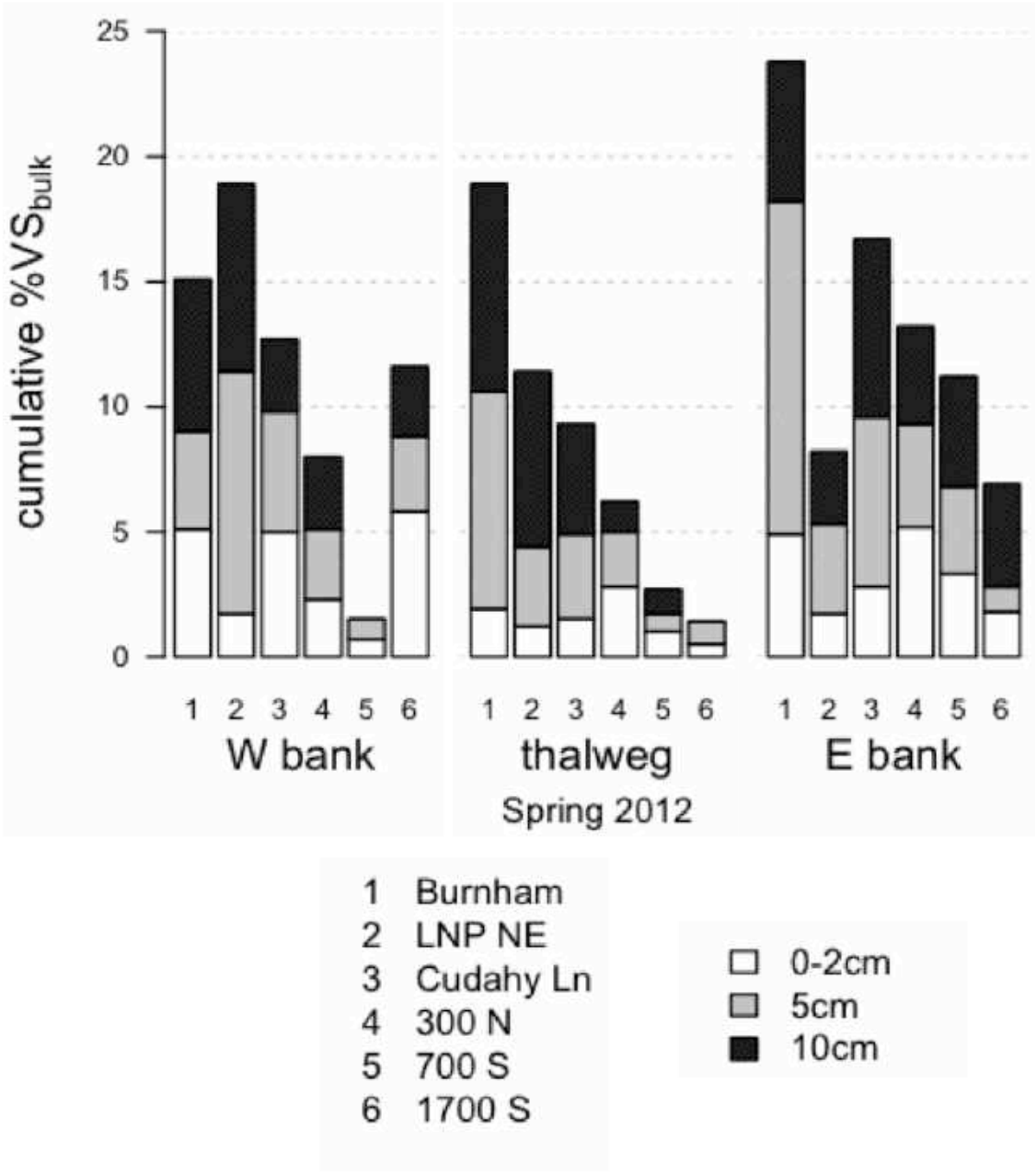

Fig. 60. River-wide sediment %VS
Note: highest surface sediment (0–2 cm) %VS at SOD site at 1700 S-W bank during Spring 2012

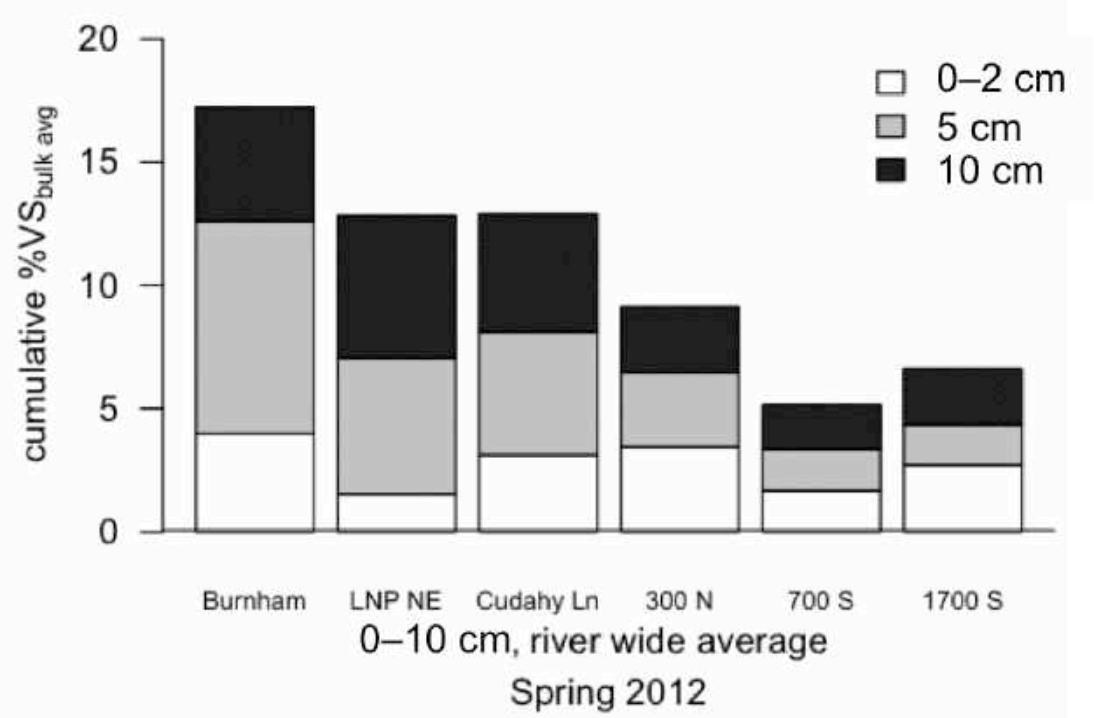

Fig. 61. Cumulative river-wide mean %VS in the top 10 cm of sediment column

5.4.3 CPOM and FPOM

221 sediment samples from the LJR were analyzed for course particulate organic matter (CPOM). CPOM includes all OM greater than 1 mm in size and represents terrestrial leaf litter and macrophyte debris since twigs, bark, and plastic were removed from the samples prior to analysis. To clarify, the parameter used to quantify the amount of CPOM is the percentage of the %VS found as CPOM ($\%VS_{CPOM}$). This parameter allows easy visualization of the relative amount of CPOM, but needs to be combined with $\%VS_{bulk}$ and $\%TS_{bulk}$ when calculating the standing stock of CPOM. River-wide $\%VS_{CPOM}$ data are provided in Appendix D.

Fig. 62 shows the cumulative sediment column $\%VS_{CPOM}$ for all sites across the width of the river. The highest concentrations of CPOM were found in the thalweg. Over 50% of sediment OM was present as CPOM from the Cudahy Ln site upstream in the

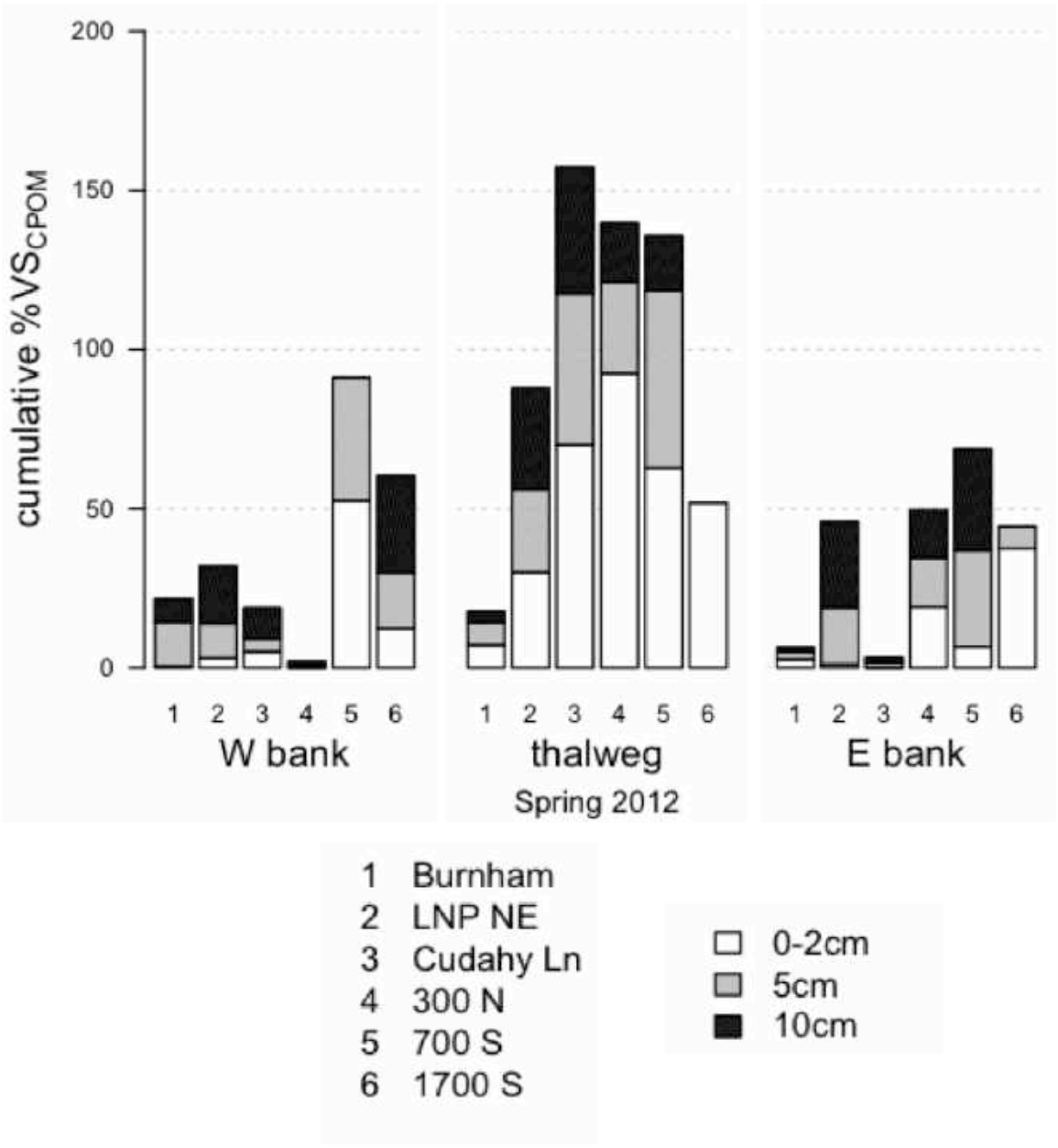

Fig. 62. River-wide cumulative sediment $\%VS_{CPOM}$

thalweg surface sediments (Reaches 2–3). Burnham Dam sediments had very little CPOM across the width of the river and sediment OM was composed of fine particulate organic matter (FPOM). The mean $\%VS_{CPOM}$ was 19% for the LJR.

The relative percentage of CPOM decreased with depth in the thalweg (Fig. 62, center). Fig. 60 above does not show a decrease in %VS with depth in the thalweg and it is hypothesized that the decreases in CPOM with depth are a result of biological CPOM processing to FPOM over time. Although the only macroinvertebrates observed in sediment cores in the LJR were worms, an estimated 60% of the CPOM ingested by shredders is excreted as FPOM in feces (Welch 1968). Bacteria and fungi are most likely responsible for the majority of CPOM conditioning and breakdown in the LJR.

Fig. 63 provides the river-wide average $\%VS_{bulk}$ (left) and $\%VS_{CPOM}$ (right). The river-wide average $\%VS_{CPOM}$ decreased with distance downstream in the LJR while the amount of $\%VS_{bulk}$ increased. The 700 S site is located downstream of the 1300 S and 900 S stormwater discharges, and these sediments had the highest concentration of CPOM, but it also had the least amount of sediment %VS.

All CPOM found in Reach 1 were assumed to be “leaf skeletons” or macrophyte remnants since twigs and sticks were removed from the sediment samples as part of sampling methodology. The identification of the source of FPOM is inconclusive since FPOM includes all algae, microbes, and degraded CPOM. The river-wide mean 10 cm depth integrated sediment column $\%VS_{CPOM}$ for the Burnham Dam, LNP NE, Cudahy Ln., 300 N, 700 S, and 1700 S sites were 4%, 18%, 18%, 25%, 30%, and 23%, respectively. The 300 N, 700 S, and 2100 S sites are located downstream of tributaries and stormwater outfalls and had elevated CPOM:FPOM ratios in the range of 0.5, similar

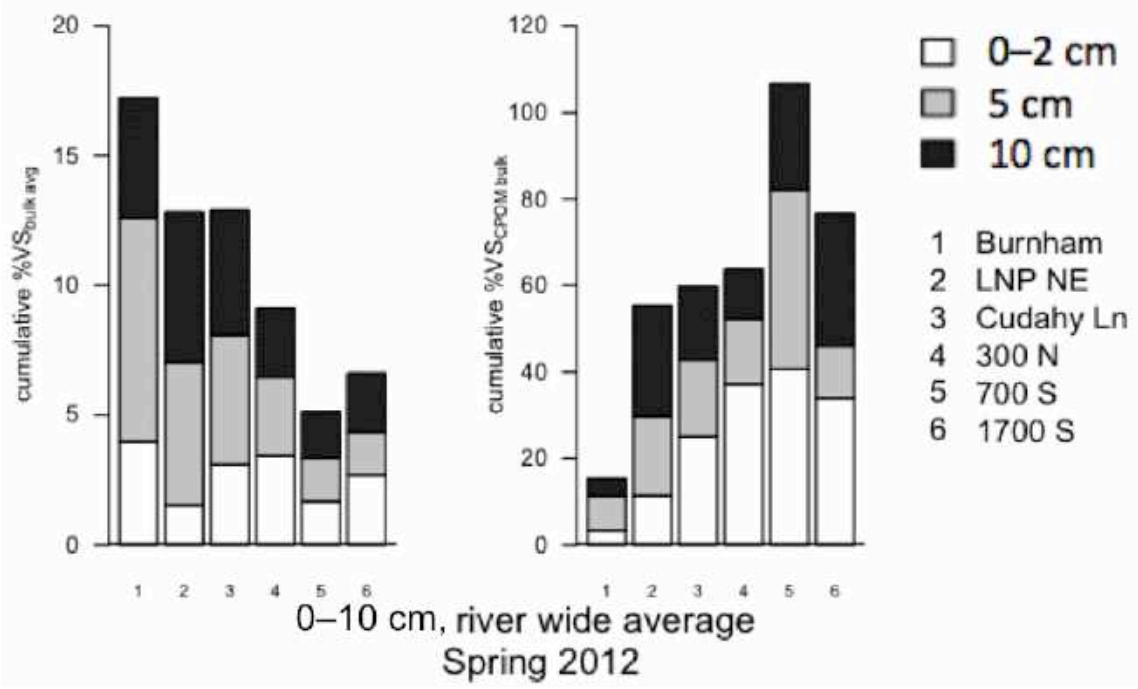

Fig. 63. River-wide average sediment $\%VS_{bulk}$ and $\%VS_{CPOM}$

to a much smaller 2nd order stream (Vannote et al. 1980). It is hypothesized that urban leaf matter is the source of this CPOM. The decrease in $\%VS_{CPOM}$ within Reach 1 resulted in CPOM:FPOM ratios dropping sharply to 0.05 at Burnham Dam and is most likely a result of two factors:

- CPOM originating from urban stormwater and entering Reach 1 as bedload has already undergone conditioning in Reaches 2 and 3 and is predominately FPOM.
- There is less riparian vegetation in Reach 1, resulting in less bank litterfall.

Riparian vegetation loads of OM are assumed to be insignificant given the scale of the urban watershed draining to the Jordan River (Imberger et al. 2011). Since algae are smaller than 1 mm in size, upstream eutrophication cannot be responsible for the CPOM aspect of the OM found in the Lower Jordan River.

The sediment surface area of Reaches 1, 2, and 3 account for 46%, 25%, and 29% of the total sediment surface area of the LJR (Section 5.7.1). Interestingly, the OM present in the top 0–2 cm of Reaches 1, 2, and 3 accounted for 47%, 27%, and 26% of the total OM in the surface sediments of the LJR after normalizing to an aerial OM standing stock. At depths of 5 and 10 cm, the OM present in Reach 1 accounted for over 60% of the OM in the LJR. This means that the surface sediments were very similar in terms of aerial OM content in all three reaches in the Spring of 2012, but the subsurface sediments in Reach 1 were more organically enriched compared to Reaches 2 and 3. This consistent surface sediment layer was attributed to upstream erosion associated with the large snowmelt in 2011 that decreased SOD and %VS throughout the LJR due to an influx of silt and sand prior to the 2012 sampling event.

5.4.4 Sediment column OM turnover estimates

Fig. 64 provides an estimate of the cumulative years required to oxidize the carbon and ammonia associated with the sediment OM based on measured SOD fluxes. It should be noted that readily biodegradable dissolved organic carbon (DOC) and methane will be utilized to denitrify water column nitrate at the sediment water interface, slightly decreasing the total amount of DO required to oxidize sediment derived OM (Chapra 2008). This results in a conservative estimation of the time required to oxidize OM under these assumptions. In addition, many of the organics are refractory and will take years to breakdown or will never contribute to an oxygen demand. One of the interesting aspects of Fig. 64 is the 1:1 relationship between cumulative years and depth. Reaches 1–3, the Surplus Canal backwater (R4 BW), and Reach 8 all follow the 1:1 relationship although they have very different wet sediment densities, OM contents, and SOD fluxes. These

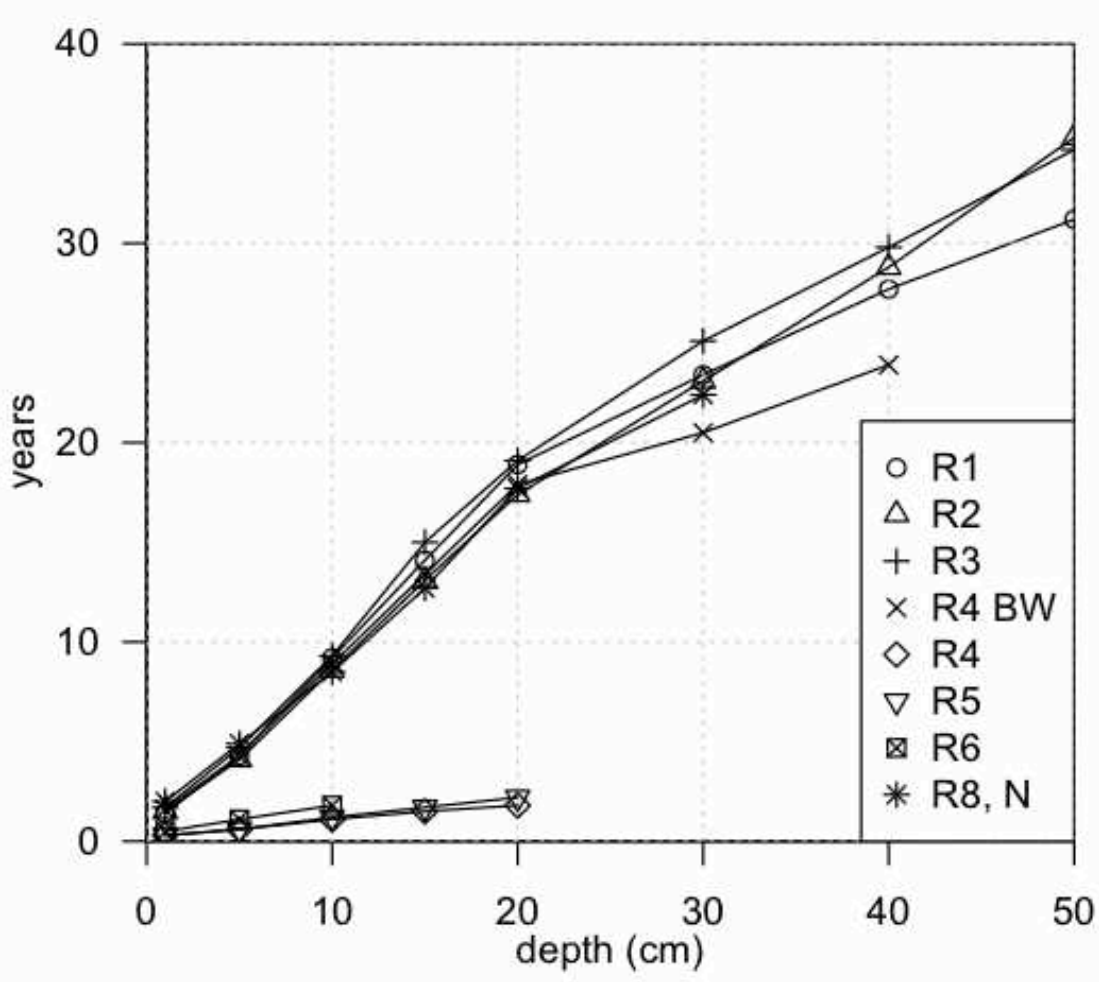

Fig. 64. Theoretical years to oxidize sediment column OM

rates coincide very closely with an annual cycle, suggesting that any reductions in OM loads to the LJR will improve WQ by reducing SOD. These OM load reductions could be achieved by reducing external loads from stormwater and tributaries, decreasing instream primary production, or both.

5.5 Dissolved Nutrient Fluxes

5.5.1 Ambient WQ

Provided in Table 22 are the ambient dissolved nutrient concentrations at the sites evaluated for nutrient fluxes. The LJR had a 3-year average ambient ammonium-N,

Table 22. Average nutrient concentrations measured during nutrient flux sampling

ambient dissolved nutrient concentration during nutrient flux sampling (mg/L)							
site	date	NH_4-N	NO_2-N	NO_3-N	TIN	PO_4-P	N:P
State Canal	2/6/13	3	0.3	6.3	9.6	0.95	22
Burnham	6/12/12	0.13	0.06	3.76	4	0.53	17
Burnham	6/14/13	0.33	0.13	2.95	3.4	0.55	14
LNP NE	6/3/10	1.49	0.23	0.06	1.8	0.12	33
LNP NE	4/3/12	0.4	0.08	1.83	2.3	0.29	18
LNP NE	6/15/12	0.39	0.16	3.95	4.5	0.65	15
LNP NE	6/15/13	0.33	0.11	3.1	3.5	0.53	15
Cudahy	6/3/10	1.33	0.24	0.06	1.6	0.1	36
Cudahy	6/13/12	0.21	0.15	3.53	3.9	0.61	14
Cudahy	6/13/13	0.27	0.16	2.96	3.4	0.56	13
300 N	6/7/10	0.06		0.59	0.7	0.07	21
300 N	4/14/12	0.17	0.08	2.31	2.6	0.43	13
300 N	6/12/13	0.1	0.06	2.42	2.6	0.43	13
700 S	6/14/12	0.1	0.07	3.32	3.5	0.58	13
700 S	6/10/13	0.11	0.05	2.17	2.3	0.36	14
900 S-N	6/8/10	0.05		0.57	0.6	0.11	12
900 S-S	6/8/10	0.08		0.64	0.7	0.1	16
1700 S-N	5/24/10	0.08	0.05	1.16	1.3	0.12	24
1700 S-N	4/16/12	0.13	0.07	2.1	2.3	0.49	10
1700 S-N	6/10/13	0.06		2.93	3	0.46	14
2600 S	6/2/10	5.64	1.13	0.22	7	0.29	53
5400 S	1/12/11	0.04		3.91	4	0.74	12
7600 S	1/15/11	0.03		1.85	1.9	0.1	42
9000 S	1/20/11	0.04		1.67	1.7	0.1	38
LJR avg.		0.31	0.11	2.13	2.5	0.37	15

Note: nitrite-N, nitrate-N, and phosphate-P DL = 0.05 mg/L
ammonium-N DL = 0.015 mg/L

nitrate-N, and orthophosphate-P concentrations of 0.3, 2.1, and 0.4 mg/L, respectively. These dissolved nutrient concentrations are higher than the total nitrogen (TN) and total phosphorus (TP) concentrations of 1.5 mg-N/L and 0.075 mg-P/L, indicating the potential for eutrophication in a lotic system (Dodd et al. 1998). The extremely high ammonium concentrations measured in State Canal and at the 2600 S site were coupled with high sediment OM content and extremely high SOD fluxes.

Generally, WQ scientists assume that nitrite concentrations are negligible in surface waters (Stanley and Hobbie 1981). The high nitrite concentrations found in Reach 1 and at the 2600 S site suggest incomplete nitrification in the water column or inhibited denitrification at the sediment–water interface. The organically enriched anaerobic sediments found in these river sections would be ideal for the microbial dissimilatory nitrate reduction metabolism carried out via fermentation that has been shown to result in nitrite accumulation in large rivers (Kelso et al. 1997). For perspective, aerobic surface waters tend to have nitrite concentrations less than 0.002 mg-N/L, or two orders of magnitude lower than measured in the LJR (Lewis and Morris 1986).

Both dissolved nitrogen and phosphorus were found in concentrations high enough for unrestricted phototrophic growth, but the elevated N:P ratios imply that phosphorus is the limiting nutrient. These ratios are even higher in the UJR upstream of all POTW discharges (7600 S and 9000 S), implying that P reductions from POTW loads to the Jordan River and the upstream Utah Lake will reduce eutrophication by limiting the availability of dissolved phosphorus. Additional external sources of nutrients to the Jordan River include groundwater, urban runoff, agriculture, and tributaries.

5.5.2 Sediment nutrient fluxes

Table 23 provides the 3-year average sediment nutrient fluxes for each site visited more than once in the LJR. Data from all nutrient flux sampling events can be found in Appendix G. The sediments were a source of ammonium at all sites in the LJR, suggesting sediment OM decay. Although the sediments were a source of ammonia-N, the sediments were a net sink for total dissolved inorganic nitrogen (TIN) due to the denitrification of nitrate loads originating from WWTP discharges. Nitrate removal was observed during all sampling events with the exception of two sites (LNP NE, 2012 and 300 N, 2010).

In Chesapeake Bay, silty sediments had increased ammonia and phosphorus fluxes compared to sandy substrate (Reay et al. 1995). Tidal flat sediments having less than 0.3% TOC (0.6% VS) had positive nitrate fluxes and exhibited positive ammonia fluxes at %TOC greater than 1.3% (2.6% VS) (Henriksen et al. 1983). The average %TOC in the surface sediments for Reaches 1–3 were all greater than 1.3% (Fig. 59 converted to %TOC), suggesting that the organically enriched sediments in the LJR are expected be a source of ammonia, not nitrate. Positive sediment phosphate fluxes were

Table 23. Average sediment nutrient fluxes in the Lower Jordan River

	average sediment flux ($g/m^2/d$)			
site	NH_4-N	NO_3-N	TIN	PO_4-P
Burnham	0.03	-0.69	-0.66	-0.08
LNP NE	0.04	-0.11	-0.09	0.06
Cudahy Ln	0.22	-0.28	-0.13	0.07
DWQ	0.04	-0.03	0.00	0.05
700 S	0.07	-0.27	-0.20	0.06
1700 S-N	0.14	-0.14	-0.04	0.11

Note: data from 16 sampling events over 3 years

characteristic of all sites in the LJR except the Burnham Dam site. This suggests that phosphorus loads from the sediments will most likely continue for some time following a decrease in anthropogenic phosphorus and OM loads (Larsen et al. 1981).

Table 24 provides average aerial sediment nutrient fluxes to Reaches 1–3 in the LJR, and Table 25 provides annual hydraulic reach sediment derived nutrient loads to the LJR. The sediments add over 5,000 kg of phosphate-P and 12,000 kg of ammonia-N to the LJR, but remove over 33,000 kg of nitrate-N from the water column. This results in the sediments removing roughly 21,000 kg of dissolved nitrogen from the water column annually. The LJR sediment derived ammonia and phosphate loads accounted for 5% and 1% of the total nutrient loadings discharged from the three online POTWs (Section 5.7.8).

Table 26 provides sediment fluxes measured in other freshwater and estuarine sediments under dark aerobic conditions. Fluxes of ammonia, nitrate, and phosphate can

Table 24. Sediment nutrient fluxes in the Lower Jordan River

	average sediment flux ($g/m^2/d$)			
site	NH_4-N	NO_3-N	TIN	PO_4-P
Reach 1	0.098	-0.361	-0.263	0.016
Reach 2	0.038	-0.028	0.010	0.052
Reach 3	0.106	-0.203	-0.098	0.087
Lower River	0.081	-0.197	-0.117	0.051

Table 25. Sediment nutrient loads to the Lower Jordan River

	Sediment Nutrient loading (kg/year)			
	Reach 1	Reach 2	Reach 3	LJR load
NH_4-N	6,455	1,352	4,332	12,139
NO_3-N	-23,738	-985	-8,343	-33,065
TIN	-17,283	368	-4,010	-20,925
PO_4-P	1,051	1,839	2,112	5,002

Note: data from 16 sampling events over 3 years

Table 26. Nutrient flux comparisons

Surface Water	Average sediment flux ($g/m^2/day$) NH_4-N	NO_3-N	PO_4-P	SOD	ref.
Anacostia River	0.205	-0.036	0.002	-2.2	1
Chester River	0.117	-0.006	0.011	-2.4	1
Potomac River	0.135	-0.007	0.009	-1.9	1
Chesapeake Bay	0.144	0.029	0.013		2
Chesapeake Bay	0.056	-0.011	0.011	-0.6	3
Yaquina Bay	-0.014	-0.135			4
Tagus Estuary		-0.018		-1.2	5
Firth of Thames Bay	0.342	0.026	0.012		6
Pacific cont. shelf	0.006	-0.01			7
WWTP biofilm nitri.		1 to 3			8
Lower Jordan River	0.081	-0.197	0.051	-1.9	9
Lower Jordan River	0.28	-0.551	0.216	-3.3	10

ref. and notes:
1 (Boynton et al. 2003) drains to Chesapeake Bay
2 (Boynton and Kemp 1985) one-year study
3 (Cowan and Boynton 1996) multi-year study
4 (Larned 2003) estuary wide flux
5 (Cabrita et al. 2000) largest wetland in Portugal
6 (Giles et al. 2006) mussel aquaculture sediments
7 (Christensen et al. 1987) offshore ocean sediments
8 (USEPA 1993) POTW design
9 This study, 2010 to 2013, 3-year average
10 This study, 2010 to 2013, 3-year maximum

vary considerably depending on historic water quality, sediment OM content, and sediment size. These parameters tend to be synergistic, such as large amounts of organic matter depositing with fine sediments while decomposing and influencing ambient WQ through nutrient cycling. Alternatively, sandy sediments may be downstream of a POTW discharging ammonia, which may lead to sediment and water column nitrification coupled with ambient DO deficits.

Sediment ammonia fluxes in the LJR were similar to degraded tributaries feeding Chesapeake Bay. Negative nitrate fluxes, or denitrification, in the LJR are the highest in

Table 26 This is hypothesized to be a result of elevated ambient nitrate concentrations originating from POTW discharges coupled with a source of sediment derived rbCOD diffusing from the anaerobic sediments in the LJR. Phosphorus fluxes were also higher in the LJR compared to the other waters presented in Table 26. The extremely high average P flux of 0.216 $g/m^2/d$ was measured at the 1700 S site in 2013 in a thick benthal deposit, highlighting the influence of benthal deposits on ambient WQ.

All surface waters are unique, and the nutrient dynamics occurring at the sediment–water interface coupled with ambient WQ, presence of toxins, sediment quality, current and historical nutrient and OM loadings, and trophic status all need to be taken into account to adequately describe the complex biochemical reactions influencing water quality.

5.5.3 Water column nutrient rates

The nutrient dynamics occurring in the WC during dark conditions are provided in Table 27. Ammonium and phosphorus were added to the WC during the degradation of water column BOD. Assuming the Redfield ratio, roughly 0.08 mg NH_4-N/L and 0.012 mg-P/L are added to the water column for every -1 g-DO/m^3/d as WC_{dark}.

Table 27. 3-year average dark WC rates in the LJR

	average WC dark metabolism rate ($g/m^3/d$)			
site	NH_4-N	NO_3-N	TIN	PO_4-P
Burnham	0.15	0.85	0.99	0.13
LNP NE	0.12	0.29	0.41	0.05
Cudahy Ln	-0.19	0.89	0.71	0.06
DWQ	-0.16	0.34	0.18	-0.09
700 S	0.09	1.59	1.68	0.27
1700 S-N	0.01	-0.42	-0.41	-0.05

Nitrate production rates associated with the two-step biological nitrification were high at all sites except the 1700 S-N site. The elevated nitrate production rates highlight the river's natural ability to transform ammonium-N into the less toxic nitrate-N (Malecki et al. 2004). The water column is oxygenated, contains abundant inorganic carbon, and has low rbCOD, allowing the slow growing autotrophic nitrifiers to establish a niche. Upstream of the South Valley WRF discharge (7600 S and 9000 S) the WC removed ammonia, nitrate, and phosphate (Table 28). Downstream of the discharge (5400 S), the WC behaved as a source of both ammonia and nitrate while removing less phosphate than upstream sites.

5.5.4 Fluxes in relation to other fluxes, SOD, WC_{dark}, and OM

Table 29 provides statistical relationships between sediment fluxes, WC rates, and other parameters measured during this research. The slope describes the sediment flux or WC rate for a particular dissolved nutrient in relation to ambient ammonia concentrations, surficial sediment %VS, and the simultaneously measured SOD and WC_{dark}. Positive slopes imply that the parameters are positively related and negative slopes indicate the opposite. Relationships between sediment fluxes and OM decay surrogates were all statistically significant ($p < 0.05$) with the exceptions of sediment P fluxes and sediment %VS and SOD. Correlations between water column rates, ambient

Table 28. Upper Jordan River dark WC nutrient dynamics

		Upper River WC dark metabolism rate ($g/m^3/d$)			
site	date	NH_4-N	NO_3-N	TIN	PO_4-P
5400 S	1/12/11	0.196	1.44	1.636	-0.039
7600 S	1/15/11	-0.025	-0.501	-0.526	-0.377
9000 S	1/20/11	-0.013	-0.125	-0.138	-0.365

Table 29. Relationships between fluxes and various OM decay surrogates

	Slope		p value		
Test	Sed.	WC	Sed.	WC	N
NO_3-N:NH_4-N	-	-	0.0006	0.75	27
PO_4-P:NH_4-N	-	+	0.002	0.35	26
PO_4-P:%VS	+		0.06		19
NH_4-N:%VS	+		0.01		19
NO_3-N:%VS	-		0.03		19
PO_4-P:SOD	+		0.05		25
PO_4-P:WC_{dark}		+		0.4	25
NH_4-N:SOD	+		0.01		25
NH_4-N:WC_{dark}		-		0.5	25
NO_3-N:SOD	-		0.03		25
NO_3-N:WC_{dark}		+		0.8	25

Notes: 0–2 cm %VS

ammonia concentrations, and WC_{dark} were all statistically insignificant ($p > 0.05$). The lack of correlations between water column rates and OM decay surrogates was a result of the vast majority of nutrients found in the water column originated from POTW loads.

Although insignificant, the negative and positive relationships between ammonia losses and nitrate production with increased WC_{dark} suggests water column nitrification, which was a prevalent water column metabolism in the LJR (Table 27). The positive correlations between sediment ammonia and phosphorus fluxes in relation to %VS and SOD is a result of OM decay. This is also supported by the inverse relationship between sediment nitrate removal, or denitrification, and sediment %VS. Denitrification at the sediment–water interface was the dominant nitrogen transformation measured in the LJR (Table 23).

5.5.5 Anoxic fluxes

Dissolved oxygen was removed from the SOD chambers through the addition of sodium sulphite to mimic anoxic conditions associated with an acute low DO event.

These events may occur during the die off of an upstream algal bloom or following a large urban storm event following an extended dry spell. By removing DO in the chamber, nitrification will stop, denitrification may increase, and polyphosphate accumulating organisms (PAOs) might release orthophosphate if rbCOD is available.

Fig. 65 provides a bar chart for sediment ammonia fluxes during aerobic (white bars) and anoxic (grey bars) conditions. Sediment ammonia fluxes increased during anoxia at all sites except the Cudahy Ln site, which had the highest ammonium fluxes measured in 2013. Anoxia resulted in a site average 15% increase in sediment ammonia fluxes in the LJR. When Cudahy Ln and the 1700 S sites are excluded, anoxia resulted in a 11% increase in ammonia fluxes. The 1700 S site had sediment %TS and %VS of 38% and 6% (Fig. 60, west bank) and a high CH_4 oxygen demand of 1.8 g-DO/m^2/d (see Chapter 5.6, west bank) in the west bank depositional zone where nutrient fluxes were measured. The benthal deposits present in depositional zones found in Reach 3, although less plentiful than downstream, are a source of ammonia to the LJR.

The removal of nitrate by the sediments increased at all sites during anoxia except the LNP NE and 700 S sites (Fig. 66). Anoxia resulted in a 3% increase in nitrate removal at the sediment–water interface and was associated with increased denitrification. The small increase in sediment denitrification during anoxia compared to background conditions is hypothesized to be a result of the sediments being anaerobic very close to the sediment–water interface during normal conditions. This would result in anoxic conditions influencing the sediment metabolism minimally since the sediments are already anaerobic.

Sediment phosphate fluxes decreased at all sites following anoxia (Fig. 67) except

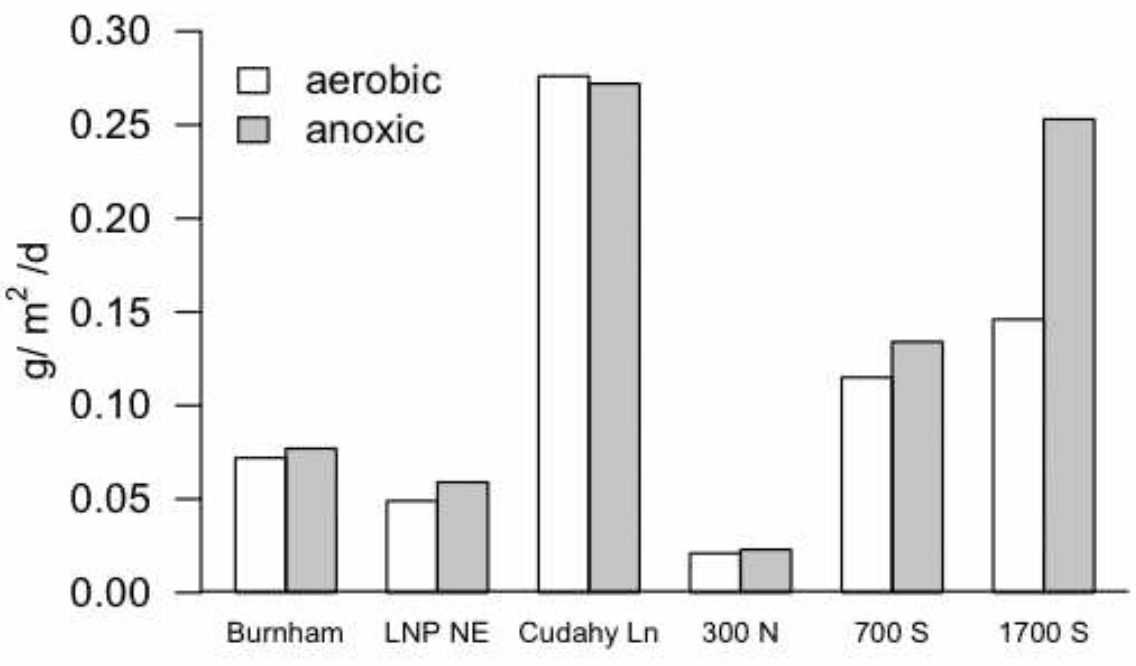

Fig. 65. Ammonia-N fluxes during anoxic conditions

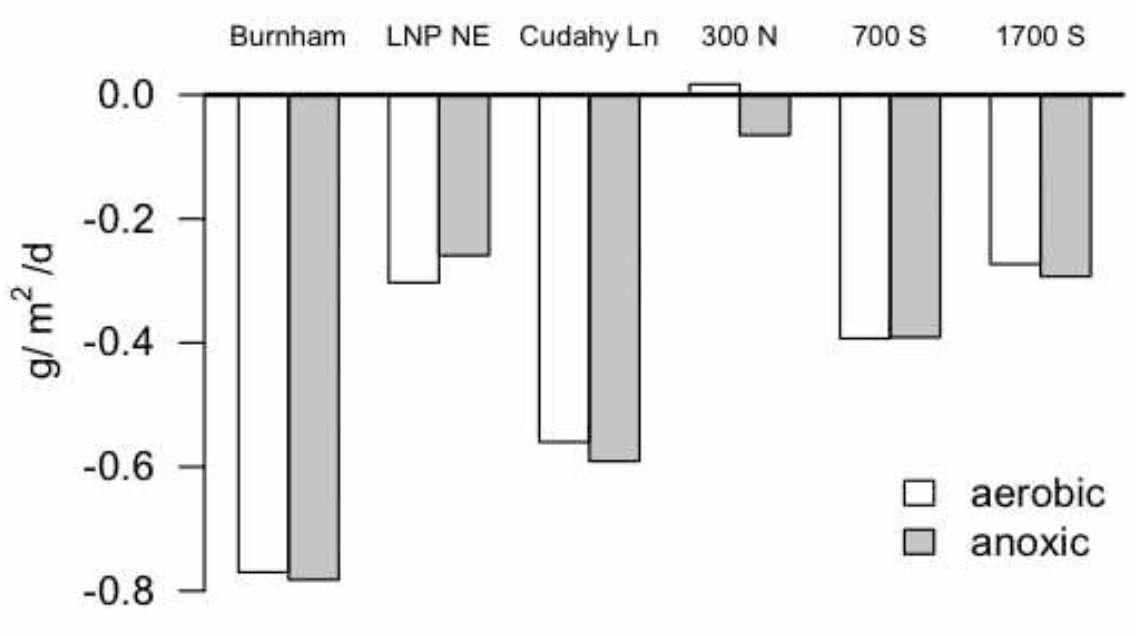

Fig. 66. Nitrate-N fluxes during anoxic conditions

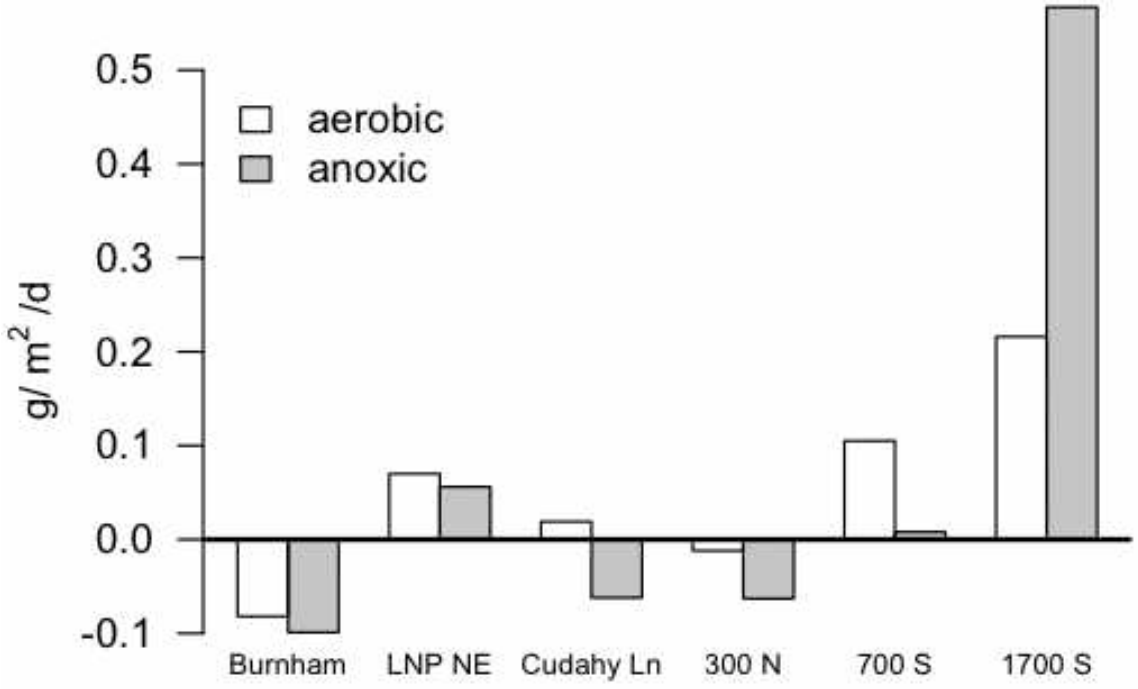

Fig. 67. Phosphate-P fluxes during anoxic conditions

for the 1700 S site. Although the other sites did not exhibit this large additional flux, the high phosphorus flux measured during aerobic conditions at the 1700 S suggest that benthal deposits found throughout the LJR are a source of dissolved phosphorus from the decay of sediment OM.

The onset of brief periods of anoxia in the Lower Jordan River will influence nutrient dynamics at the sediment–water interface slightly, but the general trend was that background fluxes were relatively uninfluenced by the 3-hour anoxic periods. This is most likely a result of the oxic-anoxic interface being very shallow in the sediment column (<2 cm).

5.5.6 pH lowering fluxes

The neutralizing of pH in the chambers while measuring nutrient fluxes was conducted to investigate the potential of increased nutrient loadings following changes in

water chemistry. Ammonia fluxes increased at all sites except the Burnham Dam site following pH lowering (Fig. 68). The increased ammonia fluxes are hypothesized to be a result of ion exchange between sorbed ammonium and the surface of organic and clay sediments. As pH decreases, additional hydronium ions, H_3O^+, are available to replace sediment sorbed ammonium cations (Mcnevin and Barford 2001).

The flux of orthophosphate from the sediments increased following reductions in pH at all sites except the 300 N site (Fig. 69). The calcareous inorganic sediments found in the LJR contain calcium bound P that could be liberated during decreases in ambient pH as part of the sediment buffering capacity. The average increase in DP fluxes from the sediments following the lowering of pH from 8 to 7 was 0.055 g-P/m^2/day (300 N excluded). This additional sediment phosphate load is greater than the suggested

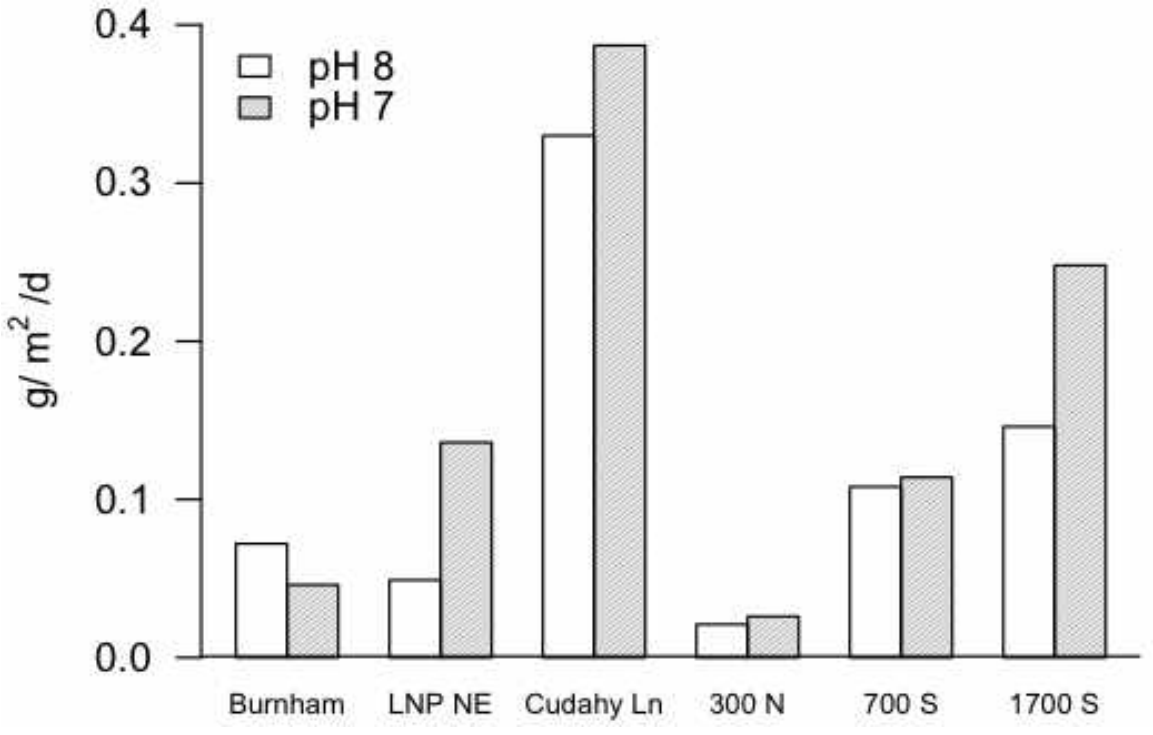

Fig. 68. Ammonia-N sediment flux following pH lowering

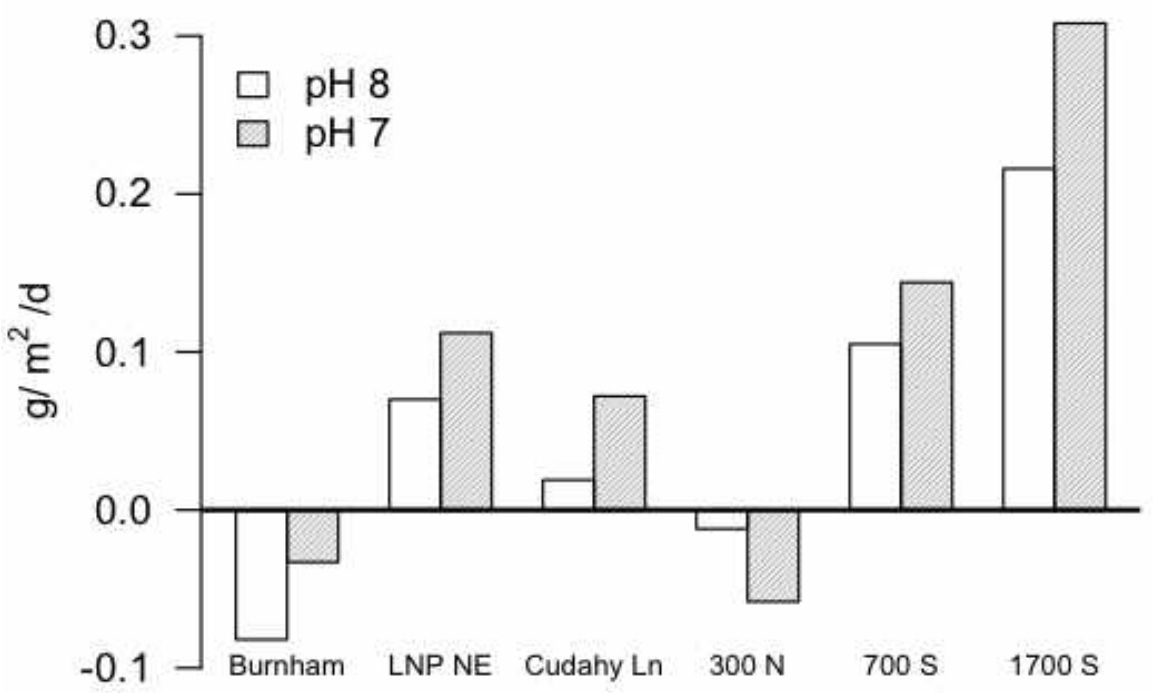

Fig. 69. Phosphate-P sediment flux following pH lowering

threshold concentration of 0.05 mg-P/L for a river draining to a lake (USEPA 1986), although with a LJR average ambient DP concentration of 0.37 mg-P/L (Table 22) the effects of sediment derived nutrient enrichment are minimal compared to the POTW nutrient discharge loads.

5.6 Methane Fluxes

5.6.1 River-wide sediment methane fluxes

The majority, up to 90%, of methane produced in the sediments is oxidized in the anoxic and aerobic zones of the uppermost sediment layers during diffusion (Wetzel 2001, pg. 642; Kuivila et al. 1988; Lidstrom and Somers 1984). Dissolved methane that is not oxidized in the sediments will be oxidized in the water column, further depleting ambient DO (Chapra 2008, pg. 458).

Fig. 70 provides the cumulative oxygen demand associated with methane production in the sediments ($CH_{4,OD}$) at three locations across the width of the river at depths of 0–2, 5, and 10 cm. Additional data can be found in Appendix H. The surface sediments were the most active in producing methane compared to deeper sediments. The east bank and thalweg at 1700 S produced no methane in the gravely sand substrate, but the benthal deposit near the west bank produced methane at fluxes similar to Reach 1. Surprisingly, the sediments at the LNP NE site produced very little methane across the

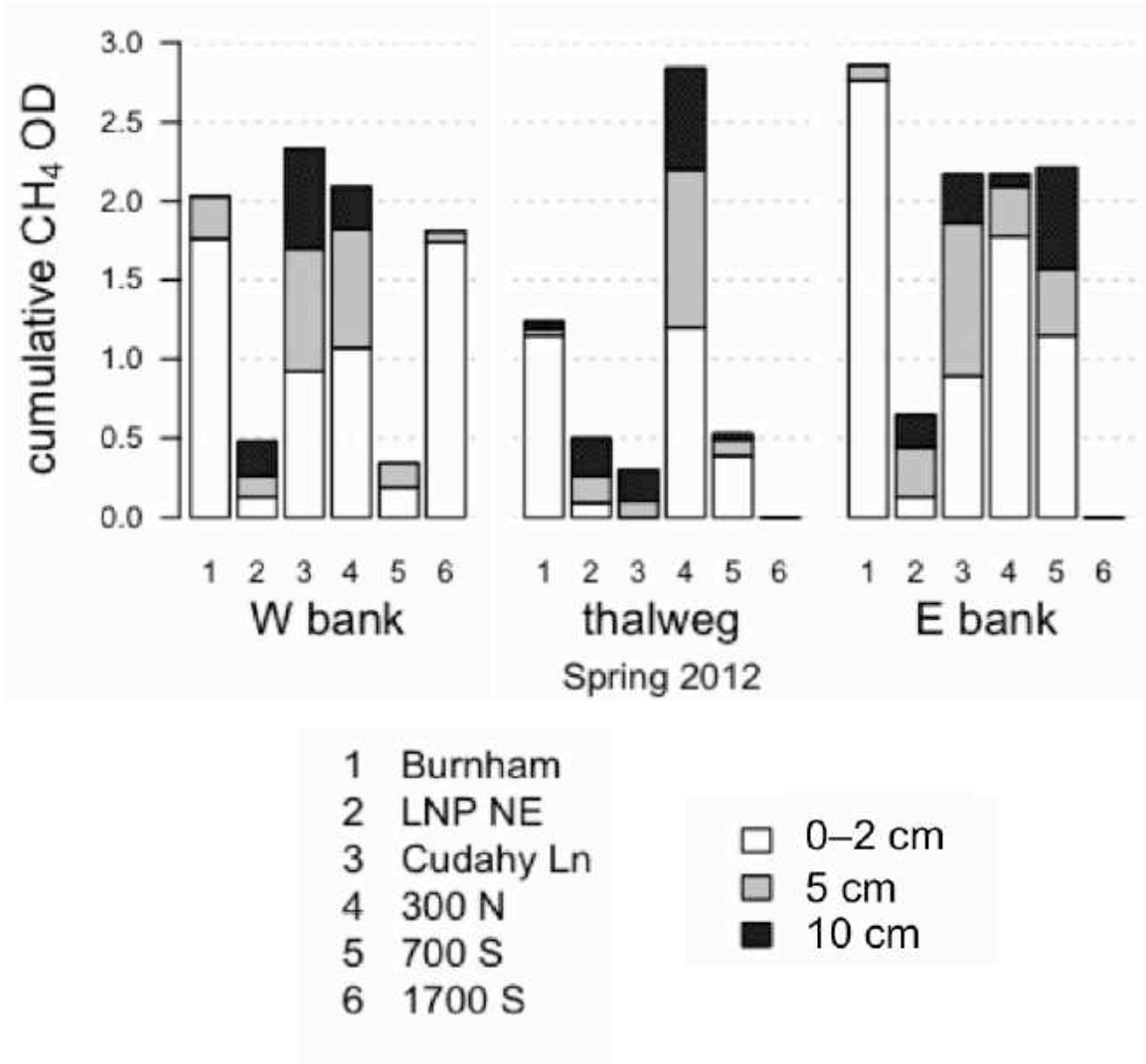

Fig. 70. Sediment column methane oxygen demand in the Lower Jordan River

width of the river and showed higher methane production rates at depths of 5 and 10 cm compared to the surface sediments. This was attributed to the influx and deposition of inorganic sediments from the 2011 high water event at this site.

Fig. 71 provides the river-wide average methane fluxes measured in 2012. The surface sediments were active in methane production throughout the LJR and were contributing to ambient oxygen deficits. The highest river-wide average surface sediment methane flux was measured at the Burnham Dam site in Reach 1 in the depositional zone located at the end of the Jordan River proper.

5.6.2 Swamp gas composition

Jordan River sediment biogas was composed of 60% methane by volume on average (Fig. 72). Prior researchers found methane contents ranging from 55–69% by

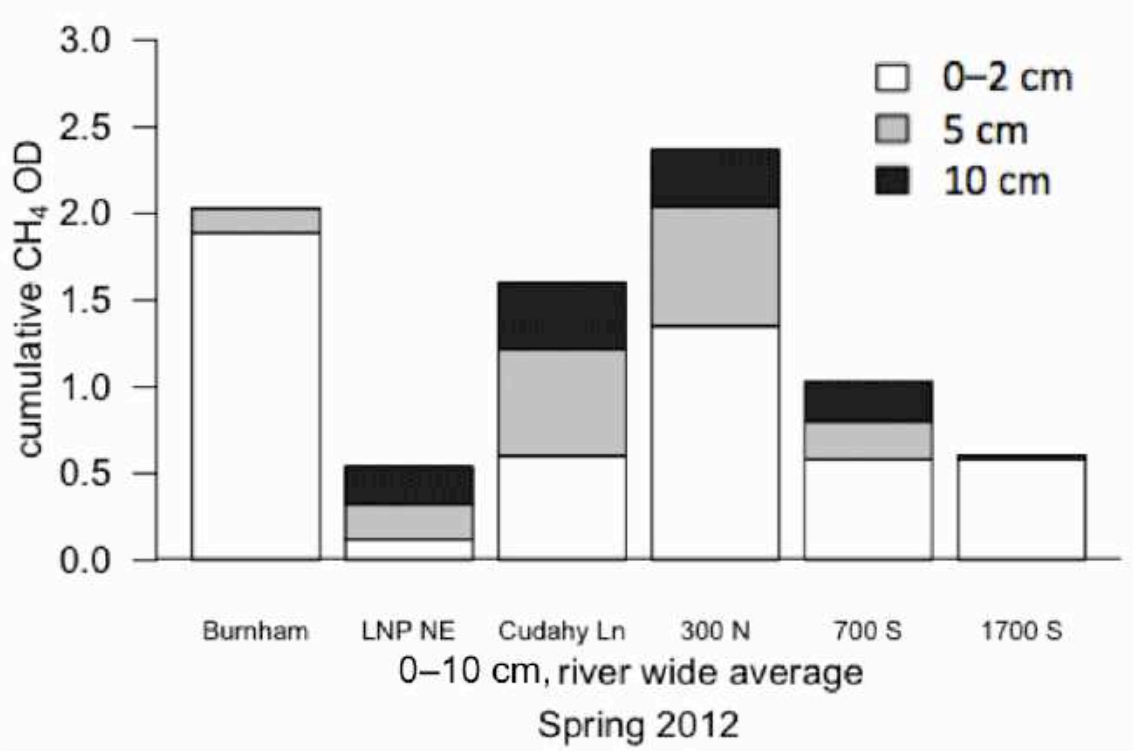

Fig. 71. River-wide average sediment column methane oxygen demand in the LJR

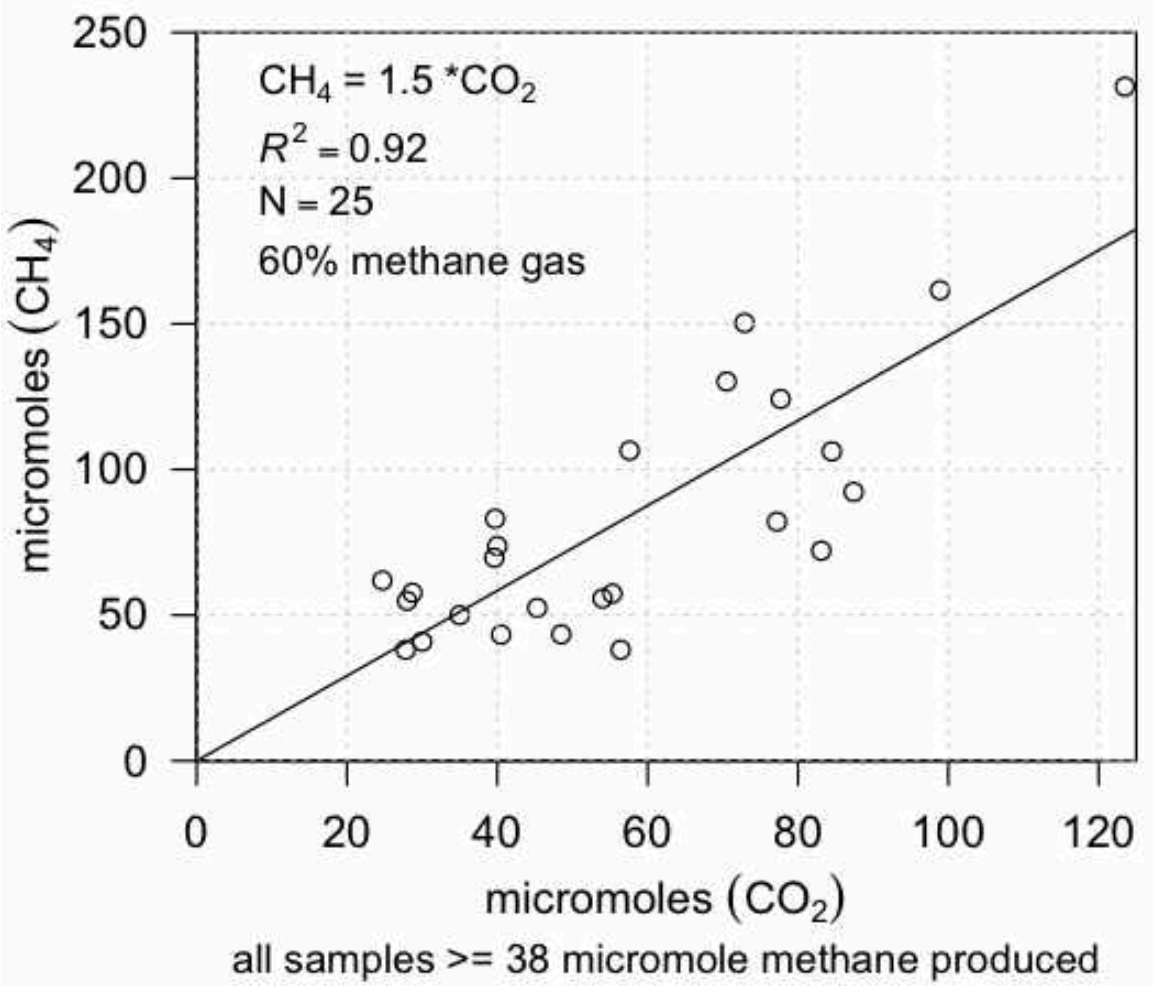

Fig. 72. Methane content of Lower Jordan River sediment gas

volume in the hypereutrophic Lake Postilampi, Finland (Huttunen et al. 2001). Typical methane concentrations found in biogas produced in a well-maintained POTW anaerobic digester is 60–70% methane (Appels et al. 2008; Deublein and Steinhauser 2008). The significance of this relationship is that for every mg of CH_4 gas oxidized at the sediment–water interface, a total of 1.67 mg of organic C was degraded in the sediments with 0.67 mg of CO_2 dissolving into the water column while contributing no additional ambient oxygen demand.

5.6.3 Sediment methane fluxes and %VS

Fig. 73 shows the relationship between the rate of sediment methane production and $\%VS_{bulk}$ at sediment depths of 0–2, 5, and 10 cm. Sediment methane fluxes were positively correlated with increased organic matter loadings (Kelly and Chynoweth 1981).

The surface sediments were the most active sediment layer in terms of methane production. The relationship between surface sediment %VS (0–2 cm) and the mass of methane produced per mass of wet sediment per day was

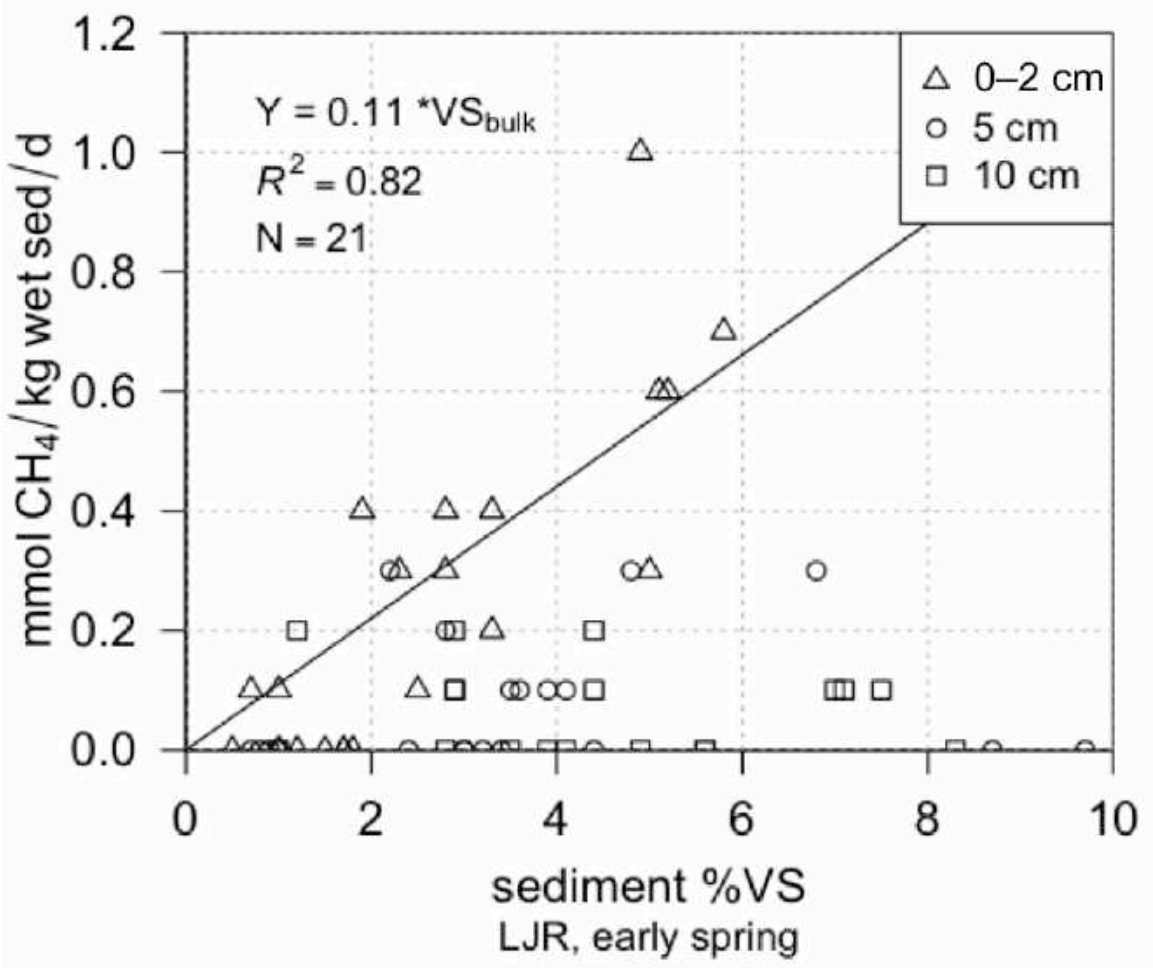

Fig. 73. Methane oxygen demand at different sediment depths

$$\frac{mmol\ CH_4}{kg\ wet\ sed * day} = 0.11 * \%VS \quad (23)$$

This relationship can be used to estimate the mass of methane produced in the surface sediments, but is not normalized to an aerial sediment flux. The sediments at depths of 5–20 cm (20 cm data not shown in Fig. 73) did produce methane in the LJR but at much slower rates, and the rates were decoupled from sediment OM content. Other studies observed that organic matter present in the top 20 cm of the sediment column served as substrate for methane generation, but methane production decreased with depth (Kelly and Chynoweth 1981). The surface sediments are the most recently deposited material and are more biologically active than deeper sediments that have already gone through a biological stabilization process (Fair et al. 1941).

After normalizing the Y-axis data points in Fig. 73 to an aerial estimate of methane oxygen demand, the relationship with 0–2 cm %VS becomes

$$CH_4OD = 0.32 * \%VS \quad (24)$$

$$CH_4OD = DO\ required\ to\ oxidize\ methane\ flux\ \left({}^{g\ DO}/_{m^2 * day}\right)$$

The above relationship can be used to estimate the surface sediment methane flux oxygen demand using sediment %VS as a surrogate in the LJR to help populate the Jordan River QUAL2kw model.

5.6.4 SOD and methane relationship

Methane oxidation associated with the top 0–2 cm of the sediments accounted for 56% of the measured SOD (Fig. 74). The remaining 44% of the SOD was associated with

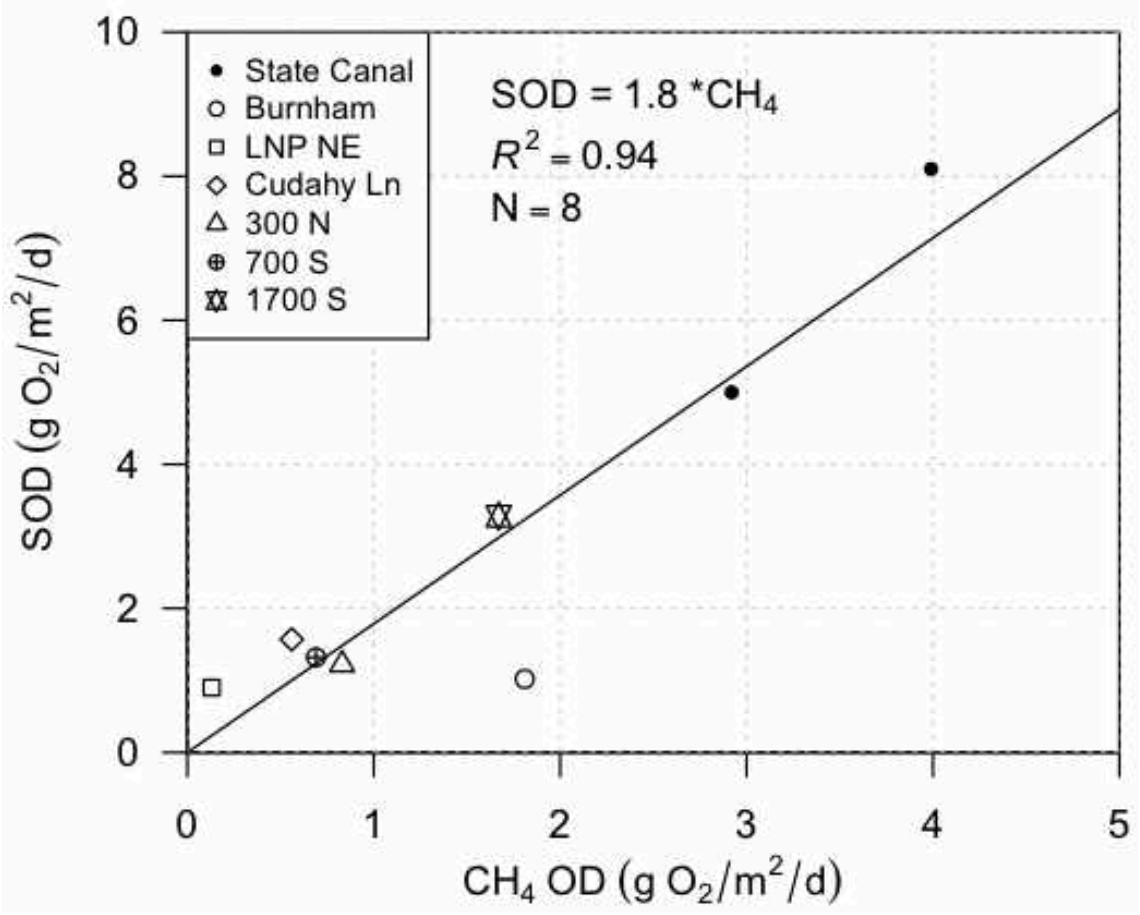

Fig. 74. Methane oxygen demand for different sediment depths

the faster aerobic metabolism at the sediment–water interface (Kristensen et al. 1995). The flux of other reduced chemicals, such as sulphide, will also exhibit an OD measured as SOD.

The sediments would require 2.5 to 4.8 years to cycle sediment OM under anaerobic conditions. This is much longer than the annual cycle (Fig. 64). The slower anaerobic sediment metabolism suggests that not all OM will be degraded in the sediments and recalcitrant OM will accumulate. This was observed in Fig. 73 where OM 5 cm and deeper did not undergo methanogenesis in a linear fashion.

5.6.5 Methanogenesis temperature dependency

Temperature dependencies were not observed for SOD, but were measured in the water column (Section 5.1.5 and 5.1.7). Table 30 provides Q_{10} values for methanogenesis rates in serum bottles collected during the winter months in State Canal, where the Q_{10} was roughly 2 at all eight tests. A Q_{10} of 2 implies that the metabolism will decrease by 50% if the temperature drops 10 °C and will double if the temperature increases by 10 °C.

A wide range in Q_{10} ratios ranging from 1.3 to 28 have been reported for methanogens. Additional factors such as quantity and quality of available substrates have been shown to heavily influence methanogenic activity at low temperatures (Kelly and Chynoweth 1981; Rath et al. 2002; van Hulzen et al. 1999). Temperature variations associated with SOD are assumed to be driven by the anaerobic sediment metabolism (Di Toro et al. 1990).

The general relationships between temperature and various metabolisms measured in the Jordan River during this study are provided on the following page.

Table 30. Q_{10} for methane production measured in State Canal

State Canal	Q_{10}
SOD_1	1.8
SOD_2	2.4
0–2 cm	1.9
0–2 cm	2
10 cm	1.8
0–2 cm	1.6
5 cm	1.9
10 cm	1.9
Mean	1.9

- WC_{dark} decreased with decreased ambient water temperature
- SOD was not influenced by decreased ambient water temperature
- sediment methane production measured in a laboratory setting consistently decreased by half when temperature decreased by 10 °C

This implies that other processes are occurring in the sediments of the Jordan River to maintain an annually consistent SOD flux. These may be attributed to

- Additional seasonal organic matter loadings occuring during autumn leaf shedding and during winter as urban stormwater runoff to provide additional substrate for sediment decomposition.
- Sediment methane production being always inhibited due to sediment diffusion limitations, leading to a constant annual flux of methane.

Both of these hypotheses are most likely occurring in the LJR.

5.6.6 Nutrient and methane fluxes

Sediment ammonia and phosphate fluxes were positively related to 0–2 cm methane fluxes ($p = 0.004$ and $p = 0.005$). Positive correlations between the amount of swamp gas and dissolved ammonia and phosphorus fluxes from the sediments were expected since all three of these parameters are associated with the anaerobic decay of OM.

Fig. 75 shows the relationship between nitrate consumption measured in the chambers and methane fluxes measured in serum bottles. The axes in this plot are presented as millimoles. Methane fluxes were a better predictor of sediment denitrification compared to ammonia and phosphorus fluxes. The dotted green line represents the theoretical stoichiometric relationship for denitrification utilizing methane.

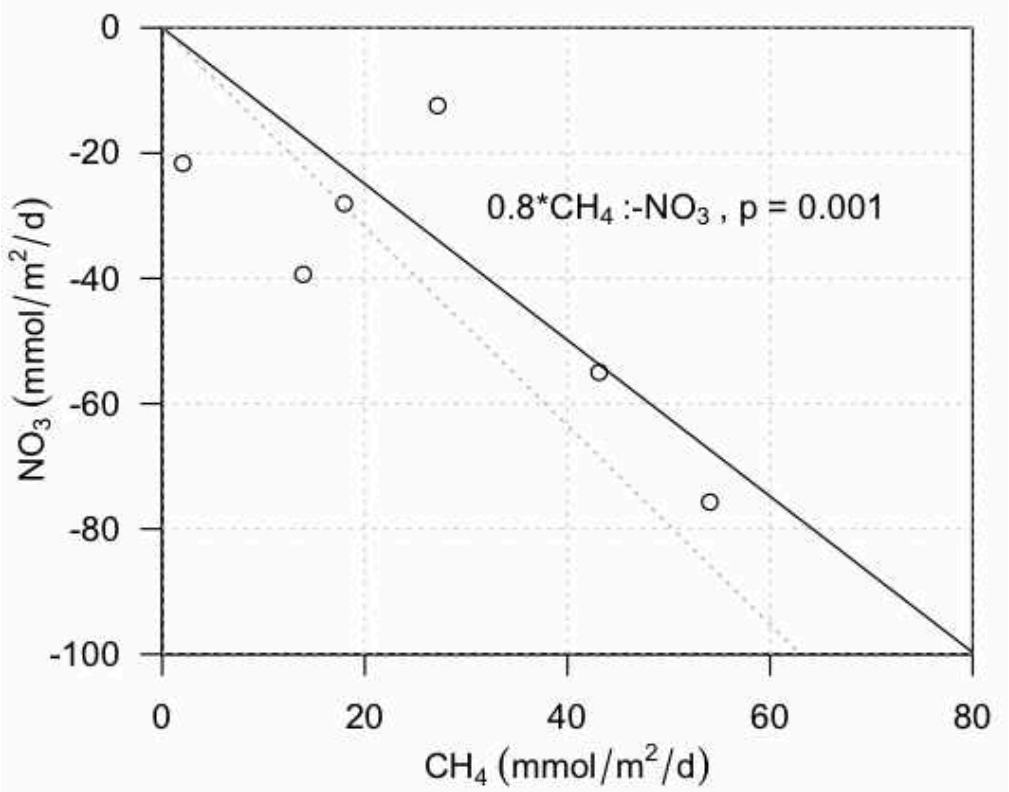

Fig. 75. 0–2 cm methane and nitrate molar fluxes

Fig. 75 predicts 0.8 moles of methane released from the sediments for every 1 mole of nitrate denitrified to dinitrogen gas. The ideal stoichiometric equation requires 0.63 moles of methane to reduce 1 mole of nitrate (Ahn et al. 2006).

$$5CH_4 + 8NO_3^- + 8H^+ \rightarrow 5CO_2 + 4N_2 + 14H_2O$$

Methane oxidized using nitrate as an electron acceptor will not be measured as an oxygen demand in the SOD chambers. The sediment methane fluxes calculated using lab techniques accounted for 50% of the SOD or 100% of the denitrification occurring at the sediment water interface. Other researchers calculated 42% of SOD being a result of methane oxidation (Gelda et al. 1995). In reality, methane is most likely being oxidized at the sediment–water interface utilizing both DO and nitrate as electron acceptors.

5.7 Jordan River DO and OM Mass Balances

5.7.1 Jordan River bathymetry

Jordan River cross sections were mapped at six sites and are provided in Fig. 76. The associated river-wide sediment sampling locations are represented by the black dots. The cross sections are presented as the river flows with the left and right representing the west and east banks, respectively. Bathymetry was obtained by measuring the depth of the Jordan River across the width at 2-feet intervals. Site bathymetry and calculated average flow velocities are provided in Table 31. The increase in calculated flow velocity in Reach 1 is a result of the cross-sectional area decreasing due to decreasing mean depths, a result of sedimentation behind Burnham Dam. The Lower Jordan River is managed for flood control in Salt Lake City and has very consistent mean daily flow rates throughout the year with the exception of storm events.

The river lengths and widths used to calculate standing stocks of OM in the Lower and Upper Jordan River are provided in Tables 32 and 33. These values were also used to calculate sediment derived nutrient loads to the LJR.

5.7.2 SOD chamber calculated OM decay rates

Estimates for OM degradation due to the seasonal average SOD and WC_{dark} using DO as a surrogate for decay are provided in Table 34. Assumptions used to convert an oxygen demand to the mass of oxidized dry OM are provided below Table 34. An estimated 355,896 kg/OM was oxidized in the LJR in the water column and at the sediment–water interface. SOD accounts for 54% of the ambient DO deficit in this scenario.

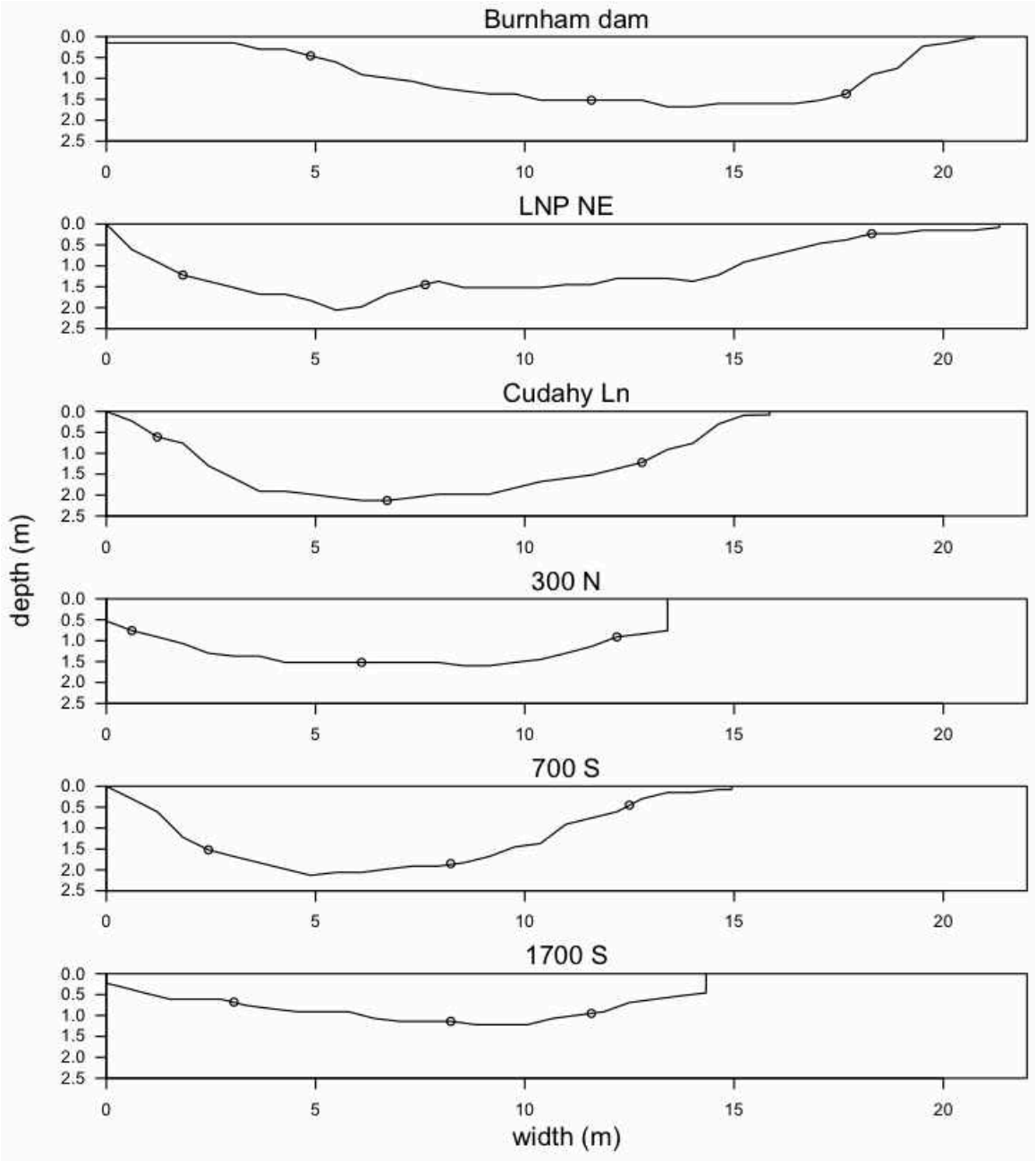

Fig. 76. Lower Jordan River cross sections and sediment sampling locations
Note: circles identify sediment sampling locations

Table 31. Site bathymetry and hydraulics

	mean depth (m)	width (m)	area (m^2)	flow* (cfs)	flow velocity (cm/sec)
Burnham Dam	1.0	21.0	18	235	37
LNP NE	1.2	21.0	20	240	34
Cudahy Ln	1.5	15.4	22	240	30
300 N	1.3	13.6	13	240	53
700 S	1.3	15.1	21	190	26
1700 S	0.9	14.5	19	165	24

*Mean annual daily flow = 250 cfs, 500 N (Salt Lake County gauge 960)
*Mean annual daily flow = 130 cfs, 1700 S (USGS gauge 10171000)

Table 32. Lower Jordan River hydraulic reach lengths, widths and depths

	length (m)	width (m)	% area of LJR	depth (m)
Reach 1	9000	20	46	1.5
Reach 2	7250	15	25	1.2
Reach 3	7250	15	29	1

Note: TMDL lengths (Table 1.1), measured widths
Note: Burnham to Burton dam section omitted from R1
Note: field measured depths

Table 33. Upper Jordan River hydraulic reach lengths and widths

	length (m)	width (m)	% area of UJR	depth (m)
Reach 4	14,150	19	25	0.8
Reach 5	2,750	17	5	0.8
Reach 6	18,000	15	32	0.5
Reach 7	6,750	11	12	0.3
Reach 8	15,450	38	27	1.2

Note: TMDL lengths (Table 1.1), Google Earth widths

Table 34. OM load estimates to and in the LJR

LJR annual SOD and BOD calculated OM decay loads (kg dry OM/year)				
	Reach 1	Reach 2	Reach 3	LJR
BOD_1	88,452	38,329	36,855	163,636
SOD	98,280	47,912	46,069	192,260
total	186,732	86,241	82,924	355,896

$BOD_1 = WC_{dark}$
used glucose equivalents to back calculate OM load
assumed BOD of 1.2 mg/L/d
assumed SOD = 2, 1.8, 1.5 for R1, R2, R3
$C_6H_{12}O_6 + 6O_2 = 6CO_2 + 6H_2O$
0.375 g-C/g DO
2 g-OM/g C
kg OM/year = (kg DO/day)*(12 kg C/32 kg DO)*(2 kg OM/kg C)*(364 d/yr)

5.7.3 NDM chamber OM production estimate

Using the seasonal average chamber NDM for the three sites in the UJR, a steady state annual OM load can be estimated using the following relationship:

$$\frac{kg\ dry\ OM}{yr} = NDM\left(\frac{g\ C}{2.67\ g\ O_2}\right)\left(\frac{g\ OM}{g\ C}\right)\left(\frac{365\ d}{yr}\right)\left(\frac{kg}{1000\ g}\right) * l * w \qquad (25)$$

$l = \ length\ of\ river\ (m)$
$w = \ average\ width\ of\ river\ (m)$

The instream production of OM based on the average UJR chamber derived NDM of 3 g-DO/m^2/d would produce roughly 540,000 kg dry OM/year (Table 35). This could account for 44% of the 1,221,491 kg OM/year estimated to enter the LJR at the Surplus Canal diversion (Utah DWQ 2013, Table 2.6, row A[1]).

The Surplus Canal diversion channels up to 90% of the annual stream flow from the LJR, but the majority of this water is diverted during spring runoff and base flow diversions are typically 50%. If 50% of the OM produced in the UJR entered the LJR

Table 35. UJR instream OM loads from primary production

kg OM/yr (chamber NDM)	
Reach 4	220,517
Reach 5	38,346
Reach 6	221,461
Reach 7	60,902
UJR total	541,225

during the 9 months of baseflow and the spring snowmelt is ignored, then 203,000 kg/yr of dry OM enters the LJR as macrophyte stocks, detached periphyton (metaphyton), and phytoplankton produced in the UJR. This would account for 17% of the OM load estimated to enter the LJR at the Surplus Canal diversion (Utah DWQ 2013, Table 3.9 upstream loads).

It should be noted that the Surplus Canal is an overflow weir and the LJR has an underflow dam design to direct additional flows associated with storm events and spring runoff down the Surplus Canal, not the LJR. The difference in dam design results in bedload CPOM entering the LJR, not the Surplus Canal. Therefore, if the remnants of yesterdays upstream primary production are transported downstream as bedload CPOM, not suspended sestonic matter, then the amount of OM entering the LJR will be higher than predicted with a 50% dilution based solely on streamflow diversions.

5.7.4 GW adjusted single-station OM production estimate

Upper Jordan River hydraulic reach based dry OM loads associated with primary production (PP) using the NDM estimated from the single-station diurnal DO model adjusted for GW having a DO concentration of 1 mg-DO/L are shown in Table 36. Instream contributions could account for 41% of the 1,221,491 kg OM/yr loading estimate to the UJR (Utah DWQ 2013, Table 2.6, row A^1).

Table 36. UJR GW adjusted OM production load estimate

	kg OM/yr (single-station GW adj. NDM)	
	avg NDM (g DO/m^2/d)	kg dry OM/yr
Reach 4	3.5	256,380
Reach 5	2.2	28,471
Reach 6	1.8	135,393
Reach 7	3.8	77,399
UJR total		497,644

NDM*(g C/2.67 g O)*(2 g OM/g C)*(365 d/yr)*length*width*(kg/1000 g)

5.7.5 Sediment column OM standing stock (Spring 2012)

Table 37 provides aerial depth integrated river-wide standing stock OM estimates. This table is cumulative; therefore the 10 cm depth includes OM present in the sediments at 0–2 and 5 cm depths. The $OM_{aerial,sum}$ is the dry mass of OM present in the wet sediments at each depth per square meter. The $OM_{aer,stretch,sum}$ and $CPOM_{aer,stretch,sum}$ represent the amount of dry OM and CPOM found in the river stretches defined in Table 32.

The surface sediments had similar OM standing stocks during the Spring of 2012. The lowest 0–2 cm OM standing stocks were found in the sandy surface sediments of LNP NE and 700 S following the 2011 UJR high water event. The amount of OM present at 5 cm and 10 cm depths steadily increased with distance downstream from the Surplus Canal diversion. The mass of OM in the top 10 cm doubled between 700 S and LNP NE, consistent with observed ambient DO deficits.

Table 38 provides Reach based sediment OM estimates for the top 10 cm of the sediment column calculated using the values found in Table 32. These values can be used to describe the existing stockpiles of sediment OM in the LJR.

Table 37. Site and river stretch sediment OM standing stocks

River-wide mean OM standing stock (depth cumulative)				
	depth (cm)	$OM_{aerial,sum}$	$OM_{aer,stretch,sum}$	$CPOM_{aer,stretch,sum}$
Burnham	0–2	71	3,953	133
	5	338	18,832	1,304
	10	576	32,118	1,857
LNP NE	0–2	42	1,902	216
	5	324	14,757	2,572
	10	580	26,474	5,580
Cudahy	0–2	66	5,016	1,256
	5	263	19,895	3,904
	10	470	35,535	6,568
300 N	0–2	61	5,245	2,182
	5	190	16,217	4,176
	10	314	26,776	5,963
700 S	0–2	43	2,179	885
	5	140	7,157	2,953
	10	271	13,815	4,587
1700 S	0–2	63	2,410	818

$OM_{aerial,sum}$ = g-OM/m^2/summed depth
$OM_{aer,stretch,sum}$ = Kg OM/river stretch/summed depth
$CPOM_{aer,stretch,sum}$ = Kg CPOM/river stretch/summed depth

Table 38. Reach based sediment OM standing stocks

$OM_{aerial,reach,summed}$ (kg dry OM, depth summed)				
depth	Reach 1	Reach 2	Reach 3	LJR OM
0-2	107,378	59,917	59,229	226,525
5	554,725	185,273	157,817	897,814
10	976,009	305,905	304,609	1,586,523

5.7.6 Riparian vegetation autumn leaf litter load estimate

Slow and fast leaf decay rates range from 0.5% to 1.5% of the mass per day (Cummins 1974; Sedell et al. 1974). This would require 1.25 years to degrade 90% of the mass of a slowly degrading leaf and 5 months for a rapidly degraded specie.

A crude estimate for fall leaf litter loads associated with riparian vegetation abutting the LJR is provided in Table 39. Based on aerial photography, the percent of the length of the LJR abutted by leaf shedding trees was visually estimated for all three hydraulic reaches. The trees are assumed to extend 3 meters over the river on both the east and west banks. The trees are assumed to drop a conservatively high 400 g-OM/m^2/yr during the fall leaf shedding and all leafs falling into the river settle to the sediments (Benfield 1997). For comparison, average annual riparian litterfall in the wet maritime climate of the Puget Sound, WA, was between 350–400 g-OM/m^2/yr (Roberts and Bibly 2009). In addition, it is assumed that 50% of the leaf litter that falls 3 meters onto land will laterally deposit in the river due to wind.

Table 39. Riparian leaf litter contribution to SOD estimate

	LJR Riparian vegetation leaf litter load estimate		
	% length	load (kg OM//yr)	SOD cycle (d)
Reach 1	10	3,240	12
Reach 2	35	8,190	62
Reach 3	30	8,100	64
total	24	19,530	37

% length = visual estimate of riparian vegetation
riparian vegetation estimated must drop leafs to be considered
load = fall leaf litter load, assume 400 g-OM/m^2/yr (Benfield 1997)
assume tree cover extends 3 m over river and all leafs enter river, both sides
assume 50% of leaf litter falling 3m into the riparian zone enters river
SOD cycle = days to oxidize leaf litter in sediments

Reach 1 is devoid of trees due to the alkaline soils associated with the flood plains of the Great Salt Lake, leading to a low percent length (% length) of the river abutted by riparian vegetation. If the leaf litter were evenly distributed over the sediments in each hydraulic reach and were completely oxidized at measured SOD fluxes, then the days required to oxidize riparian leaf litter in the sediments are provided in the last column of Table 39 as the "SOD cycle." These assumptions allow a comparison of riparian OM loads to the LJR and measured SOD decomposition rates.

Riparian vegetation litterfall would be degraded and oxidized to CO_2 in only 12 days in Reach 1. It takes an estimated 60 days for the sediments in Reaches 2 and 3 to cycle riparian leaf litter under these assumptions. When the full 19,530 kg dry OM is distributed evenly in the LJR, the sediments cycle the carbon in 37 days. 37 days is only 1/10 of a year, highlighting the reality of external and upstream OM loads degrading WQ in the urban LJR.

Low order pristine streams with a forest canopy have been shown to receive over 44% of the annual OM load as direct leaf litter (Fisher and Likens 1973). Although riparian leaf litter does add OM to the LJR, it is less than 2% of the estimated TMDL load to the LJR per the aforementioned assumptions.

The litterfall estimate accounts for 9% of the 0–2 cm sediment standing stock of OM measured during the Spring of 2012. Limiting riparian vegetation should not be viewed as a positive influence in urban WQ due to the meager OM load generated. The role of riparian habitat in providing shade and structure far outweigh the negative effects of the OM load associated with the urban riparian zone (Gregory et al. 1991).

5.7.7 OM loading and turnover estimate for the LJR

Fig. 77 shows the various types of OM observed in the LJR at different depths in the water column. In a lotic system, OM will settle, move downstream, break apart, and decay at different rates.

Table 40 provides a mass balance for OM in the LJR comparing data collected by the Utah DWQ and this research (Utah DWQ 2013). The rationale is that all OM that enters the LJR is either oxidized in the water column (WC_{dark}), remains suspended, and exits the LJR at Burnham Dam (VSS at Burnham), or settles to the bottom where it is either oxidized as SOD or accumulates as %VS. "BOD_1+SOD" was estimated in Section 5.7.2. "0–2 cm sediment VS" was the standing stock of sediment OM measured in the LJR during the Spring of 2012 and was estimated in Section 5.7.5. "NPDOC at Burnham" dam was calculated assuming 5 mg-C/L, a value typically measured in the LJR during this research (data not shown). "VSS at Burnham" dam is the mass of suspended dry OM that exits the LJR and was calculated assuming a volatile suspended solids (VSS) concentration of 8 mg VSS/L (Utah DWQ 2013, Fig. 3.2).

The "Utah DWQ" parameter is the TMDL estimated OM loads to the LJR (Utah DWQ 2013, Table 3.9). The "% unaccounted" is the percentage of the Utah DWQ estimate not accounted for in relation to the "measured total." The "forced total" parameter includes the OM found in the top 0–5 cm of the sediment column.

The parameters missing from this estimate include bedload CPOM, LWD, and the accumulation of sediment OM present in the backwaters of flow control structures. 49% of the "measured total" was associated with instream degradation processes (BOD_1+SOD), and 20% was associated with suspended VSS transported downstream

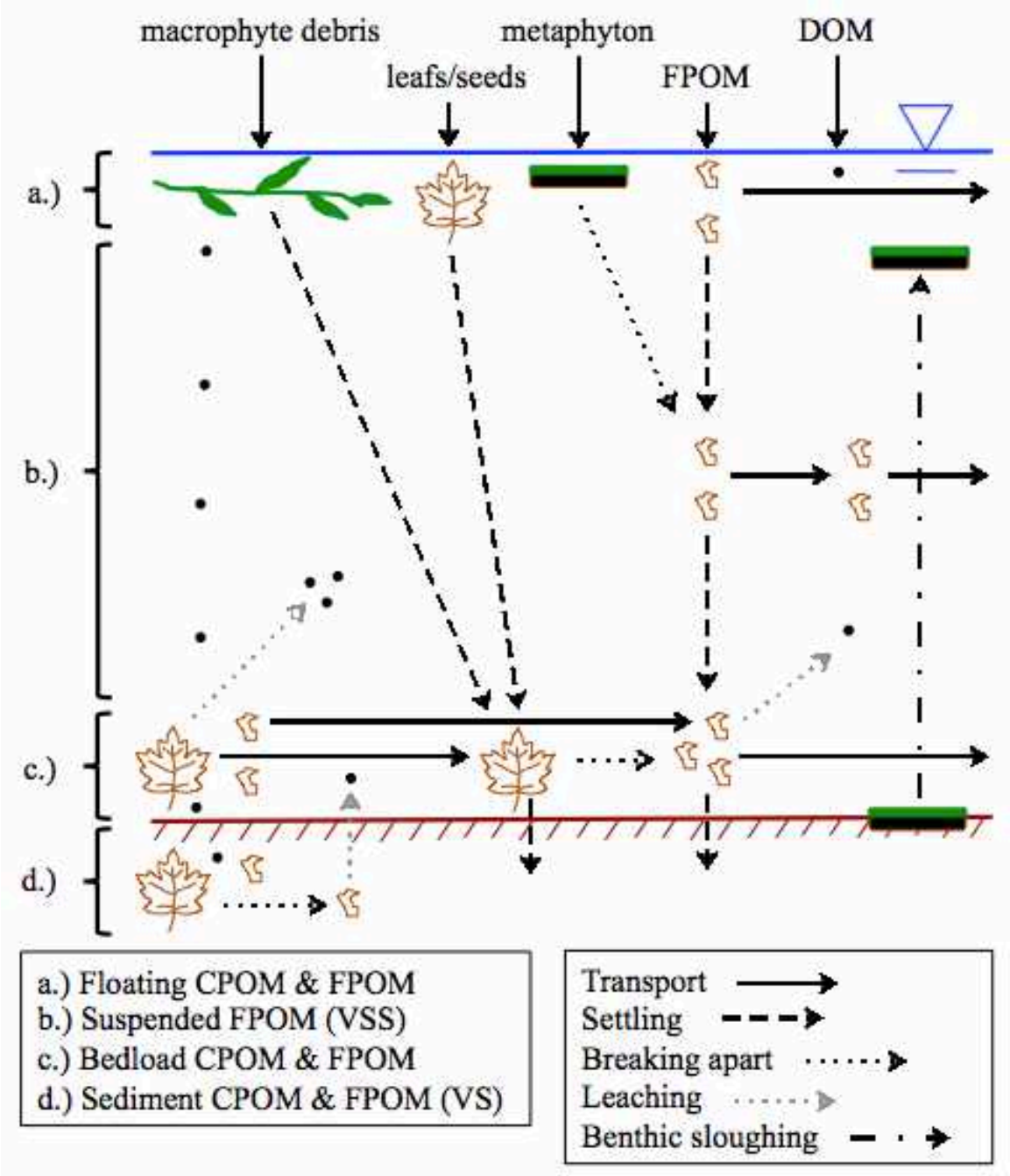

Fig. 77. OM loading schematic for mass balance

Table 40. OM load estimates to and within the LJR

LJR OM budget (kg dry OM/year)		Note:
BOD_1 + SOD	355,896	
0–2 cm sediment VS	226,525	a.
NPDOC at Burnham	176,601	b.
VSS at Burnham	141,281	c.
measured total	900,303	
Utah DWQ	2,225,523	d.
% unaccounted	60%	
Utah DWQ	1,004,031	e.
% unaccounted	10%	
forced total	1,394,992	f. and g.
% unaccounted	14%	

Notes:
a.) may be twice as high depending on time of year and other factors
b.) (5 g-C/m^3)(2 g-OM/g C)(200 cfs)(0.028 m^3/ft^3)(3153600 sec/yr)(kg/1000 g)
c.) (8 g VSS/m^3)(200 cfs)(0.028 m^3/ft^3)(3153600 sec/yr)(kg/1000 g)
d.) UJR and LJR loads
e.) LJR loads
f.) assumes top 5 cm of sediment contribute VS
g.) LJR load and 1/2 UJR load

into State Canal. The remaining 31% of the "measured total" was associated with surface sediment OM. 60% of the Upper and Lower Jordan River Utah DWQ OM load estimate is unaccounted for in relation to the "measured total." This large discrepancy may be attributed to the exclusion of OM associated with large woody debris (doubtful), bedload CPOM, and areas of extreme deposition. Another possibility is that the active sediment layer contributing to SOD and OM retention is deeper than 2 cm.

14% of the Utah DWQ organic load is missing when the UJR OM load is reduced by 50% and OM present in the top 0–5 cm are included in the standing stock of sediment OM. SOD would require 1.2 years to oxidize OM found in the top 0–2 cm of the

sediment column in this scenario, suggesting that OM is accumulating in the sediments, which is occurring, as shown by the presence of OM at depths greater than 5 cm (Fig. 60).

Fig. 78 provides a mass balance for the OM loading estimate. The red, green, and, black arrows represent loadings to the LJR, transport out of the system, and instream decay, respectively. Positive values mean OM is being added and negative values

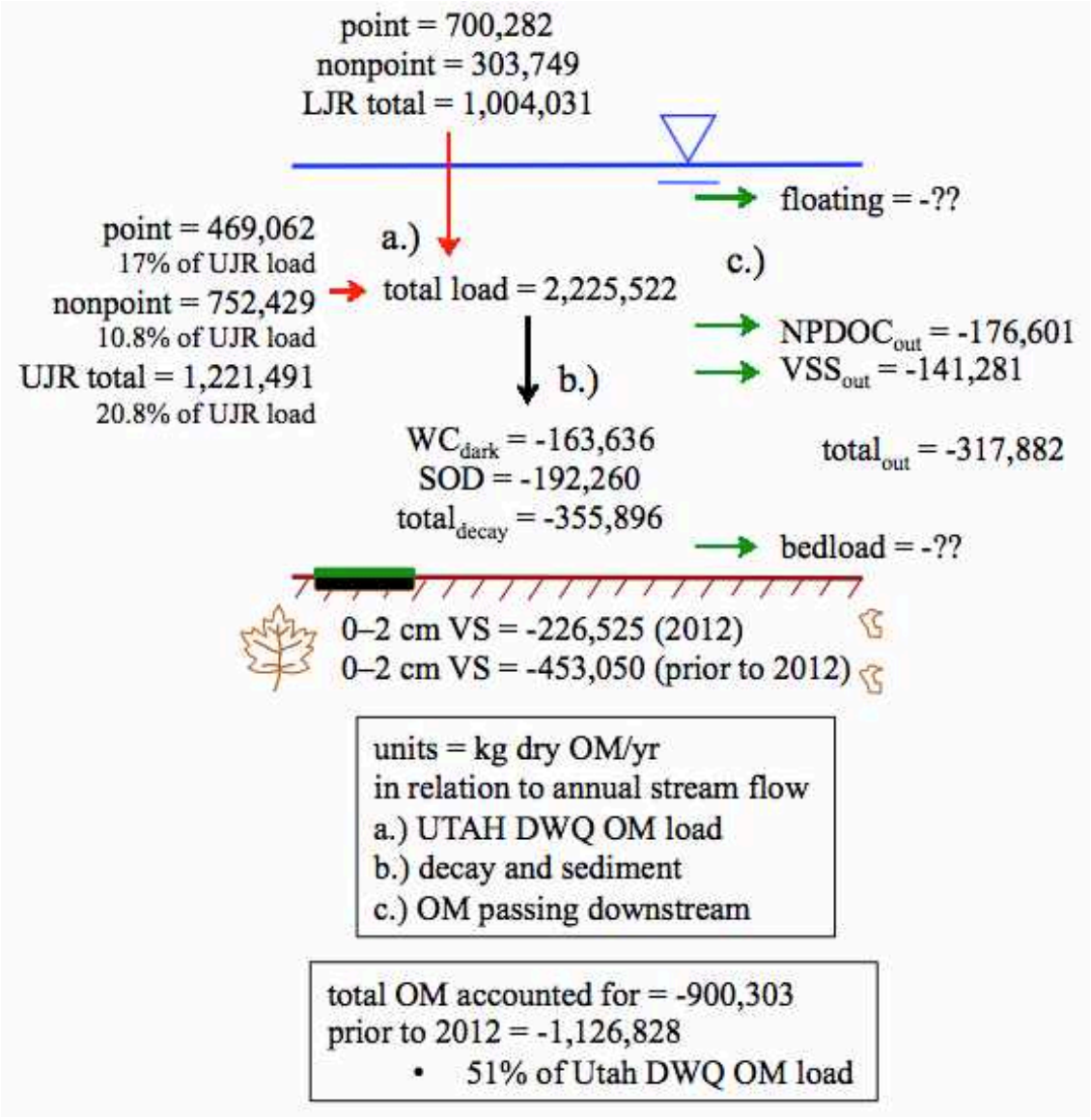

Figure 78. OM loading schematic for mass balance

represent OM losses.

The annual UJR chamber NDM OM production estimate was roughly 546,600 kg dry OM/year. This estimate would account for 57% of the Utah DWQ OM load in the UJR being a result of instream primary production with the benthos being the predominate source of primary production compared to phytoplankton. The annual UJR NDM OM estimated using the single-station diurnal DO model adjusted for GW resulted in a load of 286,400 kg dry OM/year, or 30% of the Utah DWQ UJR annual OM load. Although these estimates differ, the range of instream OM associated with photosynthesis ranges between 30–57% of the current estimated OM load to the UJR. Either way, the UJR River is a significant source of OM to the LJR as a result of eutrophication.

5.7.8 Sediment vs. POTW nutrient load comparison

Table 41 provides annual ammonium and orthophosphate loads to the Jordan River from POTW effluent calculated using average discharge concentrations and flow rates. Table 42 shows the percentage of the ambient dissolved nutrients in the LJR water column resulting from sediment OM decay compared to POTW discharges. The first column compares the LJR sediment load and the South Davis-S WWTP discharge in Reach 1. The sediments in the LJR are responsible of 36% and 43% of the ambient dissolved nutrients when the upstream WWTP discharges are ignored. The internal cycling of nutrients between the sediments and WC accounted for 28% and 21% of the total loads of the total N and P to the St. Johns River (Malecki et al. 2004).

The relatively low flow (3 MGD vs. 30+ MGD) of South Davis-S (SD-S) WWTP is the reason why the sediments are responsible for over 1/3 ambient dissolved nutrients in the LJR under this scenario. In reality, nutrients associated with POTW discharges are

Table 41. Nutrient loads associated with POTW discharges

WWTP nutrient loading (kg/year)			discharge (mg/L)		flow
	NH_4-N	PO_4-P	NH_4-N	PO_4-P	MGD
SD-S WWTP	21,840	6,552	5	1.5	3
CVWRF	128,419	228,301	1.8	3.2	49
SVWRF	83,866	135,117	1.8	2.9	32
Total	234,125	369,970			

Table 42. Sediment nutrient and POTW load comparison

% of sediment nutrient load vs. WWTP load			
	SD-S WWTP	SD-S + 1/2 CVWRF	all 3 POTWs
NH_4-N	36	12	5
PO_4-P	43	4	1

Note: % = sed. load/(sed. load + WWTP load)

already present in the WC at the start of the Lower Jordan River. To account for this, the second column includes South Davis-S and 50% of the effluent from CVWRF since the other 50% is assumed to be diverted down Surplus Canal during base flow conditions. In this scenario 12% and 4% of the ambient ammonium and phosphate were a result of OM decay in the sediments. The final column compares the sediments in the LJR to the annual nutrient loads associated with all three of the POTWs. In this scenario only 5% and 1% of the ambient nutrients were a result of sediment OM decay. The sediments are a source of the macronutrients N and P, but the contribution associated with POTW loads is much greater in the Jordan River.

CHAPTER 6

CONCLUSIONS

The key conclusions and linkages from the results of this research are provided in Fig. 79. The following descriptions summarize the five main research topics in terms of the relationship to the other topics and are presented in a clockwise fashion.

SOD in the Jordan River is a result of the oxidation of OM. Positive ammonium and orthophosphate sediment fluxes indicate OM decay, and the associated ammonia load will create a future NBOD demand in the water column during biological nitrification. Surficial sediment %VS was a reliable surrogate to estimate SOD in the silty sediments of the LJR, and 50% of the volatile matter was present as organic carbon. Roughly 1/3 of the surficial sediment OM found in Reaches 2 and 3 were present as CPOM, suggesting leaf litter associated with riparian vegetation and a terrestrial load associated with urban stormwater. Methane production in the surficial sediments could account for 50% of the observed SOD. The autotrophic NDM of the UJR may contribute up to 55% of the OM estimated by the Utah DWQ to enter the UJR (Utah DWQ 2013). This upstream OM load associated with eutrophication contributes to the DO deficits in the LJR.

Sediment ammonia and orthophosphate fluxes were positively related to sediment OM, while nitrate fluxes were inversely related to sediment OM due to denitrification. Dissolved ammonia and phosphorus fluxes were also positively related to methane fluxes. The strongest correlation between sediment methane and nutrient fluxes was

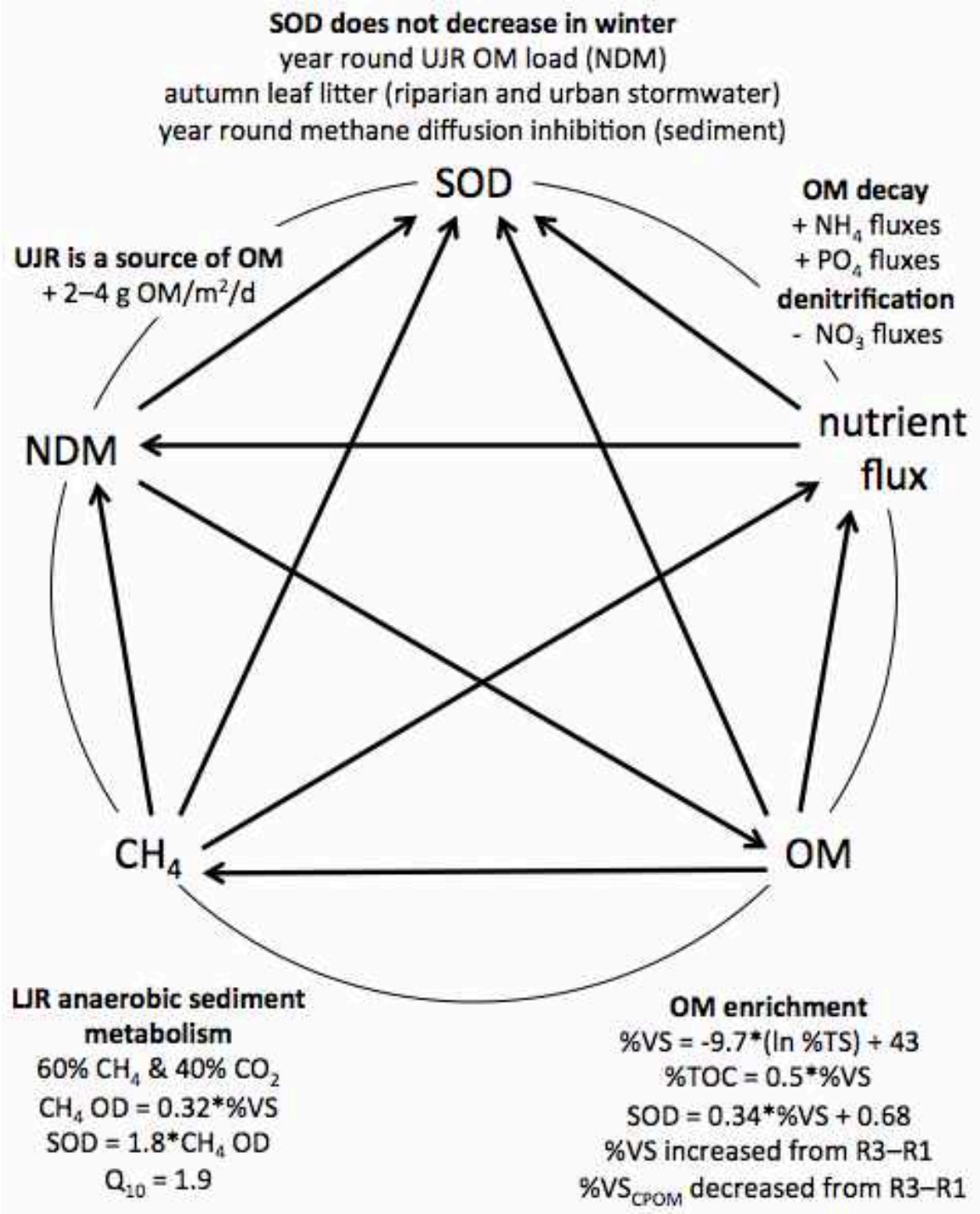

Fig. 79. Research linkages and key observations

denitrification, where denitrification fluxes were similar to the stoichiometric methane fluxes required to support the observed denitrification rates.

Sediment methane fluxes were positively related to sediment OM, and the swamp gas produced was roughly 60% methane and 40% carbon dioxide. Sediment methanogenesis was inversely related to ambient water temperature, unlike SOD and NDM.

In general, NDM was inversely related to positive ammonia, orthophosphate, and methane fluxes in the LJR. The UJR maintained a positive annual NDM, even upstream of WWTP discharges where ambient nutrient concentrations are the lowest in the river, yet high enough to support phototrophic growth. This implies that nonpoint sources, Utah Lake, and groundwater are providing ample nutrient loads to support eutrophication in the UJR.

Provided below are the objectives for this research and a list of observations and conclusions:

Objective 1: Measure seasonal SOD at locations representative of reach based sediment characteristics, downstream and upstream of wastewater and stormwater discharge points, and in other local surface waters.

- SOD fluxes increased with distance downstream in Reaches 3 to 1 (R_3 = -1.5, R_2 = -1.9, and R_3 = -2.3 g-DO/m^2/day).
- Reach 1 SOD fluxes suggest polluted sediments in regards to OM enrichment.
- The sediments were responsible for over 50% of the ambient DO deficit in the LJR during summer months during the majority of the sampling events

and over 75% of the DO deficit during more than half of the sampling events.

- SOD decreased for 1 year throughout the LJR following an influx of inorganic sediments associated with upstream erosion resulting from the unusually large snowpack in the Wasatch Mountains in the winter of 2010–2011.
- SOD fluxes did not decrease during the cold winter temperatures, but water column respiration (WC_{dark}) rates decreased.
- The upstream Utah Lake's water column was more active in terms of ambient lake dark metabolism compared to the sediments, implying that Utah Lake is a source of phytoplankton and sestonic OM to the downstream Jordan River.
- The downstream State Canal had the highest SOD fluxes measured (-6 to -8 g-DO/m^2/d), implying that the sediments downstream of the DO impaired LJR are increasingly enriched with OM along a gradient driven by topography

Objective 2: Evaluate the flux and fate of nutrients as they interact with the sediments and water column using SOD chambers during in situ conditions and after manipulating chamber DO and pH.

- During ambient dark conditions, the LJR sediments released ammonia and orthophosphate at average fluxes of 0.08 g-N/m^2/d and 0.05 g-P/m^2/d as a result of OM decay. The sediments removed nitrate at a flux of -0.2 g-N/m^2/d due to denitrification at the sediment–water interface.

- The WC produced nitrate at an average rate of 0.53 g-N/m^3/d during ambient conditions (WC nitrification).
- Anoxic conditions increased sediment ammonia and denitrification fluxes by roughly 10% and 3%, respectively. Phosphorus fluxes tended to decrease under anoxic conditions.
- Lowering pH from 8 to 7 units resulted in an additional PO_4-P sediment flux of 0.055 g-P/m^2/d.
- The sediments are a source of macronutrients in the LJR and will continue to be for some time due to OM decay.

Objective 3: Evaluate the contribution of primary production to DO dynamics and organic carbon fixation using transparent SOD chambers and diurnal ambient water quality data.

- The benthos were responsible for the majority of stream respiration and primary production (65% of light and dark metabolism).
- The UJR is a year round source of instream produced OM at a NDM flux between 2–4 g-DO/m^2/d (chamber measured).
- The single-station diurnal DO NDM model predicted autotrophic conditions in the UJR after adjusting for low DO groundwater intrusion (NDM = 1–4 g-DO/m^2/d in the UJR).
- 30–57% of the estimated Utah DWQ UJR OM load is a result of instream primary production (546,638 kg OM/year). A portion of this OM is a direct result of eutrophication.

Objective 4: Obtain sediment core samples at locations selected for SOD studies

and quantify the bulk sediments and fine/coarse particulate organic matters in terms of %TOC, %TS, and %VS to establish correlations between SOD and these parameters.

- %VS is a great surrogate for sediment OM in the LJR and 50% of the %VS is organic carbon (%TOC = 0.502 * %VS), whereas 37% of the %VS in the upstream Utah Lake is organic carbon.
- The surface sediments had a higher water content compared to the more compact subsurface sediments.
- 0–10 cm sediment column OM standing stocks increased from Reach 3 to 1.
- 0–10 cm sediment column $\%VS_{CPOM}$ decreased from Reach 3 to 1, suggesting CPOM may be from stormwater (FPOM sources are inconclusive since it may be degraded CPOM).
- Over 33% of the OM found in the surface sediments of Reaches 2 and 3 were CPOM.
- Surface sediment %VS is a practical surrogate for estimating SOD without chambers in the LJR (SOD = 0.34 * %VS + 0.68).

Objective 5: Evaluate methane fluxes from the sediments in the Lower Jordan River.

- Sediment gas composition was 60% CH_4 and 40% CO_2.
- The surface sediments (0–2 cm) produced the most methane compared to deeper sediment depths (5, 10, 15, and 20 cm).
- Methane production was positively related to surface sediment OM (CH_4 OD = 0.32 * $\%VS_{bulk}$).

- Sediment methanogenesis had a Q_{10} of 1.9.
- Methane fluxes from the top 0–2 cm of the sediment column could account for 56% of the observed SOD (SOD = 1.8 * CH_4 OD).
- Denitrification at the sediment–water interface was related to methane fluxes (1 mole of nitrate reduced for every 0.8 moles of methane).

APPENDIX A

SOD AND WC_{dark} DATA TABLES

Table 43. SOD measurements (a)

site	date	SOD_1	SOD_2	SOD_{avg}
State Canal	2/6/13	-5	-8.13	-6.57
Burnham	9/10/11	-1.32	-1.72	-1.52
Burnham	6/12/12	-1.02		-1.02
Burnham	6/14/13	-1.90	-4.80	-3.35
LNP NE	7/3/09	-4.17	-1.68	-2.93
LNP NE	10/10/09	-1.61	-1.71	-1.66
LNP NE	10/16/12	-1.77	-2.16	-1.97
LNP NE	1/9/10	-3.46	-2.6	-3.03
LNP NE	6/3/10	-2.67	-2.72	-2.70
LNP NE	7/16/10	-3.37		-3.37
LNP NE	8/24/10	-1.65		-1.65
LNP NE	12/25/10	-2.04	-2.88	-2.46
LNP NE	9/12/11	-1.63	-2.01	-1.82
LNP NE	4/3/12	-0.64	-1.15	-0.90
LNP NE	6/15/12	-1.78	-1.62	-1.70
LNP NE	6/15/13	-1.50		-1.50
LNP SW	7/3/09	-3.33	-2.5	-2.92
LNP Upper-N	8/25/09	-2.27	-2.11	-2.19
Cudahy Ln	10/10/09	-1.99	-2.38	-2.19
Cudahy Ln	1/16/10	-2.27	-2.8	-2.54
Cudahy Ln	6/3/10	-3.54	-3.04	-3.29
Cudahy Ln	6/13/12	-1.23	-1.92	-1.58
Cudahy Ln	6/13/13	-2.42	-4.17	-3.30
1700 N	9/14/11	-1.88	-2.24	-2.06
DWQ	6/29/09	-1.55	-1.84	-1.70
DWQ	1/17/10	-1.15	-1.15	-1.15
DWQ	6/7/10	-2.83	-3.53	-3.18
DWQ	7/15/10	-1.84		-1.84
DWQ	8/31/10	-4.15	-1.12	-2.64
DWQ	1/6/11	-1.14	-2.05	-1.60
DWQ	2/8/12	-0.78	-0.72	-0.75
DWQ	4/14/12	-0.73	-1.72	-1.23
300 N	6/12/13	-2.02	-2.65	-2.34
700 S	6/14/12	-1.1	-1.54	-1.32
700 S	6/10/13	-1.25	-1.78	-1.51

Note: g $DO/m^2/day$

Table 44. SOD measurements (b)

site	date	SOD_1	SOD_2	SOD_{avg}
900 S-N	6/26/09	-1.88	-0.69	-1.29
900 S-N	1/14/10	-2.11	-1.98	-2.05
900 S-N	6/8/10	-1.66		-1.66
900 S-S	6/26/09	-1.1	-1.96	-1.53
900 S-S	1/14/10	-1.02	-0.82	-0.92
900 S-S	6/8/10	-1.05	-0.79	-0.92
1300 S	9/13/11	-2.26		-2.26
1700 S-N	6/25/09	-1.05		-1.05
1700 S-N	6/26/09	-0.72	-0.49	-0.61
1700 S-N	7/8/09	-0.92	-0.75	-0.84
1700 S-N	1/10/10	-1.02	-1.88	-1.45
1700 S-N	5/24/10	-1.52	-2.12	-1.82
1700 S-N	9/15/11	-1.68	-1.8	-1.74
1700 S-N	4/16/12	-3.4	-3.16	-3.28
1700 S-N	6/10/13	-2.05	-3.28	-2.66
1700 S-S	7/14/10	-1		-1.00
1700 S-S	1/3/11	-0.63	-1.58	-1.11
2100 S	8/25/10	-1.09		-1.09
2100 S	1/7/11	-1.25	-2.14	-1.70
2300 S	7/7/09	-1.44	-1.08	-1.26
2300 S	1/17/10	-3.56	-3.66	-3.61
2600 S	6/2/10	-4.69		-4.69
2780 S-E	8/25/09	-1.85	-1.35	-1.60
2780 S-E	1/23/10	-5.07	-2.11	-3.59
2780 S-W	8/25/09	-2.42	-3.5	-2.96
2780 S-W	1/23/10	-2.5		-2.50
3600 S	8/26/09	-1.3	-0.64	-0.97
5400 S	7/16/09	-3.06	-1.67	-2.37
5400 S	1/12/10	-3.38	-2.66	-3.02
5400 S	7/19/10	-2.65		-2.65
5400 S	9/2/10	-0.11	-8.32	-4.22
5400 S	1/12/11	-2.16	-5.44	-3.80
7600 S	7/20/10	-6.69		-6.69
7600 S	9/1/10	-1.49	-0.66	-1.08
7600 S	1/15/11	-3.02	-5.37	-4.20
7800 S	7/16/09	-2.51	-0.2	-1.36
7800 S	1/12/10	-1.19		-1.19

Note: g $DO/m^2/day$

Table 45. SOD measurements (c)

site	date	SOD_1	SOD_2	SOD_{avg}
9000 S	7/16/09	-2.65		-2.65
9000 S	1/16/10	-0.99	-0.79	-0.89
9000 S	7/21/10	-0.82		-0.82
9000 S	9/3/10	-1.98	-0.85	-1.42
9000 S	1/20/11	-1.36		-1.36
SR-154	7/19/09	-2.44	-1.09	-1.77
14600 S	7/17/09	-1.67	-2.13	-1.90
US-73	7/17/09	-2.43	-1.94	-2.19
US-73	1/24/10	-0.49	-1.16	-0.83

Note: g DO/m^2/day

Table 46. SOD measurements (Utah Lake)

site	date	SOD_1	SOD_2	SOD_{avg}
Ut LK outlet	9/30/11	-1	-0.9	-0.95
Provo Bay	9/14/10		-5.21	-5.21
Geneva Steel	9/24/10	-2.09	-2.49	-2.29
Outside marina	8/2/12	-1.42	-1.19	-1.31
Goshen Bay	8/3/12	-1.42	-1.41	-1.42
Provo Bay entrance	8/3/12	-1.54	-1.12	-1.33
Goshen Bay entrance	8/4/12	-0.65	-1.06	-0.86
Pelican Point	8/4/12		-1.97	-1.97

Note: g DO/m^2/day

Table 47. WC_{dark} oxygen demand measurements

	WC_{dark} (g/m^3/day) or (mg/L/day)								
	Summer 2009	Jan. 2010	Jun. 2010	July 2010	Aug. 2010	Jan. 2011	Sept. 2011	June 2102	June 2103
Burnham							-0.58	-0.89	-0.49
LNP NE	-0.64	0	0	-0.96	-0.90	-0.92	-1.27	-0.78	-0.86
LNP SW	-0.11								
Cudahy	-0.57	0	-0.08					-0.73	-0.71
1700 N							-0.86		
300 N	0	0	0	-0.63	-1.31	0		0.00	-0.11
700 S								-1.70	-0.72
900 S-N	-0.87	0	-0.42						
900 S-S	-0.42	0	0						
1300 S							-0.30		
1700 S	-1.02	0	0	-0.92	-1.95	-0.96	-1.32	-0.89	-0.88
2100 S				-1.31	-2.62	-2.66			
2300 S	-0.30	0							
2600 S			-1.43						
2780 S-E	-0.87	0							
2780 S-W	0	0							
3600 S	-2.30								
5400 S	-3.88	-0.30		-1.57	-1.57	-0.70			
7600 S				-1.57	-0.22	-0.48			
7800 S	-2.60	0							
9000 S	-4.19	0		-1.35	-2.14	-0.09			
SR-154	-2.60								
US-73	-1.17	0							

APPENDIX B

DIURNAL DO PROFILES FOR SINGLE-STATION NDM

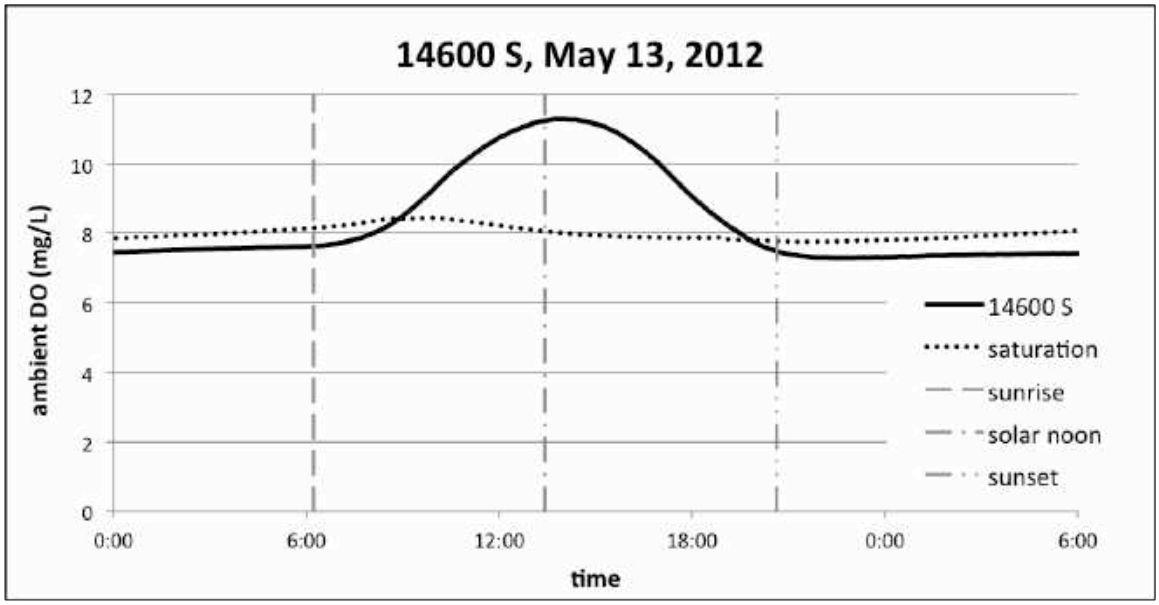

Fig. 80. 14600 S, 5-13-2012

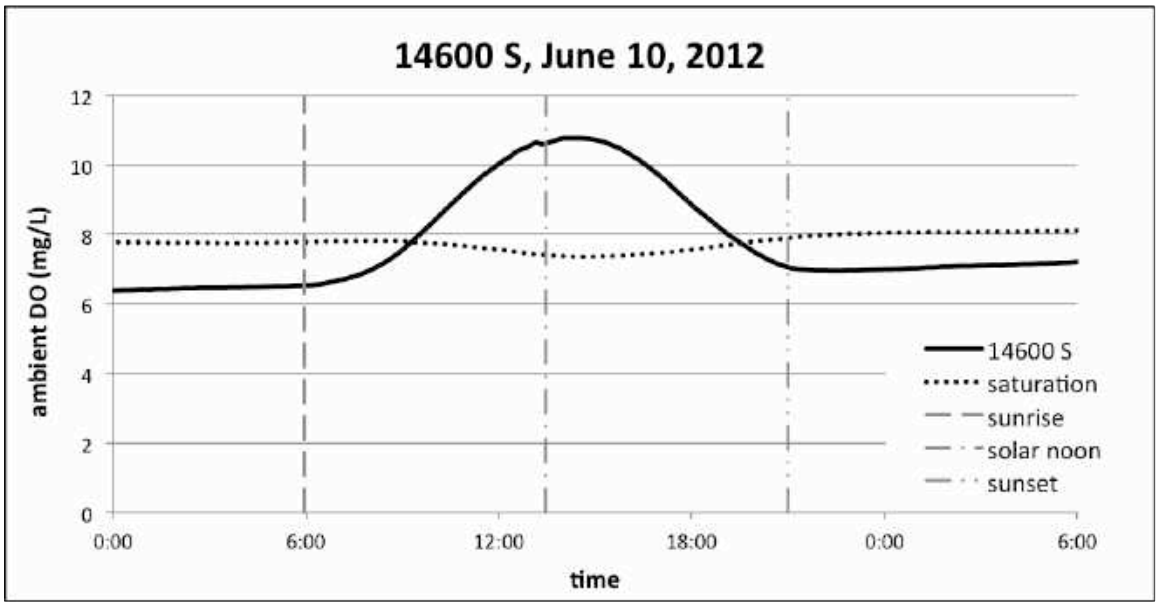

Fig. 81. 14600 S, 6-10-2012

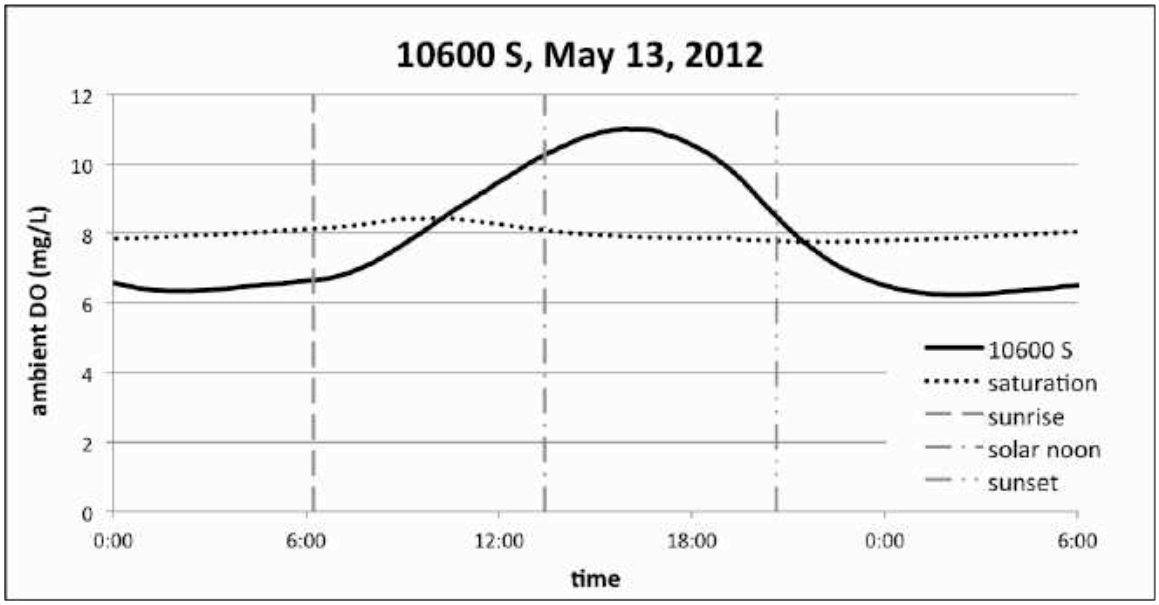

Fig. 82. 10600 S, 5-13-2012

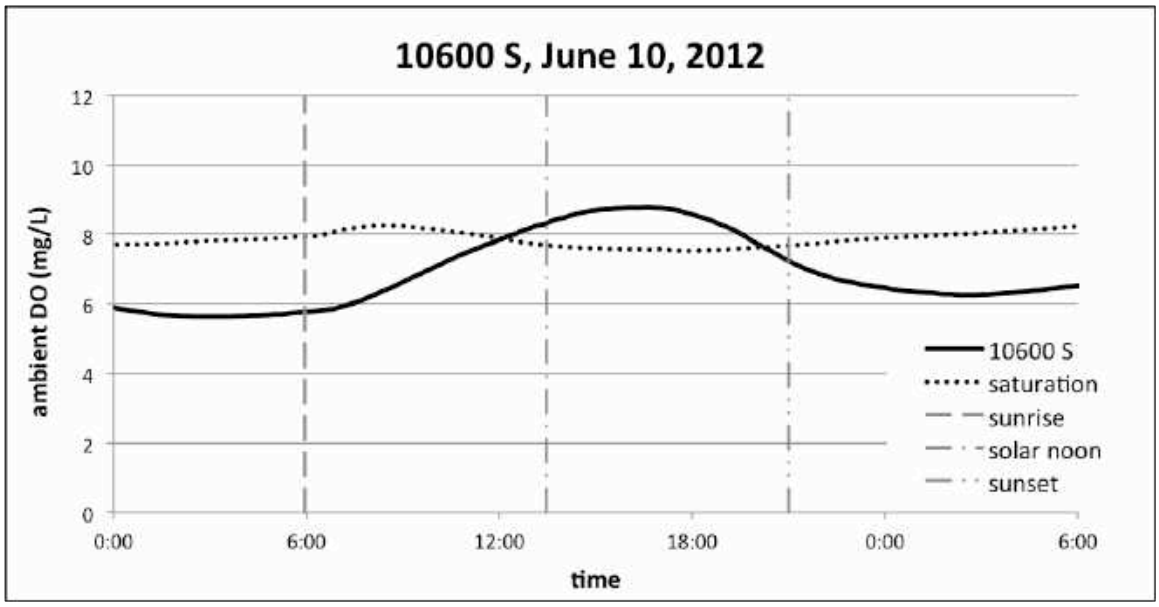

Fig. 83. 10600 S, 6-10-2012

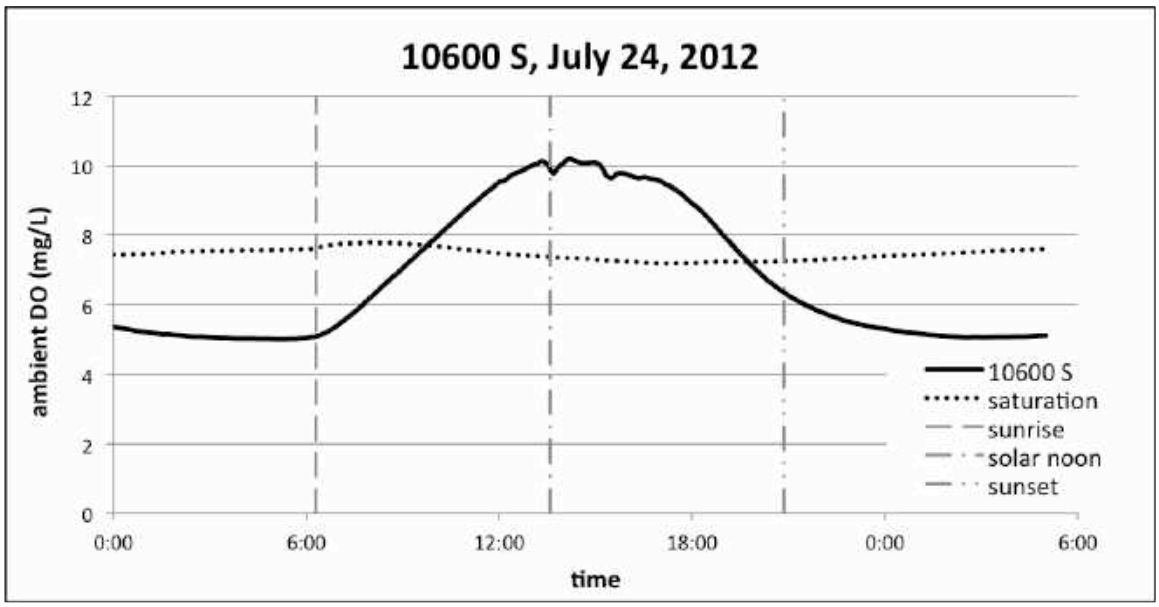

Fig. 84. 10600 S, 7-24-2012

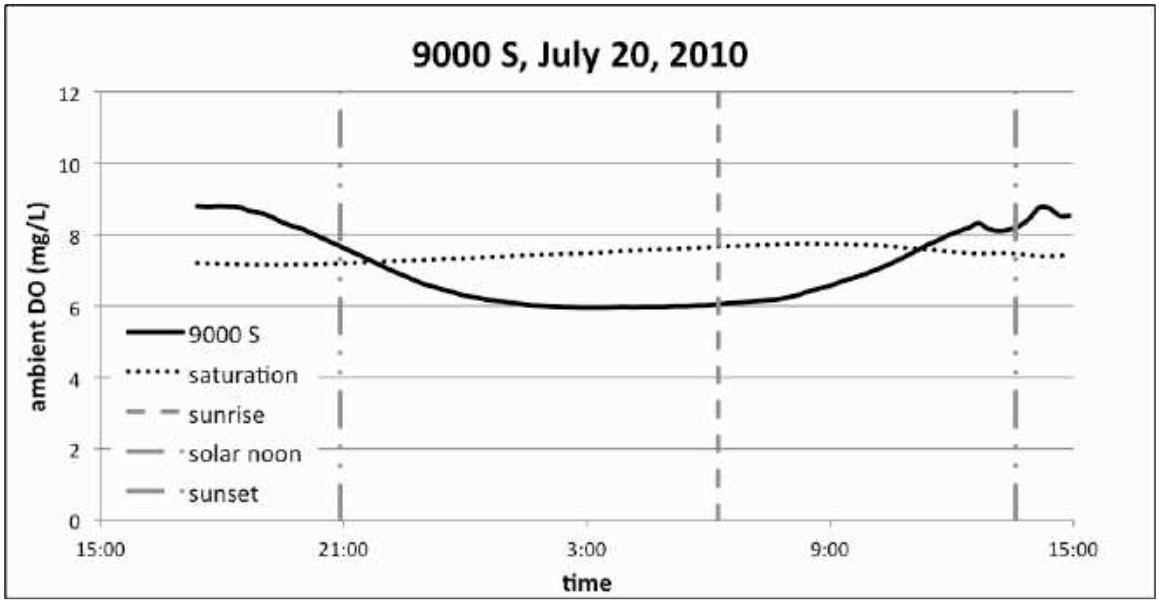

Fig. 85. 9000 S, 7-20-2010

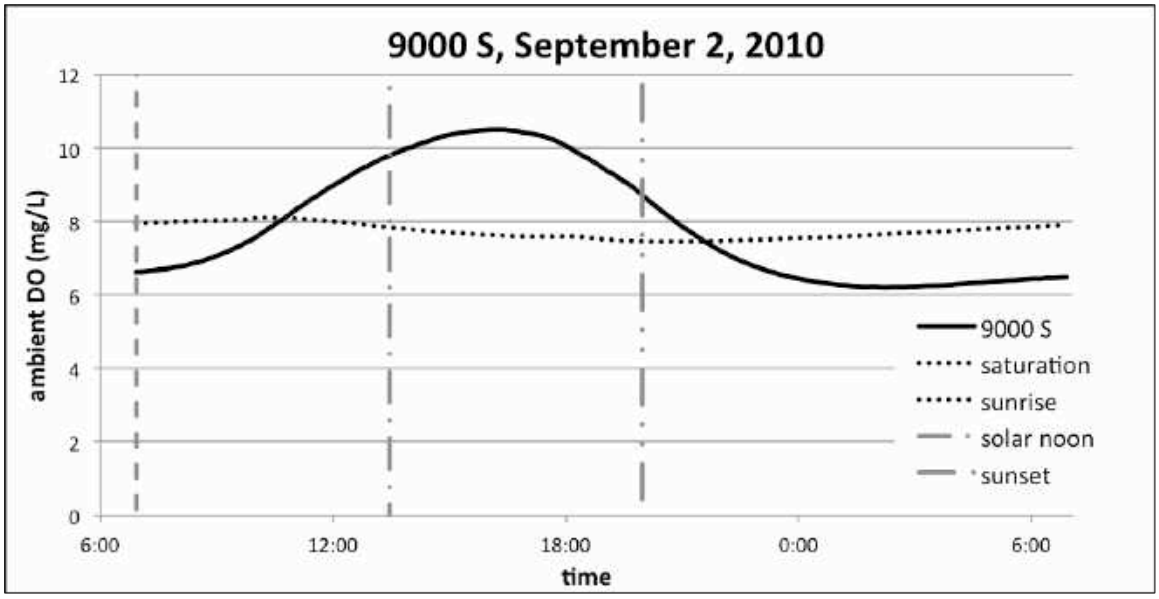

Fig. 86. 9000 S, 9-2-2010

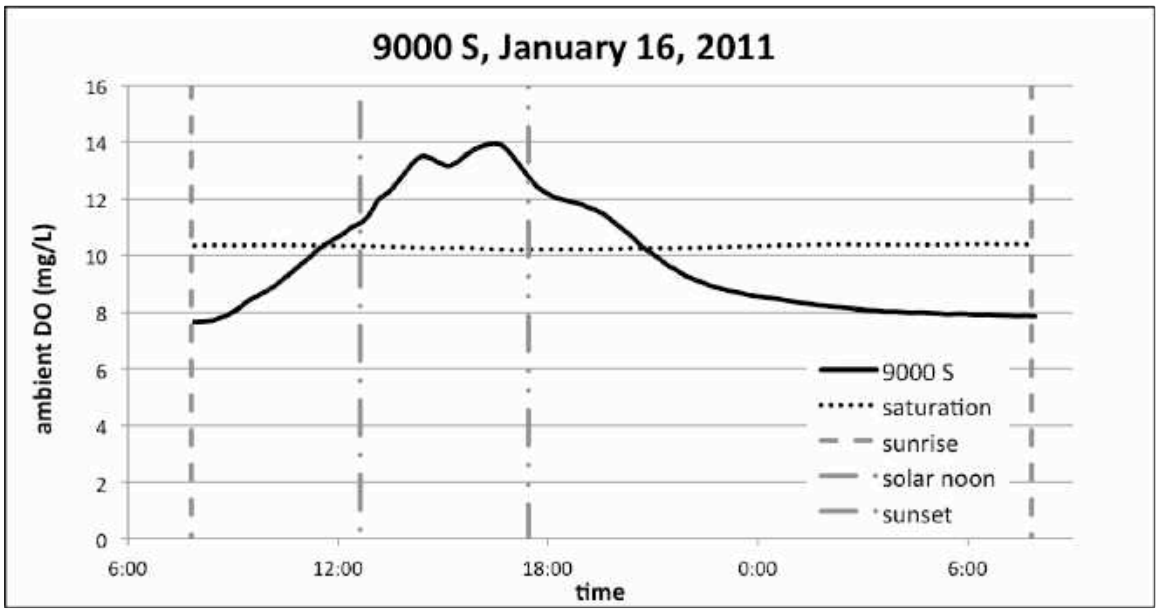

Fig. 87. 9000 S, 1-16-2011
Note: y-axis increased to 16 mg/L

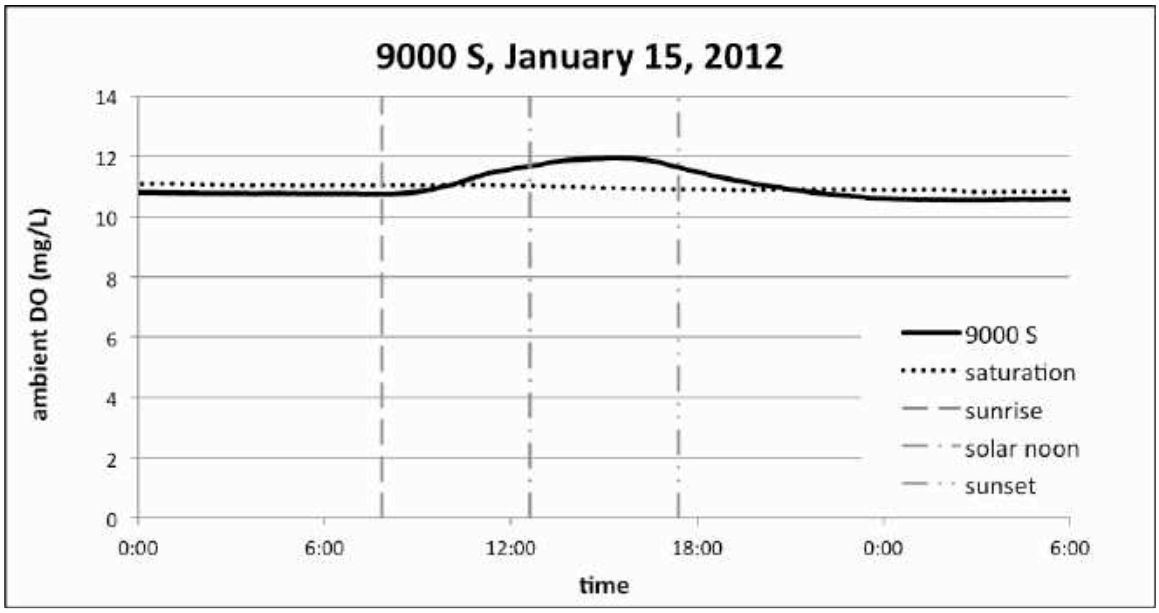

Fig. 88. 9000 S, 1-15-2012
Note: y-axis increased to 14 mg/L

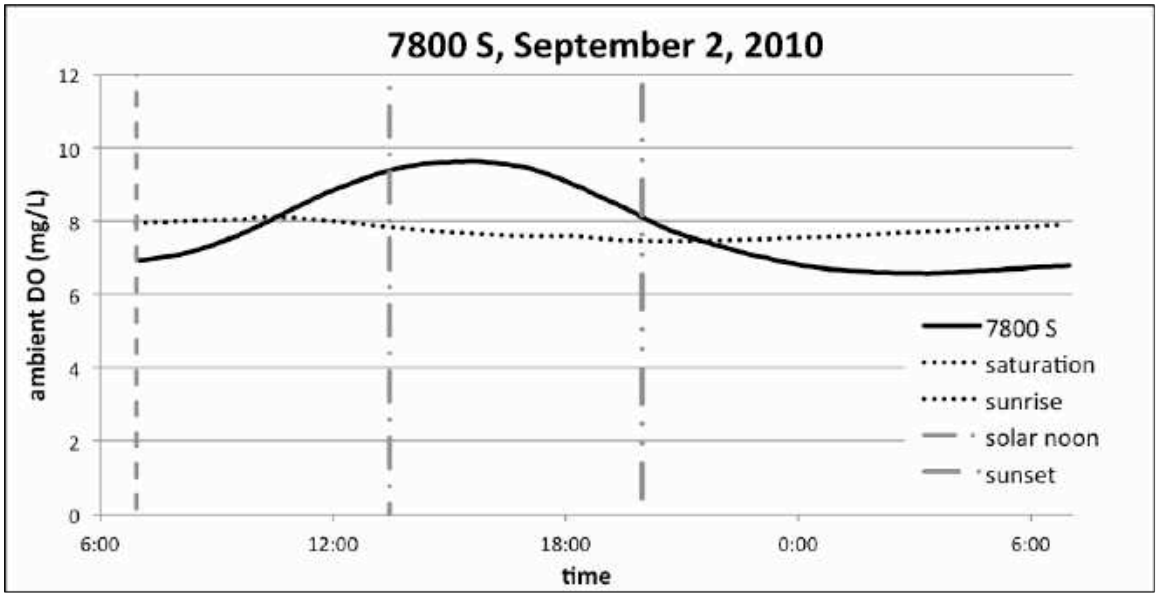

Fig. 89. 7800 S, 9-2-2010

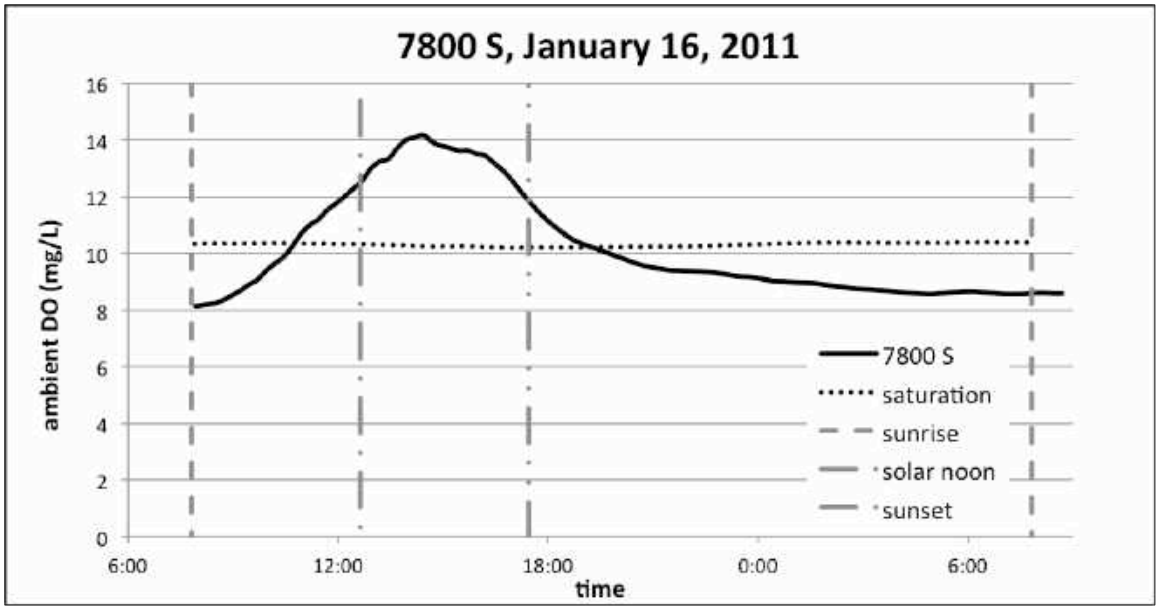

Fig. 90. 7800 S, 1-16-2011
Note: y-axis increased to 16 mg/L

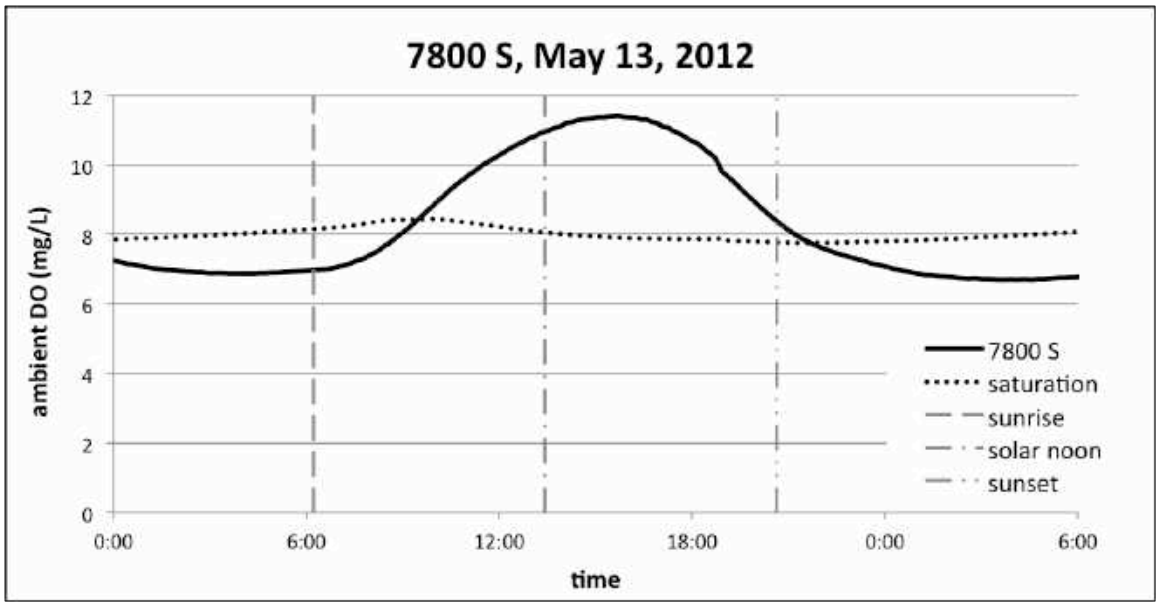

Fig. 91. 7800 S, 5-13-2012

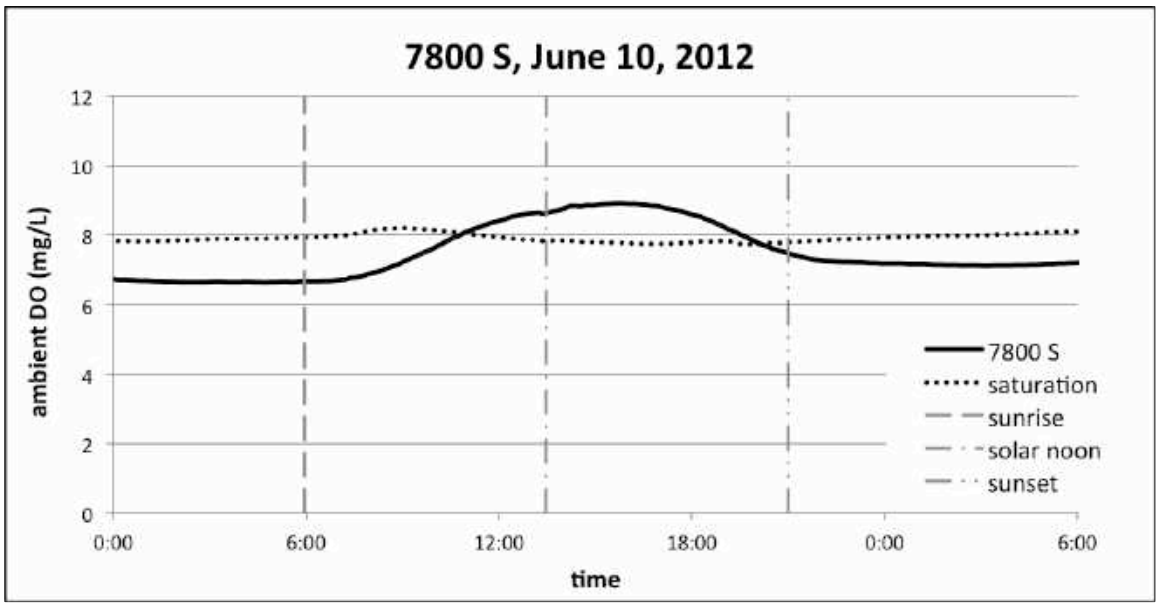

Fig. 92. 7800 S, 6-10-2012

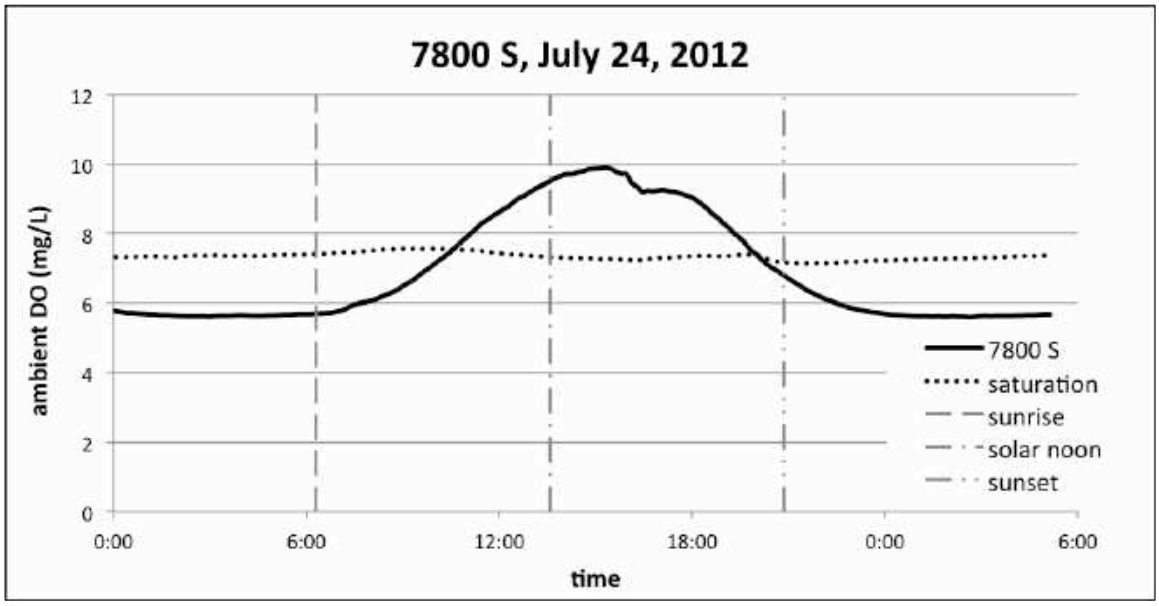

Fig. 93. 7800 S, 7-24-2012

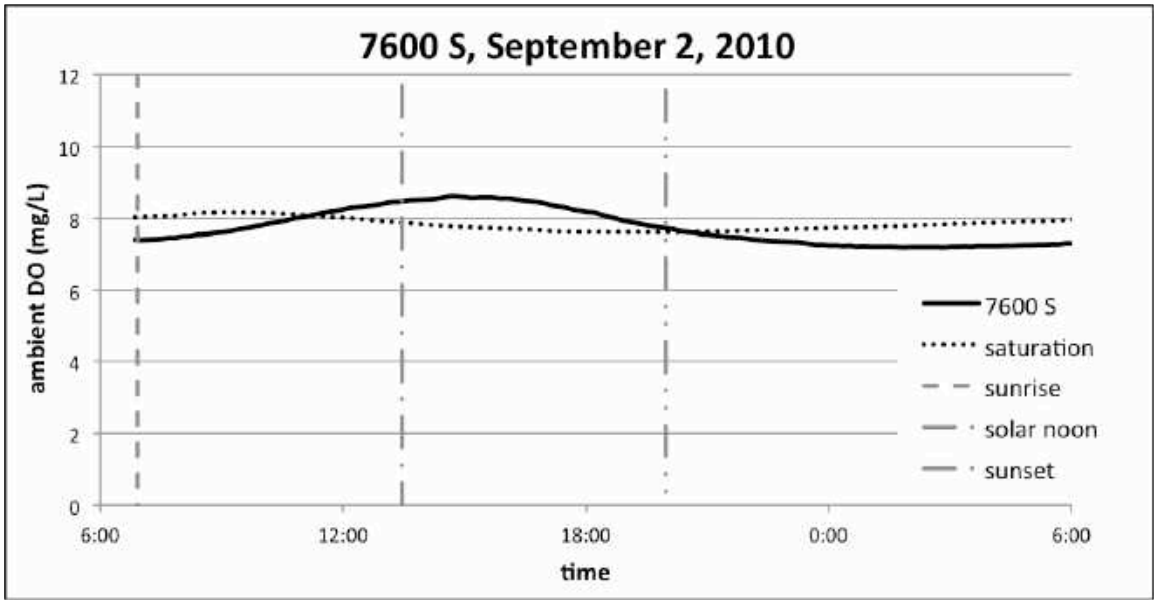

Fig. 94. 7600 S, 9-2-2010

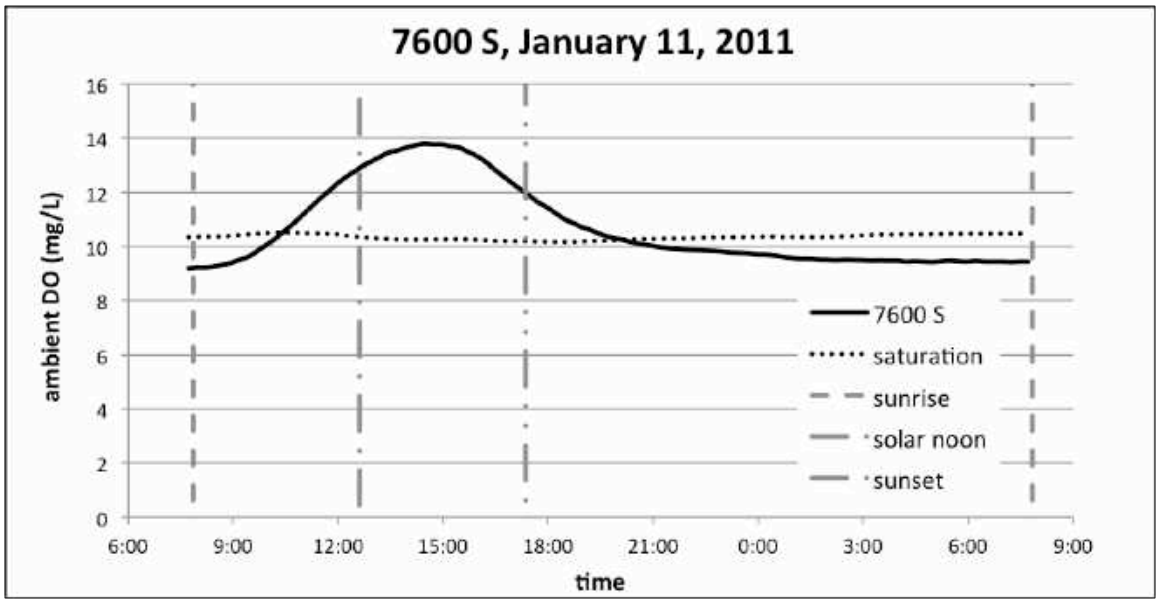

Fig. 95. 7600 S, 1-11-2011
Note: y-axis increased to 16 mg/L

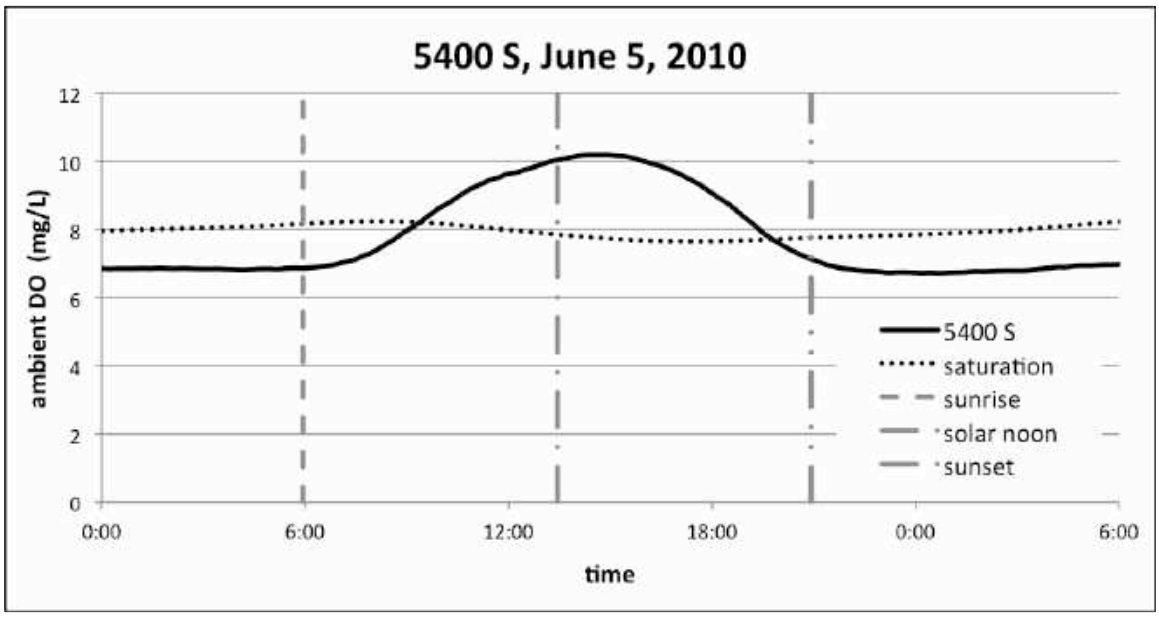

Fig. 96. 5400 S, 6-5-2010

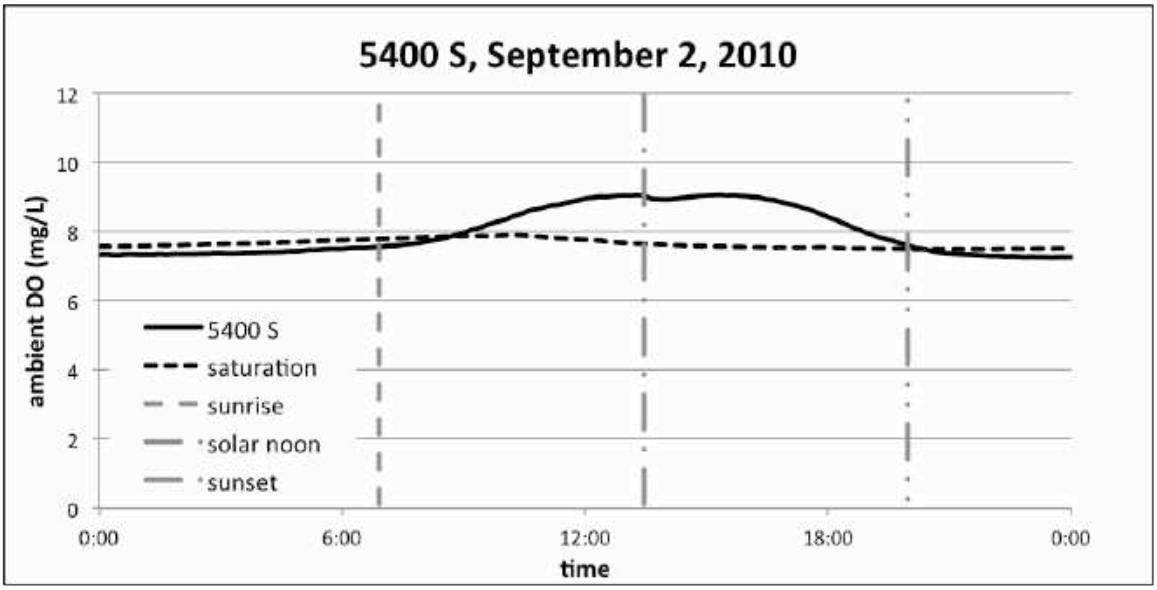

Fig. 97. 5400 S, 9-2-2010

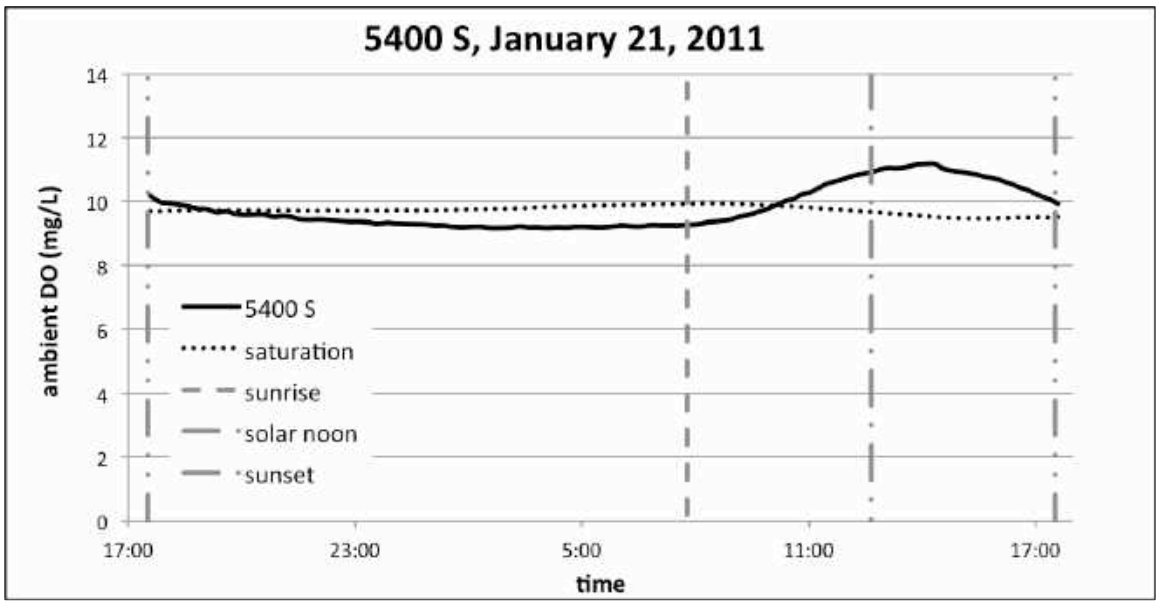

Fig. 98. 5400 S, 1-21-2011
Note: y-axis increased to 14 mg/L

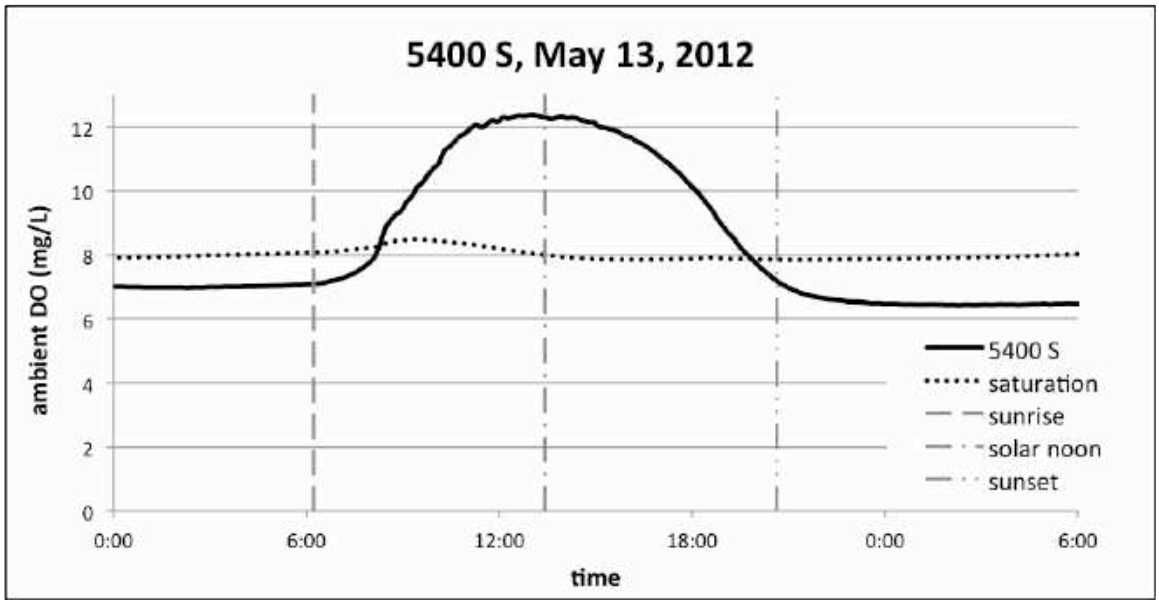

Fig. 99. 5400 S, 5-13-2012

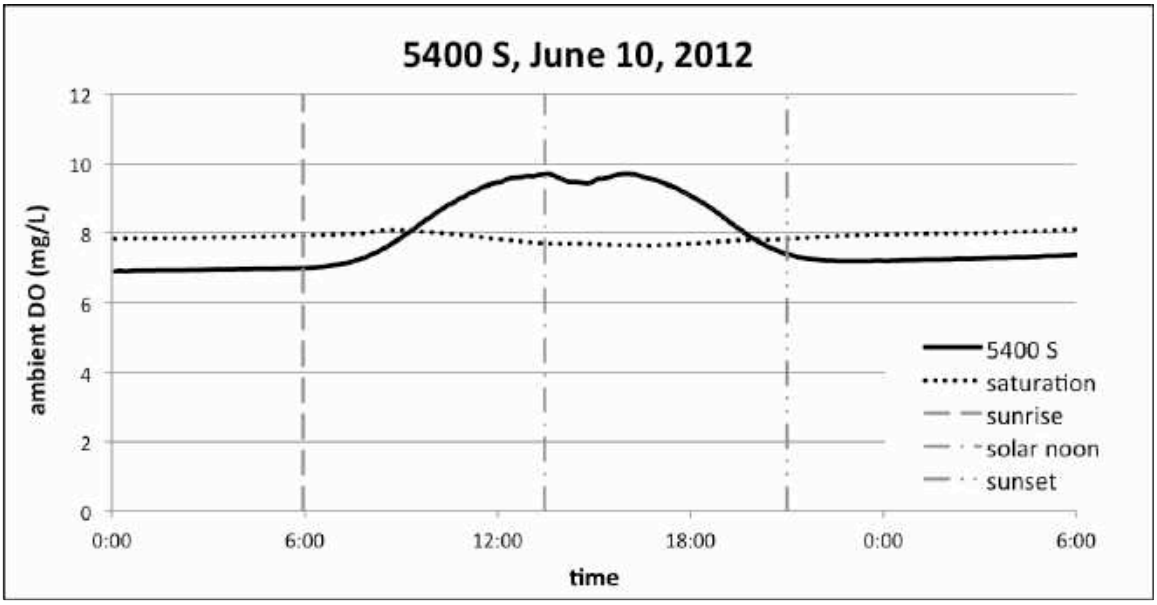

Fig. 100. 5400 S, 6-10-212

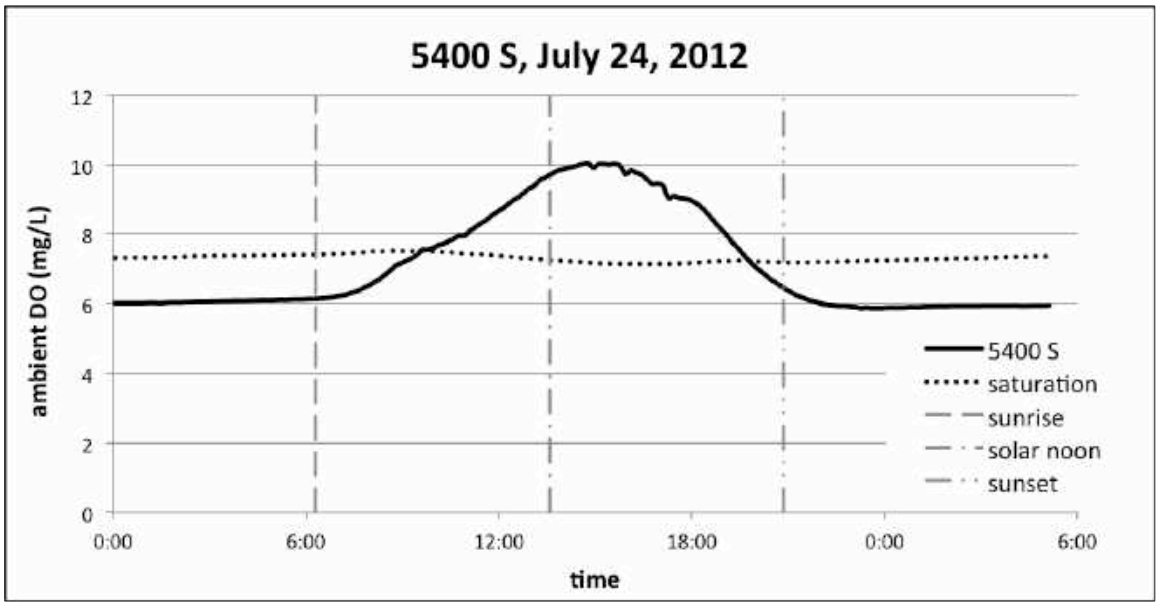

Fig. 101. 5400 S, 7-24-2012

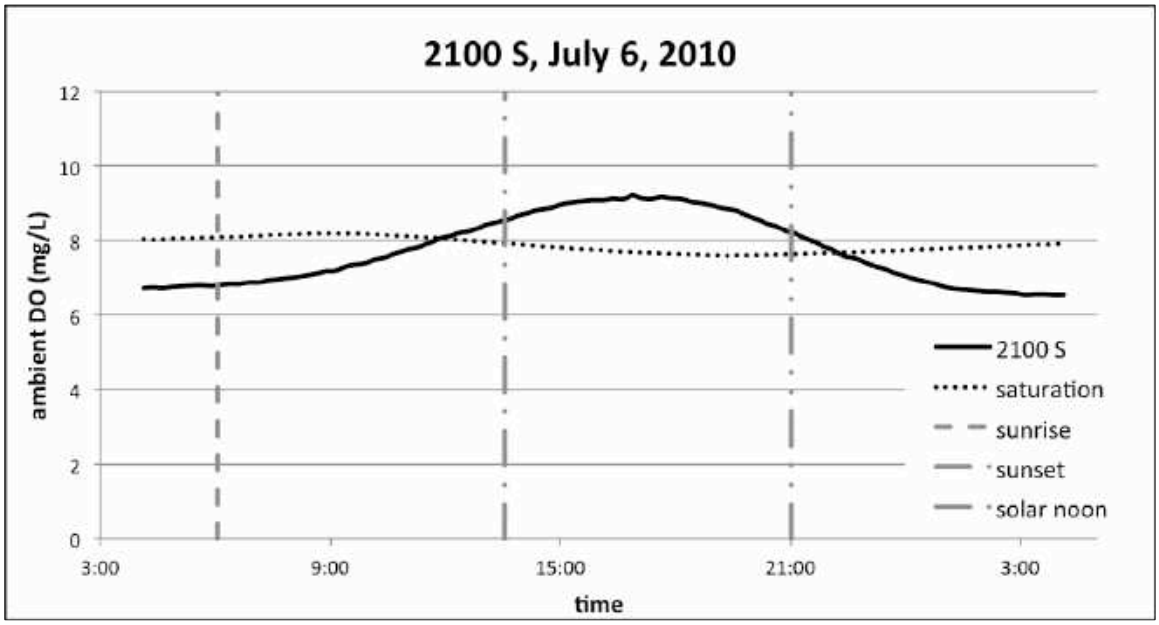

Fig. 102. 2100 S, 7-6-2010

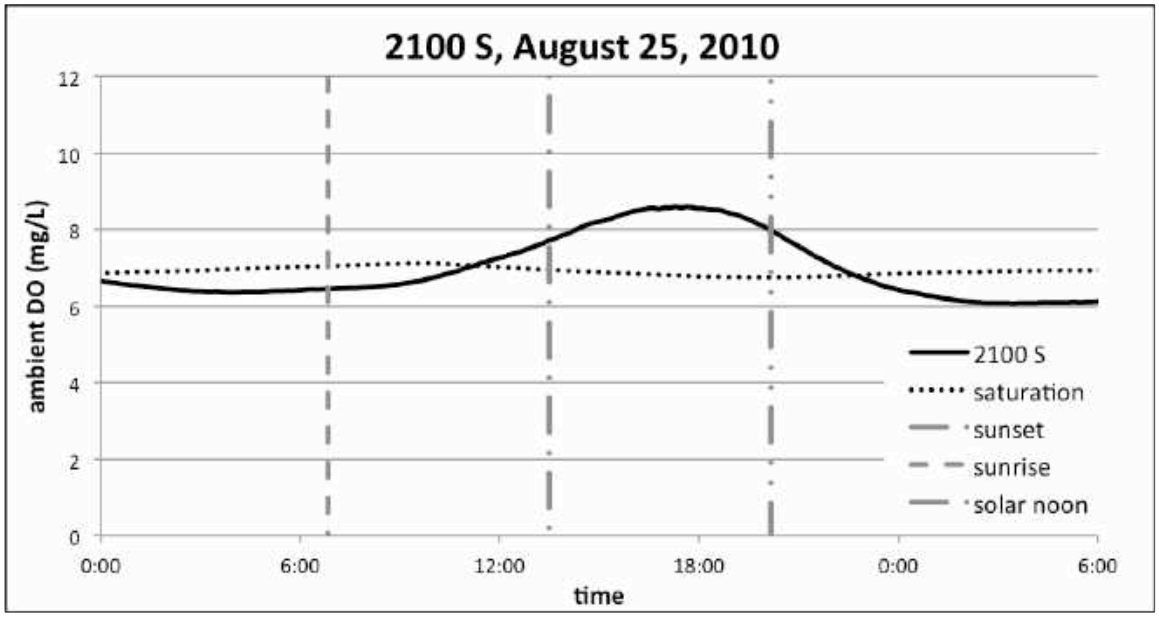

Fig. 103. 2100 S, 8-25-2010

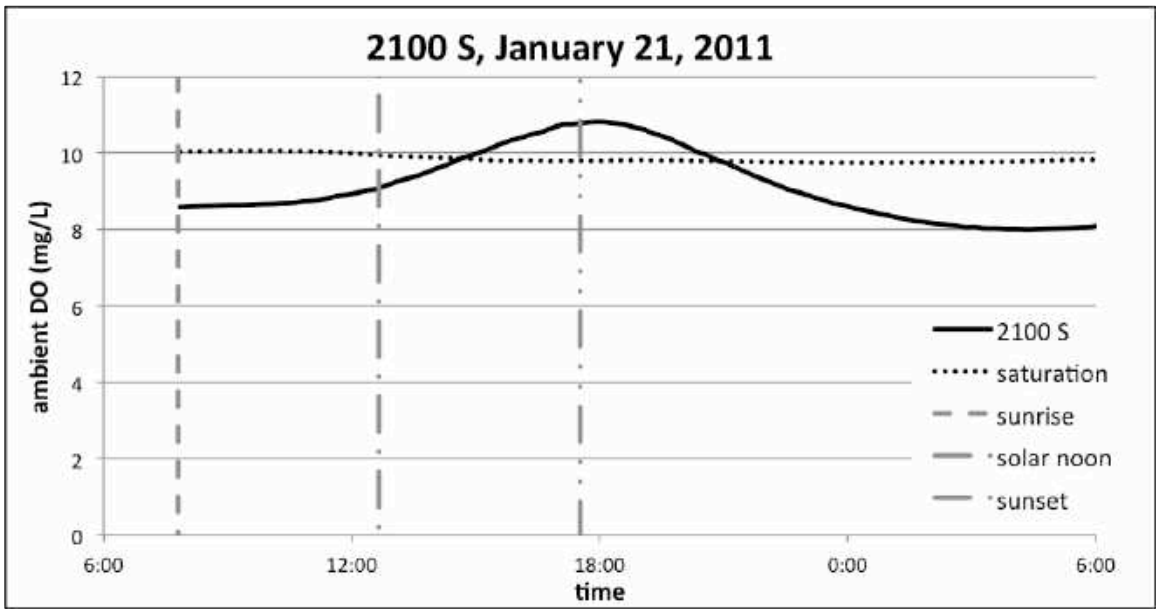

Fig. 104. 2100 S, 1-21-2011

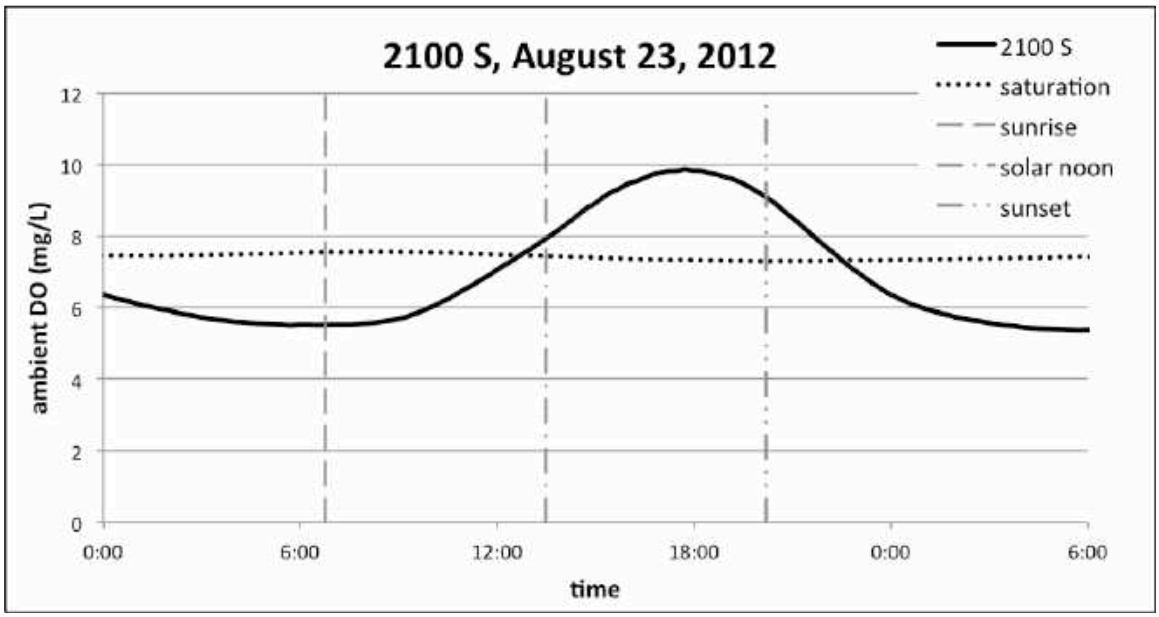

Fig. 105. 2100 S, 8-23-2012

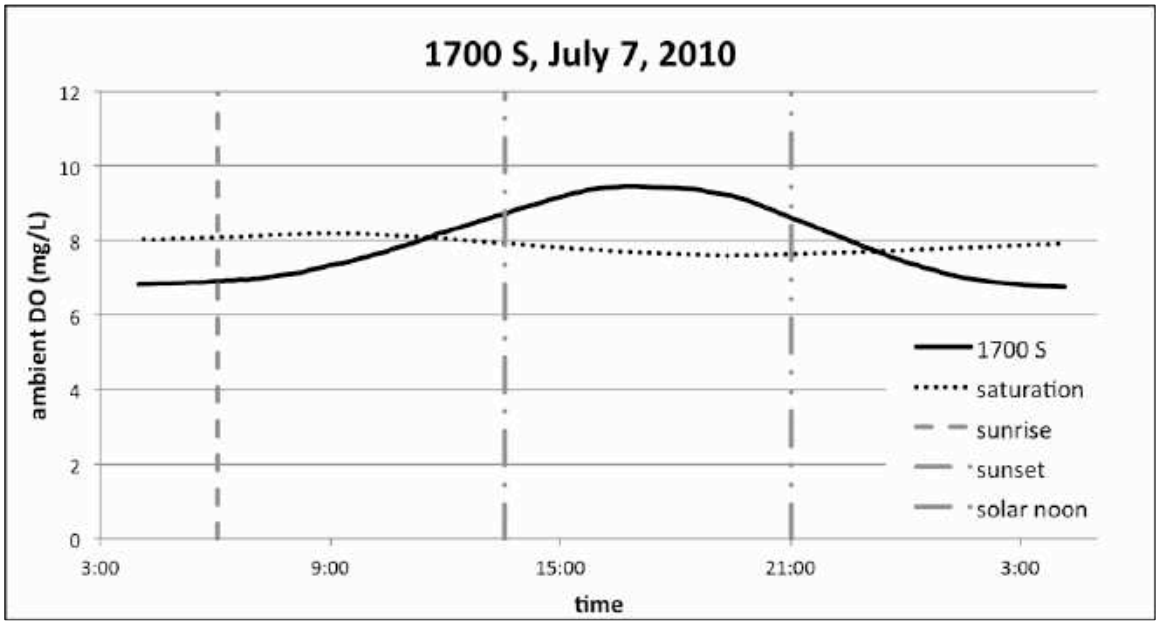

Fig. 106. 1700 S, 7-7-2010

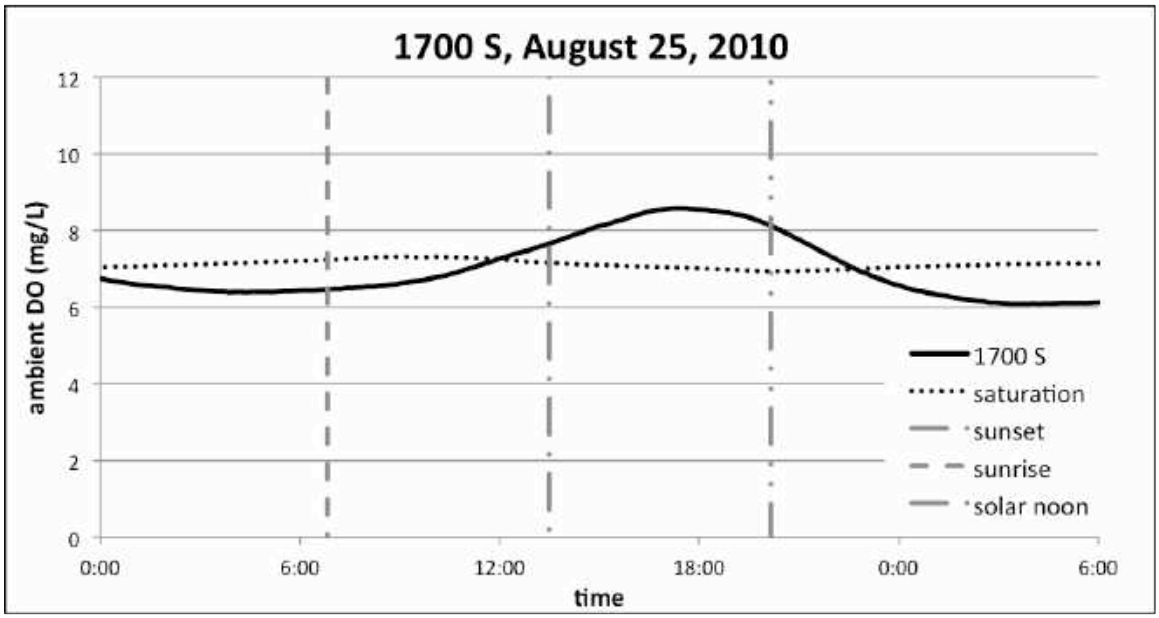

Fig. 107. 1700 S, 8-25-2010

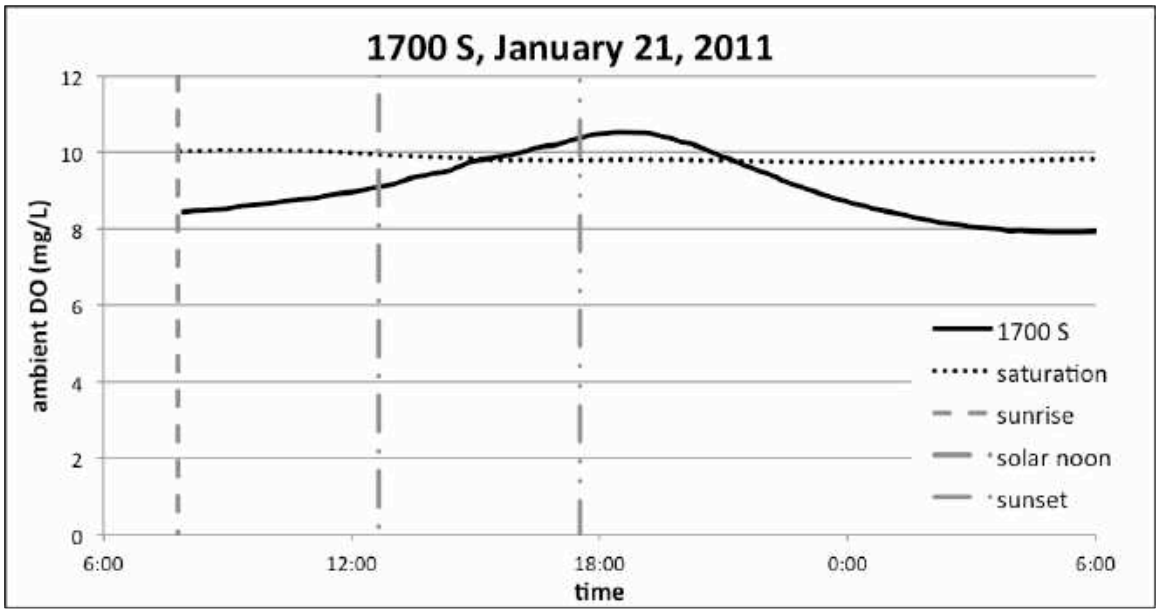

Fig. 108. 1700 S, 1-21-2011

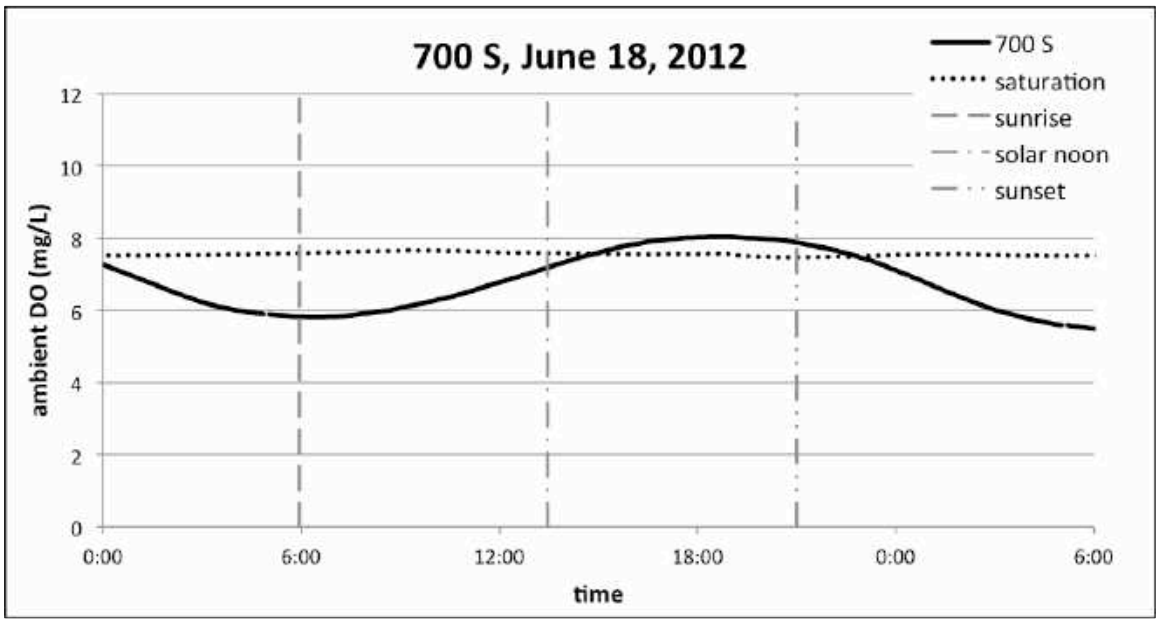

Fig. 109. 700 S, 6-18-2012

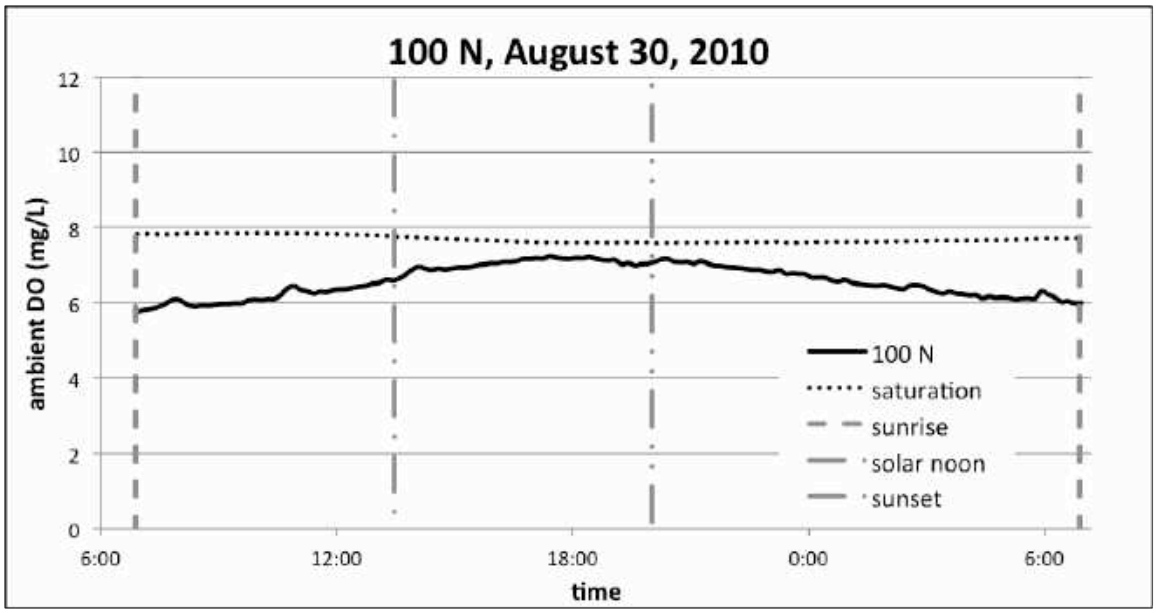

Fig. 110. 100 N, 8-30-2010

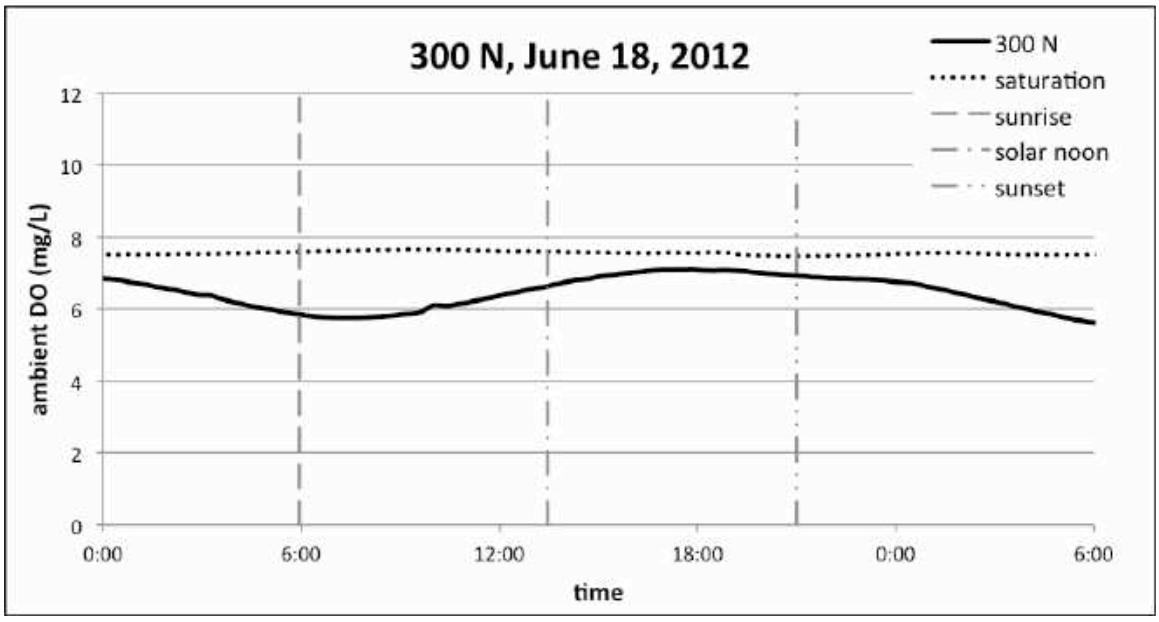

Fig. 111. 300 N, 6-18-2012

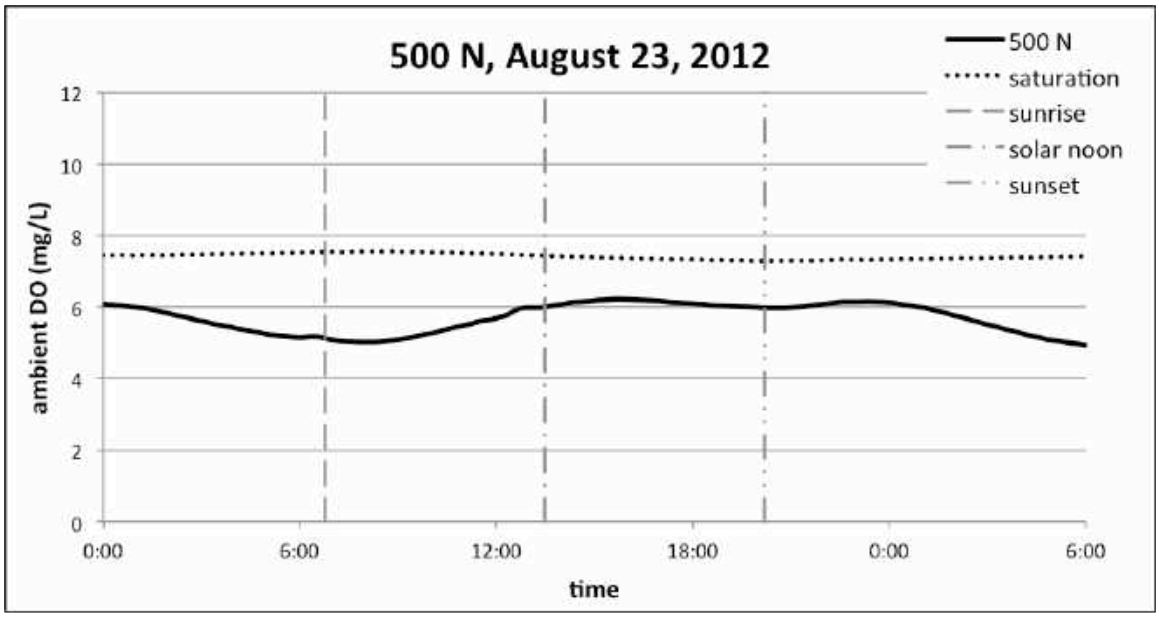

Fig. 112. 500 N, 8-23-2012

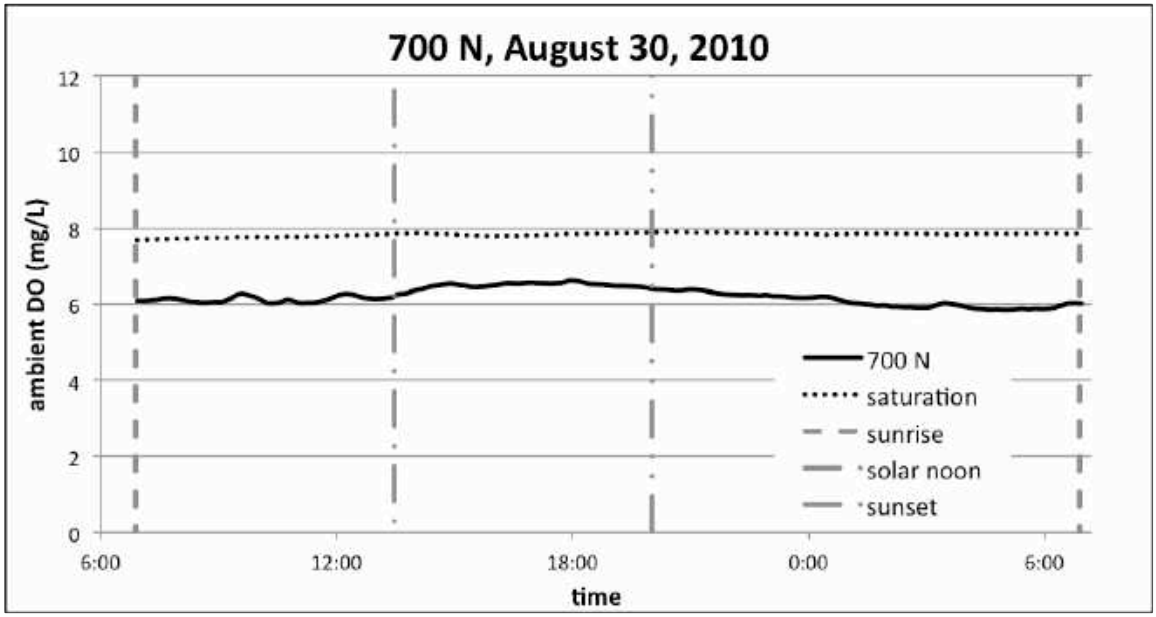

Fig. 113. 700 N, 8-30-2010

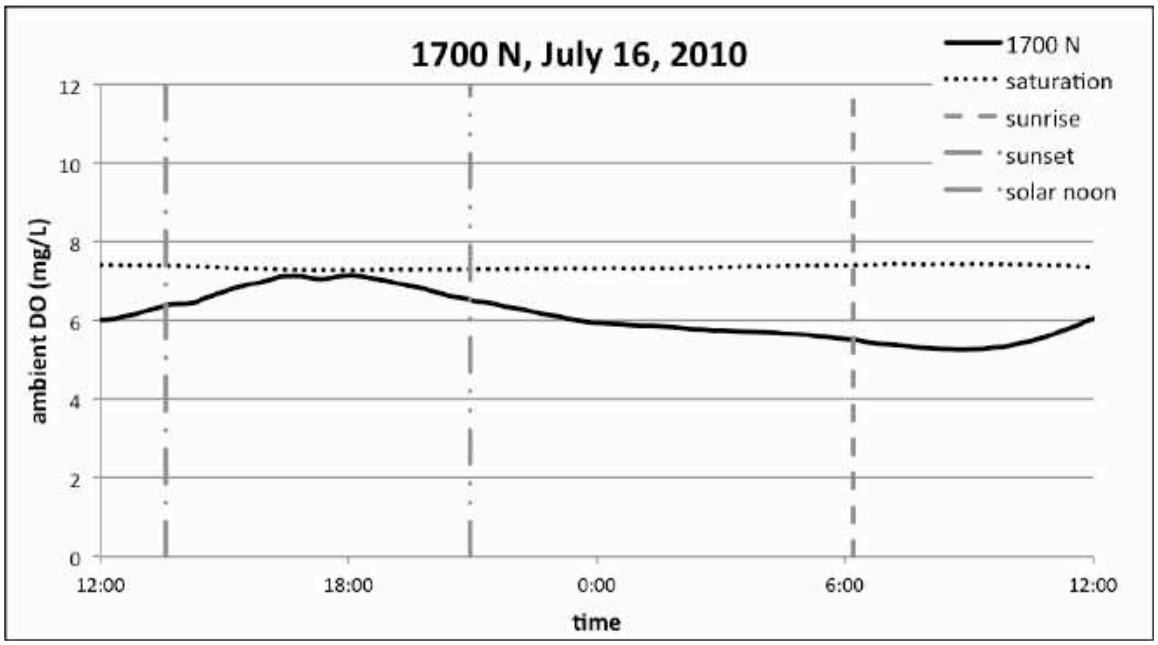

Fig. 114. 1700 N, 7-16-2010

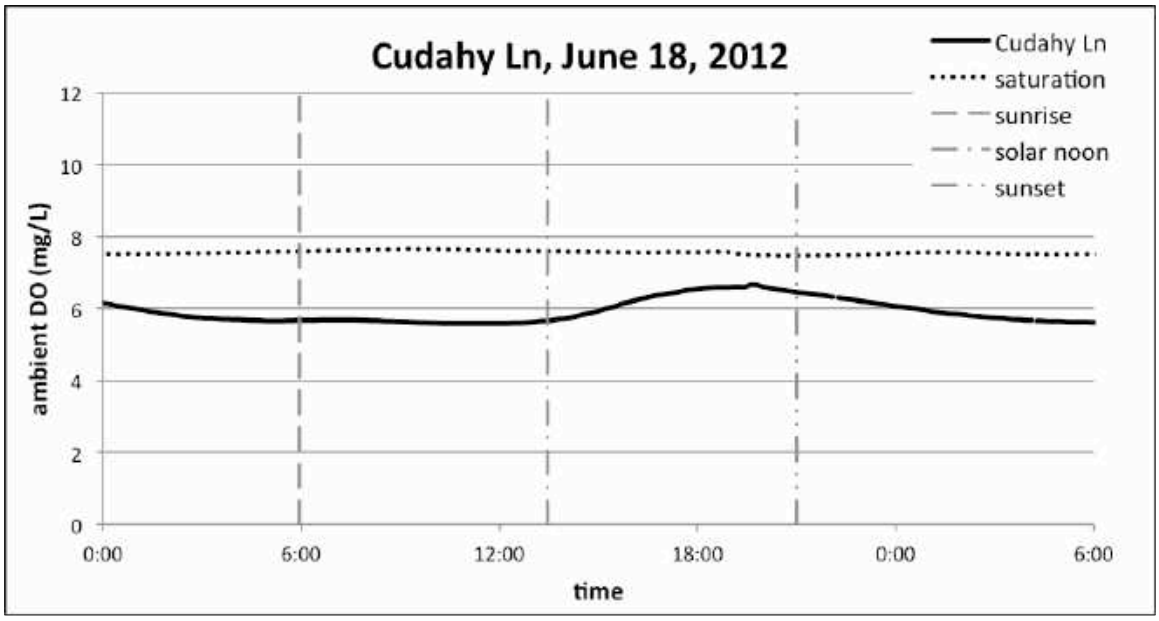

Fig. 115. Cudahy Lane, 6-18-2012

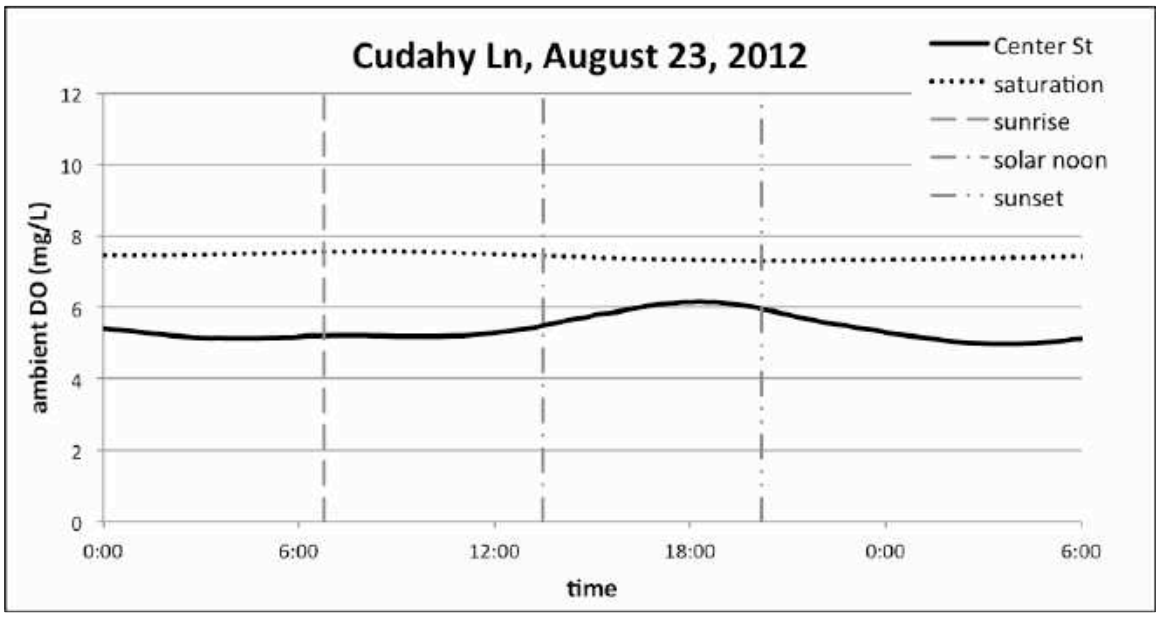

Fig. 116. Cudahy Lane, 8-23-2012

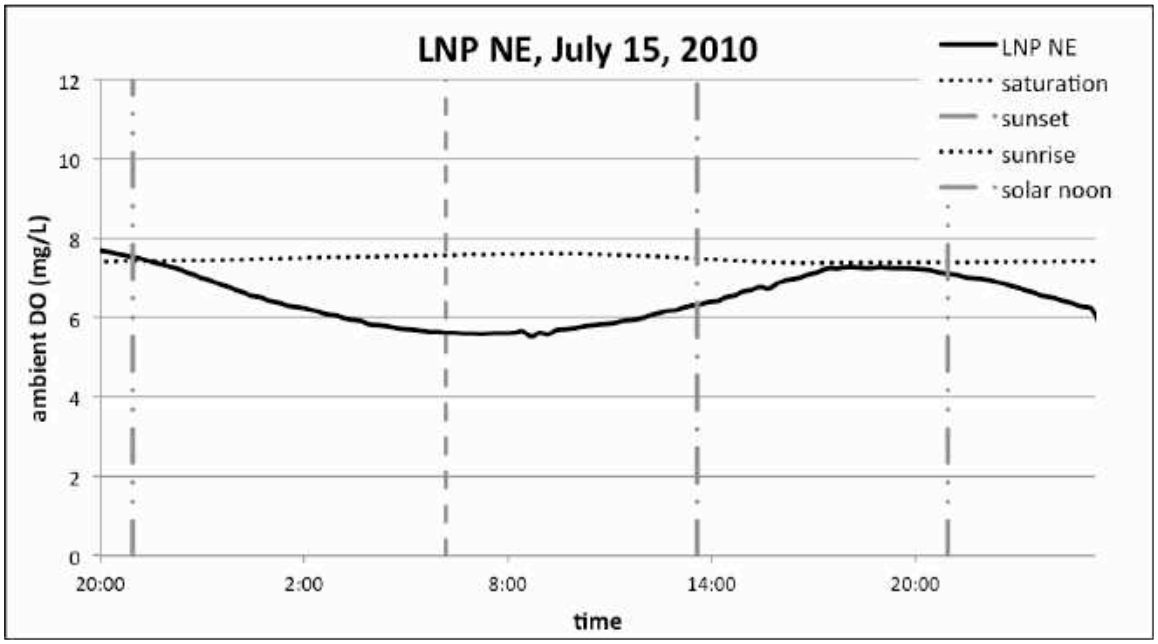

Fig. 117. LNP NE, 7-15-2010

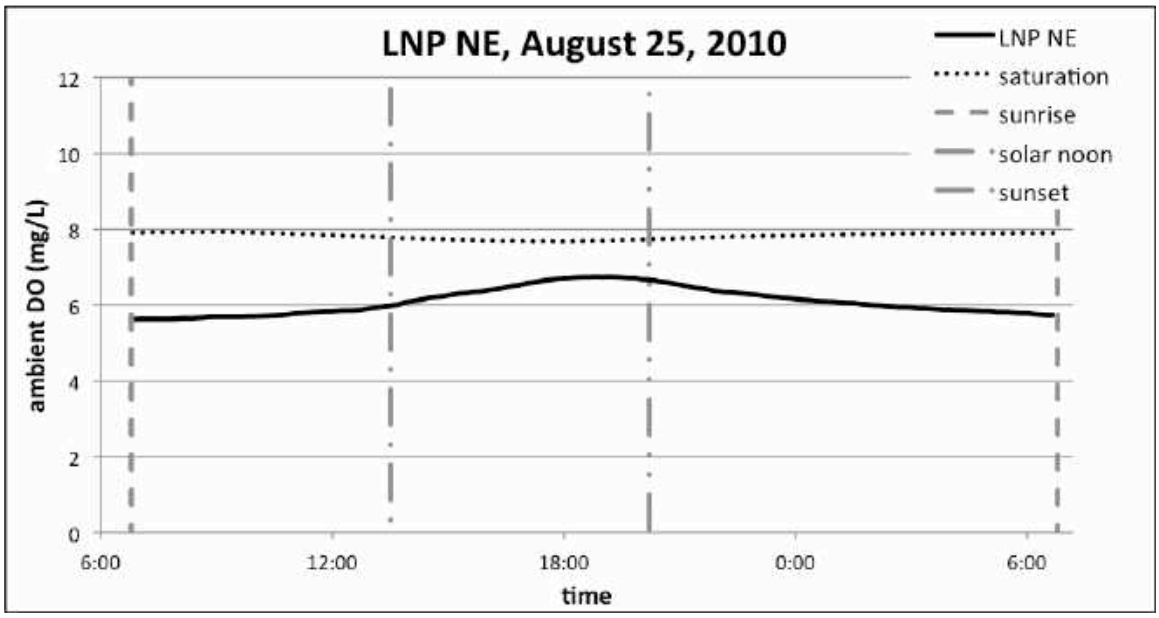

Fig. 118. LNP NE, 8-25-2010

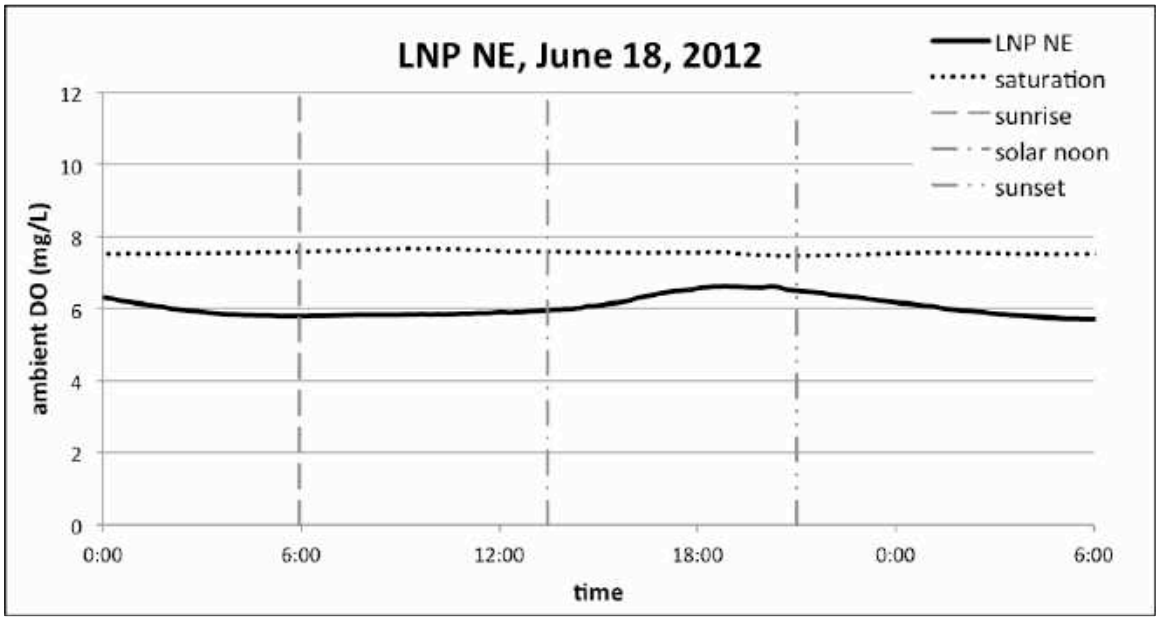

Fig. 119. LNP NE, 6-18-2012

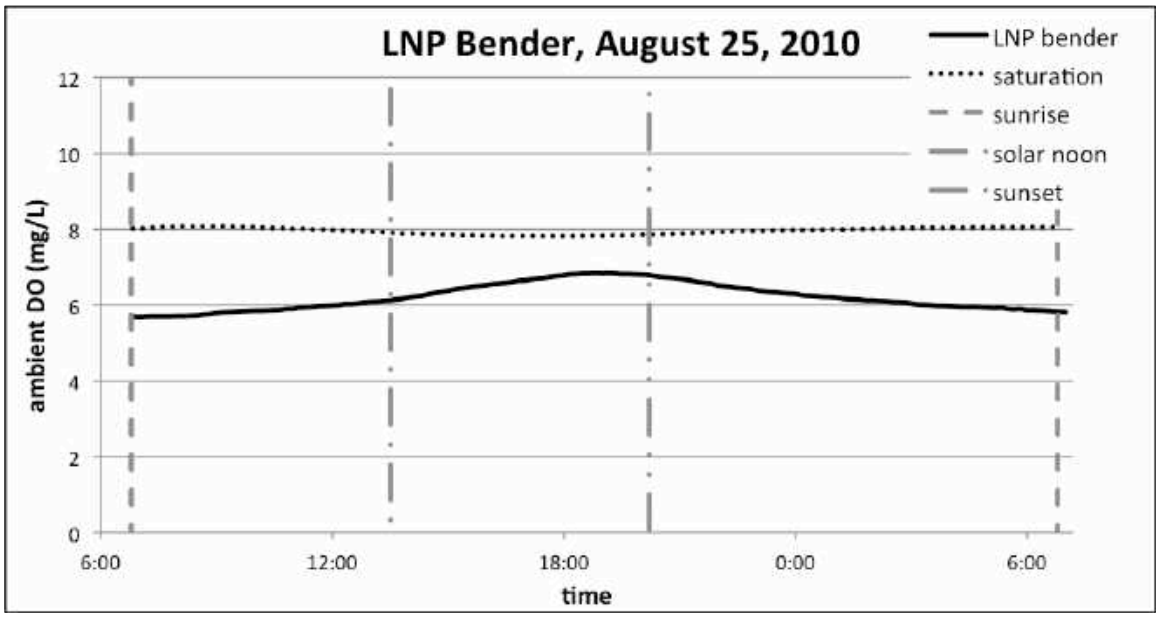

Fig. 120. LNP Bender, 8-25-2010

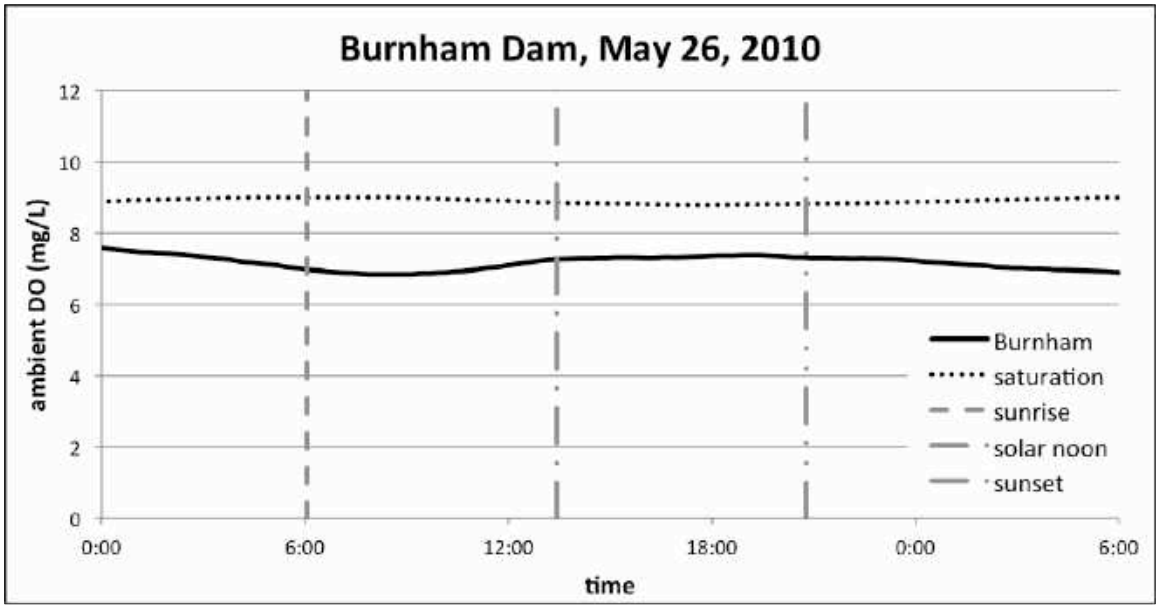

Fig. 121. Burnham Dam, 5-26-2010

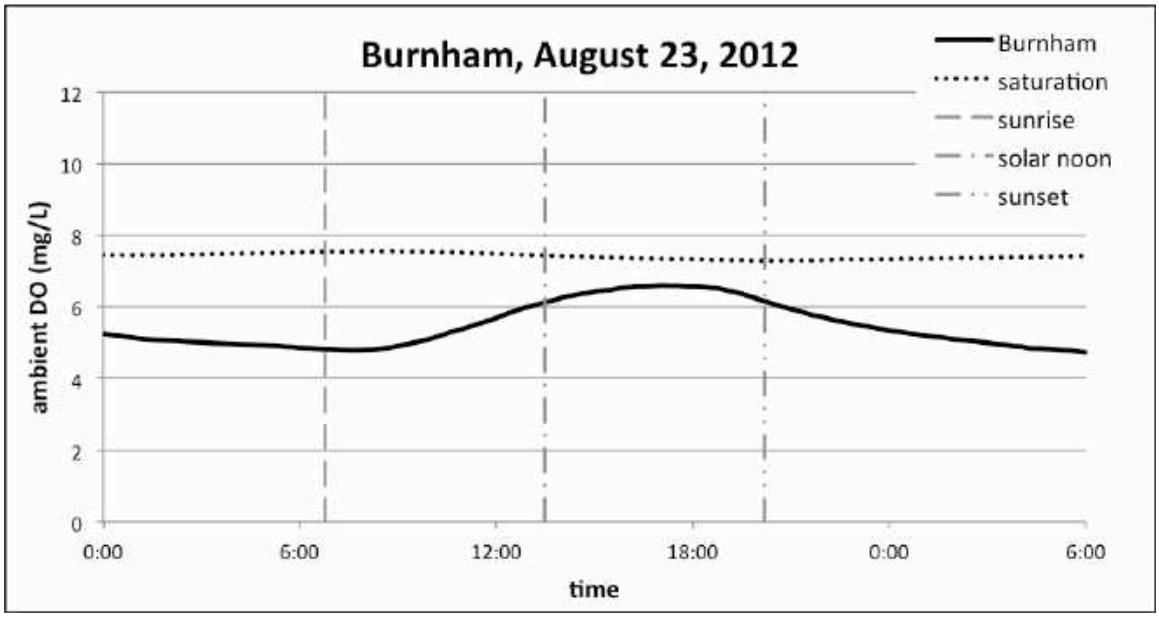

Fig. 122. Burnham Dam, 8-23-2012

APPENDIX C

SEDIMENT %TS AND %VS

Table 48. Sediment %TS and %VS (a)

site	reach	date	depth	%TS	%VS	note
LNP NE	1	5/20/10	0–2	46	4.5	
LNP NE	1	5/20/10	10	40	9.7	
LNP NE	1	5/20/10	20	56	4.4	
LNP NE	1	5/20/10	30	68	3.4	
Cudahy Ln	1	5/20/10	0–2	40	6.3	
Cudahy Ln	1	5/20/10	20	57	6.0	
Cudahy Ln	1	5/20/10	30	54	7.5	
1700 N	2	5/20/10	0–2	48	4.5	
1700 N	2	5/20/10	10	57	5.5	
1700 N	2	5/20/10	20	65	4.0	
1700 N	2	5/20/10	30	76	2.1	
300 N	2	5/20/10	0–2	53	3.3	
300 N	2	5/20/10	10	75	2.4	
300 N	2	5/20/10	20	55	8.4	
300 N	2	5/20/10	30	68	4.0	
900 S-N	3	5/24/10	0–2	62	2.6	
900 S-N	3	5/24/10	10	69	2.6	
900 S-N	3	5/24/10	20	69	2.1	
900 S-N	3	5/24/10	30	73	2.2	
900 S-S	3	5/20/10	0–2	72	1.2	
900 S-S	3	5/20/10	10	77	1.9	
900 S-S	3	5/20/10	20	76	0.7	
900 S-S	3	5/20/10	30	72	3.6	
1700 S	3	5/24/10	0–2	78	1.1	
1700 S	3	5/24/10	20	81	0.4	
1700 S	3	5/24/10	30	75	0.6	
1700 S-Pool	3	5/24/10	0–2	30	6.7	pool
1700 S-Pool	3	5/24/10	10	83	0.5	pool
1700 S-Pool	3	5/24/10	20	65	3.3	pool
Lehi		5/25/10	0–2	45	5.6	
Lehi		5/25/10	10	67	2.4	
Lehi		5/25/10	20	68	3.2	
Lehi		5/25/10	30	71	3.0	
LNP NE	1	6/3/10	0–2	47	5.6	
LNP NE	1	6/3/10	10	57	5.9	

Table 49. Sediment %TS and %VS (b)

site	reach	date	depth	%TS	%VS	note
LNP NE	1	6/3/10	20	66	3.9	
LNP NE	1	6/3/10	30	63	5.2	
LNP NE	1	6/3/10	40	71	3.0	
LNP NE	1	6/3/10	50	76	2.3	
Cudahy Ln	1	6/3/10	0–2	38	6.7	
Cudahy Ln	1	6/3/10	10	58	6.5	
Cudahy Ln	1	6/3/10	20	49	8.4	
Cudahy Ln	1	6/3/10	30	59	6.1	
Cudahy Ln	1	6/3/10	40	61	5.5	
Cudahy Ln	1	6/3/10	50	74	3.0	
900 S-N	3	6/8/10	0–2	52	5.0	
900 S-N	3	6/8/10	10	67	3.8	
900 S-N	3	6/8/10	20	70	2.4	
900 S-N	3	6/8/10	30	63	4.0	
900 S-N	3	6/8/10	40	62	4.4	
900 S-N	3	6/8/10	50	71	2.2	
900 S-N	3	6/8/10	60	67	3.9	
900 S-N	3	6/8/10	70	62	8.5	
900 S-N	3	6/8/10	0–2	64	5.7	
900 S-N	3	6/8/10	10	73	1.9	
900 S-N	3	6/8/10	20	72	2.0	
900 S-S	3	6/8/10	0–2	72	1.2	
900 S-S	3	6/8/10	10	78	1.0	
900 S-S	3	6/8/10	20	84	0.8	
900 S-S	3	6/8/10	30	68	3.9	
900 S-S	3	6/8/10	40	65	2.5	
900 S-S	3	6/8/10	50	70	4.7	
2100 S	3	6/11/10	0–2	72	0.9	
2100 S	3	6/11/10	6	78	0.4	
2100 S	3	6/11/10	12	74	0.6	
2100 S	3	6/11/10	18	73	0.8	
2100 S	3	6/11/10	24	74	1.0	
2100 S	3	6/11/10	30	73	1.7	
2100 S	3	6/11/10	40	73	2.0	
2100 S	3	6/11/10	50	76	1.5	
2100 S	3	6/11/10	60	78	1.3	
2100 S	3	6/11/10	0–2	90	0.8	
2100 S	3	6/11/10	5	89	0.4	
2100 S	3	6/11/10	10	93	0.4	

Table 50. Sediment %TS and %VS (c)

site	reach	date	depth	%TS	%VS	note
2100 S	3	6/11/10	20	89	0.4	
2100 S	3	6/11/10	30	82	0.8	
1900 S	3	7/13/10	0–2	69	1.6	
1900 S	3	7/13/10	5	76	1.1	
1900 S	3	7/13/10	10	83	0.6	
1900 S	3	7/13/10	20	69	2.6	
1900 S	3	7/13/10	27	83	0.8	
1300 S	3	7/14/10	0–2	47	10.2	
1300 S	3	7/14/10	5	53	11.2	
1300 S	3	7/14/10	10	72	4.1	
1300 S	3	7/14/10	20	60	7.0	
1300 S	3	7/14/10	30	64	10.2	
1700 S-S	3	7/15/10	0–2	71	1.7	
1700 S-S	3	7/15/10	5	81	0.7	
1700 S-S	3	7/15/10	10	84	1.0	
1700 S-S	3	7/15/10	20	83	0.4	
1700 S-S	3	7/15/10	30	76	1.0	
300 N	2	7/16/10	0–2	34	6.8	
300 N	2	7/16/10	5	55	5.2	
300 N	2	7/16/10	10	56	5.5	
300 N	2	7/16/10	20	65	3.5	
300 N	2	7/16/10	30	70	3.5	
300 N	2	7/16/10	45	79	2.4	
HC		8/9/10	0–2	67	1.5	
HC		8/9/10	5	67	3.0	
HC		8/9/10	10	41	9.4	
HC		8/9/10	20	76	1.9	
HC		8/9/10	30	78	1.1	
gas bubble		8/9/10	0–2	21	13.1	
gas bubble		8/9/10	5	29	11.7	
gas bubble		8/9/10	10	40	10.3	
gas bubble		8/9/10	20	29	17.5	
gas bubble		8/9/10	30	55	5.1	
1700 N	3	8/9/10	0–2	55	3.3	
1700 N	3	8/9/10	5	54	8.2	
1700 N	3	8/9/10	10	52	8.3	
1700 N	3	8/9/10	20	62	4.8	
1700 N	3	8/9/10	30	61	5.4	
above center St	2	8/9/10	0–2	37	7.2	

Table 51. Sediment %TS and %VS (d)

site	reach	date	depth	%TS	%VS	note
above center St	2	8/9/10	5	41	9.5	
above center St	2	8/9/10	10	47	7.8	
above center St	2	8/9/10	20	75	2.3	
above center St	2	8/9/10	30	67	4.6	
LNP NE	1	8/9/10	0–2	29	8.9	
LNP NE	1	8/9/10	5	37	9.0	
LNP NE	1	8/9/10	10	55	4.9	
LNP NE	1	8/9/10	30	53	7.4	
LNP NE	1	1/3/11	0–2	43	7.8	
LNP NE	1	1/3/11	5	41	9.7	
LNP NE	1	1/3/11	10	44	8.5	
LNP NE	1	1/3/11	20	52	7.1	
LNP NE	1	1/3/11	30	57	4.8	
LNP NE	1	1/3/11	40	60	4.5	
LNP NE	1	1/3/11	50	71	2.8	
LNP NE	1	1/3/11	0–2	45	6.9	tray 1
LNP NE	1	1/3/11	5	54	5.4	tray 1
LNP NE	1	1/3/11	0–2	43	7.7	tray 2
LNP NE	1	1/3/11	5	48	7.1	tray 2
300 N	2	1/6/11	0–2	31	10.5	
300 N	2	1/6/11	5	46	7.9	
300 N	2	1/6/11	10	65	4.4	
300 N	2	1/6/11	20	70	4.4	
300 N	2	1/6/11	30	74	2.3	
LNP NE	1	1/6/11	0–2	48	5.3	tray 1
LNP NE	1	1/6/11	5	58	5.4	tray 1
LNP NE	1	1/6/11	0–2	51	4.6	tray 2
LNP NE	1	1/6/11	5	56	5.6	tray 2
1700 S-S	3	1/7/11	0–2	77	1.0	
1700 S-S	3	1/7/11	5	77	1.1	
1700 S-S	3	1/7/11	10	79	1.1	
1700 S-S	3	1/7/11	20	85	0.5	
1700 S-S	3	1/7/11	30	86	0.5	
1700 S-S	3	1/7/11	0–2	44	4.3	tray 1
1700 S-S	3	1/7/11	5	75	0.9	tray 1
1700 S-S	3	1/7/11	0–2	57	2.5	tray 2
1700 S-S	3	1/7/11	5	79	0.9	tray 2
2100 S	3	1/7/11	0–2	90	0.5	
2100 S	3	1/7/11	5	91	0.2	

Table 52. Sediment %TS and %VS (e)

site	reach	date	depth	%TS	%VS	note
2100 S	3	1/7/11	10	91	0.1	
2100 S	3	1/7/11	20	86	0.4	
2100 S	3	1/7/11	30	89	0.8	
2100 S	3	1/7/11	0–2	83	1.0	tray 1
2100 S	3	1/7/11	5	86	0.6	tray 1
2100 S	3	1/7/11	0–2	86	0.5	tray 2
2100 S	3	1/7/11	5	86	0.7	tray 2
7600 S		1/15/11	0–2	86	0.7	
7600 S		1/15/11	5	88	0.4	
7600 S		1/15/11	10	89	0.4	
7600 S		1/15/11	20	92	0.4	
5400 S		1/12/11	0–2	87	0.6	
5400 S		1/12/11	5	92	0.4	
5400 S		1/12/11	10	92	0.4	
5400 S		1/12/11	20	93	0.3	
9000 S		1/20/11	0–2	84	0.6	
9000 S		1/20/11	5	88	0.4	
9000 S		1/20/11	10	93	0.3	
LNP NE		2/24/11	0–2	44	6.2	
LNP NE	1	2/24/11	5	53	5.9	
LNP NE	1	2/24/11	10	53	6.3	
LNP NE	1	2/24/11	20	54	6.8	
LNP NE	1	2/24/11	30	70	2.5	
LNP NE	1	2/24/11	40	63	4.6	
LNP NE	1	2/24/11	50	64	4.6	
LNP NE	1	2/24/11	60	73	2.2	
1700 N	2	2/24/11	0–2	41	6.0	
1700 N	2	2/24/11	5	52	6.2	
1700 N	2	2/24/11	10	51	7.7	
1700 N	2	2/24/11	20	66	3.8	
1700 N	2	2/24/11	30	68	3.0	
1700 N	2	2/24/11	40	66	3.8	
1700 N	2	2/24/11	50	72	2.4	
100 N	2	2/24/11	0–2	42	7.8	
100 N	2	2/24/11	5	56	7.0	
100 N	2	2/24/11	10	53	6.9	
100 N	2	2/24/11	20	74	1.4	
100 N	2	2/24/11	30	81	1.3	
100 N	2	2/24/11	40	74	2.2	

Table 53. Sediment %TS and %VS (f)

site	reach	date	depth	%TS	%VS	note
900 S-N	3	2/24/11	0–2	52	4.3	
900 S-N	3	2/24/11	5	53	6.7	
900 S-N	3	2/24/11	10	71	1.8	
900 S-N	3	2/24/11	20	69	2.5	
900 S-N	3	2/24/11	30	72	1.4	
HC		2/24/11	0–2	23	16.8	
HC		2/24/11	5	38	16.1	
HC		2/24/11	10	35	24.9	
HC		2/24/11	20	55	5.2	
HC		2/24/11	30	70	1.7	
HC		2/24/11	40	80	1.0	
HC		2/24/11	45	84	0.8	
LNP NE	1	4/14/11	0–2	60	2.3	
LNP NE	1	4/14/11	5	59	4.0	
LNP NE	1	4/14/11	10	43	9.1	
LNP NE	1	4/14/11	20	62	4.5	
LNP NE	1	4/14/11	30	70	3.7	
LNP NE	1	4/14/11	40	65	5.2	
100 N	2	4/14/11	0–2	48	6.4	
100 N	2	4/14/11	5	61	4.5	
100 N	2	4/14/11	10	73	3.2	
100 N	2	4/14/11	20	73	3.0	
100 N	2	4/14/11	30	72	3.3	
LNP NE	1	7/18/11	0–2	57	3.4	
LNP NE	1	7/18/11	5	72	1.2	
LNP NE	1	7/18/11	10	69	2.0	
LNP NE	1	7/18/11	15	49	8.5	
LNP NE	1	7/18/11	20	55	7.6	
LNP NE	1	7/18/11	30	65	4.9	
LNP NE	1	7/18/11	40	69	4.6	
LNP NE	1	7/18/11	50	67	4.6	
2500 S		7/23/11	0–2	69	1.4	
2500 S		7/23/11	5	72	2.0	
2500 S		7/23/11	10	69	3.4	
2500 S		7/23/11	15	71	2.5	
2500 S		7/23/11	20	65	4.3	
2500 S		7/23/11	30	61	5.8	
2500 S		7/23/11	40	51	7.8	
1300 S	3	7/25/11	0–2	36	12.1	

Table 54. Sediment %TS and %VS (g)

site	reach	date	depth	%TS	%VS	note
1300 S	3	7/25/11	10	58	6.1	
1300 S	3	7/25/11	15	67	4.5	
1300 S	3	7/25/11	20	62	6.4	
1300 S	3	7/25/11	25	54	10.2	
LNP NE	1	8/16/11	0–2	55	4.7	
LNP NE	1	8/16/11	5	61	4.4	
LNP NE	1	8/16/11	10	55	6.1	
LNP NE	1	8/16/11	15	60	4.7	
LNP NE	1	8/16/11	20	70	2.3	
LNP NE	1	8/16/11	30	70	1.9	
LNP NE	1	8/16/11	40	63	3.9	
LNP NE	1	8/16/11	50	73	2.7	
LNP NE	1	8/16/11	0–2	65	3.2	33' E
LNP NE	1	8/16/11	5	61	7.2	33' E
LNP NE	1	8/16/11	10	55	8.1	33' E
LNP NE	1	8/16/11	15	71	8.8	33' E
LNP NE	1	8/16/11	30	47	10.3	33' E
LNP NE	1	8/16/11	40	64	5.5	33' E
LNP NE	1	8/16/11	50	76	2.9	33' E
LNP NE	1	8/16/11	0–2	66	2.3	58' E
LNP NE	1	8/16/11	5	49	11.8	58' E
LNP NE	1	8/16/11	10	59	5.0	58' E
LNP NE	1	8/16/11	15	64	4.6	58' E
LNP NE	1	8/16/11	20	73	1.4	58' E
Burnham	1	9/12/11	0–2	57	4.0	
Burnham	1	9/12/11	5	58	4.6	
Burnham	1	9/12/11	10	60	5.0	
Burnham	1	9/12/11	15	58	6.2	
Burnham	1	9/12/11	20	62	5.3	
Burnham	1	9/12/11	30	66	3.4	
Burnham	1	9/12/11	40	72	3.0	
1300 S	3	9/13/11	0–2	71	1.4	
1300 S	3	9/13/11	5	43	15.1	
1300 S	3	9/13/11	10	43	17.6	
1300 S	3	9/13/11	20	55	10.1	
1300 S	3	9/13/11	25	63	5.4	
1700 N	2	9/14/11	0–2	41	6.5	
1700 N	2	9/14/11	5	54	5.8	
1700 N	2	9/14/11	10	57	5.4	

Table 55. Sediment %TS and %VS (h)

site	reach	date	depth	%TS	%VS	note
1700 N	2	9/14/11	15	72	2.2	
1700 N	2	9/14/11	20	58	6.8	
1700 N	2	9/14/11	30	59	6.7	
1700 N	2	9/14/11	40	63	4.9	
1700 S-N	3	9/14/11	0–2	45	4.9	
1700 S-N	3	9/14/11	5	64	4.1	
1700 S-N	3	9/14/11	10	69	3.0	
1700 S-N	3	9/14/11	15	72	2.6	
1700 S-N	3	9/14/11	20	68	3.5	
1700 S-N	3	9/14/11	25	85	0.5	
1300 S	3	1/10/12	0–2	56	2.2	
1300 S	3	1/10/12	5	76	2.0	
1300 S	3	1/10/12	10	75	2.2	
1300 S	3	1/10/12	15	74	2.0	
1300 S	3	1/10/12	20	74	2.6	
1300 S	3	1/10/12	30	46	15.8	
1700 N	2	1/18/12	0–2	76	0.6	
1700 N	2	1/18/12	5	82	0.6	
1700 N	2	1/18/12	10	83	0.5	
1700 N	2	1/18/12	15	37	13.0	
1700 N	2	1/18/12	20	49	8.0	
1700 N	2	1/18/12	30	37	16.0	
1700 N	2	1/18/12	40	33	18.1	
1700 N	2	1/18/12	0–2	73	0.7	29' W
1700 N	2	1/18/12	5	79	0.7	29' W
1700 N	2	1/18/12	10	76	1.4	29' W
1700 N	2	1/18/12	15	80	0.6	29' W
1700 N	2	1/18/12	20	83	0.6	29' W
1700 N	2	1/18/12	30	67	7.6	29' W
1700 N	2	1/18/12	40	80	1.2	29' W
1700 N	2	1/18/12	50	57	13.8	29' W
1700 N	2	1/18/12	0–2	71	0.9	43' W
1700 N	2	1/18/12	5	75	0.7	43' W
1700 N	2	1/18/12	10	77	0.6	43' W
1700 N	2	1/18/12	15	73	1.4	43' W
1700 N	2	1/18/12	20	74	1.1	43' W
1700 N	2	1/18/12	30	80	1.5	43' W
1700 N	2	1/18/12	40	79	0.9	43' W
1700 N	2	1/18/12	50	69	4.6	43' W

Table 56. Sediment %TS and %VS (i)

site	reach	date	depth	%TS	%VS	note
Rose Park	2	1/25/12	0–2	66	2.4	
Rose Park	2	1/25/12	5	72	2.5	
Rose Park	2	1/25/12	10	73	2.8	
Rose Park	2	1/25/12	15	73	2.1	
Rose Park	2	1/25/12	20	75	1.6	
Rose Park	2	1/25/12	0–2	66	1.3	15' W
Rose Park	2	1/25/12	5	75	1.0	15' W
Rose Park	2	1/25/12	10	73	1.3	15' W
Rose Park	2	1/25/12	15	77	0.7	15' W
Rose Park	2	1/25/12	20	75	1.1	15' W
Rose Park	2	1/25/12	40	65	5.2	15' W
Rose Park	2	1/25/12	50	70	3.1	15' W
Rose Park	2	1/25/12	60	75	2.4	15' W
Rose Park	2	1/25/12	70	70	4.4	15' W
Rose Park	2	1/25/12	0–2	79	0.8	28' W
Rose Park	2	1/25/12	5	79	0.7	28' W
Rose Park	2	1/25/12	10	76	1.0	28' W
Rose Park	2	1/25/12	15	78	1.9	28' W
Rose Park	2	1/25/12	20	76	2.6	28' W
Rose Park	2	1/25/12	30	76	1.0	28' W
Rose Park	2	1/25/12	40	81	0.5	28' W
Rose Park	2	1/25/12	0–2	75	1.3	40' W
Rose Park	2	1/25/12	5	81	1.0	40' W
Rose Park	2	1/25/12	10	77	2.7	40' W
Rose Park	2	1/25/12	15	77	1.0	40' W
Rose Park	2	1/25/12	20	61	8.4	40' W
Rose Park	2	1/25/12	30	68	3.3	40' W
Rose Park	2	1/25/12	40	66	6.1	40' W
Rose Park	2	1/25/12	50	64	3.0	40' W
300 N	2	2/8/12	0–2	64	2.5	
300 N	2	2/8/12	5	65	3.0	
300 N	2	2/8/12	10	69	3.5	
300 N	2	2/8/12	15	68	3.7	
300 N	2	2/8/12	20	78	1.7	
300 N	2	2/8/12	0–2	75	1.0	17' W
300 N	2	2/8/12	5	74	2.4	17' W
300 N	2	2/8/12	10	60	4.9	17' W
300 N	2	2/8/12	15	66	3.5	17' W
300 N	2	2/8/12	20	71	3.3	17' W

Table 57. Sediment %TS and %VS (j)

site	reach	date	depth	%TS	%VS	note
300 N	2	2/8/12	30	67	8.2	17' W
300 N	2	2/8/12	0–2	65	3.5	28' W
300 N	2	2/8/12	5	69	4.2	28' W
300 N	2	2/8/12	10	82	1.7	28' W
300 N	2	2/8/12	15	86	1.0	28' W
300 N	2	2/8/12	0–2	58	3.3	46' W
300 N	2	2/8/12	5	59	4.4	46' W
300 N	2	2/8/12	10	54	5.6	46' W
300 N	2	2/8/12	15	68	2.7	46' W
300 N	2	2/8/12	20	69	1.9	46' W
LNP NE	1	4/2/12	0–2	71	1.7	
LNP NE	1	4/2/12	5	76	3.6	
LNP NE	1	4/2/12	10	76	2.9	
LNP NE	1	4/2/12	15	82	1.6	
LNP NE	1	4/2/12	0–2	79	1.2	45' E
LNP NE	1	4/2/12	5	78	3.2	45' E
LNP NE	1	4/2/12	10	58	7.0	45' E
LNP NE	1	4/2/12	15	67	5.7	45' E
LNP NE	1	4/2/12	20	64	8.1	45' E
LNP NE	1	4/2/12	0–2	75	1.7	64' E
LNP NE	1	4/2/12	5	61	9.7	64' E
LNP NE	1	4/2/12	10	58	7.5	64' E
LNP NE	1	4/2/12	15	60	6.7	64' E
LNP NE	1	4/2/12	20	56	11.3	64' E
300 N	2	5/14/12	0–2	61	2.3	
300 N	2	5/14/12	5	66	2.8	
300 N	2	5/14/12	10	67	2.9	
300 N	2	5/14/12	15	70	2.9	
300 N	2	5/14/12	20	68	3.3	
300 N	2	5/14/12	0–2	74	1.2	18' W
300 N	2	5/14/12	5	79	1.2	18' W
300 N	2	5/14/12	10	74	1.6	18' W
300 N	2	5/14/12	15	69	3.0	18' W
300 N	2	5/14/12	20	72	2.4	18' W
300 N	2	5/14/12	0–2	64	2.8	28' W
300 N	2	5/14/12	5	77	2.2	28' W
300 N	2	5/14/12	10	82	1.2	28' W
300 N	2	5/14/12	15	73		28' W
300 N	2	5/14/12	20	81	1.2	28' W

Table 58. Sediment %TS and %VS (k)

site	reach	date	depth	%TS	%VS	note
300 N	2	5/14/12	0–2	50	5.2	46' W
300 N	2	5/14/12	5	59	4.1	46' W
300 N	2	5/14/12	10	65	3.9	46' W
300 N	2	5/14/12	15	76	3.6	46' W
300 N	2	5/14/12	20	82	0.5	46' W
1700 S-N	3	5/16/12	0–2	38	5.8	
1700 S-N	3	5/16/12	5	62	3.0	
1700 S-N	3	5/16/12	15	71	2.8	
1700 S-N	3	5/16/12	20	73	2.5	
1700 S-N	3	5/16/12	0–2	81	0.5	27' W
1700 S-N	3	5/16/12	5	84	0.9	27' W
1700 S-N	3	5/16/12	0–2	80	1.8	38' W
1700 S-N	3	5/16/12	5	82	1.0	38' W
1700 S-N	3	5/16/12	10	63	4.1	38' W
700 S	3	5/16/12	0–2	58	3.3	
700 S	3	5/16/12	5	65	3.5	
700 S	3	5/16/12	10	64	4.4	
700 S	3	5/16/12	15	60	7.0	
700 S	3	5/16/12	20	73	1.9	
700 S	3	5/16/12	0–2	77	1.0	22' E
700 S	3	5/16/12	5	88	0.7	22' E
700 S	3	5/16/12	10	73	1.0	22' E
700 S	3	5/16/12	15	70	3.1	22' E
700 S	3	5/16/12	20	73	2.1	22' E
700 S	3	5/16/12	0–2	80	0.7	30' E
700 S	3	5/16/12	5	85	0.8	30' E
Burnham	1	5/29/12	0–2	50	4.9	
Burnham	1	5/29/12	5	40	13.3	
Burnham	1	5/29/12	10	63	5.6	
Burnham	1	5/29/12	15	70	3.6	
Burnham	1	5/29/12	20	76	2.8	
Burnham	1	5/29/12	0–2	65	1.9	30' E
Burnham	1	5/29/12	5	44	8.7	30' E
Burnham	1	5/29/12	10	47	8.3	30' E
Burnham	1	5/29/12	15	56	5.5	30' E
Burnham	1	5/29/12	20	56	5.3	30' E
Burnham	1	5/29/12	0–2	47	5.1	52' E
Burnham	1	5/29/12	5	60	3.9	52' E
Burnham	1	5/29/12	10	52	6.1	52' E

Table 59. Sediment %TS and %VS (l)

site	reach	date	depth	%TS	%VS	note
Burnham	1	5/29/12	15	55	5.8	52' E
Burnham	1	5/29/12	20	60	5.2	52' E
Cudahy Ln	1	6/6/12	0–2	64	2.8	
Cudahy Ln	1	6/6/12	5	52	6.8	
Cudahy Ln	1	6/6/12	10	55	7.1	
Cudahy Ln	1	6/6/12	15	56	7.0	
Cudahy Ln	1	6/6/12	20	61	5.3	
Cudahy Ln	1	6/6/12	0–2	74	1.5	30'
Cudahy Ln	1	6/6/12	5	69	3.4	30'
Cudahy Ln	1	6/6/12	10	67	4.4	30'
Cudahy Ln	1	6/6/12	15	72	3.3	30'
Cudahy Ln	1	6/6/12	20	73	2.8	30'
Cudahy Ln	1	6/6/12	0–2	49	5.0	48'
Cudahy Ln	1	6/6/12	5	54	4.8	48'
Cudahy Ln	1	6/6/12	10	66	2.9	48'
Cudahy Ln	1	6/6/12	15	70	2.2	48'
Cudahy Ln	1	6/6/12	20	74	2.4	48'
HC		6/2/10	0–2	23	11.4	
HC		6/2/10	10	59	5.1	
HC		6/2/10	20	63	4.4	
HC		6/2/10	30	81	1.5	

Table 60. Hydraulic reach average sediment %TS

	%TS (2010–2013 samples)									
depth (cm)	0–2	5	10	15	20	30	40	50	# sites	# depths
Reach 1 avg.	51	54	56	60	63	62	65	72	35	163
Reach 2 avg.	58	66	67	69	70	68	69	66	29	157
Reach 3 avg.	63	70	72	75	73	72	71	76	35	170
Reach 4, BW	41	49	49	54	58	69	66		5	33
Reach 4, 5400 S	87	92	92	92	93				1	5
Reach 5, 7600 S	86	88	89	90	92				1	5
Reach 6, 9000 S	84	88	93						1	3
Reach 8, US-173	45	56	67	68	68	71			1	6

Note: data compiled from 542 samples

Table 61. Hydraulic reach average sediment %VS

%VS (2010–2013 samples)								
depth (cm)	0–2	5	10	15	20	30	40	50
Reach 1 avg.	4.8	6.6	6.2	5.8	5.4	5.0	4.4	3.3
Reach 2 avg.	3.8	3.5	3.6	3.6	3.4	4.5	4.5	5.4
Reach 3 avg.	3.1	3.3	2.8	3.4	2.5	3.7	3.0	2.8
Reach 4, backwater	8.9	8.2	8.4	7.3	6.7	3.0	4.4	
Reach 4, 5400 S	0.6	0.4	0.4	0.4	0.3			
Reach 5, 7600 S	0.7	0.4	0.4	0.4	0.4			
Reach 6, 9000 S	0.6	0.4	0.3					
Reach 8, US-173	5.6	4.0	2.4	2.8	3.2	3.0		

Note: data compiled from 538 samples

APPENDIX D

SPRING 2012 RIVER-WIDE SEDIMENT CHARACTERIZATION

Table 62. River-wide sediment analysis (a)

Burnham Dam, 5/29/11						
depth	bank	$\%TS_{bulk}$	$\%VS_{bulk}$	$\%VS_{CPOM}$	$\%TOC_{bulk}$	TOC:VS
0–2	E	50	4.9	2.6	2.6	0.53
5	E	40	13.3	2.5		
10	E	63	5.6	1.4		
15	E	70	3.6	1.1		
20	E	76	2.8	0.8		
0–2	T	65	1.9	7.1	1.2	0.63
5	T	44	8.7	7.1		
10	T	47	8.3	3.7		
15	T	56	5.5	3.2	2.9	0.53
20	T	56	5.3	0.3		
0–2	W	47	5.1	0.4	2.8	0.55
5	W	60	3.9	14	2.1	0.54
10	W	52	6.1	7.4	3.7	0.61
15	W	55	5.8	4.5	3.8	0.66
20	W	60	5.2	6.3	3.4	0.65

Note: E = east bank, T = thalweg, and W = west bank

Table 63. River-wide sediment analysis (b)

700 S, 5/16/12						
depth	bank	$\%TS_{bulk}$	$\%VS_{bulk}$	$\%VS_{CPOM}$	$\%TOC_{bulk}$	TOC:VS
0–2	E	58	3.3	6.7	1.4	0.42
5	E	65	3.5	30.2	1.5	0.43
10	E	64	4.4	31.8	2.2	0.5
15	E	60	7	19	3.6	0.51
20	E	73	1.9	8.6	0.8	0.42
0–2	T	77	1	62.7		
5	T	88	0.7	55.8		
10	T	73	1	17.3		
15	T	70	3.1	24.5	2.1	0.68
20	T	73	2.1	13.6		
0–2	W	80	0.7	52.5		
5	W	85	0.8	38.6		

Table 64. River-wide sediment analysis (c)

LNP NE, 4/2/12						
depth	bank	$\%TS_{bulk}$	$\%VS_{bulk}$	$\%VS_{CPOM}$	$\%TOC_{bulk}$	TOC:VS
0–2	E	71	1.7	1		
5	E	76	3.6	18		
10	E	76	2.9	27		
15	E	82	1.6	10		
0–2	T	79	1.2	30		
5	T	78	3.2	26		
10	T	58	7	32		
15	T	67	5.7	12		
20	T	64	8.1	19		
0–2	W	75	1.7	3		
5	W	61	9.7	11		
10	W	58	7.5	18		
15	W	60	6.7	4		
20	W	57	11.3	39		

Table 65. River-wide sediment analysis (d)

LNP NE, 8/26/11						
depth	bank	$\%TS_{bulk}$	$\%VS_{bulk}$	$\%VS_{CPOM}$	$\%TOC_{bulk}$	TOC:VS
0–2	E		4.7		2.5	0.53
5	E		4.4		1.9	0.43
10	E		6.1		2.5	0.41
15	E		4.7		2.2	0.47
20	E		2.3		1	0.43
30	E		1.9		1	0.53
40	E		3.9		2	0.51
50	E		2.7		1.4	0.52
0–2	T		7.2		2.7	0.38
10	T		8.1		3.5	0.43
30	T		10.3		4.3	0.42
40	T		5.5		1.6	0.29
10	W		5		2.7	0.54
20	W		1.4		0.4	0.29

Table 66. River-wide sediment analysis (e)

Cudahy Ln, 6/6/12						
depth	bank	$\%TS_{bulk}$	$\%VS_{bulk}$	$\%VS_{CPOM}$	$\%TOC_{bulk}$	TOC:VS
0–2	E	64	2.8	0	1.2	0.43
5	E	52	6.8	1.7	3.5	0.51
10	E	55	7.1	1.7	3.9	0.55
15	E	56	7	2.5	3.8	0.54
20	E	61	5.3	0.7	2.8	0.53
0–2	T	74	1.5	70		
5	T	69	3.4	47.6		
10	T	67	4.4	39.7	2.4	0.55
15	T	72	3.3	27.9		
20	T	73	2.8	40.3		
0–2	W	49	5	5.1	2.3	0.46
5	W	54	4.8	4.1	2.4	0.5
10	W	66	2.9	9.7	1.4	0.48
15	W	70	2.2	4.7	0.8	0.36
20	W	75	2.4	7.1		

Table 67. River-wide sediment analysis (f)

1700 S, 5/16/12						
depth	bank	$\%TS_{bulk}$	$\%VS_{bulk}$	$\%VS_{CPOM}$	$\%TOC_{bulk}$	TOC:VS
0–2	E	80	1.8	37.6		
10	E	63	4.1	6.8	2	0.49
0–2	T	81	0.5	51.9		
0–2	W	38	5.8	12.4	2.4	0.53
5	W	62	3	17.4		
15	W	71	2.8	30.6		
20	W	73	2.5	4		

Table 68. River-wide sediment analysis (g)

300 N, 5/24/12						
depth	bank	$\%TS_{bulk}$	$\%VS_{bulk}$	$\%VS_{CPOM}$	$\%TOC_{bulk}$	TOC:VS
0–2	W	61	2.3	0	0.9	0.39
5	W	66	2.8	0.9	1.2	0.43
10	W	67	2.9	1.2	1.5	0.52
15	W	70	2.9	36.5		
20	W	69	3.3	18.7		
0–2	T	74	1.2	92.4		
5	T	79	1.2	28.8		
10	T	74	1.6	18.6	0.8	0.5
15	T	69	3	45.1	2	0.67
20	T	72	2.4	15.1		
0–2	T	64	2.8	54.8	1.4	0.5
5	T	77	2.2	27.6		
10	T	82	1.2	32.9		
20	T	81	1.2	16.9		
0–2	E	50	5.2	19.2		
5	E	59	4.1	15.4	2.3	0.56
10	E	65	3.9	15	2.5	0.64
15	E	76	3.6	6.5		
20	E	82	0.5	30.1		

APPENDIX E

JORDAN RIVER SEDIMENT PORE WATER AND C:N RATIOS

Table 69. Lower Jordan River pore water

site info.	depth (cm)	%TS	%VS	pore water concentrations (mg/L) NPDOC	NH_4-N	PO_4-P
Burnham	0–2	28	10.1	46.8	3.5	5.3
5/24/13	5	33	10.6	50.8	25.1	5.8
	10	52	7.7	79.4	37.5	8.7
LNP NE	0–2	57	3.1		5.6	3.6
5/24/13	5	69	2.7	55.4	55.6	5.1
	10	57	5.9	109.0	124.9	2.6
	15	59		101.5	170.4	3.2
	20	53	7.7	96.6	174.0	3.1
Cudahy Ln	0–2	34	7.8	62.7	2.3	4.9
5/24/13	5	43	7.3	76.1	47.7	5.6
	10	56	4.7	73.1	107.3	3.3
	15	54	6.9	87.1		6.1
	20	61	6.2	125.4	151.1	5.6
300 N	0–2	66	3.3	83.9	8.6	3.7
5/24/13	5	69		85.8	15.7	4.0
	10	59	6.2	63.8	17.3	4.9
	15	85		66.6	10.9	4.0
700 S	0–2	59	3.7	38.5	12.8	7.2
5/24/13	5	66	4.9	54.6	44.7	4.6
	10	67	4.8	91.1	65.5	6.0
	15	72	3.1	70.8	91.9	5.1
	20	71	2.6	63.4	81.0	4.5
1700 S-N	0–2	59	1.8	30.0	7.0	8.6
5/24/13	5	65	2.2	46.2	11.0	8.5
	10	69	2.7	76.4	14.0	6.8
	15	77	1.5	127.0	17.0	8.3
	20	77	1.0	58.9	10.7	6.4

Notes: dilluted all samples with 200 mL Milli-Q water

$[(H_2O \text{ mass})(x) + (200)(0)] / (200 + H_2O \text{ mass}) = y$

x = pore water nutrient concentration

y = dilluted measurement

NO_2-N non detect

NO_3-N below detection limits

Table 70. Upper Jordan River sediment pore water (a)

site	location (ft)	depth (cm)	NH_4-N (mg/L)	NO_3-N (mg/L)	PO_4-P (mg/L)	NPDOC (mg/L)	DO (mg/L)	pH
5400 S		ambient	0.28	2.83	0.81	4.3	8.9	8.8
5400 S	15	30	0.06	0.82	0.09	3.9	2.2	7.6
5400 S	15	60	0.03	0.21	0.05	3.2	2.23	7.5
5400 S	15	90	0.09	2.81	0.04	2.2	2.6	7.4
5400 S	29	30	0.16	0.58	0.1	4.4	3.2	7.7
5400 S	29	60	0.08	0.24	0.05	4.4	3	7.3
5400 S	29	90	0.03	0.22	0.05	2.9	2.3	7.5
5400 S	48	30	0.01	3.21	0.05	5.6	3	7.4
5400 S	48	60	0.06	4.13	0.04	2.7	2.5	7.3
5400 S	48	90	0.04	4.06	0.05	2.9	2.3	7.2
5400 S	eddy	30	0.05	3.73	0.06	1.8	2.8	7.9
5400 S	eddy	60	0.09	3.94	0.14	5.3	2.5	7.7
5400 S	eddy	90	0.01	3.47	0.14	6.6	4.3	7.6
7600 S		ambient	0.57	1.07	0.08	5.6		
7600 S	15	30	0.14	0.28	0.05	2.9		
7600 S	15	60	0.07	0.29	0.04	3.8		
7600 S	15	90	0.26	0.31	0.03	3.7		
7600 S	15	30	0.14	0.33		3.3		
7600 S	15	60	0.05	0.31	0.04	3.6		
7600 S	15	90	0.23	0.11	0.04	3.1		
7600 S	eddy	30	0.12	0.1	0.05	2.7		
7600 S	eddy	60	0.07	0.11	0.03	3.6		
7600 S	eddy	90	0.08	0.87	0.04	3.4		

Note: 5400 S sampled on 7-22-2012
7600 S sampled on 7-27-2012

Table 71. Upper Jordan River sediment pore water (b)

site	location (ft)	depth (cm)	NH_4-N (mg/L)	NO_3-N (mg/L)	PO_4-P (mg/L)	NPDOC (mg/L)	DO (mg/L)	pH
9000 S		ambient	0.06	1.1	0.08	5.6	8.3	8.2
9000 S	17	30	0.05	0.73	0.04	4.3	1.7	7.5
9000 S	17	60	0.06	0.9	0.03	6	1.8	7.3
9000 S	17	90	0.09	0.88	0.03	8.4	1.8	7.3
9000 S	27	30	0.02	0.62	0.04	1.8	2.3	7.3
9000 S	27	60	0.05	0.77	0.03	2.3	1.8	7.3
9000 S	27	90	0.04	0.8	0.03	2.3	1.7	7.3
9000 S	45	30	0.03	0.6	0.04	1.9	1.9	7.3
9000 S	45	60	0.04	0.64	0.04	2.1	1.8	7.3
9000 S	45	90	0.03	0.72	0.03	1.8	1.9	7.3
9000 S	15	30	0.07	1.04	0.05	4	2.5	7.6
9000 S	15	60	0.05	1.03	0.03	2.5	1.8	7.6
9000 S	15	90	0.05	1.11	0.03	2.1	2.2	7.6
10600 S		ambient	0.03	1.1	0.14	4.3	8.2	8.7
10600 S	9	30	0.01	1.32	0.05	1.3	3.3	8.1
10600 S	9	60	0.02	1.09	0.04	1.5	3.5	7.9
10600 S	9	90	0.02	1.53	0.03	2.8	3	7.8
10600 S	22	30	0.01	1.43	0.04	1.6	2.8	7.7
10600 S	22	60	0.01	1.52	0.03	1.5	2.4	7.7
10600 S	22	90	0.02	1.48	0.04	1.7	3.2	7.6
10600 S	38	30	0.04	0.65	0.06	3.1	3.5	7.6
10600 S	38	60	0.01	0.91	0.06	2.6	3.2	7.5
10600 S	38	90	0.01	1.53	0.04	1.5	3.3	7.5

Note: 9000 S sampled on 7-18-2012
10600 S sampled on 7-23-2012

Table 72. Upper Jordan River sediment pore water (c)

site	location (ft)	depth (cm)	NH_4-N (mg/L)	NO_3-N (mg/L)	PO_4-P (mg/L)	NPDOC (mg/L)	DO (mg/L)	pH
10600 S	stream	30	0.06	0.15	0.05	5.7	3.1	8
10600 S	stream	60	0.09	0.06	0.09	4.3	3.4	7.7
10600 S	stream	90	0.02	0.31	0.06	3	3.8	7.5
14600 S		ambient	0.06	0.75	0.05	3.7	7.6	8.4
14600 S	15	30	0.03	2.07	0.06	1.6	6.2	8
14600 S	15	60	0.02	2.13	0.06	1.5	6.5	7.8
14600 S	15	90	0.02	2.22	0.06	1.4	6.8	7.8
14600 S	20	30	0.02	1.91	0.05	1.4	7	7.8
14600 S	20	60	0	2.2	0.04	0.8	6.9	7.7
14600 S	20	90	0.01	1.99	0.05	1	6.8	7.6

Note: 10600 S sampled on 7-23-2012
14600 S sampled on 7-24-2012

Table 73. Sediment C:N molar ratios and stable isotope data

site	$^{13}C/^{12}C_{PDB}$	$^{15}N/^{14}N_{AIR}$	organic C (%)	organic N (%)	C:N ratio
Burnham	-26.7	8.8	3.9	0.32	11.9
LNP NE	-25.8	6.9	1.8	0.14	13.4
Cudahy Ln.	-23.9	9	5.4	0.46	11.7
Redwood Rd.	-25.5	8.4	3.8	0.35	10.9
300 N	-26.1	8.1	4.9	0.41	12.1
700 S	-22.5	-	0.4	0.03	11.7
1300 S	-20.7	-	3.1	0.11	28.3
1300 S	-25.8	7.7	1.9	0.13	14
1700 S	-25.3	-	1.3	0.1	12.3
2300 S	-20.5	8.3	1	0.09	11.6
900 S	-20.5	-	0.7	0.05	14.9
(stormwater pond)	-22.8	-	0.9	0.05	19
Mill Cr.	-24.2	6.1	1.9	0.18	10.6
(below CVWRF)	-23.5	5.6	1.7	0.15	11.3
Mill Cr.	-25.8	3.6	3.1	0.18	16.7
(above CVWRF)	-26	3.6	3.2	0.2	15.8
algal mat	-18.8	9.6	28.3	2.7	10.5
(900 S pond)	-18.9	9.3	28.9	2.72	10.6
gutter leaves	-27.3	1.8	45.4	0.62	73.2
(U of U)	-27.5	1.6	45.9	0.61	74.6

APPENDIX F

JORDAN RIVER AND UTAH LAKE SEDIMENT MINERALOGY

Table 74. Lower Jordan River sediment mineralogy (a)

site	% carbonates	% clays	% feldspars	% silica oxides	% other
LNP NE	21	17	21	42	0
Cudahy Ln	18	18	26	39	0
1700 N	20	14	22	45	0
300 N	11	11	29	41	8
900 S-N	14	10	22	54	0
900 S-S	4	10	28	39	19
1700 S	7	7	33	51	2
2300 S	19	12	23	46	0
US-173	40	21	15	24	0
Lower Jordan River avg	13	12	26	44	4
*Utah Lake outlet	63	9	10	13	5
**Utah Lake avg	50	8	15	19	6

* Utah Lake sample taken 2 miles east of Saratoga Springs

** Utah Lake avg consists of 12 samples

Table 75. Lower Jordan River sediment mineralogy (b)

Sediment mineral composition by % mass (top 0–2 cm)									
	LNP NE	Cudahy Ln	1700 N	300 N	900 S-N	900 S-S	1700 S	2300 S	US 173
calcite	13.2	11.5	12.2	9.6	8.8	3.8	2.4	12.2	34.1
aragonite	2.4	2.6	2.8	0.9	2.6	0.3	2.4	2.9	2
dolomite	4.9	3.9	4.6	0.4	2.2	0.2	2.3	4.2	3.8
smectite	0.3	0.2	0.2	0.5	0.1	0.1		0.1	0.3
illite	11.7	11.3	9.8	4.1	6.3	3.8	4.2	8.3	12.4
kaolinite	3.7	4.7	3.1	3.8	2.3	3.7	0.8	2.7	5
chlorite	1.3	1.5	1.1	2.6	0.8	2.3	2.3	0.8	2.9
quartz	40.4	37.5	43.7	41	53.3	38.5	47.4	45.5	23.4
amphibole	1.2	1.2	1		1		3.3	0.9	0.9
plagioclase	10.1	12.2	10.5	3.8	9.7	2.6	17.2	9.4	7.8
K-feldspar	10.9	13.4	11.1	25.3	12.4	25.3	15.4	13.1	7.5
magnetite							2.1		
pyrite	0.1			0.2					
zeolite				8.1		19.3			

Table 76. Utah Lake sediment mineralogy

site #	site	% carbonate	% clay	% feldspar	% silica oxide	% other
1	Provo Bay	58	8	14	16	4
1	Provo Bay (3–6 cm)	67	10	10	9	5
2	Entrance to Provo Bay	13	5	24	52	6
4	S.W. Goshen Bay	48	8	15	23	6
5	Goshen Bay	56	11	13	15	4
6	Geneva Steel	41	7	14	34	4
7	Geneva Steel	51	8	16	19	6
8	2 miles E. Saratoga Springs	63	9	10	13	5
10	1 mile E. f Pelican	36	4	17	38	5
11	Midlake	62	11	11	10	6
11	Midlake	69	10	9	7	5
11	Midlake (2–4 cm)	65	9	11	9	6

APPENDIX G

SEDIMENT NUTRIENT FLUXES AND WATER COLUMN RATES

Table 77. Nutrient dynamics (a)

		WC_{dark} ($g/m^3/day$)			SOD_{avg} ($g/m^2/day$)		
site	date	NH_4-N	NO_3-N	PO_4-P	NH_4-N	NO_3-N	PO_4-P
State Can.	2/6/13	-0.14	0.82	-0.02	2.46	-1.06	0.92
Burnham	6/12/12	0.12	0.88	1	0	-0.62	-0.07
Burnham	6/14/13	0.17	0.82	0.23	0.07	-0.98	-0.08
LNP NE	6/3/10	0.07	0.07	0.07	-0.14	-0.01	0.04
LNP NE	4/3/12	0.23	0.29	-0.09	-0.05	-0.1	0.03
LNP NE	6/15/12	0.3	0.86	0.1	0.02	-0.02	0.06
LNP NE	6/15/13	-0.02	-0.07	-0.02	0.05	-0.3	0.07
Cudahy Ln	6/3/10	-0.07	0	0	-0.12	-0.01	0.17
Cudahy Ln	6/13/12	-0.53	2.41	0.16	0.17	-0.28	0.02
Cudahy Ln	6/13/13	0.03	0.27	0.03	0.33	-0.6	0.02
300 N	6/7/10	-0.14	0.24	-0.31	0.12	0.01	0.15
300 N	4/14/12	-0.31	0.58	-0.1	0.06	-0.11	0.02
300 N	6/12/13	-0.02	0.21	0.14	0.02	0.02	-0.01
700 S	6/14/12	0.16	2.36	0.4	0.04	-0.15	0.01
700 S	6/10/13	0.03	0.82		0.11	-0.39	
900 S-N	6/8/10	0	-0.31	0.07	-0.01	-0.13	0.01
900 S-S	6/8/10	0.07	0.14	-0.24	-0.08	-0.03	0.09
1700 S-N	5/24/10	-0.07	0	-0.07	0.06	-0.07	0.15
1700 S-N	4/16/12	0.04	-0.58	-0.14	0.14	-0.17	-0.02
1700 S-N	6/10/13	0.05	-0.67	0.07	0.15	-0.2	0.22

Table 78. Nutrient dynamics (b)

		SOD_1 ($g/m^2/day$)			SOD_2 ($g/m^2/day$)		
site	date	NH_4-N	NO_3-N	PO_4-P	NH_4-N	NO_3-N	PO_4-P
State Can.	2/6/13	2.44	-0.67	-0.24	2.49	-1.45	2.09
Burnham	6/12/12	-0.02	-0.66	-0.09	0.01	-0.57	-0.05
Burnham	6/14/13	0.03	-0.56	-0.11	0.12	-1.4	-0.06
LNP NE	6/3/10	-0.09	-0.02	0.04	-0.18	0	0.04
LNP NE	4/3/12	-0.06	-0.05	0.02	-0.04	-0.14	0.05
LNP NE	6/15/12	-0.02	-0.12	0.05	0.07	0.09	0.07
LNP NE	6/15/13				0.05	-0.3	0.07
Cudahy Ln	6/3/10	-0.11	0	0.27	-0.12	-0.02	0.07
Cudahy Ln	6/13/12	0.19	-0.2	0.07	0.14	-0.36	-0.04
Cudahy Ln	6/13/13	0.28	-0.54	-0.05	0.38	-0.65	0.09
300 N	6/7/10	0.09	0.03	0.12	0.15	-0.01	0.17
300 N	4/14/12	0.08	-0.11	0.02	0.03	-0.11	0.02
300 N	6/12/13	0.03	-0.04	-0.01	0.02	0.07	-0.02
700 S	6/14/12	0.03	-0.3	0.01	0.06	0.01	0.02
700 S	6/10/13	0.08	-0.4		0.14	-0.39	
900 S-N	6/8/10	0	-0.19	-0.04	-0.02	-0.06	0.05
900 S-S	6/8/10	-0.11	-0.02	0.08	-0.04	-0.04	0.1
1700 S-N	5/24/10	0.05	-0.09	0.24	0.07	-0.05	0.05
1700 S-N	4/16/12	0.14	-0.2	0	0.14	-0.13	-0.03
1700 S-N	6/10/13	0.07	-0.08	0.07	0.22	-0.33	0.36

Table 79. Nutrient dynamics (c)

		WC_{dark} ($g/m^3/day$)			SOD_{avg} ($g/m^2/day$)		
site	date	NH_4-N	NO_3-N	PO_4-P	NH_4-N	NO_3-N	PO_4-P
2600 S	6/2/10	0.07	-0.07	0.07	-0.72	0.05	0.42
5400 S	1/12/11	0.2	1.44	-0.04	-0.05	-0.54	-0.03
5400 S*	1/12/11				-0.03	-0.34	-0.08
7600 S	1/15/11	-0.03	-0.5	-0.38	-0.01	-0.34	0.14
7600 S*	1/15/11				-0.01	0.17	0.07
9000 S	1/20/11	-0.01	-0.13	-0.37	-0.08	-0.03	0.07
9000 S*	1/20/11				0.02	-0.07	0.09

Note: * identifies TOD chamber

Table 80. Nutrient dynamics (d)

		SOD_1 ($g/m^2/day$)			SOD_2 ($g/m^2/day$)		
site	date	NH_4-N	NO_3-N	PO_4-P	NH_4-N	NO_3-N	PO_4-P
2600 S	6/2/10	-0.5	0.03	0.37	-0.94	0.06	0.46
5400 S	1/12/11	-0.03	-0.45	-0.04	-0.06	-0.62	-0.01
5400 S*	1/12/11	-0.01	-0.45	-0.06	-0.05	-0.24	-0.11
7600 S	1/15/11	0.04	-0.21	0.17	-0.05	-0.47	0.12
7600 S*	1/15/11	0.02	0.14	0.08	-0.03	0.2	0.06
9000 S	1/20/11	-0.13	-0.03	0.08	-0.03	-0.03	0.06
9000 S*	1/20/11	-0.01	0	0.1	0.06	-0.14	0.07

Note: * identifies TOD chamber

APPENDIX H

SEDIMENT METHANE PRODUCTION

Table 81. Lower Jordan River sediment methane production (a)

site	depth (cm)	location	%VS	CH_4 (mmol/kg wet sed./day)	CO_2	$CH_{4,OD}$ (g DO/m^2/d)
Burnham	0–2	8' E	4.9	0.635	0.611	3.55
Burnham	5	8' E	13.3	0.042	0.206	0.21
Burnham	10	8' E	5.6	0	0.122	0
Burnham	0–2	30' E	1.9	0.213	0.837	1.34
Burnham	5	30' E	8.7	0	0.162	0
Burnham	10	30' E	8.3	0.048	0.125	0.26
Burnham	0–2	52' E	5.1	0.431	0.509	2.36
Burnham	5	52' E	3.9	0.116	0.286	0.71
LNP NE	0–2	18' W	1.7	0.038	0.147	0.25
LNP NE	5	18' W	3.6	0.089	0.172	0.61
LNP NE	10	18' W	2.9	0.06	0.248	0.41
LNP NE	15	18' W	1.6	0.049	0.146	0.35
LNP NE	20	18' W	1.4	0.052	0.189	0.37
LNP NE	0–2	45' W	1.2	0.026	0.113	0.18
LNP NE	5	45' W	3.2	0.049	0.19	0.34
LNP NE	10	45' W	7	0.078	0.318	0.47
LNP NE	15	45' W	5.7	0.083	0.27	0.53
LNP NE	20	45' W	8.1	0.098	0.689	0.61
LNP NE	0–2	64' W	1.7	0.038	0.109	0.26
LNP NE	5	64' W	9.7	0.041	0.12	0.25
LNP NE	10	64' W	7.5	0.071	0.176	0.43
LNP NE	15	64' W	6.7	0.075	2.606	0.46
LNP NE	20	64' W	11.3	0.116	0.235	0.69

Note: Burnham dam sampled on 5-29-2012
LNP NE sampled on 4-2-2012

Table 82. Lower Jordan River sediment methane production (b)

site	depth (cm)	location	%VS	CH_4 (mmol/kg wet sed./day)	CO_2	$CH_{4,OD}$ (g DO/m^2/d)
Cudahy	0–2	8' E	2.8	0.178	0.377	1.11
Cudahy	5	8' E	6.8	0.387	0.266	2.21
Cudahy	10	8' E	7.1	0.131	0.396	0.77
Cudahy	0–2	30' E	1.5	0	0.114	0
Cudahy	5	30' E	3.4	0.042	0.077	0.28
Cudahy	10	30' E	4.4	0.09	0.126	0.58
Cudahy	0–2	48' E	5	0.182	0.192	1.01
Cudahy	5	48' E	4.8	0.273	0.481	1.57
Cudahy	10	48' E	2.9	0.426	1.127	2.71
300 N	0–2	8' W	2.3	0.269	0.25	1.64
300 N	5	8' W	2.8	0.268	0.284	1.71
300 N	10	8' W	2.9	0.207	0.351	1.32
300 N	0–2	28' W	2.8	0.531	0.46	3.34
300 N	5	28' W	2.2	0.332	0.395	2.28
300 N	10	28' W	1.2	0.082	0.134	0.58
300 N	0–2	46' W	5.2	0.305	0.328	1.7
300 N	5	46' W	4.1	0.065	0.124	0.39
300 N	10	46' W	3.9	0.039	0.067	0.25

Note: Cudahy Ln sampled on 6-6-2012
300 N sampled on 5-14-2012

Table 83. Lower Jordan River sediment methane production (c)

site	depth (cm)	location	%VS	CH_4 (mmol/kg wet sed./day)	CO_2	$CH_{4,OD}$ (g DO/m^2/d)
700 S	0–2	8' E	3.3	0.226	0.291	1.36
700 S	5	8' E	3.5	0.093	0.337	0.59
700 S	10	8' E	4.4	0.207	0.462	1.3
700 S	0–2	18' E	1	0.039	0.113	0.27
700 S	5	18' E	0.7	0	0.073	0
700 S	10	18' E	1	0	0.075	0
700 S	0–2	32' E	0.7	0.026	0.12	0.18
700 S	5	32' E	0.8	0	0.089	0
1700 S-N	0–2	10' W	5.8	0.654	0.47	3.29
1700 S-N	5	10' W	3	0.047	0.106	0.29
1700 S-N	10	10' W	2.8	0	0.085	0
1700 S-N	0–2	27' W	0.5	0	0.034	0
1700 S-N	5	27' W	0.9	0	0.028	0
1700 S-N	0–2	38' W	1.8	0	0.025	0
1700 S-N	5	38' W	1	0	0.041	0
1700 S-N	10	38' W	4.1	0	0.079	0

Note: 700 S sampled on 6-6-2012
1700 S- N sampled on 5-16-2012

REFERENCES

Ahn, Y. H. (2006). "Sustainable nitrogen elimination biotechnologies: A review." *Process Biochem.*, 41(8), 1709–1721.

Allan, J. D. (1995). *Stream ecology*, Chapman & Hall, New York.

Amon, R. M., and Benner, R. (1996). "Bacterial utilization of different size classes of dissolved organic matter." *Limnol. Oceanogr.*, 41(1), 41–51.

APHA, AWWA, WEF. (2005). *Standard Methods for the Examination of Water and Wastewater*, (A. D. Eaton, L. S. Clesceri, E. W. Rice, and A. E. Greenberg, Eds.), Americal Public Health Association, Washington, DC.

Appels, L., Baeyens, J., Degrève, J., and Dewil, R. (2008). "Principles and potential of the anaerobic digestion of waste-activated sludge." *Prog. Energ. Combust.*, 34(6), 755–781.

Baines, S. B., and Pace, M. L. (1991). "The production of dissolved organic matter by phytoplankton and its importance to bacteria: Patterns across marine and freshwater systems." *Limnol. Oceanogr.*, 36(6), 1078–1090.

Baity, H. G. (1938). "Some factors affecting the aerobic decomposition of sewage sludge deposits." *Sewage Work J.*, 10(3), 539–568.

Ball, D. F. (1964). "Loss-On-Ignition as an estimate of organic matter and organic carbon in non-calcareous soils." *J. Soil Sci.*, 15(1), 84–92.

Banks, R. B., and Herrera, F. F. (1977). "Effect of Wind and Rain on Surface Reaeration." *J. Environ. Eng.*, 103(3), 489–504.

Barcelona, M. J. (1983). "Sediment oxygen demand fractionation, kinetics and reduced chemical substances." *Water Res.*, 17(9), 1081–1093.

Bastviken, D., Cole, J., Pace, M., and Tranvik, L. (2004). "Methane emissions from lakes: Dependence of lake characteristics, two regional assessments, and a global estimate." *Global Biogeochem. Cy.*, 18(4), 1–12.

Beaudoin, A. (2003). "A comparison of two methods for estimating the organic content of sediments." *J. Paleolimnol.*, 29(3), 387–390.

Beck, M. B. (1987). “Water quality modeling: A review of the analysis of uncertainty.” *Water Resour. Res.*, 23(8), 1393–1442.

Benfield, E. F. (1997). “Comparison of litterfall input to streams.” *J. N. Am. Benthol. Soc.*, 16(1), 104–108.

Bernhardt, E. S., and Palmer, M. A. (2007). “Restoring streams in an urbanizing world.” *Freshw. Biol.*, 52(4), 738–751.

Berthelson, C. R., Cathcart, T. P., and Pote, J. W. (1996). “In situ measurement of sediment oxygen demand in catfish ponds.” *Aquac. Eng.*, 15(4), 261–271.

Bertrand-Krajewski, J.-L., Chebbo, G., and Saget, A. (1998). “Distribution of pollutant mass vs volume in stormwater discharges and the first flush phenomenon.” *Water Res.*, 32(8), 2341–2356.

Biggs, B. J., and Close, M. E. (1989). “Periphyton biomass dynamics in gravel bed rivers: The relative effects of flows and nutrients.” *Freshw. Biol.*, 22(2), 209–231.

Booth, D. B. (1990). “Stream-channel incision following drainage-basin urbanization.” *J. Am. Water Resour. As.*, 26(3), 407–417.

Bott, T. L., Brock, J. T., Baattrup-Pedersen, A., Chambers, P. A., Dodds, W. K., Himbeault, K. T., Lawrence, J. R., Planas, D., Snyder, E., and Wolfaardt, G. M. (1997). “An evaluation of techniques for measuring periphyton metabolism in chambers.” *Can. J. Fish. Aquat. Sci.*, 54(3), 715–725.

Bott, T. L., Brock, J. T., Cushing, C. E., Gregory, S. V., King, D., and Petersen, R. C. (1978). “A comparison of methods for measuring primary productivity and community respiration in streams.” *Hydrobiologia*, 60(1), 3–12.

Bott, T. L., Brock, J. T., Dunn, C. S., Naiman, R. J., Ovink, R. W., and Petersen, R. C. (1985). “Benthic community metabolism in four temperate stream systems: An inter-biome comparison and evaluation of the river continuum concept.” *Hydrobiologia*, 123(1), 3–45.

Bouck, G. R., Nebeker, A. V., and Stevens, D. G. (1976). *Mortality, saltwater adaptation and reproduction of fish during gas supersaturation*. US Environmental Protection Agency, Office of Research and Development, Environmental Research Laboratory, Duluth, MN, 1-64.

Boughton, W. C., and Neller, R. J. (1981). “Modifications to stream channels in the Brisbane Metropolitan Area, Australia.” *Environ. Conserv.*, 8(4), 299–305.

Boulton, A. J., Findlay, S., Marmonier, P., Stanley, E. H., and Valett, H. M. (1998). “The functional significance of the hyporheic zone in streams and rivers.” *Annu. Rev. Ecol.*

Syst., 29, 59–81.

Boyd, J. (2000). "New face of the Clean Water Act: A critical review of the EPA's new TMDL rules." *Duke Environ. Law Policy Forum*, 11(39), 39–87.

Boynton, W. R., and Kemp, W. M. (1985). "Nutrient regeneration and oxygen consumption by sediments along an estuarine salinity gradient." *Mar. Ecol.-Prog. Ser.*, 23(1), 45–55.

Bratbak, G., and Dundas, I. (1984). "Bacterial dry matter content and biomass estimations." *Appl. Environ. Microb.,* 48(4), 755–757.

Bridge, J. W. (2005). *High resolution in-situ monitoring of hyporheic zone biogeochemistry*. Environment Agency, Almondsbury, UK, 1–51.

Brunke, M., and Gonser, T. (1997). "The ecological significance of exchange processes between rivers and groundwater." *Freshw. Biol.*, 37(1), 1–33.

Butcher, R. W. (1947). "Studies in the ecology of rivers: VII. The algae of organically enriched waters." *J. Ecol.*, 35, 186–191.

Butts, T. A. (1974). *Measurements of sediment oxygen demand characteristics of the Upper Illinois Waterway*. Illinois State Water Survey, Urbana, IL, 1–36.

Butts, T. A., and Evans, R. L. (1978). *Sediment oxygen demand studies of selected northeastern Illinois streams*. Illinois State Water Survey, Urbana, IL.

Cabrita, M. T., and Brotas, V. (2000). "Seasonal variation in denitrification and dissolved nitrogen fluxes in intertidal sediments of the Tagus estuary, Portugal." *Mar. Ecol. Prog. Ser.*, 202, 51–65.

Caldwell, J. M., and Doyle, M. C. (1995). *Sediment oxygen demand in the Lower Willamette River, Oregon, 1994*. US Department of the Interior, US Geological Survey, Portland, OR, 1–19.

Callender, E., and Hammond, D. E. (1982). "Nutrient exchange across the sediment-water interface in the Potomac River estuary." *Estuar. Coast. Shelf Sci.*, 15(4), 395–413.

Carlson, R. E. (1977). "A trophic state index for lakes." *Limnol. Oceanogr.*, 22(2), 361–369.

Casas, J. J. (1996). "Environmental patchiness and processing of maple leaf litter in a backwater of a mountain stream: Riffle area vs. debris dams." *Arch. Hydrobiol.,* 136(4), 489–508.

Casey, R. J. (1990). *Sediment oxygen demand during the winter in the Athabasca River and the Wapiti-Smoky River system, 1990*. Alberta Environment, Standards and Approvals Division and Environmental Assessment Division, Edmonton, AB, 1–59.

Casper, P., Maberly, S. C., Hall, G. H., and Finlay, B. J. (2000). "Fluxes of methane and carbon dioxide from a small productive lake to the atmosphere." *Biogeochemistry*, 49(1), 1–19.

Cavinder, T. (2002). *Reaeration rate determination with a diffusion dome*. United States Environmental Protection Agency, Athens, GA, 1–11.

Cerco, C. F. (1989). "Estimating estuarine reaeration rates." *J. Environ. Eng. (New York),* 115(5), 1066–1070.

Chapman, A. D., and Schelske, C. L. (1997). "Recent appearance of Cylindrospermopsis (cyanobacteria) in five hypereutrophic Florida lakes." *J. Phycol.*, 33(2), 191–195.

Chapra, S. C. (2008). *Surface water-quality modeling*. Waveland Press, Long Grove, IL, 1-844.

Chapra, S. C., and Di Toro, D. M. (1991). "Delta method for estimating primary production, respiration, and reaeration in streams." *J. Environ. Eng. (New York)*, 117(5), 640–655.

Chiaro, P. S., and Burke, D. A. (1980). "Sediment oxygen demand and nutrient release." *J. Environ. Eng. (New York)*, 106(1), 177–195.

Christensen, J. P., Smethie, W. M., Jr, and Devol, A. H. (1987). "Benthic nutrient regeneration and denitrification on the Washington continental shelf." *Deep Sea Res. A*, 34(5), 1027–1047.

Churchill, M. A., Elmore, H. L., and Buckingham, R. A. (1962). "The prediction of stream reaeration rates." *Int. J. Air Water Pollut.*, 6, 467–504.

Cleveland, C. C., and Liptzin, D. (2007). "C:N:P stoichiometry in soil: Is there a 'Redfield ratio' for the microbial biomass?." *Biogeochemistry*, 85(3), 235–252.

Copeland, B. J., and Duffer, W. R. (1964). "Use of a clear plastic dome to measure gaseous diffusion rates in natural waters." *Limnol. Oceanogr.*, 9(4), 494–499.

Covar, A. P. (1976). "Selecting the proper reaeration coefficient for use in water quality models." United States Environmental Protection Agency, Cincinnati, OH, 340–343.

Cowan, J. L. W., and Boynton, W. R. (1996). "Sediment-water oxygen and nutrient exchanges along the longitudinal axis of Chesapeake Bay: Seasonal patterns, controlling factors and ecological significance." *Estuaries*, 19(3), 562–580.

Cox, B. (2003). "A review of dissolved oxygen modelling techniques for lowland rivers." *Sci. Total Environ.*, 314, 303–334.

Cummins, K. W. (1974). "Structure and function of stream ecosystems." *BioScience*, 24(11), 631–641.

Cushing, C. E., Minshall, G. W., and Newbold, J. D. (1993). "Transport dynamics of fine particulate organic matter in two Idaho streams." *Limnol. Oceanogr.*, 38(6), 1101–1115.

Dauer, D. M., Rodi, A. J., and Ranasinghe, J. A. (1992). "Effects of low dissolved oxygen events on the macrobenthos of the lower Chesapeake Bay." *Estuaries*, 15(3), 384–391.

Dean, W. E., Jr. (1974). "Determination of carbonate and organic matter in calcareous sediments and sedimentary rocks by loss on ignition: Comparison with other methods." *J. Sediment, Res. A Sediment Petrol Process*, 44(1), 242–248.

Deletic, A. (1998). "The first flush load of urban surface runoff." *Water Res.*, 32(8), 2462–2470.

DeSimone, L. A., and Howes, B. L. (1996). "Denitrification and nitrogen transport in a coastal aquifer receiving wastewater discharge." *Environ. Sci. Technol.*, 30(4), 1152–1162.

Deublein, D., and Steinhauser, A. (2008). *Biogas from Waste and Renewable Resources*. John Wiley & Sons, Weinheim, Germany, 1-433.

Di Toro, D. M., Paquin, P. R., Subburamu, K., and Gruber, D. A. (1990). "Sediment oxygen demand model: methane and ammonia oxidation." *J. Environ. Eng. (New York)*, 116(5), 945–986.

Diaz, R. J., and Rosenberg, R. (2008). "Spreading dead zones and consequences for marine ecosystems." *Science*, 321(5891), 926–929.

Dillon, P. J., and Rigler, F. H. (1974). "The phosphorus-chlorophyll relationship in lakes." *Limnol. Oceanogr.*, 19(5), 767–773.

Dodds, W. K. (2006). "Nutrients and the 'dead zone': The link between nutrient ratios and dissolved oxygen in the northern Gulf of Mexico." *Front. Ecol. Environ.*, 4(4), 211–217.

Dodds, W. K. (2007). "Trophic state, eutrophication and nutrient criteria in streams." *Trends Ecol. Evol.*, 22(12), 669–676.

Dodds, W. K., Jones, J. R., and Welch, E. B. (1998). "Suggested classification of stream

trophic state: Distributions of temperate stream types by chlorophyll, total nitrogen, and phosphorus." *Water Res.*, 32(5), 1455–1462.

Doyle, M. C., and Lynch, D. D. (2005). *Sediment Oxygen Demand in Lake Ewauna and the Klamath River, Oregon, June 2003*. US Department of the Interior, US Geological Survey, Reston, VA, 1–24.

Dubrovsky, N. M., Burow, K. R., Clark, G. M., Gronberg, J. M., Hamilton, P. A., Hitt, K. J., Mueller, D. K., Munn, M. D., Nolan, B. T., Puckett, L. J., Rupert, M. G., Short, T. M., Spahr, N. E., Sprague, L. A., and Wilber, W. G. (2010). *The quality of our nation's water*. US Department of the Interior, US Geological Survey, Reston, VA, 1-174.

Edmondson, W. T., and Lehman, J. T. (1981). "The effect of changes in the nutrient income on the condition of Lake Washington." *Limnol. Oceanogr.*, 26(1), 1–29.

Edwards, R. W., and Rolley, H. (1965). "Oxygen consumption of river muds." *Journal of Ecology*, 53(1), 1–19.

Ellis, B. K., Stanford, J. A., and Ward, J. V. (1998). "Microbial assemblages and production in alluvial aquifers of the Flathead River, Montana, USA." *J. North. Am. Benthol. Soc.*, 17(4), 382–402.

Ellis, J. B. (1977). "The characterization of particulate solids and quality of water discharged from an urban catchment." *IAHS-AISH P.*, (123), 283–291.

Ensign, S. H., and Doyle, M. W. (2006). "Nutrient spiraling in streams and river networks." *J. Goephys. Res. Biogeosci.*, 111(G04009), 1–13.

Fair, G. M., Moore, E. W., and Thomas, H. A., Jr. (1941). "The natural purification of river muds and pollutional sediments." *Sewage Work. J.*, 13(2), 270–307.

Fillos, J., and Swanson, W. R. (1975). "The release rate of nutrients from river and lake sediments." *J. Water Pollut. Control Fed.*, 47(5), 1032–1042.

Fischer, H., Wanner, S. C., and Pusch, M. (2002). "Bacterial abundance and production in river sediments as related to the biochemical composition of particulate organic matter (POM)." *Biogeochemistry*, 61(1), 37–55.

Fisher, M. M., Reddy, K. R., and James, R. T. (2005). "Internal nutrient loads from sediments in a shallow, subtropical lake." *Lake and Reserv. Manag.*, 21(3), 338–349.

Fisher, S. G., and Likens, G. E. (1973). "Energy flow in Bear Brook, New Hampshire: An integrative approach to stream ecosystem metabolism." *Ecol. Monogr.*, 43(4), 421–439.

Fisher, T. R., Carlson, P. R., and Barber, R. T. (1982). "Sediment nutrient regeneration in three North Carolina estuaries." *Estuar. Coast. Shelf Sci.*, 14(1), 101–116.

Forja, J. M., and Gómez-Parra, A. (1998). "Measuring nutrient fluxes across the sediment-water interface using benthic chambers." *Mar. Ecol. Prog. Ser.*, 164, 95–105.

Gardiner, R. D., Auer, M. T., and Canale, R. P. (1984). "Sediment Oxygen Demand in Green Bay (Lake Michigan)." *Proc., Environmental Engineering.* ASCE, Los Angeles, CA, 514–519.

Gelda, R. K., Auer, M. T., and Effler, S. W. (1995). "Determination of sediment oxygen demand by direct measurement and by inference from reduced species accumulation." *Mar. Freshw. Res.*, 46(1), 81–88.

Gessner, M. O., Chauvet, E., and Dobson, M. (1999). "A perspective on leaf litter breakdown in streams." *Oikos*, 85(2), 377–384.

Giles, H., Pilditch, C. A., and Bell, D. G. (2006). "Sedimentation from mussel (Perna canaliculus) culture in the Firth of Thames, New Zealand: Impacts on sediment oxygen and nutrient fluxes." *Aquaculture*, 261(1), 125–140.

Gleick, P. H. (1993). *Water in Crisis*. Pacific Institute for Studies in Development, Environment, and Security, Stockholm Environment Institute. Oxford University Press, Inc., New York, NY, 11–24.

Glew, J. (1988). "A portable extruding device for close interval sectioning of unconsolidated core samples." *J. Paleolimnol.*, 1(3), 235–239.

Glew, J. R., Smol, J. P., and Last, W. M. (2001). *Tracking environmental change using lake sediments. Volume 1: Basin analysis, coring, and chronological techniques*. Kluwer Academic Publishers, Dordrecht, The Netherlands, 73–105.

Goonetilleke, A., Thomas, E., Ginn, S., and Gilbert, D. (2005). "Understanding the role of land use in urban stormwater quality management." *J. Environ. Manage.*, 74(1), 31–42.

Grace, M. R., and Imberger, S. J. (2006). *Stream metabolism: Performing & interpreting measurements*. *Water Studies Centre Monash University, Murray Darling Basin Commission and New South Wales Department of Environment and Climate Change*, Water Studies Centre Monash University, Murray Darling Basin Commission and New South Wales Department of Environment and Climate Change 204.

Gregory, S. V., Swanson, F. J., McKee, W. A., and Cummins, K. W. (1991). "An ecosystem perspective of riparian zones." *BioScience*, 41(8), 540–551.

Groffman, P. M., and Crawford, M. K. (2003). “Denitrification potential in urban riparian zones.” *J. Environ. Qual.*, 32(3), 1144–1149.

Gromaire-Mertz, M. C., Garnaud, S., Gonzalez, A., and Chebbo, G. (1999). “Characterisation of urban runoff pollution in Paris.” *Water Sci. Technol.*, 39(2), 1–8.

Hall, R. O., and Tank, J. L. (2005). “Correcting whole-stream estimates of metabolism for groundwater input.” *Limnol. Oceanogr. Methods*, 3, 222–229.

Hatt, B. E., Fletcher, T. D., Walsh, C. J., and Taylor, S. L. (2004). “The influence of urban density and drainage infrastructure on the concentrations and loads of pollutants in small streams.” *Environ. Manage.*, 34(1), 112–124.

Hauer, F. R., and Lamberti, G. A. (2007). *Methods in stream ecology*. Academic Press, Burlington, MA.

Heaney, J. P., and Huber, W. C. (1984). “Nationwide assessment of urban runoff impact on recieving water quality.” *J. Am. Water Resour. As.*, 20(1), 35–42.

Heckathorn, H. A., and Gibs, J. (2010). *Sediment Oxygen Demand in the Saddle River and Salem River Watersheds, New Jersey, July–August 2008*. U.S. Department of the Interior, U.S. Geological Survey, Reston, VA.

Heiri, O., Lotter, A. F., and Lemcke, G. (2001). “Loss on ignition as a method for estimating organic and carbonate content in sediments: Reproducibility and comparability of results.” *J. Paleolimnol.*, 25(1), 101–110.

Henriksen, K., Rasmussen, M. B., and Jensen, A. (1983). “Effect of bioturbation on microbial nitrogen transformations in the sediment and fluxes of ammonium and nitrate to the overlaying water.” *Ecological Bulletins*, 35, 193–205.

Higashino, M., Gantzer, C. J., and Stefan, H. G. (2004). “Unsteady diffusional mass transfer at the sediment/water interface: Theory and significance for SOD measurement.” *Water Res.*, 38(1), 1–12.

Hilton, J., and Irons, G. P. (1998). *Determining the causes of "apparent eutrophication" effects*. Environment Agency R&D technical report, 21.

Hilton, J., O'Hare, M., Bowes, M. J., and Jones, J. I. (2006). “How green is my river? A new paradigm of eutrophication in rivers.” *Sci. Total Environ.*, 365(1), 66–83.

Hogsett, M., and Goel, R. (2013). “Dissolved oxygen dynamics at the sediment–water column interface in an urbanized stream.” *Environ. Eng. Sci.*, 30(10), 594–605.

Huttunen, J. T., Lappalainen, K. M., Saarijärvi, E., Väisänen, T., and Martikainen, P. J. (2001). “A novel sediment gas sampler and a subsurface gas collector used for

measurement of the ebullition of methane and carbon dioxide from a eutrophied lake." *Sci. Total Environ.,* 266(1), 153–158.

Huttunen, J. T., Vaisanen, T. S., Hellsten, S. K., and Martikainen, P. J. (2006). "Methane fluxes at the sediment-water interface in some boreal lakes and reservoirs." *Boreal Environ. Res.*, 11(1), 27–34.

Imberger, S. J., Thompson, R. M., and Grace, M. R. (2011). "Urban catchment hydrology overwhelms reach scale effects of riparian vegetation on organic matter dynamics." *Freshw. Biol.*, 56(7), 1370–1389.

Imberger, S. J., Walsh, C. J., and Grace, M. R. (2008). "More microbial activity, not abrasive flow or shredder abundance, accelerates breakdown of labile leaf litter in urban streams." *J. North Am. Benthol. Soc.*, 17(3), 549–561.

Jenkins, J. (2005). *The humanure handbook*. Joseph Jenkins, Inc., Grove City, PA.

Kaplan, L. A., and Bott, T. L. (1982). "Diel fluctuations of DOC generated by algae in a piedmont stream." *Limnol. Oceanogr.*, 27(6), 1091–1100.

Kelly, C. A., and Chynoweth, D. P. (1981). "The contributions of temperature and of the input of organic matter in controlling rates of sediment methanogenesis." *Limnol. Oceanogr.*, 26(5), 891–897.

Kelso, B., Smith, R. V., Laughlin, R. J., and Lennox, S. D. (1997). "Dissimilatory nitrate reduction in anaerobic sediments leading to river nitrite accumulation." *J. Appl. Environ. Mircobial.*, 63(12), 4679–4685.

Konen, M. E., Jacobs, P. M., Burras, C. L., Talaga, B. J., and Mason, J. A. (2002). "Equations for predicting soil organic carbon using loss-on-ignition for North Central U.S. soils." *Soil Sci. Soc. Am. J.*, 66(6), 1878–1881.

Kristensen, E., Ahmed, S. I., and Devol, A. H. (1995). "Aerobic and anaerobic decomposition of organic matter in marine sediment: Which is fastest?" *Limnol. Oceanogr.*, 40(8), 1430–1437.

Kuivila, K. M., Murray, J. W., Devol, A. H., Lidstrom, M. E., and Reimers, C. E. (1988). "Methane cycling in the sediments of Lake Washington." *Limnol. Oceanogr.*, 33(4), 571–581.

Larned, S. T. (2003). "Effects of the invasive, nonindigenous seagrass Zostera japonica on nutrient fluxes between the water column and benthos in a NE Pacific estuary." *Mar. Ecol. Prog. Ser.*, 254, 69–80.

Larsen, D. P., Schults, D. W., and Malueg, K. W. (1981). "Summer internal phosphorus supplies in Shagawa Lake, Minnesota." *Limnol. Oceanogr.*, 26(4), 740–753.

Lee, G. F., Rast, W., and Jones, R. A. (1978). "Water Report: Eutrophication of water bodies: Insights for an age old problem." *Environ. Sci. Technol.*, 12(8), 900–908.

Leipe, T., Tauber, F., Vallius, H., Virtasalo, J., Uścinowicz, S., Kowalski, N., Hille, S., Lindgren, S., and Myllyvirta, T. (2010). "Particulate organic carbon (POC) in surface sediments of the Baltic Sea." *Geo-Marine Letters*, 31(3), 175–188.

Leu, H.-G., Ouyang, C. F., and Pai, T.-Y. (1997). "Effects of flow velocity and depth on the rates of reaeration and BOD removal in a shallow open channel." *Water Sci. Technol.*, 35(8), 57–67.

Lewis, W. M., and Morris, D. P. (1986). "Toxity of nitrite to fish: A review." *Trans. Am. Fish. Soc.*, 115(2), 183–195.

Lidstrom, M. E., and Somers, L. (1984). "Seasonal study of methane oxidation in Lake Washington." *J. Appl. Environ. Microbiol.*, 47(6), 1255–1260.

Litke, D. W. (1999). *Review of phosphorus control measures in the United States and their effects on water quality*. US Geological Survey, Denver, CO, 43.

Ludsin, S. A., Kershner, M. W., Blocksom, K. A., Knight, R. L., and Stein, R. A. (2001). "Life after death in Lake Erie: Nutrient controls drive fish species richness, rehabilitation." *Ecol. Appl.*, 11(3), 731–746.

Lytle, D. A., and Poff, N. L. (2004). "Adaptation to natural flow regimes." *Trends Ecol. Evol.*, 19(2), 94–100.

Machelor Bailey, E. K., Stankelis, R. M., Smail, P. W., Greene, S., Rohland, W. R., and Boynton, W. R. (2003). *Dissolved oxygen and nutrient flux estimation from sediments in the Anacostia River*. University of Maryland Center for Environmental Science, Solomons, MD, 1–97.

Mackenthun, A. A., and Stefan, H. G. (1998). "Effect of flow velocity on sediment oxygen demand: Experiments." *J. Environ. Eng. (New York)*, 124(3), 222–230.

Mackereth, F. J. H. (1966). "Some chemical observations on post-glacial lake sediments." *Philos. Trans. R. Soc. Lond., B., Biol. Sci.*, 250(765), 165–213.

Madenjian, C. P. (1990). "Patterns of oxygen production and consumption in intensively managed marine shrimp ponds." *Aquac. Res.*, 21(4), 407–417.

Makepeace, D. K., Smith, D. W., and Stanley, S. J. (1995). "Urban stormwater quality: Summary of contaminant data." *Crit. Rev. Environ. Sci. Technol.*, 25(2), 93–139.

Malcolm, I. A., Soulsby, C., Youngson, A. F., Hannah, D. M., McLaren, I. S., and Thorne, A. (2004). "Hydrological influences on hyporheic water quality:

Implications for salmon egg survival." *Hydrol. Process.*, 18(9), 1543–1560.

Malecki, L. M., White, J. R., and Reddy, K. R. (2004). "Nitrogen and phosphorus flux rates from sediment in the lower St. Johns River estuary." *J. Environ. Qual.*, 33(4), 1545–1555.

Marsden, M. W. (1989). "Lake restoration by reducing external phosphorus loading: The influence of sediment phosphorus release." *Freshw. Biol.*, 21(2), 139–162.

Matlock, M. D., Kasprzak, K. R., and Osborn, G. S. (2003). "Sediment oxygen demand in the Arroyo Colorado River." *J. Am. Water Resour. As.*, 39(2), 267–275.

McDonnell, A. J., and Hall, S. D. (1969). "Effect of environmental factors on benthal oxygen uptake." *J. Water Pollut. Control Fed.*, 41(8), 353–363.

McDowell, W. H., and Fisher, S. G. (1976). "Autumnal processing of dissolved organic matter in a small woodland stream ecosystem." *Ecology*, 57(3), 561–569.

McGroddy, M. E., Daufresne, T., and Hedin, L. O. (2004). "Scaling of C: N: P stoichiometry in forests worldwide: Implications of terrestrial Redfield-type ratios." *Ecology*, 85(9), 2390–2401.

McNevin, D., and Barfprd, J. (2001). "Inter-relationship between adsorption and pH in peat biofilters in the context of a cation-exchange mechanism." *Water Res.*, 35(3), 736–744.

Meentemeyer, V., Box, E. O., and Thompson, R. (1982). "World patterns and amounts of terrestrial plant litter production." *BioScience*, 32(3), 125–128.

Melillo, J. M., Naiman, R. J., Aber, J. D., and Eshleman, K. N. (1983). "The influence of substrate quality and stream size on wood decomposition dynamics." *Oecologia*, 58(3), 281–285.

Meyer, J. L., Paul, M. J., and Taulbee, W. K. (2005). "Stream ecosystem function in urbanizing landscapes." *J. North. Am. Benthol. Soc.,* 24(3), 602–612.

Miller, W., and Boulton, A. J. (2005). "Managing and rehabilitating ecosystem processes in regional urban streams in Australia." *Hydrobiologia*, 552(1), 121–133.

Minshall, G. W. (1978). "Autotrophy in stream ecosystems." *BioScience*, 28(12), 767–771.

Minshall, G. W., Petersen, R. C., Bott, T. L., Cushing, C. E., Cummins, K. W., Vannote, R. L., and Sedell, J. R. (1992). "Stream ecosystem dynamics of the Salmon River, Idaho: An 8th-order system." *J. North Am. Benthol. Soc*., 11(2), 111–137.

Mueller, D. K., and Helsel, D. R. (1996). *Nutrients in the nations waters–Too much of a good thing?* US Geological Survey, Denver, CO, 1–31.

Murphy, P. J., and Hicks, D. B. (1986). *In-situ method for measuring sediment oxygen demand*. (K. J. Hatcher, Ed.), Sediment Oxygen Demand: Processes, Modeling and Measurement, Athens, GA, 307–323.

Naiman, R. J., and Bilby, R. E. (1998). *River Ecology and Management*. Springer Verlag, New York, NY.

Nakamura, Y., and Stefan, H. G. (1994). "Effect of flow velocity on sediment oxygen demand: Theory." *J. Environ. Eng. (New York)*, 120(5), 996–1016.

Newbold, J. D., Elwood, J. W., O'Neill, R. V., and Winkle, W. V. (1981). "Measuring nutrient spiralling in streams." *Can. J. Fish. Aquat. Sci.*, 38(7), 860–863.

Newbold, J. D., Mulholland, P. J., Elwood, J. W., and O'Neill, R. V. (1982). "Organic carbon spiralling in stream ecosystems." *Oikos*, 38(3), 266–272.

O'Connor, D. J., and Dobbins, W. E. (1956). "The mechanism of reaeration in natural streams." *T. Am. Soc. Civ. Eng.*, 123(1), 641–666.

Odum, H. T. (1956). "Primary production in flowing waters." *Limnol. Oceanogr.*, 1(2), 102–117.

Olsen, L. M., Ozturk, M., and Sakshaug, E. (2006). "Photosynthesis-induced phosphate precipitation in seawater: Ecological implications for phytoplankton." *Mar. Ecol. Prog. Ser.*, 319, 103–110.

Owens, M., Edwards, R. W., and Gibbs, J. W. (1964). "Some reaeration studies in streams." *Air Water Pollut*., 8, 469-486.

Paerl, H. W., Pinckney, J. L., Fear, J. M., and Peierls, B. L. (1998). "Ecosystem responses to internal and watershed organic matter loading: Consequences for hypoxia in the eutrophying Neuse River Estuary, North Carolina, USA." *Mar. Ecol. Prog. Ser.*, 166, 17–25.

Parr, L. B., and Mason, C. F. (2003). "Long-term trends in water quality and their impact on macroinvertebrate assemblages in eutrophic lowland rivers." *Water Res.*, 37(12), 2969–2979.

Parr, L. B., and Mason, C. F. (2004). "Causes of low oxygen in a lowland, regulated eutrophic river in Eastern England." *Sci. Total Environ.*, 321(1), 273–286.

Pascoal, C., and Cassio, F. (2004). "Contribution of fungi and bacteria to leaf litter decomposition in a polluted river." *J. Appl. Environ. Microbiol.*, 70(9), 5266–5273.

Pauer, J. J., and Auer, M. T. (2000). "Nitrification in the water column and sediment of a hypereutrophic lake and adjoining river system." *Water Res.*, 34(4), 1247–1254.

Paul, M. J., and Meyer, J. L. (2001). "Streams in the urban landscape." *Annu. Rev. Ecol. Syst.*, 333–365.

Pelletier, G. J., Chapra, S. C., and Tao, H. (2006). "QUAL2Kw – A framework for modeling water quality in streams and rivers using a genetic algorithm for calibration." *Environ. Model. Softw.*, 21(3), 419–425.

Pimentel, D., Zuniga, R., and Morrison, D. (2005). "Update on the environmental and economic costs associated with alien-invasive species in the United States." *Ecol. Econ.*, 52(3), 273–288.

Pusch, M., Fiebig, D., Brettar, I., Eisenmann, H., Ellis, B. K., Kaplan, L. A., Lock, M. A., Naegeli, M. W., and Traunspurger, W. (1998). "The role of micro-organisms in the ecological connectivity of running waters." *Freshw. Biol.*, 40(3), 453–495.

Rath, A. K., Ramakrishnan, B., and Sethunathan, N. (2002). "Temperature dependence of methane production in tropical rice soils." *Geomicrobiol. J.*, 19(6), 581–592.

Reay, W. G., Gallagher, D. L., and Simmons, G. M. (1995). "Sediment-water column oxygen and nutrient fluxes in nearshore environments of the lower Delmarva Peninsula, USA." *Mar. Ecol. Prog. Ser.*, 118, 215–215.

Redfield, A. C. (1934). "On the proportions of organic derivations in sea water and their relation the the composition of plankton." James Johnstone Memorial Volume, Liverpool, UK, 176–192.

Refsgaard, J. C., van der Sluijs, J. P., Højberg, A. L., and Vanrolleghem, P. A. (2007). "Uncertainty in the environmental modelling process – A framework and guidance." *Environ. Model. Softw.*, 22(11), 1543–1556.

Reid, M., Thoms, M., Rowan, J. S., Duck, R. W., and Werritty, A. (2006). "Linking pattern and process: the effects of hydraulic conditions on cobble biofilm metabolism in an Australian upland stream." *IAHS-AISH P*, 322–330.

Renfro, W. C. (1963). "Gas-bubble mortality of fishes in Galveston Bay, Texas." *Trans. Am. Fish. Soc.*, 92(3), 320–322.

Ro, K. S., and Hunt, P. G. (2006). "New Unified Equation for Wind-Driven Surficial Oxygen Transfer into Stationary Water Bodies." *Biol. Eng. Trans.*, 49(5), 1615–1622.

Roberts, M. L., and Bilby, R. E. (2009). "Urbanization alters litterfall rates and nutrient inputs to small Puget Lowland streams." *J. North Am. Benthol. Soc.*, 28(4), 941–954.

Rolley, H., and Owens, M. (1967). "Oxygen consumption rates and some chemical properties of river muds." *Water Res.*, 1(11), 759–766.

Rudolfs, W. (1932). "Relation between biochemical oxygen demand and volatile solids of the sludge deposits in the Connecticut River." *Sewage Work. J.*, 4(2), 315–321.

Rutherford, J. C., Wilcock, R. J., and Hickey, C. W. (1991). "Deoxygenation in a mobile-bed river–I. Field studies." *Water Res.*, 25(12), 1487–1497.

Ryder, D. S., and Miller, W. (2005). "Setting goals and measuring success: Linking patterns and processes in stream restoration." *Hydrobiologia*, 552(1), 147–158.

Sedell, J. R., Triska, F. J., Hall, J. D., Anderson, N. H., and Lyford, J. H. (1974). "Sources and fates of organic inputs in coniferous forest streams." *Integrated research in the coniferous forest biome. Seattle: Bulletin of the Coniferous Forest Biome Ecosystem Analysis Studies, University of Washington.* 57–69.

Segers, R. (1998). "Methane production and methane consumption: a review of processes underlying wetland methane fluxes." *Biogeochemistry*, 41(1), 23–51.

Spencer, R. G. M., Pellerin, B. A., Bergamaschi, B. A., Downing, B. D., Kraus, T. E. C., Smart, D. R., Dahlgren, R. A., and Hernes, P. J. (2007). "Diurnal variability in riverine dissolved organic matter composition determined by in situ optical measurement in the San Joaquin River (California, USA)." *Hydrol. Process.*, 21(23), 3181–3189.

Stackelberg, von, N. O., and Neilson, B. T. (2012). "A collaborative approach to calibration of a riverine water quality model." *J. Water Res. Pl.-ASCE*, 140(3), 393–405.

Stanley, D. W., and Hobbie, J. E. (1981). "Nitrogen recycling in a North Carolina coastal river." *Limnol. Oceanogr.*, 26(1), 30–42.

Streeter, H. W., and Phelps, E. B. (1958). *A study of the pollution and natural purification of the Ohio River*. United States Public Health Service, Washington, DC, 1–80.

Stringfellow, W., Herr, J., Litton, G., Brunell, M., Borglin, S., Hanlon, J., Chen, C., Graham, J., Burks, R., Dahlgren, R., Kendall, C., Brown, R., and Quinn, N. (2009). "Investigation of river eutrophication as part of a low dissolved oxygen total maximum daily load implementation." *Water Sci. Technol.*, 59(1), 9.

Stumm, W., and Morgan, J. J. (1996). *Aquatic Chemistry*. John Wiley & Sons, New York, NY.

Sweeney, B. W., Bott, T. L., Jackson, J. K., Kaplan, L. A., Newbold, J. D., Standley, L.

J., Hession, W. C., and Horwitz, R. J. (2004). "Riparian deforestation, stream narrowing, and loss of stream ecosystem services." *Proc. Natl. Acad. Sci. U.S.A.*, 101(39), 14132–14137.

Tchobanoglous, G., Burton, F. L., and Stensel, H. D. (2003). *Wastewater Engineering*. McGraw Hill, New York.

Tenore, K. R. (1972). "Macrobenthos of the Pamlico river estuary, North Carolina." *Ecol. Monogr.*, 42(1), 51–69.

Thomas, N. A. (1970). *Sediment oxygen demand investigations of the Willamette River*. Water Pollution Control Administration, National Field Investigations Center, Memorandum Report, Portland, OR.

Todd, M. J., Vellidis, G., Lowrance, R. R., and Pringle, C. M. (2009). "High sediment oxygen demand within an instream swamp in Southern Georgia: Implications for low dissolved oxygen levels in coastal blackwater streams." *J. Am. Water Resour. Assoc.*, 45(6), 1493–1507.

Tsivoglou, J. B., Cohen, S. D., Shearer, S. D., and Godsil, P. J. (1968). "Tracer measurement of stream reaeration. II. Field studies." *Water Environ. Res.*, 40(2), 285–305.

Uchrin, C. G., and Ahlert, W. K. (1985). "In situ sediment oxygen demand determinations in the Passaic River (NJ) during the late summer/early fall 1983." *Water Res.*, 19(9), 1141–1144.

USEPA. (1978). *Rates, constants, and kinetics formulations in surface water quality modeling*. United States Environmental Protection Agency, Athens, GA.

USEPA. (1985). *Rates, constants, and kinetics formulations in surface water quality modeling*. United States Environmental Protection Agency, Athens, GA, 1-471.

USEPA. (1986). *Quality criteria for water*. United States Environmental Protection Agency, Washington, DC, 1–477.

USEPA. (1993). *Nitrogen control*. United States Environmental Protection Agency, Washington, DC, 1–326.

USEPA. (2001). "METHOD 1684 Total, Fixed, and Volatile Solids in Water, Solids, and Biosolids." United States Environmental Protection Agency, Washington, DC, 1-16.

USEPA. (2006). *Wadeable Streams Assessment: A Collaborative Survey of the Nation's Streams*. United States Environmental Protection Agency, Washington, DC, 1–113.

USEPA. (2008). *State Adoption of Numeric Nutrient Standards (1998–2008)*. United

States Environmental Protection Agency, Washington, DC, 1–96.

USEPA. (2010a). *Methane and nitrous oxide emissions from natural sources*. United States Environmental Protection Agency, Washington, DC, 1–194.

USEPA. (2010b). *National Lakes Assessment*. United States Environmental Protection Agency, Office of Water and Office of Research and Development, Washington, DC, 1–118.

Utah DWQ. (2007). *Utah Lake TMDL: Pollutant Loading Assessment & Designated Beneficial Use Impairment Assessment*. Prepared by PSOMAS and SWCA, Salt Lake City, UT, 1–88.

Utah DWQ. (2013). *Jordan River Total Maximum Daily Load Water Quality Study - Phase 1*, Prepared by Cirrus Ecological Solutions, LC, Logan, UT and Stantec Consulting Inc., Salt Lake City, UT, 170.

Utley, B. C., Vellidis, G., Lowrance, R., and Smith, M. C. (2008). "Factors affecting sediment oxygen demand dynamics in blackwater streams of Georgia's coastal plain." *J. Am. Water Resour. Assoc.*, 44(3), 742–753.

Van Hulzen, J. B., Segers, R., Van Bodegom, P. M., and Leffelaar, P. A. (1999). "Temperature effects on soil methane production: an explanation for observed variability." *Soil Biol. Biochem.,* 31(14), 1919–1929.

Vannote, R. L., Minshall, G. W., Cummins, K. W., Sedell, J. R., and Cushing, C. E. (1980). "The river continuum concept." *Can. J. Fish. Aquat. Sci.*, 37(1), 130–137.

Vollenweider, R. A. (1971). *Scientific fundamentals of the eutrophication of lakes and flowing waters, with particular reference to nitrogen and phosphorus as factors in eutrophication*. Organisation for Economic Co-operation and Development, Paris.

Vollenweider, R. A. (1976). "Advances in defining critical loading levels for phosphorus in lake eutrophication." *Mem. Ist. Ital. Idrobiol.*, 33, 53–83.

Walker, R. R., and Snodgrass, W. J. (1986). "Model for Sediment Oxygen Demand in Lakes." *J. Environ. Eng. (New York)*, 112(1), 25–43.

Wallace, J. B., Whiles, M. R., Eggert, S., Cuffney, T. F., Lugthart, G. J., and Chung, K. (1995). "Long-term dynamics of coarse particulate organic matter in three Appalachian Mountain streams." *J. North Am. Benthol. Soc.*, 14(2), 217–232.

Walsh, C. J., Roy, A. H., Feminella, J. W., Cottingham, P. D., Groffman, P. M., and Morgan, R. P., II. (2005). "The urban stream syndrome: Current knowledge and the search for a cure." *J. North Am. Benthol. Soc.*, 24(3), 706–723.

Wang, W. (1981). “Kinetics of sediment oxygen demand.” *Water Res.*, Elsevier, 15(4), 475–482.

Webster, J. R., and Benfield, E. F. (1986). “Vascular plant breakdown in freshwater ecosystems.” *Annu. Rev. Ecol. Syst.*, 17, 567–594.

Webster, J. R., Wallace, J. B., and Benfield, E. F. (1995). *River and Stream Ecosystems of the World*. (C. E. Cushing, K. W. Cummins, and G. W. Minshall, Eds.), Los Angeles, CA, 117–187.

Welch, H. E. (1968). “Relationships between assimiliation efficiencies and growth efficiencies for aquatic consumers.” *Ecology*, 49(4), 755–759.

Wetzel, R. G. (2001). *Limnology: Lake and river ecosystems*. Elsevier, San Diego, CA.

Wetzel, R. G., and Likens, G. E. (2000). *Limnological analysis*. Springer, New York, NY.

Wright, K. K., Baxter, C. V., and Li, J. L. (2005). “Restricted hyporheic exchange in an alluvial river system: implications for theory and management.” *J. North Am. Benthol. Soc.*, 24(3), 447–460.

Young, R. G., Matthaei, C. D., and Townsend, C. R. (2008). “Organic matter breakdown and ecosystem metabolism: functional indicators for assessing river ecosystem health.” *J. North Am. Benthol. Soc.*, 27(3), 605–625.

Ziadat, A. H., and Berdanier, B. W. (2004). “Stream depth significance during in-situ sediment oxygen demand measurements in shallow streams.” *J. Am. Water Resour. Assoc.*, 40(3), 631–638.

Progress Report to the Jordan River Farmington Bay Water Quality Council

December 21, 2017

Nitrogen sources and transformations within the Jordan River, Utah

and

Microbial community response to energy and nutrient availability in the Jordan River, Utah

Prepared by

J. Follstad Shah[1,2,*], R. Smith[3,4], R. Gabor[4], S. Weintraub[6], Y. Jameel[4] & M. Navidomskis[5]
[1]Environmental & Sustainability Studies, [2]Department of Geography, [3]Department of Biology, [4]Department of Geology & Geophysics, [5]Department of Civil Engineering, University of Utah; [6]Neon, Inc.

[*]Jennifer Follstad Shah, Ph.D., 801-585-5730, jennifer.shah@envst.utah.edu

Table of Contents

Executive Summary

The Jordan River is a 4th order river that runs through the Salt Lake Valley of north-central Utah, USA. The river suffers impairment in the form of low dissolved oxygen in some of parts of its flowpath. Low dissolved oxygen is likely due to excess organic matter and nutrients fueling microbial respiration.

We obtained funding[1] from the Jordan River Farmington Bay Water Quality Council, the innovative Urban Transitions and Arid-region Hydro-sustainability (iUTAH) Program, and the University of Utah Undergraduate Research Opportunties Program (UROP) to answer the following six research questions:

1. *What proportion of N entering the river is sourced from WRF effluent?*
2. *Is N being transformed along the Jordan River flowpath via dissimilatory N uptake?*
3. *Is wastewater effluent a source of N for in-stream biota?*
4. *Are substrates supporting microbial community metabolism in the Jordan River primarily of terrestrial or aquatic origin?*
5. *What is the quality of the organic matter within the Jordan River?*
6. *Are microbial communities in the Jordan River limited by C, N, and/or P?*

We collected data in spring, summer, and fall of 2016 from 18 sites along the Jordan River, 2 sites along the oil drain canal, 1 wetland of the Great Salt Lake, and 4 water reclamation facility (WRF) effluent discharge sites. This spatial and temporal design was selected to assess broad scale effects of WRF inputs to the system and fine scale dynamics of nutrient transformations at times when the river varied with respect to hydrology and temperature.

Main findings include the following:

- TDN inputs from WRF effluent discharge represented between 46-92% of total dissolved nitrogen (TDN) loads in Jordan River locations immediately downstream of WRF sites, with the majority of the load generally occurring as NO_3-N.
- We find evidence of mass nitrogen and phosphorus removal from the water column between water reclamation facilities, suggesting that biotic uptake is occurring and influences downstream nutrient loads.
- ^{15}N-NO_3 becomes less enriched along an intensively studied flowpath, suggesting either that N fixation is occurring or novel inputs of less enriched in ^{15}N-NO_3 are entering the system.
- Origination of fine particulate organic matter (POM) is difficult to discern due to likely contamination by entrained sediment, which confounded distinction in ^{2}H values between biofilm and riparian leaf end members.
- ^{15}N of POM and dissolved organic matter (DOM) become enriched downstream of the Central Valley WRF, but the effects of effluent on POM are less clear and we lack data on DOM ^{15}N in relation to other WRFs.

[1] Funding from the Jordan River Farmington Bay Water Quality Council supported, in part or in full, data collection and analysis for research questions 3-6.

- Fluorescence Index (FI) values, derived from emission-excitation matrices (EEMs), are very high for the Jordan River relative to other aquatic systems. High FI values are typically associated with microbially sourced organic matter. Elevated FI values downstream of WRFs relative to upstream sites in all seasons indicate that WRF inputs influence organic matter composition in the Jordan River.
- Ecoenzyme activities indicate that most of the organic matter in the river supporting microbial metabolism is labile.
- Microbial communities in the water column and sediment differ with respect to C, which is in adequate supply in the water column but appears to be limiting in the sediment in some seasons. Microbial communities in the water column and sediment are similar because N appears to be in adequate supply and both communities are limited with respect to P at some times of the year.

This research has contributed to the professional training of three undergraduate students, one graduate student, and two postdoctoral scholars. To date, we have presented our work at 8 conferences and have one manuscript in preparation for submission to the Journal of the American Water Resources Association in late January 2018.

Introduction

The Jordan River is a 4th order river that runs through the Salt Lake Valley of north-central Utah, USA. The river originates at the outlet of Utah Lake and drains into wetlands of the Great Salt Lake. Roughly 44% of the surface area of the 805 mi^2 Jordan River watershed is urban.

The Jordan River suffers impairment related to water temperature and concentrations of total dissolved and suspended solids (TDS and TSS, respectively), dissolved oxygen (DO), and pathogens (e.g., e coli) at levels to the detriment of human health and wildlife (Jensen and Rees 2005). DO concentrations are < 4 mg/L at some locations along the river's 58-mile course (Arens and Adams 2012).

Excess nutrient loading to streams and rivers also is an issue in many urban watersheds (Bernhardt et al. 2009; Kaushal et al. 2011). Eutrophication can promote blooms of nuisance algae, including taxa that produce toxins. Nutrient loading from water reclamation facilities (WRFs) are of concern within the Jordan River due to the number of WRFs and their contribution towards river flow via effluent. Twelve WRFs discharge into Utah Lake, the Jordan River itself, one of the major tributaries of the Jordan River, or a canal draining directly into the Great Salt Lake (Fig. 1). The three WRFs discharging directly into the Jordan River or the Mill Creek tributary contribute between 13 and 29% of the river's flow directly downstream of a given effluent outfall. These three direct WRF contributions constitute 20% of the river's flow above the surplus canal in spring and 43% in summer.

WRFs treat highly concentrated wastewater through a series of settling and mixing processes and vary widely in nitrogen (N) removal efficiency depending on which technologies are used (Townsend-Small et al. 2011; Schmidt et al. 2016). However, the contribution of WRFs to the overall load of N to the Jordan River and the extent to which the river can transform N inputs from organic to inorganic forms or remove N from the system via N_2 gas efflux is not clear. It also is not known whether biota assimilate N inputs from WRFs into biomass.

Microbial communities are responsible for the majority of organic matter and nutrient transformations in streams and rivers (Mallin et al. 2011, Sinsabaugh and Follstad Shah 2012). Microbial community metabolism is heterotrophic. This process can deplete oxygen within aquatic ecosystems, particularly in the presence of high supply of organic matter and nutrients. Debate exists whether organic matter supply in the Jordan River is largely due to in-stream production by autotrophs (i.e., algae, macrophytes) or inputs from terrestrial sources (i.e., plant litter, sediment in run-off, solids in waste water effluent). Furthermore, the quality of organic matter within the system has not been well characterized. It also is unclear whether microbial communities in the Jordan River are limited by an imbalance in organic matter, nitrogen and/or phosphorus at various times or locations, despite generally high supply of these resources.

Research Questions

We have asked the following research questions, in two complementary studies, in an effort to better understand the biogeochemistry and ecology of the Jordan River:

<u>'Intensive' study: Tracking nitrogen sources and transformations within the Jordan River</u>

1. *What proportion of N entering the river is sourced from WRF effluent?*
2. *Is N being transformed along the Jordan River flowpath via dissimilatory N uptake?*
3. *Is wastewater effluent a source of N for in-stream biota?*

Note: The innovative Urban Transitions and Aridregion Hydrosustainability (iUTAH) Program funded this study.

'Extensive' study: Microbial communities response to energy and nutrient supply within the Jordan River

7. *Are substrates supporting microbial community metabolism in the Jordan River (suspended solids and benthic organic matter) primarily of terrestrial or aquatic origin?*
8. *What is the quality of the organic matter within the Jordan River?*
9. *Are microbial communities in the Jordan River limited by C, N, and/or P?*

Methods

Study Design

For the intensive study, we established ten study sites, at 1 km intervals, within a 10 km stretch of the Jordan River beginning just downstream of the Central Valley Water Reclamation Facility (Figure 1, Table 1). These sites were sampled synoptically (i.e., within a single day) during each sampling campaign. We deemed the proximity of sites and synoptic sampling necessary to monitor change in N inputs from the WRF, given that processing of these inputs could occur rapidly and over small spatial scales.

For the extensive study, we established ten study sites along the Jordan River flowpath (Figure 1, Table 1), including a site just downstream of the Utah Lake outlet, sites above and below each WRF, one site within the oil drain canal just upstream of the Farmington Bay inlet and one wetland site. The last two 'river' sites were located within the oil drain canal because this is where the Salt Lake City WRF discharges effluent. The wetland site was included as a point of comparison for the riverine and canal sites.

Effluent from the four WRFs along the Jordan River flowpath was sampled in conjunction with field site sampling.

Samples were collected from the intensive and extensive sites in spring (late May and early June), summer (mid August), and fall (late October) of 2016. These dates were selected because they represent times that differ in terms of hydrology (high flow in spring and summer, low flow in fall) and dominant sources of organic matter inputs (i.e., autotrophic vs. terrestrial).

Analytical Techniques

Chemistry and stable isotopes of water

Wastewater effluent is often nutrient rich and enriched in $\delta^{15}N$ compared with other sources such

as precipitation, fertilizer and soil N, due to mass-dependent fractionation during waste production (Kendall et al. 2007). Denitrification within aquatic habitats can further enrich $\delta^{15}N$ within the water column as microbes preferentially use ^{14}N (Kendall et al. 2007). Hence, we are using measures of riverine nutrient concentrations, hydrologic flow volume, and stable isotope analyses (natural abundance) to quantify the contribution of effluent to N loading to the river, compared with other sources (Research Question 1), the degree to which N is transformed downstream via biotic processes (Research Question 2), and the extent to which biota assimilate N from WRF inputs (Research Question 3). We are using a mass balance approach to quantify WRF contributions of nutrients and water to the river, based on nutrient concentrations within the river and effluent sources combined with flow volumes for the river and effluent discharge (Research Question 1). We are quantifying changes in the natural abundance of $_{15}N\text{-}NO_3$ in the water column downstream of the Central Valley WRF to determine if denitrification is occurring along the Jordan River flowpath, which would result in a loss of N gas to the atmosphere (Research Question 2). We are measuring the natural abundance of ^{15}N in particulate organic matter within the water column, biofilms, and sediments to infer whether N inputs from WRFs are being assimilated by biota within the Jordan River (Research Question 3).

Elemental content and stable isotopes of biofilms, organic matter, and sediment

We are quantifying the natural abundance of a suite of stable isotopes (^2H, ^{13}C, and ^{15}N) and the C:N ratios of biofilms, fine particulate organic matter (FPOM) in the water column and sediments (^{13}C and ^{15}N only), and senesced leaves of riparian plants to infer whether organic matter within Jordan River is primarily of aquatic or terrestrial origin (Research Question 4). This suite of stable isotopes was chosen for several reasons. First, the natural abundance of deuterium (^2H) produced in aquatic (-250 $^0/_{00}$) vs. terrestrial (-150 $^0/_{00}$) habitats generally differs by ~ 100 dell units ($^0/_{00}$; Doucett et al. 2007). Second, measurement of ^{13}C and ^{15}N combined with C:N ratios also can distinguish between organic matter derived from algal vs. terrestrial production (Finlay and Kendall 2007). Third, measurement of ^{13}C and ^{15}N may help to determine if organic matter has an anthropogenic signature. Human diets are now rich in products derived from corn, a C4 plant that is more enriched (-13 $^0/_{00}$) in ^{13}C relative to C3 plants (-27 $^0/_{00}$), such as riparian shrubs and trees, and freshwater autotrophs (-18 to -35 $^0/_{00}$; Finlay and Kendall 2007). In addition, fecal matter is typically enriched in ^{15}N (+15-20 $^0/_{00}$) relative to the atmosphere or N fixed by biota (0 $^0/_{00}$; Kendall et al. 2007).

Ecoenzyme expression and excitation-emission matrices

We are inferring the quality of organic C fueling microbial community metabolism (Research Question 5) using two complementary approaches: measurement of ecoenzyme activity rates associated with the hydrolysis of labile and recalcitrant organic matter (Table 2) and quantification of dissolved organic C (DOC) concentrations combined with multi-wave fluorescence spectroscopy to create excitation-emission matrices (EEMs). Microbes generally express more POX relative to BG when available organic matter is recalcitrant (Sinsabaugh and Follstad Shah 2011). EEMs represent a simple index used to identify the types of organic matter present in samples and distinguish between likely sources of organic matter to rivers (McKnight et al. 2001).

Microbes generally produce and release enzymes proportional to energy or nutrient requirements (Sinsabaugh and Follstad Shah 2012; Table 2). When the availability of energy and nutrient resources meet microbial maintenance and growth demands, the ratios of ecoenzymes related to C, N, and P resources is approximately 1:1:1 (Sinsabaugh et al. 2009). Deviations from these ratios indicate whether microbial communities are energy or nutrient limited (Sinsabaugh and Follstad Shah 2012). We have measured the activity rates of five ecoenzymes associated with microbial acquisition of C, N, and P using high throughput fluorescence spectroscopy to address whether these resources are balanced or imbalanced relative to microbial stoichiometric requirements (Research Question 6).

Results

What proportion of N entering the river is sourced from WRF effluent?

Total dissolved nitrogen (TDN) loads (kg day^{-1}) within the Jordan River ranged from 150-4734 kg N day^{-1}in spring and 512-6847 kg N day^{-1} in summer, with the greatest increase in loads for both seasons occurring downstream of the Mill Creek tributary (Fig. 2). This tributary carries the effluent from the Central Valley WRF. TDN inputs from WRF effluent discharge represented between 46-92% of total dissolved nitrogen (TDN) loads (kg day^{-1}) in Jordan River locations immediately downstream of WRF sites in spring and summer (Fig. 3). The majority of the load from all WRFs occurred as NO_3-N in all seasons, with the exception of the Salt Lake City WRF. Loads from this WRF were dominated by NH_4-N in summer and were split almost equally between NH_4-N and dissolved organic N (DON) in fall (Fig. 4). NO_3-N also was the predominant form of N within the intensively studied reach of the river in spring and summer, while DON loads were generally greater than NH_4-N in this area (Fig. 5). DON and NH_4-N loads were similar, while NO_3-N loads remained higher (Fig. 5). NO_3-N loads ranged between approximately 1000-2500 kg day^{-1}, but loads as high as 4000-5000 kg day^{-1} were observed in fall (Fig. 5)

Is N being transformed along the Jordan River flowpath via dissimilatory N uptake?

We found a positive correlation between $\delta^{15}N\text{-}NO_3$ and $\delta^{18}O\text{-}NO_3$ for water samples collected in spring along the intensively sampled reach ($r^2 = 0.67$; Fig. 6). The slope for this relationship was 0.45, which is close to the value (0.50) expected if N is being transformed via denitrification along the downstream flowpath. However, we found that samples became less enriched in $^{15}N\text{-}NO_3$ along the flowpath, suggesting either that N fixation is occurring or novel inputs of less enriched in $^{15}N\text{-}NO_3$ are entering the system (e.g., leaf litter from N_2-fixing species, such as Russian olive [*Elaeagnus angustifolia*], groundwater recharge). Analyses of $\delta^{15}N\text{-}NO_3$ and $\delta^{18}O\text{-}NO_3$ for water samples collected in summer and fall do not show this trend, however. When combined with longitudinal trends in $\delta^{15}N\text{-}NO_3$ and $\delta^{18}O\text{-}NO_3$ our results suggest that denitrification does not have a strong impact on nitrate removal in the water column. Instead, nitrification may be favored.

Is wastewater effluent a source of N for in-stream biota?

$\delta^{15}N$ of fine particulate organic matter (POM) measured in our study was quite variable, ranging from 3-12 ‰ (Fig. 7). $\delta^{15}N$ of POM derived from effluent discharged from the Jordan Valley

WRF consistently had lower (depleted) values than the river, while effluent discharged from the Central Valley WRF consistently had higher (enriched) values than the river. Effluent from the South Valley WRF had $\delta^{15}N$ of POM values lower than the river in spring and fall, but higher values in summer. $\delta^{15}N$ of POM values just downstream of WRFs sometimes declined in response to lower effluent inputs (e.g., downstream of Jordan Valley WRF in fall), but sometimes increased (e.g., downstream of Jordan Valley WRF in summer) relative to upstream river $\delta^{15}N$ of POM signatures. These data indicate we cannot correlate $\delta^{15}N$ of POM signatures to effluent discharge. However, downstream of the Central Valley WRF, $\delta^{15}N$ of POM values were always enriched, suggesting a consistent influence of effluent inputs on POM signatures at this location. It is possible these differences are due to differences in technology used at the various WRFs along the river.

Because dissolved N in the river is not isotopically distinct from N in wastewater effluent, we were not able to quantify the proportion of N in POM sourced from effluent. The broader question here, however, relates to the potential for uptake of wastewater-derived nutrients within the stream channel. To that end, we do find evidence of mass nitrogen and phosphorus removal from the water column between water reclamation facilities (Fig. 3), suggesting that biotic uptake is occurring and influences downstream nutrient loads.

$\delta^{15}N$ of POM values measured in 2013 (Kelso and Baker 2017) and 2016 were of a similar range but values in 2016 were usually more enriched relative to values in 2013 (Fig. 7). $\delta^{15}N$ of POM values for both 2013 and 2016 were much more depleted relative to $\delta^{15}N$ of DOM measured in 2013 (Kelso and Baker 2017). $\delta^{15}N$ of DOM was 6 ‰ greater downstream of the Central Valley WRF relative to upstream in summer of 2013. These data suggest that the N signature of effluent discharge is more evident in the river's DOM pool as compared to the POM pool. However, we do not have data on the $\delta^{15}N$ of DOM within effluent, so this conclusion is uncertain.

We have not reported $\delta^{13}C$ values of POM or C:N ratio of POM because many of our samples had highly enriched $\delta^{13}C$ values, suggesting contamination of carbonates within the POM matrix presumably due to suspended solids in the river. We could not correct for these carbonates through acid digestion given the small quantity of POM collected on filters.

Are substrates supporting microbial community metabolism in the Jordan River primarily of terrestrial or aquatic origin?

We did not find distinction between the $\delta^{2}H$ values of biofilms and riparian vegetation, as expected (Figs. 8-9). Contamination of biofilms by entrained sediment enriched in ^{2}H is one possible reason for this outcome. However, we found that FPOM $\delta^{2}H$ values were similar in both 2013 (measured by J. Kelso) and 2016 (our study) (Fig. 9). FPOM from both years of sample collection and DOM (measured in 2013 by J. Kelso) also had similar $\delta^{2}H$ values (Fig. 9). Mean annual flow in the Jordan River at 1700 S. was 20.6 $ft^3\ s^{-1}$ for 2013 and 34.6 $ft^3\ s^{-1}$ for 2016 (USGS 2017). Differences in flow in these years may have altered the relative contribution of terrestrial vs. aquatic sources to dissolved and particulate organic matter pools, but it is not possible to distinguish between contributions from various sources without isotopic distinction in biofilm and riparian vegetation end-members.

Fluorescence Index (FI) is one type of index that can be calculated from excitation-emission matrices (EEMs). FI values from Antarctica (a purely microbial source) are approximately 1.8-2.0. FI values from the Suwannee River (with intact wetland) are approximately 1.1-1.2. Hence, lower FI values are associated with plant material and higher FI values are associated with microbial biomass or material sourced from microbes. The Jordan River has very high FI values – as high or higher than values observed from microbe dominated communities of Antarctica (Fig. 10). These results suggest that microbes may constitute a significant fraction of dissolved organic carbon (DOC) in the water column. However, EEMs have not been commonly used in urban river systems. Such systems may contain constituents that augment FI values relative to systems without large human populations. That said, our results spurred us to examine the methods used to generate FI values, which may lead to a modification of the analysis used to measure FI. We will re-analyze our data, should this modification be deemed appropriate. Regardless of the actual value of FI, our data suggest that WRFs influence FI values, given that FI values were generally elevated downstream of WRFs relative to upstream sites. Lowest FI values in the Jordan River were observed just downstream of Utah Lake, upstream of the Jordan Basin WRF, and in the Unit 1 wetland. Higher rates of primary production in all of these areas relative to other parts of the Jordan River may be one mechanism leading to similarity in FI values. FI values were lowest in the Jordan River in spring, during high hydrologic flow, and generally increased through summer and fall. Highest FI values in fall as compared to other seasons suggest terrestrial sources do not contribute significantly to dissolved organic matter loads, contrary to previous reports (UDWQ 2015).

What is the quality of the organic matter within the Jordan River?

High FI values (Fig. 10), as discussed previously, suggest that DOC in the Jordan River water column is very labile. BG:POX ratios (Fig. 11) also show much greater rates of ecoenzyme expression related acquisition of C from labile sources (i.e., glucose) relative to more recalcitrant sources (i.e., lignin). Ecoenzyme expression was measured on unfiltered water samples, so these data are reflective of both dissolved and particulate forms of organic matter.

Are microbial communities in the Jordan River limited by C, N, and/or P?

Ecoenzyme activities in water derived from the river, effluent, oil drain, and wetland were highly variable both spatially and temporally (Fig. 11). Activities of ecoenzymes associated with C and N acquisition (BG, NAG+LAP) were high in effluent, resulting in elevated activities downstream. This pattern was not evident with respect to activities of ecoenzymes associated with P acquisition (AP). AP activities along the river's flow path in summer were the mirror opposite of activities in spring and fall, while longitudinal patterns of BG and NAG+LAP were generally similar through time. Regression analyses of ecoenzyme activities (Fig. 12) showed consistent positive relationships between C and N acquisition, explaining between 54-85% of the variation. Slopes had values less than 1, suggesting the river is more limited with respect to N relative to C. Relationships between C and P acquisition and N and P acquisition were positive in summer, but explained less variation (27% for C:P, 11% for N:P). These positive relationships in summer may result from higher temperatures driving higher metabolic rates, and thus higher growth rates (Sinsabaugh and Follstad Shah 2011). High growth rate requires greater P uptake given that ribosomes are rich in P. In contrast, negative relationships were evident in spring and

fall, explaining between 15-26% of the variation. Negative relationships in spring and fall are indicative of greater allocation to P relative to C and N, which typically occurs when P is limiting growth. Hence, ecoenzyme expression in the water column of the Jordan River shows that microbial communities perceive differences in resource supply relative to metabolic needs and are responding most to P availability.

Ecoenzyme activities in sediment derived from the river, oil drain, and wetland were highly variable both spatially and temporally (Fig. 13). However, longitudinal variation in patterns of BG, NAG+LAP, and AP showed greater concordance as compared to patterns in the water column. Correlation in longitudinal patterns were supported by consistent positive relationships in relationships between BG vs. NAG+LAP, BG vs. AP, and NAG+LAP vs. AP, which explained between 11-51% of the variation (data not shown). BG vs. NAG+LAP and BG vs. AP slopes were close to or greater than 1, indicating either matched allocation of energy to C and N acquisition or greater allocation of energy towards C acquisition. NAG+LAP vs. AP slopes were approximately 1 in spring and fall, indicating matched allocation of energy to N and P acquisition, but 0.74 in summer indicative of greater allocation to P when growth rate demands are highest.

In summary, microbial communities in the water column and sediment differ with respect to C, which is in adequate supply in the water column but appears to be limiting in the sediment in some seasons. Microbial communities in the water column and sediment are similar because N appears to be in adequate supply and both communities are limited with respect to P at some times of the year.

Project Presentations

Oral Presentations

Smith, R.M., Follstad Shah, J.J., Weintraub, S., Gabor, R., Jameel, Y., Navidomskis, M. Seasonal variation in organic matter quality and microbial ecology along the Jordan River, Utah. Salt Lake County Watershed Symposium, November 16, 2017, Salt Lake City, Utah.

Follstad Shah, J.J., Gabor, R., Jameel, Y., Smith, R.M., M., Weintraub, S. Evidence of groundwater connectivity in the Jordan River despite flow regulation and effluent inputs. Salt Lake County Watershed Symposium, November 15, 2017, Salt Lake City, Utah.

Smith, R.M. Biogeochemical cycling of carbon and nutrients in an effluent-dominated river. University of Utah Department of Biology Annual Retreat August 26, 2016, Salt Lake City, Utah.

Follstad Shah, J.J., Smith, R.M., Gabor, R., Jameel, Y., Navidomskis, M., Weintraub, S. Do microbes of the Jordan River yo-yo diet? Salt Lake County Watershed Symposium, November 15, 2016, Salt Lake City, Utah.

Gabor, R. Relationships between microbial activity, nutrients, and organic matter chemistry in urban-impacted rivers. 253rd American Chemical Society National Meeting & Exposition, April 3, 2017, San Francisco, California.

Follstad Shah, J.J., Smith, R.M., Gabor, R., Jameel, Y., Navidomskis, M., Weintraub, S. Microbial community response to energy and nutrient flows within a semi-arid, effluent dominated urban river system. 2017 Spring American Water Resources Association Meeting – Connecting the dots: the emerging science of aquatic system connectivity, April 30-May 3, 2017, Snowbird, Utah.

Poster Presentations

Smith, R.M., Follstad Shah, J.J., Gabor, R., Navidomskis, M. Sources and cycling of nitrogen in the Jordan River, Annual Global Change & Sustainability Science Center Research Symposium, February 8, 2017, Salt Lake City, Utah.

Navidomskis, M , Follstad Shah, J.J., Smith, R.M., Gabor, R. Sources and cycling of nitrogen in the Jordan River. Salt Lake County Watershed Symposium, November 15, 2016, Salt Lake City, Utah.

Smith, R.M., Follstad Shah, J.J., Gabor, R., Navidomskis, M. Sources and processing of nitrogen in an effluent-dominated river. Association for the Sciences of Limnology & Oceanography 2017 meeting: Mountains to the Sea, Feb 26-Mar 3, 2017, Honolulu Hawaii.

Follstad Shah, J.J., Smith, R.M., Gabor, R., Jameel, Y., Navidomskis, M., Weintraub, S. Microbial community response to energy and nutrient flows within a semi-arid, effluent dominated urban river system. 2017 Spring Run-off Conference, Utah State University, March 28, 2017, Logan, Utah.

Acknowledgements

We extend thanks to several individuals for their support: water reclamation facility operators for their assistance in accessing effluent discharge sites and providing ancillary data needed for our study; our undergraduate research technicians, Mickey Navidomskis, Lily Wetterlin, and Nick Storey for their help with sample collection, processing, and analysis; Dr. Gabe Bowen, Dr. Paul Brooks, and Dr. Diane Pataki for access to their laboratory spaces and equipment; Dr. Suvankar Chakraborty for his expertise and assistance in running stable isotope analyses; Sagarika Banerjee for her help conducting $^{15}N\text{-}NO_3$ analyses using the denitrifier method; and Cindy Brown and Kim Peterson for accounting and administration services.

References

Arens, H. N. and C. A. Adams. 2012. Jordan River Total Maximum Daily Load (TMDL): Phase 1. Oral presentation at the Salt Lake County Watershed Symposium, September, 2012, Salt Lake City, UT. http://www.waterquality.utah.gov/TM accessed December 7, 2015.

Bernhardt, E. S., Band, L. E., Walsh, C. J., & Berke, P. E. (2008). Understanding, managing, and minimizing urban impacts on surface water nitrogen loading. *Annals of the New York Academy of Sciences*, *1134*, 61–96. http://doi.org/10.1196/annals.1439.014

Doucett, R. R., J. C. Marks, D. W. Blinn, M. Caron, and B. A. Hungate. 2007. Measuring terrestrial subsidies to aquatic food webs using stable isotopes of hydrogen. Ecology 88:1587-1592.

Finlay, J. C. and C. Kendall. 2007. Stable isotope tracing of temporal and spatial variability in organic matter sources to freshwater ecosystems. Pages 283-333 in R. Michener and K. Lajtha (eds.), Stable Isotopes in Ecology and Environmental Science, Second Edition, Blackwell Publishing, Malden, Massachusetts, USA.

Jensen, S.F. and N. Rees. 2005. Jordan River Watershed water quality TMDL assessment. State of Utah Division of Water Quality. 75 pp. http://slco.org/watershed/pdf/wqJrTMDL.pdf accessed December 7, 2015.

Kaushal SS, Delaney-Newcomb K, Findlay SE, et al (2014) Longitudinal patterns in carbon and nitrogen fluxes and stream metabolism along an urban watershed continuum. Biogeochemistry 121:23–44. doi: 10.1007/s10533-014-9979-9

Kelso, J., M. Baker (2017). FPOM and DOM isotope values, HydroShare, http://www.hydroshare.org/resource/4eb5c9c871e34aa4ae6951ce6d15020d

Kendall, C., Elliott, E.M., and Wankel, S.D., 2007. Tracing anthropogenic inputs of nitrogen to ecosystems, Chapter 12, In: R.H. Michener and K. Lajtha (Eds.), Stable Isotopes in Ecology and Environmental Science, 2nd edition, Blackwell Publishing, p. 375- 449.

Mallin, M. a., Johnson, V. L., Ensign, S. H., & MacPherson, T. a. (2006). Factors contributing to hypoxia in rivers, lakes, and streams. *Limnology and Oceanography*, *51*(1, part 2), 690–701. http://doi.org/10.4319/lo.2006.51.1_part_2.0690

Schmidt, C. E., Robinson, R. S., Fields, L., & Nixon, S. W. (2016). Changes to nitrate isotopic composition of wastewater treatment effluent and rivers after upgrades to tertiary treatment in the Narragansett Bay watershed, RI. *Marine Pollution Bulletin*. http://doi.org/10.1016/j.marpolbul.2016.02.010

McKnight, D. M., E. W. Boyer, P. K. Westeroff, P. T Doran, T. Kulbe, and D. T. Andersen. 2001. Spectrofluorometric characterization of dissolved organic matter for indication of precursor organic material and aromaticity. Limnology & Oceanography 46:38-38.

Sinsabaugh, R. L. and J. J. Follstad Shah. 2011. Ecoenzymatic stoichiometry of recalcitrant organic matter decomposition: the growth rate hypothesis in reverse. Biogeochemistry 102:31-43.

Sinsabaugh, R. L. and J. J. Follstad Shah. 2012. Ecoenzymatic stoichiometry and ecological theory. Annual Reviews of Ecology, Evolution, and Systematics 43:313-343.

Utah State Division of Water Quality (UDWQ). 2015. Jordan River Research 2010-2015.

United States Geologic Survey (USGS). 2017. National Water Information System. https://nwis.waterdata.usgs.gov/ accessed December 20, 2017.

Townsend-Small, A., Pataki, D. E., Tseng, L. Y., Tsai, C.-Y., & Rosso, D. (2011). Nitrous oxide emissions from wastewater treatment and water reclamation plants in southern California. *Journal of Environmental Quality*, *40*(5), 1542–1550. http://doi.org/10.2134/jeq2011.0059

Tables

Table 1. List of study sites and their locations.

Site Name	River Kilometer (starting at Utah lake outlet)	Intensive Site	Extensive Site	WRF
Willow Park (Lehi, UT)	5.6		x	
Bangeter Highway (13900 S)	21		x	
Jordan Basin Effluent	22			x
Jordan River Rotary Park	23		x	
Garner Village (7800 S)	36		x	
South Valley Effluent	37			x
Zagg foot bridge (7200 S)	38		x	
3300 S	49		x	
Central Valley Effluent	50			x
Cesar Chaves Drive	51		x	
1700 S	53	x		
California Avenue	54	x		
Indiana Avenue	56	x		
Poplar Grove Road (400 S)	57	x		
200 S	58	x		
North Temple	59	x		
Cottonwood Park (400 N)	60	x		
Redwood Road (700 N)	61	x		
Rose Park Library (1000 N)	62	x	x	
Joust Court Golf Course	63	x		
Northwest Middle School	64	x		
Salt Lake City Effluent	65			x
Oil Drain at Cudahey Lane	70		x	
Oil Drain in Great Salt Lake Wetlands	79.4		x	
Great Salt Lake Unit 1 Wetland	NA		x	

Table 2. Microbial ecoenzymes and their ecological roles.

Ecoenzyme	**Code**	**Ecological Role**
β-1,4-glucosidase	BG	Carbon acquisition via cellulose degradation; hydrolyzes glucose from cellobiose
β-1,4-N-acetylglucosaminidase	NAG	Carbon and nitrogen acquisition via chitin and peptidoglycan degradation; hydrolyzes glucosamine from chitobiose
Leucine aminopeptidase	LAP	Nitrogen acquisition via proteolysis; hydrolyzes leucine and other hydrophobic amino acids from the N terminus of polypeptides
Acid (alkaline) phosphatase	AP	Phosphorus acquisition via hydrolysis of phosphate from phosphosaccharides or phospholipids
Phenol oxidase	POX	C acquisition via the oxidative degradation of lignin

Figures

Cover Figure: Jordan Valley Water Reclamation Facility effluent discharge into the Jordan River.

Figure 1. Map of study area.

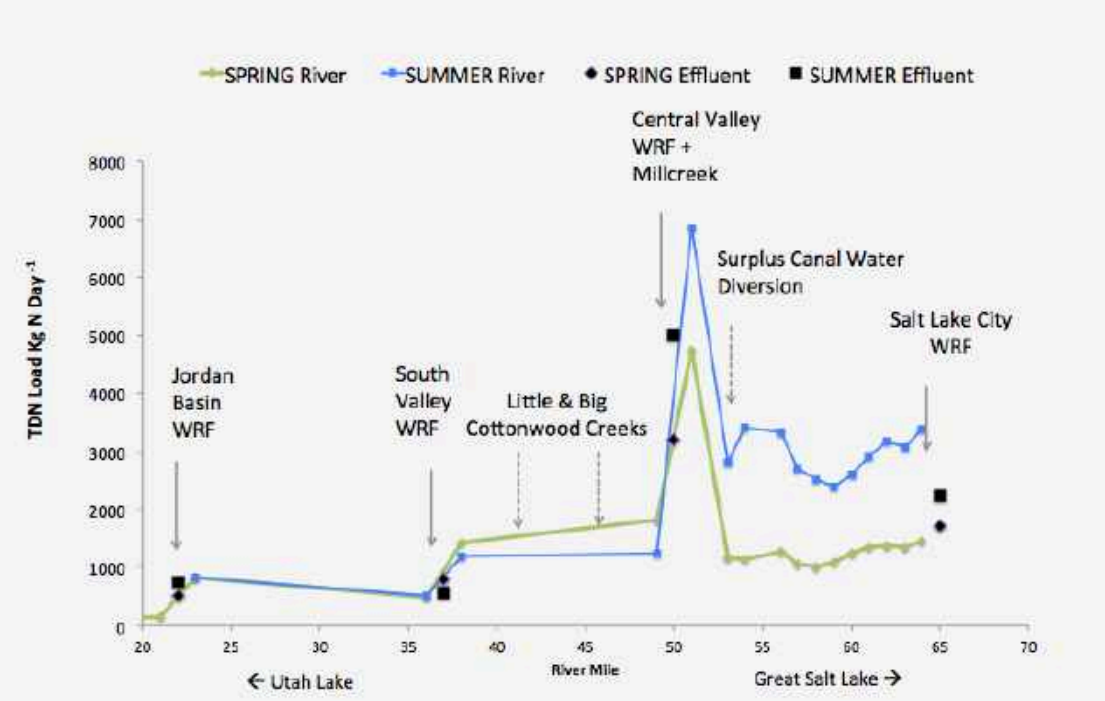

Figure 2. Total dissolved nitrogen (TDN) load of the Jordan River in spring (green line) and summer (blue line) of 2016. TDN loads from water reclamation facilities are shown as triangles (spring) and squares (summer). Data for fall are not available due to failure of equipment used to measure river discharge.

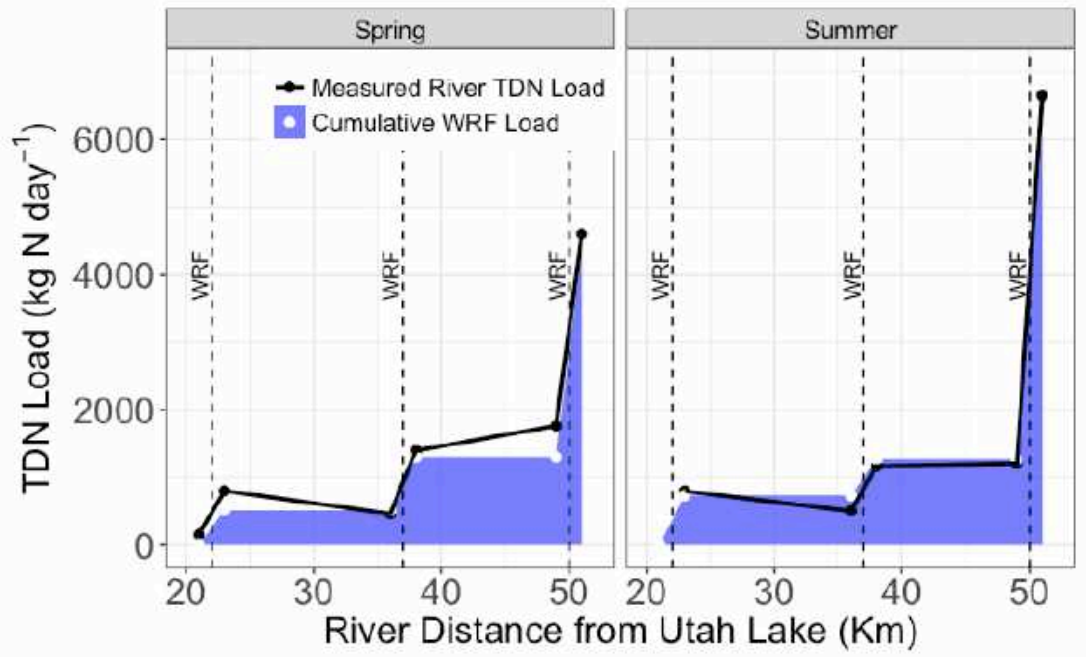

Figure 3. Measured river (TDN) load plotted alongside cumulative loads from three water reclamation facilities between Utah Lake and 1700 S in spring and summer of 2016. Load data for fall is not available due to lack of flow data.

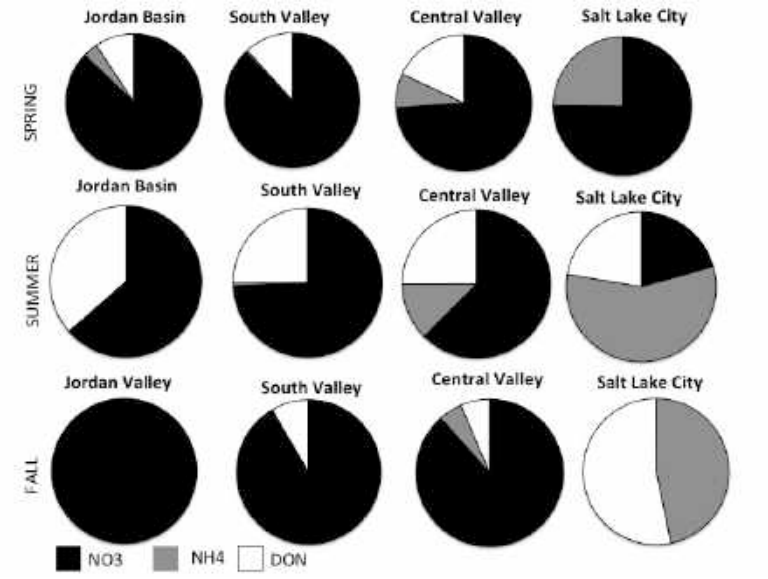

Figure 4. Composition of N inputs to the Jordan River from four water reclamation facilities in spring, summer, and fall of 2016.

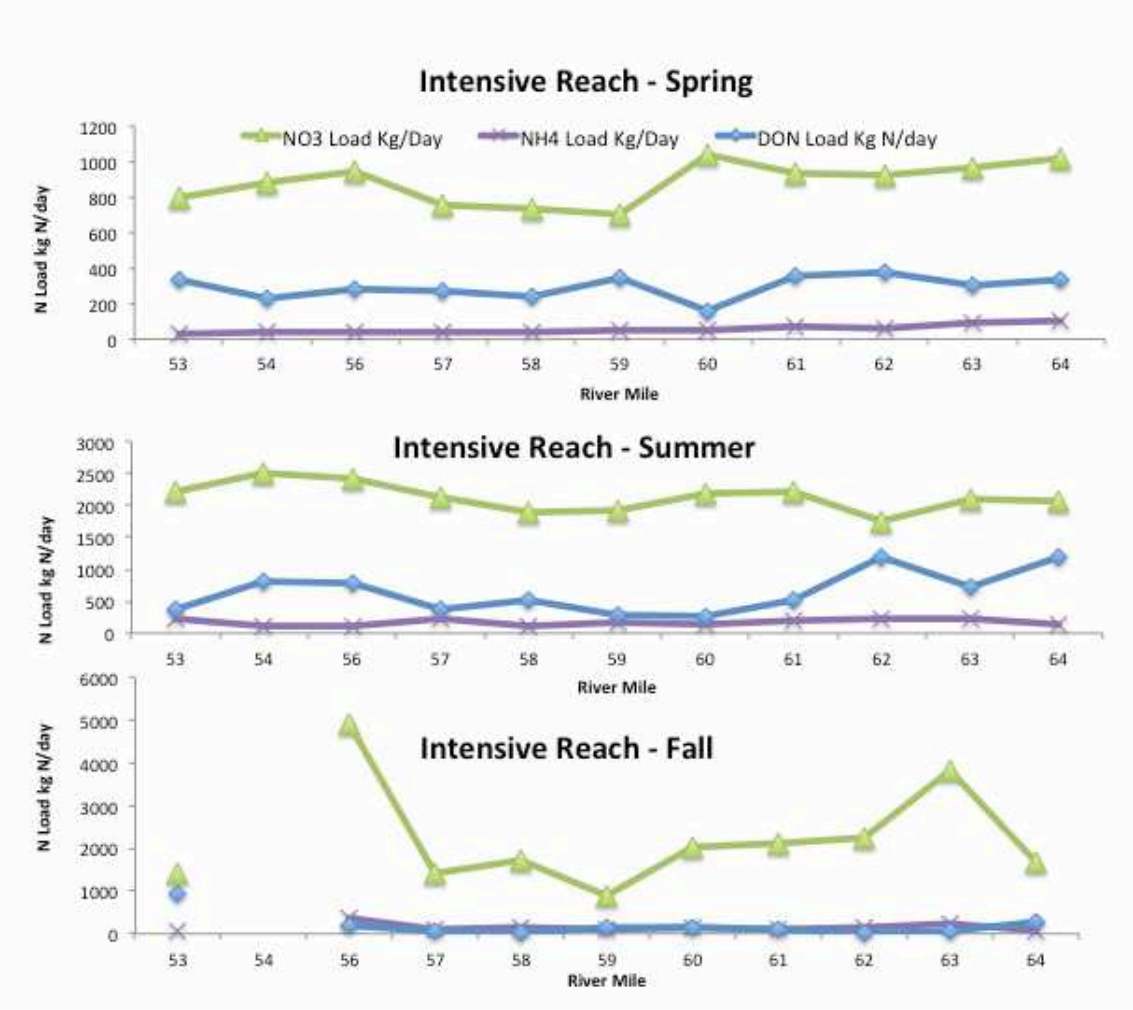

Figure 5. Loads of NO_3-N, NH_4-N, and dissolved organic N (DON) at the ten sites within the intensively studied reach in spring, summer, and fall 2016.

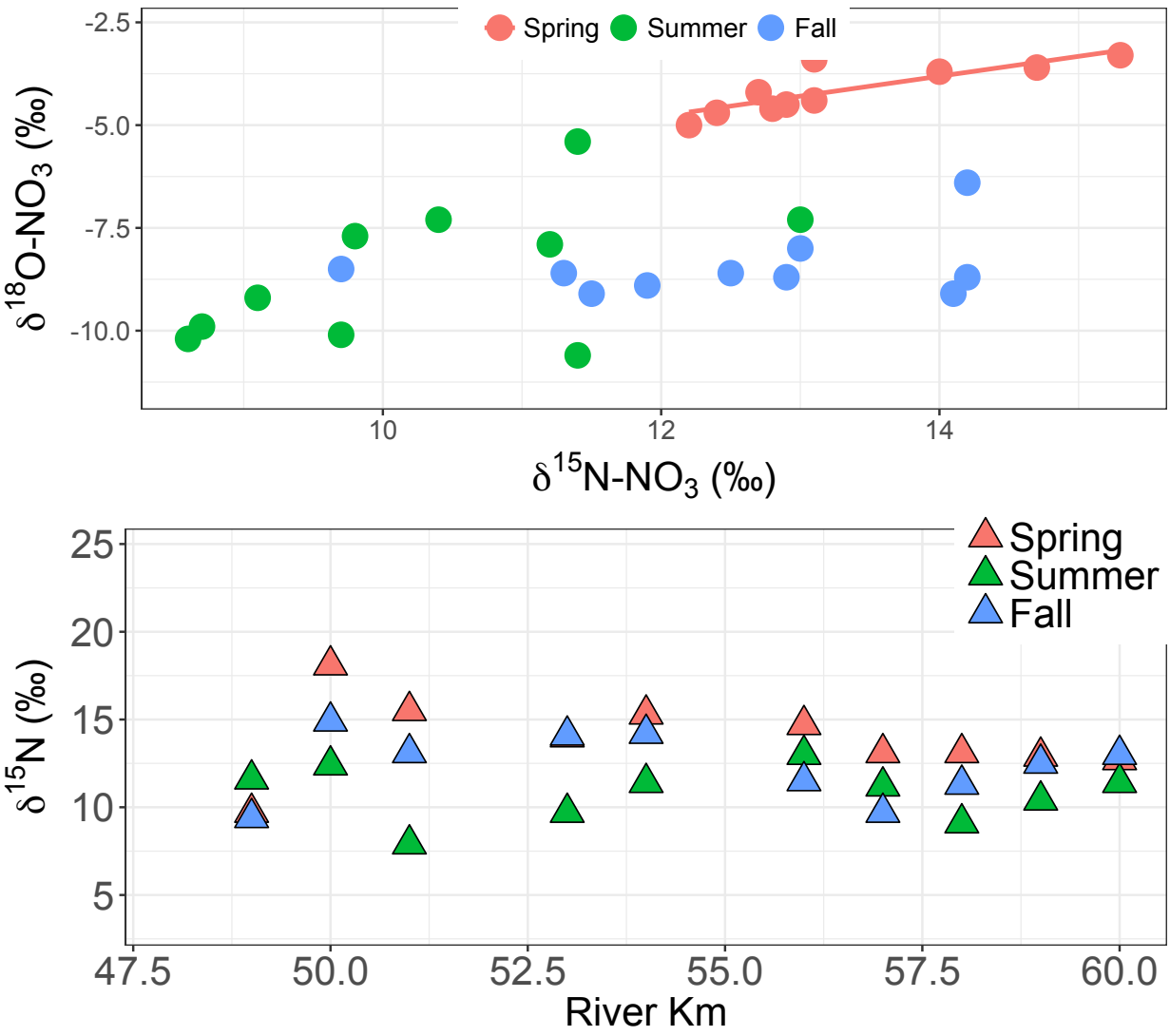

Figure 6. δ^{15}N-NO_3^- vs. δ^{18}O-NO_3 for the ten study sites within the intensively sampled reach of the Jordan River for spring, summer and fall (upper graph). Dual enrichment of δ^{15}N-NO_3 and δ^{18}O-NO_3 in spring (r^2=0.45, $p<0.05$) theoretically signifies potential removal from the water column, as denitrifying microbes preferentially convert isotopically lighter forms of NO_3^- to N_2O. This trend is initially apparent in spring, however this relationship is not present in fall or summer seasons. Additionally, for this relationship to truly signify NO_3^- removal, dual enrichment would need to occur in the downstream direction. Instead, we see a decreasing trend of δ^{15}N-NO_3^- downstream, net NO_3^- production in this reach (lower graph).

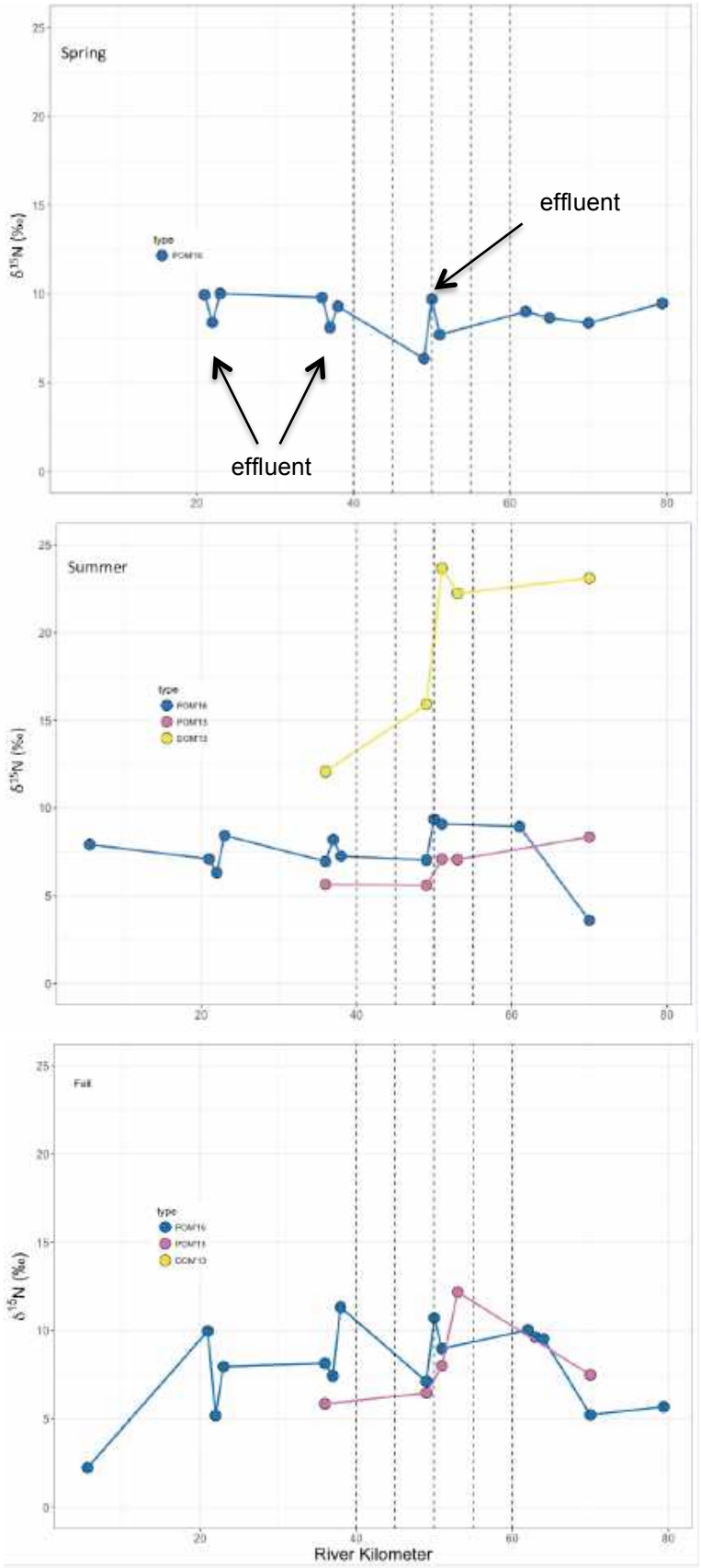

Figure 7. $\delta^{15}N$ of fine particulate organic matter (POM) in spring, summer, and fall of 2016 (blue symbols and line). These data are compared to $\delta^{15}N$ of POM (pink symbols and line) and dissolved organic matter (DOM; yellow symbols and line) measured in 2013 (Kelso & Baker 2017). Locations of effluent discharge measures are identified for spring, but corresponding measures are shown for summer and fall as well.

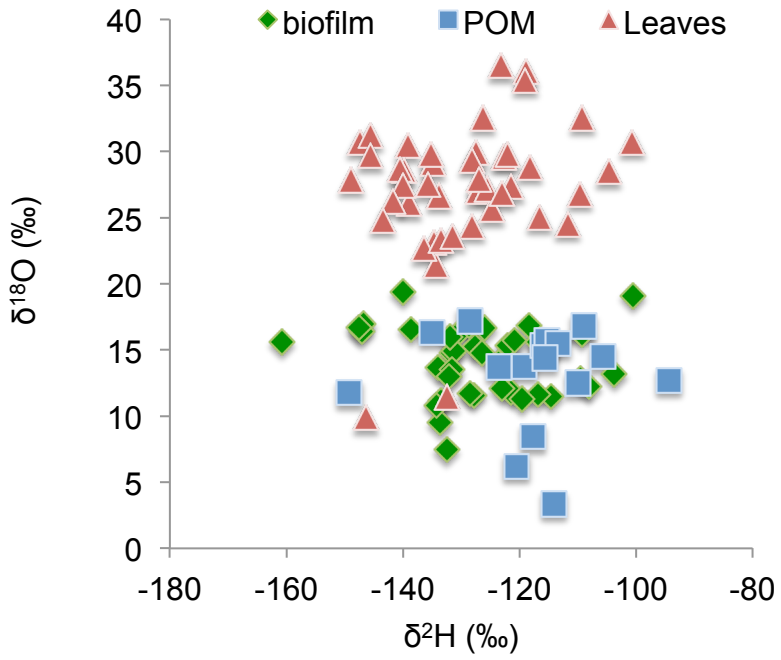

Figure 8. Values of δ^2H and $\delta^{18}O$ for biofilms (green diamonds), riparian leaves (red triangles), and fine particulate organic matter (POM; blue squares) from the water column of the Jordan River.

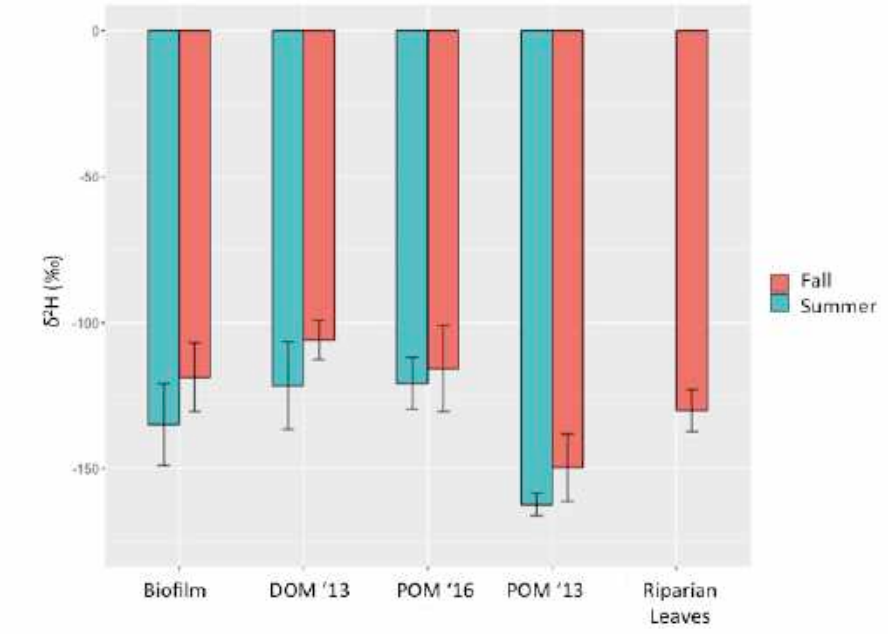

Figure 9. Similarity in δ^2H values in summer (green) and fall (orange) for biofilms, dissolved organic matter (DOM, measured in 2013), fine particulate organic matter (measured in both 2013 and 2016), and riparian leaves. Measurements from 2013 are from Kelso and Baker (2017).

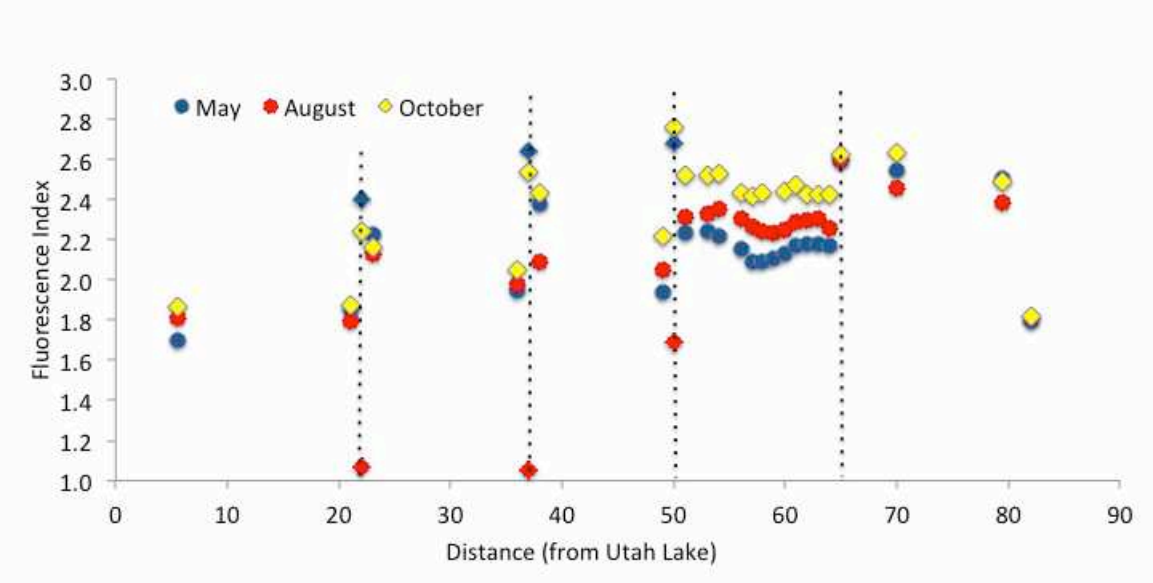

Figure 10. Fluorescence Index (FI) of dissolved organic carbon (DOC) collected from the Jordan River (circles) and water reclamation facilities (diamonds along dashed vertical lines) in spring (blue), summer (red), and fall (yellow). FI values were derived from excitation-emission matrix (EEM) analyses.

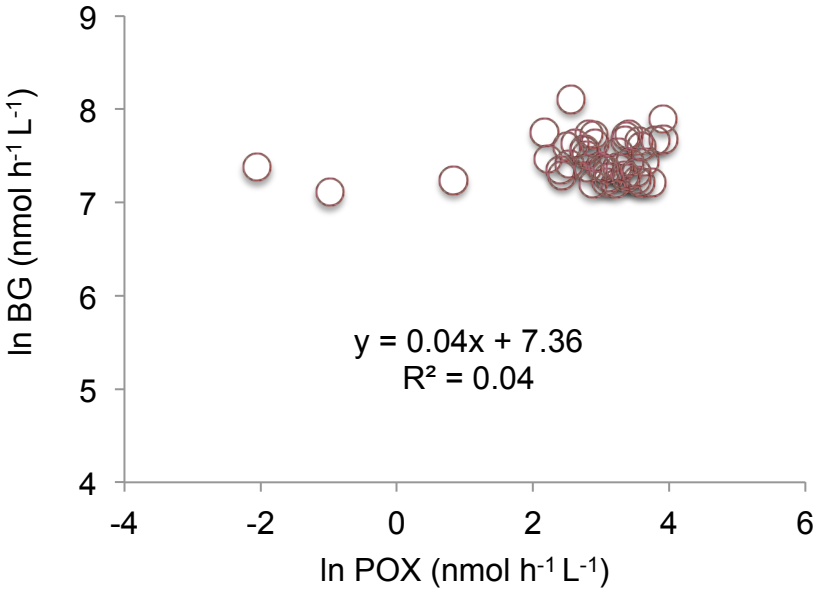

Figure 11. Microbial expression of β-1,4-glucosidase (BG) is greater than expression of phenol oxidase (POX) by a magnitude of ~100 times, but shows less variation in activity rates.

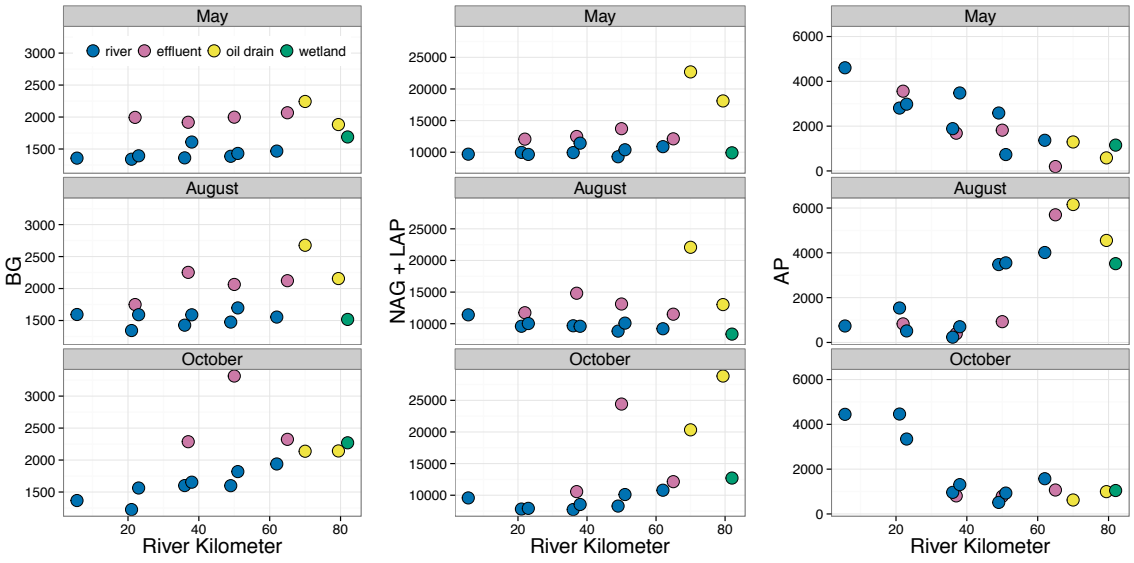

Figure 11. Activities (nmol L^{-1} h^{-1}) of ecoenzymes associated with acquisition of C (β-1,4-glucosidase, BG), N (β-1,4-N-acetylglucosaminidase, NAG; leucine aminopeptidase, LAP), and P (alkaline phosphatase, AP) are variable both spatially and temporally in water derived from the river (blue circles), effluent (pink circles), oil drain (yellow circles), and wetland (green circles).

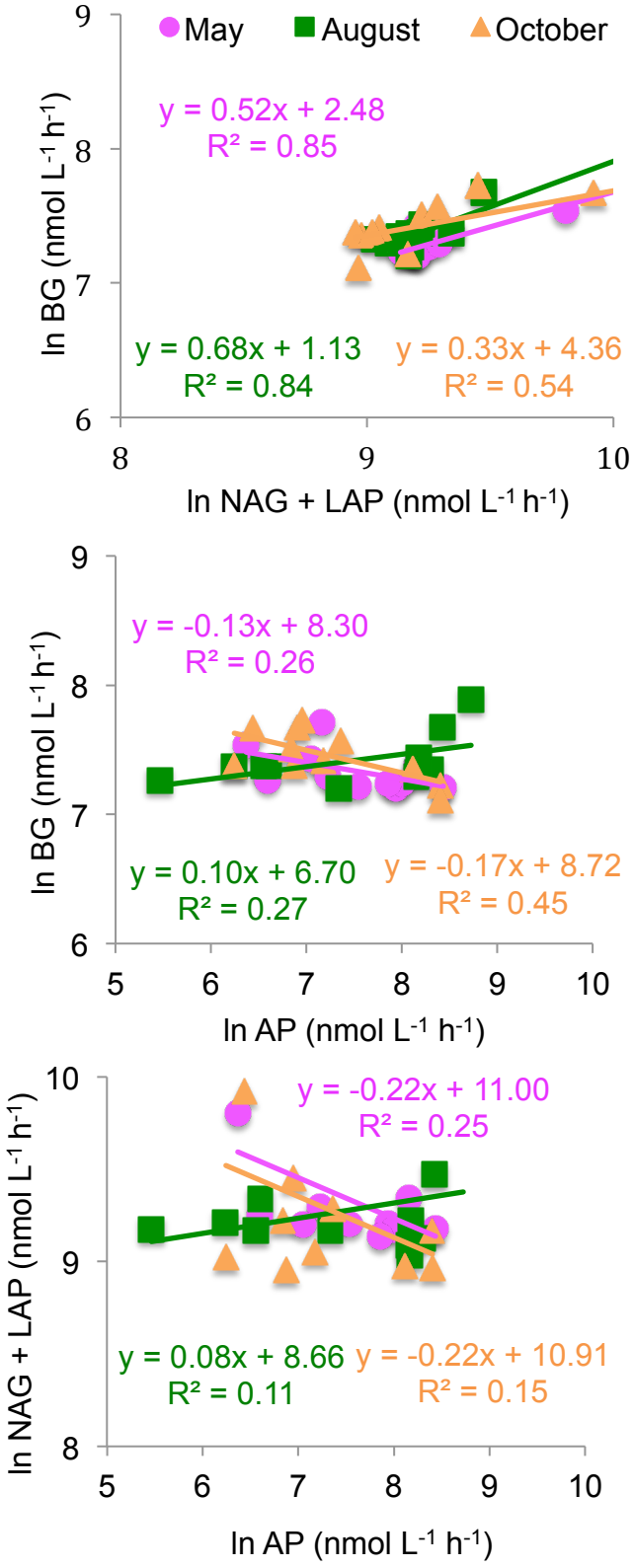

Figure 12. Ecoenzyme ratios of Jordan River water column samples in spring, summer, and fall. BG refers to β-1,4-glucosidase, which is associated with labile C acquisition. , NAG+LAP refers to β-1,4-N-acetylglucosaminidase and leucine aminopeptidase, which are associated with acquisition of N. AP refers to alkaline phosphatase, which is associated with acquisition of P. The graph show C:N (upper), C:P (middle), and N:P (lower) relationships.

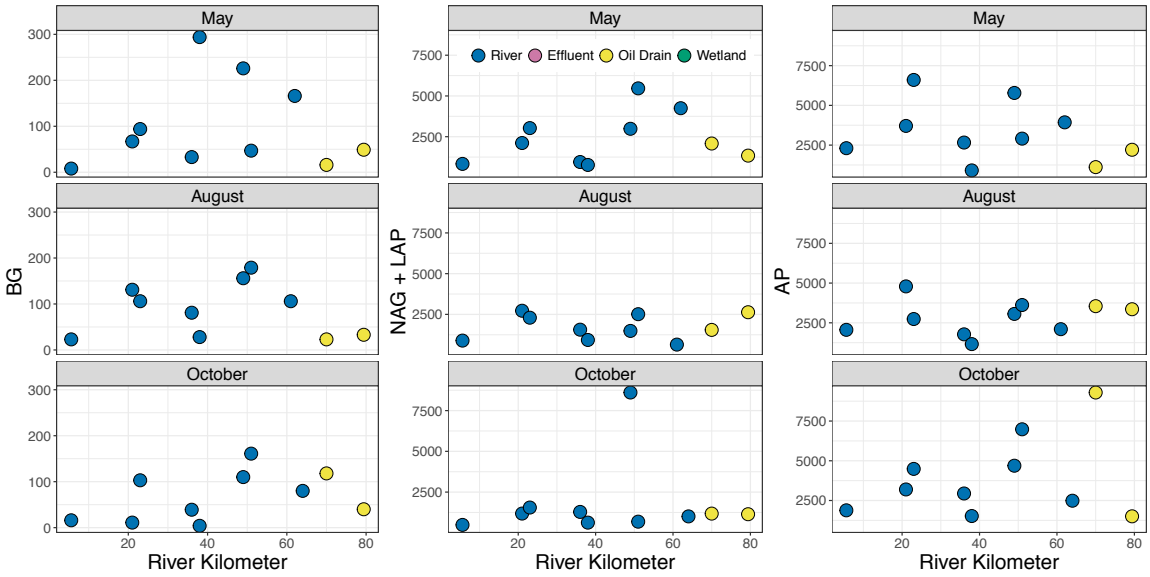

Figure 13. Activities (nmol L^{-1} h^{-1}) of ecoenzymes associated with acquisition of C (β-1,4-glucosidase, BG), N (β-1,4-N-acetylglucosaminidase, NAG; leucine aminopeptidase, LAP), and P (alkaline phosphatase, AP) are variable both spatially and temporally in sediment from the river (blue circles), oil drain (yellow circles), and wetland (green circles).

Understanding Nitrogen Dynamics at Selected Sites in The Jordan River and The Great Salt Lake Wetlands

ANNUAL PROJECT REPORT

Abstract: Nitrogen contamination in surface water is a widespread problem. The purpose of this research was to establish protocols to study nitrogen dynamics at selected sites in the Jordan River and the Great Salt Lake (GSL) wetlands. Three sites in the Jordan River and three in the GSL wetlands were chosen to demonstrate the developed protocols. Results strongly indicate that Jordan River sediments are very active in ammonia oxidation and, more importantly, in nitrate reduction. Results also indicate that sediments are actively producing and consuming methane gas, thus affecting dissolved oxygen dynamics in the Jordan River. Wetland sediments also demonstrated active nitrification and denitrification. We normalized the rate data to the actual functional gene copy numbers to compare different sites. This could represent a significant leap forward in understanding nitrogen dynamics in wetlands. Based on nutrient flux chamber experiments, it is also concluded that wetland sediments in general serve as source of ammonium and sink of nitrate.

Dr. Ramesh Goel, Shaikha Abedin and Scott Teeters

November, 2014

From
Dr. Ramesh Goel
Associate Professor
Civil & Environmental Engineering
University of Utah

To: Dr. Theron Miller

Subject: Research status report for the project titled "Understanding Nitrogen Dynamics at Selected Sites in The Jordan River and The Great Salt Lake Wetlands**".**

Dear Dr. Miller

I am pleased to update you on the progress of our research on nitrogen dynamics in the Jordan River for the titled project. This project has primarily four independent tasks. Our initial work focused on protocol development and student training. The four tasks are listed below.

Task 1: *Estimate the contribution of biological processes to nitrogen fate, including that due to anaerobic ammonia oxidation*.

Task 2*: Evaluate the presence of other nitrogen cycling bacteria*.

Task 3*: Determine methane formation rates in Jordan River sediments.*

Task 4*: Determine nutrient fluxes though nutrient flux experiments at three GSL wetland sites*:

1.0 Methodology

1.1 Sampling Locations: To execute the tasks stated above, three sites in the Jordan River were chosen based on recommendations by Dr. Theron Miller. For the nutrient flux experiments, three GSL wetland sites were also selected. The Jordan River sites are; (i) 1300 S, (ii) Center Street and, (III) Legacy Nature Preserve (LNP). The three wetland sites are, (i) Ambassador, (ii) Turpin- GSLI-013 and, (III) Bear River Nature Preserve Unit 5C

1.2 Sample collection: For the Jordan River samples, sediments were collected from near the mid-width of the river. For the wetland sites, samples were collected from a distance of 10~20 feet from the bank depending upon the accessibility. A core sampler with a 2.5 inch diameter and length of 3 feet was used to collect sediment samples. Sediments were collected from a depth of 0-10 cm from the top assuming that nitrifying bacteria would be present in the top layer of 0-5 cm and denitrifying bacteria would be present below, although both can simultaneously co-exist in the top layer as well. Each of the 5 cm deep samples were separated and kept in different sampling containers. The samples were transported to the lab in an ice cooler for further processing.

1.3 Nitrification protocol

For nitrification experiments, the top 5-cm sediment sub-core was homogenized aseptically with a laboratory-scale spatula. A predetermined amount of the homogenized slurry was placed in a 600 ml sterile beaker as shown in the left panel in Figure 1. The mixture was aerated with a low airflow rate and stirred continuously. Ammonia-nitrogen stock solution was added to start the nitrification process to accomplish a predetermined final ammonium nitrogen concentration. For each experiment, a sterile pipette was used to remove 25 ml of the slurry, with duplicates, and the ammonia nitrogen, nitrate nitrogen and nitrite nitrogen concentrations were measured. Total solids and volatile solids were also measured according to standard methods.

Figure 1: *Preparation for nitrification and denitrification (On left: sediment being stirred in a beaker for nitrification. On right: a serum bottle for denitrification experiment).*

To evaluate the role of abiotic processes in ammonium fate, experiments were also conducted in the presence of a nitrification inhibitor (50 mg/L allylthiourea). For the inhibition of nitrification, another batch was prepared in a serum bottle and 50 mg/L allylthiourea was added. At first, allylthiourea was added with sediment and deionized water, and the bottle was shaken for about 3 hours to inhibit the nitrification process. The same target concentration of ammonia-nitrogen, as used in the other experiment, was added after 3 hour of mixing and then the slurry samples were collected at specified time intervals. The concentrations for NO_3-N in the raw data were obtained directly from the ion chromatograph, NO_2-N was obtained using the nitrite colorimeter method, and NH_3-N using HACH high range and low range test kits.

1.4 Denitrification protocol

Two sets of serum bottle denitrification experiments were performed: one without any carbon source, and the other with sodium acetate as a source of organic carbon. For each set-up, 6-9 serum bottles were used and duplicates were taken at each sampling time. After homogenizing the sediment sample in the same manner as we did for nitrification tests, equal amounts of weighed samples were taken into each serum bottle. After adding a fixed amount of sediment and deionized water or acetate solution to the serum bottles, the serum bottles were capped with 20 mm aluminum crimp caps and 20 mm butyl rubber-teflon faced septa. In order to make the system anoxic, dinitrogen gas was pumped into the serum bottle for

about 15 to 20 minutes. As a source of nitrate nitrogen, sodium nitrate stock solution was added into each serum bottle after 20 minutes of purging with N_2 gas using a 5ml syringe to accomplish a final nitrate nitrogen concentration of 3.5 mg/L. One of the serum bottles was opened after the addition and mixing of nitrate stock and it was considered a time zero hour sample. The rest of the bottles were kept on a shaker to be sampled subsequently.

1.5 Methane fluxes and methane oxidation in Jordan River

Serum bottle sediment methane production batch tests were conducted following the method developed by our group (Hogsett 2013). Briefly, a known mass of wet sediments was transferred into a 75 mL serum bottle. Jordan River water was then added to the serum bottle so that the final volume of the sediment/water mixture was 30 mL, with 45 mL of headspace to allow standardized use of the ideal gas equation. The serum bottles were capped with 20 mm aluminum crimp caps and 20 mm butyl rubber-teflon faced septa. After sealing the bottles, the sediment slurry and headspace were purged for 15 minutes with nitrogen gas while gently mixing the slurry every 5 minutes to create anaerobic conditions.

The sediment serum bottles were left undisturbed to incubate at 20°C in a dark cabinet for a time period of five days. Gas samples of 200 microliters were collected with a gas tight syringe (Hamilton #81156) and injected into an Agilent Technology gas chromatograph 7890A with a thermal conductivity detector (TCD) at a detector temperature of 150°C. Gas separation was carried out using a 30 meter capillary column (Agilent GS-Carbon plot) at an isothermal oven temperature (30°C) over 5 minutes. The carrier gas was helium at 27 cm/sec with an injector temperature of 185°C and 1:30 split. The methane peak was observed at 2.6 minutes and carbon dioxide occurred at 4 minutes. The calibration curves for CH_4 and CO_2 were within the range of 0.02-25% in terms of partial pressure of the gas sample. The methane and carbon dioxide percentages were then used in the gas equations shown below. The percent of carbon dioxide can be substituted for methane in the following equations to estimate sediment production of the more soluble CO_2.

The following equations provide the parameters and units required to utilize the ideal gas law in this serum bottle study. Absolute pressure is calculated as the sum of atmospheric and relative headspace pressures.

$$\mu mol\ CH^4 = \frac{\left\{(P_{amb} + P_{HS})\left(10^3\ {}^{Pa}/_{kPa}\right)\right\}\left\{(V_{HS})\left({}^{L}/_{10^3\ mL}\right)\left(\frac{m^3}{10^3\ L}\right)\right\}\left\{\left(10^6\ {}^{\mu mol}/_{mole}\right)\left({}^{\%CH_4}/_{10^2}\right)\right\}}{\left(8.314\ {}^{J}/_{K * mol}\right)(T_{amb})}$$

$$\mu mol\ CH^4 = \frac{(P_{amb} + P_{HS})(V_{HS})(\%CH_4)(10)}{(8.314)(T_{amb})}$$

$\mu mol\ CH_4 = micromoles\ methane\ in\ headspace\ of\ bottle$

$P_{amb} = ambient\ atmospheric\ pressure\ (kPa) \cong 85.6$

$P_{HS} = serum\ bottle\ headspace\ pressure\ (kPa)$

$V_{HS} = serum\ bottle\ headspace\ volume\ (mL)$

$\%CH_4 = headspace\ methane\ as\ percent\ volume\ (GC\ output)$

$T_{amb} = ambient\ room\ temperature\ (K) \cong 293$

After determining the number of micromoles of methane produced in the sediment bottle, this value was normalized to wet sediment mass and days of incubation to calculate the wet sediment methane production rate (Y).

$$Y = \frac{(\mu mol\ CH_4)\left({}^{mol}/_{10^6\ \mu mol}\right)}{(m_{wet})\left({}^{kg}/_{10^3}\right)(t)} = \frac{mol\ CH_4}{(m_{wet})(t)(10^3)}$$

$Y = \frac{mol\ CH_4}{(kg\ wet\ sediment)(day)}$, $t = time\ (days)$, $m_{wet} = wet\ mass\ of\ sediments\ (g)$

1.6 Nutrient flux experiments on the wetlands samples

Transparent rectangular acrylic chambers (10”×10”×36”) were used to measure the daytime nutrient dynamics at the sediment-water interface and within the water column. These chambers were deployed in duplicate for a total of four chambers per site. The sediment chamber has both an open top and open bottom to measure nutrient dynamics in the water column while interacting with the sediments. The water column chamber has an open top and closed bottom to measure nutrient dynamics in the water column only.

The sediment chamber was carefully pressed into the sediment (5-10cm deep) to avoid sediment disturbance. The water column chamber was filled with water to match the depth within the sediment chamber. It was stabilized with a wooden post adjacent to the corresponding sediment chamber. The water column in each chamber was thoroughly mixed with a low flow submergible pump (5 L/min for 10 minutes). A minimum sampling time of six hours was suggested with samples being collected every two hours. The primary information sought from the chamber installation is data on the related fluxes of NH_3-

N, NO_3-N, NO_2-N and PO_4-P from the sediments. After experiments under ambient conditions, chamber contents were spiked with low but known concentrations of ammonium, nitrate and phosphate as well.

The rate of change of the dissolved nutrients for each chamber was calculated using the slope of the concentration (mg/l) versus time (day). The final rates and fluxes are expressed in terms of g/m^3/day and g/m^2/day, respectively. The water column (WC) rate was calculated initially since the field-observed rate describes the nutrient dynamics occurring in the water column.

$$WC_{light} = \frac{dC}{dt}$$

WC_{light} = WC nutrient rate during daytime conditions (g/m^3/d)

dC = Change of nutrient concentration in chamber (mg/L)dt = length of sampling event (day)

1.7 Pore Water Concentration

Pore water concentrations were calculated using the following methodology.

The nutrient concentrations were taken from unspiked serum bottle test samples, as will be described later. In this case, 50 mL deionized water (pH ~ 7) was added to 10 grams of sediment sample, made into a slurry, and a 10 mL sample was immediately filtered for analysis by IC in order to prevent major concentration changes due to desorption. Total solids content of wet sediments was determined by heating a known weight of wet sediments at 103 degree centigrade overnight.

$$V_{Pore\ Water} = \frac{m_{wet\ sed} * (1 - \%TS)}{\rho_{water}}, V_{Pore\ Water} = Volume\ of\ pore\ water\ (mL)$$

$m_{wet\ sed}$ = mass of wet sediment (g), $\%TS = Percent\ total\ solids = = \frac{m_{dry\ sed} - m_{dish}}{m_{wet\ sed} - m_{dish}}$

$m_{dry\ sed} = mass\ of\ sediment\ after\ 12\ hours\ of\ drying\ at\ 106℃\ and\ pulverizing$ (g)

$m_{dish} = mass\ of\ weighing\ dish\ after\ ignition\ to\ remove\ organic\ mass\ (g)$

$\rho_{water} = density\ of\ water, assumed\ to\ be\ 0.997\ g/mL$

The pore water volume is then applied to the concentrations determined from HACH kits for ammonia and the ion chromatograph for nitrate, nitrite, and phosphate.

$$C_{Pore\ Water} = Sample\ Concentration * \frac{V_{Total}}{V_{Pore\ Water}}$$

$$Sample\ Concentration = Concentration\ measured\ by\ IC\ or\ HACH\ (\frac{mg}{L})$$

$V_{Total} = Total\ unspiked\ serum\ bottle\ volume = 50\ mL + V_{Pore\ Water}$

$C_{Pore\ Water} = Pore\ Water\ Concentration\ (\frac{mg}{L})$

1.8 Serum Bottle Tests and Genomic Characterization

The serum bottle tests were conducted the day after sampling for each site. In each case, roughly 10 g of sediment sample was made into a slurry with 50 mL of deionized water in a serum bottle and left to react for twelve hours on the shaker at room temperature. The final NH4-N concentration was 0.5 mg/L. If it was needed, NH4-N stock was added to achieve the target final concentration. Experiments were performed in duplicate. However, due to the ammonia pore water concentrations of the sediments, it was difficult to consistently reach 0.5 mg/L NH_4-N. Nevertheless, the same spike amount was used for each trial. The following equations were used to determine serum bottle nitrification rates.

$m_{VS} = m_{wet\ sed} * \%\ TS * \%\ VS_{dry} = mass\ of\ volatile\ solids$

$\%\ VS_{dry} = \frac{m_{dry\ sed} - m_{ign\ sed}}{m_{dry\ sed} - m_{dish}}$ = Percent volatile solids of dry sediment

$m_{ign\ sed} = Mass\ of\ sediment\ ignited\ at\ 550℃\ for\ one\ hour\ after\ drying$

$$C_{VS}\ \left(\frac{g}{L}\right) = concentration\ of\ volatile\ suspended\ solids = \frac{m_{VS}}{50\ mL + V_{pore\ water}} \times (\frac{1000\ mL}{L})$$

$$Rate\ of\ Disappearance\ \left(\frac{mg\ NH4 - N}{g\ VSS * day}\right) = \frac{\left(\frac{dC_{serum}}{dt} * 24\frac{hours}{day}\right)}{C_{VS}}$$

$$\frac{dC_{serum}}{dt} = Change\ in\ nutrient\ concentration\ in\ serum\ bottle\ over\ time\ reacted\ (\frac{mg}{L * hr})$$

From here, the serum bottle rates were standardized to incorporate genomic data. Real time PCR was conducted to quantify ammonium monooxygenase gene (amoA) copy numbers present in each DNA sample. AAs one copy of amoA is present in each AOB general, the number of amoA gene copy numbers directly represents the number of ammonia oxidizers in sediments. The following methodology was used to normalize rate data to amoA gene copy numbers for comparison purposes.

$$\frac{\#\ amoA\ Gene\ Copies}{mg\ VS} = \frac{\#\ amoA\ Gene\ Copies}{m_{DNA\ Ext} * \%TS * \%VS}$$

$\#\ AmoA\ Gene\ Copies = Number\ of\ AmoA\ copies\ reported\ using\ real\ time\ PCR$

$m_{DNA\ Ext} = Mass\ of\ sediment\ used\ in\ DNA\ Extraction$ (mg)

From here, the genomic data was incorporated into the nitrification serum bottle results to help explain the nutrient flux data from each site. Nitrification rates per amoA gene can be calculated for each site using the equations below. Similar strategy was used for denitrification rate data using nir gene.

$$\frac{mg\ NH4-N}{AmoA\ Copy * L\ * day} = \frac{(\frac{dC_{serum}}{dt} * 24\frac{hours}{day})}{m_{VS} * (\frac{\#\ AmoA\ Gene\ Copies}{mg\ VS})}$$

1.9 Molecular tools for the presence of other nitrogen cycling bacteria.

Both ammonia oxidizers and denitrifiers were targeted in this research. Table 1 presents details on biomarkers that were employed to profile these bacteria. DNA was extracted from 0.25–0.40 g sediments using a MO Bio Power Soil extraction kit, and concentrations were measured in ng/µl using a NanoDrop ND-1000 UV-Vis Spectrophotometer.

Quantitative PCR (q-PCR) was performed to quantify amoA and nirS genes. Each qPCR reaction contains 10 µL of 2×SYBR green master mix (Life Technologies), 1 µM of forward primer and 1 µM of reverse primer, 1 µL of BSA (0.1 mg/mL) and 1 µL of cDNA template (10 to 100 ng). The primer sequences and annealing temperatures used in qPCR are summarized in Table 1

Table 1: q-PCR primer and size for selected genes

Enzyme	Primer	Size, bp	Reference
Ammonium monooxygenase (AMO, α subunit) for **ammonia oxidizers**	F:GGGTTTCTACTGGTGGT R:CCCCTCKGSAAAGCCTTCTTC	491	Rotthauwe *et al.*, 1997
Heme containing nitrite reductase (NirS or cd_1NIR) for **denitrifiers**	Cd3a: AACGYSAAGGARACSGG R3cd: GASTTCGGRTGSGTCTTSAYGAA	425	Throbäck *et al.*, 2004

1.10 Nutrient flux experiments.

We installed square limnocorrals at three wetland sites in June and August to estimate nutrient flux and to record the response of the water column against spiked nutrients. The budget for this task was not included in this project. The strategy included installing the sediment (open at the bottom) and water column (i.e closed at the bottom) chambers in the morning session, monitor nutrient flux for 4 hours and then spike the chambers with low concentrations of ammonium, nitrate and phosphate and, monitor their fate for the next 4~5 hours.

Nutrient flux sampling involved visiting different sampling sites and installing limnocorrals to monitor nutrient changes throughout the day with the goal of determining how the nutrients interact with sediment. Four limnocorral chambers were used for each site- two water chambers and two sediment chambers. The water column chambers were filled with ambient water. A water pump was placed in each water column to mix the water before sampling and to use as an easy way to extract water samples. The sediment chambers were built and installed similarly, but with the exception that these chambers had no acrylic bottom and could be inserted directly into the sediment so that the ambient water was in contact with the wetland's sediment floor. Pumps for sediment columns were installed as to not disturb the sediment during mixing.

The columns were typically installed between 9-10 AM on sampling days and were sampled at 1-2 hour intervals- four samples over the course of four hours including a time zero sample were collected. After four hours of sample collection at varying time intervals, the water and sediment chambers were both spiked to add 0.5 mg/L NH_4-N, 0.5 mg/L NO_3-N, and 0.1 mg/L PO_4-P to observe any fluxes previously below detection limits and record the effects of raised nutrient concentrations in the wetlands. The spiked chambers were sampled over the same interval of four hours as well. The time of each sample was recorded in order to determine a concentration regression for flux calculations.

The sediment nutrient flux was determined by measuring concentration changes in the water column compared to concentration changes in water exposed to the sediments. The concentration changes in the water column were subtracted from the concentration changes in the sediment column to calculate sediment nutrient flux using the following equations:

$$WC_{light} = \frac{dC_{WC}}{dt}$$

WC_{light} = Water Column (WC) nutrient rate during daytime conditions ($g/m^3/d$)

dC_{WC} = Change of nutrient concentration in water column (mg/L)

dt = length of sampling event (day)

The sediment nutrient flux is calculated next by subtracting out the activity in the WC and normalizing the chamber working volume to the area of sediments enclosed in the chamber. Since the entire depth of the WC is used, the normalization factor becomes equal to the depth of the WC in meters. Note that dC/dt and WC_{light} are in the units mg/L/day and g/m^3/day, which are equivalent.

$$Sed_{flux} = \left(\frac{dC_{SD}}{dt} - WC_{light}\right) \times \frac{V}{A}$$

Sed_{flux} = Sediment nutrient flux during daytime conditions ($g/m^2/d$)

dC_{SD}/dt = Change of nutrient concentration in sediment column (mg/L/hr)

V= Volume of water within chamber, varies with depth (L)

A= Sediment surface area within the chamber (0.0645 m^2)

$$d = \frac{V}{A} \times \frac{m^3}{1000\ L}$$

d = depth of ambient WC (m)

Negative sediment flux for nutrients describes the sediment as a nutrient sink while positive sediment fluxes describe the sediment as a nutrient source. Due to low nutrient concentrations for many sites, only statistically significant concentration change rates were used to determine sediment fluxes- no flux results for a site indicates no detectable, statistically significant changes in concentration are occurring.

2.0 RESULTS AND DISCUSSION

2.1 Nitrification Potential

Figure 2 shows the results of nitrification using the sediments from three sites along the Jordan River. The graphs show that ammonia decreased over time, while an increase in nitrate was recorded. In general, nitrite accumulation was not observed, signifying complete nitrification to nitrate. Over the duration of the experiment (25 hours), NH_4^+-N concentration decreased from 2.5 to 0.2 mg/L for LNP, from 1.5 to 0.3 mg/L for Center Street and from 1.8 to 0.8 mg/L for the 1300 S site respectively.

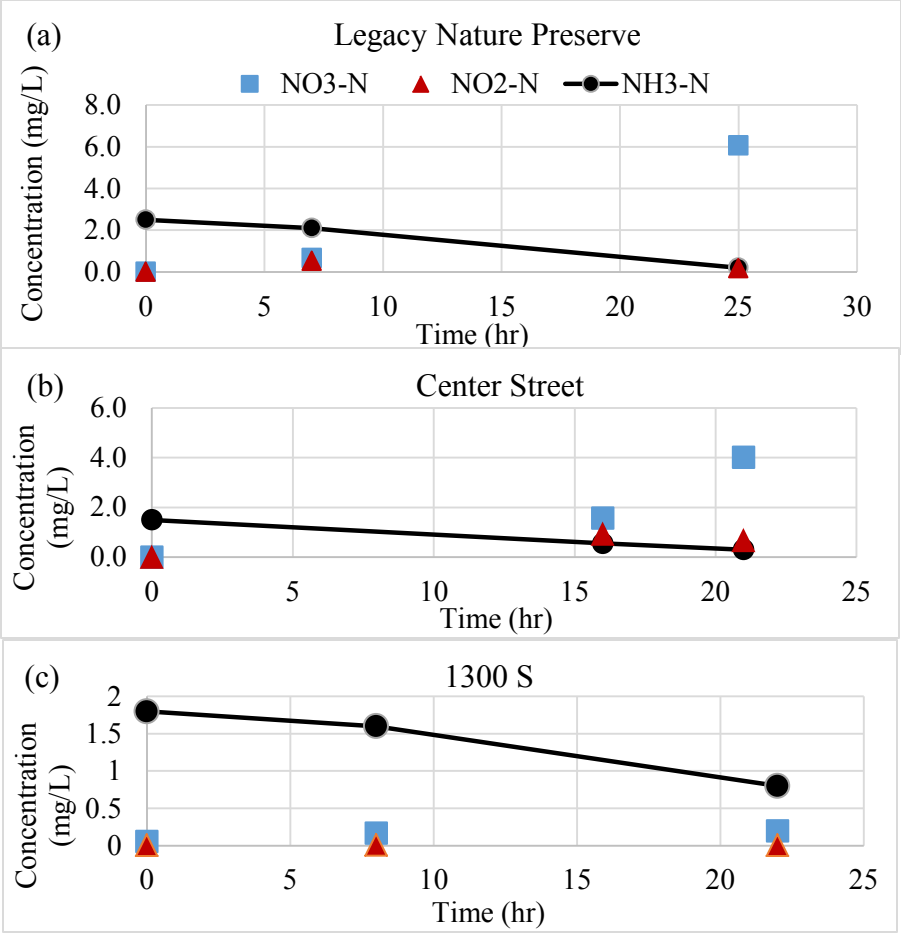

Figure 2: Results showing nitrification for (a) Legacy Nature Preserve, (b) Center Street and (c) 1300 S

The corresponding increases in NO_3^--N concentrations were 0 to 6.1 mg/L for LNP, from 0 to 4.0 mg/L for Center Street and from 0.06 to 0.2 mg/L for the 1300 S site respectively. The increases in NO_3^--N concentrations were nonstoichiometric, especially for the LNP and Center Street sites. Ammonium, being a cation, can be absorbed by the negatively-charged soil colloids. It is possible that the sorbed ammonium ions were released into the solution during the later hours of the experiments and were nitrified, thus enabling higher concentrations of nitrate. As a negative control, a known nitrification inhibitor, allylthiourea, was used. In the negative control, the concentration of NH_4^+-N did not change over the period of the experiment, indicating that the loss of ammonium in the experimental serum bottles was primary due to biological activity. Furthermore, the pH of the mixed slurry in all experimental and negative control bottles was close to neutral. Hence, the formation of free ammonia can also be neglected for all practical purposes. Nitrification rates in terms of mg-N/g VSS/day for the Center Street and 1300 S sites were 0.251 and 0.178 respectively. The same rate for the LNP site was 0.468 mg-N/g VSS/day, which is almost two orders of magnitude higher than the rates for the other two sites.

Ammonia oxidizers are responsible for the oxidation of NH_4^+-N to nitrite, which in turn is oxidized to nitrate by nitrite oxidizers. The functional gene responsible for this NH_4^+-N oxidation to nitrite is called ammonia monooxygenase (amoA gene). To further confirm the presence of nitrification, the amoA gene was targeted. Furthermore, to compare between the different sites, the amoA gene was also quantified in the river sediments using the advanced quantitative polymerase chain reaction (qPCR) technique. Figure 3 shows amoA gene copy numbers normalized to mg of sediments for all three sampled sites.

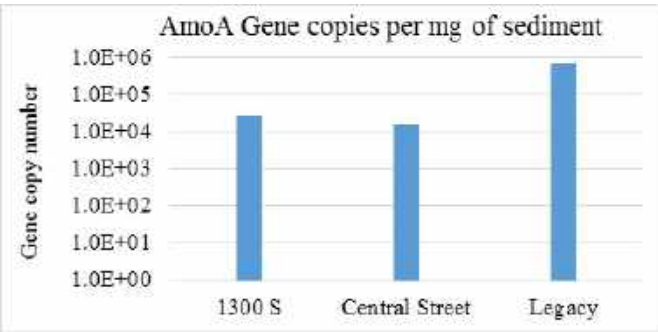

Figure 3: AmoA gene copy numbers obtained from qPCR for the Jordan River sediments

It is clear from Figure 3 that the number of amoA gene copies in the sediments for the 1300 S and Center Street sites was almost identical which agrees with the similar nitrification rates that were recorded for these two sites. However, the amoA gene copy number, and thus the number of ammonia oxidizers, at the LNP site was almost one order of magnitude higher than the copy numbers for the other two sites. This coincides well with the nitrification rates in which a much higher nitrification rate for the LNP site was estimated.

Figure 4 shows the results of nitrification using the sediments from three GSL wetlands sites (Turpin, Bear River unit 5 and Ambassador. All three sites showed active nitrification. The sediments from Turpin and Ambassador were spiked with higher ammonium nitrogen concentration in the range of 2.5 mg/L whereas the sediments from the Bear River were subjected to low concentration. It was due to miscommunication between two students working on the project. Nevertheless, the results show active nitrification for all three sites. Based on the VS data and the kinetic rates, the specific nitrification rates in terms of mg-N/g VS/day for Turpin, Bear River and Ambassador were 0.261, 0.299 and 0.251 respectively. Hence, Bear River site enabled the highest specific nitrification rate. It is also noticeable that, the net decreases in ammonium nitrogen concentration for all three sites were not completely associated with corresponding increases in nitrite and nitrate nitrogen concentrations and perhaps, this was due to simultaneously denitrification in the sediments even if the sediments were aerobic because some micro-anoxic zones still existed in the sediments.

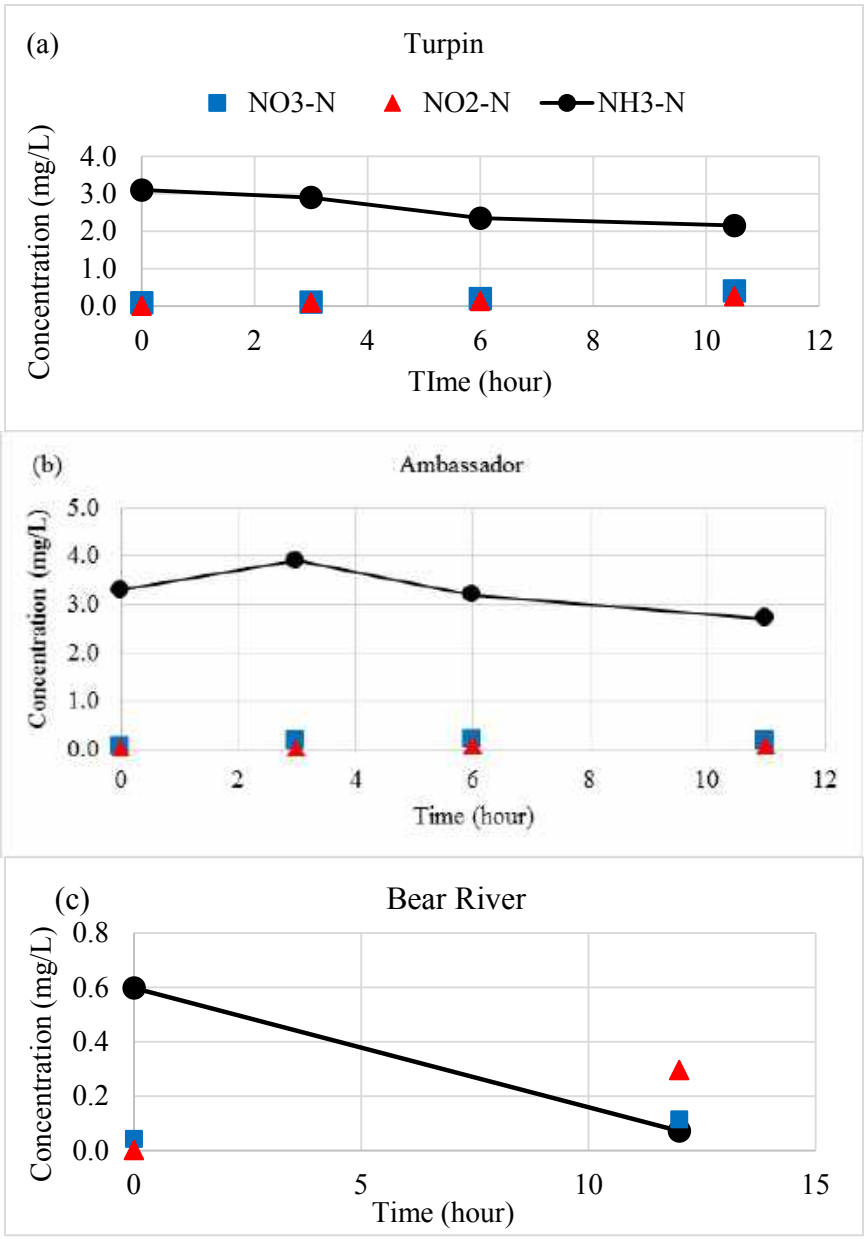

Figure 4: Nitrification experiment results for (a) Turpin, (b) Ambassador and (c) Bear River Unit 5,

Denitrification Potential

2.2.1 Jordan River Sites

Experiments were conducted with and without organic carbon (acetate) added. The sediment slurry samples were spiked with known concentrations of NO_3^-N. Figure 5 shows plots of different nitrogen

species measured during the denitrification serum bottle tests for the three Jordan River sites without a carbon source added.

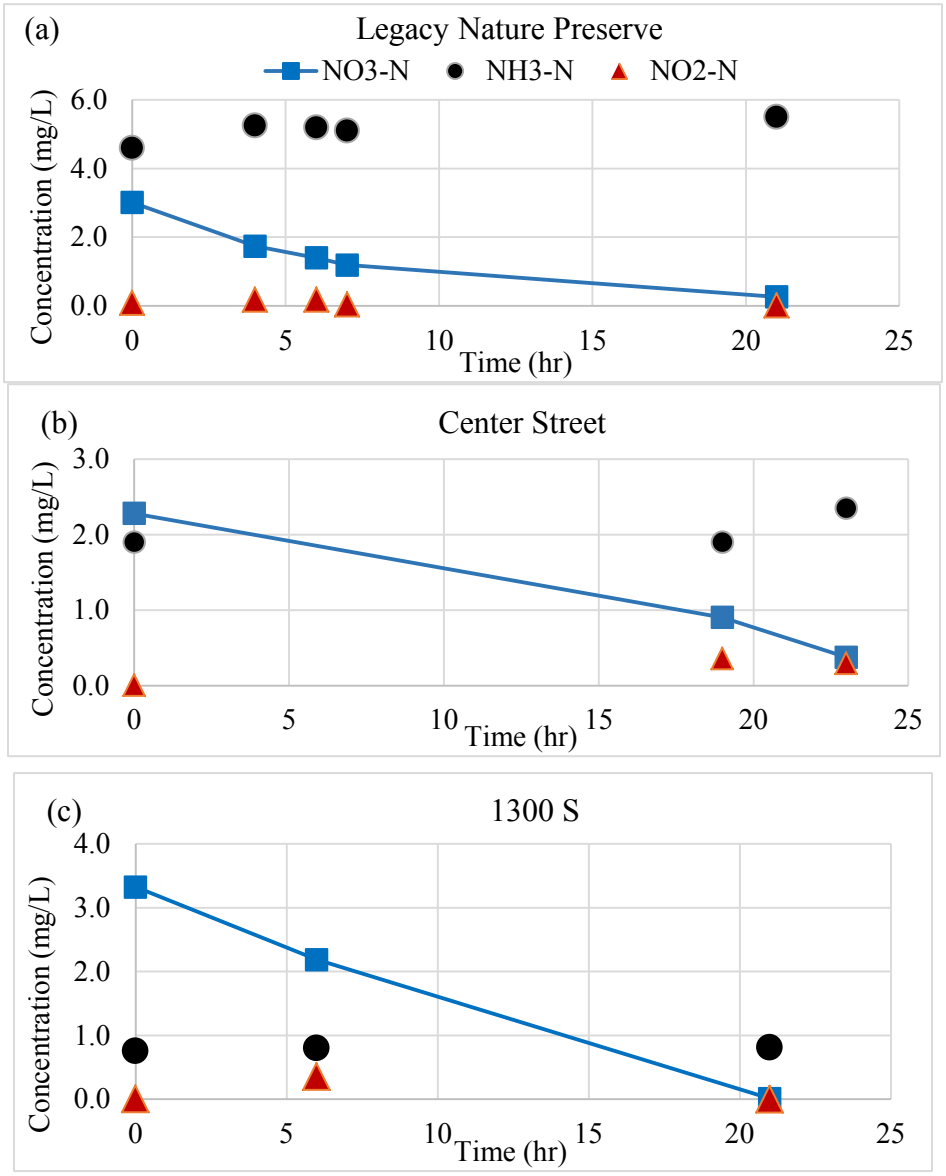

Figure 5: Results showing denitrification using sediments from (a) Legacy nature preserve, (b) Center Street and (c) 1300 S, Jordan River.

As evident from figure 5, NO_3^-N concentration decreased in all three batch tests corresponding to different sites. The decreases in NO_3^--N concentrations were 3.0 to 0.26 mg/L for LNP, from 2.3 to 0.37 mg/L for Center Street and from 3.3 to 0.01 mg/L for the 1300 S site respectively, representing significant denitrification activities in the sediments. NO_2^-N concentrations in all three batch experiments were fairly constant, denoting complete denitrification. Furthermore, except for the Center Street site, the

NH_4^+-N concentrations in other two batches were also fairly constant, hence ruling out the possibility of nitrate conversion to ammonium through dissimilatory nitrate reduction to ammonium (DNRA). For the Center Street site, an increase in NH_4^+-N concentration was observed beyond 20 hours which could be due to release of ammonium from sediments as a result of decay processes and/or DNRA.

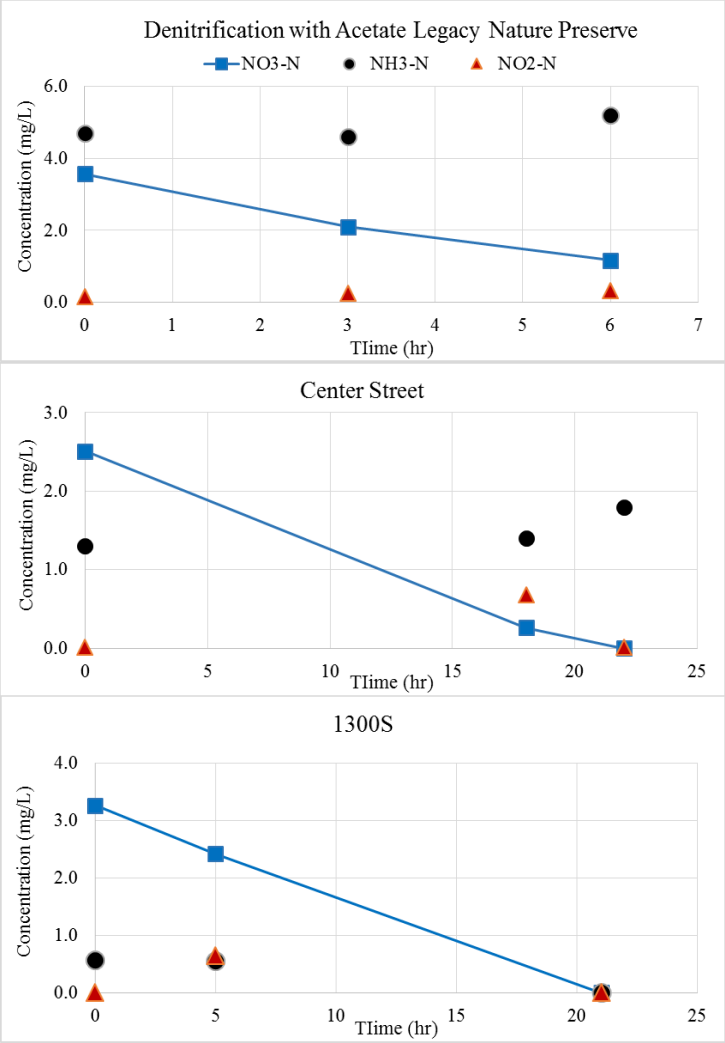

Figure 6 shows denitrification kinetics for all three river sites when experiments were conducted with an external carbon source added to the serum bottles. Except for the LNP site, the addition of acetate did not make much difference in denitrification kinetics. However, for the LNP site, denitrification was significantly enhanced by the addition of acetate. For the Center Street and 1300 S sites, the denitrification rates were 0.847 and 0.713 mg-N/g VS/day respectively without acetate added and were 1.10 and 0.734 mg-N/g VS/day respectively with acetate added. On the other hand, for the LNP site, the denitrification rate increased from 1.092 to 2.11 mg-N/g VS/day in the batch without acetate to the batch with acetate.

Figure 6: Results showing denitrification with added carbon source

The second step of denitrification, which is nitrite reduction to nitric oxide is mediated by the enzyme nitrite reductase (nirS). We estimated the nirS gene copy numbers for all three sites in the Jordan River. The nirS gene copy numbers for 1300 S, Center Street, and LNP sites were 8.84×10^5, $7.5 \times 10^5$and, 1.12×10^7 respectively. Looking at the nirS gene copy numbers, it is not surprising to observe higher denitrification rates for the LNP site especially with supplemented carbon source.

2.2.2 Wetland Sites

Figure 7 shows denitrification kinetics for all three wetland sites without carbon source added. Surprisingly, all three wetland sites showed faster denitrification kinetics as compared to all three Jordan River Sites. The denitrification rates in terms of mg-N/g VS/day for Turpin, Ambassador, and Bear River site were 1.35, 2.40, and 0.313 respectively.

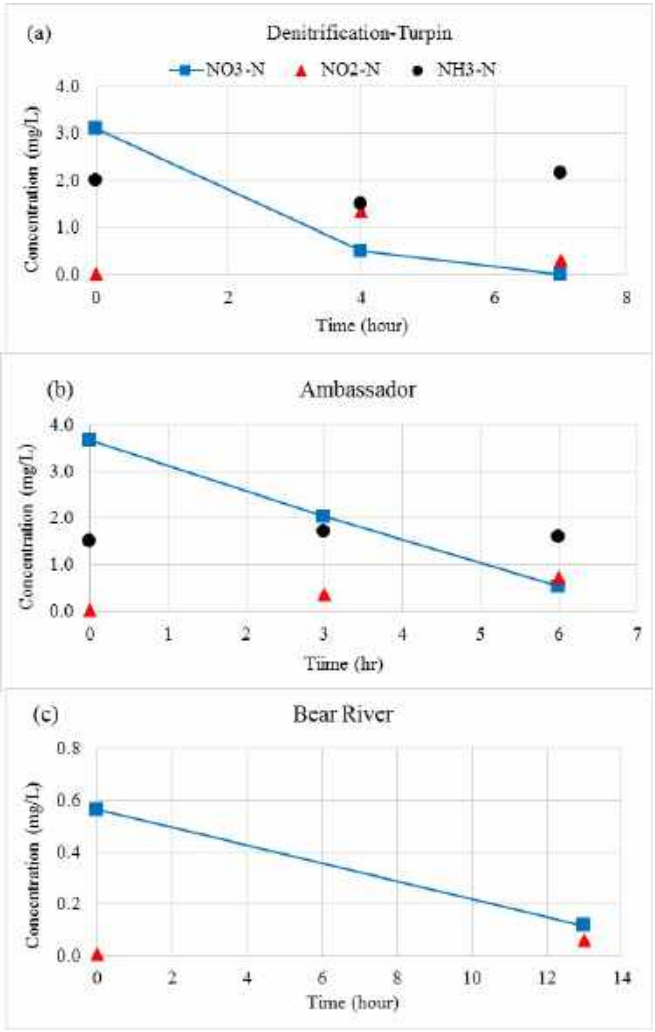

Figure 7: Results showing denitrification without added carbon source

Ammonia nitrogen concentration in denitrification serum bottles were fairly constant demonstrating the denitrified nitrate did not go to ammonium through DNRA. Furthermore, slight or no nitrite accumulation was observed in serum bottles indicating nitrate reduction did not stop at nitrite and proceeded further.

Denitrification tests were also conducted with an added readily biodegradable carbon source for denitrifiers. The addition of acetate significantly enhanced denitrification rates to 1.87 and 4.56 for Turpin and Ambassador, respectively. Bear River Site displayed a rate of 0.242 mg-N/g VS/day, indicating that denitrification rates did not increase with added acetate (graphs not shown).

In summary, the following conclusions can be made from the data for the river and wetlands sites in regard to nitrification and denitrification.

1. All tested river sites showed strong possibility of nitrification and denitrification potential with the LNP site showing the most promise.
2. The nitrification and denitrification rate data was well supported with the functional gene copy numbers.
3. The rate data along with the functional gene copy numbers can easily be used to model ammonia and nitrate dynamics in the Jordan River. However, similar data from more sites will be needed.

3.0 Nutrient fluxes from Wetland sediments

Nutrient flux using in-situ chambers were evaluated at three wetland sites under two conditions; (1) under ambient conditions and, (2) under nutrient-spiked conditions. Furthermore, sampling was performed in early summer (May, 2014) and late summer/early fall (August, 2014) to evaluate seasonal effects on nutrient fluxes. Table 2 depicts the concentrations of major nitrogen and phosphorus ions in pore water. The general trend was that the pore water concentrations increased from May to August for all three ions measured. This was perhaps due to decay activities which generally take place in sediments and, in fact, becomes significant in later summer. Furthermore, the Ambassador site in general showed higher concentrations of ammonium, nitrate, and phosphate.

Table 2: Pore water nutrient concentrations

	NH_4-N, mg/L		NO_3-N, mg/L		PO_4-P, mg/L	
	May	August	May	August	May	August
Bear	1.63	2.71	0.46	0.36	1.4	0.587
Turpin	1.56	3.25	0.79	0.49	0.331	0.421
Ambassador	2.12	9.32	0.32	0.39	2.6	4.39

3.1 Nutrient fluxes

NH4-N fluxes in g/m2/day				
	May		August	
	Non-spike	Spiked	Non-spike	Spiked
Bear River	ND	0.013	ND	-0.148
Turpin	ND	-0.199	0.122	-0.055
Ambassador	0.062	0.045	0.083	0.133

Table 3: NH4-N fluxes at all wetland sites. All flux values are reported in terms of g/m2/day based on the area covered by the sediment chamber base. Table 3 shows ammonium nitrogen fluxes under spiked and unspiked conditions for May and August sampling events. The positive values denote flux from sediments to the water column and the negative values represent the opposite. For the Bear River, the May and August fluxes under unspiked conditions were negligible. For the ambassador site, sediments contributed to ammonium to the water column under all conditions as evident by positive flux values. For Turpin site, May unspiked sampling event enabled negligible flux and a high positive ammonium nitrogen flux was recorded under unspiked condition during August sampling. This could perhaps be due to diagenesis activities that start in sediments in Fall leading to nutrient release from biomass to the surroundings. For the same site, i.e. Turpin, both May and August fluxes under spiked conditions were negative representing sink of ammonium to sediments. The Bear River wetland site enabled positive flux in May and a high negative flux in August under spiked conditions.

Table 4: Nitrate and phosphate fluxes at the sampled wetland sites in May and August

PO4-P fluxes in g/m2/day				
	May		August	
	Non-spike	Spiked	Non-spike	Spiked
Bear River	ND	-0.048	0.015	0.03
Turpin	-0.043	-0.069	-0.063	-0.127
Ambassador	ND	-0.055	ND	-0.122

NO3-N fluxes in g/m2/day				
	May		August	
	Non-spike	Spiked	Non-spike	Spiked
Bear River	ND	-0.182	ND	0.051
Turpin	ND	-0.182	ND	-0.163
Ambassador	ND	-0.276	0.026	-0.089

Table 4 shows nitrate nitrogen and phosphorus fluxes under spiked and unspiked conditions for sampling conducted in May and August. Except for August sampling for the Bear River site in which case a positive flux of nitrate nitrogen was recorded under both conditions, sediments consumed nitrate resulting in negative fluxes of nitrate nitrogen in all other cases. In our experiments, chambers were installed in sediments with minimum or no submerged vegetation. Hence, nitrate consumption by SAV can be neglected. The serum bottle tests with sediments collected from all these three sites showed strong denitrification activities. Hence, it can be concluded that the negative fluxes of nitrate (i.e from water column to sediments) were perhaps due to continuous denitrification activity in sediments.

In case of phosphorus also, sediments served as sink. It is less likely that major biological activity, such as through polyphosphate accumulation in bacteria, would have contributed to phosphate sink in sediments. The likely reasons could be; (1) co-precipitation of phosphate with other metals ions during sampling but this needs to be verified by studying the chemistry of water column and biogeochemistry of top sediment layer and/or, (2) sorption of phosphate on suspended minerals followed by settling.

Conclusions

1. In general, sediments serve as a source of ammonium nitrogen but sink for nitrate and phosphate.
2. Biological activities, especially those mediated by bacteria, are one of the pathways through which nutrients display their fate in wetlands. However, evidence are strong that biological processes can sometime be major player and this fact should be incorporated into wetland management efforts.
3. To clearly illustrate the mechanisms related to the fate of nitrogen and phosphorus, a control volume approach incorporating lab scale stable isotope experiments would be needed.
4. Using the control volume approach listed above, a nutrient budget should be developed based on the hydrological model of the wetlands. For example, can we comfortably estimate the nutrient load a certain segment of GSL wetland can handle?

5. The efforts should also include characterizing sediments, for example their organic carbon contents, mineralogy and their potential to resuspend followed by settling.

Ongoing works/Future directions

- Molecular analyses -- PCR, qPCR, Terminal restriction fragment length polymorphism (TRFLP) for amoA, nirS, nirK will be done for all six sites
- Methane formation rates will be measured

Reference

- Arp D.J., Sayavedra-Soto L.A., Hommes N.G. 2002. Molecular biology and biochemistry of ammonia oxidation by Nitrosomonas europaea. Arch Microbiol, 178(4): 250-255.
- Cebron A, Berthe T, and Garnier J. 2003. Nitrification and Nitrifying Bacteria in the Lower Seine River and Estuary (France). Applied and Environmental Microbiology, 69(12): 7091–7100.
- Knowles R. 1982 (March). Denitrification. Microbiological Reviews, 46(1): 43-70.
- Rittmann, B.E., Perry, M.L., *Environmental Biotechnology: Principles and Applications.* McGraw-Hill.
- Zeglin L.H., Taylor A.E., and Bottomley P.J. 2011. Bacterial and archaeal amoA gene distribution covaries with soil nitrification properties across a range of land uses. Environmental Microbiology Reports, 3(6): 717–726.

An Ecological Assessment of the Jordan River: 2013-2018

Volume II

Biological Integrity

Prepared by

Theron Miller, PhD

WFWQC

And

David Richards, PhD

OreoHelix Ecological

Prepared for

Wasatch Front Water Quality Council

August 2019

Executive Summary

Introduction

The Jordan River, named after the biblical River Jordan, is a unique river that originates from shallow, highly-regulated Utah Lake, the last freshwater remnant of pluvial Lake Bonneville. It flows from the lake for approximately 51 miles as it is fed by numerous cold-water Wasatch Front Range tributaries until it ultimately nourishes several impounded and sheetflow wetlands reliant on its waters on the southern fringe of Farmington Bay, Great Salt Lake. The physical, chemical, and biological integrity of the Jordan River that make up its ecological integrity are intimately linked via feedback loops that do not act independently. It is now apparent to the Council that the river's ecological integrity has been debased.

In this volume, Volume II we present our research and findings on the biological integrity of the Jordan River. In Volume I, we presented research and findings on the physical and chemical integrity of the river.

Biological Integrity Research

Algal Assemblages

In addition to the extensive physical and chemical integrity-based research documented in Volume I, we also conducted the most comprehensive biological integrity research on the Jordan River, to date. Our focus was on algae and macroinvertebrates as they relate to water quality and ecosystem function.

In addition to the Rushforth and Rushforth (2009) and Miller (2009) algal assemblage analyses, additional algae assemblage analysis included the following study:

> In **Chapter 7: "Jordan River Phytoplankton Assemblages: Rushforth and Rushforth 2009 Data Revisited",** we revisited Rushforth and Rushforth (2009) and Miller (2009) reports and reanalyzed some of their data using several traditional statistical approaches, ecological indices, and multivariate community level models. Our results confirm that the phytoplankton assemblages significantly varied both spatially and temporally and that the source of phytoplankton in the river was primarily eutrophic Utah Lake in the Jordan River in 2009. Results of these analyses provide alternative interpretations of phytoplankton assemblages in the river and confirms our conclusion that the Jordan River cannot function properly due to major anthropogenic disturbances.

Macroinvertebrate Assemblages

Several Jordan River Assessment Units were designated impaired for Benthic-Macroinvertebrate Bioassessments, in the DWQ 2016 Integrated Report. This designation led us to evaluate macroinvertebrate bioassessment methods used for impairment listing, analyze existing macroinvertebrate data, and conduct additional macroinvertebrate studies. Several studies were conducted and are included in this volume:

In **Chapter 8: "Real and Perceived Macroinvertebrate Assemblage Variability in the Jordan River, UT can Affect Water Quality Assessments"** we showed that seasonality, field sampling error, subsampling, taxonomic resolution, and the river continuum can affect our understanding of macroinvertebrate assemblage relationships in the Jordan River and can confound generalized water quality assessment models and potentially lead to costly erroneous conclusions.

In **Chapter 9: "Is Reliance on a Single Bioassessment Metric for Assessing Water Quality in Utah's Rivers and Streams Prudent?"** we demonstrated that even though the RIVPACS O/E model exclusively relied upon by DWQ has the potential to be a useful summary metric, DWQ's dependence on this model as a stand-alone metric is not recommended. O/E models rely on far too many assumptions, constraints, and inherent errors that necessitates their inclusion into a more comprehensive and informative macroinvertebrate multimetric based program. In addition, it has been verified that the presently used O/E models are not relevant for evaluating benthic macroinvertebrate assemblage integrity in the Jordan River.

In **Chapter 10: "Jordan River Macroinvertebrate Assemblages: Preliminary Findings"**, we found that macroinvertebrate assemblage integrity in the Jordan River has suffered from severe bottlenecks and hysteresis; however, given the resilience of life to perturbation, several macroinvertebrate taxa have endured, including two invasive mollusks that now dominate the ecosystem. Those native and invasive taxa that remain are temperature, sediment, and organic pollution tolerant and are not likely negatively affected by nutrients.

In **Chapter 11: "Upper Jordan River Macroinvertebrate Assemblage"** our findings were both confirmatory and surprising: 1) Macroinvertebrate densities were abnormally low at most locations and do not reflect the amount of nutrients potentially available to the food web; 2) densities were greatest in stable, less- embedded but atypically uncommon cobble habitat; 3) the majority of habitat of the upper Jordan River has unstable very fine to small sized substrate which reduces invertebrate densities; and 4) the upper Jordan River is dominated by two highly invasive mollusk taxa, the New Zealand mudsnail and the Asian clam. These findings support our conclusion that the upper Jordan River is a severely impaired analog of its former self and for the most part is not much biologically different than the Surplus Canal.

In **Chapter 12: "A snail, a clam, and the River Jordan"** we showed that two invasive mollusks, the New Zealand mudsnail and the Asian clam are undoubtedly the most important and dominant biota in the now novel Jordan River ecosystem and together co-regulate: seasonal nitrogen, phosphorus, ammonia, and carbon cycling; SOD; microbial community structure; and stream metabolism. The snail and clam are almost certainly seasonally controlling most other ecosystem functions as well, (e.g. water quality) despite their roles being unnoticed to most researchers and managers.

New EPA ammonia criteria documents were released in 2013 that created more stringent ammonia criteria if native mussels were present in streams that contain elevated concentrations of ammonia. Yet, if these mussels weren't present, the ammonia criteria would be slightly relaxed. This resulted in several studies:

In **Chapter 13: "Apparent extinction of native mussels in Lower Mill Creek and Mid-Jordan River, UT."** we found that native mussels are likely extinct in the Jordan River and that ammonia criteria need to reflect these findings. Our report(s) and published results helped DWQ revise ammonia criteria for the Jordan River.

In **Chapter 14: "Numeric Water Quality Criteria Recalculation for Several Toxicants Related to Central Valley Water Reclamation Facility Discharge into Mill Creek, Salt Lake County, UT. Part 1: Ammonia",** we recalculated ammonia criteria for Mill Creek and lower Jordan River based on taxa that were expected to occur in these waters according to EPA guidelines.

Fisheries Studies

We are also conducting the most comprehensive fish surveys in the Jordan River in the last twenty years and will relate our findings to the river's ecological integrity, particularly in relation to temperature, dissolved oxygen, ammonia, and macroinvertebrates, and more relevantly to the Council and DWQ water quality standards.

Chapter 7

Jordan River Phytoplankton Assemblages: Rushforth and Rushforth 2009 Data Revisited

By:

David C. Richards, Ph.D.

OreoHelix Ecological

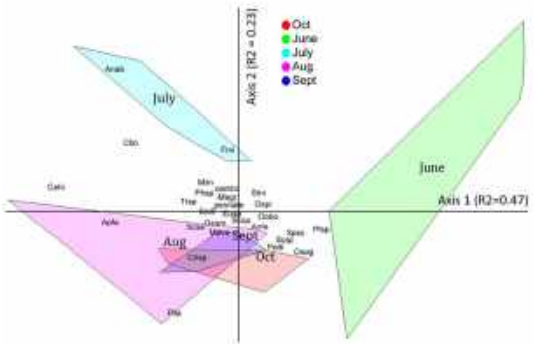

Summary

The Jordan River often has very high densities of transient phytoplankton that makes it an atypical mid-order river in the western USA. Rushforth and Rushforth (2009) and Miller (2009) conducted the most comprehensive analysis of phytoplankton assemblages in the Jordan River, to date. However, they provided no traditional statistical analysis or assemblage level statistical analysis of their data that would help verify and solidify their conclusions or to provide further insights. We revisited Rushforth and Rushforth (2009) and Miller (2009) reports and reanalyzed some of their data using several traditional statistical approaches, ecological indices, and multivariate community level models. Our results confirm that the phytoplankton assemblages significantly varied both spatially and temporally and that the source of phytoplankton in the river was primarily eutrophic Utah Lake in the Jordan River in 2009. Results of these analyses provide alternative interpretations of phytoplankton assemblages in the river and confirms our conclusion that the Jordan River cannot function properly due to major anthropogenic disturbances.

TABLE OF CONTENTS

List of Figures

List of Tables

List of Appendices

Introduction

Phytoplankton assemblages in the Jordan River are atypical. Most mid-order rivers in the world characteristically have no or very few resident planktonic primary producers due to constant downstream flows that preclude their establishment because they are unable to swim against the current. Exceptions are rivers that have upstream water sources with long enough retention times that allow phytoplankton assemblages to develop and flourish, which then can be passively transported downstream. One such source is Utah Lake.

Utah Lake is a very large, ≈ 100,000-acre, shallow, desert, lake and is a small remnant of ancient Lake Bonneville. Utah Lake is nutrient rich from natural geologic sources that have accumulated over the millennia and from more recent geologic times, anthropogenic sources. The lake is a highly regulated analog of its past and has undergone catastrophic ecosystem shifts and hysteresis (Richards and Miller 2017). These conditions are ideal for phytoplankton growth and periodic blooms. Utah Lake is the source and primary contributor of the Jordan River. Consequently, Rushforth and Rushforth (2009) and Miller (2009) concluded that phytoplankton assemblages in the Jordan River originate almost exclusively in Utah Lake.

The Jordan River is also nutrient rich and shallow, has undergone ecosystem shifts and is highly impaired (Richards 2018a). Because it receives ample solar radiation that can penetrate even to its deepest pools (i.e. photic or compensation zone), the river should have very high levels of autochthonous primary production. Autochthonous primary production in rivers typically occurs in the form of attached benthic algae (periphyton), aquatic vegetation (macrophytes), or from decomposition of allochthonous organic matter that originated from outside of the river. However, periphyton and macrophytes are uncommon in the Jordan River. For much of its length, the river has unstable substrates composed of shifting fines, sands, and gravels that do not allow long term attachment of periphyton or macrophytes (Miller 2009). Thus, understanding the Jordan River's atypical phytoplankton assemblages as a component of its primary production is extremely important to our understanding of its ecology and how phytoplankton assemblages relate to water quality.

Justification

Rushforth and Rushforth (2009) and Miller (2009) conducted the most extensive surveys of phytoplankton in the Jordan River, to date. They provided great insights into autecological phytoplankton taxa distribution and abundances in the river, which contributed greatly to our knowledge of the ecology of the Jordan River. However, they did not incorporate statistical tests to help verify their conclusions, nor did they analyze their data from a synecological assemblage (community) perspective. In this chapter, we statistically re-examine Rushforth and Rushforth (2009) data and then conduct additional synecological assemblage analyses to help supplement and increase our knowledge of phytoplankton in the Jordan River.

Methods

We transcribed data from Rushforth and Rushforth (2009) appendices into Excel spreadsheets and then filtered and prepared these data for statistical analysis. Rushforth and Rushforth (2009) locations were not georeferenced in their report, therefore, we approximated latitude and longitude from site descriptions. Sample site locations are presented in Figure 1. We only used data that were collected from the Jordan River or State Canal and omitted samples from Little Cottonwood Creek, Mill Creek, and Surplus Canal from this analysis. Rushforth and Rushforth (2009) collected samples on a monthly basis from June through October 2009. Therefore, we considered seasonal comparisons and contrasts based on months to be valid because samples were collected on a mostly uniform schedule (≈ 30 days in between sampling events). Spatial and temporal statistical analyses included: nonparametric k-sample equality of medians tests; linear regression; multivariate community ecology analysis including non-metric multidimensional scaling (NMS), multiple response permutation procedure (MRPP), and indicator species analysis (ISA). We also calculated several richness and diversity indices for statistical comparisons including; taxa richness (S); effective number of taxa (ENT); evenness (E), and Shannon's (H) and Simpson's (D) diversity. We developed box plots and used non-parametric tests using medians and percentiles instead of means and confidence intervals because much of the data were not normally distributed, fractional, and/or zero truncated for all single variate analyses, although we $\log_{10}$ transformed abundances (biovolume) (μ^3 cells ml^{-1}) to conduct linear regressions of abundances vs. distances downstream. We used latitude values as a surrogate for distance downstream from Utah Lake. All statistics were conducted using Stata 15.1 (StataCorp 2018) and PC-ORD 7.1 (McCune and Mefford 2018).

Figure 1. General locations (black circles) of phytoplankton samples from Rushforth (2009) reanalyzed in this chapter.

Results

A total of forty-four phytoplankton taxa were observed from the Rushforth and Rushforth (2009) samples that we reanalyzed. Species area curve estimates predicted that at least 50 taxa (Chao2 bias corrected method (McCune and Mefford 2018)) and as many as 56 taxa (second-order jackknife estimate (McCune and Mefford 2018)) may have occurred in the Jordan River during sampling periods in 2009.

Seasonal Trends

Phytoplankton abundances, richness, and diversity differed seasonally. The following sections illustrate these seasonal differences and similarities. Equality of medians tests for differences in monthly abundances, richness, and diversity analysis are in

Appendix 1.

Abundance (biovolume)

Phytoplankton abundance (biovolume) (μ^3 cells ml^{-1}) was by far much greater in July than the other months (Figure 2). June and October on the other hand, had significantly lower abundances than the median (Figure 2).

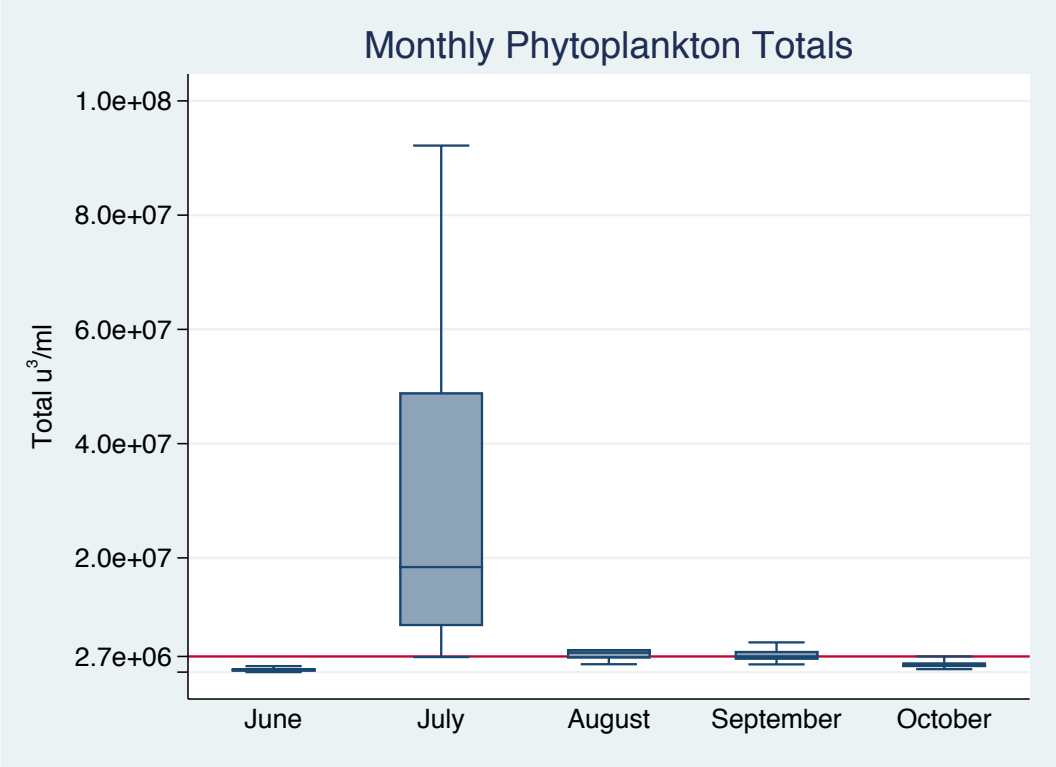

Figure 2. Jordan River monthly biovolume (abundance μ^3 cells ml^{-1}). Red line = median biovolume = 2,743,210 μ^3 cells ml^{-1}. Boxes are 25th to 75th percentiles; solid line in boxes = median; error bars = upper and lower quartiles ± 1.5 inter quartile range; and circles = outliers.

Phytoplankton Richness and Diversity

There was very low monthly (β)richness and diversity in the phytoplankton assemblages in the Jordan River (Figure 3 and Figure 4). The mean number of taxa was 8.95 (std err. = 0.35), while the mean effective number of taxa (ENT) was only 2.6 (std. err. = 0.35). June had below median taxa richness but about median ENT (Figure 3). July had above median richness but contrarily, the lowest median ENT (Figure 3), due to greater abundances (Figure 2) and dominance of a few cyanophytes. August had above median richness and ENT (Figure 3). September had the greatest richness and ENT (Figure 3), despite having median abundances (Figure 2). October had the fewest taxa and below median ENT (Figure 3), primarily because it had below median abundances (Figure 2). July had the fewest ENT (Figure 3).

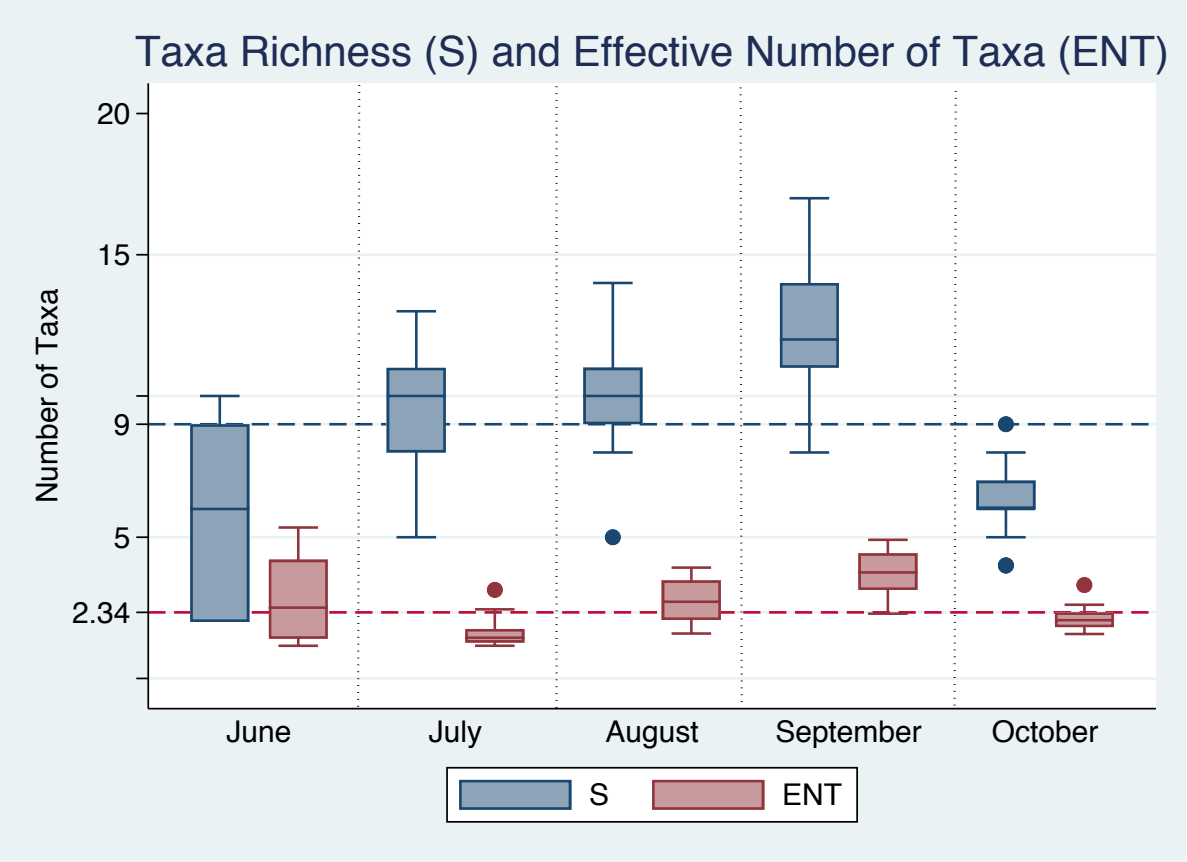

Figure 3. Monthly differences in taxa richness (S) and effective number of taxa (ENT). Red dashed line = median S = 9; blue dashed line = ENT = 2.34. Boxes are 25th to 75th percentiles; solid line in boxes = median; error bars = upper and lower quartiles ± 1.5 inter quartile range; and circles = outliers.

Phytoplankton Diversity

July assemblages were significantly less diverse than the other four months using all three indices (Figure 4). July was when the cyanophyte blooms occurred in Utah Lake and dominated Jordan River water downstream and when total phytoplankton biovolumes were orders of magnitude greater than other months (Figure 2).

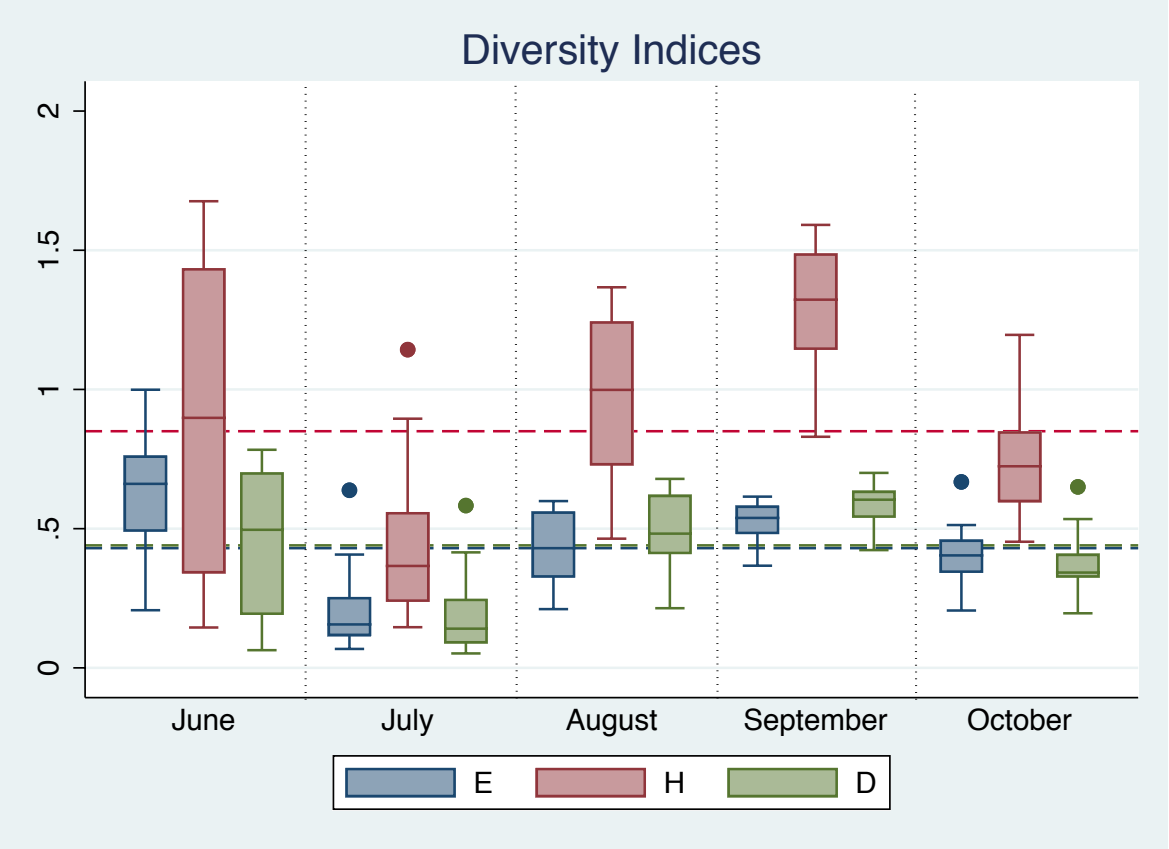

Figure 4. Monthly differences in three diversity indices; Evenness (E), Shannon Diversity (H), and Simpson Diversity (D). Red dashed line = median H = 0.85; blue dashed line = median E = 0.43; green dashed line = median D = 0.44. Boxes are 25th to 75th percentiles; solid line in boxes = median; error bars = upper and lower quartiles $\pm$ 1.5 inter quartile range; and circles = outliers.

Algal Abundance vs. Distance Downstream from Utah Lake

Total cell counts (μ^3 cells ml^{-1}) ($\log_{10}$ transformed) significantly decreased from Utah Lake outlet downstream during each month, except in June (Figure 5 and Table 1). See Appendix 5 for full regression results.

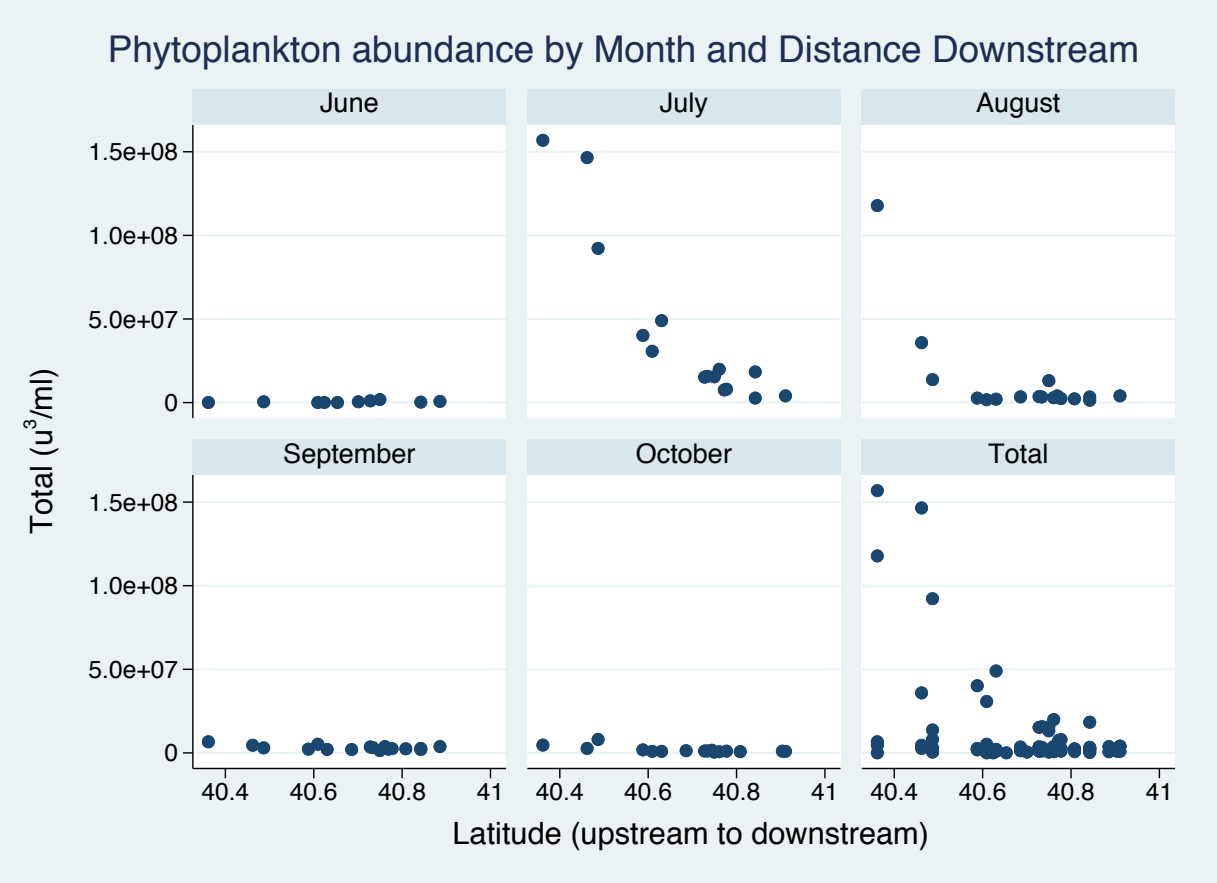

Figure 5. Monthly relationships between total phytoplankton cells ((μ^3 cells ml^{-1}) and distance downstream (latitude).

Table 1. Linear regression results of total cell counts (μ^3 cells ml^{-1}) (log_{10}) vs latitude (distance downstream). See Appendix 5 for full regression results.

Month	R^2	p-value
June	0.32	0.09
July	0.86	< 0.01
August	0.50	< 0.01
September	0.26	0.04
October	0.60	< 0.01

These regression results support Rushforth (2009) and Miller (year) conclusions that much of the phytoplankton in the Jordan River is transient and originates in Utah Lake starting in July and going

through at least October, even though phytoplankton biovolume was much less, and had greater ENT and diversity in August, September and October than July (Figure 2).

Jordan River Phytoplankton Assemblages

Jordan River phytoplankton taxa may not function independently from other taxa in the assemblage. Therefore, ecological analyses of assemblages were conducted to better understand relationships between entire assemblages and their environment. Cluster analysis were initially used to help determine dis(similarities) among samples. The cluster analysis of samples coded by month is in Appendix 3.

Non-Metric Multidimensional Scaling (NMS)

After exploring a dozen or so NMS models using different transformations, distance measures, and removal of individual taxa that had very low occurrences, we decided on a best fit model. The final two-dimensional model using a Sorenson-Bray distance measure had a very good final stress of 9.85 (final instability < 0.00001; number of iterations = 77; Axis 1 R^2 = 0.47; axis 2 R^2 = 0.23). Additional statistical measures of fit for NMS model are in Appendix 6. Because the final stress = 9.85 there was little chance of misinterpreting the ordination of samples and taxa (McCune and Mefford 2018).

Seventeen taxa that had < 5 taxa per sample were removed from the NMS analyses. This helped improve the ordination[1]. The final NMS model used 75 sites and 28 taxa. The seventeen taxa that were removed from the final model were:

Actinastrum species,

Ankistrodesmus convolutes,

Asterionella formosa,

Cosmarium species,

Crucigenia irregularis,

Crucigenia rectangularis,

Dinobryon divergens,

Fragilaria crotonensis,

Gomphosphaeria species,

[1] There is always a trade-off when deleting rare and uncommon taxa from multivariate analyses. The rare and uncommon taxa that were removed from the final multivariate models, although not highly influential in assemblage analyses, may be important when examining other ecological or water quality effects in the future.

Lyngbya birgei,

Merismopedia species,

Pandorina morum,

Scenedesmus bijuga,

Scenedesmus species,

Staurastrum species,

Stigeoclonium polymorphum, and

Tabellaria fenestrata.

NMS results showed that phytoplankton assemblages were significantly different between all months. June assemblages were highly variable and assemblages in the lower sections of the river significantly differed from assemblages in the upper sections. July and August upstream assemblages also differed from downstream assemblages and were more variable than mostly homogenous September and October assemblages did not differ much spatially. (Figure 6; Figure 7). Sample label codes are in Appendix 9

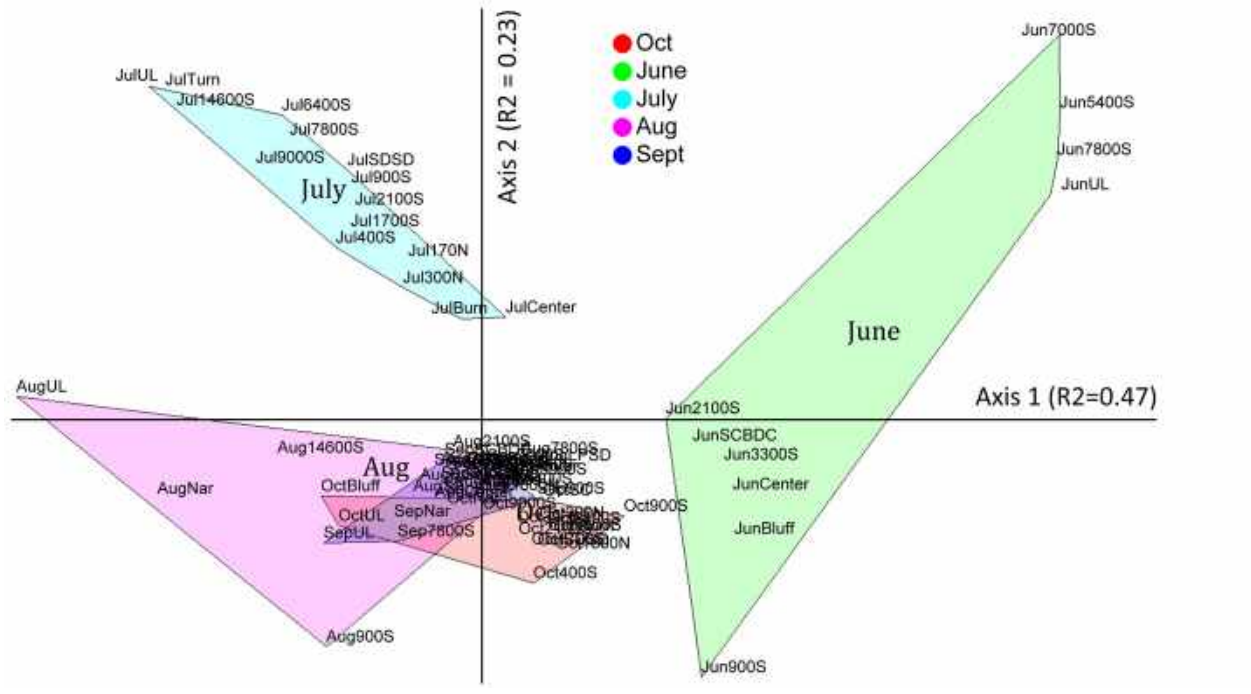

Figure 6. Axis 1 and Axis 2 of best fit Non-Metric Multidimensional Scaling (NMS) ordination of phytoplankton assemblages in the Jordan River showing dis(similarities) by months and location. Upstream assemblages separated farthest away from the center (origin) of the ordination, while downstream assemblages tended to ordinate towards the center. This was most apparent for June, July and August assemblages. September and October assemblages were very similar and showed very little spatial variability. Labels are coded with month first, then location (see Appendix 9).

Several individual phytoplankton differed in their abundances both spatially and temporally, while other taxa were more ubiquitous (Figure 7).

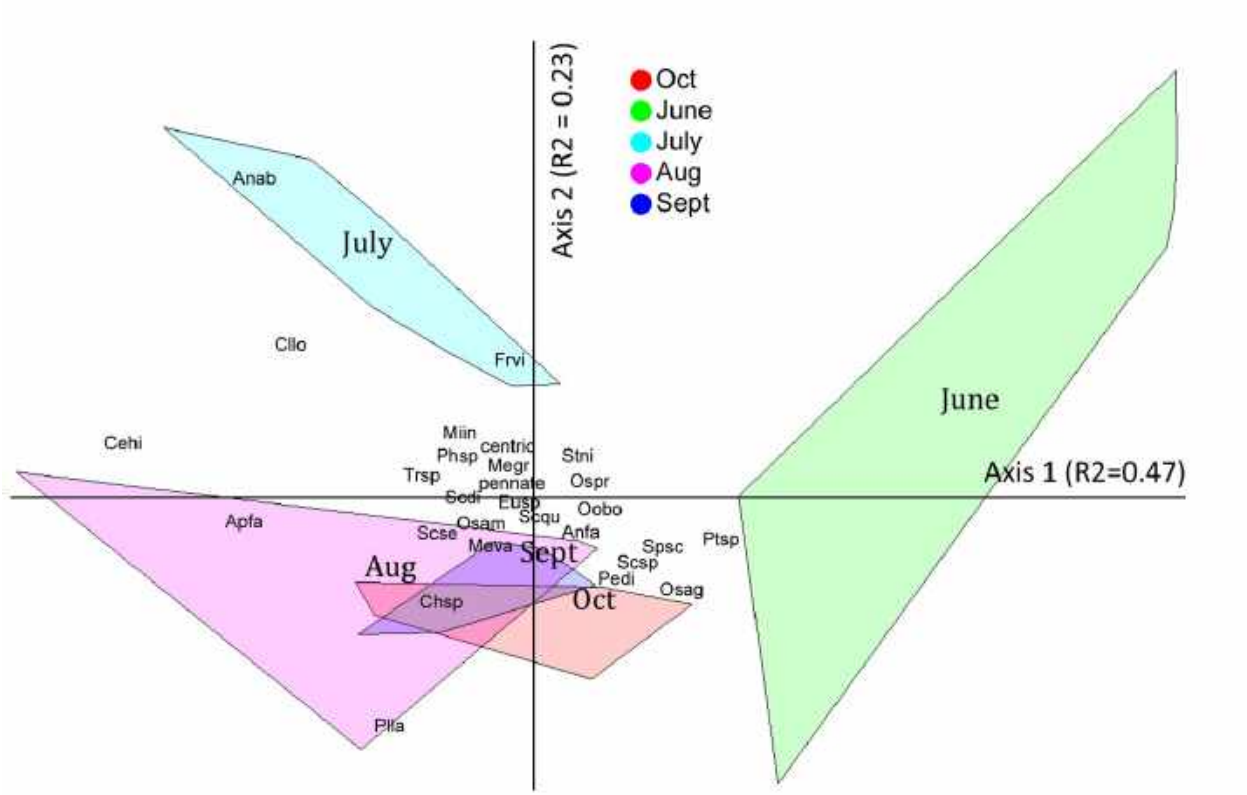

Figure 7. Axis 1 and Axis 2 of NMS showing taxa dis(similarities). See Appendix 2 for taxa codes and Figure 8 for ordination of cyanophytes.

Multiple response permutation procedure (MRPP)

Multiple response permutation procedure (MRPP) results supported NMS results and showed that Jordan River phytoplankton assemblages significantly differed between months, including significant difference between September and October that were not readily apparent in NMS ordination (A = 0.288; P < 0.001; Table 2).

Table 2. MRPP pairwise comparisons of phytoplankton assemblages between months.

Compared			*T*	*A*	P-value
July	vs.	August	-17.40	0.25	> 0.01
July	vs.	September	-20.05	0.34	> 0.01
July	vs.	October	-18.91	0.34	> 0.01
July	vs.	June	-11.16	0.18	> 0.01

August	vs.	September	-1.73	0.02	0.06
August	vs.	October	-8.81	0.11	> 0.01
August	vs.	June	-11.19	0.15	> 0.01
September	vs.	October	-9.88	0.14	> 0.01
September	vs.	June	-14.90	0.21	> 0.01
October	vs.	June	-12.67	0.20	> 0.01

Indicator Species Analysis

It was not difficult to find significant monthly indicator taxa, since entire phytoplankton assemblages differed by month (see NMS and MRPP results above). The only month that we could not find significant indicator taxa was October. Table 3 lists the significant indicator taxa for June, July, August, and September. Appendix 7 has values for all taxa including non-significant indicators.

Table 3. Significant monthly phytoplankton indicators in the Jordan River, 2009. P values < 0.06 were considered significant.

June

Taxon	IV	Mean	Std dev	P
Pteromonas species	35.1	11.6	5.68	< 0.01
Scenedesmus species	14.1	7.3	4.01	0.04

July

Taxon	IV	Mean	Std dev	P
Anabaena spiroides	98.6	25.4	7.61	< 0.01
Centric diatoms	38.8	26.2	3.30	< 0.01

August

Taxon	IV	Mean	Std dev	P

Chlamydomonas species	54.5	16.7	4.84	< 0.01
Melosira varians	42.2	24.1	4.64	< 0.01
Pennate diatoms	32.7	24.2	2.33	< 0.01
Aphanizomenon flos-aquae	67.9	44.0	7.34	< 0.01
Melosira granulata	30.1	17.6	4.14	0.01

September

Taxon	IV	Mean	Std dev	P
Scenedesmus quadricauda	57.3	20.2	5.21	< 0.01
Phacus species	36.7	15.1	4.33	< 0.01
Ankistrodesmus species	14.3	6.7	3.97	0.03
Oscillatoria princeps	15.2	8.6	3.96	0.06

Cyanophyta (Blue Green Algae, cyanobacteria) Assemblages

The six most common and abundant cyanophytes in the Jordan River were: *Aphanizomenon flos-aquae, Anabaena spiroides*, *Microcystis incerta*, *Oscillatoria agardhii*, *Oscillatoria amphibia* and *Oscillatoria princeps*. We superimposed Hilltop Overlays onto the NMS ordination axes from Figure 6 to illustrate associations among these six taxa shown in Figure 8 (See Appendix 8 for a brief introduction to Hilltop Overlays). We used a flexibility = 8.2; Std. dev. = 2.0; and a hilltop percent of range = 15% to best illustrate these associations. *Microcystis* and *Anabaena* co-occurred and were closely associated in the upstream sections of the river in July. *Aphanizomenon* dominated assemblages in August near the Utah Lake outlet. The three *Oscillatoria* taxa exhibited classic competitive exclusion where *O. princeps* occurred primarily in July at the furthest downstream reaches, *O. agardhii* occurred mostly in June downstream, and *O. amphibia* occurred mostly in late summer, early autumn throughout the river (Figure 8).

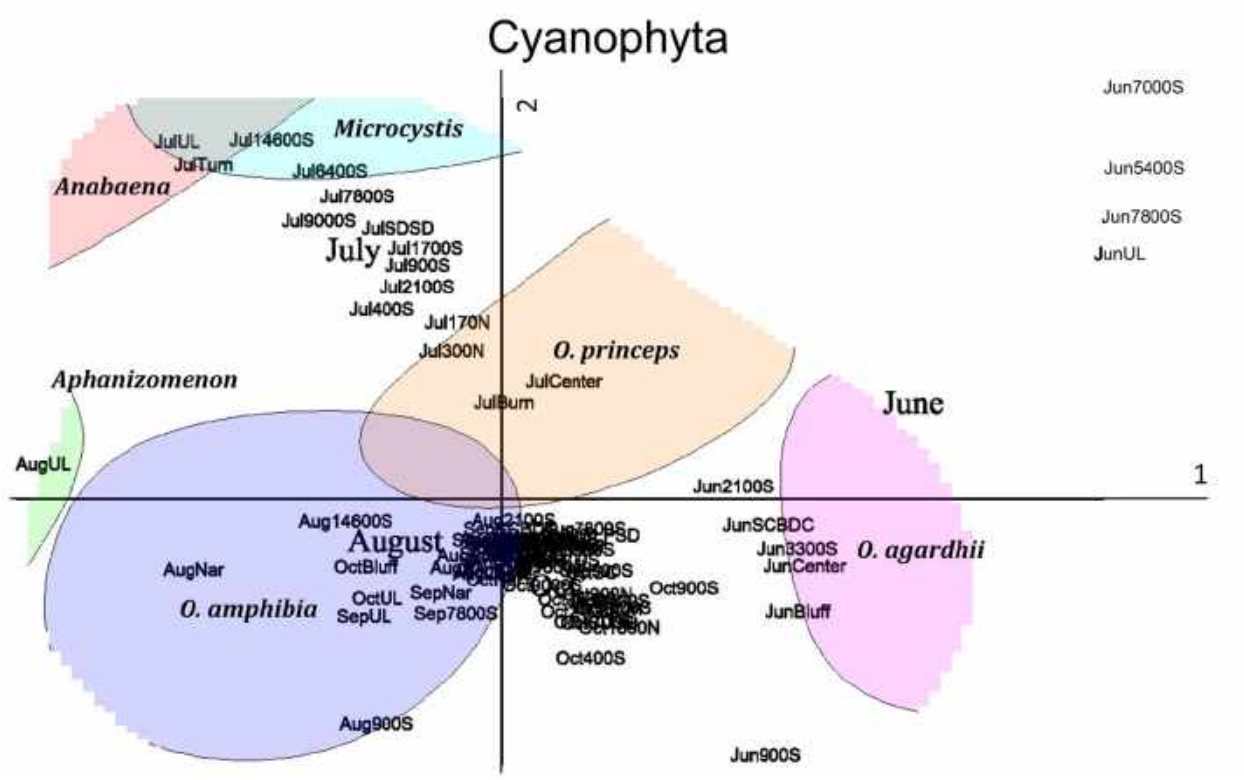

Figure 8. Associations of the six most common cyanophytes in the Jordan River, 2009 Aphanizomenon flos-aquae, Anabaena spiroides, Microcystis incerta, Oscillatoria agardhii, Oscillatoria amphibia and Oscillatoria princeps using Hilltop Overlays from the NMS ordination axes (Figure 6). Sample labels are coded with month first, then location (see Appendix 9). See Appendix 8 for description of hilltop overlays.

Discussion

The analyses presented here support findings by Rushforth and Rushforth (2009) and Miller (2009). These analyses also provide needed statistical backing of their conclusions, as well as additional useful tools for developing water quality metrics (e. g. indicator taxa and range values of richness and diversity indices). These statistical evaluations clearly show spatial and temporal differences in phytoplankton assemblages in the Jordan River. Phytoplankton assemblages in the Jordan are, for the most part, transient and clearly originate in Utah Lake as was documented by Rushforth and Rushforth (2009) and Miller (2009) and, as was expected, based on river ecological theory (Hynes 1970; Vannote et al. 1980).

This analysis also clearly showed decreased phytoplankton abundance as flows moved downstream from the lake to about 9000 South. However, reasons for this decline are not fully understood. Several reasons that most likely are the causes of these decreases have been suggested by Miller (2009) including cell death resulting in cells not being counted by Rushforth and Rushforth (2009); dilution from incoming sources as the river water progressed downstream. However, it seems unlikely that phytoplankton cells died so abruptly during transport from Utah Lake downstream, an estimated transit time of << 2 days. There are more than enough available nutrients in the water column to keep cells nourished and alive during their passive journey downstream. An important factor that may have been over looked is the filter feeding invasive clam, *Corbicula*. Richards (2018b) and Wasatch Front Water

Quality Council members (including Dr. Miller) have documented this clam occurring at very high densities, often >> 10,000 m^{-2}. Richards (2018b) suggested that during peak activity (summer months), *Corbicula* could filter the entire Jordan River water column in < 2 days. Densities of *Corbicula* in 2009 are unknown but we suggest that even though researchers did not report high densities, they were quite abundant by that time period (Richards 2018b).

From this and other research conducted on the Jordan River by WFWQC and OreoHelix; primary production from attached benthic algae (periphyton) and macrophytes appears to be severely limited, mostly due to unsuitable shifting substrates in the upper Jordan River and primarily hardpan clay substrates in the lower sections of the Jordan River. The river also has an overabundance of nutrients. As we have reported elsewhere, the Jordan River is obviously out of balance, is not a properly functioning ecosystem, and is now a low-quality analog of its former self (Richards 2018a; 2018b; 2018c; 2018d; 2018e; Richards and Miller in press). The primary reasons for this are:

1) channelization,
2) Dewatering,

3) loss of beaver dams,

4) increased nutrients and,

5) increased temperatures.

The Jordan River, prior to settlement, was highly sinuous, filled to carrying capacity with beaver dams, and connected to its floodplain. These three phenomena interacted to reduce sediment loads (e.g. beaver ponds and connection to floodplains during regular flood events) that exposed solid stable substrates (primarily cobbles). This in turn allowed the establishment of periphyton and macrophytes that kept primary production in balance with the rest of the ecosystem functions, including secondary production and fisheries.

Finally, our reanalysis showed that there was very little richness or diversity in the phytoplankton assemblages in the Jordan River. This is in sharp contrast to what Richards and Miller (2017) and Richards (2018f) found in Utah Lake in 2016, where they estimated that there were more than 150 phytoplankton taxa. However, phytoplankton richness and diversity are not expected to be high because of their transient nature in flowing waters, such as the Jordan River.

Recommendations

Based on the analyses presented in this report and those from Rushforth and Rushforth (2009) and Miller (year), we highly recommend the following:

1. Measure primary production, especially on stable cobble substrates.
2. Redo phytoplankton surveys conducted by WFWQC and Rushforth and Rushforth (2009).
3. Measure effects of *Corbicula* on regulating phytoplankton, nutrients, and water quality.

4. Conduct ecological models that relate nutrients, primary production, secondary production, and fisheries in the Jordan River. This will require survey data that were collected concurrently or less than a few years apart.

Literature Cited

Hynes, Hugh Bernard Noel. 1970. The Ecology of Running Waters. University of Toronto Press.

McCune, B. and M. J. Mefford. 2018. PC-ORD. Multivariate Analysis of Ecological Data. Version 7.07. Wild Blueberry Media, Corvallis, Oregon, U.S.A.

Miller 2009. Phytoplankton studies in the Jordan River. Wasatch Front Water Quality Council.

Miller, T. G. 2014. A Physical, Chemical and Biological Assessment of the Jordan River: 2009-2013. Wasatch Front Water Quality Council

Richards, D. C. and T. Miller. 2017. A preliminary analysis of Utah Lake's unique foodweb with a focus on the role of nutrients, phytoplankton, zooplankton, and benthic invertebrates on HABs. Utah Lake Research 2016. Progress Report. Wasatch Front Water Quality Council, Salt Lake City, UT.

Richards, D.C. 2018a. Jordan River macroinvertebrate assemblages: preliminary findings. Draft Report to Wasatch Front Water Quality Council. Salt Lake City, UT. OreoHelix Consulting. Vineyard, UT.

2018b. A snail, a clam, and the River Jordan: A revealing novel. Version 1.5. Technical Report Submitted to The Wasatch Front Water Quality Council. OreoHelix Consulting, Vineyard, UT.

2018c. Jordan River fisheries studies. Part 2: Lower Jordan River, Surplus and State Canal fisheries. Draft Report to Wasatch Front Water Quality Council. Salt Lake City, UT. OreoHelix Consulting. Vineyard, UT.

2018d. Jordan River fisheries studies. Part 1: Upper Jordan River Brown Trout redd surveys. Draft Report to Wasatch Front Water Quality Council. Salt Lake City, UT. OreoHelix Consulting. Vineyard, UT.

2018e. The Jordan River: How to regulate an analog ecosystem. Scientific presentation at the Twelve Annual Salt Lake County Watershed Symposium, Salt Lake City, UT.

2018f. Relationships between phytoplankton richness and diversity, zooplankton abundance, and cyanoHABs dominance in Utah Lake, 2016. Draft Technical Report to Wasatch Front Water Quality Council. Salt Lake City, UT. OreoHelix Consulting. Vineyard, UT.

Richards, D.C. and T. Miller. In Press. Apparent extinction of native mussels in Lower Mill Creek and Mid-Jordan River, UT. Western North American Naturalist

Rushforth, S.R. and S.J. Rushforth. 2009. Assessment of the phytoplankton of the Jordan River: June-October 2019. Rushforth Phycology. Orem, UT.

StataCorp 2018. Stata/IC 15.1 for Mac (64-bit Intel). Revision 17Dec2018. College Station, TX

Vannote R.L., G.W. Minshall, K.W. Cummins, J.R. Sedell, and C.E. Cushing. 1980. The River Continuum Concept. Canadian Journal of Fisheries and Aquatic Sciences. 37. Ottawa, 130-137.

Appendices

Appendix 1. Equality of medians test results for monthly phytoplankton abundance (μ^3/ml), richness (S), effective number of taxa (ENT), evenness (E), Shannon Diversity (H), and Simpson Diversity (D).

Abundance (biovolume)

Greater than the median	DATE June	July	August	September	October	Total
no	**10**	**1**	**5**	**8**	**14**	**38**
yes	**0**	**14**	**12**	**9**	**2**	**37**
Total	**10**	**15**	**17**	**17**	**16**	**75**

Pearson chi2(**4**) = **33.2004** Pr = **0.000**
Fisher's exact = **0.000**

Taxa Richness (S)

Greater than the median	Month June	July	August	September	October	Total
no	**9**	**7**	**7**	**2**	**17**	**42**
yes	**1**	**10**	**11**	**16**	**0**	**38**
Total	**10**	**17**	**18**	**18**	**17**	**80**

Pearson chi2(**4**) = **35.5962** Pr = **0.000**
Fisher's exact = **0.000**

Effective number of taxa (ENT)

Greater than the median	Month					
	June	July	August	September	October	Total
no	**5**	**15**	**6**	**1**	**13**	**40**
yes	**5**	**2**	**12**	**17**	**4**	**40**
Total	**10**	**17**	**18**	**18**	**17**	**80**

Pearson chi2(**4**) = **30.9281** Pr = **0.000**
Fisher's exact = **0.000**

Evenness (E)

Greater than the median	Month					
	June	July	August	September	October	Total
no	**2**	**16**	**9**	**2**	**11**	**40**
yes	**8**	**1**	**9**	**16**	**6**	**40**
Total	**10**	**17**	**18**	**18**	**17**	**80**

Pearson chi2(**4**) = **29.1948** Pr = **0.000**
Fisher's exact = **0.000**

Shannon Diversity (H)

Greater than the median	Month					
	June	July	August	September	October	Total
no	**5**	**15**	**6**	**1**	**13**	**40**
yes	**5**	**2**	**12**	**17**	**4**	**40**
Total	**10**	**17**	**18**	**18**	**17**	**80**

Pearson chi2(**4**) = **30.9281** Pr = **0.000**
Fisher's exact = **0.000**

Simpson Diversity (D)

Greater than the median	Month					
	June	July	August	September	October	Total
no	**3**	**16**	**6**	**1**	**14**	**40**
yes	**7**	**1**	**12**	**17**	**3**	**40**
Total	**10**	**17**	**18**	**18**	**17**	**80**

Pearson chi2(**4**) = **38.1752** Pr = **0.000**
Fisher's exact = **0.000**

Appendix 2. Jordan River, 2009 phytoplankton taxa list and abbreviations used in this chapter.

Taxon	Abbreviations
Actinastrum species	Ansp
Anabaena spiroides	Anab
Ankistrodesmus convolutus	Anco
Ankistrodesmus falcatus	Anfa
Aphanizomenon flos-aquae	Apfa
Asterionella formosa	Asfo
centric diatoms	centric
Ceratium hirundinella	Cehi
Chlamydomonas species	Chsp
Closteriopsis longissima	Cllo
Cosmarium species	Cosp
Crucigenia irregularis	Crir
Crucigenia rectangularis	Crre
Dinobryon divergens	Didi
Euglena species	Eusp

Fragilaria crotonensis	Frcr
Fragilaria virescens	Frvi
Gomphosphaeria species	Gosp
Lyngbya birgei	Lybi
Melosira granulata	Megr
Melosira varians	Meva
Merismopedia species	Mesp
Microcystis incerta	Miin
Oocystis borgei	Oobo
Oscillatoria agardhii	Osag
Oscillatoria amphibia	Osam
Oscillatoria princeps	Ospr
Pandorina morum	Pamo
Pediastrum	Pedi
pennate diatoms	pennate
Phacus species	Phsp
Pleurosira laevis	Plla
Pteromonas species	Ptsp
Scenedesmus bijuga	Scbi
Scenedesmus dimorphus	Scdi
Scenedesmus quadricauda	Scqu
Scenedesmus species	Scsp
Schroederia setigera	Scse
Sphaerocystis schroeteri	Spsc
Spirogyra species	Spsp
Staurastrum species	Stsp

Stephanodiscus niagarae	Stni
Stigeoclonium polymorphum	Stop
Tabellaria fenestrata	Tafe
Trachellomonas species	Trsp

Appendix 3. Cluster Analysis Dendogram showing relations between phytoplankton assemblages including monthly relationships colored coded.

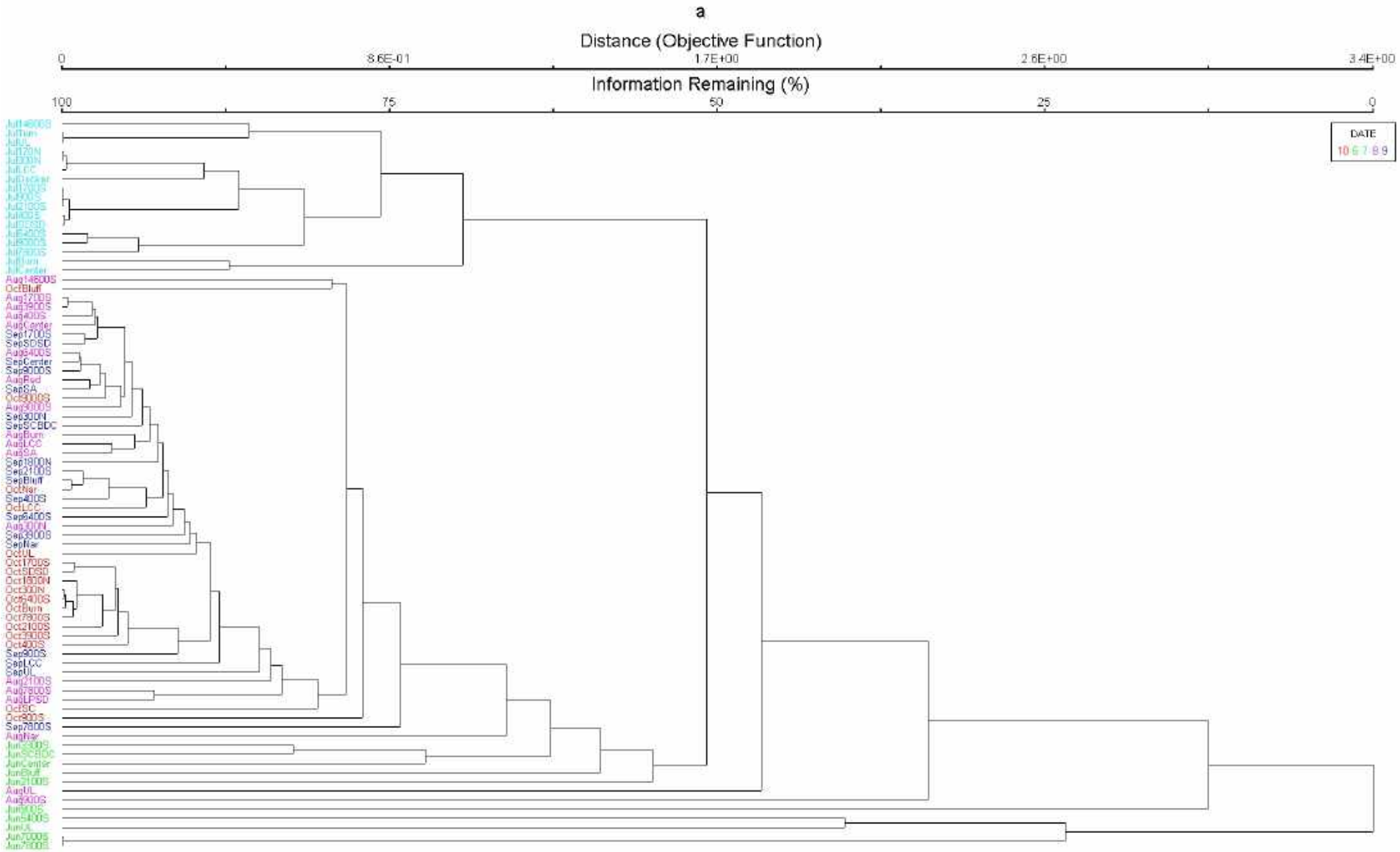

Appendix 4. Descriptive statistics including diversity indices for each sample.

July

Number	Name	Mean	Stand.Dev.	Sum	Minimum	Maximum	S	E	H`	D
1	Jul14600S	2.05E+06	1.34E+07	9.22E+07	0	8.97E+07	10	0.068	0.156	0.0519
2	Jul170N	1.67E+05	9.65E+05	7.50E+06	0	6.47E+06	9	0.255	0.56	0.2486
3	Jul1700S	3.48E+05	2.16E+06	1.57E+07	0	1.45E+07	10	0.152	0.349	0.1435
4	Jul2100S	3.38E+05	2.07E+06	1.52E+07	0	1.39E+07	11	0.166	0.397	0.1619
5	Jul300N	1.79E+05	9.89E+05	8.04E+06	0	6.62E+06	11	0.296	0.71	0.3124
6	Jul400S	4.44E+05	2.70E+06	2.00E+07	0	1.81E+07	13	0.163	0.418	0.1773
7	Jul6400S	1.09E+06	7.09E+06	4.90E+07	0	4.76E+07	10	0.074	0.17	0.0575
8	Jul7800S	6.84E+05	4.39E+06	3.08E+07	0	2.95E+07	8	0.112	0.233	0.0829
9	Jul900S	3.42E+05	2.12E+06	1.54E+07	0	1.43E+07	11	0.153	0.366	0.1408
10	Jul9000S	8.95E+05	5.73E+06	4.03E+07	0	3.84E+07	8	0.114	0.237	0.0874
11	JulBurn	8.85E+04	3.77E+05	3.98E+06	0	2.32E+06	6	0.638	1.143	0.5829
12	JulCenter	5.87E+04	2.99E+05	2.64E+06	0	1.98E+06	9	0.407	0.895	0.4148
13	JulDecker	2.18E+05	1.36E+06	9.82E+06	0	9.11E+06	10	0.157	0.362	0.1366
14	JulLCC	1.78E+05	9.87E+05	7.99E+06	0	6.62E+06	10	0.306	0.705	0.3064
15	JulSDSD	4.09E+05	2.54E+06	1.84E+07	0	1.71E+07	11	0.156	0.375	0.1386
16	JulTurn	3.25E+06	2.12E+07	1.46E+08	0	1.42E+08	5	0.091	0.146	0.0533
17	JulUL	3.49E+06	2.17E+07	1.57E+08	0	1.46E+08	7	0.15	0.291	0.1342

August

Number	Name	Mean	Stand.Dev.	Sum	Minimum	Maximum	S	E	H`	D
1	Aug14600S	3.05E+05	1.81E+06	1.37E+07	0	1.21E+07	9	0.211	0.464	0.2143
2	Aug1700S	7.38E+04	3.24E+05	3.32E+06	0	1.96E+06	14	0.432	1.141	0.5594
3	Aug2100S	8.07E+04	2.99E+05	3.63E+06	0	1.46E+06	10	0.593	1.367	0.6788
4	Aug300N	5.34E+04	2.16E+05	2.40E+06	0	1.23E+06	9	0.577	1.267	0.6219
5	Aug3900S	7.70E+04	3.30E+05	3.47E+06	0	2.05E+06	11	0.5	1.198	0.5792

6	Aug400S	6.61E+04	3.22E+05	2.98E+06	0	2.10E+06	10	0.421	0.97	0.4629
7	Aug6400S	4.69E+04	1.86E+05	2.11E+06	0	1.14E+06	11	0.562	1.348	0.637
8	Aug7800S	3.79E+04	1.46E+05	1.71E+06	0	8.21E+05	8	0.599	1.245	0.6558
9	Aug900S	2.93E+05	1.51E+06	1.32E+07	0	9.95E+06	5	0.493	0.794	0.4027
10	Aug9000S	6.12E+04	2.63E+05	2.75E+06	0	1.55E+06	11	0.477	1.144	0.5765
11	AugBurn	9.02E+04	4.33E+05	4.06E+06	0	2.78E+06	10	0.416	0.957	0.4766
12	AugCenter	7.54E+04	3.86E+05	3.40E+06	0	2.55E+06	11	0.364	0.873	0.4081
13	AugLPSD	3.07E+04	1.16E+05	1.38E+06	0	6.38E+05	9	0.592	1.302	0.6684
14	AugLCC	1.00E+05	5.52E+05	4.51E+06	0	3.69E+06	9	0.324	0.712	0.3186
15	AugNar	7.97E+05	3.97E+06	3.59E+07	0	2.49E+07	11	0.303	0.727	0.4389
16	AugRed	4.92E+04	2.34E+05	2.21E+06	0	1.51E+06	11	0.428	1.027	0.4878
17	AugSA	8.98E+04	4.92E+05	4.04E+06	0	3.26E+06	13	0.257	0.659	0.3259
18	AugUL	2.62E+06	1.31E+07	1.18E+08	0	8.22E+07	9	0.313	0.687	0.4327

September

Number	Name	Mean	Stand.Dev.	Sum	Minimum	Maximum	S	E	H`	D
1	Sep1700S	7.00E+04	3.00E+05	3.15E+06	0	1.92E+06	14	0.48	1.268	0.5779
2	Sep1800N	5.55E+04	2.25E+05	2.50E+06	0	1.46E+06	12	0.583	1.448	0.6214
3	Sep2100S	7.91E+04	3.26E+05	3.56E+06	0	2.14E+06	15	0.55	1.489	0.6086
4	Sep300N	5.71E+04	2.12E+05	2.57E+06	0	1.32E+06	14	0.599	1.581	0.6768
5	Sep3900S	4.66E+04	1.70E+05	2.10E+06	0	1.00E+06	12	0.615	1.527	0.6894
6	Sep400S	8.33E+04	3.30E+05	3.75E+06	0	2.14E+06	17	0.533	1.511	0.6366
7	Sep6400S	4.74E+04	1.98E+05	2.13E+06	0	1.23E+06	11	0.542	1.299	0.5994
8	Sep7800S	1.16E+05	4.56E+05	5.21E+06	0	2.71E+06	11	0.553	1.326	0.6399
9	Sep900S	3.01E+04	1.26E+05	1.35E+06	0	8.21E+05	9	0.608	1.335	0.5989
10	Sep9000S	5.09E+04	2.02E+05	2.29E+06	0	1.23E+06	11	0.55	1.319	0.6361
11	SepBluff	6.72E+04	3.22E+05	3.02E+06	0	2.14E+06	12	0.445	1.107	0.4779
12	SepCenter	4.36E+04	1.77E+05	1.96E+06	0	1.09E+06	12	0.535	1.329	0.6205
13	SepLCC	7.93E+04	3.40E+05	3.57E+06	0	2.14E+06	10	0.509	1.173	0.5776
14	SepNar	1.01E+05	5.12E+05	4.56E+06	0	3.37E+06	11	0.367	0.879	0.423

15	SepSDSD	6.13E+04	2.82E+05	2.76E+06	0	1.82E+06	13	0.445	1.142	0.5184
16	SepSCBDC	8.27E+04	2.96E+05	3.72E+06	0	1.73E+06	14	0.603	1.591	0.7003
17	SepSA	4.82E+04	2.17E+05	2.17E+06	0	1.39E+06	10	0.49	1.128	0.539
18	SepUL	1.49E+05	6.93E+05	6.72E+06	0	3.97E+06	8	0.399	0.83	0.5093

AVERAGES: 0.7048E+05 0.2991E+06 0.3171E+07 0.000 0.1869E+07 12.0 0.523 1.293 0.5917

October

Number	Name	Mean	Stand.Dev.	Sum	Minimum	Maximum	S	E	H`	D
1	Oct1700S	2.43E+04	1.20E+05	1.09E+06	0	7.98E+05	8	0.461	0.959	0.4442
2	Oct1800N	1.77E+04	9.57E+04	7.95E+05	0	6.38E+05	6	0.408	0.731	0.3409
3	Oct2100S	2.49E+04	1.34E+05	1.12E+06	0	8.89E+05	7	0.381	0.742	0.3528
4	Oct300N	2.30E+04	1.25E+05	1.04E+06	0	8.21E+05	4	0.429	0.595	0.3389
5	Oct3900S	2.86E+04	1.55E+05	1.29E+06	0	1.03E+06	6	0.379	0.68	0.3423
6	Oct400S	1.52E+04	8.30E+04	6.82E+05	0	5.47E+05	7	0.307	0.598	0.3255
7	Oct6400S	2.14E+04	1.18E+05	9.64E+05	0	7.75E+05	6	0.333	0.597	0.324
8	Oct7800S	2.06E+04	1.05E+05	9.26E+05	0	6.84E+05	5	0.462	0.743	0.4103
9	Oct900S	1.16E+04	5.22E+04	5.20E+05	0	2.96E+05	6	0.513	0.92	0.5345
10	Oct9000S	4.12E+04	2.18E+05	1.85E+06	0	1.44E+06	6	0.404	0.724	0.3725
11	OctBluff	1.80E+05	1.05E+06	8.08E+06	0	7.02E+06	4	0.372	0.516	0.2368
12	OctBurn	1.96E+04	1.10E+05	8.80E+05	0	7.30E+05	5	0.341	0.549	0.2914
13	OctLCC	4.65E+04	2.79E+05	2.09E+06	0	1.87E+06	9	0.206	0.453	0.1961
14	OctNar	6.10E+04	3.10E+05	2.74E+06	0	2.05E+06	6	0.476	0.852	0.4177
15	OctSDSD	2.28E+04	1.17E+05	1.03E+06	0	7.75E+05	7	0.437	0.85	0.406
16	OctSC	3.34E+04	1.30E+05	1.50E+06	0	7.30E+05	6	0.668	1.196	0.65
17	OctUL	1.02E+05	6.06E+05	4.60E+06	0	4.06E+06	6	0.259	0.464	0.2153

June

Number	Name	Mean	Stand.Dev.	Sum	Minimum	Maximum	S	E	H`	D
1	Jun2100S	2.34E+04	8.32E+04	1.05E+06	0	4.51E+05	7	0.738	1.436	0.7027
2	Jun3300S	1.18E+04	4.39E+04	5.31E+05	0	2.50E+05	9	0.64	1.405	0.6769
3	Jun5400S	205.333	999.622	9240	0	5880	2	0.946	0.655	0.4628
4	Jun7000S	1136	7368.643	51120	0	49440	2	0.209	0.145	0.0636
5	Jun7800S	1229.333	7402.213	55320	0	49440	2	0.489	0.339	0.19
6	Jun900S	3.93E+04	2.42E+05	1.77E+06	0	1.62E+06	5	0.207	0.334	0.1564
7	JunBluff	1.25E+04	3.73E+04	5.61E+05	0	1.73E+05	9	0.763	1.676	0.7833
8	JunCenter	6446.4	30451.602	290088	0	201600	8	0.531	1.104	0.4929
9	JunSCBDC	1.48E+04	5.26E+04	6.67E+05	0	3.17E+05	10	0.682	1.569	0.7043
10	JunUL	234.667	1101.589	10560	0	5520	2	0.999	0.692	0.499

Appendix 5. Regression results for total cells (μ^3 cells ml^{-1}) vs. distance downstream

```
. by date, sort : regress logTotal lat

-------------------------------------------------------------------------------
-> date = June

      Source |       SS           df       MS      Number of obs   =        10
-------------+----------------------------------   F(1, 8)         =      3.81
       Model |  1.98303092         1  1.98303092   Prob > F        =    0.0867
    Residual |  4.16216731         8  .520270914   R-squared       =    0.3227
-------------+----------------------------------   Adj R-squared   =    0.2380
       Total |  6.14519824         9  .682799804   Root MSE        =     .7213

------------------------------------------------------------------------------
    logTotal |      Coef.   Std. Err.      t    P>|t|     [95% Conf. Interval]
-------------+----------------------------------------------------------------
         lat |    2.992519   1.532805     1.95   0.087    -.5421359    6.527173
       _cons |   -116.4411   62.33064    -1.87   0.099    -260.1758    27.29365
------------------------------------------------------------------------------
```

-> date = July

Source	SS	df	MS	Number of obs	=	15
				F(1, 13)	=	81.03
Model	3.35245978	1	3.35245978	Prob > F	=	0.0000
Residual	.537840622	13	.041372356	R-squared	=	0.8617
				Adj R-squared	=	0.8511
Total	3.8903004	14	.2778786	Root MSE	=	.2034

logTotal	Coef.	Std. Err.	t	P>|t|	[95% Conf.	Interval]
lat	-3.127484	.3474309	-9.00	0.000	-3.878063	-2.376905
_cons	134.5736	14.13486	9.52	0.000	104.0371	165.1102

-> date = August

Source	SS	df	MS	Number of obs	=	17
				F(1, 15)	=	15.16
Model	2.06959383	1	2.06959383	Prob > F	=	0.0014
Residual	2.04726706	15	.136484471	R-squared	=	0.5027
				Adj R-squared	=	0.4696
Total	4.1168609	16	.257303806	Root MSE	=	.36944

logTotal	Coef.	Std. Err.	t	P>|t|	[95% Conf.	Interval]
lat	-2.40879	.618583	-3.89	0.001	-3.727268	-1.090311
_cons	104.6973	25.17086	4.16	0.001	51.04685	158.3477

-> date = September

Source	SS	df	MS	Number of obs	=	17
				F(1, 15)	=	5.20
Model	.123484943	1	.123484943	Prob > F	=	0.0376
Residual	.356247834	15	.023749856	R-squared	=	0.2574
				Adj R-squared	=	0.2079
Total	.479732777	16	.029983299	Root MSE	=	.15411

logTotal	Coef.	Std. Err.	t	P>|t|	[95% Conf.	Interval]
lat	-.5970481	.2618381	-2.28	0.038	-1.155143	-.0389534
_cons	30.75807	10.65412	2.89	0.011	8.049353	53.46679

```
-> date = October

      Source |       SS           df       MS      Number of obs   =        16
-------------+----------------------------------   F(1, 14)        =     20.62
       Model |  .858423417         1  .858423417   Prob > F        =    0.0005
    Residual |  .582964601        14  .041640329   R-squared       =    0.5956
-------------+----------------------------------   Adj R-squared   =    0.5667
       Total |  1.44138802        15  .096092535   Root MSE        =    .20406

------------------------------------------------------------------------------
    logTotal |      Coef.   Std. Err.      t    P>|t|     [95% Conf. Interval]
-------------+----------------------------------------------------------------
         lat |  -1.561235   .3438543    -4.54   0.000    -2.298729   -.8237406
       _cons |   69.6433   13.98938     4.98   0.000     39.63906    99.64754
------------------------------------------------------------------------------
```

Appendix 6. NMS results

Ordination of sites in taxa space. 75 sites, 28 taxa

6 = Number of tie blocks in dissimilarity matrix.

30 = Number of elements involved in ties.

2775 = Total number of elements in dissimilarity matrix.

1.081 = Percentage of elements involved in ties.

STRESS IN RELATION TO DIMENSIONALITY (Number of Axes)

Stress in real data Stress in randomized data

250 run(s) Monte Carlo test, 250 runs

Axes	Minimum	Mean	Maximum	Minimum	Mean	Maximum	p	n

1	17.480	35.417	56.956	27.408	43.736	56.957	0.0040	0
2	9.849	11.833	18.000	12.032	17.060	40.902	0.0040	0
3	6.452	6.778	9.668	8.656	10.880	12.981	0.0040	0
4	5.126	5.264	5.874	7.317	8.409	9.955	0.0040	0
5	3.998	4.214	4.670	5.768	6.846	8.087	0.0040	0
6	3.365	3.531	4.245	4.632	5.674	6.597	0.0040	0

---

p = proportion of randomized runs with stress < or = observed stress

i.e., p = (1 + n)/(1 + N)

n = no. permutations <= observed

N = no. permutations

Conclusion: a 2-dimensional solution is recommended.

Now rerunning the best ordination with that dimensionality.

Selected file CONFIG2.GPH for the starting configuration for

the final run.

File containing starting coordinates:

CONFIG2.GPH

9.85062 = final stress for 2-dimensional solution

0.00000 = final instability

77 = number of iterations

MEASURES OF FIT

R≤n (nonmetric fit) = 0.9903 Intrinsic measure for NMS. Null: all points co-located.

R≤l (linear fit) = 0.9745 Null: all ordination distances equal.

R≤m (metric fit) = 0.6971 Null: no linear relationship with observed dissimilarities.

CHANCE-CORRECTED EVALUATIONS

Improvement: I = 0.7672

Null model: final configuration no better than initial random configuration.

Interpretation: 0 = random expectation, 1 = perfect fit, <0 = worse than random expectation

Basis: 2 dimensions

250 = number of random initial configurations used

42.3100 = average initial stress

9.8506 = final stress

Association: A = 0.3181

Null model: relationships among columns no stronger than expected chance, based on shuffling within columns.

Interpretation: 0 = random expectation, 1 = perfect fit, <0 = worse than random expectation

Basis: 2 dimensions

500 = number of randomizations used

14.4464 = average final stress from randomizations

9.8506 = final stress

Final configuration (ordination scores) for this run

sites Axis

Name	1	2
Jul14600S	0.1768	-1.6579

Aug14600S	-0.6995	-0.5007
Jul170N	0.2618	-0.6807
Jul1700S	0.2698	-1.0204
Aug1700S	-0.2546	0.0396
Sep1700S	-0.241	0.0621
Oct1700S	-0.2412	0.5179
Sep1800N	-0.2261	0.2112
Oct1800N	-0.1861	0.6044
Jun2100S	0.5332	0.543
Jul2100S	0.2609	-0.9854
Aug2100S	-0.1758	0.0026
Sep2100S	-0.3049	0.0585
Oct2100S	-0.2474	0.4497
Jul300N	0.1654	-0.6167
Aug300N	-0.1447	0.1505
Sep300N	-0.1605	0.1424
Oct300N	-0.1393	0.4669
Jun3300S	0.5657	0.8498
Aug3900S	-0.2635	0.0201
Sep3900S	-0.0971	0.2529
Oct3900S	-0.2185	0.411
Jul400S	0.0918	-0.9321
Aug400S	-0.2931	0.1163
Sep400S	-0.2879	-0.0001
Oct400S	-0.3365	0.6214
Jun5400S	2.5805	0.8409

Jul6400S	0.3322	-1.4743
Aug6400S	-0.123	0.1982
Sep6400S	-0.1678	0.2377
Oct6400S	-0.1357	0.5062
Jun7000S	2.8077	0.613
Jun7800S	2.4332	0.9671
Jul7800S	0.2688	-1.252
Aug7800S	-0.0017	0.2282
Sep7800S	-0.6027	0.0948
Oct7800S	-0.1506	0.5285
Jun900S	-0.1346	1.3912
Jul900S	0.3088	-1.0212
Aug900S	-1.1215	0.1863
Sep900S	-0.0769	0.3901
Oct900S	0.1211	0.6978
Jul9000S	0.1743	-1.2972
Aug9000S	-0.1869	0.1144
Sep9000S	-0.1197	0.1446
Oct9000S	-0.2758	0.2715
JunBluff	0.3729	1.0946
SepBluff	-0.3435	0.1135
OctBluff	-0.6896	-0.2641
AugBurn	-0.3712	-0.0002
JulBurn	0.2395	-0.3529
OctBurn	-0.1413	0.5458
JunCenter	0.4994	0.961

JulCenter	0.3731	-0.2271
AugCenter	-0.3781	0.0954
SepCenter	-0.1149	0.2128
AugLPSD	0.0268	0.3001
AugNar	-1.1661	-0.7438
SepNar	-0.5527	0.0286
OctNar	-0.3626	0.15
AugRed	-0.2083	0.1976
OctSDSD	-0.2254	0.5399
JulSDSD	0.356	-1.1207
SepSDSD	-0.2476	0.1291
JunSCBDC	0.5036	0.7332
SepSCBDC	-0.2229	0.001
AugSA	-0.4254	0.0121
SepSA	-0.1896	0.1903
OctSC	-0.0644	0.4122
JulTurn	0.0738	-1.8933
JunUL	2.3079	1.0471
AugUL	-1.2704	-1.4572
SepUL	-0.8226	-0.1205
OctUL	-0.7277	-0.1238
JulUL	0.0339	-1.9531

Principal axes rotation of 2-dimensional solution.

Configuration after rotation is listed below.

Final configuration (ordination scores) for this run

sites Axis

Name	1	2
Jul14600S	-1.0706	1.2782
Aug14600S	-0.846	-0.1559
Jul170N	-0.3082	0.661
Jul1700S	-0.5472	0.9025
Aug1700S	-0.1482	-0.2108
Sep1700S	-0.1226	-0.2165
Oct1700S	0.2053	-0.5332
Sep1800N	-0.005	-0.3094
Oct1800N	0.3059	-0.5535
Jun2100S	0.761	0.0069
Jul2100S	-0.5282	0.8718
Aug2100S	-0.1201	-0.1284
Sep2100S	-0.1695	-0.2601
Oct2100S	0.152	-0.4903
Jul300N	-0.3291	0.5472
Aug300N	0.0079	-0.2086
Sep300N	-0.0089	-0.2143
Oct300N	0.2394	-0.4244
Jun3300S	1.0044	-0.1827
Aug3900S	-0.1684	-0.2036
Sep3900S	0.1146	-0.2455

Oct3900S	0.1441	-0.4426
Jul400S	-0.6072	0.7131
Aug400S	-0.1198	-0.2916
Sep400S	-0.1999	-0.2072
Oct400S	0.2137	-0.6736
Jun5400S	2.3966	1.2736
Jul6400S	-0.8306	1.2626
Aug6400S	0.0573	-0.2261
Sep6400S	0.0546	-0.2858
Oct6400S	0.2702	-0.449
Jun7000S	2.3903	1.5955
Jun7800S	2.3852	1.08
Jul7800S	-0.7145	1.0626
Aug7800S	0.1631	-0.1597
Sep7800S	-0.3501	-0.4997
Oct7800S	0.2759	-0.4752
Jun900S	0.9079	-1.0627
Jul900S	-0.5207	0.9312
Aug900S	-0.6444	-0.9366
Sep900S	0.2274	-0.3262
Oct900S	0.5863	-0.3972
Jul9000S	-0.8127	1.026
Aug9000S	-0.0474	-0.214
Sep9000S	0.021	-0.1865
Oct9000S	0.004	-0.387
JunBluff	1.0468	-0.4914

SepBluff	-0.1567	-0.326
OctBluff	-0.6688	-0.313
AugBurn	-0.2578	-0.2671
JulBurn	-0.0878	0.4174
OctBurn	0.2948	-0.4806
JunCenter	1.0384	-0.3076
JulCenter	0.0956	0.4262
AugCenter	-0.1938	-0.3384
SepCenter	0.0734	-0.2304
AugLPSD	0.2346	-0.1891
AugNar	-1.3449	-0.3231
SepNar	-0.3631	-0.4177
OctNar	-0.1437	-0.3651
AugRed	-0.0024	-0.2871
OctSDSD	0.2322	-0.537
JulSDSD	-0.5595	1.0343
SepSDSD	-0.0789	-0.2679
JunSCBDC	0.8774	-0.1465
SepSCBDC	-0.154	-0.1612
AugSA	-0.2866	-0.3146
SepSA	0.0054	-0.2686
OctSC	0.252	-0.3326
JulTurn	-1.3116	1.3674
JunUL	2.3558	0.9343
AugUL	-1.9308	0.0971
SepUL	-0.6577	-0.5084

OctUL	-0.5943	-0.4379
JulUL	-1.3823	1.3802

Appendix 7. Indicator species results.

June				
Taxon	IV	Mean	Std dev	P
Ptsp	35.1	11.6	5.68	0.002
Spsc	14.1	7.3	4.01	0.042
Osag	15.1	8.2	3.95	0.079
Anfa	13.7	9.1	4.05	0.1134
Lybi	10.0	6.3	1.44	0.1274
Scsp	10.1	7.2	3.92	0.223
Didi	4.7	5.9	3.36	0.3523
Frvi	6.8	7.4	4.26	0.4271
Frcr	6.5	7.3	3.88	0.4625
Oobo	7.7	9.6	4.35	0.6093

July				
taxon	IV	Mean	Std dev	P
Anab	98.6	25.4	7.61	0.0002
centric	38.8	26.2	3.30	0.0028
Crre	11.8	6.0	3.45	0.0994
Stsp	5.9	6.3	1.43	0.5495
Scbi	4.4	6.1	3.27	0.5755
Cosp	3.9	5.9	3.39	0.7039

August				
taxon	IV	Mean	Std dev	P
Chsp	54.5	16.7	4.84	0.0002
Meva	42.2	24.1	4.64	0.0022
pennate	32.7	24.2	2.33	0.0024
Apfa	67.9	44.0	7.34	0.0036
Megr	30.1	17.6	4.14	0.012
Stop	12.3	6.6	3.83	0.1844
Plla	30.1	23.1	8.44	0.1876
Cllo	10.2	12.7	5.67	0.6263
Cehi	11.4	20.2	7.80	0.91
Osam	6.5	8.9	4.47	0.6323
Miin	6.2	8.5	4.14	0.6723
Crir	3.6	5.9	3.35	1
Mesp	3.8	6.1	3.45	1

September				
taxon	IV	Mean	Std dev	P
Scqu	57.3	20.2	5.21	0.0002
Phsp	36.7	15.1	4.33	0.0018
Ansp	14.3	6.7	3.97	0.0328
Ospr	15.2	8.6	3.96	0.0606

Scdi	15.2	8.5	4.12	0.0718
Scse	15.3	9.3	4.39	0.0884
Eusp	19.6	16.1	4.44	0.1836
Gosp	11.1	5.5	3.73	0.192
Pamo	10.4	6.6	3.83	0.199
Stni	13.1	11.4	4.71	0.2895
Pedi	11.6	9.5	4.98	0.3111
Trsp	8.2	9.9	4.24	0.5837
Asfo	5.6	6.3	1.46	1
Spsp	5.6	6.3	1.43	1
Tafe	5.6	6.3	1.45	1

Appendix 8. Brief introduction to Hilltop Overlays superimposed on NMS ordination axes.

Description of Hilltop Overlays from PCORD (McCune and Mefford 2018):

> "A hilltop plot is a way of showing more than one nonlinear response surface at a time on a single graph. One of the first uses was in Nelson et al. (2015). In PC-ORD, response surfaces are superimposed on an ordination as an overlay. This enables simultaneous measurement and display of one- and two-dimensional, non-linear community–trait–environment associations.
>
> For each selected overlay variable, we trace a particular contour that is specified as a percentage of that variable's range. Each contained area is a "hilltop", and multiple partially transparent hilltops are superimposed on one ordination. The resulting diagram shows the maxima of many nonlinear overlay variables (e.g. traits, species abundances, or environmental variables) in a single figure.

Because the hilltops are based on a contoured response surface, you can better understand the basis for hilltop plots by reading about contour overlays. The chief difference in use between the hilltops and the contour plots is that contour plots can be shown for only one variable at a time, while one can graph many hilltops on the same ordination. This comes at a loss of information in that most of the contour plot is discarded when converting to a hilltop.

Flexibility – This controls how tightly the response surfaces fit individual points. The default is to specify a flexibility of 8.2, which in many cases is a reasonable compromise between a surface that is too smooth and one that is overfitting individual points or small groups of points"

Appendix 9. Site codes for multivariate analyses. Months data collected were placed before the site abbreviation.

SITE	Abbreviation
14600 South	14600S
170 North	170N
1700 South	1700S
1800 North	1800N
2100 South	2100S
300 North	300N
3300 South	3300S
3900 South	3900S
400 South	400S
5400 South	5400S
6400 South	6400S
7000 South	7000S
7800 South	7800S
900 South	900S
9000 South	9000S
Bluffdale Road	Bluff
Burnham Dam	Burn

Center Street	Center
Decker Drain	Decker
Legacy Preserve S Davis	LPSD
Little Cottonwood Creek	LCC
Mil Creek downstream	MCd
Mill Creek upstream	Mcu
Narrows	Nar
Redwood Rd 1800 N	Red
SDSD	SDSD
State Canal Burnham Duck Club	SCBDC
Surplus at Airport	SA
Surplus Canal	SC
Turner Dam	Turn
Utah Lake	UL

Chapter 8

Real and Perceived Macroinvertebrate Assemblage Variability in the Jordan River, Utah can Affect Water Quality Assessments

By

David C. Richards, Ph. D.

OreoHelix Ecological

Summary

Seasonality, field sampling error, subsampling, taxonomic resolution, and the river continuum affects our understanding of macroinvertebrate assemblage relationships in the Jordan River and confounds generalized water quality assessment models and conclusions.

Introduction

The Jordan River flows from Utah Lake and into the Great Salt Lake through the most densely populated area of Utah. By any measure; this river has been compromised. Its headwater source, Utah Lake, has undergone a catastrophic ecosystem shift in the last century and is now a shallow, eutrophic, highly regulated, agricultural-centric-use reservoir. More often than not, water needs to be physically pumped out of Utah Lake and into the Jordan River to maintain baseline flows. Tributaries to the Jordan River also primarily consist of Utah Lake water conveyed through a convoluted and difficult to resolve system of canals and dams. Most clean cold waters from its tributaries originating in the Wasatch Range no longer reach the Jordan River but instead are diverted for agricultural or culinary uses. Several spring tributaries that occur alongside the Jordan River are rapidly being appropriated and contaminated by residential and industrial users.

Historically, the Jordan River regularly flooded its impermanent banks and meandered across its valley forming many braided channels along its course terminating in the Great Salt Lake. The Jordan River naturally followed the river continuum with steeper gradients and larger substrata upstream and more meandering channels, lower gradients, and finer sediments along its downstream reaches. Physical, chemical, and biological conditions reflected this natural gradient. Although not formally quantified and akin to Utah Lake; the Jordan River has also undergone a catastrophic ecosystem shift and will continue to function as a highly regulated and restrained urban stream into the foreseeable future.

Macroinvertebrates are perhaps the most useful biological indicators of conditions in rivers and streams, including the Jordan River and are the cornerstone of most water quality assessment programs throughout the world. The Utah Department of Water Quality (UDWQ) relies on macroinvertebrates as their sole determinant of the biological component of their water quality assessments of the Jordan River. UDWQ has delineated the Jordan River into eight Assessment Units (AU) for water quality assessment purposes. Six out of the eight Jordan River AUs are considered impaired based on a macroinvertebrate metric, O/E (UDWQ 2016). However, it goes without saying that many natural factors can contribute to differences in macroinvertebrate assemblages including seasonal shifts and changes in the river continuum from upstream to down. In addition, it is well known that many other ‘sampling errors’ can affect interpretation of assemblages including the level of taxonomic resolution and associated error, subsampling effects, and actual field sampling error.

In this preliminary analysis, I highlight differences in macroinvertebrate assemblages in the Jordan River based on spatial and temporal factors, and sampling error, and then show how these differences can affect water quality assessments.

Methods

Data set

Available data were required that used comparable macroinvertebrate sampling methods and standardized taxonomic resolution and which focused on water quality assessment in the Jordan River. Twenty-five samples were chosen from the USU/USGS BugLab Mapit website: http://wmc6.bluezone.usu.edu. These samples were collected by UDWQ for water quality assessment from 2000 until 2006. Several of the samples were collected from the same site at different years (Table 1).

Table 4.UDWQ Macroinvertebrate dataset used in this report. Data were obtained from USU/USGS BugLab Mapit website. Note: Latitude/Longitude for samples 114429, 115117, 117487, 118510, 121480, 126843, 127668, and 129968 (Bluffdale Road crossing) are incorrect in the USU/USGS website. The correct latitude/longitude for these samples is 40.48717, -111.93626.

UDWQ Sample ID	Station	Location	Lat	Long	Month	Day	Year
114429	499460	Bluffdale Road crossing	40.48638916	-111.0852814	May	2	2000
114433	499088	Newstate Canal Road crossing	40.9056015	-111.9336014	May	3	2000
114442	499417	7800 South	40.6094017	-111.9203033	May	13	2000
115117	499460	Bluffdale Road crossing	40.48638916	-111.0852814	Oct	12	2000
117487	499460	Bluffdale Road crossing	40.48638916	-111.0852814	Mar	30	2001
118510	499460	Bluffdale Road crossing	40.48638916	-111.0852814	Oct	18	2001
121480	499460	Bluffdale Road crossing	40.48638916	-111.0852814	Apr	3	2003
124961	499088	Newstate Canal Road crossing	40.9056015	-111.9336014	Nov	24	2003
126843	499460	Bluffdale Road crossing	40.48638916	-111.0852814	Oct	20	2004
127346	499088	Newstate Canal Road crossing	40.9056015	-111.9336014	Dec	1	2004
127666	4992290	1700 South	40.73361206	-111.9227753	Nov	10	2005
127667	4994101	6800 South	40.62333298	-111.9199982	Nov	10	2005

127668	499460	Bluffdale Road crossing	40.48638916	-111.0852814	Oct	4	2005
127669	499088	Newstate Canal Road crossing	40.9056015	-111.9336014	Nov	10	2005
129968	499460	Bluffdale Road crossing	40.48638916	-111.0852814	Oct	19	2006
140272	4992890	3900/4100 South Crossing	40.68611145	-111.9202805	Sep	26	2007
140273	4991890	500 North Crossing	40.78027725	-111.9377747	Sep	25	2007
140274	4994270	9000 South Crossing	40.58750153	-111.9119415	Sep	27	2007
140275	4994520	Bangerter Highway Crossing	40.52338028	-111.9210205	Sep	28	2007
141615	4994100	6400 South	40.71722412	-111.5163879	Oct	30	2008
142102	4992480	Mill Creek above confluence with Jordan River at USGS Gage Station	40.70861053	-111.9196701	Nov	9	2009
142111	4991820	Cudahy Lane above Davis S WWTP	40.84116745	-111.9499969	Nov	16	2009
142112	4991800	1000 ft below South Davis WWTP	40.84500122	-111.9524994	Nov	16	2009
142113	4992880	3300 S Crossing above confluence with Mill Creek	40.71611023	-111.9255524	Nov	9	2009
142114	4992320	1100 W 2100 S below confluence with Mill Creek	40.72499847	-111.9250031	Nov	9	2009

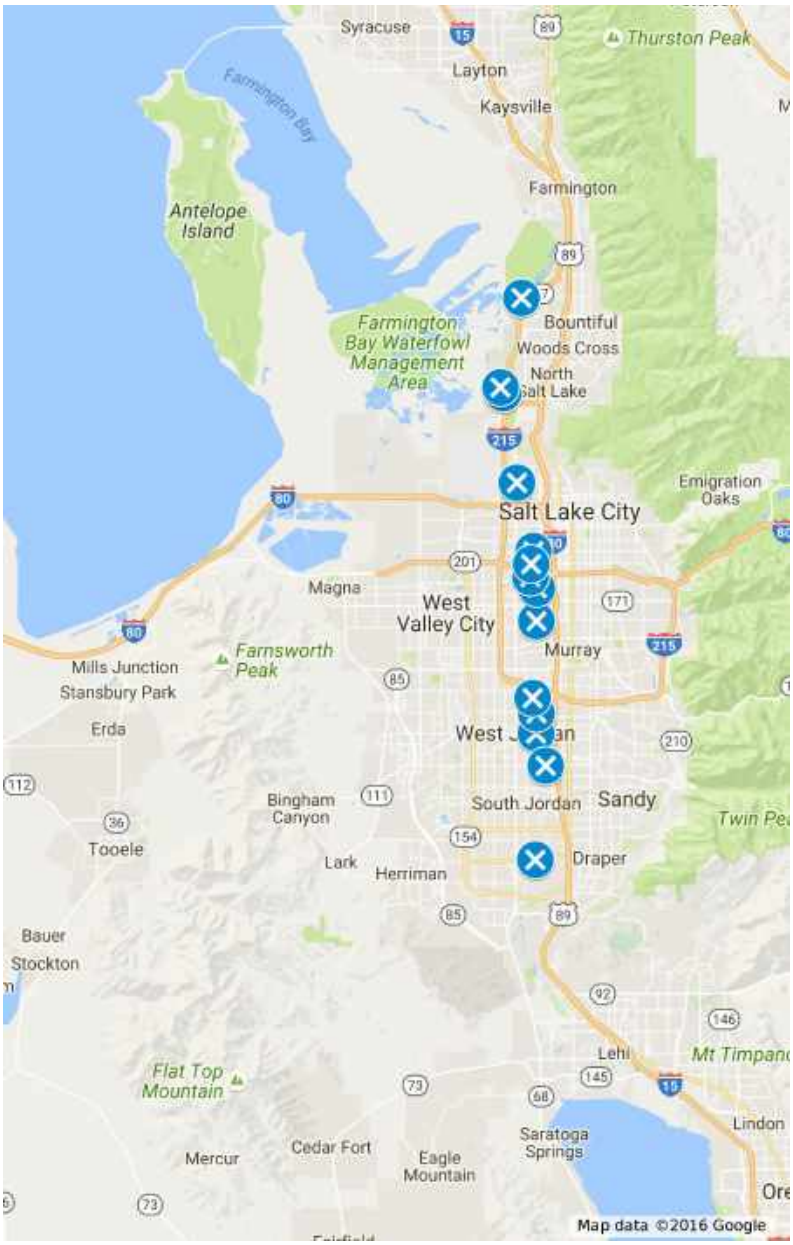

Figure 9. Map of macroinvertebrate sample locations on the Jordan River used in this analysis. Refer to UDWQ website for maps of their Jordan River assessment units.

Statistical Methods

Non metric multidimensional scaling (NMS), multiple response permutation procedure (MRPP), and Indicator Species Analyses (ISA) were performed on the macroinvertebrate dataset using PC-ORD Version 6.0 (McCune and Mefford 2011). A Sorensen Bray distance measure on log + 1 transformed macroinvertebrate abundances was used. Taxa were filtered and 'rolled up' to lower taxonomic resolution when appropriate and taxa that occurred in less than 2 of the 25 samples were eliminated. NMS and MRPP were evaluated by; month, year, UDWQ assessment unit, and % laboratory subsampled (lab split). Simple box plots of taxa abundances at each of the UDWQ assessment units were also produced.

Results

Taxa List for Jordan River

The following is a taxa list for the Jordan River based on the samples analyzed (Table 2). Richards 2016 includes a more robust list for the Jordan River.

Table 5. Complete taxa list from all samples analyzed in this report.

Aeshna

Aeshnidae

Ambrysus

Amphipoda

Anax walsinghami

Antocha monticola

Argia

Argia emma

Baetidae

Baetis

Bivalvia

Caecidotea

Caenis

Centrarchidae

Chironomidae

Chironominae

Clitellata

Coenagrionidae

Collembola

Corbicula fluminea

Corixidae

Curculionidae

Dina parva

Diptera

Dubiraphia

Elmidae

Ephemerellidae

Ephemeroptera

Erpobdellidae

Fallceon quilleri

Ferrissia

Ferrissia rivularis

Fluminicola coloradoensis

Gammarus

Gastropoda

Glossiphonia complanata

Gyraulus

Gyrinus

Helobdella stagnalis

Hemerodromia

Heptageniidae

Hetaerina

Hetaerina americana

Hyalella

Hyalella azteca

Hydrobiidae

Hydropsyche

Hydropsychidae

Hydroptila

Hydroptilidae

Isoperla

Lebertia

Lepidostoma

Leptoceridae

Leptohyphidae

Leptophlebiidae

Microcylloepus pusillus

Microcylloepus similis

Nemata

Nephelopsis obscura

Oligochaeta

Ophiogomphus

Optioservus

Optioservus quadrimaculatus

Orconectes virilis

Ordobrevia nubifera

Orthocladiinae

Physa

Pisidium

Planorbidae

Plecoptera

Potamopyrgus antipodarum

Probezzia

Psychoda

Sigara

Simuliidae

Simulium

Simulium vittatum group

Sperchon

Sperchonidae

Stenelmis

Tanypodinae

Trichoptera

Tricorythodes

Tricorythodes minutus

Trombidiformes

Turbellaria

Macroinvertebrate Assemblage Differences in the Jordan River

The best NMS ordination using all 25 samples for the entire Jordan River had a final stress of 10.17 for a 3-D solution, a final instability of < 0.00001 for 91 iterations. R^2 values for Axis 1 =0.51, Axis 2 = 0.28, and Axis 3 = 0.12 for a cumulative R^2 of 0.90 (Figure 2 and 3). There was an observable statistically significant difference in macroinvertebrate assemblages between months (Figure 2 and 3, MRPP; *A* = 0.10, p = 0.002). For additional MRPP comparisons between months see Appendix 2.

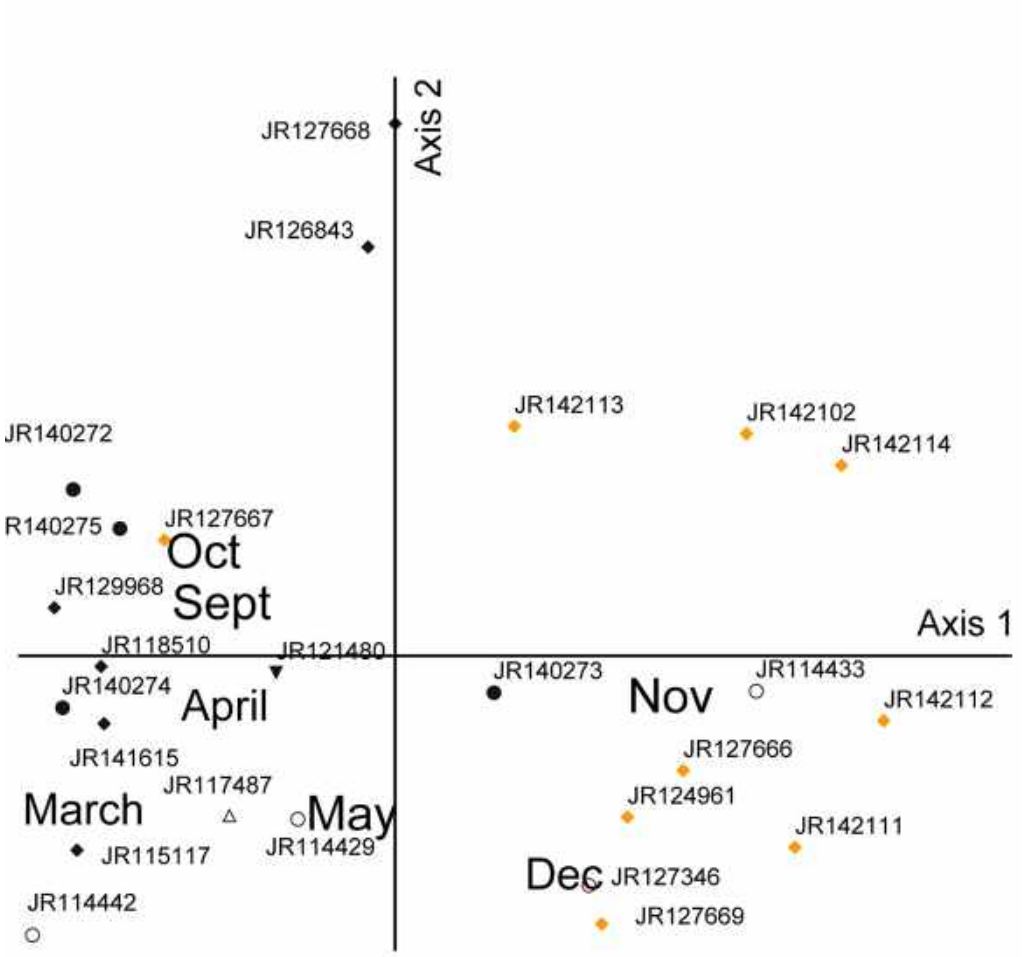

Figure 10. NMS ordination axes 1and 2 with month centroids added.

JR127668 (Jordan River at Bluffdale Road crossing October 2005) and JR126843 (Jordan River at Bluffdale Road crossing October 2004) separated out by themselves along Axis 2 in the upper left quadrant (Figure 2)(See following NMS/MRPP sections for addition comparisons).

JR142102 was the sample collected from Mill Creek near the confluence with the Jordan River and was similar to JR142114 the Jordan River at 1100W 2100 S below the confluence with Mill Creek in Figure 2 but the Mill Creek sample separated away from other samples in Figure 3 (axis 1 vs. axis 3) except for JR142113 the Jordan River sample collected at 3300 South just upstream of confluence with Mill Creek.

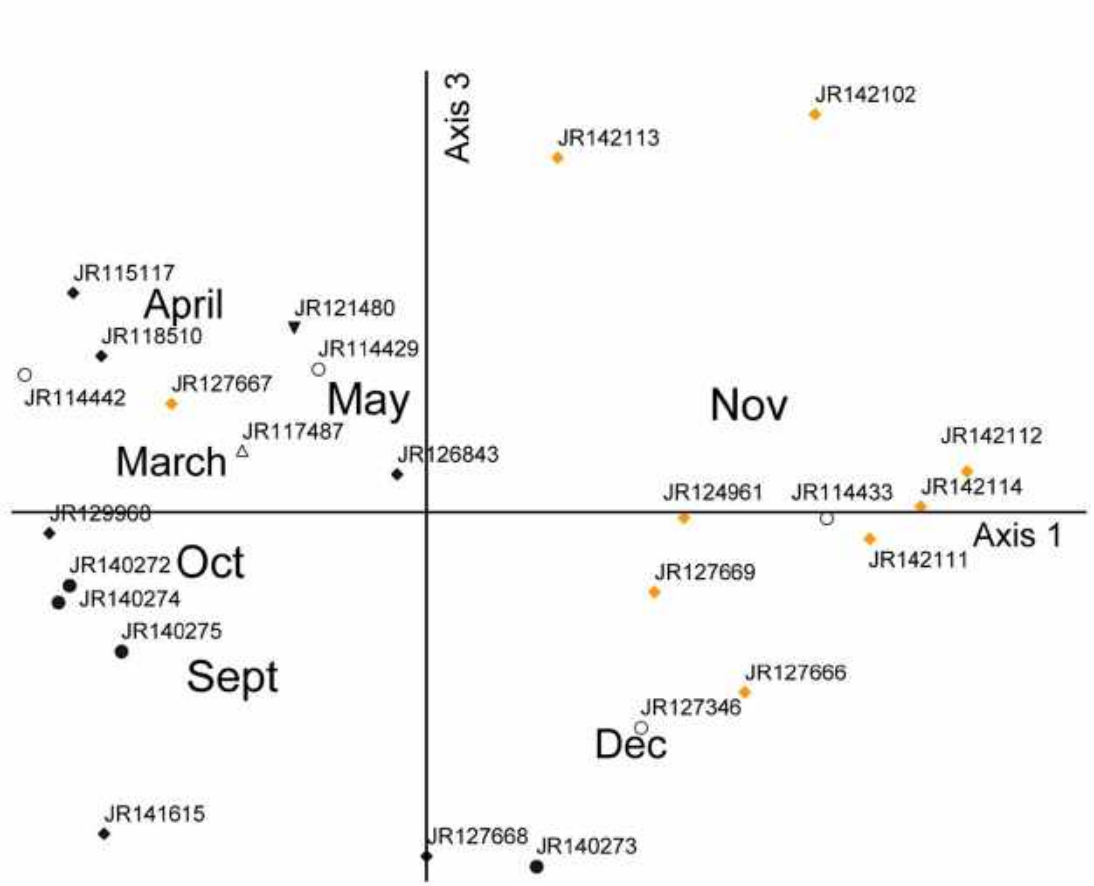

Figure 11. NMS ordination axes 1and 3 with month centroids added.

Macroinvertebrate assemblages also clearly differed between UDWQ Assessment Units, with Unit 1 (furthest downstream unit) and Unit 2 significantly differing than the other units (Figure 4, MRPP; A = 0.15, $p < 0.001$). The largest within unit variability in assemblages was Assessment Unit 7, the upstream unit and Assessment Unit 4, which also included a Mill Creek sample (labelled JR142102). For addition MRPP comparisons see Appendix 2.

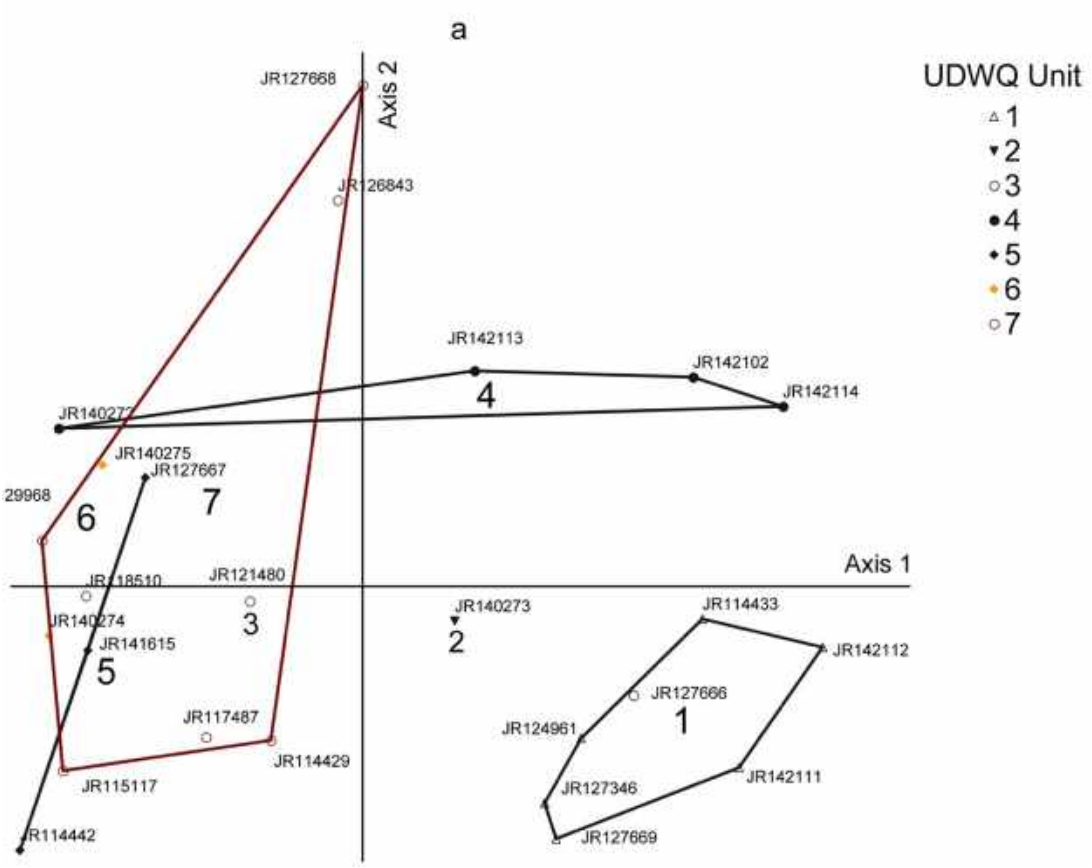

Figure 12. NMS ordination axes 1 and 3 with UDWQ Assessment Unit centroids added. UDWQ Units 1, 2, 3, 4, 6, and 7 were listed as impaired (UDWQ 2016).JR142102 is a sample collected from Mill Creek near the Jordan River.

UDWQ listed Units, 1, 2, 3, 4, 6, and 7 as impaired but not Unit 5 however, the NMS results (Figure 4) suggest that Unit 5 macroinvertebrate assemblage was not much different than Units 3, 6, and 7. Note JR140272 (Unit 4) was much different than the other samples from Unit 4. This could be because the sample was collected in September compared with the other samples that were collected in November or because of spatial longitudinal differences

Macroinvertebrate assemblages were also significantly affected by lab split (% subsampled) (Figure 5).

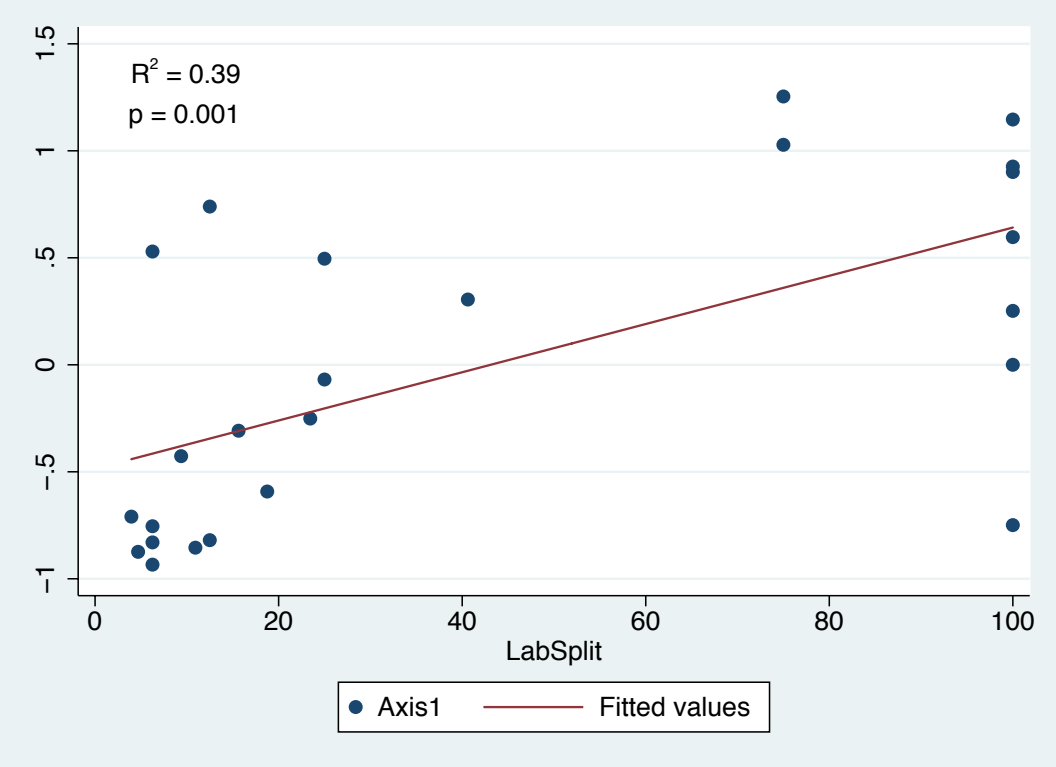

Figure 13. Linear fit model of NMS axis 1 vs. Lab Split. Y axis is NMS axis 1 score.

Taxa Abundances in Assessment Units

As expected and predicted by the River Continuum Concept, individual taxa varied in abundances between UDWQ Assessment Units (Figure 6).

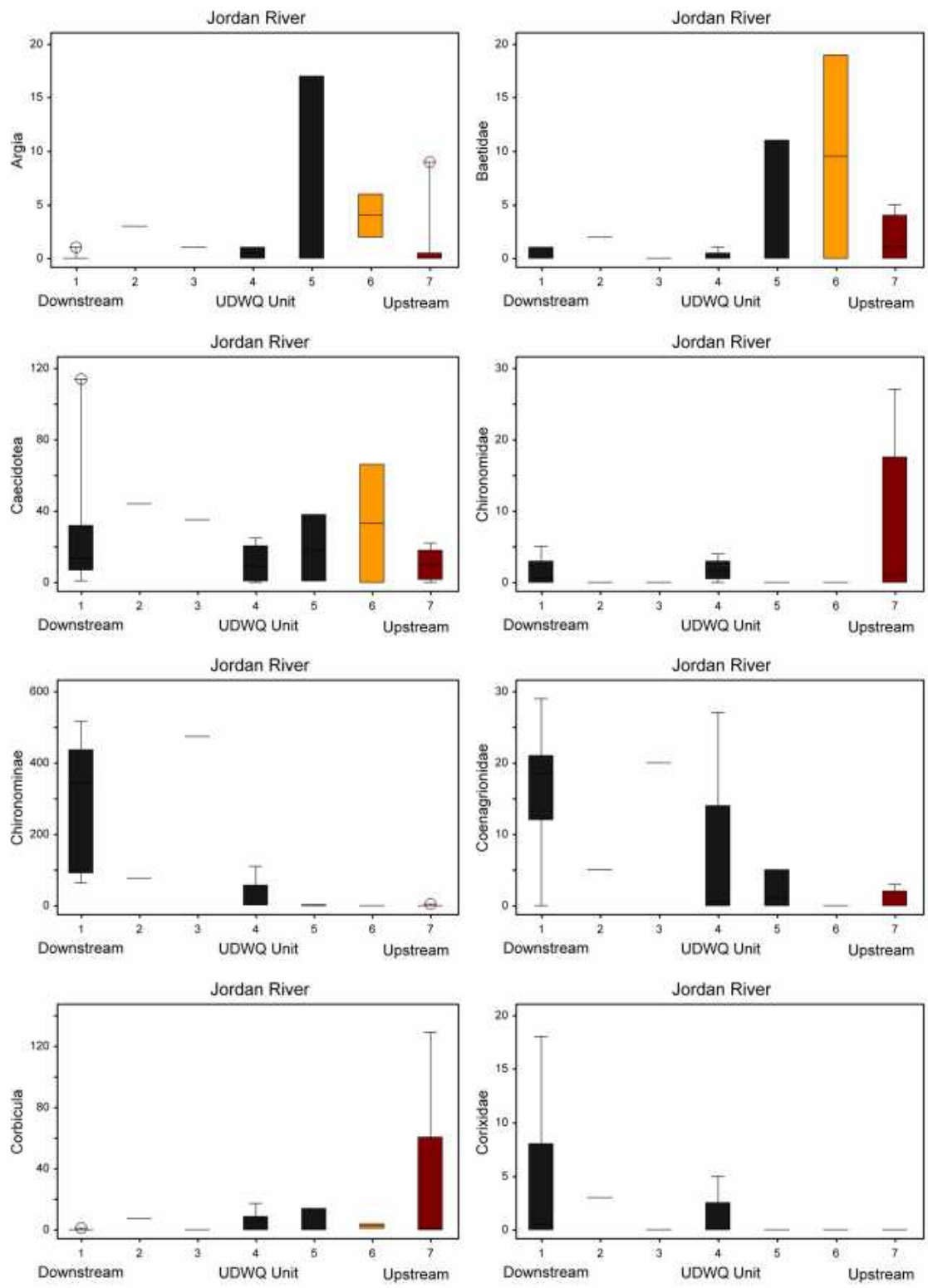
Jordan River
Argia
Baetidae
Caecidotea
Chironomidae
Chironominae
Coenagrionidae
Corbicula
Corixidae
Downstream
UDWQ Unit
Upstream

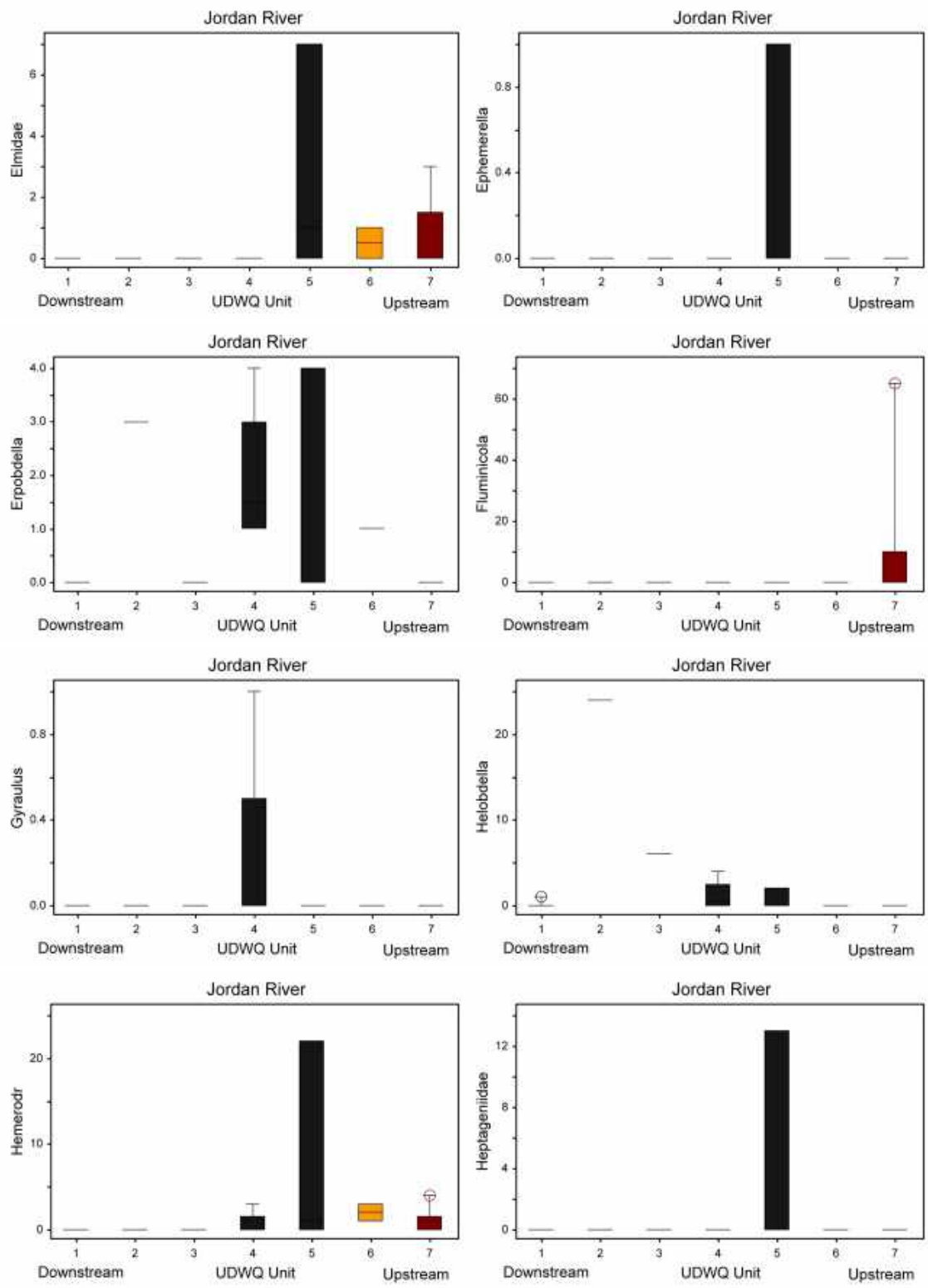
Jordan River
Elmidae
Ephemerella
Erpobdella
Fluminicola
Gyraulus
Helobdella
Hemerodr
Heptageniidae
Downstream
UDWQ Unit
Upstream

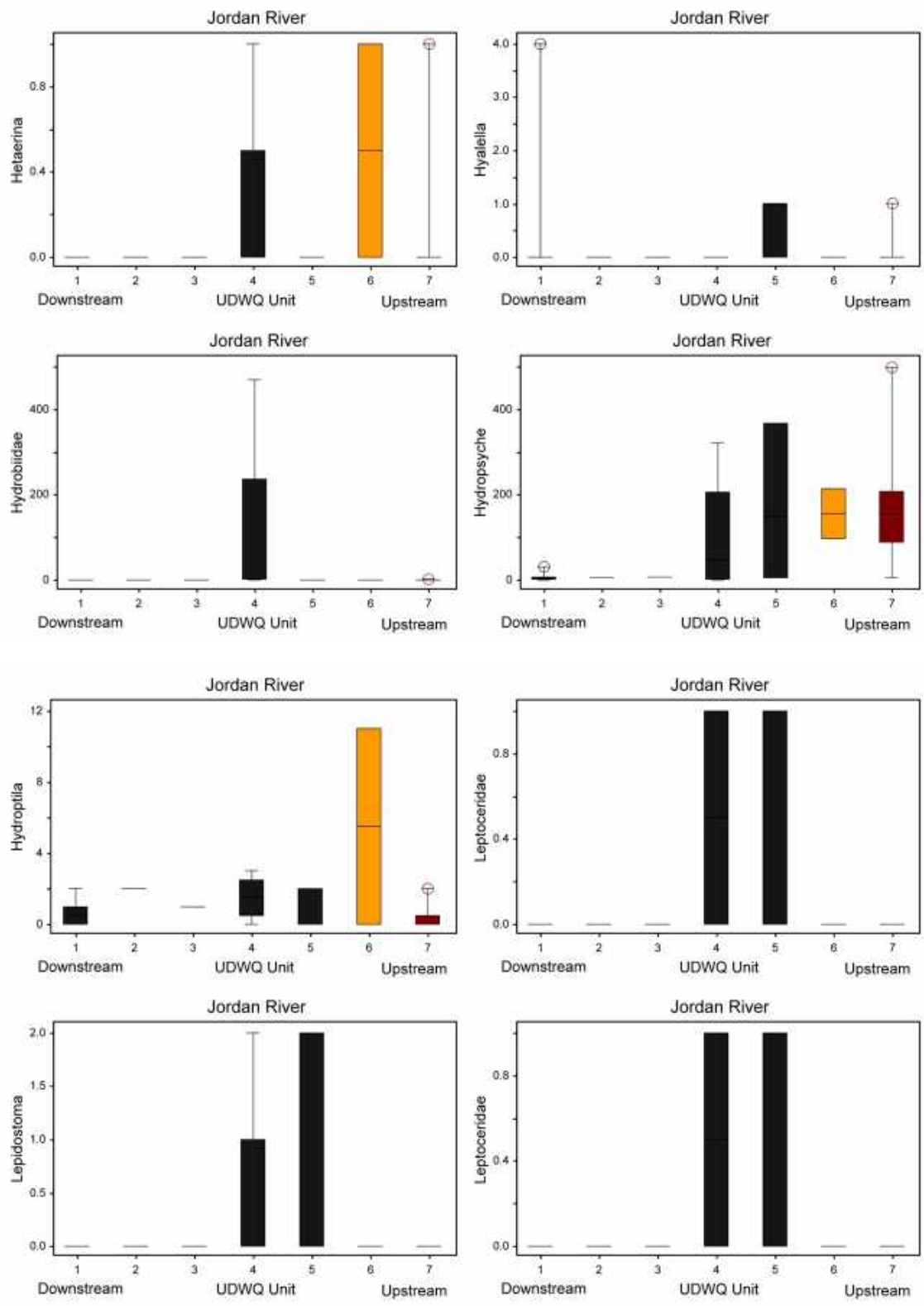
Jordan River
Hetaerina
Hyalella
Hydrobiidae
Hydropsyche
Hydroptila
Leptoceridae
Lepidostoma
Leptoceridae
Downstream
UDWQ Unit
Upstream

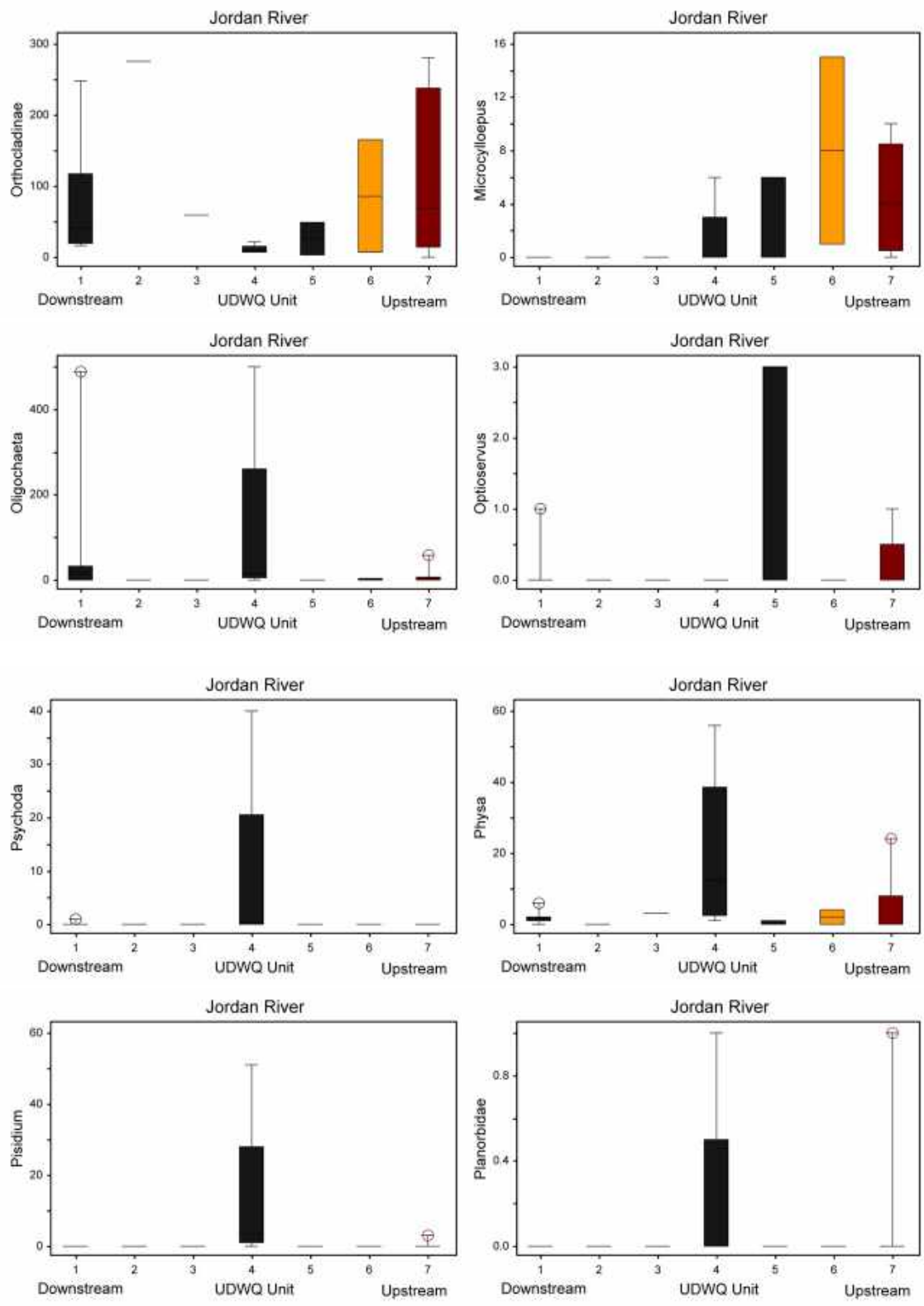
Jordan River
Orthocladinae
Microcylloepus
Oligochaeta
Optioservus
Psychoda
Physa
Pisidium
Planorbidae
Downstream
UDWQ Unit
Upstream

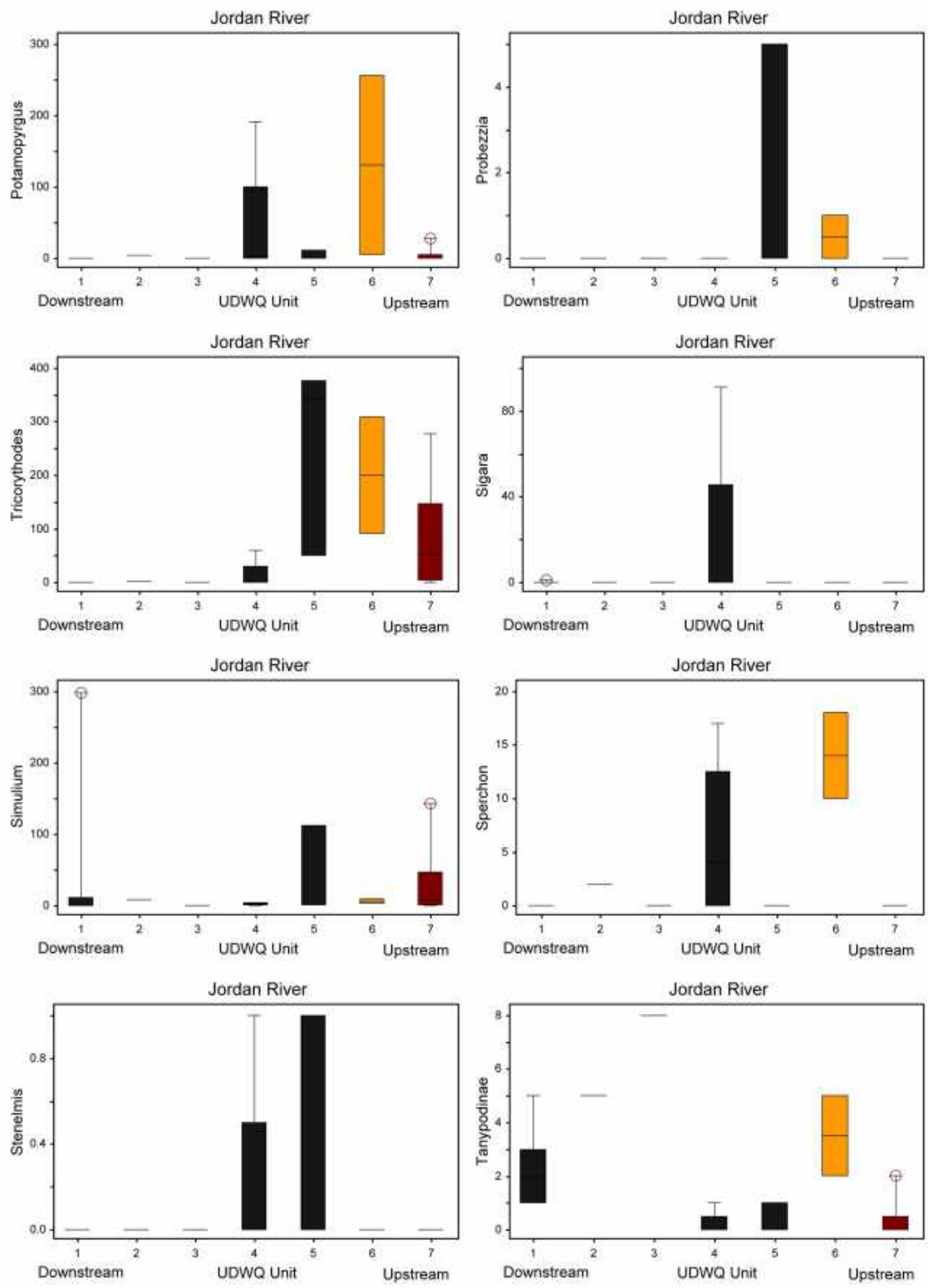
Jordan River
Potamopyrgus
Probezzia
Tricorythodes
Sigara
Simulium
Sperchon
Stenelmis
Tanypodinae
Downstream
UDWQ Unit
Upstream

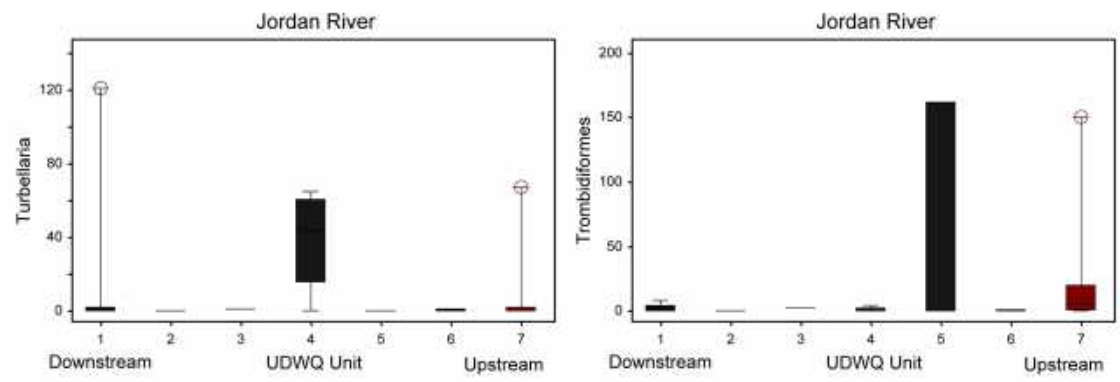

Figure 14. Macroinvertebrate taxa abundances for each of the seven UDWQ assessment units. Box plots are 25th to 75th centiles, range, and outliers.

Jordan River Assemblages Upstream vs. Downstream

Jordan River macroinvertebrate assemblages clearly and significantly differed between upstream Unit 7 and downstream Unit 1 and within these sections due to sampling, seasonal, and annual effects and water quality effects, particularly the major water diversion at 2100 South (Surplus Canal), which could have affected assemblages in the furthest downstream Units 1 and 2. The best fit NMS ordination resulted in a very good final stress = 8.02, final instability < 0.001, using 49 iterations for a 2-D solution (Figure 7). Axis 1 R^2 = 0.41 and Axis 2 R^2= 0.51 for a cumulative R^2 = 0.92. MRPP A = 0.2, p < 0.001.

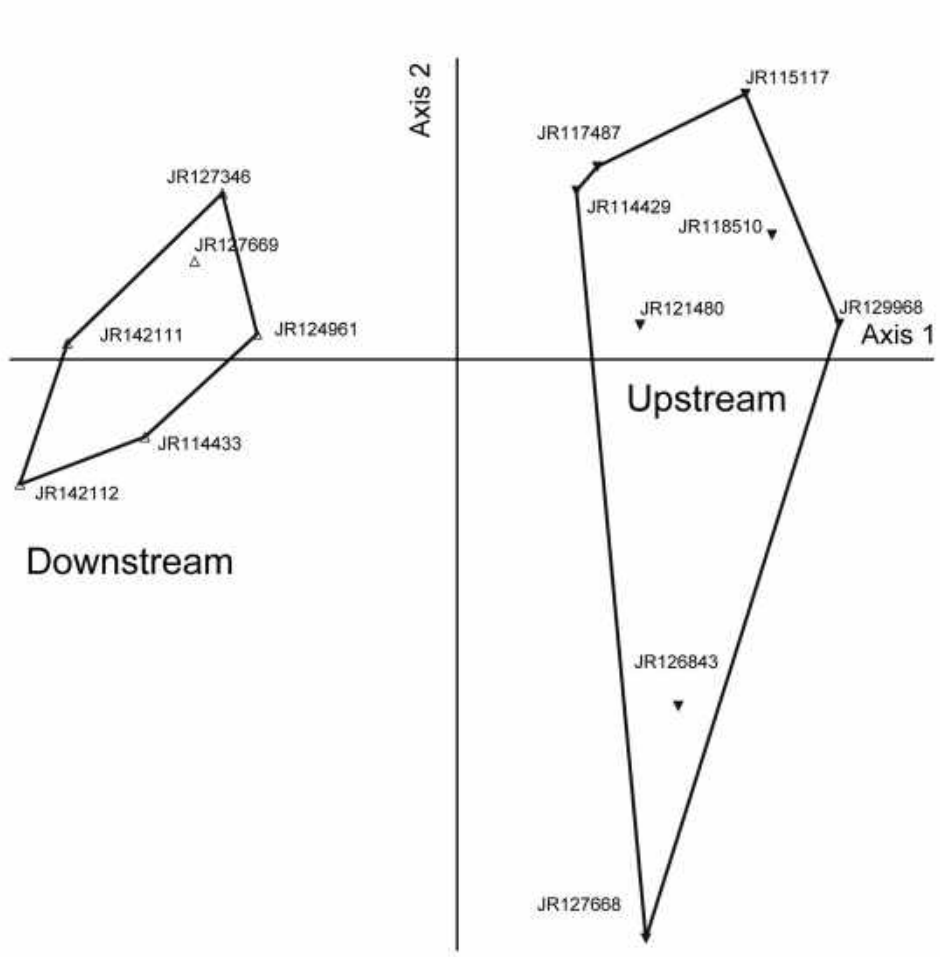

Figure 15. NMS Axis 1 and 2 for Jordan River macroinvertebrate samples from UDWQ Assessment Unit 1 (furthest downstream) and Assessment Unit 7 (furthest upstream).

One of the reasons upstream (Unit 1) and downstream (Unit 7) assemblages differed so much was because a large proportion of the Jordan River is diverted into Surplus Canal at 2100 South and flows are greatly diminished downstream. However, the Jordan River also changes character naturally from upstream to downstream and the taxa clearly showed this (Figure 6).

Indicator Taxa

Several taxa were significantly more abundant either upstream or downstream and are useful indicators using Indicator Taxa Analysis (Table 3).

Table 6. Taxa that were significant indicators of either upstream or downstream macroinvertebrate assemblages using Indicator Taxa Analysis.

Downstream				
Taxon	Observed	IV	IV	p

	Indicator Value (IV)	Mean	Std Dev	
Chironominae	93.6	45.6	11	0.0018
Tanypodinae	83.4	42	10.75	0.0048
Coenagrionidae	70.7	42	10.94	0.0204
Corixidae	50	23.6	10.99	0.0566

Upstream				
Taxon	Observed Indicator Value (IV)	IV Mean	IV Std Dev	p
Hydropsyche	78.2	55.3	6.51	0.0004
Microcylloepus	75	35.3	11.33	0.0138
Tricorythodes	75	35.5	11.21	0.016
Hemerodromia	62.5	31.6	11.89	0.0316

As shown earlier in Figure 2, the most variability in assemblages occurred in the Upstream section (assessment unit 7). This was primarily due to two samples, JR126843 collected October 2004 and JR127668 collected October 2005. This variability prompted the following multivariate analysis.

Annual Assemblage Differences in Upstream Unit 7 in October

The macroinvertebrate samples collected from Assessment Unit 7 in October were also clearly and statistically different between years. 2004 and 2005 October samples were much different than 2000, 2001, and 2006 samples. The best fit NMS ordination had an extremely low and highly accurate final stress of 0.0001, < 0.0001 instability, using 26 iterations for a 1-D solution. Axis 1 R^2 was 0.67.

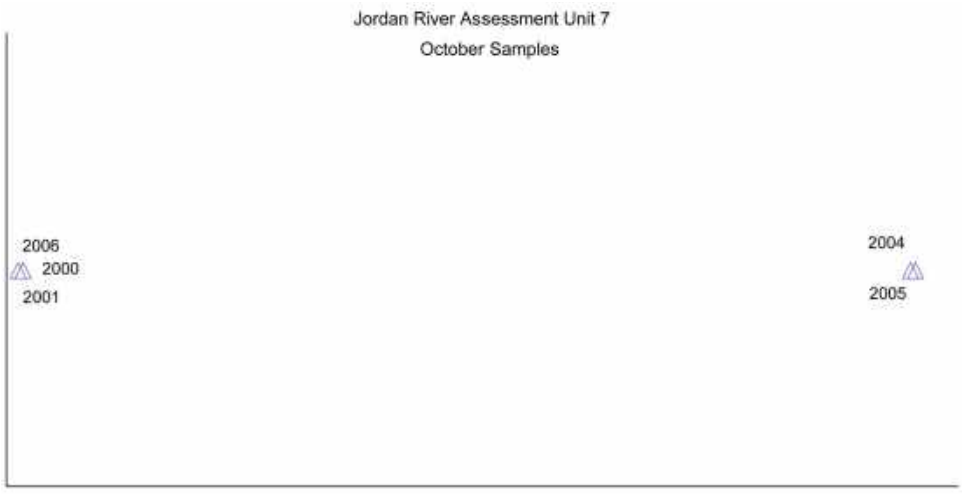

Figure 16. NMS ordination Axis 1 for macroinvertebrate samples collected by UDWQ at Assessment Unit 7 in October at five different years.

Taxa responsible for these differences were mostly more Tricorythodes, Hydropsyche, Orthocladinae, Argia, and Oligochaetes in the 2000, 2001, and 2006 samples vs. more Physa, Corbicula, Fluminicola, Caecidotea, and Coenagrionidae found in the 2004 and 2005 samples (Table 4).

Table 7. Correlations (r)between macroinvertebrate taxa and Axis 1 of the NMS ordination of UDWQ Assessment Unit 7 October samples.

Taxon	r
Tricoryt	-0.988
Hydropsy	-0.881
Orthocla	-0.831
Oligocha	-0.666
Argia	-0.545
Hemerodr	-0.433
Dina	-0.412
Elmidae	-0.406
Hydrobii	-0.406
Hydropti	-0.406
Optioser	-0.406

Simulium	-0.192
Chrnmida	-0.166
Baetidae	-0.096
Trombidi	0.243
Potamopy	0.304
Turbella	0.49
Microcyl	0.549
Coenagri	0.72
Caecidot	0.882
Fluminic	0.98
Corbicul	0.993
Physa	0.996

The NMS axis was also strongly correlated with percent lab split (r = 0.75) which was a function of the number of individuals encountered in a sample. The more individuals in a sample, the greater the percentage needed to be subsampled (labsplit) to meet standardized count criteria. Richards 2016 showed the relationship between labsplit, evenness and taxa richness and how these can negatively affect O/E scores.

Table 8. Sample ID, year, and % subsampled UDWQ macroinvertebrate samples from Assessment Unit7 collected in October.

Sample ID	Year	Lab-Split (% subsampled)
JR115117	2000	12.50
JR118510	2001	6.25
JR126843	2004	25.00
JR127668	2005	100.00
JR129968	2006	4.68

Discussion and Conclusion

Although the Jordan River is obviously impaired; much of the differences in macroinvertebrate samples in the Jordan River can be explained by seasonality, sampling error, subsampling effects, and the river continuum. It is more difficult to explain why there were more Physa, Corbicula, Fluminicola, Caecidotea, and Coenagrionidae found in the 2004 and 2005 upstream samples and more Tricorythodes, Hydropsyche, Orthocladinae, Argia, and Oligochaetes in the 2000, 2001, and 2006 upstream samples even though all of these samples were collected in October. Tricorythodes, Orthocladinae, and Argia are short lived taxa and their abundances can change annual more so than the other taxa. Physa are more typically found in the slower, shoreline sections. Perhaps samples were taken along the shoreline in 2004/2005. Corbicula are now abundant throughout the Jordan River and because they are relatively long lived they should have been collected in all samples particularly in 2006 if they recently became established. Fluminicola also have overlapping generations and should have been collected in all years. The most likely explanation for these differences is sampling error, including the effects of laboratory subsampling.

Many of the samples were collected at assessment unit boundaries. Samples collected at boundaries need to be consistently included in the unit immediately upstream because macroinvertebrate assemblages are determined by upstream conditions not downstream conditions. Future samples should be centered within the unit not at the boundaries. UDWQ Assessment Unit boundaries should be adjusted based on changes in macroinvertebrate assemblages and not on other less informative variables (e.g. fish assemblages, DO, convenient landmarks, etc.) and after more samples are collected and analyzed. O/E assessments and other water quality assessments need to reflect this, which can substantially improve assessment conclusions.

Differences in Unit 7 October samples could easily have been due to annual variation in taxa abundances and were also likely due to the percentage subsampled (lab- split). Other factors could have been involved such as sampling error (e.g. location differences, uneven compositing from non-riffle habitat, or taxonomic resolution). It is also possible that some type of impairment affected these assemblages in differing years, however I am not aware of any changes in Unit 7 during these years, particularly 2004 and 2005. Further investigation into any events such as high flow years, dewatering, habitat alterations needs to be conducted. The very discernable differences in assemblages reported from samples collected in the same assessment unit and the same month certainly affected any water quality assessments even if no perturbation occurred during the years sampled. At this time, it is unknown if UDWQ used the same O/E scoring criteria for all assessment units to conclude that most units in the Jordan River were impaired. However, the most recent UDWQ Integrative Report (2016) states that O/E models are based on at least eleven ‘watershed’ based climate/environmental variables without defining ‘watershed’. The Jordan River watershed drains over 3800 square miles with elevations ranging from 11,900 ft. to 4200 ft. (http://www.utahcleanwater.org/jordan-river-watershed.html) and the Jordan River is an atypical unique river because its headwaters is a very large, shallow, slightly saline, eutrophic lake. Assigning impaired status to UDWQ Jordan River Assessment Units could have been inappropriate if UDWQ used the entire Jordan River watershed, as was detailed in their 2016 IR, to

develop O/E models and averaged watershed “E” (expected) taxa probabilities of capture for final O/E scores.

Finally, highly regulated urban rivers such as the Jordan River cannot be compared to reference rivers or hypothetical ‘average watershed’ macroinvertebrate assemblages. Highly regulated, urban rivers and their macroinvertebrate assemblages will never be able to achieve reference condition or expected (E) values because they have been irreversibly altered and compromised. New assessment methods need to be developed to assess and monitor the desired unnatural conditions of urban rivers, including the Jordan River.

Recommendations

Because this was a preliminary analysis, more documentation and analyses of the physical and chemical conditions of the Jordan River is highly recommended. Physical and chemical data were likely collected by UDWQ at the same time macroinvertebrate samples were collected. Additional macroinvertebrate samples and physical and chemical data are also needed to assess conditions, particularly if no samples have been collected in the last several years. Regulatory metrics such as the O/E metric need to be adjusted to reflect sampling error, natural variability, and ‘watershed’ representativeness in the assemblages. O/E metrics also need to be revised to account for the now inescapable permanent condition of the Jordan River; a highly regulated and exceedingly managed urban river. UDWQ Assessment Units should be adjusted based on the best bio-predictors of water quality, macroinvertebrates.

Literature Cited

McCune, B. and J. Mefford. 2011. PC-ORD. Multivariate Analysis of Ecological Data. Version. 6.22. MjM Software, Gleneden Beach, Oregon.

Richards, D. C. 2016. Is reliance on RIVPACS O/E models for monitoring water quality in Utah prudent? Draft Technical Report to: Jordan River/Farmington Bay Water Quality Council. OreoHelix Consulting. August 14. 32 pages.

UDWQ. 2016. Utah’s Draft 2016 Integrated Report. Salt Lake City, Utah. Utah Department of Environmental Quality.

Appendices

Appendix 10. NMS sample Axes 1,2, and 3

JR114429	-0.25146	-0.41853	0.33293
JR114433	0.92628	-0.08856	-0.01144
JR114442	-0.93414	-0.71781	0.32096
JR115117	-0.81923	-0.50179	0.50770
JR117487	-0.42682	-0.41176	0.14353
JR118510	-0.75473	-0.02641	0.36261
JR121480	-0.30773	-0.04072	0.42941
JR124961	0.59670	-0.41396	-0.01281
JR126843	-0.06890	1.05133	0.08723
JR127346	0.49564	-0.58994	-0.49939
JR127666	0.73958	-0.29589	-0.41694
JR127667	-0.59258	0.29737	0.25318
JR127668	0.00020	1.36699	-0.79838
JR127669	0.52903	-0.68851	-0.18530
JR129968	-0.87418	0.12582	-0.05000
JR140272	-0.83012	0.43177	-0.16770
JR140273	0.25204	-0.09307	-0.81922
JR140274	-0.85499	-0.13335	-0.20668
JR140275	-0.70967	0.33032	-0.32007
JR141615	-0.74947	-0.17336	-0.74556
JR142102	0.90119	0.57110	0.92485
JR142111	1.02803	-0.49350	-0.06050
JR142112	1.25422	-0.16619	0.09322
JR142113	0.30475	0.58850	0.82399

JR142114	1.14637	0.49017	0.01440

Appendix 11. NMS macroinvertebrate Axes 1, 2 and 3.

Aeshnida	0.85117	-0.37234	-0.27905
Ambrysus	-0.59258	0.29737	0.25318
Argia	-0.41477	0.14812	-0.07331
Baetidae	-0.39807	0.02388	-0.24702
Caecidot	0.14818	-0.00292	-0.04674
Chrnmida	0.13199	-0.08282	0.30684
Chrnmina	0.57648	-0.22309	-0.15906
Clitella	0.64614	-0.41472	-0.32886
Coenagri	0.57951	-0.06881	-0.08094
Corbicul	-0.31674	0.50076	-0.31858
Corixida	0.80561	-0.10376	0.05252
Dina par	-0.62135	-0.32342	0.47741
Diptera	0.43318	-0.28181	-0.01784
Elmidae	-0.63837	-0.03233	0.09106
Ephemere	-0.74947	-0.17336	-0.74556
Ephemero	-0.25146	-0.41853	0.33293
Erpobdel	-0.11132	0.22246	-0.10709
Ferrissi	0.29696	-0.13489	-0.71412
Fluminic	-0.02888	1.23414	-0.42567
Gyraulus	1.14637	0.49017	0.01440
Helobdel	0.49781	-0.02410	-0.39367
Hemerodr	-0.64541	0.16762	0.03120
Heptagen	-0.93414	-0.71781	0.32096
Hetaerin	-0.42637	0.34821	0.15131
Hyalella	-0.09146	-0.38090	-0.28363

Hydrobii	0.34928	0.45914	0.58030
Hydropsy	-0.37914	-0.00201	0.07180
Hydropti	-0.03496	0.06211	-0.03480
Lebertia	0.47221	0.27085	-0.31673
Lepidost	-0.22236	0.20757	0.03922
Leptocer	0.02727	0.30067	0.08650
Leptohyp	-0.75473	-0.02641	0.36261
Leptophl	-0.42682	-0.41176	0.14353
Microcyl	-0.53569	0.40419	-0.03814
Nemata	0.08958	0.19893	0.63402
Oligocha	0.48947	0.00855	0.23847
Optioser	-0.41315	-0.20076	-0.23970
Orthocla	-0.00670	-0.13473	-0.00156
Physa	0.48292	0.44196	0.03948
Pisidium	0.10703	0.61922	0.37580
Planorbi	0.44746	0.03582	0.17367
Potamopy	-0.43404	0.37628	-0.36245
Probezzi	-0.66578	0.17722	0.12491
Psychoda	0.98250	0.45989	0.68808
Sigara	1.16071	0.40293	0.02488
Simulium	-0.21914	-0.04498	-0.01282
Sperchon	-0.48511	0.26817	-0.08780
Stenelmi	-0.14391	0.44293	0.53858
Tanypodi	0.31493	-0.22715	-0.22922
Tricoryt	-0.69888	-0.12650	0.02404
Trombidi	-0.20189	0.12506	0.10621
Turbella	0.49961	0.37988	0.28728

Appendix 12.MRPP results by month.

Month

```
Chance-corrected within-group agreement, A =  0.10072408

     A = 1 - (observed delta/expected delta)

     Amax = 1 when all items are identical within groups (delta=0)

     A = 0 when heterogeneity within groups equals expectation by chance

     A < 0 with more heterogeneity within groups than expected by chance


    Probability of a smaller or equal delta, p =  0.00244195
```

PAIRWISE COMPARISONS

Note: p values not corrected for multiple comparisons.

	T	A	p
May vs. October	0.25213146	0.00884007	0.35708513
May vs. November	0.05271432	0.00152494	0.42022471
May vs.September	1.55764143	0.06474327	0.06907140
October vs.November	4.64619396	0.10481584	0.00154419
October vs. September	0.86654643	0.02600541	0.18612781
November vs.September	4.08158040	0.12323943	0.00353617

Appendix 13. MRPP by UDWQ Assessment Unit

```
Identifiers for excluded groups:
         2
         3


    Groups were defined by values of: UDWQ Uni
    Input data has:   23 Samples by   52 Taxa
    Weighting option: C(I) = n(I)/sum(n(I))
    Distance measure: Sorensen (Bray-Curtis)


   GROUP:   1
Identifier:   7
   Size:   8   0.52998185  = Average distance
Members:
 JR114429 JR115117 JR117487 JR118510 JR121480 JR126843 JR127668 JR129968


   GROUP:   2
Identifier:   1
   Size:   6   0.42141123  = Average distance
Members:
 JR114433 JR124961 JR127346 JR127669 JR142111 JR142112


   GROUP:   3
Identifier:   5
   Size:   3   0.59540733  = Average distance
Members:
 JR114442 JR127667 JR141615
```

```
   GROUP:   4
Identifier:   4
   Size:   4   0.61634908  = Average distance
Members:
 JR140272 JR142102 JR142113 JR142114

   GROUP:   5
Identifier:   6
   Size:   2   0.42817768  = Average distance
Members:
 JR140274 JR140275

    Test statistic: T =   -4.9146274
      Observed delta =   0.51636069
      Expected delta =   0.60872260
    Variance of delta =   0.35318691E-03
    Skewness of delta =   -0.50886650

    Chance-corrected within-group agreement, A =  0.15173070
     A = 1 - (observed delta/expected delta)
     Amax = 1 when all items are identical within groups (delta=0)
     A = 0 when heterogeneity within groups equals expectation by chance
     A < 0 with more heterogeneity within groups than expected by chance

    Probability of a smaller or equal delta, p =  0.00008412
```

PAIRWISE COMPARISONS

Note: p values not corrected for multiple comparisons.

Groups (identifiers)

Compared	T	A	p
7 vs. 1	-6.69399161	0.17355259	0.00012495
7 vs. 5	0.66847261	-0.01898252	0.72674698
7 vs. 4	-2.38142907	0.06656315	0.02730797
7 vs. 6	-0.47524985	0.01958275	0.24143208
1 vs. 5	-4.14904785	0.17225330	0.00240940
1 vs. 4	-3.84048188	0.11366991	0.00274305
1 vs. 6	-3.76897841	0.22797295	0.00809950
5 vs. 4	-1.48355332	0.07606936	0.08465916
5 vs. 6	0.40392234	-0.02181514	NaN
4 vs. 6	-0.75705657	0.07703657	0.21191159

********** MRPP finished **********

10 Aug 2016, 16:59:52

Appendix 14. MRPP by Year

Identifiers for excluded groups:

2006

2008

Groups were defined by values of: Year

Input data has: 23 Samples by 52 Taxa

```
    Weighting option: C(I) = n(I)/sum(n(I))

    Distance measure: Sorensen (Bray-Curtis)


   GROUP:   1

Identifier: 2000

   Size:   4   0.57616850  = Average distance

Members:

 JR114429 JR114433 JR114442 JR115117


   GROUP:   2

Identifier: 2001

   Size:   2   0.36443168  = Average distance

Members:

 JR117487 JR118510


   GROUP:   3

Identifier: 2003

   Size:   2   0.49666446  = Average distance

Members:

 JR121480 JR124961


   GROUP:   4

Identifier: 2004

   Size:   2   0.69450498  = Average distance

Members:

 JR126843 JR127346


   GROUP:   5
```

```
Identifier: 2005
   Size:   4   0.59811219  = Average distance
Members:
 JR127666 JR127667 JR127668 JR127669

   GROUP:   6
Identifier: 2007
   Size:   4   0.45090043  = Average distance
Members:
 JR140272 JR140273 JR140274 JR140275

   GROUP:   7
Identifier: 2009
   Size:   5   0.52126362  = Average distance
Members:
 JR142102 JR142111 JR142112 JR142113 JR142114

    Test statistic: T =   -3.0722786
      Observed delta =   0.53122804
      Expected delta =   0.60577188
    Variance of delta =   0.58871135E-03
    Skewness of delta =   -0.31823663

    Chance-corrected within-group agreement, A =  0.12305597
     A = 1 - (observed delta/expected delta)
     Amax = 1 when all items are identical within groups (delta=0)
     A = 0 when heterogeneity within groups equals expectation by chance
     A < 0 with more heterogeneity within groups than expected by chance
```

Probability of a smaller or equal delta, p = 0.00316615

PAIRWISE COMPARISONS

Note: p values not corrected for multiple comparisons.

Groups (identifiers)

Compared	T	A	p
2000 vs. 2001	0.03763096	-0.00161876	0.45489719
2000 vs. 2003	0.03227199	-0.00273200	0.43564372
2000 vs. 2004	-0.05221852	0.00378331	0.42477378
2000 vs. 2005	-0.68636818	0.03125192	0.19663127
2000 vs. 2007	-2.15130341	0.08303194	0.02093223
2000 vs. 2009	-2.30615495	0.10649360	0.03155842
2001 vs. 2003	-1.14584772	0.08272332	NaN
2001 vs. 2004	-0.76802794	0.08283086	NaN
2001 vs. 2005	-1.43872743	0.12195933	0.08751927
2001 vs. 2007	-1.85908602	0.10849158	0.04403912
2001 vs. 2009	-2.78681255	0.20321745	0.01496853
2003 vs. 2004	0.78856413	-0.10042125	NaN
2003 vs. 2005	-0.24282238	0.01758170	0.39029419
2003 vs. 2007	-1.65612660	0.12478133	0.06245641
2003 vs. 2009	-1.55599105	0.07758326	0.07148734
2004 vs. 2005	0.81794716	-0.08024633	0.78591231
2004 vs. 2007	-0.74756948	0.04883706	0.21328981
2004 vs. 2009	-0.63125946	0.03532870	0.25122520

```
  2005 vs.  2007   -1.72772094  0.08789296  0.06336632

  2005 vs.  2009   -2.75126544  0.09534575  0.01382705

  2007 vs.  2009   -3.88369488  0.19817894  0.00538565

------------------------------------------------------------------

****************************** MRPP finished ******************************

10 Aug 2016, 17:02:10
```

Appendix 15. NMS axis 1 and 2 Jordan River UDWQ Asssessment Unit 7

```
JR114429   0.33746   0.47649

JR114433  -0.88169  -0.22025

JR115117   0.81374   0.75000

JR117487   0.39611   0.54699

JR118510   0.88902   0.35158

JR121480   0.51490   0.09774

JR124961  -0.56378   0.07215

JR126843   0.62465  -0.98037

JR127346  -0.66254   0.46975

JR127668   0.53183  -1.63792

JR127669  -0.74071   0.27884

JR129968   1.07759   0.10265

JR142111  -1.10054   0.04588
```

JR142112 -1.23603 -0.35351

Appendix 16. NMS axis 1 and 2 Jordan River UDWQ Asssessment Unit 7 October Samples

Samples Number	Name	Axis 1
1	JR115117	-0.8240
2	JR118510	-0.8127
3	JR126843	1.2191
4	JR127668	1.2304
5	JR129968	-0.8127

Chapter 9

Is Reliance on a Single Bioassessment Metric for Assessing Water Quality in Utah's Rivers and Streams Prudent?

By

David C. Richards, Ph. D.

OreoHelix Ecological

SUMMARY

Utah is blessed with many irreplaceable rivers and streams despite being the 2nd driest state in the USA. Utah's human population, water demands, and booming economy are growing exponentially throughout much of the state and are completely depend on increasingly limited clean water supplies. Evaluating and protecting the health of Utah's rivers and streams is now crucial and will become even more so into the foreseeable future and is reliant on whose citizens and economy are well positioned to appreciate and fund protection.

The State of Utah Department of Water Quality (UDWQ) is responsible for assessing, monitoring, and protecting the 'physical, chemical, and biological integrity' of its waters based on the Clean Water Act (CWA) and by UDWQ's designated 'beneficial uses' under state law. Biological integrity is the cornerstone upon which the health of a river or stream is measured, and biological assessments are one of the most important and useful management tools available for restoring and maintaining biological integrity. Bioassessments have been developed for many years and are widely used by management agencies for wadeable waters throughout the world, however, Utah is the only state in the western USA that entrusts its river and stream bioassessments entirely to a single taxa richness based metric, "River Invertebrate Prediction and Classification System" (RIVPACS O/E). All other western state water quality programs in the region integrate multimetric methods. O/E models are complex and are based on many assumptions and generalizations; some of which lead to a poor evaluation of biological integrity. An impaired listing based on O/E can have significant economic penalties on water users. Consequently, the reliance on any single metric such as O/E in a bioassessment program may not be prudent.

A statistical evaluation of O/E as it relates to evenness and other metrics and the effects of subsampling on these metrics was conducted. A discussion of the consequences of a > 50% probability of capture criterion in O/E models and their ability to actually monitor biological integrity is also discussed, as well as some other concerns including a comparison between bioassessment programs in UT and surrounding states.

Macroinvertebrate datasets were obtained from the Bureau of Land Management/Utah State University Buglab database and the Utah Department of Water Quality data that were used in their 2016 draft Integrated Report. Compatible data were merged and filtered to reduce spatial variability. Several metrics reported by the Buglab were examined; O/E score, Taxa Richness, % Labsplit, Abundance, Shannon Diversity, Simpson Diversity and Evenness. Pairwise correlations, linear and quadratic Ordinary Least Squares (OLS) regressions, simultaneous quantile regressions at the 25th, 50th, and 75th quantiles and Path Diagrams and Structural Equation Models (SEM) were developed.

Evenness and taxa richness were the most important metrics directly and indirectly effecting O/E scores. SEM results suggest that a 1 standard deviation change in evenness (0.14) equaled a 0.96 standard deviation change in O/E scores = 0.22 (0.18 to 0.26, 95% CIs). As little of a change in evenness of approximately 5% can lead to a change from an O/E score of 0.76 (fully supporting) to 0.69 (not supporting) and unrelated to impairment.

A hypothetical but realistic example of the effects of evenness and subsampling on taxa richness resulted in a detection of all taxa in the completely even sample compared to a detection of < 50% of the taxa in an uneven sample when in fact all the same taxa occurred in the original uneven and even samples. Thus, natural fluctuations in evenness in a river or stream without a loss or extinction event resulting from human caused impairment could trigger an unjustified management response from 'fully supporting' to 'not supporting'. A real-world example is the Jordan River, listed as impaired by UDWQ. Analysis showed that O/E scores should have been rated higher if the effects of subsampling and evenness were considered.

Reliance on a complicated, computationally expensive, generalized, non-site-specific metric such as that produced by a RIVPACS O/E model may not be prudent. Replacing the O/E metric with one or several of the other correlated metrics should be considered. At the minimum, these metrics should also be included in a bioassessment program. The decision to use a probability of capture $\geq$ 50% in an O/E model has very strong negative consequences for assessing the biological integrity of Utah's river or streams. Uncommon and rare taxa should always be included in ecological assessments. Detection of impacts will be enhanced by including these taxa because they are often the first to become extinct due to human disturbance. Uncommon and rare taxa have also been shown to disproportionally contribute to ecosystem function and integrity. Their unmeasured loss could fail to warn of an impending ecological shift.

Many RIVPAC O/E users continue to insist that a reduction in O/E scores reflects the extent to which taxa have become locally extinct due to human activities. This is clearly not the case. In many instances, taxa weren't lost; they just weren't found. To continue to assume that native taxa have become locally extinct because O/E scores have decreased reflects a gross misinterpretation of RIVPACS O/E models. There is also no shortage of additional informative metrics used by other state water quality management agencies, including those with fewer resources and human populations than Utah. Utah should follow suit, otherwise it will lag far behind.

Even though a RIVPACS O/E model has the potential to be a useful summary metric: its use as a stand-alone metric is not recommended. O/E relies on too many assumptions, constraints, and inherent errors that necessitates its inclusion into a more comprehensive macroinvertebrate multimetric program. Fewer incorrect assessments of impairment will be made by incorporating the O/E metric into a multimetric program than if used alone. Unfortunately, all metrics are affected by the evenness of a sample and subsampling. This phenomenon needs to be considered in any bioassessment program. The O/E probability of capture < 50% constraint results in a poor evaluation of macroinvertebrate assemblages and thus fails to measure true biological integrity. With Utah's booming economy and exponentially growing population, UDWQ now has the opportunity to build a bioassessment program worthy of its unique rivers and streams.

Table of Contents

List of Figures

List of Tables

List of Appendices

Introduction

Utah is blessed with many irreplaceable rivers and streams, including well known rivers such as the Provo, Bear, Weber, Green, Virgin, San Juan, and Colorado Rivers. Utah is also the 2nd driest state in the USA with human population and water demands increasing exponentially throughout much of the state, particularly along the Wasatch Front in the Greater Salt Lake City metropolitan area. At the same time, Utah's booming economy driven by high tech, high paying jobs has been called "the new economic Zion" (Newsweek 2010). Evaluating and protecting the health of Utah's rivers and streams is vital and will become ever more important into the foreseeable future in a state whose citizens and economy are well positioned to appreciate and fund protection.

"The most direct and effective measure of integrity of a water body is the status of its living systems".

(Karr and Chu 1997)

The State of Utah Department of Water Quality (UDWQ) is responsible for assessing, monitoring, and protecting the 'physical, chemical, and biological integrity of its waters based on the Clean Water Act (CWA) and by UDWQ's designated 'beneficial uses' under state law. Physical and chemical integrity are manifested in biological integrity. The natural biotic community can only be maintained when physical and chemical conditions are suitable and in good condition. Biological integrity is the cornerstone upon which the health of a river or stream is measured. Although physical and chemical integrity have not been well expressed by regulatory agencies; the definition and understanding of biological integrity has been conferred at length by aquatic ecologists and subsequently simplified for adoption by regulators. One of the most widely recognized definitions of biological integrity is from Karr and Dudley (1981) (adapted from Frey 1977), "the capability of supporting and maintaining a balanced, integrated, adaptive community of organisms having a species composition, diversity, and functional organization comparable to that of the natural habitat of the region". This definition implies that aquatic ecosystems operate on several levels. These parts that sustain and contribute to an aquatic ecosystem's functioning are quantifiable (Karr 1991) and need to be understood in the context of their surrounding environments and evolutionary history (Wikipedia 2014). Of course, the definition of biological integrity presented here is a condensed version taken from Karr and Dudley (1981) and there are many other aspects and definitions of biological integrity that are often ignored by management agencies but should be considered including for example, genetics and metapopulation dynamics.

Biological assessments and biocriteria are one of the most important and useful management tools available for restoring and maintaining the biological integrity of rivers and streams. Bioassessments rely on empirical knowledge of how a wide range of biological attributes responds to varying degrees of human influence (Karr 1993; Karr and Chu 1997). The most useful bioassessments explicitly embrace

several attributes of the biotic assemblages including: taxa richness, indicator taxa (e.g., tolerant and intolerant groups), and assessments of processes such as trophic structure, feeding strategies and other taxa traits. Simply stated, the goal of bioassessments is to measure and evaluate the consequences of human actions on biological systems (Karr 1993; Karr and Chu 1997).

Bioassessments have a long history and are widely used by management agencies primarily for wadeable waters (i.e. streams and small rivers) worldwide. However, Utah is the only state in the western USA that entrusts its river and stream bioassessments entirely to a single taxa-richness based metric, "River Invertebrate Prediction and Classification System" (RIVPACS O/E). All other western state water quality programs understand that river and stream ecosystems operate on several complex ecological levels and understand the importance of combining and utilizing a suite of metrics, which typically include several richness, diversity, trait, and functional metrics but may or may not include a RIVPACS O/E model.

The O/E metric is simply the relationship between the observed (O) taxa and the expected (E) taxa in a river or stream. If the number of observed taxa is less than the number of expected taxa, managers often conclude a loss of taxa and diversity and hence a loss of biological integrity and compromised water quality. However, the RIVPACS O/E model is mathematically complex and relies on several summary and averaged watershed descriptors in model construction to predict "E", under least-impaired, reference conditions. In contrast, other commonly used taxa richness, diversity, and evenness metrics are straight forward, easy to calculate, and do not rely on average watershed descriptors for development.

RIVPACs O/E models also integrate a 'probability of capture' in the development of the "E" component. UDWQ uses a 50% probability of capture level (UDWQ 2016), which effectively eliminates invertebrate taxa that occur in < 50% of its 'reference' streams. This has important consequences and can severely misjudge levels of impairment and eliminate the ability to monitor taxa that may be unique to a river or stream and which are a fundamental part of its biological integrity; i.e. taxa that are not cosmopolitan and ubiquitous. In addition, because costs of taxonomic identification are purportedly large, invertebrate samples collected by management agencies are subsampled before metrics are calculated, including O/E scores. The effects of subsampling on O/E and other metrics may be substantial and can be affected by how evenly taxa abundances occur in a river or stream and represented in a sample (evenness). Effects of subsampling and evenness can then contribute to a misinterpretation of these metrics potentially resulting in unreliable assessments of water quality.

Justification

UDWQ is the only state in the western USA that relies on a single metric, O/E, for evaluating the complex biological integrity of Utah's many diverse rivers and streams. UDWQ uses O/E to determine whether to list a river or stream as biologically impaired or not. An impaired listing based on O/E can have significant economic penalties on water users, therefore the reliance on any single metric such as O/E in a bioassessment may not be prudent. A statistical evaluation of O/E as it relates to evenness and other metrics and the effects that subsampling has on these metrics was needed. A discussion of the consequences of a > 50% probability of capture criterion on actually monitoring biological integrity also needed to be addressed, as well as a comparison between bioassessment programs in UT and surrounding states.

Methods

Dataset

Macroinvertebrate datasets were obtained from the Bureau of Land Management/Utah State University Buglab database and the Utah Department of Water Quality data that were used in their 2016 draft Integrated Report. The Buglab dataset included all samples that were analyzed in their lab for the UDWQ bioassessment program from May 11, 1998 to October 16, 2014 (N = 1341 samples). The UDWQ dataset included samples collected from May 12, 2009 to October 16, 2014 (N = 797 samples). The two datasets were merged for a total of 513 samples. UDWQ has determined that 'mountain' and 'desert' expected number of taxa (E) are substantially different and developed their O/E scores accordingly. To help eliminate the effects of this bias, the dataset was filtered to include only the following 'mountain' management units: Bear River, Jordan River, Uinta Basin, Utah Lake, and Weber River. The dataset was then filtered to remove all samples that were not sub sorted to help understand the effects of subsampling and resulted for a final sample size of 262. BLM/USUS Buglab randomly splits a percentage of the sample to obtain 600 random individuals. They then computationally resample 300 of these organisms before calculating their metrics.

Statistical Analyses

Histograms were examined for normality for the following metrics that were *a priori* expected to be redundant and correlated:

1. O/E score
2. Taxa Richness
3. % Labsplit
4. Abundance
5. Shannon Diversity
6. Simpson Diversity and,

7. Evenness

All of the metrics were approximately normally distributed, except two, % Labsplit and Abundance. Transformations were not considered necessary. Pearson product-moment pairwise correlations with p-values were then calculated for the seven metrics.

Linear and quadratic Ordinary Least Squares (OLS) regressions were then computed for combinations of the metrics (predictor variables) that were most correlated with O/E scores (dependent variable) (%Labsplit and Abundance omitted). Simultaneous quantile regressions were also performed at the 25th, 50th, and 75th quantiles to examine if relationships between the dependent variable O/E score varied at different predictor values. Because standard regression analyses such as OLS cannot adequately evaluate indirect effects of a predictor variable on a response variable (e.g. O/E), Path Diagrams and Structural Equation Models (SEM) were developed for the most promising combinations of predictors. Both OLS and SEM are confirmatory statistical models and were used as such. All statistical analyses were conducted using Stata 14.1 for Mac (StataCorp 2016).

Results

Metric Correlations

There were strong significant correlations between many of the subsample derived metrics including those with O/E scores (Table 1). Taxa richness, Shannon and Simpson diversity and evenness metrics were strongly correlated with O/E (Table 1). The two diversity metrics are based on taxa richness and evenness and as expected were strongly correlated.

Table 9. Pearson correlations between richness and diversity metrics (= significant at p < 0.05)*

	O/E score	Richness	LabSplit	Abundance	ShannonD	Simpson
Richness	0.7581*					
LabSplit	-0.1295*	-0.1425*				
Abundance	-0.0896	-0.1095	-0.3895*			
ShannonD	0.7029*	0.8678*	-0.1152	-0.0965		
Simpson	0.6007*	0.724*	-0.0874*	-0.072	0.9453*	
Evenness	0.5612*	0.6581*	-0.071	-0.0566	0.9408*	0.9661*

Summary Statistics

The following three tables (Tables 2-4) are summary statistics for taxa richness, evenness, and O/E scores.

Table 10. Summary statistics for taxa richness metric.

Richness*

Percentiles		Smallest		
1%	6	4		
5%	8	6		
10%	10	6	Obs	262
25%	13	6	Sum of Wgt.	262
50%	19		Mean	18.9542
		Largest	Std. Dev.	6.681435
75%	24	34		
90%	28	34	Variance	44.64157
95%	29	34	Skewness	.0542729
99%	34	35	Kurtosis	2.274394

Table 11. Summary statistics for evenness metric.

Evenness*

Percentiles		Smallest		
1%	.2484093	.061079		
5%	.4228132	.1969372		
10%	.4709411	.2484093	Obs	262
25%	.5750272	.2599899	Sum of Wgt.	262
50%	.6802697		Mean	.6538558
		Largest	Std. Dev.	.1367357
75%	.754016	.86718		
90%	.8037984	.8762848	Variance	.0186967
95%	.8310941	.8844925	Skewness	-.9792063
99%	.8762848	.8874369	Kurtosis	4.237731

Table 12. Summary statistics for O/E score metric.

OE_SCORE

	Percentiles	Smallest		
1%	.4	.3		
5%	.5	.399		
10%	.607	.4	Obs	262
25%	.754	.411	Sum of Wgt.	262
50%	.908		Mean	.9069275
		Largest	Std. Dev.	.2336467
75%	1.084	1.354		
90%	1.211	1.36	Variance	.0545908
95%	1.288	1.419	Skewness	-.1137977
99%	1.36	1.423	Kurtosis	2.504571

The BLM/USU Buglab estimated total abundances in the filtered dataset ranged between 965 and 211,604 individuals/m^2 and the proportion of the samples used for subsampling ranged between 1.14 and 87.5%.

OLS regression

The best OLS regression model at predicting O/E scores included two predictors, richness and evenness and resulted in an R^2 of 0.58 (Table 1, Figures 1 and 2). There was very little difference in either a linear or quadratic model, therefore only the more easily interpretable linear model results are included in Table 5. OLS models were also computed with no constant (forcing the fit through the origin) because it was assumed that when richness and evenness were zero, so were O/E scores. Models without constants produced substantially lower coefficient standard errors indicating an improvement of OLS models over those that included constants although models with or without constants produced slopes that were significantly greater than zero. However, interpretation of OLS models without a constant is more difficult compared with models with constants that produce statistically relevant R^2 values. Therefore, only the OLS model that included the estimated constant is reported (Table 5). Simultaneous quantile regression coefficients were not significantly different than the final OLS coefficients indicating relatively consistent prediction of the OLS model throughout the range of data.

Table 13. OLS regression results of O/E score as a function of taxa richness and evenness.

```
. regress oe_score richness  evenness
```

Source	SS	df	MS		
Model	8.28553352	2	4.14276676	Number of obs	= 262
Residual	5.96265445	259	.023021832	F(2, 259)	= 179.95
				Prob > F	= 0.0000
Total	14.248188	261	.054590758	R-squared	= 0.5815
				Adj R-squared	= 0.5783
				Root MSE	= .15173

oe_score	Coef.	Std. Err.	t	P>|t|	[95% Conf.	Interval]
richness	.0239824	.001867	12.85	0.000	.0203059	.0276589
evenness	.1876308	.0912297	2.06	0.041	.0079845	.3672772
_cons	.329677	.0460416	7.16	0.000	.2390135	.4203405

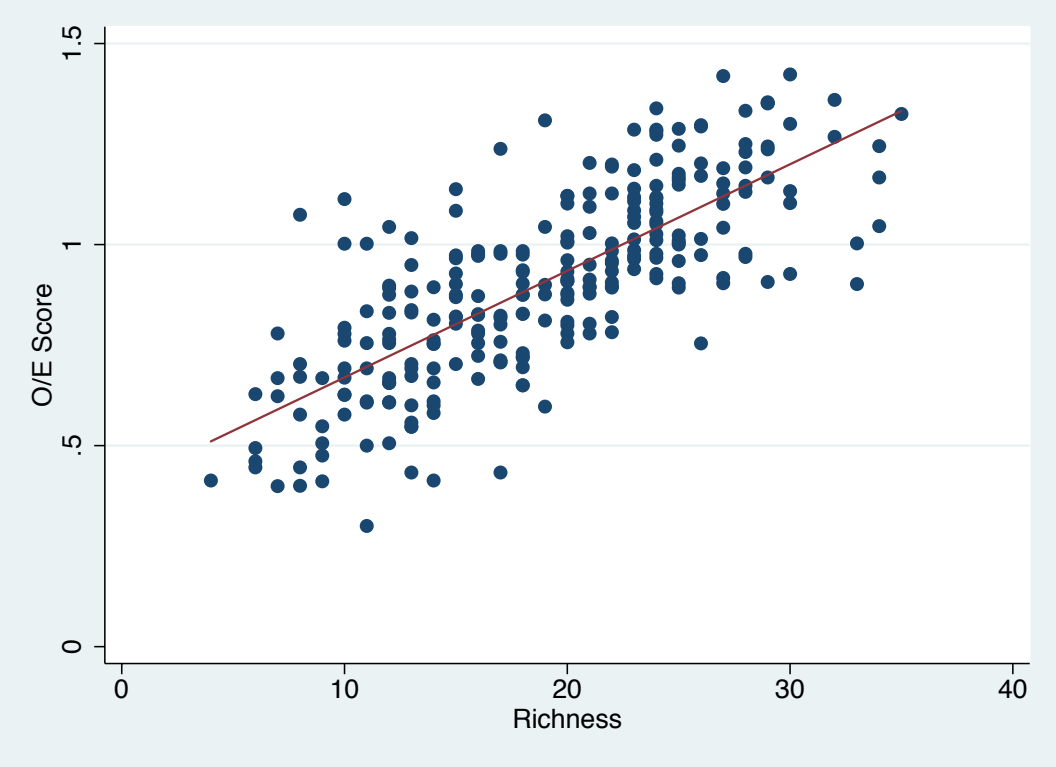

Figure 17. Relation of O/E scores to taxa richness. Red line is OLS regression linear fit. See Table 5 for OLS results.

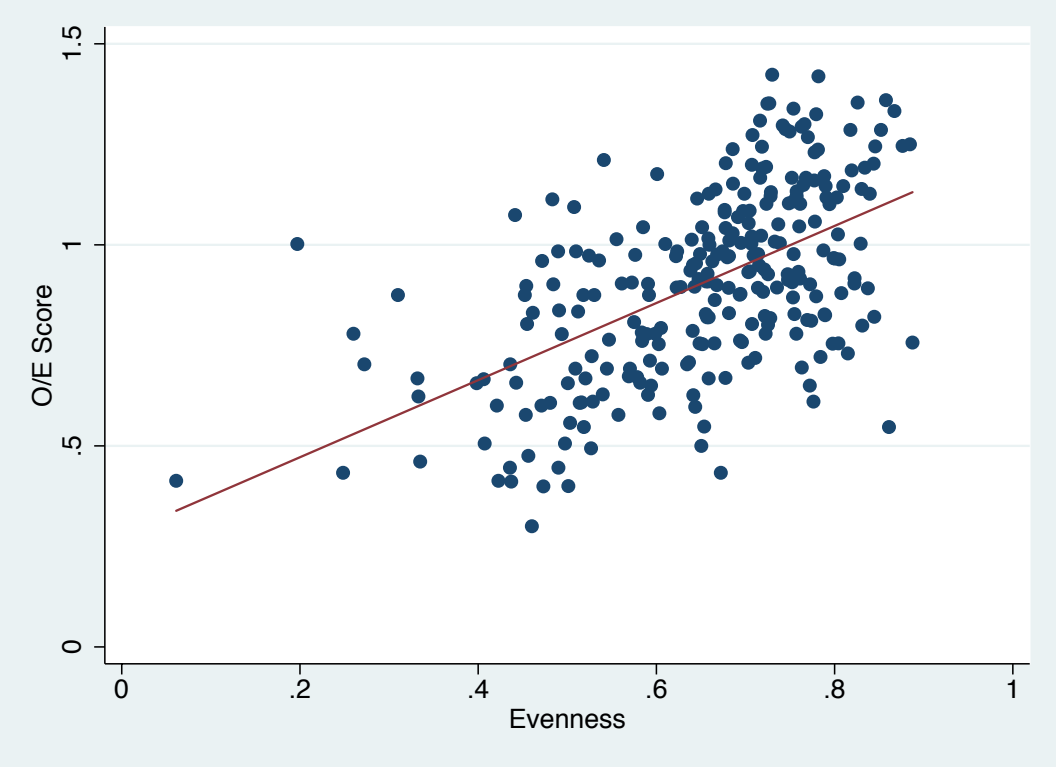

Figure 18. Relation of O/E scores to evenness. Red line is OLS regression linear fit. See Table 5 for OLS results

The linear relationship between O/E and taxa richness was much less variable than the relation between O/E and evenness as shown in Table 5 (standard errors and 95% CIs of p-values) and Figures 1 and 2.

Structural Equation Models

SEMs and path diagrams were conducted using all seven of the predictor metrics of O/E scores. The best SEM also included only richness and evenness as predictors of O/E scores (Figure 3 and Tables 3 - 6). This SEM model was a good predictor of O/E scores and also produced the same as the OLS model above, R^2 = 0.58. Richness had a strong direct effect on O/E (0.69) and evenness had significant but lesser direct effect (0.11). However, evenness had a direct effect on richness (0.66) and therefore an indirect effect on O/E scores for a total effect on O/E of 0.56 similar to the effect richness had on O/E scores (0.69) (Figure 3, Tables 6-9).

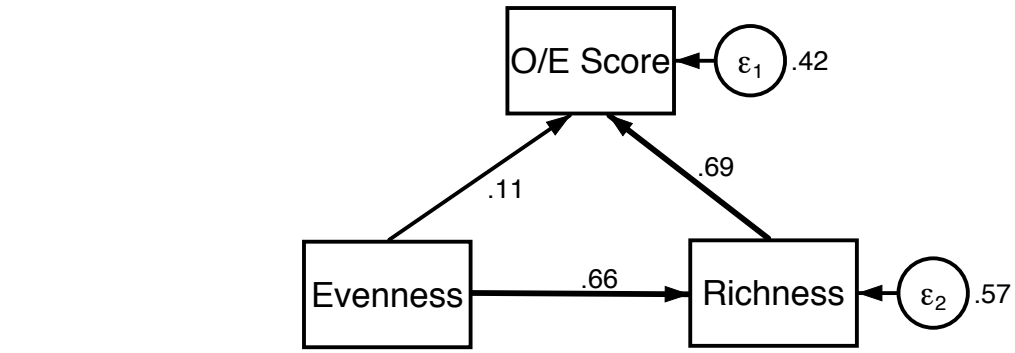

O/E: R^2 = 0.58
Richness: R^2 = 0.43
Overall: R^2 = 0.44

O/E Total Effects
Richness = 0.69
Evenness = 0.56

Figure 19. Structural Equation Model (SEM) and path diagram of the direct and indirect effects of richness and evenness metrics on O/E scores (values in the figure are standardized).

Table 14. Standardized SEM results of the effects of richness and evenness on O/E scores.

Structural equation model — Number of obs = **262**
Estimation method = **ml**
Log likelihood = **-520.69055**

Standardized	Coef.	OIM Std. Err.	z	P>|z|	[95% Conf.	Interval]
Structural						
oe_score <-						
richness	.6858081	.0454566	15.09	0.000	.5967148	.7749015
evenness	.1098061	.0529155	2.08	0.038	.0060937	.2135186
_cons	1.413707	.2305396	6.13	0.000	.961858	1.865557
richness <-						
evenness	.6581465	.0309963	21.23	0.000	.5973949	.7188982
_cons	-.3109353	.2184783	-1.42	0.155	-.7391449	.1172743
var(e.oe_score)	.4184851	.0377126			.3507295	.4993301
var(e.richness)	.5668432	.0408002			.4922607	.6527257

Table 15. Standardized SEM direct effects of richness and evenness on O/E scores.

Direct effects

	OIM Coef.	Std. Err.	z	P>|z|	[95% Conf.	Interval]
Structural						
oe_score <-						
richness	**.0239824**	**.0018563**	**12.92**	**0.000**	**.0203441**	**.0276207**
evenness	**.1876308**	**.0907059**	**2.07**	**0.039**	**.0098506**	**.3654111**
richness <-						
evenness	**32.15957**	**2.272838**	**14.15**	**0.000**	**27.70489**	**36.61425**

Table 16. Standardized SEM indirect effects of richness and evenness on O/E scores.

Indirect effects

	OIM Coef.	Std. Err.	z	P>|z|	[95% Conf.	Interval]
Structural						
oe_score <-						
richness	**0**	(no path)				
evenness	**.7712634**	**.0808391**	**9.54**	**0.000**	**.6128218**	**.9297051**
richness <-						
evenness	**0**	(no path)				

Table 17.Standardized SEM total effects of richness and evenness on O/E scores.

Total effects

	OIM Coef.	Std. Err.	z	P>|z|	[95% Conf.	Interval]
Structural						
oe_score <-						
richness	**.0239824**	**.0018563**	**12.92**	**0.000**	**.0203441**	**.0276207**
evenness	**.9588942**	**.0873777**	**10.97**	**0.000**	**.7876371**	**1.130151**
richness <-						
evenness	**32.15957**	**2.272838**	**14.15**	**0.000**	**27.70489**	**36.61425**

The interpretation of the SEM standardized loadings (coefficients) for total effects on O/E scores is fairly straight forward. A 1 standard deviation change in taxa richness results in a 0.23 standard deviation change in O/E score (Table 9). Likewise, a 1 standard deviation change in evenness (0.14) (Table 3) equals a 0.96 standard deviation change in O/E scores = 0.22 (Table 4 and Table 9). The 95% CIs of evenness coefficients are quite wide; 0.79 to 1.13 (Table 9). This suggests that if evenness changes by 1 std. dev., O/E scores could change between 0.18 and 0.26.

The relationship between O/E and taxa richness was much less variable than the relation between O/E and evenness in SEM as shown in Table 6 (standard errors and 95% CIs of p-values).

Effects of evenness on taxa richness: hypothetical example

The following tables, Table 7 and Table 8 are hypothetical invertebrate samples that both have the same number of individuals, N = 30,000, a typical number of individuals that occur in a UDWQ river or stream sample. The abundance and proportional abundance of each of the 30 taxa is the same (evenness = 1.0) in idealized Table 1. In Table 8, abundances and proportion abundances are exaggerated with one taxon, 'dd' having substantially more individuals.

On average a random 300 count subsample from the sample taxa pool in Table 7 would result in 30 observed taxa, which is the actual true number of taxa in the taxa pool. In contrast, the number of taxa observed from a random 300 count subsample taken from the sample taxa pool in Table 8 would only be 14. This would be a > 50% reduction in taxa observed even though there were still 30 taxa in the original sample and there was no loss of taxa from the site.

Table 18. Hypothetical invertebrate sample with 30,000 individuals and equal proportional abundances. A fixed 330 count subsample would result in 10 individuals counted per taxon and the total number of taxa observed = 30.

Taxon	Abundance	Proportion Abundance	300 Count	Taxa Counted
a	1000	0.033	10	1
b	1000	0.033	10	1
c	1000	0.033	10	1
d	1000	0.033	10	1
e	1000	0.033	10	1
f	1000	0.033	10	1
g	1000	0.033	10	1
h	1000	0.033	10	1
i	1000	0.033	10	1
j	1000	0.033	10	1
k	1000	0.033	10	1
l	1000	0.033	10	1

m	1000	0.033	10	1
n	1000	0.033	10	1
o	1000	0.033	10	1
p	1000	0.033	10	1
q	1000	0.033	10	1
r	1000	0.033	10	1
s	1000	0.033	10	1
t	1000	0.033	10	1
u	1000	0.033	10	1
v	1000	0.033	10	1
w	1000	0.033	10	1
z	1000	0.033	10	1
y	1000	0.033	10	1
z	1000	0.033	10	1
aa	1000	0.033	10	1
bb	1000	0.033	10	1
cc	1000	0.033	10	1
dd	1000	0.033	10	1
Total Taxa Counted				**30**

Table 19. Hypothetical invertebrate sample with 30,000 individuals and unequal proportional abundances[2]. A fixed 300 count subsample would result in a variable number of individuals counted per taxon and the total number of taxa observed would equal 14.

[2] Although the proportion abundances in Table 11 are exaggerated, real samples are virtually never completely even (e.g. Table 10). This is because individual taxa abundances vary widely both spatially and temporally, sometimes biweekly in the case of short lived taxa. A high turnover taxon can be absent from a sample either because they are in the egg stage or aerial adults, while one to two weeks later their early instar abundances can

Taxon	Abundance	Proportion Abundance	300 count	Taxa Counted
a	10	< 0.000	0.1	0
b	20	0.001	0.2	0
c	30	0.001	0.3	0
d	40	0.001	0.4	0
e	49	0.002	0.49	0
f	60	0.002	0.6	1
g	70	0.002	0.7	1
h	80	0.003	0.8	1
i	90	0.003	0.9	1
j	100	0.003	1	1
k	10	0.000	0.1	0
l	20	0.001	0.2	0
m	30	0.001	0.3	0
n	40	0.001	0.4	0
o	50	0.002	0.5	0
p	60	0.002	0.6	1
q	70	0.002	0.7	1
r	80	0.003	0.8	1
s	90	0.003	0.9	1
t	100	0.003	1	1
u	10	0.000	0.1	0

dominate the sample. Younger, smaller instars are always more abundant than older, larger instars or adults and there are always both inter and intraspecific population abundance dynamics occurring.

v	20	0.001	0.2	0
w	30	0.001	0.3	0
z	40	0.001	0.4	0
y	50	0.002	0.5	1
z	50	0.002	0.5	0
aa	50	0.002	0.5	1
bb	50	0.002	0.5	0
cc	50	0.002	0.5	1
dd	28551	0.952	285.51	1
Total Taxa Counted				**14**

Jordan River O/E Bioassessment Example

The Jordan River flows from Utah Lake and into the Great Salt Lake through the most densely populated area of Utah. By any measure, this river has been compromised. Subsequently, six out of the eight Jordan River UDWQ Assessment Units (Units 1, 2, 3, 4, 6, and 7) were considered impaired due to O/E scores in the UDWQ 2016 Integrated Report. However, a synthesis of the BLM/USU Buglab database revealed there were potentially >> 200 macroinvertebrate taxa in the Jordan River (Table 12). These taxa occurred at various probability of captures (see Discussion section on probability of capture problems). Some taxa were highly abundant and widely distributed throughout the length of the river, while other taxa were rare and uncommon spatially and abundance based (Table 13).

Table 20. List of taxa found in Jordan River using BLM/USU Buglab database. Accessed July 11, 2016.

Taxon	**Taxon**	**Taxon**
Ablabesmyia	Cheumatopsyche	Ephemera
Acari	Chironomidae	Ephemerella
Aeshna	Chironominae	Ephemerellidae
Aeshnidae	Chironomini	Ephydridae
Ambrysus	Chrysops	Erpobdella punctata
Amphipoda	Cinygmula	Erpobdellidae

Anagapetus	Cladotanytarsus	Eukiefferiella
Anax	Cleptelmis addenda	Fallceon quilleri
Anax walsinghami	Clitellata	Ferrissia
Ancyronyx	Coenagrionidae	Ferrissia rivularis
Antocha	Coleoptera	Fluminicola coloradoensis
Antocha monticola	Collembola	Fossaria
Apedilum	Corbicula	Gammarus
Apsectrotanypus	Corisella	Gastropoda
Argia	Corixidae	Glossiphonia complanata
Argia emma	Corticacarus	Glossiphoniidae
Asellidae	Corydalus	Glossosoma
Atherix lantha	Corynoneura	Gomphidae
Atrichopogon	Crangonyx	Gyraulus
Baetidae	Cricotopus	Gyrinus
Baetis	Cricotopus bicinctus group	Hagenius
Baetis tricaudatus	Cricotopus trifascia group	Haliplidae
Baetisca	Cricotopus/Orthocladius	Harnischia
Berosus	Cryptochironomus	Helisoma
Bezzia/Palpomyia	Cryptotendipes	Helobdella stagnalis
Bivalvia	Curculionidae	Helodon
Boyeria	Diamesa	Hemerodromia
Brachycentrus	Dicrotendipes	Heptagenia elegantula/solitaria
Buenoa	Didymops	Heptageniidae
Caecidotea	Dina dubia	Hesperocorixa
Caenis	Diptera	Hesperoperla pacifica
Callibaetis	Dolichopodidae	Hetaerina

Calopteryx	Drunella coloradensis/flavilinea	Hetaerina americana
Cambarinae	Drunella doddsii	Hetaerina vulnerata
Centroptilum/Procloeon	Dubiraphia	Heterlimnius corpulentus
Ceratopogonidae	Elmidae	Hyalella azteca
Ceratopsyche	Enchytraeidae	Hydrobiidae
Chauliodes	Enochrus	Hydrophilidae
Chelifera	Epeorus	Hydrophilus

Hydropsychidae	Nephelopsis obscura	Probezzia
Hydroptila	Nigronia	Procladius
Hydroptilidae	Nilothauma	Promoresia
Hygrobates	Notonectidae	Prostoma
Hygrobatidae	Odonata	Protzia
Ischnura	Oecetis	Psectrocladius
Isonychia	Oligochaeta	Pseudocloeon
Isoperla	Oligostomis	Pseudosmittia
Kiefferulus	Ophiogomphus	Psychoda
Labrundinia	Optioservus	Pteronarcys
Laccophilus	Optioservus quadrimaculatus	Pyrgulopsis
Laccophilus maculosus	Orconectes virilis	Pyrgulopsis kolobensis
Lepidostoma	Ordobrevia nubifera	Pyrgulopsis pilsbryana
Leptoceridae	Orthocladiinae	Rhantus
Leptohyphidae	Orthocladius	Rheopelopia
Leptophlebiidae	Ostracoda	Rheosmittia
Leuctridae	Oxyethira	Rheotanytarsus
Libellula	Pagastia	Rhithrogena

Libellulidae	Pantala hymenaea	Rhyacophila
Lopescladius	Parakiefferiella	Rhyacophila brunnea/vemna group
Lumbriculidae	Paraleptophlebia	Rhyacophila vofixa group
Lymnaeidae	Parametriocnemus	Robackia
Macronychus	Parapsyche elsis	Saetheria
Macrostemum	Paratanytarsus	Sepedon
Micrasema	Pentaneurini	Sialis
Microcylloepus	Perlesta	Sigara
Microcylloepus pusillus	Phaenopsectra	Simuliidae
Microcylloepus similis	Philopotamidae	Simulium
Micropsectra	Phylocentropus	Simulium vittatum group
Microtendipes	Physa	Sperchon
Muscomorpha	Pisidiidae	Sperchonidae
Naididae	Pisidium	Stagnicola
Nanocladius	Planariidae	Stempellinella
Nectopsyche	Planorbidae	Stenelmis
Nemata	Plauditus	Stenochironomus
Nemouridae	Polypedilum	Stenonema
Neoplasta	Pomacea bridgesi	Stictochironomus
Neothremma	Potamopyrgus antipodarum	Stratiomyidae
Neozavrelia	Potthastia	Sublettea

Synorthocladius		
Tabanidae		
Taeniopterygidae		
Taeniopteryx		

Tanypodinae		
Tanytarsini		
Tanytarsini		
Tanytarsus		
Thienemanniella		
Thienemannimyia		
Tipulidae		
Torrenticola		
Tribelos		
Trichoptera		
Tricorythodes		
Tricorythodes minutus		
Trombidiformes		
Tropisternus		
Tubificidae		
Turbellaria		
Tvetenia		
Wiedemannia		
Wiedemannia		
Xylotopus		
Zaitzevia		
Zapada columbiana		
Zapada columbiana/oregonensis group		
Zygoptera		

The family Chironomidae accounted for 53% of the Dominant Family entries (N = 17/32) and Hydropsychidae and Leptohyphidae each accounted for 16% (5/32)(Table 13). These three families

accounted for a total of 84% of the entries. Percent dominance by abundance ranged from 13% to 95% (Table 13).

Table 21. Jordan River evenness score, Dominant Family, % Dominant Family, Dominant Taxon, and % Dominant Taxon from 32 BLM/USU Buglab samples.

Evenness	Dominant Family	% Dominant Family	Dominant Taxon	% Dominant Taxon
0.44	Chironomidae	17.51	Oligochaeta	75.06
0.62	Chironomidae	13.03	Oligochaeta	54.38
0.38	Leptohyphidae	74.65	Tricorythodes	74.65
0.38	Chironomidae	88.35	Chironominae	77.37
0.50	Hydrobiidae	63.29	Hydrobiidae	63.29
0.58	Hydropsychidae	48.03	Hydropsyche	48.03
0.60	Chironomidae	61.95	Orthocladiinae	47.94
0.47	Leptohyphidae	64.84	Tricorythodes	64.84
0.66	Hydropsychidae	50.12	Hydropsyche	35.95
0.59	Hydropsychidae	37.52	Tricorythodes	32.90
0.53	Leptohyphidae	66.74	Tricorythodes	66.74
0.65	Hydrobiidae	39.10	P.antipodarum	39.10
0.57	Hydropsychidae	74.93	Hydropsyche	62.47
0.56	Chironomidae	53.49	Orthocladiinae	50.18
0.69	Leptohyphidae	39.71	Tricorythodes	39.71
0.59	Chironomidae	44.75	Orthocladiinae	39.97
0.53	Leptohyphidae	47.84	Tricorythodes	46.40
0.57	Chironomidae	57.02	Orthocladiinae	55.18
0.73	Chironomidae	42.35	Orthocladiinae	38.45
0.78	Simuliidae	34.11	Simulium	34.11

0.73	Corbiculidae	46.39	Corbicula fluminea	46.39
0.46	Hydropsychidae	73.32	Hydropsyche	65.47
0.49	Chironomidae	89.56	Chironominae	53.09
0.60	Chironomidae	53.83	Simulium	41.35
0.68	Asellidae	26.89	Turbellaria	28.52
0.63	Chironomidae	48.06	Chironominae	38.69
0.40	Chironomidae	94.49	Chironominae	69.01
0.57	Chironomidae	61.47	Chironominae	52.91
0.67	Chironomidae	72.51	Chironominae	37.31
0.57	Chironomidae	78.40	Orthocladiinae	39.77
0.44	Chironomidae	49.49	Chironominae	46.27
0.39	Chironomidae	89.02	Chironominae	69.93

Only four samples were comparable between the two data sets. O/E scores and evenness are in Table 14.

Table 22.Four Jordan River sites with O/E scores and evenness values that were compatible between the two datasets.

Sample	Site	O/E score	Evenness
142111	Jordan River at Cudahy Lane	0.446	na
142112	Jordan River 1000 ft below South Davis Treatment Plant	0.446	0.44
142113	Jordan River at 3300 S Crossing	0.557	0.50
142114	Jordan River 1100 W 2100 S below confluence with Mill Creek	0.445	0.62

The % Dominant taxon was Oligochaeta (segmented worms) at 54% of the total abundance in the Jordan River Sample 142114(collected 9 November 2009)(Table 15). There were at least fifteen taxa in the subsampled results (Table 15) and likely more in the entire sample but were not counted due to dominance by Oligochaeta.

Table 23. Taxa observed in the Jordan River sample 142114. Oligochaeta comprised 54% of total abundances.

Taxon	**Taxon**
Bivalvia	Lebertia
Caecidotea	Leptoceridae
Chironomidae	Oligochaeta
Chironominae	Orthocladiinae
Coenagrionidae	Physa
Erpobdellidae	Pisidium
Gammarus	Planorbidae
Gyraulus	Potamopyrgus antipodarum
Helobdella stagnalis	Psychoda
Hydrobiidae	Sigara
Hydropsyche	Tanypodinae
Hydroptilidae	Turbellaria

Results from the OLS and SEM models showed that evenness had a strong effect on taxa richness and O/E scores, thus there were likely more taxa in the complete original Jordan River samples than in the subsamples. Even though the Jordan River is obviously impaired (i.e. it is a highly regulated, dewatered urban/industrial system); O/E scores should have been higher in most of the Jordan River samples if the effects of subsampling and evenness were considered.

Discussion

There were strong effects of evenness and richness metrics on O/E scores, which apparently often affect biological assessments. Taxa richness obviously effects O/E scores because the O/E model is mostly based on this metric. Evenness directly effects taxa richness in a subsample and consequently directly and indirectly effects O/E scores. These effects need to be accounted for by water quality agencies before assigning an assessment score.

The unexplained variability in richness (E_2 = 0.57 in Figure 3) due to its relationship with evenness in the SEM and hence some of the unexplained variability in O/E scores was likely in part due to: 1) natural variability in richness in the different stream types and conditions, 2) varying levels of impairment, and more concerning, 3) the assumptions and variables that went into development of the O/E models. Taxa richness is often greater in mid elevation streams compared to headwaters or lower elevation streams (i.e. the river continuum). Richness is also greater in reference streams than impaired streams, which is why richness is the most widely used metric in bioassessments. A larger data set than the one used in these analyses would have allowed for the separation of stream types and varying levels of impairment and there likely would have been a much stronger relation between evenness and richness and these two variables with O/E. Nothing can be done about the assumptions and subsequent effects of the PRISM variables on the O/E scores evaluated in this analysis except to completely redo the models. RIVPAC O/E models as used by UDWQ rely on at least eleven 'watershed' based climate/environmental variables without defining 'watershed'. For example, the Jordan River watershed drains over 3800 square miles with elevations ranging from 11,900 ft. to 4200 ft. (http://www.utahcleanwater.org/jordan-river-watershed.html). Assigning impaired status to UDWQ Jordan River Assessment Units could have been inappropriate if UDWQ used the entire Jordan River watershed, as was detailed in their 2016 IR, to develop O/E models and averaged watershed "E" (expected) taxa probabilities of capture for final O/E scores (see Richards 2016a for more discussion on Jordan River macroinvertebrate assemblages in relation to water quality assessments using O/E).

Simple correlations showed that several commonly used and easily calculable metrics; taxa richness, Shannon's and Simpsons diversity indices, and evenness were significantly and strongly correlated with O/E scores (Table 1). This suggests that reliance on a complicated and computationally expensive, non-transparent, metric such as that produced by a RIVPACS O/E model may not be prudent and that replacing the O/E metric with one or several of the other correlated metrics should be considered. At the minimum, these metrics should be included in a bioassessment program and used to supplement O/E scores.

Implications of Evenness on O/E Scores and UDWQ bioassessments

UDWQ uses a mean O/E score of $\geq$ 0.76 as 'fully supporting' and in general, a score of $\leq$ 0.69 as 'not supporting' (UDWQ Integrated Report 2016). If the SEM standardized loadings (coefficients) for the total effects of evenness on O/E scores in Table 9 are reasonable, then that would suggest that a 0.07 decrease in O/E score from 0.76 (fully supporting) to 0.69 (not supporting) would only require a decrease in evenness of about 0.044 (0.037 to 0.053). As discussed in footnote 2, page 108, taxa abundances in macroinvertebrate samples are rarely if ever even, and this relatively small change in evenness could easily trigger an assessment from 'fully supporting' to 'not supporting'.

RIVPACS O/E 'Probability of Capture' is Problematic

RIVPACS O/E models include a 'probability of capture' (P_c) component. P_c is the probability that a taxon occurs at a reference site and is used in the development of the "E" expected taxa list. To reduce 'noise' in results and to ease interpretation, many users, including UDWQ, use a $P_C \geq 50\%$. That is, the probability of a taxon occurring at a site is estimated to be greater than 50%. The decision to use a $P_c \geq$

50% has very strong negative implications for assessing the biological integrity of a river or stream in UT. Many ecologists agree that uncommon and rare taxa should be included in ecological assessments and by including these taxa detection of impacts is improved (Turak and Koop 2003; Nijboer and Schmidt-Kloiber 2004). It is also widely recognized that rare taxa are the first to become extinct due to human disturbance (Leitao 2016). Uncommon and rare taxa have also been shown to disproportionally contribute to ecosystem function and integrity (Leitao 2016). For example, native bivalves are extremely important for maintaining water quality via their filter feeding activity and of much concern for developing NH_3 criteria. However, bivalves do not occur in >50% of Utah's reference sites and unionids are likely on the brink of extinction in UT (Richards 2016b). A $P_C \geq 50\%$ may easily overlook many, many, taxa that are unique to Utah's rivers and streams including threatened and endangered species, important ecosystems providers, or simply an unknown number of taxa that occur in < 50% of reference streams. These taxa are the true measure of biological integrity and without which will result in a homogenous, biodiversity -limited condition lacking integrity. These taxa are also the most likely to be most sensitive to impacts because their niche breadth is much narrower that taxa that have P_cs > 50%. There is a well-known saying in ecology; 'rare is common, and common is rare' (Pimm et al. 2014). Modifications to RIVPACS O/E models have allowed researchers and managers in England to monitor rare species and to flag Red Data Book threatened species (http://www.ceh.ac.uk/services/rivpacs-reference-database), however they use much lower P_cs. Utah should consider the same.

Misinterpretation of O/E

Many RIVPAC O/E users continue to insist that a reduction in O/E scores reflects the extent to which taxa have become locally extinct due to human activities (UDWQ Integrate Report 2016). This is clearly not the case. The analyses included in this report highlight the fact that subsampling and evenness have significant effects on the number of taxa observed, especially the more uneven a sample and subsample. Taxa weren't lost; they just weren't found. They may not have even decreased in abundance. It is possible that other taxa could have disproportionally increased in abundance for whatever reason and that the 'lost' taxa simply weren't counted. To continue to assume that native taxa have become locally extinct because O/E scores have decreased reflects a gross misinterpretation of RIVPACS O/E models.

Additional Bioassessment Metrics in Use

There is no shortage of metrics in use by water quality management agencies throughout the USA including; richness, diversity, trait, and functional metrics. Each of these metrics addresses different aspects of biological integrity and combined into a suite can be highly useful in water quality assessments. Utah is the only state in the western USA that relies solely on a single metric, O/E. This can be analogous to a physician relying solely on body temperature to assess a person's health. Although measuring body temperature is highly useful, used alone, it cannot assess other ailments (e.g. broken leg, gunshot wound, cancer, etc.). BLM/USU Buglab processes the vast majority of UDWQ invertebrate samples and in addition to calculating O/E scores, automatically provides UDWQ with several dozen potentially useful metrics (Table 12). Surrounding states also include a suite of metrics in their bioassessment programs (Appendices 1-6). By not incorporating simple, easy to use and pertinent metrics, it appears that UDWQ now lags far behind surrounding states in its bioassessment program.

Several of these states also include separate multimetric indices using diatoms and fish metrics. At this time, UT does not use either.

Table 24. Condensed list of metrics that are routinely generated by BLM/ USU Buglab for UDWQ's bioassessment program.

Richness (metrics summarizing all unique taxa in a sample)	Richness
	Abundance
	Shannon's Diversity
	Simpson's Diversity
	Evenness
	# of EPT Taxa
	EPT Taxa Abundance
Dominance Metrics (metrics summarizing all most abundant taxa in a sample)	Dominant Family
	Abundance of Dominant Family
	Dominant Taxa
	Abundance of Dominant Taxa
Tolerance Indices (indices based on the indicator species concept in which taxa are assigned tolerance values)	Hilsenhoff Biotic Index
	# of Intolerant Taxa
	Intolerant Taxa abundance
	# of Tolerant Taxa
	Tolerant Taxa abundance
	USFS Community Tolerance Quotient (d)
Functional Feeding Groups (classification of organisms based on morphological or behavioral adaptations for where and how food is acquired)	# of shredder taxa
	Shredder Abundance
	# of scraper taxa
	Scraper abundance
	# of collector-filterer taxa
	Collector-filterer abundance
	# of collector-gatherer taxa
	Collector-gatherer abundance
	# of predator taxa

	Predator abundance
Functional Traits	# of clinger taxa
	"# of" Long-lived Taxa
Compositional Metrics (richness and abundance of various taxonomic groups)	# of Ephemeroptera taxa
	Ephemeroptera abundance
	# of Plecoptera taxa
	Plecoptera abundance
	# of Trichoptera taxa
	Trichoptera abundance
	# of Coleoptera taxa
	Coleoptera abundance
	# of Elmidae taxa
	Elmidae abundance
	# of Megaloptera taxa
	Megaloptera abundance
	# of Diptera taxa
	Diptera abundance
	# of Chironomidae taxa
	Chironomidae abundance
	# of Crustacea taxa
	Crustacea abundance
	# of Oligochaete taxa
	Oligochaete abundance
	# of Mollusca taxa
	Mollusca abundance
	# of Insect taxa
	Insect abundance

Economics vs. Bioassessment Quality.

All western USA states near UT had the same time frame allotted by EPA for developing their bioassessment programs. It does not appear that economic hardship or small population (taxpayer base) were factors in UDWQs decision to rely on a RIVPACs O/E metric as its sole measure of biological integrity (Table 13 and Appendices). Contrarily, Utah now seems economically poised to lead other states in the region in developing relevant and useful bioassessments. “According to the 2007 State New Economy Index, Utah is ranked the top state in the nation for Economic Dynamism, determined by "the degree to which state economies are knowledge-based, globalized, entrepreneurial, information technology-driven and innovation-based". In 2010, Utah was ranked number one in Forbes' list of "Best States For Business"(Badenhausen 2010). A November 2010 article in Newsweek magazine highlighted Utah and particularly the Salt Lake City area's economic outlook, calling it "the new economic Zion", and examined how the area has been able to bring in high-paying jobs and attract high-tech corporations to the area during a recession (Dokoupil 2010). As mentioned in the introduction and based on the U.S. Census Bureau statistics, Utah has one of the fastest growing populations of any U.S. state, 2nd in 2013. Table 13 compares surrounding states estimated gross state product and estimated population.

Table 25. Estimated gross state product and population for Utah and surrounding states (2010 data).

State	Gross State Product ($ billions)	Rank	Population (millions)	Rank
Utah	130.5	3	3.0	3
Colorado	257.6	2	5.5	2
Wyoming	38.4	8	0.6	8
Arizona	259.0	1	6.3	1
New Mexico	79.7	5	2.1	5
Idaho	58.2	6	1.7	6
Montana	44.3	7	1.0	7
Nevada	126	4	2.9	4

Conclusion

Even though RIVPACS O/E models have the potential to be useful summary metrics, their use as a stand-alone metric is not recommended. O/E models rely on far too many assumptions, constraints, and inherent errors that necessitates their inclusion into a more comprehensive and informative macroinvertebrate multimetric based program. By incorporating the O/E metric into a multimetric program fewer incorrect assessments of impairment will be made than if it used alone. Unfortunately,

all metrics are affected by the evenness of a sample and subsampling. This phenomenon needs to be considered in any bioassessment program. O/E probability of capture < 50% results in a poor evaluation of macroinvertebrate assemblages and thus fails to measure biological integrity. All states in the region other than Utah incorporate multimetric indices and several include the O/E metric, even states with fewer citizens and less resources. With Utah's booming economy and exponentially growing population, UDWQ now has the opportunity to build a bioassessment program worthy of its unique rivers and streams.

Literature Cited

Badenhausen, Kurt (October 13, 2010). "The Best States For Business And Careers". Forbes.

Dokoupil, Tony (November 8, 2010). "How Utah Became an Economic Zion". Newsweek.

Leitao, R. P. et al. 2016. Rare species contribute disproportionately to the functional structure of species assemblages. Proceedings of the Royal Society B: Biological Sciences. Vol. 283. Issue 1828.

Nijboer, R. C. and A. Schmidt-Kloiber. 2004. The effect of excluding taxa with low abundances or taxa with small distribution ranges on ecological assessment. Hydrobiologia. Vol. 515 1:347-363.

Pimm, S. L. et al. 2014. The biodiversity of species and their rates of extinction, distribution, and protection. Science. Vol. 344. Issue 6187. Review.

Richards, D. C. 2016a. Real and Perceived Macroinvertebrate Assemblage Variability in the Jordan River, Utah can Effect Water Quality Assessments. Draft Technical Report. Submitted to the Jordan River/Farmington Bay Water Quality Council. Salt Lake City, UT. Oreohelix Consulting, Vineyard, UT.

Richards, D. C. 2016b. Recalculation of Ammonia Criteria for Central Valley Water Reclamation Facility's Discharge into Mill Creek, Salt Lake County, UT based on Native Unionoida Surveys and Metapopulation Dynamics. Final Report. Submitted to the Jordan River/Farmington Bay Water Quality Council. Salt Lake City, UT. Oreohelix Consulting, Moab, UT.

Turak, E. and K. Koop. 2003. Use of rare macroinvertebrate taxa and multiple-year data to detect low-level impacts in rivers. Aquatic ecosystem health and management. 167-175

Appendices

Metrics used by other states

Appendix 17. Bioassessment metrics used by Montana (MDEQ 2016)

Ephemeroptera taxa

Plecoptera taxa

% EPT

% Non-insect

% Predator

Burrower taxa %

Hilsenhoff Biotic Index

% EPT excluding Hydropsychidae and Baetidae % Chironomidae

% Crustacea and Mollusca

Shredder Taxa

% Predator

EPT taxa

% Tanypodinae

% Orthocladiinae of Chironomidae

Predator taxa

% Filterers and Collectors

O/E

Appendix 18. Bioassessment metrics used by Wyomng (Hargett 2011)

Richness and Diversity Metrics

- % Chironomidae Taxa of Total Taxa
- % Diptera Taxa of Total TaxaX
- % Ephemeroptera Taxa of EPT Taxa
- % Ephemeroptera Taxa of Total Taxa
- No. Ephemeroptera Taxa
- No. EPT
- No. EPT Taxa (less Arctopsychidae and Hydropychidae)
- No. EPT Taxa (less Baetidae, Arctopsychidae, Hydropychidae and Tricorythodes)
- No. EPT Taxa (less Baetidae and Tricorythodes)
- Shannon Diversity (E)

Composition Metrics

- % Ephemeroptera (less Baetidae and Tricorythodes)
- % EPT (less Arctopsychidae and Hydropsychidae)
- % EPT (less Baetidae and Tricorythodes)
- % Tricorythodes of Ephemeroptera

Life History Metrics

- No. Semivoltine Taxa
- No. Univoltine Taxa
- Ratio of Multivoltine Taxa to Unvoltine Taxa +Semivoltine Taxa

Functional Feeding Group/Habitat Metrics

- % Clinger
- % Collector-gatherer
- % Filterer Taxa of Total Taxa
- % Scraper
- % Scraper Taxa of Total Taxa

No. Burrower Taxa

No. Predator Taxa

No. Scraper Taxa

Tolerance Metrics

BCICTQa

HBI

Appendix 19. Bioassessment metrics used by Idaho(IDEQ 2011). In addition, IDEQ is developing and intermittent stream index.

% Chironomidae

% clingers

% Ephemeroptera

% Ephemeroptera and Plecoptera % filterers

% EPT

% EPT, excl. Hydropsychidae

% filterers (adjusted)

% Multivoltine

% non-insects

% Predators

% Scrapers

% Tolerant

% tolerant (adjusted)

Becks Biotic index

Clinger taxa (adjusted)

EPT Taxa

EPT taxa (adjusted)

HBI (adjusted)

Insect Taxa

Non-insect % of taxa

Non-insect % of taxa (adjusted)

Scraper taxa

Semi-voltine taxa

Simpson's index

Sprawler taxa

Sprawler taxa (adjusted)

Swimmer & Climber Taxa

Tolerant taxa

O/E

Appendix 20. Some Bioassessment metrics used by Arizona(Jones and Woods 2010). In addition, ADEQ is developing and intermittent stream index.

Total taxa

Diptera taxa

HBI

% Stoneflies

% Scrapers

Scraper taxa

Caddisfly taxa

Mayfly taxa

%Mayflies

%Dominant taxa

Appendix 21. Bioassessment metrics used by New Mexico (NMED 2006)

Clinger Taxa

Coleoptera %

Ephemeroptera Taxa

EPT Taxa

Evenness

Intolerant Percent

Plecoptera %

Plecoptera Taxa

Scraper %

Scraper Taxa

Sensitive EPT %

Shannon DI (log2)

Sprawler Taxa

Swimmer Taxa

Taxonomic Richness

Trichoptera Taxa

O/E

Appendix 22. Bioassessment metrics used by Colorado(Jessup 2009)

Numerous including O/E. See Jessup (2009)

Appendix Literature Cited

Hargett, E. G. 2011. The Wyoming stream integrity index (WSII) multimetric indices for assessment of wadeable streams and large rivers in Wyoming. Wyoming Department of Environmental Quality. Cheyenne, WY.

Idaho Department of Environmental Quality. 2011. Biological assessment frameworks and index development for rivers and streams in Idaho. IDEQ. Boise, Idaho.

Jessup, B. Recalibration of the macroinvertebrate multi-metric index for Colorado. Colorado Department of Public Health and Environment. Water Quality Control Division. Denver, CO.

Jones, J. and J. Woods 2007 to 2010. A statewide assessment of Arizona's streams. Arizona Department of Environmental Quality.

MDEQ 2008. An assessment of the ecological conditions of the streams and rivers of Montana using environmental monitoring and assessment program (EMAP) method. Montana Department of Environmental Quality. Helena MT.

NMED. 2006. Benthic macroinvertebrate stream condition indices for New Mexico wadeable streams. New Mexico Environmental Department. Santa Fe, New Mexico.

Chapter 10

Jordan River Macroinvertebrate Assemblages: Preliminary Findings

By:

David C. Richards, Ph.D.

OreoHelix Ecological

Summary

The Jordan River has undergone unprecedented anthropogenic caused catastrophic ecosystem shifts resulting in macroinvertebrate assemblages that have most certainly suffered from severe bottlenecks and hysteresis; however, several macroinvertebrate taxa have endured or even prospered. Those that remain are temperature, sediment, and organic pollution tolerant. Only a handful of taxa are effective members of the riffle habitat type community including: the mayfly *Tricorythodes* sp., the caddisfly, *Hydropsyche* sp., two groups of midges, caecitoid sow bugs, flatworms and segmented worms, simuliid blackflies, and two highly invasive species, the New Zealand mudsnail, *Potamopyrgus antipodarum*, and the Asian clam, *Corbicula fluminea*. Overall densities in riffle type habitats are low compared with most eutrophic (i.e. productive) rivers, indicating degraded habitat that hinders their ability to regulate much needed ecosystem services. However, macroinvertebrates continue to govern almost all ecosystem functions including; nutrient cycling, organic matter decomposition, and are the major transfer link between food-web trophic levels in the Jordan River.

Analyses presented in this chapter were based on fifty samples collected by several county, state, and federal agencies focused on the use of macroinvertebrates as water quality indicators, starting in 1999. A few highlights of this analysis are as follows. Most of the dominant taxa were significantly spatially distributed within in the river continuum and were subject to seasonal and annual variability. Tolerance values for individual taxa were derived from the literature and applied to Jordan River taxa showed that dominant taxa were more: 1) organic pollution tolerant, 2) very fine sediment (< 0.06 mm) intolerant, 3) fine sediment > 0.06 mm tolerant, and 4) temperature tolerant than the overall assemblage. Remaining riffle habitats were so embedded with sediment that individual taxa and assemblages in riffle habitats did not differ from reach wide habitats and along with additional results presented here, lead us to conclude that sedimentation is their limiting factor. Sedimentation also likely negatively affected macroinvertebrate abundances (densities) in the river, which are well below average densities found in most rivers of North America. Isolation from other sediment dominated, warm-water rivers has likely resulted in reduced resilience to perturbation and increased extinction probability. This analysis supplements our ongoing collaborative research on the Jordan River and guides us toward comprehensive studies based on our conclusion that despite their anthropogenically induced setbacks; macroinvertebrates continue to be the most important component of ecosystem function and services, including their role in regulating water quality and their usefulness as indicators of water quality conditions in the Jordan River.

Table of Contents

List of Figures

List of Tables

Appendices

Introduction

The Jordan River is a highly polluted, highly regulated, irrigational conveyance canal, more often than not, severely dewatered via pumps and diversion dams. The river has been known as the most polluted river in Utah and perhaps at times, in the country (Giddings and Stephens 1999). Ecologically, the river has undergone what is known as 'catastrophic ecosystem shift' (Scheffer et al. 2001), and 'ecological hysteresis' (Scheffer and Carpenter 2003). The Jordan River is now a severely impaired analog river ecosystem and can never regain its past condition (Richards 2018b, Dakos et al. 2015). But it wasn't always this way.

History of Jordan River

Pre Mormon-Settlement

It is hard to imagine what conditions were like along the Jordan River corridor prior to Mormon settlement. However, a report by National Audubon Society (2000) to the U.S. Fish and Wildlife Service sheds some light on its past:

> "Before the area was urbanized, mammals such as bighorn sheep, mule deer, coyote, wolves, beaver, muskrat and jack rabbits would have been seen along the river. A "varmint hunt" was organized by John D. Lee around 1848, after the arrival of Mormon settlers. The final count of the hunt included "two bears, two wolverines, two wildcats, 783 wolves, 409 foxes, 31 minks, nine eagles, 530 magpies, hawks and owls, and 1,026 ravens."

It is difficult to conceive that bears (grizzly or black), wolves, and even wolverines occupied what is now Salt Lake City Greater Metropolitan Area and were common along the Jordan River floodplain. As has been reported National Audubon Society (and others); beavers where once abundant along the river and they are occasional still found, in some locations. Beavers affect river ecosystem functioning more than any other invertebrate, other than humans. They are the prototypical ecosystem engineers (Wright et. al. 2002).

Figure 20. Active beaver dam on Jordan River near W 14200 South, November 2018. As was much more common in the past, this beaver dam acts as a sediment trap and cobbles downstream of the dam are virtually unembedded for at least 50 meters downstream.

The Jordan River prior to Mormon settlement was a sinuous, low gradient meandering river with a wide floodplain and riparian ecosystem filled with willows and cottonwood trees; ideal beaver food, housing, and dam building material. Unquestionably, beaver dams dominated the river ecosystem and its riparian community. These dams, among other things, acted as sediment traps for sands and other fine sediments; a major component of the geological material within the floodplain. Directly below the dams, unembedded cobble riffle habitat dominated for several tens of meters, similar to what can be found today in upstream sections of the Jordan River near Bluffdale.

Utah Lake, the main source of the Jordan River, provided much cooler water to the river than it does at present and was fed by numerous unaltered and unimpeded springs and groundwater recharge. The combination of beaver dams and unembedded cobble riffles provided superior habitat for native fish species, including the Bonneville cutthroat trout, which no longer exists in the Jordan. Spring floods and summer storm events periodically removed beaver dams and the system began anew on a semi regular basis. Macroinvertebrate diversity and abundances reflected these conditions and along with beavers, governed Jordan River ecosystem function.

Post-Settlement

Named after the Biblical 'River Jordan' in the Middle East that drains the Sea of Galilee (aka Utah Lake) into the Dead Sea (aka Great Salt Lake); the post-settlement story of the Jordan River has been one of neglect and abuse. On the second day after arrival in 1847, Mormon settlers began diverting City Creek, a tributary of the Jordan River and industrious, utilitarian citizens haven't stopped diverting most of its

waters ever since. The Jordan River completely stopped flowing during the drought of 1901-1902 (Hooton 1989). The river again ran dry when Utah Lake levels dropped during the droughts of 1934 and 1992 when the pumps along the river became useless (Hooton 1989). Large sections of the river were straightened and channelized throughout Salt Lake County. Subsequently, natural meanders in the river were cut off and the channel slope increased. Remarkably, the Jordan River channel was deliberately and physically shifted to the opposite sides of the flood plain within the Cities of Midvale and Murray (Watershed Planning and Restoration Program 1992).

Raw, untreated sewage was dumped into the Jordan River for well over 100 years (Deseret News 1972). Agricultural and livestock runoff entered the river continuously and at least 40 smelters contaminated the river with heavy metals, mostly arsenic and lead (USEPA http://epa.gov/region8/superfund/ut/murray/index.html). There are two Superfund sites along the river in the City of Midvale that comprise almost 1000 acres that have contaminated the river with lead, arsenic, chromium, cadmium, iron, manganese, and zinc (http://www.epa.gov/region8/superfund/ut/midvale/) (http://www.epa.gov/region8/superfund/ut/midvale/RiparianFactSheetOct08.pdf). About 700 million US gallons of uranium contaminated shallow ground water from a uranium mill and storage facility near Mill Creek and the Jordan River may still remain (USEPA http://www.eia.doe.gov/cneaf/nuclear/page/umtra/salt_lake_title1.html). In addition, an unprecedented 3 million cells per 100 milliliters of fecal coliform were documented in the Jordan River in 1962 (Deseret News 1972). Pharmaceuticals are now of major concern in the Jordan River and it is estimated that at least twenty chemicals can be found in macroinvertebrate and fish tissue in the river (Richards 2018b). As a consequence, macroinvertebrate diversity, abundance, and community (assemblage) structure were devastated and their efficient and critical role in ecosystem functioning drastically diminished as a result of human economic activity along the Jordan River.

Macroinvertebrates in the Jordan River

It is a testament to life's tenacity in the face of adversity that a few macroinvertebrate taxa survived these hard times and that some of the more tolerant taxa continue to exist. Macroinvertebrates are the most important biological and ecological component of every temperate river ecosystem in the world, including the Jordan River. They link primary production (e.g. plants, algae, etc.) with higher level production (e.g. fish, birds, etc.), direct nutrient spiraling, govern algal community structure, reduce and decompose organic matter, and regulate water quality. They are responsible for maintaining ecosystem function and provide underappreciated ecosystem services. Macroinvertebrates are also arguably the single most influential metric defining the ecological management of aquatic resources throughout the world (Monaghan 2016). Virtually every governmental water quality agency, from city to federal, tribal, NGO, and citizen action groups use macroinvertebrate-based metrics and indices to monitor water quality.

Given their crucial importance to ecosystem function and superior value as water quality indicators; macroinvertebrate life history, ecology, assemblage structure, and contribution to ecosystem function in the Jordan River are poorly understood. Only rudimentary generalizations can be made at this time. In

this report, we begin to synthesize macroinvertebrate data from several sources to further understand their role in the Jordan River and help guide management decisions.

Methods

Dataset

We queried the BLM/USU National Aquatic Monitoring Center MAPIT -a Mapping Application for Freshwater Invertebrate Taxa for all samples in their database from Utah that contained the word Jordan River. We then downloaded this dataset. Several entries were from locations other than the Jordan River and were removed from the dataset, including entries from Mill Creek, City Creek, and a canal near the upper Jordan River. This resulted in a total of forty-seven (47) useful samples from the Jordan River starting from 1999 until 2015. Samples in this dataset were collected from three agency programs whose repository is MAPIT: EMAP-West, UT-DEQ (DWQ), and USU/BLM-BUGLAB. In addition, Salt Lake County Watershed Planning and Restoration Program, Salt Lake City has a well-staffed active macroinvertebrate monitoring program and provided us with three of their most recent (2017) datasets from the Jordan River.

We then combined the datasets (N = 50). The level of taxonomic identification varied from each source and time period; therefore, higher resolution taxa were combined to coarser level taxonomic groups during statistical analyses[3]. Figure 21 shows the locations of the samples along the Jordan River. Latitude and longitude coordinates for sample sites are in Appendix 1.

[3]Samples in the dataset labeled Jordan River at NewState Canal Road Crossing retrieved from the USU/BLM BugLab MAPIT database collected by UDWQ have latitude- longitude coordinates that puts them in State Canal north of SDSD treatment facility. These samples were analyzed in this report assuming that the location description was correct and that the latitude- longitude was incorrect. However, this assumption could have resulted in inaccurate or misleading results in our analyses. In the past we have found numerous instances when latitude- longitude or location descriptions collected by UDWQ and stored in the MAPIT database were obviously incorrect or did not concur.

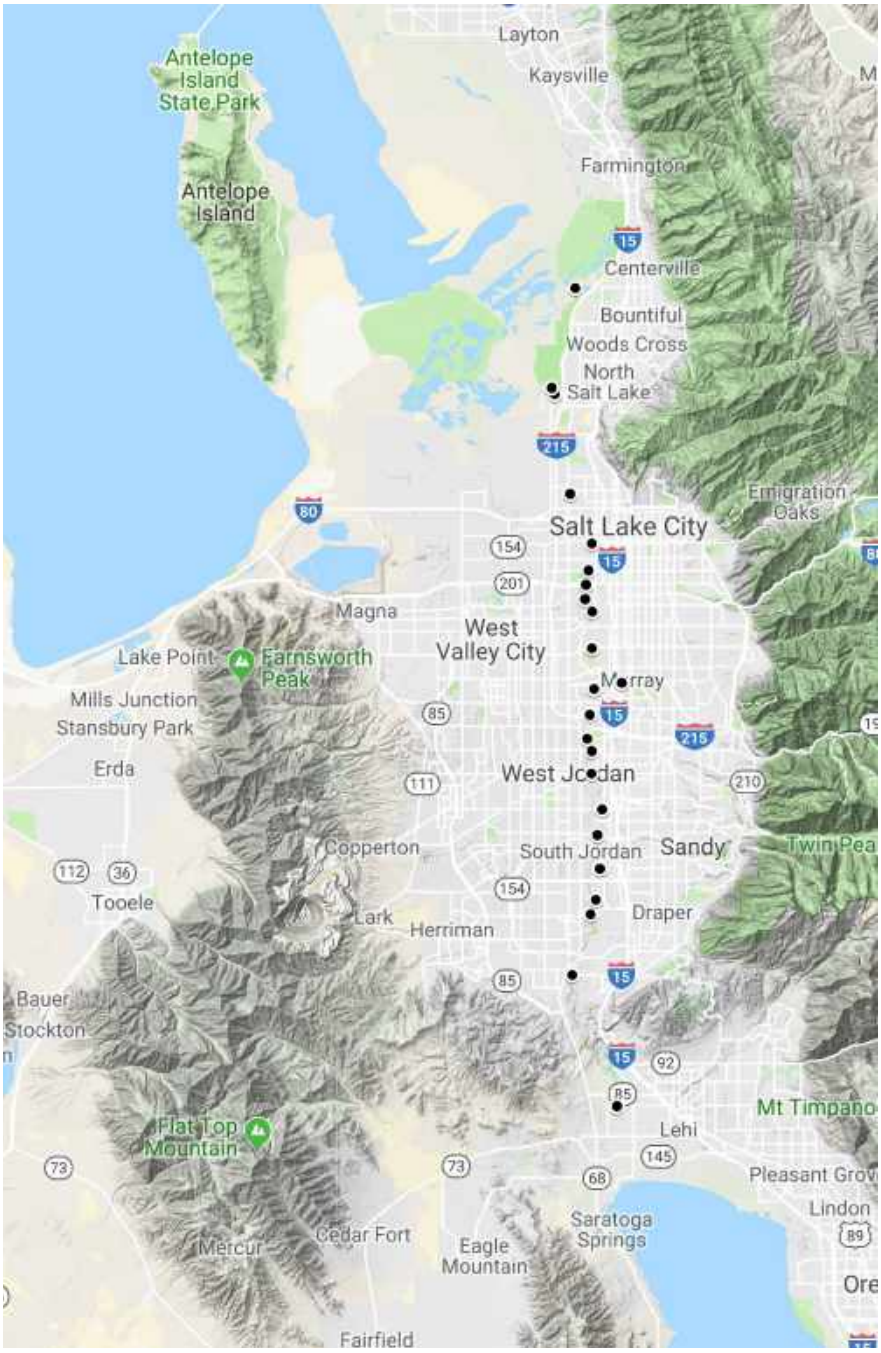

Figure 21. Location (black dots) of macroinvertebrate samples from the Jordan River analyzed in this report. Map created using Google Maps.

Statistical Analyses

We used several statistic methods to analyze the data including: Calculations of richness and diversity indices (i.e. Shannon's Diversity, Evenness, Taxa Richness, and Effective Number of Taxa); several tolerance indices (organic pollution HBI, sediment indices, and temperature indices); and linear regression on $\log_{10}$+1 transformed densities vs. latitude, month, and year. We also used three multivariate community ecology statistical methods: Non-metric multidimensional scaling (NMS),

multiple response permutation procedure (MRPP), and cluster analysis. More detail of each statistical method is presented at the beginning of each section of the report. All analyses were conducted using either Stata 15.1 (StataCorp 2018) or PC-Ord 6.1 (McCune and Mefford 2011).

Results

A list of the Jordan River macroinvertebrate taxa that were reported from the datasets used in our analyses is presented in Table 26.

Table 26. List of macroinvertebrate taxa found in the Jordan River from datasets used in this analysis. Note: Many taxa were not identified to either species or genus level and were likely duplicates.

Order	**Family**	**Genus**	**Lowest Taxon Identified**
Amphipoda			Amphipoda
	Gammaridae	*Gammarus*	*Gammarus lucustris*
	Hyalellidae	*Hyalella*	*Hyalella azteca*
			Hyalella sp.
Arhynchobdellida	Erpobdellidae		Erpobdellidae
		Dina	*Dina dubia*
			Dina parva
		Erpobdella	*Erpobdella punctata*
			Erpobdella sp.
		Nephelopsis	*Nephelopsis obscura*
Basommatophora	Ancylidae	*Ferrissia*	*Ferrissia rivularis*
			Ferrissia sp.
	Lymnaeidae		Lymnaeidae
		Fossaria	*Fossaria sp.*
		Stagnicola	*Stagnicola sp.*
	Physidae	*Physa*	*Physa sp.*
	Planorbidae		Planorbidae
		Gyraulus	*Gyraulus sp.*
Coleoptera	Curculionidae		Curculionidae

	Elmidae		Elmidae
		Cleptelmis	*Cleptelmis addenda*
		Dubiraphia	*Dubiraphia sp.*
		Microcylloepus	*Microcylloepus sp.*
			Microcylloepus pusillus
			Microcylloepus similis
		Optioservus	*Optioservus sp.*
			Optioservus quadrimaculatus
		Ordobrevia	*Ordobrevia nubifera*
		Stenelmis	*Stenelmis sp.*
		Zaitzevia	*Zaitzevia sp.*
	Gyrinidae	*Gyrinus*	*Gyrinus sp.*
Collembola			Collembola
Decapoda	Cambaridae	*Orconectes*	*Orconectes virilis*
Diptera			Diptera
	Ceratopogonidae		Ceratopogonidae
			Ceratopogoninae
		Probezzia	*Probezzia sp.*
		Bezzia/Palpomyia	*Bezzia/Palpomyia*
	Chironomidae		Chironomidae
			Chironominae
			Orthocladiinae
		Apedilum	*Apedilum sp.*
		Brillia	*Brillia sp.*
		Cricotopus	*Cricotopus sp.*
			Cricotopus bicinctus group

			Cricotopus trifascia group
		Cryptochironomus	*Cryptochironomus sp.*
		Diamesa	*Diamesa sp.*
		Eukiefferiella	*Eukiefferiella sp.*
		Nanocladius	*Nanocladius sp.*
		Orthocladius	*Orthocladius sp.*
		Parakiefferiella	*Parakiefferiella sp.*
		Polypedilum	*Polypedilum sp.*
		Thienemanniella	*Thienemanniella sp.*
		Pentaneurini sp.	*Pentaneurini sp.*
		Tanypodinae	Tanypodinae
		Micropsectra	*Micropsectra sp.*
	Empididae	*Hemerodromia*	*Hemerodromia sp.*
	Psychodidae	*Psychoda*	*Psychoda sp.*
	Simuliidae		Simuliidae
		Simulium	*Simulium sp.*
	Stratiomyidae		Stratiomyidae
	Tipulidae	*Antocha*	*Antocha monticola*
Ephemeroptera			Ephemeroptera
	Baetidae		Baetidae
		Baetis	*Baetis sp.*
			Baetis tricaudatus
		Callibaetis	*Callibaetis sp.*
		Fallceon	*Fallceon sp.*
			Fallceon quilleri
	Caenidae	*Caenis*	*Caenis sp.*

	Ephemerellidae		Ephemerellidae
		Drunella	*Drunella doddsii*
	Heptageniidae		Heptageniidae
		Heptagenia	*Heptagenia elegantula/solitaria*
	Leptohyphidae		Leptohyphidae
		Tricorythodes	*Tricorythodes sp.*
			Tricorythodes minutus
	Leptophlebiidae		Leptophlebiidae
Hemiptera	Corixidae		Corixidae
		Corisella	*Corisella sp.*
		Sigara	*Sigara sp.*
	Naucoridae	*Ambrysus*	*Ambrysus sp.*
	Notonectidae	*Notonecta*	Notonecta
Hoplonemertea	Tetrastemmatidae	*Prostoma*	Prostoma
Isopoda	*Caecidotea*		Caecidotea
	Asellidae		*Asellidae*
Lepidoptera	Crambidae	*Petrophila*	*Petrophila sp.*
Neotaenioglossa	Hydrobiidae		Hydrobiidae
		Fluminicola	*Fluminicola coloradoensis*
		Pyrgulopsis	*Pyrgulopsis sp.*
			Pyrgulopsis kolobensis
			Pyrgulopsis pilsbryana
	Tateidae	*Potamopyrgus*	*Potamopyrgus antipodarum*
Odonata	Aeshnidae		Aeshnidae
		Aeshna	*Aeshna*
		Anax	*Anax sp.*

			Anax walsinghami
	Calopterygidae	*Hetaerina*	*Hetaerina sp.*
			Hetaerina americana
			Hetaerina vulnerata
	Coenagrionidae		Coenagrionidae
		Argia	*Argia sp.*
		Argia	*Argia emma*
		Ischnura	*Ischnura sp.*
	Gomphidae	*Ophiogomphus*	*Ophiogomphus sp.*
Plecoptera			Plecoptera
	Nemouridae	*Zapada*	*Zapada sp.*
	Perlodidae	*Isoperla*	*Isoperla sp.*
	Taeniopterygidae		Taeniopterygidae
Rhynchobdellida	Glossiphoniidae		Glossiphoniidae
		Glossiphonia	*Glossiphonia complanata*
		Helobdella	*Helobdella stagnalis*
Trichoptera			Trichoptera
	Hydropsychidae		Hydropsychidae
		Hydropsyche	*Hydropsyche sp.*
	Hydroptilidae		Hydroptilidae
		Hydroptila	*Hydroptila sp.*
	Lepidostomatidae	*Lepidostoma*	*Lepidostoma sp.*
	Leptoceridae		Leptoceridae
		Nectopsyche	*Nectopsyche sp.*
	Rhyacophilidae	*Rhyacophila*	*Rhyacophila sp.*

			Acari
			Trombidiformes
Acari (Trombidiformes)	Hygrobatidae		*Hygrobatidae*
		Corticacarus	*Corticacarus sp.*
		Hygrobates	*Hygrobates sp.*
	Lebertiidae	*Lebertia*	*Lebertia sp.*
	Sperchonidae		Sperchonidae
		Sperchon	*Sperchon sp.*
Bivalvia			Bivalvia
	Corbiculidae	*Corbicula*	*Corbicula sp.*
			Corbicula fluminea
	Pisidiidae		Pisidiidae
		Pisidium	*Pisidium sp.*
Nemotoda			*Nemata*
Veneroida			Ostracoda
Platyhelminthes	Trepaxonemata		Trepaxonemata
	Turbellaria		Turbellaria
Oligochaeta			Oligochaeta
Ostracoda			Ostracoda

Taxa Richness

A total of about 45 taxa were reported from the Jordan River in the dataset (β- diversity), which only included targeted riffle and reach-wide habitats. Estimated total taxa that may have occurred in these two habitats throughout the river (β- diversity), ranged from 52 to 61 taxa based on several estimator

methods (McCune and Mefford 2011). Mean estimated total number of taxa per sample (α-diversity) was a very low 12.62 m^{-2} (std. err. = 3.19, min = 6, max = 21). Mean effective number of taxa per sample (ENT) (Shannon Diversity Index exponentiated) (α-diversity) was extremely low at 4.05 m^{-2} (std. err. = 1.58, minimum = 2.01, maximum = 9.64). This extreme low effective number of approximately 4 taxa m^{-2} is very troubling and shows that the river is severely impaired. Several factors responsible for this low ENT are discussed throughout this report, including the following section on densities estimates.

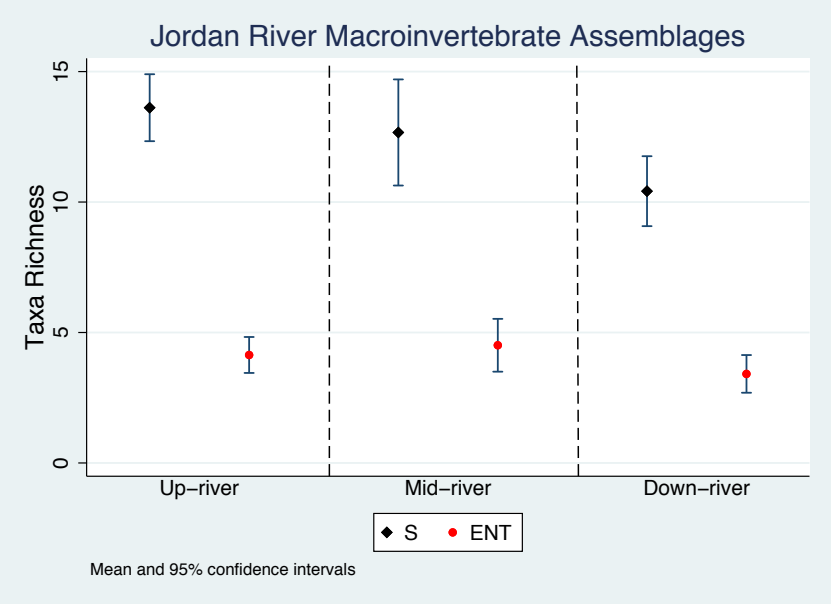

Figure 22. Taxa richness (S) and effective number of taxa (ENT) at three generalized sections of the Jordan River. Mean and 95% CIs are illustrated.

Density

Macroinvertebrate densities in the river were highly left skewed with a median of 3,686 m^{-2}. Some samples had as few as 51 m^{-2} individuals or as much as 47,720 m^{-2} (Figure 23). Some of this variability was in part due to the effects of different: 1) field methods used, 2) amounts of area sampled, and 3) laboratory subsampling on standardizing densities. Standardized densities from subsampling typically are over estimated. However, our estimated median densities = 3,686 m^{-2} from targeted riffle/reach wide habitats is on the very low end, particularly for highly productive rivers such as the Jordan River. Riffle and run habitats almost always have the highest diversity and abundances (densities) of any type of habitat in a river or stream. On average, macroinvertebrate densities in riffles throughout North America range between 10,000 and 30,000 m^{-2} (Jackson et al. 2005). Low abundances (densities) in more than half of the samples could have major impacts on Jordan River ecosystem function and needs to be further explored (see following section, Densities: upstream vs downstream).

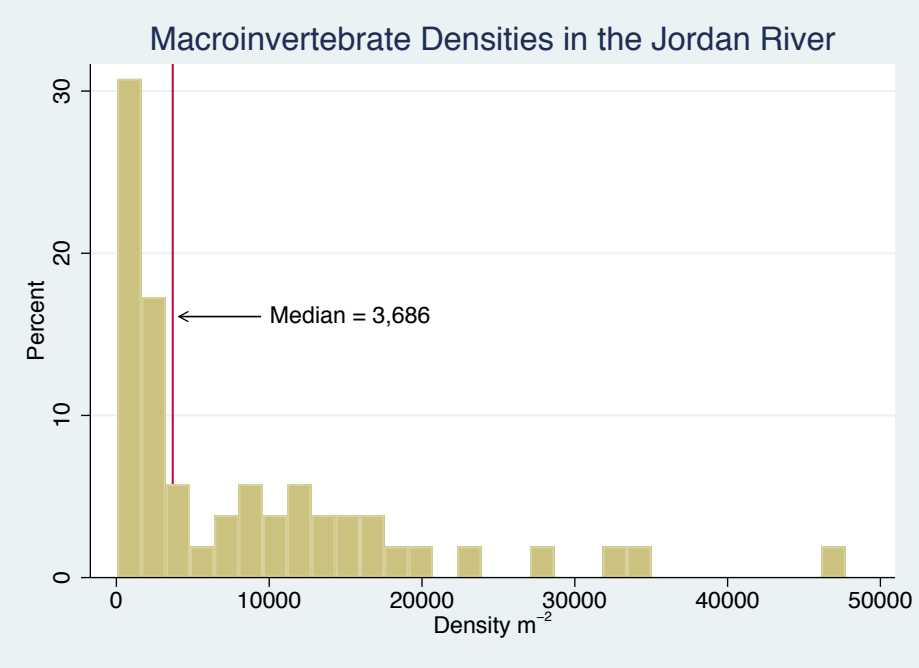

Mean	Std. error	Median	25th	75th	Min	Max
8,581	1,416	3,686	1,327	13,174	51	47,720

Figure 23. Distribution of macroinvertebrate densities in the Jordan River per sample analyzed (per sample = m^{-2}; α-diversity).

Macroinvertebrate evenness and diversity (H) was low but was comparable throughout the river, although diversity was lower downstream than upstream, but not significantly (Figure 24).

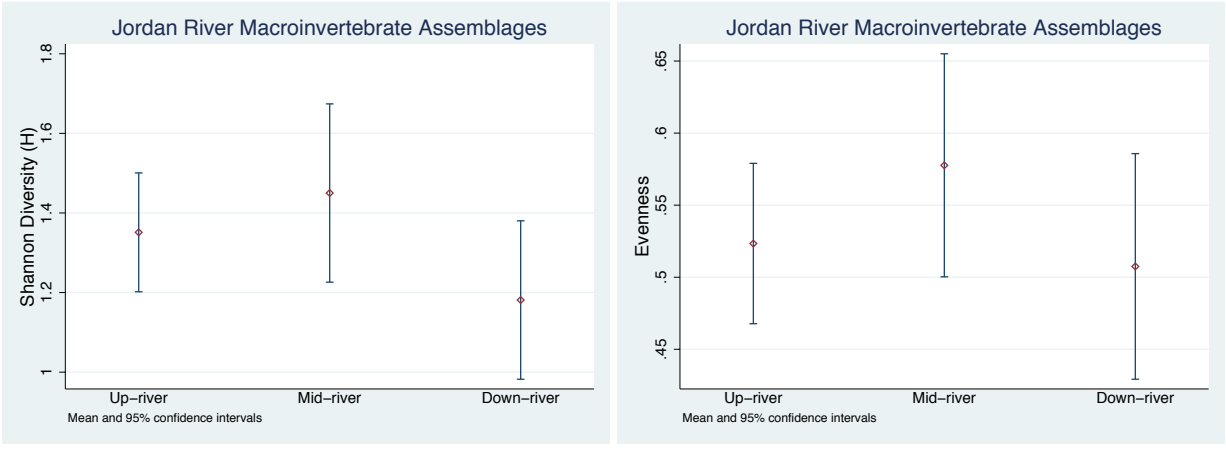

Figure 24. Macroinvertebrate diversity, and evenness based on three generalized sections of the Jordan River: Up-river, mid-river, and down-river. Mean and 95% CIs are illustrated.

Dominance

Just a handful of taxa dominated the Jordan River as measured by abundance. Dominance by a few taxa is a clear indicator that the river has major impairment(s). Throughout this report we discuss some of the dominant taxa and factors influencing their abundance.

Densities Upstream to downstream

Macroinvertebrate densities (raw) were significantly greater in the most upstream sites (Bangerter Rd. crossing area) than the furthest downstream sites (New State Canal crossing area) (Figure 25). This was primarily due to more cobble habitat upstream with some upstream locations having unembedded or slightly embedded cobble riffles as compared to thick silt and organic matter layer on top of mostly clay hardpan in the downstream sections.

The extreme lack of suitable macroinvertebrate habitat in downstream sections of the Jordan River reduced abundances (densities) and severely limited macroinvertebrate ability to perform essential ecosystem functions such as; nutrient cycling, regulation of primary producers including algae, tertiary and high trophic levels in the food web, and decomposition of organic matter. The furthest downstream sections of the Jordan River are extremely habitat limited for secondary producers such as macroinvertebrates and fish assemblages.

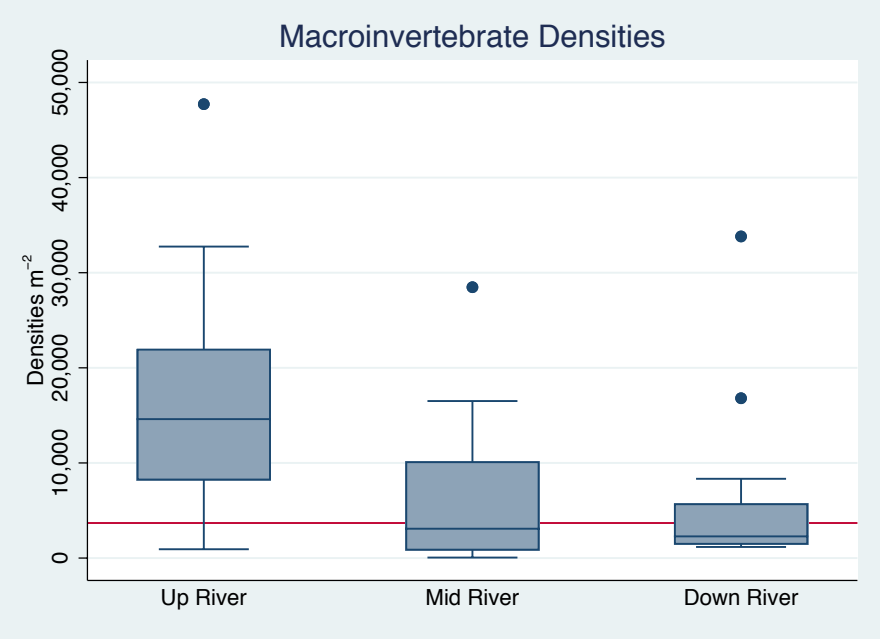

Figure 25. Comparison of macroinvertebrate densities between up-river, mid-river, and down-river sites. Red line is median = 3,686 m^{-2}.

Densities were $\log_{10}$+1 transformed for the following density analyses. The best fit (lowest log-likelihood, AIC, and BIC ratios) linear regression model for density was distance downstream (lat), month, year, and interactions between month and year. This model produced a significant $R^2 = 0.69$.

Although distance downstream only had a near significant effect on density (p = 0.06) it was important in the model (Figure 26). Densities varied across years with highest density estimates in 2006 and a decreasing trend through 2017(Figure 26). However, there were no data available from 2010 through 2015 or for 2016 and it is unknown whether these missing years may have had higher densities. Cyclic density patterns occur often in rivers, particularly for short lived taxa such as those that dominate Jordan River assemblages. Densities appeared to be stable across months except for February with lower densities and March with higher densities than average (Figure 26). For reasons not assessed in this report, no samples were reported in the databases for summer months.

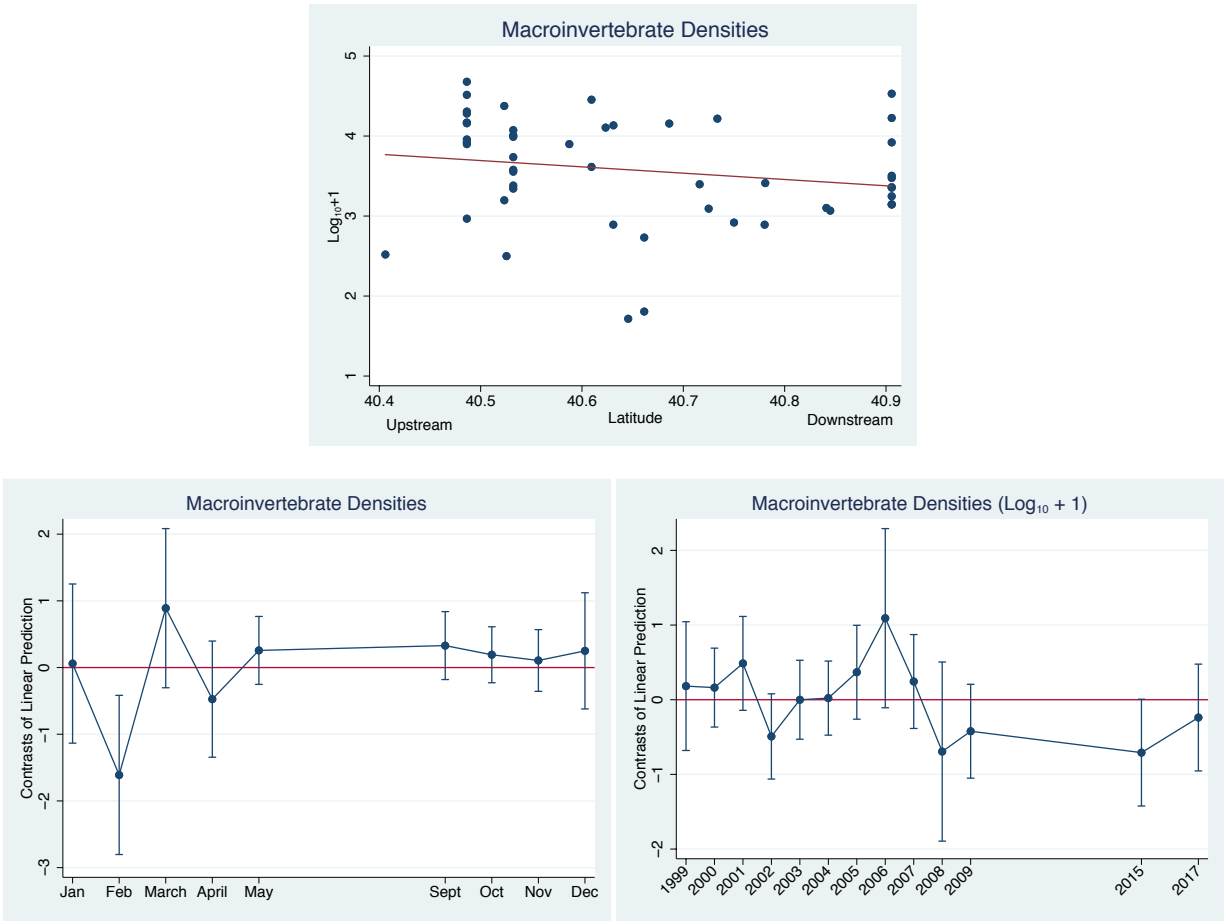

Figure 26. Macroinvertebrate densities (log_{10}+1) from upstream (left) to downstream (right), monthly, and yearly in the Jordan River.

Densities of Dominant Taxa

The macroinvertebrate assemblage in the river was dominated by just a dozen or so taxa, primarily by *Hydropsyche* sp., *Tricorythodes* sp., Chironomidae, and Orthocladiinae (Table 27). These four taxa are also those that dominated the very low effective number of taxa, ENT metric. Dominance by just a few taxa is a direct result of impaired conditions in the river. Densities for all taxa reported are in Table 27.

Table 27. Mean densities m^{-2} of taxa found in Jordan River from datasets used in this analysis listed in order of abundance. Taxa were 'rolled up' to account for differences in taxonomic identification or for specimens that could not be identified at higher taxonomic resolution.

	Taxon	Common Name	Mean density m^{-2}
1	Hydropsyche sp.	Caddisfly	2110.22
2	*Tricorythodes sp.*	Mayfly	1871.04
3	Chironomidae	Midge	1363.52
4	Orthocladiinae	Midge	1018.75
5	*Potamopyrgus antipodarum*	New Zealand mudsnail	478.50
6	Simuliidae	Blackfly	291.97
7	Oligochaeta	Segmented worm	278.17
8	Caecidotea	Sow bug	261.93
9	Acari	Mite	241.29
10	Coenagrionidae	Damselfly	77.21
11	Turbellaria	Flatworm	67.78
12	*Corbicula sp.*	Asian clam	64.25
13	Elmidae	Riffle beetle	54.97
14	Hydrobiidae	Snail	35.01
15	Baetidae	Mayfly	27.60
16	Hirudinea	Leech	21.51
17	Empididae	Fly	20.49
18	Physidae	Snail	19.76
19	Hydroptilidae	Caddisfly	14.94
20	*Fluminicola coloradoensis*	Snail	10.64
21	Leptohyphidae	Mayfly	8.82
22	Nemata	Nematode	7.60
23	Pisidiidae	Fingernail clam	6.87
24	Amphipoda	Scud	6.56
25	Ceratopogonidae	Biting midge	4.11

26	Corixidae	Water boatman	3.88
27	Tetrastemmatidae	Worm	3.84
28	Ancylidae	Snail	3.15
29	Leptophlebiidae	Mayfly	2.20
30	Calopterygidae	Damselfly	2.14
31	Aeshinidae	Dragonfly	1.29
32	*Orconectes virilis*	Invasive crayfish	1.08
33	Trichoptera	Caddisfly	0.81
34	Leptoceridae		0.52
35	Caenidae		0.37
36	Lymnaeidae		0.32
37	Planorbidae		0.30
38	*Isoperla sp.*		0.12
39	Ephydridae		0.10
40	Hydrophilidae		0.06
41	Lepidostomatidae		0.05
42	Dytiscidae		0.04
43	Ephemerellidae		0.03
44	Notonectidae		0.03

Community Ecology

Several well-known and valid multivariate ecological assemblage methods can be used to understand complex interactions between macroinvertebrate taxa and environmental conditions. We used three of the most commonly used and informative methods: 1) Non-parametric Multidimensional Scaling (NMS) which is akin to Principal Components Analysis (PCA), 2) Multiple Response Permutation Procedure (MRPP) which is akin to Analysis of Similarity (ANOSIM), and 3) cluster analysis. Taxa with low occurrences were either omitted or combined, mostly to family level or coarser, for the community (assemblage) ecological analyses. Assemblages generally grouped by month, year, and location. Changes in assemblage structure can have significant effects on interactions between taxa and ecosystem functioning. These changes shown in assemblage structure in the multivariate analyses that follow need

to be accounted for in any ecological and water quality analysis. Cluster analysis results are in Appendix 30.

NMS

The best NMS model was a 3-dimensional model that used a Sorensen-Bray distance measure with a final stress = 12.99; final instability < 0.000; and number of iterations = 66. The cumulative R^2 = 0.65 with Axis 1 R^2 = 0.35; Axis 2 R^2 = 0.19, and Axis 3 R^2 = 0.12. Axis 2 clearly showed the difference between assemblages from furthest upstream sites vs. furthest downstream sites but not for sites in between (Figure 27 and Figure 28). NMS didn't show any differences in assemblages between months or years (not shown).

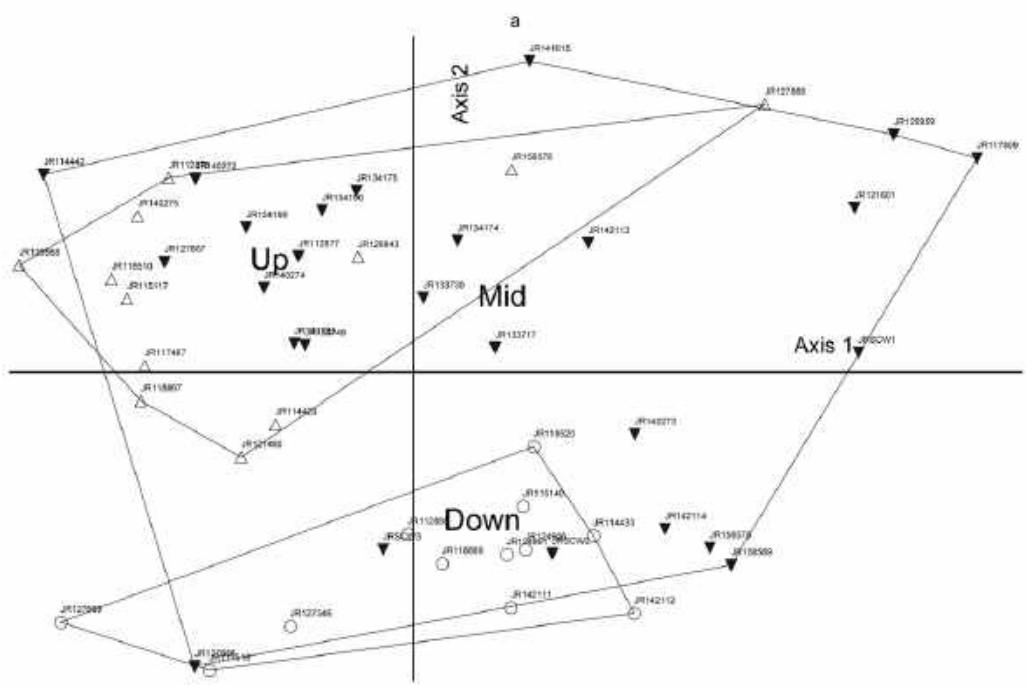

Figure 27. NMS axis 1 and 2 showing differences between furthest upstream and furthest downstream macroinvertebrate assemblages but not between mid reaches of the river.

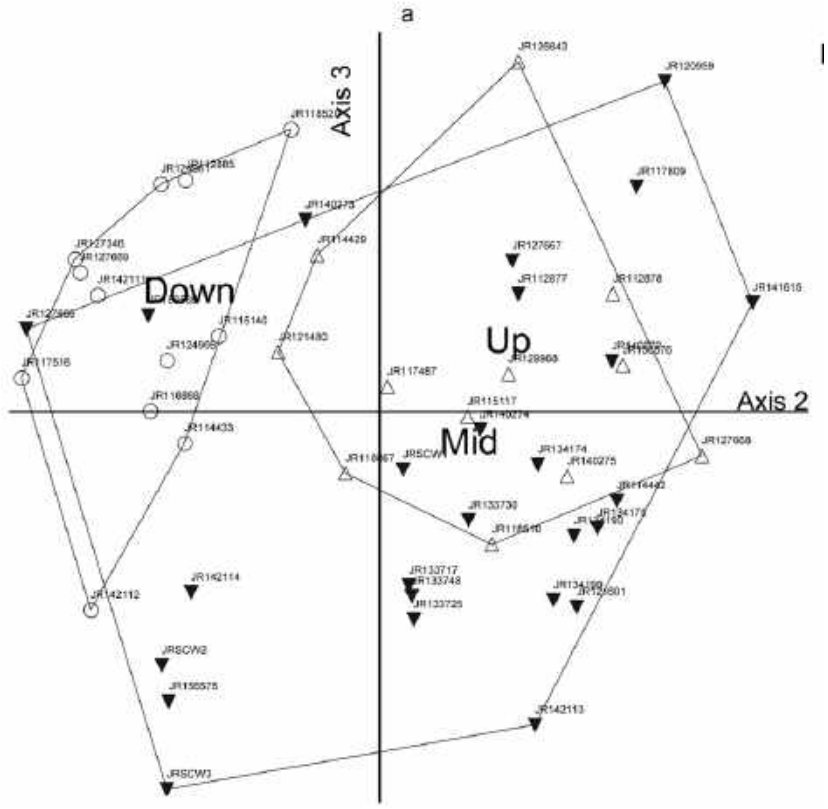

Figure 28. NMS axis 2 and 3 showing differences between furthest upstream and furthest downstream macroinvertebrate assemblages but not between mid reaches of the river.

Correlations, *r* between macroinvertebrate taxa and NMS axes are in Appendix 24.

MRPP results were consistent with NMS results and showed that assemblages differed significantly between furthest upstream sites and furthest downstream sites but were also significantly different from midstream site assemblages ($A = 0.08$, $p < 0.001$):

1. Upstream vs midstream ($p < 0.001$)
2. Upstream vs. downstream ($p < 0.001$)
3. Midstream vs. downstream ($p < 0.001$)

MRPP also showed that there were several significant ($p << 0.07$) monthly differences in assemblages between:

1. May and October
2. October and November
3. May and September
4. November and September.

and there were several significant ($p << 0.07$) yearly differences in assemblages between:

- 1999 and 2002
- 1999 and 2004
- 1999 and 2009
- 2004 and 2009
- 2004 and 2017
- 2003 and 2005
- 2005 and 2017
- 2007 and 2009

These assemblage results show that locational, seasonal, and annual variability must be accounted for when analyzing macroinvertebrate data in the Jordan River. For example, if these factors are not the focus of interest in an analysis, then they should be modeled as random factors. Or if water quality comparisons are to be made, then variability caused by these factors must be adequately addressed.

Assemblages and Habitat

Jordan River macroinvertebrate assemblages did not differ between targeted riffles or reach-wide types of habitat using NMS or MRPP ($A = 0.002$, $p = 0.29$). These findings were similar to individual dominant taxa relationships with habitat that we present in following sections (Assemblages and Habitat, Sediment Tolerance) and suggests that cobble riffle habitats, which almost universally have the greatest macroinvertebrate diversity and densities of any habitat in a properly functioning stream (Hauer and Lamberti 2007), do not support assemblages that differ from reach-wide runs composed of mostly sands and gravels in the Jordan River. This phenomenon is a direct result of anthropogenically induced cobble habitats becoming extremely embedded with naturally occurring sands and fines that under natural

conditions would have been removed from cobble riffles on a regular basis, either from flood events, beaver pond sediment entrapment, or both.

Indicator Species by General Location

Indicator species analysis based on upstream, midstream, and downstream classification showed that several taxa could be used as significant indicators of those sections (Table 28).

Table 28. Significant indicator taxa for three loosely grouped sections of the Jordan River: Upstream, Mid-river, and Down-river.

Upstream indicators				
Taxon	IV	Mean	Std.Dev.	P-value
Elmidae	81.6	29.5	8.08	0.0002
Hydropsychidae	85.1	50.4	9.50	0.0004
Empididae	47.8	19.5	7.33	0.0038
Orthocladinae	64.8	39.6	8.10	0.007
Tricorythodes	49.7	30.3	7.62	0.023
Corbicula	49.4	29.1	9.17	0.0308
Mid-river Indicators				
Taxon	IV	Mean	Std.Dev.	P-value
Hirudinea	51.8	27.4	6.98	0.007
Ceratopogonidae	30.8	14.3	6.39	0.0176
Down-river indicators				
Chironomidae	82.9	51.4	11.64	0.0036

Dominant Taxa Density Relationships with Latitude, Month, and Year

Linear regression models were developed for the twelve most dominant taxa in the river using $\log_{10}$ +1 transformed densities vs. latitude, month, year, and interactions. Best fit models were chosen using log likelihood, Akaike's Information Criteria, and Bayesian Information Criteria. Densities (abundances) of most of these taxa were significantly affected by latitude, month, year, and their interactions, which often explained a substantial amount of abundance (density) variability (please examine R^2 values for each taxon). Month and year linear contrasts with grand means were then made using the best fit

models and then graphed to illustrate the differences in taxa densities (log_{10} + 1) among months and among years.

Trichorythodes sp., Tricho Mayfly

All three predictors; latitude, month, and year best described *Tricorythodes* sp. densities with an R^2 = 0.74. Note the drop off in densities after 40.7 latitude starting downstream of Surplus Canal Diversion at 21st South (Figure 29 and Figure 30). *Tricorythodes* sp. densities were also lowest during late autumn through winter most likely because of eggs stages and earlier instar, which weren't detected during sampling. Also note the decrease in abundance after 2009 (Figure 29). This could have been caused by erratic sampling dates and different methods, etc. but needs further investigation.

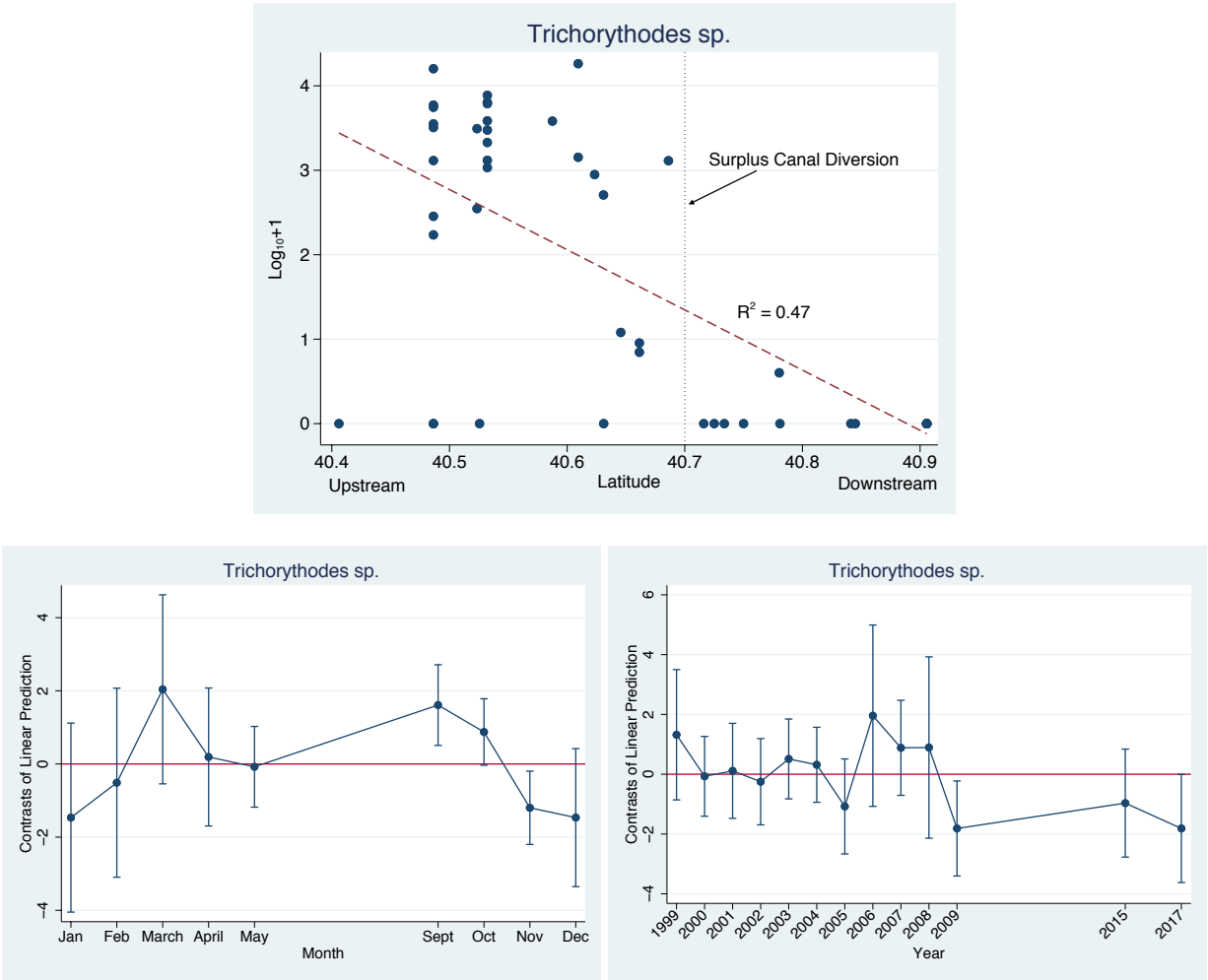

Figure 29. Tricorythodes sp. relation to latitude, Month, and Year. Red line for latitude figure = linear trend. Red line for month and year are the grand means (log_{10}); Circles = means; error bars = 95% CIs.

Further analysis of *Tricorythodes* sp. density differences between upstream of 40.7 latitude and downstream samples supported those shown in Figure 29. Densities significantly dropped to near zero downstream of the Surplus Canal Diversion (21st South, Latitude > 40.7) as compared to upstream (Figure 30).

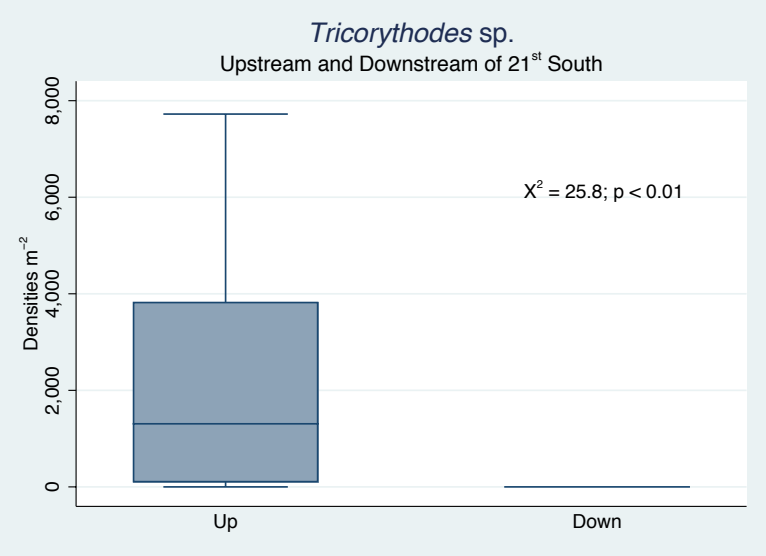

Figure 30. Comparison of Tricorythodes sp. densities in the Jordan River upstream and downstream of latitude 40.7 where substantial flows of the river are diverted into the Surplus Canal. Non- parametric Kruskal-Wallis X^2 ranks test results are in figure.

The cursory results of analyses on *Tricorythodes* sp. shown above emphasize the importance of this taxon as an indicator of conditions in the Jordan River as they are affected by the Surplus Canal Diversion. More than one environmental factor may be responsible for reduced tricho mayfly densities including those presented in following sections.

Hydropsychidae

Upstream to downstream (latitude), habitat, month, year, and month-year interactions were the best predictor of *Hydropsyche* sp. (Hydropsychidae) densities ($R^2 = 0.74$) (Figure 31). Densities decreased from upstream to down, most likely due to loss of suitable stable habitat (see sections: Sediment Tolerance, and Habitat). Slight but not significant lower densities were found from autumn through winter. This was possibly due to non-detectable egg or very small instars. Notice decline *Hydropsyche* sp. starting in 2006-2008, similar to other taxa declines.

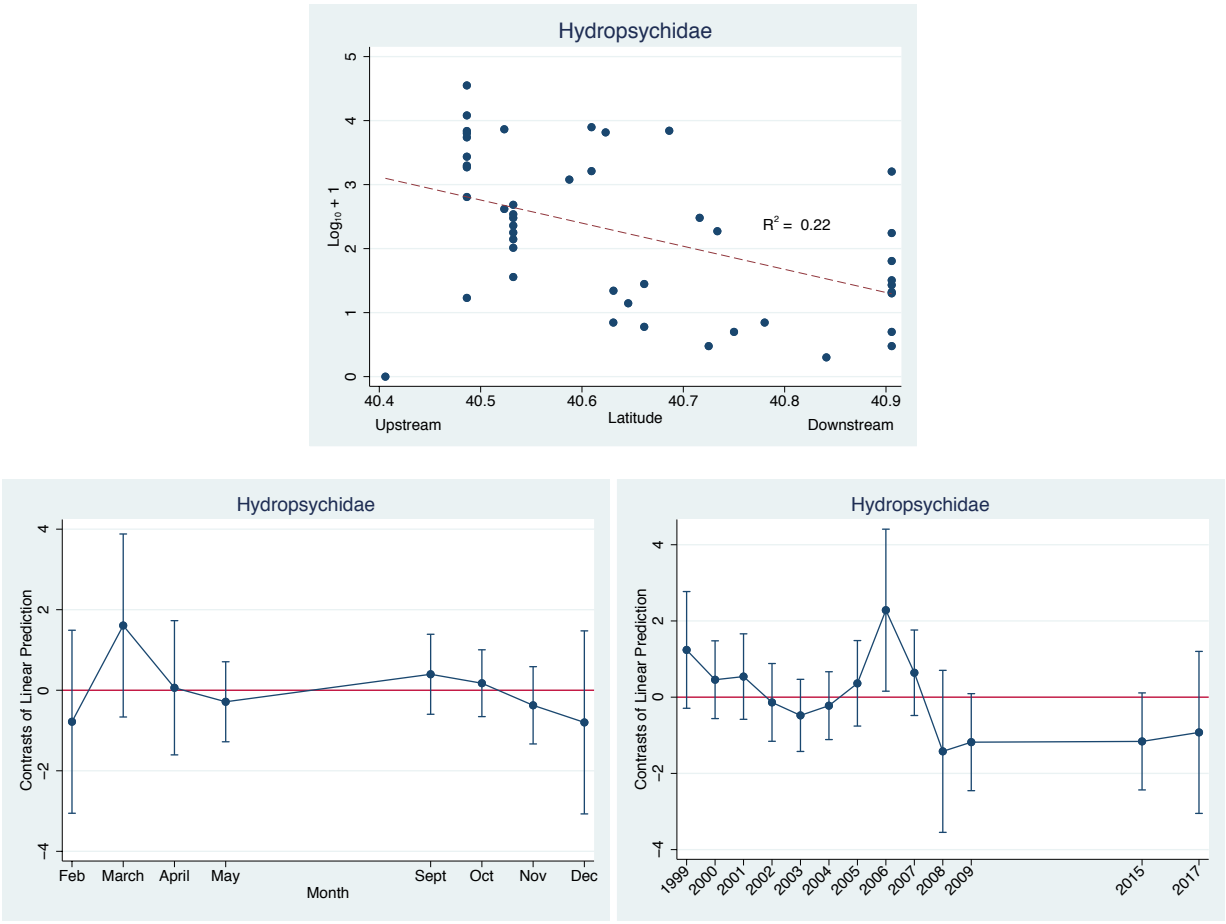

Figure 31. Hydropsyche sp. (Hydropsychidae) density (log_{10}) relation to latitude, Month, and Year. Red line for latitude figure = linear trend. Red line for month and year figures are the grand means (log_{10}); Circles = means; error bars = 95% CIs.

Chironomidae, midges

Chironomids were the third most abundant taxon in the dataset and had slightly increasing densities from upstream to down, reverse of many of the dominant taxa. There were no significant seasonal or annual patterns of midge densities, however, notice the non-significant decline in chironomids starting in 2006 or earlier, which is a consistent pattern with many of the taxa. This decline needs to be investigated further. Lack of taxonomic resolution beyond family level of Chironomidae was an extreme deficiency on the part of the goals of researchers who contributed to the database. Chironomids are one of the most diverse taxonomic groups of macroinvertebrates and there could have been perhaps as many chironomid species in the Jordan River as there were all other non-chironomid taxa combined.

This deficiency resulted in much less ability on our part to evaluate the role of macroinvertebrates in the Jordan River ecosystem.

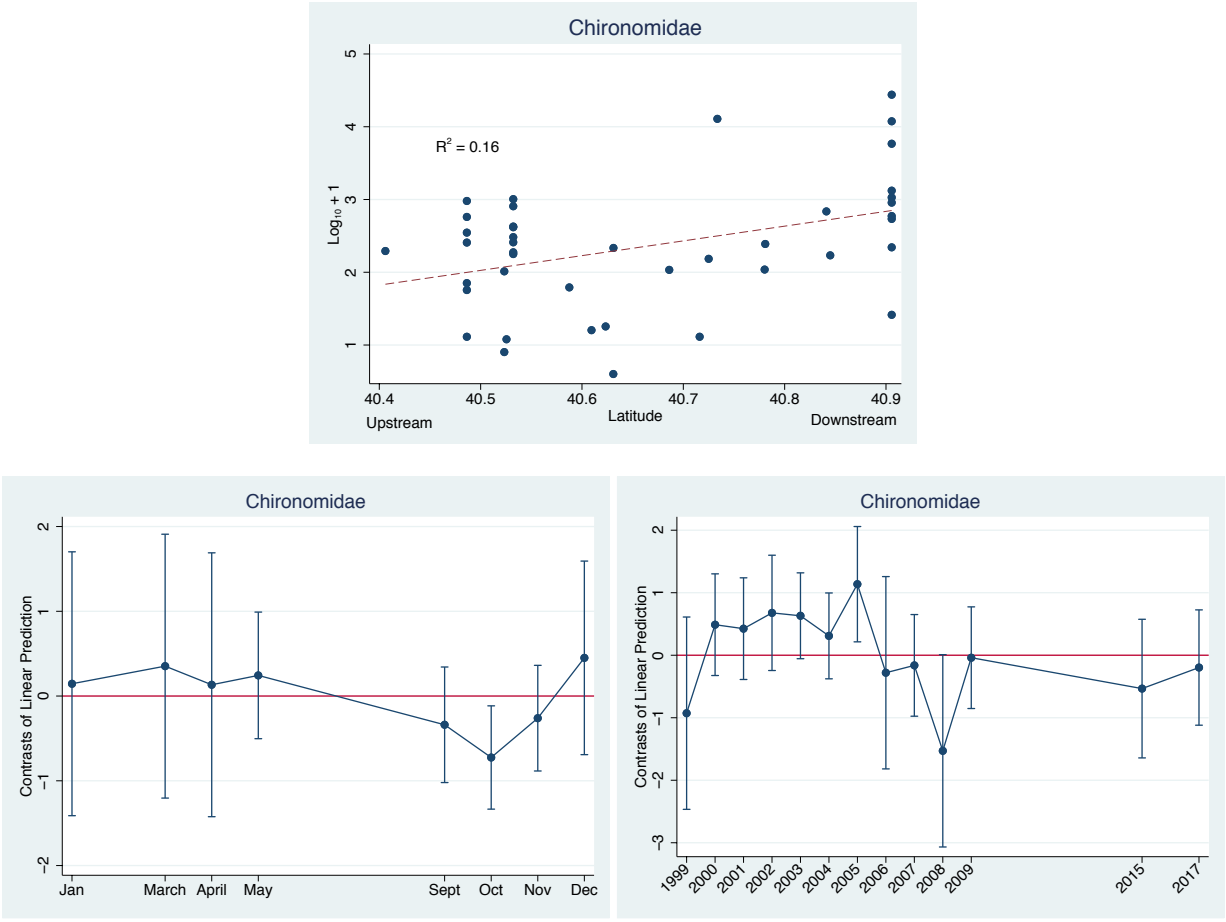

Figure 32. Chironomidae density (log_{10}) relation to latitude, Month, and Year. Red line for latitude figure = linear trend. Red line for month and year figures are the grand means (log_{10}); Circles = means; error bars = 95% CIs.

Orthocladinae, subfamily of midges

Orthoclad densities did not appear to vary upstream to downstream and had stable densities throughout the year, except possibly in February (R^2 = 0.74). Note drop off after 2007 or so. Need to find out the cause(s), but sampling effort, taxonomic effort, a potential missed cycle (4 year cycle ?), or several types of impairment are suspect.

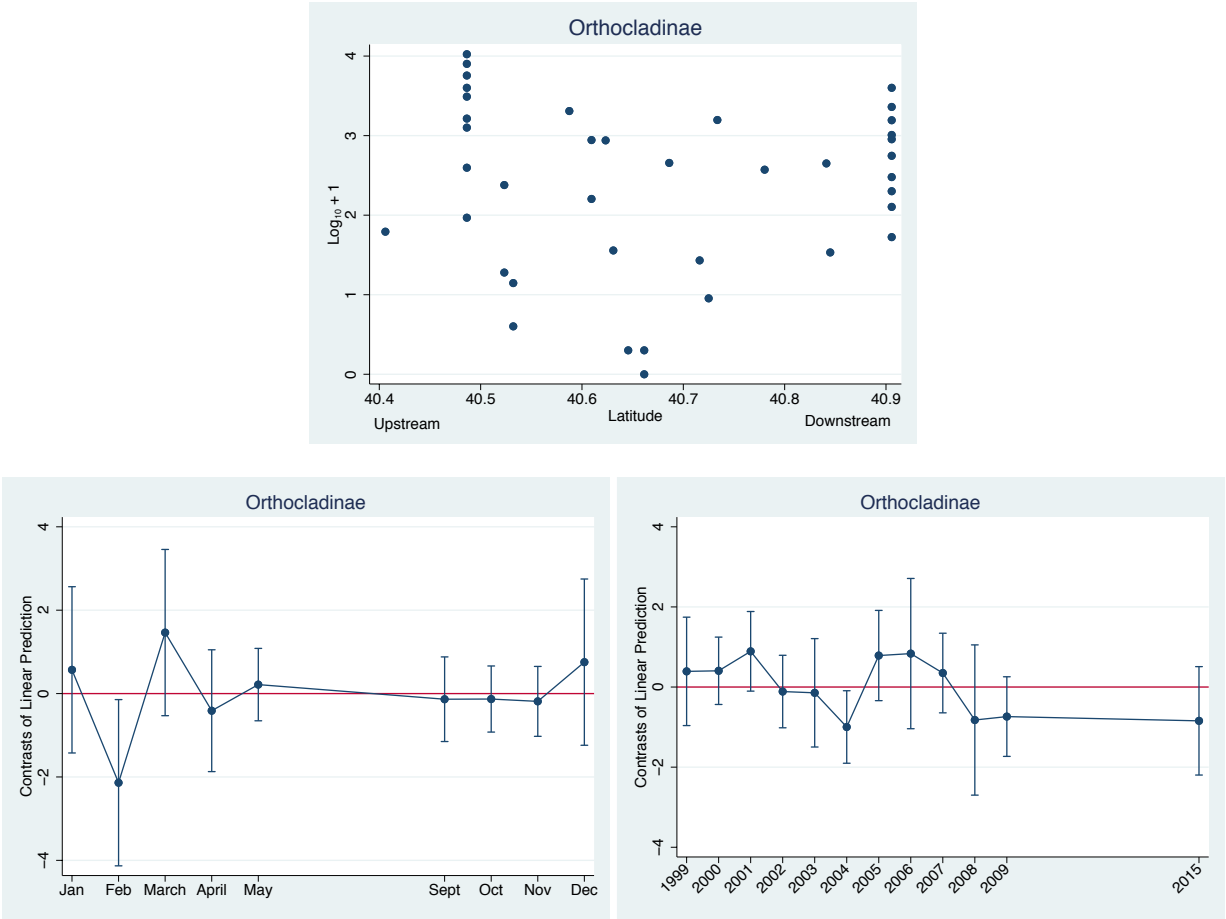

Figure 33. Orthocladinae density (log_{10}) relation to latitude, Month, and Year. Red line for latitude figure = linear trend. Red line for month and year figures are the grand means (log_{10}); Circles = means; error bars = 95% CIs.

Potamopyrgus antipodarum, New Zealand Mudsnail

There were not enough comparative samples to generate a very rigorous regression model (N =13) for mudsnail densities, however the best fit linear regression suggested that mudsnails densities (log_{10} +1) were not significantly affected by distance downstream (latitude), month or year (Figure 34). However, the combination of the three predictors provided a non-significant R^2 = 0.38. The analysis suggests that mudsnail densities have been steady since 2004 even though in many waterbodies where this snail has invaded, their populations have crashed after reaching extreme high densities (Moore et. al. 2012).

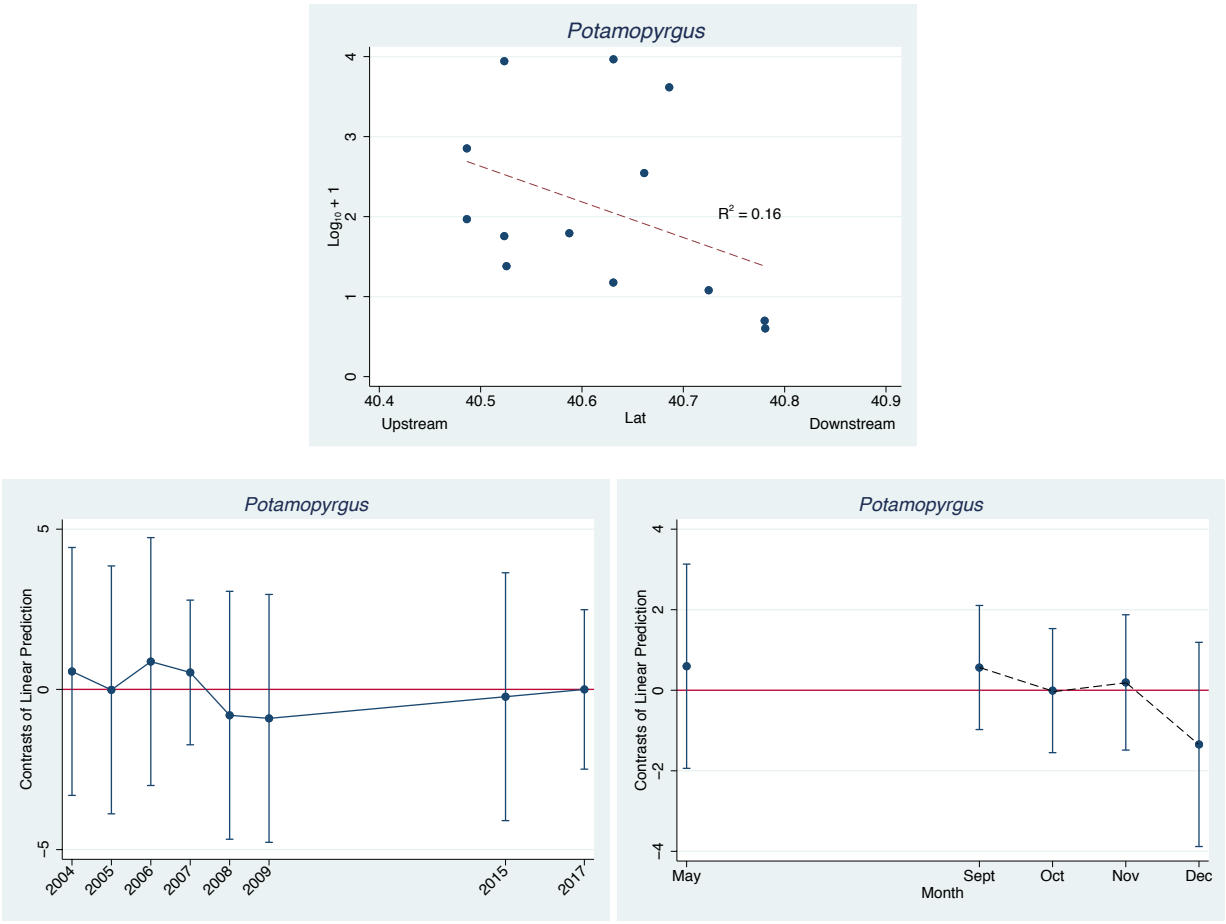

Figure 34. Potamopyrgus density (log_{10}) relation to latitude, Month, and Year. Red line for latitude figure = linear trend. Red line for month and year figures are the grand means (log_{10}); Circles = means; error bars = 95% CIs.

Not enough seasonal sampling data were available for a robust analysis but from experience, *Potamopyrgus* densities can remain high throughout the year with higher abundances of smaller individuals occurring when temperatures are conducive for birthing. Much more research is needed to understand how New Zealand mudsnails alter ecosystem function in the Jordan River. Richards (2017a, 2017b, 2018a, 2018b) reported the most detailed descriptions of the potential effects of mudsnails in the Jordan River, to date.

Figure 35.Typical densities of New Zealand mudsnails, Potamopyrgus antipodarum on semi embedded cobble in Jordan River.

Simuliidae, Blackflies

Blackfly density (abundance) significantly varied from upstream to downstream (latitude) and among months and years (plus interactions) (R^2 = 0.75) (Figure 36).

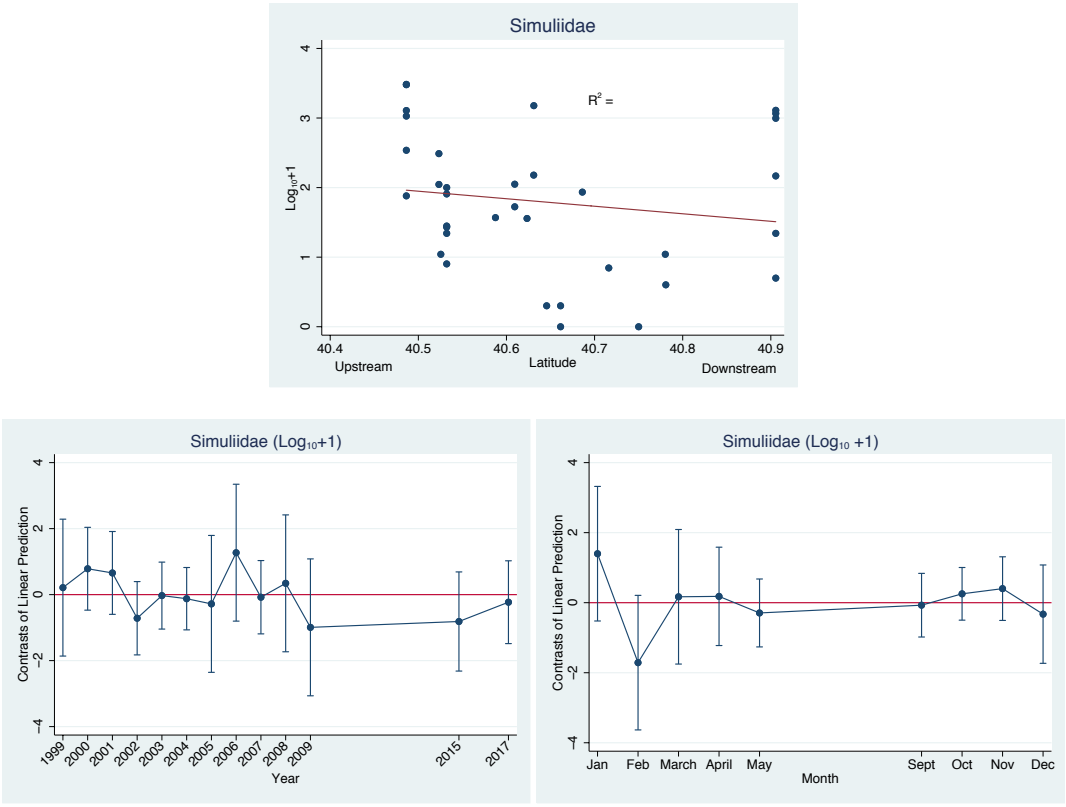

Figure 36. Simuliidae density (log_{10}) relation to latitude, Month, and Year. Red line for latitude figure = linear trend. Red line for month and year figures are the grand means (log_{10}); Circles = means; error bars = 95% CIs.

Oligochaeta, segmented worms

Oligochaete worm densities varied significantly among months and years (plus interactions) but not from upstream to downstream (R^2 = 0.76) (Figure 37). Oligochaete are extremely important to ecosystem function and are one of the primary taxa for breaking down organic matter. It appeared that oligochaetes were the only major taxon to increase in abundance from 2007. We have also recently become aware that polychaetes inhabit the Jordan River and may have been misidentified as oligochaetes. This is another deficiency in taxonomic resolution that needs to be rectified.

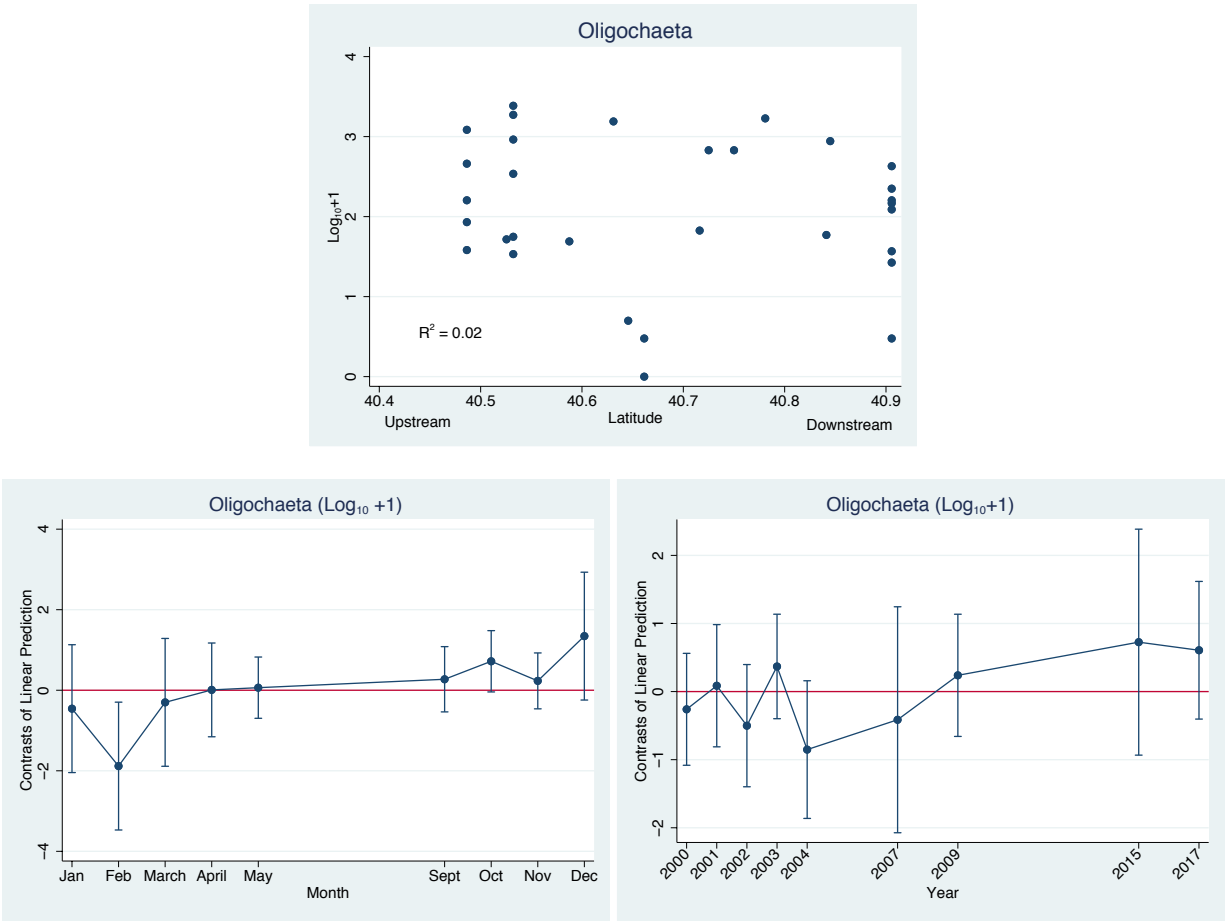

Figure 37. Oligochaeta density (log_{10}) relation to latitude, Month, and Year. Red line for latitude figure = linear trend. Red line for month and year figures are the grand means (log_{10}); Circles = means; error bars = 95% CIs.

Caecidotea, sow bugs

Sow bugs (pill bugs) density was significantly affected by latitude (upstream-downstream), month, year, and month-year interactions (R^2 = 0.71). These taxa are common and widespread throughout the river and are important detritivores that tolerate warm temperatures and sediments.

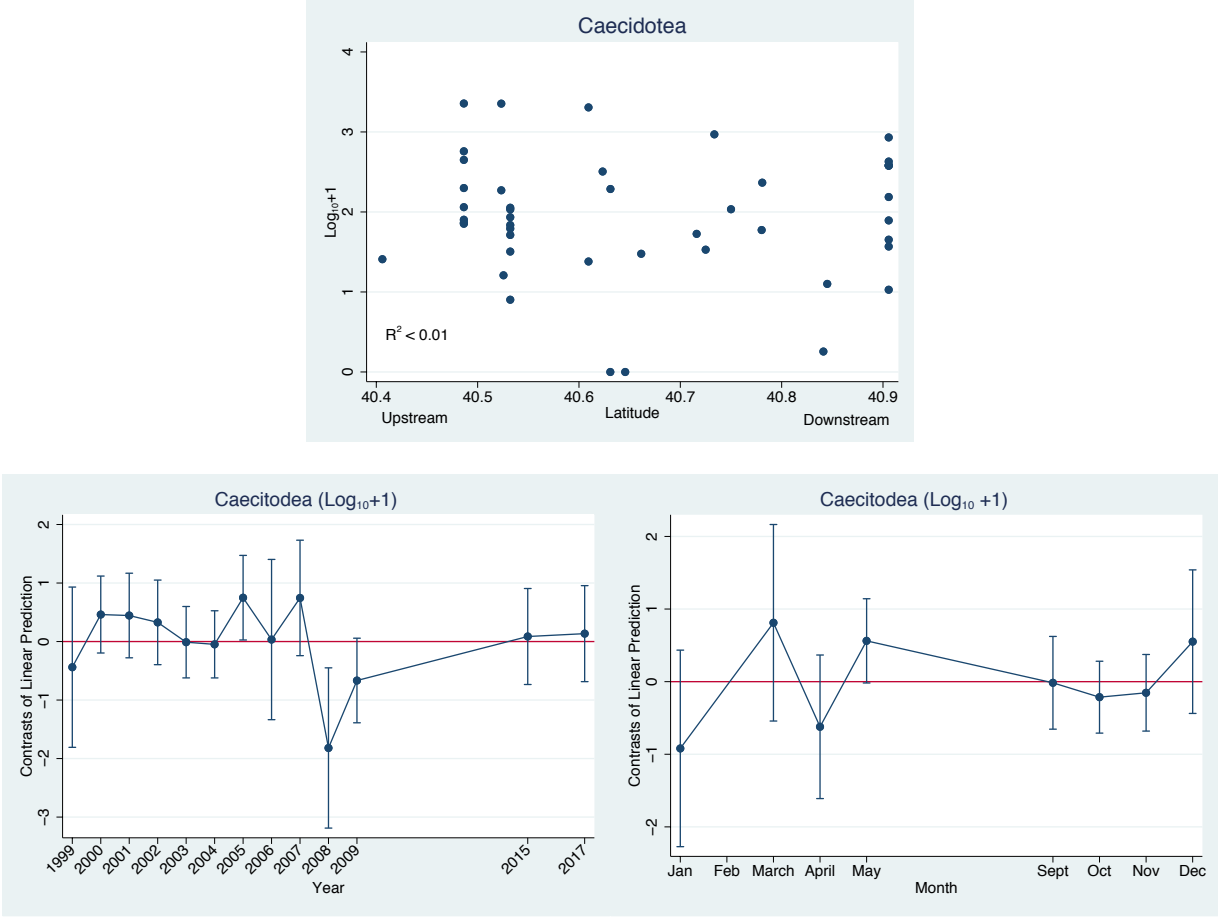

Figure 38.Caecitodea density (log_{10}) relation to latitude, Month, and Year. Red line for latitude figure = linear trend. Red line for month and year figures are the grand means (log_{10}); Circles = means; error bars = 95% CIs.

Acari, mites

Mite densities were also significantly affected by latitude, month, year, and month-year interactions (R2 = 0.78) (Figure 39). Very little is known about the ecology and function of these predators in the Jordan River.

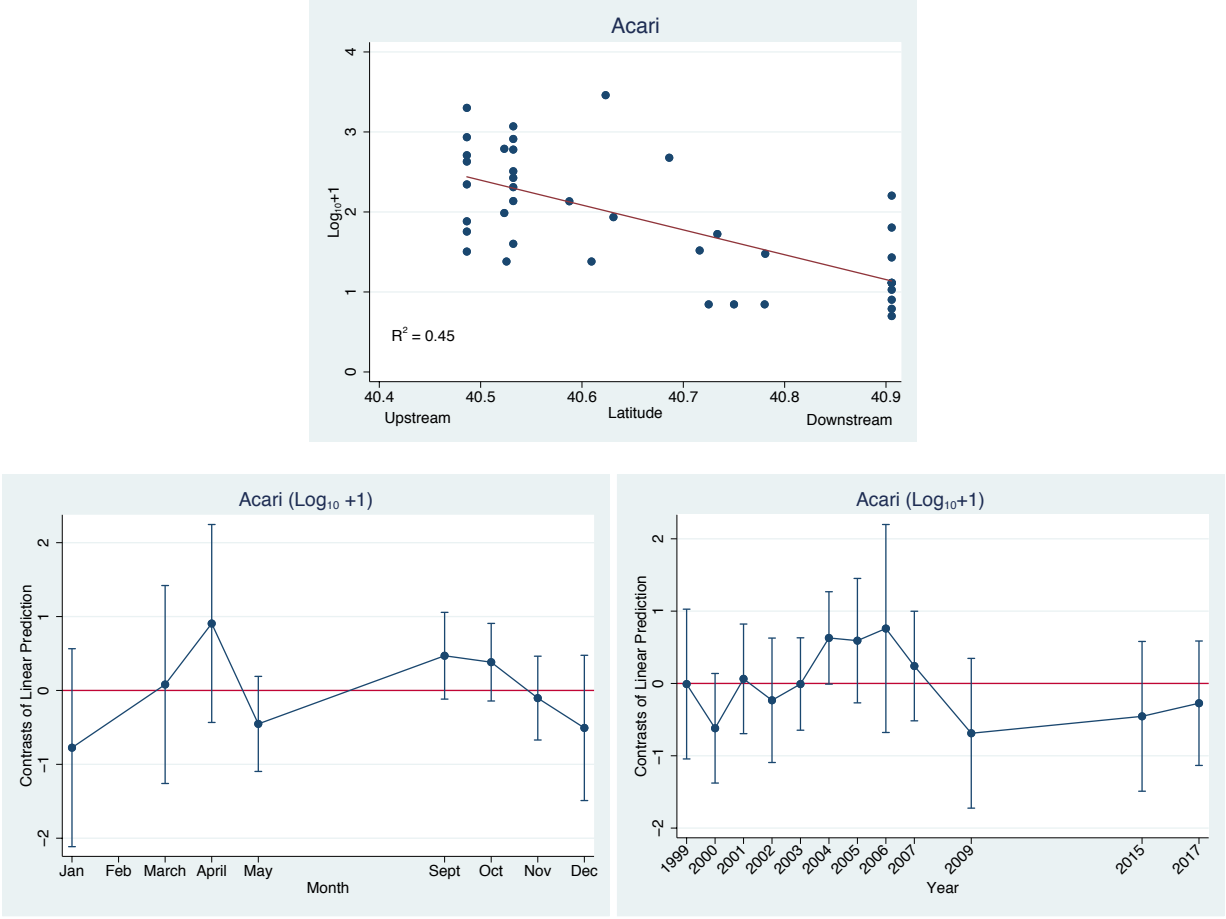

Figure 39. Acari density (log_{10}) relation to latitude, Month, and Year. Red line for latitude figure = linear trend. Red line for month and year figures are the grand means (log_{10}); Circles = means; error bars = 95% CIs.

Coenagrionidae, damselflies

The best fit linear regression model for Coenagrionidae densities (log_{10}+1) was month, year, and month-year interaction which explained most of their variability (R^2 = 0.89) (Figure 40). Distance downstream (latitude) was not a good predictor of damselfly densities.

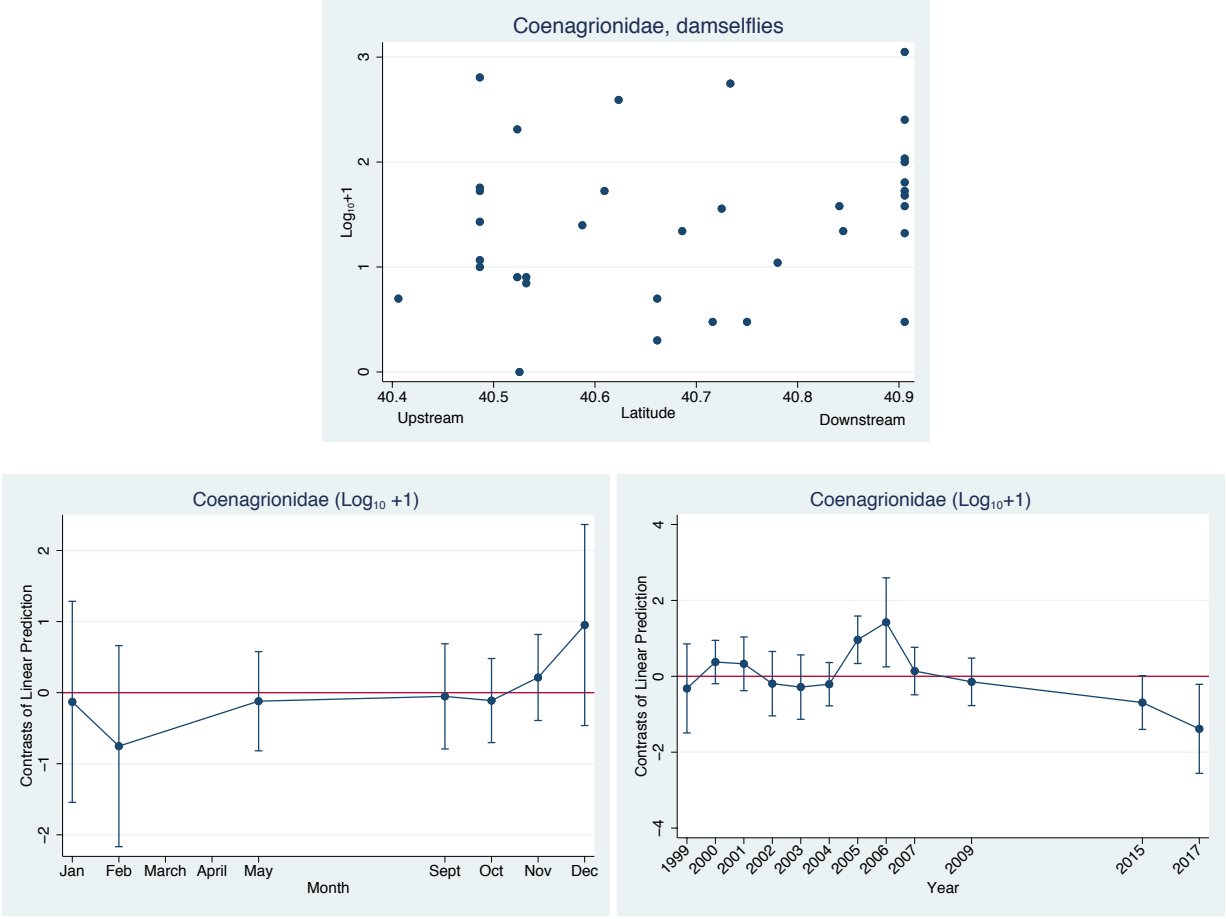

Figure 40. Coenagrionidae density (log_{10}) relation to latitude, Month, and Year. Red line for latitude figure = linear trend. Red line for month and year figures are the grand means (log_{10}); Circles = means; error bars = 95% CIs.

Turbellaria, flatworms

The best fit linear regression model for flatworm densities (log_{10}+1) was distance downstream (latitude), month, year, and month-year interaction with an R^2 = 0.88, although distance downstream was not significant (Figure 41). Very little is known about flatworm ecology in the Jordan River but given their high abundances their effects on ecosystem function are likely substantial.

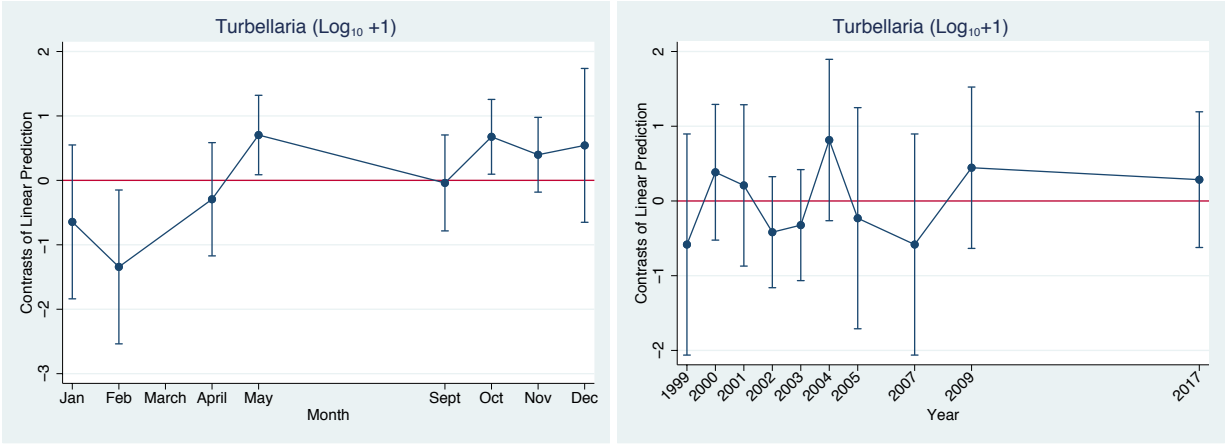

Figure 41. Turbellaria density (log_{10}) relation to latitude, Month, and Year. Red line for latitude figure = linear trend. Red line for month and year figures are the grand means (log_{10}); Circles = means; error bars = 95% CIs.

Corbicula sp., invasive Asian clams

The best fit linear regression model for *Corbicula* sp. densities (log_{10}+1) was distance downstream (latitude), month, year, and month-year interaction with an $R^2 = 0.68$. Although distance downstream was not significant in the four-predictor model, distance downstream was when modelled by itself, $R^2 = 0.24$ ($p = 0.07$) (Figure 42).

Sample data used in these analyses were collected from mostly targeted cobble riffles (N = 35) and reach wide sections (N = 10). *Corbicula* sp. occurs primarily in gravelly/sandy runs and pools will low amounts of organic matter (Richards 2018a). Therefore, *Corbicula* densities presented here are very low estimates and are not representative of the entire Jordan River.

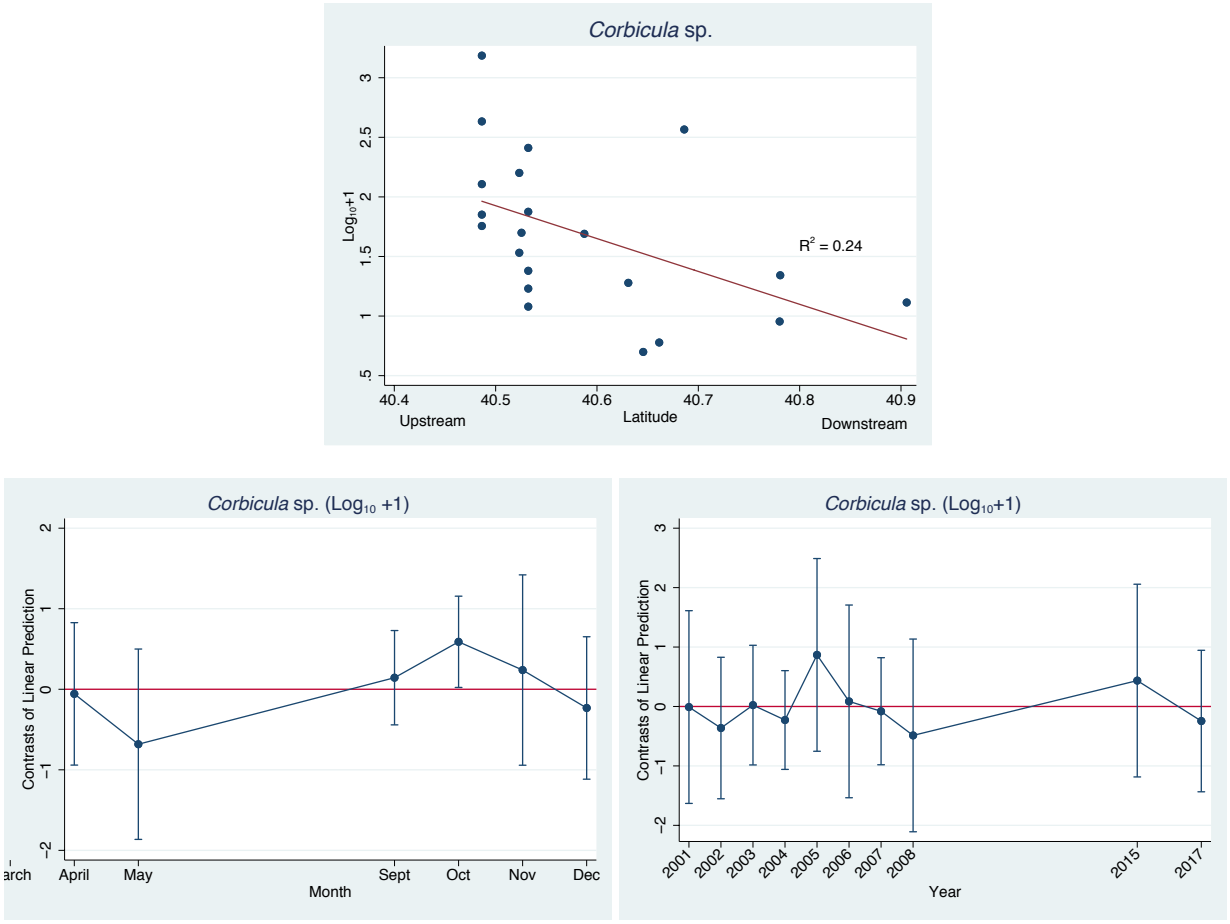

Figure 42.Corbicula density (log_{10}) relation to latitude, Month, and Year. Red line for latitude figure = linear trend. Red line for month and year figures are the grand means (log_{10}); Circles = means; error bars = 95% CIs.

Richards (2017a, 2017b, 2018a, 2018b) and Richards and Miller (in press) reported the most detailed descriptions of the potential effects of *Corbicula* (and *Potamopyrgus*) in the Jordan River, to date. Findings from these reports solidify our conclusion that the invasive clam, *Corbicula* and to a lesser extent the invasive mudsnail, *Potamopyrgus* are the dominant macroinvertebrate taxa in the Jordan River and likely regulate entire ecosystem function and water quality.

Organic Pollutants, Sediment and Temperature Pollution Effects on Macroinvertebrate Assemblages

Water Quality Indices

Simplified metrics such as RIVPACS O/E models or generalized but comprehensive reports such as those provided by macroinvertebrate taxonomy labs do not always guide managers in determining the types of pollutants or pollution that may be responsible for observed macroinvertebrate assemblage composition. Relying on a single metric cannot possibly assist in causal inference. Several types of pollution or pollutants may be acting individually or synergistically. Comprehensive reports are more useful but unless managers critically evaluate individual metrics or indices based on some understanding of macroinvertebrate ecology and life history then important relationships are invariably overlooked.

We examined and compared several metrics and indices that measure three types of processes known to affect macroinvertebrate assemblages: Organic enrichment, sedimentation, and temperature. We calculated and compared these metrics using taxa presence and taxa abundances. Family level taxonomic resolution is not as useful as species or genus level resolution for developing any type of metric (USEPA 2006, Richards 2016, Sweeney et. al. 2011). Therefore, we used the lowest practical taxonomic resolution as was possible in evaluation and comparisons of these metrics.

Hilsenhoff Biotic Index, HBI

The Hilsenhoff Biotic Index (HBI) is the most widely used and abused metric for evaluating organic enrichment. The Hilsenhoff Biotic Index (HBI) estimates overall tolerance of the community in a sampled area, weighted by the relative abundance of each taxonomic group (family, genus, etc.). Organisms are assigned a tolerance number from 0 to 10 pertaining to that group's known sensitivity to organic pollutants; 0 being most sensitive, 10 being most tolerant. Even though HBI values are sometimes strongly correlated with other indices (e. g. sedimentation or temperature indices), HBI was only developed to measure organic pollutant effects.

The mean taxa based HBI for all taxa found in the Jordan River = 5.77 (std. err. = 0.17; median = 6) which resulted in a ‘fair’ water quality score (Table 29, Table 30). However, the abundance based mean 4.98 (std. error < 0.00) and median = 4 (Table 29) resulted in a ‘good’ water quality score (Table 30). These results show that riverwide; less-tolerant (more sensitive) individuals were more abundant than more-tolerant individuals to organic pollution (Figure 43). This was most likely due to the two most dominant (abundant) taxa in the river samples, the mayfly *Tricorythodes* sp. and the caddisfly, *Hydropsyche* sp. Both taxa have lower than average Jordan River macroinvertebrate assemblage HBI tolerance values of 4 and both taxa decrease in abundance from up-river to down river (see section Dominant Taxa Density Relationships with Latitude, Month, and Year). Appendix 26 provides HBI values for all 83 of the Jordan River taxa that had HBI values.

Table 29. Descriptive statistics for HBI abundance and taxa based.

HBI	mean	se(mean)	median	p25	p75	min	max
Abundance based	4.98	0.00	4	4	6	1	9
Taxa based	5.77	0.17	6	5	6	1	9

Table 30. Hilsenhoff Biotic Index Values as they relate to organic pollution. From Hilsenhoff 1987.

HBI Value	Water Quality	Degree of Organic Pollution
0.00-3.50	Excellent	No apparent organic pollution
3.51-4.50	Very Good	Slight organic pollution
4.51-5.50	Good	Some organic pollution
5.51-6.50	Fair	Fairly significant organic pollution
6.51-7.50	Fairly Poor	Significant organic pollution
7.51-8.50	Poor	Very significant organic pollution
8.51-10.00	Very Poor	Severe organic pollution

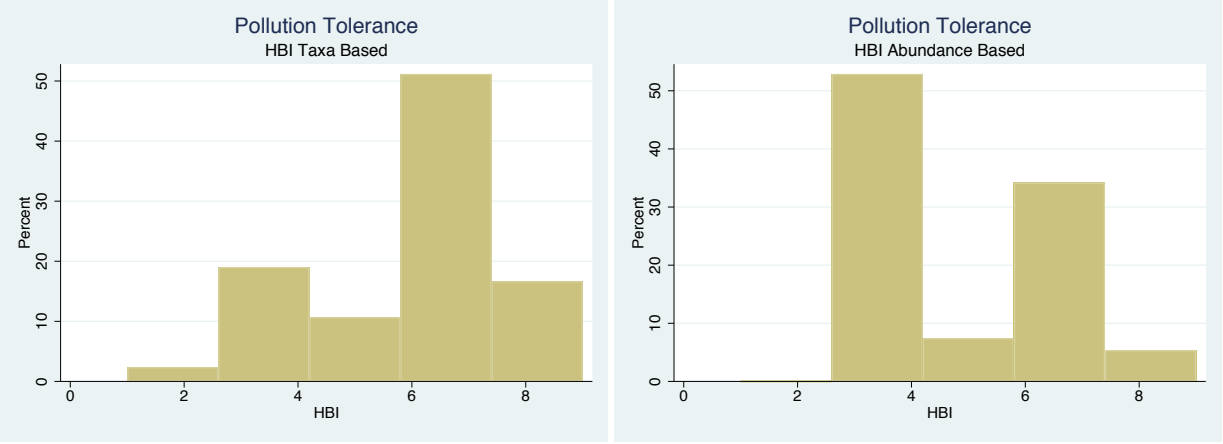

Figure 43. Comparison of taxa based (left) vs. abundance based (right) macroinvertebrate pollution tolerance (HBI) distributions. There was a shift from a median of 6 for taxa based HBI to median of 4 for abundance based HBI.

Sediment Tolerance

Eight sedimentation metrics were used to examine relationships between macroinvertebrates and sedimentation: 1) Biological sedimentation tolerance index (BSTI) developed by Hubler et al. (2016), and 2) General Linear Model Maximum (GLMMAX), 3) GLMCL, 4) GAMMAX, 5) GAMCL, 6) Weighted Average (WA), and 8) 75% Cumulative Distribution (CD75) developed by USEPA (2006).

The biological sediment tolerance index (BSTI) is based on macroinvertebrate taxa and sediment conditions found in Oregon and in our opinion, is one of the most robust and statistically valid sediment indices available. The BSTI, unlike other sediment tolerance indices, uses fine sediments < 0.06 mm, which are typically silt and clay but can also contain fractionated organic matter. Unfortunately, because of the ecoregional differences between Oregon macroinvertebrate taxa and the Jordan River taxa, only

45 of the taxa in the Jordan River had useable BSTI values. Appendix 26 provides BSTI sediment tolerance values for all 45 of the Jordan River taxa.

Taxa-based BSTI for all taxa found in JR = 16.05 % fines (std. dev. = 1.71%) (Table 31). However, the BSTI weighted average abundances for all taxa found in JR = 9.32 % fines (< 0.06 mm) (Table 32). As occurred in the HBI scores, this discrepancy was due to the two most dominant (abundant) taxa in the samples, the mayfly *Tricorythodes* sp. and the caddisfly, *Hydropsyche* sp. Both taxa have lower than average Jordan River macroinvertebrate assemblage BSTI values of 10 and 6, respectively and are apparently less tolerant to fine sediments < 0.06 mm than most other taxa in the river.

However, both *Tricorythodes* sp. and *Hydropsyche* sp. are very tolerant of sands and fines > 0.06 mm (Table 33; Table 34; Appendix 27; Table 38). *Hydropsyche* sp. sediment tolerance is about 33% sands and fines > 0.06 mm (Appendix 27; Blinn and Ruiter 2006, 2009, and 2013). *Tricorythodes* sp. appears to be able to tolerate > 97% sedimentation (Table 38 and Appendix 27). It needs to be remembered that the majority of samples used in these analyses were targeted riffle or riffle- run habitats and that *Hydropsyche* sp. prefer to live on stable substrates such as those found in cobble riffles and *Tricorythodes* sp. prefers slower sections of the river where sands and fines dominate with low amounts of silt/clay/OM and adequate DO.

Table 31. Taxa- based sediment tolerance values. See Hubler et al. (2016) for a description of the BSTI and USEPA for a description of the four other sediment indices.

% Fines < 0.06 mm (silts/clay/OM)

Index	Mean	S.E.	Median	25th	75th	min	max
BSTI	16.05	1.71	13	8	23	1	63

% Sands and fines > 0.06 mm

Index	Mean	S.E.	Median	25th	75th	min	max
GLMMAX	63.85	8.47	78.95	34.30	97.10	0.00	97.10
GAMMAX	60.86	7.18	72.60	32.40	97.10	0.00	97.10
WA	32.77	1.73	29.60	26.10	39.50	10.00	58.30
CD75	46.71	2.55	41.00	35.70	58.85	12.40	76.20
Mean	53.01	5.42	58.95	32.18	77.93	4.48	85.16

Table 32. Abundance- based sediment tolerance values. See Hubler et al. (2016) for a description of the BSTI and USEPA for a description of the four other sediment indices.

% Fines < 0.06 mm (silts/clay/OM)

Index	Mean	S.E.	Median	25th	75th	min	max
BSTI	9.49	0.01	8.00	6.00	10.00	1.00	63.00

% Sands and fines > 0.06 mm

Index	Mean	S.E.	Median	25th	75th	min	max
GLMMAX	96.20	0.02	97.10	97.10	97.10	0.00	97.10
GAMMAX	92.45	0.03	97.10	97.10	97.10	0.00	97.10
WA	33.04	0.01	28.80	28.10	39.50	10.00	58.30
CD75	49.24	0.01	41.00	41.00	60.60	12.40	76.20
Mean	67.73	0.02	66.00	65.83	73.58	5.60	82.18

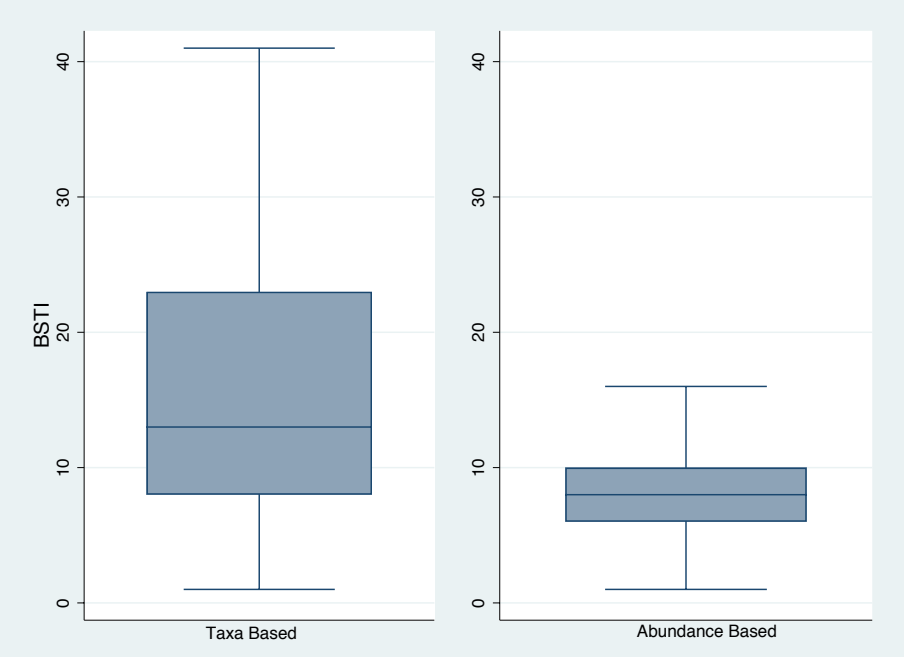

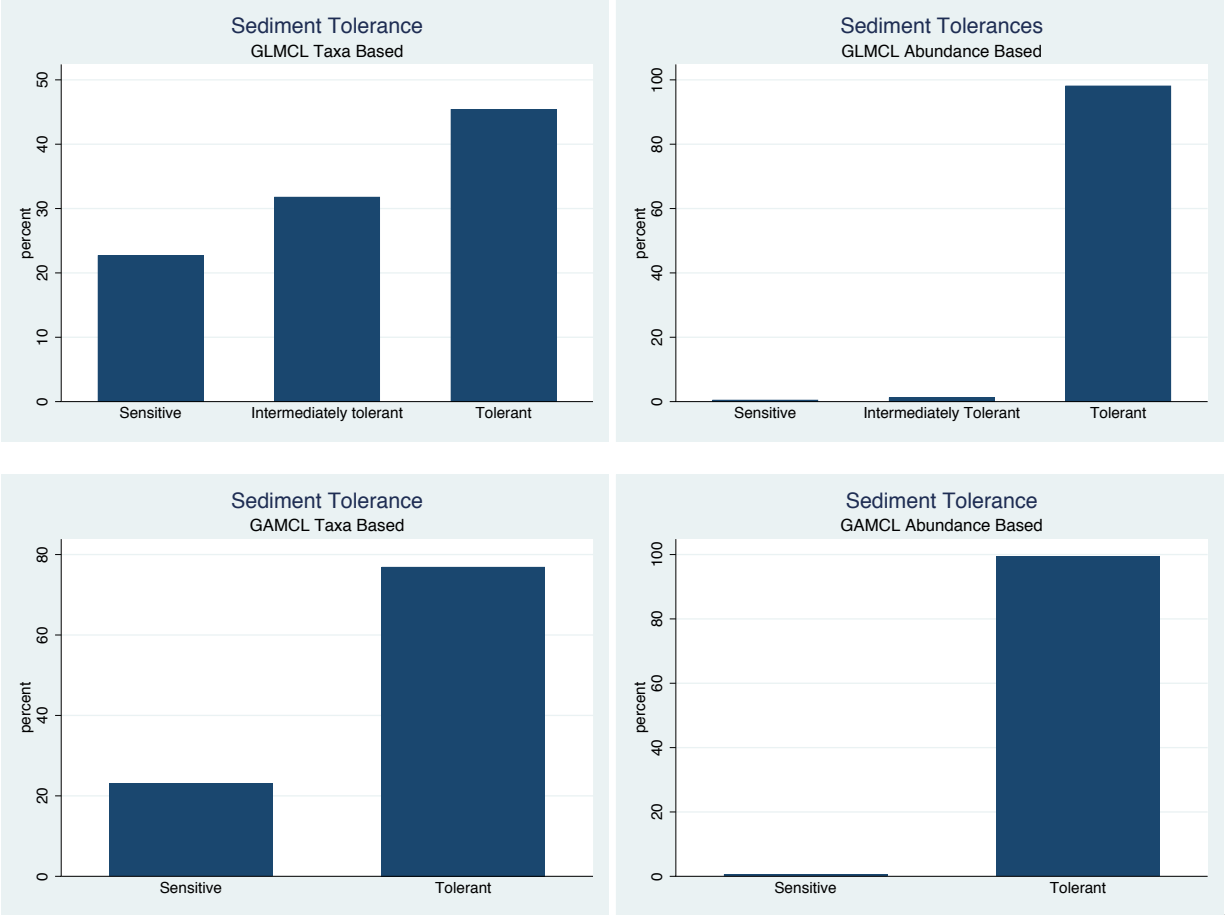

Figure 44. Comparisons of three sediment indices on taxa-based vs. abundance-based macroinvertebrate assemblages in the Jordan River. See Hubler et al. (2016) for a description of the BSTI and USEPA for a description of the four other sediment indices.

Table 33. GLMCL tolerance groups for taxa found in samples analyzed in this report. See USEPA (2006) for a description of GLMCL derivation and interpretation.

Sensitive	**Intermediately Tolerant**	**Tolerant**
Baetis sp.	*Ambrysus sp.*	*Argia emma*
Brillia sp.	*Antocha monticola*	*Fallceon quilleri*
Eukiefferiella sp.	*Caenis sp.*	*Fallceon sp.*
Lebertia sp.	*Hyalella azteca*	*Hemerodromia sp.*
Ordobrevia nubifera	*Hydroptila sp.*	*Physa sp.*
	Optioservus sp.	*Pisidium sp.*
	Parakiefferiella sp.	Simuliidae
		Simulium sp.

Tricorythodes minutus

Tricorythodes sp.

Table 34. GAMCL tolerance groups for taxa found in samples analyzed in this report. See USEPA (2006) for a description of GAMCL derivation and interpretation.

Sensitive	**Tolerant**
Baetis sp.	*Ambrysus sp.*
Brillia sp.	*Antocha monticola*
Eukiefferiella sp.	*Argia emma*
Lebertia sp.	*Caenis sp.*
Optioservus sp.	*Fallceon quilleri*
Ordobrevia nubifera	*Fallceon sp.*
	Hemerodromia sp.
	Hyalella azteca
	Hydroptila sp.
	Hygrobates sp.
	Microcylloepus pusillus
	Microcylloepus similis
	Microcylloepus sp.
	Parakiefferiella sp.
	Physa sp.
	Simuliidae
	Simulium sp.
	Tricorythodes minutus
	Tricorythodes sp.
	Pisidium sp.

Temperature Tolerance

Six metrics were used to examine relationships between macroinvertebrates and temperature: 1) General Linear Model Maximum (GLMMAX), 2) GLMCL, 3) GAMMAX, 4) GAMCL, 5) Weighted Average (WA), and 6) 75% Cumulative Distribution (CD75), all six based on USEPA (2006) values.

As with HBI and the USEPA (2006) sediment indices; tolerance values differed between taxa-based and abundance-based analyses (Table 35; Figure 45). Mean and median abundance- based temperature tolerances were greater than mean and median taxa-based tolerances using GLMMAX and GAMMAX indices (Table 35). There was also a lower percentage of sensitive and intermediately tolerant taxa when GLMCL and GAMCL categories were applied compared with taxa-based results (Figure 45).

Table 35. Temperature tolerance values. See USEPA (2006) for a description of derivation and interpretation of indices.

Taxa based

index	mean	se	median	25th	75th	min	max
GLMMAX	19.63	1.60	22.3	14	29.1	2	29.1
GAMMAX	19.24	1.69	22	13.8	29.1	2	29.1
WA	15.84	0.37	15.2	14.1	17.8	11	19.4
CD75	18.86	0.41	18.8	17.5	20.4	13.1	22.9

Abundance based

index	mean	se	median	25th	75th	min	max
GLMMAX	27.31	0.01	29.1	29.1	29.1	2	29.1
GAMMAX	27.22	0.01	29.1	29.1	29.1	2	29.1
WA	17.75	0.00	18.5	18.5	18.5	11	19.4
CD75	21.45	0.00	22.4	22.4	22.4	13.1	22.9

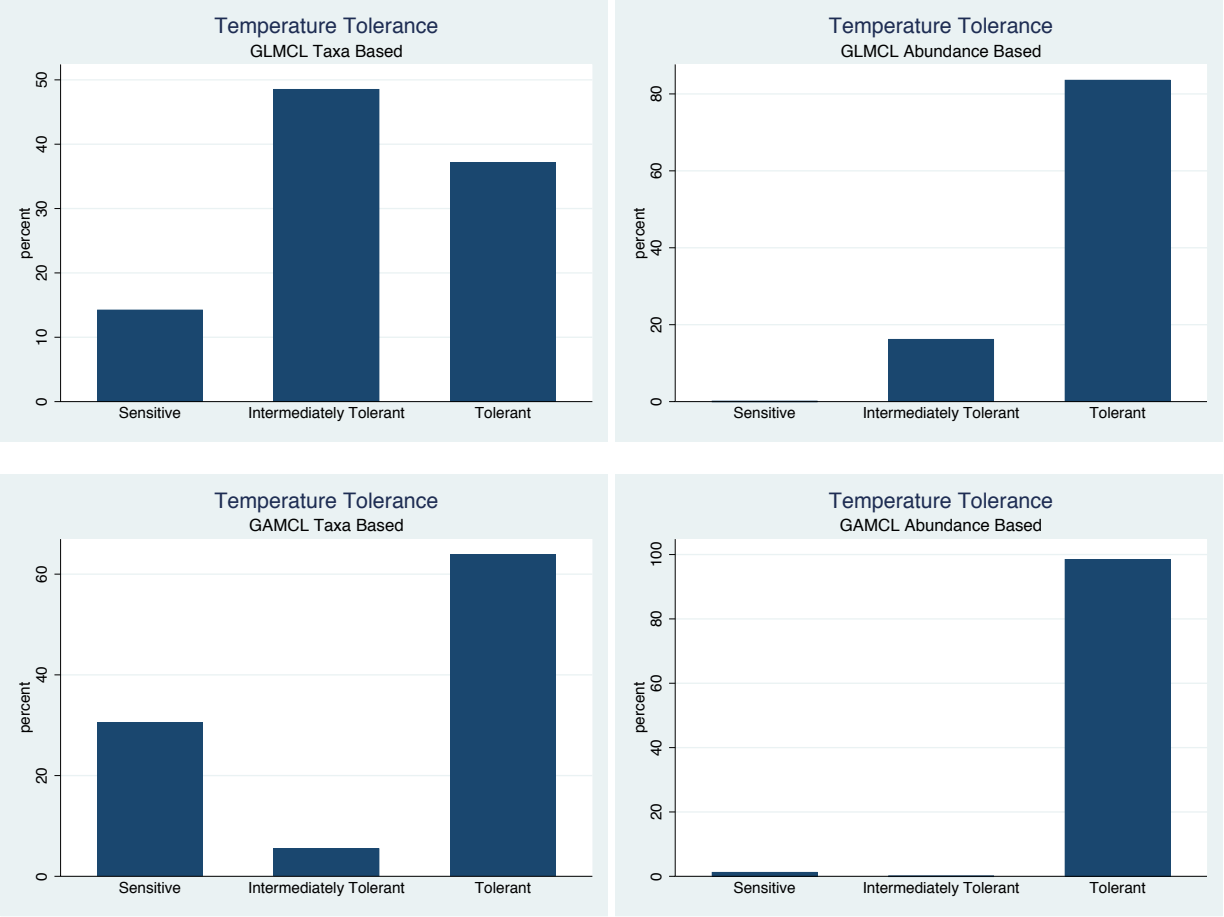

Figure 45. Comparison of taxa-based vs. abundance-based temperature tolerance groups. See USEPA (2006) for a description of derivation and interpretation of indices.

The following two tables list sensitive, intermediately tolerant, and tolerant taxa to temperature using GMCL (Table 36) and GAMCL (Table 37). These taxa can be used to create multimetric indices for the Jordan River to monitor water quality and to further our understanding of the functioning of the river.

Table 36. GLMCL based temperature tolerances. See USEPA (2006) for a description of derivation and interpretation of indices.

Sensitive	**Intermediately Tolerant**	**Tolerant**
Diamesa sp.	*Argia sp.*	*Ambrysus sp.*
Eukiefferiella claripennis group	Baetidae	*Caenis sp.*
Eukiefferiella devonica group	*Baetis sp.*	*Cricotopus bicinctus group*
Eukiefferiella sp.	*Baetis tricaudatus*	*Cricotopus sp.*
Lebertia sp.	*Brillia sp.*	*Cricotopus trifascia group*
	Cleptelmis addenda	*Cryptochironomus sp.*

	Hemerodromia sp.	*Dubiraphia sp.*
	Hyalella azteca	*Fallceon sp.*
	Hydroptila sp.	*Microcylloepus pusillus*
	Nanocladius sp.	*Physa sp.*
	Optioservus sp.	*Tricorythodes sp.*
	Ordobrevia nubifera	
	Pisidium sp.	
	Simuliidae	

Table 37. GAMCL based temperature tolerances. See USEPA (2006) for a description of derivation and interpretation of indices.

Sensitive	**Intermediately Tolerant**	**Tolerant**
Baetidae	*Cleptelmis addenda*	*Ambrysus sp.*
Baetis sp.	*Optioservus sp.*	*Argia emma*
Baetis tricaudatus		*Argia sp.*
Brillia sp.		*Caenis sp.*
Diamesa sp.		*Cricotopus bicinctus group*
Eukiefferiella claripennis group		*Cricotopus sp.*
Eukiefferiella devonica group		*Cricotopus trifascia group*
Eukiefferiella sp.		*Cryptochironomus sp.*
Lebertia sp.		*Dubiraphia sp.*
Nanocladius sp.		*Fallceon quilleri*
Parakiefferiella sp.		*Fallceon sp.*
		Hemerodromia sp.
		Hyalella azteca
		Hydroptila sp.
		Hydroptilidae
		Microcylloepus pusillus

Ordobrevia nubifera

Physa sp.

Pisidium sp.

Simuliidae

Simulium sp.

Tricorythodes minutus

Tricorythodes sp.

Tolerances of 12 dominant taxa

A summary table of organic pollution, sedimentation, and temperature tolerances for the twelve most dominant taxa in the Jordan River is in

Table 38. Unfortunately, tolerance values have not been established for most of the twelve dominant taxa. A more thorough literature review may provide additional values, but values will need to be adjusted due to different methods used to develop indices. In addition, tolerance values will need to be made at the species or genus level in order to provide meaningful indices.

Table 38. Organic pollution (HBI), Sediment (BSTI, Glmmax, Gammax, WA, and CD75), and temperature (Glmmax, Gammax, WA, and CD75) values for the twelve most dominant taxa in the Jordan River samples analyzed. See Hilsenhoff (1987), Hubler et al. (2016), and USEPA (2006) for a description of derivation and interpretation of indices.

Taxon	Organic	% Sediment					Temperature ^{0}C			
	HBI	BSTI	GLMMAX	GAMMAX	WA	CD75	GLMMAX	GAMMAX	WA	CD75
Hydropsyche sp.	4	6	na	na	28.1	41	na	na	na	na
Tricorythodes sp.	4	10	97.1	97.1	39.5	60.6	29.1	29.1	18.5	22.4
Chironomidae	8	na	na	na	na	na	na	na	na	na
Orthocladiinae	6	8	na	na	na	na	na	na	na	na
Potamopyrgus antipodarum	na	na	na	na	na	na	na	na	na	na
Simuliidae	6	8	97.1	77.5	28.8	40	17.6	17.6	14.8	17.7

Oligochaeta	5	10	na	na	na	na	na	na	na	na
Caecidotea	8	27	na	na	na	na	na	na	na	na
Acari	6	na	na	na	na	na	na	na	na	na
Coenagrionidae	9	25	na	na	na	na	na	na	na	na
Turbellaria	na	8	na	na	na	na	na	na	na	na
Corbicula sp.	6	na	na	na	na	na	na	na	na	na

We suggest that closely monitoring these twelve taxa will provide ecologists and managers with water quality and ecosystem function assessment measures far superior to those being used at present by state agencies.

Functional Feeding Groups

There is a disproportionally high number of predator taxa in the river compared to other rivers in the region, although predator taxa did occur at low densities typical of rivers in the region (Figure 46). Collectors gatherers and collector filterer densities dominate the river with a near absence of shredders (Figure 46). This is due to food resource availability. Most of the macroinvertebrate food resources in the river are either loosely attached to the substrates or suspended in the water column. Shredders are near absent indicating that in riffle habitats, CPOM is mostly absent or that embeddedness disfavors predators. There are many problems and difficulties using FFG's to interpret ecosystem function in the Jordan River that need to be addressed before they can be confidently interpreted.

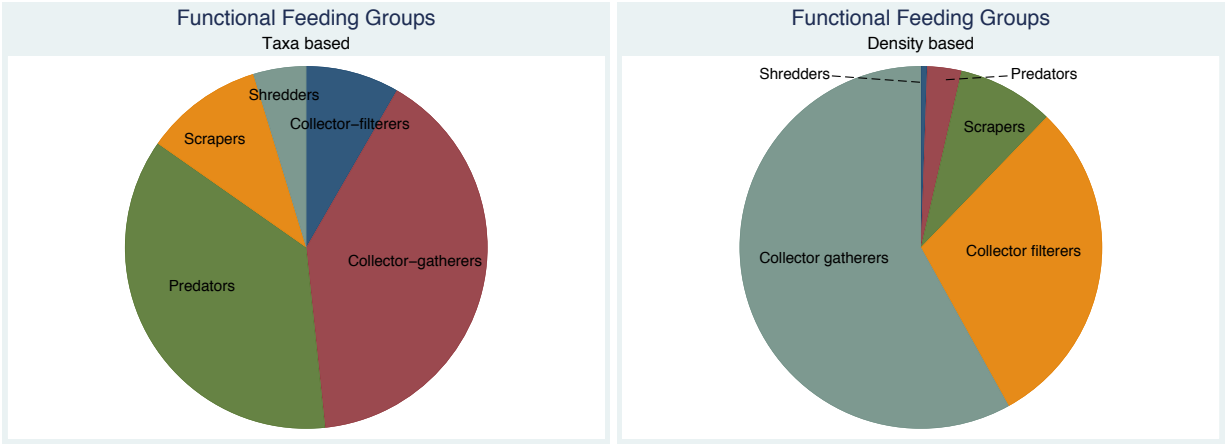

Figure 46. Taxa-based vs. abundance (density)-based functional feeding groups in the Jordan River based on samples analyzed in this report.

Habitat

Suitable habitat, in the form of substrate, along with temperature, are two of the most important factors in a macroinvertebrate taxon's fundamental niche. Suitable habitat also directly determines

assemblage structure and composition. Substrate habitat in the Jordan River, as illustrated throughout this report, is severely impaired from sedimentation, both naturally and anthropogenically. Typically, in most streams including streams and rivers in Utah; riffles are composed of cobbles or sometimes boulders often with little embeddedness. This is obviously not the case for the Jordan River.

Macroinvertebrate densities were noticeably lower in reach wide habitats than in riffle habitats but not significantly (Figure 47;Table 39).

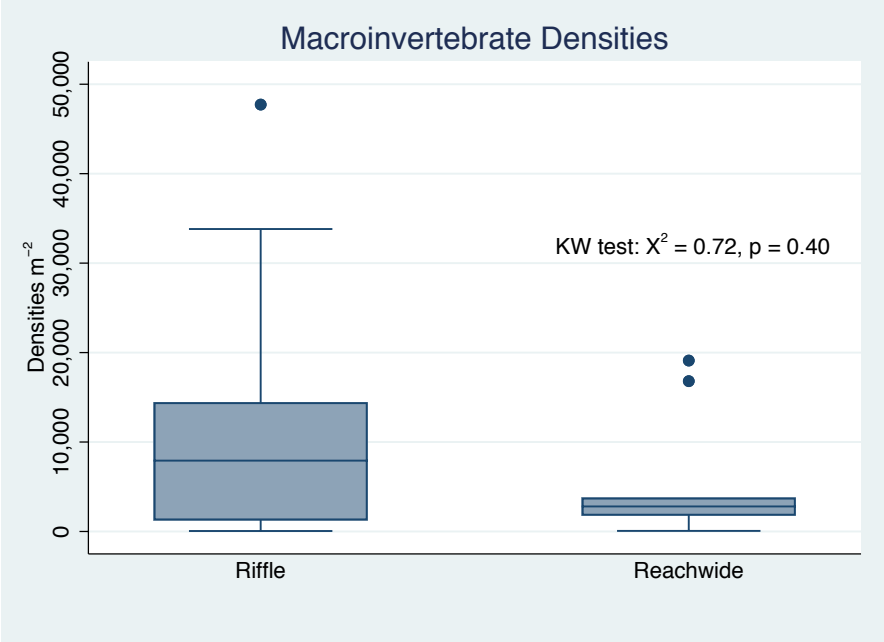

Figure 47. Comparison of macroinvertebrate densities between targeted riffle and reach wide habitats in the Jordan River.

Table 39. Descriptive statistics of macroinvertebrate densities between targeted riffle and reach wide habitats in the Jordan River

Habitat	N	mean	se	median	25th	75th
Riffle	35	10333.22	1938.21	7921.50	1237.83	14453.33
Reach wide	10	5344.78	2142.64	2796.66	1765.83	3786.01
Total	45	9224.68	1601.32	3786.01	1261.26	14313.51

We performed nonparametric Kruskal-Wallis tests on raw densities and t-tests on $\log_{10}$+1 transformed densities for each of the twelve dominant taxa vs. habitat type. There were no significant differences for any taxon density between riffles and reach wide habitats except for Hydropsychidae which had significantly less densities in reach wide habitat (Figure 48). Several taxa appeared to have lower densities in reach wide habitat including; Acari, *Corbicula*, *Potamopyrgus*, and Simuliidae but none were significantly lower (Figure 48).

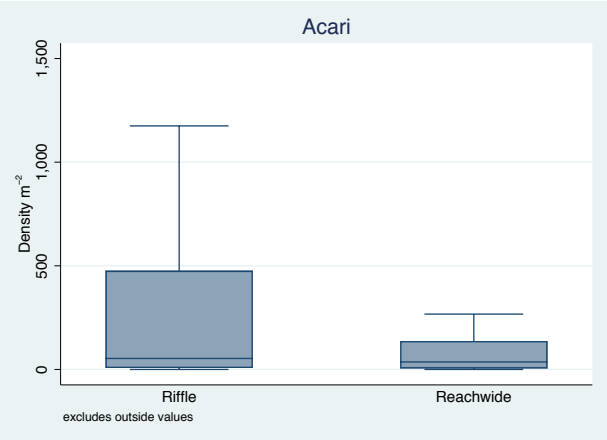
Acari
Density m^{-2}
0
500
1,000
1,500
Riffle
Reachwide
excludes outside values

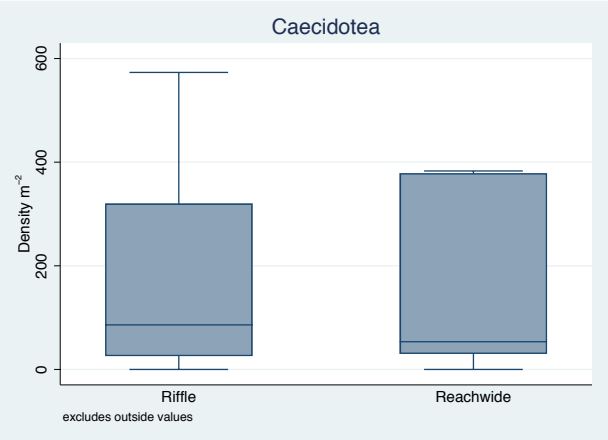
Caecidotea
Density m^{-2}
0
200
400
600
Riffle
Reachwide
excludes outside values

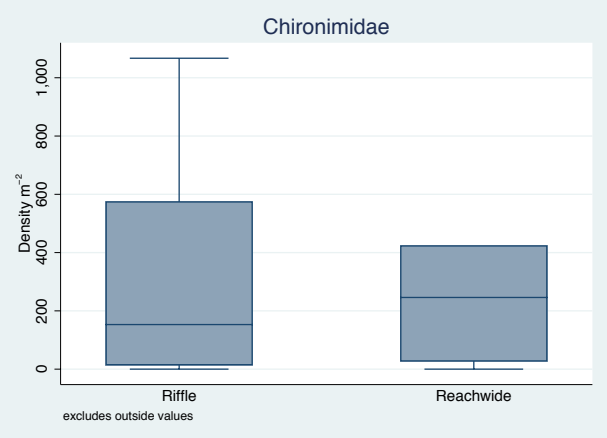
Chironimidae
Density m^{-2}
0
200
400
600
800
1,000
Riffle
Reachwide
excludes outside values

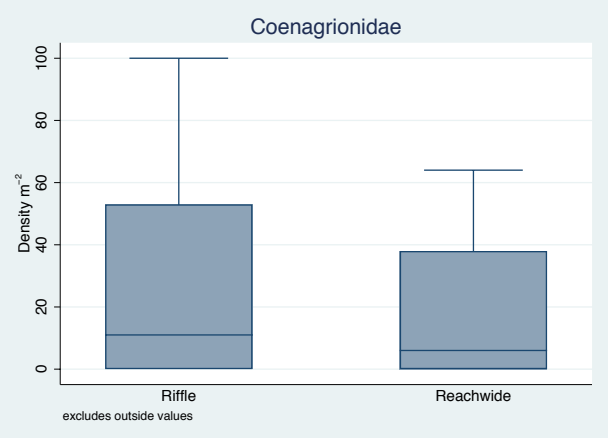
Coenagrionidae
Density m^{-2}
0
20
40
60
80
100
Riffle
Reachwide
excludes outside values

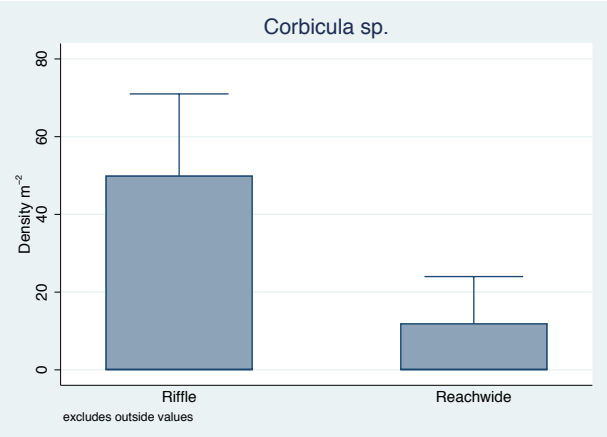
Corbicula sp.
Density m^{-2}
0
20
40
60
80
Riffle
Reachwide
excludes outside values

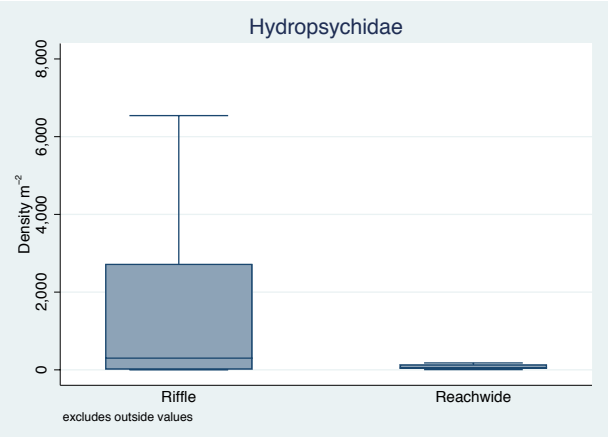
Hydropsychidae
Density m^{-2}
0
2,000
4,000
6,000
8,000
Riffle
Reachwide
excludes outside values

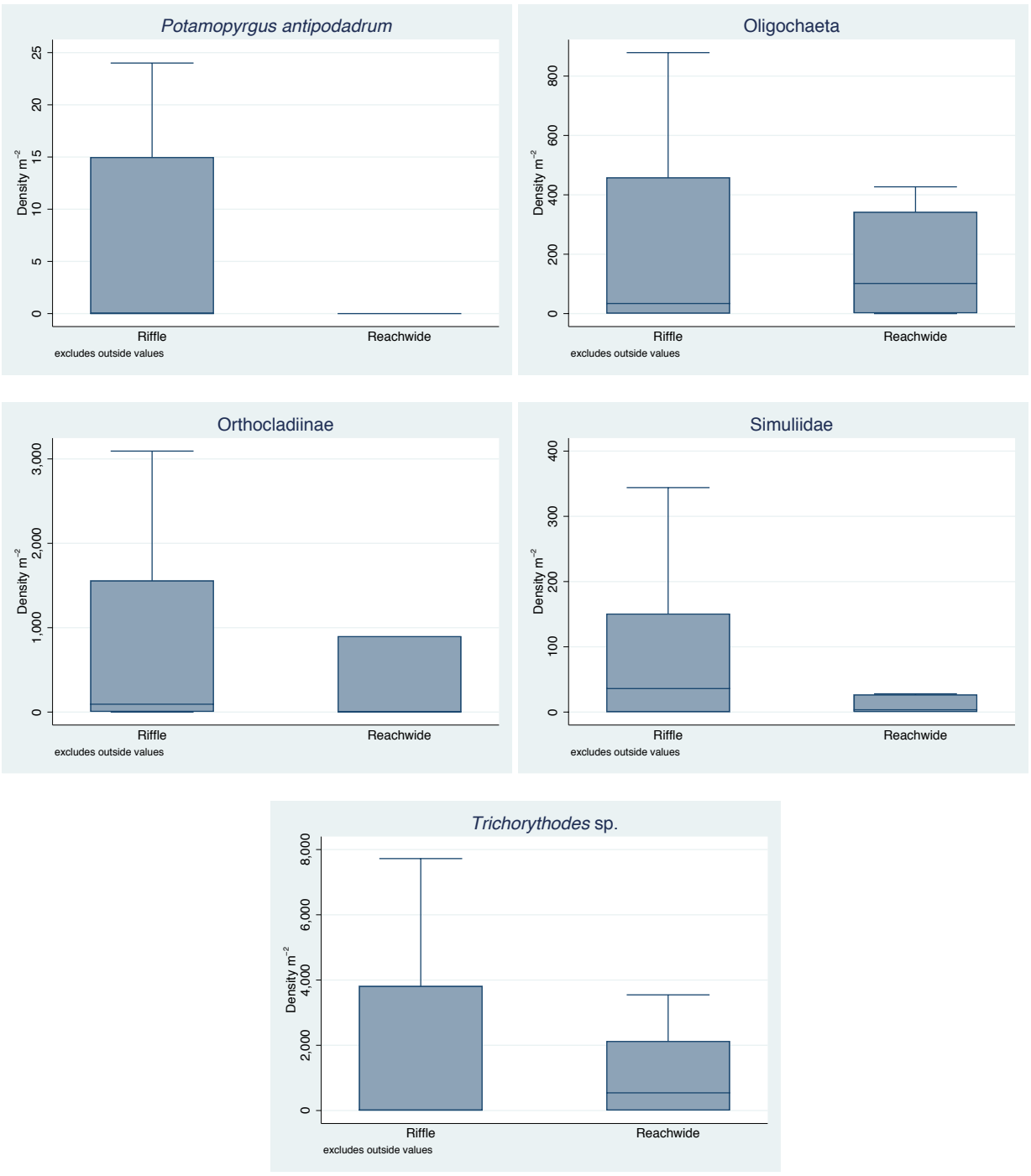

Figure 48. Comparison of twelve most dominant taxa densities between targeted riffle and reach wide habitats in the Jordan River. Note: there was only one reach wide sample for Potamopyrgus.

These results and those presented in the Assemblage and Habitat section lead us to conclude that given all of the anthropogenic bottlenecks that macroinvertebrates have survived; sedimentation is likely the number one limiting factor.

Discussion

From this investigation and our experience conducting research on the Jordan River, and throughout the drainage, and in rivers and streams throughout the western USA; the Jordan River has undergone major anthropogenic caused catastrophic ecosystem shifts resulting in macroinvertebrate assemblages that have most certainly suffered from severe bottlenecks and hysteresis. However, several taxa have endured or even prospered.

Targeted riffles/reach wide vs. what is really there

The datasets used in these analyses were either from targeted riffles or reach wide habitats near riffles, most of which were embedded with sands and fines. This type of habitat is not representative of the entire river and comprises perhaps < 5 % of Jordan River habitat. Unembedded cobble habitat, which is essential for macroinvertebrate diversity and abundance, occurs even less frequently in the river and is difficult to find unless specifically searching for it. The majority of habitat in the Jordan River upstream of the Surplus Canal Diversion near 21st South is embedded riffle runs or pools filled with fines and organic matter (personal observations). The majority of habitat downstream of Surplus Canal is even more embedded runs and pools filled with increased amounts of organic matter that often has elevated levels of methane and decreased levels of dissolved oxygen. Thus, the majority of habitat in the Jordan River is not conducive to a diverse and abundant macroinvertebrate assemblage and only those taxa that are sediment tolerant in the upstream sections and sediment, hardpan clay, and low DO tolerant downstream can be found. Suitable habitat is their limiting factor.

Temperature tolerance also determines which taxa can survive in the river. However, given that the Jordan River is mostly a warm-water river and that upstream sections are now experiencing increased temperatures and will continue to do so into the future; only those taxa and assemblages that tolerate warm temperatures will survive. Isolated cold- water, spring- fed sections will be the exceptions. This is not to say that temperature is a type of impairment, *per se*. The reality is that warm water is now the norm in this analog system and temperature should no longer be considered an impairment. The new norm is that the analog Jordan River is a sediment- laden, warm-water ecosystem with a macroinvertebrate assemblage that reflects this condition, but it also reflects region wide taxa diversity (gamma diversity). Only taxa that occur in the region or that are unintentionally or intentionally introduced are able to colonize the river and only those taxa that are sediment and temperature tolerant will survive.

Macroinvertebrate taxa populations that survive in the river are now isolated from other populations because there are very few waters in the drainage or region with environmental conditions similar to the Jordan River. Isolation results in increased extinction risk. These populations are now governed by isolated or metapopulation dynamics and if the former, are much more susceptible to extinction than the later. Most of the nearby streams in the sub basin are cold-water streams with less stream embeddedness and have been diverted away from the Jordan River. Warm-water Utah Lake, the main source of the Jordan River is also severely impaired and not a potential source for stream dwelling macroinvertebrates. This predicament also means that macroinvertebrate assemblages in the river have low resilience to future disturbance (Dakos et al. 2015).

Given its isolation, unique set of conditions, and compromised resistance and resilience; all efforts should be made to protect what few macroinvertebrates survive in the river. Even though there are only 4 or so effective taxa in the river in any given section, a few dozen other taxa occur at low abundances and efforts should be made to insure their survival. Each one of these remaining taxa provide unique contributions to continued ecosystem function.

Macroinvertebrates have been poorly monitored and studied in the Jordan River in spite of the critical importance. This results in an extremely poor understanding of the river's ecology and function particularly in reference to water quality. It is imperative to begin ecological research on the macroinvertebrate assemblages in the river and initiate a robust monitoring program. Other ecosystem and water quality parameters are easily measured and interpreted such as temperature, DO, nutrients, sedimentation, etc. But these are relatively meaningless or are vaguely useful unless they can be directly related to the biota that live in the river.

Taxonomic Resolution and Tolerance Indices

All of the samples analyzed had taxonomic issues whether different levels of taxonomic resolution used or difficulty in identification of missing key body parts. In addition, each sample used different sampling methods, area sampled, or subsampling effort. These problems have been a major impediment to accuracy and precision in determining population dynamics, ecologic function, and water quality assessment in most locations. A potential solution to these problems is the use of DNA barcoding, which is now a common and superior method in use in other ecological fields and is beginning to take hold in stream macroinvertebrate studies (Sweeney et al. 2011).

Tolerance indices are widespread, and ecologists are developing newer indices on a regular basis. At this time, however, most indices, including those used in these analyses are not robust enough and have inherent problems. Thus, they have limited use and should be used with a dash of skepticism (Monaghan 2016, Richards 2016). There is a real need to improve nutrient, temperature, and sediment tolerant indices that are taxon specific to the Jordan River. Nutrient biotic indices are in short supply and methods used by Smith et. al. (2006) for developing a nutrient biotic index in New York may provide useful for the Jordan River. Likewise, tolerance values for different type of conditions can be developed specifically for Jordan River macroinvertebrates similar to what Blinn and Ruiter (2006, 2009, 2013) have done for caddisflies in Washington and Arizona.

Loss of Important Natives

The Jordan River has lost many unique native taxa during its encounter with utilitarian settlers. The most important being its molluskan fauna. Almost twenty species of snails, clams, and mussels once flourished in its waters. Most have been extirpated. Richards (2017a, 2017b, 2018a, 2018b) and Richards and Miller (in press) give detailed accounts of these taxa in the Jordan River drainage.

Another important taxon that apparently no longer exists in the Jordan River drainage is the burrowing mayfly *Ephoron album* (Family: Polymitarcidae). This species is well known throughout the U.S. for its extreme high densities that often force motorists to use their headlights and windshield wipers during cloud forming adult emergences. *Ephoron album* was reported by Edmunds et. al. (1956) as very

abundant in the Jordan River and canals in 1947. Unfortunately, USU/BLM MAPIT has no records of this mayfly from the Jordan River and reasons for its apparent disappearance are unknown. This is but one example of once common taxa that have disappeared from the river and their ecological importance lost and unrecorded.

Lost Aquatic Entomologist Heritage

The University of Utah has a rich history of influential aquatic entomologists. Dr. Ardin Gaufin was a world renown Plecoptera (stonefly) expert; Dr. George Edmunds, was a world renown Ephemeroptera (mayfly) expert, to name a few. The Jordan River is just a few short miles from U of U. We suggest that U of U restarts their heritage aquatic entomology program and focus studies on the Jordan River.

Invasives

The Jordan River is now home to at least three ecosystem altering invasive macroinvertebrates: the Asian clam, *Corbicula fluminea*, New Zealand mudsnail, *Potamopyrgus antipodarum*; and the crayfish, *Orconectes virillis*. Both *Corbicula* and *Potamopyrgus* occur at very high densities, >10,000 m^{-2} and > 250,000 m^{-2} respectively in some locations in the river. *Orconectes* is rapidly expanding throughout the river and in abundance (personal observation). Richards (2018a; 2018b) provides the most up to date survey report of these two invasives in the river. These mollusks are now the analogs to the unique and diverse native mollusk assemblages that once inhabited the Jordan River.

Chronic dredging and Sediment Pulses

The river experiences acute and chronic dredging throughout its entire length. This obviously has severe negative consequences on macroinvertebrates. Subsequently, only short-lived and/or rapid colonizer taxa can survive dredging. In November 2018, when conducting macroinvertebrate and salmonid redd surveys, we witnessed a sediment pulse of dark anoxic fine material in upstream portions of the river. This plume lasted for several days and eventually covered the entire substrate for many kilometers with fine, anoxic, material. Apparently, the plume was a result of flushing of irrigation canals west of the river and occurs on a regular basis. City of South Jordan park managers reported a major fish die-off as a consequence of the plume which even included a die-off of the pollution tolerant invasive carp that dominates the river. We continue to monitor the effects of the plume on macroinvertebrates but assume that regular flushing of sediments from canals into the river have severe negative effects on macroinvertebrates.

Additional Studies

The Wasatch Front Water Quality Council and OreoHelix Consulting are continuing to collect ecological data from the Jordan River, including macroinvertebrate data. We have and continue to collect samples from gravel riffles, runs, and pools to supplement past surveys that focused on cobble riffles. At this point, we have collected fourteen samples from the river that are near taxonomic and preliminary analysis completion.

The Salt Lake County Watershed Planning and Restoration Program, in our opinion, collects samples and monitors the Jordan River better than any other agency at this time. An example of an assessment by SLCWPR from 500 North of the Jordan River is in Appendix 31. This is one of the most comprehensive analyses, albeit limited number of samples, to date. SLCWPR also considers the river to be impaired based on their macroinvertebrate results however, some of their scoring is biased toward cold-water condition assumptions and needs to be adjusted for actual Jordan River conditions. We will continue to work with this enthusiastic and qualified group into the future and share expertise.

Macroinvertebrate assemblages as causes of impairments

The lack of a fully functioning macroinvertebrate assemblage in the Jordan River may actually be the cause of and not the result of several of the types of impairments reported for the river including; low DO, abundant periphyton growth and assemblage structure, and organic matter accumulation. Without a full suite of macroinvertebrate taxa, these types of impairments cannot be properly managed by the remaining macroinvertebrates. As a result, these types of impairment often go uncontrolled. In addition, the two invasive mollusks, *Corbicula* and *Potamopyrgus* are now provide most of the valuable biological functioning and ecosystem services to the river but do so at a cost, which often is oxygen consumption and ammonia production (Richards 2018a; 2018b).

Conclusion

The Jordan River is now a reduced analog of its former self and cannot return to its historical condition. Despite their trials and tribulations, macroinvertebrates continue to be the major regulator of the Jordan River's ecosystem function, although their reduced diversity and abundances preclude them from functioning at anywhere near efficiency. Macroinvertebrate assemblages in the river continue to provide valuable ecosystem services but again, at a bargain-basement rate. Unfortunately, these essential assemblages are severely understudied, precluding any valid assessment of conditions affecting them or guidance on how to manage conditions in the river to improve their ability to function more efficiently.

This report is the most comprehensive analysis of Jordan River macroinvertebrate assemblages to date and illuminates their importance to the ecosystem and their response to pollutants and pollution. Although the dataset analyzed in this report was one of the most valid and complete datasets available for direct comparisons, many problems and inconsistencies allowed for only generalized analysis and conclusions. Much more research is urgently needed.

Recommendations

Several recommendations for future research surfaced from this analysis and from our experiences as aquatic entomologists, malacologists, and stream ecologists working on the Jordan River and throughout the western USA. They are as follows:

1. Much more macroinvertebrate ecological research is desperately needed. This includes comprehensive life history, ecological, and water quality related studies particularly for the most dominant taxa.

2. DNA barcoding needs to begin for macroinvertebrate taxa in the Jordan River. Initial costs of barcoding are relatively low compared to recent years and the cost effectiveness of using DNA barcoding compared to taxonomic identification is substantial. Much more accurate and precise analyses will result, which in turn will lead to more scientifically valid water quality regulations.

3. Tolerance indices including; temperature, sedimentation, organic pollution, pharmaceuticals, and nutrient indices need to be refined and developed specifically for the Jordan River.

4. Data in the USU MAPIT database needs to be reviewed and QA/QC'd by UDWQ. On more than one occasion when using MAPIT, the UDWQ macroinvertebrate data repository, we have found discrepancies between latitude-longitude coordinates and narrative descriptions of locations. These errors are difficult to remedy and can have important scientific and economic consequences for water quality managers who may rely on this data for management decisions.

5. Data recently collected by WFWQC and future collections need to be combined with data used in this analysis and from other sources to better understand macroinvertebrate assemblages as they relate to water quality in the Jordan River. This will be an ongoing process.

6. Periodic sampling of riffles or reach wide habitats, every five or six years, then applying a single metric determination (RIVPACS O/E models) as routinely done by UDWQ are inadequate to determine responses of macroinvertebrates to water quality impairment or ecosystem function in the Jordan River. Efforts should be made to address this problem.

7. Wasatch Front Water Quality Council needs to work more closely with Salt Lake County Watershed Planning and Restoration group. Combined efforts will help understand water quality conditions in the Jordan River as they pertain to macroinvertebrates.

Acknowledgements

We are sincerely grateful to the Wasatch Front Water Quality Council for continued support of our ongoing studies of macroinvertebrate assemblages in the Jordan River. Without this organization, limited understanding of the Jordan River ecosystem as it pertains to water quality would be severely lacking and regulations would be determined based on limited scientific validity. We also appreciate the generous donation of data from Salt Lake County Watershed Planning and Restoration and encourage them to continue to conduct the most scientifically valid assessments possible. Last but not least, we

thank WFWQC technicians Frank Fluckiger and W. D. Robinson for their dedicated assistance braving adverse conditions to bring home the data unharmed.

Literature Cited

Blinn, D. W. and D. E. Ruiter. 2009. Caddisfly (Trichoptera) assemblages along major river drainages in Arizona. Western North American Naturalist. 69(3): 299-308.

Blinn, D. W. and D. E. Ruiter. 2013.Tolerance Values and Effects of Selected Environmental Determinants on Caddisfly (Trichoptera) Distribution in Northwest and North Central Washington, USA. Western North American Naturalist. 3(3): 270-294.

Blinn, D.W. and D.E. Ruiter. 2006. Tolerance values of stream caddisflies (Trichoptera) in the lower Colorado River Basin, USA. The Southwestern Naturalist. 51(3): 326-337.

Dakos ,V., Carpenter S.R., van Nes E.H., and M.Scheffer 2015 Resilience indicators: prospects and limitations for early warnings of regime shifts. Phil. Trans. R. Soc. B 370: 20130263. http://dx.doi.org/10.1098/rstb.2013.0263.

Deseret News. 1972. “Pollution unit calls for river action”. 16 Nov 1972.

Elise M. Giddings and Doyle Stephens. 1999. Selected aquatic biological investigations in the Great Salt Lake Basins, 1875-1998. U.S. Geological Survey, Water-Resources Investigations Report 99-4132 National Water-Quality Assessment Program. Salt Lake City, Utah.

Gaufin, A. R. 1957, Limnological analysis of Jordan, Price, Provo and Weber Rivers: Salt Lake City, Utah, University of Utah, 7 p.

Giddings, E.M. and D. Stephens. 1999. Selected aquatic biological investigations in the Great Salt Lake Basins, 1875-1998, National Water-Quality Assessment Program. U.S. Geological Survey. Water-Resources Investigations Report 99-4132. Salt Lake City, UT.

Hauer, R.F. and G.A. Lamberti. 2007. Methods in stream ecology. 2nd edition. Academic Press.

Hilsenhoff, W.L. 1977. Use of arthropods to evaluate water quality of streams. Tech. Bull. Wisconsin Dept. Nat. Resour. 100. 15pp.

Hilsenhoff, W.L. 1982. Using a Biotic Index to Evaluate Water Quality in Streams. Tech. Bull. Wisc. Dept. Nat. Res. 132p.

Hilsenhoff, W.L. 1987. An improved biotic index of organic stream pollution. Great Lakes Entomol. 20:31-39.

Hilsenhoff, W.L. 1988. Rapid field assessment of organic pollution with a family-level biotic index. J. N. Am. Benthol. Soc. 7(1):65-68.

Hinshaw, R.N., 1967, The pollutional degradation of the Jordan River as shown by aquatic invertebrates: Salt Lake City, University of Utah, Master of Science thesis, 121 p.

Holden, P.B., and Crist, L.W., 1987, Fishery and macroinvertebrate studies of the Jordan River in Salt Lake County, November 1986: prepared by BIO/WEST, Inc. for Central Valley Water Reclamation Facility Board, Salt Lake City, Utah, 92 p.

Jackson, J.K., A.D. Huryn, D.L. Strayers, D.L.Courtemanch, and B.W. Sweeney. 2005. Atlantic coast rivers of the northeastern United States. In Benke, A.C. and C.E. Cushing eds.: Rivers of North America. Elsevier Inc.

Mangum, F.A., 1995, Aquatic ecosystem inventory, Macroinvertebrate analysis: State of Utah, Department of Environmental Quality, Division of Water Quality Ambient Streams and Special Project Streams, 139 p.

McCune, B. and J. Mefford. 2011. PC-ORD. Multivariate Analysis of Ecological Data. Version. 6.22. MjM Software, Gleneden Beach, Oregon.

Monaghan KA (2016) Four Reasons to Question the Accuracy of a Biotic Index; the Risk of Metric Bias and the Scope to Improve Accuracy. PLoS ONE 11(7): e0158383. doi:10.1371/journal. pone.0158383

Moore, J. W., D. B. Herbst, W. N. Heady, and S. M. Carlson. 2012. Stream community and ecosystem responses to the boom and bust of an invading snail. Biological Invasions. DOI 10.1007/s10530-012-0240-y.

Nabrotzky, F., 1987, Macroinvertebrate analysis and water quality data for wetlands of the Jordan River in Salt Lake County: Salt Lake City-County Health Department, Division of Environmental Health, Bureau of Water Quality, Salt Lake City, 33 p.

National Audubon Society. 2000. The Jordan River natural conservation corridor report. Prepared for the Mitigation Commission and the U.S. Fish and Wildlife Service.

Richards, D. C. 2016a. Does phylogeny predict sensitivity to ammonia in freshwater animals using USEPA ammonia criteria data?

Richards, D.C. 2016b. Real and perceived macroinvertebrate assemblage variability in the Jordan River, Utah can affect water quality assessments. Technical Report to Jordan River/Farmington Bay Water Quality Council. OreoHelix Consulting, Vineyard, UT.

Richards, D.C. 2017a. Lower Mill Creek and Mid-Jordan River native mussel survey 2017: As it relates to the Central Valley Water Reclamation Facility Discharge. Report to: Wasatch Front Water Quality Council. Salt Lake City, UT. OreoHelix Consulting, Vineyard, UT.

Richards, D. C. 2017b. Native Unionoida Surveys, Distribution, and Metapopulation Dynamics in the Jordan River-Utah Lake Drainage, UT. Report to: Wasatch Front Water Quality Council. Salt Lake City, UT. OreoHelix Consulting, Vineyard, UT. Version 1.5 May, 26, 2017.

Richards, D. C. 2018a. A snail, a clam, and the River Jordan: A revealing novel. Version 1.5. Technical Report Submitted to The Wasatch Front Water Quality Council. OreoHelix Consulting, Vineyard, UT.

Richards, D. C. 2018b. The Jordan River: How to regulate an analog ecosystem. Scientific presentation at the Twelve Annual Salt Lake County Watershed Symposium, Salt Lake City, UT

Richards, D.C. and T. Miller. In Press. Apparent extinction of native mussels in Lower Mill Creek and Mid-Jordan River, UT. Western North American Naturalist.

Scheffer M, Carpenter S, Foley JA, Folke C, Walkerk B, Walker B. 2001 Catastrophic shifts in ecosystems. Nature 413, 591–596. (doi:10.1038/35098000).

Scheffer M, Carpenter SR. 2003 Catastrophic regime shifts in ecosystems: linking theory to observation. Trends Ecol. Evol. 18, 648–656. (doi:10.1016/j.tree. 2003.09.002).

StataCorp. 2018. Stata/IC 15.1 for Mac (64-bit Intel). College Station, TX.

Sweeney, B.W., J.M. Battle, J.K. Jackson, and T. Dapkey. Can DNA barcodes of stream macroinvertebrates improve descriptions of community structure and water quality? J.N.Am.Benthol.Soc. 30(1): 195-216.

U.S. Environmental Protection Agency, 1973, Jordan River Study, Utah, June-August 1972: Report S&A/TSB-16, Technical Support Branch, Surveillance and Analysis Division, Region 8, Denver, Colo., 67 p.

U.S.E.P.A. 2006. Estimation and application of macroinvertebrate tolerance values. EPA/600/P-04/116F. National Center for Environmental Assessment Office of Research and Development. U.S. Environmental Protection Agency. Washington, DC 20460

Watershed Planning and Restoration Program. 1992. Jordan River Stability Study. Salt Lake County, Utah, December 1992,

Wright, J.P., C.G. Jones, A.S. Flecker. 2002. An ecosystem engineer, the beaver, increases species richness at the landscape scale. Ecosystems Ecology. 132(1): 96-101.

Additional Literature

23. Alexander, Charles P. 1925. An entomological survey of the Salt Fork of the Vermilion River in 1921, with a bibliography of aquatic insects. Bull. Illinois Nat. Hist. Surv. 15:435-535.

65. Clifford, Hugh F. 1966. Some limnological characteristics of six Ozark Streams. Missouri Dept. Conserv., Div. Fish., D-J Series No. 4:1-55.

87. Edmunds, George F., Jr. 1948. The nymph of Ephoron album (Ephemeroptera). Entomol. News 59:12-14.

92. Edmunds, George F., Jr., Lewis T. Nielsen, and Joseph R. Larsen. 1956. The life history of Ephoron album (Say) (Ephemeroptera: Polymitarcidae). Wasmann J. Biol. 14:145-153.

100. Edmunds, George F., and Guy G. Musser. 1960. The mayfly fauna of Green River in the Flaming Gorge Reservoir Basin, Wyoming and Utah. Univ. Utah Anthropol. Pap. 43:111-123.

133. Koss, Richard W. 1970. A list of the mayflies (Ephemeroptera) in the Michigan State University Entomology Museum. Mich. Entomol. 3:98-101.

138. Lehmkuhl, D. M. 1974. Thermal regime alteration and vital environmental physiological signals in aquatic organisms. IN Thermal Ecology, J. W. Gibbons and R. R. Scharits (eds.), A.E.C. Symp. Ser. (CONF 730505) p:216-222.

151. McCafferty, W. P. 1975. The burrowing mayflies (Ephemeroptera: Ephemeroidea) of the United States. Trans. Am. Entomol. Soc. 101:447-504.

158. Minshall, G. Wayne, and Douglas A. Andrews. 1973. An ecological investigation of the Portneuf River, Idaho: A semiarid-land stream subjected to pollution. Freshwater Biol. 3:1-30.

159. Morgan, Anna H. 1911. May-flies of Fall Creek. Ann. Entomol. Soc. Am. 4:93-119, 7 pl.

173. Jensen, Steven Leroy. 1966. The mayflies of Idaho (Ephemeroptera). M. S. Thesis, Univ. Utah, Salt Lake City.

191. Peters, William L. 1976. Unpublished observations.

Appendices

Appendix 23. Month, year, latitude and longitude for macroinvertebrate samples analyzed in this report. Several samples were collected from the same locations.

Site	Month	Year	Latitude	Longitude
JR156569	10	2015	40.4060288	-111.90001
JR114429	5	2000	40.4863892	-111.93605
JR115117	10	2000	40.4863892	-111.93605
JR117487	3	2001	40.4863892	-111.93605
JR118510	10	2001	40.4863892	-111.93605
JR118867	5	2002	40.4863892	-111.93605
JR121480	4	2002	40.4863892	-111.93605
JR126843	10	2004	40.4863892	-111.93605
JR127668	10	2005	40.4863892	-111.93605
JR129968	10	2006	40.4863892	-111.93605
JR140275	9	2007	40.5233803	-111.92102
JR156576	10	2015	40.5233803	-111.92102
JRSCW1	11	2017	40.5255437	-111.921745
JR133717	10	2003	40.5321999	-111.917
JR133725	10	2003	40.5321999	-111.917
JR133730	9	2003	40.5321999	-111.917
JR133748	9	2003	40.5321999	-111.917
JR134174	9	2004	40.5321999	-111.917
JR134175	10	2004	40.5321999	-111.917
JR134190	9	2004	40.5321999	-111.917
JR134199	10	2004	40.5321999	-111.917
JR140274	9	2007	40.5875015	-111.91194

JR114442	5	2000	40.6094017	-111.9203
JR127667	11	2005	40.623333	-111.92
JR141615	10	2008	40.630924	-111.92378
JRSCW3	11	2017	40.6310774	-111.923699
JR117809	4	2002	40.6455994	-111.9217
JR120959	2	2002	40.6613998	-111.9185
JR121601	5	2004	40.6613998	-111.9185
JR140272	9	2007	40.6861115	-111.92028
JR142113	11	2009	40.7161102	-111.92555
JR142114	11	2009	40.7249985	-111.925
JR127666	11	2005	40.7336121	-111.92278
JR156575	10	2015	40.7500114	-111.92015
JR140273	9	2007	40.7802773	-111.93777
JRSCW2	12	2017	40.7808607	-111.93824
JR142111	11	2009	40.8411675	-111.95
JR142112	11	2009	40.8450012	-111.9525
JR114433	5	2000	40.9056015	-111.9336
JR117516	5	2001	40.9056015	-111.9336
JR118520	11	2001	40.9056015	-111.9336
JR118868	5	2002	40.9056015	-111.9336
JR124961	11	2003	40.9056015	-111.9336
JR127346	12	2004	40.9056015	-111.9336
JR127669	11	2005	40.9056015	-111.9336

Appendix 24. Correlations, r between macroinvertebrate taxa and NMS axes.

Axis 1	Axis 2	Axis 3

Taxon	r	Taxon	r	Taxon	r
Isoperla	0.411	Tricoryt	0.345	Simuliid	0.294
Pyrgulop	0.210	Elmidae	0.265	Corbicul	0.244
Corixida	0.207	Acari	0.264	Coenagri	0.209
Notonect	0.177	Ephemere	0.261	Pyrgulop	0.191
Ancylida	0.144	Lepidost	0.261	Physidae	0.190
Fluminic	0.114	Pyrgulop	0.255	Fluminic	0.180
Tetraste	0.101	Fluminic	0.240	Chironom	0.170
Hydrobii	0.084	Hydropsy	0.240	Isoperla	0.168
Ephemere	0.070	Corbicul	0.218	Caenidae	0.148
Lepidost	0.070	Empidida	0.203	Ancylida	0.135
Turbella	0.034	Pisidiid	0.200	Planorbi	0.123
Pisidiid	0.021	Lymnaeid	0.178	Amphipod	0.118
Lymnaeid	0.014	Calopter	0.140	Orthocla	0.116
Oligocha	-0.003	Hydrobii	0.129	Acari	0.107
Corbicul	-0.028	Isoperla	0.104	Aeshinid	0.096
Caenidae	-0.041	Leptocer	0.102	Ephemere	0.092
Nemata	-0.070	Ceratopo	0.089	Lepidost	0.092
Planorbi	-0.072	Hydropti	0.086	Leptocer	0.091
Leptocer	-0.106	Leptohyp	0.078	Orconect	0.058
Aeshinid	-0.121	Nemata	0.064	Empidida	0.056
Physidae	-0.128	Physidae	0.045	Turbella	0.048
Trichopt	-0.128	Potamopy	0.040	Trichopt	0.033
Ceratopo	-0.138	Trichopt	0.026	Elmidae	0.030
Leptophl	-0.161	Leptophl	0.007	Hydropsy	0.026
Potamopy	-0.169	Hirudine	-0.015	Leptophl	0.022

Simuliid	-0.179	Baetidae	-0.018	Ceratopo	0.014
Leptohyp	-0.181	Caecidot	-0.037	Calopter	-0.010
Orconect	-0.202	Planorbi	-0.052	Caecidot	-0.062
Baetidae	-0.212	Simuliid	-0.069	Lymnaeid	-0.074
Hirudine	-0.224	Ancylida	-0.071	Leptohyp	-0.115
Amphipod	-0.255	Turbella	-0.076	Hydropti	-0.142
Calopter	-0.279	Tetraste	-0.093	Pisidiid	-0.165
Chironom	-0.300	Orconect	-0.143	Corixida	-0.208
Hydropti	-0.337	Notonect	-0.148	Nemata	-0.224
Acari	-0.346	Orthocla	-0.171	Notonect	-0.248
Empidida	-0.360	Amphipod	-0.180	Potamopy	-0.252
Coenagri	-0.409	Corixida	-0.196	Hydrobii	-0.258
Elmidae	-0.446	Caenidae	-0.242	Baetidae	-0.266
Caecidot	-0.449	Oligocha	-0.242	Tricoryt	-0.279
Orthocla	-0.456	Coenagri	-0.247	Tetraste	-0.348
Hydropsy	-0.505	Aeshinid	-0.284	Hirudine	-0.351
Tricoryt	-0.516	Chironom	-0.431	Oligocha	-0.540

Appendix 25. Indicator Species Analysis: Up-river indicators

Taxon	Maxgroup	IV	Mean	Std.Dev.	P-value
Elmidae	1	81.6	29.5	8.08	0.0002
Hydropsy	1	85.1	50.4	9.50	0.0004

Empidida	1	47.8	19.5	7.33	0.0038
Orthocla	1	64.8	39.6	8.10	0.007
Tricoryt	1	49.7	30.3	7.62	0.023
Corbicul	1	49.4	29.1	9.17	0.0308
Baetidae	1	32.7	22.1	7.40	0.0924
Fluminic	1	15.6	11.1	5.45	0.1646
Calopter	1	16.1	11.7	5.63	0.1716
Simuliid	1	44.3	37.7	8.99	0.2124
Acari	1	47.5	41.7	8.56	0.2312
Caecidot	1	46.9	44.4	8.31	0.3393
Planorbi	1	8.1	7.6	3.71	0.3531
Physidae	1	29.2	29.1	8.33	0.4185
Potamopy	1	20.0	21.0	8.21	0.4511
Trichopt	1	7.9	9.3	4.62	0.4567
Leptophl	1	8.3	6.0	2.24	0.4723
Leptohyp	1	8.3	6.0	2.24	0.4855
Pyrgulop	1	6.4	7.2	3.31	0.6289
Orconect	1	5.5	8.7	4.48	0.8052

Indicator Species Analysis: Mid stream indicators

Taxon	Maxgroup	IV	Mean	Std.Dev.	P-value
Hirudine	2	51.8	27.4	6.98	0.007
Ceratopo	2	30.8	14.3	6.39	0.0176
Nemata	2	26.1	17.0	6.93	0.1042

Pisidiid	2	27.2	17.6	7.22	0.1084
Tetraste	2	15.4	9.3	5.07	0.141
Isoperla	2	11.5	8.3	4.56	0.3091
Hydrobii	2	22.4	19.4	7.52	0.3299
Ancylida	2	11.1	10.7	5.17	0.3945
Oligocha	2	33.4	32.6	7.64	0.4047
Hydropti	2	25.8	26.8	7.67	0.4687
Leptocer	2	12.0	11.5	5.71	0.4831
Lymnaeid	2	7.7	7.4	3.77	0.6253
Ephemere	2	3.8	6.0	2.24	1
Lepidost	2	3.8	6.0	2.24	1
Notonect	2	3.8	6.0	2.24	1

Indicator Species Analysis: Downstream indicators

Taxon	Maxgroup	IV	Mean	Std.Dev.	P-value
Chironom	3	82.9	51.4	11.64	0.0036
Coenagri	3	54.9	39.3	9.62	0.0754
Caenidae	3	16.7	7.3	3.53	0.1094
Aeshinid	3	11.9	12.1	5.74	0.4853
Corixida	3	10.8	14.1	6.41	0.6947
Amphipod	3	11.5	18.2	7.39	0.8316
Turbella	3	20.0	29.7	8.24	0.9204

Appendix 26

Biological sediment tolerance index (2016) and Hilsenhoff Biotic Index (HBI) for organic pollution (Hilsenhoff 1987) values for Jordan River macroinvertebrate taxa that had associated values. BSTI tolerance values are based on % fines < 0.06 mm (silt, sand, fine OM) and HBI values have ranges from 1 to 10 with 1 being the least tolerant to organic pollution and 10 being the most tolerant.

Taxon	BSTI (%FN)	Taxon	HBI
Ordobrevia nubifera	1	Ephemerellidae	1
Diamesa sp.	2	Leptophlebiidae	2
Antocha monticola	5	*Antocha monticola*	3
Baetidae	6	*Microcylloepus pusillus*	3
Baetis sp.	6	*Microcylloepus similis*	3
Baetis tricaudatus	6	*Cleptelmis addenda*	4
Hydropsyche sp.	6	Elmidae	4
Hydropsychidae	6	*Eukiefferiella devonica group*	4
Hemerodromia sp.	7	*Gyrinus sp.*	4
Orthocladiinae	8	Heptageniidae	4
Orthocladius sp.	8	*Hydropsyche sp.*	4
Simuliidae	8	Hydropsychidae	4
Simulium sp.	8	Leptohyphidae	4
Turbellaria	8	*Microcylloepus sp.*	4
Trombidiformes	9	*Optioservus sp.*	4
Ephydridae	10	*Parakiefferiella sp.*	4
Oligochaeta	10	*Tricorythodes minutus*	4
Tricorythodes minutus	10	*Tricorythodes sp.*	4
Tricorythodes sp.	10	*Aeshna*	5

Ceratopogonidae	11	Aeshnidae	5
Ceratopogoninae	11	*Ambrysus sp.*	5
Optioservus sp.	12	*Brillia sp.*	5
Tanypodinae	12	Corixidae	5
Prostoma	14	*Diamesa sp.*	5
Cleptelmis addenda	16	Oligochaeta	5
Fluminicola coloradoensis	16	*Simulium sp.*	5
Ferrissia rivularis	17	*Stenelmis sp.*	5
Hydroptila sp.	17	Acari	6
Hydroptilidae	17	*Anax sp.*	6
Microcylloepus pusillus	17	*Anax walsinghami*	6
Microcylloepus similis	17	*Apedilum sp.*	6
Microcylloepus sp.	17	*Argia emma*	6
Asellidae	21	*Argia sp.*	6
Physa sp.	21	Baetidae	6
Coenagrionidae	25	*Baetis sp.*	6
Dubiraphia sp.	25	*Baetis tricaudatus*	6
Corisella sp.	26	*Bezzia/Palpomyia*	6
Corixidae	26	*Caenis sp.*	6
Caecidotea	27	Ceratopogonidae	6
Corbicula fluminea	27	Ceratopogoninae	6
Corbicula sp.	27	Chironominae	6
Hyalella azteca	27	*Corbicula fluminea*	6
Gammarus lucustris	28	*Corbicula sp.*	6

Curculionidae	41	*Cricotopus trifascia group*	6
Callibaetis sp.	63	*Dubiraphia sp.*	6
		Ephydridae	6
		Eukiefferiella sp.	6
		Ferrissia rivularis	6
		Fossaria sp.	6
		Gammarus lucustris	6
		Hemerodromia sp.	6
		Hetaerina americana	6
		Hetaerina sp.	6
		Hetaerina vulnerata	6
		Hydroptila sp.	6
		Hydroptilidae	6
		Lebertia sp.	6
		Orconectes virilis	6
		Orthocladiinae	6
		Pisidium sp.	6
		Probezzia sp.	6
		Simuliidae	6
		Sperchon sp.	6
		Stagnicola sp.	6
		Turbellaria	6
		Callibaetis sp.	7
		Cricotopus bicinctus group	7

		Cricotopus sp.	7
		Nanocladius sp.	7
		Tanypodinae	7
		Asellidae	8
		Caecidotea	8
		Chironomidae	8
		Cryptochironomus sp.	8
		Eukiefferiella claripennis group	8
		Glossiphoniidae	8
		Gyraulus sp.	8
		Helobdella stagnalis	8
		Hyalella azteca	8
		Nemata	8
		Physa sp.	8
		Prostoma	8
		Sperchonidae	8
		Coenagrionidae	9

Appendix 27. Sediment tolerance values for macroinvertebrate taxa that were reported in this analysis.

Taxon	BSTI	GLMMAX	GLMCL	GAMMAX	GAMCL	WA	CD75

Acari	na	na	na	na	na	na	na
Aeshna	na	na	na	na	na	na	na
Aeshnidae	na	na	na	na	na	na	na
Ambrysus sp.	na	48.1	i	47.1	t	37	47.6
Anax sp.	na	na	na	na	na	na	na
Anax walsinghami	na	na	na	na	na	na	na
Antocha monticola	5	65.7	i	73.6	t	40.9	57.1
Apedilum sp.	na	na	na	na	na	na	na
Argia emma	na	97.1	t	97.1	t	40.4	66.7
Argia sp.	na	na	na	na	na	na	na
Asellidae	21	na	na	na	na	na	na
Baetidae	6	na	na	na	na	na	na
Baetis sp.	6	0	s	0	s	24.2	34.3
Baetis tricaudatus	6	na	na	na	na	na	na
Bezzia/Palpomyia	na	na	na	na	na	na	na
Brillia sp.	na	0	s	0	s	20.2	31.4
Caecidotea	27	na	na	na	na	na	na
Caenis sp.	na	64.8	i	72.6	t	54.2	68.6
Callibaetis sp.	63	na	na	na	na	na	na
Ceratopogonidae	11	na	na	na	na	na	na
Ceratopogoninae	11	na	na	na	na	na	na
Chironomidae	na	na	na	na	na	na	na
Chironominae	na	na	na	na	na	na	na
Cleptelmis addenda	16	na	na	na	na	na	na
Clitellata	na	na	na	na	na	na	na
Coenagrionidae	25	na	na	na	na	na	na
Collembola	na	na	na	na	na	na	na

Corbicula fluminea	27	na	na	na	na	na	na
Corbicula sp.	27	na	na	na	na	na	na
Corisella sp.	26	na	na	na	na	na	na
Corixidae	26	na	na	na	na	na	na
Corticacarus sp.	na	na	na	na	na	na	na
Cricotopus bicinctus group	na	na	na	na	na	na	na
Cricotopus sp.	na	na	na	na	na	na	na
Cricotopus trifascia group	na	na	na	na	na	na	na
Cryptochironomus sp.	na	na	na	na	na	na	na
Curculionidae	41	na	na	na	na	na	na
Diamesa sp.	2	na	na	na	na	na	na
Dina dubia	na	na	na	na	na	na	na
Dina parva	na	na	na	na	na	na	na
Dubiraphia sp.	25	na	na	na	na	na	na
Elmidae	na	na	na	na	na	na	na
Enochrus sp.	na	na	na	na	na	na	na
Ephemerellidae	na	na	na	na	na	na	na
Ephemeroptera	na	na	na	na	na	na	na
Ephydridae	10	na	na	na	na	na	na
Erpobdella punctata	na	na	na	na	na	na	na
Erpobdella sp.	na	na	na	na	na	na	na
Eukiefferiella claripennis group	na	na	na	na	na	na	na
Eukiefferiella devonica group	na	na	na	na	na	na	na
Eukiefferiella sp.	na	0	s	0	s	22.7	32.4
Fallceon quilleri	na	97.1	t	97.1	t	42.1	60.6
Fallceon sp.	na	97.1	t	97.1	t	42.1	60.6
Ferrissia rivularis	17	na	na	na	na	na	na

Fluminicola coloradoensis	16	na	na	na	na	na	na
Fossaria sp.	na	na	na	na	na	na	na
Gammarus lucustris	28	na	na	na	na	na	na
Glossiphonia complanata	na	na	na	na	na	na	na
Glossiphoniidae	na	na	na	na	na	na	na
Gyraulus sp.	na	na	na	na	na	na	na
Gyrinus sp.	na	na	na	na	na	na	na
Helobdella stagnalis	na	na	na	na	na	na	na
Hemerodromia sp.	7	97.1	t	64.8	t	33.7	55.2
Heptageniidae	na	na	na	na	na	na	na
Hetaerina americana	na	na	na	na	na	na	na
Hetaerina sp.	na	na	na	na	na	na	na
Hetaerina vulnerata	na	na	na	na	na	na	na
Hyalella azteca	27	86.3	i	97.1	t	58.3	76.2
Hydrobiidae	na	na	na	na	na	na	na
Hydrophilus sp.	na	na	na	na	na	na	na
Hydropsyche sp.	6	na	na	na	na	28.1	41
Hydropsychidae	na	na	na	na	na	28.1	41
Hydroptila sp.	17	71.6	i	97.1	t	38.1	55.2
Hydroptilidae	17	na	na	na	na	na	na
Hygrobates sp.	na	na	na	97.1	t	31.2	41
Lebertia sp.	na	0	s	0	s	22.4	29.8
Leptohyphidae	na	na	na	na	na	na	na
Leptophlebiidae	na	na	na	na	na	na	na
Microcylloepus pusillus	17	na	na	32.4	t	29.6	34.3
Microcylloepus similis	17	na	na	32.4	t	29.6	34.3
Microcylloepus sp.	17	na	na	32.4	t	29.6	34.3

Nanocladius sp.	na	na	na	60.8	na	28.2	49
Nemata	na	na	na	na	na	na	na
Nephelopsis obscura	na	na	na	na	na	na	na
Oligochaeta	10	na	na	na	na	na	na
Optioservus sp.	12	34.3	i	30.4	s	26.3	37.1
Orconectes virilis	na	na	na	na	na	na	na
Ordobrevia nubifera	1	0	s	0	s	10	12.4
Orthocladiinae	8	na	na	na	na	na	na
Orthocladius sp.	8	na	na	na	na	24.8	38.1
Parakiefferiella sp.	na	62.8	i	70.6	t	37.6	57.1
Physa sp.	21	97.1	t	97.1	t	38.3	57.1
Pisidium sp.	na	97.1	t	97.1	7	42.5	67
Potamopyrgus antipodarum	na	na	na	na	na	na	na
Probezzia sp.	na	na	na	na	na	na	na
Prostoma	14	na	na	na	na	na	na
Pyrgulopsis sp.	na	na	na	na	na	na	na
Sigara sp.	na	na	na	na	na	na	na
Simuliidae	8	97.1	t	77.5	t	28.8	40
Simulium sp.	8	97.1	t	77.5	t	28.8	40
Sperchon sp.	na	na	na	na	na	25.9	37.1
Sperchonidae	na	na	na	na	na	25.9	37.1
Stagnicola sp.	na	na	na	na	na	na	na
Stenelmis sp.	na	na	na	na	na	na	na
Tanypodinae	12	na	na	na	na	na	na
Trepaxonemata	na	na	na	na	na	na	na
Tricorythodes minutus	10	97.1	t	97.1	t	39.5	60.6
Tricorythodes sp.	10	97.1	t	97.1	t	39.5	60.6

Trombidiformes	9	na	na	na	na	na	na
Turbellaria	8	na	na	na	na	na	na

Appendix 28. Summary statistic of macroinvertebrate samples including mean, std. dev., sum, maximum and minimum densities, and alpha: richness (S), evenness (E), Shannon Diversity (H), and Simpson Diversity (D).

Sample ID	Mean	Stand.Dev.	Sum	Min	Max	S	E	H	D`
JR112877	89.57	336.14	4120.00	0.00	1624.00	9.00	0.58	1.27	0.68
JR112878	182.23	952.50	8382.70	0.00	6360.00	8.00	0.39	0.81	0.40
JR112885	65.04	252.22	2992.00	0.00	1291.00	9.00	0.55	1.21	0.66
JR114429	172.18	656.83	7920.18	0.00	3996.00	13.00	0.56	1.44	0.67
JR114433	30.28	88.83	1393.00	0.00	403.00	10.00	0.76	1.76	0.80
JR114442	619.10	2919.06	28478.67	0.00	18293.00	6.00	0.49	0.88	0.51
JR115117	314.20	1211.10	14453.00	0.00	5573.00	8.00	0.57	1.18	0.66
JR115140	49.89	168.57	2295.00	0.00	905.00	12.00	0.65	1.61	0.74
JR117487	440.25	1590.09	20251.65	0.00	7986.00	13.00	0.56	1.44	0.70
JR117516	365.34	1833.52	16805.54	0.00	11885.00	10.00	0.36	0.84	0.44
JR117809	1.11	2.85	51.00	0.00	14.00	11.00	0.85	2.05	0.84
JR118510	711.84	2902.43	32744.70	0.00	15943.00	16.00	0.48	1.32	0.62
JR118520	38.39	176.68	1766.00	0.00	1164.00	8.00	0.54	1.13	0.53
JR118867	415.33	1667.00	19105.37	0.00	10543.00	10.00	0.57	1.31	0.64
JR118868	69.33	243.73	3189.00	0.00	1323.00	12.00	0.59	1.48	0.72
JR120704	3.72	14.76	171.00	0.00	96.00	11.00	0.62	1.48	0.64
JR120959	1.37	4.42	63.00	0.00	28.00	12.00	0.75	1.87	0.76
JR121480	320.85	1019.71	14758.86	0.00	5694.00	13.00	0.68	1.73	0.76
JR121601	11.70	53.30	538.00	0.00	350.00	15.00	0.45	1.21	0.54
JR124906	30.44	114.80	1400.40	0.00	557.00	11.00	0.57	1.36	0.68
JR124961	49.16	211.92	2261.33	0.00	1067.00	14.00	0.42	1.10	0.58
JR126843	197.07	578.47	9065.00	0.00	3013.00	14.00	0.70	1.85	0.80
JR127346	181.12	885.68	8331.67	0.00	5840.00	12.00	0.39	0.97	0.47
JR127666	358.86	1899.37	16507.33	0.00	12827.00	12.00	0.36	0.89	0.38

JR127667	277.13	1049.76	12748.00	0.00	6542.00	14.00	0.58	1.53	0.67
JR127668	20.14	71.67	926.33	0.00	430.00	9.00	0.71	1.56	0.71
JR127669	735.05	4069.64	33812.34	0.00	27573.00	7.00	0.39	0.76	0.33
JR129968	1037.33	5269.65	47717.23	0.00	35470.00	17.00	0.37	1.04	0.43
JR133717	52.26	206.56	2404.00	0.00	1076.00	14.00	0.51	1.34	0.65
JR133725	257.66	1006.35	11852.53	0.00	6387.00	14.00	0.56	1.49	0.65
JR133730	77.98	320.80	3587.00	0.00	2133.00	15.00	0.56	1.51	0.62
JR133748	221.35	943.74	10182.00	0.00	6148.00	16.00	0.49	1.34	0.59
JR134174	47.91	198.76	2204.00	0.00	1312.00	17.00	0.52	1.47	0.61
JR134175	82.30	442.51	3785.59	0.00	2997.00	12.00	0.35	0.87	0.36
JR134190	118.54	572.91	5452.60	0.00	3853.00	13.00	0.45	1.14	0.48
JR134199	212.72	1146.86	9784.98	0.00	7723.00	10.00	0.34	0.79	0.36
JR140272	311.20	1184.05	14315.00	0.00	6941.00	15.00	0.55	1.48	0.67
JR140273	16.90	59.94	777.46	0.00	373.00	16.00	0.60	1.66	0.71
JR140274	172.20	648.48	7921.00	0.00	3819.00	17.00	0.52	1.47	0.68
JR140275	516.87	1723.56	23775.95	0.00	8758.00	15.00	0.61	1.65	0.74
JR141615	16.89	77.61	777.00	0.00	509.00	16.00	0.43	1.19	0.53
JR142111	27.43	119.35	1261.60	0.00	686.00	12.00	0.44	1.08	0.58
JR142112	25.38	131.26	1167.61	0.00	879.00	8.00	0.43	0.89	0.41
JR142113	54.22	233.99	2494.22	0.00	1560.00	21.00	0.47	1.43	0.58
JR142114	26.91	103.12	1237.78	0.00	676.00	18.00	0.55	1.60	0.67
JR156569	7.15	30.27	328.68	0.00	196.00	9.00	0.59	1.29	0.60
JR156571	255.72	1523.45	11763.00	0.00	10270.00	6.00	0.23	0.42	0.22
JR156575	18.00	100.45	828.11	0.00	676.00	12.00	0.28	0.70	0.32
JR156576	34.21	87.49	1573.49	0.00	416.00	16.00	0.75	2.07	0.84
JRSCW1	6.83	14.77	314.14	0.00	58.00	14.00	0.86	2.27	0.88
JRSCW2	56.12	252.95	2581.42	0.00	1687.00	13.00	0.49	1.24	0.55

JRSCW3	295.71	1386.65	13602.68	0.00	9254.00	13.00	0.46	1.17	0.51
----------	----------	----------	----------	----------	----------	------	-------	------	-------
AVERAGES:	186.50	822.30	8581.00	0.00	5100.00	12.50	0.53	1.32	0.60

Appendix 29. Temperature tolerance values for macroinvertebrate taxa that occurred in this analysis.

Taxon	GLM MAX	GL MC L	GAM MAX	GA MCL	Weighted Average	CD75	ID Occurre nce	ID -ISA
Acari	na	na	na	na	na	na	2b	5
Aeshna	na	na	na	na	na	na	na	na
Aeshnidae	na	na	na	na	na	na	na	na
Ambrysus sp.	29.1	t	29.1	t	18.9	22.7	1a	4
Anax sp.	na	na	na	na	na	na	na	na
Anax walsinghami	na	na	na	na	na	na	na	na
Antocha monticola	na	na	na	na	na	na	2a	2
Apedilum sp.	na	na	na	na	na	na	1b	4
Argia emma	22.5	i	25	t	18.5	22	1b	4
Argia sp.	22.5	i	25	t	18.5	22	1b	4
Asellidae	na	na	na	na	na	na	na	na
Baetidae	14	i	13.8	s	14.1	17	2b	na
Baetis sp.	14	i	13.8	s	14.1	17	2a	2
Baetis tricaudatus	14	i	13.8	s	14.1	17	2b	5
Bezzia/Palpomyia	na	na	na	na	na	na	2a	2
Brillia sp.	8.6	i	2	s	12	14.6	2a	2
Caecidotea	na	na	na	na	na	na	na	4

Caenis sp.	29.1	t	29.1	t	18.2	19.8	1a	4
Callibaetis sp.	na	na	na	na	na	na	1a	4
Ceratopogonidae	na	na	na	na	na	na	2a	2
Ceratopogoninae	na	na	na	na	na	na	2b	5
Chironomidae	na	na	na	na	na	na	na	5
Chironominae	na	na	na	na	na	na	na	na
Cleptelmis addenda	14.6	i	14	i	na	na	2b	2
Clitellata	na	na	na	na	na	na	na	na
Coenagrionidae	na	na	na	na	na	na	1a	4
Collembola	na	na	na	na	na	na	na	na
Corbicula fluminea	na	na	na	na	na	na	na	na
Corbicula sp.	na	na	na	na	na	na	na	na
Corisella sp.	na	na	na	na	na	na	na	na
Corixidae	na	na	na	na	na	na	1a	4
Corticacarus sp.	na	na	na	na	na	na	na	na
Cricotopus bicinctus group	29.1	t	29.1	t	15.2	18.8	1b	5
Cricotopus sp.	29.1	t	29.1	t	15.2	18.8	1b	5
Cricotopus trifascia group	29.1	t	29.1	t	15.2	18.8	1b	5
Cryptochironomus sp.	29.1	t	29.1	t	17.6	21.5	1b	4
Curculionidae	na	na	na	na	na	na	na	na
Diamesa sp.	2	s	2	s	11	13.1	2a	2
Dina dubia	na	na	na	na	na	na	na	na
Dina parva	na	na	na	na	na	na	na	na
Dubiraphia sp.	29.1	t	27.2	t	16.8	19.8	1a	4
Elmidae	na	na	na	na	na	na	2a	na

Enochrus sp.	na	na	na	na	na	na	na	na
Ephemerellidae	na	na	na	na	na	na	2a	2
Ephemeroptera	na	na	na	na	na	na	na	na
Ephydridae	na	na	na	na	na	na	na	na
Erpobdella punctata	na	na	na	na	na	na	na	2
Erpobdella sp.	na	na	na	na	na	na	na	2
Eukiefferiella claripennis group	2	s	2	s	13.4	16.1	2b	5
Eukiefferiella devonica group	2	s	2	s	13.4	16.1	2a	2
Eukiefferiella sp.	2	s	2	s	13.4	16.1	2a	2
Fallceon quilleri	29.1	t	29.1	t	19.4	22.2	1a	4
Fallceon sp.	29.1	t	29.1	t	19.4	22.2	1a	4
Ferrissia rivularis	na	na	na	na	na	na	1b	4
Fluminicola coloradoensis	na	na	na	na	na	na	2b	2
Fossaria sp.	na	na	na	na	na	na	na	5
Gammarus lucustris	na	na	na	na	na	na	1b	5
Glossiphonia complanata	na	na	na	na	na	na	1a	4
Glossiphoniidae	na	na	na	na	na	na	1a	na
Gyraulus sp.	na	na	na	na	na	na	1b	5
Gyrinus sp.	na	na	na	na	na	na	na	na
Helobdella stagnalis	na	na	na	na	na	na	1b	2
Hemerodromia sp.	22.3	i	22.8	t	17.3	19.6	2b	5
Heptageniidae	na	na	na	na	na	na	2b	2
Hetaerina americana	na	na	na	na	na	na	na	na

Hetaerina sp.	na	na	na	na	na	na	na	na
Hetaerina vulnerata	na	na	na	na	na	na	na	na
Hyalella azteca	20.1	i	21.2	t	16.5	19.1	1a	5
Hydrobiidae	na	na	na	na	na	na	2b	na
Hydrophilus sp.	na	na	na	na	na	na	na	5
Hydropsyche sp.	na	na	na	na	na	na	2b	5
Hydropsychidae	na	na	na	na	na	na	2b	5
Hydroptila sp.	22.5	i	25	t	17.8	20.4	2b	5
Hydroptilidae	22.5	i	25	t	17.8	20.4	2b	5
Hygrobates sp.	na	na	na	na	4.70	7.6	1b	a
Lebertia sp.	2	S	2	S	12.8	15.2	2a	2
Leptohyphidae	na	na	na	na	na	na	na	na
Leptophlebiidae	na	na	na	na	na	na	2b	2
Microcylloepus pusillus	29.1	t	29.1	t	19.2	22.9	1b	4
Microcylloepus similis	na	na	na	na	na	na	1b	4
Microcylloepus sp.	na	na	na	na	na	na	1b	4
Nanocladius sp.	15.1	i	16.5	s	14.3	18.2	na	na
Nemata	na	na	na	na	na	na	na	na
Nephelopsis obscura	na	na	na	na	na	na	na	na
Oligochaeta	na	na	na	na	na	na	na	na
Optioservus sp.	16.8	i	17.1	i	14.9	17.5	1b	5
Orconectes virilis	na	na	na	na	na	na	na	na
Ordobrevia nubifera	17.1	i	17.1	t	16	18	2b	na
Orthocladiinae	na	na	na	na	na	na	1b	2

Orthocladius sp.	na	na	na	na	na	na	1b	5
Parakiefferiella sp.	na	na	2	s	13.4	17.8	1b	5
Physa sp.	29.1	t	29.1	t	16.9	19.5	1b	4
Pisidium sp.	17.1	i	17.1	t	15	18.2	2b	5
Potamopyrgus antipodarum	na	na	na	na	na	na	1b	na
Probezzia sp.	na	na	na	na	na	na	1b	5
Prostoma	na	na	na	na	na	na	1b	5
Pyrgulopsis sp.	na	na	na	na	na	na	na	na
Sigara sp.	na	na	na	na	na	na	na	na
Simuliidae	17.6	i	17.6	t	14.8	17.7	2b	5
Simulium sp.	17.6	i	17.6	t	14.8	17.7	2b	5
Sperchon sp.	na	na	na	na	14.3	17.8	2b	5
Sperchonidae	na	na	na	na	na	na	2b	5
Stagnicola sp.	na	na	na	na	na	na	na	na
Stenelmis sp.	na	na	na	na	na	na	na	na
Tanypodinae	na	na	na	na	na	na	1b	5
Trepaxonemata	na	na	na	na	na	na	na	na
Tricorythodes minutus	29.1	t	29.1	t	18.5	22.4	1b	4
Tricorythodes sp.	29.1	t	29.1	t	18.5	22.4	1b	4
Trombidiformes	na	na	na	na	na	na	na	na
Turbellaria	na	na	na	na	na	na	2a	2

Appendix 30. Cluster analyses

```
Linkage method:    CENTROID

Distance measure:  Sorensen (Bray-Curtis)

Total sum of squares:    0.3795953E+10

 Percent chaining =  43.22
```

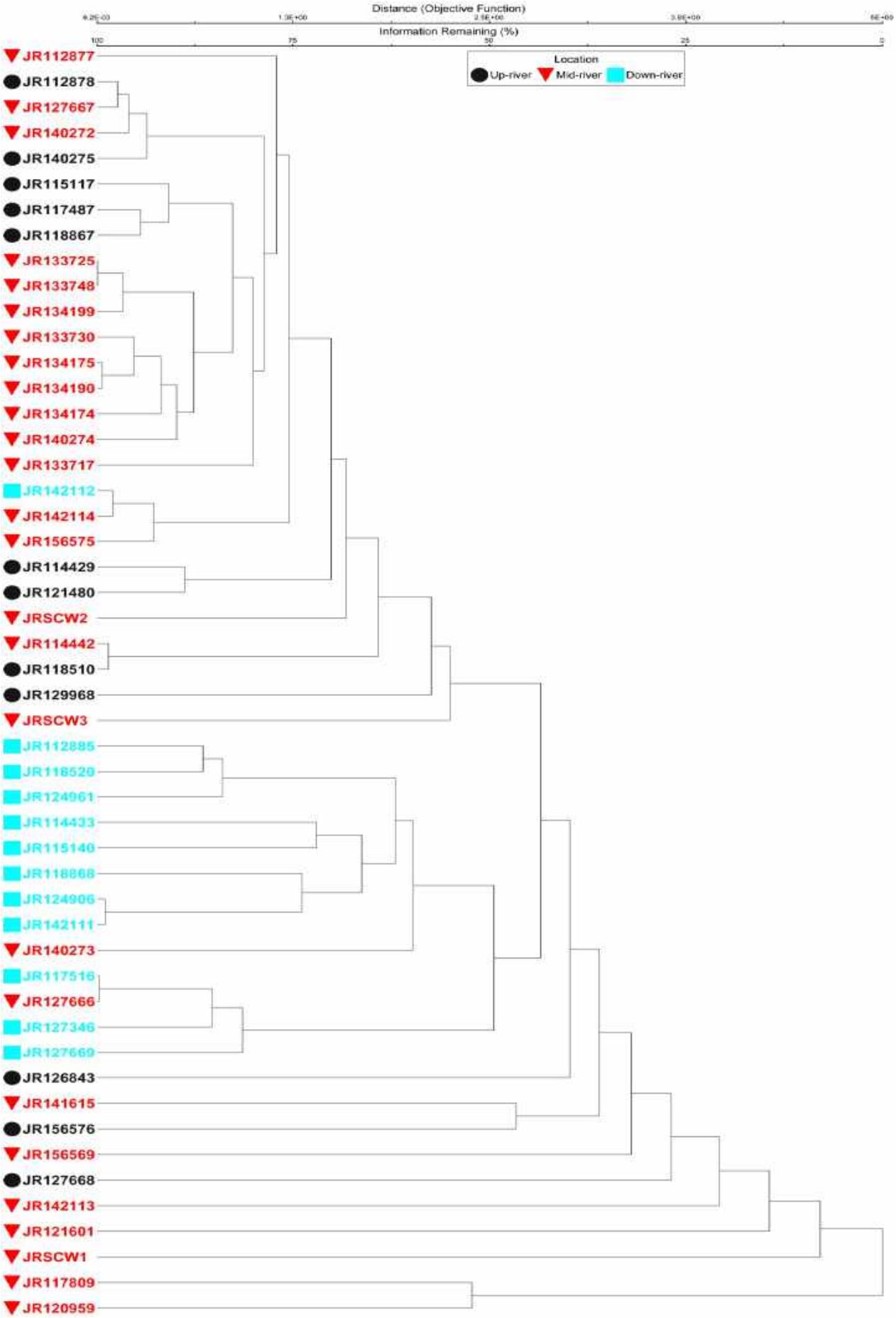
Distance (Objective Function)
Information Remaining (%)
Location
Up-river
Mid-river
Down-river
JR112877
JR112878
JR127667
JR140272
JR140275
JR115117
JR117487
JR118867
JR133725
JR133748
JR134199
JR133730
JR134175
JR134190
JR134174
JR140274
JR133717
JR142112
JR142114
JR156575
JR114429
JR121480
JRSCW2
JR114442
JR118510
JR129968
JRSCW3
JR112885
JR118520
JR124961
JR114433
JR115140
JR118868
JR124906
JR142111
JR140273
JR117516
JR127666
JR127346
JR127669
JR126843
JR141615
JR156576
JR156569
JR127668
JR142113
JR121601
JRSCW1
JR117809
JR120959

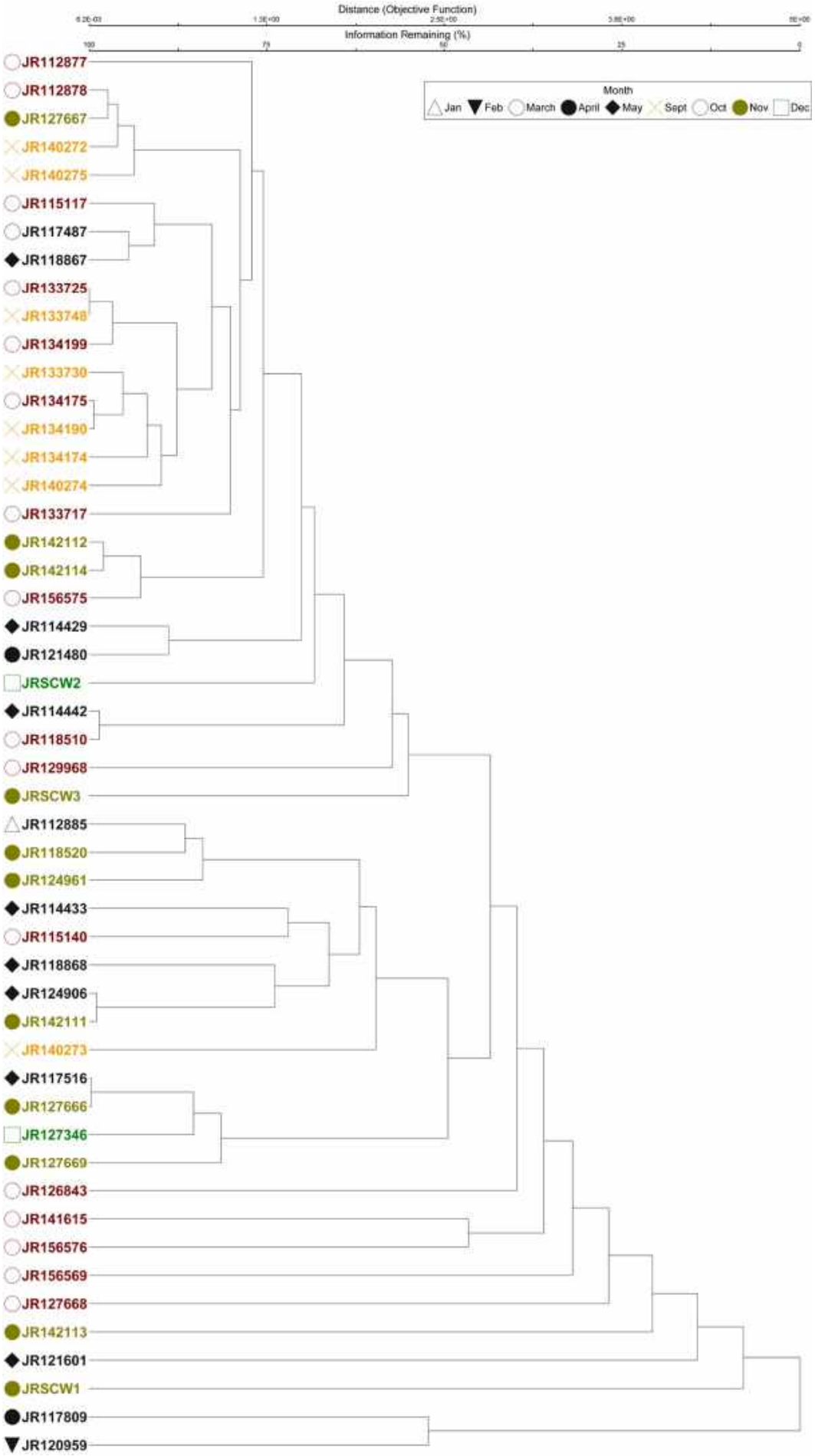
Distance (Objective Function)
Information Remaining (%)
Month
Jan
Feb
March
April
May
Sept
Oct
Nov
Dec
JR112877
JR112878
JR127667
JR140272
JR140275
JR115117
JR117487
JR118867
JR133725
JR133748
JR134199
JR133730
JR134175
JR134190
JR134174
JR140274
JR133717
JR142112
JR142114
JR156575
JR114429
JR121480
JRSCW2
JR114442
JR118510
JR129968
JRSCW3
JR112885
JR118520
JR124961
JR114433
JR115140
JR118868
JR124906
JR142111
JR140273
JR117516
JR127666
JR127346
JR127669
JR126843
JR141615
JR156576
JR156569
JR127668
JR142113
JR121601
JRSCW1
JR117809
JR120959

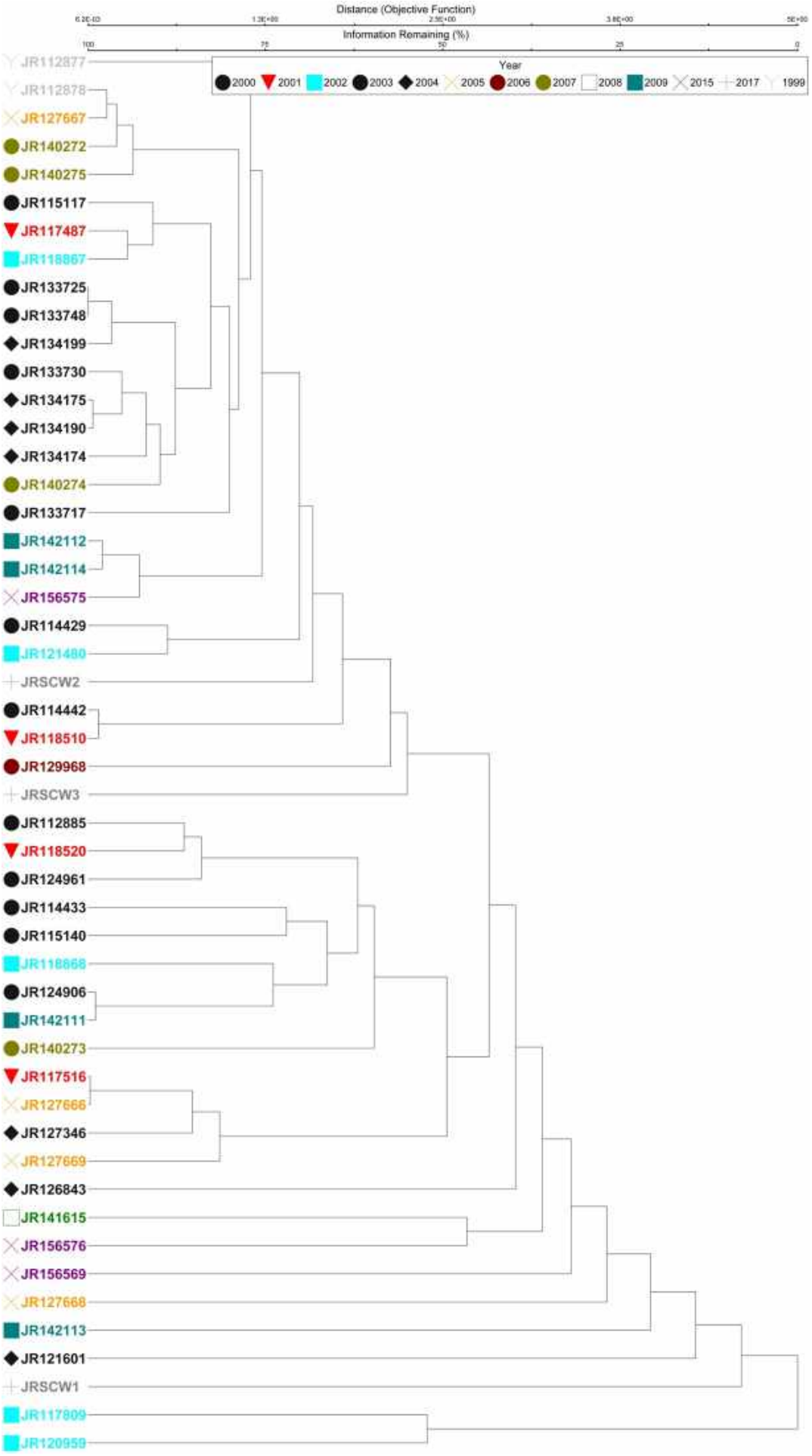
Distance (Objective Function)
Information Remaining (%)
Year
2000
2001
2002
2003
2004
2005
2006
2007
2008
2009
2015
2017
1999
JR112877
JR112878
JR127667
JR140272
JR140275
JR115117
JR117487
JR118867
JR133725
JR133748
JR134199
JR133730
JR134175
JR134190
JR134174
JR140274
JR133717
JR142112
JR142114
JR156575
JR114429
JR121480
JRSCW2
JR114442
JR118510
JR129968
JRSCW3
JR112885
JR118520
JR124961
JR114433
JR115140
JR118868
JR124906
JR142111
JR140273
JR117516
JR127666
JR127346
JR127669
JR126843
JR141615
JR156576
JR156569
JR127668
JR142113
JR121601
JRSCW1
JR117809
JR120959

Month

PAIRWISE COMPARISONS

Note: p values not corrected for multiple comparisons.

Groups (identifiers)

Compared			T	A	p
10	vs.	5	-1.67836672	0.01758062	0.06587330
10	vs.	4	0.20548324	-0.00341144	0.51365844
10	vs.	11	-2.53031434	0.02304250	0.01982259
10	vs.	12	-0.34016021	0.00604862	0.30609137
10	vs.	9	0.19803133	-0.00234180	0.51019934
5	vs.	4	0.75292591	-0.02586693	0.75916988
5	vs.	11	0.23347381	-0.00324636	0.53767410
5	vs.	12	0.88658988	-0.03025806	0.81508503
5	vs.	9	-2.84433727	0.05377584	0.01342494
4	vs.	11	0.40874157	-0.00950311	0.52153180
4	vs.	12	1.35682962	-0.04823357	NaN
4	vs.	9	-0.65238184	0.02554186	0.21564205
11	vs.	12	0.88624053	-0.02549582	0.85370625
11	vs.	9	-4.06818097	0.06131477	0.00129807
12	vs.	9	-1.03861619	0.04218901	0.13838409

Appendix 31. Example of Salt Lake County Watershed Planning and Restoration, Salt Lake City macroinvertebrate assessments in the Jordan River. Used with permission.

Jordan River @ 500 N, JR_08.77, December 8, 2017

Benthic macroinvertebrate community

Site Summary		
Biological Condition Gradient (BCG) assignment	**6**	Extreme changes in structure and ecosystem function
Karr Benthic Index of Biological Integrity (BIBI)	**14**	Very poor biological integrity

Potential benthic community stressors	Undoubtedly	Probably	Maybe	Not indicated	Uncertain
Thermal	**X**				
Dissolved oxygen		**X**			
Nutrient enrichment		**X**			
Toxins		**X**			
Substrate disturbance by floods		**X**			
Substrate embedding and fine sediment	**X**				
Overall habitat complexity low	**Very poor**				

General observations:
New Zealand mud snail and Asiatic clam present. Caecidotea, the highly tolernat aquatic sowbug common.
Severely distorted feeding groups
Cold water biota absent
Semivoltine taxa are all tolerant taxa
BCG attribute 6 taxa present
0.5% by abundance of sensitive taxa
98.5% are tolerant BCG attribute 4 & 5 taxa
Assigned a solid BCG level 6

Metric response	Very poor	Poor	Fair	Good	Excellent
Decreases (D) with declining water/habitat quality	Very low	Low	Medium	High	Very high
Increases (I) with declining water/habitat quality	Very high	High	Medium	Low	Very Low

	Site value	Comments
Gross community composition and abundance		
Total taxa richness	24	
Total abundance (per square meter)	2617	
EPT taxa richness	2	
Warm water biota		
Warm water biota richness	9	
% Warm water biota	19	
Cold water biota		
Cold water biota richness	0	
% Cold water biota	0	
Ubiquitous western montane cold water taxa		
% Baetis bicaudatus	0	
% Drunella doddsii	0	
% Megarcys	0	
% Parapsyche elsis	0	
% Neothremma	0	
Semivoltine, k-selected or long-lived taxa		
Semivoltine taxa richness	3	
% Semivoltine taxa	1.3	
Multivoltine, r-selected or short-lived taxa		

Multivoltine taxa richness	17	
% Multivoltine taxa	31	
Size potential at maturity		
% Small size at maturity	23	
% Medium size at maturity	76	
% Large size at maturity	1	
Insect orders and Chironomidae		
Mayflies		
% Ephemeroptera (mayflies)	9.1	
% Baetis tricaudatus (tolerant mayfly)	2.3	too extreme even for B. tricaudatus complex
% Fallceon (tolerant mayfly)	6.7	
Stoneflies		
% Plecoptera (stoneflies)	0	
Perlidae	0	
Nemouridae taxa richness	0	
Caddisflies		
% Trichoptera (caddisflies)	0	
Rhyacophila taxa richness	0	
% Coleoptera (beetles)	0	
% Diptera (true flies)	10.9	
% Chironomidae (midges)	10.7	
% Simuliidae (blackflies)	0.2	
% Non-insects by abundance		
% Non-insect invertebrates	80	
% Trepaxonemata (flatworms)	3	
% Prostoma (nemerteans)	0.5	
% Oligochaeta (segmented worms)	65	
% Hirudinea (leeches)	0.2	

% Mollusca (bivalves and snails)	2
% Fluminicola (native snail)	0
% Potamopyrgus (NZ mud snail)	0.2
% Corbicula (Asiatic clam)	0.8
% Crustacea	8.9
% Amphipoda (scuds)	0
% Caecidotea (aquatic sowbugs)	8.9
Feeding group taxa richness	
Collector richness	18
Predator richness	4
Shedder richness	0
Scraper or grazer richness	1
% Feeding group by abundance	
% Collector	94
% Predator	3.8
% Shredder	0
% Scraper or Grazer	0.7
Biological Condition Gradient (BCG) Attributes	
% of total taxa richness	
Attribute 1 % of total taxa richness	0
Attribute 2+3 % of total taxa richness	4.2
Attribute 4+5 % of total taxa richness	88
Attribute 6 % of total taxa richness	8.3
% by abundance	
% Attribute 1 by abundance	0
% Attribute 2-3 by abundance	0.5
% Attribute 4+5 by abundance	98.5

% Attribute 6 by abundance	1

Karr Benthic Index of Biological Integrity (BIBI original traits and 10-50 scoring scale)

Modified by Wisseman 2018

METRIC	**Site value**	**Score**
Total number of taxa	24	3
Number Ephemeroptera taxa	2	1
Number Plecoptera taxa	0	1
Number Trichoptera taxa	0	1
Number of long-lived taxa	3	1
Number of intolerant taxa	0	1
% Tolerant taxa	21	3
% Predator	3.8	1
Number of clinger taxa	9	1
% Dominance (3 taxa)	80	1
Karr BIBI TOTAL SCORE		**14**
BIOLOGICAL CONDITION CATEGORY	**Very Poor**	

Chapter 11

Upper Jordan River Macroinvertebrate Assemblage: November 2018

By:

David C. Richards, Ph.D.

OreoHelix Ecological

Summary

Understanding benthic macroinvertebrate assemblages is critical to managing water quality in the upper Jordan River. However, very little research has been done regarding this. We collected and analyzed fifteen macroinvertebrate samples from the upper Jordan River in November 2018. Results were both confirmatory and surprising: 1) Densities were extremely low at most locations and do not reflect the amount of nutrients available to the food web; 2) densities were greatest in stable less embedded cobble habitat; 3) the majority of the upper Jordan River has unstable small sized substrate which reduces densities; and 4) the upper Jordan River is dominated by two highly invasive mollusk taxa, the New Zealand mudsnail and the Asian clam. These findings support our conclusion that the upper Jordan River is a severely impaired analog of its former self, and for the most part ecologically is not much different than the conveyance canal, Surplus Canal. Surprisingly two newly identified taxa were found in the river; the polychaete, *Capitella capitata* and the mayfly, *Baetis adonis*. More research is needed to understand the macroinvertebrate assemblages and their role in ecosystem function and water quality.

Table of Contents

List of Figures

List of Tables

Appendices

Introduction

Benthic macroinvertebrates are crucially important to river ecosystem function. They are the most important biological and ecological component of every temperate river ecosystem in the world, including the Jordan River. They link primary production (e.g. plants, algae, etc.) with higher level production (e.g. fish, birds, etc.), direct nutrient spiraling, govern algal community structure, reduce and decompose organic matter, and regulate water quality. They are responsible for maintaining ecosystem function and provide underappreciated ecosystem services. Macroinvertebrates are also arguably the single most influential metric defining the ecological management of aquatic resources throughout the world (Monaghan 2016), including the Jordan River.

Very few studies have been conducted on macroinvertebrates in the Jordan River despite their importance to ecosystem function. All studies to date focused on macroinvertebrates as water quality indicators and those sample collections focused on cobble-riffle habitats (Richards 2018b). No studies that we are aware of collected samples from multiple locations during a single time period on the river and analyzed such data from an ecological assemblage-wide perspective or examined multimetric indicators. Without such knowledge of macroinvertebrate assemblages, prudent management of water quality conditions in the river is pointless.

Methods

Field and Lab

Fifteen benthic macroinvertebrate samples were collected from the upper Jordan River in early November 2018 (Table 40). Thirteen 0.5 m^2 samples were collected using a shovel and net method described in Richards (2018b). Two samples (BB-5; JR-10) were collected by scraping several large cobbles for a total surface area $\approx$ 0.5 m^2. Five of the samples labeled BB were from the 'Big Bend' section of the Jordan River where a multi-agency restoration project is scheduled to occur. These samples will provide baseline macroinvertebrate data to help monitor the success of the restoration project. Samples were preserved in 70% isopropyl and delivered to River Continuum Concepts, Manhattan, MT. Invertebrates were identified to the lowest practical level, typically genus or species using a 700-subsample method. Map locations and latitudinal/longitudinal coordinates are in Figure 49 and Table 40.

Figure 49. Map of sample sites (black dots).

Table 40. Site names and latitude and longitude. BB = 'Big Bend' section of the Jordan River; JR = Jordan River.

Site	Latitude	Longitude
BB-1	40.596243	-111.91571
BB-2	40.596322	-111.915902
BB-3	40.596762	-111.91686
BB-4	40.596417	-111.91511
BB-5	40.591419	-111.91247
JR-1a	40.490588	-111.92999
JR-1b	40.492599	-111.92591
JR-2	40.491006	-111.92941
JR-7a	40.525511	-111.9206

JR-7b	40.526750	-111.919353
JR-8	40.53203	-111.91849
JR-9	40.538161	-111.91642
JR-10	40.544091	-111.91681
JR-11a	40.550855	-111.91542
JR-11b	40.551497	-111.91185

Statistics

Several statistical methods were used to help understand macroinvertebrate assemblages in the river. Multivariate (community level) methods included: non-metric multidimensional scaling (NMS); multiple response permutation procedure (MRPP); and indicator species analysis (ISA) (McCune and Mefford 2018). Kruskal-Wallis rank tests, nonparametric equality of means tests, and box plots were used to compare relationships between several metrics including: taxa richness (S), effective number of taxa (ENT), evenness (E), Shannon diversity (H), Simpson diversity (D), total density (m^{-2}), and individual taxa density (m^{-2}). Box plots included; medians, 25^{th} and 75^{th} percentiles, and upper and lower adjacent values. Nonparametric tests were also conducted for comparisons with habitat type, substrate type, % dominant taxon. In addition, several dozen regression analyses were used to find the best fit model of relationships between densities of select taxa and habitat, substrate, depth, and % embeddedness. Because density estimates were essentially count data and left-skewed, regression methods examined included negative binomial truncated at zero, Poisson truncated at zero, and linear regression. Best fits were determined by comparing AIC, BIC, and -2 log likelihood scores. All statistics were conducted using Stata 15.1 (StataCorp 2018) and PC-ORD 7.1 (McCune and Mefford 2018). Note: Limited samples size (N = 15) requires caution when interpreting results.

Results

Taxa

Forty-four taxa were found in the upper Jordan River in November 2018 (Table 41).

Table 41. Macroinvertebrate taxa collected in fifteen benthic samples from the upper Jordan River, November 2018.

Non-Insects	
Platyzoa	Tricladida
	Nemertia
Nematoda	Nematoda/Nemata

Hydrazoa	*Hydra sp.*
Annelida	
Oligochaeta	Oligochaeta
Hirudinea	*Helobdella stagnalis*
	Erpobdella
Polychaeta	
	Capitella capitata
Mollusca	
Gastropoda	
	Potamopyrgus antipodarum
	Physa
	Lymnaea
Bivalvia	
	Pisidium sp.
	Corbicula fluminea
Arthropoda	*Acari*
Crustacea	
Cladocera	Daphnia (ephippia)
	Daphnia galeata mendotae
Amphipoda	*Gammarus*
Isopoda	*Caecidotea*
Copepoda	Copepoda
Ostracoda	Ostracoda

INSECTS

Ephemeroptera	
Baetidae	*Baetis sp.*
	Baetis adonis

	Fallceon quilleri
Leptohyphidae	*Tricorythodes sp.*
Odonata	
Coenagrionidae	*Argia sp.*
Calopterygidae	*Hetaerina americana*
Lepidoptera	
Crambidae	*Petrophila sp.*
Trichoptera	
Hydroptilidae	Hydroptilidae (pupae)
	Hydroptila sp.
Hydropsychidae	*Hydropsyche sp.*
Coleoptera	
Elmidae	*Microcylloepus sp.*
	Stenelmis sp.
	Ordrobrevia sp.
Diptera	
Tipulidae	Antocha
Chironomidae	Chironomidae (pupae/partial)
	Tanypodinae
	Orthocladiinae
	Chironominae
	Chironomini
	Tanytarsini
Ceratopogonidae	Bezzia/Palpomyia (complex)
	Probezzia sp.
Simuliidae	Simulium sp.
Empididae	Hemerodromia sp.

Brachycera	Ephydridae

The estimated number of taxa based on our samples ranged from 54 to up to a maximum of 76 (Table 42).

Table 42. Estimated number of taxa based on several commonly used estimators.

```
44 = Number of taxa observed

54 = First-order jackknife estimate

61 = Second-order jackknife estimate

64 = Chao2 estimate, classic form

56 = Chao2 estimate, bias corrected form

76 = Upper 95% bound, Chao2 estimate
```

Assemblages

Multivariate analyses showed that assemblages significantly differed, mostly based on substrate and habitat types. Eleven taxa that had only one occurrence were removed from the dataset prior to analyses. The best fit NMS model was a one-dimensional model with a final stress of 7.64; final stability < 0.001; at 41 iterations. Additional NMS model fit criteria are in Appendix 33. The single NMS axis had an $R^2 = 0.85$. There is little room for misinterpreting assemblage relationships in Figure 50, given a one-dimensional model with very low final stress and large R^2.

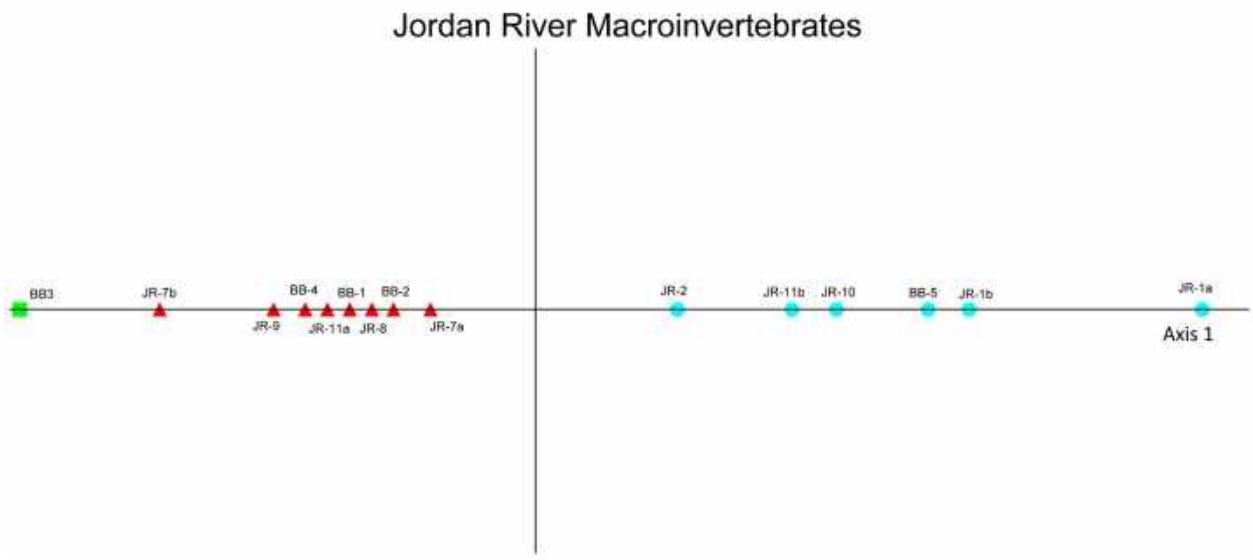

Figure 50. Best- fit NMS model of macroinvertebrate assemblages in the upper Jordan River, November 2018. Substrate: blue circle = cobble; red triangle=silt/sand/gravel; green square=highly erosional unstable sand/gravel.

Assemblages were most affected by substrate type (cobble vs. ≤ gravel size). Sample JR-1a ordinated on the far-right side of the NMS axis, while sample BB-3 ordinated on the furthest left side of the axis (Figure 50). JR-1a was the furthest upstream sample and was comprised of mostly unembedded cobbles just downstream (10 m) of a spring creek. The cobbles had well established algal growth. JR-1a had the highest densities of any site (> 25,000 m^{-2}). BB-3 was located at a highly erosional run directly downstream of a pool. Substrate was slightly greater at BB-3 than other riffle, runs, or pools. BB-3 had the lowest densities (86 m^{-2}). All samples that ordinated on the right side of the origin had cobble substrates, while all samples on the left side had ≤ gravel substrates. Samples also ordinated well by habitat (not shown) but not as distinctly as by substrate.

Multiple response permutation procedure (MRPP) also showed that assemblages significantly differed based on habitat (A = 0.10; p = 0.03) and substrate (A = 0.25; p < 0.01). Indicator species analysis (ISA) showed that several taxa were significantly associated with riffle habitat including: triclads, oligochaetes, *Potamopyrgus*, Caecidotea, and *Fallceon quilleri*. ISA also showed that many taxa were significantly associated with cobble substrate including: triclads, Nemertia, nematodes, oligochaetes, *Potamopyrgus*, Pisidium, Caecidotea, *Baetis adonis*, *Fallceon quilleri*, *Hydropsyche* sp., *Stenelmis* sp., orthoclads, Chironomini, and Hemerodromia.

Metrics by Substrate Type

Taxa richness (S) was greater on cobble substrate but the effective number of taxa (ENT) was not (Figure 51).

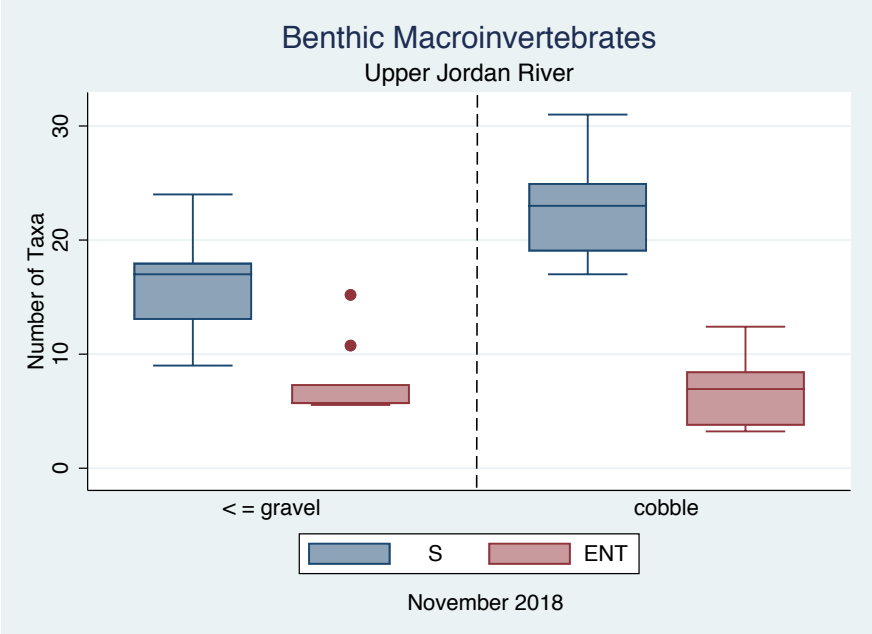

Figure 51. Taxa richness (S) was significantly greater on cobbles although the effective number of taxa (ENT) was not.

Evenness (E) was lower on cobble habitat than ≤ gravel but not significantly. There were no significant differences of Shannon and Simpson diversity indices between cobble and gravel substrate (Figure 52).

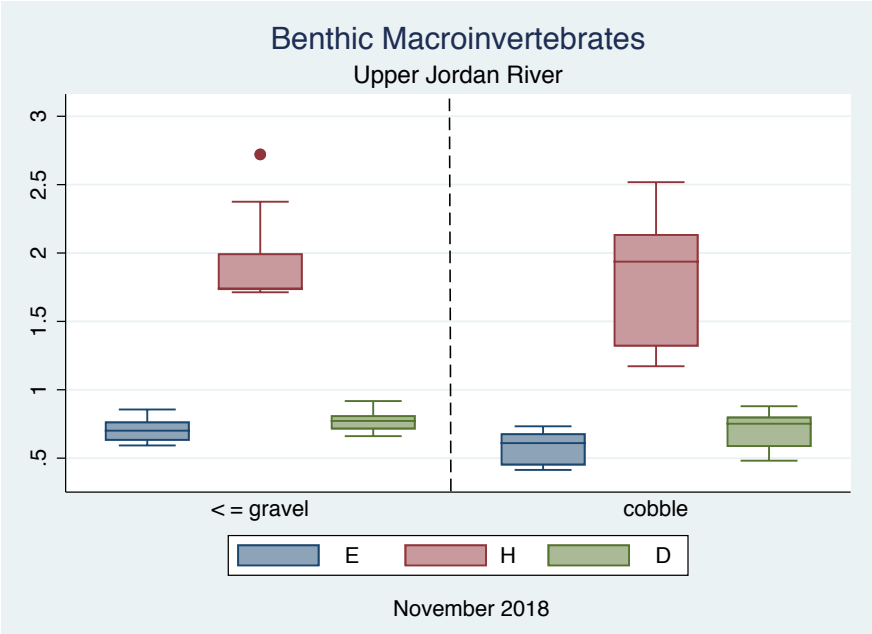

Figure 52. Evenness (E), Shannon diversity (H), and Simpson diversity (D) relationships between ≤ gravel sized substrates and cobble substrates. There were no significant differences, but E was noticeably lower on cobbles.

Percent dominant taxa did not significantly differ between substrate types (Figure 53).

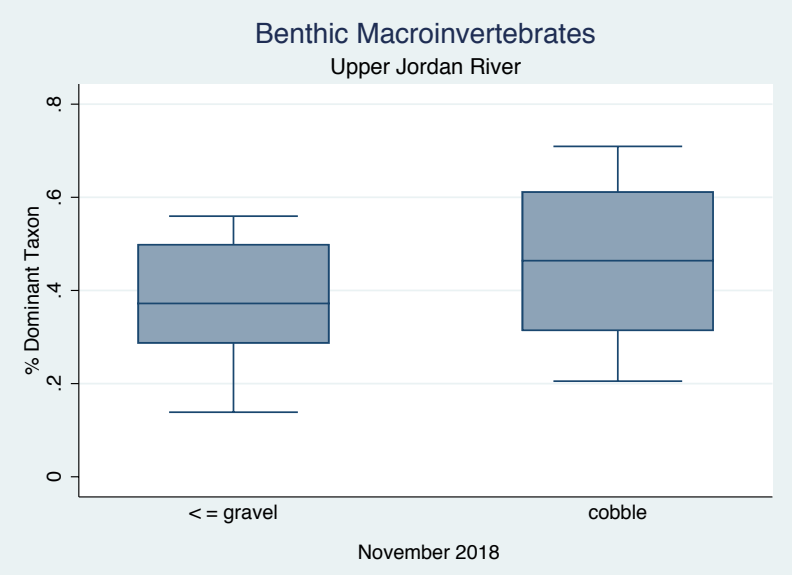

Figure 53. Percent dominant taxa relationships between ≤ gravel sized substrates and cobble substrates. No significant difference.

Metrics by Habitat Type

There were no significant differences in taxa richness (S) and ENT between habitat types, although run habitats appeared to have slightly higher richness and ENT (Figure 54).

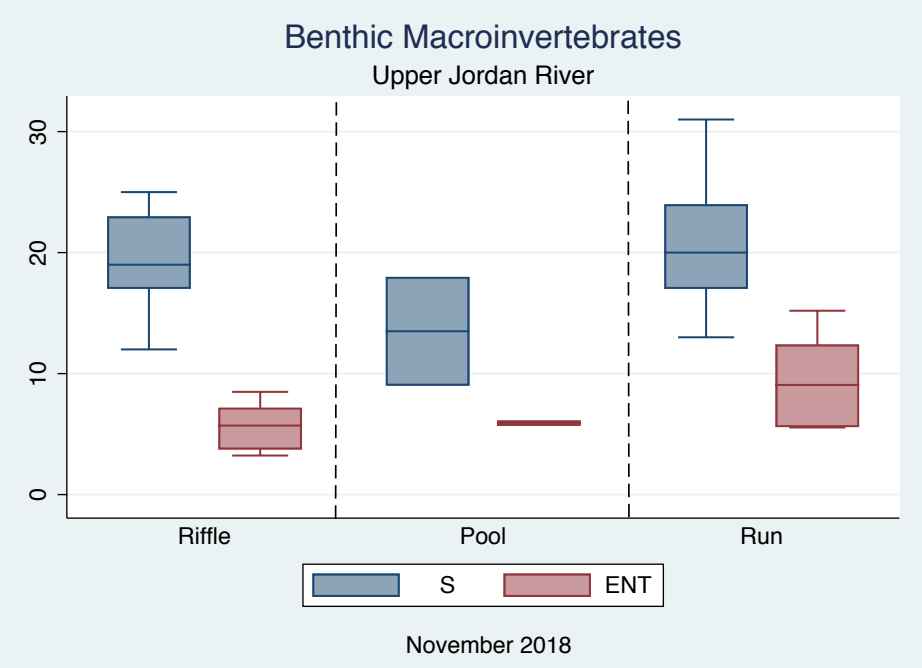

Figure 54. Relationships between Taxa richness (S) and effective number of taxa (ENT) and three habitat types. There were no significant differences.

There were also no significant differences in evenness, Shannon, and Simpson diversity indices between habitats, although run habitats had slightly greater values for all three indices (Figure 55).

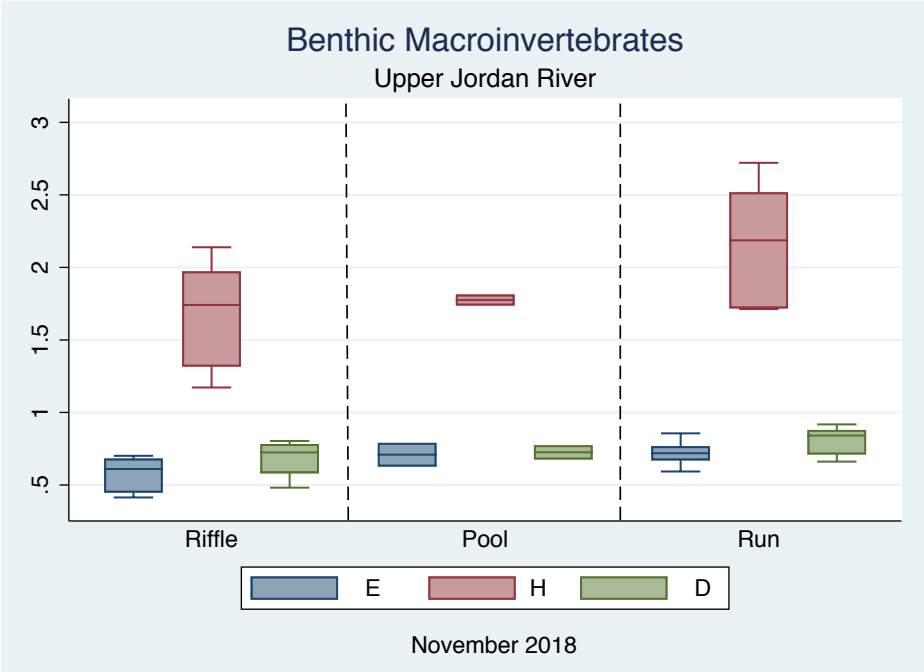

Figure 55. Evenness (E), Shannon diversity (H), and Simpson diversity (D) relationships between three habitat types. There were no significant differences.

Percent dominant taxon was lowest in run habitat and highest in riffle habitat but not significantly (Figure 56).

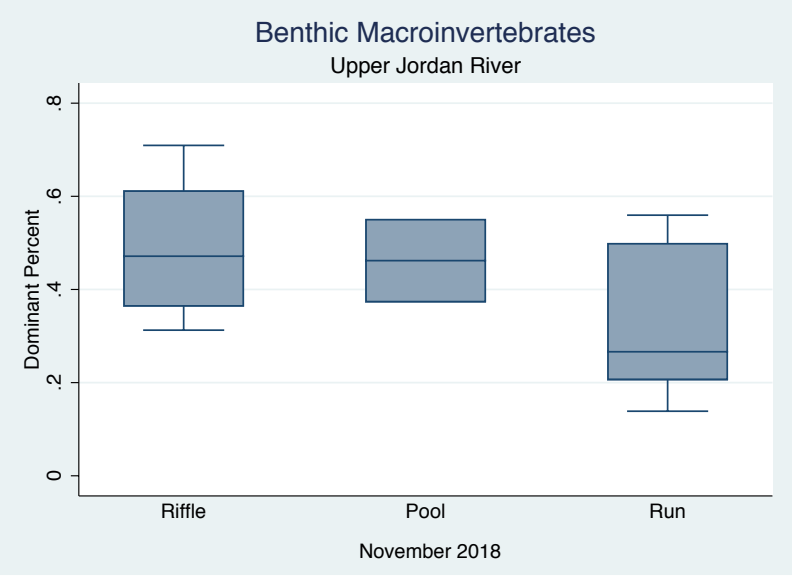

Figure 56. Percent dominant taxa relationships between three habitat types. No significant differences.

Densities

Densities were unusually low throughout most of the upper Jordan River (Figure 57) although cobble-riffle habitats had normal densities compared with other rivers throughout North America (Richards 2018b; Jackson et al. 2005)(Table 43; Figure 58).

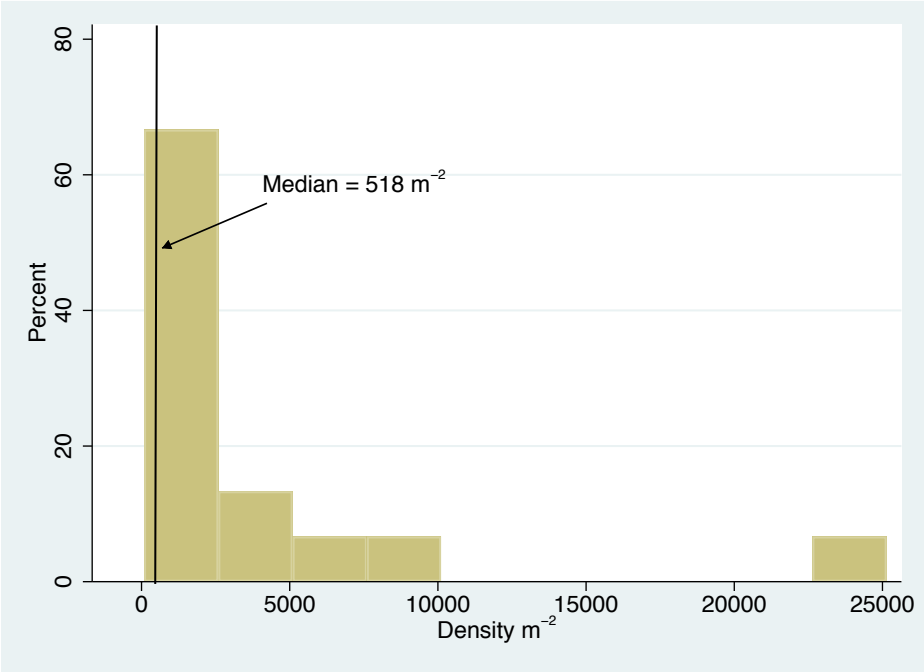

Figure 57. Distribution of macroinvertebrate densities in the upper Jordan River, November 2018.

Low densities highlight the serious problem of unstable ≤ gravel sized substrates, high levels of embeddedness, and the lack of suitable cobble habitat in the river. Although cobble habitat provided the greatest densities, they were still low considering nutrient availability and for primary production potential to be great.

Table 43. Descriptive statistics of macroinvertebrate densities (m^{-2}) between ≤ gravel and cobble sized substrates. JR-1a removed.

substrate	Mean	se(mean)	Median	Max	Min
< = gravel	396	53	420	606	86
cobble	8418	3471	5404	25142	2270
Average	3605	1681	518		

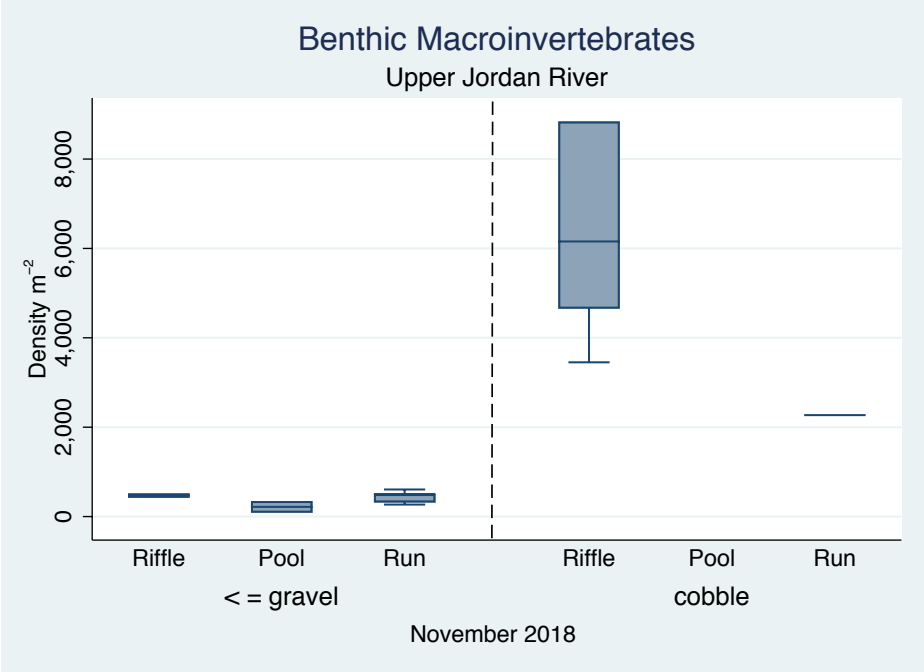

Figure 58. Macroinvertebrate densities (m-2) at three habitat types and two substrate types. Significant difference by habitat and by substrate. One outlier was excluded that had a density = 25,142 m^{-2}.

Densities (log_{10} transformed) were significantly negatively related to % embeddedness (Table 44).

Table 44. Relationship between macroinvertebrate density (Log_{10}) and % embeddedness.

Source	SS	df	MS		
				Number of obs	= 15
				F(1, 13)	= 6.63
Model	2.25934657	1	2.25934657	Prob > F	= 0.0230
Residual	4.42711891	13	.340547608	R-squared	= 0.3379
				Adj R-squared	= 0.2870
Total	6.68646548	14	.477604677	Root MSE	= .58356

logDensity	Coef.	Std. Err.	t	P>|t|	[95% Conf.	Interval]
embeddedness	-.0128373	.0049839	-2.58	0.023	-.0236044	-.0020702
_cons	3.953226	.3846016	10.28	0.000	3.122345	4.784107

An outlier, Site JR -1a had the highest density of any sample and had 50% embeddedness. This high density was mostly because it was a well-established cobble riffle just downstream of a spring fed creek. Contrarily, JR-1b was also a cobble-riffle habitat with 0% embeddedness but was recently exposed habitat from a beaver dam directly upstream (Figure 59) and didn't have as much of an established periphyton assemblage as did JR-1a.

Figure 59. Site JR-1b recently exposed cobble-riffle directly below beaver dam. Cobbles did not have sufficient time to be colonized by macroinvertebrates compared with JR-1a cobble-riffle.

Individual Taxa

Two new taxa unreported from the Jordan River were found in the samples: the polychaete *Capitella capitata* and the mayfly (Family Baetidae), *Baetis adonis*. Polychaetes are primarily salt-water taxa but a few, including *C. capitata* are sometimes found in freshwater. *Baetis adonis* was likely previously identified as *B. tricaudatus*.

Capitella capitata

We could not find any significant relationships between *C. capitata* and habitat, substrate, or depth but this polychaete was significantly negatively associated with % embeddedness (R^2 = 0.69)(Figure 60) and the best fit regression model that included habitat as a predictor produced an R^2 = 0.79 (Table 45).

Table 45. Best fit linear regression of Capitella capitata densities as a function of % embeddedness and habitat type.

Source	SS	df	MS	Number of obs	=	15
				F(3, 11)	=	14.03
Model	5932.82638	3	1977.60879	Prob > F	=	0.0004
Residual	1550.90695	11	140.991541	R-squared	=	0.7928
				Adj R-squared	=	0.7362
Total	7483.73333	14	534.552381	Root MSE	=	11.874

Capcap	Coef.	Std. Err.	t	P>|t|	[95% Conf.	Interval]
embeddedness	-.6509342	.1047939	-6.21	0.000	-.8815841	-.4202843
habitat						
Pool	-5.325606	9.643239	-0.55	0.592	-26.55023	15.89902
Run	13.21684	6.802243	1.94	0.078	-1.754797	28.18847
_cons	59.77301	7.970624	7.50	0.000	42.22978	77.31623

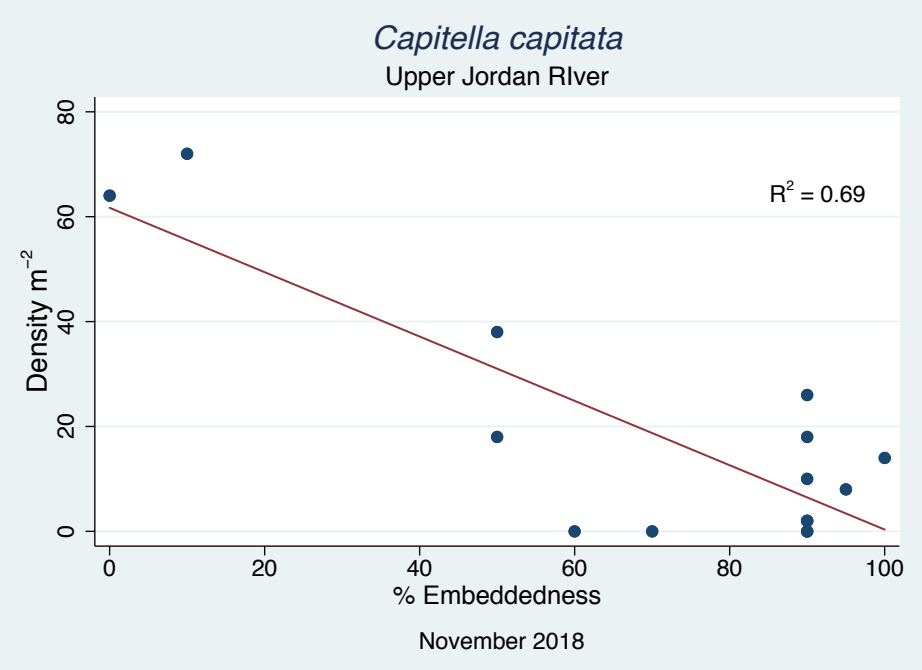

Figure 60. Relationship between Capitella capitata and % embeddedness.

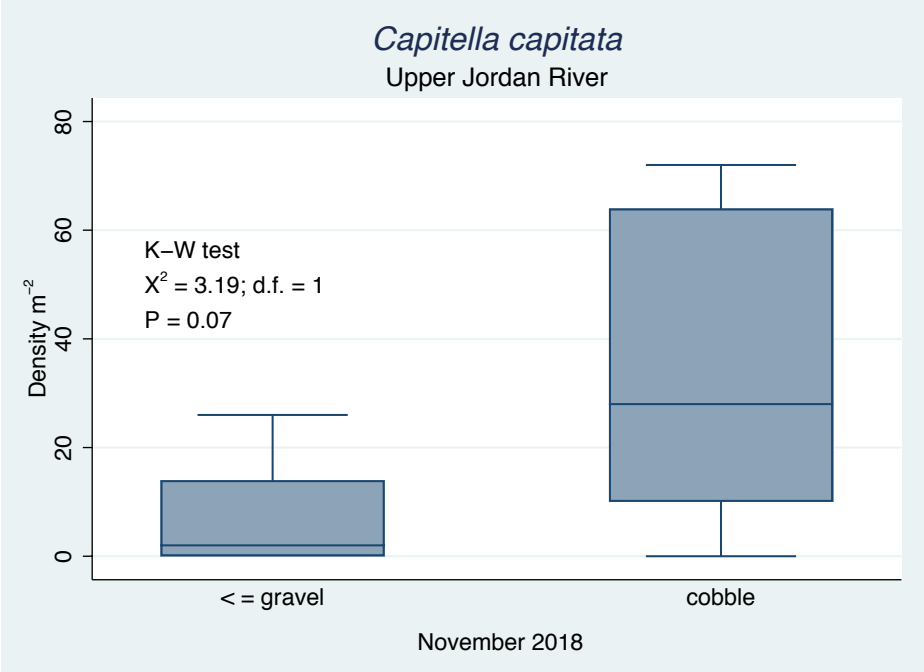

Figure 61. Capitella capitata densities as a function of substrate type. Densities were near significantly higher in cobble habitat.

Baetis adonis

The best predictor for *B. adonis* from this limited data set was % embeddedness (R^2 = 0.50) and similar to *C. capitata, B. adonis* was negatively associated with embedded substrates (Figure 62; Table 46).

Table 46. Best fit linear of Baetis adonis densities and % embeddedness.

Source	SS	df	MS		
				Number of obs	= 15
				F(1, 13)	= 12.89
Model	2461017.26	1	2461017.26	Prob > F	= 0.0033
Residual	2482632.34	13	190971.719	R-squared	= 0.4978
				Adj R-squared	= 0.4592
Total	4943649.6	14	353117.829	Root MSE	= 437

Badonis	Coef.	Std. Err.	t	P>|t|	[95% Conf.	Interval]
embeddedness	-13.39796	3.732208	-3.59	0.003	-21.4609	-5.335013
_cons	1175.655	288.0094	4.08	0.001	553.4485	1797.862

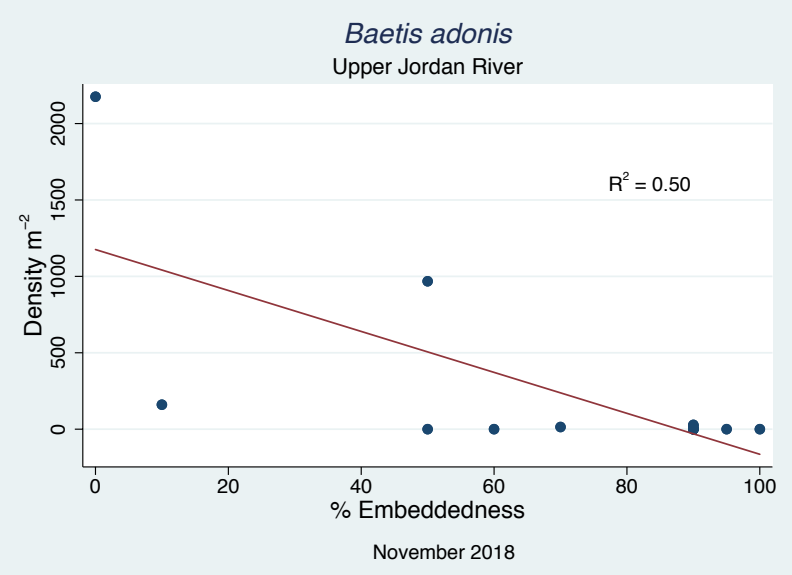

Figure 62. Relationship between Baetis adonis densities and % embeddedness.

Baetis adonis was mostly found in the upstream sites JR-1a, JR-1b, and JR-2, in cobble habitat (Figure 63).

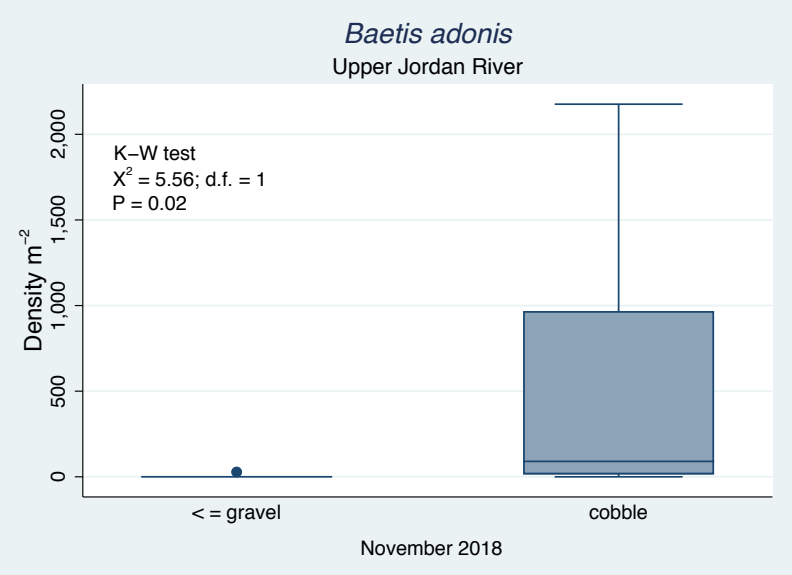

Figure 63. Relationship between Baetis adonis densities and substrate type. Densities were significantly greater in cobble habitat.

Potamopyrgus antipodarum, New Zealand Mudsnail

The invasive New Zealand mudsnail, *Potamopyrgus antipodarum* dominates the analog upper Jordan River by abundance (density). These snails on average were 26% of total abundances and as high as 71% total abundances (Figure 64; Table 47). Their proportional abundances were also greatest in cobble-riffle habitat (Figure 64; Table 47).

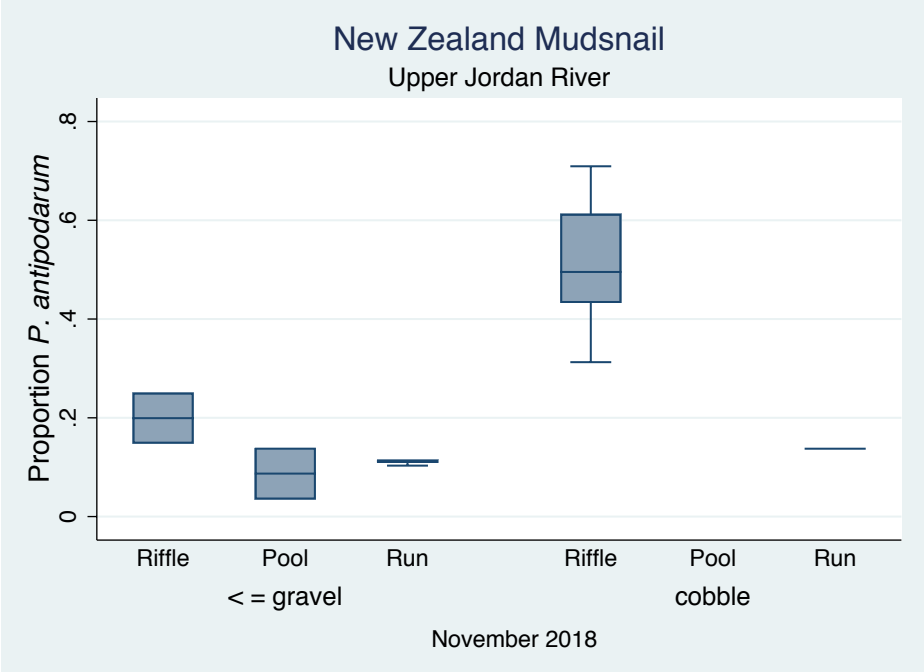

Figure 64. Proportion P. antipodarum compared with all taxa densities by substrate and habitat.

Table 47. Proportion P. antipodarum compared with all taxa densities by substrate.

substrate	mean	se(mean)	median	max	min
< = gravel	0.13	0.02	0.12	0.25	0.03
cobble	0.45	0.08	0.46	0.71	0.14
Total	0.26	0.05	0.15	0.71	0.03

Corbicula fluminea, Asian clam

The invasive Asian clam, *Corbicula fluminea*, didn't occur at high densities in the upper Jordan River. Although, due to its large size compared to the other taxa, its overall biomass was likely higher than all other taxa, except possibly *P. antipodarum (*Table 48*)*.

Table 48. Corbicula fluminea densities by habitat and substrate types.

habitat	mean	se(mean)	p50	max
Riffle	**14**	**4.535574**	**22**	**26**
Pool	**6.5**	**5.5**	**6.5**	**12**
Run	**6.5**	**1.839384**	**5**	**13**
Total	**10**	**2.426049**	**6**	**26**

substrate	mean	se(mean)	p50	max
< = gravel	**9.444444**	**2.749298**	**6**	**22**
cobble	**10.83333**	**4.777842**	**7.5**	**26**
Total	**10**	**2.426049**	**6**	**26**

Discussion

The upper Jordan River is an impaired analog of its past. Richards (2018b) discussed how channelization, dewatering, disconnect from its floodplain, sedimentation, and loss of beaver dams caused the river to cease to function as a healthy river. Richards (2018b) also evaluated macroinvertebrate assemblages from past studies that support these findings.

Several new and supportive key findings in this report are discussed. It is abundantly clear that unstable ≤ gravel sized substrates in the upper Jordan River cannot adequately support macroinvertebrate assemblages at densities normally found in properly functioning rivers with more stable substrates. The Jordan River is considered eutrophic and should support densities much greater than 20,000 m^{-2}; particularly given that many of the taxa we found in the upper Jordan River were short-lived, small-sized taxa including chironomids, snails, and annelids. However, median densities for the entire upper Jordan River were about 500 m^{-2}, densities in ≤ gravel sized substrate only averaged around 400 m^{-2}, and on stable cobble substrates only 5000 to 8000 m^{-2}. The upper Jordan River is dominated by erosional gravel habitat with an overabundance of fine sediments. Unembedded cobble habitat is sparse (Richards 2018c), consequently for most of its length, the river does not provide near the densities of macroinvertebrates that it would if conditions were similar to its past. These severe low macroinvertebrate densities prevent the river from providing essential ecosystem services including uptake (spiraling) of an overabundance of nutrients, either from the water column or from benthic algae. The severe lack of macroinvertebrates also negatively affects higher trophic levels. Most fishes in the upper Jordan River depend on benthic macroinvertebrates throughout their life cycle. Without adequate food resources, the river cannot hope to support viable game fisheries. If stable cobble substrates with limited embeddedness were established, then macroinvertebrate densities would dramatically increase, and fisheries would flourish.

Substrate and habitat covary and some of the macroinvertebrate taxa associated with cobble riffles in this report may occur there only because gravel riffles and runs provide limited habitat. Almost all taxa that we found were associated with cobbles with limited embeddedness.

A single dominant macroinvertebrate taxon signals poor function and impaired water quality. The highly invasive New Zealand mudsnail, *Potamopyrgus antipodarum*, completely dominates much of the benthic assemblages in the upper Jordan River. This snail is an analog of the native snails that once thrived in the river (Richards 2004) but functions differently than native snails in the region (Richards 2004). New Zealand mudsnails are considered to be a 'lawn mower' type grazers rapidly moving across

their environment, unless surrounded by inhospitable habitat (e.g. lone cobble surrounded by shifting sands). Mudsnails typically only superficially graze benthic algae (Richards 2004). Native conspecifics, including the pebble snail, *Fluminicola coloradensis* and spring snails, *Pyrgulopsis* sp., typically are slower, more thorough grazers and often have different food resource preferences than *P. antipodarum* (Richards 2004). The New Zealand mudsnail is also a known competitor with other native taxa including mayflies (Ephemeroptera) and caddisflies (Trichoptera) and may reduce their abundances (Kerans et. al. 2005). Two of the most common and important taxa groups in the upper Jordan River are three mayfly species, *Baetis adonis*, *Fallceon quilleri*, and *Tricorythodes* sp., and two caddisfly taxa, *Hydropsyche* sp. and *Hydroptila* sp. New Zealand mudsnails more than likely are competing with these taxa for food resources and more importantly for limited space on stable cobble substrate. Based on our research with New Zealand mudsnails (e.g. Richards 2004) and other benthic invertebrate taxa throughout western U. S., we conclude that densities of native mayflies and caddisflies would likely be greater in the absence of *Potamopyrgus antipodarum* in the upper Jordan River. Native mayfly and caddisfly taxa also have somewhat different functional roles than *P. antipodarum* and more than likely these roles are being hindered by its presence. As a result, functioning of the upper Jordan River ecosystem is altered to a lower state with less resistance and resilience due to the effects of this invasive snail.

The invasive Asian clam, *Corbicula fluminea* also has substantial ecosystem altering effects in the upper Jordan River. Richards (2008b) gives a detailed description of these effects in the Jordan River, as well as the effects of New Zealand mudsnails.

Fifteen samples are a low N, therefore results of this study should be interpreted with caution. We anticipate collecting between 15 and 20 additional samples from the upper Jordan River in March 2019 to supplement these results. There was a major toxic pulse of very fine anoxic sediments in the river during our sampling (Richards 2018a and 2018c). Effects of these chronic spills are unknown but may have influenced macroinvertebrate assemblages. Samples that will be collected in 2019 may shed light onto this catastrophe.

In addition, direct comparisons between Richards 2018a and this report are not feasible without losing valuable information because of the large differences in taxonomic resolution and field methods. For example, this study used a higher taxonomic resolution than was available in Richards 2018b.

One surprising finding was the addition of two previously unidentified or misidentified species: *Capitella capitata* and *Baetis adonis*. As far as we know, neither *C. capitata* nor *B. adonis* have been reported in Utah and certainly have not been reported in the Jordan River. Brett Marshall, director of River Continuum Concepts and a highly qualified aquatic macroinvertebrate taxonomist, cross referenced and taxonomically verified these species. Both species superficially resemble other closely related taxa. *Capitella capitata* is very similar morphologically to oligochaete worms and *B. adonis* is very similar morphologically to *B. tricaudatus.* More work needs to be done to better understand their life history, ecology, and water quality tolerances in the Jordan River. Because *B. adonis* is very similar to B. *tricaudatus* and easily misidentified as such, at this time there is no way of knowing what the ratios of the two species were in past studies in the Jordan River, which could have important implications for water quality managers and ecologists studying the river. Both species have been DNA sequenced from

other locations and their sequences are available online. We will collect specimens in 2019 and have them sequenced to further confirm their taxonomy.

Formal species traits analyses will be conducted after additional samples are collected in 2019. Richards (2018b) reported that most taxa in the Jordan River (including those found in this study) are temperature and sediment tolerant. We will use additional traits; including indices for sediment, nutrient, functional feeding groups, and life history traits to better understand macroinvertebrate assemblages in the upper portion of the river as they relate to ecosystem function and water quality.

As reported in this report and others by us, the Jordan River is an analog ecosystem not representative of its former self or even representative of a true river (Richards 2019a). Consequently, based on our extensive research in the Jordan River drainage, we see no noticeable ecological differences between the upper Jordan River macroinvertebrate assemblages in gravel habitats which dominate the river and the Surplus Canal assemblages. This is a big problem. The Surplus Canal was created as a conveyance canal and is not managed as a fishery or considered a functioning ecosystem. To have the upper Jordan River's macroinvertebrate assemblages closely resemble assemblages in a conveyance canal shows just how impaired conditions in the upper Jordan River are.

Recommendations

Based on this report and our past and continuing extensive research on the Jordan River and other rivers throughout the western USA, we recommend the following:

1. Continued collection of macroinvertebrate samples from the upper Jordan River, starting in spring 2019. Conduct formal traits analyses related to water quality. Use this information to inform and direct water quality standards.
2. Continued compilation and ecological analyses of macroinvertebrate data from the upper Jordan River focusing on ecosystem function, food web, and water quality. Use this information to inform and direct water quality standards.
3. Conduct life history and ecological studies on the two analog invasive mollusk species in the river, *Potamopyrgus antipodarum* and *Corbicula fluminea*. Focus studies on their effects on nutrient spiraling and water quality. Use this information to inform and direct water quality standards.
4. Conduct DNA sequencing of the two newly identified species in the river, *Capitella capitata* and *Baetis adonis.* Conduct research on their life histories and water quality requirements.

Acknowledgements

We sincerely appreciate the dedicated work of the Wasatch Front Water Quality field technicians, Frank Fluckiger and W. D. Robinson. We also sincerely appreciate the continued financial support of the WFWQC, without whom so very little would be known about the Jordan River ecosystem and its water quality.

Literature Cited

Jackson, J.K., A.D. Huryn, D.L. Strayers, D. L. Courtemanch, and B.W. Sweeney. 2005. Atlantic coast rivers of the northeastern United States. In Benke, A.C. and C.E. Cushing eds.: Rivers of North America. Elsevier Inc.

Kerans, B., M.F. Dybdahl, M.M. Gangloff, and J. Jannot. 2005 Potamopyrgus antipodarum: Distribution, density, and effects on native macroinvertebrate assemblages in the Greater Yellowstone Ecosystem. Journal of North American Benthological Society. 24(1): 123-138.

McCune, B. and M. J. Mefford. 2018. PC-ORD. Multivariate Analysis of Ecological Data. Version 7.07. Wild Blueberry Media, Corvallis, Oregon, U.S.A.

Monaghan, K. A. 2016. Four Reasons to Question the Accuracy of a Biotic Index; the Risk of Metric Bias and the Scope to Improve Accuracy. PLoS ONE 11(7): e0158383. doi:10.1371/journal. pone.0158383

Richards, D. C. 2004. Competition between the threatened Bliss Rapids Snail, *Taylorconcha serpenticola* (Hershler et al.) and the invasive aquatic snail, *Potamopyrgus antipodarum* (Gray). Ph.D. dissertation. Department of Ecology, Montana State University, Bozeman, MT. 177 pp.

Richards, D.C. 2018a. Jordan River macroinvertebrate assemblages: preliminary findings. Draft Report to Wasatch Front Water Quality Council. Salt Lake City, UT. OreoHelix Consulting. Vineyard, UT.

2018b. A snail, a clam, and the River Jordan: A revealing novel. Version 1.5. Technical Report Submitted to The Wasatch Front Water Quality Council. OreoHelix Consulting, Vineyard, UT.

2018c. The Jordan River: How to regulate an analog ecosystem. Scientific presentation at the Twelve Annual Salt Lake County Watershed Symposium, Salt Lake City, UT.

StataCorp 2018. Stata/IC 15.1 for Mac (64-bit Intel). Revision 17Dec2018. College Station, TX

Appendices

Appendix 32. Descriptive statistics for benthic macroinvertebrates from upper Jordan River, November 2018. S = taxa richness; E = evenness; H = Shannon diversity; D = Simpson diversity. Habitat: 1 = riffle; 2 = pool; 3 = run. Substrate: 1 = silt/sand/gravel; 2 = sand/gravel/large gravel; 3 = cobble.

Site	Density m^{-2}	Dominant Taxon Density m^{-2}	S	E	H	D	Habitat	Substrate	Depth (cm)	% Embedded	% Dominant
BB-1	420	198	17	0.61	1.73	0.72	1	1	11	90	0.47
BB-2	518	188	12	0.7	1.74	0.77	1	1	18	90	0.36
BB-3	86	32	9	0.79	1.74	0.77	2	2	65	60	0.37
BB-4	348	192	18	0.63	1.81	0.68	2	1	63	95	0.55
BB-5	6156	3774	19	0.45	1.32	0.58	1	3	40	50	0.61
JR-1a	25142	17834	17	0.41	1.17	0.48	1	3	35	50	0.71
JR-1b	8840	2764	23	0.63	1.97	0.8	1	3	16	0	0.31
JR-2	2270	466	31	0.73	2.52	0.88	3	3	18	10	0.21
JR-7a	606	84	24	0.86	2.72	0.92	3	1	23	90	0.14
JR-7b	268	134	13	0.67	1.72	0.71	3	1	60	90	0.5
JR-8	504	282	18	0.59	1.71	0.66	3	1	30	100	0.56
JR-9	316	78	22	0.77	2.38	0.87	3	1	53	90	0.25

JR-10	4652	2012	23	0.68	2.14	0.78	1	3	17	70	0.43
JR-11a	504	144	17	0.71	2	0.81	3	1	30	90	0.29
JR-11b	3452	1710	25	0.59	1.9	0.72	1	3	30	90	0.5

Appendix 33.

MEASURES OF FIT

R^2n (nonmetric fit) = 0.9942 Intrinsic measure for NMS. Null: all points co-located.

R^2l (linear fit) = 0.9826 Null: all ordination distances equal.

R^2m (metric fit) = 0.8462 Null: no linear relationship with observed dissimilarities.

CHANCE-CORRECTED EVALUATIONS

Improvement: I = 0.8600

Null model: final configuration no better than initial random configuration.

Interpretation: 0 = random expectation, 1 = perfect fit, <0 = worse than random expectation

Basis: 1 dimension

250 = number of random initial configurations used

54.6090 = average initial stress

7.6477 = final stress

Association: A = 0.7842

Null model: relationships among columns no stronger than expected chance, based on shuffling within columns.

Interpretation: 0 = random expectation, 1 = perfect fit, <0 = worse than random expectation

Basis: 1 dimension

500 = number of randomizations used

```
35.4453 = average final stress from randomizations

 7.6477 = final stress
```

Appendix 34. NMS ordination by site.

JR-BB-01	-0.56511
JR-BB-02	-0.43132
JR-BB-03	-1.56685
JR-BB-04	-0.70008
JR-BB-05	1.19128
JR-01a	2.02286
JR-01b	1.3155
JR-02	0.42955
JR-07a	-0.31924
JR-07b	-1.14211
JR-08	-0.49604
JR-09	-0.79631
JR-10	0.91306
JR-11a	-0.63211
JR-11b	0.77694

Appendix 35. NMS ordination by taxon.

Triclad	1.30755

Nemert	0.53014
Nematoda	1.15799
Oligoch	0.91532
Heloblst	0.18107
Erpobdella	0.32125
Capcap	0.62801
Potamopyrgus	1.63575
Physa	0.42532
Pisidium	1.39239
Corbicula	0.14133
Acari	0.4084
Daphnia (eph	-0.11831
Gammarus	0.51053
Caecidotea	1.63087
Baetissp.	0.4571
Baetisadonis	1.45834
Fallceon qui	0.87919
Tricorythode	0.48661
Argia sp.	0.86193
Petrophila s	0.99046
Hydroptila s	0.9282
Hydropsyche	1.08562
Microcylloep	0.84034
Stenelmis sp	1.55199
Chironpupa	0.48101

Tanypodinae	0.64711
Orthocladiin	0.70807
Chironomini	0.64655
Bezzia/Palpo	0.97364
Probezzia sp	0.85273
Simulium sp.	1.39032
Hemerodromia	1.22649

Chapter 12

A Snail, a Clam, and the River Jordan: *A Revealing Novel*

The river Rhine, it is well known,

Doth wash your city of Cologne;

But tell me, Nymphs, what power divine

Shall henceforth wash the river Rhine?

Samuel Taylor Coleridge 1772-1834

Cover photos:

Asian clam: http://www.corpi.ku.lt/databases/index.php/aquanis/species/view/id/1018

New Zealand mud snail: Dr. Dan Gustafson, Montana State University.

Technical Report

Submitted to The Wasatch Front Water Quality Council

By David C. Richards, Ph.D., OreoHelix Ecological

March 1, 2018

Ancient Chinese Fortune Cookie Proverb: *Unexpected good luck sometimes comes in small packages that are often hard to see unless you are willing to open your eyes.*

Summary

For better or worse, the invasive 'good luck' clam, *Corbicula fluminea* and New Zealand mudsnail, *Potamopyrgus antipodarum* are well established in the Jordan River, UT. Both the snail and the clam reach some of the highest densities recorded (>>5000 m^{-2} for *Corbicula*; 250,000 to 500,000 m^{-2} for *Potamopyrgus*). Based on literature review presented in this report and recent mollusk surveys conducted in the Jordan River by OreoHelix Consulting and the Wasatch Front Water Quality Council; it is now apparent that the filter-feeder/pedal- feeder *Corbicula* and the grazer, *Potamopyrgus* dominate ecosystem functions in the Jordan River. *Corbicula* can filter out the entire water column FPOM (including algae, bacteria, nutrients) in the Jordan River in about a day in locations where its densities are high, as it does in many rivers. *Corbicula* filtration rates can range from about 0.4 to 3.0 cubic meters of water m^{-2} hr^{-1}, depending on temperatures. It has also been suggested that *Corbicula* can decrease the likelihood of cyanoHABS and increase water clarity that promote reestablishment of native aquatic vegetation. On good days, *Corbicula*'s organic matter consumption rates in the Jordan River can be from 0.33 to 6.2 metric tons km^{-1} day^{-1}. The 'good luck' clam is also likely responsible for among other things: enhancing nutrient cycling, reducing turbidity, increasing light penetration, and reducing phytoplankton abundance; all of which are improvements in the degraded Jordan River's water quality. However, these benefits performed free of monetary expenditure come with some ecological and water quality costs, primarily dissolved oxygen consumption and ammonia respiration. *Corbicula* O_2 consumption rates can range from 1 to 16 mg m^{-2} hr^{-1} and CO_2 respiration rates range from 1 to 14 mg m^{-2} hr^{-1}. *Corbicula*'s consumption rates of nitrogen and phosphorus in the Jordan River range between 0.75 to 2.12 mg m^{-2} day^{-1} N and 0.27 to 0.95 mg m^{-2} day^{-1} P. Excretion rates were calculated to be from 75 to 1,426 μmol m^{-2} day^{-1} NH_4 and from 15 to 286 μmol m^{-2} day^{-1} P in the river. As with all mollusks, *Corbicula* contributes to the reduction of the greenhouse gas CO_2 in the production of $CaCO_3$ based shells. It is quite feasible that *Corbicula* sequesters ≈ 10 metric tons C km^{-1} $year^{-1}$ in sections of the Jordan River, via shell production.

The New Zealand mudsnail, *Potamopyrgus* can have production rates ≈ 1500 mg AFDM m^{-2} day^{-1}; excretion rates ≈ 8 mg N m^{-2} day^{-1}; and egestion rates ≈ 200 mg N m^{-2} day^{-1} in the Jordan River. Although much is still to be learned about its role in the Jordan River, it likely has similar rates as *Corbicula* but on a smaller scale.

Corbicula and *Potamopyrgus* are undoubtedly the most important and dominant biota in the now **novel** Jordan River ecosystem and together co-regulate seasonal nitrogen, phosphorus, and carbon cycling, microbial community structure, and stream metabolism. The snail and clam are almost certainly seasonally controlling most other ecosystem functions as well, (e.g. water quality), despite their roles being unnoticed to most researchers and managers.

Table of Contents

Introduction

Over the millennia, physical and chemical conditions in the Jordan River, Utah drainage have created a freshwater mollusk hotspot in an otherwise depauperate western United States, providing ideal habitat for mussels, clams, and snails, including the globally invasive Asian clam[4], *Corbicula fluminea* and New Zealand mudsnail, *Potamopyrgus antipodarum* (Richards 2017a; 2017b). *Corbicula fluminea* densities and biomass in the now highly regulated and degraded Jordan River[5], UT often occur at greater levels than have been reported elsewhere in the world (Richards 2017a, Richards 2017b, Phelps 1994; Karatayev et al. 2003; Ilarri et al. 2011; Beaver et al. 1991). This species of clam often reaches densities >> 5000/m^{-2} in several sections of the Jordan River, particularly downstream of its confluence with Mill Creek (Richards 2017a, Richards 2017b). Invasive New Zealand mudsnails, *Potamopyrgus antipodarum* are extremely abundant throughout the Jordan River and have been estimated to exceed densities >>250,000 m^{-2}, particularly in upstream sections (Richards personal observation).

When bivalves (mussels and clams) such as *Corbicula*[6] or snails such as *Potamopyrgus*[7] reach high enough densities and biomass, they transition into ecosystem engineers and keystone species (Prins and Escaravage 2005). They then control and oft times transform most ecological functions by:

- altering water quality;
- enhancing nutrient cycling;
- reducing turbidity and increase light penetration;
- reducing phytoplankton abundance
- regulating bacteria and fungi assemblages;
- controlling key processes such as oxidation of organic matter; and
- altering N:P ratios, nutrient chemistry, sediment oxygen demand (SOD), and; biological oxygen demand (BOD)(see following sections for citations).

Thus, their dominance in an aquatic ecosystem is considered by ecologists and managers to be a double-edged sword; on one side, ecosystem altering invasive species that may cause certain types of water quality degradation; on the other side, naturalized resident species such as

[4] *Corbicula* is known as the 'good luck clam' in many parts of Asia.
[5] The Jordan River, UT was named after the Biblical 'River Jordan' in the Mideast.
[6] The species of *Corbicula* found in the Jordan River is *Corbicula fluminea* but in this report will be referred to as *Corbicula*.

[7] The New Zealand mudsnail found in the Jordan River is *Potamopyrgus antipodarum* but in this report will simply be referred to as *Potamopyrgus*.

Corbicula and *Potamopyrgus*, that replace inefficient natives and that may vastly improve overall water quality, depending on conditions, and doing so with zero monetary expenditures by citizens.

The effects of *Corbicula* and *Potamopyrgus* on ecosystem processes are well known throughout the world. It is also known that these clams and snails have occupied most sections of the Jordan River at unbelievably high densities/biomass for well over a decade, undoubtedly having huge ecological and water quality effects. However, *Corbicula* and *Potamopyrgus* and their role in the ecological functioning of the Jordan River continues to be ignored and their effects are all but invisible to most Jordan River researchers and managers, despite this knowledge. Jordan River managers and scientists studying the effects of nutrient loads on water quality and ecosystem processes in the river always seem to come up short explaining inconsistencies in data interpretation, typically resulting in conclusions that are mostly vague, unsatisfactory, incomplete, and on occasion, wrong (e.g. Follstad Shah et al. 2017; others). The most likely explanation for these incorrect assessments is the failure to include the effects of *Corbicula* and *Potamopyrgus*.

Justification

Researchers and managers have been blind to the very large effects that the ecosystem engineers, *Corbicula* and *Potamopyrgus* are having on nutrient cycling, water quality, and ecosystem functions in the Jordan River. This has often resulted in misinformed and erroneous conclusions, and likely misdirected management decisions. This technical report describes known effects of *Corbicula* and other bivalves (used as surrogates for *Corbicula*) and *Potamopyrgus* on ecological processes and water quality in waters outside of Utah based on literature review. This knowledge is then applied to the most recent and only intensive surveys of *Corbicula* distribution and abundance in the Jordan River, as reported by Richards (2017a; 2017b) and the Wasatch Front Water Quality Council and by personal observations by Richards while conducting ecological studies, including mollusk surveys on the Jordan River. The review and analyses validates the large effect that *Corbicula* and *Potamopyrgus* are having on the river's nutrient cycle, water quality, and ecosystem function and will guide scientists and managers to a better understanding of the river and their ability to manage the river accordingly.

Report Sections

This report is presented in several sections. The first section of the review focuses on *Corbicula*'s water column filter feeding ecology and its ecosystem effects. The second section of the review focuses on the clam's pedal feeding ecology and its ecosystem effects. The third section focuses on *Potamopyrgus* ecology and ecosystem effects and the fourth section applies what was learned in the first three sections to *Corbicula* and *Potamopyrgus* populations in the Jordan River. This fourth section on effects of *Corbicula* in the Jordan River is primarily focused on portions of the mid-Jordan River downstream of its confluence with Mill Creek to about 900

South. This portion of the river contained the highest *Corbicula* densities found by Richards 2017a and 2017b and members of the Wasatch Front Water Quality Council, and is likely where *Corbicula* has the most influence. The fourth section addressing the effects of *Potamopyrgus* on the Jordan River ecosystem focuses more on sections upstream of its confluence with Mill Creek, where its known densities are highest.

Review of *Corbicula* Ecology and Ecosystem Effects

Corbicula, a keystone species, ecosystem engineer is well known to alter food web structure, often times shifting the structure towards a microbial based food web (Prins and Escaravage 2005). *Corbicula* are self-fertilizing, simultaneous hermaphrodites and release up to 2,000 juveniles per day, and more than 100,000 in a lifetime. Juveniles are ≈1 mm in length and take from one to four years to reach maturity and reach a length of about 5 cm. Table 1 is a summary of *Corbicula* life history characteristics.

Table 49. Summary of some *Corbicula* life history characteristics. From Sousa et al. 2008 Table 1 (and adapted from McMahon 2002).

Life history characteristics	*C. fluminea*
Life span	1 to 5 years
Age at maturity	3 to 9 months
Reproductive mode	Hermaphroditic
Growth rate	Rapid
Fecundity	68 678
Juvenile size release	250 µm
Position of broods	Inner demibranchs
Type of released larvae (juveniles)	D-shaped configuration
Type of brooding	Synchronous
Juvenile survivorship	Low
Adult survivorship	Usually low
Number of reproductive events	Usually two but may vary
Assimilated energy respired	11 - 42 %
Non-respired energy transferred to growth	58 - 71 %
Non-respired energy transferred to reproduction	5 - 15 %
Turnover time	73 - 91 days
Habitat requirements	Intolerant to high salinity values and even moderate hypoxia conditions (this species is usually restricted to well-oxygenated areas). Tolerate low water temperatures and prefer sandier sediments mixed with silt and clay (which enhance the organic matter content). However, in some ecosystems this species can be found in all types of sediments (with or without submerged vegetation) (Sousa et al. 2008)

Corbicula filter large amounts of water and thus process large amounts of suspended materials (FPOM) and nutrients, which are used by the clams for growth and reproduction or excreted in

dissolved form or deposited as feces or pseudofeces[8] (Ostroumov 2005; Cohen et al. 1984; Beaver et al. 1991; Arnott and Vanni 1996; Newell et al. 2005). As a result, *Corbicula* enhances nutrient cycling (Lauritsen and Mozley 1989, Cohen et al. 1984; Boltovskoy et al. 1995). Not only does *Corbicula* alter water column processes, it also alters benthic/sediment processes. This is because *Corbicula* has two distinct feeding mechanisms: 1) filtering- feeding water column particulate organic matter (POM) (Lauritsen 1986a; Leff et al. 1990; Boltovsky et al. 1995) and, 2) pedal feeding sediment organic matter (OM) using cilia on their foot to collect subsurface organic matter (Cleland 1988; Reid et al. 1992, Hakenkamp and Palmer 1999).

Corbicula can influence nutrient fluxes through one of five main pathways:

1. regeneration of dissolved nutrients directly into the water column;
2. sequestration of nutrients bound up in tissue and shell;
3. burial of particulate in sediments;
4. regeneration of dissolved nutrients from sediments; or,
5. denitrification from sediments (Konrad 2013).

Water Column Filter-feeding

Corbicula often dominate the benthic invertebrate community both numerically and in terms of biomass (Lauritsen and Mozley 1989; Poff et al. 1993). *Corbicula* perform both the function of removing particles from the water column and regulating other biota involved in water purification, including algae, bacteria, and fungi in the sediments (Ostroumov 2002a; Newell 1988; Newell & Ott 1998). They thus control the key process of oxidation of organic matter in an aquatic system when clams occur at high densities, particularly the major oxidizer, bacteria, (Wetzel 2001; Sorokin et al. 1997; Ostroumov 2005). *Corbicula* can directly reduce the amount of particulate organic matter (POM) available to be remineralized by pelagic consumers and bacterioplankton (Cloern 1982; Officer et al. 1982; Newell et al. 2005). *Corbicula* also actively select particles to digest or reject as pseudofeces as illustrated in Figure 65.

[8] *Pseudofeces are mucous-enveloped, partially or undigested filtered POM.*

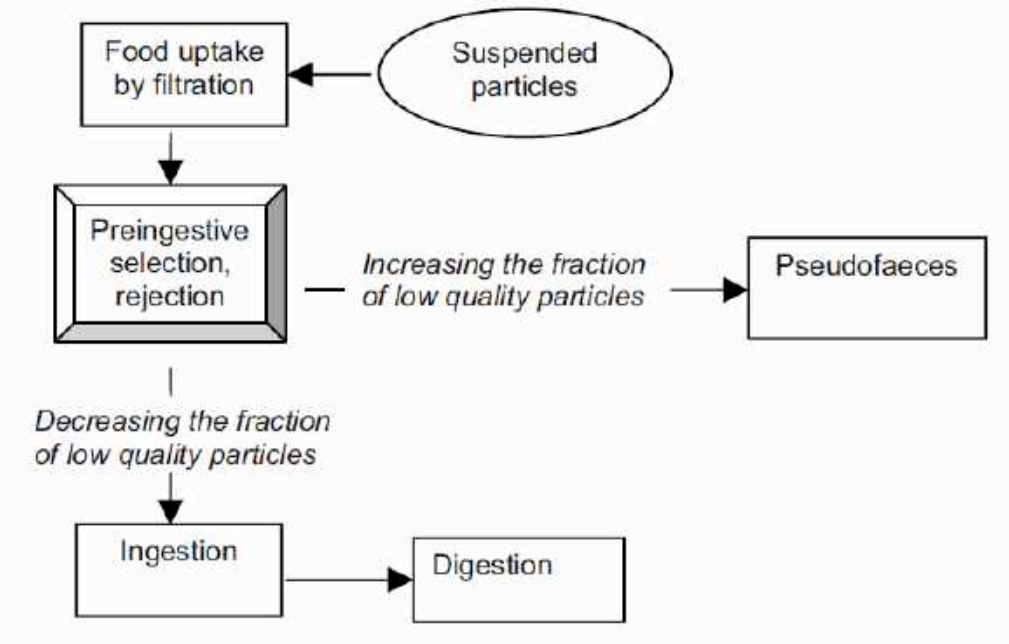

Figure 65. A conceptual model of food processing by *Corbicula* actively filter feeding and particle selecting for rejection as pseudofeces or digestion (from Dame and Olenin (2005)).

Filtration Rates

Bivalves are world renowned for the ability to filter large volumes of water (Table 50) and *Corbicula* filtration rates are some of the highest recorded for filter feeders (Cohen et al. 1984; Beaver et al. 1991; Lauritsen 1986) (Table 51; Table 52).

Table 50. Estimates of filter feeder clearance times (number of days for water column to be filtered). Note: Only 4 of the taxa in table are non- bivalves. From Ostroumov (2005).

System	Organism	% vol	Time (d)	References; comments
Lake Baikal, Russia	*Baikalospongia bacillifera*, *B. intermeda*, *Lubomirskia baikalensis*	100	1.2	Savarese et al., 1997; littoral zone, 12-m depth
Lake Punnus-jarvi, Russia	Zooplankton (various)	100	3	Andronikova (1976, 1978) – cit. in Gutelmaher (1986)
Lake Tuakitoto, New Zealand	*Hyridella menziesi* (bivalve)	100	1.4	Ogilvie and Mitchell, (1995)
Sphagnum bog-pond; Wisconsin, USA	*Spongilla lacustris* (sponge)	130	1	Frost (1978); areas of high biomass 31.8 g m^{-2}
Laholm Bay in the Kattegat, Denmark	*Cardium edule*, *Mya arenaria*	50-100	3	Loo and Rosenberg (1989); area 60 km^2
Northern San Francisco Bay, USA	*M. arenaria*	100	ca. 1	Nichols (1985)
South San Francisco Bay, USA	*Potamocorbula amurensis*	100	0.6	Cloern (1982); water volume $2500 \cdot 10^6$ m^3
North Inlet (South Carolina, USA)	*Crassostrea virginica*	100	0.8-6.1	Dame et al. (1980); volume $22 \cdot 10^6$ m^3
Carlingford Lough, Ireland	*C. gigas*, *Tapes semidiscussata*, *Mytilus edulis*	100	87.5	Ball et al. (1997); cit. in Dame et al. (2001); volume of water $196 \cdot 10^6$ m^3
Narragansett Bay (Rhode Island, USA)	*Mercenaria mercenaria*	100	32.1	Pilson (1985); volume of water $2724 \cdot 10^6$ m^3
Oosterschelde, The Netherlands	*Mytilus edulis*, *Cerastoderma edule*	100	3.7	Smaal et al. (1986); volume of water $2740 \cdot 10^6$ m^3
Western Wadden	*M. edulis*, *C. edule*	100	5.8	Dame et al. (1991a); Van

Sea, The Netherlands				Stralen (1995); cit. in Dame et al. (2001); volume of water $4020 \cdot 10^6$ m^3
Ria de Arosa, Spain	*M. edulis*	100	12.4	Tenore et al.(1982); cit. in Dame et al. (2001); volume of water $4335 \cdot 10^6$ m^3
Chesapeake Bay, USA	*C. virginica*	100	87.5	Newell (1988) ; volume27 $300 \cdot 10^6$ m^3
Marina da Gama	several species	100	1.1	Davies et al. (1989) volume $0.025 \cdot 10^6$ m^3
Kertinge Nor, Denmark	*Ciona intestinalis* (ascidian)	100	0.8-5	Petersen and Riisgård (1992) ; volume $11\ 000 \cdot 10^6$ m^3
Bay of Brest, France	multiple species	100	2.8-6	Hily (1991); volume $1480 \cdot 10^6$ m^3
Marennes-Oléron, France	*C. gigas, M. edulis*	100	2.9	Héral et al. (1988); Bacher (1989) - cit. in Dame et al. (2001); volume $675 \cdot 10^6$ m^3
Königshafen, Germany	*M. edulis, C. gigas*	100	0.9-2.8	Asmus and Asmus (1991); volume $7.2 \cdot 10^6$ m^3

Table 51. Filtration rates *Corbicula* fluminea clearance time (amount of days for the water column to be filtered) from Karatayev et al. (2005)

Water body	Days	Source
Potamac River, USA	3-4	Cohen et al. 1984
Upper Chowan River, USA	1-1.5	Lauritsen 1986
Meyers Branch Stream, USA	1	Leff et al. 1990
Clear Fork of the Trinity River, USA	0.01	McMachon and Bogan 2001

Table 52. *Corbicula* filtration rates (from Lauritsen (1986) Table 1).

	Algal Volume (mm^3/L)				
	0.33	0.67	1.33	2.00	2.67
Mean filtration rate (ml/hr)	782.3	656.5	489.0	420.2[a]	277.8
1 SE	69.6	55.5	53.6		82.5
Mean volume ingested (mm^3)	0.23	0.41	0.64		0.80
1 SE	0.01	0.03	0.06		0.07

A clearance rate model developed by Fulford et al. (2007) predicted that at historic oyster biomass levels oysters would be able to filter the entire volume of Chesapeake Bay in about 27 d (annual average), and in about 9 d at peak summer clearance rates. This is consistent with previous estimates of water filtration by oysters reported by Newell (1988) but likely much less than would occur from the better filter-feeder, *Corbicula*. Cohen et al. (1984) showed that *Corbicula* at moderate densities (≈1400 m^{-2}) compared to mid-Jordan River densities (section: *Corbicula* and *Potamopyrgus* in the Jordan River) were able to filter the entire volume of water in a reach of the Potomac River (3.0 x 10^7 m^3) in 3 to 4 days or an estimated 8.9 x 10^6 m^3 day^{-1}. Cohen et al. (1984) also showed that on average, one *Corbicula* was able to remove 30% of phytoplankton chlorophyll *a* from a 2 -L river water sample in 2 hours. Beaver et al. (1991) reported that *Corbicula* filtrations rates in a hypereutrophic lake were approximately 0.5 to 0.7 L hr^{-1} $clam^{-1}$ and at moderate densities (1310 to 2621 m^{-2}) reduced chlorophyll *a* concentrations > 60% in 7 days.

Particle Size Ingestion

Corbicula typically have a lower ingestion size limit of < 1 µm and upper size limit of about 20 µm for filtered POM (McMahon and Bogan 2001; Way et al. 1990) but can consume algae with a spherical diameter from 50 µm up to 170 µm (Boltovskoy et al. 1995). However, larger sized POM or higher concentrations of POM favor the production of pseudofeces and/or reduced filtration rates (Beaver et al. 1991; Lauritsen 1986; Way et al. 1990). Because of this particle ingestion size range, they can effectively remove a large majority of or even completely deplete detritus, bacteria and algae from the water column when they occur at high densities/biomass (Mikheev 1994, McMahon 1999, Boltovskoy et al. 1995; Cloern, 1982 Fréchette and Bourget 1985; Dame and Olenin 2005). Consequently, *Corbicula* play a key role in the stability of aquatic ecosystems (Herman and Scholten 1990; Kotta et al 2005; Dame and Olenin 2005). *Corbicula* has been shown to initiate pseudofeces production at 17 to 20 mg l^{-1} TSS (Fuji 1979, Hornbach et al. 1984, Way et al. 1990; Appendix 37). See Appendix 37 for a detailed description of the effects of inorganic suspended matter on bivalves, including *Corbicula* and native mussels in the Jordan River.

Filter-feeding Selectivity

Corbicula is considered to be mostly a non-selective, filter-feeder (Lauritsen 1986; Way et al. 1990; Beaver et al. 1991). Several feeding studies have suggested that *Corbicula* grow equally well on green algae and diatoms and assimilation and net production efficiencies of *Corbicula* fed the cyanobacteria, *Anabaena oscillaroides* were not significantly different than those fed chlorophytes (Lauritsen 1986; Beaver et al. 1991). The Lauritsen (1986) study found that the lowest filtration rates and the highest assimilation efficiencies were with another cyanobacteria, *Anabaena flos-aquae*. *Corbicula* are even thought to have reduced the severity of cyanoHABs in the Potomac River (Phelps 1994).

Nutrient Ingestion and Excretion

Corbicula can digest and assimilate N from different sources of POM with efficiencies from ≈20 to 90% (Newell et al. 2005). Some nitrogen and phosphorus regeneration is a direct result of *Corbicula* excretion from filter feeding on phytoplankton (Newell et al. 2005). High densities of *Corbicula* in eutrophic systems are completely capable of reducing water column phosphorus (TP) levels (Beaver et al. 1991). Boltovskoy et al. suggested that *Corbicula* needed roughly 66 to 673 mg C m^{-2} h^{-1} (mean: 289) for respiration only and that phytoplankton ingestion alone may only supply 2 to 51% of organic matter C required for respiration.

Nutrients excreted into the water column by *Corbicula* in dissolved inorganic form may be readily available to phytoplankton and periphyton (Arnott and Vanni 1996; Hakenkamp and Palmer 1999). Nitrogen excretion (g^{-1} dry weight) is size dependent; smaller bivalves excrete less than larger bivalves however, smaller bivalves may excrete more P per gram dry weight than larger bivalves (Arnott and Vanni 1996; Hakenkamp and Palmer 1999). Thus small clams relative to medium or large clams can excrete at significantly lower N:P ratios, however, excreted N:P in all size classes can often be lower than that which occurs in the water column and may shift phytoplankton towards N limitation (Arnott and Vanni 1996). This can have direct effects on species-specific phytoplankton growth rates, which may allow cyanobacteria to outcompete algal phytoplankton. However, *Corbicula* filter feed both cyanobacteria and algae and net effects need to be calculated.

Newell et al. (2005) reported <u>average ammonium excretion rates of</u> *Corbicula*:

$$\cong 6.0\ \mu mol\ NH_4^{+}\ g^{-1}\ DW\ h^{-1}\ (DW = dry\ tissue\ weight)$$

and <u>average phosphorus excretion rates</u>

$$\cong 1.2\ \mu mol\ P\ g^{-1}\ DW\ h^{-1}\ (DW = dry\ tissue\ weight)$$

Lauritsen and Mozley (1989) reported NH_3 excretion rates between 357 and 8642 μmol m^{-2} day^{-1} and PO_4 (orthophosphate) rates between 161 and 3924 μmol m^{-2} day^{-1} in a coastal plain river in Virginia-North Carolina. They estimated that an average size clam of 20 mg DFW would excrete 2.06 μmol NH_3 hr^{-1} in summer and 0.95 μmol NH_3 hr^{-1} in winter and 0.36 μmol PO_4 hr^{-1} in summer and 0.02 μmol PO_4 hr^{-1} in winter. Thus, P recycling by *Corbicula* can be greater than all other sources including; zooplankton, point sources, tributary loading, atmospheric inputs, sediments, and macrophytes (Arnott and Vanni 1996).

Konrad (2013) discussed approaches for evaluating the effects of bivalve filter feeding on nutrient dynamics. A summary of these is provided in Appendix 36.

O_2 consumption and CO_2 respiration

Hokenkamp and Palmer 1999 reported that *Corbicula* consumes high rates of O_2 and respires high rates of CO_2, which contributes strongly to total metabolism in streambeds and significant utilization of OM resources. However, the benefit of *Corbicula* on reducing hypoxia depends on a reduction in the flux of organic detritus to benthic sediments that creates biochemical oxygen demand (BOD) through heterotrophic respiration and decomposition of organic material (Konrad 2013). With respect to carbon dynamics, *Corbicula* may be the single most important species in a stream.

Boltovskoy et al. (1995) estimated *Corbicula* densities between 450 and 4500 m^{-2} (mean 2000 m^{-2}) and 66 to 673 mg C m^{-2} h^{-1} (mean: 289 mg C m^{-2} h^{-1}) required for respiration only, which translates to approximately 16 to 162 (mean 69) g C m^{-2} day^{-1}. These densities were similar to those found by Richards 2017a in the Jordan River.

Turbidity

Filter feeding by *Corbicula* also reduces turbidity, increases water clarity, and thereby increases nutrient mineralization rates and light availablity to microphytobenthos and SAV (Buttner 1986; Lauritsen and Mozley 1989; Phelps 1994; Newell et al. 2005; Buttner 1986; Lauritsen and Mozley 1989; Phelps 1994; Beaver et al. 1991; Newell 2004; Newell & Koch 2004). Phelps (1994) suggested that it was *Corbicula* filter feeding at high clearance rates that reduced turbidity, increased light availability to bottom sections of the Potomac River, and allowed aquatic vegetation to reestablish.

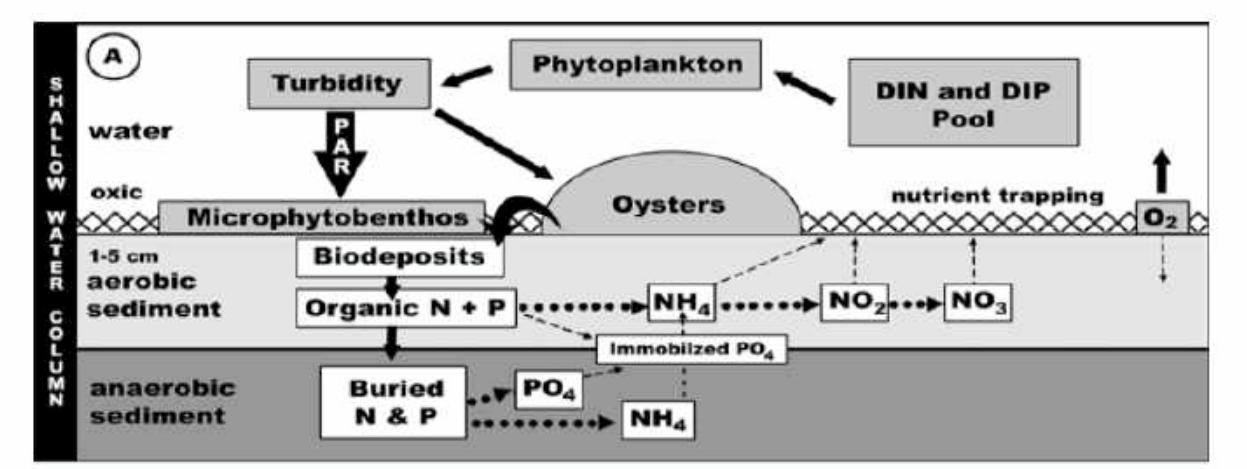

Figure 66. An additional conceptualization of bivalves (oysters) on nutrient cycling (from Newell et al. 2005). The Jordan River is a shallow, often eutrophic water body and this figure is a good representation by replacing 'oysters' with *Corbicula* in the illustration.

Sediments and Biodeposition

Most researchers focus on nutrient regeneration of bivalve filter-feeding, however one of the more important effects of bivalve feeding is the repackaging of small seston particles into large aggregates of feces and pseudofeces, known as biodeposition (Newell et al. 2005; more). Particles in bivalve feces are tightly bound in a mucoid matrix and voided as pelleted strings that can be as long as several millimeters (Kautsky and Evans 1987, Widdows et al. 1998; Newell et al. 2005). Feces and pseudofeces sinking velocities can be up to 40 times faster than that of non-aggregated particles, although pseudofeces are less tightly bound in mucus than feces and may disaggregate when voided (Kautsky and Evans 1987, Widdows et al. 1998; Newell et al. 2005). Table 5 displays the enormous amount of biodeposits and bio-sediment formation rates that bivalves are capable of. Table 6. shows how a bivalve (oyster) was seasonally capable of removing up to several metric tons (5%) of N inputs and more than a ton (35%) of P inputs to a watershed per month (based on oysters at 1 g dry weight m^{-2}). *Corbicula* is assumed to be a much more efficient filterer than most oysters and can occur in the Jordan River up to 9.9 g dry weight m^{-2}, which suggests it could be removing N and P at much greater rates than shown in Table 6.

Table 53. Biosediments formation by suspension-feeders. From Ostroumov 2005.

System	Organisms	Amount	Comments	References
Laholm Bay	*Cardium edule*	N: 199 t y^{-1} C: 1449 t y^{-1}	per 60 km^2; 0-10 m depth	Loo and Rosenberg (1989)
	M. arenaria	N: 36 t·y^{-1} C: 262 t·y^{-1}		
	C. edule + *M. arenaria*	N: 235 t y^{-1} C: 1711 t·y^{-1} C: 29 g·m^{-2} y^{-1}		
Rocky shores	*Mytilus edulis*	11.9 kg ·m^{-2} y^{-1} (dry weight),	of 11.9 kg, faeces 9.2 kg, pseudofaeces 2.7	Tsuchiya (1980)
Norwegian-Greenland Sea, depth 2020-2630 m	sponge *Thenea abyssorum*, biomass up to 1524 mg AFDW m^{-2}	0.6-2.2 mg C·m^{-2} ·d^{-1}	The poriferan community possibly adds up to 10% to the vertical particle flux	Witte et al. (1997)
	T. abyssorum	up to 0.7 g C m^{-2} y^{-1}	-	author's estimate based on the data (Witte et al. 1997)
Baltic coastal ecosystem	M. edulis	1092 g ·m^{-2} y^{-1} dry weight, including C 80.7 g ·m^{-2} ·y^{-1} N 10.4 g. m^{-2} .y^{-1} P 1.6 g .m^{-2} .y^{-1}	Total sedimentation (total amount of all types of sedimenting material) was 3521 g ·m^{-2} ·y^{-1} dry weight	Kautsky and Evans, 1987;
Marine/ estuarine	*M. edulis*	60 g ·m^{-2} ·h^{-1}	-	Widdows et al., 1998
NETHERLANDS	bivalves	25 g ·m^{-2} ·h^{-1}	-	Smaal et al. 1986
Marine/ estuarine	M. chilensis	18 g·m^{-2} ·h^{-1}	-	Jaramillo et al., 1992; cit. in Ostroumov et al., 2001

Table 54. Newell et al. 2005: Total monthly N and P (kg) inputs and removal by oysters in an estuary. Note: This table was based on oysters but exemplifies the contribution bivalves (such as *Corbicula)* have

on nutrient removal. Also note that the nutrient removal values are for 1 bivalve (Oyster) = 1.0 g DW. *Corbicula* in the Jordan River range from mean = 1.1 g DW m^{-2} up to 9.9 g DW m^{-2} (see section: *Corbicula* and *Potamopyrgus* in the Jordan River).

	Total-N inputs (kg)	Total-P inputs (kg)	Monthly nutrient removal for oysters at a density of 1 m^{-2} on 1,736 ha oyster bottom			
			N (kg)	P (kg)	% N inputs	% P inputs
Jan	281,450	5,245	0	0	0.0	0.0
Feb	261,970	4,837	0	0	0.0	0.0
Mar	312,350	5,351	106	38	0.0	0.7
Apr	292,500	5,338	226	82	0.1	1.5
May	243,930	6,022	552	200	0.2	3.3
Jun	148,250	4,641	1,207	436	0.8	9.4
Jul	75,480	4,059	3,887	1,405	5.1	34.6
Aug	80,810	4,274	4,038	1,460	5.0	34.2
Sep	99,140	4,587	2,331	843	2.4	18.4
Oct	97,940	4,015	449	162	0.5	4.0
Nov	114,500	4,344	218	79	0.2	1.8
Dec	254,270	6,373	66	24	0.0	0.4
Total	2,262,580	59,085	13,080	4,728	0.6	8.0

Corbicula biodeposits have been shown to contain ≈ 2 to 3 times as much C, N, and P per unit weight as particles settling-out naturally from the water column (Newell et al. 2005)(Table 55).

Table 55. Example of Bivalve (oyster) Carbon, nitrogen, and phosphorus biodeposits vs. seston (From Newell et al. 2005, Table 1).

	Biodeposits	Seston Material
Carbon (mg C g^{-1})	34.8 ± 3.15	14.6 ± 1.19
Nitrogen (mg N g^{-1})	4.8 ± 0.44	2.1 ± 1.19
Phosphorus (mg P g^{-1})	0.58 ± 0.085	0.32 ± 0.028
C:N:P ratio (molar)	154:18:1	117:14:1

Although some algae are undigested and passed as feces or pseudofeces (Hill and Knight 1981; Galtsoff 1964, Cohen et al. 1984), overall, "*Corbicula* biodeposition enhances net ecosystem losses of N and P via sediment burial and bacterially mediated, coupled nitrification-denitrification" (Newell et al. 2005). Microphytobenthos may then compete with nitrifying bacteria for N, potentially reducing coupled nitrification-denitrification, they retain N and P within sediments, further reducing net regeneration to the water column. (Newell et al. 2005).

Biodeposition can stimulate microbial metabolism sufficiently to cause the sediments to become anaerobic when *Corbicula* are at very high population densities or in locations with low water circulation (Newell 2004). When this occurs, nutrients are regenerated primarily as NH_4^+ and

PO_4 ^{3}, with little or no loss due to burial and denitrification (Newell et al. 2005). Also, under these conditions, *Corbicula* may show several signs of density dependence because it has low tolerance of hypoxia relative to other freshwater bivalves of North America (Johnson & McMahon, 1998; Matthews & McMahon, 1999).

As reported in the Water Column section of this report, Cohen et al. (1984) showed that *Corbicula* removed vast quantities of phytoplankton from Potomac River water. They also demonstrated that pheopigment concentration in the sediment was proportional to clam biomass, thus verifying that *Corbicula* deposit some partially digested phytoplankton on the bottom as feces or pseudofeces. Cohen et al. (1984) also reported that Prokopovich (1969) found that the mucoidlike mass of the pseudofeces of *Corbicula* was a strong binding agent of sediment and that it would probably require a bottom-scouring storm to resuspend the excreted, partially decomposed algae.

Clams can experience variation in oxygen availability depending on the habitats occupied (e.g. pools versus riffles), diel or seasonal factors, and/or location. Additionally, clams in streams can be exposed to low oxygen waters during periods of low flow, during the release of water from dams, and/or a significant effect of DO level on final burial depth (Saloom and Duncan 2005).

Newell et al. (2005) described the major chemical pathway of bivalve deposits as they relate to benthic-water column coupling and the inter relationship between aerobic and anaerobic microbe communities that have evolved in association with bivalve deposits:

> "Natural sediments have well-developed microbial communities inhabiting distinct zones of oxygen content (Henriksen and Kemp 1988). Therefore, bivalve biodeposits that settle on sediments with an oxic surface layer are subject to initial decomposition by aerobic bacteria Organic materials are oxidized to CO_2, PO_4^{3-}, and NH_4^+, and other aerobic bacteria further oxidize NH_4^+ to NO_2^- and NO_3^-. Some of the NO_2^- and NO_3^- diffuses down into underlying anaerobic sediments, and some diffuses out of the sediment and enters the water-column nutrient pool. In the underlying anaerobic sediments, denitrifying bacteria use the oxidized forms of N as terminal electron acceptors, reducing the NO_2^- and NO_3^- to N_2 gas (Henriksen and Kemp 1988, Seitzinger 1988, Risgaard-Petersen et al.1994). Absent N fixation, N_2 is unavailable to plants and passes to the atmosphere. Denitrification can only occur where there is a close juxtaposition between oxygenated sediments that support nitrifying bacteria and anaerobic sediments that support denitrifying bacteria (Kristensen 1988). Bacterial degradation of particulate organic N and P from bivalve biodeposits that settle to anoxic sediments is solely via anaerobic pathways. Because the initial nitrification step is precluded, all regenerated N remains as NH_4 $^+$, and there is negligible sorption of PO^4 to iron complexes (Krom and Berner 1981). The microbial communities associated with sediments are a crucial element mediating nutrient regeneration processes from biodeposits."

In addition, total N flux from bivalve respiration and deposits can range from ≈ 1 to 5 mmol N m^{-2} h^{-1} (Dame et al. 1989; 1991a; Asmus and Asmus 1991; Magni et al. 2000; Newell et al.

2005). Dame et al. (1989) estimated that oyster biodeposits transferred ≈189 g N m^{-2} y^{-1} from the water to the sediments, most of which was regenerated as NH_4^+ (125 g N m-2 y-1)(Newell et al. 2005). Dame et al. (1989) also calculated that bivalves were responsible for a net retention of 98 g P m^{-2} yr^{-1}, which was either incorporated into fauna and flora or buried in the sediments, with little P release (Newell et al. 2005; Konrad 2013). Newell et al. (2005) concluded that because sediment N and P regeneration are less than 100% efficient due to burial and denitrification, bivalve feeding reduces recycling and reduces system-level phytoplankton production and biomass.

Body tissue and Shell Carbon Consumption and Fixation Rates

Corbicula is an extremely fast growing bivalve. It can grow from a 1 mm juvenile to a 5 cm adult within a year and develop very thick shells. These clams require constantly large amounts of carbon to incorporate into their shells ($CaCO_3$) during their growth. Carbon sources for shell development include organic carbon filtered from the water column or pedal fed from the substrate or from CO_2 dissolved in the water (Baker 2010). By now everyone is aware that CO_2 is a major greenhouse gas that effects many stream functions, including metabolism and water quality. *Corbicula* fix carbon into refractory proteins that are part of their shells but more importantly they fix carbon in the shells themselves, which are approximately 12% carbon by weight (Baker 2010). Unlike the carbon contained in plant and animal tissue that can return to CO_2 to the atmosphere in a few years or less, carbon fixed as $CaCO_3$ can persist for tens to hundreds of years as shells or indefinitely as limestone. Shell decay rates are mostly dependent on water chemistry and flow (Strayer and Malcom 2007).

Several studies have measured freshwater bivalve shell production, including *Corbicula* (Aldridge & McMahon, 1978; Strayer et al., 1981; Vincent, Vaillancourt and Lafontaine, 1981; Vincent and Lafontaine, 1984). Only a few have measured shell decay (Strayer et al., 1981; Strayer and Malcom 2007). Aldridge & McMahon (1978) found that shell production was approximately 30 times organic production, suggesting that the populations of *Corbicula* that have been studied had shell production rates of 18–400 g shells m^{-2} $year^{-1}$. Dense populations of *Corbicula* might therefore produce more than 1 kg shells m^{-2} $year^{-1}$ and are capable of producing large amounts >10 kg m^{-2} $year^{-1}$ of spent shells (Stayer and Malcom 2007). C, N, and P concentrations in bivalve tissues can vary seasonally and differ between body tissue and shells (Arnott and Vanni 1996). Zebra mussels are about 5 to 10% dry weight as tissue compared to shell dry weight.

Corbicula and water quality

Bivalves, including *Corbicula*, are a severely underestimated key component for maintaining and improving water quality in an aquatic ecosystem (Huang et al. 2005; Fulford et al. 2007)(Table

56 and Table 57). Their role is powerful, labile, and subject to subtle adjustment and regulation (Ostroumov 2005). However, their role in maintaining Jordan River water quality is overlooked by every agency other than the Council.

Table 56. Water filtration by suspension-feeders may influence other biotic and abiotic processes that are involved in water purification. From Ostroumov 2005.

Water purification	Biotic/ Abiotic	Suspension-feeders influence
Chemical oxidation by oxygen	Abiotic	Suspension-feeders remove some suspended matter from water column; by increasing light penetration, they help benthic algae to carry out photosynthesis and to produce oxygen; availability of oxygen is especially important at the bottom where the organic matter is accumulated
Photodegradation of organic matter and pollutants	Abiotic	Suspension-feeders via filtration increase the water transparency and light penetration into water
Pollutant sorption by sediments	Abiotic	The sorption of pollutants by sediments depends on the percentage of organic matter in the sediments; suspension-feeders produce pellets rich in organics and by doing so increase the percentage and amount of organic matter in the sediments; as a result, the capacity of sediments to adsorb pollutants increases.
Pollutant sorption by pellets	Abiotic	Suspension-feeders produce pellets (faeces, pseudofaeces) which are the additional centers for adsorption of pollutants
Sedimentation of particles of seston	Abiotic	Suspension-feeders remove small particles from water and aggregate them into bigger particles of pellets; the latter sediment faster than the small particles
Material accumulation by aquatic organisms	Biotic	Suspension-feeders produce shells, which contain C and other elements that stay on the bottom for long time. It is important in terms of biomineralization and cycling of carbonates bound in shells.
Oxidative biodegradation of organic molecules by bacteria and fungi	Biotic	By removing bacteria and fungi from water suspension-feeders participate in regulating the abundances of many species in the ecosystem. As a result, suspension-feeders contribute to the control of the rate of processes performed by bacteria and fungi (e.g., Ostroumov, 2000 e, 2001d)
Recycling nutrients making them available to organisms involved in water purification	Biotic	Suspension-feeders actively participate in recycling nutrients. E.g., they excrete N and P. By doing so they contribute to recycling.
Decreasing sediment erodibility	Biotic/ Abiotic	Sediment erodibility depends on the epifaunal bivalves (Widdows et al. 2000)

Table 57. Some key facts and principles that characterize suspension-feeders as part of water- filtering biomachinery maintaining water quality and some features of aquatic ecosystem. From Ostroumov 2005.

Key facts	Comment / Consequences	Fundamental principles concerning the role of suspension-feeders
The amount of water filtered (per unit of biomass of animals or per unit of area or per unit of time) is very significant	Significant contribution to the removal of particles (seston) from water; contribution to water purification	Large-scale repair of water quality
There are several taxa of suspension-feeders which filter water	Increase in reliability of the biomachinery of water filtration	Contribution to the stability of water quality in ecosystem; maintaining stability of habitats of many aquatic species
The higher the concentration of particles, the lower the filtration rate and relative grazing pressure	Positive feedbacks that in turn may lead to the increase in heterogeneity of parts of the water column	Suspension-feeders have a potential to contribute to creating habitat heterogeneity (in terms of patchiness of concentrations of suspended matter in water)
The amount of suspension that is being filtered out of water is usually more than needed for metabolism	A significant amount of the formerly suspended matter is finally packed, ejected and/or excreted as pellets	Suspension-feeders provide some ecological services to the system (by upgrading water quality); ecological taxation: suspension-feeders pay ecological tax to the community (ecosystem)
Suspension-feeders produce pellets	The pellets gravitate towards the bottom or the lower layers	Acceleration of migration of elements through the water
	of the water column	column of the ecosystem; pellets-mediated acceleration of the removal of particles (seston) from water column
Suspension-feeders remove bacteria and fungi	Regulatory effect (control) on planktonic bacteria and fungi; regulatory impact on benthos benthic community	Contribution to the regulation of ecosystem metabolism

Review of *Potamopyrgus* Ecology and Ecosystem Effects

Potamopyrgus densities in the western U.S. can often exceed 300,000 m^{-2} (Richards et al. 2001; Richards 2004; Cross et al. 2010; Arango et al. 2009) and have been reported as high as 500,000 m^{-2} in a tributary of the Snake River in Yellowstone National Park (Hall et al. 2003). Richards (personal observations) has estimated that this snail can far exceed 250,000 m^{-2} in the Jordan River, particularly on submerged aquatic vegetation where they can be 500,000 m^{-2}. Although it is thought to be primarily a parthenogenic livebearer in the western USA (M. Dybdahl, Washington State University, personal communication), males have been found to comprise from 1- 3% of a population in SW Montana. In the western USA, adult *Potamopyrgus* are typically 4 to 5 mm shell length. *Potamopyrgus* often comprises 85% to 95% of the invertebrate assemblages both in biomass and abundance in many rivers in the western USA (Bowler 1991, Richards et al. 2001, Shannon et al. 2003), although for unknown reasons this snail undergoes widely varying 'boom and bust' population density cycles (Richards unpublished data, Moore et al. 2012).

Hall et al. (2003) and Hall et al. (2006) documented *Potamopyrgus* diverting > 75% of gross primary production in a river in Yellowstone National Park. Their data showed that *Potamopyrgus* consumed nearly 100% of the algal primary production and that algal growth rates were slower with increased *Potamopyrgus* biomass, which suggested that *Potamopyrgus* was consuming high-turnover algal taxa and that its impacts on the aquatic environment were comparable to that of the zebra mussel (Dreissenia polymorpha) in the eastern USA (Hall et al. 2003). Hall et al. (2003) also showed that *Potamopyrgus* can dominate carbon and nitrogen cycles in productive streams, which the Jordan River certainly is. See Table 58 for values generated by (Hall et al. 2003). Arango et al. (2009) showed that heavy grazing by *Potamopyrgus* dominated the nitrogen cycle in a stream of similar size to the Jordan River and changed periphyton composition by reducing the proportion of green algae and increasing the proportion of nitrogen-fixing diatoms. Arango et al. (2009) also showed that nitrogen fixation rates increased disproportionately to nitrogen-fixing algal cells, indicating that these snails increased nitrogenase efficiency, probably by improving light and (or) nutrient availability to nitrogen fixers. Thus, *Potamopyrgus* has the potential to alter ecosystem function and affect whole ecosystem processes wherever it occurs in high densities (Alonso and Castro-Diez 2012), including the Jordan River.

Table 58. Hall et. al (2003) Table 1 *Potamopyrgus* production values.

Table 1. Mean abundance, biomass, secondary production, and scaled excretion and egestion fluxes of *Potamopyrgus antipodarum* relative to native invertebrates in Polecat Creek, WY, during July and August 2001

	Abundance	Biomass	Production	Excretion	Egestion	
	indiv/m^2	gAFDM/m^2	mgAFDM/m^2/d	mgN/m^2/h	gAFDM/m^2/d	mg/Nm^2/d
Potamopyrgus	48 3000	34.5	1490	7.8	4.1	190
Native primary consumer taxa	950	0.95	41	0.17*	**	8.7*

*Estimates based on Grimm (1988) **Not estimated

Corbicula and *Potamopyrgus* in the Jordan River

The Jordan River is fairly shallow (< 2 m), eutrophic, and the water column is well mixed. It is also, heavily urbanized, degraded, and regulated (Richards 2017b). However, its water chemistry continues to be ideal for mollusk production, including the now resident clam, *Corbicula* and snail, *Potamopyrgus*. Both *Corbicula* and *Potamopyrgus* reach much higher than average densities and biomass in sections of the Jordan River than elsewhere in the world (Table 59; other citations throughout this report). The following sections discuss rate estimates and effects of the snail and clam in the Jordan River[9].

Corbicula in the Jordan River

Corbicula densities and biomass are both spatially and temporally variable in the Jordan River (Richards 2017a; 2017b; Table 59). Results in this section were based on density estimates from mostly riffle and run habitats between the Jordan River's confluence with Mill Creek and 900 S, the area intensively surveyed by Richards (2017a). However, *Corbicula* densities upstream of Mill Creek confluence are within the range reported in Table 59. Pool habitats almost always have very low densities of live clams.

Table 59. Descriptive statistics of live *Corbicula* m^{-2} in the Jordan River. Based on Richards 2017a.

11a. Live clams and empty shells m^{-2} in run habitat

	N	Mean	Std. Error	Median	25th	75th	Maximum

[9] Note: All of the values in all of the tables for Jordan River are rough estimates. Values in tables should be considered reasonably accurate but not precise. There were many variables that effected these estimates. Some estimates were based on data for other bivalve taxa (e.g.oysters). Temperature effects, seasonal effects, and individual *Corbicula* biomass variability, etc. need to be accounted for. Field data collection is critically needed to verify and adjust.

54th South to Mill Creek	7	271	76	297	85	444	575
Mill Creek to 21st South	12	449	279	122	79	348	3,502
17th South to 13th South	9	4,175	1,670	2,180	1,245	4,880	16,400
13th South to 9th South	13	1,014	467	250	39	1,366	6,100
Total	41	1,416	453	353	85	1,366	16,400

11b. Live clams m^{-2} in run habitat

	N	Mean	Std. Error	Median	25th	75th	Maximum
54th South to Mill Creek	7	175	49	150	53	275	367
Mill Creek to 21st South	12	179	66	99	33	258	837
17th South to 13th South	9	2,635	1,287	956	650	3,420	12,400
13th South to 9th South	13	676	295	130	13	1,100	3,700
Total	41	875	323	262	40	837	12,400

11c. Empty shells m^{-2} in run habitat

	N	Mean	Std. Error	Median	25th	75th	Maximum
54th South to Mill Creek	7	97	38	78	17	147	300
Mill Creek to 21st South	12	271	218	43	28	90	2,665
17th South to 13th South	9	1,540	432	1,224	595	1,712	4,000
13th South to 9th South	13	338	179	110	25	350	2,400
Total	41	541	149	110	31	512	4,000

11d. Live clams and empty shells m^{-2} in pool habitat. N = 7 samples

	Mean	Std. Error	Median	25th	75th	Maximum
Live clams	4	1	6	1	6	8

Empty shells	5	1	6	3	7	10
Live clams and empty shells	10	2	10	4	15	16

Corbicula prefer well oxygenated sediments (Belanger et al. 1985; Richards 2017a; 2017b) and their populations are often much lower or absent in sediments of high organic and low oxygen content (Aldridge and McMahon 1978; McMahon 1979; Eng 1979). This is similar to what Richards 2017a and 2017b reported; high abundances in run habitat, low to absent abundances in slower pool habitats with high organic and low oxygen contents.

Estimated Water Column Filtration Rates for *Corbicula* in the Jordan River

Karatayev et al. (2005) stated that in small water body streams (e.g. Jordan River), *Corbicula* could filter the volume of water equivalent to that of the entire waterbody from 16 min to 4 days (see Table 3).

Based on Karatayev et al. (2005) estimates, **it should only take *Corbicula* ≤ 1 day to filter the entire water column in sections of Jordan River where the clam is at high densities and less than a week in other locations**. Lauritsen (1986) estimated average sized *Corbicula* water column filtering rates at three temperatures shown in Table 60.

Table 60. *Corbicula* filtrations rates reported by Lauritsen (1986) at three temperatures (Similarly sized clams (mean shell length=22.4 mm) were used for testing. At 8^0 C, only data from clams that opened their shells were analyzed).

	Temperature		
	8°C	20°C	31°C
Mean filtration rate (ml/hr)	245.9	905.8	951.3
1 SE	47.4	43.6	78.9
n	4	4	4

Filtration rates were estimated for *Corbicula* in the Jordan River using Lauritsen (1986) rates (Table 60) and density estimates from Table 59. Results are presented in Table 61.

Table 61. Estimated filtration rates of *Corbicula* in the Jordan River at 3 temperature means and standard errors from rates published by Lauritsen (1986).

Corbicula Density	*8° C*	20 °C	21° C

(m^{-2})	$m^3\ m^{-2}\ hr^{-1}$	$m^3\ m^{-2}\ hr^{-1}$	$m^3\ m^{-2}\ hr^{-1}$
Median = 650	0.16 (± 0.01)	0.59 (± 0.03)	0.62 (± 0.05)
Mean = 1,435	0.35 (± 0.02)	1.301 (± 0.06)	1.37 (± 0.10)
75th = 1,223	0.30 (± 0.01)	1.11 (± 0.05)	1.16 (± 0.09)
95th = 3,700	0.91 (± 0.04)	3.35 (± 0.15)	3.52 (± 0.28)
99th = 12,400	3.05 (± 0.16)	11.23 (± 0.50)	11.80 (± 0.93)

Estimated N and P consumption rates for *Corbicula* in the Jordan River

Table 14 contains monthly and daily nitrogen and phosphorus consumption rates based on Newell et al. 2005.

Table 62. Monthly and daily Nitrogen and Phosphorus consumption rates (mg m^{-2}) for *Corbicula* in the Jordan River during summer months (June-September = 122 days) based on Newell et al. (2005). See Table 6 from Newell et al. (2005) monthly consumption rates adjusted by mean and se for *Corbicula* density adjusted biomass.

	Month		***Day***	
Corbicula Biomass[1] ($g\ m^{-2}$)	***N*** *mg* m^{-2} *(± SE)*	***P*** *mg* m^{-2} *(± SE)*	***N*** *mg* m^{-2} *(± SE)*	***P*** *mg* m^{-2} *(± SE)*
Mean	189.84 (145.19, 234.49)	68.63 (52.47, 84.79)	1.56 (1.19,1.92)	0.56 (0.43,0.70)
-1 SE	120.18 (91.91, 148.44)	43.45 (33.21, 53.68)	0.99 (0.75,1.22)	0.36 (0.27,0.44)

+1 SE	259.11 (198.17, 320.05)	93.67 (71.61,115.73)	2.12 (1.62,2.62)	0.77 (0.59,0.95)

Estimated O_2 Consumption Rates for *Corbicula* in the Jordan River

Table 63 contains estimated O_2 consumption and CO_2 respiration rates for *Corbicula* in the river based on Hakenkamp and Palmer (1999) rates.

Table 63. Estimated O_2 consumption and CO_2 respiration rates (mg m^{-2} hr^{-1}) by *Corbicula* in run habitat sections of the Jordan River downstream CVWRF to 900 South.

Corbicula Density (m^{-2})[a]	*Corbicula* Dry Weight (g m^{-2})[b]	O_2 consumption (mg m^{-2} hr^{-1})[b]	CO_2 respiration (mg m^{-2} hr^{-1})[c]
Median = 650	0.52	1.01	0.85
Mean (± SE) = 1,436 (910, 1962)	1.15 (0.73, 1.57)	2.01 (1.34, 2.67)	1.70 (1.14, 2.27)
75^{th} = 1,223	0.98	1.74	1.45
95^{th} = 3,700	2.96	4.87	4.14
99^{th} = 12,400	9.92	15.86	13.48

[a]Jordan River *Corbicula* density estimates downstream of CVWRF in non-pools (from Richards 2017)(see Table 59 for more descriptive stats on density estimates).
[b]Based on Hakenkamp and Palmer (1999) *Corbicula* dry weight estimates and regression model: oxygen consumed = 0.19 + (1.58 X *Corbicula* dry weight (g)).
[c]Based on Bott (2007) Respiratory Quotient: 1 mol CO_2 respired/1 mol O_2 consumed = 0.85

Based on these estimates of high O_2 consumption rates and CO_2 respiration rates, it is obvious that *Corbicula* contributes strongly to total metabolism in the water column and streambed sediments in the Jordan River. Because every 1 mole of oxygen consumed by *Corbicula* is roughly equivalent to the release of 1 mole of carbon in the form of carbon dioxide (Respiratory Quotient = 0.85; e.g., Bott 1996), the high respiration rate found for *Corbicula* reflects significant utilization of organic matter resources (Hakenkamp and Palmer 1999). These CO_2 respiration rates combined with the as of yet unmeasured amount of sequestering of C into their shells, and results from Hakenkamp and Palmer (1999), clearly shows that *Corbicula* is likely the single most important species in the Jordan River with respect to carbon dynamics and stream metabolism.

Total O_2 consumption rates in the Jordan River obviously need to include *Corbicula* consumption rates but also need to account for other sources (i.e. decomposition of dead phytoplankton, microbes, plant and animal matter, and benthic algae, etc). This report has shown that *Corbicula* can remove vast amounts of small POM including phytoplankton and zooplankton and microbes from the water column and OM from the sediments, which otherwise would have contributed significantly to O_2 demand in the Jordan River. In addition, *Corbicula* reduces turbidity by consuming vast amounts of suspended solids in the water column, which allows more light to reach the benthos, which in turn allows photosynthetic benthic algae to grow and respire O_2 during daylight hours. The net result would be that the proportion of the total O_2 demand in the river contributed by *Corbicula* O_2 consumption rates would be substantially lower. However, as stated earlier, the benefit of *Corbicula* on reducing hypoxia depends on a reduction in the flux of organic detritus to benthic sediments that creates biochemical oxygen demand (BOD) through heterotrophic respiration and decomposition of organic material (Konrad 2013).

Estimated Ammonium and Phosphorus Excretion Rates in the Jordan River

Newell et al. (2005) reported average ammonium excretion rates of *Corbicula*:

$$\cong 6.0\ \mu mol\ NH_4^{+}\ g^{-1}\ DW\ h^{-1}\ (DW = dry\ tissue\ weight)$$

and phosphorus excretion rates:

$$\cong 1.2\ \mu mol\ P\ g^{-1}\ DW\ h^{-1}\ (DW = dry\ tissue\ weight)$$

Table 64. contains *Corbicula* ammonium and phosphorus excretion rates based on these values.

Table 64. Estimated average ammonium (NH_4^+) and phosphorus (P) excretion rates of *Corbicula* in the mid-Jordan River

Density (m^{-2})[a]	Dry weight ($g\ m^{-2}$)[b]	NH_4^+ excretion ($\mu mol\ m^{-2}\ day^{-1}$)[b]	P excretion ($\mu mol\ m^{-2}\ day^{-1}$)[b]
Median = 650	0.52	75	15
Mean (± SE) = 1,436 (910,1962)	1.15 (0.73 1.57)	165 (105, 226)	33 (21, 45)
75^{th} = 1,223	0.98	141	28
95^{th} = 3,700	2.96	426	85

99th = 12,400	9.92	1,426	286

Estimated Sediment Organic Matter Consumption Rates in Jordan River

Table 65 contains estimated *Corbicula* organic matter rates in the Jordan River based on these values.

Table 65. Estimated organic matter (OM) consumption rates (mass unit area^{-1} day^{-1}) by *Corbicula* pedal feeding in the Jordan River.

Density[1]	g m^{-2} day^{-1}	kg km^{-1} day^{-1}	metric tons km^{-1} year^{-1}
Mean (± SE)	7 (6, 10)	72 (46, 986)	26 (17, 36)
Median	3	33	12
75th	6	61	22
95th	19	185	68
Maximum	62	6,200	226

Boltovskoy et al. (1995) estimated *Corbicula* densities between 450 and 4500 m^{-2} (mean 2000 m^{-2}) and 66 to 673 mg C m^{-2} h^{-1} (mean: 289 mg C m^{-2} h^{-1}) required for respiration only, which translates to approximately 16 to 162 (mean 69) g C m^{-2} day^{-1}.

Carbon Consumption and Fixation Rates of *Corbicula* in the Jordan River

Aldridge and McMahon (1978) showed that *Corbicula* had shell production rates of 18–400 g shells m^{-2} year^{-1} and that dense populations of *Corbicula* are capable of producing large amounts >10 kg shells m^{-2} year^{-1} (Stayer and Malcom 2007). Baker (2010) estimated that *Corbicula* shells were approximately 12% carbon by weight (Baker 2010). This suggests that average densities in the Jordan River, *Corbicula* are capable of sequestering ≈ 1 kg C m^{-2} year^{-1}. This could equate to ≈ 10 metric tons C km^{-1} year^{-1} in some sections of the Jordan River.

Potamopyrgus in the Jordan River

Hall et al. (2003) estimated production, excretion, and egestion rates for *Potamopyrgus* in a highly productive stream at snail densities 500,000 m^{-2}. Densities of *Potamopyrgus* in the Jordan River are within this range and the Jordan River is likely much more productive than the river

examined by Hall et al. (2003). Therefore, the estimates made by Hall et al. (2003) are probably similar for the Jordan River. Assuming these values are reasonably accurate, then *Potamopyrgus* in the Jordan River can have production rates ≈ 1500 mg AFDM m^{-2} day^{-1}; excretion rate ≈ 8 mg N m^{-2} day^{-1}; and egestion rates ≈ 200 mg N m^{-2} day^{-1}. At these high rates, *Potamopyrgus* is most certainly co-dominating nitrogen and carbon cycles with *Corbicula* in the Jordan River and likely with other ecosystem functions, including those that affect water quality. Much more research is needed on nutrient and carbon rates and other ecosystem effects of *Potamopyrgus* to the river.

Corbicula and Potamopyrgus in the Jordan River

Individually, *Corbicula* and *Potamopyrgus* have major ecosystem effects in the Jordan River as shown throughout this report. However, both co-occur in the river with potentially synergistic effects. For example, as illustrated in Figure 67, *Corbicula* filter feed (ingest) vast amounts of POM, nutrients, bacteria, etc. from the water column, which decreases turbidity, increases light penetration, and transform nutrients (TN and TP) into more biologically available forms (e.g. NH_4 and PO_4). The increased light penetration can allow benthic photosynthetic algae, SAV, and epiphytes on SAV to prosper, which *Potamopyrgus* readily grazes (doesn't graze SAV). The effects of grazing are to stimulate algae and epiphyte production by reducing standing stock and increasing readily used nutrients via snail excretion. Reduction of epiphyte biomass also allows SAV to increase production. Increased primary-autotrophic production mitigated by *Corbicula* and *Potamopyrgus* in combination, accelerates nutrient cycling in the river.

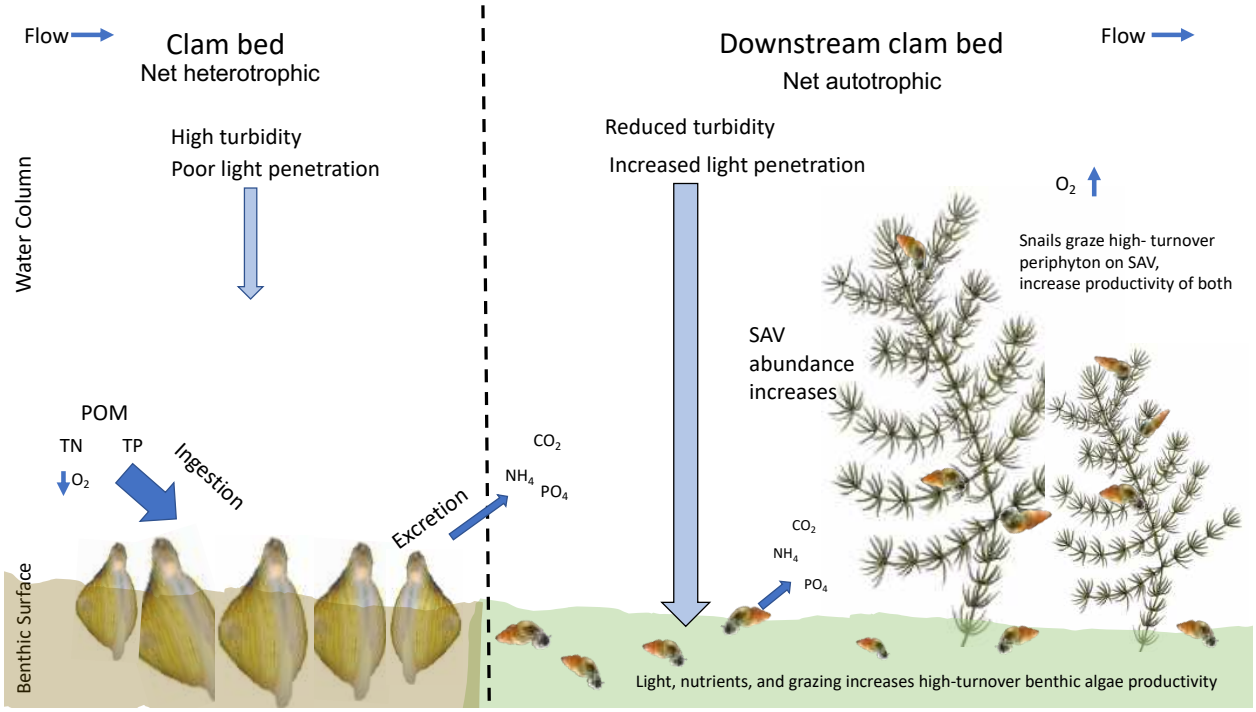

Figure 67. Potential synergistic effects of *Corbicula* and *Potamopyrgus* on nutrient cycling in the Jordan River. See text above for description.

Figure 67 is but one example of the potential synergistic effects of *Corbicula* and *Potamopyrgus* on the Jordan River's ecosystem. Much more research is needed to determine the interaction effects between these snails and clams and the Jordan River ecosystem.

Discussion and Conclusion

Results from this report clearly show that the invasive 'good luck clam' *Corbicula fluminea* and the New Zealand mudsnail, *Potamopyrgus antipodarum* co-dominate ecosystem functions in the Jordan River with pathways that have been well described in the literature. These snails and clams can mitigate improved water quality in the Jordan River, free of monetary expenditures. Contrary to the current Jordan River paradigm; microbial assemblages do not govern ecosystem functioning in the Jordan River. It is both *Corbicula* and *Potamopyrgus* that co-regulate the community structure of aerobic and anaerobic microbes. The effects of the snails and clams on the Jordan River's metabolism, nutrient cycling, cyanoHABS, etc. should now be well apparent to researchers and managers and when taken into account, explain the vast majority of unexplained variability and discrepancies reported in past research. *Corbicula* and *Potamopyrgus* are here to stay in the Jordan River and for better or worse, are now integral components of what is considered by restoration and conservation ecologists to be a 'novel ecosystem'. A novel ecosystem is the establishment of an ecosystem that differs in composition and/or function from the past system and is an almost inevitable consequence of changing species distributions and environmental alteration through climate and land use change (Root and Schneider 2006; Harris et al. 2006; Hobbs et al. 2009). The novel Jordan River ecosystem is now dependent on the services of two once invasive species but who are now residents to maintain and improve its current ecological state and provide resilience to anthropogenic nutrient inputs; the grazer, *Potamopyrgus* and the filter-feeding, benthic-feeding, pseudofeces-forming bivalve, *Corbicula*.

Recommendations

1. Conduct field research to verify and update estimated values calculated for Jordan River from literature and presented in this report. Specifically, estimate densities of *Corbicula* and *Potamopyrgus* in sections not surveyed by OreoHelix Consulting and The Wasatch Front Water Quality Council. Conduct in situ experiments using the most up to date methods for estimating: carbon, nitrogen, and phosphorous filtering and consumption rates, excretion rates, and carbon fixation rates, etc. (see Same and Olenin 2005; . Relate these findings to water chemistry values in the Jordan River and determine the effects of the clam and snail. Update all Jordan River reports with this new information. Inform researchers and managers.

2. The Clean Water Act explicitly provides for the protection and propagation of our nation's fish and shellfish, of which *Corbicula* and *Potamopyrgus* obviously are the latter. UDWQ does not differentiate between native and invasive species in their monitoring or protection and is thus responsible for the snails and clams continued

persistence and viability. However, *Corbicula* or *Potamopyrgus* could be having trade-off between positive and negative impacts (e.g.O_2 depletion, lower N:P) in the Jordan River when their densities reach a certain, as of yet determined level. An possible solution would be to harvest *Corbicula*, either recreationally or commercially at a yet to be determined rate, as they do in many places in the world. However, these clams may be considered unsafe for consumption because of toxic substances in their tissues (e.g. metals, *E. coli*). If toxicants are a problem in the Jordan River then it stands to reason that a major impairment in the Jordan River is not nutrients (*Corbicula* and *Potamopyrgus* take care of this) but toxic substances, including *E. coli*, which should be considered a management priority by water quality managers.

3. Consider aquaculture use of *Corbicula* in Jordan River to reduce nutrient inputs from POTWs. Nutrient trading schemes are being considered between municipal waste water treatment facilities and the extra market value of nutrient removal offered by bivalve aquaculturalists in Chesapeake Bay and monitored by EPA. (Newell 2004). *Corbicula* harvesting would also be a measurable contribution to reducing CO_2 emissions and the effects global climate change.

Acknowledgements

A big thanks to our mollusk surveyors: W.D. Robinson and Frank Fluckinger and the Wasatch Front Water Quality Council for sponsoring this important paradigm shift.

Literature Cited

Aldridge D.W. & McMahon R.F. (1978) Growth, fecundity, and bioenergetics in a natural population of the Asiatic freshwater clam, *Corbicula manilensis* Philippi, from north central Texas. Journal of Molluscan Studies, 44, 49–70.

Alonso, A. and P. Castro-Diez. 2012. The exotic aquatic mud snail *Potamopyrgus antipodarum* (Hydrobiidae, Mollusca): state of the art of a worldwide invasion. Aquat. Sci. 74: 375-383.

Arango, C. P., Riley, L. A. , Tank, J. L., and R. O.Hall. 2009.Herbivory by an invasive snail increases nitrogen fixation in a nitrogen-limited stream. Canadian Journal of Fisheries and Aquatic Sciences, 2009, 66(8): 1309-1317, https://doi.org/10.1139/F09-079.

Asmus RM Asmus H 1991 Mussel beds, limiting or promoting phytoplankton? J Exp Mar Biol Ecol 148: 215-232

Baker, P. and S. Baker. 2010. Carbon fixation by hard clam aquaculture in Florida. Florida Sea Grant College Program. PD-09-10. http://shellfish.ifas.ufl.edu/projects/shellfish-farm-environment/carbon-fixation/.

Beaver, J. R., Crisman, T. L., and R. J. Brock. 1991. Grazing effects of an exotic bivalve (*Corbicula fluminea*) on hypereutrophic lake water. Lake and Reservoir Management. 7(1): 45-51.

Boltovskoy, D., Izaguirre, Ir. And N. Correa. 1995. Feeding selectivity of *Corbicula fluminea* (Bivalvia) on natural phytoplankton. Hydrobiologia. 312: 171-182.

Bott, T.L .2007. Primary productivity and community respiration. In: Hauer FR, Lamberti GA (eds) Methods in stream ecology. Academic Press, San Diego, page 668.

Bowler, P. A. 1991. The rapid spread of the freshwater hydrobiid snail *Potamopyrgus antipodarum* (Gray) in the Middle Snake River, southern Idaho. Proceedings of the Desert Fishes Council. 21: 173-182.

Bowler, P.A. 2001. Photophobic reactions in Hydrobiid snails from the Owens Valley, California, and the first record of the New Zealand Mudsnail, *Potamopyrgus antipodarum* (Gray, 1843) from the Owens River. Proceedings of the Desert Fishes Council 32: 51-52

Buttner, J. K . 1986. Biology of *Corbicula* in catfish rearing ponds. In: Proceedings of the Second International *Corbicula* Symposium, JC Britton (Ed). American Malacological Union, Hattiesburg. Am Malacol Bull 2 (Special ed.) pp 211-218.

Cleland JD (1988) Ecological and physiological considerations of deposit-feeding in freshwater bivalve, *Corbicula* fluminea. Masters Thesis, University of Texas, Arlington.

Cohen, R. R. H., Dresler, P.V., Phillips, E. J.P. and R. L. Cory. 1984. The effect of the Asiatic clam, *Corbicula* fluminea, on phytoplankton of the Potomac River, Maryland. Limnol. Oceanogr. 29(1):170-180.

Cross, W. F., Rosi-Marshall, E. J., Behn, K. E. et al. 2010. Invasion and production of New Zealand mud snails in the Colorado River, Glen Canyon. Biol. Invasions. 12: 3033-3043.

Dame RF Spurrier JD Wolaver TG 1989 Carbon, nitrogen and phosphorus processing by an oyster reef. Mar Ecol Prog Ser 54: 249-256

Dame RF Dankers N Prins TC Jongsma H Smaal AC 1991a The influence of mussel beds on nutrients in the western Wadden Sea and eastern Scheldt estuaries. Estuaries 14: 130-138

Fulford, R. S., Breitburg, D. L., Newell, R. I. E., Kemp, W.M., and M. Luckenbach. 2007. Effects of oyster population restoration strategies on phytoplankton biomass in Chesapeake Bay: a flexible modeling approach. Marine Ecology Progress Series. 336: 43-61.

Hall, Tank, J. L., and M. F. Dybdahl. 2003. Exotic snails dominate nitrogen and carbon cycling in a highly productive stream. Front. Ecol. Environ. 1(8): 407-411.

Hall, R. O., Dybdahl, M. F., and M. C. VanderLoop. 2006. Extremely high secondary production of introduced snails in rivers. Ecological Applications. 16(3): 1121-1131.

Hakenkamp, C.C. and M. A. Palmer 1999. Introduced bivalves in freshwater ecosystems: the impact of *Corbicula* on organic matter dynamics in a sandy stream. Oecologia. 119: 445-451.

Harris, J.A. et al. (2006) Ecological restoration and global climate change. Rest. Ecol. 14, 170–176.

Henriksen K Kemp WM 1988 Nitrification in estuarine and coastal marine sediments. In: Nitrogen Cycling in Coastal Marine Environments. TH Blackburn J Sorensen (Eds). Wiley and Sons, Chichester, England, pp 205-249

Hobbs, R. J. , Higgs, E., and J. A. Harris. 2009. Novel ecosystems: implications for conservation and restoration. Trends in Ecology and Evolution. doi:10.1016/j.tree.2009.05.012.

Huang, S.C., Jeng, S., and H. L. Hsieh. 2005. The function of filter-feeding bivalves in aquatic ecosystems: using Tapeng Bay as an example. Journal of the Fisheries Society of Taiwan. 32(1): 17.

Isom BG (1986) Historical review of Asiatic clam (*Corbicula*) invasion and biofouling of waters and industries in the Americans. In: Britton JC (ed) Proceedings of the Second International *Corbicula* Symposium (American Malacological Bulletin special edition 2). American Malacological Union, Hattiesburg, pp 1±6

Konrad, C. P. year. 2013. Approaches for evaluating the effects of bivalve filter feeding on nutrient dynamics in Puget Sound, Washington. USGS. Scientific Investigations Report 2013–5237.

Kristensen E 1988 Benthic fauna and biogeochemical processes in marine sediments, microbial activities and fluxes. In: Nitrogen Cycling in Coastal Marine Environments. TH Blackburn and J Sorensen (Eds). Wiley and Sons, Chichester, England, p 275-299

Krom MD Berner RA 1981 The diagenesis of phosphorus in a nearshore marine sediment. Geochim Cosmo Acta 45: 207-216

Lauritsen, D. D. 1986. Filter-feeding in *Corbicula* fluminea and its effect upon seston removal. J. N. Am. Benthological Society. 5:165-172.

Lauritsen, D. D., and S.C. Mozley. 1989. Nutrient excretion by the Asiatic clam *Corbicula* fluminea. J. North. Amer. Benthol. Soc. 8:134-139.

Leff, Laura G.; Burch, Jarrett L.; and McArthur, J. Vaun .1990. Spatial Distribution, Seston Removal, and Potential Competitive Interactions of the Bivalves *Corbicula* Fluminea and Elliptio Complanata, in a Coastal Plain Stream. Freshwater Biology 24(2), 409-416. doi: 10.1111/j.1365-2427.1990.tb00720.x Retrieved from https://digitalcommons.kent.edu/bscipubs/50

Magni P Montani S Takada C Tsutsumi H 2000 Temporal scaling and relevance of bivalve nutrient excretion on a tidal flat of the Seto Inland Sea, Japan. Mar Ecol Prog Ser 198: 139-155

McMahon, R.F. and A.E. Bogan. 2001 Mollusca: Bivalvia. In: Ecology and Classification of North American Freshwater Invertebrates, 2nd Edition, JH Thorp AP Covich (Eds.), Academic Press, Inc., pp 331-430.

McMahon R.F. 2002. - Evolutionary and physiological adaptations of aquatic invasive animals: r selection versus resistance. Can. J. Fish. Aquat. Sci., 59, 1235-1244.

Moore, J. W., Herbst, D. B., Heady, W. N. and S. M. Carlson. 2012. Stream community and ecosystem responses to the boom and bust of an invading snail. Biol. Invasions. DOI 10.1007/s10530-012-0240-y.

Newell RIE (1988) Ecological changes in Chesapeake Bay: Are they the result of overharvesting the American oyster,
Crassostrea virginica? In: Lynch MP, Krome EC (eds) Understanding the estuary: advances in Chesapeake Bay research. Chesapeake Research Consortium, Gloucester Point, VA, p 536–546

Newell RIE (2004) Ecosystem influences of natural and cultivated populations of suspension-feeding bivalve molluscs: a review. J Shellfish Res 23:51–61

Newell RIE, Koch EW (2004) Modeling seagrass density and distribution in response to changes in turbidity stemming
from bivalve filtration and seagrass sediment stabilization. Estuaries 27:793–806

Newell RIE, Langdon CJ (1996) Mechanisms and physiology of larval and adult feeding. In: Kennedy VS, Newell RIE, Eble AF (eds) The eastern oyster Crassostrea virginica. Maryland Sea Grant College, College Park, MD, p 185–230

Newell RIE, Ott J (1998) Macrobenthic communities and eutrophication. In: Malone TC, Malej A, Harding LW,
Smodlaka N, Turner RE (eds) Ecosystems at the land–sea 60 margin: drainage basin to coastal sea. Coast Estuar Stud 55: 265–293

Newell RIE, Fisher TR, Holyoke RR, Cornwell JC (2005) Influence of eastern oysters on nitrogen and phosphorus regeneration in Chesapeake Bay, USA. In: Dame R, Olenin S (eds) The comparative roles of suspension feeders in ecosystems. NATO Science Series: IV Earth and Environmental Sciences, Vol 47. Springer, Netherlands, p 93–120

Newell, R. I. E. 2004. Ecosystem influences of natural and cultivated populations of suspension-feeding bivalve molluscs: a review. Journal of Shellfish Research. 23(1): 51-61.

Phelps, H. I. 1994. The Asiatic Clam (*Corbicula* fluminea) invasion and system -level ecological change in the Potomac River estuary near Washington, D.C. Estuaries. 17(3):614-621.

Poff, NL, Palmer MA, Angermeier PL, Vadas Jr RL, Hakenkamp CC, Bely A, Arensburger P, Martin AP (1993) The size struc- ture of a metazoan community in a Piedmont stream. Oecologia 95:202±209

Prokopovich, N. P. 1969. Deposition of clastic sediments by clams. J. Sediment. Petrol. 30:891-901.

Reid, R.G.B, McMahon RF Foighil DO Finnigan R 1992 Anterior inhalant currents and pedal feeding in bivalves. Veliger 35: 93-104

Richards, D. C. 2017a. Lower Mill Creek and Mid-Jordan River Native Mussel Survey 2017: As it pertains to the Central Valley Water Reclamation Facility Discharge. Report to: Wasatch Front Water Quality Council. Salt Lake City, UT.

Richards, D. C. 2017b. Native Unionoida Surveys, Distribution, and Metapopulation Dynamics in the Jordan River-Utah Lake Drainage, UT. Report to: Wasatch Front Water Quality Council. Salt Lake City, UT. OreoHelix Consulting, Vineyard, UT. Version 1.5 May, 26, 2017. Available at: http://wfwqc.org/wp-content/uploads/2017/04/Native-Unionoida-Surveys-and-Metapopulation-Dynamics-in-the-Jordan-River-Utah-Lake-drainage-UT-Version-1.5-compressed.pdf. With supporting documentation at: http://wfwqc.org/wp-content/uploads/2017/10/Appendix-8-Native-Mussels-Spreadsheet-FINAL-read-only.xlsx.

Richards, D. C., L. D. Cazier, and G. T. Lester. 2001. Spatial distribution of three snail species, including the invader *Potamopyrgus antipodarum*, in a freshwater spring. Western North American Naturalist.61: 375-380

Richards, D. C., T. Arrington, S. Sing, and B. L. Kerans. In revision. Competition and coexistence between an invasive aquatic snail and its threatened native congener. American Malacological Society Bulletin.

Richards, D. C. and T, Arrington. In review. Spatial and environmental relationships of three snail taxa in a freshwater spring: with estimates of their abundance. Journal North American Benthological Society.

Richards, D. C., C. M. Falter, G. T. Lester, and R. Myers. In revision. Mollusk survey of Hells Canyon reservoirs and free flowing Snake River, Idaho and Oregon, USA: with focus on rare and listed taxa, including a newly described Taylorconcha sp. American Malacological Society Bulletin.

Richards, D. C., P. O'Connell, and D. C. Shinn. In preparation. Growth Rates of the threatened Bliss Rapids Snail, Taylorconcha serpenticola and the invasive New Zealand mudsnail *Potamopyrgus antipodarum* at six temperatures.

Richards, D. C. 2010. Mollusk diversity and estimated predation rates by gastropod shell borehole drillers on Turritella spp. at Playa Grande, Las Baulas National Park, Costa Rica. American Malacological Society Newsletter. Vol. 41. No. 2. Pg 5-7.

Richards, D. C. and T. Arrington. 2008. Evaluation of Threatened Bliss Rapids Snail, Taylorconcha serpenticola susceptibility to exposure: potential impact of 'load following' from hydroelectric facilities. American Malacological Society Bulletin.

Richards, D. C. In review. Some life history studies of the threatened Bliss Rapids snail and invasive New Zealand mudsnail. Western North American Naturalist.

Richards, D. C. and D. C. Shinn. 2004. Intraspecific competition and development of size structure in the invasive snail, *Potamopyrgus antipodarum*. American Malacological Society Bulletin. 19. 1.2.

Richards, D. C., P. O'Connell, and D. C. Shinn. 2004. Simple control method for the New Zealand mudsnail, *Potamopyrgus antipodarum*. Journal North American Fisheries Management. 24:114-117.

Richards, D. C., L. D. Cazier, and G. T. Lester. 2001. Spatial distribution of three snail species, including the invader *Potamopyrgus antipodarum*, in a freshwater spring. Western North American Naturalist.61: 375-380.

Risgaard-Petersen N Rysgaard S Nielsen LP Revsbech NP 1994 Diurnal variation of denitrification and nitrification in sediments colonized by benthic microphytes. Limnol Oceanogr 39: 573-579

Root, T.L. and Schneider, S.H. (2006) Conservation and climate change: the challenges ahead. Conserv. Biol. 20, 706 708.

Seitzinger SP 1988 Denitrification in freshwater and coastal marine ecosystems, ecological and geochemical significance. Limnol Oceanogr 33: 702-724

Shannon, J. P., E. P. Benenati, H. Kloeppel, and D. C. Richards. 2003. Monitoring the aquatic food base in the Colorado River, Arizona during June and October 2002. Annual Report. Grand Canyon Monitoring and Research Center. USGS. Cooperative Agreement-02WRAG0028.

Sousa, R., Antunes, C., and L. Guilhermino. 2008. Ecology of the invasive clam Corbicula fluminea (Muller, 1774) in aquatic ecosystems: an overview. Ann. Limnol.-Int. J. Lim. 44(2): 85-94.

Strayer D.L., Cole J.J., Likens G.E. & Buso D.C. (1981) Biomass and annual production of the freshwater mussel Elliptio complanata in an oligotrophic softwater lake. Freshwater Biology, 11, 435–440.

Strayer, D. L. and H. M. Malcom. 2007. Shell decay rates of native and alien freshwater bivalves and implications for habitat engineering. Freshwater Biology. 52: 1611-1617.

Vincent, Vaillancourt & Lafontaine, 1981

Vincent B. & Lafontaine N. (1984) Cycle de developpement, croissance et production de Sphaerium striatinum (Bivalvia: Pisidiidae) dans le Saint-Laurent (Quebec). Canadian Journal of Zoology, 62, 2418–2424.

Way, C.M., Hornbach, D. J., Miller, Way, C. A. , Payne, B. S., and A. C. Miller. 1990. Dynamics of filter-feeding in *Corbicula fluminea* (Bivalvia: Corbiculidae). Can. J. Zool. 68: 115-120.

1 Appendices

Appendix 36. Summary of approaches for assessing the effects of bivalve filter feeding on nutrient dynamics. From Konrad 2013.

Approach	Key data requirements	Typical temporal scale	Temporal scaling	Typical spatial resolution	Spatial scaling
1. Nutrient mass balance	Mass of bivalve harvested in area of interest	Life-span of bivalve	Can be scaled down to a "typical" year by calculating mean annual nutrient uptake	Area of bivalve bed harvested	Can be scaled over larger areas where bivalve densities are known and growth rates are comparable
2. Spatially aggregated model based on clearance rates	Filter feeding rates representative of area of interest	Synoptic–same as period used to calculate filtration rate	Can be scaled over longer periods by adjusting filtration rate to account for temporal variability in seston, temperature, metabolic demand of bivalve, etc.	Same as area used to calculate filtration rate	Can be scaled over larger areas by adjusting filtration rate for variability in seston, temperature, bivalve density, etc.
3. Spatially aggregated biophysical indicators	Rates of primary production, filter feeding, and mixing for area of interest	Seasonal–same as period used to calculate rates in key data requirements	Can be scaled over time by adjusting rates to account for temporal variability	Area of estuary where rates (key data requirements) are relatively homogeneous	Scaling over larger area requires rates appropriate for the area
4. Biophysical model in a spatial framework	Spatially distributed rates of primary production, filter feeding, and mixing	Seasonal–same as period used to calculate rates in key data requirements	Can be scaled over time by adjusting rates to account for temporal variability	Area of estuary where rates (key data requirements) are relatively homogeneous	Scaling over larger areas requires appropriate spatial distributions of rates and parameters
5. Biogeochemistry in a low trophic level model	Rates of primary production (as function of nutrient concentrations) and filter feeding by bivalve, dissolved nutrient flux from bivalve (soluble and solid) and from sediment diagensis, denitrification, rates of other filter feeders and associated nutrient fluxes to sediment and water column	Seasonal–same as period used to calculate rates in key data requirements	Can be scaled over time by adjusting rates to account for temporal variability	Area of estuary where rates (key data requirements) are relatively homogeneous	Scaling over larger areas requires appropriate spatial distributions of rates and parameters
6. Spatially aggregated, bioenergetics model with full trophic dynamics	Spatially distributed rates of primary production, filter feeding, higher level predation, and decomposition	Seasonal–same as period used to calculate rates in key data requirements	Can be scaled over time by adjusting rates to account for temporal variability	Area of estuary where rates (key data requirements) are relatively homogeneous	Scaling over larger areas requires appropriate spatial distributions of rates and parameters
7. Spatially explicit ecosystem model	Spatially distributed rates of all significant biological and physical processes (may be a subset of all those listed for other approaches)	Seasonal–same as period used to calculate rates in key data requirements	Can be scaled over time by adjusting rates to account for temporal variability	Area of estuary where rates (key data requirements) are relatively homogeneous	Scaling over larger areas requires appropriate spatial distributions of rates and parameters

Appendix 37. Effects of inorganic suspended matter on mussel population viability in the utah lake/jordan river drainage: a preliminary literature review.

Version 1.2

Effects of Inorganic Suspended Matter on Mussel Population Viability in the Utah Lake/Jordan River Drainage: A Preliminary Literature Review

Addendum
To:

Richards (2016) "Recalculation of Ammonia Criteria for Central Valley Water Reclamation Facility's Discharge into Mill Creek, Salt Lake County, UT based on Native Unionoida Surveys and Metapopulation Dynamics"

and

Richards (2016) "Recalculation of Ammonia Criteria for Timpanogos Special Service District and the Cities of Orem and Provo Water Reclamation Facilities Discharge into Utah Lake based on Native Unionoida Surveys and Metapopulation Dynamics"

Submitted to:

Jordan River Farmington bay Water Quality Council

Salt Lake City, UT, USA

Submitted by:

David C. Richards, Ph. D.

OreoHelix Consulting

Moab, UT 84532

Email: oreohelix@icloud.com

Phone: 406.580.7816

March 2, 2016

Introduction

Detailed analyses of native mussel population surveys and viability in the Utah Lake/Jordan River drainage were presented to the Jordan River Farmington Bay Water Quality Council in several reports including, Richards (2016) "*Recalculation of Ammonia Criteria for Central Valley Water Reclamation Facility's Discharge into Mill Creek, Salt Lake County, UT based on Native Unionoida Surveys and Metapopulation Dynamics*" and Richards (2016) "*Recalculation of Ammonia Criteria for Timpanogos Special Service District and the Cities of Orem and Provo Water Reclamation Facilities Discharge into Utah Lake based on Native Unionoida Surveys and Metapopulation Dynamics*". Because of the large number and combination of stressors and factors examined in these reports that were considered responsible for the near extinction of the two once abundant native mussel taxa in this drainage, *Margaritifera falcata* and *Anodonta nuttalliana/californiensis*, only a limited discussion on the effects of suspended inorganic matter (SIM) on their viability was included. A brief literature review on the importance of SIM to native mussel population viability in Utah Lake/Jordan River drainage follows.

Literature Review

High concentrations of inorganic solids (sand, silt, clay, etc.) often originate from erosion related to agriculture, forestry, and urbanization, and can alter feeding patterns, substrate composition, and food web dynamics (Waters 1995). Concentrations of suspended inorganic matter (SIM)(e.g. suspended inorganic solids) are well known to affect mussel respiration, growth, parasite infestation and reproduction (Box and Mossa 1999, Robinson et al. 1984, Alexander 1994, Rosewarne et al 2013, and Tokumon et al. 2016). These effects subsequently can reduce native mussel population viability and increase extinction risk.

Feeding is strongly impeded for many filter feeding bivalves due to high levels of SIM (Robinson et al. 1984, Jorgensen 1996, Lei et al. 1996, Cheung and Shin 2005, Velasco and Navarro 2005, and Tokumon et al. 2016). The reasons for negative effects of SIM on mussel feeding are numerous and can include decreases in the proportion of organic material (i.e. food) in suspension, which can then result in much higher energy expenditures in sorting out and eliminating energetically unprofitable particles (Jorgensen 1990, Velasco and Navarro 2005, Safi and Hayden 2010). Tokumon et al. (2016) suggested that water pumping activity of the invasive bivalve, *Limnoperna fortunei* (Family Mytilidea) did not differ noticeably at different SIM concentrations, but at low sediment loads the production of pseudofaeces was moderate whereas at at high concentrations mussels expelled mucus-embedded strings of material at noticeably higher rates. This indicates that the ability of mussels to sort and ingest organic particles from total suspended solids can be reduced severely by SIM (Robinson et al. 1984, Berg et al 1996, Baker et al 1998).

Gascho Landis et al. (2013) showed that total suspended solids (TSS) interfered with fertilization and caused reproductive failure of *Ligumia subrostrata* (Family Unionidae). They found that clearance rates dropped abruptly and remained uniformly low at a threshold level of total suspended solids > 8 mg l^{-1}. Gascho Landis et al. (2013) proposed that "reduced clearance rates could decrease the chance of females encountering suspended sperm during filter feeding, or an increase in pseudofeces production could bind sperm in mucus and lead to its egestion before fertilization". They also concluded that "interruption of fertilization coincident with high TSS (total suspended solids) is a potential mechanism to explain the lack of mussel recruitment in many locations".

TSS can have profound effects on reproduction. In the Gascho Landis et al. (2013) study, the percentage of brooding *Ligumia subrostrata* females decreased sharply with increasing TSS and complete reproductive failure occurred in hypereutrophic ponds with TSS > 20 mg l^{-1}. They found that the proportion of females that became gravid during the experiment was strongly related to TSS best characterized by an exponential decline. At the lowest mean TSS, the majority of females were gravid, but this percentage declined rapidly with increasing mean TSS. No gravid unionid females were found at TSS >20 mg l^{-1} (Gascho Landis et al. 2013). Gascho Landis et al. (2013) also reported that *L. subrostrata* mussels were largely extirpated from lakes with the shallowest Secchi depths (hyper- eutrophic lakes), possibly indicating a threshold above which increased nutrients and resultant organic solids have a negative effect.

In other studies, decreased clearance rates (the volume of water cleared of particles per unit time) for 3 unionid species subjected to intermittent exposure to extremely high levels of suspended sediment was proposed as a cause of decreased growth or starvation (Aldridge et al. 1987). Recruitment strength of *Margaritifera margaritifera*, the European version of *M. falcata* was negatively related to turbidity and deposited sediment, but the mechanism for this relationship was unclear (Osterling et al. 2010). Others have also shown that unionid filter feeding is often disrupted at levels > 20 mg l^{-1} (Hornbach et al. 1984, Way et al. 1990).

Even relatively pollution tolerant invasive Asian clams (*Corbicula* sp.) and fingernail clams (Sphaerium) initiated pseudofeces production at 17 to 20 mg l^{-1} TSS (Fuji 1979, Hornbach et al. 1984, Way et al. 1990). Invasive Zebra mussels (*Dreissena polymorpha*) can initiate pseudofeces production at 27 mg l^{-1} (Lei et al. 1996, Schneider et al. 1998) and TSS loads dominated by inorganic particles can decrease their growth rates (Osterling et al. 2007).

SIM and Native Mussel Viability in the Utah Lake/Jordan River Drainage

Total suspended solids in Utah Lake and Jordan River proper, although relatively low compared to many other waters in the world (Meybeck 2003), have levels that are likely detrimental to native mussel viability. By itself, high levels of TSS could explain the absence of *Margaritifera falcata* and the near extirpation of *Anodonta nuttalliana/ californiensis* from this drainage. Combined with the other factors reported in the Richards 2016 reports; the likelihood of recolonization of either taxon in the drainage is near zero.

Jordan River Farmington Bay Water Quality Council researchers reported TSS levels of 56.3 mg l^{-1} (VSS = 11.7 mg l^{-1}) in Utah Lake at its outlet into the Jordan River. Background TSS levels are typically between 23 and 38 mg l^{-1} (VSS about 5 mg l^{-1}) downstream in the Jordan River. These TSS levels are well within and above the known ranges that have been shown to severely affect mussel reproduction (see Literature Review above). High levels of TSS in Beer Creek that supports one of the last remaining *Anodonta nuttalliana/ californiensis* populations could also partially explain why no apparent reproduction has been observed. TSS will likely continue to negatively affect remaining native mussel viability and their recolonization potential in the Utah Lake/Jordan River drainage until TSS levels are drastically reduced from sources such as erosion related to agriculture, forestry, industrialization, and urbanization.

Literature Cited

Aldridge, D. W., Payne, B. S., A. C. Miller. 1987. The effects of intermittent exposure to suspended solids and turbulence on 3 species of freshwater mussels. Environmental Pollution 45:17–28.

Alexander, J. E., Thorp, J. H. and R. D. Fell. 1994. Turbidity and temperature effects on oxygen consumption in the Zebra Mussel (*Dreissena polymorpha*). Canadian Journal of Fisheries and Aquatic Sciences. 51: 179-184.

Baker, S. M. Levinton, J. S. , Kurdziel, J. P. and S. E. Shumway. 1998. Selective feeding and biodeposition by zebra mussels and their relation to changes in phytoplankton composition and seston load. Journal of Shellfish Research. 17: 1207-1213.

Berg, D. J., Fisher, S. W. and P. F. Landrum. 1996. Clearance and processing of algal particles by zebra mussels (*Dreissena polymorpha*). Journal of Great Lakes Research. 22: 779-788.

Box, J.B. and J. Mossa. 1999. Sediment, land use, and freshwater mussels: prospects and problems. Journal of the North American Benthological Society, 18, 99–117.

Cheung, S. and P. Shin. 2005. Size effects of suspended particles on gill damage in green-lipped mussel. Marine Pollution Bulletin. 51: 801-810.

Fuji, A. 1979. Phosphorous budget in a natural population of *Corbicula* japonica Prime in a poikilohaline lagoon, Zyusan-Ko. Bulletin of the Faculty of Fisheries Hokkaido University 30:34–49.

Gascho Landis, A. M. Haag, W. R. and J. A. Stoeckel. 2013. High suspended solids as a factor in reproductive failure of a freshwater mussel. Freshwater Science. 32: 70-81.

Hornback, D. J. , Way, C. M. Wissing, T. E., and A. J. Burky. 1984. Effects of particle concentration and season on the filtration rates of the freshwater clam, Sphaerium striatinum Lamarck (Bivalvia, Pisidiidae). Hydrobiologia. 108:83–96.

Jorgensen, C. B. 1990. Bivalve filter feeding: hydrodynamics, bioenergetics, physiology and ecology. Olsen and Olsen. Fredensborg. Denmark.

Jorgensen, C. B. 1996. Bivalve filter feeding revisited. Marine Ecology Progress Series. 142: 287-302.

Lei, J., Payne, B. S. and S. Y. Wang. 1996. Filtration dynamics of the Zebra Mussel, *Dreissena polymorpha*. Canadian Journal of Fisheries an Aquatic Sciences. 53: 29-37.

Meybeck, M., Laroche,L, Durr, H. H., and J. P. M. Syvitski. 2003. Global variability of daily total suspended solids and their fluxes in rivers. Global and Planetary Change. 39:65-93.

Osterling, E. M. Bergman, E. , Greenberg, L. A., Baldwin, B. S., and E. L. Mills. 2007. Turbidity-mediated interactions between invasive filter-feeding mussels and native bioturbating mayflies. Freshwater Biology 52:1602–1610.

Robinson, W. E., Wehling, W.E., and M. P. Morse. 1984. The effect of suspended clay on feeding and digestive efficiency of the surf clam, *Spisula solidissima* (Dilwyn). Journal of Experimental Marine Biology and Ecology, 14: 1-12.

Rosewarne, P. J., Svendsen, J. C., Mortimer, R. J. G. and A. M. Dunn. 2013. Muddied waters: suspended sediment impacts on gill structure and aerobic scope in an endangered native and an invasive freshwater crayfish. Hydrobiologia. 722: 61-74.

Safi, K. A., and B. Hayden. 2010. Differential grazing on natural planktonic populations by the mussel *Perna canaliculus*. Aquatic Biology. 11: 113-125.

Schneider, D. W., Madon, S. p., Stoeckel, J. A., and R. E. Sparks. 1998. Seston quality controls zebra mussel (Dreissena polymorpha) energetics in turbid rivers. Oecologia (Berlin). 117:331–341.

Tokumon, R. , Cataldo, D., and D. Boltovskoy. 2016. Effects of suspended inorganic matter on filtration and grazing rates of the invasive mussel *Limnoperna fortunei* (Bivalvia: Mytiloidea). Journal of Molluscan Studies. 82: 201-204.

Velasco, L. A. and J. M. Navarro. 2005. Feeding physiology of two bivalves under laboratory and field conditions in response to variable food concentrations. Marine Ecology Progress Series. 201: 115-124.

Way, C. M., Hornbach, D. J., Payne, B. S., and A. C. Miller. 1990. Dynamics of filter feeding in *Corbicula fluminea* (Bivalvia, Corbiculidae). Canadian Journal of Zoology 68:115–120.

Waters, T. F. 1995. Sediment in streams: sources, biological effects, and control. American Fisheries Society, Bethesda, Maryland.

Chapter 13

Apparent extinction of native mussels in Lower Mill Creek and Mid-Jordan River, UT

This chapter, Richards, D.C. and T. Miller. 2019. Apparent extinction of native mussels in Lower Mill Creek and Mid-Jordan River, UT. Western North American Naturalist. 79(1): 72-74. is included as a pdf attachment to this volume

Western North American Naturalist 79(1), © 2019, pp. 72–84

Apparent extinction of native mussels in Lower Mill Creek and Mid-Jordan River, Utah

DAVID C. RICHARDS[1,*] AND THERON MILLER[2]

[1]*OreoHelix Consulting, Vineyard, UT* [2]*Wasatch Front Water Quality Council, Salt Lake City, UT*

ABSTRACT.—Native mussels likely occurred in Mill Creek and the Jordan River, Utah, in the past. However, human-induced impacts have virtually eliminated the possibility of their continued existence in these waters. We conducted an intensive native mussel survey upstream and downstream of a water reclamation facility discharge into Mill Creek and the Jordan River to determine its effects on mussel populations. The survey was conducted from September to October 2017 and resulted in approximately 7.6 m^3 of >4 mm-sized substrate particles being thoroughly examined at near 100% efficiency. We then used statistical models to estimate population densities as a function of probability of detection and search efficiencies based on this and other surveys. Regrettably, no live or recently dead native mussels were found. Given that our survey methods provided near perfect search efficiency, native mussel densities were estimated to be <<0.03 per m^2, which is much lower than what we consider to be a viable population density. Combined with multiple lines of evidence from other surveys, this low density strongly points toward the conclusion that native mussels are extinct in the survey area. Reasons for the demise of native mussels in Mill Creek and the Jordan River are numerous, and these factors need to be aggressively addressed if native mussels are to survive in the drainage.

RESUMEN.—Es probable que en el pasado habitaran mejillones nativos en el río Mill Creek y Jordan en Utah. Sin embargo, los impactos ocasionados por el hombre han eliminado prácticamente la posibilidad de su existencia en estas aguas. Llevamos a cabo un estudio intensivo de mejillones nativos, río abajo y río arriba en una instalación de descarga de agua reciclada en Mill Creek y en el río Jordan para determinar sus efectos en las poblaciones de mejillones. El estudio se llevó a cabo en septiembre y octubre del año 2017, en los cuales, se examinaron minuciosamente aproximadamente, 7.6 m^3 de partículas de sustrato de tamaño >4 mm, con una eficacia cercana al 100%. Posteriormente, utilizamos modelos estadísticos para estimar las densidades poblacionales en función de su probabilidad de detección y de la eficiencia de búsqueda, basada en este y en otros muestreos. Desafortunadamente, no encontramos mejillones nativos vivos o recientemente muertos. Debido a que, nuestros métodos de muestreo proporcionaron una eficacia de búsqueda casi perfecta, se estimó que la densidad de mejillones nativos es <<0.03 m^{-2}, mucho menor a lo que consideramos como una densidad poblacional viable, y cuando se combina con múltiples evidencias de otros muestreos, indica que los mejillones nativos están extintos en el área de estudio. Las razones de la desaparición de los mejillones nativos en los ríos Mill Creek y el Jordan son numerosas, y tales factores necesitan abordarse intensivamente para que los mejillones nativos puedan sobrevivir en el drenaje.

North America supports the richest diversity of freshwater mollusks (clams, mussels, and snails) on the planet, with at least 700 species of snails and 300 species of freshwater mussels (Johnson et al. 2013, FMCS 2015). Freshwater mollusks serve vital functions in freshwater ecosystems, are excellent indicators of water quality, and are increasingly recognized as important ecosystem providers (Huryn et al. 1995, Covich et al. 1999, Ostroumov 2005, Fulford et al. 2007, Brown and Lydeard 2010, Johnson et al. 2013). Unfortunately, freshwater mollusks are one of the most disproportionally imperiled groups on earth. Approximately 72% of North American freshwater mussel taxa are considered endangered, threatened, or species of concern (NatureServe 2014). This alarming decline is almost entirely due to human activities (Williams et al. 1993).

The greatest diversity of North America's freshwater mussels occurs in the southeastern USA, whereas in the western half of North America the mussel fauna is relatively depauperate. However, the area consisting of the

*Corresponding author: oreohelix@icloud.com

313

Chapter 14

Numeric Water Quality Criteria Recalculation for Several Toxicants Related to Central Valley Water Reclamation Facility Discharge into Mill Creek, Salt Lake County, UT

Part 1: Ammonia

by

David C. Richards, Ph.D.

OreoHelix Consulting

Summary

EPA regulations allow states to adopt water quality criteria that reflect site-specific conditions based on sound scientific rational. One EPA recommended site-specific method is the 'Recalculation Procedure' that best reflects the species that reside at a site and is used to edit the taxonomic composition of a toxicity dataset used for Species Sensitivity Distributions. The underlying premise of the Recalculation Procedure is, "taxonomy has value in predicting sensitivity".

It is well documented that ammonia (NH_3) can be highly toxic to aquatic organisms, particularly Unionoida mussels, non-pulmonate snails, and other sensitive species, and that ammonia criteria need to be developed by state water quality management agencies to protect these species. However, these taxa may be absent at a site and costs to treatment facilities and citizens to implement ammonia criteria based on taxa that are absent may be unnecessary, an economic burden, or misdirected from projects that could actually benefit the aquatic habitat of these sites.

The Jordan River/ Farmington Bay Water Quality Council contracted Dr. David C. Richards, OreoHelix Consulting to initiate an ammonia Recalculation Procedure and Deletion Process based on taxa that are 'resident' to the sections of Mill Creek and downstream sections of the Jordan River, UT that could potentially be affected by Central Valley Water Reclamation Facilities discharge using EPA recommended procedures. For the purpose of this recalculation, the 'site' was designated as the degraded section of Mill Creek upstream of CVWRF to the bridge at Interstate -15 (UDWQ designated 'non game fishery') and downstream in the Jordan River to 2100 South, Salt Lake City (UDWQ designated 'warm water fishery').

The most relevant and useful macroinvertebrate datasets available for the site were selected, as were amphibian and fish datasets. ITIS, the taxonomic system recommended by EPA was used for consistency. Taxa were determined to be 'resident' or 'not resident' based on EPA guidelines. This deletion and recalculation process adhered to EPAs guidelines including those for 'critical species' acute values, species sensitivity distributions, and chronic values were calculated using EPA methods. Recalculation criteria were slightly lower but similar and consistent with EPA's recent ammonia criteria that were based on mussel and rainbow trout absence; further justification for recalculating NH_3 criteria for CVWRF's discharge into Mill Creek. Several problems need to be addressed to further improve recalculations and to evaluate EPAs reliance on these guidelines and methods. There is an urgent need to determine residency status of fish and amphibian taxa in the Mill Creek site. The reliance of surrogate taxa for invasive, ecosystem altering taxa that occur in Mill Creek is also very problematic and questionable and the determination of Unionoida residency continues to plague recalculation efforts. One major concern is the absence of error estimates in any of the EPA recommended steps in the process, which likely results in imprecise criteria values. Nevertheless, the determination of resident taxa in the Mill Creek site and many of the calculations derived in this recalculation process can now be easily used for recalculation of any toxicant of concern by CVWRF, as long as there is ample sensitivity data in the national ECOTOX database. A thorough rechecking of the calculations to verify accuracy,

particularly during the deletion process is recommended, as is verification of truly resident taxa. Further statistical analyses to test the supposition that there is use or value in presuming relationships between phylogeny and NH_3 sensitivity is highly recommended, as are future criteria recalculations that incorporate error estimates. Finally, laboratory ammonia toxicity tests are urgently needed on several species including *Anodonta* (native mussel), *Corbicula* (invasive clam), *Pisidium* sp., a native clam whose within- family surrogate is one of the most ammonia sensitive species which doesn't occur at the site, and *P. antipodarum* (New Zealand mudsnail), whose family level surrogate is the highly sensitive *Fluminicola* (pebblesnail), which also doesn't occur at the site.

Table of Contents

List of Figures

List of Tables

List of Appendices

> ***"A statement of a criterion as a number that is not to be exceeded any time or place is not acceptable because few, if any, people who use criteria would take it literally and few, if any, toxicologists would defend a literal interpretation." (USEPA 2010, page 4)***

Introduction

Site Specific Water Quality Criteria and The Recalculation Procedure

EPA regulation at 40 CFR § 131.11(b)(l)(ii) "provides that states and tribes may adopt water quality criteria that "… reflect site-specific conditions." (USEPA 2013b, 2013c). "Site-specific criteria are intended to come closer than the national criteria recommendations to providing the intended level of protection to the aquatic life at the site, usually by taking into account the biological and/or chemical conditions (i.e., the species composition and/or water quality characteristics) at the site. Site-specific criteria, as with all water quality criteria, must be based on a sound scientific rationale and protect the designated use" (USEPA 2013c). Additionally, "EPA's decision to approve or disapprove site-specific criteria is not based on whether the resulting criteria are more or less stringent than EPA guidance" (USEPA 2013c).

One of the methods that EPA recommends for adoption of site-specific water quality criteria is the 'Recalculation Procedure'; "intended to provide flexibility to States to derive site-specific criteria that best reflect the species that reside at a site" (USEPA 2013a). "The Recalculation Procedure is used to edit the taxonomic composition of the toxicity dataset used for the Species Sensitivity Distribution (SSD) upon which a site-specific criterion is based, in order to better match the assemblage that resides at the site (USEPA 2013c). The underlying premise of the Recalculation Procedure is that "taxonomy has value in predicting sensitivity[10]," (USEPA 2013a). A site-specific Species Sensitivity Distribution (SSD) can be adjusted to reflect the taxonomy of species that reside at a site. "The core of the procedure is the Deletion Process, which involves removing tested species from the SSD. The recommended procedure allows deletion of nonresident tested species if and only if they are not appropriate surrogates of resident untested species – based on taxonomy."

Justification

It is well documented that ammonia (NH_3) can be highly toxic to aquatic organisms, particularly Unionoida mussels, non-pulmonate snails, and other sensitive species, and that ammonia criteria need to be developed by state water quality management agencies to protect these species (USEPA 2013b). However, Unionoida, non-pulmonate snails, and other sensitive taxa that were used to develop EPAs 2013 ammonia criteria may be absent at site specific locations and the cost to treatment facilities and

[10] This assumption has not been tested and is subject to much debate by ecologists and toxicologists. Richards (2016) Technical Memo suggests there is little or no evidence for this assumption based on NH_3 sensitivities using EPAs NH_3 national criteria dataset.

citizens to implement ammonia criteria based on taxa that are absent may be unnecessary, an economic burden, or misdirected from projects that could actually benefit the aquatic habitat of these sites.

In response to the new EPA 2013 proposed NH_3 criteria and the need to potentially reevaluate the Central Valley Water Reclamation Facility (CVWRF) ammonia discharge limits into Mill Creek; the Jordan River Farmington Bay Water Quality Council, Salt Lake City, UT contracted Dr. David C. Richards, OreoHelix Consulting, Moab UT to initiate a Recalculation Procedure and Deletion Process based on taxa that are 'resident' to the sections of Mill Creek and downstream sections of the Jordan River that could potentially be affected by CVWRF discharge. These analyses are in addition and supplementation to the extensive mollusk survey that Richards (2016) and colleagues conducted in Mill Creek and nearby water bodies and which, based on these intensive surveys and other researchers, concluded that the status of Unionoida mussels in Mill Creek and the Jordan River is currently likely to be 'non-present'. If any isolated populations do exist, their survival is likely in severe jeopardy (Richards 2015). Being as Unionoida mussels are not considered residents of the Mill Creek site, Richards 2015 suggested that NH_3 recalculation values be based on those recommended in Appendix N in the USEPA 2013b document. The recalculations presented here that are based on resident taxa other than mussels can be used as further evidence that NH_3 criteria recalculations are justified.

Central Valley Water Reclamation Facility

The Central Valley Water Reclamation Facility (CVWRF) at 800 West Central Valley Road (3190 South) in Salt Lake City, UT is the largest treatment facility in the greater Salt Lake City area. The CVWRF was designed and built to treat 75 million gallons of wastewater/day and serves over half a million people in Salt Lake County. CVWRF discharges treated water directly into Mill Creek approximately 400 m upstream of its confluence with the Jordan River. CVWRF management and operators are required by law to protect Mill Creek and the Jordan River environment receiving waters under the Clean Water Act, whose goal is 'to maintain and improve the physical, chemical, and biological integrity' of these waters for present and future generations (http://www.cvwrf.org/brochure/page3.php). The CVWRF Mission Statement reflects this ethic and as stated is to "Improve the Utah environment by treating wastewater and recovering resources, safely, efficiently and sustainably". CVWRF has worked closely with UDWQ throughout its history meeting these goals (http://www.cvwrf.org).

Methods

Site Description and Designation of Site Area

In the USEPA (2013c) Technical Support document (EPA 800-R-13-003), EPA states that; "In the general context of site-specific criteria, a "site" may be a region, watershed, waterbody, or segment of a waterbody". Exactly how the site is defined is a matter of state discretion, for example a site may be designated as, "A segment of a stream, river, lake reservoir, or wetland" or "Some specified distance upstream and downstream of a point-source discharge." (EPA 800-R-13-003). Additionally, USEPA (2013a) states that, "Use of the Recalculation Procedure does not sidestep the need to protect downstream uses".

In a collaborative effort, CVWRF, the Jordan River Farmington Bay Water Quality Council and UDWQ, determined that for the purpose of this reevaluation of ammonia criteria, the 'site' would be designated as follows:

Upstream boundary: Upstream of CVWRF to Interstate 15 bridge.

Downstream boundary: Extent of CVWRF physical, chemical, and biological influence in Jordan River at 2100 South, Salt Lake City.

UDWQ Designated Beneficial Uses of Mill Creek and the Jordan River Downstream

Mill Creek from I-15 to its confluence with the Jordan River (UDWQ Assessment Unit: Mill Creek- 1) is designated by UDWQ as *3C*, "Protected for nongame fish and other aquatic life, including the necessary aquatic organisms in their food chain." The section of the Jordan River from the confluence with Mill Creek downstream to 2100 South (UDWQ's Assessment Unit, Jordan-4) is designated as Use Class *3B* "warm water fishery and other aquatic life, including the necessary aquatic organisms in their food chain".

Table 66. Designated Beneficial Uses of Mill Creek and Jordan River at the recalculation site (Downloaded from Utah DEQ: DWQ: Beneficial Uses and Water Quality Assessment Map: HTTP://wq.deq.utah.gov.) Beneficial Use Classes: 2B = Infrequent primary contact recreation (e.g. wading, fishing); 3B = Warm water fishery/aquatic life; 3C = Protected for nongame fish and other aquatic life, included the necessary aquatic organisms in their food chain; 4 = Agricultural uses (crop irrigation and stock watering).

Unit Name	Unit ID	Beneficial Use Class	Unit Description
Mill Creek-1	UT16020204-026	2B, 3C, and 4	Mill Creek from confluence with Jordan River to Interstate 15 crossing
Jordan River-4	UT16020204-004	2B, 3B, and 4	Jordan River from 2100 South to the confluence with Little Cottonwood Creek

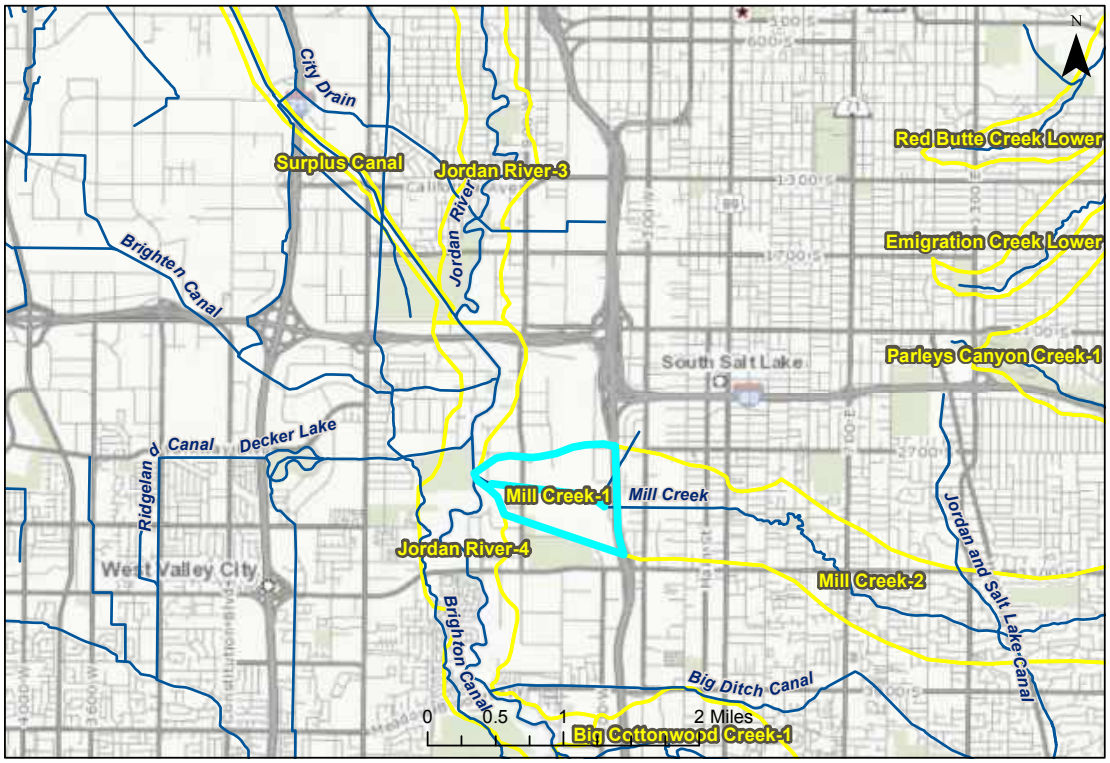

undefined: 0
undefined: 0
undefined: 414
undefined: 414
undefined: 414
Assessment Unit Name: Mill Creek-1
Unit ID: UT16020204-026
Unit Description: Mill Creek from confluence with Jordan River to Interstate 15 crossing
Beneficial Uses: Use Class 2B = Infrequent primary contact recreation (e.g. wading, fishing); Use Class 3C = Nongame fishery/aquatic life; Use Class 4 = Agricultural uses (crop irrigation and stock watering)
undefined: 1.032
Watershed Management Unit: Jordan River
undefined:
undefined:
2010 Assessment: Assessment Category 2 = Not impaired: assessed beneficial uses are supported, at least 1 use not assessed
Beneficial Use: Cause of Impairment:
TMDL Required: 303d Cause of Impairment: n/a
TMDL Approved: Cause of Impairment: n/a
Aquatic Habitat Impairment: n/a
undefined: 2
undefined:
undefined: 2
undefined:
undefined: 2

Figure 68. Beneficial use and water quality assessment map: UDWQ management unit, Mill Creek-1.

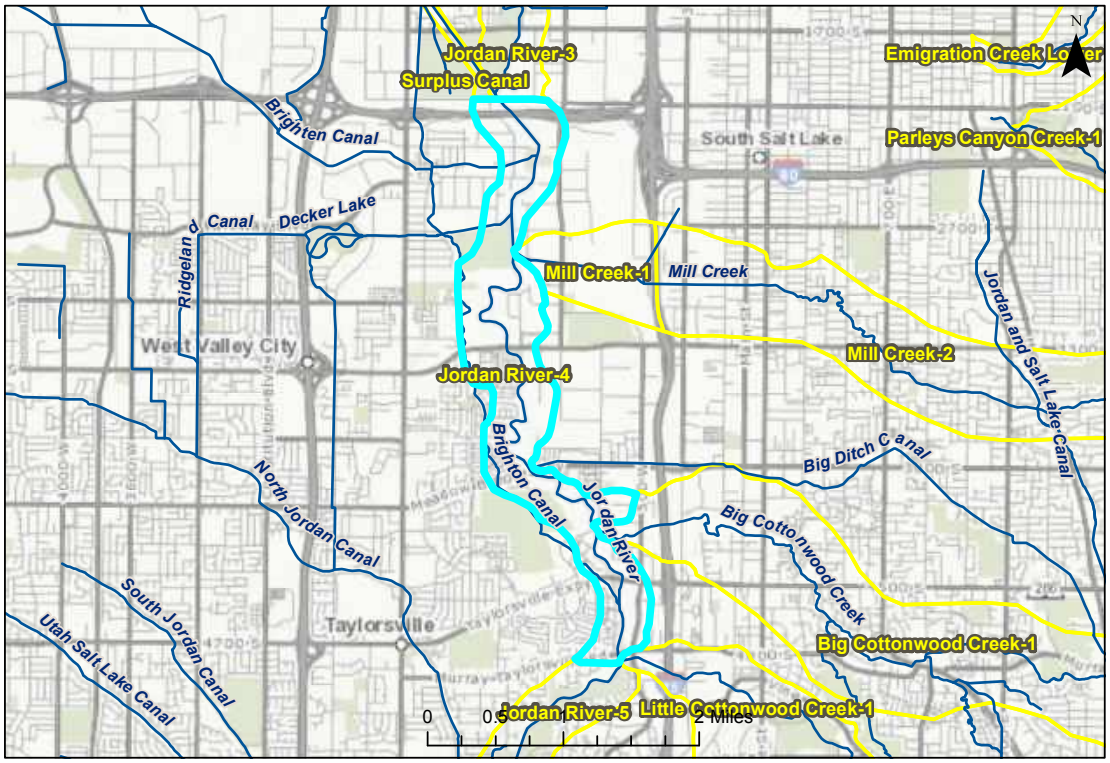

undefined: 0
undefined: 0
undefined: 496
undefined: 496
undefined: 496
Assessment Unit Name: Jordan River-4
Unit ID: UT16020204-004
Unit Description: Jordan River from 2100 South to the confluence with Little Cottonwood Creek
Beneficial Uses: Use Class 2B = Infrequent primary contact recreation (e.g. wading, fishing); Use Class 3B = Warm water fishery/aquatic life; Use Class 4 = Agricultural uses (crop irrigation and stock watering)
undefined: 6.287
Watershed Management Unit: Jordan River
undefined:
undefined:
2010 Assessment: Assessment Category 5 = Impaired: TMDL required (303d list)
Beneficial Use: Cause of Impairment: Use Class 3B: Benthic-Macroinvertebrate Bioassessments; Use Class 4: Total Dissolved Solids
TMDL Required: 303d Cause of Impairment: poor Benthic Macro-invertebrate Community, Total Dissolved Solids
TMDL Approved: Cause of Impairment: n/a
Aquatic Habitat Impairment: n/a
undefined: 5
undefined:
undefined: 2
undefined:

Figure 69. Beneficial use and water quality assessment map: UDWQ management unit, Jordan-4.

Mill Creek

Mill Creek, Salt Lake County, UT originates in the Wasatch mountains and then flows through the City of Salt Lake where it joins the Jordan River, which then empties into Farmington Bay of the Great Salt Lake. After leaving the Wasatch mountains and USFS lands, where it is relatively unimpaired, most of Mill Creek waters are captured for culinary purposes for use by the citizens of Salt Lake City. Remaining waters in Mill Creek are then supplemented and often dominated by waters transported directly from Utah Lake via the Jordan and Salt Lake Canal. After the water quality in Mill Creek has been compromised by waters from hyper eutrophic Utah lake, it then flows through a heavily urbanized, residential, and industrial landscape before entering the Jordan River. For the most part, this heavily impacted downstream section of Mill Creek:

1) has been channelized,

2) has been vastly dewatered and lost its natural ability to create meanders and floodplains has been curtailed,

3) has degraded integrity (river continuum) as flows and habitat have been altered,

4) has numerous industrial point source discharges,

5) experiences large urban and industrial runoff events,

6) is dominated by highly invasive taxa (including carp, Asian clams, and New Zealand mudsnails, black rats are frequently encountered along its banks, etc.),

7) has substrates that are predominately embedded with fine organic matter often > 50 cm thick (Richards 2015)

8) has trash that often comprises a significant portion of the substrate (Richards 2015) and

9) is designated by UDWQ as water quality impaired.

By all standards the section of Mill Creek that flows through Salt Lake City is in poor condition and has been poorly managed in the past. The macroinvertebrate assemblages and fish taxa resident to Mill Creek clearly reflect these conditions (see the following section *Species Datasets and Taxonomic System Used* and the *Results* section).

Species Datasets and Taxonomic System Used

“Perhaps the most important condition in defining species residency is that the taxa that occur at the site cannot be determined merely by a one-time sampling downstream and/or upstream of the site” (USEPA 2013c, page 5).

The most pertinent datasets available were used in the deletion process. The most important and inclusive macroinvertebrate data sets available and examined included:

1. Four sampling events in Mill Creek between 2014 and 2016 using 1 m^2 500-micron mesh kick samples, 8-12 replicates/event, collected by Dr. Richards, OreoHelix Consulting, Moab, UT and processed and taxonomic identifications completed by Brett Marshall, Adjunct Senior Aquatic Entomologist with the National Academy of Sciences at his laboratory River Continuum Concepts, Manhattan, MT. The level of taxonomic resolution performed by this lab was much greater than other available datasets from all other sources and helped to improve the likelihood of including all 'resident' taxa need for the deletion process.
2. A one-time sampling event conducted by UDWQ, November 2009 with a single upstream of CVWRF discharge composite sample and a single downstream of discharge composite sample. Taxonomic resolution was at standard bioassessment levels.
3. All macroinvertebrate data available from the Western Center for Monitoring and Assessment of Freshwater Ecosystems, BLM/USU National Aquatic Monitoring Center "MAPIT-Mapping Application for Freshwater Invertebrate Taxa" database (http://wmc6.bluezone.usu.edu). Taxonomic resolution was typically only to standard bioassessment levels.

Summaries of amphibian and fish species known to occur (resident) at the site were compiled from the Jordan River Commission website: http://jordanrivercommission.com; (http://jordanrivercommission.com/wp-content/uploads/2011/04/Fish-Species-of-the-Jordan-River-2011.pdf) for fish and (http://jordanrivercommission.com/wp-content/uploads/2011/11/Amphibians-of-the-Jordan-River-2011.pdf) for amphibians. The Jordan River Commission is a clearinghouse for species that occur in the area. It appears that no formal fish or amphibian surveys have been conducted at the site in recent years. As additional fish and amphibian data becomes available the deletion process and NH_3 recalculations will be updated.

"Because the Deletion Process is taxonomy based, it is important that one taxonomic system be used consistently in the derivation of national and site-specific criteria. The system that U.S. EPA uses is the Integrated Taxonomic Information System (ITIS; www.itis.gov)." This system was used for the deletion process and recalculation procedure reported in this document.

The Process

Resident Species

Whether a taxon was considered resident or not in the site was based on EPAs (2013a) definitions:

"the equivalent terms "resident" or "occur at the site" includes life stages and species that:

a. are usually present at the site,

b. are present at the site only seasonally due to migration,

c. are present at the site intermittently because they periodically return to or extend their ranges into the site,

d. were present at the site in the past, are not currently present at the site due to degraded conditions, but are expected to return to the site when conditions improve, or

e. are present in nearby bodies of water, are not currently present at the site due to degraded conditions, but are expected to be present at the site when conditions improve.

The terms "resident" or "occur at the site" do not include life stages and species that:

a. were once present at the site but cannot exist at the site now due to permanent alterations of the habitat or other conditions that are not likely to change within reasonable planning horizons, or

b. are still-water life stages or species that are found in a flowing-water site solely and exclusively because they are washed through the site by stream flow from a still-water site" (USEPA 2013a).

Resident "critical species"

EPA defines a 'critical species' as on that is listed as threatened or endangered under section 4 of the Endangered Species Act and suggests that the Deletion Process should not be undertaken unless toxicity data are available for at least one species in each class of aquatic plants or animals that contains a critical species (2013a). This requirement was met.

Deletion process

"Based on taxonomy, U.S. EPA (1994) provided the Recalculation Procedure with a step-by-step protocol for deciding which nonresident tested species to retain or delete. For any particular nonresident tested species, the decision process begins at the genus level: the species is either

(a) deleted,

(b) retained as a surrogate for resident untested species in the genus, or

(c) a decision is postponed.

If the decision is postponed, then the next higher taxonomic level is considered. For a nonresident tested species, this hierarchical process stops once the decision to delete or retain is made – that is, the decision to delete or retain is not reconsidered or reversed at a higher taxonomic level." (USEPA 2013a). "The Deletion Process is designed to ensure that:

1. Each species, genus, family, order, class, and phylum that occurs both at the site and in the national toxicity dataset is retained in the site-specific toxicity dataset.
2. Each species, genus, family, order, class, and phylum that occurs at the site but not in the national toxicity dataset is represented in the site-specific dataset by at least one species most closely related to it from the national dataset" (USEPA 2013a).

EPAs underlying Deletion Process principle is as follows:

> "1. Looking within a genus, are all of its resident species tested? (That is, are they in the national toxicity dataset?) If so, then delete the nonresident tested species in that genus. If not, retain them as surrogates.
>
> 2. Moving up to the family level, does every resident genus in a family contain at least one tested species? (That is, are all of its resident genera tested?) If so, then delete the tested species in the family's nonresident genera. If not, retain them. (Note that this is not asking whether every resident species in the family is tested. Rather it asks whether every resident genus in the family appears in the national toxicity dataset.)
>
> 3. Moving up each subsequent level, to order, class, and phylum, the concept remains parallel. Does every resident family in an order contain at least one tested species? Does every resident order in a class contain at least one tested species? Does every resident class in a phylum contain at least one tested species? In each case, if so, delete the nonresident. If not, retain as surrogates" (USEPA 2013a).

The specific steps used in the deletion process for determining Genus Mean Acute Values (GMAV) followed *Appendix 2. Longer Statement of the Deletion Process* (USEPA 2013a). See Appendix 3 for explanation of the steps used.

Acute

The primary method for calculating acute values was first to use the GMAVs for genera retained in the deletion process (Appendices 5, 7, and 8). Then the Final Acute Value (FAV) was calculated using the formulas provided in *Section IV. Final Acute Value, parts J – O*, page 16 in the USEPA 2010 Guidelines. The steps are listed below:

J. For each genus for which one or more SMAVs are available, the Genus Mean Acute Value (GMAV) should be calculated as the geometric mean of the SMAVs available for the genus.

K. Order the GMAVs from high to low.

L. Assign ranks, R, to the GMAVs from "1" for the lowest to "N" for the highest. If two or more GMAVs are identical, arbitrarily assign them successive ranks.

M. Calculate the cumulative probability, P, for each GMAV as R/(N+1).

N. Select the four GMAVs which have cumulative probabilities closest to 0.05 (if there are less than 59 GMAVs, these will always be the four lowest GMAVs).

O. Using the selected GMAVs and Ps, calculate

$$S^2 = \frac{\sum((\ln GMAV)^2) - ((\sum \ln GMAV))^2 / 4}{\sum (F) - ((\sum (\sqrt{P}))^2 / 4)}$$

$$L = (\sum (\ln GMAV) - S(\sum (\sqrt{P}))) / 4$$

$$A = S(\sqrt{0.05}) + L$$

$$FAV = e^A$$

An alternative method was used to develop SSDs that included important error estimates. This method is recommended by USEPA CADDIS EcoTox Volume 4: Data analyses, Species Sensitivity Distributions (SSDs) (https://www3.epa.gov/caddis/da_advanced_2.html)(Updated 22Feb2016). The probit regression SSD_Generator_V1.xlt provided by CADDIS was used. Statistical steps used to generate SSDs and FAVs using this alternative method are as follows:

1) Calculated the geometric mean and $\log_{10}$ of the mean for each taxon.

2) Converted ranks to proportions: Proportion=(rank-0.5)/Number of taxa.

3) Transformed proportions to probit. The probit is the inverse cumulative distribution function of the normal distribution with a mean of 5 and a standard deviation of 1. A mean of 5 was chosen to ensure that all probit values are non-negative.

4) Calculated the slope and intercept for Log_{10}Mean (X axis) * Probit (Y axis).

5) Calculated the $\log_{10}$ central tendency (Pred) for the regression line:

$\log_{10}$ Central Tendency=(Probit-Intercept)/Slope.

Prediction intervals were calculated after Neter et al. 1990.

6) Calculated the Mean Squared Error (MSE): For each taxon, subtracted the observed $\log_{10}$ mean (Obs) from the $\log_{10}$ central tendency (Pred), square, added these values and divided by n-2.

7) Calculated the Corrected Sum of Squares (CSSQ): For each taxon, squared each probit value then sum (sum of squares). Next, summed the probit values for all taxa, squared this result and divided by the number of taxa (average sum squared). Subtracted the average sum squared from the total sum of squares to get the CSSQ.

8) Calculated the Grand Mean (average of all $\log_{10}$ exposure values).

9) Calculated the Point Error: $[(MSE/(Slope^2))*(1+(1/n)+((Pred-Grand\ Mean)^2)]/CSSQ)$

10) Calculated the prediction intervals (PI) using the critical t value:

logPI=logCentralTendency +/- tCrit*(SQRT(PointError)) and finally,

11) Back converted results from log value: 10^{value}

Chronic

According to USEPA (2010) *Guidelines for Deriving Numerical National Water Quality Criteria for the Protection Of Aquatic Organisms and Their Uses* (page 19); "Depending on the data that are available concerning chronic toxicity to aquatic animals, the Final Chronic Value (*FCV*) might be calculated in the same manner as the Final Acute Value or by dividing the Final Acute Value by the Final Acute-Chronic Ratio (*ACR*)."

The later method was preferred therefore, the *FCV* was calculated by dividing the *FAV* by a Final-Acute-Chronic Ratio (*ACR*) developed using the deletion process and from Table F.1. Species, Genus and Taxon-specific *ACR*s for Freshwater Aquatic Animals Exposed to Ammonia (EPA 2013b). See Appendix 11 for the taxon specific ACRs for NH_3 used in the recalculation process. The *CMC* or Criterion Maximum Concentrations was calculated following EPA guidelines and was equal to one-half the Final Acute Value and the *CCC* or Criterion Continuous Concentration was set equal to the lowest of the Final Chronic Values" (USEPA 2010, page 29.)

Results

Acute

Final Acute Value (FAV)

Three Final Acute Values (*FAV*s) were calculated; the first with *Fluminicola* sp. resident, the second with *Fluminicola* sp. non- resident, and the third with three species that are considered rare in the Jordan River removed; Golden shiner (*Notemigonus crysoleucas*), Pebblesnail (*Fluminicola coloradensis*), and June sucker (*Chasmistes liorus*). The *FAV* with *Fluminicola* sp. resident was **66.89**, the *FAV* with *Fluminicola* not resident was **69.77**, and the *FAV* with three rare taxa removed was **75.28**. Tables 1 -3 contain the formulas, calculations and FAVs.

*Table 67. Methods and values used to calculate FAV with Fluminicola **resident** (N = total number of GMAVs in data set = 45)*

Rank	GMAV	ln(GMAV)	$ln(GMAV)^2$	P=R/(n+1)	√P
1	62.15	4.129551	17.05319	0.0217391	0.147442
2	63.02	4.143452	17.1682	0.0434783	0.2085144
3	71.56	4.270536	18.23748	0.0652174	0.255377
4	72.55	4.284276	18.35502	0.0869565	0.2948839
Sum		**16.827815**	**70.81389**	**0.2173913**	**0.9062173**

$S^2 = [70.8138 - (16.8278)^2/4] / [0.2174– (0.9062)^2/4] = 1.6593$

S = 1.2881

L = [16.8278 - (1.2881)(0.9062)]/4 = 3.9151

A = (1.2881)(√0.05) +3.9151 = 4.2032

FAV = $e^{4.2032}$ = 66.89

*Table 68. Methods and values used to calculate FAV with Fluminicola **not resident**. (N = total number of GMAVs in data set = 44)*

Rank	GMAV	ln(GMAV)	$ln(GMAV)^2$	P=R/(n+1)	√P
1	63.02	4.143452	17.1682	0.0222222	0.1490712
2	71.56	4.270536	18.23748	0.0444444	0.2108185
3	72.55	4.284276	18.35502	0.0666667	0.2581989
4	74.25	4.307438	18.55402	0.0888889	0.2981424
Sum		**17.005702**	**72.31472**	**0.2222222**	**0.916231**

$S^2 = [72.31472- (17.005702)^2/4] / [0.2222222– (0.916231)^2/4] = 1.3151$

S = 1.1468

L = [17.005702- (1.2454)(0.916231)]/4 = 3.9887

A = (1.1468)(√0.05) + 3.9887= 4.2452

FAV = $e^{4.2452}$ = 69.77

Table 69. Methods and values used to calculate FAV with three rare or not resident taxa removed. (N = total number of GMAVs in data set = 43)

Rank	GMAV	ln(GMAV)	ln(GMAV)^2	P=R/(n+1)	√P
1	71.56	4.2705	18.2374	0.0232	0.1524
2	72.55	4.2842	18.3550	0.0465	0.2156
3	74.25	4.3074	18.5540	0.0697	0.2641
4	89.06	4.4893	20.1539	0.0930	0.3049
Sum		**17.3515**	**75.3004**	**0.2325**	**0.9372**

S^2 = [75.3004- (17.3515)^2/4] / [0.2326– (0.9373)^2/4] = 2.4191

S = 1.5553

L = [17.3515- (1.5553)(0.9373)]/4 = 3.9734

A = (1.5553)(√0.05) + 3.9734= 4.321

FAV = $e^{4.321}$ = 75.28

Critical Species

The federally listed June sucker (*Chasmistes liorus*) is an unlikely but possible resident of the site. The surrogate for the June sucker included in the National Toxicity Dataset, *Chasmistes brevirostris* was therefore, included in the calculations at the genus level for the analyses that included *Flumincola* sp. as a resident and as not resident but not for analyses with the three rare or absent taxon deleted.

Alternative Species Sensitivity Distributions (SSDs)

The alternative probit regresssion *FAV*s had lower predicted mean values than those that were calculated and presented in Tables 1 -3 but were well within the prediction intervals (Table 5). There was no statistically significant difference between values using probit regression. Complete SSD results using probit regression are in Appendices 9, 10, and 11.

Table 70. Mean and lower and upper 95% prediction intervals for FAVs developed using probit regression species sensitivity distribution methods used by EPAs CADDIS EcoTox program (https://www3.epa.gov/caddis/da_advanced_2.html). Mean and prediction intervals are for the 5th percentile GMAVs.

	Mean	Lower 95% PI	Upper 95% PI
Fluminicola "resident"	46.247	28.256	75.693
Fluminicola "not resident"	47.792	28.825	79.238
Three rare or absent taxa removed	49.00	28.99	82.82

The *FAV* developed using EPA Appendix N. Table N.2 with mussels absent/RBT present was **48.21**, whereas with mussels absent/RBT absent the FAV was **76**. Therefore, the deletion and recalculation process resulted in similar but consistently lower *FAV* values than those reported by EPA based on mussels and RBT absent. These lower FAV values were likely a result of the most sensitive taxa and their surrogates (e.g *Fluminicola* (Pebblesnail), *Notemigonus* (Golden shiner), *Pseudacris* (Spring peeper), and *Hybognathus* sp. (Rio Grande silvery minnow)) having disproportionally more weight on the Mill Creek/Jordan River dataset with fewer taxa than with the more robust EPA dataset, which included a greater number of taxa. The number of taxa in a dataset affects EPA FAV calculations.

Chronic

The Acute Chronic Ratio (*ACR*) was calculated using taxa that had *ACR* values reported in USEPA 2013b (see Appendix 11, Table 6). Geometric means of the *ACR*s and 95% confidence intervals were 12.4556 (7.6054, 20.3989). The estimated Final Chronic Value (*FCV*) was 5.319 (3.248, 8.712); and the Criterion Continuous Concentration (*CCC*) was 5.319 (3.248, 8.712) (Table 6). The Chronic Maximum Concentrations (*CMC*s) were 33.45 with *Fluminicola* resident, 34.89 with *Fluminicola* not resident, and 37.64 for three rare or absent taxa removed.

Table 71. Taxa whose Acute Chronic Ratios were used to calculate chronic values.

Fluminicola sp.	7.94
Musculium transversum	42.5
Pimephales promelas	19.24
Ictalurus punctatus	4.8
Cyprinus carpio	8.1
Hyalella azteca	15.81
Lepomis cyanellus	6.468

Lepomis macrochirus	28.51
Micropterus dolomieui	13.61
Actinopterygii	8.973

Geometric mean = **12.4556 (7.6054, 20.3989)**

Final Chronic Value (*FCV*)= **5.319 (3.248, 8.712)**

Criterion Continuous Concentration (CCC) = *FCV* = **5.319 (3.248, 8.712)**

Criterion Maximum Concentration (CMC):

With *Fluminicola* sp. *CMC* = 0.5*66.89 = **33.45**

Without *Fluminicola* sp. *CMC* = 0.5*69.77 = **34.89**

Without three rare or absent taxa *CMC* = 0.5*75.28 = **37.64**

EPA (2013b) *CMC* excluding mussels and RBT = **38**.

Discussion

Results of this deletion and recalculation process were similar to and somewhat consistent with EPAs NH_3 criteria based solely on mussel and RBT presence/absence (USEPA 2013b). These results also bolster the decision to recalculate NH_3 criteria for CVWRFs discharge into Mill Creek. Several problems need to be addressed to further improve these calculations and to justify EPAs reliance on these methods. There is an urgent need to determine residency status of fish taxa in the Mill Creek site and particularly to determine if the June sucker (*Chasmistes liorus*) should be considered a resident, as well as Golden shiner (*Notemigonus)*. Amphibian surveys are also needed. The use of *Fluminicola* sp. (pebblesnail) as a surrogate for other taxa particularly the highly invasive New Zealand mudsnails (*Potamopyrgus antipodarum*) and Asian clams (*Corbicula* sp.) is problematic. *Fluminicola* sp. (i.e. *F. coloradensis*) likely do not occur in the site (they are more of a cold water species) and their use as surrogates to protect highly invasive, ecosystem-altering species such as *P. antipodarum* and *Corbicula* sp. is highly questionable and the continued use of these surrogates by EPA is possibly quite detrimental to critically evaluating the biological integrity of the Mill Creek site. The determination of Unionoida residency at the site is still in effect for any recalculation procedure until regulators can acknowledge or confirm that these taxa are no longer residents. For all practical purposes, Unionoida were assumed to be 'not resident' in the Mill Creek site because; 1) none of the macroinvertebrate datasets used in the analyses contained Unionoida species eventhough other bivalves were collected, 2) Richards (2015) intensive surveys did not find any individuals, and 3) there are no other recent reports of their residency.

One of the most important deficiencies exposed during this EPAs deletion and recalculation process was the absence of error estimates in any of the EPA recommended steps: starting from the untested premise that taxonomy (or more correctly phylogeny) has value in determining sensitivy to NH_3; to the highly variable within- species NH_3 sensitivies; and continuing through each succesive step to the derivations of final criteria values. Unfortunately, these systematic errors were likely multiplicative throughout each step of the process. In a brief technical memo to JR/FBWQC, Richards (2016) analyzed taxa from EPA's NH_3 criteria development report (USEPA 2013b) and showed that phylogeny had little or no ammonia sensivity predictive value, even between different phyla. In addition, the probit regression species sensitivity distributions (SSD) developed in this report and recommended by the EPA CADDIS program included prediction interval estimates. These model estimates suggested that any single point estimates, although potentionally accurate, likely were imprecise and unless addressed and accounted for could have costly consequences to citizens and to the aquatic environments of Utah, if enforced. As an additional example, by incorporating a basic understanding of the importance of model error, the geometric means of Acute Chronic Ratios (ACRs) calculated for chronic criteria in this report included error estimates (e.g. confidence intervals). For example, the *Criterion Continuous Concentration (CCC)* estimate based on geometric means of ACRs had a mean of 5.319 and 95% CIs between 3.248 to 8.712, quite a wide range when considering potential costs to society and environmental protection. In contrast, no error estimates were possible using point estimate formulas provided by and recommended by EPA. Hence, the precision of these estimates remains unknown, as is their ecological relevance. There also was also a paucity of chronic ammonia data, even at the national level on which to base criteria, which likely added to imprecise final values.

Conclusion and Recommendations

Results of this 'draft' Deletion and Recalculation Procedure for NH_3 in the Mill Creek site are strong evidence to support CVWRF ammonia recalculations. The determination of 'resident' taxa in the Mill Creek site completed in this report and many of the calculations derived therein can subsequently be used to recalculate any toxicant of concern by CVWRF, as long as there is ample sensitivity data in the national EcoTox database. A thorough rechecking of the calculations provided in this draft is recommended to verify accuracy, particularly the deletion process and determination of truly resident taxa. Further statistical analyses are needed to test the supposition that there is value in using phylogenic relationships for evaluating NH_3 sensitivty, as is the informed choice of requiring future criteria recalculations to include error estimates. Amphibian and fish surveys at the site in the near future to determine residency are highly recommended. Annual macroinvertebrate collections including mollusk surveys to monitor changes should also be considered. Finally, laboratory ammonia toxicity tests are urgently needed to be conducted on several species, particularly *Anodonta* (native mussel), *Corbicula* (invasive clam), *Pisidium* sp. a native clam whose within- family surrogate is one of the most NH_3 sensitive species and doesn't occur at the site, and for *P. antipodarum* (New Zealand mudsnail), whose family level surrogate is the highly sensitive *Fluminicola* (pebblesnail), which also doesn't occur at the site.

Literature Cited

Neter, J., W. Wasserman and M.H. Kutner. 1990. Applied Linear Statistical Models, 3rd ed. Irwin, Boston, MA. 1184 pp.

Posthuma, L., G.W. Suter II, and TP Traas. 2002. Species Sensitivity Distributions in Ecotoxicology. Lewis Publishers, Boca Raton, FL. 587 pp.

Richards, D. C. 2015. Recalculation of Ammonia Criteria for Central Valley Water Reclamation Facility's Discharge into Mill Creek, Salt Lake County, UT based on Native Unionoida Surveys and Metapopulation Dynamics. Final Draft Report. To: Jordan River/Farmington Bay Water Quality Council. Salt Lake City, UT. 92 pages.

Richards, D. C. 2016. Does phylogeny predict sensitivity to ammonia in freshwater animals using USEPA ammonia criteria data? Technical Memo. To: Jordan River/Farmington Bay Water Quality Council. Salt Lake City, UT. 15 pages.

United States Environmental Protection Agency. 1985. Ambient water quality criteria for ammonia - 1984. EPA-440/5-85-001. National Technical Information Service, Springfield, VA

United States Environmental Protection Agency. 1999. 1999 Update of ambient water quality criteria for ammonia. EPA-822-R-99-014. National Technical Information Service, Springfield, VA.

United States Environmental Protection Agency. 2009. Draft 2009 update aquatic life ambient water quality criteria for ammonia – freshwater. EPA-822-D-09-001. Office of Water, Office of Science and Technology, Washington, DC.

United States Environmental Protection Agency. 2010. Guidelines for deriving numerical national water quality criteria for the protection of aquatic organisms and their uses. EPA-PB85-227049.

United States Environmental Protection Agency. 2013a. The revised deletion process for the site-specific recalculation procedure for aquatic life criteria. EPA 823-R-13-001. National Technical Information Service, Springfield, VA.

United States Environmental Protection Agency. 2013b. Aquatic life ambient water quality criteria for ammonia-freshwater. EPA 822-R-13-001.

United States Environmental Protection Agency. 2013c. Technical support document for conducting and reviewing freshwater mussel occurrence surveys fo the development of site-specific water quality criteria for ammonia. EPA 800-R-13-003.

U.S. Environmental Protection Agency (EPA). 2005. Methods/indicators for determining when metals are the cause of biological impairments of rivers and streams: species sensitivity distributions and chronic exposure-response relationships from laboratory data. Cincinnati, Ohio, U.S. EPA, Office of Research and Development, National Center for Environmental Assessment.

Acknowledgements

The author would like to thank, Dr. Tim Graham for QA/QC of the deletion process, Brett Marshall, River Continuum Concepts, Manhattan, MT for his above and beyond the call of duty taxonomic identification efforts, and the JRFBWQC for funding.

Appendices

Appendix 38 Acute toxicity of ammonia to aquatic animals including SMAV (mg TAN/L). Ammended from Appendix A, EPA 822-R-13-001.

Phylum	Class	Order	Family	Genus	Species	SMAV (mg TAN/L)
Annelida	Citellata	Haplotaxida	Tubificidae	*Limnodrilus*	*Limnodrilus hoffmeisteri*	170.2
Annelida	Citellata	Lumbriculida	Lumbriculidae	*Lumbriculus*	*Lumbriculus variegatus*	218.7
Annelida	Clitellata	Oligochaeta	Naididae	*Tubifex*	*Tubifex tubifex*	216.5
Arthropoda	Branchiopoda	Cladocera	Chydoridae	*Chydorus*	*Chydorus sphaericus*	162.6
Arthropoda	Branchiopoda	Cladocera	Daphnidae	*Ceriodaphnia*	*Catostomus platyrhynchus*	136.2
Arthropoda	Branchiopoda	Cladocera	Daphnidae	*Ceriodaphnia*	*Ceriodaphnia acanthina*	154.3
Arthropoda	Branchiopoda	Cladocera	Daphnidae	*Ceriodaphnia*	*Ceriodaphnia dubia*	134.2
Arthropoda	Branchiopoda	Cladocera	Daphnidae	*Daphnia*	*Daphnia magna*	**157.7**
Arthropoda	Branchiopoda	Cladocera	Daphnidae	*Daphnia*	*Daphnia pulicaria*	**99.0**
Arthropoda	Branchiopoda	Cladocera	Daphnidae	*Simocephalus*	*Simocephalus vetulus*	142.9
Arthropoda	Insecta	Coleoptera	Elmidae	*Stenelmis*	*Stenelmis sexlineata*	735.9
Arthropoda	Insecta	Diptera	Chironomidae	*Chironomus*	*Chironomus riparius*	1029.0
Arthropoda	Insecta	Diptera	Chironomidae	*Chironomus*	*Chironomus tentans*	451.8
Arthropoda	Insecta	Ephemeroptera	Baetidae	*Callibaetis*	*Callibaetis skokianus*	364.6
Arthropoda	Insecta	Ephemeroptera	Baetidae	*Callibaetis*	*Callibaetis* sp.	166.7

Arthropoda	Insecta	Ephemeroptera	Ephemereliidae	*Drunella*	*Drunella grandis*	442.4
Arthropoda	Insecta	Odonata	Coenagrionidae	*Enallagma*	*Enallagma* sp.	164.0
Arthropoda	Insecta	Odonata	Coenagrionidae	*Erythromma*	*Erythromma najas*	2515.0
Arthropoda	Insecta	Odonata	Libellulidae	*Pachydiplax*	*Pachydiplax longipennis*	233.0
Arthropoda	Insecta	Plecoptera	Perlodidae	*Skwala*	*Skwala americana*	192.4
Arthropoda	Insecta	Trichoptera	Limnephilidae	*Philarctus*	*Philarctus quaeris*	994.5
Arthropoda	Malacostraca	Amphipoda	Crangonyctidae	*Crangonyx*	*Crangonyx pseudogracilis*	270.5
Arthropoda	Malacostraca	Amphipoda	Crangonyctidae	*Crangonyx*	*Crangonyx* sp.	122.2
Arthropoda	Malacostraca	Amphipoda	Hyalellidae	*Hyalella*	*Hyalella azteca*	192.6
Arthropoda	Malacostraca	Decapoda	Cambaridae	*Orconectes*	*Orconectes immunis*	1550.0
Arthropoda	Malacostraca	Decapoda	Cambaridae	*Orconectes*	*Orconectes nais*	303.8
Arthropoda	Malacostraca	Decapoda	Cambaridae	*Procambarus*	*Procambarus clarkii*	138.0
Arthropoda	Malacostraca	Isopoda	Asellidae	*Asellus*	*Asellus aquaticus*	378.2
Arthropoda	Malacostraca	Isopoda	Asellidae	*Caecidotea*	*Caecidotea racovitzai*	387.0
Chordata	Actinopterygii	Acipenseriformes	Acipenseridae	*Acipenser*	*Acipenser brevirostrum*	156.7
Chordata	Actinopterygii	Cypriniformes	Catostomidae	*Catostomus*	*Catostomus commersonii*	157.5
Chordata	Actinopterygii	Cypriniformes	Catostomidae	*Chasmistes*	*Chasmistes brevirostris*	69.4
Chordata	Actinopterygii	Cypriniformes	Catostomidae	*Deltistes*	*Deltistes luxatus*	56.6

Chordata	Actinopterygii	Cypriniformes	Cyprinidae	*Campostoma*	*Campostoma anomalum*	115.9
Chordata	Actinopterygii	Cypriniformes	Cyprinidae	*Cyprinella*	*Cyprinella lutrensis*	196.1
Chordata	Actinopterygii	Cypriniformes	Cyprinidae	*Cyprinella*	*Cyprinella spiloptera*	83.8
Chordata	Actinopterygii	Cypriniformes	Cyprinidae	*Cyprinella*	*Cyprinella whipplei*	80.9
Chordata	Actinopterygii	Cypriniformes	Cyprinidae	*Cyprinus*	*Cyprinus carpio*	106.3
Chordata	Actinopterygii	Cypriniformes	Cyprinidae	*Hybognathus*	*Hybognathus amarus*	72.6
Chordata	Actinopterygii	Cypriniformes	Cyprinidae	*Notemigonus*	*Notemigonus crysoleucas*	63.0
Chordata	Actinopterygii	Cypriniformes	Cyprinidae	*Notropis*	*Notropis topeka*	96.7
Chordata	Actinopterygii	Cypriniformes	Cyprinidae	*Pimephales*	*Pimephales promelas*	159.2
Chordata	Actinopterygii	Cyprinodontiformes	Poeciliidae	*Gambusia*	*Gambusia affinis*	219.3
Chordata	Actinopterygii	Cyprinodontiformes	Poeciliidae	*Poecilia*	*Poecilia reticulata*	74.7
Chordata	Actinopterygii	Gasterosteiformes	Gasterosteidae	*Gasterosteus*	*Gasterosteus aculeatus*	281.5
Chordata	Actinopterygii	Perciformes	Centrarchidae	*Lepomis*	*Lepomis cyanellus*	150.8
Chordata	Actinopterygii	Perciformes	Centrarchidae	*Lepomis*	*Lepomis gibbosus*	77.5
Chordata	Actinopterygii	Perciformes	Centrarchidae	*Lepomis*	*Lepomis macrochirus*	104.5
Chordata	Actinopterygii	Perciformes	Centrarchidae	*Micropterus*	Micropterus dolomieu	150.6
Chordata	Actinopterygii	Perciformes	Centrarchidae	*Micropterus*	*Micropterus salmoides*	86.0
Chordata	Actinopterygii	Perciformes	Centrarchidae	*Micropterus*	*Micropterus treculii*	54.5

Chordata	Actinopterygii	Perciformes	Cichlidae	*Oreochromis*	*Oreochromis mossambicus*	185.2
Chordata	Actinopterygii	Perciformes	Moronidae	*Morone*	*Morone chrysops*	144.0
Chordata	Actinopterygii	Perciformes	Moronidae	*Morone*	*Morone saxatilis*	246.2
Chordata	Actinopterygii	Perciformes	Moronidae	*Morone*	*Morone saxatilis x chrysops*	70.2
Chordata	Actinopterygii	Perciformes	Percidae	*Etheostoma*	*Etheostoma nigrum*	71.5
Chordata	Actinopterygii	Perciformes	Percidae	*Etheostoma*	*Etheostoma spectabile*	77.2
Chordata	Actinopterygii	Perciformes	Percidae	*Sander*	*Sander vitreus*	117.1
Chordata	Actinopterygii	Salmoniformes	Salmonidae	*Oncorhynchus*	*Oncorhynchus aguabonita*	112.1
Chordata	Actinopterygii	Salmoniformes	Salmonidae	*Oncorhynchus*	*Oncorhynchus clarkii*	78.9
Chordata	Actinopterygii	Salmoniformes	Salmonidae	*Oncorhynchus*	*Oncorhynchus gorbuscha*	180.7
Chordata	Actinopterygii	Salmoniformes	Salmonidae	*Oncorhynchus*	*Oncorhynchus kisutch*	87.1
Chordata	Actinopterygii	Salmoniformes	Salmonidae	*Oncorhynchus*	*Oncorhynchus mykiss*	82.9
Chordata	Actinopterygii	Salmoniformes	Salmonidae	*Prosopium*	*Prosopium williamsoni*	51.9
Chordata	Actinopterygii	Salmoniformes	Salmonidae	*Salmo*	*Salmo salar*	183.3
Chordata	Actinopterygii	Salmoniformes	Salmonidae	*Salvelinus*	*Salvelinus fontinalis*	156.3
Chordata	Actinopterygii	Salmoniformes	Salmonidae	*Salvelinus*	*Salvelinus namaycush*	159.3
Chordata	Actinopterygii	Scorpaeniformes	Cottidae	*Cottus*	*Cottus bairdii*	222.2
Chordata	Actinopterygii	Siluriformes	Ictaluridae	*Ictalurus*	*Ictalurus punctatus*	142.4

Chordata	Amphibia	Anura	Hylidae	*Pseudacris*	*Pseudacris crucifer*	61.2
Chordata	Amphibia	Anura	Hylidae	*Pseudacris*	*Pseudacris regilla*	83.7
Chordata	Amphibia	Anura	Pipidae	*Xenopus*	*Xenopus laevis*	122.5
Chordata	Amphibia	Anura	Ranidae	*Rana*	*Rana pipiens*	96.4
Mollusca	Bivalvia	Unionoida	Unionidae	*Actinonaias*	*Actinonaias ligamentina*	63.9
Mollusca	Bivalvia	Unionoida	Unionidae	*Actinonaias*	*Actinonaias pectorosa*	79.5
Mollusca	Bivalvia	Unionoida	Unionidae	*Alasmidonta*	*Alasmidonta heterodon*	>109.0
Mollusca	Bivalvia	Unionoida	Unionidae	*Epioblasma*	*Epioblasma capsaeformis*	31.1
Mollusca	Bivalvia	Unionoida	Unionidae	*Fusconaia*	*Fusconaia masoni*	47.4
Mollusca	Bivalvia	Unionoida	Unionidae	*Lampsilis*	*Lampsilis abrupta*	26.0
Mollusca	Bivalvia	Unionoida	Unionidae	*Lampsilis*	*Lampsilis cardium*	50.5
Mollusca	Bivalvia	Unionoida	Unionidae	*Lampsilis*	*Lampsilis fasciola*	48.1
Mollusca	Bivalvia	Unionoida	Unionidae	*Lampsilis*	*Lampsilis higginsii*	41.9
Mollusca	Bivalvia	Unionoida	Unionidae	*Lampsilis*	*Lampsilis rafinesqueana*	70.0
Mollusca	Bivalvia	Unionoida	Unionidae	*Lampsilis*	*Lampsilis siliquoidea*	55.4
Mollusca	Bivalvia	Unionoida	Unionidae	*Lasmigona*	*Lasmigona subviridis*	23.4
Mollusca	Bivalvia	Unionoida	Unionidae	*Potamilus*	*Potamilus ohiensis*	>109.0
Mollusca	Bivalvia	Unionoida	Unionidae	*Pyganodon*	*Pyganodon grandis*	70.7

Mollusca	Bivalvia	Unionoida	Unionidae	*Utterbackia*	*Utterbackia imbecillis*	46.9
Mollusca	Bivalvia	Unionoida	Unionidae	*Venustaconcha*	*Venustaconcha ellipsiformis*	23.1
Mollusca	Bivalvia	Unionoida	Unionidae	*Villosa*	*Villosa iris*	34.2
Mollusca	Bivalvia	Verenoida	Sphaeriidae	*Musculium*	*Musculium transversum*	89.4
Mollusca	Gastropoda	Hygrophila	Lymnaeidae	*Lymnaea*	*Lymnaea stagnalis*	88.6
Mollusca	Gastropoda	Hygrophila	Physidae	*Physa*	*Physa gyrina*	164.5
Mollusca	Gastropoda	Hygrophila	Planorbidae	*Planorbella*	*Planorbella*	211.6
Mollusca	Gastropoda	Neotaenioglossa	Hydrobiidae	*Fluminicola*	*Fluminicola* sp.	> 62.15
Mollusca	Gastropoda	Sorbeocncha	Pleuroceridae	*Pleurocera*	*Pleurocera uncialis*	68.5
Platyhelminthes	Trepaxonemata	Tricladida	Dendrocoelidae	*Dendrocoelum*	*Dendrocoelum lacteum*	119.5

Appendix 39. Mill Creek/Jordan River 'resident' taxa including common names and status for several species.

Phylum	**Class**	**Order**	**Family**	**Genus**	**Species**	**Common Name**	**Status**
Annelida	Clitellata	Arhynchobdellida	Erpobdellidae	*unidentified*	*unidentified*	leech	
Annelida	Clitellata	Oligochaeta	unidentified	*unidentified*	*unidentified*	aquatic worm	
Annelida	Clitellata	Oligochaeta	Naididae	*unidentified*	*unidentified*	aquatic worm	
Annelida	Clitellata	Rhynchobdellida	Glossiphoniidae	*Helobdella*	stagnalis	leech	

Annelida	Hirudinea	Rhynchobdellida	Glossiphoniidae	*Glossiphonia*	*complanata*	leech	
Arthropoda	Arachnida	Trombidiformes	Lebertiidae	*Lebertia*	*sp.*	mite	
Arthropoda	Entognatha	Collembola	unidentified	*unidentified*	*unidentified*	springtail	
Arthropoda	Insecta	Coleoptera	Elmidae	*Stenelmis*	*sp.*	riffle beetle	
Arthropoda	Insecta	Diptera	Ceratopogonidae	*Palpomyia/Bezzia*	*sp.*	Biting midge	
Arthropoda	Insecta	Diptera	Ceratopogonidae	*Probezzia*	*sp.*	Biting midge	
Arthropoda	Insecta	Diptera	Chironomidae	*unidentified*	*unidentified*	midge	
Arthropoda	Insecta	Diptera	Chironomidae	*unidentified*	*unidentified*	midge	
Arthropoda	Insecta	Diptera	Chironomidae	*Chironomus*	*sp.*	midge	
Arthropoda	Insecta	Diptera	Chironomidae	*Cricotopus*	*sp.*	midge	
Arthropoda	Insecta	Diptera	Chironomidae	*Cryptochironomus*	*sp.*	midge	
Arthropoda	Insecta	Diptera	Chironomidae	*Dicrotendipes*	*sp.*	midge	
Arthropoda	Insecta	Diptera	Chironomidae	*Glptotendipes*	*sp.*	midge	
Arthropoda	Insecta	Diptera	Chironomidae	*Parachironomus*	*sp.*	midge	
Arthropoda	Insecta	Diptera	Chironomidae	*Paratanytarsus*	*sp.*	midge	
Arthropoda	Insecta	Diptera	Chironomidae	*Paratendipes*	*sp.*	midge	

Arthropoda	Insecta	Diptera	Chironomidae	*Phaenopsectra*	*sp.*	midge	
Arthropoda	Insecta	Diptera	Chironomidae	*Procladius*	*sp.*	midge	
Arthropoda	Insecta	Diptera	Chironomidae	*Prodiamesa*	*sp.*	midge	
Arthropoda	Insecta	Diptera	Chironomidae	*Rheocricotopus*	*sp.*	midge	
Arthropoda	Insecta	Diptera	Chironomidae	*Thienemanniella*	*sp.*	midge	
Arthropoda	Insecta	Diptera	Chironomidae	*Tvetenia*	*sp.*	midge	
Arthropoda	Insecta	Diptera	Psychodidae	*Pericoma*	*sp.*	sewer fly	
Arthropoda	Insecta	Diptera	Psychodidae	*Psychoda*	*sp.*	sewer fly	
Arthropoda	Insecta	Diptera	Simuliidae	*Simulium*	*sp.*	black fly	
Arthropoda	Insecta	Diptera	Simuliidae	*Simulium*	*vittatum*	black fly	
Arthropoda	Insecta	Ephemeroptera	Baetidae	*Baetis*	*sp.*	mayfly	
Arthropoda	Insecta	Ephemeroptera	Caenidae	*Caenis*	*sp.*	mayfly	
Arthropoda	Insecta	Hemiptera	Corixidae	*Corisella*	*sp.*	water boatman	
Arthropoda	Insecta	Hemiptera	Corixidae	*Hesperocorixa*	*sp.*	water boatman	
Arthropoda	Insecta	Hemiptera	Corixidae	*Sigara*	*sp.*	water boatman	
Arthropoda	Insecta	Odonata	Calopterygidae	*Hetaerina*	*sp.*	Damselfly	
Arthropoda	Insecta	Odonata	Coenagrionidae	*unidentified*	*unidentified*	Damselfly	
Arthropoda	Insecta	Odonata	Coenagrionidae	*Argia*	*sp.*	Damselfly	

Arthropoda	Insecta	Odonata	Coenagrionidae	*Ischnura*	*sp.*	Damselfly	
Arthropoda	Insecta	Odonata	Corduliidae	*unidentified*	*unidentified*	Dragonfly	
Arthropoda	Insecta	Trichoptera	Hydropsychidae	*Cheumatopsyche*	*sp.*	caddis fly	
Arthropoda	Insecta	Trichoptera	Hydropsychidae	*Hydropsyche*	*sp.*	caddis fly	
Arthropoda	Insecta	Trichoptera	Hydroptilidae	*Hydroptila*	*sp.*	caddis fly	
Arthropoda	Insecta	Trichoptera	Leptoceridae	*unidentified*	*unidentified*	caddis fly	
Arthropoda	Malacostraca	Amphipoda	Gammaridae	*Gammarus*	*sp.*	scud	
Arthropoda	Malacostraca	Amphipoda	Hyalellidae	*Hyalella*	*sp.*	scud	
Arthropoda	Malacostraca	Copepoda	unidentified	*unidentified*	*unidentified*	copepod	
Arthropoda	Malacostraca	Isopoda	Asellidae	*Asellus*	*sp.*	sow bug	
Arthropoda	Malacostraca	Isopoda	Asellidae	*Caecidotea*	*sp.*	sow bug	
Chordata	Actinopterygii	Cypriniformes	Catostomidae	*Catostomus*	*ardens*	Utah sucker	common
Chordata	Actinopterygii	Cypriniformes	Catostomidae	*Catostomus*	*platyrhynchus*	Mountain sucker	uncommon
Chordata	Actinopterygii	Cypriniformes	Catostomidae	*Chasmistes*	*liorus*	June sucker	rare
Chordata	Actinopterygii	Cypriniformes	Cyprinidae	*Cyprinus*	*carpio*	Common carp	common
Chordata	Actinopterygii	Cypriniformes	Cyprinidae	*Gila*	*atraria*	Utah chub	uncommon
Chordata	Actinopterygii	Cypriniformes	Cyprinidae	*Notemigonus*	*crysoleucas*	Golden shiner	rare
Chordata	Actinopterygii	Cypriniformes	Cyprinidae	*Pimephales*	*promelas*	Fathead minnow	rare

Chordata	Actinopterygii	Cypriniformes	Cyprinidae	*Rhinichthys*	*osculus*	speckled dace	locally common
Chordata	Actinopterygii	Cypriniformes	Cyprinidae	*Richardsonius*	*balteatus*	redside shiner	locally common
Chordata	Actinopterygii	Cyprinodontiformes	Poeciliidae	*Gambusia*	*affinis*	Mosquito fish	common
Chordata	Actinopterygii	Perciformes	Centrarchidae	*Lepomis*	*cyanellus*	Green sunfish	common
Chordata	Actinopterygii	Perciformes	Centrarchidae	*Lepomis*	*macrochirus*	Bluegill	uncommon
Chordata	Actinopterygii	Perciformes	Centrarchidae	*Micropterus*	*salmoides*	Largemouth bass	uncommon
Chordata	Actinopterygii	Perciformes	Centrarchidae	*Pomoxis*	*nigromaculatus*	Black crappie	uncommon
Chordata	Actinopterygii	Perciformes	Moronidae	*Morone*	*chrysops*	White bass	common
Chordata	Actinopterygii	Perciformes	Percidae	*Perca*	*flavescens*	Yellow perch	uncommon
Chordata	Actinopterygii	Perciformes	Percidae	*Stiozostedion*	*vitreum*	Walleye	uncommon
Chordata	Actinopterygii	Siluriformes	Ictaluridae	*Ameiurus*	*melas*	Black bullhead	common
Chordata	Actinopterygii	Siluriformes	Ictaluridae	*Ictalurus*	*punctatus*	Channel catfish	common
Chordata	Amphibia	Anura	Hylidae	*Pseudacris*	*triseriatea maculata*	Boreal chorus frog	common
Chordata	Amphibia	Anura	Ranidae	*Rana*	*catesbeiana*	American bullfrog	common

Chordata	Amphibia	Anura	Ranidae	*Rana*	*luteiventris (pretiosa)*	Northern spotted frog	rare
Chordata	Amphibia	Anura	Ranidae	*Lithobates*	*pipiens*	Northern leopard frog	rare
Mollusca	Bivalvia	Verenoida	Cyrenidae	*Corbicula*	*sp.*	Asian clam	
Mollusca	Bivalvia	Verenoida	Sphaeriidae	*Pisidium*	*sp.*	fingernail clam	
Mollusca	Gastropoda	Hygrophila	Physidae	*Physa*	*sp.*	Physa snail	
Mollusca	Gastropoda	Hygrophila	Planorbidae	*unidentified*	*unidentified*	Planorbid snail	
Mollusca	Gastropoda	Hygrophila	Planorbidae	*unidentified*	*unidentified*	Planorbid snail	
Mollusca	Gastropoda	Hygrophila	Planorbidae	*Gyraulus*	*sp.*	Planorbid snail	
Mollusca	Gastropoda	Neotaenioglossa	Hydrobiidae	*unidentified*	*unidentified*	Hydrobiid snail	
Mollusca	Gastropoda	Neotaenioglossa	Hydrobiidae	*Potamopyrgus*	*antipodarum*	New Zealand mudsnail	common
Nemotoda	unidentified	unidentified	unidentified	*unidentified*	*unidentified*	Nemotode	
Platyhelminthes	Trepaxonemata	Tricladida	unidentified	*unidentified*	*unidentified*	Flatworm	
Platyhelminthes	Turbellaria	unidentified	unidentified	*unidentified*	*unidentified*	Flatworm	

Appendix 2. Longer Statement of the Deletion Process

In contrast to the Appendix 1 version, which operates on the list of tested species, comparing it to the list of resident species, this version operates on a single combined list. Use of a single list was found to have certain advantages, which furthered the development of an automated spreadsheet for determining retention or deletion of tested species. Appendices 1 and 2 are intended to yield identical results.

Steps A through J are performed sequentially so that the appropriate entry is made in the site- specific toxicity dataset column for each species; the entry indicates whether the species is or is not included in the site-specific toxicity dataset. This version of the Deletion Process is organized so that, beginning with Step D, each species that does not have an entry in the site- specific toxicity dataset column is addressed at the genus level before any species is addressed at the family level. Then, the order, class, and phylum taxonomic levels are addressed sequentially. The number of species that need to be addressed decreases as higher and higher taxonomic levels are addressed.

Step A: Make a table that lists all of the species in the (possibly modified) national toxicity dataset, all of the species that occur at the site, and all surrogates that are used for critical species at the site in taxonomic order by species, genus, family, order, class, and

phylum using the current version of ITIS. If a surrogate species is listed in the table, the species that it is a surrogate for should not be listed in the table. Fill in each column for each species, except do not put anything in the last column on the right, which is titled “In site-specific toxicity dataset?”

Step B: For each species that has a "No" in the national toxicity dataset column, enter "N-1" in the site-specific toxicity dataset column.

1. N = "No" and means that the species is not in the site-specific toxicity database.

Step C: For each species that has a "Yes" in the "Occur at the site?" column and a "Yes" in the national toxicity dataset column, enter "Y-2" in the site-specific toxicity dataset column.

Each species that does not yet have an entry in the site-specific toxicity dataset column has a "No" in the "Occur at the site?" column and a "Yes" in the national toxicity dataset column.

Step D: Look down the column titled "Genus" and every time a genus name appears more than once, draw a circle around all of the multiple entries for that one genus. The species in the circled genera are the only species that will be addressed in this Step D. For each species that is in a circled genus and does not already have an entry in the site-specific toxicity dataset column, look at the circled genus that that species is in and do one of the following regarding the site-specific toxicity dataset column:

1. Enter "N-3" if all of the species in that genus that occur at the site are already in the site-specific toxicity dataset.
2. Enter "Y-4" if one or more of the species in that genus that occur at the site are not in the site-specific toxicity dataset species occurring at the site.

Step E: Look down the column titled "Family" and every time a family name appears more than once, draw a circle around all of the multiple entries for that one family. The species in the circled families are the only species that will be addressed in this Step E. For each species that is in a circled family and does not already have an entry in the site-specific toxicity dataset column, look at the circled family that that species is in and do one of the following regarding the site-specific toxicity dataset column:

1. Enter "N-5" if all of the genera in that family that occur at the site are already represented in the site-specific toxicity dataset.
2. Enter "Y-6" if one or more of the genera in that family that occur at the site are not represented in the site-specific toxicity dataset.

This step will not result in an entry for tested species in families having no species occurring at the site.

Step F: Look down the column titled "Order" and every time an order name appears more than once, draw a circle around all of the multiple entries for that one order. The species in the circled orders are the only species that will be addressed in this Step F. For each species that is in a circled order and does not already have an entry in the site-specific toxicity dataset column, look at the circled order that that species is in and do one of the following regarding the site-specific toxicity dataset column:

1. Enter "N-7" if all of the families in that order that occur at the site are already represented in the site-specific toxicity dataset.
2. Enter "Y-8" if one or more of the families in that order that occur at the site are not represented in the site-specific toxicity dataset.

This step will not result in an entry for tested species in orders having no species occurring at the site.

Step G: Look down the column titled "Class" and every time a class name appears more than once, draw a circle around all of the multiple entries for that one class. The species in the circled classes are the only species that will be addressed in this Step G. For each species that is in a circled class and does not already have an entry in the site-specific toxicity dataset column, look at the circled class that that species is in and do one of the following regarding the site-specific toxicity dataset column:

1. Enter "N-9" if all of the orders in that class that occur at the site are already represented in the site-specific toxicity dataset.
2. Enter "Y-10" if one or more of the orders in that class that occur at the site are not represented in the site-specific toxicity dataset.

This step will not result in an entry for tested species in classes having no species occurring at the site.

Step H: Look down the column titled "Phylum" and every time a phylum name appears more than once, draw a circle around all of the multiple entries for that one phylum. The species in the circled phyla are the only species that will be addressed in this Step H. For each species that is in a circled phylum and does not already have an entry in the following regarding the site-specific toxicity dataset column:

1. Enter "N-11" if all of the classes in that phylum that occur at the site are already represented in the site-specific toxicity dataset.

2. Enter "Y-12" if one or more of the classes in that phylum that occur at the site are not represented in the site-specific toxicity dataset.

Step I: For each species for which no entry has been made in the site-specific toxicity dataset column, enter "N-13" because the phylum does not occur at the site.

Aspects of a completed table that are easy to review. a. Every "N" should have an odd number after it.

b. Every "Y" should have an even number after it.

c. Every species that has "No" in the national toxicity database column should have "N-1" in the site-specific database column.

d. Every species that has "Y-2" in the site-specific toxicity database column should have "Yes" in the "Occur at the site?" column and in the national toxicity dataset column.

Appendix 41. The deletion process. Taxa occurrence in Mill Creek/Jordan River site, taxa in national toxicity dataset, and determination for inclusion in site toxicity dataset with Fluminicola sp, resident (see Appendix 3 for description of deletion methods and N and Y values in the "Include in Site Toxicity Dataset?" column. Taxa are color coded to help interpret deletion methods used in Appendix 3)

Phylum	Class	Order	Family	Genus	Species	Occurs at site?	In National Toxicity Dataset?	Include in Site Toxicity Dataset?
Annelida	Clitellata	Arhynchobdellida	Erpobdellidae	*?*	*?*	Yes	No	N-1
Annelida	Clitellata	Lumbriculida	Lumbriculidae	*Lumbriculus*	*variegatus*	?	Yes	Y-10
Annelida	Clitellata	Oligochaeta	?	*?*	*?*	Yes	?	Y-8
Annelida	Clitellata	Oligochaeta	Naididae	*?*	*?*	Yes	?	Y-6
Annelida	Clitellata	Oligochaeta	Naididae	*Limnodrilus*	*hoffmeisteri*	?	Yes	Y-6
Annelida	Clitellata	Oligochaeta	Naididae	*Tubifex*	*tubifex*	?	Yes	Y-6
Annelida	Hirudinea	Rhynchobdellida	Glossiphoniidae	Helobdella	stagnalis	Yes	No	N-1
Annelida	Hirudinea	Rhynchobdellida	Glossiphoniidae	Glossiphonia	*complanata*	Yes	No	N-1
Arthropoda	Arachnida	Trombidiformes	Lebertiidae	Lebertia	*?*	Yes	No	N-1
Arthropoda	Branchiopoda	Cladocera	Chydoridae	*Chydorus*	*sphaericus*	No	Yes	Y-12
Arthropoda	Branchiopoda	Cladocera	Daphnidae	*Ceriodaphnia*	*acanthina*	No	Yes	Y-12
Arthropoda	Branchiopoda	Cladocera	Daphnidae	*Ceriodaphnia*	*dubia*	No	Yes	Y-12
Arthropoda	Branchiopoda	Cladocera	Daphnidae	*Daphnia*	*magna*	No	Yes	Y-12

Arthropoda	Branchiopoda	Cladocera	Daphnidae	*Daphnia*	*pulicaria*	No	Yes	Y-12
Arthropoda	Branchiopoda	Cladocera	Daphnidae	*Simocephalus*	*vetulus*	No	Yes	Y-12
Arthropoda	Entognatha	Collembola	?	?	*?*	Yes	No	N-1
Arthropoda	Insecta	Coleoptera	Elmidae	*Stenelmis*	*?*	Yes	?	Y-4
Arthropoda	Insecta	Coleoptera	Elmidae	*Stenelmis*	*sexlineata*	?	Yes	Y-4
Arthropoda	Insecta	Diptera	Ceratopogonidae	*Palpomyia/Bezzia*	*?*	Yes	No	N-1
Arthropoda	Insecta	Diptera	Ceratopogonidae	*Probezzia*	*?*	Yes	No	N-1
Arthropoda	Insecta	Diptera	Chironomidae	*?*	*?*	Yes	?	Y-6
Arthropoda	Insecta	Diptera	Chironomidae	*?*	*?*	Yes	?	Y-6
Arthropoda	Insecta	Diptera	Chironomidae	*Chironomus*	*riparius*	?	Yes	Y-4
Arthropoda	Insecta	Diptera	Chironomidae	*Chironomus*	*?*	Yes	?	Y-4
Arthropoda	Insecta	Diptera	Chironomidae	*Chironomus*	*tentans*	?	Yes	Y-4
Arthropoda	Insecta	Diptera	Chironomidae	*Cricotopus*	*sp*	Yes	No	N-1
Arthropoda	Insecta	Diptera	Chironomidae	*Cryptochironomus*	*?*	Yes	No	N-1
Arthropoda	Insecta	Diptera	Chironomidae	*Dicrotendipes*	*?*	Yes	No	N-1
Arthropoda	Insecta	Diptera	Chironomidae	*Glptotendipes*	*?*	Yes	No	N-1
Arthropoda	Insecta	Diptera	Chironomidae	*Parachironomus*	*?*	Yes	No	N-1
Arthropoda	Insecta	Diptera	Chironomidae	*Paratanytarsus*	*?*	Yes	No	N-1
Arthropoda	Insecta	Diptera	Chironomidae	*Paratendipes*	*?*	Yes	No	N-1

Arthropoda	Insecta	Diptera	Chironomidae	*Phaenopsectra*	*?*	Yes	No	N-1
Arthropoda	Insecta	Diptera	Chironomidae	*Procladius*		Yes	No	N-1
Arthropoda	Insecta	Diptera	Chironomidae	*Prodiamesa*		Yes	No	N-1
Arthropoda	Insecta	Diptera	Chironomidae	*Rheocricotopus*	*?*	Yes	No	N-1
Arthropoda	Insecta	Diptera	Chironomidae	*Thienemanniella*	*?*	Yes	No	N-1
Arthropoda	Insecta	Diptera	Chironomidae	*Tvetenia*	*?*	Yes	No	N-1
Arthropoda	Insecta	Diptera	Psychodidae	*Pericoma*	*?*	Yes	No	N-1
Arthropoda	Insecta	Diptera	Psychodidae	Psychoda	*?*	Yes	No	N-1
Arthropoda	Insecta	Diptera	Simuliidae	Simulium	*?*	Yes	No	N-1
Arthropoda	Insecta	Diptera	Simuliidae	Simulium	*vittatum*	Yes	No	N-1
Arthropoda	Insecta	Ephemeroptera	Baetidae	*Baetis*	*?*	Yes	No	N-1
Arthropoda	Insecta	Ephemeroptera	Baetidae	*Callibaetis*	*skokianus*	No	Yes	Y-6
Arthropoda	Insecta	Ephemeroptera	Baetidae	*Callibaetis*	sp.	No	Yes	Y-6
Arthropoda	Insecta	Ephemeroptera	Caenidae	*Caenis*	*?*	Yes	No	N-1
Arthropoda	Insecta	Ephemeroptera	Ephemereliidae	*Drunella*	*grandis*	No	Yes	Y-8
Arthropoda	Insecta	Hemiptera	Corixidae	*Corisella*	*?*	Yes	No	N-1
Arthropoda	Insecta	Hemiptera	Corixidae	*Hesperocorixa*	*?*	Yes	No	N-1
Arthropoda	Insecta	Hemiptera	Corixidae	*Sigara*	*?*	Yes	No	N-1
Arthropoda	Insecta	Odonata	Calopterygidae	*Hetaerina*	*?*	Yes	No	N-1

Arthropoda	Insecta	Odonata	Coenagrionidae	*?*	*?*	Yes	?	Y-6
Arthropoda	Insecta	Odonata	Coenagrionidae	*Argia*	*?*	Yes	No	N-1
Arthropoda	Insecta	Odonata	Coenagrionidae	*Enallagma*	sp.	?	Yes	Y-6
Arthropoda	Insecta	Odonata	Coenagrionidae	*Erythromma*	*najas*	?	Yes	Y-6
Arthropoda	Insecta	Odonata	Coenagrionidae	*Ischnura*	*?*	Yes	No	N-1
Arthropoda	Insecta	Odonata	Corduliidae	*?*	*?*	Yes	No	N-1
Arthropoda	Insecta	Odonata	Libellulidae	*Pachydiplax*	*longipennis*	No	Yes	Y-8
Arthropoda	Insecta	Plecoptera	Perlodidae	*Skwala*	*americana*	No	Yes	Y-10
Arthropoda	Insecta	Trichoptera	Hydropsychidae	*Cheumatopsyche*	*?*	Yes	No	N-1
Arthropoda	Insecta	Trichoptera	Hydropsychidae	*Hydropsyche*	*?*	Yes	No	N-1
Arthropoda	Insecta	Trichoptera	Hydroptilidae	*Hydroptila*	*?*	Yes	No	N-1
Arthropoda	Insecta	Trichoptera	Leptoceridae	*?*	*?*	Yes	No	N-1
Arthropoda	Insecta	Trichoptera	Limnephilidae	*Philarctus*	*quaeris*	No	Yes	Y-8
Arthropoda	Malacostraca	Amphipoda	Crangonyctidae	*Crangonyx*	*pseudogracilis*	?	Yes	Y-2
Arthropoda	Malacostraca	Amphipoda	Crangonyctidae	*Crangonyx*	sp.	Yes	Yes	Y-2
Arthropoda	Malacostraca	Amphipoda	Gammaridae	*Gammarus*	*?*	Yes	No	N-1
Arthropoda	Malacostraca	Amphipoda	Hyalellidae	*Hyalella*	*azteca*	Yes	Yes	Y-2
Arthropoda	Malacostraca	Copepoda	?	*?*	*?*	Yes	?	Y-10
Arthropoda	Malacostraca	Decapoda	Cambaridae	*Orconectes*	*nais*	No	Yes	Y-10

Arthropoda	Malacostraca	Decapoda	Cambaridae	*Orconectes*	*immunis*	No	Yes	Y-10
Arthropoda	Malacostraca	Decapoda	Cambaridae	*Procambarus*	*clarkii*	No	Yes	Y-10
Arthropoda	Malacostraca	Isopoda	Asellidae	*Asellus*	*?*	Yes	?	Y-4
Arthropoda	Malacostraca	Isopoda	Asellidae	*Asellus*	*aquaticus*	?	Yes	Y-4
Arthropoda	Malacostraca	Isopoda	Asellidae	*Caecidotea*	*?*	Yes	?	Y-4
Arthropoda	Malacostraca	Isopoda	Asellidae	*Caecidotea*	*racovitzai*	?	Yes	Y-4
Chordata	Actinopterygii	Acipenseriformes	Acipenseridae	*Acipenser*	*brevirostrum*	No	Yes	N-9
Chordata	Actinopterygii	Cypriniformes	Catostomidae	*Catostomus*	*ardens*	Yes	No	N-1
Chordata	Actinopterygii	Cypriniformes	Catostomidae	*Catostomus*	*commersonii*	No	Yes	Y-4
Chordata	Actinopterygii	Cypriniformes	Catostomidae	*Catostomus*	*platyrhynchus*	Yes	Yes	Y-2
Chordata	Actinopterygii	Cypriniformes	Catostomidae	*Chasmistes*	*brevirostris*	No	Yes	Y-4
Chordata	Actinopterygii	Cypriniformes	Catostomidae	*Chasmistes*	*liorus*	Yes	No	N-1
Chordata	Actinopterygii	Cypriniformes	Catostomidae	*Deltistes*	*luxatus*	No	Yes	N-5
Chordata	Actinopterygii	Cypriniformes	Cyprinidae	*Campostoma*	*anomalum*	No	Yes	Y-6
Chordata	Actinopterygii	Cypriniformes	Cyprinidae	*Cyprinella*	*lutrensis*	No	Yes	Y-6
Chordata	Actinopterygii	Cypriniformes	Cyprinidae	*Cyprinella*	*spiloptera*	No	Yes	Y-6
Chordata	Actinopterygii	Cypriniformes	Cyprinidae	*Cyprinella*	*whipplei*	No	Yes	Y-6
Chordata	Actinopterygii	Cypriniformes	Cyprinidae	*Cyprinus*	*carpio*	Yes	Yes	Y-2
Chordata	Actinopterygii	Cypriniformes	Cyprinidae	*Gila*	*atraria*	Yes	No	N-1

Chordata	Actinopterygii	Cypriniformes	Cyprinidae	*Hybognathus*	*amarus*	No	Yes	Y-6
Chordata	Actinopterygii	Cypriniformes	Cyprinidae	*Notemigonus*	*crysoleucas*	Yes	Yes	Y-2
Chordata	Actinopterygii	Cypriniformes	Cyprinidae	*Notropis*	*topeka*	No	Yes	Y-6
Chordata	Actinopterygii	Cypriniformes	Cyprinidae	*Pimephales*	*promelas*	Yes	Yes	Y-2
Chordata	Actinopterygii	Cypriniformes	Cyprinidae	*Rhinichthys*	*osculus*	Yes	No	N-1
Chordata	Actinopterygii	Cypriniformes	Cyprinidae	*Richardsonius*	*balteatus*	Yes	No	N-1
Chordata	Actinopterygii	Cyprinodontiformes	Poeciliidae	*Gambusia*	*affinis*	Yes	Yes	Y-2
Chordata	Actinopterygii	Cyprinodontiformes	Poeciliidae	*Poecilia*	*reticulata*	No	Yes	N-5
Chordata	Actinopterygii	Gasterosteiformes	Gasterosteidae	*Gasterosteus*	*aculeatus*	No	Yes	N-9
Chordata	Actinopterygii	Perciformes	Centrarchidae	*Lepomis*	*cyanellus*	Yes	Yes	Y-2
Chordata	Actinopterygii	Perciformes	Centrarchidae	*Lepomis*	*gibbosus*	No	Yes	N-3
Chordata	Actinopterygii	Perciformes	Centrarchidae	*Lepomis*	*macrochirus*	Yes	Yes	Y-2
Chordata	Actinopterygii	Perciformes	Centrarchidae	*Micropterus*	*salmoides*	Yes	Yes	Y-2
Chordata	Actinopterygii	Perciformes	Centrarchidae	*Micropterus*	*treculii*	No	Yes	N-3
Chordata	Actinopterygii	Perciformes	Centrarchidae	*Micropterus*	dolomieu	No	Yes	N-3
Chordata	Actinopterygii	Perciformes	Centrarchidae	*Pomoxis*	*nigromaculatus*	Yes	No	N-1
Chordata	Actinopterygii	Perciformes	Cichlidae	*Oreochromis*	*mossambicus*	No	Yes	N-7
Chordata	Actinopterygii	Perciformes	Moronidae	*Morone*	*chrysops*	Yes	Yes	Y-2
Chordata	Actinopterygii	Perciformes	Moronidae	*Morone*	*saxatilis*	No	Yes	N-3

Chordata	Actinopterygii	Perciformes	Moronidae	*Morone*	*saxatilis x chrysops*	No	Yes	N-3
Chordata	Actinopterygii	Perciformes	Percidae	*Etheostoma*	*nigrum*	No	Yes	Y-6
Chordata	Actinopterygii	Perciformes	Percidae	*Etheostoma*	*spectabile*	No	Yes	Y-6
Chordata	Actinopterygii	Perciformes	Percidae	*Perca*	*flavescens*	Yes	No	N-1
Chordata	Actinopterygii	Perciformes	Percidae	*Sander*	*vitreus*	No	Yes	Y-6
Chordata	Actinopterygii	Perciformes	Percidae	*Stiostedion*	*vitreum*	Yes	No	N-1
Chordata	Actinopterygii	Salmoniformes	Salmonidae	*Oncorhynchus*	*kisutch*	No	Yes	N-9
Chordata	Actinopterygii	Salmoniformes	Salmonidae	*Oncorhynchus*	*aguabonita*	No	Yes	N-9
Chordata	Actinopterygii	Salmoniformes	Salmonidae	*Oncorhynchus*	*clarkii*	No	Yes	N-9
Chordata	Actinopterygii	Salmoniformes	Salmonidae	*Oncorhynchus*	*gorbuscha*	No	Yes	N-9
Chordata	Actinopterygii	Salmoniformes	Salmonidae	*Oncorhynchus*	*mykiss*	No	Yes	N-9
Chordata	Actinopterygii	Salmoniformes	Salmonidae	*Prosopium*	*williamsoni*	No	Yes	N-9
Chordata	Actinopterygii	Salmoniformes	Salmonidae	*Salmo*	*salar*	No	Yes	N-9
Chordata	Actinopterygii	Salmoniformes	Salmonidae	*Salvelinus*	*fontinalis*	No	Yes	N-9
Chordata	Actinopterygii	Salmoniformes	Salmonidae	*Salvelinus*	*namaycush*	No	Yes	N-9
Chordata	Actinopterygii	Scorpaeniformes	Cottidae	*Cottus*	*bairdii*	No	Yes	N-9
Chordata	Actinopterygii	Siluriformes	Ictaluridae	*Ameiurus*	*melas*	Yes	No	N-1
Chordata	Actinopterygii	Siluriformes	Ictaluridae	*Ictalurus*	*punctatus*	Yes	Yes	Y-2
Chordata	Amphibia	Anura	Hylidae	*Pseudacris*	*crucifer*	No	Yes	Y-4

Chordata	Amphibia	Anura	Hylidae	*Pseudacris*	*regilla*	No	Yes	Y-4
Chordata	Amphibia	Anura	Hylidae	*Pseudacris*	*triseriatea maculata*	Yes	No	N-1
Chordata	Amphibia	Anura	Pipidae	*Xenopus*	*laevis*	No	Yes	N-7
Chordata	Amphibia	Anura	Ranidae	*Rana*	*cateseiana*	Yes	No	N-1
Chordata	Amphibia	Anura	Ranidae	*Rana*	*luteiventris*	Yes	No	N-1
Chordata	Amphibia	Anura	Ranidae	*Rana*	*pipiens*	Yes	Yes	Y-2
Mollusca	Bivalvia	Unionoida	Unionidae	*Actinonaias*	*ligamentina*	No	Yes	N-9
Mollusca	Bivalvia	Unionoida	Unionidae	*Actinonaias*	*pectorosa*	No	Yes	N-9
Mollusca	Bivalvia	Unionoida	Unionidae	*Alasmidonta*	*heterodon*	No	Yes	N-9
Mollusca	Bivalvia	Unionoida	Unionidae	*Epioblasma*	*capsaeformis*	No	Yes	N-9
Mollusca	Bivalvia	Unionoida	Unionidae	*Fusconaia*	*masoni*	No	Yes	N-9
Mollusca	Bivalvia	Unionoida	Unionidae	*Lampsilis*	*abrupta*	No	Yes	N-9
Mollusca	Bivalvia	Unionoida	Unionidae	*Lampsilis*	*cardium*	No	Yes	N-9
Mollusca	Bivalvia	Unionoida	Unionidae	*Lampsilis*	*fasciola*	No	Yes	N-9
Mollusca	Bivalvia	Unionoida	Unionidae	*Lampsilis*	*higginsii*	No	Yes	N-9
Mollusca	Bivalvia	Unionoida	Unionidae	*Lampsilis*	*rafinesqueana*	No	Yes	N-9
Mollusca	Bivalvia	Unionoida	Unionidae	*Lampsilis*	*siliquoidea*	No	Yes	N-9
Mollusca	Bivalvia	Unionoida	Unionidae	*Lasmigona*	*subviridis*	No	Yes	N-9
Mollusca	Bivalvia	Unionoida	Unionidae	*Potamilus*	*ohiensis*	No	Yes	N-9

Mollusca	Bivalvia	Unionoida	Unionidae	*Pyganodon*	*grandis*	No	Yes	N-9
Mollusca	Bivalvia	Unionoida	Unionidae	*Utterbackia*	*imbecillis*	No	Yes	N-9
Mollusca	Bivalvia	Unionoida	Unionidae	*Venustaconcha*	*ellipsiformis*	No	Yes	N-9
Mollusca	Bivalvia	Unionoida	Unionidae	*Villosa*	*iris*	No	Yes	N-9
Mollusca	Bivalvia	Verenoida	Cyrenidae	*Corbicula*	*?*	Yes	No	N-1
Mollusca	Bivalvia	Verenoida	Sphaeriidae	*Musculium*	*transversum*	No	Yes	Y-6
Mollusca	Bivalvia	Verenoida	Sphaeriidae	*Pisidium*	*?*	Yes	No	N-1
Mollusca	Gastropoda	Hygrophila	Lymnaeidae	*Lymnaea*	*stagnalis*	?	Yes	N-7
Mollusca	Gastropoda	Hygrophila	Physidae	*Physa*	*?*	Yes	?	Y-4
Mollusca	Gastropoda	Hygrophila	Physidae	*Physa*	*gyrina*	?	Yes	Y-4
Mollusca	Gastropoda	Hygrophila	Planorbidae	*?*	*?*	Yes	?	Y-6
Mollusca	Gastropoda	Hygrophila	Planorbidae	*?*	*?*	Yes	?	Y-6
Mollusca	Gastropoda	Hygrophila	Planorbidae	*Gyraulus*	*?*	Yes	No	N-1
Mollusca	Gastropoda	Hygrophila	Planorbidae	*Planorbella*	*trivolvis*	?	Yes	Y-6
Mollusca	Gastropoda	Neotaenioglossa	Hydrobiidae	*?*	*?*	Yes	?	Y-6
Mollusca	Gastropoda	Neotaenioglossa	Hydrobiidae	*Fluminicola*	sp.	No	Yes	Y-6
Mollusca	Gastropoda	Neotaenioglossa	Hydrobiidae	*Potamopyrgus*	*antipodarum*	Yes	No	N-1
Mollusca	Gastropoda	Sorbeocncha	Pleuroceridae	*Pleurocera*	*uncialis*	No	Yes	N-9
Nemotoda	?	?	?	*?*	*?*	Yes	No	N-1

Platyhelminthes	Trepaxonemata	Tricladida	?	*?*	*?*	Yes	?	Y-8
Platyhelminthes	Trepaxonemata	Tricladida	Dendrocoelidae	*Dendrocoelum*	*lacteum*	?	Yes	Y-8
Platyhelminthes	Turbellaria	?	?	*?*	*?*	Yes	No	N-1

Phylum	**Class**	**Order**	**Family**	**Genus**	GMAV (mg TAN/L)
Annelida	Clitellata	Lumbriculida	Lumbriculidae	*Lumbriculus*	218.7
Annelida	Clitellata	Oligochaeta	Naididae	*Limnodrilus*	170.2
Annelida	Clitellata	Oligochaeta	Naididae	*Tubifex*	216.5
Arthropoda	Branchiopoda	Cladocera	Chydoridae	*Chydorus*	162.6
Arthropoda	Branchiopoda	Cladocera	Daphnidae	*Ceriodaphnia*	143.9
Arthropoda	Branchiopoda	Cladocera	Daphnidae	*Daphnia*	125
Arthropoda	Branchiopoda	Cladocera	Daphnidae	*Simocephalus*	142.9
Arthropoda	Insecta	Coleoptera	Elmidae	*Stenelmis*	735.9
Arthropoda	Insecta	Diptera	Chironomidae	*Chironomus*	681.8
Arthropoda	Insecta	Ephemeroptera	Baetidae	*Callibaetis*	246.5
Arthropoda	Insecta	Ephemeroptera	Ephemereliidae	*Drunella*	442.4

Arthropoda	Insecta	Odonata	Coenagrionidae	*Enallagma*	164
Arthropoda	Insecta	Odonata	Coenagrionidae	*Erythromma*	2515
Arthropoda	Insecta	Odonata	Libellulidae	*Pachydiplax*	233
Arthropoda	Insecta	Plecoptera	Perlodidae	*Skwala*	192.4
Arthropoda	Insecta	Trichoptera	Limnephilidae	*Philarctus*	994.5
Arthropoda	Malacostraca	Amphipoda	Crangonyctidae	*Crangonyx*	181.8
Arthropoda	Malacostraca	Amphipoda	Hyalellidae	*Hyalella*	192.6
Arthropoda	Malacostraca	Decapoda	Cambaridae	*Orconectes*	686.2
Arthropoda	Malacostraca	Decapoda	Cambaridae	*Procambarus*	138
Arthropoda	Malacostraca	Isopoda	Asellidae	*Asellus*	378.2
Arthropoda	Malacostraca	Isopoda	Asellidae	*Caecidotea*	387
Chordata	Actinopterygii	Cypriniformes	Catostomidae	*Catostomus*	146.5
Chordata	Actinopterygii	Cypriniformes	Cyprinidae	*Campostoma*	115.9
Chordata	Actinopterygii	Cypriniformes	Cyprinidae	*Cyprinella*	110
Chordata	Actinopterygii	Cypriniformes	Cyprinidae	*Cyprinus*	106.3
Chordata	Actinopterygii	Cypriniformes	Cyprinidae	*Hybognathus*	72.55
Chordata	Actinopterygii	Cypriniformes	Cyprinidae	*Notropis*	96.72
Chordata	Actinopterygii	Cypriniformes	Cyprinidae	*Pimephales*	159.2
Chordata	Actinopterygii	Cyprinodontiformes	Poeciliidae	*Gambusia*	219.3

Chordata	Actinopterygii	Perciformes	Centrarchidae	*Lepomis*	106.9
Chordata	Actinopterygii	Perciformes	Centrarchidae	*Micropterus*	89.06
Chordata	Actinopterygii	Perciformes	Moronidae	*Morone*	134.8
Chordata	Actinopterygii	Perciformes	Percidae	*Etheostoma*	74.25
Chordata	Actinopterygii	Perciformes	Percidae	*Sander*	117.1
Chordata	Actinopterygii	Siluriformes	Ictaluridae	*Ictalurus*	142.4
Chordata	Amphibia	Anura	Hylidae	*Pseudacris*	71.56
Chordata	Amphibia	Anura	Ranidae	*Rana*	96.38
Mollusca	Bivalvia	Verenoida	Sphaeriidae	*Musculium*	89.36
Mollusca	Gastropoda	Hygrophila	Physidae	*Physa*	164.5
Mollusca	Gastropoda	Hygrophila	Planorbidae	*Planorbella*	211.6
Platyhelminthes	Trepaxonemata	Tricladida	Dendrocoelidae	*Dendrocoelum*	119.5

Appendix 42. Taxa used for Acute Recalculation and genus level GMAVs including Fluminicola sp.

Phylum	**Class**	**Order**	**Family**	**Genus**	GMAV (mg TAN/L)

Annelida	Clitellata	Lumbriculida	Lumbriculidae	*Lumbriculus*	218.7
Annelida	Clitellata	Oligochaeta	Naididae	*Limnodrilus*	170.2
Annelida	Clitellata	Oligochaeta	Naididae	*Tubifex*	216.5
Arthropoda	Branchiopoda	Cladocera	Chydoridae	*Chydorus*	162.6
Arthropoda	Branchiopoda	Cladocera	Daphnidae	*Ceriodaphnia*	143.9
Arthropoda	Branchiopoda	Cladocera	Daphnidae	*Daphnia*	125
Arthropoda	Branchiopoda	Cladocera	Daphnidae	*Simocephalus*	142.9
Arthropoda	Insecta	Coleoptera	Elmidae	*Stenelmis*	735.9
Arthropoda	Insecta	Diptera	Chironomidae	*Chironomus*	681.8
Arthropoda	Insecta	Ephemeroptera	Baetidae	*Callibaetis*	246.5
Arthropoda	Insecta	Ephemeroptera	Ephemereliidae	*Drunella*	442.4
Arthropoda	Insecta	Odonata	Coenagrionidae	*Enallagma*	164
Arthropoda	Insecta	Odonata	Coenagrionidae	*Erythromma*	2515
Arthropoda	Insecta	Odonata	Libellulidae	*Pachydiplax*	233
Arthropoda	Insecta	Plecoptera	Perlodidae	*Skwala*	192.4
Arthropoda	Insecta	Trichoptera	Limnephilidae	*Philarctus*	994.5
Arthropoda	Malacostraca	Amphipoda	Crangonyctidae	*Crangonyx*	181.8
Arthropoda	Malacostraca	Amphipoda	Hyalellidae	*Hyalella*	192.6
Arthropoda	Malacostraca	Decapoda	Cambaridae	*Orconectes*	686.2

Arthropoda	Malacostraca	Decapoda	Cambaridae	*Procambarus*	138
Arthropoda	Malacostraca	Isopoda	Asellidae	*Asellus*	378.2
Arthropoda	Malacostraca	Isopoda	Asellidae	*Caecidotea*	387
Chordata	Actinopterygii	Cypriniformes	Catostomidae	*Catostomus*	146.5
Chordata	Actinopterygii	Cypriniformes	Catostomidae	*Chasmistes*	146.5
Chordata	Actinopterygii	Cypriniformes	Cyprinidae	*Campostoma*	115.9
Chordata	Actinopterygii	Cypriniformes	Cyprinidae	*Cyprinella*	110
Chordata	Actinopterygii	Cypriniformes	Cyprinidae	*Cyprinus*	106.3
Chordata	Actinopterygii	Cypriniformes	Cyprinidae	*Hybognathus*	72.55
Chordata	Actinopterygii	Cypriniformes	Cyprinidae	*Notemigonus*	63.02
Chordata	Actinopterygii	Cypriniformes	Cyprinidae	*Notropis*	96.72
Chordata	Actinopterygii	Cypriniformes	Cyprinidae	*Pimephales*	159.2
Chordata	Actinopterygii	Cyprinodontiformes	Poeciliidae	*Gambusia*	219.3
Chordata	Actinopterygii	Perciformes	Centrarchidae	*Lepomis*	106.9
Chordata	Actinopterygii	Perciformes	Centrarchidae	*Micropterus*	89.06
Chordata	Actinopterygii	Perciformes	Moronidae	*Morone*	134.8
Chordata	Actinopterygii	Perciformes	Percidae	*Etheostoma*	74.25
Chordata	Actinopterygii	Perciformes	Percidae	*Sander*	117.1
Chordata	Actinopterygii	Siluriformes	Ictaluridae	*Ictalurus*	142.4

Chordata	Amphibia	Anura	Hylidae	*Pseudacris*	71.56
Chordata	Amphibia	Anura	Ranidae	*Rana*	96.38
Mollusca	Bivalvia	Verenoida	Sphaeriidae	*Musculium*	89.36
Mollusca	Gastropoda	Hygrophila	Physidae	*Physa*	164.5
Mollusca	Gastropoda	Hygrophila	Planorbidae	*Planorbella*	211.6
Mollusca	Gastropoda	Neotaenioglossa	Hydrobiidae	*Fluminicola*	>62.15
Platyhelminthes	Trepaxonemata	Tricladida	Dendrocoelidae	*Dendrocoelum*	119.5

Appendix 43. Some common names for species used in Acute recalculation and their SMAVs. Some common names are not ITIS recognized.

Common Name	**Species**	**SMAV (mg TAN/L)**
Spring peeper	*Pseudacris crucifer*	61.18
Pebblesnail	*Fluminicola sp.*	62.15
Golden shiner	*Notemigonus crysoleucas*	63.02
Shortnose sucker	*Chasmistes brevirostris*	69.36
Johnny darter	*Etheostoma nigrum*	71.45
Rio Grande silvery minnow	*Hybognathus amarus*	72.55

Orangethroat darter	*Etheostoma spectabile*	77.17
Steelcolor shiner	*Cyprinella whipplei*	80.94
Pacific tree frog	*Pseudacris regilla*	83.71
Spotfin shiner	*Cyprinella spiloptera*	83.80
Largemouth bass	*Micropterus salmoides*	86.02
Great pond snail	*Lymnaea stagnalis*	88.62
Long fingernail clam	*Musculium transversum*	89.36
Lithobates pipiens	*Rana pipiens*	96.38
Topeka shiner	*Notropis topeka*	96.72
Bluegill	*Lepomis macrochirus*	104.50
Carp	*Cyprinus carpio*	106.30
Central stoneroller	*Campostoma anomalum*	115.90
Walleye	*Sander vitreus*	117.10
Flatworm species	*Dendrocoelum lacteum*	119.50
Amphipod sp.	*Crangonyx sp.*	122.20
Mountain sucker	*Catostomus platyrhynchus*	136.20
Red swamp crayfish	*Procambarus clarkii*	138.00
Channel catfish	*Ictalurus punctatus*	142.40

White bass	*Morone chrysops*	144.00
Green sunfish	*Lepomis cyanellus*	150.80
White sucker	*Catostomus commersonii*	157.50
Fathead minnow	*Pimephales promelas*	159.20
Damselfly sp.	*Enallagma sp.*	164.00
Physa snail	*Physa gyrina*	164.50
Mayfly species	*Callibaetis sp.*	166.70
Aquatic oligochaete worm	*Limnodrilus hoffmeisteri*	170.20
Perlodid stonefly	*Skwala americana*	192.40
Amphipod sp.	*Hyalella azteca*	192.60
Red shiner	*Cyprinella lutrensis*	196.10
Marsh ramshorn	*Planorbella trivolvis*	211.60
Aquatic oligochaete worm	*Tubifex tubifex*	216.50
Aquatic oligochaete worm	*Lumbriculus variegatus*	218.70
Mosquito fish	*Gambusia affinis*	219.30
Blue dasher dragonfly	*Pachydiplax longipennis*	233.00
Northern river crangonyctid	*Crangonyx pseudogracilis*	270.50
Water nymph crayfish	*Orconectes nais*	303.80

Mayfly species	*Callibaetis skokianus*	364.60
Aquatic sowbug (not ITIS)	*Asellus aquaticus*	378.20
Aquatic sowbug (not ITIS)	*Caecidotea acovitzai*	387.00
Mayfly species	*Drunella grandis*	442.40
Midge species	*Chironomus tentans*	451.80
Riffle beetle	*Stenelmis sexlineata*	735.90
Caddisfly species	*Philarctus quaeris*	994.50
Midge species	*Chironomus riparius*	1029.00
Calico crayfish(not ITIS)	*Orconectes immunis*	1550.00
Red eyed damselfly (not ITIS)	*Erythromma najas*	2515.00

Appendix 44. Genera used for Acute Recalculation

Genus	GMAV (mg TAN/L)
Fluminicola	62.15
Notemigonus	63.02
Pseudacris	71.56
Hybognathus	72.55

Etheostoma	74.25
Micropterus	89.06
Musculium	89.36
Rana	96.38
Notropis	96.72
Cyprinus	106.3
Lepomis	106.9
Cyprinella	110
Campostoma	115.9
Sander	117.1
Dendrocoelum	119.5
Daphnia	125
Morone	134.8
Procambarus	138
Ictalurus	142.4
Simocephalus	142.9
Ceriodaphnia	143.9
Catostomus	146.5

Chasmistes	146.5
Pimephales	159.2
Chydorus	162.6
Enallagma	164
Physa	164.5
Limnodrilus	170.2
Crangonyx	181.8
Skwala	192.4
Hyalella	192.6
Planorbella	211.6
Tubifex	216.5
Lumbriculus	218.7
Gambusia	219.3
Pachydiplax	233
Callibaetis	246.5
Asellus	378.2
Caecidotea	387
Drunella	442.4

Chironomus	681.8
Orconectes	686.2
Stenelmis	735.9
Philarctus	994.5
Erythromma	2515

Appendix 45. The deletion process. Taxa occurrence in Mill Creek/Jordan River site, taxa in national toxicity dataset, and determination for inclusion in site toxicity dataset with three rare or absent taxa removed (see Appendix 3 for description of deletion methods and N and Y values in the "Include in Site Toxicity Dataset?" column. Taxa are color coded to help interpret deletion methods used in Appendix 3)

Phylum	Class	Order	Family	Genus	Species	Occurs at site?	In National Toxicity Dataset?	Include in Site Toxicity Dataset?
Annelida	Clitellata	Arhynchobdellida	Erpobdellidae	*?*	*?*	Yes	No	N-1
Annelida	Clitellata	Lumbriculida	Lumbriculidae	*Lumbriculus*	*variegatus*	?	Yes	Y-10
Annelida	Clitellata	Oligochaeta	?	*?*	*?*	Yes	?	Y-8
Annelida	Clitellata	Oligochaeta	Naididae	*?*	*?*	Yes	?	Y-6
Annelida	Clitellata	Oligochaeta	Naididae	*Limnodrilus*	*hoffmeisteri*	?	Yes	Y-6

Annelida	Clitellata	Oligochaeta	Naididae	*Tubifex*	*tubifex*	?	Yes	Y-6
Annelida	Hirudinea	Rhynchobdellida	Glossiphoniidae	Helobdella	stagnalis	Yes	No	N-1
Annelida	Hirudinea	Rhynchobdellida	Glossiphoniidae	Glossiphonia	*complanata*	Yes	No	N-1
Arthropoda	Arachnida	Trombidiformes	Lebertiidae	Lebertia	*?*	Yes	No	N-1
Arthropoda	Branchiopoda	Cladocera	Chydoridae	*Chydorus*	*sphaericus*	No	Yes	Y-12
Arthropoda	Branchiopoda	Cladocera	Daphnidae	*Ceriodaphnia*	*acanthina*	No	Yes	Y-12
Arthropoda	Branchiopoda	Cladocera	Daphnidae	*Ceriodaphnia*	*dubia*	No	Yes	Y-12
Arthropoda	Branchiopoda	Cladocera	Daphnidae	*Daphnia*	*magna*	No	Yes	Y-12
Arthropoda	Branchiopoda	Cladocera	Daphnidae	*Daphnia*	*pulicaria*	No	Yes	Y-12
Arthropoda	Branchiopoda	Cladocera	Daphnidae	*Simocephalus*	*vetulus*	No	Yes	Y-12
Arthropoda	Entognatha	Collembola	?	?	*?*	Yes	No	N-1
Arthropoda	Insecta	Coleoptera	Elmidae	*Stenelmis*	*?*	Yes	?	Y-4
Arthropoda	Insecta	Coleoptera	Elmidae	*Stenelmis*	*sexlineata*	?	Yes	Y-4
Arthropoda	Insecta	Diptera	Ceratopogonidae	*Palpomyia/Bezzia*	*?*	Yes	No	N-1
Arthropoda	Insecta	Diptera	Ceratopogonidae	*Probezzia*	*?*	Yes	No	N-1
Arthropoda	Insecta	Diptera	Chironomidae	*?*	*?*	Yes	?	Y-6
Arthropoda	Insecta	Diptera	Chironomidae	*?*	*?*	Yes	?	Y-6
Arthropoda	Insecta	Diptera	Chironomidae	*Chironomus*	*riparius*	?	Yes	Y-4
Arthropoda	Insecta	Diptera	Chironomidae	*Chironomus*	*?*	Yes	?	Y-4

Arthropoda	Insecta	Diptera	Chironomidae	*Chironomus*	*tentans*	?	Yes	Y-4
Arthropoda	Insecta	Diptera	Chironomidae	*Cricotopus*	*sp*	Yes	No	N-1
Arthropoda	Insecta	Diptera	Chironomidae	*Cryptochironomus*	*?*	Yes	No	N-1
Arthropoda	Insecta	Diptera	Chironomidae	*Dicrotendipes*	*?*	Yes	No	N-1
Arthropoda	Insecta	Diptera	Chironomidae	*Glptotendipes*	*?*	Yes	No	N-1
Arthropoda	Insecta	Diptera	Chironomidae	*Parachironomus*	*?*	Yes	No	N-1
Arthropoda	Insecta	Diptera	Chironomidae	*Paratanytarsus*	*?*	Yes	No	N-1
Arthropoda	Insecta	Diptera	Chironomidae	*Paratendipes*	*?*	Yes	No	N-1
Arthropoda	Insecta	Diptera	Chironomidae	*Phaenopsectra*	*?*	Yes	No	N-1
Arthropoda	Insecta	Diptera	Chironomidae	*Procladius*		Yes	No	N-1
Arthropoda	Insecta	Diptera	Chironomidae	*Prodiamesa*		Yes	No	N-1
Arthropoda	Insecta	Diptera	Chironomidae	*Rheocricotopus*	*?*	Yes	No	N-1
Arthropoda	Insecta	Diptera	Chironomidae	*Thienemanniella*	*?*	Yes	No	N-1
Arthropoda	Insecta	Diptera	Chironomidae	*Tvetenia*	*?*	Yes	No	N-1
Arthropoda	Insecta	Diptera	Psychodidae	*Pericoma*	*?*	Yes	No	N-1
Arthropoda	Insecta	Diptera	Psychodidae	Psychoda	*?*	Yes	No	N-1
Arthropoda	Insecta	Diptera	Simuliidae	Simulium	*?*	Yes	No	N-1
Arthropoda	Insecta	Diptera	Simuliidae	Simulium	*vittatum*	Yes	No	N-1
Arthropoda	Insecta	Ephemeroptera	Baetidae	*Baetis*	*?*	Yes	No	N-1

Arthropoda	Insecta	Ephemeroptera	Baetidae	*Callibaetis*	*skokianus*	No	Yes	Y-6
Arthropoda	Insecta	Ephemeroptera	Baetidae	*Callibaetis*	sp.	No	Yes	Y-6
Arthropoda	Insecta	Ephemeroptera	Caenidae	*Caenis*	*?*	Yes	No	N-1
Arthropoda	Insecta	Ephemeroptera	Ephemereliidae	*Drunella*	*grandis*	No	Yes	Y-8
Arthropoda	Insecta	Hemiptera	Corixidae	*Corisella*	*?*	Yes	No	N-1
Arthropoda	Insecta	Hemiptera	Corixidae	*Hesperocorixa*	*?*	Yes	No	N-1
Arthropoda	Insecta	Hemiptera	Corixidae	*Sigara*	*?*	Yes	No	N-1
Arthropoda	Insecta	Odonata	Calopterygidae	*Hetaerina*	*?*	Yes	No	N-1
Arthropoda	Insecta	Odonata	Coenagrionidae	*?*	*?*	Yes	?	Y-6
Arthropoda	Insecta	Odonata	Coenagrionidae	*Argia*	*?*	Yes	No	N-1
Arthropoda	Insecta	Odonata	Coenagrionidae	*Enallagma*	sp.	?	Yes	Y-6
Arthropoda	Insecta	Odonata	Coenagrionidae	*Erythromma*	*najas*	?	Yes	Y-6
Arthropoda	Insecta	Odonata	Coenagrionidae	*Ischnura*	*?*	Yes	No	N-1
Arthropoda	Insecta	Odonata	Corduliidae	*?*	*?*	Yes	No	N-1
Arthropoda	Insecta	Odonata	Libellulidae	*Pachydiplax*	*longipennis*	No	Yes	Y-8
Arthropoda	Insecta	Plecoptera	Perlodidae	*Skwala*	*americana*	No	Yes	Y-10
Arthropoda	Insecta	Trichoptera	Hydropsychidae	*Cheumatopsyche*	*?*	Yes	No	N-1
Arthropoda	Insecta	Trichoptera	Hydropsychidae	*Hydropsyche*	*?*	Yes	No	N-1
Arthropoda	Insecta	Trichoptera	Hydroptilidae	*Hydroptila*	*?*	Yes	No	N-1

Arthropoda	Insecta	Trichoptera	Leptoceridae	*?*	*?*	Yes	No	N-1
Arthropoda	Insecta	Trichoptera	Limnephilidae	*Philarctus*	*quaeris*	No	Yes	Y-8
Arthropoda	Malacostraca	Amphipoda	Crangonyctidae	*Crangonyx*	*pseudogracilis*	?	Yes	N-3
Arthropoda	Malacostraca	Amphipoda	Crangonyctidae	*Crangonyx*	sp.	Yes	Yes	Y-2
Arthropoda	Malacostraca	Amphipoda	Gammaridae	*Gammarus*	*?*	Yes	No	N-1
Arthropoda	Malacostraca	Amphipoda	Hyalellidae	*Hyalella*	*azteca*	Yes	Yes	Y-2
Arthropoda	Malacostraca	Copepoda	?	*?*	*?*	Yes	No	Y-10
Arthropoda	Malacostraca	Decapoda	Cambaridae	*Orconectes*	*nais*	No	Yes	Y-10
Arthropoda	Malacostraca	Decapoda	Cambaridae	*Orconectes*	*immunis*	No	Yes	Y-10
Arthropoda	Malacostraca	Decapoda	Cambaridae	*Procambarus*	*clarkii*	No	Yes	Y-10
Arthropoda	Malacostraca	Isopoda	Asellidae	*Asellus*	*?*	Yes	?	Y-4
Arthropoda	Malacostraca	Isopoda	Asellidae	*Asellus*	*aquaticus*	?	Yes	Y-4
Arthropoda	Malacostraca	Isopoda	Asellidae	*Caecidotea*	*?*	Yes	?	Y-4
Arthropoda	Malacostraca	Isopoda	Asellidae	*Caecidotea*	*racovitzai*	?	Yes	Y-4
Chordata	Actinopterygii	Acipenseriformes	Acipenseridae	*Acipenser*	*brevirostrum*	No	Yes	Y-12
Chordata	Actinopterygii	Cypriniformes	Catostomidae	*Catostomus*	*ardens*	Yes	No	N-1
Chordata	Actinopterygii	Cypriniformes	Catostomidae	*Catostomus*	*commersonii*	No	Yes	Y-4
Chordata	Actinopterygii	Cypriniformes	Catostomidae	*Catostomus*	*platyrhynchus*	Yes	Yes	Y-2
Chordata	Actinopterygii	Cypriniformes	Catostomidae	*Chasmistes*	*brevirostris*	No	Yes	N-5

Chordata	Actinopterygii	Cypriniformes	Catostomidae	*Deltistes*	*luxatus*	No	Yes	N-5
Chordata	Actinopterygii	Cypriniformes	Cyprinidae	*Campostoma*	*anomalum*	No	Yes	Y-6
Chordata	Actinopterygii	Cypriniformes	Cyprinidae	*Cyprinella*	*lutrensis*	No	Yes	Y-6
Chordata	Actinopterygii	Cypriniformes	Cyprinidae	*Cyprinella*	*spiloptera*	No	Yes	Y-6
Chordata	Actinopterygii	Cypriniformes	Cyprinidae	*Cyprinella*	*whipplei*	No	Yes	Y-6
Chordata	Actinopterygii	Cypriniformes	Cyprinidae	*Cyprinus*	*carpio*	Yes	Yes	Y-2
Chordata	Actinopterygii	Cypriniformes	Cyprinidae	*Gila*	*atraria*	Yes	No	N-1
Chordata	Actinopterygii	Cypriniformes	Cyprinidae	*Hybognathus*	*amarus*	No	Yes	Y-6
Chordata	Actinopterygii	Cypriniformes	Cyprinidae	*Notropis*	*topeka*	No	Yes	Y-6
Chordata	Actinopterygii	Cypriniformes	Cyprinidae	*Pimephales*	*promelas*	Yes	Yes	Y-2
Chordata	Actinopterygii	Cypriniformes	Cyprinidae	*Rhinichthys*	*osculus*	Yes	No	N-1
Chordata	Actinopterygii	Cypriniformes	Cyprinidae	*Richardsonius*	*balteatus*	Yes	No	N-1
Chordata	Actinopterygii	Cyprinodontiformes	Poeciliidae	*Gambusia*	*affinis*	Yes	Yes	Y-2
Chordata	Actinopterygii	Cyprinodontiformes	Poeciliidae	*Poecilia*	*reticulata*	No	Yes	N-3
Chordata	Actinopterygii	Gasterosteiformes	Gasterosteidae	*Gasterosteus*	*aculeatus*	No	Yes	N-9
Chordata	Actinopterygii	Perciformes	Centrarchidae	*Lepomis*	*cyanellus*	Yes	Yes	Y-2
Chordata	Actinopterygii	Perciformes	Centrarchidae	*Lepomis*	*gibbosus*	No	Yes	Y-6
Chordata	Actinopterygii	Perciformes	Centrarchidae	*Lepomis*	*macrochirus*	Yes	Yes	Y-2
Chordata	Actinopterygii	Perciformes	Centrarchidae	*Micropterus*	*salmoides*	Yes	Yes	Y-2

Chordata	Actinopterygii	Perciformes	Centrarchidae	*Micropterus*	*treculii*	No	Yes	Y-6
Chordata	Actinopterygii	Perciformes	Centrarchidae	*Micropterus*	dolomieu	No	Yes	Y-6
Chordata	Actinopterygii	Perciformes	Centrarchidae	*Pomoxis*	*nigromaculatus*	Yes	No	N-1
Chordata	Actinopterygii	Perciformes	Cichlidae	*Oreochromis*	*mossambicus*	No	Yes	N-7
Chordata	Actinopterygii	Perciformes	Moronidae	*Morone*	*chrysops*	Yes	Yes	Y-2
Chordata	Actinopterygii	Perciformes	Moronidae	*Morone*	*saxatilis*	No	Yes	N-3
Chordata	Actinopterygii	Perciformes	Moronidae	*Morone*	*saxatilis x chrysops*	No	Yes	N-3
Chordata	Actinopterygii	Perciformes	Percidae	*Etheostoma*	*nigrum*	No	Yes	Y-6
Chordata	Actinopterygii	Perciformes	Percidae	*Etheostoma*	*spectabile*	No	Yes	Y-6
Chordata	Actinopterygii	Perciformes	Percidae	*Perca*	*flavescens*	Yes	No	N-1
Chordata	Actinopterygii	Perciformes	Percidae	*Sander*	*vitreus*	No	Yes	Y6
Chordata	Actinopterygii	Perciformes	Percidae	*Stiostedion*	*vitreum*	Yes	No	N-1
Chordata	Actinopterygii	Salmoniformes	Salmonidae	*Oncorhynchus*	*kisutch*	No	Yes	N-9
Chordata	Actinopterygii	Salmoniformes	Salmonidae	*Oncorhynchus*	*aguabonita*	No	Yes	N-9
Chordata	Actinopterygii	Salmoniformes	Salmonidae	*Oncorhynchus*	*clarkii*	No	Yes	N-9
Chordata	Actinopterygii	Salmoniformes	Salmonidae	*Oncorhynchus*	*gorbuscha*	No	Yes	N-9
Chordata	Actinopterygii	Salmoniformes	Salmonidae	*Oncorhynchus*	*mykiss*	No	Yes	N-9
Chordata	Actinopterygii	Salmoniformes	Salmonidae	*Prosopium*	*williamsoni*	No	Yes	N-9
Chordata	Actinopterygii	Salmoniformes	Salmonidae	*Salmo*	*salar*	No	Yes	N-9

Chordata	Actinopterygii	Salmoniformes	Salmonidae	*Salvelinus*	*fontinalis*	No	Yes	N-9
Chordata	Actinopterygii	Salmoniformes	Salmonidae	*Salvelinus*	*namaycush*	No	Yes	N-9
Chordata	Actinopterygii	Scorpaeniformes	Cottidae	*Cottus*	*bairdii*	No	Yes	N-9
Chordata	Actinopterygii	Siluriformes	Ictaluridae	*Ameiurus*	*melas*	Yes	No	N-1
Chordata	Actinopterygii	Siluriformes	Ictaluridae	*Ictalurus*	*punctatus*	Yes	Yes	Y-2
Chordata	Amphibia	Anura	Hylidae	*Pseudacris*	*crucifer*	No	Yes	Y-6
Chordata	Amphibia	Anura	Hylidae	*Pseudacris*	*regilla*	No	Yes	Y-6
Chordata	Amphibia	Anura	Hylidae	*Pseudacris*	*triseriatea maculata*	Yes	No	N-1
Chordata	Amphibia	Anura	Pipidae	*Xenopus*	*laevis*	No	Yes	N-7
Chordata	Amphibia	Anura	Ranidae	*Rana*	*cateseiana*	Yes	No	N-1
Chordata	Amphibia	Anura	Ranidae	*Rana*	*luteiventris*	Yes	No	N-1
Chordata	Amphibia	Anura	Ranidae	*Rana*	*pipiens*	Yes	Yes	Y-2
Mollusca	Bivalvia	Unionoida	Unionidae	*Actinonaias*	*ligamentina*	No	Yes	N-9
Mollusca	Bivalvia	Unionoida	Unionidae	*Actinonaias*	*pectorosa*	No	Yes	N-9
Mollusca	Bivalvia	Unionoida	Unionidae	*Alasmidonta*	*heterodon*	No	Yes	N-9
Mollusca	Bivalvia	Unionoida	Unionidae	*Epioblasma*	*capsaeformis*	No	Yes	N-9
Mollusca	Bivalvia	Unionoida	Unionidae	*Fusconaia*	*masoni*	No	Yes	N-9
Mollusca	Bivalvia	Unionoida	Unionidae	*Lampsilis*	*abrupta*	No	Yes	N-9
Mollusca	Bivalvia	Unionoida	Unionidae	*Lampsilis*	*cardium*	No	Yes	N-9

Mollusca	Bivalvia	Unionoida	Unionidae	*Lampsilis*	*fasciola*	No	Yes	N-9
Mollusca	Bivalvia	Unionoida	Unionidae	*Lampsilis*	*higginsii*	No	Yes	N-9
Mollusca	Bivalvia	Unionoida	Unionidae	*Lampsilis*	*rafinesqueana*	No	Yes	N-9
Mollusca	Bivalvia	Unionoida	Unionidae	*Lampsilis*	*siliquoidea*	No	Yes	N-9
Mollusca	Bivalvia	Unionoida	Unionidae	*Lasmigona*	*subviridis*	No	Yes	N-9
Mollusca	Bivalvia	Unionoida	Unionidae	*Potamilus*	*ohiensis*	No	Yes	N-9
Mollusca	Bivalvia	Unionoida	Unionidae	*Pyganodon*	*grandis*	No	Yes	N-9
Mollusca	Bivalvia	Unionoida	Unionidae	*Utterbackia*	*imbecillis*	No	Yes	N-9
Mollusca	Bivalvia	Unionoida	Unionidae	*Venustaconcha*	*ellipsiformis*	No	Yes	N-9
Mollusca	Bivalvia	Unionoida	Unionidae	*Villosa*	*iris*	No	Yes	N-9
Mollusca	Bivalvia	Verenoida	Cyrenidae	*Corbicula*	*?*	Yes	No	N-1
Mollusca	Bivalvia	Verenoida	Sphaeriidae	*Musculium*	*transversum*	No	Yes	Y-6
Mollusca	Bivalvia	Verenoida	Sphaeriidae	*Pisidium*	*?*	Yes	No	N-1
Mollusca	Gastropoda	Hygrophila	Lymnaeidae	*Lymnaea*	*stagnalis*	?	Yes	N-7
Mollusca	Gastropoda	Hygrophila	Physidae	*Physa*	*?*	Yes	?	Y-2
Mollusca	Gastropoda	Hygrophila	Physidae	*Physa*	*gyrina*	?	Yes	Y-2
Mollusca	Gastropoda	Hygrophila	Planorbidae	*?*	*?*	Yes	?	Y-6
Mollusca	Gastropoda	Hygrophila	Planorbidae	*?*	*?*	Yes	?	Y-6
Mollusca	Gastropoda	Hygrophila	Planorbidae	*Gyraulus*	*?*	Yes	No	N-1

Mollusca	Gastropoda	Hygrophila	Planorbidae	*Planorbella*	*trivolvis*	?	Yes	Y-6
Mollusca	Gastropoda	Neotaenioglossa	Hydrobiidae	*Fluminicola*	sp.	No	Yes	N-9
Mollusca	Gastropoda	Sorbeocncha	Pleuroceridae	*Pleurocera*	*uncialis*	No	Yes	N-9
Nemotoda	?	?	?	*?*	*?*	Yes	No	N-1
Platyhelminthes	Trepaxonemata	Tricladida	?	*?*	*?*	Yes	?	Y-8
Platyhelminthes	Trepaxonemata	Tricladida	Dendrocoelidae	*Dendrocoelum*	*lacteum*	?	Yes	Y-8
Platyhelminthes	Turbellaria	?	?	*?*	*?*	Yes	No	N-1

Appendix 46. EPA (2013b) Appendix N. Table N.5 and N. 7 site specific criteria based on mussel present/absent and RBT present/absent.

Table N.5. 2013 Acute Criterion Recalculations for Site-specific Criteria.

Acute Criterion Duration (1 hr average) at pH 7 and 20°C (mg TAN/L)	**Acute Criterion Magnitude (CMC) Oncorhynchus spp. (Rainbow Trout) Present**	**Acute Criterion Magnitude (CMC) Oncorhynchus spp. (Rainbow Trout) Absent**
Mussels Present	17	17
Mussels Absent	24	38
Frequency: Criteria values not to be exceeded more than once in three years.		

Table N.7. Chronic Criterion Recalculations for Site-Specific Criteria.

Chronic Criterion Duration (30-day average) at pH 7 and 20°C (mg TAN/L)	Chronic Criterion Magnitude (CCC) Fish ELS Present	Chronic Criterion Magnitude (CCC) Fish ELS Absent
Mussels Present	1.9	1.9
Mussels Absent	6.5	7.1
Not to exceed 2.5 times the CCC as a 4-day average within the 30-day averaging period.		
Frequency: Criteria values not to be exceeded more than once in three years.		

Appendix 47 Results of Species Sensitivity Distributions probit regressions using EPA CADDIS Volume 4: Data Analysis SSD_Generator_V1.xlt ***Fluminicola resident*** *(https://www3.epa.gov/caddis/da_software_ssdmacro.html)*

Genus	GMAV NH_3 (mg TAN/L)	Taxon Log Exposure Geometric Mean	Proportion	Rank	Probit	Probit Predicted	Difference
Fluminicola	62.15	1.7934	1%	1	2.7135	3.7155	1.0042
Notemigonus	63.02	1.7995	3%	2	3.1661	3.7325	0.3208

Pseudacris	71.56	1.8547	6%	3	3.4068	3.8874	0.2310
Hybognathus	72.55	1.8606	8%	4	3.5798	3.9042	0.1052
Etheostoma	74.25	1.8707	10%	5	3.7184	3.9324	0.0458
Micropterus	89.06	1.9497	12%	6	3.8361	4.1542	0.1012
Musculium	89.36	1.9511	14%	7	3.9394	4.1583	0.0479
Rana	96.38	1.9840	17%	8	4.0326	4.2505	0.0475
Notropis	96.72	1.9855	19%	9	4.1180	4.2548	0.0187
Cyprinus	106.3	2.0265	21%	10	4.1974	4.3700	0.0298
Lepomis	106.9	2.0290	23%	11	4.2721	4.3768	0.0110
Cyprinella	110	2.0414	26%	12	4.3429	4.4117	0.0047
Campostoma	115.9	2.0641	28%	13	4.4105	4.4754	0.0042
Sander	117.1	2.0686	30%	14	4.4756	4.4880	0.0002
Dendrocoelum	119.5	2.0774	32%	15	4.5385	4.5127	0.0007
Daphnia	125	2.0969	34%	16	4.5996	4.5676	0.0010
Morone	134.8	2.1297	37%	17	4.6593	4.6596	0.0000
Procambarus	138	2.1399	39%	18	4.7178	4.6882	0.0009
Ictalurus	142.4	2.1535	41%	19	4.7753	4.7265	0.0024
Simocephalus	142.9	2.1550	43%	20	4.8321	4.7308	0.0103
Ceriodaphnia	143.9	2.1581	46%	21	4.8884	4.7393	0.0222

Catostomus	146.5	2.1658	48%	22	4.9443	4.7611	0.0335
Chasmistes	146.5	2.1658	48%	22	4.9443	4.7611	0.0335
Pimephales	159.2	2.2019	52%	24	5.0557	4.8625	0.0373
Chydorus	162.6	2.2111	54%	25	5.1116	4.8882	0.0499
Enallagma	164	2.2148	57%	26	5.1679	4.8987	0.0725
Physa	164.5	2.2162	59%	27	5.2247	4.9024	0.1039
Limnodrilus	170.2	2.2310	61%	28	5.2822	4.9439	0.1144
Crangonyx	181.8	2.2596	63%	29	5.3407	5.0243	0.1001
Skwala	192.4	2.2842	66%	30	5.4004	5.0934	0.0942
Hyalella	192.6	2.2847	68%	31	5.4615	5.0947	0.1345
Planorbella	211.6	2.3255	70%	32	5.5244	5.2094	0.0992
Tubifex	216.5	2.3355	72%	33	5.5895	5.2373	0.1240
Lumbriculus	218.7	2.3398	74%	34	5.6571	5.2497	0.1660
Gambusia	219.3	2.3410	77%	35	5.7279	5.2530	0.2255
Pachydiplax	233	2.3674	79%	36	5.8026	5.3269	0.2263
Callibaetis	246.5	2.3918	81%	37	5.8820	5.3956	0.2366
Asellus	378.2	2.5777	83%	38	5.9674	5.9175	0.0025
Caecidotea	387	2.5877	86%	39	6.0606	5.9456	0.0132
Drunella	442.4	2.6458	88%	40	6.1639	6.1087	0.0030

Chironomus	681.8	2.8337	90%	41	6.2816	6.6361	0.1257
Orconectes	686.2	2.8365	92%	42	6.4202	6.6440	0.0501
Stenelmis	735.9	2.8668	94%	43	6.5932	6.7292	0.0185
Philarctus	994.5	2.9976	97%	44	6.8339	7.0964	0.0689
Erythromma	2515	3.4005	99%	45	7.2865	8.2277	0.8859

PARAMETERS	
Slope	2.808
Intercept	-1.320
R^2	0.885
Grand Mean	2.250
Sum SQ	232.822
CSSQ	4.912
MSE	0.117
T critical	1.681
N	45
df	43

Proportion	Probit	Log Central Tendency	SSQ	Log Upper PI	Log Lower PI	Central Tendency	Upper PI	Lower PI
0.05	3.355	1.665	0.016	1.879	1.451	46.247	75.693	28.256
0.1	3.718	1.794	0.016	2.006	1.583	62.299	101.332	38.301
0.2	4.158	1.951	0.015	2.160	1.742	89.365	144.554	55.247
0.4	4.747	2.161	0.015	2.368	1.954	144.774	233.281	89.847
0.5	5.000	2.251	0.015	2.458	2.044	178.207	287.044	110.637
0.7	5.524	2.438	0.015	2.645	2.230	273.967	442.021	169.806
0.8	5.842	2.551	0.015	2.760	2.342	355.371	574.850	219.689
0.9	6.282	2.707	0.016	2.919	2.496	509.765	829.187	313.392
0.95	6.645	2.837	0.016	3.051	2.623	686.698	1123.977	419.541

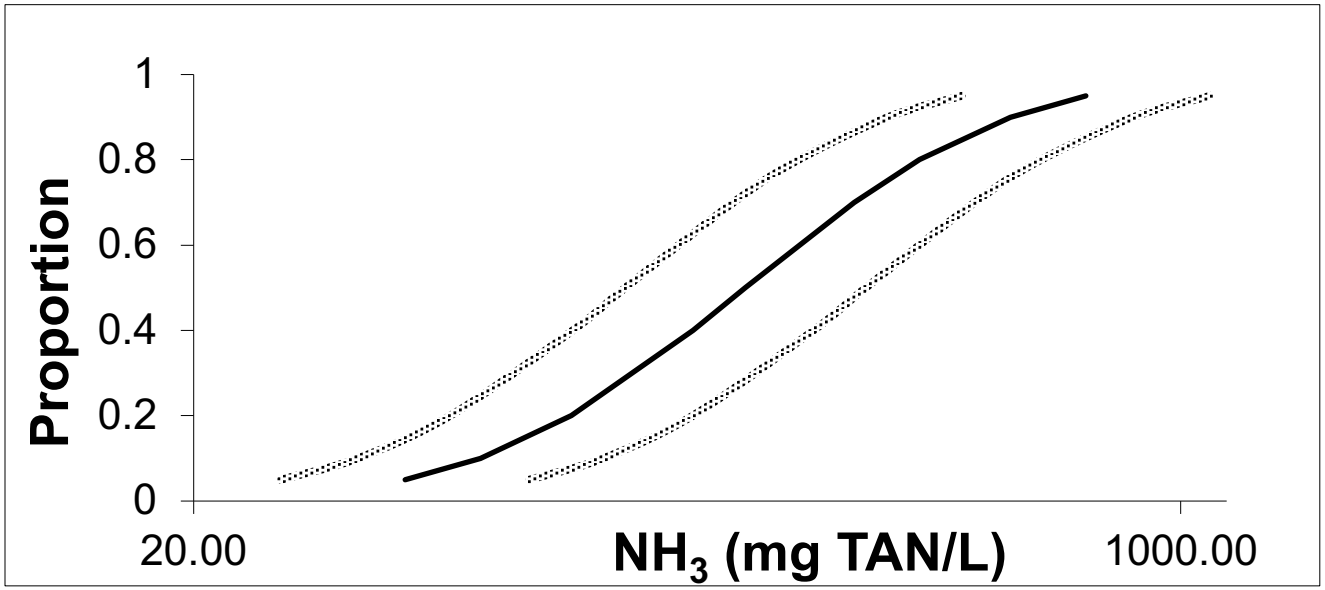

Appendix 48. Results of Species Sensitivity Distributions probit regressions using EPA CADDIS Volume 4: Data Analysis SSD_Generator_V1.xlt ***Fluminicola not resident*** *(https://www3.epa.gov/caddis/da_software_ssdmacro.html)*

Genera	MGAV NH_3 (mg TAN/L)	MGAV Log NH_3 (mg TAN/L) Geometric Mean	Proportion	Rank	Probit	Probit Predicted	Difference
Notemigonus	63.02	1.7995	1%	1	2.7220	3.6947	0.9460

Pseudacris	71.56	1.8547	3%	2	3.1762	3.8506	0.4549
Hybognathus	72.55	1.8606	6%	3	3.4179	3.8675	0.2021
Etheostoma	74.25	1.8707	8%	4	3.5919	3.8959	0.0925
Micropterus	89.06	1.9497	10%	5	3.7313	4.1192	0.1505
Musculium	89.36	1.9511	13%	6	3.8497	4.1233	0.0749
Rana	96.38	1.9840	15%	7	3.9538	4.2161	0.0688
Notropis	96.72	1.9855	17%	8	4.0476	4.2205	0.0299
Cyprinus	106.3	2.0265	19%	9	4.1338	4.3364	0.0411
Lepomis	106.9	2.0290	22%	10	4.2139	4.3433	0.0167
Cyprinella	110	2.0414	24%	11	4.2893	4.3784	0.0079
Campostoma	115.9	2.0641	26%	12	4.3609	4.4425	0.0067
Sander	117.1	2.0686	28%	13	4.4293	4.4552	0.0007
Dendrocoelum	119.5	2.0774	31%	14	4.4951	4.4801	0.0002
Daphnia	125	2.0969	33%	15	4.5588	4.5353	0.0006
Morone	134.8	2.1297	35%	16	4.6208	4.6279	0.0001
Procambarus	138	2.1399	38%	17	4.6814	4.6567	0.0006
Ictalurus	142.4	2.1535	40%	18	4.7408	4.6953	0.0021
Simocephalus	142.9	2.1550	42%	19	4.7993	4.6996	0.0099
Ceriodaphnia	143.9	2.1581	44%	20	4.8571	4.7081	0.0222

Catostomus	146.5	2.1658	47%	21	4.9144	4.7301	0.0340
Chasmistes	146.5	2.1658	47%	21	4.9144	4.7301	0.0340
Pimephales	159.2	2.2019	51%	23	5.0285	4.8322	0.0385
Chydorus	162.6	2.2111	53%	24	5.0856	4.8581	0.0517
Enallagma	164	2.2148	56%	25	5.1429	4.8686	0.0752
Physa	164.5	2.2162	58%	26	5.2007	4.8724	0.1078
Limnodrilus	170.2	2.2310	60%	27	5.2592	4.9142	0.1191
Crangonyx	181.8	2.2596	63%	28	5.3186	4.9951	0.1047
Skwala	192.4	2.2842	65%	29	5.3792	5.0647	0.0989
Hyalella	192.6	2.2847	67%	30	5.4412	5.0659	0.1408
Planorbella	211.6	2.3255	69%	31	5.5049	5.1814	0.1046
Tubifex	216.5	2.3355	72%	32	5.5707	5.2095	0.1305
Lumbriculus	218.7	2.3398	74%	33	5.6391	5.2219	0.1741
Gambusia	219.3	2.3410	76%	34	5.7107	5.2253	0.2356
Pachydiplax	233	2.3674	78%	35	5.7861	5.2997	0.2366
Callibaetis	246.5	2.3918	81%	36	5.8662	5.3688	0.2474
Asellus	378.2	2.5777	83%	37	5.9524	5.8942	0.0034
Caecidotea	387	2.5877	85%	38	6.0462	5.9225	0.0153
Drunella	442.4	2.6458	88%	39	6.1503	6.0867	0.0041

Chironomus	681.8	2.8337	90%	40	6.2687	6.6176	0.1217
Orconectes	686.2	2.8365	92%	41	6.4081	6.6255	0.0472
Stenelmis	735.9	2.8668	94%	42	6.5821	6.7113	0.0167
Philarctus	994.5	2.9976	97%	43	6.8238	7.0810	0.0661
Erythromma	2515	3.4005	99%	44	7.2780	8.2198	0.8870

PARAMETERS	
Slope	2.826
Intercept	-1.391
R^2	0.878
GrandMean	2.261
SumSQ	229.606
CSSQ	4.698
MSE	0.124
Tcrit	1.682
N	44
df	42

Proportion	Probit	Log Central Tendency	SSQ	Log Upper PI	Log Lower PI	Central Tendency	Upper PI	Lower PI
0.05	3.355	1.679	0.017	1.899	1.460	47.792	79.238	28.825
0.1	3.718	1.808	0.017	2.025	1.591	64.253	105.833	39.010
0.2	4.158	1.964	0.016	2.178	1.749	91.950	150.568	56.152
0.4	4.747	2.172	0.016	2.384	1.959	148.488	242.162	91.049
0.5	5.000	2.261	0.016	2.474	2.049	182.528	297.556	111.967
0.7	5.524	2.447	0.016	2.660	2.234	279.815	456.954	171.344
0.8	5.842	2.559	0.016	2.773	2.345	362.334	593.339	221.266
0.9	6.282	2.715	0.017	2.932	2.498	518.518	854.091	314.791
0.95	6.645	2.843	0.017	3.063	2.624	697.117	1155.868	420.439

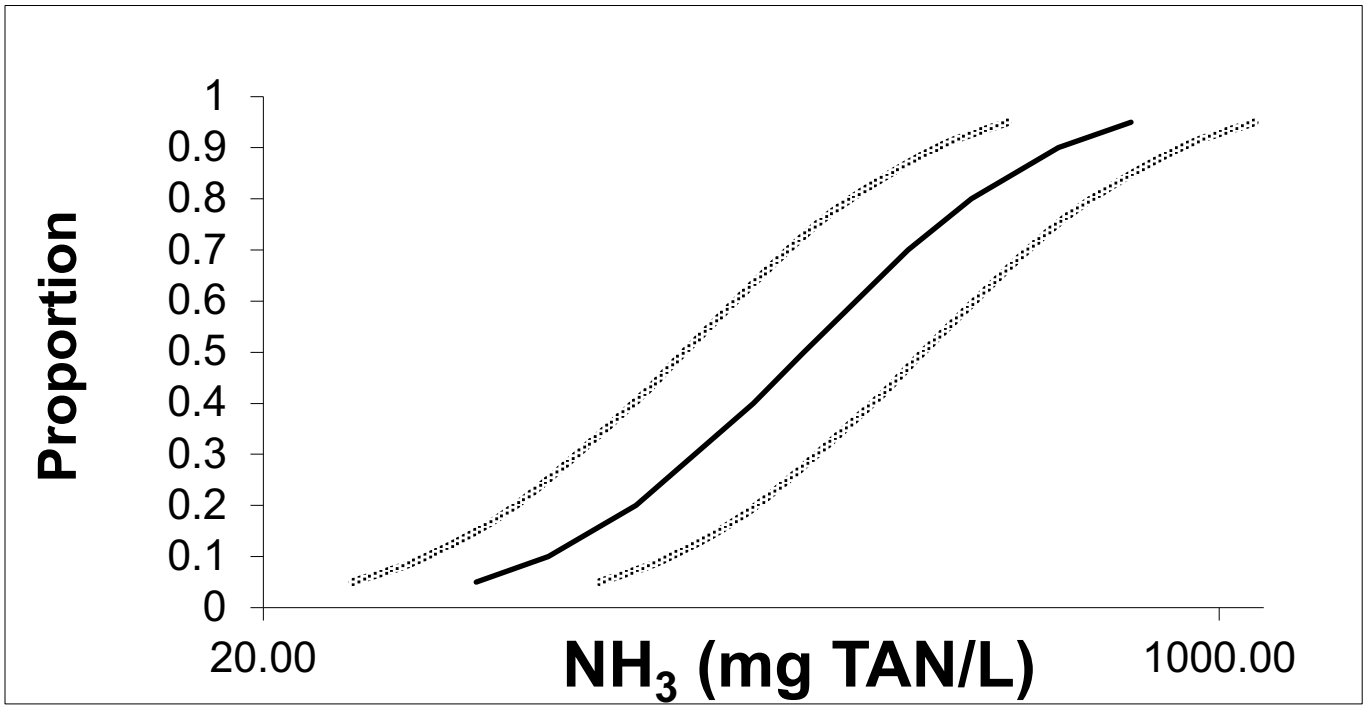

Appendix 49. Results of Species Sensitivity Distributions probit regressions using EPA CADDIS Volume 4: Data Analysis SSD_Generator_V1.xlt ***with three rare and not resident taxa removed*** *(https://www3.epa.gov/caddis/da_software_ssdmacro.html)*

Taxa	GMAV (mg TAN/L)	Log GMAV Geometric	Proportion	Rank	Probit	Probit Predicted	Difference^2

		Mean					
Pseudacris	71.56	1.8547	1%	1	2.7398	3.8184	1.1635
Hybognathus	72.55	1.8606	4%	2	3.1973	3.8353	0.4070
Etheostoma	74.25	1.8707	6%	3	3.4412	3.8636	0.1784
Micropterus	89.06	1.9497	8%	4	3.6170	4.0861	0.2200
Musculium	89.36	1.9511	11%	5	3.7581	4.0902	0.1103
Rana	96.38	1.9840	13%	6	3.8781	4.1827	0.0928
Notropis	96.72	1.9855	15%	7	3.9838	4.1870	0.0413
Cyprinus	106.3	2.0265	18%	8	4.0792	4.3026	0.0499
Lepomis	106.9	2.0290	20%	9	4.1669	4.3095	0.0203
Cyprinella	110	2.0414	23%	10	4.2485	4.3444	0.0092
Campostoma	115.9	2.0641	25%	11	4.3255	4.4083	0.0069
Sander	117.1	2.0686	27%	12	4.3987	4.4209	0.0005
Dendrocoelum	119.5	2.0774	30%	13	4.4687	4.4458	0.0005
Daphnia	125	2.0969	32%	14	4.5363	4.5008	0.0013
Morone	134.8	2.1297	35%	15	4.6018	4.5932	0.0001
Procambarus	138	2.1399	37%	16	4.6656	4.6219	0.0019

Ictalurus	142.4	2.1535	39%	17	4.7281	4.6603	0.0046
Simocephalus	142.9	2.1550	42%	18	4.7896	4.6645	0.0156
Ceriodaphnia	143.9	2.1581	44%	19	4.8502	4.6731	0.0314
Catostomus	146.5	2.1658	46%	20	4.9104	4.6950	0.0464
Pimephales	159.2	2.2019	49%	21	4.9702	4.7967	0.0301
Chydorus	162.6	2.2111	51%	22	5.0298	4.8225	0.0430
Enallagma	164	2.2148	54%	23	5.0896	4.8330	0.0659
Physa	164.5	2.2162	56%	24	5.1498	4.8368	0.0980
Limnodrilus	170.2	2.2310	58%	25	5.2104	4.8784	0.1102
Crangonyx	181.8	2.2596	61%	26	5.2719	4.9591	0.0978
Skwala	192.4	2.2842	63%	27	5.3344	5.0284	0.0936
Hyalella	192.6	2.2847	65%	28	5.3982	5.0297	0.1358
Planorbella	211.6	2.3255	68%	29	5.4637	5.1448	0.1017
Tubifex	216.5	2.3355	70%	30	5.5313	5.1728	0.1285
Lumbriculus	218.7	2.3398	73%	31	5.6013	5.1852	0.1732
Gambusia	219.3	2.3410	75%	32	5.6745	5.1885	0.2362
Pachydiplax	233	2.3674	77%	33	5.7515	5.2626	0.2389
Callibaetis	246.5	2.3918	80%	34	5.8331	5.3315	0.2516
Asellus	378.2	2.5777	82%	35	5.9208	5.8552	0.0043

Caecidotea	387	2.5877	85%	36	6.0162	5.8834	0.0177
Drunella	442.4	2.6458	87%	37	6.1219	6.0470	0.0056
Chironomus	681.8	2.8337	89%	38	6.2419	6.5762	0.1118
Orconectes	686.2	2.8365	92%	39	6.3830	6.5840	0.0404
Stenelmis	735.9	2.8668	94%	40	6.5588	6.6696	0.0123
Philarctus	994.5	2.9976	96%	41	6.8027	7.0380	0.0553
Erythromma	2515	3.4005	99%	42	7.2602	8.1730	0.8333

PARAMETERS	
Slope	2.817
Intercept	-1.406
R^2	0.870
GrandMean	2.274
SumSQ	221.677
CSSQ	4.469
MSE	0.132
Tcrit	1.684
N	42
df	40

Proportion	Probit	Log Central Tendency	SSQ	Log Upper PI	Log Lower PI	Central Tendency	Upper PI	Lower PI
0.05	3.355	1.690	0.018	1.918	1.462	49.000	82.821	28.991
0.1	3.718	1.819	0.018	2.044	1.594	65.943	110.659	39.297
0.2	4.158	1.975	0.017	2.197	1.753	94.481	157.534	56.665
0.4	4.747	2.184	0.017	2.404	1.964	152.820	253.671	92.064
0.5	5.000	2.274	0.017	2.494	2.054	187.983	311.900	113.298
0.7	5.524	2.460	0.017	2.681	2.240	288.589	479.742	173.601
0.8	5.842	2.573	0.017	2.795	2.351	374.019	623.625	224.317
0.9	6.282	2.729	0.018	2.954	2.504	535.880	899.253	319.340
0.95	6.645	2.858	0.018	3.086	2.630	721.173	1218.936	426.675

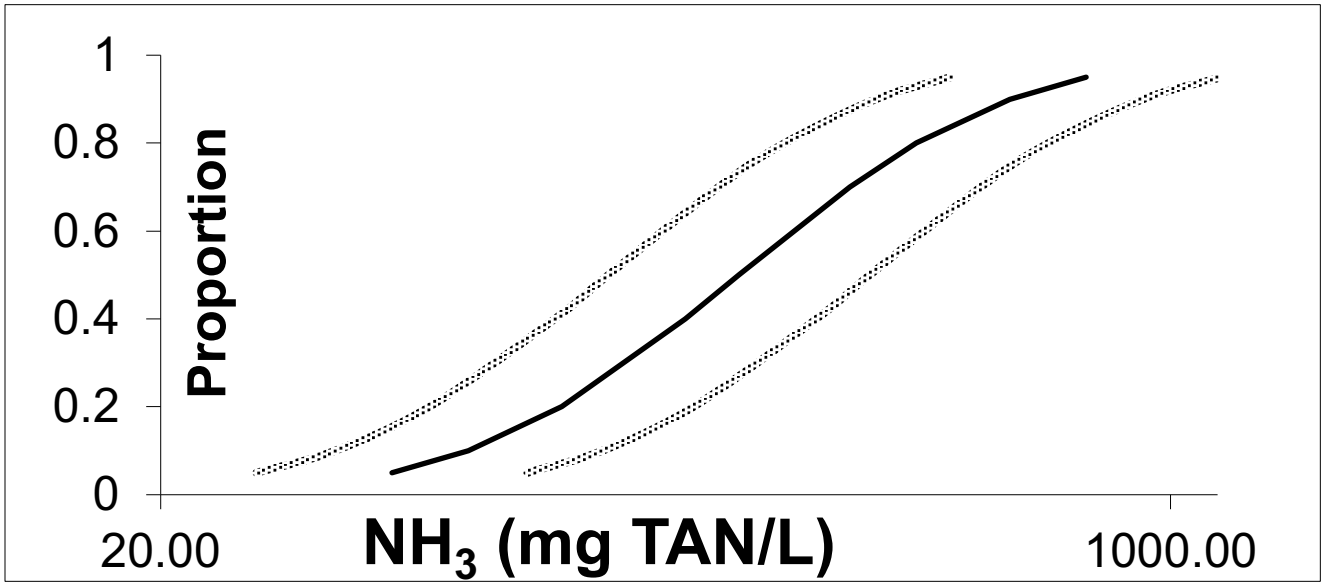
1
0.8
0.6
0.4
0.2
0
Proportion
20.00
NH3 (mg TAN/L)
1000.00

Volume II: Biological Integrity of the Jordan River

Appendix 50. Species, Genus, and Taxon-specific Acute Chronic Ratios (ACRs) for Freshwater Aquatic Animals Exposed to Ammonia (from Table F.1. USEPA 2013b).

Table F.1. Species, Genus and Taxon-specific ACRs for Freshwater Aquatic Animals Exposed to Ammonia

Species Scientific Name	Acute and Chronic Test Endpoint	pH	Temp	Normalized Values	Reference	ACR	SMACR	GMACR	TSACR (Family)	TSACR (Class)
Class Gastropoda (Family: Lithoglyphidae)										
Fluminicola sp.	LC50	8.25	20.2	>62.15	Besser 2011	7.94	7.94	7.94	7.94	7.94
	EC20 - Change in Length	8.22	20.1	7.828						
Class Bivalvia (Families Unionidae and Pasidiidae)										
Lampsilis fasciola	EC50	8.5	20	69.63	Wang et al. 2007b	49.45	49.45	21.13	15.52	25.68
	EC20 - Survival	8.2	20	1.408	Wang et al. 2007a					
Lampsilis siliquoidea	EC50	8.2	20	28.99	Wang et al. 2007a	9.028	9.028			
	EC20 - Survival	8.25	20	3.211	Wang et al. 2011					
Villosa iris	EC50	8.4	20	23.29	Wang et al. 2007b	11.4	11.4	11.4		
	EC50	8.3	20	68.4	Wang et al. 2007b					
	EC20 - Survival	8.2	20	3.501	Wang et al. 2007a					

Musculium transversum	EC50	8.1	14.6	109	West 1985; Arthur et al. 1987	42.5	42.5	42.5	42.5	
	EC20 - Survival	7.8	21.8	2.565	Sparks and Sandusky 1981					
Class Branchiopda (Family: Daphniidae)										
Ceriodaphnia acanthina	EC50	7.06	24	154.3	Mount 1982	2.406	2.406	3.073	5.113	5.113
	EC20 - Reproduction	7.15	24.5	64.1						
Ceriodaphnia dubia	EC50	7.8	25	152.9	Nimmo et al. 1989	3.924	3.924			
	EC20 - Reproduction	7.8	25	38.96						
Daphnia magna	EC50	8.5	20	296.9	Gersich and Hopkins 1986	8.186	8.507	8.507		
	EC20 - Reproduction	8.45	19.8	36.27	Gersich et al. 1985					
	EC50	8.34	19.7	419.1	Reinbold and Pescitelli 1982a	8.841				
	EC20 - Reproduction	7.92	20.1	47.4						
Class Malacostraca (Family: Dogielinotidae)										
Hyalella azteca	EC50	8.3	25	461.2	Ankley et al. 1995	15.81	15.81	15.81	15.81	15.81
	EC20 - Biomass	8.04	25	29.17	Borgmann 1994					

Table F.1. Species, Genus and Taxon-specific ACRs for Freshwater Aquatic Animals Exposed to Ammonia

Species Scientific Name	Acute and Chronic Test Endpoint	pH	Temp	Normalized Values	Reference	ACR	SMACR	GMACR	TSACR (Family)	TSACR (Class)
Class Actinopterygii (Families Salmonidae, Catostomidae, Cyprinidae, Ictaluridae and Centrarchidae)										
Oncorhynchus clarkii	LC50	7.81	13.1	132.3	Thurston et al. 1978					
O. clarkii henshawi	EC20 - Survival	7.57	13.7	25.83	Koch et al. 1980	5.122	5.122			
Oncorhynchus mykiss	LC50	7.4	14.5	31.47	Calamari et al. 1981					
	EC20 - Survival	7.4	14.5	3.246	Calamari et al. 1977, 1981	9.696		5.518	5.518	
	LC50	7.67	7.7	40.4	Thurston et al. 1981a		5.945			
	EC20 - 5 yr Life Cycle	7.7	7.5-10.5	>11.08	Thurston et al. 1984a	3.646				
Catostomus commersoni	LC50	8.16	15	176.6						
	LC50	8.14	15.4	166.3	Reinbold and Pescitelli 1982c	14.75	14.75	14.75	14.75	
	EC20 - Biomass	8.32	18.6	11.62	Reinbold and Pescitelli 1982a					
Notropis topeka	LC50	8.09	13.2	147.3	Adelman et al. 2009 (EC20 from Appendix C)					
	EC20 - Growth Rate	8.07	12.4	17.45		8.437	8.437	8.437		
	LC50	7.76	19	139.3						
	LC50	7.83	22	158.7						

Pimephales promelas	LC50	7.91	18.9	178.9	Thurston et al. 1983, 1986	36.53	19.24	19.24	10.96	8.973
	LC50	7.94	19.1	162.3						
	LC50	8.06	22	205						
	LC50	8.03	22.1	216.3						
	EC20 - LC Hatchability	8	24.2	4.784						
	LC50	8.14	22	141.2	Mayes et al. 1986	11.35				
	EC20 - Survival	8	24.8	12.43						
	LC50	7.78	25.9	117.3	Swigert and Spacie 1983	17.17				
	LC50	7.8	25.6	126.8						
	EC20 - Biomass	7.82	25.1	7.101						
Cyprinus carpio	LC50	7.72	28	133.9	Hasan and MacIntosh 1986	8.1	8.1	8.1		
	EC20 - Growth: Weight	7.85	23	16.53	Mallet and Sims 1994					
Ictalurus punctatus	LC50	7.8	25.7	97.67	Swigert and Spacie 1983	4.8	4.8	4.8	4.8	
	EC20 - Biomass	7.76	26.9	20.35						
Lepomis cyanellus	LC50	7.72	22.4	144.3	McCormick et al. 1984	12.18	6.468	13.58	13.59	
	EC20 - Biomass	7.9	22	11.85						
	LC50	8.28	26.2	62.07	Reinbold and Pescitelli 1982a	3.437				

Table F.1. Species, Genus and Taxon-specific ACRs for Freshwater Aquatic Animals Exposed to Ammonia										
Species Scientific Name	**Acute and Chronic Test Endpoint**	**pH**	**Temp**	**Normalized Values**	**Reference**	**ACR**	**SMACR**	**GMACR**	**TSACR (Family)**	**TSACR (Class)**
	EC20 - Survival	8.16	25.4	18.06						
Lepomis macrochirus	LC50	7.6	21.7	93.31	Smith et al. 1984	28.51	28.51			
	EC20 - Biomass	7.76	22.5	3.273						
Micropterus dolomieui	LC50 (pH 6.5)	6.53	22.3	269.2	Broderius et al. 1985		13.61	13.61		
	EC20 (pH 6.5) - Biomass	6.6	22.3	8.65		31.12				
	LC50 (pH 7.0)	7.16	22.3	144.3						
	EC20 (pH 7.0) - Biomass	7.25	22.3	9.726		14.84				
	LC50 (pH 7.5)	7.74	22.3	105.2						
	EC20 (pH 7.5) - Biomass	7.83	22.3	15.77		6.67				
	LC50 (pH 8.5)	8.71	22.3	126						
	EC20 (pH 8.5) - Biomass	8.68	22.3	11.31		11.14				

Western North American Naturalist 79(1), © 2019, pp. 72–84

Apparent extinction of native mussels in Lower Mill Creek and Mid-Jordan River, Utah

David C. Richards[1,*] and Theron Miller[2]

[1]*OreoHelix Consulting, Vineyard, UT*
[2]*Wasatch Front Water Quality Council, Salt Lake City, UT*

Abstract.—Native mussels likely occurred in Mill Creek and the Jordan River, Utah, in the past. However, human-induced impacts have virtually eliminated the possibility of their continued existence in these waters. We conducted an intensive native mussel survey upstream and downstream of a water reclamation facility discharge into Mill Creek and the Jordan River to determine its effects on mussel populations. The survey was conducted from September to October 2017 and resulted in approximately 7.6 m^3 of >4 mm-sized substrate particles being thoroughly examined at near 100% efficiency. We then used statistical models to estimate population densities as a function of probability of detection and search efficiencies based on this and other surveys. Regrettably, no live or recently dead native mussels were found. Given that our survey methods provided near perfect search efficiency, native mussel densities were estimated to be $<<0.03$ per m^2, which is much lower than what we consider to be a viable population density. Combined with multiple lines of evidence from other surveys, this low density strongly points toward the conclusion that native mussels are extinct in the survey area. Reasons for the demise of native mussels in Mill Creek and the Jordan River are numerous, and these factors need to be aggressively addressed if native mussels are to survive in the drainage.

Resumen.—Es probable que en el pasado habitaran mejillones nativos en el río Mill Creek y Jordan en Utah. Sin embargo, los impactos ocasionados por el hombre han eliminado prácticamente la posibilidad de su existencia en estas aguas. Llevamos a cabo un estudio intensivo de mejillones nativos, río abajo y río arriba en una instalación de descarga de agua reciclada en Mill Creek y en el río Jordan para determinar sus efectos en las poblaciones de mejillones. El estudio se llevó a cabo en septiembre y octubre del año 2017, en los cuales, se examinaron minuciosamente aproximadamente, 7.6 m^3 de partículas de sustrato de tamaño >4 mm, con una eficacia cercana al 100%. Posteriormente, utilizamos modelos estadísticos para estimar las densidades poblacionales en función de su probabilidad de detección y de la eficiencia de búsqueda, basada en este y en otros muestreos. Desafortunadamente, no encontramos mejillones nativos vivos o recientemente muertos. Debido a que, nuestros métodos de muestreo proporcionaron una eficacia de búsqueda casi perfecta, se estimó que la densidad de mejillones nativos es $<<0.03$ m^{-2}, mucho menor a lo que consideramos como una densidad poblacional viable, y cuando se combina con múltiples evidencias de otros muestreos, indica que los mejillones nativos están extintos en el área de estudio. Las razones de la desaparición de los mejillones nativos en los ríos Mill Creek y el Jordan son numerosas, y tales factores necesitan abordarse intensivamente para que los mejillones nativos puedan sobrevivir en el drenaje.

North America supports the richest diversity of freshwater mollusks (clams, mussels, and snails) on the planet, with at least 700 species of snails and 300 species of freshwater mussels (Johnson et al. 2013, FMCS 2015). Freshwater mollusks serve vital functions in freshwater ecosystems, are excellent indicators of water quality, and are increasingly recognized as important ecosystem providers (Huryn et al. 1995, Covich et al. 1999, Ostroumov 2005, Fulford et al. 2007, Brown and Lydeard 2010, Johnson et al. 2013). Unfortunately, freshwater mollusks are one of the most disproportionally imperiled groups on earth. Approximately 72% of North American freshwater mussel taxa are considered endangered, threatened, or species of concern (NatureServe 2014). This alarming decline is almost entirely due to human activities (Williams et al. 1993).

The greatest diversity of North America's freshwater mussels occurs in the southeastern USA, whereas in the western half of North America the mussel fauna is relatively depauperate. However, the area consisting of the

*Corresponding author: oreohelix@icloud.com

Fig. 1. The Jordan River flows north from its origin at the outlet of Utah Lake to its confluence with the Great Salt Lake. Mill Creek flows west from its origin in the Wasatch Mountains to its confluence with Jordan River. Both water bodies flow through the highly urbanized Salt Lake City metropolitan area. Numerous canals and several other tributaries are also shown. The survey area was near the confluence of Mill Creek with Jordan River. The Central Valley Water Reclamation Facility (CVWRF) is located approximately 0.8 km upstream of the confluence of Mill Creek with Jordan River.

Great Basin, Snake River Basin, and Bonneville Basin, including the Great Salt Lake and Jordan River–Utah Lake drainages, is a freshwater molluscan hotspot (Hershler and Sada 2002, Hovingh 2004). There are at least 70 mollusk taxa reported from Utah (Oliver and Bosworth 1999), many of which are freshwater endemics to the Bonneville Basin, and the evolution and distribution of this unique diversity are strongly linked with the geological and geomorphic history of pluvial Lake Bonneville (Hershler and Sada 2002, Polhemus and Polhemus 2002, Mock et al. 2004) (Fig. 1).

Two species of native mussels, the Floater, *Anodonta* sp. (Family: Unionidae) and the Western Pearlshell, *Margaritifera falcata* (Family: Margaritiferidae), probably occurred in the Jordan River, Utah, and its tributaries, including Mill Creek (Richards 2017, UDWQ 2017b). Taxonomy of *Anodonta* sp. is presently being reevaluated (Mock et al. 2004). Unfortunately, severely degraded conditions along with secondary host-dependent, dispersal-limited population dynamics and absence of past monitoring and legal protection have jeopardized the mussels' continued existence in these waters and waters throughout the west (USEPA 2013a, Richards 2017). There are no historical records of *M. falcata* occurring in Mill Creek or the Jordan River, and there is only one historical record, from 1942, of *Anodonta* sp. potentially occurring at a single location in the Jordan River (UDWQ 2017b), although *M. falcata* (formerly *Margaritana margaritifera*) was collected from Big Cottonwood Creek, a tributary of the Jordan River, a few miles upstream of Mill Creek in the 1880s (Natural History Museum of Utah, Salt Lake City specimens examined).

Prior to this study, Richards (2017) conducted the most extensive native mussel surveys in the Jordan River drainage to date, but did not find any live or recently dead native

mussels in Mill Creek or the Jordan River. However, Richards (2017) did find several highly weathered *Anodonta* sp. shell fragments, indicating that this species could have occurred in these or nearby waters in the past. Even though Richards (2017) concluded that native mussels were likely absent in Mill Creek and the Jordan River, absolute determination of absence is not possible without an unfeasibly complete and thorough examination of the entire creek and river beds (USEPA 2013a, 2013b, Richards 2017). Alternatively, probability of detection and survey efficiency statistical models in conjunction with knowledge of native mussel ecology and population dynamics can be employed to help validate a presence or absence conclusion (Smith 2006, Richards 2017, Richards and Miller 2017, UDWQ 2017a).

The United States Environmental Protection Agency (USEPA) recently recommended methods for surveying mussels (USEPA 2013b), and the Utah Division of Water Quality (UDWQ 2017a) developed mussel probability of detection (POD) standards for Utah waters. USEPA and UDWQ recommendations came in response to new USEPA ammonia criteria based on mussel sensitivities from published toxicity tests (USEPA 2013a). The POD criteria developed by UDWQ were based on survey search efficiencies and seemingly based on biological meaningful densities in order to determine presence or absence of native mollusks on a site-specific basis using Smith et al. (2001) and Smith (2006) statistical models. Search efficiency (SE) is also termed detectability, which is the probability of detecting an individual mussel in the survey area (Smith 2006).

We adapted USEPA-recommended methods to conduct an intensive and intrusive survey of native mussels in sections of Mill Creek and the mid-Jordan River upstream and downstream of a water treatment facility to determine whether native mussels occurred in this area and if so, whether their densities were affected by the facility's "zone of influence" (Richards and Miller 2017). We then calculated several PODs, SEs, and density estimates following Smith et al. (2001) and Smith (2006), and we compared our results with POD criteria developed by UDWQ. In addition, we produced a multiple-lines-of-evidence analysis based on results from our mussel surveys conducted over the past several years and from available historic survey data collected by other qualified researchers.

STUDY AREA

The Jordan River drainage is in north central Utah and drains an area of over 9842 km^2 (Fig. 1). Elevations range from 3637 m in the Wasatch Range to 1280 m where the Jordan River enters the Great Salt Lake. Average precipitation ranges from 31 $cm \cdot year^{-1}$ in the lower valleys to over 127 $cm \cdot year^{-1}$ in the higher elevations. Much of the precipitation occurs as snow, which contributes to the rivers as snowmelt during spring and summer. The Jordan River flows north from Utah Lake for about 82 km through the most populous, industrialized, and urbanized area of Utah, including Salt Lake City, before entering the Great Salt Lake. Major tributaries to the Jordan River include Big Cottonwood, Little Cottonwood, Red Butte, Mill, Parleys, and City Creeks. However, most of these tributaries were diverted and heavily modified by Mormon settlers in the Salt Lake Valley, starting in the mid-1800s (Bancroft 1889, Alexander 2003), and most remain disconnected from the Jordan River.

Mill Creek originates in the Wasatch Mountains and then flows through the City of South Salt Lake where it joins the Jordan River (Fig. 1). After leaving the Wasatch Mountains and United States Forest Service lands, where it is relatively unimpaired, most Mill Creek waters are captured and diverted for municipal use by the citizens of Salt Lake City. Remaining waters in Mill Creek are then supplemented and often dominated by waters transported directly from highly eutrophic Utah Lake via the Jordan and Salt Lake Canals. After water quality has been compromised by Utah Lake water, Lower Mill Creek flows through a heavily urbanized, residential, and industrial landscape before joining the Jordan River. By all standards, the sections of Mill Creek and the Jordan River that we surveyed are in poor condition, are poorly managed, and are of eroded integrity (Richards and Miller 2017).

The Central Valley Water Reclamation Facility (CVWRF) at 800 West Central Valley Road (3190 South) in Salt Lake City, Utah, is the largest treatment facility in the greater Salt Lake City area and was built to treat 75 million gallons of wastewater per day, serving over half a million people in Salt Lake County. CVWRF discharges treated water directly into Mill Creek approximately 400 m upstream of its confluence with the Jordan River. Discharge from the facility is required to meet state and

federal water quality standards, including new ammonia criteria that were primarily based on native mussel presence or absence (USEPA 2013a, 2013b, UDWQ 2017a). An ammonia "zone of influence" was designated by UDWQ to extend from CVWRF discharge downstream in Mill Creek and the Jordan River to about the bridge crossing at 900 South, approximately 3.5 km (Richards and Miller 2017).

Methods

We conducted intrusive excavation surveys as suggested by UDWQ (2017a) and USEPA (2013b) using 2 methods: (1) shovel-netting for wadeable sections of the area, and (2) suction dredging for deeper, nonwadeable sections of the area. The survey was conducted between 16 September 2017 and 24 October 2017 (Appendixes 1 and 2 include dates, Universal Transverse Mercator [UTM] coordinates, survey method, area [m^2], substrate types, and depths [cm] for the Jordan River and Mill Creek, respectively).

Wadeable Sections

We used a flat-bottom shovel with a 10-cm depth line marked across the blade to survey wadeable sections of the survey area. One surveyor demarcated a 0.5-m^2 area of substrate using the known width of the shovel blade and then sank the shovel down to a penetrable depth (up to 10 cm) and scooped all sediment in the 0.5-m^2 area into a heavy-framed 1-mm-mesh benthic net held by a second surveyor standing directly downstream of the first surveyor. Net contents were then taken on shore and sieved through 4-mm-mesh sieves into large plastic trays and closely examined for mollusks (bivalves and gastropods). We used a grid layout and randomly selected grids for sampling. We collected 132 shovel/net substrate samples (0.5 m^2 each) at 79 locations for a total of 66 m^2 (approximately 6.6 m^3) (Appendixes 1, 2).

Nonwadeable Sections

We used a shoreline-based suction dredge sampler fitted with a handheld 7.62-cm-diameter suction hose to sample nonwadeable sections of the survey area on several occasions. We attached a 22.23-cm-wide by 20.32-cm-tall (3.79-L) aluminum large-mouth funnel to the end of the hose (end diameter of the funnel = 387.77 cm^2). One surveyor pushed the funnel into the soft-bottomed substrate to a depth up to 10 cm while wading and while the suction pump was running. The funnel was pushed into substrate 13 times in adjacent locations to cover a 0.5-m^2 area while suction contents were being pumped into a 189.27-L barrel on shore. The pump was powerful enough to collect sediments up to large gravel size (and presumably large mussels). To ensure that enough sediment was collected, a line was drawn along the outside of the 189.27-L barrel to mark a volume of 0.05 m^3 (0.5 m^2 × 0.1 m substrate depth), and dredging continued until sediments filled the barrel to that line. Sediments were gravel size or smaller at all but one site; therefore, by measuring content volume in the barrel we estimated that we sampled at least a 0.5-m^2 area. The substrate at one of the deeper sites was mostly medium to large cobbles; consequently, we dredged approximately a 4.0-m^2 area to ensure adequate coverage. A total of approximately 9.7 m^2 of substrate was sampled from 7 locations in deeper-water habitats using the suction dredge method (Appendixes 1, 2). All suction dredge locations within the deeper-water sites were randomly chosen, similar to methods used in the wadeable sections.

Statistical Models

We used the Smith (2006) quantitative mussel survey formula (eq. 4, p. 703)

$$\mathrm{POD} = 1 - e^{-\beta\alpha\mu},$$

where POD = probability of detecting at least one individual mussel; β = search efficiency (SE), α = search area = 75.7 m^2, and μ = density (m^{-2}), to develop a probability of detection (POD) model as a function of density at a search efficiency between 0.75 and 1.00. We then compared our model results with UDWQ (2017a) criteria that recommend surveying enough area with 100% search efficiency and 90% POD at their predetermined biologically meaningful density of 0.1 m^{-2}. We also modeled these relationships from other data sources as multiple lines of evidence for presence/absence determination. Other sources included Richards (2017) survey data, the Bureau of Land Management/Utah State University MAPIT database, and the UDWQ (2017a) report.

RESULTS

No live or recently dead native mussels (*Anodonta* sp. or *M. falcata*) were found in the survey area, despite our intensive survey efforts. Therefore, we could not evaluate the effects of CVWRF on native mussel populations within the study area because none were found either upstream or downstream of the facility. Only one tiny, well-weathered *Anodonta* fragment was found in Mill Creek. It is unknown whether this shell fragment represented an individual that once lived in the survey area or one that was deposited via past high-flow events from an upstream source, including Utah Lake, a former *Anodonta* stronghold (UDNR 2007).

Probabilities of Detection (POD), Search Efficiencies (SEs), and Density Estimates

Using the Smith (2006) equation, we determined that estimated mussel densities only had to be ≥ 0.04 m^{-2} at an unrealistically low search efficiency of 0.75 for our survey to obtain a UDWQ-recommended POD of 0.90 (Fig. 2). However, excavation methods (e.g., shovel-nets, suction dredges) are considered the most effective sampling methods for detecting mussels (USEPA 2013b), and when sieved materials are thoroughly examined, survey results closely approach 100% search efficiency. Thus, we assumed that our search efficiency was ≥ 0.99, which equated to a density estimate of 0.03 m^{-2} at POD = 0.90 (Fig. 2). In other words, we should have observed at least one mussel if they occurred in the survey area at densities ≥ 0.03 m^{-2}. At UDWQ's recommended biologically meaningful density of 0.1 m^{-2}, our estimated POD was 1.00, even at the unrealistically low search efficiency of 0.75 (Fig. 2). That is, even if after close examination we missed observing 1 out of 4 mussels in our viewing trays, we still would have found mussels if they occurred at density levels ≥ 0.1 m^{-2}.

Multiple Lines of Evidence from Other Native Mussel Surveys

This survey produced no live or recently dead native mussels, and our POD, SEs, and density estimate models suggested that native mussels were absent from the survey area. However, concluding absence (extinction) of Utah's native mussels from an area where they should occur based on a single survey does not seem wise. The following analyses from other mussel surveys on Mill Creek and Jordan River provided multiple lines of evidence that further helped determine whether native mussels were present or absent in the survey area.

THE RICHARDS (2017) UTAH LAKE–JORDAN RIVER DRAINAGE MUSSEL SURVEY—Richards (2017) conducted extensive visual and limited excavation surveys in Mill Creek, the Jordan River, and other locations within the Utah Lake–Jordan River drainage in 2015 and 2016. Analysis of the Richards (2017) unpublished data for the Jordan River and Lower Mill Creek produced probability of detection (POD) and search efficiency relationships as a function of density that also support an absence conclusion. As an example, mussel densities only needed to be at a biologically unsustainable density of 0.001 visible mussels m^{-2}, even at an extremely low search efficiency of 0.07 (i.e., only 7 out of 100 mussels needed to be observed on the substrate surface) in Mill Creek when data were modeled at POD = 0.90 (Fig. 3). Similarly, mussel densities in the Jordan River only had to be at a density of 0.0005 m^{-2} to have a POD = 0.90, again with an extremely low search efficiency of 0.08 (i.e., 8 out of 100 observed) (Fig. 4). At a UDWQ-suggested biologically meaningful density = 0.1 m^{-2} and POD = 0.90, search efficiencies based on Richards' (2017) data only needed to be 1 visible mussel out of 1000 in Mill Creek and 4 visible mussels out of 10,000 in the Jordan River (Figs. 3, 4). These very low search efficiency requirements are well below what other mussel experts report for the proportion of mussel populations visible on the substrate surface. For example, USEPA (2013) reported that 50% of a mussel community was present at the substrate surface, and Smith (2006) reported that 30% to 50% of 2 species of the family Unionidae (river mussels) were visible on the substrate surface. These results are further evidence that native mussels are absent or may occur at extremely low, unsustainable densities in the survey area.

USU–BLM MAPIT DATABASE.—The MAPIT database (Mapping Application for Freshwater Invertebrate Taxa; http://wmc6.bluezone.usu.edu), developed by the Bureau of Land Management and Utah State University's National

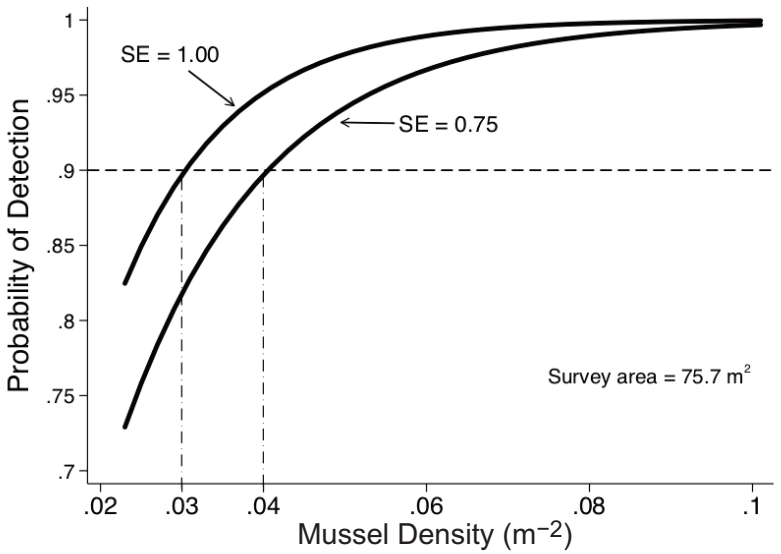

Fig. 2. Relationship between probability of detection (POD) and mussel density (m^{-2}) at search efficiencies (SEs) between 0.75 and 1.00 in our Mill Creek and mid-Jordan River survey area (75.7 m^2). Even at a very poor search efficiency of 0.75, densities only needed to be 0.04 m^{-2} for a UDWQ-recommended POD of 0.90 (dashed and dotted lines). However, we assumed that our search efficiency was ≥0.99, which equates to a density estimate of 0.03 m^{-2} at UDWQ-recommended POD = 0.90 (dashed and dotted lines). At UDWQ-recommended biologically meaningful density = 0.1 m^{-2}, our estimated POD was 1.00, even if we had a very poor search efficiency of 0.75. Model based on Smith (2006).

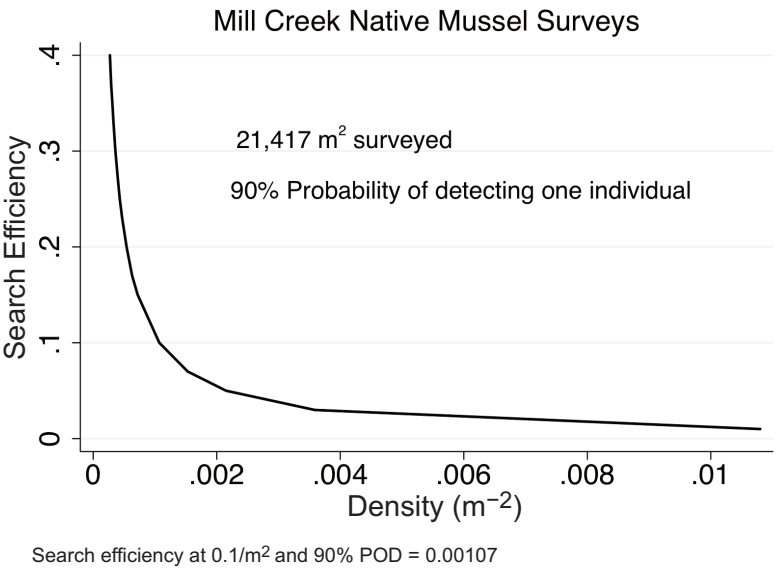

Fig. 3. Ninety percent probabilities of detecting at least one individual native mussel (e.g., *Anodonta* sp.) during the Mill Creek survey at various search efficiencies and corresponding densities, given the Richards (2017) survey of 21,417 m^2. As an example, Richards' (2017) data had a 90% probability of detecting at least one individual if densities were 0.001 m^{-2} with a search efficiency of approximately 0.07 (7%). Estimates are based on mussel distributions from Smith (2006). The formula for the graph is $0.90 = 1 - e^{-\beta\alpha\mu}$, where 0.90 is a 90% probability of detecting at least one individual mussel, β = search efficiency, α = search area = 21,417 m^2, and μ = density (m^{-2}).

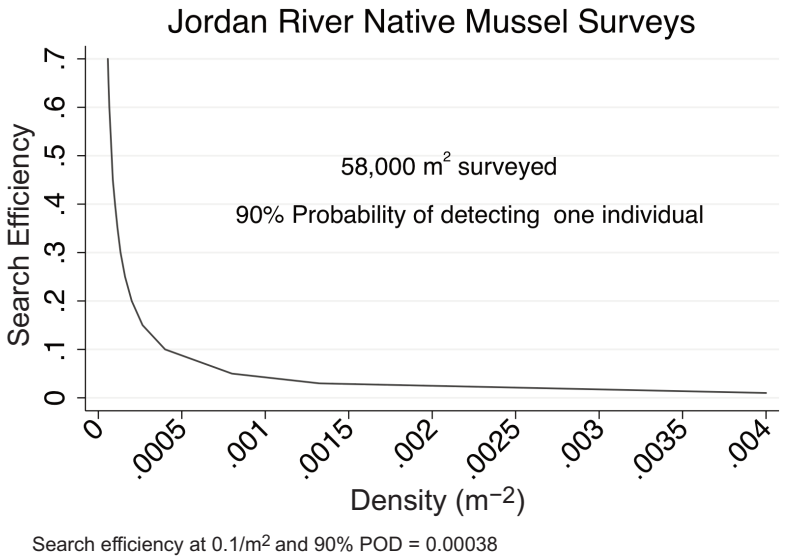

Fig. 4. Ninety percent probabilities of detecting at least one individual native mussel (e.g., *Anodonta* sp.) in the Jordan River at various search efficiencies and corresponding densities, given that Richards (2017) sampled 58,000 m^2 of river. As an example, there was a 90% probability of detecting at least one individual if densities were 0.0005/m^2 and a search efficiency of approximately 0.078 (approximately 8%). Estimates are based on mussel distributions from Smith (2006). The formula for the graph is $0.90 = 1 - e^{-\beta\alpha\mu}$, where 0.90 is a 90% probability of detecting at least one individual mussel, β = search efficiency, α = search area = 58,000 m^2, and μ = density (m^{-2}).

Aquatic Monitoring Center, has an extensive set of benthic invertebrate survey data compiled from several water quality management agencies, including EMAP–West, NAQWA, USU/BLM–BUGLAB, and UDWQ. We queried this database for the presence of native mussels from samples collected in the Jordan River and Mill Creek and then calculated the total survey areas (m^2) sampled. The MAPIT database produced 80 Mill Creek macroinvertebrate data sets for a total of 65.97 m^2 sampled with no native mussels reported. MAPIT also produced 55 Jordan River macroinvertebrate data sets for a total of 40.38 m^2 sampled, but again no native mussels were reported. Most of the water quality monitoring programs, including USU/BLM–BUGLAB and UDWQ, employ standardized benthic invertebrate sampling methods. These methods typically involve the use of Hess or Surber samplers that do not target native mussel collection. However, their protocols direct surveyors to specifically include mussels "when encountered," and other bivalves such as *Corbicula* sp. and Sphaeriidae were reported in their MAPIT data sets. Therefore, we consider these data sets to be valid supportive information for determining presence/absence. Subsequently, we developed useful and reliable POD, SE, and density models from the 2 MAPIT data sets (Figs. 5, 6). As an example from the models (Figs. 5, 6), mussel densities needed to be $\geq$0.11 m^{-2} for mussels in the Jordan River and $\geq$0.07 m^{-2} for mussels in Mill Creek, at a UDWQ-recommended POD = 0.90, to be detected at a very low SE of 0.50. We could not determine search efficiencies for methods used in the MAPIT data but assume that they are at least 0.50. These MAPIT-based models also support our survey findings that live or recently dead native mussels in Mill Creek and the Jordan River are likely absent.

UDWQ HISTORIC MUSSEL SPECIFIC SURVEYS.—UDWQ (2017b) recently completed a report based on a literature review of historical mussel presence/absence locations in Utah. They found no records of *M. falcata* in Mill Creek or the Jordan River and no *Anodonta* records from lower Mill Creek or the mid-Jordan River in our survey area. However, UDWQ (2017b) did report one *Anodonta* data point from the Jordan River dated 1942. It appears that this record was collected from an old Jordan River channel that is no

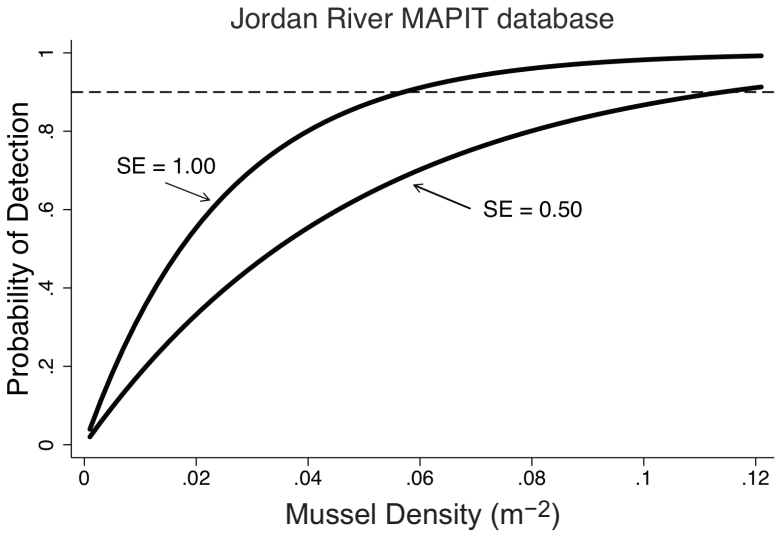

Fig. 5. Bureau of Land Management/Utah State University MAPIT data set for Jordan River. $N = 55$ sample events, 40.38 m^2 sampled.

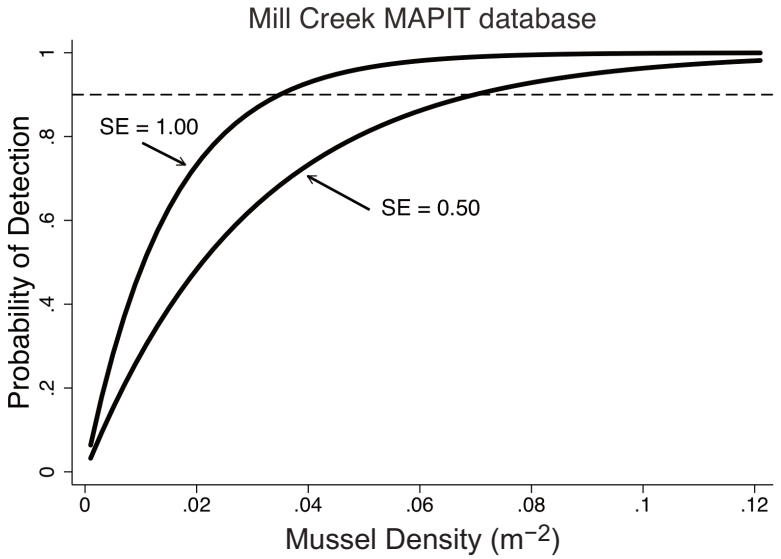

Fig. 6. Bureau of Land Management/Utah State University MAPIT data set for Mill Creek. $N = 80$ sample events, 65.97 m^2 sampled.

longer occupied by the present Jordan River channel, or it is possible that the latitude/longitude coordinates were not reported correctly. The UDWQ (2017b) historical data review is consistent with our survey findings that native mussels are absent from the survey area and likely the entire lower Mill Creek and Jordan River, although we caution that very few mussel-specific surveys other than those presented here and by Richards (2017) have been conducted in Utah waters.

DISCUSSION

The combined analyses presented here provide a strong multiple-lines-of-evidence

conclusion that native mussels in Mill Creek and the Jordan River are likely absent. This apparent extinction of native mussels in our survey area and their continued demise throughout the Utah Lake–Jordan River drainage as reported by Richards (2017) are of great ecological and societal concern. Reasons for their rapid decline in Utah and throughout the United States are numerous and cumulative, and are discussed at length by Richards (2017) and others (Strayer 1999, 2013, Johnson et al. 2013). It does not appear that the Central Valley Water Reclamation Facility discharge was responsible for the apparent extinction of native mussels in the survey area, nor that native mussels will return in the foreseeable future (Richards 2017, Richards and Miller 2017).

If per chance native mussels do survive undetected in the Jordan River or Mill Creek, they do so at what we suggest are critically low, unsustainable densities. Both native mussel taxa, *Anodonta* sp. and *M. falcata*, require secondary fish hosts to reproduce. Consequently, suitable fish host densities and mussel densities both need to be sufficiently great for mussel viability (i.e., biologically meaningful densities) (Strayer 2013, Richards 2017), but neither appears to be sufficient in the Jordan River or Mill Creek (Richards 2017). As far as we know, biologically meaningful densities for either mussel taxon have not been adequately evaluated or equivocally determined. For example, a mussel density of 0.1 m^{-2} could be sufficient if fish host density were extremely high but would be considered unsustainable if fish host densities were low or if there were no connectivity between populations (i.e., isolated populations vs. metapopulations). The POD models developed by Smith (2006) were based on several distribution assumptions that, although necessary for model development, are not always representative of mussel population distributions. As an example, the Smith (2006) models were based on Poisson probability distributions, which implies that mussels at very low densities have a spatially random distribution (Smith 2006). We suggest that mussel density distributions are often not spatially random but are often highly spatially autocorrelated, especially when populations become small and isolated. That is, it is more likely to encounter a mussel where other mussels occur. We are also advocates of the axiom that "nothing in the universe is random," although things may appear to be random in the absence of useful information. However, assuming that the Smith (2006) models provide reasonable statistical relationships between POD, SE, and mussel density and that the models are extremely useful for understanding mussel population viability, biologically meaningful densities still need to be determined. Smith (2006) stated, "The determination of a biologically meaningful threshold should involve multiple considerations including legal mandates, life history, population viability, and comparisons of densities throughout a local watershed, region, or range." These factors clearly need to be addressed before biologically meaningful densities can be determined for native mussels in the Jordan River drainage. Much of this information is available. For example, Richards (2017) discussed life histories and population viability dynamics (including metapopulation viability dynamics) at length and provided density estimates of native mussels throughout much of the drainage. Sadly, the prognosis is not good. Native mussel populations appear to be in steep decline throughout the region, and only a few small, isolated populations of *Anodonta* still exist in the Utah Lake–Jordan River drainage. The Western Pearlshell mussel, *Margaritifera falcata*, may no longer exist.

Even though native mussels in all likelihood are absent from lower Mill Creek and the mid-Jordan River, the invasive clam *Corbicula fluminea* thrives. Although not the focus of this survey, we have accumulated the most data to date on *Corbicula* densities in relation to habitat conditions in Mill Creek and the Jordan River (Richards and Miller 2017). We estimated that *Corbicula* densities can sometimes exceed 12,000 m^{-2} as live individuals and >16,000 m^{-2} as live and empty shells in ideal Jordan River habitat. Ideal habitat for *Corbicula* appears to be runs with moderate flow and mostly small- to medium-sized gravels of sufficient depth to allow the clams to secure themselves. It is well known that *Corbicula* is a very strong competitor and predator on native mussels and is likely a major contributor to the continued demise of native mussels in our survey area and other invaded locations (Phelps 1994, Strayer 1999, Strayer 2013, Richards 2017).

Our mussel survey methods also weren't designed as fish surveys, although we have conducted fish surveys in the past. We did not observe many potential fish hosts during our mussel survey. We captured only 2 individuals, one small burbot (*Lota lota*) and one fathead minnow (*Pimephales promelas*), in the survey and only rarely saw other fish swimming by, mostly common carp (*Cyprinus carpio*). Richards (2017) discussed at length how secondary fish host densities must be high enough for successful glochidium (larval mussel) attachment and juvenile recruitment, including fish host densities in Mill Creek and the Jordan River. We suggest that Mill Creek and the Jordan River no longer have high enough densities of fish hosts for mussel viability.

Finally, Mill Creek and the Jordan River have been physically degraded for many decades. Both water bodies have been channelized and diverted and no longer function as natural systems (Richards and Miller 2017). Most sections of these waters in the survey area continue to be dredged on a regular basis, eliminating whole age classes of extant native mussel populations, making recruitment almost nonexistent, and sending population viability spiraling to zero in these locations, even without the other factors that negatively influence their populations.

Conclusion

Results of this native mussel survey combined with other surveys provide multiple lines of evidence that show that native mussels in lower Mill Creek and the mid-Jordan River are likely extinct or are so extremely rare and cryptic that as far as is known, no live individuals have ever been documented in Mill Creek nor have any been documented in the Jordan River since 1942. Reasons for their rapid decline, decreased population viability, and potential complete demise throughout the Jordan River drainage are numerous, and immediate steps need to be taken if they are to survive in remaining occupied habitats.

Acknowledgments

We extend thanks to our mussel survey technicians W.D. Robinson and Frank Fluckinger and to the Wasatch Front Water Quality Council for funding this important research.

Literature Cited

Alexander, T.G. 2003. Utah, the right place. Revised and updated edition. Utah Division of State History. Gibb Smith [publisher], Layton, UT.

Bancroft, H.H. 1889. The works of Hubert Howe Bancroft. Volume XXVI, History of Utah. 1540–1886. The History Company, San Francisco, CA.

Brown, K.M., and C. Lydeard. 2010. Mollusca: Gastropoda. Pages 277–306 *in* J.H. Thorp and A.P. Covich, editors, Ecology and classification of North American freshwater invertebrates. Academic Press, New York, NY.

Covich, A.P., M.A. Palmer, and T.A. Crowl. 1999. The role of benthic invertebrate species in freshwater ecosystems. BioScience 49:119–127.

[FMCS] Freshwater Mollusk Conservation Society. 2015. Freshwater Mollusk Conservation Society [website]. https://molluskconservation.org

Fulford, R.S., D.L. Breitburg, R.I.E. Newell, W.M. Kemp, and M. Luckenbach. 2007. Effects of oyster population restoration strategies on phytoplankton biomass in Chesapeake Bay: a flexible modeling approach. Marine Ecology Progress Series 336: 43–61.

Hershler, R., and D.W. Sada. 2002. Biogeography of Great Basin aquatic snails of the genus *Pyrgulopsis.* Smithsonian Contributions to the Earth Sciences 33:255–276.

Hovingh, P. 2004. Intermountain freshwater mollusks, USA (*Margaritifera, Anodonta, Gonidea, Valvata, Ferrissia*): geography, conservation, and fish management implications. Monographs of the Western North American Naturalist 2:109–135.

Huryn, A.D., A.C. Benke, and G.M. Ward. 1995. Direct and indirect effects of geology on the distribution, biomass, and production of the freshwater snail *Elimia.* Journal of the North American Benthological Society 14:519–534.

Johnson, P.D., A.E. Bogan, K.M. Brown, N.M. Burkhead, J.R. Cordeiro, J.T. Garner, P.D. Hartfield, D.A.W. Lepitzki, G.L. Mackie, E. Pip, et al. 2013. Conservation status of freshwater gastropods of Canada and the United States. Fisheries 38:247–282.

Mock, K.E., J.C. Brim-Box, M.P. Miller, M.E. Downing, and W.R. Hoeh. 2004. Genetic diversity and divergence among freshwater mussel (*Anodonta*) populations in the Bonneville Basin of Utah. Molecular Ecology 13:1085–1098.

NatureServe. 2014. NatureServe Explorer. http://explorer.natureserve.org

Oliver, G.V., and W.R. Bosworth III. 1999. Rare, imperiled, and recently extinct or extirpated mollusks of Utah: a literature review. State of Utah Department of Natural Resources, All U.S. Government Documents (Utah Regional Depository). Paper 531. http://digitalcommons.usu.edu/govdocs/531

Ostroumov, S.A. 2005. Suspension-feeders as factors influencing water quality in aquatic ecosystems. Pages 147–164 *in* R. Dame and S. Olenin, editors, The comparative roles of suspension feeders in ecosystems. NATO Science Series: IV Earth and Environmental Sciences Volume 47. Springer, Netherlands.

Phelps, H.I. 1994. The Asiatic clam (*Corbicula fluminea*) invasion and system-level ecological change in the

Potomac River estuary near Washington, D.C. Estuaries 17:614–621.

Polhemus, D.A., and J.T. Polhemus. 2002. Basins and ranges: the biogeography of aquatic true bugs (Insecta: Heteroptera) in the Great Basin. Smithsonian Contributions to the Earth Sciences 33:235–254.

Prins, T., and V. Escaravage. 2005. Can bivalve suspension feeders affect pelagic food web structure? Pages 31–51 *in* R. Dame and S. Olenin, editors, The comparative roles of suspension feeders in ecosystems. NATO Science Series: IV Earth and Environmental Sciences Volume 47. Springer, Netherlands.

Richards, D.C. 2017. Native Unionoida surveys, distribution, and metapopulation dynamics in the Jordan River–Utah Lake Drainage, UT. Report to Wasatch Front Water Quality Council, Salt Lake City, UT. OreoHelix Consulting, Vineyard, UT. Version 1.5. 26 May 2017. http://wfwqc.org/wp-content/uploads/2017/04/Native-Unionoida-Surveys-and-Metapopulation-Dynamics-in-the-Jordan-River-Utah-Lake-drainage-UT-Version-1.5-compressed.pdf. Supporting documentation: http://wfwqc.org/wp-content/uploads/2017/10/Appendix-8-Native-Mussels-Spreadsheet-FINAL-read-only.xlsx

Richards, D.C., and T. Miller. 2017. Lower Mill Creek and Jordan River native mussel surveys. Scope of Work (SOW) and Sampling and Analysis Plan (SAP), Draft Final. Version 2.0. 14 August 2017. Wasatch Front Water Quality Council, Salt Lake City, UT.

Smith, D.R. 2006. Survey design for detecting rare freshwater mussels. Journal of the North American Benthological Society 25:701–711.

Smith, D.R., R.F. Villella, D.P. Lemarié, and S. Von Oettingen. 2001. How much excavation is needed to monitor freshwater mussels? Pages 203–218 *in* R.A. Tankersley, D.I. Warmolts, G.T. Watters, B.J. Armitage, P.D. Johnson, and R.S. Butler, editors, Freshwater Mollusk Symposium Proceedings. Ohio Biological Survey, Columbus, OH.

Strayer, D.L. 1999. Effects of alien species on freshwater mollusks in North America. Journal of the North American Benthological Society 18:74–98.

Strayer, D.L. 2013. Freshwater mussel ecology: a multifactor approach to distribution and abundance. Freshwater Ecology Series. University of California Press, Oakland, CA. 204 pp.

[USEPA] United States Environmental Protection Agency. 2013a. Aquatic life ambient water quality criteria for ammonia-freshwater 2013. USEPA, Office of Water, Office of Science and Technology, Washington, DC. EPA-822-R-13-001.

[USEPA] United States Environmental Protection Agency. 2013b. Technical support document for conducting and reviewing freshwater mussel occurrence surveys for the development of site-specific water quality criteria for ammonia. U.S. Environmental Protection Agency Office of Water Office of Science and Technology Standards and Health Protection Division National Water Quality Standards Branch Washington, DC. August 2013. EPA 800-R-13-003.

[UDNR] Utah Department of Natural Resources. 2007. Utah sensitive species list. State of Utah Department of Natural Resources, Division of Wildlife Resources. 14 December 2007.

[UDWQ] Utah Division of Water Quality. 2017a. Adoption of USEPA 2013 ammonia criteria for the protection of aquatic life in Utah. 12 March. Review draft v.0.1. Utah Division of Water Quality, Salt Lake City, UT. https://documents.deq.utah.gov/water-quality/standards-technical-services/us-epa/DWQ-2017-002062.pdf

[UDWQ] Utah Division of Water Quality. 2017b. Utah and Colorado water survey for mussels and snails. Final report. Original draft—1 July 2017. Revised draft. Utah Division of Water Quality, Salt Lake City, UT. https://documents.deq.utah.gov/water-quality/facilities/utah-colorado-water-survey/DWQ-2017-008943.pdf

Williams, J.D., M.L. Warren Jr., K.S. Cummings, J.L. Harris, and R.J. Neves. 1993. Conservation status of freshwater mussels of the United States and Canada. Fisheries 18:6–22.

Received 8 March 2018
Revised 7 May 2018
Accepted 6 June 2018
Published online 8 April 2019

APPENDIX 1. Jordan River 2017 site data. Locations are given in relation to the confluence with Mill Creek. All shovel sample areas equal 0.5 m^2, whereas all suction dredge sample areas were between 0.5 and 4.0 m^2. Samples were collected between 23 September 2017 and 23 October 2017. Substrate codes: CPOM = coarse particulate organic matter, FPOM = fine particulate organic matter, OM = organic matter, and SAV = submerged aquatic vegetation.

UTM 12T			
Easting (m)	Northing (m)	Substrate	Depth (cm)
1A. DOWNSTREAM OF MILL CREEK CONFLUENCE (IMPACTED SITES); METHOD = SHOVEL			
422033.54	4509629.59	Cobble/gravel/sand	60
422039	4509711.02	CPOM/garbage/OM/pea gravel	62
422003	4509839	*Corbicula*/peagravel	55
421949	4509831	*Corbicula*/peagravel	62
421956.91	4509950.37	*Corbicula*/peagravel/CPOM	50–80
422031.98	4509980.84	clay/gravel	50–80
422057.83	4510004.51	OM/silt/sand/*Corbicula*	50–70
422120.14	4510254.91	silt/sand/CPOM	50–90
422074	4510333.88	CPOM/silt/sand	70–100
422445.97	4510750.23	CPOM/silt/anaerobic	40–100
422480.56	4510716.21	OM/silt/sand	70–100
422453.14	4510645.01	peagravel/silt	70–120
422231.91	4510739.51	CPOM/silt	50–90
422210.96	4510756.82	CPOM/silt/fine sand	70–110
422223	4510790.25	silt/CPOM/fines	70–110
422235.72	4510806	silt/CPOM/fines	70–100
422246.02	4510923.75	silt/CPOM/fines	65–100
422319.9	4511415.2	deep OM/CPOM/garbage	60–100
422393.17	4511375.5	sand/CPOM/cobble	65
422280.64	4511422.33	OM/silt/clay/garbage	35
422222.28	4511382.05	OM/silt/clay/garbage	50
421964.7	4507219.29	sand/gravel	10
421963.81	4507324.34	silt/sand/gravel	34
421946.32	4507474.33	OM/silt/sand/gravel	82
422156.14	4507695.2	silt/sand/gravel	90
422016.53	4507623.26	silt/sand/gravel	117
422276	4508124.34	OM/silt/sand	110
421936.27	4508567.51	cobble/gravel/*Corbicula*	60
421805.52	4508909.21	sand/peagravel/*Corbicula*	95
421870.73	4509030.97	CPOM/silt/sand/peagravel/*Corbicula*	75
421924.25	4509240.47	roots/CPOM/FPOM/silt	100
422357	4511306	silt/CPOM	90–120
422306	4511288	silt/CPOM/FPOM/clay	60–120
422259	4511255	silt/CPOM/FPOM/clay	70–120
422142	4511074	FPOM/clay/silt	90–140
422249	4510953	silt/CPOM/FPOM/clay	70–120
422211	4510743	CPOM/FPOM/silt/muck/sand	90–130
422209	4510747	CPOM/FPOM/silt/muck/sand	100–130
422207	4510750	muck	70–120
1B. DOWNSTREAM OF MILL CREEK CONFLUENCE (IMPACTED SITES); METHOD = SUCTION DREDGE			
422259.92	4508110.23	cobbles/sand/silt/garbage/CPOM	90–130
422246.65	4508078.02	cobbles/sand/silt/garbage/CPOM	90–140
1C. UPSTREAM OF MILL CREEK CONFLUENCE (CONTROL SITES); METHOD = SHOVEL			
421879.36	4505831.52	peagravel/gravel	30–40
421886.68	4505935.81	gravel/clay	50–80
421730.66	4506092.01	gravel/SAV/sand	40–80
422847	4503923	large gravel/peagravel/sand	50–100
422817	4503986	peagravel/gravel/small cobble/sand	50–120
421939	4500685	small cobble/gavel/sand/silt/ SAV	40–90
421947	4500715	large gravel/peagravel/hard pan	30–60

Appendix 2. Mill Creek 2017 site data. Locations are given in relation to the Central Valley Water Reclamation Facility (CVWRF). All shovel sample areas equal 0.5 m^2, whereas all suction dredge sample areas were between 0.5 and 4.0 m^2. Samples were collected between 18 September 2017 and 21 September 2017. Substrate codes: CPOM = coarse particulate organic matter, FPOM = fine particulate organic matter, OM = organic matter, and SAV = submerged aquatic vegetation.

UTM 12T			
Easting (m)	Northing (m)	Substrate	Depth (cm)
2a. Upstream of CVWRF (control sites); method = shovel			
422656.00	4506771.71	CPOM/FPOM/clay	70
422676.10	4506768.19	CPOM/FPOM/clay	60
422704.00	4506764.00	clay	60
422726.00	4506761.00	SAV/silt/sand/CPOM/FPOM	75
422772.00	4506757.00	silt/SAV/CPOM/FPOM	60
422805.00	4506756.00	sand/silt/OM/trash/slag	60
422826.00	4506753.00	CPOM/sand/SAV	60
422861.00	4506747.00	hard clay/SAV	60
422877.00	4506745.00	hard clay	60–70
422925.00	4506741.00	hard clay/silt	60–70
422948.00	4506736.00	tree branches/CPOM	50–70
422978.00	4506733.00	sand/silt/clay	65
423604.92	4506540.01	gravel	65
423533.48	4506541.77	gravel	50
423402.69	4506634.96	sand/gravel	60
423377.19	4506643.72	silt/sand/veg/roots	60–70
423548.12	4506539.82	roots/silt/sand/CPOM	60–70
423579.90	4506539.59	gravel	60
2b. Downstream of CVWRF (impacted sites); method = shovel			
422074.00	4506876.00	silt/sand/clay	125
422064.00	4506881.00	silt/sand/clay	110
422059.00	4506885.00	silt/sand	90
422006.00	4506930.00	gravel/sand/silt	90
422001.00	4506934.00	sand/gravel/trash	100
422135.00	4506847.00	gravel/sand/silt/FPOM	90–100
422162.00	4506836.00	gravel/sand/silt/FPOM	90–100
422170.00	4506834.00	gravel/sand/silt/FPOM	90–100
422178.00	4506833.00	gravel/sand/silt/FPOM	90–100
422220.00	4506823.00	gravel/sand/silt/FPOM	90–100
422301.00	4506815.00	gravel/sand/cobble	90–100
422425.00	4506800.00	gravel/sand/cobble	90–100
422431.00	4506799.00	gravel/sand/cobble	90–100
422481.00	4506791.00	gravel/sand/cobble	90–100
422500.00	4506791.00	gravel/sand/cobble	90–100
2c. Downstream of CVWRF (impacted sites); method = suction dredge			
422005.00	4506933.00	FPOM/silt/sand/gravel	120
422003.00	4506928.00	FPOM/silt/sand/gravel	130
421993.00	4506940.00	FPOM/silt/sand/gravel	130
421992.00	4506946.00	FPOM/silt/sand/gravel	100
421989.00	4506949.00	FPOM/silt/sand/gravel	125